Birla Central Library
PILANI (Rajasthan)

Class No :- 621·55
Book No :- D953S
Accession No :- 37199

SCIENTIFIC FOUNDATIONS OF VACUUM TECHNIQUE

SCIENTIFIC FOUNDATIONS
OF
VACUUM TECHNIQUE

SAUL DUSHMAN, Ph.D.
Formerly Assistant Director, Research Laboratory
General Electric Company
Schenectady, N. Y.

NEW YORK JOHN WILEY & SONS, INC.
LONDON CHAPMAN & HALL, LIMITED

COPYRIGHT, 1949
BY GENERAL ELECTRIC COMPANY

All Rights Reserved
This book or any part thereof must not be reproduced in any form without the written permission of the publisher.

SECOND PRINTING, AUGUST, 1949

PRINTED IN THE UNITED STATES OF AMERICA

Dedicated to the
Memory of My Parents

PREFACE

In 1922, the writer published a small volume entitled *The Production and Measurement of High Vacua.* This work consisted of a revision of a series of articles which had appeared in the *General Electric Review* during 1920–1921. The following quotation is taken from the Preface to that volume:

"The subject of high vacua has become of such technical and scientific importance that it is hardly necessary to apologize for attempting to incorporate the information available on this topic into a convenient form for reference.

"Naturally the author has drawn to a large extent upon the results of numerous investigations carried out in this laboratory by Dr. Langmuir and his associates. To Dr. Langmuir, especially, he wishes to express his sincere gratitude for constant encouragement and helpful suggestions.

"He also feels greatly indebted to Dr. Whitney for constant interest in the present undertaking, and for placing at his disposal the facilities of the laboratory for pursuing various lines of purely scientific work."

To Dr. W. D. Coolidge, the former Director of the Research Laboratory, and Dr. C. G. Suits, the present Director, the writer feels likewise indebted for encouraging him in an extensive revision of the earlier work and for their continued interest in the present undertaking.

During the quarter century that has intervened, the subject of vacuum technique has increased in importance to such an extent as to necessitate not only a complete revision of the material in the previous volume but also the addition of a number of new topics.

The industrial and scientific importance of the investigations in this field that have been published during the past twenty-five years, and which are being increased almost daily, was emphasized by the large attendance at the Symposium on Vacuum Technique held at Cambridge, Mass., October 30–31, 1947, under the sponsorship of the National Research Corporation and Division of Industrial and Engineering Chemistry of the American Chemical Society.

The interest in vacuum technique which was initiated by the development of the incandescent-filament vacuum lamp and received an additional impetus by the subsequent developments in the study and production of electronic devices was accelerated by certain extremely important problems which arose during the second world war.

The importance of vacuum technique both in purely scientific investigations and in industry is evident from a brief summary of some of the most striking applications. In the electronic field we have the vast range of devices from the smallest receiving tube to the 100-kw transmitting tube, in the field now designated nucleonics we have high-voltage devices such as the cyclotron, betatron, and synchrotron, as well as 2-million-volt X-ray tubes. Moreover, the industrial utilization of vacuum distillation, vacuum dehydration, and vacuum fusion of metals has increased to a significant extent. In short, vacuum technique has emerged from the purely scientific environment of the research laboratory and has entered the engineering stage on a scale that could not have been conceived even as recently as two decades ago.

In this treatise the writer has not dealt specially with experimental procedures for using vacuum technique in the same manner as in Strong's book, *Procedures in Experimental Physics*, or the more recent work by Bachman, *Techniques in Experimental Electronics*. He has attempted to present a survey of fundamental ideas in physics, chemistry, and (to a smaller extent) metallurgy, which will be found useful to both scientists and engineers in dealing with problems in the production and measurement of high vacua.

The writer appreciates the criticisms, suggestions, and information which he has received from a number of his associates in the Research Laboratory and from friends engaged in the industrial applications of vacuum technology. Every effort has been made to give credit to those individuals and organizations, in connection with the specific topics.

Finally, the writer wishes to express his appreciation of the help in typing the manuscript, and for subsequent details which had to be worked out while the volume was going through the press, to Miss Constance Edwards, his former secretary, Miss Gloria Feola, his present secretary, Mrs. Rose Hunton, and Miss Jean Oldham.

CONTENTS

CHAPTER 1 KINETIC THEORY OF GASES

1 Fundamental Postulates of the Kinetic Theory of Gases, *1.* 2 Ideal Gas Laws, *1.* 3 Avogadro Number, *7.* 4 Molecular Velocities. Maxwell-Boltzmann Distribution Law, *9;* Added Note 1: Relation between Molecular Velocities and Velocity of Sound, *13.* Added Note 2: Determination of Avogadro Constant from Distribution of Particles in Brownian Motion, *14.* 5 Rate at Which Molecules Strike a Surface, *17.* 6 Rate of Evaporation and Vapor Pressure, *18.* 7. Free Paths of Molecules, *24.* 8 Relation between Coefficient of Viscosity, Mean Free Path, and Molecular Diameter, *28.* Added Note 3: Viscosity at Low Pressures, *39.* Added Note 4: Molecular Diameters, *41.* 9 Heat Conductivity of Gases, *44.* 10 Thermal Conductivity at Low Pressures, *48.* 11 Langmuir's Film Theory of Heat Conduction, *59.* 12 Thermal Transpiration (Thermomolecular Flow), *65.* 13 Thermal Diffusion, *67.* 14 Theory of Diffusion of Gases, *74.* Added Note 5: Maxwell-Loschmidt Method for Determination of Diffusion Coefficients, *77.* Added Note 6: Effect of Pressure of Gas on Rates of Evaporation of Metals, *78.* 15 Random Motions and Fluctuations, *81.*

CHAPTER 2 FLOW OF GASES THROUGH TUBES AND ORIFICES

1 Viscous Flow of Gases, *84.* Added Note: Turbulent Flow, *88.* 2 "Free Molecule" Flow, *90.* 3 Flow at Intermediate Pressures, *111.* 4 Flow of Gases through Porous Diaphragms, *118.* 5 Rate of Exhaust through a Tube or Orifice, *121.*

CHAPTER 3 MECHANICAL PUMPS

1 Historical Review, *126.* 2 General Remarks on Operation of Pumps, *128.* 3 Design of High-Vacuum Systems, *134.* 4 Earlier Types of Mechanical Pumps, *136.* 5 Commercial Types of Rotary Oil Pumps, *141.* 6 Molecular Pumps, *151.* 7 Determination of Speed of Pump, *159.*

CHAPTER 4 STEAM-JET EJECTORS AND MERCURY-VAPOR PUMPS

1 Steam-Jet Ejectors, *169.* 2 Diffusion of Gases in a Vapor Stream, *176.* 3 The Gaede Diffusion Pumps, *182.* 4 The Langmuir Condensation Pump, *184.* 5 Multistage Pumps, *191.* 6 Performance Characteristics of Mercury-Vapor Pumps as Influenced by Different Factors, *193.* 7 Effect of Design of Nozzles, *198.* 8 Role of Diffusion and Condensation in Vapor-Stream Pumps, *204.* 9 Design of Cooling Trap and Substitutes for Liquid Air, *214.*

CHAPTER 5 VAPOR PUMPS USING ORGANIC LIQUIDS

1 Investigation of Suitable Liquids, *218.* Note on the Mean Free Paths in Oil Vapors, *225.* 2 Non-Fractionating Oil-Vapor Pumps, *226.* 3

Fractionating Types of Oil-Vapor Pumps, *230.* 4 Jet Design and Baffles, *241.* 5 Stability of Oils, Ultimate Vacuum of Oil-Vapor Pumps, *249.* 6 Use of Silicone Oils, *253.*

CHAPTER 6 MANOMETERS FOR LOW GAS PRESSURES

1 Application of Electrical Discharge in Gas at Low Pressures, *258.* 2 Mercury (and Other Liquid) Manometers, *260.* 3 Mechanical Manometers, *272.* 4 Viscosity Manometers, *279.* 5 Radiometer Type of Gauges, *293.* 6 Heat Conductivity Manometers, *313.* 7 Ionization Gauges, *332.* 8 General Remarks on Gauges, *366.* 9 Leak Detectors, *370.*

CHAPTER 7 SORPTION OF GASES AND VAPORS BY SOLIDS

1 Adsorption, Absorption, Occlusion, and Sorption, *387.* 2 Some Typical Adsorption Isotherms, *390.* 3 Parabolic and Hyperbolic Equations for Adsorption Isotherm, *396.* 4 Other Expressions for the Adsorption Isotherm, *416.* 5 Multimolecular Adsorption, *425.* 6 Temperature Variation of Adsorption, *434.* 7 Heat of Sorption, *445.* 8 Rate of Sorption, *451.* 9 Surface of Adsorbents, *454.*

CHAPTER 8 SORPTION OF GASES BY "ACTIVE" CHARCOAL, SILICATES (INCLUDING GLASSES), AND CELLULOSE

1 Preparation and Structure of Activated Charcoal, *466.* 2 Sorption Data at Higher Pressures, *472.* 3 Sorption Data at Low Pressures, *488.* 4 Use of Charcoal at Low Temperatures in High-Vacuum Systems, *493.* 5 Sorption by Silica Gel and Silicates, *498.* 6 Evolution and Sorption of Gases by Glass, *509.* 7 Diffusion of Gases through Quartz and Glasses, *531.* 8 Sorption and Desorption Phenomena in Cellulose, *538.*

CHAPTER 9 GASES AND METALS

1 Introductory Remarks, *547.* 2 Physical Adsorption and Chemisorption, *547.* 3 General Remarks on Sorption of Gases by Metals, *552.* 4 Solubility of Hydrogen in Metals of Group A, *553.* 5 Solubility of Hydrogen in Metals of Group B, *572.* 6 Derivation of Relations for the Solubility of Hydrogen in Metals, *589.* 7 Solubility of Hydrogen in Palladiumlike Metals and Palladium Black, *591.* 8 Solubility of Nitrogen in Metals, *596.* 9 Solubility of Oxygen and Other Gases, *600.* 10 Diffusion of Gases through Metals, *607.* 11 Rates of Sorption and Desorption; Calculation of Diffusion Constants, *618.* 12 Earlier Investigations on Degassing of Metals, *624.* 13 Investigation on Degassing of Metals by Norton and Marshall, *633.* 14 Determination of Oxygen Content of Metals from Composition of Gases Evolved, *637.* 15 Embrittlement of Metals by Hydrogen, *640.* 16 Observations on Gases in Cast Metals, *644.* 17 Analysis of Gases in Metals, *648.*

CHAPTER 10 CHEMICAL AND ELECTRICAL CLEAN-UP OF GASES AT LOW PRESSURES

1 General Remarks, *654.* *Part A, Chemical Clean-up.* 2 Clean-up of Gases by Evaporated Metals, *656.* 3 Technical Getters, *668.* 4 Clean-up by Zirconium and Titanium, *670.* 5 Reactions between Gases at Low Pressures and Incandescent Filaments, *673.* *Part B, Electrical Clean-up of Gases.* 6 Phenomena in Cold-Cathode Discharge Tubes, *687.* 7 Clean-up

in Electrodeless Discharges, *698.* 8 Electron Emission and Space-Charge Phenomena in Hot-Cathode Low-Pressure Devices, *699.* 9 Clean-up in Hot-Cathode Discharges, *704.* 10 Clean-up Phenomena in Vacuum Incandescent Lamps, *716.* 11 Electrical Clean-up in Hot-Cathode Tubes at Very Low Pressures, *724.* 12 Production of Extremely High Vacuum in Sealed-off Devices, *730.*

CHAPTER 11 VAPOR PRESSURES AND RATES OF EVAPORATION

1 Thermodynamical Relations, *740.* 2 Vapor-Pressure Data and Rates of Evaporation for Metals and Carbon, *743.* 3 General Remarks on Vacuum Distillation of Metals and Deposition of Films, *757.* 4 Vapor Pressures and Evaporation Phenomena of Alloys, *764.* 5 Vapor Pressures of Oxides and Other Inorganic Compounds, *778.* 6 Vapor Pressures at Low Temperatures, *781.* 7 Boiling Point of Liquid Air, *786.* 8 Vapor Pressures of Oils, Greases, and Waxes, *789.*

CHAPTER 12 DISSOCIATION PRESSURES OF OXIDES, HYDRIDES, AND NITRIDES AND RATES OF OXIDATION

1 Free and Total Energy, *793.* 2 Free and Total Energy of Formation of Water Vapor, *798.* 3 Dissociation Pressures of Oxides of Silver, Mercury, and Palladium, *803.* 4 Dissociation and Reduction of Oxides of Copper, *805.* 5 Dissociation of Oxides of Iron and Their Reduction by Hydrogen, *810.* 6 Dissociation and Reduction of Oxides of Nickel and Cobalt, *817.* 7 Dissociation and Reduction of Oxides of Manganese, Chromium, Molybdenum, and Tungsten, *819.* 8 Reduction of Oxides by Carbon Monoxide, Other Reducing Atmospheres, and Carbon, *822.* 9 Dissociation of Hydrides of the Alkali and Alkaline-Earth Metals, *828.* 10 Dissociation Pressures of Nitrides, *830.* 11 Parabolic Law of Rates of Oxidation, *835.* 12 Logarithmic Law of Rates of Oxidation, *849.* 13 Ionic Theory of Rates of Oxidation, *852.*

SIGNIFICANCE OF REFERENCE ABBREVIATIONS, *855*

NAME INDEX, *857*

SUBJECT INDEX, *869*

CHAPTER 1[1]

KINETIC THEORY OF GASES

1. FUNDAMENTAL POSTULATES OF THE KINETIC THEORY OF GASES

For a proper understanding of phenomena in gases, more especially at low pressures, it is essential to consider these phenomena from the point of view of the kinetic theory of gases. This theory rests essentially upon two fundamental assumptions. The first of these postulates is that matter is made up of extremely small particles or molecules, and that the molecules of the same chemical substance are exactly alike as regards size, shape, mass, and so forth. The second postulate is that the molecules of a gas are in constant motion, and this motion is intimately related to the temperature. In fact, the temperature of a gas is a manifestation of the amount or intensity of molecular motion.

In the case of monatomic molecules (such as those of the rare gases and vapors of most metals) the effect of increased temperature is evidenced by increased translational (kinetic) energy of the molecules. In the case of diatomic and polyatomic molecules increase in temperature also increases rotational energy of the molecule about one or more axes, as well as vibrational energy of the constituent atoms with respect to mean positions of equilibrium. However, in the following discussion only the effect on translational energy will be considered.

2. IDEAL GAS LAWS

According to the kinetic theory a gas exerts pressure on the enclosing walls because of the impact of molecules on these walls. Since the gas suffers no loss of energy through exerting pressure on the solid wall of its enclosure, it follows that each molecule is thrown back from the wall with the same speed as that with which it impinges, but in the reverse direction; that is, the impacts are perfectly elastic.

---

[1] In connection with this chapter the writer has made use of the following treatises. The abbreviations used for these references in this volume are indicated in parentheses.

1. E. H. Kennard, *Kinetic Theory of Gases with an Introduction to Statistical Mechanics*, McGraw-Hill Book Company, New York, 1938 (EHK).
2. L. B. Loeb, *Kinetic Theory of Gases*, McGraw-Hill Book Company, New York, 2nd ed., 1934 (LBL).
3. J. H. Jeans, *An Introduction to the Kinetic Theory of Gases*, The Macmillan Company, New York, 1940 (JHJ).
4. S. Chapman and T. G. Cowling, *The Mathematical Theory of Non-Uniform Gases*, Cambridge, England, The University Press, 1939 (CC).

Suppose a molecule of mass m to approach the wall with velocity v. Since the molecule rebounds with the same speed, the change of momentum per impact is $2mv$. If ν molecules strike unit area in unit time with an average velocity v, the total impulse exerted on the unit area per unit time is $2m\nu v$. But the pressure is defined as the rate at which momentum is imparted to a unit area of surface. Hence,

$$2m\nu v = P. \tag{1a}$$

It now remains to calculate ν. Let n denote the number of molecules per unit volume. It is evident that at any instant we can consider the molecules as moving in six directions corresponding to the six faces of a cube. Since the velocity of the molecules is v, it follows that, on the average, $(n/6)v$ molecules will cross unit area in unit time.

Equation 1*a* therefore becomes

$$P = \tfrac{1}{3}mnv^2. \tag{1b}$$

Since

$$mn = \rho, \tag{2}$$

where ρ denotes the density, equation 1*b* can be expressed in the form

$$P = \tfrac{1}{3}\rho v^2, \tag{3}$$

which shows that, at constant temperature, the pressure varies directly as the density, or inversely as the volume. This is known as Boyle's law.

Also, from equation 1*b* it follows that the total kinetic energy of the molecules in volume V is

$$\tfrac{1}{2}mnv^2V = \tfrac{3}{2}PV. \tag{4}$$

Now it is a fact that no change in temperature occurs if two different gases, originally at the same temperature, are mixed. This result is valid independently of the relative volumes. Consequently, the average kinetic energy of the molecules must be the same for all gases at any given temperature and the rate of increase with temperature must be the same for all gases. We may therefore define temperature in terms of the average kinetic energy of the molecules, and this suggestion leads to the relation

$$\tfrac{1}{2}mv^2 = \tfrac{3}{2}kT, \tag{5}$$

where T is the absolute temperature (degrees Kelvin), defined by the relation $T = 273.16 + t$ (t = degrees Centigrade), and k is a *universal constant,* known as the Boltzmann constant.

Combining equation 5 with 4, it follows that

$$P = nkT. \tag{6}$$

This is an extremely useful relation, as will be shown subsequently, for the determination of n for given values of P and T. Also, from equation 2 and the last equation, it follows that

$$P = \frac{k}{m} \rho T, \tag{7a}$$

that is,

$$\frac{P}{\rho} = \frac{k}{m} T, \tag{7b}$$

which is known as Charles' law.

Lastly, let us consider *equal* volumes of any two different gases at the same values of P and T. Since P and V are respectively the same for each gas, and $\frac{1}{2}mv^2$ is constant at constant value of T, it follows from equations 4 and 6 that n must be the same for both gases. That is, *equal volumes of all gases at any given values of temperature and pressure contain an equal number of molecules.* This was enunciated as a fundamental principle by Avogadro in 1811, but it required about 50 years for chemists to understand its full significance.

On the basis of Avogadro's law the molecular mass, M, of any gas or vapor is defined as that *mass in grams,* calculated for an ideal gas, which occupies, at 0° C and 1 atmosphere, a volume[2]

$$V_0 = 22{,}414.6 \quad \text{cm}^3.$$

This is therefore designated the *molar volume,* and the *equation of state for an ideal gas* can be written in the form

$$PV = \frac{W}{M} \cdot R_0 T, \tag{8a}$$

---

[2] The values given for V_0 and other constants in this and subsequent sections are those recommended by R. T. Birge, *Reports on Progress in Physics,* Vol. VIII, 90, 1941. The original paper gives, for each constant, the probable error. While the values are stated to the same number of decimal points as by Birge, it is evident that for most calculations values rounded out to an accuracy of 0.1 per cent are sufficiently satisfactory. [A more recent discussion (*Am. J. Phys.,* **13,** 63, 1945) leaves the 1941 values substantially unaltered.]

As far as possible the notation used for the constants is the same as that given by Birge. For R_0, the molar gas constant, writers on the kinetic theory of gases often use the notation R_M or R. On the other hand, R is also used to designate R_0/M.

where W = mass in grams.
M = molecular mass in grams.
R_0 = a *universal constant.*
V = volume of W grams at pressure P and absolute temperature T.

It is convenient to express the last equation in the form

$$PV = n_M \cdot R_0 T, \tag{8b}$$

where n_M denotes the *number of moles* (corresponding to M in grams) in the volume V under the given conditions of temperature and pressure.

Obviously the exact value to be used for R_0 must depend upon the units in which P, V, T, and W are expressed.

In the cgs system the *unit of pressure* is 1 dyne per cm^2. This is designated, according to the most recent terminology,[3] 1 *microbar* (= 10^{-6} bar).

The standard atmosphere (A_0) is defined as the pressure exerted per square centimeters by a mercury column 760 mm in height, at 0° C. Since the density of mercury at 0° C is 13.595 g/cm^3, it follows that

$$\begin{aligned} 1\ A_0 &= 76 \times 13.595 = 1033.22\ \text{g} \cdot \text{cm}^{-2} \\ &= 1033.2 \times 980.67 = 1.01325 \cdot 10^6\ \textit{microbar}. \end{aligned}$$

Hence, 10^6 microbar = 1 bar = 750.06 mm Hg, and 10^3 microbar = 1 *millibar* = 0.75 mm Hg.

In vacuum technology the units of pressure commonly used are the following:[4]

---

[3] Formerly the designations used were as follows: 1 bar (ca. 1915), and 1 barye (1920–1930, approximately); and what is now designated 1 bar was termed a megabar.

[4] In German literature, 1 Tor (or 1 Torr) is used to designate 1 mm Hg pressure. In engineering literature the following units are frequently used:

$$\begin{aligned} 1\ A_0 &= 29.921\ \text{in. Hg at } 32^\circ\ \text{F} \\ &= 14.696\ \text{lb/in.}^2\ \text{(psi)}. \\ x\ \text{psig} &= x\ \text{lb/in.}^2\ \textit{on gauge} \\ &= x\ \text{lb/in.}^2\ \textit{above}\ \text{atmospheric pressure.} \end{aligned}$$

Also, in the mks system,

$$1\ \text{newton} = 10^5\ \text{dynes},$$

and

$$1\ \text{newton/cm}^2 = 0.1\ \text{bar} = 10^5\ \text{microbars}.$$

While the notation P will be used to designate pressure, in general, the notations P_b, P_{atm}, $P_{\mu b}$, P_{mm}, and P_μ will be used to designate the pressure in bars, atmospheres, microbars, millimeters, and microns, respectively.

$$1 \text{ mm Hg} = 1333.22 \text{ microbar} = 1.333 \text{ millibar.}$$

$$1 \text{ micron} = 1\ \mu = 10^{-3} \text{ mm Hg}$$
$$= 1.3332 \text{ microbars.}$$

$$10^{-3} \text{ micron} = 1\ \text{m}\mu = 1.333 \cdot 10^{-3} \text{ microbar.}$$

Hence, 1 microbar = 0.75 μ.

The unit of volume in the cgs system is 1 cm^3, and that of mass, 1 g. In industrial operations, these are commonly replaced by the liter, cubic foot (cu ft), and ounce (or pound) avoirdupois.

For temperature we have the absolute Centigrade or Kelvin scale ($T = t° \text{ C} + 273.16$) or the absolute Fahrenheit scale[5] ($T_F = t° \text{ F} + 459.7$).

It should be observed, as a matter of considerable practical importance, that (to within 0.12 per cent) there is approximately the same relation between liters and cubic feet as between grams and ounces avoirdupois; that is,

1 liter = 0.035316 cu ft (reciprocal = 28.316),

and

1 gram = 0.035274 oz av (reciprocal = 28.3495).

Ratio = 1.0012.

By means of these conversion factors we obtain the following values for R_0:[6]

$$R_0 = \frac{760 \times 22.415}{273.16} = 62.364 \text{ mm} \cdot \text{liter} \cdot \text{deg}^{-1}\ \text{K} \cdot \text{g-mole}^{-1}$$

$$= \frac{1.01325 \times 10^6 \times 22{,}415}{273.16} = 8.3146 \cdot 10^7 \text{ erg} \cdot \text{deg}^{-1}\ \text{K} \cdot \text{g-mole}^{-1}$$

$$= 62.364 \times 0.035316 = 2.2024 \text{ mm} \cdot \text{cu ft} \cdot \text{deg}^{-1}\ \text{K} \cdot \text{g-mole}^{-1}$$

$$= 2.2024 \times 28.3495 = 62.439 \text{ mm} \cdot \text{cu ft} \cdot \text{deg}^{-1}\ \text{K} \cdot \textit{oz}\text{-mole}^{-1}$$

$$= 62.439 \times 16 = 999.024 \text{ mm} \cdot \text{cu ft} \cdot \text{deg}^{-1}\ \text{K} \cdot \text{lb-mole}^{-1}$$

$$= \frac{760 \times 22.415 \times 1.0012}{(459.7 + 32)} = 34.687 \text{ mm} \cdot \text{cu ft} \cdot \text{deg}^{-1}\ T_F \cdot \text{oz-mole}^{-1}.$$

It will be observed that the last three relations refer to the molecular weight expressed in oz av or lb av.

---

[5] T_F is designated "degrees Rankine."

[6] Values in other units may be deduced in a similar manner.

In dealing with gases at low pressures, it is convenient to express the *quantity of gas* ($Q = PV$) in the following units:

$$1\ \mu \cdot l = \text{quantity of gas in 1 liter at 1 micron.}$$

$$1\ \text{mm} \cdot \text{cu ft} = \text{quantity in 1 cubic foot at 1 mm.}$$

$$1\ \text{mm} \cdot l = 10^3\ \mu \cdot l.$$

Since the amount (or mass) of gas in a given volume depends upon the temperature as well as the pressure, we shall assume, unless otherwise stated, that we are dealing with an ideal gas at room temperature, that is, 25° C.[7]

Let Q_l and Q_c designate the number of *micron · liters* and *mm · cu ft*, respectively. Then, at 25° C,

$$Q_l = \frac{10^{-3}}{62.364 \times 298.16} = 5.3779 \cdot 10^{-8}\ Q_l \text{ g-mole}$$

$$= 5.3779 \cdot 10^{-8}\ Q_l M \text{ g},$$

$$Q_c = \frac{1}{2.2024 \times 298.16} = 1.5228 \cdot 10^{-3}\ Q_c \text{ g-mole}$$

$$= 1.5228 \cdot 10^{-3}\ Q_c M \text{ g},$$

$$Q_c = \frac{1}{62.439 \times 298.16} = 5.3715 \cdot 10^{-5}\ Q_c M' \text{ oz av},$$

where M' = molecular weight in oz av. (M' for $O_2 = 32.0$.)

Introducing the mechanical equivalent of heat,

$$J_{15} = 4.1855 \cdot 10^7 \text{ erg} \cdot \text{cal}_{15}{}^{-1},$$

we obtain the relation

$$J_{15}R_0 = \frac{8.3146}{4.1855}$$

$$= 1.98647 \text{ cal}_{15} \cdot \text{deg}^{-1} \cdot \text{g-mole}^{-1}.$$

---

[7] The following additional conversion factors will be found useful:

$$1\ \mu \cdot l\ (25° \text{ C}) = 0.9162 \text{ micron} \cdot \text{liter at } 0° \text{ C}$$

$$= 1.205 \text{ atm} \cdot \text{mm}^3 \text{ at } 0° \text{ C}$$

$$= 1.316 \text{ atm} \cdot \text{mm}^3 \text{ at } 25° \text{ C}$$

$$= 3.240 \cdot 10^{16} \text{ molecules (see section 3)}$$

$$= 0.0353 \text{ micron} \cdot \text{cu ft at } 25° \text{ C}.$$

From the values given above for R_0 the following relations are derived for the density:

$$\begin{aligned}\rho = mn = \frac{M}{V_0} = \frac{MP_{\mu b}}{R_0 T} \qquad\qquad (9)\\ = 1.2027 \cdot 10^{-8} \frac{MP_{\mu b}}{T} \quad \mathrm{g} \cdot \mathrm{cm}^{-3}\\ = 1.6035 \cdot 10^{-5} \frac{MP_{mm}}{T} \quad \mathrm{g} \cdot \mathrm{cm}^{-3}\end{aligned}$$

where $P_{\mu b}$ = pressure in microbars.

P_{mm} = pressure in millimeters of mercury.

$\rho_1{}^0$ = density at 1 microbar and 0° C

$= 4.403 \cdot 10^{-11} M$.

Values of $\rho_1{}^0$ for a number of gases are given in the fourth column of Table 3.

In terms of *cubic feet* and *millimeters of mercury,*

$$\begin{aligned}\rho &= \frac{MP_{mm}}{2.2024T} = 0.45405MP_{mm}/T \quad \mathrm{g/cu\ ft}\\ &= \frac{M'P_{mm}}{34.687T_F} = 0.02883M'P_{mm}/T_F \ \mathrm{oz/cu\ ft.}\end{aligned}$$

3. AVOGADRO NUMBER

Avogadro's law states that the number of molecules per gram-molecular mass is a constant, which is designated N_A. Although a number of different methods have been used for the determination of this constant, the most accurate method depends upon the determination of both the Faraday (F) and the charge of the electron (e).

For the deposition of one gram-equivalent the most accurate value is

$$F = 96{,}488 \text{ absolute coulombs.}$$

Assuming that each univalent ion has a charge equal in magnitude to that of one electron,

$$N_A = \frac{F}{e}.$$

The accepted value of the charge of the electron is

$$e = 4.8025 \cdot 10^{-10} \text{ absolute esu}$$

$$= 10 \frac{e}{c} \text{ absolute coulombs,}$$

where c = velocity of light = $2.99776 \cdot 10^{10}$ cm · sec^{-1}. Hence

$$e = 1.60203 \cdot 10^{-19} \text{ absolute coulomb}$$

and

$$N_A = 6.0228 \cdot 10^{23} \text{ mole}^{-1}.$$

From equations 2.6 and 2.8 it follows that for the molar volume

$$P = \frac{N_A kT}{V}$$

and hence

$$k = \frac{R_0}{N_A} \tag{1}$$

$$= 1.3805 \cdot 10^{-16} \quad \text{erg} \cdot \text{deg}^{-1} \text{ K.}$$

From equation 2.5 it also follows that the *average kinetic energy per molecule* is given by

$$\tfrac{1}{2}mv^2 = \tfrac{3}{2}kT = 2.0707 \cdot 10^{-16}T \quad \text{erg}$$

$$= 5.6565 \cdot 10^{-14} \quad \text{erg at } 0° \text{ C.} \tag{2}$$

The mass per molecule is evidently

$$m = \frac{M}{N_A}$$

$$= 1.66035 \cdot 10^{-24}M \quad \text{g.} \tag{3}$$

The second and third columns in Table 3 give, respectively, values of M and m for a number of gases.

From equation 2.6 it follows that

$$n = \text{number of molecules per cm}^3$$

$$= 7.244 \cdot 10^{15} \frac{P_{\mu b}}{T} \quad \text{where } P \text{ is given in microbars} \tag{4a}$$

$$= 9.656 \cdot 10^{18} \frac{P_{mm}}{T} \quad \text{where } P \text{ is given in millimeters.} \tag{4b}$$

Table 1 gives values of n for a series of values of T and $P_{\mu b}$ or P_{mm}. The value $n = 2.687 \cdot 10^{19}$ is known as the Loschmidt number.

TABLE 1

NUMBER OF MOLECULES PER CM^3

T	$P_{\mu b}$	P_{mm}	n
273.16	$1.0133 \cdot 10^6$	760	$2.687 \cdot 10^{19}$
298.16	$1.0133 \cdot 10^6$	760	$2.462 \cdot 10^{19}$
273.16	$1.333 \cdot 10^3$	1	$3.536 \cdot 10^{16}$
298.16	$1.333 \cdot 10^3$	1	$3.240 \cdot 10^{16}$
273.16	1.000	$7.50 \cdot 10^{-4}$	$2.653 \cdot 10^{13}$
298.16	1.000	$7.50 \cdot 10^{-4}$	$2.430 \cdot 10^{13}$

4. MOLECULAR VELOCITIES. MAXWELL-BOLTZMANN DISTRIBUTION LAWS

It is evident that there must be a non-uniform distribution of velocities among all the molecules in a given volume because of the constant occurrence of collisions. J. C. Maxwell and L. Boltzmann showed that it is possible to determine the law according to which the molecular velocities are distributed at any given temperature.

The form of the distribution law differs according to the particular type of velocity distribution of interest. If we let $\dot{x}$, $\dot{y}$, and $\dot{z}$ designate the components, along the three coordinate axes, of the randomly directed velocity v, then

$$v^2 = \dot{x}^2 + \dot{y}^2 + \dot{z}^2, \tag{1}$$

and the distribution function, $f_{\dot{x}}$, with respect to, say, $\dot{x}$ is given by the relation

$$\frac{1}{N}\frac{dN}{d\dot{x}} = f_{\dot{x}} = \left(\frac{m}{2\pi kT}\right)^{1/2} \epsilon^{-m\dot{x}^2/(2kT)}, \tag{2}$$

where N = number of molecules in the volume under consideration.

The distribution function for all three components of v has the form

$$\frac{1}{N}\frac{dN}{d\dot{x}\,d\dot{y}\,d\dot{z}} = f_{\dot{x}\dot{y}\dot{z}} = \left(\frac{m}{2\pi kT}\right)^{3/2} \epsilon^{-\frac{m(\dot{x}^2+\dot{y}^2+\dot{z}^2)}{2kT}}. \tag{3}$$

With respect to the polar coordinates θ and ϕ,

$$\frac{1}{N}\frac{dN}{dv\,d\theta\,d\phi} = f_{v\theta\phi} = \left(\frac{m}{2\pi kT}\right)^{3/2} \epsilon^{-mv^2/(2kT)} \sin\theta. \tag{4}$$

The most important distribution function is that with respect to *v in a random direction*, which is given by the relation

$$\frac{1}{N}\frac{dN}{dv} = f_v = \frac{4}{\sqrt{\pi}}\left(\frac{m}{2kT}\right)^{3/2} v^2 \epsilon^{-mv^2/(2kT)}. \tag{5}$$

Differentiating f_v with respect to v, it is observed that the maximum value occurs for

$$v = \alpha = \sqrt{\frac{2kT}{m}}. \tag{6}$$

Hence α corresponds to the value of the *most probable velocity,* which is given by the relation

$$\alpha = \sqrt{\frac{2R_0T}{M}} = 12{,}895\sqrt{\frac{T}{M}} \quad \text{cm} \cdot \text{sec}^{-1}. \tag{7}$$

In terms of $c = v/\alpha$, we can express equation 5 in the form

$$\frac{dy}{dc} = \frac{1}{N}\frac{dN}{dc} = f_c = \frac{4c^2}{\sqrt{\pi}}\epsilon^{-c^2}, \tag{8}$$

where c varies from 0 to ∞, and dy $(= f_c\,dc)$ corresponds to the fraction of the total number of molecules which have values of c ranging between c and $c + dc$. Hence

$$\int_0^1 dy = \int_0^\infty f_c\,dc = 1. \tag{9a}$$

From the last equation we derive the value of the *arithmetical average velocity,* $v_a = \alpha c_a$, where

$$c_a = \frac{\int_0^\infty cf_c\,dc}{\int_0^\infty f_c\,dc} = \frac{2}{\sqrt{\pi}} = 1.1284,$$

and

$$v_a = \sqrt{\frac{8R_0T}{\pi M}} \quad \text{from equation 7}$$

$$= 14{,}551\sqrt{\frac{T}{M}} \quad \text{cm} \cdot \text{sec}^{-1}. \tag{10}$$

The *root-mean square velocity,* v_r, corresponds to the square root of the average value of v^2 as derived from equation 2.5 and is therefore given by the relation

$$v_r = \sqrt{\frac{3R_0T}{M}}$$

$$= 15{,}794\sqrt{\frac{T}{M}} \quad \text{cm} \cdot \text{sec}^{-1} \tag{11}$$

$$= c_r\alpha$$

and

$$c_r = \sqrt{\tfrac{3}{2}} = 1.2247$$
$$= 1.0854 c_a.$$

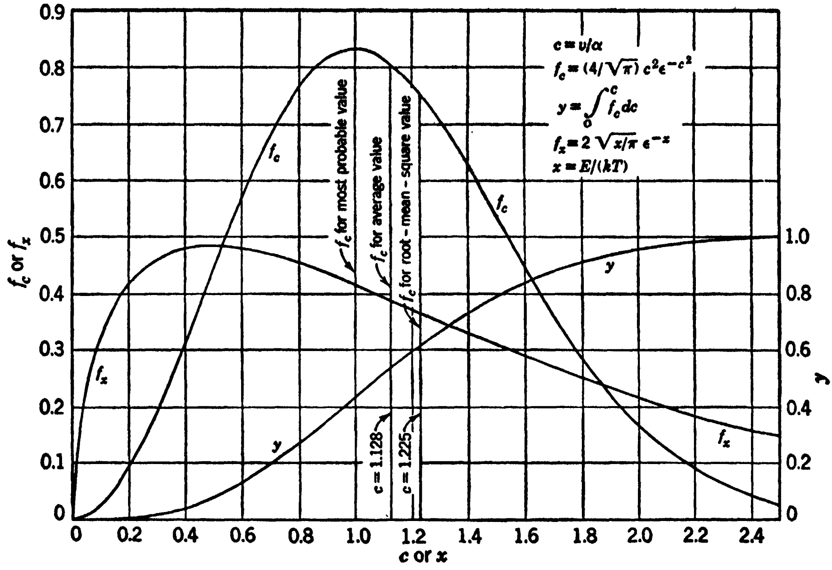

FIG. 1. Plots illustrating Maxwell-Boltzmann distribution laws. Plot f_c shows distribution function for random velocity, c expressed in terms of the most probable velocity α; plot f_x shows distribution function for energy, E, in terms of $x = E/(kT)$; y corresponds to the fraction of the total number of molecules for which the random velocity (expressed in terms of α) is less than or equal to a given value c.

The second column in Table 2 gives values of f_c for a series of values of c, and Fig. 1 shows a plot of these data, on which the values of f_c are indicated for the values $c = 1$, 1.1284, and 1.2247, respectively.

The integral

$$y = \frac{N_c}{N} = \int_0^c f_c\, dc \tag{9b}$$

gives the *fraction of the total number of molecules* which have a random velocity *equal to or less* than that corresponding to the value c, or to $v = \alpha c$. The third and fourth columns in Table 2[8] show values of y and of Δy, where Δy gives the fraction of the total number which have velocities (in terms of α as a unit) ranging between c and the immediately preceding value of c. Thus, 8.35 per cent of the molecules have velocities between $c = 1$ and $c = 1.1$, and 42.76 per cent have velocities equal to or less than the most probable value. The values in parentheses are those of $(1 - y)$. A plot of y versus c is shown in Fig. 1.

---

[8] A similar table is given in appendix B, p. 578, of *Gaseous Conductors* by J. D. Cobine, McGraw-Hill Book Company, 1941.

It is evident that y corresponds to the area under the curve for f_c from the origin to the given value of c.

From equation 5 the distribution formula for translational energy (E) can be derived. It has the form

$$\frac{1}{N}\frac{dN}{dE} = f_E = \frac{2}{\sqrt{\pi}}\frac{1}{kT}\sqrt{\frac{E}{kT}}\,\epsilon^{-E/(kT)}. \tag{12}$$

Substituting the variable $x = E/(kT)$, the last equation becomes

$$\frac{1}{N}\frac{dN}{dx} = f_x = \sqrt{\frac{4x}{\pi}}\,\epsilon^{-x}. \tag{13}$$

TABLE 2

Values of f_c, y, and f_x, Illustrating Application of Distribution Laws

c	f_c	y	Δy	x	f_x
0	0	0		0	0
0.1	0.0223	0.0008	0.0008	0.05	0.2401
0.2	.0867	.0059	.0051	0.1	.3229
0.3	.1856	.0193	.0134	0.2	.4131
0.4	.3077	.0438	.0245	0.3	.4578
0.5	.4393	.0812	.0374	0.4	.4785
0.6	.5668	.1316	.0504	0.5	.4839
0.7	.6775	.1939	.0623	0.6	.4797
0.8	.7613	.2663	.0724	0.7	.4688
0.9	.8129	.3453	.0790	0.8	.4535
1.0	.8302	.4276	.0823	0.9	.4352
1.1	.8142	.5101	.0835	1.0	.4152
1.2	.7697	.5896	.0795	1.2	.3722
1.3	.7036	.6634	.0738	1.4	.3294
1.4	.6232	.7286	.0642	1.6	.2882
1.5	.5350	.7878	.0602	1.8	.2502
1.6	.4464	.8369	.0491	2.0	.2160
1.7	.3624	.8772	.0403	2.2	.1855
1.8	.2862	.9096	.0324	2.5	.1464
1.9	.2204	.9348	.0252	3.0	.0973
2.0	.1652	.9540	.0192	3.5	.0637
2.2	.0864	.9784	.0244	4.0	.0413
2.5	.0272	.9941	.0157	4.5	.0266
3.0	.0024	$(4.2 \cdot 10^{-4})$	.0055	5.0	.0170
4.0	$4.1 \cdot 10^{-6}$	$(5.1 \cdot 10^{-7})$		6.0	.0069
5.0	$7.8 \cdot 10^{-10}$	$(7.9 \cdot 10^{-11})$		7.0	.0027
6.0	$1.9 \cdot 10^{-14}$	$(4.4 \cdot 10^{-16})$		8.0	.0011

The last two columns in Table 2 give values of f_x as a function of x, and Fig. 1 shows a plot of this function. By differentiating f_x with respect to x and equating the result to zero, it is readily shown that f_x has a maximum value for $x = 0.5$; that is, f_E has a maximum value for $E = \frac{1}{2}kT$. On the other hand, as stated in equation 2.5, $E_{\text{av}} = \frac{3}{2}kT$.

Since

$$x = \frac{mv^2}{\alpha^2} = mc^2, \tag{14}$$

it is possible, from the plot for y in Fig. 1, to determine the fraction of the total number of molecules which have an energy equal to or less than that corresponding to a given value of E.

It follows from the equations above that the value of v for which f_v is a maximum increases with $\sqrt{T}$, while that of E for which f_E is a maximum increases with T.

Values of v_a, at 0° C and 25° C, for a number of gases and vapors, are given in Table 3.

ADDED NOTE 1. RELATION BETWEEN MOLECULAR VELOCITIES AND VELOCITY OF SOUND

It is of interest to note that the relations for α, v_a, and v_r can also be expressed in terms of the velocity of sound, which we shall designate by u.

Since

$$\rho = \frac{MP}{R_0 T} = P\rho_1,$$

where ρ_1 = density at 1 microbar, and $P = P_{\mu b}$, we can write the relations for molecular velocities in the forms

$$\alpha = \sqrt{2\frac{P}{\rho}} = \sqrt{\frac{2}{\rho_1}}, \tag{15}$$

$$v_a = \sqrt{\frac{8}{\pi}\cdot\frac{P}{\rho}} = 4\sqrt{\frac{1}{2\pi\rho_1}}, \tag{16}$$

$$v_r = \sqrt{3\frac{P}{\rho}} = \sqrt{\frac{3}{\rho_1}}. \tag{17}$$

On the other hand,

$$u = \sqrt{\gamma\frac{P}{\rho}} = \sqrt{\frac{\gamma}{\rho_1}}, \tag{18}$$

where $\gamma = C_p/C_v$ = ratio of specific heats (per gram-mole) at constant pressure and constant volume. Hence

$$\frac{v_a}{u} = \sqrt{\frac{8}{\pi\gamma}}, \tag{19}$$

and

$$\frac{\alpha}{u} = \sqrt{\frac{2}{\gamma}}. \tag{20}$$

For mercury and other monatomic gases, $\gamma = 1.667$; for diatomic gases (such as H_2, N_2, O_2, etc.), $\gamma = 1.40$ (approximately). Hence,

$$\frac{v_a}{u} = 1.236 \quad \text{for monatomic gases}$$

$$= 1.349 \quad \text{for diatomic gases,}$$

and

$$\frac{u}{\alpha} = 0.9124 \quad \text{for monatomic gas.}$$

Thus the velocity of sound in a gas approaches molecular velocities very closely.

ADDED NOTE 2. DETERMINATION OF AVOGADRO CONSTANT FROM DISTRIBUTION OF PARTICLES IN BROWNIAN MOTION

Under high magnification, all suspensions of very fine particles in gases or liquids exhibit "Brownian" motions. Einstein (1905) suggested that the motion of these particles is essentially that to be expected, on the basis of the kinetic theory of gases, of "large molecules," and therefore subject *to the same laws as gas molecules.* That is, the average energy per particle at any given temperature T is $\frac{3}{2}kT$, and the average velocity of the particles is given by the relation

$$v_a = \sqrt{8kT(\pi m)}, \tag{21}$$

where m = mass of particle.

Application of the Boltzmann-Maxwell laws leads to the following relation for the distribution of particles at different levels in a gravitational field:

$$\frac{n}{n_0} = \epsilon^{-m'gh/(kT)} \tag{22}$$

where n_0 = number of particles per cm^3 at $h = 0$.

n = number of particles per cm^3 at height h (cm).

g = 981 dynes.

m' = apparent mass of particles, which is different from the actual mass because of the buoyancy of the medium.

Let m = actual mass of particle. Then

$$m' = m\left(1 - \frac{\rho'}{\rho}\right), \tag{23}$$

where ρ' = density of the medium and ρ = density of the particles.

Actually m' is determined from the rate of settling of the particles, by application of Stokes' law.

Thus it is possible to determine k (and consequently the value of $N_A = R_0/k$) from observations on the value of m' and the relation between n/n_0 and h. Using a fine suspension of gum arabic in water, Perrin obtained the value $N_A = 6.8 \times 10^{23}$.

Equation 22 has been applied to the determination of the variation with altitude of the density of the atmosphere.

Assuming an average temperature of $T = 230°$ K at higher altitudes,

$$\frac{m'}{k} = \frac{M}{R_0} = \frac{29 \times 10^{-7}}{8.315},$$

and hence

$$\log P_{mm} = \log 760 - \frac{29 \times 981 \times 10^{-5}H}{2.303 \times 8.315 \times 230}$$
$$= 2.8808 - 6.452 \cdot 10^{-5}H, \tag{24}$$

where P_{mm} is the pressure at the altitude H (in meters) above sea level.

Figure 2 shows plots of P_{mm} versus the height in kilometers (AA') as calculated by C. N. Warfield.[9] The plot A is satisfactorily represented over the range 20 to 40 kilometers by equation 24. According to this relation the pressure should decrease to one-tenth its value at any given altitude for an increase in altitude of 15,500 meters.

Plot B represents observations made by N. R. Best, E. Durand, D. I. Gale, and R. J. Havens.[10] Evidently these determinations lie below those calculated by Warfield (plot A'). The linear plot C corresponds to the extension of equation 24 to altitudes above 40 kilometers.

---

[9] *Technical Note* 1200, National Advisory Committee for Aeronautics, 1947.

[10] *Phys. Rev.*, **70**, 985 (1946).

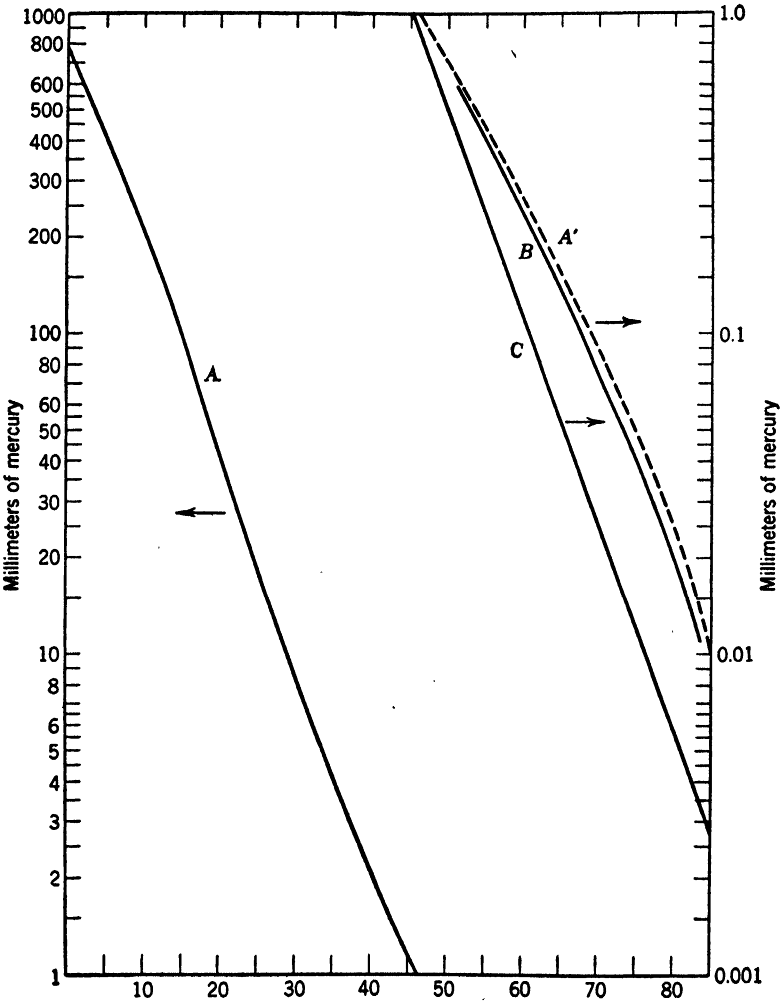

FIG. 2. Variation in pressure of atmosphere with height. (1 kilometer = 0.6214 statute mile = 3281 feet.) Plots A and A' from data by NACA (1947); plot B from data in *Phys. Rev.*, 1946; plot C, pressure calculated according to equation 4.24. Appropriate scales of pressure are indicated by arrows.

5. RATE AT WHICH MOLECULES STRIKE A SURFACE

It was shown by O. E. Meyer that the number of molecules of a gas at rest as a whole that strike unit area per unit time is given by the relation

$$\nu = \tfrac{1}{4} n v_a. \tag{1}$$

Substituting for n and v_a, from equations 3.4 and 4.10, we obtain the relations

$$\nu = 2.635 \cdot 10^{19} \frac{P_{\mu b}}{\sqrt{MT}} \quad \mathrm{cm}^{-2} \cdot \mathrm{sec}^{-1} \tag{2a}$$

$$= 3.513 \cdot 10^{22} \frac{P_{mm}}{\sqrt{MT}} \quad \mathrm{cm}^{-2} \cdot \mathrm{sec}^{-1}. \tag{2b}$$

G = mass of gas incident on unit area per unit time

$$= m\nu = \tfrac{1}{4} \rho v_a \tag{3}$$

$$= 1.6604 \cdot 10^{-24} M\nu \tag{4}$$

$$= P_{\mu b} \sqrt{\frac{M}{2\pi R_0 T}} = P_{\mu b} \sqrt{\frac{\rho_1}{2\pi}} \tag{5}$$

$$= 4.375 \cdot 10^{-5} P_{\mu b} \sqrt{\frac{M}{T}} \quad \mathrm{g} \cdot \mathrm{cm}^{-2} \cdot \mathrm{sec}^{-1} \tag{6a}$$

$$= 5.833 \cdot 10^{-2} P_{mm} \sqrt{\frac{M}{T}} \quad \mathrm{g} \cdot \mathrm{cm}^{-2} \cdot \mathrm{sec}^{-1}. \tag{6b}$$

The *volume* which strikes *unit area per unit time* is given by

$$F = \frac{\nu}{n} = \frac{v_a}{4} = 3638 \sqrt{\frac{T}{M}} \quad \mathrm{cm}^3 \cdot \mathrm{sec}^{-1} \cdot \mathrm{cm}^{-2} \tag{7}$$

and is therefore a constant at all pressures, but varies with $\sqrt{T/M}$.

In the literature, especially that originating in Germany, the last relation is expressed in the form

$$F = \frac{1}{4} \sqrt{\frac{8 R_0 T}{\pi M}} = \frac{1}{\sqrt{2\pi \rho_1}}. \tag{8}$$

The last four columns of Table 3 give values of ν_1 and G_1, the values calculated for a pressure of 1 microbar, and of ν_1' and G_1', the values calculated for a pressure of 1 mm—all at 0° C.

The equations given above for ν and G are also applicable to the effusion of gases *at low pressures* through small holes in *very thin plates.* The requisite condition for the application of Meyer's relation to effusion is that the diameter of the opening should be small compared with the mean free path.[11]

A comparison of relative values of ν or G for different gases or vapors streaming through such a hole makes it possible to obtain relative values of M, since, for constant values of P and T, ν varies *inversely* as $\sqrt{M}$, and G directly as $\sqrt{M}$.

A good check on the above equations was obtained by M. Knudsen[12] in some experiments in which hydrogen, oxygen, and carbon dioxide, at pressures ranging from 10 to 0.001 cm of Hg, were made to flow into a vacuum through a 0.025-mm hole in a 0.0025-mm-thick platinum strip.

Equation 7 shows that the volume per unit area per unit time, measured at the pressure P, is always the same. It follows that $FP_{\mu b}$ *corresponds to the volume measured at 1 microbar.* Hence, if $P_{\mu b1}$ and $P_{\mu b2}$ ($>P_{\mu b1}$) denote the pressures on the two sides of a very thin-walled orifice of area A, the net *quantity* of gas (Q) flowing through the orifice per unit time is given by

$$\begin{aligned} FA(P_{\mu b2} - P_{\mu b1}) &= Q_2 - Q_1 \\ &= Q, \end{aligned} \tag{9}$$

where Q = volume in cubic centimeters per second, measured at 1 microbar. That is, Q denotes microbars × cm³ per unit time.

Similarly, if the pressure is measured in microns (denoted in this volume by P_μ), then Q denotes microns × cm³ per unit time, and $10^{-3}Q$ denotes the number of micron · liters per unit time.

6. RATE OF EVAPORATION AND VAPOR PRESSURE

An interesting application of equation 5.5 was first made by I. Langmuir[13] to the determination of vapor pressures from rates of evaporation in high vacua. Since this subject is discussed more fully in a subsequent chapter it will be sufficient in the present connection to quote from Langmuir's original paper, "The Vapor Pressure of Metallic Tungsten."

> Let us consider a surface of metal in equilibrium with its saturated vapor. According to the kinetic theory we look upon the equilibrium *as a balance between the rate of evaporation and rate of condensation.* That is, we conceive of these two processes going on simultaneously *at equal rates.*

---

[11] See discussion in EHK, pp. 63–66, also section 7 of this chapter.

[12] *Ann. Physik,* **28**, 75 (1909).

[13] *Phys. Rev.,* **2**, 329 (1913).

TABLE 3.

MASSES, VELOCITIES, AND RATES OF INCIDENCE OF MOLECULES

Note: ν_1 = rate of incidence of molecules per cm^2 per sec, at 0° C and 1 microbar.
ν_1' = rate of incidence of molecules per cm^2 per sec, at 0° C and 1 mm.
G_1 = mass of gas corresponding to ν_1 ($\text{g} \cdot \text{cm}^{-2} \cdot \text{sec}^{-1}$).
G_1' = mass of gas corresponding to ν_1' ($\text{g} \cdot \text{cm}^{-2} \cdot \text{sec}^{-1}$).
m = mass of molecule in grams; $\rho_1{}^0$ = density of gas at 0° C and 1 microbar ($\text{g} \cdot \text{cm}^{-3}$).
v_a = average velocity ($\text{cm} \cdot \text{sec}^{-1}$).

				$10^{-4} \cdot v_a$					
Gas or Vapor	M	$10^{23}m$	$10^{10}\rho_1{}^0$	0° C	25° C	$10^{-17}\nu_1$	$10^{-20}\nu_1'$	10^5G_1	$10^2G_1'$
H_2	2.016	0.3347	0.8878	16.93	17.70	11.23	14.97	0.3759	0.5012
He	4.003	0.6646	1.7631	12.01	12.56	7.969	10.63	0.5297	0.7062
CH_4	16.04	2.663	7.063	6.005	6.273	3.981	5.308	1.060	1.414
NH_3	17.03	2.827	7.498	5.829	6.089	3.865	5.152	1.092	1.456
H_2O	18.02	2.992	7.936	5.665	5.919	3.756	5.007	1.124	1.498
Ne	20.18	3.351	8.886	5.355	5.594	3.550	4.733	1.190	1.586
CO	28.01	4.651	12.34	4.543	4.746	3.012	4.016	1.402	1.868
N_2	28.02	4.652	12.34	4.542	4.745	3.011	4.015	1.402	1.868
Air	28.98*	4.811	12.77	4.468	4.668	2.962	3.950	1.425	1.900
O_2	32.00	5.313	14.09	4.252	4.442	2.819	3.758	1.497	1.996
A	39.94	6.631	17.59	3.805	3.976	2.523	3.363	1.675	2.230
CO_2	44.01	7.308	19.38	3.624	3.787	2.403	3.204	1.756	2.342
CH_3Cl	50.49	8.383	22.23	3.385	3.356	2.244	2.991	1.881	2.508
SO_2	64.06	10.64	28.21	3.004	3.139	1.992	2.656	2.118	2.825
Cl_2	70.91	11.77	31.23	2.856	2.984	1.893	2.524	2.229	2.973
Kr	83.7	13.90	36.85	2.629	2.747	1.743	2.324	2.422	3.229
C_7H_{16}	100.2	16.63	44.12	2.403	2.510	1.593	2.123	2.650	3.533
Xe	131.3	21.80	57.82	2.099	2.193	1.392	1.856	3.034	4.044
CCl_4	153.8	25.54	67.72	1.939	2.026	1.286	1.714	3.283	4.377
Hg†	200.6	33.31	(88.33)	1.698	1.774	(1.126	1.501	3.750	4.998)

* Calculated from the value $\rho = 1.293 \cdot 10^{-3}$ at 0° C and 760 mm.

† Since the vapor pressure of mercury at 0° C is $1.85 \cdot 10^{-4}$ mm (= 0.247 μb), the values given in parentheses have no physical significance. Actual values at 0° C, corresponding to saturation pressure, are as follows: $\rho = 21.79 \cdot 10^{-10}$; $\nu = 2.777 \cdot 10^{16}$; $G = 9.249 \cdot 10^{-6}$.

At temperatures so low that the vapor pressure of a substance does not exceed a millimeter, we may consider that the actual rate of evaporation of a substance is independent of the presence of vapor around it. That is, the rate of evaporation in a high vacuum is the same as the rate of evaporation in presence of saturated vapor. Similarly we may consider that the rate of condensation is determined only by the pressure of the vapor.

The rate at which molecules will, in general, condense on a surface is given by $\alpha\nu$, where α is known as the *accommodation coefficient.*[14] It represents the ratio between the rate at which molecules actually condense on the surface and the rate at which they strike the surface. If we let μ denote the rate at which molecules evaporate from the surface, then, at equilibrium,

$$\mu = \alpha\nu. \tag{1a}$$

Langmuir[15] has shown that for metal atoms condensing on the surface of a metal the value of α may be assumed to be equal to 1. In a much more recent paper on the vapor pressures of high-boiling-point organic liquids, F. H. Verhoek and A. L. Marshall[16] have shown that the same assumption is justified in respect to these liquids. Hence, we may, in practically all cases of evaporation, express the relation for rate of evaporation in the form

$$\mu = \nu = \tfrac{1}{4}nv_a. \tag{1b}$$

For the purpose of calculating the vapor pressure of a metal from a determination of loss of weight per unit area per unit time it is convenient to express equations 5.6*a* and 5.6*b* in the forms

$$P_{\mu b} = 2.286 \cdot 10^4 G \sqrt{\frac{T}{M}} \tag{2a}$$

and

$$P_{mm} = 17.14 G \sqrt{\frac{T}{M}}, \tag{2b}$$

where G = rate of evaporation in $\text{g} \cdot \text{cm}^{-2} \cdot \text{sec}^{-1}$.

As an illustration of the application of these equations, Table 4 gives values of G for tungsten[17] and tantalum[18] at a series of temperatures (degrees K) together with calculated values of $P_{\mu b}$.[19]

For the evaporation from a wire of diameter d' (in *mils*) the *loss in weight per second per centimeter length* is given by

$$G_l = 2.54 \cdot 10^{-3}\pi d'G.$$

---

[14] This topic is discussed more fully in subsequent sections.

[15] *Phys. Rev.*, **2**, 329 (1913), and subsequent papers.

[16] *J. Am. Chem. Soc.*, **61**, 2737 (1939).

[17] H. A. Jones and I. Langmuir, *Gen. Elec. Rev.*, **30**, 310, 354, and 408 (1927).

[18] D. B. Langmuir and L. Malter, *Phys. Rev.*, **55**, 748 (1939).

[19] See Table 11.2 for vapor pressures and rates of evaporation for the metals and carbon.

TABLE 4

RATES OF EVAPORATION AND VAPOR PRESSURES OF TUNGSTEN AND TANTALUM

	T	G	$P_{\mu b}$
Tungsten $M = 183.92$			
	2600	$8.41 \cdot 10^{-9}$	$7.23 \cdot 10^{-4}$
	2800	$1.10 \cdot 10^{-7}$	$9.81 \cdot 10^{-3}$
	3000	$9.95 \cdot 10^{-7}$	$9.18 \cdot 10^{-2}$
	3200	$6.38 \cdot 10^{-6}$	$6.08 \cdot 10^{-1}$
	3400	$3.47 \cdot 10^{-5}$	3.41
Tantalum	2400	$3.04 \cdot 10^{-9}$	$2.58 \cdot 10^{-4}$
$M = 180.88$	2600	$5.54 \cdot 10^{-8}$	$4.90 \cdot 10^{-3}$
	2800	$6.61 \cdot 10^{-7}$	$6.07 \cdot 10^{-2}$
	3000	$5.79 \cdot 10^{-6}$	$5.40 \cdot 10^{-1}$
	3200	$3.82 \cdot 10^{-5}$	3.77

Hence equations 2*a* and 2*b* assume the forms

$$P_{\mu b} = 2.865 \cdot 10^6 \frac{G_l}{d'} \sqrt{\frac{T}{M}}. \tag{3a}$$

$$P_{mm} = 2.148 \cdot 10^3 \frac{G_l}{d'} \sqrt{\frac{T}{M}}. \tag{3b}$$

Equations 2*a* and 2*b* have also been applied by Knudsen and subsequent investigators to the determination of vapor pressures from *rates of effusion through a small orifice.*

Thus let us consider the case in which molecules evaporating from a hot surface pass through a small orifice into another chamber in which they are condensed. If the pressure of residual gas in this "cool" compartment is extremely low and the *radius of the opening is less than L,* the mean free path of the evaporating molecules in the "hot" compartment, then the rate at which molecules pass through the hole is equal to the rate at which they strike this opening.[20] Consequently, the vapor pressure for any given temperature will be given by equation 2*a* or 2*b*, where G represents the weight passing through the orifice per *unit area, per unit time.*

These equations are, however, strictly applicable only if the thickness (l) of the wall, in which the orifice of area πa^2 is located, is vanishingly small compared to a. If the orifice consists of a short tube for which l/a is appreciable, then a correction factor has to be applied, and instead of equation 5.3 we have the relation

---

[20] The conditions for the validity of the equations for rate of effusion are discussed by I. Estermann in his article "Molecular Beam Technique," *Rev. Modern Phys.*, **18,** 300 (1946).

$$G = K(\tfrac{1}{4}\rho v_a) = KP_{\mu b}\sqrt{\frac{\rho_1}{2\pi}}, \tag{4}$$

where K is a function of l/a which is less than 1 for $l/a > 0$. The manner in which the value of K varies with l/a is discussed subsequently in Chapter 2, section 2. Hence, if G' denotes the actual loss in weight, at temperature T, of material of molecular mass M, through an opening of area A, over a period of t seconds, then

$$P_{\mu b} = 2.286 \cdot 10^4 \cdot \frac{G'}{KAt}\sqrt{\frac{T}{M}}. \tag{5a}$$

$$P_{mm} = 17.14\,\frac{G'}{KAt}\sqrt{\frac{T}{M}}. \tag{5b}$$

These equations have been applied by a number of investigators for the determination of vapor pressure at low temperatures, where the values are of the order of a fraction of a millimeter of mercury. The method has been used, for instance, by A. C. Egerton for such metals as zinc, cadmium, mercury,[21] and lead.[22]

As an illustration let us consider one such determination made for mercury vapor. In this case the area of the opening was $A = 0.0335$ cm^2. At 33.7° C, the loss of mercury through this orifice was 0.7867 g over a period of 2370 minutes. To correct for the fact that l/a was not negligible, the value of K was found (by means of the relations given in Chapter 2, section 2) to be 0.93.[23]

Hence the corrected value of G is given by

$$G = \frac{0.7867}{2370 \times 60 \times 0.0335 \times 0.93}$$

$$= 1.651 \cdot 10^{-4}\ \text{g} \cdot \text{cm}^{-2}\,\text{sec}^{-1}.$$

Since $T = 306.9$, and $M = 200.6$, it follows from equation 2*b* that $P_{mm} = 3.77 \cdot 10^{-3}$.

Another interesting application of the above relations, and one which is of increasing importance in industrial chemistry, is provided by the comparatively recent development of *high-vacuum distillation* for the separation of certain organic compounds in the pure state from naturally occurring oils. The great advantage of this process arises from the fact that these organic compounds are unstable at higher temperatures and therefore they can be distilled only at lower temperatures, at which the vapor pressures are in the range of 10^{-4} to 10^{-6} atmosphere.[24]

---

[21] *Phil. Mag.*, Series 6, **33**, 33 (1917).

[22] *Proc. Roy. Soc. London*, **A**, **103**, 469 (1923).

[23] Egerton and other investigators designate $\sqrt{2\pi}/A$ as a "resistance," and the effect of the correction is that of increasing this resistance in the ratio $1/K$.

In this operation, evaporation takes place from a very thin film of liquid, which is renewed continuously, and condensation occurs on an adjacent cooled surface. In a sufficiently high vacuum (pressure of residual gas less than 1 micron) the rate of transfer of distilland is in accordance with equations 5.6*a* and 5.6*b*. As the pressure of residual gas is increased, however, the rate of distillation is decreased because of collisions between the molecules of the distilland and those of the gas. This is illustrated by the data shown in Table 5, taken from Hickman's paper.

TABLE 5

VARIATION OF RATE OF DISTILLATION WITH PRESSURE*

(Hickman)

Pressure (μ) of Residual Gas (air)	W ($\text{g} \cdot \text{sec}^{-1} \cdot \text{m}^{-2}$)		
	$P_\mu = 1$ $T = 368$	$P_\mu = 3$ $T = 383$	$P_\mu = 10$ $T = 393$
0.3	0.6	1.85	6.4
4.0	.46	1.59	5.7
7.0	.38	1.37	5.2
10.0	.32	1.18	4.6
15.0	.25	0.95	3.8
25.0	.21	0.70	2.1
50.0	.12	0.40	1.67

* The values given for T were taken from a plot of log P_{mm} versus $1/T$ and are therefore only approximate values, which accounts for the fact that values of W calculated by means of equation *i* for extremely low pressure are slightly less for 3 and 10 μ than those given in the first row.

The distilland used was Octoil, which has the chemical formula $C_6H_4COO(C_8H_{17})_2$, and molecular weight $M = 390.3$. From equation 5.6*b*, it follows that the rate of evaporation, W, in grams per second *per square meter* at pressure P_μ, is

$$W = 0.5833 P_\mu \sqrt{\frac{390.3}{T}}, \qquad (i)$$

where T is the absolute temperature corresponding to the vapor pressure of P_μ.

---

[24] A comprehensive review of this topic has been published by K. C. D. Hickman, one of the pioneers in this field, in *Chem. Revs.*, **34**, 51 (1944).

It is evident from these observations as well as observations of a similar nature mentioned in the next section that molecules leaving the surface of the distilland are prevented from reaching the surface of condensation because of collisions with the molecules of the residual gas. As a result of such collisions many of the molecules leaving the hot film are driven back, the number of such molecules increasing with the magnitude of residual pressure. We are thus led to the concept of free path as the distance that a molecule can travel without suffering a collision.

7. FREE PATHS OF MOLECULES[25]

Although the individual molecules in a gas at rest possess very high velocities, as shown previously, it is a matter of ordinary observation that gases diffuse into one another very slowly. This is explained on the kinetic point of view by assuming that the molecules do not travel continuously in straight lines, but undergo frequent collisions. The term "collision" naturally leads to the notion of *free path.* This may be defined as the distance traversed by a molecule between successive collisions. Since, manifestly, the magnitude of this distance is a function of the velocities of the molecules, we are further led to use the expression "mean free path" (denoted by L), which is defined as the average distance traversed by all the molecules between successive collisions.

However, this definition assumes that the molecules actually collide like billiard balls; that is, the molecules are assumed to be rigid elastic spheres possessing definite dimensions and exerting no attractive or repulsive forces on one another. But this concept can certainly not be in accord with the facts. We have every reason to believe that the structure of atoms and molecules is exceedingly complex. It is probably impossible to state definitely the diameter of a hydrogen atom or molecule, much less that of a polyatomic molecule. Also there is no doubt that the molecules exert attractive forces on one another for certain distances and repulsive forces when they approach exceptionally close. Otherwise how could we explain surface tension, discrepancies from Boyle's law, and a host of related phenomena? To speak of collisions among molecules, such as these, is impossible. What meaning, therefore, shall we assign to the free path under these conditions?

Let us consider at $t = 0$ a group of N_0 "tagged" molecules moving in a given direction. As time goes on, these molecules will suffer random collisions and a number will disappear from the original group. Let N

---

[25] See EHK, pp. 101–102.

denote the number which, after a period t, are still identified with the original group, and let ω denote the collision frequency. Then

$$-dN = N\omega\, dt. \tag{1}$$

Integrating this equation we obtain the result,

$$N = N_0\epsilon^{-\omega t}. \tag{2}$$

If we let l $(= v_a t)$ designate the path that has been traversed by a molecule without suffering collision during the interval t, then the last equation can be written in the form

$$N = N_0\epsilon^{-\omega l/v_a}. \tag{3}$$

Furthermore we can write

$$\omega = \frac{v_a}{L}, \tag{4}$$

where L is a distance covered between collisions. Then it follows that equation 3 assumes the form

$$\phi(l) = \frac{N}{N_0} = \epsilon^{-l/L}. \tag{5}$$

That is, $\phi(l)$ is the *fraction* of the original group of molecules that are still traveling without having suffered a collision in the distance l.

Furthermore it follows from equation 3 that

$$\psi(l)\, dl = \frac{dN}{N_0} = \frac{\omega}{v_a}\, \epsilon^{-\omega l/v_a}\, dl = \frac{1}{L}\, \epsilon^{-l/L}\, dl \tag{6}$$

represents the fraction of all the free paths that have a length between l and $l + dl$. (Hence the omission of the negative sign in the differentiation.)

It follows from the last relation that the *average* value of the free path is

$$l_a = \int_0^\infty l\psi(l)\, dl = \frac{1}{L}\int_0^\infty l\epsilon^{-l/L}\, dl = L. \tag{7}$$

For $l = L$, $\phi(l) = \epsilon^{-1} = 0.3679.$ This result shows that 63.21 per cent of the molecules collide with other molecules in a distance equal to or less than L. Furthermore it is seen from equation 2 that this 63.21 per cent of collisions occur in the interval $\tau = 1/\omega$. Thus $1/\omega$ is a constant of the same nature as the "decay" constant in radioactive disintegrations, while $1/L$ may be regarded as an "absorption" coefficient similar to the coefficient that measures the decrease in intensity of a beam of light in passing through a medium.

Equation 5 indicates an experimental method for the determination of L which has been used by M. Born[26] and F. Bielz,[27] and which is described by R. G. J. Fraser.[28]

A beam of silver atoms is sent into nitrogen or air and a determination is made of the amount of silver deposited by the beam in a given time t on a surface distant l from the source. If we let I_0 designate the intensity of the beam at the source, then the intensity at the collector is

$$I = I_0 \epsilon^{-l/L_P}, \tag{8}$$

where L_P is the mean free path of silver atoms in the gas at the pressure in the collecting chamber.

Measurements of the mean free path of potassium in nitrogen have also been reported by J. J. Weigle and M. S. Plesset.[29]

As Fraser points out,[30]

> With non-condensible gases, it is not possible to measure I_0 directly. We assign therefore to I_0 [in equation 8] a different meaning: namely, the intensity which the beam would have if it were not, as is actually the case, weakened through scattering by the alien molecules present in the collimator chamber. Now, clearly I_0 is directly proportional to the quantity of gas issuing from the source slit per second; but so also is the pressure P in the collimator chamber, if a constant pump speed is assumed. We can therefore set $I_0 = c \cdot P$. On the other hand, L_P is inversely proportional to P; that is, $L_P = L/P$, where if P is measured say in microns of mercury, L is the mean free path at a pressure of 1 micron. I can therefore be expressed as a function of the pressure P; thus if l is the distance between source slit and image slit,
>
> $$I = c \cdot P \cdot e^{-P \cdot l/L}, \tag{9}$$
>
> it being assumed that the pressure in the observation chamber is negligibly small. I is a maximum for that value of P which makes $P \cdot l/L = 1$. To make a measurement, the intensity is plotted as a function of the pressure in the collimator chamber, and the value of the latter at the maximum intensity is observed. Then $L_P = L/P = l$. At this value of P, $I = 0.3679 I_0$.

It is of interest to observe, as Fraser emphasizes, that the requisite condition for obtaining a directional effect of the molecules passing through the slit is that L_P *must not be less than* d, the width of the slit.[31]

The determination of mean free path for hydrogen has been carried out by F. Knauer and O. Stern.[32] The value they obtained, however, is only about 0.44 times that derived from viscosity relations (see discussion in the following section). The reason, as Fraser points out,

---

[26] *Physik. Z.*, **21**, 578 (1920).

[27] *Z. Physik*, **32**, 81 (1925).

[28] *Molecular Rays*, Cambridge University Press, 1931; also *Molecular Beams*, Methuen and Company, London, 1937.

[29] *Phys. Rev.*, **36**, 373 (1930).

[30] *Op. cit.*, p. 75.

[31] See also LBL, p. 307.

[32] *Z. Physik*, **53**, 766 (1929).

> is that the standard methods require an intimate encounter in order that the molecules may exchange energy and momentum in amounts capable of affecting the viscosity or heat conductivity of the gas. The molecular ray method on the other hand counts as a collision an approach of two molecules sufficiently close to deflect them very slightly out of their paths; with narrow slits angular deflections of less than 10^{-4} are detectable.

In this connection the reader will find an interesting description of the many uses of molecular beams in a paper by John B. Taylor.[33] As he states, "Molecular beams, narrow rays of molecules formed by a slit system and moving in one direction in an evacuated apparatus, may be used to advantage in many types of research." Among these are determinations of molecular velocities (involving experimental tests of the validity of the Maxwell-Boltzmann distribution law), mean free paths, vapor pressures, accommodation coefficients, and mechanism of chemical reactions and of adsorption.[34]

Evidently the mean free path must depend upon the molecular diameter, and simple considerations indicate that the length of the mean free path must vary inversely as the total cross-sectional area of the molecules per unit volume. Again, the magnitudes of the coefficients of viscosity, heat conductivity, and diffusivity of gases are intimately bound up with the length of the free path; whether it be transference of momentum from one layer to another as in viscosity, or transference of increased kinetic energy of the molecules as in heat conductivity, the rate of this transference must depend upon the number of collisions which each molecule experiences as it passes from point to point. It is therefore to be expected that there should exist very similar relations between the values of the mean free path and those of the coefficients of viscosity, heat conductivity, and diffusion. However, in attempting to deduce such relations, the theoretical physicist has found himself confronted with the problem regarding the laws governing the variation with distance of attractive and repulsive forces between molecules. As a result of successive attacks on this problem, by a number of investigators, the exact forms of these relations have been modified from time to time. In the following discussion the writer has been guided to a great extent by the conclusions stated in the treatise by Chapman and

---

[33] *J. Ind. Eng. Chem.*, **23**, 1228 (1931). Also see W. H. Bessey and O. C. Simpson, *Chem. Revs.*, **30**, 239 (1942).

[34] An excellent and comprehensive review of molecular-beam technique has been published by I. Estermann, *Rev. Modern Phys.*, **18**, 300 (1946). This gives a very complete bibliography of references on the subject.

Cowling, which undoubtedly represents the most comprehensive treatment of the whole problem.

8. RELATION BETWEEN COEFFICIENT OF VISCOSITY, MEAN FREE PATH, AND MOLECULAR DIAMETER

A gas streaming through a narrow-bore tube experiences a resistance to flow, so that the velocity of this flow decreases uniformly from the center outwards until it reaches zero at the walls. Each layer of gas parallel to the direction of flow exerts a tangential force on the adjacent layer, tending to decrease the velocity of the faster-moving and to increase that of the slower-moving layers. The property of a gas (or liquid) by virtue of which it exhibits this phenomenon is known as *internal viscosity.*

As a simple working hypothesis we may assume, as Newton did, that the internal viscosity is directly proportional to the velocity gradient in the gas. Furthermore, the viscosity must depend upon the nature of the fluid, so that in a more viscous fluid the tangential force between adjacent layers, for constant velocity gradient, will be greater than in a less viscous fluid. We thus arrive at the following definition of the *coefficient of viscosity:*

The coefficient of viscosity is defined as the tangential force per unit area for unit rate of decrease of velocity with distance (that is, per unit velocity gradient).

With this definition we are in a position to deduce the approximate form of the relation between the coefficient of viscosity and the free path.

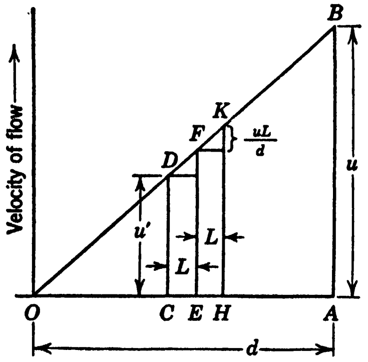

FIG. 3. Diagram illustrating the derivation of simple relation between coefficient of viscosity (η) of a gas and the molecular mean free path (L).

Let u denote the velocity of flow of the gas at a distance d from a stationary surface. In uniform flow along a surface, the velocity will decrease uniformly to zero as the surface is approached. We can therefore represent (see Fig. 3) the velocity at distance $OA = d$ by the ordinate $AB = u$ and velocities at intermediate distances by the corresponding ordinates of the line OB.

We shall imagine the gas divided into layers parallel to the surface, each having a depth equal to the free path, L.

Let us denote the tangential force per unit area between adjacent layers by B. By definition:

$$B = \eta \times \text{velocity gradient}$$

$$= \eta \times \frac{u}{d}, \tag{1}$$

where η denotes the coefficient of internal viscosity.

But, according to the kinetic theory, the tangential force per unit area is measured by the rate at which momentum is transferred per unit area between adjacent layers.

Owing to the relative motion of the layers, the molecules moving from a faster- into a slower-moving layer possess more momentum in the direction of flow than those moving in the opposite direction.

Let us consider any layer, CE or EH, of thickness equal to L. We have chosen this particular value of the thickness so that we may be justified, as a first approximation, in assuming that the molecules starting at either of the planes CD or HK reach the plane EF without suffering collision, that is, without change of momentum.

The momentum, parallel to the surface, of any molecule reaching the plane EF from the plane CD is $m(u' + v)$, where u' denotes the velocity of flow at the plane CD and v is the mean velocity of the molecules.

The momentum, parallel to the surface, of a molecule reaching the plane EF from the plane HK is

$$m\left(u' + v + 2\frac{uL}{d}\right).$$

The number of molecules that cross unit area per unit time in any direction in a gas at rest is equal to $\frac{1}{6}nv$, and this must be the same for the molecules traveling in a direction perpendicular to the plane EF, for the velocity of flow is assumed to be so small that the density remains constant throughout the different layers.

Hence the net rate of transference of momentum across unit area of the plane EF is equal to

$$B = \frac{1}{3}mnv\frac{uL}{d}. \tag{2}$$

From equations 1 and 2 it follows that

$$\eta = \tfrac{1}{3}mnvL = \tfrac{1}{3}\rho vL. \tag{3}$$

The dimensions of η are evidently $ml^{-1}t^{-1}$, and in the cgs system the unit of viscosity is 1 poise = 1 $\text{g} \cdot \text{cm}^{-1} \cdot \text{sec}^{-1}$ = 1 $\text{dyne} \cdot \text{sec} \cdot \text{cm}^{-2}$. This is the unit of coefficient of viscosity used in this volume.

In deducing the last equation it has been assumed that all the molecules possess the same velocity v and the same free path L. Introducing the law of distribution of velocities, Boltzmann (1881) deduced the the relation

$$\eta = 0.3502 \rho v_a L_B, \tag{4}$$

where v_a = average velocity, and L_B is defined as the average free path.

O. E. Meyer, in his *Kinetic Theory of Gases*, used a different method of calculation and derived a relation of the form

$$\eta = 0.3097 \rho v_a L_M, \tag{5}$$

where L_M is also defined as the average free path.

From these equations an interesting conclusion may be deduced regarding the dependence of viscosity on pressure. As has been mentioned, it is evident from very simple considerations that L must vary inversely as the number of molecules present per unit volume. Consequently the product ρL is constant and independent of the pressure. The velocity, v, depends only upon the temperature and molecular weight. It therefore follows that, for any gas at constant temperature, the *viscosity is independent of the pressure* and *must increase with the temperature.* The confirmation of these two deductions has been justly regarded as one of the most signal triumphs of the kinetic theory of gases. As is well known, the viscosity of all ordinary liquids *decreases* with increase in temperature. That the viscosity of gases must increase with temperature was therefore regarded as a remarkable conclusion.

At both extremely low pressures and very high pressures, the conclusion that the viscosity is independent of the pressure is not in accord with the observations, but this is due to the fact that the same derivation as has been presented above is not valid under those conditions where either attractive forces between the molecules come into play or the pressure is so low that a molecule can travel over the whole distance between the walls of the enclosure without suffering collision.

Both relations 4 and 5 have been used by physicists, until comparatively recently, for deriving values of L from η. However, the work of S. Chapman and D. Enskog, since about 1911, has led to the following relations which are discussed by Chapman and Cowling[35] in their treatise.

To derive a more exact relation between η and L it is necessary to introduce the relation between L and δ, the molecular diameter, which has been shown to be of the form

---

[35] CC, Chapter 12, p. 218.

$$L = \frac{1}{\sqrt{2} \cdot \pi n \delta^2}, \tag{6}$$

where n = number of molecules per cubic centimeter.

For smooth rigid elastic spherical molecules, it is shown that

$$\eta = \frac{5}{16\delta^2}\left(\frac{kmT}{\pi}\right)^{\frac{1}{2}}. \tag{7}$$

Substituting in this equation the relations $v_a = \sqrt{8kT/\pi m}$ and $\rho = mn$, it follows that

$$\eta = \frac{0.491\rho v_a}{\sqrt{2} \cdot \pi n \delta^2}.$$

A further approximation leads to the conclusion that the right-hand side of the last equation should be multiplied by the factor 1.016, and consequently

$$\eta = \frac{0.499\rho v_a}{\sqrt{2} \cdot \pi n \delta^2}. \tag{8}$$

Combining this with equation 6, the result is the relation, used in the following discussion,

$$\eta = 0.499\rho v_a L. \qquad (9)^{36}$$

It follows directly from equation 7 that, for two gases having approximately equal values of δ, the viscosities should be in the same ratio as the square roots of the molecular masses.

This conclusion has been confirmed by observations on the relative viscosities of H_2 and D_2 (deuterium).[37] At room temperature $\eta_{D_2}/\eta_{H_2} = 1.39$, which is approximately equal to $\sqrt{2}$.

The difference between equation 9 and the equations of Boltzmann and Meyer arises from the fact that the two latter investigators failed to take into account the existence of forces of attraction and repulsion between molecules. The accurate form of the relation between η and δ

---

[36] This and equation 6 are those used by E. H. Kennard (see EHK, p. 147 et subseq.).

[37] A.C. Torrey, *Phys. Rev.*, **47**, 644 (1935), A. B. Van Cleave and O. Maass, *Can. J. Research*, (B) **12**, 57 (1935); **13**, 384 (1935).

has been a topic of considerable discussion by theoretical physicists.[38]

One interesting contribution to this subject, to which reference is made in a subsequent section, is the model suggested by W. Sutherland.[39] Let us assume that the molecules are "smooth rigid elastic spheres surrounded by fields of attractive force."

The relation between coefficient of viscosity and molecular diameter then has the form

$$\eta = \frac{(5/16\delta_m^2)(kmT/\pi)^{1/2}}{1 + C/T}, \tag{10}$$

where the constant C is a measure of the strength of the attractive forces between the molecules. In this equation the notation δ_m has been introduced to indicate that the value of the molecular diameter derived in this manner is different from the value δ used in equation 7. From a comparison with equation 7 it follows that equation 10 is equivalent to the relation

$$\eta = \frac{0.499\rho v_a}{\sqrt{2}\cdot\pi n\delta_m^2(1 + C/T)} \tag{11}$$

$$= \frac{0.499\rho v_a L_m}{1 + C/T}, \tag{12}$$

where

$$\delta_m^2 = \frac{\delta^2}{1 + C/T}. \tag{13}$$

and

$$L_m = \frac{1}{\sqrt{2}\cdot\pi n\delta_m^2} = L\left(1 + \frac{C}{T}\right). \tag{14}$$

Equation 10 leads to the relation, used for calculating C, which has the form

$$\frac{\eta_T}{\eta_0} = \left(\frac{T}{T_0}\right)^{1/2}\left(\frac{1 + C/T_0}{1 + C/T}\right), \tag{15}$$

---

[38] This topic is discussed at length by Chapman and Cowling in their treatise on this subject. It will be observed that

$$L_M = 1.611L = 1.131L_B$$

and

$$L_B = 1.425L.$$

[39] See CC, section 10.41.

where η_T and η_0 are the values of the coefficient of viscosity measured at T and T_0 respectively. Equation 15 is also often expressed in the form

$$\eta_T = \frac{KT^{3/2}}{C + T}, \tag{16}$$

where $K = \eta_0(C + T_0) \cdot T_0^{-3/2}$.

By combining equations 16 and 11 it is seen that the value of δ_m thus deduced is independent of T and actually corresponds to the value of the molecular diameter at infinitely high temperature, whereas, as pointed out below, the value of δ decreases with increase in T. For this reason equations 11 and 12 were used formerly by many writers on this subject (and are quoted by some authorities even in recent publications). However, following the procedure of Chapman and Cowling, and of Kennard, equations 8 and 9 are used in the following discussion for the calculations of the values of δ and L, and respectively. The conversion to values deduced by application of Sutherland's theory may then be made by means of equations 13 and 14.

From equation 9 the following numerical relations are derived:

$$L = 1.1451 \cdot 10^4 \frac{\eta}{P_{\mu b}} \sqrt{\frac{T}{M}} \quad \text{cm} \tag{17a}$$

$$= 8.589 \cdot \frac{\eta}{P_{mm}} \sqrt{\frac{T}{M}} \quad \text{cm}, \tag{17b}$$

where $P_{\mu b}$ and P_{mm} denote the pressure in microbars and millimeters of mercury, respectively, and η is expressed in poises. These relations have been used to calculate values of L and, from these, values of δ given in Tables 6 and 7.

From equation 8 we obtain the following relations for δ^2 and $S_c = \pi\delta^2$, the latter being defined as *the mean equivalent cross section for viscosity:*[40]

$$\delta^2 = 2.714 \cdot 10^{-21} \frac{\sqrt{MT}}{\eta_T} \quad \text{cm}^2. \tag{18}$$

$$\pi\delta^2 = 8.524 \cdot 10^{-21} \frac{\sqrt{MT}}{\eta_T} \quad \text{cm}^2. \tag{19}$$

Where δ has been determined by some other method,[41] an approximate calculation of L may be made by means of the relations

---

[40] EHK, p. 147.

[41] See Added Note 4 at the end of this section.

$$L = \frac{3.107 \cdot 10^{-17}T}{P_{\mu b}\delta^2} \text{ cm} \tag{20a}$$

$$= \frac{2.331 \cdot 10^{-20}T}{P_{mm}\delta^2} \text{ cm.} \tag{20b}$$

Another useful magnitude is the *collision frequency* per molecule, which is given by the relation

$$\omega = \frac{v_a}{L} \tag{21}$$

$$= 1.271 \frac{P_{\mu b}}{\eta} \text{ sec}^{-1} \tag{22a}$$

$$= 1.694 \cdot 10^3 \frac{P_{mm}}{\eta} \text{ sec}^{-1}. \tag{22b}$$

Values of ω are shown in the lowest row in Table 6.

Although Sutherland's equation 16 has been used most frequently to express the temperature variation of viscosity, several other relations have been derived in the literature. The simplest of these is the *exponential relation*

$$\eta_T = aT^x, \tag{23}$$

where a and x are constants characteristic of each gas. This relation has been recommended especially for relatively small ranges of temperature.

Equations 16 and 23 as well as some other relations have been tested by W. Licht, Jr., and D. G. Stechert[42] for a number of typical gases and vapors, using for this purpose data published in the Landolt-Börnstein tables.[43]

According to these investigators, "For twenty-four representative gases and vapors at atmospheric pressure Sutherland's equation has been found to fit extensive experimental data with an average error of less than 1 per cent." Values of the constants C and K in equation 16 and of a and x in equation 23, taken from the original discussion, are shown in Table 8. These constants were used by the writer to derive values of η_{25} shown in the fifth and eighth columns of the table.

---

[42] *J. Phys. Chem.*, **48**, 23 (1944).

[43] *Physikalisch-Chemische Tabellen*, 5th edition, Julius Springer, Berlin, 1923–1935.

The values of C given in Table 6 are those deduced by A. E. Schuil,[44] and it is of interest to compare them with those given in Table 8.

In deriving the values of L and δ shown in Tables 6 and 7, the values of η used are those given by Kennard[45] for 15° C. Values for 0° C and 25° C (η_0 and η_{25}, respectively) were derived from the values for 15° C by means of equation 23 using the values of x, taken from Kennard's table, which are given in the second row of the table. The values of δ were derived from those of η_0 and therefore apply strictly only at 0° C.

Combining equation 23 with equation 7, it follows that at room temperature δ varies as $T^{-0.5(x-0.5)}$. Since x is greater than 0.5, it also follows that the calculated value of δ must decrease with increase in temperature.

An interesting method of calculating values of L for air as a function of the temperature has been used by Hsue-Shen Tsien.[46]

From equations 9 and 4.18 it follows that

$$L = 1.255 \frac{\eta}{\rho} \frac{\sqrt{\gamma}}{u}.$$

Thus L may be expressed in terms of the "kinematic viscosity," η/ρ, and the velocity of sound, u. By means of this relation, Tsien has calculated values of the mean free path for air for the range 0° C to 500° C. A few of the values thus deduced (in centimeters) are as follows:

t°C:	0	20	40	100	200	300	400	500
$10^6 L(P/P_0)$:	5.89	6.48	7.06	8.78	11.73	14.86	17.78	20.83

In the lower row, P_0 denotes the standard pressure, 1 atmosphere, and P any other value of the pressure in atmospheres. The value 5.89 for 0° C is to be compared with the value 5.98 given for $10^6 L_0^{760}$ in Table 6.

In the tables the following notation has been used:

L_0^1 = mean free path in cm at 0° C and 1 mm of Hg.

L_{25}^1 = mean free path in cm at 25° C and 1 mm of Hg.

L_t^P = mean free path in cm at t° C and P mm of Hg.

ω = collision frequency (sec^{-1}) at 25° C and 760 mm of Hg.

---

[44] *Phil. Mag.*, **28**, 679 (1939). This paper gives data on values of η for gases and vapors over the range 0° C to 250° C.

[45] EHK, p. 149.

[46] *J. Aeronautical Sciences*, **13**, 653 (1946).

TABLE 6

MEAN FREE PATHS, MOLECULAR DIAMETERS, AND RELATED DATA FOR A NUMBER OF GASES

Gas:	H_2	He	Ne	Air	O_2	A	CO_2	Kr	Xe
$10^7\eta_{15}$	871	1943	3095	1796	2003	2196	1448	2431	2236
x	0.69	0.64	0.67	0.79	0.81	0.86	0.95	0.85	0.92
$10^7\eta_0$	839	1878	2986	1722	1918	2097	1377	2372	2129
$10^7\eta_{25}$	892	1986	3166	1845	2059	2261	1496	2502	2308
$10^3L_0{}^1$	8.39	13.32	9.44	4.54	4.81	4.71	2.95	3.69	2.64
$10^6L_0{}^{760}$	11.04	17.53	12.42	5.98	6.33	6.20	3.88	4.85	3.47
$10^3L_{25}{}^1$	9.31	14.72	10.45	5.09	5.40	5.31	3.34	4.06	2.98
$10^6L_{25}{}^{760}$	12.26	19.36	13.75	6.69	7.10	6.67	4.40	5.34	3.93
$10^8\delta$	2.75	2.18	2.60	3.74	3.64	3.67	4.65	4.15	4.91
C	84.4	80	56	112	125	142	254	188	252
$10^{-14}N_S$	15.22	24.16	17.12	8.24	8.71	8.54	5.34	6.69	4.78
$10^{-9}\omega$	14.45	7.16	1.68	6.98	6.26	5.70	8.61	6.48	5.71

TABLE 7

MEAN FREE PATHS, MOLECULAR DIAMETERS, AND RELATED DATA FOR WATER AND MERCURY VAPORS

	$t°$ C	P_{mm}	$10^5\eta_0$	$10^3L_t{}^1$	$L_t{}^P$	$10^8\delta_t$	$10^{-14}N_S$
H_2O	0	4.58	8.69	2.90	$6.34 \cdot 10^{-4}$	4.68	5.27
	15	12.79	9.26				
	25	23.76	9.64	3.37	$1.42 \cdot 10^{-4}$		
Hg	219.4	31.57	46.66	6.28	$1.99 \cdot 10^{-4}$	4.27	6.32
	150.0	2.807	39.04	4.87	$1.74 \cdot 10^{-3}$	4.50	5.70
	100.0	0.2729	33.56	3.93	$1.44 \cdot 10^{-2}$	4.70	5.22
	25.0	0.0018	25.40	2.66	1.45	5.11	4.42
	0.0		16.2(J)			6.26(J)	

P_{mm} = vapor pressure at $t°$ C.

In the case of H_2O, for which values of L and δ for a series of temperatures are given in Table 7, the Sutherland relation was used with $C = 650$ and $\eta_{15} = 9.26 \cdot 10^{-5}$ cgs unit.

In the case of Hg (see Table 7), the values of η used are based on that given by H. Braune, R. Basch, and W. Wentzel[47] for $t = 219.4°$ C. Values at other temperatures were derived by means of Sutherland's relation, with $C = 942.2$.[48] It should be observed that in their publication the authors used equation 11 to calculate values of δ_m.

---

[47] *Z. physik. Chem.*, **137**, **A**, 447 (1928).

[48] Value given by Braune, et al., *loc. cit.*, which differs somewhat from that given in Table 8.

TABLE 8

CHARACTERISTIC CONSTANTS FOR VISCOSITY-TEMPERATURE FUNCTIONS

Substance	Temperature Range ° C	Sutherland Equation			Exponential Equation		
		C	10^6K	$10^5\eta_{25}$	10^6a	x	$10^5\eta_{25}$
Ammonia	−77–441	472	15.42	10.30	0.274	1.041	10.30
Argon	−183–827	133	19.00	22.67	2.782	0.766	21.83
Benzene	0–313	403	10.33	7.58	0.299	0.974	7.71
Carbon dioxide	−98–1052	233	15.52	15.03	1.057	0.868	14.86
Helium	−258–817	97.6	15.13	19.66	4.894	0.653	20.18
Hydrogen	−258–825	70.6	6.48	9.04	1.860	0.678	8.85
Mercury	218–610	996	63.00	25.03	0.573	1.082	27.20
Methane	18–499	155	9.82	11.14	1.360	0.770	10.92
Nitrogen	−191–825	102	13.85	17.80	3.213	0.702	17.60
Oxygen	−191–829	110	16.49	20.78	3.355	0.721	20.42
Water vapor	0–407	659	18.31	9.84	0.170	1.116	9.82

The value of η for 0° C is quoted by J. H. Jeans (from Kaye and Laby, *Physical Constants*, 1936 edition) in his book (p. 183).

In addition, the tables give values of N_S, the number of molecules per square centimeter to form a monomolecular layer at 0° C. On the assumption that the spacing is that of a close-packed (face-centered) lattice,[49]

$$N_S = \frac{2}{\sqrt{3}\delta^2} = \frac{1.154}{\delta^2}. \tag{24}$$

Formulas for the viscosity of mixed gases are given by Kennard.[50] As he points out, the viscosity of a binary mixture does not necessarily lie between the values for the pure components; it may be below or above both these values.

The relations for collision frequency per unit volume between molecules are of importance in many problems of interaction between molecules.

Let Z_{AA} and Z_{AB} denote the number of collisions between *like* and *unlike* molecules, respectively, per cubic centimeter, per second. Then,

$$\begin{aligned} Z_{AA} &= n^2\delta^2\sqrt{\frac{4\pi R_0 T}{M}} \\ &= 3.232 \cdot 10^4 n^2\delta^2\sqrt{\frac{T}{M}} \quad \mathrm{cm}^{-3}\cdot\mathrm{sec}^{-1}, \end{aligned} \tag{25}$$

---

[49] See Added Note 4 at the end of this section, and Table 9.

[50] EHK, pp. 160–162.

$$
\begin{aligned}
Z_{AB} &= n_A n_B \delta_{AB}^2 \sqrt{8\pi R_0 T\left(\frac{1}{M_A} + \frac{1}{M_B}\right)} \\
&= 4.5712 \cdot 10^4 n_A n_B \delta_{AB}^2 \sqrt{T\left(\frac{1}{M_A} + \frac{1}{M_B}\right)} \quad \text{cm}^{-3} \cdot \text{sec}^{-1} \qquad (26) \\
&= 2.398 \cdot 10^{36} P_A P_B \delta_{AB}^2 \cdot T^{-3/2} \sqrt{\frac{1}{M_A} + \frac{1}{M_B}}, \qquad (27)
\end{aligned}
$$

where n_A = number of molecules per cm^3, of A at pressure P_A (microbars), with similar definition for n_B, and $\delta_{AB} = \frac{1}{2}(\delta_A + \delta_B)$.

For instance, for nitrogen ($M = 28.02$, $\delta = 3.62 \cdot 10^{-8}$) at $T = 298.2$,

$$
\begin{aligned}
Z &= 8.157 \cdot 10^{16} \quad \text{cm}^{-3} \cdot \text{sec}^{-1} \text{ at 1 microbar} \\
&= 8.357 \cdot 10^{28} \quad \text{cm}^{-3} \cdot \text{sec}^{-1} \text{ at 1 atmosphere.}
\end{aligned}
$$

For the *mean free paths* of the molecules A and B in a mixture, the following general relations have been derived:

$$\frac{1}{L_A} = \sqrt{2}\pi n_A \delta_A^2 + \pi n_B \delta_{AB}^2 \sqrt{1 + \frac{v_B^2}{v_A^2}}, \qquad (28)$$

$$\frac{1}{L_B} = \sqrt{2}\pi n_B \delta_B^2 + \pi n_A \delta_{AB}^2 \sqrt{1 + \frac{v_A^2}{v_B^2}}, \qquad (29)$$

where v_A and v_B refer to the *average velocity* of each type of molecule.

For $T_A = T_B$, equation 28 becomes

$$\frac{1}{L_A} = \sqrt{2}\pi n_A \delta_A^2 + \pi n_B \delta_{AB}^2 \sqrt{1 + \frac{m_A}{m_B}}, \qquad (30)$$

and similarly for $1/L_B$.

For δ_A very much smaller than δ_B, $m_A \ll m_B$, and $n_A \ll n_B$,

$$\frac{1}{L_A} = \sqrt{2}\pi n_A \delta_A^2 + \pi n_B \delta_{AB}^2. \qquad (31)$$

For δ_A very much smaller than δ_B,

$$\frac{1}{L_A} = \pi n_B \delta_{AB}^2 = \tfrac{1}{4}\pi n_B \delta_B^2. \qquad (32)$$

For n_A very much less than n_B, and T_A *not identical with* T_B,

$$
\begin{aligned}
\frac{1}{L_A} &= \pi n_B \delta_{AB}^2 \sqrt{1 + \left(\frac{v_B}{v_A}\right)^2} \qquad (33) \\
&= \pi n_B \delta_{AB}^2 \sqrt{1 + \frac{T_B}{T_A}\frac{M_A}{M_B}}.
\end{aligned}
$$

The last equation has been used by W. Gaede[51] to calculate the mean free path of nitrogen (A) in the blast of a mercury-vapor pump. In this case we may assume: $T_A = 300°$ K, and the temperature of the mercury vapor $T_B = 400°$ K. At this temperature the pressure of mercury vapor is about 1 mm. Hence, $n_B = 2.414 \cdot 10^{16}$.

From the data in Tables 6 and 7,

$$10^8 \cdot \delta_{AB} = \tfrac{1}{2}(3.78 + 4.70) = 4.24.$$

Substituting these values, and those for M_A and M_B, in equation 33, the result is $L_A = 6.73 \cdot 10^{-3}$ cm, whereas, from the data for L_t^1 in Table 7, the value derived for the mean free path of mercury molecules in the saturated vapor at 400° K is $L = 4.4 \cdot 10^{-3}$ cm.

ADDED NOTE 3. VISCOSITY AT LOW PRESSURES

As mentioned previously the coefficient of viscosity is not independent of pressure when the pressure decreases to a low value. Under those conditions it was observed by Kundt and Warburg (1875) that the damping of a vibrating surface by the surrounding gas is decreased, as if the gas were slipping over the surface. If one surface is at rest, and another surface, at a distance d, is moving parallel to the first surface with a uniform velocity, u, the viscous drag upon each surface at normal pressures is given in accordance with the definition of η by the relation

$$B = \frac{\eta u}{d}. \tag{34}$$

At low pressures, however, the observed value of the tangential force B is less than that given by the last equation, corresponding to an increase in the value of d. That is, the equation assumes the form

$$B = \frac{\eta u}{d + 2\zeta}, \tag{35}$$

where ζ is known as the *coefficient of slip.*

Considerations based on the kinetic theory of gases lead to the relation

$$\zeta = \left(\frac{2 - f}{f}\right)\frac{\eta}{P_{\mu b}}\sqrt{\frac{\pi R_0 T}{2M}}, \tag{36a}$$

which, combined with equation 9 above, leads to the relation

$$\zeta = 2 \cdot 0.499 \frac{(2 - f)}{f} L, \tag{36b}$$

---

[51] *Ann. Physik,* **46,** 357 (1915).

where f is a numerical coefficient which has a maximum value of 1. It was introduced by Maxwell with an interpretation given by Kennard as follows:[52]

> The value of f, the transfer ratio for momentum, will presumably depend upon the character of the interaction between the gas molecules and the surface; it may vary with the temperature. We can imagine a surface that is absolutely smooth and reflects the molecules "specularly" with no change in their tangential velocities; in such a case $f = 0$ and $\zeta = \infty$, viscosity being unable to get a grip upon the wall at all. On the other hand, we can imagine the molecules to be reflected without regard to their directions of incidence and therefore with complete loss of their initial average tangential velocity.

In this case $f = 1$, and $\zeta = L$.[53]

More generally, $\zeta = \beta L$, where β is of the order of unity, and at very low pressures, where $L \gg d$, equation 35 becomes

$$B = \frac{\eta u}{2\beta L} = \frac{u}{\beta} \cdot \frac{\rho v_a}{4} \tag{37a}$$

$$= \frac{u}{\beta} \cdot P_{\mu b} \sqrt{\frac{M}{2\pi R_0 T}} \tag{37b}$$

Thus, at very low pressures the rate of transference of momentum from a moving surface to another surface adjacent and parallel is *directly proportional to the pressure* and to the velocity of the moving surface. This conclusion was applied by I. Langmuir[54] to the design of a *molecular gauge* for the measurement of low pressures, which is described in Chapter 6.

The quantity $\rho v_a/4$, which as noted previously corresponds to the mass of gas incident on unit area per unit time, has been designated by Kennard as the *free-molecule* viscosity of the gas between the plates.

The concept of coefficient of slip has also been used to interpret observations on the flow of gases at very low pressures, through capillaries. This topic will be discussed in the following chapter.

---

[52] EHK, p. 297.

[53] A. Timiriazeff, *Ann. Physik*, **40**, 971 (1913), assumed that f, which may be regarded as an accommodation coefficient for transfer of momentum, has the same value for any gas-surface combination as α, the accommodation coefficient for heat transfer (discussed in the following section); but B. Baule, *Ann. Physik*, **44**, 145 (1914), disagreed with this assumption and concluded that the value of the ratio between ζ and L (denoted by β in equations 37 below) must be a complicated function of the diameters of the molecules in the gas and those constituting the surface. The theoretical investigations on this topic are discussed by Kennard and Loeb (LBL, pp. 296–300). Loeb quotes results obtained by R. A. Millikan, *Phys. Rev.*, **21**, 217 (1923), which lead to values of f ranging from 0.87 to 1.00.

[54] *Phys. Rev.*, **1**, 337 (1913).

ADDED NOTE 4. MOLECULAR DIAMETERS

Mention has been made in the previous section of the two relations for deducing values of δ and of δ_m from viscosity measurements. These relations are as follows:

$$\delta^2 = 2.714 \cdot 10^{-21} \frac{\sqrt{MT}}{\eta} \tag{18}$$

and

$$\delta_m{}^2 = \frac{\delta^2 T}{C + T}. \tag{13}$$

As illustrated in Table 7 by the values of δ for mercury, these values exhibit a considerable decrease with increase in temperature, and in this case it is found that $\delta_m = 2.50 \cdot 10^{-8}$. The variation with T is obviously greater for those molecules for which the Sutherland constant, C, has a large value.

In spite of the fact that the values of δ thus deduced exhibit a variation with T, the writer has followed Chapman and Cowling in choosing equation 18 rather than 13. While, as pointed out by Chapman and Cowling, such a variation in the value of δ with T "receives a simple explanation on the hypothesis that the molecules are centers of repulsive forces, not hard spheres," it is of interest to compare the results obtained by means of equation 18 with those obtained by means of 13 and also by other methods.

There are several such methods, and only a few of the more important ones can be mentioned briefly, together with some of the results deduced.

Application of the van der Waals Equation. Near the critical temperature and pressure the behavior of gases can be described very satisfactorily by a modified form of equation 2.8, deduced by van der Waals, which is as follows:

$$\left(P + \frac{a}{V^2}\right)(V - b) = R_0T. \tag{38}$$

In this equation V is the volume per mole, the term a/V^2 is a correction term which takes into account the attractive forces between the molecules, and the constant b is a measure of the actual volume of the total number of molecules in accordance with the relation.

$$\frac{b}{4} = N_A \cdot \frac{4}{3} \cdot \frac{\pi\delta^3}{8}. \tag{39}$$

Hence,

$$\delta^3 = \frac{3b}{2\pi N_A} = 7.929 \cdot 10^{-25} b. \tag{40}$$

The value[55] of the constant b may be determined for any given gas from the values of the critical temperature (T_c) and critical pressure (P_c) by means of the relation

$$b = \frac{R_0 T_c}{8P_c}. \tag{41}$$

From the Density of the Solid or Liquid. Assuming that the molecules are closely packed, as in a face-centered cubic lattice, the projected area per molecule is given by the relation[56]

$$\frac{1}{N_S} = \sigma = \frac{4\sqrt{3}}{2}\left(\frac{m}{4\sqrt{2}\rho}\right)^{2/3} = \frac{10^{-15}}{6.537}\left(\frac{M}{\rho}\right)^{2/3} \tag{42}$$

where m = mass of molecule = M/N_A.

ρ = density of *condensed* phase.

But, according to equation 24,

$$\sigma = \frac{\sqrt{3}}{2}\delta^2 = 0.866\delta^2 \tag{43}$$

Hence,

$$\delta = 1.122\left(\frac{m}{\rho}\right)^{1/3} = 1.329 \cdot 10^{-8}\left(\frac{M}{\rho}\right)^{1/3}. \tag{44}$$

Equation 42 has been used to calculate the number of molecules per unit area required to form a unimolecular layer (or monolayer). (See last column of Table 9.)

Cross Section for Collision with Electrons.[57] A cathode-ray beam of initial intensity I_0 is decreased to intensity I, after passing through a layer of the gas of thickness x, in accordance with the relation

$$I = I_0 \epsilon^{-\alpha x}, \tag{45}$$

where, as shown previously in equation 7.5, α is a measure of $1/L_e$, where L_e = mean free path for electrons = $4\sqrt{2}L$. Hence it follows from equation 6 that

---

[55] Values of b for a large number of gases and vapors are given in the *Handbook of Chemistry and Physics*, published by Chemical Rubber Publishing Company, Cleveland, Ohio. Since these values are expressed in terms of the volume at 0° C and 1 atm as unity, they should be multiplied by 22,415 to give values for use in equation 40. See also *Handbook of Chemistry*, by N. A. Lange, Handbook Publishers, Sandusky, Ohio, 1941, p. 1307.

[56] H. K. Livingston, *J. Am. Chem. Soc.*, **66**, 569 (1944); also S. Brunauer, *The Adsorption of Gases and Vapors*, Princeton University Press, Princeton, 1942, p. 287.

[57] These observations are discussed very fully by H. A. Stuart, *Molekülstruktur*, Julius Springer, Berlin, 1934, p. 49 et subseq.

$$\alpha = \frac{n\pi\delta^2}{4} \tag{46}$$

Thus the collision cross section is given by α/n. However, as has been observed experimentally, the value of α varies in a rather complex manner with the potential used to accelerate the electrons, with the result that it is actually impossible to assign a definite value to δ as derived from electron-collision measurements.

The structure of molecules has also been determined from measurements of dipole moments and from electron-diffraction experiments, all of which are discussed at length by H. A. Stuart[58] in his book.

TABLE 9

VALUES OF MOLECULAR DIAMETER (CM $\times 10^{-8}$)

Gas	From η δ_0	From η δ_m	From b	From ρ	Electron Collision	$10^{-14} \cdot N_S$ from ρ
H_2	2.75	2.10	2.76	4.19	2.2	6.58
He	2.18	1.69	2.66	4.21	1.70	6.49
Ne	2.60	2.16	2.38	3.40	2.2	9.98
A	3.67	2.42	2.94	4.15	3.6	6.71
O_2	3.64	2.50	2.93	3.73	3.4	8.30
Hg	6.26	2.50	2.38	3.26		10.86
CO_2	4.65	3.32	3.24	4.05	4.4	7.04
H_2O	4.68	2.45	2.89	3.48	3.8	9.53
C_6H_6	7.65	4.71	4.51	5.89		3.33
CH_4	4.19	3.31	3.24	4.49		5.73
C_2H_6	5.37	3.87	3.70	5.01		4.60
C_3H_8	6.32	4.45	4.06	5.61		3.67
n-C_4H_{10}	7.06	4.84	4.60	6.10		3.18
n-C_5H_{12}	7.82	5.05	4.89	6.45		2.78
n-C_6H_{14}	8.42	5.22	5.16	6.74		2.54

Table 9 gives, for comparison, values of δ for a number of gases and vapors as deduced by at least four different relations. The second and third columns give values of δ_0 and δ_m as deduced by means of equations 18 and 13, respectively, from the values of η (extrapolated to 0° C) and the values of C given by E. Schuil.[59] The fourth column gives values of δ calculated by means of equation 40 from the values of the van der Waals constant, b; the fifth column gives values deduced by means of equation 44 from values of ρ at extremely low temperatures (in general for the solid state). The sixth column gives values, derived from observed values of α by means of equation 46, for 36-volt electrons,[60] and the last column gives values of N_S calculated by means of equation 43 from the values of δ in the fifth column.[61] The values thus derived are to be compared with those deduced in Tables 6 and 7 from kinetic-theory values of δ.

---

[58] *Op. cit.*

[59] *Phil. Mag.*, **28**, 679 (1939).

9. HEAT CONDUCTIVITY OF GASES

The kinetic theory of gases achieved a great triumph when it led to the conclusion that the viscosity is independent of the pressure. It led to still further important results when it predicted the existence of simple relations between the properties of viscosity, heat conductivity, and diffusivity.

From the kinetic point of view it is the same whether the molecules transfer momentum from one layer to another or translational energy. The equations are quite analogous.

As in the case of viscosity, we consider any two layers *CE, EH* (Fig. 3), each of thickness L, between two plates whose temperatures are T_1 and T_2 and distance apart d. Let c_v denote the heat capacity *per unit mass* at constant volume. The relative temperature drop between the planes *CD* and *HK* is equal to

$$2(T_1 - T_2)\frac{L}{d}\cdot$$

Hence the heat transferred per unit area is

$$E = \frac{1}{6}nv \cdot 2mc_v\frac{(T_1 - T_2)L}{d} \tag{1}$$

$$= \frac{1}{3}\rho vc_v \cdot L\,\frac{(T_1 - T_2)}{d}\cdot$$

Therefore the coefficient of heat conductivity

$$\lambda = \tfrac{1}{3}\rho v_a L c_v. \tag{2}$$

If c_v is expressed in calories per gram, the unit of λ is 1 cal $\cdot$ cm^{-1} $\cdot$ sec^{-1} $\cdot$ deg^{-1}.

Comparing the last equation with 8.3 it follows that

$$\lambda = \eta c_v. \tag{3}$$

As in the case of the relation for η, a more careful consideration of the mechanism of energy transfer by means of the molecules leads to the relation

---

[60] H. A. Stuart, *op. cit.*, p. 51.

[61] See also P. H. Emmett and S. Brunauer, *J. Am. Chem. Soc.*, **59**, 1553 (1937).

$$\lambda = \epsilon \eta c_v, \tag{4}$$

where, according to A. Eucken,[62]

$$\epsilon = \frac{9\gamma - 5}{4} \tag{5}$$

and γ = ratio of specific heat at constant pressure to that at constant volume.

For monatomic gases $\gamma = 5/3$, and for polyatomic gases γ tends to approach the value 1, with increase in total number of atoms per molecule.

Hence

$$1 \leqslant \epsilon \leqslant 2.5.$$

Table 10 gives data published by W. G. Kannuluik and L. K. Martin,[63] on values of λ_0 (conductivity at 0° C) and of ϵ, as derived from observation by means of equation 4 and as calculated by means of equation 5.

Similar data for these gases and a number of others are given in the treatise by Chapman and Cowling.[64]

One important conclusion that follows from equation 4 is that the thermal conductivity of a gas is *independent of pressure*, which is valid as long as the pressure is higher than the range in which molecular flow occurs. (See the following section.)

With regard to the variation in λ with T the following remarks may be made. To a first approximation the variation in value of λ follows that in the value of η, since ϵ exhibits only a slight variation with T. However, for larger ranges of T, account must be taken of the increase with T in the value of c_v. Denoting the *molecular* specific heat, at

---

[62] *Physik. Z.*, **14**, 324 (1913). Also see LBL, pp. 234–252.

[63] *Proc. Roy. Soc. London*, A, **144**, 496 (1934). See also the following references on this topic:

H. Gregory and C. T. Archer, *Proc. Roy. Soc. London*, A, **110**, 91 (1926); **121**, 285 (1928).

H. Gregory and S. Marshall, *Proc. Roy. Soc. London*, A, **114**, 354 (1927); **118**, 594 (1928).

B. G. Dickins, *Proc. Roy. Soc. London*, A, **143**, 517 (1934).

H. A. Daynes, *Gas Analysis by Measurements of Thermal Conductivity*, Cambridge University Press, 1933, gives a very comprehensive table of relative thermal conductivities (air = 1) for a large number of gases, including hydrocarbons.

[64] CC, p. 241.

TABLE 10*

VALUES OF HEAT CONDUCTIVITY COMPARED WITH COEFFICIENTS OF VISCOSITY

Gas	$10^5\lambda_0$	$10^5\eta_0$	$c_v(\text{cal} \cdot \text{g}^{-1})$	ϵ (obs.)	ϵ (calc.)
He	34.3	18.76	0.746	2.45	2.44
Ne	11.12	29.81	0.150	2.50	2.44
A	3.82	21.02	0.0745	2.44	2.44
H_2	41.3	8.50	2.43	2.00	1.90
Air	5.76	17.22	0.171	1.96	1.91
O_2	5.83	19.31	0.157	1.92	1.95
CO	5.37	16.65	0.178	1.81	1.91
CO_2	3.43	13.74	0.153	1.64	1.72
N_2O	3.61	13.66	0.155	1.71	1.73

* To convert values of λ_0 from $\text{cal} \cdot \text{cm}^{-1} \cdot \text{sec}^{-1} \cdot \text{deg}^{-1}$ to *watts* $\cdot \text{cm}^{-1} \cdot \text{deg}^{-1}$ multiply values in Table 10 by 4.186.

constant volume, by C_v, the following relations are given by J. R. Partington and W. G. Shilling[65] for different gases.

GAS	$\gamma = C_p/C_v$	C_v
Air	1.4034	$4.924 + 1.7 \cdot 10^{-4}T + 3.1 \cdot 10^{-7}T^2$
N_2	1.405	$4.924 + 1.7 \cdot 10^{-4}T + 3.1 \cdot 10^{-7}T^2$
O_2	1.396	$4.924 + 1.7 \cdot 10^{-4}T + 3.1 \cdot 10^{-7}T^2$
CO	1.404	$4.924 + 1.7 \cdot 10^{-4}T + 3.1 \cdot 10^{-7}T^2$
H_2	1.408	$4.659 + 7.0 \cdot 10^{-4}T$
CO_2	1.302	$5.547 + 4.5 \cdot 10^{-3}T - 1.02 \cdot 10^{-6}T^2$
H_2O	—	$6.901 - 1.19 \cdot 10^{-3}T + 2.34 \cdot 10^{-6}T^2$
Hg, A, etc.	1.667	2.990

Since the variation in η with T is given by the Sutherland relation, equation 8.16, it follows that, in terms of λ_0 in $\text{cal} \cdot \text{cm}^{-1} \cdot \text{sec}^{-1} \cdot \text{deg}^{-1}$,

$$\lambda_T = 4.186\lambda_0 \cdot \frac{(C + 273.2)}{(273.2)^{3/2}} \cdot \frac{\sqrt{T}(1 + \alpha T + \beta T^2)}{1 + C/T}, \tag{6}$$

where α and β are determined from the expression for C_v as a function of T, and λ_T is expressed in *watts* $\cdot \text{cm}^{-1} \cdot \text{deg}^{-1}$. For *hydrogen*,

$$\lambda_T = 1.369 \cdot 10^{-4} \sqrt{T} \left(\frac{1 + 1.50 \cdot 10^{-4} T}{1 + 84.4/T} \right);$$

---

[65] The *Specific Heats of Gases*, 1924. See also G. N. Lewis and M. Randall, *Thermodynamics*, McGraw-Hill Book Company, 1923, p. 80. The most recent publication is *Bull.* 30, Cornell University Engineering Experiment Station, October, 1942, which gives specific heats of a number of gases over a wide range of pressures and temperatures.

for *argon*,

$$\lambda_T = 1.470 \cdot 10^{-5} \frac{\sqrt{T}}{1 + 142/T};$$

for *nitrogen*,

$$\lambda_T = 2.009 \cdot 10^{-5} \sqrt{T} \left(\frac{1 + 3.45 \cdot 10^{-5} T + 6.30 \cdot 10^{-8} T^2}{1 + 104/T} \right).$$

Similar expressions for gases for which λ has not been determined can be derived, as is evident, from determinations of η, using the observed values of C and values of ϵ calculated from those of γ by means of equation 5.

It will be observed that the heat conductivities of hydrogen and helium are much greater than those of heavier gases, such as oxygen and carbon dioxide.

For the case of a wire of radius a and length l, suspended along the axis of a cylinder of radius r, the *energy loss per unit time* due to thermal conduction by the gas is[66]

$$E = \frac{2\pi a l \lambda_m (T - T_0)}{a \ln (r/a)} = \frac{2\pi \lambda_m l (T - T_0)}{\ln (r/a)}, \tag{7}$$

where $T - T_0$ is the difference in temperature and r/a is not "excessively" large,[67] while λ_m is the average conductivity over the temperature range $T - T_0$.

The units in which E is expressed are usually in terms of watts $\cdot$ cm^{-2}.

The *energy loss per unit area* per unit time is

$$E_0 = \frac{\lambda_m (T - T_0)}{a \ln (r/a)}, \tag{8}$$

and the *energy loss per unit length of wire* per unit time is

$$E_l = \frac{2\pi \lambda_m (T - T_0)}{\ln (r/a)}. \tag{9}$$

Hence

$$E_l = 2\pi a E_0. \tag{10}$$

Since the total energy loss from a heated wire is the sum of that lost by radiation (which varies as $T^4 - T_0{}^4$) and that lost by conduction of the gas, the former has to be subtracted from the total energy loss in order to obtain the amount due to the latter. Furthermore, in the case of short wires especially, a correction has to be made for the loss by conduction at the ends.

---

[66] $\ln = \log_e = 2.303 \log_{10}$.

[67] The exact meaning of this requirement will appear in the subsequent discussion.

For wires of low emissivity, such as platinum, operating at a temperature below about 500° C, the loss due to radiation is negligible compared to that due to conduction.

Since the thermal conduction loss in the case of mixtures varies with both the nature of the gas and the composition, this has been applied to the analysis of gases.[68]

An instrument devised for this purpose by G. A. Shakespear,[69] known as a *katharometer*, consists of a platinum spiral filament in a copper block. This instrument has been used extensively by English investigators for determinations of rates in gaseous reactions and for experiments on thermal transpiration (which is discussed in section 12).[70]

10. THERMAL CONDUCTIVITY AT LOW PRESSURES

As mentioned in the previous section, the heat conductivity of gases should theoretically be independent of pressure. That this is at least approximately confirmed by observation is illustrated by the data shown in Table 11 obtained by B. G. Dickins.[71]

The values under W represent the total heat loss (in calories) by conduction, from a platinum wire ($a = 3.765 \cdot 10^{-3}$ cm, $l = 20.09$ cm) suspended along the axis of a Pyrex glass tube (inside radius, $r = 0.3346$ cm). The tube was maintained at about 0° C by external cooling, and Δt is the temperature differential between the wire and the wall. The pressure of the gas in millimeters of mercury is given in the third column, and the value indicated by W_∞ represents the heat loss extrapolated for $P = \infty$. The values under λ_t give the thermal heat conductivity at the mean temperature indicated in the last column. The values of λ_t (in calories) were derived by means of the relation, deduced from equation 9.7,

---

[68] See A. Farkas and H. W. Melville, *Experimental Methods in Gas Reactions*, Cambridge University Press, 1939, p. 190 (designated FM), also A. Farkas, *Orthohydrogen, Parahydrogen, and Heavy Hydrogen*, Cambridge University Press, 1935, for illustrations of the application of this method.

[69] *Proc. Roy. Soc. London*, **A**, **97**, 273 (1920). See also the comprehensive discussion of this instrument by H. A. Daynes, *Gas Analysis by Measurement of Thermal Conductivity*, Cambridge University Press, 1933.

[70] See especially a description of a modified construction by T. L. Ibbs, *Proc. Roy. Soc. London*, **A**, **99**, 385 (1921), also **107**, 470 (1925). W. E. Summerhays, *Proc. Phys. Soc. London*, **42**, 218 (1930), has used the katharometer to measure the coefficient of diffusion of water vapor.

[71] *Proc. Roy. Soc. London*, **A**, **143**, 517 (1934).

$$W_\infty = \frac{2\pi al \cdot \lambda_t \, \Delta t}{a \ln (r/a)}. \tag{1}$$

TABLE 11

VARIATION IN THERMAL CONDUCTION WITH PRESSURE (DICKINS)

Gas	Δt	P_{mm}	W	W_∞	$10^5\lambda_t$	$t°$ C
H_2	17.866	625.0	0.21323	0.21494	42.77	9.04
		442.0	.21258			
		302.3	.21145			
		229.9	.21038			
		168.2	.20875			
		129.8	.20692			
Air	23.832	91.7	0.04021	0.04052	6.044	11.94
		52.1	.03997			
		31.3	.03961			
		22.3	.03926			
		17.1	.03891			
		11.9	.03825			
CO_2	23.80	83.3	0.02461	0.02473	3.694	11.91
		40.5	.02447			
		19.2	.02417			
		11.1	.02379			

It will be observed that over a range of pressures the values of W did not exhibit any considerable decrease.

That the heat conductivity is practically constant over a large range of pressures is also shown by the plots in Fig. 4, of the energy loss (in watts) at constant temperature (about 99° C) from a platinum filament. The filament was a 14-cm length of 3-mil wire located along the axis of a glass tube 2.54 cm in diameter. The wall temperature was 0° C.

As will be observed, the heat loss in hydrogen was about 10 times that in argon. The loss at a pressure of about 1 micron was 0.006 watt. A comparison of the relative losses in the three gases at 76 cm yields values which agree, within a few per cent, with the values of λ given in Table 10.

Thus, over the range 10 to 76 cm Hg, the heat loss in hydrogen increased only about 7 per cent, whereas in the range below 5 cm the decrease was nearly 100 per cent. Careful measurements show that at very low pressures the thermal conductivity decreases linearly with the pressure.

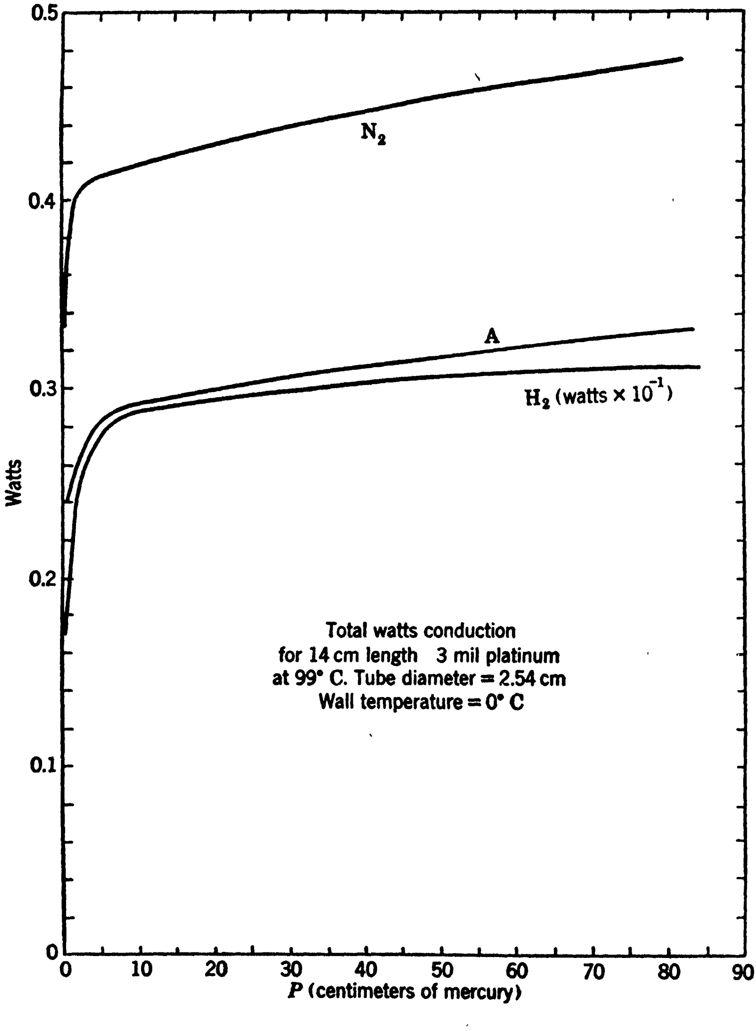

FIG. 4. Illustrating the variation in thermal conductivity with pressure, for nitrogen, argon, and hydrogen. Ordinates give values of total watts conducted from platinum filament 14 cm long and 3 mil diameter along the axis of a cylindrical glass tube, diameter = 2.54 cm. Temperature of filament = 99° C, temp. of wall = 0° C. Scale of watts for hydrogen should be multiplied by 10. Abscissas give pressures in centimeters of mercury.

The theory of heat conduction at these pressures has been developed from two different points of view. The first of these, due to M. Knudsen,[72] involves a consideration of the mechanism of energy transfer by individual molecules incident on the hot surface.

The second point of view, due to M. von Smoluchowski,[73] is based upon the concept of a temperature discontinuity which is the thermal analogue of the phenomenon of "slip" discussed in Added Note 3 at the end of section 8.

Free Molecule Conductivity (Knudsen). When molecules originally at a temperature T_i strike a hot surface at temperature T_s ($> T_i$), complete interchange of energy does not occur at the first collision. In fact it may often require many collisions for this to occur. Therefore Knudsen introduced a constant, known as the *accommodation coefficient*, designated by α, which "can be defined as standing for the fractional extent to which those molecules that fall on the surface and are reflected or re-emitted from it, have their mean energy adjusted or 'accommodated' toward what it would be if the returning molecules were issuing as a stream out of a mass of gas at the temperature of the wall."[74]

The molecules re-emitted or reflected from the hot surface consequently possess a mean energy which corresponds to a temperature lower than T_s, which we shall designate as T_r, and the accommodation coefficient is defined by the relation

$$\alpha = \frac{T_r - T_i}{T_s - T_i}. \tag{2}$$

For $\alpha = 1$, $T_r = T_s$; for $\alpha < 1$, $T_s > T_r > T_i$.

In any treatise on kinetic theory of gases it is shown that the energy transferred from a surface at temperature T is given by $E = 2kT$ (instead of $\frac{3}{2}kT$, which is the average energy of the molecules in a volume).

Let us now consider heat transfer in a monatomic gas at low pressure.

E_0 = energy transfer from hot to cold surface (at temperature T_i) per square centimeter of hot surface per second

$$= \nu \cdot 2k(T_r - T_i)$$

$$= \tfrac{1}{4}nv_i \cdot 2k(T_r - T_i)$$

---

[72] *Ann. Physik*, **31**, 205 (1910); **32**, 809 (1910); **33**, 1435 (1910); **34**, 593 (1911); and **6**, 129 (1930). See also LBL, pp. 310–325, and EHK, pp. 311–320.

[73] A number of papers published before 1911, and *Ann. Physik*, **35**, 983 (1911). Also discussed by LBL and EHK.

[74] EHK, pp. 311–312.

$$= \frac{1}{2} \cdot \frac{Pv_i}{T_i} (T_r - T_i)$$

$$= \frac{\alpha}{2} \cdot \frac{Pv_i}{T_i} (T_s - T_i), \tag{3}$$

where v_i = average velocity at T_i.

Thus the rate of energy transfer at low pressure is proportional to the pressure and the temperature difference.

For diatomic and polyatomic gases, the molecules striking the hot surface acquire not only increased translational energy but also increased amounts of both rotational and vibrational energy. The amount of the vibrational energy possessed by molecules as compared with the amount of translational energy is measured by the value of γ. A detailed calculation leads, in these cases, to the relation

$$E_0 = \frac{\alpha}{8} \left(\frac{\gamma + 1}{\gamma - 1}\right) \frac{Pv_i}{T_i} (T_s - T_i), \tag{4}$$

which for $\gamma = 5/3$ (case of monatomic gases) becomes identical with equation 3.

In this equation, α has the value[75]

$$\alpha = \frac{\alpha_1 \alpha_2}{\alpha_1 + \alpha_2 - \alpha_1 \alpha_2}, \tag{5}$$

where α_1 and α_2 are the values of the accommodation coefficient for the two surfaces.

Substituting for v_i from the relation in terms of T_i and M, equation 4 assumes the form

$$E_0 = \frac{\alpha}{2} \left(\frac{\gamma + 1}{\gamma - 1}\right) \sqrt{\frac{R_0}{2\pi M(273.2)}} \cdot P_{\mu b} \sqrt{\frac{273.2}{T_i}} (T_s - T_i)$$

$$= \alpha \Lambda_0 P_{\mu b} \sqrt{\frac{273.2}{T_i}} \cdot (T_s - T_i), \tag{6}$$

where Λ_0 = *free-molecule heat conductivity* at 0° C

$$= \frac{1}{2} \left(\frac{\gamma + 1}{\gamma - 1}\right) \sqrt{\frac{R_0}{2\pi}} \cdot \frac{1}{\sqrt{M(273.2)}}$$

$$= \frac{1.819 \cdot 10^{-4}}{\sqrt{M(273.2)}} \left(\frac{\gamma + 1}{\gamma - 1}\right) \text{ watts} \cdot \text{cm}^{-2} \cdot \text{deg}^{-1} \cdot \textit{microbar}^{-1} \tag{7}$$

---

[75] See EHK, p. 316.

$$= \frac{1.468 \cdot 10^{-5}}{\sqrt{M}} \left(\frac{\gamma + 1}{\gamma - 1}\right) \quad \text{watts} \cdot \text{cm}^{-2} \cdot \text{deg}^{-1} \cdot \textit{micron}^{-1}. \tag{8}$$

(In terms of g · cal · sec^{-1}, Λ_0 should be multiplied by 0.2389.)

Table 12 gives values of Λ_0 in *watts* · *cm*$^{-2}$ · *deg*$^{-1}$ · *micron*$^{-1}$ for a number of gases and vapors,[76] and, for comparison, values of $4.86\lambda_0$ (derived from the values in Table 10 and from other sources) which correspond to the conductivity at 0° C in terms of *watts* · *cm*$^{-1}$ · *deg*$^{-1}$.

TABLE 12

VALUES OF MOLECULAR HEAT CONDUCTIVITY

Gas	M	γ	$10^6\Lambda_0$	$4.186 \cdot 10^4\lambda_0$
H_2	2.016	1.41	60.72	17.30
He	4.003	1.67	29.35	14.36
H_2O	18.016	1.30	26.49	—
Ne	20.18	1.67	13.07	4.66
N_2	28.02	1.40	16.63	2.38
O_2	32.00	1.40	15.57	2.44
A	39.94	1.67	9.29	1.60
CO_2	44.01	1.30	16.96	1.44
Hg	200.6	1.67	4.15	—

In terms of g · cal per mole

$$R_0 = \frac{8.3144 \cdot 10^7}{4.8155 \cdot 10^7} = 1.9865 \quad \text{g} \cdot \text{cal} \cdot \text{deg}^{-1} \cdot \text{mole}^{-1}.$$

Since $\gamma + 1 = (2C_v + 1.9865)/C_v$, and $\gamma - 1 = 1.9865/C_v$, where C_v = *molar* specific heat in g · cal, at constant volume,

$$\frac{\gamma + 1}{\gamma - 1} = 1 + \frac{2C_v}{1.9865}.$$

Hence equation 7 can be expressed in the form

$$\Lambda_0 = \left(\frac{C_v}{1.9865} + \frac{1}{2}\right)\sqrt{\frac{R_0}{2\pi M(273.2)}}. \tag{9}$$

For *coaxial cylinders* of radii a and r ($r > a$), the rate of energy transfer *per unit area* from the inner cylinder or wire, at temperature T_s and at *low pressures*, is given by the relation

$$E_0 = \alpha_r \cdot \Lambda_0 P_{\mu b} \sqrt{\frac{273.2}{T_i}} \cdot (T_s - T_i) \tag{10}$$

---

[76] A table of values of γ is given by LBL, p. 445. Also see J. R. Partington and W. G. Shilling, *The Specific Heat of Gases,* 1924.

where

$$\alpha_r = \frac{\alpha}{1 - (1 - \alpha)(a/r)}, \tag{11}$$

and α is assumed to be the same for the two surfaces.[77]

It is of interest to compare the rate of energy loss in hydrogen at atmospheric pressure with that at low pressures. At 1 atm, $E_0 = 1.730 \cdot 10^{-3}$ watts $\cdot$ cm^{-1} $\cdot$ deg^{-1}, whereas, at P_μ and $T_i = 273.2$, $E_0 = 6.07 \cdot 10^{-5} P_\mu$ watts $\cdot$ cm^{-2} $\cdot$ deg^{-1}.

Jeans has pointed out[78] that according to general dynamical considerations the constant α should be determined by a relation of the form

$$\alpha = \frac{4mm'}{(m + m')^2} = 1 - \left(\frac{m - m'}{m + m'}\right)^2, \tag{12}$$

where m' = mass for molecules striking the surface for which the molecular mass is m.

For completely roughened surfaces $\alpha = 1$. Values of α which have been observed for different cases are given in Table 13.[79]

Temperature Discontinuity (Smoluchowski). At the end of section 8 mention was made of the phenomenon of "slip" which occurs in a gas at moderately low pressures. There was introduced in equation 8.35 a coefficient of slip $\zeta = \beta L$, to account for the apparent decrease in viscosity at low pressures.

An analogous phenomenon was observed by Smoluchowski in the case of thermal conduction at low pressures. For two parallel plane surfaces separated by a distance d, the *heat loss per unit area per unit*

---

[77] M. von Smoluchowski, *Ann. Physik*, **35**, 983 (1911).

[78] JHJ, p. 193.

[79] The data for platinum are from LBL, p. 321. The data for tungsten are from H. A. Jones and I. Langmuir, *Gen. Elec. Rev.*, **30**, 354 (1927), while those for "ordinary" platinum are from B. G. Dickins, *Proc. Roy. Soc. London*, **A**, **143**, 517 (1934). That the value of the accommodation coefficient is greatly affected by the nature of the surface film has been shown by K. B. Blodgett and I. Langmuir, *Phys. Rev.*, **40**, 78 (1932). In the case of a tungsten wire in hydrogen at 0.20 mm, the value of α changes from 0.534 for bare tungsten to 0.094 for tungsten with an adsorbed film of oxygen. The general problem of the interaction between molecules and solid surfaces, which is obviously involved in the interpretation of α, has received considerable attention from a number of investigators. For detailed discussion, especially with regard to the role of α in adsorption phenomena, see LBL, p. 311, etc., also J. K. Roberts, *Some Problems in Adsorption*, Cambridge University Press, 1939. Values of α for air and a number of different metals having etched, polished, and machined surfaces have been determined by M. L. Wiedmann, *Trans. Am. Soc. Mech. Eng.*, **68**, 57 (1946). These values range from 0.87 to 0.97.

TABLE 13

VALUES OF THE ACCOMMODATION COEFFICIENT FOR HYDROGEN, OXYGEN, AND CARBON DIOXIDE

Surface	H_2	O_2	CO_2
Polished Pt	0.358	0.835	0.868
Pt slightly coated with black	.556	.927	.945
Pt heavily coated with black	.712	.956	.975

	H_2	N_2	A	Hg	Air
Tungsten	0.20	0.57	0.85	0.95	
Ordinary Pt	.36	.89	.89		0.90

time may be represented at these pressures by a relation of the form

$$E_0 = \frac{\lambda_m(T_1 - T_0)}{d + 2g}, \tag{13}$$

where λ_m is the mean conductivity over the range $T_1 - T_0$.

In this equation, g is a coefficient defined by the relation

$$\Delta T = -g\frac{dT}{dx}, \tag{14}$$

where ΔT represents the temperature discontinuity at any one surface, and dT/dx is the temperature gradient normal to the surface.

As shown by Kennard,

$$\begin{aligned} g &= \frac{2-\alpha}{\alpha}\cdot\frac{2}{\gamma+1}\cdot\frac{\lambda}{\eta c_v}\cdot L \\ &= \frac{2-\alpha}{\alpha}\cdot\frac{2\epsilon}{\gamma+1}\cdot L = \beta' L, \end{aligned} \tag{15}$$

where the numerical constant ϵ has a value, according to equation 9.5, which varies between 1 and 2.5, and β' is a numerical constant of the order of unity.

Hence equation 13 may be expressed in the form

$$E_{0p} = \frac{\lambda_m(T_1 - T_0)}{d + 2\beta' L} = \frac{\lambda_m(T_1 - T_0)}{d + 2\beta' c/P}, \tag{16}$$

where α is assumed to be the same for both surfaces, also $L = c/P$, and the symbol E_{0p} indicates that the conductivity per unit area is a function of P.

For a hot wire of radius a situated along the axis of a cylindrical tube of radius r, equation 16 must be replaced by the relation

$$E_{0p} = \frac{\lambda_m(T_1 - T_0)}{a \ln (r/a) + (\beta' c/P)(a/r + 1)}, \tag{17}$$

where it is assumed that α is the same for both the wire and inside surface of the cylinder.

For very low values of P, equation 16 becomes

$$E_{0p} = \frac{\lambda_m(T_1 - T_0)}{2\beta' c} \cdot P, \tag{18}$$

and equation 17 becomes

$$E_{0p} = \frac{\lambda_m(T_1 - T_0) \cdot P}{\beta' c(1 + a/r)}. \tag{19}$$

That is, at very low pressures E_{0p} is independent of d and *varies linearly with P*. This conclusion is identical with that deduced above by Knudsen for the case of free-molecule flow. That equation 18 is identical with 6 may be shown as follows:

Substituting for β' from equation 15, for λ_m from equation 9.4, and utilizing the relation $\eta = 0.5\rho v_a L$, we obtain the result

$$\begin{aligned}
\frac{\lambda_m}{2\beta' c} &= \frac{\alpha \epsilon \eta c_v(\gamma + 1)}{(2 - \alpha)4\epsilon PL} \\
&= \left(\frac{\alpha}{2 - \alpha}\right)\frac{1}{4}(\gamma + 1)\frac{C_v}{M}\frac{1}{2}\frac{\rho v_a L}{PL} \\
&= \left(\frac{\alpha}{2 - \alpha}\right)\frac{1}{8}\left(\frac{\gamma + 1}{\gamma - 1}\right)\frac{R_0 MP}{PMR_0 T_i}\sqrt{\frac{8R_0 T_i}{\pi M}} \\
&= \left(\frac{\alpha}{2 - \alpha}\right)\frac{1}{2}\left(\frac{\gamma + 1}{\gamma - 1}\right)\sqrt{\frac{R_0}{2\pi M T_i}} \\
&= \left(\frac{\alpha}{2 - \alpha}\right)\Lambda_0\sqrt{\frac{273.2}{T_i}},
\end{aligned}$$

where $\alpha/(2 - \alpha)$ takes the place of α used in equation 6.

Equations 16 and 17 can be expressed in a form which is very convenient for calculation. We shall consider especially equation 17, which is more important in practical measurements of heat conductivity. This equation may obviously be written in the form

$$\frac{1}{E_{0p}} = \frac{a \ln r/a}{\lambda_m(T_1 - T_0)} + \frac{X}{P}. \tag{20}$$

That is, if $1/E_{0p}$ is plotted against $1/P$ a *straight line* is obtained.

From the intercept for $1/P = 0$, which we shall designate by $1/E_{0\infty}$, the value of λ_m may be obtained, while the slope is given by the relation

$$\frac{\Delta(1/E_0)}{\Delta(1/P)} = X,$$

where X is a constant determined by the relation

$$X = \frac{\beta' c(1 + a/r)}{E_{0\infty}\, a \ln (r/a)}. \tag{21}$$

Equation 20 thus applies to the transition range of pressures in which E_0 changes from being independent of pressure (at higher pressures) to varying linearly with the pressure (at very low pressures).

The validity of this conclusion can be illustrated by its application to two sets of data, of which the first is that given in Table 11.

A plot of $1/W = 1/(2\pi l a E_0)$ against $1/P$ yields, as Dickins has shown, a straight line for each gas, and the values of λ_t given in the table were deduced from the values of $1/W_\infty$ which correspond to the intercepts on the ordinate axis for $1/P = 0$. (See equation 1.)

The other set of data is that obtained by Knudsen[80] on the rate of energy transfer from a very fine tungsten wire in hydrogen. In this case, $a = 2.2 \cdot 10^{-4}$ cm, $l = 9.65$, and $r = 0.535$. Hence $2\pi a l = 0.01334$ cm^2. For the range $P_{\mu b} = 10^6$ to $P_{\mu b} = 6000$, $\Delta T = 2.98°$ C; from 6000 to 400 microbars, $\Delta T = 32.73$; and for pressures below 400 microbars, $\Delta T = 104.2°$ C.

Table 14 gives the values of $P_{\mu b}$ and $E_0/\Delta T$ in cal $\cdot$ cm$^{-2} \cdot$ deg$^{-1} \cdot$ sec^{-1}, along with the reciprocals of each of these quantities.

TABLE 14

DATA (ACCORDING TO KNUDSEN) USED IN PLOT IN FIG. 5

$P_{\mu b}$	$10^3/P_{\mu b}$	$10^5 E_0/\Delta T$	$10^{-3}\Delta T/E_0$	$10^{-3}P_{\mu b}$	$10^5/P_{\mu b}$	$10^3 E_0/\Delta T$	$\Delta T/E_0$
107.3	9.33	40.77	2.453	3.200	31.3	11.65	85.8
214.8	4.66	81.56	1.226	6.355	15.74	22.05	45.4
322.1	3.11	122.1	0.819	13.45	7.435	42.12	23.75
428.6	2.33	162.1	0.617	35.0	2.857	83.9	11.92
534.8	1.87	201.5	0.496	66.8	1.495	121.9	8.20
640.0	1.56	241.4	0.414	129.0	0.775	190.9	5.24
744.6	1.34	280.5	0.357	505.0	0.198	211.1	4.74
848.6	1.18	319.2	0.313	1016.0	0.0984	223.9	4.47
950.9	1.05	357.6	0.280	∞	0	(227)	(4.4)
1053.3	0.949	395.4	0.253				
1075.0	.930	400.9	0.249				

---

[80] *Ann. Physik*, **34**, 593 (1911).

A plot of $\Delta T/E_0$ versus $1/P_{\mu b}$ (see Fig. 5) yields a straight line, for the range $P_{\mu b} = 3.2 \cdot 10^3$ to $P_{\mu b} = 1.016 \cdot 10^6$ (2.4 mm to 762 mm) with the values

$$\frac{d(\Delta T/E_0)}{d(1/P_{\mu b})} = 2.60 \cdot 10^5; \quad \left(\frac{\Delta T}{E_0}\right)_\infty = 4.4; \quad \left(\frac{E_0}{\Delta T}\right)_\infty = 0.227.$$

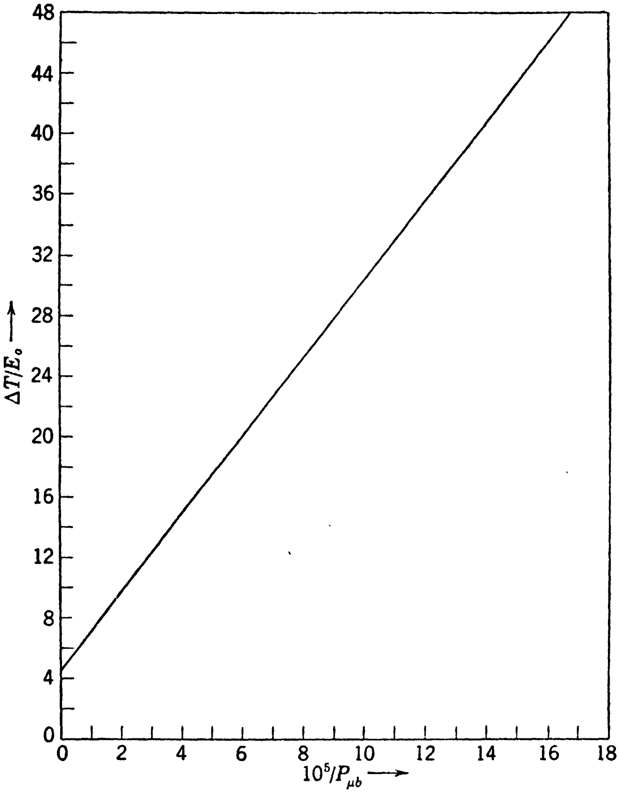

FIG. 5. Plot of $\Delta T/E_0$ versus $10^5/P_{\mu b}$ of Knudsen's data in Table 14. Ordinates give values of deg C/(cal · cm^{-2} · sec^{-1}).

In the range $P_{\mu b} = 1053.3$ to $P_{\mu b} = 107$,

$$\frac{E_0}{\Delta T} = 3.72 \cdot 10^{-6} P_{\mu b}.$$

That is, the energy loss varies linearly with P.

From the value

$$\left(\frac{E_0}{\Delta T}\right)_\infty = 0.227$$

$$= \frac{\lambda_m}{a \ln (r/a)} = \frac{\lambda_m}{2.2 \cdot 10^{-4} \ln (535/0.22)}$$

it follows that $\lambda_m = 38.9 \cdot 10^{-5}$ cal · cm^{-1} · deg^{-1} · sec^{-1}, which is in good agreement with the value given for λ_0 in Table 10.

On the other hand, it follows from the values in Table 12 that, at low pressures and 0° C,

$$\frac{E_0}{\Delta T} = \frac{60.72 \cdot 10^{-6}}{4.186} \cdot \frac{3}{4} \alpha P_{\mu b} = 1.09 \cdot 10^{-5} \alpha_r P_{\mu b} \quad \text{cal} \cdot \text{deg}^{-1} \cdot \text{cm}^{-2} \cdot \text{sec}^{-1}.$$

Hence $\alpha_r = \frac{3.72 \cdot 10^{-6}}{10.9 \cdot 10^{-6}} = 0.34$, and $\alpha = 0.34$, since a/r is negligibly small. That is, the accommodation coefficient for hydrogen on tungsten, as deduced from Knudsen's measurements, is 0.34.

It follows from the relations given above for E_{0p} that, in order to obtain the minimum dependence on pressure, a should be made as large as possible and r nearly equal to a.

11. LANGMUIR'S FILM THEORY OF HEAT CONDUCTION

In a very interesting paper published in 1912,[81] I. Langmuir formulated a theory of the mechanism of heat conduction from wires (as well as plane surfaces), which deserves a great deal more attention than it has received.

Observations on the heat losses in hydrogen from tungsten wires heated to incandescence showed that whether the wire was in a horizontal or vertical position made a difference of only a few per cent (at constant temperature) in the heat loss. "This," states Langmuir, "was strong indication that the heat loss was dependent practically only on heat conduction very close to the filament and that the convection currents had practically no effect except to carry the heat away after it passed out through the film of adhering gas."

Let us consider, first, a *plane* surface in a gas at normal pressures. Assuming that the *whole temperature drop occurs in a film of thickness B*, adjacent to the surface, the rate of energy loss (due to conduction) per unit area is given by the relation

---

[81] *Phys. Rev.*, **34**, 401 (1912). See also H. A. Jones, *Gen. Elec. Rev.*, **28**, 650 (1925).

$$W = \frac{\lambda \cdot \Delta T}{B} \quad \text{cal} \cdot \text{cm}^{-2} \cdot \text{sec}^{-1}, \tag{1}$$

where ΔT is a relatively small temperature drop. Since, as shown in equation 9.6, λ is a function of T, it follows that for a large difference in temperature, $T_2 - T_1$,

$$\begin{aligned} W &= \frac{4.186}{B} \int_{T_1}^{T_2} \lambda\, dT \quad \text{watts} \cdot \text{cm}^{-2} \\ &= \frac{4.186}{B} \left\{ \int_0^{T_2} \lambda\, dt - \int_0^{T_1} \lambda\, dT \right\} \\ &= \frac{4.186}{B} (\phi_2 - \phi_1), \end{aligned} \tag{2}$$

where $\phi = \int_0^T \lambda\, dT$.

Log-log plots of the values of 4.186ϕ versus T, as calculated by Langmuir, for both hydrogen and air, show that the data may be represented, to within an error not exceeding 2.5 per cent, in the range $1300 \geqslant T \geqslant 300$, by the following equations:[82]

$$\text{For } H_2\text{:} \quad \log (4.186\phi) = -4.965 + 1.78 \log T. \tag{3a}$$

$$\text{For air:} \quad \log (4.186\phi) = -5.877 + 1.81 \log T. \tag{3b}$$

In the case of a wire of radius a, the energy loss will occur through a film of adherent gas, the outer edge of which is at a distance b from the axis of the wire. As shown by Langmuir, the value of b satisfies the relation[83]

$$b \ln \frac{b}{a} = B, \tag{4}$$

and the energy loss *per centimeter length* of wire is given by the relation

$$W = 4.186 \frac{2\pi(\phi_2 - \phi_1)}{\ln (b/a)} \quad \text{watts} \tag{5a}$$

$$= 4.186s\,(\phi_2 - \phi_1) \quad \text{watts}, \tag{5b}$$

---

[82] Values of $4.186(\phi_2 - \phi_1)$ for hydrogen for the case in which the lower temperature is 80° K (boiling point of nitrogen) are given by K. B. Blodgett and I. Langmuir, *Phys. Rev.*, **40**, 78 (1932).

[83] In this and the following sections, $\ln x = \log_e x = 2.303 \log x$, where log refers to ordinary logarithms.

where

$$s = \frac{2\pi}{\ln (b/a)}. \tag{6}$$

Introducing into the last equation the relation expressed by equation 4, it follows that

$$\frac{a}{B} = \frac{s\epsilon^{-2\pi/s}}{\pi}. \tag{7}$$

Table 15 (taken from Langmuir's paper) gives corresponding values of s and a/B as derived by means of the last equation. Figure 6 shows a plot of these data on semi-log scale. The scales for curves I and II are indicated by arrows.

TABLE 15

VALUES OF s AS A FUNCTION OF a/B (LANGMUIR)

s	a/B	s	a/B	s	a/B	s	a/B
0.0	0.0	5.0	0.453	10	1.696	30	7.738
0.5	$0.735 \cdot 10^{-6}$	5.5	0.558	12	2.263	32	8.370
1.0	$0.594 \cdot 10^{-3}$	6.0	0.671	14	2.844	34	8.995
1.5	$0.725 \cdot 10^{-2}$	6.5	0.788	16	3.438	36	9.622
2.0	$2.752 \cdot 10^{-2}$	7.0	0.908	18	4.040	38	10.25
2.5	0.0644	7.5	1.032	20	4.645	40	10.87
3.0	0.1176	8.0	1.160	22	5.263	42	11.50
3.5	0.185	8.5	1.291	24	5.877	44	12.14
4.0	0.265	9.0	1.424	26	6.505	46	12.77
4.5	0.354	9.5	1.561	28	7.122	48	13.40
5.0	0.453	10.0	1.696	30	7.738	50	14.03

From measurements of the energy losses from platinum wires in air,[84] Langmuir derived the conclusions that, for air at 20° C and 760 mm Hg, $B = 0.043$ cm and is "surprisingly independent" of T. He also concluded that B should be proportional to the viscosity and inversely proportional to the density, "For it is the viscosity that causes the existence of the film and it is the difference of density between hot and cold gas (proportional to the density itself) that keeps the film from becoming indefinitely large." That is,

$$\begin{aligned} B &= \text{const.}\, \frac{\eta}{\rho} \\ &= \text{const.}\, v_a L = \text{const.}\, L\sqrt{\frac{T}{M}}, \end{aligned} \tag{8}$$

where v_a and L correspond to values at T_1 (the lower temperature).

---

[84] Of course, the loss due to radiation was subtracted from the total observed energy loss.

Assuming that, for air at 1 atm and 20° C, $B = 0.43$ cm, it follows from the last equation that, for H_2 at 1 atm and 20° C, $B = 3.0$ cm. On the other hand, observations on the heat losses from tungsten wires in H_2 and N_2,[85] in which the values of s were determined from the observed values of W and the values of $(\phi_2 - \phi_1)$ calculated according to equation 5*b*, lead to the values $B = 1.35$ for H_2 and 0.68 for N_2 at 750 mm pressure.

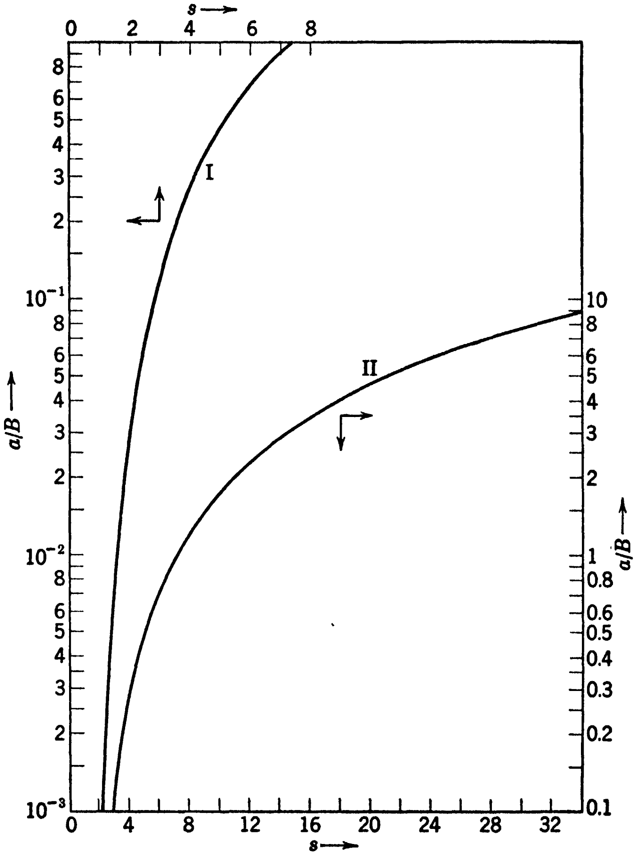

FIG. 6. Plots of a/B versus s according to data in Table 15, deduced for thermal conduction, at normal pressures, through a film surrounding a wire. Appropriate scales for curves I and II are indicated by the arrows.

---

[85] I. Langmuir and G. M. J. Mackay, *J. Am. Chem. Soc.*, **36**, 1708 (1914), and I. Langmuir, *ibid.*, **37**, 417 (1915).

As the pressure is decreased, the value of b increases and the following table[86] gives values deduced from experimentally determined values of s for the heat loss from a tungsten wire in hydrogen ($a = 0.00353$), at 20° C. The last column gives values of B calculated from those of b by

P_{mm}	s	b	B
750	1.25	0.54 cm	1.35 cm
200	0.88	9.0	32.1
100	0.72	45.0	196.3
50	0.56	530.0	

means of equation 4. It is evident that, for pressures below atmospheric, B becomes greater than the distance from wire to wall. "This means," as Langmuir states,[87] "that the heat loss from the filament is actually less than if there were no convection currents and the laws of heat conduction could be applied." The decrease in value of s at the lower pressures is actually due, as Langmuir points out, "to a temperature discontinuity at the surface of the wire, which becomes appreciable at pressures even as high as 200 mm, and increases with decrease in pressure."

The problem of heat conduction at low pressures from a wire of radius a, suspended coaxially in a glass tube of radius r, where r is very much greater than a, has been discussed from the point of view of Langmuir's film theory by H. A. Jones.[88]

Following the relations developed by M. v. Smoluchowski, which have been discussed above, Jones substitutes for equation 5a, in the case of low pressures, a relation of the form

$$W = \frac{4.186 \cdot 2\pi(\phi_2 - \phi_1)}{\ln(b/a) + y(1/a + 1/b)}, \qquad (9a)$$

where W = watts lost by conduction per unit length of wire, b = radius of the outside edge of the film, and y varies as L. Since b is very large compared to a, the last equation may be replaced by

$$W = \frac{4.186 \cdot 2\pi(\phi_2 - \phi_1)}{\ln(b/a) + y/a}. \qquad (9b)$$

Jones has applied this equation to calculate the heat loss from iron wires in hydrogen at 100 mm of Hg, and at the two temperatures, 840° K and 1045° K, respectively, between which ballasting action is obtained.

---

[86] *J. Am. Chem. Soc.*, **37**, 419 (1915).

[87] A further application of Langmuir's film theory to account for the effect of gas pressure on rate of evaporation is discussed in Added Note 6, at the end of section 14.

[88] *Gen. Elec. Rev.*, **28**, 650 (1925).

(This is the temperature range in which the current is maintained practically constant when the lamp is used in series with a load on a variable voltage source.)

The value of b has been deduced by Jones by means of equation 4 from the following semi-empirical relation for B, deduced by C. W. Rice[89] for hydrogen:

$$B = \frac{0.5442a^{0.19}}{{P_{mm}}^{0.54}} \left\{ \frac{(T + T_0)^{5/2}}{154 + T + T_0\sqrt{T - T_0}} \right\}^{0.54} \text{ cm} \qquad (10)$$

where T = temperature of the wire in deg K,

T_0 = temperature of the wall in deg K.

The values of B and b thus calculated for different values of a are given in the respective columns in Table 16.

According to Smoluchowski's views, y is proportional to the mean free path L, and Jones derives the values given in the last row of the table. According to the data in Table 16, $L = 9.32 \cdot 10^{-5}$ cm, for H_2 at 25° C and 100 mm. It follows from equations 8.17 and 8.15 that, for any other temperature, T,

$$\frac{L_T}{L_{298}} = \frac{T}{298.2}\left(\frac{1 + 84.4/298.2}{1 + 84.4/T}\right).$$

TABLE 16

FILM THICKNESS, ENERGY LOSS, AND RELATED DATA FOR IRON FILAMENTS IN HYDROGEN AT 100 MM HG AND AT TWO TEMPERATURES

$T = 840$						$T = 1045$				
a	B	$\ln b/a$	b	y/a	W	B	$\ln b/a$	b	y/a	W
0.00127	2.66	5.86	0.454	0.939	1.359	2.57	5.85	0.439	0.988	2.1
.0127	2.88	4.025	0.715	.0939	2.248	2.76	4.0	0.690	.0988	3.5
.0635	2.82	2.772	1.017	.0188	3.31	2.70	2.74	0.985	.0198	5.19
.127	2.75	2.265	1.213	.0094	4.065	2.65	2.25	1.177	.0099	6.35
$L_T = 3.06 \cdot 10^{-4}$, $y = 11.92 \cdot 10^{-4}$ cm						$L_T = 3.88 \cdot 10^{-4}$, $y = 12.55 \cdot 10^{-4}$ cm				

The values of L_T thus deduced are also given in the last line in Table 16. Thus, at 840° K, $y = 3.89L_T$, and at 1045° K, $y = 3.23L_T$.

Finally, the values of the function $4.186(\phi_2 - \phi_1)$ used in equation 9b, as deduced from equation 3a, are: 1.468 watts $\cdot$ cm^{-2} and

---

[89] *Trans. A.I.E.E.*, June, 1923, also February, 1924.

2.294 watts · cm^{-2} for $T = 840$ and $T = 1045$ respectively, and $T_0 = 293$.

The values under W give the *watts lost, by conduction, per unit length of wire.*

12. THERMAL TRANSPIRATION (THERMOMOLECULAR FLOW)

From equation 5.3,

$$G = m\nu = \frac{1}{4}\rho v_a = \rho\sqrt{\frac{R_0T}{2\pi M}},$$

it follows that the rate of efflux of a given gas through a small opening varies as $\rho\sqrt{T}$. If we have two chambers A and B, separated by a porous plug, at two different temperatures, T_A and T_B, transpiration will occur until an equilibrium state is established at which

$$\rho_A\sqrt{T_A} = \rho_B\sqrt{T_B} \tag{1}$$

and, since

$$\rho = \frac{MP_{\mu b}}{R_0T},$$

$$\frac{P_A}{P_B} = \sqrt{\frac{T_A}{T_B}}. \tag{2}$$

This is of importance in observations at low pressures. For instance, if the chamber A is a part of a system at liquid-air temperature ($T_A = 90$) and the pressure is measured by means of a gauge at room temperature ($T_B = 300$), then the real value of P_A is given by the relation

$$P_A = P_B\sqrt{\frac{90}{300}} = 0.55P_B.$$

Equation 1 or 2 is valid for two vessels *connected by small-bore tubing* provided that $2a$, the diameter, is small compared to L, the mean free path. When, however, L is very much smaller than $2a$, so that collisions between molecules become predominant over collisions against the walls, then the condition of equilibrium is $P_A = P_B$, in consequence of which

$$\frac{\rho_A}{\rho_B} = \frac{T_B}{T_A}. \tag{3}$$

There exists therefore a range of pressures in which the pressure relation changes from that given by equation 3 to that given by equation 2. The smaller the diameter of the connecting tube, the higher the pressure at which equation 2 is valid.

The theory of the phenomenon was first discussed by Maxwell (1879) and, subsequently, by M. Knudsen,[90] who derived equations for the pressure gradient along the connecting tube as a function of the tube diameter and pressure in the hot chamber. For low pressures such that L is of the same order of magnitude as a, he derived the relation

$$\frac{dP}{dT} = \frac{3}{8} \frac{k_2}{(1 + 2a/L)} \cdot \frac{P}{T}, \tag{4}$$

where k_2 is a coefficient which varies slightly with the value of $2a/L$ and tends to the value $\frac{4}{3}$ for L very large compared to a. It follows that, for $a/L = 0$, the last equation becomes identical with equation 2.[91]

F. C. Tompkins and D. W. Wheeler,[92] who investigated the problem experimentally, give the following summary of Knudsen's interpretation:

> Knudsen has shown that the phenomenon can be adequately explained by two opposing flows in the gas mass—an axial one, from the hotter to the colder region, and a surface flow along the walls in the reverse direction. At equilibrium these are equal in magnitude. He assumes that any plane surface consists of tooth-like projections of molecular dimensions, so that any molecule striking the walls is repelled in a direction which is totally independent of the angle of incidence and, after reflection, obeys the Lambert Cosine Rule for the reflection of light from a glowing body. In consequence, any unit of surface will receive a larger momentum from the collision of molecules coming from the warmer side, and therefore a tangential force along the walls is set up, tending to drive the molecules near the surface from the colder to the hotter parts. The axial flow is the ordinary passage of gas from a region of higher temperature to that of a lower one.
>
> This "double streaming" must exist at all pressures, but can only be of importance at low pressures, where Poiseuille's Law[93] is no longer valid. At higher pressures, the flows will be limited by the frequency of collisions in the gas phase and therefore the thickness of the surface layer can never be greater than that of the order of the mean free path of molecules. Consequently, as the pressure is increased the axial current becomes the main factor and then Gay-Lussac's Law will operate and there will be equality of pressure throughout the apparatus.
>
> The intermediate transition region between the two limiting cases is one of great difficulty from a theoretical point of view. Here, molecules come from points far enough away from the walls to have speeds which bear no relation to the temperature of the surface at the point of impact, and therefore the isothermal surface in the gas will not be perpendicular to the length of the tube and will become more oblique as the pressure is increased.

---

[90] *Ann. Physik*, **31**, 205, 633 (1910).

[91] It should be observed that, in deriving values of L from those of η, Knudsen used equation 8.5. This, however, does not affect the conclusion that dP/dT increases with decrease in the value of $2a/L$.

[92] *Trans. Faraday Soc.*, **29**, 1248 (1933).

[93] See discussion of this topic in Chapter 2, section 1.

For this reason Knudsen introduced the coefficient k_2, mentioned in equation 4.[94]

In their experiments Tompkins and Wheeler measured the ratio of pressure, $r = P_A/P_B$, in two vessels A and B connected by glass tubing 1 cm in diameter, for $T_B = 298°$ and $T_A = 90°$ and 193° respectively. Hydrogen was used, since it is not adsorbed to any noticeable extent by glass surfaces at these temperatures. The values observed for r at these two temperatures for a series of pressures in microns, in chamber B, are given in Table 17.

TABLE 17

VALUES OF $r = P_A/P_B$ FOR THERMAL TRANSPIRATION

$P_{\mu B}$	$T_A = 90°$	$T_A = 193°$
0	0.550 (calc.)	0.805 (calc.)
10	0.716	0.854
20	0.817	0.907
40	0.929	0.951
60	0.985	0.977
80	1.019	0.988
100	1.033	0.996
120	1.034	1.001
140	1.034	1.004

The values of r greater than unity represent, of course, experimental errors. It should be pointed out that, for $P_{\mu B} = 10$ of hydrogen and $2a = 1$, $2a/L = 1/0.931 = 1.074$.

Similar results have been obtained by J. Smittenburg[95] in his determinations of the sorption of hydrogen by nickel wire, over the range 90° K to 873° K.

These observations indicate that equation 2 yields too low a value of P_A unless $2a/L$ is of the order of magnitude of, or less than, 0.1.

13. THERMAL DIFFUSION

The thermal-diffusion effect has been described by T. L. Ibbs[96] as follows:

> If a temperature gradient is applied to a mixture of two gases of uniform concentration there is a tendency for the heavier and large molecules (mass m_1, diameter δ_1)

---

[94] A detailed discussion of Knudsen's theory is given in *Vacuum Practice*, by Louis Dunoyer, translated by J. H. Smith, D. Van Nostrand Company, New York, 1926 (designated LD).

[95] *Rec. trav. chim.*, **53**, 1065 (1934).

[96] *Physica*, **4**, 1135 (1937). This is a non-mathematical discussion of the subject, which gives a list of references to previous papers.

to move to the cold side, and for the lighter and smaller molecules (mass m_2, and diameter δ_2) to move to the hot side. The separating effect of thermal diffusion (coefficient D_T) is ultimately balanced by the mixing effect of ordinary diffusion (coefficient D_{12}) so that finally a steady state is reached and a concentration gradient is associated with the temperature gradient. The amount of thermal separation thus produced by a given difference in temperature depends upon the ratios m_1/m_2 and δ_1/δ_2, and upon the proportion by volume of the heavier gas f_1 and of the lighter gas f_2 (where $f_1 + f_2 = 1$) and also upon the nature of the field of force operating between the unlike molecules.

The effect was predicted by D. Enskog (1917) and, independently, by S. Chapman and F. W. Dootson.[97]

Following the earlier experimental investigations of T. L. Ibbs and others, K. Clusius and G. Dickel[98] devised a continuous method for separating mixtures of gases and isotopes which has been applied extensively by subsequent investigators.

In this section the discussion will be limited largely to the experimental data, since the mathematical theory is quite complex and beyond the scope of the objectives of this chapter.

The *coefficient of thermal separation* is defined by the relation

$$k_T = \frac{D_T}{D_{12}}, \tag{1}$$

where D_T and D_{12} have been defined above. Now

$$k_T = \frac{-df_1}{d \ln T} = \frac{df_2}{d \ln T}. \tag{2}$$

If k_T is a constant, then we obtain from equation 2 the relation

$$\Delta f = k_T \ln \frac{T_1}{T_2} \tag{3}$$

$$= \text{amount of separation,}$$

where T_1 and T_2 denote the hot and cold temperatures, respectively.

Figures 7 and 8 illustrate results obtained by Ibbs[99] with mixtures of H_2 and N_2. The concentrations of H_2 in the different mixtures varied from 4.7 per cent for No. 2 to 50.5 per cent for No. 7. It will be observed that these observations are in accord with equation 3 since Δf is found to be a linear function of log (T_1/T_2). Figure 8 shows the variation in value of Δf with composition for a constant value of the ratio T_1/T_2.

---

[97] *Phil. Mag.*, **33**, 248 (1917). See also JHJ, p. 251. A mathematical treatment of the subject is given by Chapman and Cowling in their treatise (CC, pp. 253–258), also by W. H. Furry, R. Clark Jones, and L. Onsager, *Phys. Rev.*, **55**, 1083 (1939), and R. C. Jones and W. H. Furry, *Rev. Modern Phys.*, **18**, 151 (1946). A "simple theory" has been published by L. J. Gillespie, *J. Chem. Phys.*, **7**, 530 (1939), and a much more elaborate mathematical discussion has been published by S. Chapman, *Proc. Roy. Soc. London*, **A**, **177**, 38 (1940–1941).

[98] *Naturwissenschaften*, **26**, 546 (1938); **27**, 148 (1939).

[99] *Proc. Roy. Soc. London*, **A**, **107**, 470 (1925).

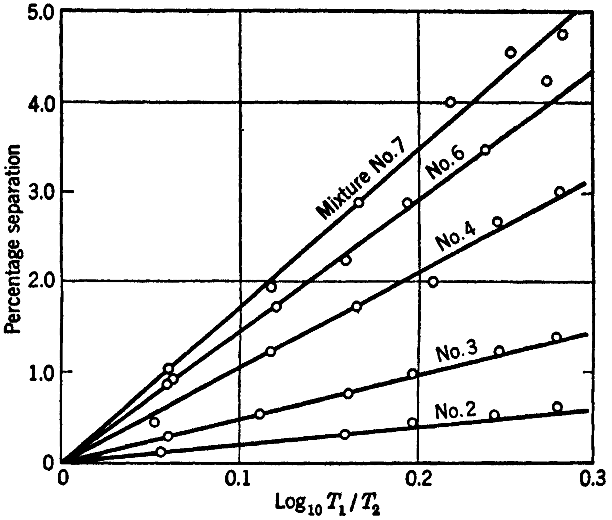

FIG. 7. Relation between degree of separation by thermal diffusion and log (T_1/T_2) for mixtures of H_2 and N_2.

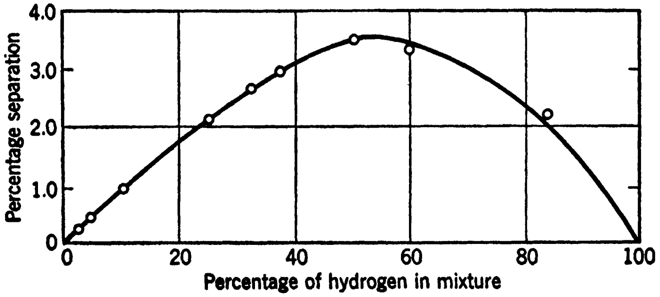

FIG. 8. Relation between composition of H_2-N_2 mixtures and degree of separation for log $(T_1/T_2) = 0.2$.

Chapman has shown that k_T can be expressed in the form[100]

$$k_T = \frac{Af_1 + Bf_2}{1 + Cf_1/f_2 + Df_2/f_1}, \tag{4}$$

---

[100] See L. J. Gillespie, *J. Chem. Phys.*, **7**, 530 (1939), for discussion of the derivation of this equation.

where the coefficients A to D are functions of the molecular weights and of the ratio δ_1/δ_2. These can be calculated from the force constants s_{12} in the relation $F = cr^{-s_{12}}$, which expresses the force of repulsion between a pair of unlike molecules as a function of $r = \frac{1}{2}(\delta_1 + \delta_2)$.

The separation in a mixture of H_2 and CO_2 was investigated by Ibbs and A. C. R. Wakeman[101] over a range of 600° C. For any given mixture it was observed that the amount of separation was in accordance with equation 3. For a constant difference in temperature, Δf increased from 0 for pure H_2 to a maximum value, $\Delta f = 0.0365$ (for $\Delta T = 600°$), for a mixture containing 61 per cent H_2.

According to Chapman, k_T in this case should be given by a relation of the form

$$k_T = \frac{5}{2}\left\{\frac{0.216f_1 + 0.139f_2}{1.275 + 1.409f_1/f_2 + 0.232f_2/f_1}\right\}, \qquad (i)$$

where f_1 refers to CO_2, and f_2 to H_2. Since this relation is deduced on the assumption that the molecules behave as rigid elastic spheres with a force relation in which s has a definite value for the interaction between the two types of molecules, it was expected that the observed values of k_T would differ from those calculated. The following table gives the results of a series of measurements. The last column gives values of a constant defined by the relation

$$R_T = \frac{k_T \text{ observed}}{k_T \text{ calc. for rigid elastic spheres}}. \qquad (5)$$

f_1	Temperature Range	k_T (calc.)	k_T (obs.)	R_T
0.469	Below 144° C	0.1575	0.0665	0.422
	Above 144° C	.1575	.0939	.596
	At 470° C	.1575	.1045	.663
0.34	Below 145° C	.1685	.0695	.415
	Above 145° C	.1685	.0929	.552

For CO_2-N_2 mixture, Chapman's expression for k_T is of the form

$$k_T = \frac{5}{2}\left\{\frac{0.163f_1 + 0.167f_2}{3.38 + 2.154f_1/f_2 + 1.480f_2/f_1}\right\}, \qquad (ii)$$

where f_1 again refers to the *heavier* gas. (In all the following equations f_1 has the same significance.)

For $f_1 = 0.494$, the value of k_T calculated $= 0.0564$, whereas the value of R_T observed varied from 0.247 for temperatures below 144° C to 0.441 for temperatures above 144° C.

---

[101] *Proc. Roy. Soc. London*, **A**, **134**, 613 (1932).

For the mixtures A-He, Ne-H_2, and N_2-He, relations similar to (*i*) and (*ii*) for k_T have been published by Ibbs and K. E. Grew.[102] All the observed values of R_T showed a decrease with decrease in temperature down to −190° C.

According to Chapman and Cowling,

$$R_T = \frac{13}{10}\left(\frac{s_{12} - 5}{s_{12} - 1}\right). \tag{6}$$

Hence observations on the values of R_T should yield values of s_{12}. In fact the observations on *thermal diffusion* of gases should reveal interesting information on the forces between molecules. Table 18 gives values of the repulsive force constant s_{12} as determined from observed values of R_T, and, for comparison, values of s_1 and s_2 for the individual gases, as determined from other phenomena.

TABLE 18

VALUES OF "FORCE" CONSTANTS FOR INTERACTION OF MOLECULES

Gases	R_T	s_{12}	s_1	s_2
O_2-H_2	0.48	7.3	7.6	11.3
N_2-A	0.47	7.2	8.8	7.35
H_2-N_2	0.58	8.2	11.3	8.8
He-A	0.65	9.0	14.6	7.35
H_2-Ne	0.74	11.4	11.3	14.5
H_2-CO_2	0.47	7.2	11.3	5.6
Ne-A	0.54	7.9	14.5	7.35
He-Ne	0.80	11.4	14.6	14.5

In 1938, as mentioned previously, Clusius and Dickel[103] devised an arrangement of hot and cold surfaces that could be utilized practically for the separation of mixtures of different gases and of isotopes. They used a long vertical tube with a hot wire along the axis. Because of thermal diffusion, the relative concentration of the heavier molecules is greater at the cold wall. Convection causes the gas at the hot surface to rise to the top, where it is deflected to the cold wall. There the gas sinks to the bottom and the cycle is then repeated. As a result, the *heavier component concentrates at the bottom*, and the lighter at the top.

For instance, in a chamber 1 meter in height, for a temperature difference of 600° C, it was possible to separate a mixture containing 40 per cent (by volume) CO_2 and 60 per cent H_2, with a yield of practically 100 per cent CO_2 at the bottom and 100 per cent H_2 at the top.

---

[102] *Proc. Phys. Soc. London*, **43**, 142 (1931).

[103] *Loc. cit.*

In a chamber 2.9 meters in height, for a temperature difference of 600° C, air (21 per cent O_2, 78 per cent N_2) could be separated, yielding 85 per cent O_2 at the bottom. Finally, from a mixture of 23 per cent HCl^{37} and 77 per cent HCl^{35}, a mixture containing 40 per cent of the heavier isotope was obtained at the bottom of the diffusion chamber.

A. Keith Brewer and A. Bramley[104] used a heated inner tube 1 cm in diameter, and an outer cooled concentric tube 2 cm in diameter, each 1 meter long. With a 350° C difference in temperature, He and Br_2 could be separated, so that after 15 minutes no Br_2 could be detected at the top. Under similar conditions a 50-50 mixture of CH_4 and NH_3 was enriched 25 per cent in NH_3 at the bottom. They deduced the following relation: "If l denotes the cylinder length, r the radius of the outer tube, and d the difference in radii, then, to a first approximation, the rate of separation varies as rd and the purity as l/d."

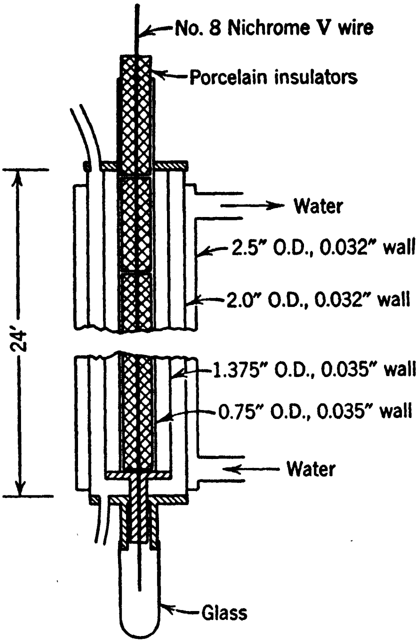

FIG. 9. Cross-sectional view of column used for thermal diffusion experiments by Nier. The column is used as a return lead for the current flowing through the Nichrome wire.

Figure 9 shows a thermal diffusion column developed by A. O. Nier[105] for the concentration of $C^{13}H_4$. A Nichrome wire is inserted along the axis of a steel tube ¾ in. in outside diameter, which is concentric with a steel tube 1¾ in. in outside diameter having a wall thickness of 0.035 in. This tube constitutes the inner wall of the annular space containing the gas, and the outer wall consists of a 2-in. outside diameter brass tube, which is water cooled as shown in the figure. The column was 24 ft in length. At the lower end, the two steel tubes were brazed concentrically to a circular steel plate. The average temperature of the outer wall was 27° C, and that of the inner approximately 375° C. The samples of methane taken at the bottom and top were analyzed by means of a mass spectrometer for the ratio of $C^{13}H_4$ to $C^{12}H_4$. At a pressure of 656 mm, and after operating for 23.5 hours, the values of this ratio at the bottom and top were 0.0215 and 0.0054 respectively, so that the ratio of $C^{13}H_4$ at the bottom to that at the top was 3.99.

---

[104] *Phys. Rev.*, **55**, 590 (1939).

[105] *Phys. Rev.*, **57**, 30 (1940).

The results obtained were found to be in agreement with conclusions deduced from theoretical considerations by W. Furry, R. Jones, and L. Onsager.[106] They derived the relation

$$\frac{C_1{}^L}{C_1{}^U} = \epsilon^x, \tag{7}$$

where

$$x = \frac{a/p^2}{1 + b/p^4}, \tag{8}$$

$C_1{}^L$ and $C_1{}^U$ represent equilibrium concentrations of $C^{13}H_4$ in the lower and upper ends of the column, respectively, a and b are constants for the gas used and the dimensions of the column, and p denotes the pressure. Thus ϵ^x corresponds to the separation factor. In the investigation under consideration, this factor was observed to pass through a maximum at $p = 0.6$ atmosphere, approximately.

The separation of $C^{13}H_4$ and $C^{12}H_4$ has also been investigated, in a column 40 ft in length, by T. I. Taylor and G. Glockler,[107] who found that the separation factor could be represented, in agreement with the theory, by the above equations.

The rate at which equilibrium is approached in such a column has been discussed by J. Bardeen,[108] and the conclusions reached have been found to be in good agreement with experimental results obtained by Nier.

Although the above discussion has dealt largely with the separation of gases which differ in value of M, it follows from the theory of thermal diffusion that it should be possible by this method to effect a certain degree of separation in a mixture of gases which have the same value of M but differ with respect to the magnitude of the molecular diameter. Results in agreement with this prediction have been obtained by F. T. Wall and C. E. Holley, Jr.[109]

[106] *Phys. Rev.*, **55**, 1083 (1939).

[107] *J. Chem. Phys.*, **8**, 843 (1940).

[108] *Phys. Rev.*, **57**, 35 (1940).

[109] *J. Chem. Phys.*, **8**, 949 (1940).

14. THEORY OF DIFFUSION OF GASES[110]

As in the case of viscosity and heat conduction, approximate kinetic theory considerations lead to the conclusion that the *coefficient of self-diffusion, D,* is given by a relation of the form

$$D = \tfrac{1}{3}v_a L, \tag{1}$$

which indicates that, at constant temperature, D varies directly as the mean free path or inversely as the pressure.

Combining equation 1 with the relation

$$\eta = \tfrac{1}{3}\rho v_a L,$$

it follows that

$$D = \frac{\eta}{\rho}.$$

Introducing the correction for persistence of velocities and that for Maxwellian distribution of velocities, it is found that the more accurate relation is

$$D = 1.342\frac{\eta}{\rho}. \tag{2}$$

According to Chapman and Enskog,[111] the coefficient in equation 2 should have a value lying between 1.200 for hard spheres and 1.543 for inverse-fifth-power repulsion. Actually observed values of D yield the following values of the coefficient:[112]

CO, 1.30; H_2, 1.37; O_2, 1.40; CO_2, 1.58.

For the derivation of a relation for the coefficient of interdiffusion, D_{12} (corresponding to the fact that molecules 1 and 2 are involved), we shall follow the Stefan-Maxwell derivation,[113] which, as will be evident, is based on the same considerations as those used in deriving equation 1 above.

The relation for the mean free path, L_1, in a mixture of two gases, designated 1 and 2, according to 8.30, is

---

[110] In addition to the treatises on kinetic theory of gases previously mentioned, there is a very comprehensive treatment of the topic by K. F. Herzfeld and H. M. Smallwood in Taylor's *Treatise on Physical Chemistry,* 2nd edition, Vol. I, p. 209, D. Van Nostrand Company, New York, 1931.

[111] EHK, pp. 195–196.

[112] JHJ, p. 216.

[113] JHJ, pp. 207–210.

$$\frac{1}{L_1} = \sqrt{2} \cdot \pi n_1 \delta_1^2 + \pi n_2 \delta_{12}^2 \sqrt{1 + \frac{m_1}{m_2}} \cdot$$

However, as Stefan and Maxwell have pointed out, the collisions between like molecules do not influence diffusion, and hence for this case the mean free paths are given by the relations

$$\frac{1}{L_1} = \pi n_2 \delta_{12}^2 \sqrt{1 + \frac{m_1}{m_2}} \tag{3}$$

and

$$\frac{1}{L_2} = \pi n_1 \delta_{12}^2 \sqrt{1 + \frac{m_2}{m_1}} \cdot \tag{4}$$

On this basis it is found that the relation for the coefficient of interdiffusion is

$$D_{12} = \frac{\sqrt{v_1^2 + v_2^2}}{3\pi n \delta_{12}^2}, \tag{5}$$

where v_1 and v_2 refer to the value of v_a, and $n = n_1 + n_2$.

It is evident that for like molecules this relation becomes

$$D_{11} = \frac{2}{3} \frac{v_a}{\sqrt{2}\pi n \delta^2} \cdot \tag{6}$$

Combining this with the relation

$$\eta = \frac{0.499 \rho v_a}{\sqrt{2} \cdot \pi n \delta^2},$$

the result is

$$D_{11} = 1.336 \frac{\eta}{\rho}, \tag{7}$$

which is in substantial agreement with equation 2.

Table 19[114] gives the values of D_{12} ($\mathrm{cm}^2 \cdot \mathrm{sec}^{-1}$) observed for several pairs of gases, at 0° C and 1 atmosphere, also values of δ_{12} calculated from the values of D_{12} by means of equation 5, and, for comparison, values of δ_{12} calculated from viscosity measurements (see Table 6) for each of the two gases.

In the case of the first six pairs which are constituted of "hard" molecules (with a value for the repulsive force constant greater than 7.4) the agreement is very satisfactory. Even in the case of "softer"

---

[114] JHJ, pp. 217–218.

TABLE 19

COEFFICIENTS OF INTERDIFFUSION AND AVERAGE MOLECULAR DIAMETERS

Gases	D_{12} (obs.)	$10^8\delta_{12}$ calc. from D_{12}	$10^8\delta_{12}$ calc. from η
H_2-air	0.661	3.23	3.23
H_2-O_2	.679	3.18	3.17
O_2-air	.1775	3.69	3.68
O_2-N_2	.174	3.74	3.70
CO-H_2	.642	3.28	3.25
CO-O_2	.183	3.65	3.70
CO_2-H_2	0.538	3.56	3.69
CO_2-air	.138	4.03	4.20
CO_2-CO	.136	4.09	4.22
N_2O-H_2	.535	3.57	3.69
N_2O-CO_2	.0983	4.53	4.66

molecules the agreement is fair, as shown by the values for the second set of five pairs.

W. E. Summerhays[115] has used the katharometer (see section 9) to measure the diffusion coefficient of water vapor in air. The value observed was $D = 0.282\ \text{cm}^2 \cdot \text{sec}^{-1}$ at 16.1° C.

As will be noted, equation 5 indicates that the interdiffusion coefficient should be independent of composition. However, a series of experiments carried out at Halle[116] to test this conclusion show that there is a variation of not over a few per cent with variation in the ratio n_1/n_2.

Mention should be made in this connection of a relation for the coefficient of interdiffusion, given by Loeb,[117] which is of the form

$$D_{12} = \beta\left(\frac{n_1}{n}\cdot\frac{\eta_2}{\rho_2} + \frac{n_2}{n}\cdot\frac{\eta_1}{\rho_1}\right), \tag{8}$$

in which β is a numerical factor, the value of which is between 1.00 and 1.50, and $n = n_1 + n_2$.

From the equations for D it follows that to a first approximation D should vary as $T^{3/2}$ and as P^{-1}. Since, however, η varies with T in accordance with Sutherland's relation, equation 8.15, it is to be expected that the exponent of T would exceed $3/2$. Lonius[118] gives the following relation for D as a function of T:

---

[115] *Proc. Phys. Soc. London*, **42**, 218 (1930).

[116] The results are summarized by A. Lonius, *Ann. Physik*, **29**, 664 (1909). See also JHJ, p. 213; LBL, pp. 273–274; and EHK, p. 197.

[117] LBL, p. 272.

[118] *Loc. cit.*

$$D_T = D\left(\frac{T}{288.2}\right)^x \frac{760}{P_{mm}}, \tag{9}$$

where D_T = value at $T°$ K and P_{mm}.

D = value at 15° C and 760 mm.

The values of x used by Lonius are as follows:

H_2-O_2	1.754
N_2-O_2	1.795
H_2-CO_2	1.74
H_2-N_2	1.707
He-A	1.75

ADDED NOTE 5. MAXWELL-LOSCHMIDT METHOD FOR DETERMINATION OF DIFFUSION COEFFICIENTS

In view of the fact that in vacuum technique the problem arises occasionally regarding the time required for gases to mix, it is of interest to review briefly one method which has been used for the determination of D for gases.

A tube of length l is divided by means of a wide-bore stopcock into two parts of equal length. This is mounted in a vertical position; the *heavier* gas (A) is put in the *lower* part, and the lighter gas (B) is put in the *upper* part. At time $t = 0$ the stopcock is opened and diffusion is allowed to occur for a definite period, t. The stopcock is then closed and the proportions of A and B are measured in each compartment.

Let U = amount of A expressed as the fraction of the total number of moles in the *lower* compartment,

Q = amount of A in *upper* compartment, expressed similarly.

Then, on the basis of the equations for diffusion,

$$U - Q = \frac{8}{\pi^2}\left\{\epsilon^{-x} + \frac{1}{9}\epsilon^{-9x} + \frac{1}{25}\epsilon^{-25x} + \cdots\right\}, \tag{10}$$

where

$$x = \frac{\pi^2}{l^2}Dt. \tag{11}$$

For instance, in the case of H_2-O_2 mixture, for l = 99.93 cm and

$t = 1800$ sec, $U = 0.5982$, $Q = 0.4018$, at 14.8° C and 749.3 mm. Hence, at 15° C and 760 mm, $D = 0.788$.[119]

Table 20 gives values of $U - Q$ for two different values of l as a function of Dt, also values of t, for $l = 100$ cm, assuming $D = 0.2$ cm$^2 \cdot$ sec^{-1}.

TABLE 20

ILLUSTRATING THE APPLICATION OF EQUATION 10

Dt	$l = 100$ cm $U - Q$	$l = 25$ cm $U - Q$	t in minutes for $D = 0.2$
100	0.9550	0.2063	8.33
200	.8401	.0425	16.67
300	.7514	.0088	25.00
400	.6771		33.34
500	.6118		41.67
700	.5014		58.67
1000	.3728		83.83
1500	.2276		125.00
2000	.1390		166.67
3000	.0518		250.00
5000	.0071		416.67

For $l = 100$, only the first term in the series on the right-hand side of equation 10 is of importance for values of $Dt > 500$. For $l = 25$, only the first term is of importance for $Dt \geqslant 100$.

Equation 11 shows that for values of l and Dt for which the first term only is sufficiently accurate t varies as l^2 for constant value of $(U - Q)$.

ADDED NOTE 6. EFFECT OF PRESSURE OF GAS ON RATES OF EVAPORATION OF METALS

In section 6, equations were derived for rates of evaporation in a *vacuum*. These equations have been applied, as illustrated in the above connection, to the calculation of vapor pressures of high-melting-point metals from observations on rate of loss in weight as a function of the temperature. However, in the presence of a gas which does not react chemically with the metal, the observed rate of evaporation is lower; as is well known, this fact was utilized by Langmuir in the invention and development of the gas-filled tungsten-filament lamp.

This phenomenon has been explained by Langmuir by assuming the existence of a film adjacent to the evaporating surface through which the atoms evaporated from the surface diffuse. Thus this theory is quite similar to that suggested by Langmuir, and discussed in section 11 above, for the effect of varying the diameter on heat conduction from a wire.

---

[119] The values of k, the diffusion constant, given by Lonius are expressed in terms of (meters)^2/hour. Therefore these should be multiplied by $1/0.36 = 2.78$ to convert them to cm^2/sec.

G. R. Fonda[120] has shown that this theory accounts very satisfactorily for his observations on the rate of evaporation of tungsten in the presence of argon at various pressures, and the following remarks on the mechanism of evaporation under these conditions are quoted from his paper.

> The filament is considered to be surrounded by tungsten vapor at the same pressure as would be present in a vacuum. The atoms of this vapor, however, instead of being projected directly from the filament, as in a vacuum, are pictured as diffusing through the stationary film of gas. Once an atom reaches the outer boundary of the film, it would be carried away in the convection current of gas and would be lost to the filament; but the path within the film is so irregular that an atom may in fact return to the filament and be deposited on it, thus leading to a reduced evaporation as compared with that in a vacuum.

Let dc/dr denote the concentration gradient at the surface of the wire, where r is the distance from the axis, and let D denote the diffusion constant. Assuming uniform distribution over the surface of the wire, the rate of diffusion *per unit length* of the wire is

$$q = 2\pi r D \frac{dc}{dr}, \tag{12}$$

where D is given by equation 5.

Since the value of n for tungsten atoms is negligible compared with that of n for argon gas, the expression for D becomes identical with equation 1, where L and v_a refer to the values of the mean free path and average velocity respectively of the tungsten atoms at the temperature of the filament. Thus D varies inversely as the pressure, P, of argon, and equation 12 becomes

$$q = \frac{Ar}{P} \frac{dc}{dr}, \tag{13}$$

where A is a proportionality constant.

For a wire of diameter $2a$ and gas film of diameter $2b$, it follows, from the same considerations as those that lead to equation 11.4 for the heat loss, that

$$\int_b^a \frac{dr}{r} = \ln \frac{b}{a}. \tag{14}$$

---

[120] *Phys. Rev.*, **31**, 260 (1928).

Let m denote the rate of evaporation in $\text{gm} \cdot \text{cm}^{-2} \cdot \text{sec}^{-1}$. Then it follows from the last two equations that

$$maP \log \frac{b}{a} = \int dc = c_a - c_b = \text{constant}, \tag{15}$$

where c_a and c_b are the concentrations of the tungsten atoms at $r = a$ and $r = b$, respectively.

Table 21 shows results obtained by Fonda for the rate of evaporation from a filament in a mixture of argon and nitrogen such as used in gas-filled lamps.

TABLE 21

RATE OF EVAPORATION (m) OF TUNGSTEN IN 86 PER CENT ARGON, 14 PER CENT NITROGEN AT 2870° K. DIAMETER OF FILAMENT $(2a) = 0.00978$ CM

P_{cm}	$10^9 m$	b (cm)	$10^9 maP_{cm} \log (b/a)$	$10^9 m/b$
0	230	—	—	—
1	57.5	9.68	3.9	—
5	23.5	2.42	6.3	—
10	20.5	1.31	9.8	15.6
25	10.3	0.63	10.4	16.2
50	5.4	0.36	9.6	14.8
70	4.2	0.28	9.6	14.8
165	2.0	0.15	8.8	13.5

The value $m = 230 \cdot 10^{-9}\ \text{g} \cdot \text{cm}^{-2} \cdot \text{sec}^{-1}$ observed for $P = 0$ is in agreement with the value $250 \cdot 10^{-9}$ observed by Langmuir, Jones, and Mackay.[121]

As Fonda states,

> the expression $maP_{cm} \log (b/a)$ is sufficiently constant at pressures above 10 cm to allow of credence being given the hypothesis developed above.
>
> The constancy of the expression has a further significance, for, as is evident from its derivation, it denotes a constant difference between the vapor pressure of tungsten at the surface of the filament and at the surface of the film of gas. For constant filament temperature this implies that the concentration of tungsten vapor at the surface of the stationary film of gas should be constant for all pressures above 10 cm. It is this vapor which constitutes that which effectively evaporates from the filament, for the rising convection currents of gas carry it off to be deposited on the bulb. The rate of evaporation at different pressures should be determined therefore by the area of the assumed film of gas if the concentration of vapor at its border is in fact a constant.

The constancy of the ratio m/b is therefore a further confirmation of the validity of the theory. Other evidence, based on the appearance of the surface of the filament, has also been shown by Fonda to be in agreement with the views expressed above.

---

[121] *Phys. Rev.*, **30**, 211 (1927).

From equation 15 it also follows that at constant pressure and for filaments of different diameters the expression $ma \log (b/a)$ should be constant. The validity of this conclusion was confirmed by Fonda in a series of observations made with both pure nitrogen and a mixture of nitrogen and argon.[122] In these cases the value actually used for B (the thickness of the film for a plane surface in gas at atmospheric pressure) was the same as that obtained from data on heat conduction in nitrogen. (See section 11.)

15. RANDOM MOTIONS AND FLUCTUATIONS[123]

Let us consider the case in which a group of N molecules start from the plane $z = 0$, at the instant $t = 0$, and diffuse through the gas. The differential equation for the diffusion is

$$\frac{dn}{dt} = D\frac{d^2n}{dz^2}. \tag{1}$$

At any instant, t, the distribution of these molecules along the z axis is given by the relation

$$dn = \frac{N}{2\sqrt{\pi D t}} \cdot \epsilon^{-z^2/4Dt}\, dz, \tag{2}$$

which satisfies the condition

$$N = \frac{N}{\sqrt{\pi}} \int_{-\infty}^{\infty} \frac{1}{2\sqrt{Dt}}\, \epsilon^{-z^2/4Dt}\, dz.$$

Hence, the average value of z is

$$z_a = \frac{1}{\sqrt{\pi}} \int_{-\infty}^{\infty} \frac{z}{2\sqrt{Dt}}\, \epsilon^{-z^2/4Dt}\, dz$$

$$= 2\sqrt{\frac{Dt}{\pi}}. \tag{3}$$

And similarly it can be shown that the root-mean-square value is given by the relation

$$z_r = \sqrt{\frac{\pi}{2}} \cdot z_a = \sqrt{2Dt}. \tag{4}$$

---

[122] *Phys. Rev.*, **21**, 343 (1923).

[123] See EHK, Chapter VII; JHJ, pp. 218–224.

That is, the *total net displacement* in any given direction varies as $\sqrt{t}$.

These equations are of special importance in the determination of diffusion coefficients from observations on the Brownian motion of small particles.

We can also express equations 3 and 4 in terms of the mean free path, L, on the basis of the relation

$$D = \tfrac{1}{3}Lv_a. \tag{14.1}$$

Substituting in the above equations, we obtain the relations

$$z_a = \sqrt{\frac{4Lv_a t}{3\pi}} \tag{5}$$

and

$$z_r = \sqrt{\frac{2Lv_a t}{3}} = \sqrt{\frac{\pi}{2}}\, z_a. \tag{6}$$

The collision frequency per molecule is

$$\omega = \frac{v_a}{L},$$

while the total length of path actually traversed by a molecule in time t is

$$l = \omega t = \frac{v_a t}{L}. \tag{7}$$

Hence

$$z_a^2 = \left(\frac{4L^2}{3\pi}\right) l \tag{8}$$

or

$$l = 2.356\,\frac{z_a^2}{L^2} \tag{9}$$

$$= 1.5\,\frac{z_r^2}{L^2}. \tag{10}$$

That is, the *total length of path varies as the square of the net displacement* from the point of origin at $t = 0$.

As an illustration of the above equations let us consider the case of molecules in air at 25° C and atmospheric pressure. Since $L = 6.69 \cdot 10^{-6}$ and $v_a = 4.67 \cdot 10^4$, it follows from equation 14.1 that $D = 0.104\ \text{cm}^2 \cdot \text{sec}^{-1}$, and for $t = 60$ sec, $z_r = 3.53$ cm, while $l = 6.98 \cdot 10^9 t = 4.19 \cdot 10^{11}$ cm.

That $l = 1.19 \cdot 10^{11} z_r$ is obviously due to the fact that after each collision the probability of a displacement towards lower (or more negative) values of z is just as great as that of a displacement towards more positive values of z.

The equations for random motion have been applied to determine the value of the Avogadro constant from observations on rates of diffusion of Brownian particles. It may be demonstrated that the rate of diffusion of spherical particles is given by the relation

$$D = \frac{R_0 T}{N_A} \cdot \frac{1}{6\pi a \eta}, \tag{11}$$

where a = radius of particle, and η = viscosity of medium.

Also, the mean square of the displacement per second

$$\frac{z^2}{t} = \frac{R_0 T}{N_A} \cdot \frac{1}{3\pi a \eta}. \tag{12}$$

Values of N_A obtained by application of these relations, though not nearly as accurate as those obtained from determinations of the unit electric charge (method used by Millikan), are in good agreement with them.

CHAPTER 2

FLOW OF GASES THROUGH TUBES AND ORIFICES

1. VISCOUS FLOW OF GASES

At normal pressures the rate of flow of gases through cylindrical capillaries is governed by the Poiseuille law. The rate at which gas flows through a tube of length l (*in centimeters*) and radius a (*in centimeters*), expressed in terms of *moles per second*, is given by the relation[1]

$$n_M = \frac{\pi}{16\eta_T} \frac{a^4}{l} \frac{P_2{}^2 - P_1{}^2}{R_0 T_m}, \tag{1}$$

where η_T = coefficient of viscosity of the gas at temperature T of the capillary, P_2 and P_1 denote the pressures (in microbars) at the two ends of the tube, and T_m is the temperature at which n_M is measured. If V_m is the rate of flow in $\text{cm}^3 \cdot \text{sec}^{-1}$ at the pressure P_m,

$$n_M R_0 T = P_m V_m.$$

In general, the rate of flow is measured at the same temperature as the gas in the capillary, and equation 1 then assumes the form

$$Q_{bl} = 10^{-3} \frac{\pi}{8\eta} \frac{a^4}{l} P_{\mu ba}(P_{\mu b2} - P_{\mu b1}) \tag{2a}$$

$$= \frac{3.926 \cdot 10^{-4}}{\eta} \frac{a^4}{l} P_{\mu ba}(P_{\mu b2} - P_{\mu b1}), \tag{2b}$$

where Q_{bl} = microbar · liters per sec, at the temperature of capillary, and $P_{\mu ba}$ = average pressure (in microbars) = $\frac{1}{2}(P_{\mu b1} + P_{\mu b2})$.

Since 1 micron · liter = 1.333 microbar · liter,

$$Q_{\mu l} = \text{number of } \textit{micron} \cdot \textit{liters per second}$$

$$= 1.333 \cdot 10^{-3} \frac{\pi}{8\eta} \frac{a^4}{l} P_{\mu a}(P_{\mu 2} - P_{\mu 1})$$

$$= \frac{5.236 \cdot 10^{-4}}{\eta} \frac{a^4}{l} P_{\mu a}(P_{\mu 2} - P_{\mu 1}), \tag{3a}$$

where P_μ = pressure in microns.

---

[1] K.F. Herzfeld and H. M. Smallwood, *Taylor's Treatise on Physical Chemistry*, Vol. 1, p. 175, 2nd edition, D. Van Nostrand Company, New York, 1931.

In terms of d_i = diameter in *inches* and l_i = length in *inches,* the last equation becomes

$$Q_{\mu l} = \frac{5.362 \cdot 10^{-4}}{\eta} \frac{d_i^4}{l_i} P_{\mu a}(P_{\mu 2} - P_{\mu 1}). \tag{3b}$$

Let B denote any other unit of pressure, and let f denote the *number of microbars per unit of pressure.* Then

$$Q_{Bl} = \text{number of } \textit{liters at 1 unit of pressure, per second,}$$

$$= 10^{-3} f \frac{\pi}{8\eta} \frac{a^4}{l} B_a(B_2 - B_1) \tag{4}$$

where $B_a = \frac{1}{2}(B_1 + B_2)$.

Table 1 gives values of f and of $\pi f/8$ for some of the more common units of pressure. The last column gives the corresponding values of $\pi f/(8\eta)$ for air at 25° C ($\eta = 1.845 \cdot 10^{-4}$ poise).

TABLE 1

CONVERSION FACTORS FOR RATE OF VISCOUS FLOW IN TERMS OF DIFFERENT UNITS OF PRESSURE

Unit of Pressure	f	$\pi f/8$	$\pi f/(8\eta)$ for Air at 25° C
1 microbar	1	0.3926	$2.128 \cdot 10^3$
1 micron	1.333	0.5236	$2.838 \cdot 10^3$
1 mm	1333	$5.236 \cdot 10^2$	$2.838 \cdot 10^6$
1 atm	$1.0133 \cdot 10^6$	$3.978 \cdot 10^5$	$2.156 \cdot 10^9$
1 $\text{kg} \cdot \text{cm}^{-2}$	$9.807 \cdot 10^5$	$3.850 \cdot 10^5$	$2.086 \cdot 10^9$
1 $\text{lb} \cdot \text{in.}^{-2}$	$6.895 \cdot 10^4$	$2.708 \cdot 10^4$	$1.467 \cdot 10^8$

For instance, for air at 25° C,

$$Q_{P_{mm}l} = \text{number of } \textit{mm} \cdot \textit{liter} \text{ per sec}$$

$$= 2.838 \cdot 10^3 \frac{a^4}{l} P_{mma}(P_{mm2} - P_{mm1}), \tag{i}$$

Also, *for air at 25° C,*

$$Q_{\mu l} = 2.907 \frac{d_i^4}{l_i} P_{\mu a}(P_{\mu 2} - P_{\mu 1}) \quad \text{micron} \cdot \text{liters} \cdot \text{sec}^{-1}, \tag{ii}$$

where P_μ = pressure in microns.

The following conversion factors are useful in calculating rates of flow for any given temperature:

$$\begin{aligned}
1\ \text{atm} \cdot \text{cm}^3 \cdot \text{sec}^{-1} &= 760\ \text{micron} \cdot \text{liter} \cdot \text{sec}^{-1}. \\
1\ \text{micron} \cdot \text{liter} \cdot \text{sec}^{-1} &= 1.316 \cdot 10^{-3}\ \text{atm} \cdot \text{cm}^3 \cdot \text{sec}^{-1} \\
&= 0.03532\ \text{micron} \cdot \text{cu ft} \cdot \text{sec}^{-1} \\
&= 2.119\ \text{micron} \cdot \text{cu ft} \cdot \text{min}^{-1}. \\
1\ \text{micron} \cdot \text{cu ft} \cdot \text{min}^{-1} &= 0.4719\ \text{micron} \cdot \text{liter} \cdot \text{sec}^{-1}.
\end{aligned}$$

As an illustration of the application of equation 4, we shall calculate the rates of flow of air at 25° C, and for $B_2 = 1$ atm, $B_1 = 0$, through two capillaries:

(1) $l = 100,\quad a = 5.52 \cdot 10^{-3}$ (diam. = 4.53 mil).

(2) $l = 100,\quad a = 3.106 \cdot 10^{-3}$ (diam. = 2.45 mil).

In the first case, $Q_{Bl} = 1 \cdot 10^{-5}$ atm · liter per sec; in the second, $Q_{Bl} = 1 \cdot 10^{-6}$ atm · liter per sec.

For the pressure (B) expressed in terms of *pounds per square inch*, l_i = length in inches, and d_m = diameter in mils,

$$\begin{aligned}
Q &= \text{rate for air at 25° C, in } \textit{atm} \cdot \textit{cm}^3 \textit{ per min} \\
&= 6.135 \cdot 10^{-4} \frac{d_m^{\ 4}}{l_i} B_a(B_2 - B_1).
\end{aligned}$$

It is convenient, especially from the point of view of the subsequent discussion, to express equation 4 in the form

$$F = \frac{Q_{Bl}}{B_2 - B_1} = \frac{\pi f}{8\eta}\left(\frac{a^4}{l}\right) B_a. \tag{5}$$

Then this quantity corresponds to the rate of *flow per unit difference of pressure*, expressed in *cm*^{3} *per sec* measured at that unit of pressure in which B_a is expressed.

Equation 5 shows that, for a given length and radius of tube, F varies linearly with the average pressure and inversely as the coefficient of viscosity.

In terms of *microbars* and *cm*^{3}, it follows from equation 2 that

$$F = \frac{\pi}{8\eta} P_{\mu ba}\left(\frac{a^4}{l}\right) \quad \text{cm}^3 \cdot \text{sec}^{-1}. \tag{6}$$

Substituting for η from the relation

$$\eta = 0.5 \rho v_a L,$$

we obtain the relation

$$F = \frac{\pi}{8} \frac{A}{l/a} \frac{a}{L_a} \frac{v_a}{4}, \tag{7}$$

where L_a is the mean free path at the average pressure $P_{\mu ba}$, and $A = \pi a^2$.

For any given gas, at constant temperature, $L = cP_{\mu b}$, where c is a constant the value of which may be determined from Table 1.6. Hence, equation 7 can also be written in the form

$$F = \frac{\pi}{8} \frac{A}{l/a} \frac{aP_{\mu ba}}{c} \frac{v_a}{4} \tag{8}$$

$$= 4.487 \cdot 10^3 \frac{a^4}{l} \frac{P_{\mu ba}}{c} \sqrt{\frac{T}{M}} \quad \text{cm}^3 \cdot \text{sec}^{-1}, \tag{9}$$

where c = mean free path at 1 microbar and T° K.

The number of molecules per second is given by

$$\nu_F = F(n_2 - n_1)$$

$$= \frac{\pi}{8} \frac{A}{l/a} \frac{aP_{\mu ba}}{c} (\nu_2 - \nu_1), \tag{10}$$

where $\nu = \frac{1}{4} n v_a$ = number of molecules incident on unit area per unit of time at pressure $P_{\mu b}$ and n = number of molecules per cubic centimeter at pressure $P_{\mu b}$.

Equation 6 shows, as stated above, that F decreases with decrease in $P_{\mu ba}$. However, as the pressure is lowered a new effect becomes of importance—that of *slip* along the walls, which was discussed at the end of section 8, Chapter 1. Under these conditions the Poiseuille law, as expressed in equation 2, must be modified to take into account the fact that the velocity of flow at the walls can no longer be assumed to be zero. The corrected equation has the form

$$Q_{bs} = \frac{\pi}{8\eta} \frac{a^4}{l} P_{\mu ba}(P_{\mu b2} - P_{\mu b1}) \left(1 + \frac{4\zeta}{a}\right), \tag{11}$$

where ζ is the coefficient of slip given by equation I.8.36; that is

$$\zeta = \beta L_a, \tag{12}$$

where β is a numerical constant of the order unity, and L_a is the mean free path corresponding to $P_{\mu ba}$.

Consequently equation 2 assumes the form

$$F = \frac{\pi}{8\eta}\frac{a^4}{l}P_{\mu ba}\left(1 + \frac{4\beta L_a}{a}\right) \tag{13}$$

$$= \frac{\pi}{8\eta}\frac{a^4}{l}P_{\mu ba} + \frac{\pi\beta}{\rho_1 v_a}\frac{a^3}{l}. \tag{14}$$

At very low pressures, the first term on the right-hand side of the last equation becomes negligible compared with the second term, which is *independent of the pressure.* The equation then becomes

$$F = \frac{\pi\beta}{\rho_1 v_a}\frac{a^3}{l}$$

$$= \frac{\pi a^2}{l/a}\frac{v_a}{4}\frac{\pi\beta}{2}. \tag{15}$$

According to Knudsen (as discussed in the following section), the value of F at low pressures is given by the relation

$$F = 0.81 \cdot \frac{8}{3}\frac{\pi a^2}{l/a}\frac{v_a}{4}. \tag{16}$$

Comparing the last two relations, it follows that $\beta = 1.375$.

However, as has also been shown by Knudsen, the laws of flow of gases at intermediate pressures, that is in the range of pressures in which slip becomes of importance, may be determined without the necessity of introducing either the concept of slip or the coefficient β. This topic will be discussed in section 3.

Before concluding this section it is essential to observe that the quantity designated in the above equations by F evidently corresponds to the quantity which in the conduction of electricity is known as *conductance.* That is, the pressure is analogous to electrical potential, and Q, to the current. In consequence of this $1/F$ *may be treated as a resistance,* and, if there are two or more tubes in series of different dimensions, the total resistance is obtained by adding the values of $1/F$ for each tube, as in dealing with electrical resistances. The practical utility of this concept will be emphasized more fully in the following section.

ADDED NOTE 1. TURBULENT FLOW

The Poiseuille law is applicable only for *viscous laminar* flow. When the velocity of the gas through a cylindrical tube exceeds a certain critical value, u_c, turbulence sets in and the pressure difference between the two ends exceeds that calculated from equation 2. As first shown by Reynolds, the value of u_c is determined by the relation

$$u_c = \frac{R_e \eta}{\rho a}, \tag{i}$$

where R_e is a dimensionless number, known as the "Reynolds number," which has the approximate numerical value 1000.

Thus, for air at 25° C and 1 atm pressure, $\eta = 1.845 \cdot 10^{-4}$ and $\rho = 1.185 \cdot 10^{-3}\ \text{g} \cdot \text{cm}^{-3}$. Hence turbulent flow will occur when the critical velocity

$$u_c \geqslant \frac{155.7}{a}\ \text{cm} \cdot \text{sec}^{-1}. \tag{ii}$$

But

$$u_c = \frac{Q_{ac}}{\pi a^2}\ \text{cm} \cdot \text{sec}^{-1}, \tag{iii}$$

where

$$\begin{aligned} Q_{ac} &= \text{atm} \cdot \text{cm}^3 \cdot \text{sec}^{-1} \\ &= 1.078 \cdot 10^9 \frac{a^4}{l} (B_2{}^2 - B_1{}^2), \end{aligned} \tag{iv}$$

and B_2 and B_1 denote the pressures in atmospheres at the two ends of the capillary. (This relation is derived from the value for $\pi f/(8\eta)$ given in the last column of Table 1.)

Consequently, at the critical velocity, the following relations must apply:

1. $Q_{ac} \geqslant 490a.$ (v)

2. Assuming $B_1 = 0$,

$$B_2{}^2 \geqslant 4.544 \cdot 10^{-7} \frac{l}{a^3}. \tag{vi}$$

In vacuum technique, $B_2 = 1$ atm, and therefore the last relation becomes

$$\frac{l}{a^3} \leqslant 2.2 \cdot 10^6.$$

That is, turbulent flow will occur at the initial stage of exhaust, if, for instance, $a = 10^{-2}$ cm and $l \leqslant 2.2$ cm, or $a = 10^{-1}$ cm and $l \leqslant 2200$ cm. Since such capillaries are not very likely to be used in evacuation it is evident that the flow will usually be turbulent until the pressure is much less than 1 atm.

Relation *v* indicates that, for $a = 1$, turbulent flow will occur for $Q_{ac} \geqslant 490$ atm · cm^3 sec^{-1}, that is, $3.724 \cdot 10^5$ micron · liters · sec^{-1}.

In an investigation on the flow of air in glass and metal capillaries, W. Ruckes[2] confirmed the validity of relation *i* with values for R_e of 1000 for glass and 400 to 500 for metal. In thèse experiments, in which capillaries were used ranging in values of a from $6.15 \cdot 10^{-3}$ cm to 0.19 cm, in values of l from 16.3 cm to 1530 cm, and in values of B_2 from 15 atm to less than 1 atm, the observed rates of flow, for values of $u < u_c$, were found to be in good agreement with those deduced from the Poiseuille law, that is, equation *iv*.

2. "FREE-MOLECULE" FLOW

At ordinary pressures the rate of flow of gases through a tube is limited by the frequency of collisions between molecules. Hence arises the necessity for introducing the coefficient of viscosity, as in the Poiseuille law. At very low pressures, however, where L is much greater than a, the rate of flow is limited, not by collisions between molecules, but by collisions of molecules against the walls. For pointing out the manner of attacking the problem of flow at these low pressures, we are indebted to the investigations of M. von Smoluchowski, M. Knudsen, W. Gaede, and P. Clausing.

The term "molecular flow" was suggested by Knudsen[3] to designate the flow of gases at pressures for which L is of the same order of magnitude as or greater than a. Under these conditions a molecule striking the inner surface of the tube at any point is repelled and suffers no collision until it strikes the walls at some other point. Knudsen assumes that any surface, no matter how smooth it may appear macroscopically, is in reality covered with projections that are of atomic or molecular dimensions and irregularly distributed over the surface. Consequently,

a gas molecule, on striking the surface, is repelled in a direction which is totally independent of the direction of incidence, and the distribution of directions of an infinitely large number of molecules after reflection from a surface follows Lambert's cosine law for the reflection of light from a glowing body.

Introducing Maxwell's distribution law, Knudsen deduced the following relations:

---

[2] *Ann. Physik*, **25**, 983 (1908). For a comprehensive discussion of the conditions of turbulent flow and for experimental determinations of the Reynolds number see also *Heat Transmission* by W. H. McAdams, Chapter V, McGraw-Hill Book Company, New York, 2nd ed., 1942.

[3] *Ann. Physik*, **28**, 75, 999 (1909), and subsequent papers.

Let $P_{\mu b1}$ and $P_{\mu b2}$ denote the pressures in microbars at the two ends of a tube. Then the quantity of gas flowing through the tube, in microbar · cm^3 · sec^{-1}, is

$$Q = \frac{P_{\mu b2} - P_{\mu b1}}{W\sqrt{\rho_1}}, \tag{1}$$

where $\rho_1 = M/R_0T$ = density at 1 microbar, and W is a factor the value of which depends upon the shape and dimensions of the tube. Thus $W\sqrt{\rho_1}$ corresponds to a "resistance."

Since $\dfrac{1}{\sqrt{2\pi\rho_1}} = \dfrac{v_a}{4}$,

where v_a = average molecular velocity

$= 14{,}551\sqrt{T/M}$ cm · sec^{-1},

it follows that we can express equation 1 in the form

$$F = \frac{Q}{P_{\mu b2} - P_{\mu b1}} = \frac{\sqrt{2\pi}}{W}\frac{v_a}{4}, \tag{2}$$

where, evidently, F corresponds to a "conductance" and designates *units of volume per unit of time.*

For an opening of area A in a *very thin* plate, the value of W is given by

$$W_0 = \frac{\sqrt{2\pi}}{A}. \tag{3}$$

Hence the conductance of an opening of area A is given by

$$F_0 = \frac{Av_a}{4}. \tag{4}$$

For a long[4] tube of length l and varying cross section A and perimeter H, the fundamental relation deduced by Knudsen is

$$F_t = \frac{4}{3}\frac{v_a}{\int_0^l \frac{H}{A^2}\,dl}. \tag{5}$$

It follows that the values of F_0 and F_t are *independent of the unit of pressure* used and depend only on the units in which v_a and the geometrical dimensions (A, H, and l) are expressed.

---

[4] That is, one for which the conductance of the tube is small compared with that of the ends. This is discussed in more detail in subsequent remarks.

Thus for A expressed in cm^2 and v_a in $\text{cm} \cdot \text{sec}^{-1}$, F denotes $\text{cm}^3 \cdot \text{sec}^{-1}$. If the pressure is expressed in microns, then Q designates $\text{micron} \cdot \text{cm}^3 \cdot \text{sec}^{-1}$.

It will be observed that F_0 corresponds to the *volume incident* on the area A, per unit time, while F_t corresponds to the volume flowing through the tube or duct per unit time.

From equation 4 it follows that, for a *circular opening* of radius a (cm) and area $A = \pi a^2$ (cm²),

$$F_0 = 3638A\sqrt{\frac{T}{M}} \quad \text{cm}^3 \cdot \text{sec}^{-1} \tag{6a}$$

$$= 11{,}428a^2\sqrt{\frac{T}{M}} \quad \text{cm}^3 \cdot \text{sec}^{-1}. \tag{6b}$$

From equation 5 we derive the following relation for a *long tube of uniform* cross section:

$$F_t = 19{,}400\frac{A^2}{Hl}\sqrt{\frac{T}{M}} \quad \text{cm}^3 \cdot \text{sec}^{-1}. \tag{7}$$

Hence, for a *cylindrical tube* of radius a (cm), length l (cm), for which l/a is greater than about 100,

$$F_t = 30{,}480\frac{a^3}{l}\sqrt{\frac{T}{M}} \quad \text{cm}^3 \cdot \text{sec}^{-1}. \tag{8}$$

For a duct of uniform *rectangular cross section* (lengths of sides a and b, in cm),

$$F_t = \frac{2}{3}\frac{a^2b^2}{(a+b)l}v_a$$

$$= 9700\frac{a^2b^2}{(a+b)l}\sqrt{\frac{T}{M}} \quad \text{cm}^3 \cdot \text{sec}^{-1}. \tag{9a}$$

For the case $a = b$ (a duct of square cross section),

$$F_t = 4850\frac{a^3}{l}\sqrt{\frac{T}{M}} \quad \text{cm}^3 \cdot \text{sec}^{-1}. \tag{9b}$$

In the case of an ellipse, $A = \pi ab$, and $H = 2\pi\sqrt{(a^2+b^2)/2}$ approximately, where a and b designate the lengths of the two semi-axes. Hence, for uniform *elliptical cross section,*

$$F_t = 43{,}100\frac{a^2b^2}{l\sqrt{a^2+b^2}}\sqrt{\frac{T}{M}} \quad \text{cm}^3 \cdot \text{sec}^{-1}, \tag{10}$$

where a, b, and l are expressed in centimeters.

Another interesting application of equation 5 is that of calculating the conductance of a *long tapered round tube* for which the radius is a_0 at one end and $a_l\ (= a_0 + bl)$ at the other end. The result of the integration is

$$F_t = \frac{2}{3}\,\frac{\pi a_0{}^2 a_l{}^2}{a_{l/2} l}\,v_a$$

$$= 30{,}480\,\frac{a_0{}^2 a_l{}^2}{a_{l/2} l}\sqrt{\frac{T}{M}}\quad \text{cm}^3 \cdot \text{sec}^{-1}, \tag{11}$$

where $a_{l/2}$ is the value of the radius halfway along the tube. It is evident that, for $a = a_0 = a_{l/2} = a_l$, the last equation becomes identical with equation 8.

For air at 25° C, $\sqrt{T/M} = 3.207$.

It should be emphasized that the relation for the conductance of an orifice is strictly applicable, as shown by Knudsen,[5] only under those conditions in which the diameter (or largest dimension of the orifice) is one-tenth or less than the mean free path for the gas molecules at the pressure of effusion. For practical purposes the relation may be applied to pressures which are ten times greater, but it is no longer valid, even approximately, if the area of the orifice is so large, or the pressure so high, that mass motion of the gas occurs.

Equations 6 and 8 can also be expressed in the following forms:

The *number of molecules* flowing through a tube per second, for a difference in pressure $P_{\mu b2} - P_{\mu b1}$,

$$(\nu_F)_t = F_t(n_2 - n_1) \tag{12a}$$

$$= \frac{8}{3} A \frac{a}{l} \frac{v_a}{4} (n_2 - n_1)$$

$$= \frac{8}{3} A \frac{a}{l} (\nu_2 - \nu_1), \tag{12b}$$

where n = number of molecules per cubic centimeter at pressure $P_{\mu b}$

ν = number of molecules striking unit area per second, at pressure $P_{\mu b}$

$= 2.635 \cdot 10^{19} P_{\mu b}/\sqrt{MT}$

$= 3.513 \cdot 10^{22} P_{mm}/\sqrt{MT}$.

---

[5] *Ann. Physik*, **28**, 75 (1909). See also discussion in EHK, pp. 64–66, and Chapter 1, section 6, of this volume.

Similarly for the case of an *orifice of area* A (cm^2),

$$(\nu_F)_0 = A(\nu_2 - \nu_1). \tag{13}$$

The mass of gas (in g · sec^{-1}) is given by

$$G' = m\nu_F.$$

$$G_t' = \frac{8}{3} A \cdot \frac{a}{l} \cdot g \sqrt{\frac{M}{T}} \, (P_{\mu b1} - P_{\mu b2}) \quad \text{for a tube,} \tag{14}$$

$$\text{where } g = \frac{2.635 \cdot 10^{19}}{6.023 \cdot 10^{23}} = 4.375 \cdot 10^{-5} \text{ for } P_{\mu b}$$

$$= \frac{3.513 \cdot 10^{22}}{6.023 \cdot 10^{23}} = 5.833 \cdot 10^{-2} \text{ for } P_{mm}.$$

$$G_0' = Ag \sqrt{\frac{M}{T}} \, (P_2 - P_1) \quad \text{for an orifice.} \tag{15}$$

It should be mentioned that, following Knudsen, many of the German writers have designated the expression $\theta = \frac{3}{8}\sqrt{\pi\rho_1/2}$ as "coefficient of external viscosity." Hence

$$\frac{1}{2\theta} = \frac{8}{3}\sqrt{\frac{1}{2\pi\rho_1}} = \frac{2}{3} v_a. \tag{16}$$

Table 2 gives values of F_t, and of F_0, calculated by means of equations 8 and 6, respectively, for a few of the more important gases, at $T = 298$ (room temperature).

TABLE 2*

VALUES OF "CONDUCTANCE" OF CYLINDRICAL TUBES AND OPENINGS AT 25° C

Gas	M	$F_t(l/a^3)$ liters · sec^{-1} $= 526.2/\sqrt{M}$	F_0A^{-1} liters · sec^{-1} $= 62.81/\sqrt{M}$	F_0a^{-2} liters · sec^{-1} $= 197.3/\sqrt{M}$
H_2	2.016	370.6	44.24	139.0
He	4.003	263.0	31.39	98.58
Air	28.98	97.75†	11.67	36.66
A	39.94	83.28	9.94	31.23

* It should be emphasized, as pointed out in the subsequent discussion, that the relations for F_t are valid, even approximately, only for $l/a > 100$. Furthermore, all the expressions for F are valid only for pressures at which the *mean free path is greater than a.*

† A useful approximation, pointed out by J. Yarwood, *High Vacuum Technique*, John Wiley & Sons, 2nd edition, 1945 (designated JY), is $F_t = 100(a^3/l)$ liters · sec^{-1}, where a and l are measured in centimeters, as above.

In terms of d_i, the diameter, and l_i the length, expressed in inches, it follows that, for *air at 25° C,*

$$F_t = 78.81\ (d_i^3/l_i) \quad \text{liters} \cdot \text{sec}^{-1}$$
$$= 167.0\ (d_i^3/l_i) \quad \text{cu ft} \cdot \text{min}^{-1},$$

and

$$F_0 = 75.28 \quad \text{liters} \cdot \text{sec}^{-1} \text{ per square inch area}$$
$$= 159.5 \quad \text{cu ft} \cdot \text{min}^{-1} \text{ per square inch area}$$
$$= 125.2 d_i^2 \quad \text{cu ft} \cdot \text{min}^{-1}.$$

That the "conductance" at low pressures is considerably less than that at high pressures is evident from the following illustration.

For the flow of air at 25° C through a tube, for which $l = 100$ and $a = 0.5$ cm, it follows from equation 1.5 that, at $P_{\mu ba} = 5.067 \cdot 10^5$ (0.5 atm),

$$F_t = 6.725 \cdot 10^5 \quad \text{cm}^3 \cdot \text{sec}^{-1}.$$

As mentioned previously, F decreases linearly with decrease in P_a for the condition of viscous flow. On the other hand, at low pressures (L large compared to a), F_t is *independent of the pressure,* and according to Table 2 its value is given, in the case under consideration, by the relation

$$F_t = 97{,}750 \frac{a^3}{l} = 122.3 \quad \text{cm}^3 \cdot \text{sec}^{-1}.$$

In the next section we shall consider at further length the relation governing the value of F for the transition region between viscous flow and molecular flow.

From the relations given above it follows that at very low pressures the ratio of the resistance of a cylindrical tube to that of the opening is given by

$$r = \frac{W_t}{W_0} = \frac{3}{8} \frac{l}{a}.$$

For $l/a = 50$, $r = 18.75$. That is, the resistance to flow offered by the walls is 18.75 times that offered by the open end. This leads to the conclusion that, for small values of l/a, the above relations for W_t give values of the total resistance to flow which are too low. Reasoning from the point of view that the *total resistance* is given by the relation

$$W = W_t + W_0$$

or

$$\frac{1}{F} = \frac{1}{F_t} + \frac{1}{F_0},$$

the corrected equation (given in the 1922 edition of the writer's book on high-vacuum technique) for the conductance of a tube was assumed to be

$$\frac{1}{F} = \left(\frac{2.394l}{d^3} + \frac{3.184}{d^2}\right)\sqrt{\rho_1}, \tag{17a}$$

where $d = 2a =$ diameter of tube, and

$$\rho_1 = \frac{M}{83.144 \cdot 10^6 T}.$$

Equation 17*a* can be expressed in the more convenient form

$$F = K'A\frac{v_a}{4} = 3638K'A\sqrt{\frac{T}{M}} \quad \text{cm}^3 \cdot \text{sec}^{-1},$$

where

$$K' = \frac{\frac{8}{3}a/l}{1 + \frac{8}{3}a/l} = \frac{1}{1 + \frac{3}{8}l/a} \tag{17b}$$

and $A = \pi a^2$.

That is, the factor K' may be regarded as representing the *ratio between the rate at which gas leaves the outlet of the tube and that at which gas strikes the inlet.*

Figure 1 represents plots of values of F, calculated, by means of equation 17*a*, for air at 20° C, drawn on log-log scale.[6] Each curve gives F as a function of l (in centimeters) for a constant value of d (in centimeters) which is indicated at the bottom of the figure. The linear portion of each curve represents the effect of the term l/d^3, while the curved portion represents the added effect of the term containing $1/d^2$. For other gases the conductance, for constant values of l and d, varies inversely as $\sqrt{M}$.

As shown by P. Clausing,[7] equation 17*a* or 17*b* is only approximate.

---

[6] These plots were first drawn by Mr. J. H. Payne for use in his investigations on the design of high-speed pumps, and Fig. 1 was published in *J. Franklin Inst.*, **211**, 691 (1931). The same data have also been plotted by Dr. M. N. States of the Central Scientific Company in a special chart.

[7] *Ann. Physik*, **12**, 961 (1932).

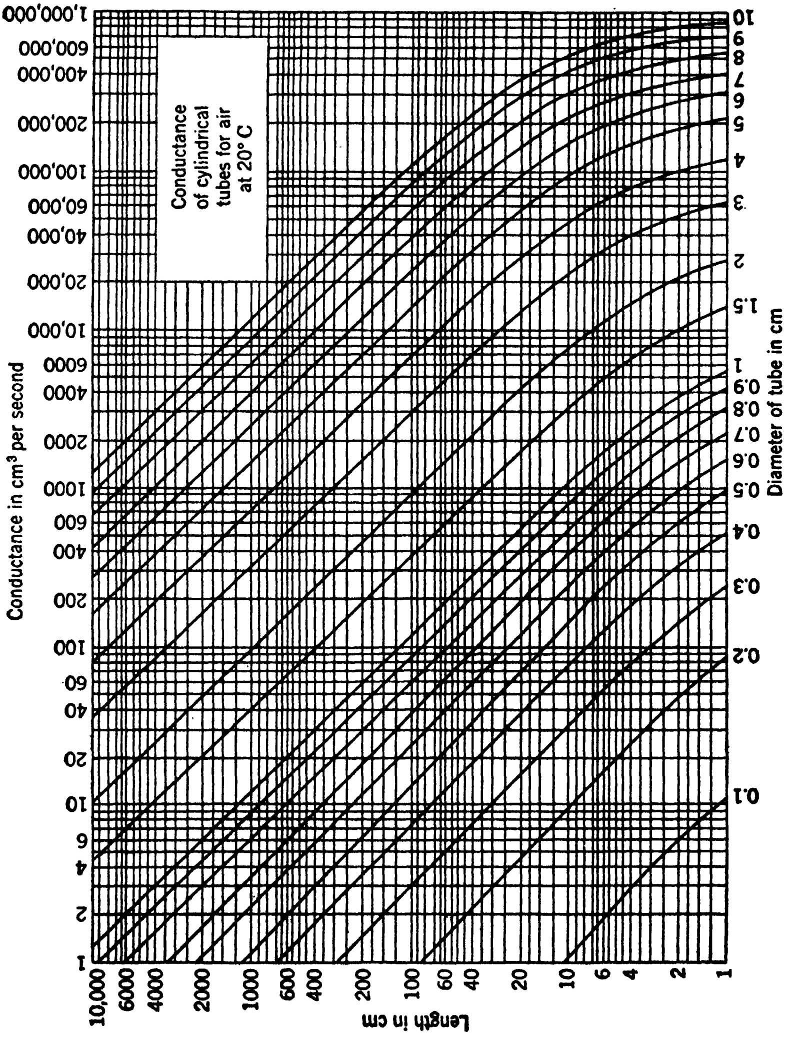

FIG. 1. Plots of conductance of cylindrical tubes for air at 20° C calculated according to equation (2.17*a*).

From a detailed investigation he deduced the relation

$$F = KA\frac{v_a}{4} = 3638KA\sqrt{\frac{T}{M}} \quad \text{cm}^3 \cdot \text{sec}^{-1}, \tag{18}$$

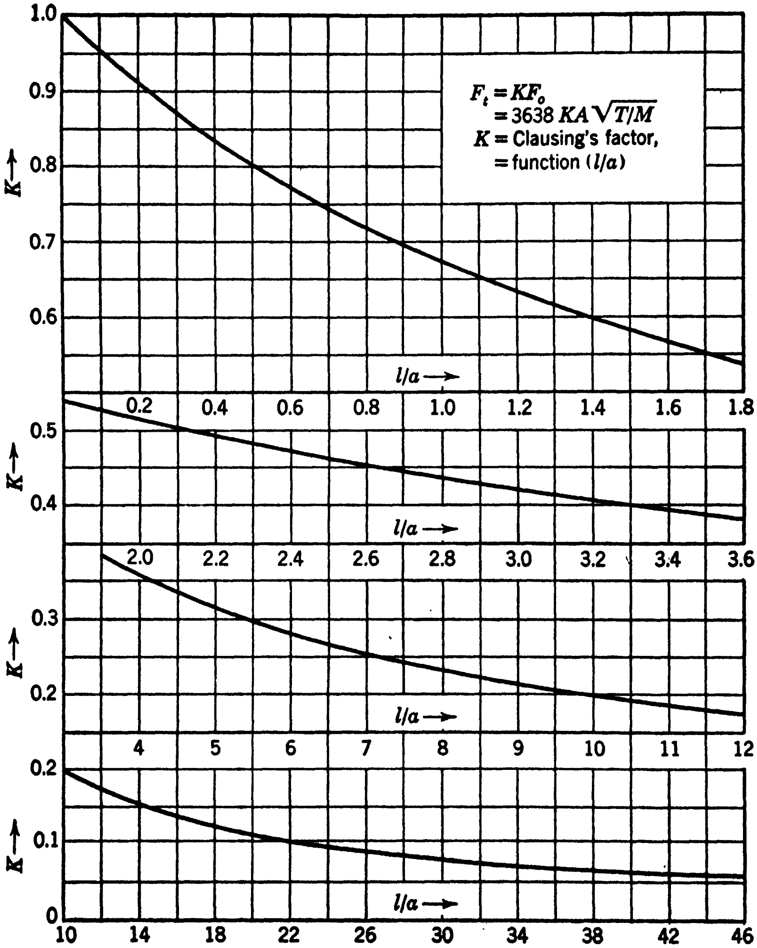

FIG. 2. Plot of Clausing's factor, K, as a function of (l/a). Scales for K and l/a are indicated for each curve.

where, as shown in Table 3, K is a dimensionless function of l/a, the value of which decreases from 1 (for $l/a = 0$) to $8a/(3l)$ for l/a very large. Clausing's values of K are given in the second and fifth columns; the values of K' deduced by means of equation 17b are given, for comparison, in the third and sixth columns. It will be observed that for low values

TABLE 3

VALUES OF CLAUSING'S FACTOR K AND THE APPROXIMATE CORRECTION K' FOR A SERIES OF VALUES OF l/a

l/a	K	K'	l/a	K	K'
0	1	1	3.2	0.4062	0.454
0.1	0.9524	0.965	3.4	.3931	.439
0.2	.9092	.931	3.6	.3809	.426
0.3	.8699	.899	3.8	.3695	.412
0.4	.8341	.870	4.0	.3589	.400
0.5	.8013	.842	5	.3146	.348
0.6	.7711	.816	6	.2807	.307
0.7	.7434	.792	7	.2537	.276
0.8	.7177	.769	8	.2316	.250
0.9	.6940	.747	9	.2131	.229
1.0	.6720	.727	10	.1973	.210
1.1	.6514	.708	12	.1719	.182
1.2	.6320	.690	14	.1523	.160
1.3	.6139	.672	16	.1367	.143
1.4	.5970	.656	18	.1240	.129
1.5	.5810	.640	20	.1135	.117
1.6	.5659	.625	30	.0797	.0817
1.7	.5518	.611	40	.0613	.0625
1.8	.5384	.597	50	.0499	.0506
1.9	.5256	.584	60	.0420	.0425
2.0	.5136	.572	70	.0363	.0367
2.2	.4914	.548	80	.0319	.0322
2.4	.4711	.526	90	.0285	.0288
2.6	.4527	.506	100	.0258	.0260
2.8	.4359	.488	1000	.002658	.002660
3.0	.4205	.470		$8a/(3l)$	$8a/(3l)$

of l/a the difference amounts to as much as 12 per cent. For l/a very large, K' tends to become equal to K. A series of plots of K versus l/a are shown in Fig. 2. The scale for l/a is indicated underneath each curve.

E. H. Kennard[8] has shown that values of K in good agreement with those deduced by Clausing are given by the following empirical relations:

For $0 \leqslant l/a \leqslant 1.50$,

$$K = \frac{1}{1 + 0.5l/a}; \tag{19a}$$

for $l/a > 1.50$,

$$K = \frac{1 + 0.4l/a}{1 + 0.95l/a + 0.15(l/a)^2}. \tag{19b}$$

---

[8] EHK, pp. 306–308.

It is important to realize that for relatively short tubes serious errors may be made if the value of F is calculated by means of equation 8. This is evident from an inspection of the data given in Table 4.

Let F_1 = value calculated by means of equation 8 and $F_2 = KF_0 = K \cdot Av_a/4$, and let

$$r = \frac{F_1}{F_2} = \frac{8}{3K} \cdot \frac{a}{l} \cdot$$

Then the value of r denotes the ratio between the value of F deduced for the condition l/a very large and the correct value deduced by means of Clausing's correction factor K. It will be observed from the last column in Table 4 that, for low values of l/a, r is much greater than 1 and approaches unity as a limiting value only for $l/a > 100$ approximately.

TABLE 4

ILLUSTRATING THE EFFECT OF NEGLECTING "END CORRECTION" IN CALCULATING CONDUCTANCE OF CYLINDRICAL TUBES

l/a	K	r
0.5	0.8013	6.656
1.0	.6720	3.968
2.0	.5136	2.597
3.0	.4205	2.114
4.0	.3589	1.857
5.0	.3146	1.695
7.0	.2537	1.502
10.0	.1973	1.352
20.0	.1135	1.175
30.0	.0797	1.115
40.0	.0613	1.087
50.0	.0499	1.069
100	.0258	1.034
1000	.00266	1.0035

From this discussion we are thus led to the following relations for the calculation of F for an orifice or cylindrical tube, in the range of very low pressures:

1. *For an orifice:*

$$F = F_0 = \frac{Av_a}{4}$$

$$= 3.638A\sqrt{\frac{T}{M}} \text{ liter} \cdot \text{sec}^{-1}$$

$$= 11.428a^2\sqrt{\frac{T}{M}} \text{ liter} \cdot \text{sec}^{-1}.$$

2. *For a tube:*

$$F = F_t = \frac{KAv_a}{4} = KF_0,$$

where K is Clausing's factor, given as a function of l/a in Table 3 or Fig. 2.

3. For a very short tube ($l/a \lesssim 1.5$):

$$K = \frac{1}{1 + 0.5\, l/a}.$$

4. For l/a *very large* (l/a approximately > 100):

$$K = \frac{8}{3}\frac{a}{l}; \quad \text{and} \quad F_t = \frac{8\pi}{3} \cdot \frac{a^3}{l}\frac{v_a}{4}$$

$$= 30.48 \frac{a^3}{l}\sqrt{\frac{T}{M}} \quad \text{liter} \cdot \text{sec}^{-1}.$$

5. For $l/a > 1.5$, a convenient approximation (maximum error about 12 per cent) is given by the relation

$$F_t = \frac{K'Av_a}{4} = \frac{\pi a^2 \cdot v_a/4}{1 + \frac{3}{8}\, l/a} = \frac{F_0}{1 + \frac{3}{8}\, l/a}$$

$$= \frac{(8\pi/3) \cdot (a^3/l) \cdot (v_a/4)}{1 + \frac{8}{3}\, a/l}.$$

This is the relation used in deriving the plots shown in Fig. 1.

Formulas for F_0 and F_t for different gases at 25° C are given in Table 2.

Clausing[8] has also deduced values of K for tubes with *rectangular section*, $a \gg b$, and $a \gg l$ (as in slits for molecular ray experiments).

$$F = 3638Kab\sqrt{\frac{T}{M}} \quad \text{cm}^3 \cdot \text{sec}^{-1} \tag{20}$$

$$= 3.668 \times 10^4\, Kab \quad \text{cm}^3 \cdot \text{sec}^{-1},$$

for air at 25° C, where a and b are expressed in centimeters.

Table 5 gives a selection of values of K.[9]

For a *short tube* of any form of uniform cross section, an *approximate* result may be obtained, as in the case of a cylindrical tube,[10] by means of the relation

---

[9] *Loc. cit.;* see also LBL, p. 306, and I. Estermann, *Rev. Modern Phys.*, **18**, 301, 1946, Table I, for more detailed data.

[10] See equations 17*a* and 17*b*.

$$\frac{1}{F_t'} = \frac{1}{F_t} + \frac{1}{F_0},$$

where F_t is the conductance deduced for a very long tube, F_0 denotes the conductance of one end, and F_t' is the conductance corrected for "end effects."

TABLE 5

VALUES OF CLAUSING'S FACTOR FOR TUBES OF RECTANGULAR CROSS SECTION

l/b	K	l/b	K
0	1.000	1.50	0.6024
0.1	0.9525	2.00	.5417
0.2	0.9096	3.00	.4570
0.4	0.8362	4.00	.3999
0.8	0.7266	5.00	.3582
1.0	0.6848	10.00	.2457
		∞	$\frac{b}{l} \ln \frac{l}{b}$

Hence, in terms of the cross-sectional area, A, in square centimeters, and H and l in centimeters,

$$F_0 = 29.54\, A_i \sqrt{\frac{\;}{M}} \quad \text{liter} \cdot \text{sec}^{-1}, \tag{22}$$

$$F_t = 125.1\, \frac{A_i^2}{H_i l_i} \sqrt{\frac{T}{M}} \quad \text{liter} \cdot \text{sec}^{-1}, \tag{23}$$

$$F_t' = \frac{29.54 A_i \sqrt{T/M}}{1 + \frac{3}{16}\,(H_i l_i / A_i)} \quad \text{liter} \cdot \text{sec}^{-1}. \tag{24}$$

It will be observed that for the dimensions expressed in *inches*, instead of in centimeters, the values deduced for F_t in equations 7, 8, 9, 10, 11, and 12 should be multiplied by $(2.54)^2 = 6.452$ to give the value of the conductance in $\text{cm}^3 \cdot \text{sec}^{-1}$.

For air at 25° C, $\sqrt{T/M} = 3.207$, and hence we derive the following relations, for the values of the *conductance for air at 25° C:*

$$F_0 = 75.3 A_i \quad \text{liter} \cdot \text{sec}^{-1}.$$

For a *long cylindrical tube* ($l_i/d_i > 50$), where d_i = diameter in inches,

$$F_t = 78.8 d_i^3/l_i \quad \text{liter} \cdot \text{sec}^{-1}.$$

For a long tube of *non-circular cross section,*

$$F_t = 401.6 A_i^2/(H_i l_i) \quad \text{liter} \cdot \text{sec}^{-1}.$$

For a *short tube* of any form of uniform cross section,

$$F_t' = \frac{F_t}{1 + 0.188\, H_i l_i / A_i} \quad \text{liter} \cdot \text{sec}^{-1}.$$

For the special case in which a tube of cross section A_1 joins a tube of *smaller cross section,* A_2, the value of the conductance at the junction, *for air at 25° C,* is

$$F_j = \frac{75.3 A_2}{1 - A_2/A_1}, \tag{25}$$[11]

where A_1 and A_2 are expressed in square inches.

For $A_2 = A_1$, $F_j = \infty$, and $1/F_j = 0$, which signifies that for this case the added resistance is zero.

For A_2 very much less than A_1, the value of the conductance approaches that for the opening of area A_2.

As illustrations of the application of the equations for molecular flow, Table 6 gives values of F_t ($\text{cm}^3 \cdot \text{sec}^{-1}$) for a number of typical cases. The temperature is assumed to be 25° C in all cases. At 25° C,

$$F_t = 1.972 \cdot 10^5 K a^2 \cdot M^{-1/2} \quad \text{cm}^3 \cdot \text{sec}^{-1}.$$

The last column in the table gives values of the *time constant,* $\Delta t_0 = 2.303 \cdot 10^3 F_t^{-1}$, which, as will be shown in the following section, corresponds to the interval of time (in seconds) required to reduce the pressure in a 1-liter volume to 10 per cent of its instantaneous value, through a tube of the dimensions given, assuming that the pressure at the inlet to the pump is maintained at zero. In this table, and Table 7 F_t corresponds to F_t' in the previous equations.

As will be observed, the values of F_t for large values of a are considerably greater than for smaller values. This is, of course, due to the a^3 factor. An increase of 10 per cent in the value of a leads to an increase of 33.1 per cent in the value of F_t (for long tubes), whereas a 10 per cent decrease in the value of l leads to an increase of only 11.1 per cent in the value of F_t.

---

[11] This relation has been widely quoted in reports issued by the Manhattan Project. Its derivation has been ascribed to Dr. R. Loevenger of Stanford University, but the writer has been unable to obtain the details of this derivation.

TABLE 6

VALUES OF "CONDUCTANCE," F_t, FOR A NUMBER OF TYPICAL CASES

a	l	l/a	K	Gas	F_t ($\text{cm}^3 \cdot \text{sec}^{-1}$)	$2303/F_t$ (sec)
0.51	3.2	6.273	0.273	H_2	$9.868 \cdot 10^3$	0.2333
(Wide-bore stopcock)				Ne	$3.120 \cdot 10^3$	0.7381
				Air	$2.620 \cdot 10^3$	0.8790
				A	$2.216 \cdot 10^3$	1.040
				Kr	$1.532 \cdot 10^3$	1.503
0.20	2.0	10.0	0.197	H_2	$1.088 \cdot 10^3$	2.116
(Narrow-bore stopcock)				Ne	$3.442 \cdot 10^2$	6.689
				Air	$2.871 \cdot 10^2$	8.021
				A	$2.445 \cdot 10^2$	9.419
				Kr	$1.690 \cdot 10^2$	13.61
0.40	40.0	100.0	0.0258	H_2	$5.709 \cdot 10^2$	4.033
				Ne	$1.805 \cdot 10^2$	12.76
				Air	$1.505 \cdot 10^2$	15.31
				A	$1.282 \cdot 10^2$	17.97
				Kr	$0.886 \cdot 10^2$	25.99
2.0	40.0	20.0	0.1135	H_2	$6.319 \cdot 10^4$	$3.645 \cdot 10^{-2}$
				Air	$1.665 \cdot 10^4$	$1.383 \cdot 10^{-1}$
5.0	20.0	4.0	0.3589	H_2	$1.248 \cdot 10^6$	$1.845 \cdot 10^{-3}$
				Air	$3.291 \cdot 10^5$	$6.998 \cdot 10^{-3}$
20.0	20.0	1.0	0.6720	H_2	$3.741 \cdot 10^7$	$6.156 \cdot 10^{-5}$
				Air	$9.860 \cdot 10^6$	$2.335 \cdot 10^{-4}$
2.5	20.0	8.0	0.2316	H_2	$2.014 \cdot 10^5$	$1.144 \cdot 10^{-2}$
				Air	$5.309 \cdot 10^4$	$4.338 \cdot 10^{-2}$
2.0	1.0	0.5	0.8013	H_2	$4.461 \cdot 10^5$	$5.163 \cdot 10^{-3}$
				Air	$1.176 \cdot 10^5$	$1.959 \cdot 10^{-2}$

The effect of the "end correction," which is really the significance of the factor K, is shown by comparing the values of F_t for the 40-cm length of tubing, 2.0-cm radius, with that for the 1-cm length. If only l were involved, F_t for the shorter tubing should be equal to $40 \times 1.665 \cdot 10^4 = 6.860 \cdot 10^5$ (for air), whereas it is actually equal to $1.176 \cdot 10^5$.

For *an opening* of radius a in a *very thin plate*, the value of F_0, in the case of *air at 25° C*, is given, as shown in Table 2, by

$$F_0 = 36.66 \cdot 10^3 a^2 \quad \text{cm}^3 \cdot \text{sec}^{-1}$$

and

$$\frac{2303}{F_0} = 6.279 \cdot 10^{-2} a^{-2} \quad \text{sec.}$$

Table 7 gives values, *for air at 25° C*, of F_0, the conductance of an opening of radius a, and of F_t, the conductance of a tube of the same radius, for different values of l/a. The corresponding values of K are given at the top of the table, and the value of $F_t = F_0K = 36.66Ka^2$ liters · sec^{-1}.

TABLE 7

VALUES OF CONDUCTANCE OF ORIFICES AND TUBES, FOR A RANGE OF VALUES OF a FOR AIR AT 25° C

a (cm)	F_0 (liters · sec^{-1})	F_t, Conductance of Tube (liters · sec^{-1}) for Air at 25° C						
		$l/a = 1$	2	4	8	12	16	30
		$K = 0.672$	0.514	0.359	0.232	0.172	0.137	0.080
0.1	0.367	0.246	0.188	0.132	0.085	0.063	0.050	0.029
0.2	1.466	0.986	0.753	0.527	0.340	0.252	0.200	0.117
0.3	3.300	2.217	1.664	1.184	0.764	0.567	0.451	0.263
0.4	5.866	3.943	3.013	2.106	1.358	1.008	0.802	0.468
0.5	9.166	6.160	4.708	3.291	2.122	1.575	1.253	0.731
0.6	13.20	8.872	6.779	4.739	3.057	2.269	1.805	1.052
0.7	17.97	12.08	9.228	6.449	4.161	3.088	2.457	1.432
0.8	23.47	15.77	12.05	8.424	5.436	4.033	3.208	1.871
0.9	29.70	19.96	15.25	10.66	6.879	5.105	4.061	2.368
1.0	36.66	24.64	18.83	13.16	8.492	6.302	5.013	2.922
2.0	146.6	98.56	75.34	52.65	33.97	25.21	20.05	11.69
3.0	330.0	221.7	166.4	118.4	76.42	56.71	45.11	26.30
4.0	586.6	394.3	301.3	210.6	135.8	100.8	80.21	46.77
5.0	916.6	616.0	470.8	329.1	212.2	157.5	125.3	73.10
6.0	1320.0	887.2	677.9	473.9	305.7	226.9	180.5	105.2
7.0	1797.0	1208.0	922.8	644.9	416.1	308.8	245.7	143.2
8.0	2347.0	1577.0	1205.0	842.4	543.6	403.3	320.8	187.1
9.0	2970.0	1996.0	1525.0	1066.0	687.9	510.5	406.1	236.8
10.0	3666.0	2464.0	1883.0	1316.0	849.2	630.2	501.3	292.2

For the range $a = 10$ to $a = 100$ cm, the values of both F_0 and F_t are obviously 100 times those given in the table for the corresponding values in the range $a = 1$ to $a = 10$.

One case of importance in vacuum-tube technique is the determination of the conductance (or "speed") of a *liquid-air* trap.

Let us consider a trap, such as that shown in Fig. 3, in which $2a_2$ = inside diameter of outer cylinder, and $2a_1$ = outside diameter of inner cylinder. For the annular space between the two cylinders, of length l, equation 2 leads to the relation

$$\frac{1}{F_c} = \frac{3}{8}\cdot\frac{4}{v_a}\cdot\frac{l}{\pi(a_2^2 - a_1^2)(a_2 - a_1)} \quad \text{cm}^{-3}\cdot\text{sec}, \tag{26}$$

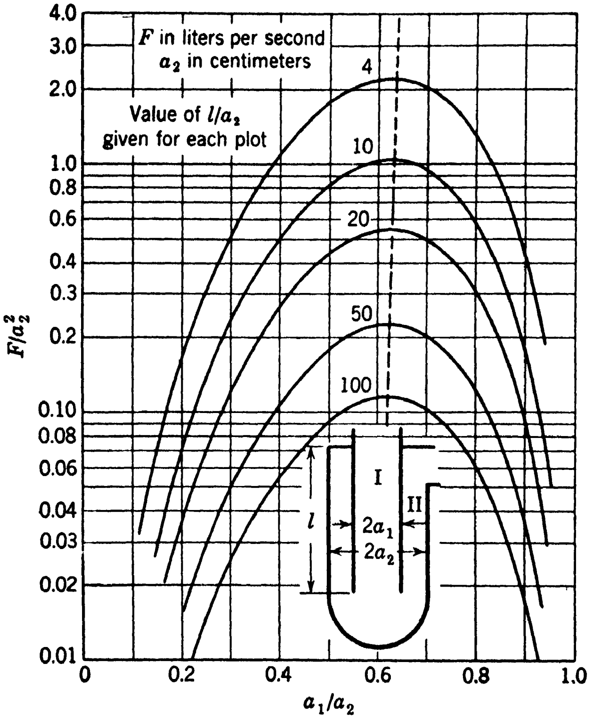

FIG. 3. Plots of F/a_2^2 versus a_1/a_2 for the "molecular" flow of air at 25° C through a liquid-air trap. The ordinates give values of F/a_2^2, where F = conductance in liters · sec^{-1} and a^2 denotes the inside radius (in centimeters) of the outer tube. The abscissas give values of a_1/a_2, where a_1 denotes the inside radius (in centimeters) of the inner tube. Each curve corresponds to the indicated value of l/a_2, where l denotes the total length (in centimeters) of the trap. For large values of l/a_2 the maxima (indicated by the dashed line) occur at the value $a_1 = 0.62a_2$.

that is,

$$F_c = 9700\pi(a_1 - a_2)^2(a_2 + a_1)\frac{1}{l}\sqrt{\frac{T}{M}} \quad \text{cm}^3\cdot\text{sec}^{-1} \tag{27}$$

$$= 97.70(a_2^2 - a_1^2)(a_2 + a_1)\frac{1}{l} \quad \text{liter}\cdot\text{sec}^{-1}$$

for air at 25° C.

It will be observed that for $a_1 = 0$ the last relation is identical with that given in Table 2.

For short tubes an approximate correction may be made by adding the resistance of the orifice to that of the annular space. Hence

$$\frac{1}{F_{c2}} = \frac{1}{F_c} + \frac{4}{v_a} \cdot \frac{1}{\pi(a_2^2 - a_1^2)}$$

$$= \frac{4}{\pi v_a} \cdot \frac{1}{(a_2^2 - a_1^2)} \left\{ 1 + \frac{3l}{8(a_2 - a_1)} \right\}.$$

Assuming that the thickness of the wall is negligible compared to a_1, the resistance of the inside cylinder is

$$\frac{1}{F_{c1}} = \frac{1 + \frac{3}{8}(l/a_1)}{a_1^2} \cdot \frac{4}{\pi v_a}.$$

Hence, the total resistance is given by

$$\frac{1}{F} = \frac{1}{F_{c2}} + \frac{1}{F_{c1}}$$

$$= \frac{4}{\pi v_a} \left\{ \frac{1}{a_2 - a_1^2} + \frac{3l}{8(a_2 - a_1)(a_2^2 - a_1^2)} + \frac{1}{a_1^2} + \frac{3}{8} \frac{l}{a_1^3} \right\}. \quad (28)$$

The problem of interest in designing a liquid-air trap is the calculation of the optimum value of the ratio a_1/a_2. J. M. Lafferty of this laboratory has treated the problem in the following manner:

Let $X = a_1/a_2$, and let $Y = l/a_2$.

Then equation 28 leads to an expression for F, the conductance of the trap, of the form

$$F = \pi a_2^2 \cdot \frac{v_a}{4} \cdot f(X, Y),$$

where

$$f(X, Y) = \frac{X^3(1 - X)(1 - X^2)}{X(1 - X) + \frac{3}{8}Y[X^3 + (1 - X)(1 - X^2)]}.$$

For air at 25° C,

$$F = 36.66 a_2^2 f(X, Y).$$

In Fig. 3 this relation has been used to plot F as a function of X for a series of values of Y. From the approximate method used for the calculation of both F_{c1} and F_{c2}, it is evident that the derived relation may be applied only for values of Y which are greater than at least 4. The dotted curve shows the values of X for maximum conductance at different values of Y. For large values of Y, the *maximum value* of $f(X, Y)$ occurs for $X^2 + X = 1$, that is, for $X = 0.618$.

Hence the *optimum conductance* of a liquid-air trap (for air at 25° C) for given values of a_2 and l is given by the relation

$$F = 0.618 \times 0.382 \times 1.33 \times 36.66 a_2{}^2/Y \tag{29}$$

$$= 11.53 a_2{}^3/l \quad \text{liter} \cdot \text{sec}^{-1},$$

where $a_1 = 0.618a_2$ and $l > 5a_2$.

To the resistance thus calculated must also be added the resistance of the extension of the inner tube and also that of the side connection. Furthermore, the wall thickness of the inside tube may not be negligible compared with the inner diameter of the tube. As illustrations, the following detailed calculations give the values of F for two different traps. For both, $2a_1$ is the *outside* diameter of the inner tube, $2a_2$ the inside diameter of the outer tube, and $2a$ the inside diameter of the inner tube.

Case I. Large Trap.

1. For the *annular space*, $a_1 = 1.59$, $a_2 = 2.38$, $l = 21.6$. Hence

$$F_1 = \frac{97.83 \times 0.79 \times 3.97}{21.6/0.79 + 2.67} \quad \text{liters} \cdot \text{sec}^{-1}$$

$$= 10{,}220 \quad \text{cm}^3 \cdot \text{sec}^{-1}$$

and

$$\frac{1}{F_1} = 9.783 \cdot 10^{-5} \quad \text{cm}^{-3} \cdot \text{sec}.$$

2. For the *inside tube*, $a = 1.40$, $l = 24.1$ (assuming that this tube extends 2.5 cm outside the annular space). Therefore $l/a = 17.22$, $K = 0.13$.

$$F_2 = 36.66 \times (1.40)^2 \times 0.13, \quad \text{liters} \cdot \text{sec}^{-1}$$

$$= 9340 \quad \text{cm}^3 \cdot \text{sec}^{-1}.$$

$$\frac{1}{F_2} = 10.71 \cdot 10^{-5} \quad \text{cm}^{-3} \cdot \text{sec}.$$

3. For the *side tube*, $a = 1.40$, $l = 2.54$, $l/a = 1.81$, $K = 0.537$.

$$F_3 = 36.66 \times (1.40)^2 \times 0.537 \quad \text{liters} \cdot \text{sec}^{-1}$$
$$= 38{,}590 \quad \text{cm}^3 \cdot \text{sec}^{-1}.$$
$$\frac{1}{F_3} = 2.592 \cdot 10^{-5} \quad \text{cm}^{-3} \cdot \text{sec}.$$

Hence,

$$\frac{1}{F} = \frac{1}{F_1} + \frac{1}{F_2} + \frac{1}{F_3} = 23.09 \cdot 10^{-5} \quad \text{cm}^{-3} \cdot \text{sec},$$

and

$$F = 4331 \quad \text{cm}^3 \cdot \text{sec}^{-1}.$$

In this calculation it is assumed that the side tube is only 1 in. long, and that the inner tube extends only 1 in. outside the ring seal at the top. If the inner tube extends 20 in. (50.8 cm), then $F_2 = 3682$ cm$^3 \cdot$ sec^{-1}, and $1/F_2 = 27.16 \cdot 10^{-5}$, with the result that

$$\frac{1}{F} = 39.54 \cdot 10^{-5} \quad \text{and} \quad F = 2529 \quad \text{cm}^3 \cdot \text{sec}^{-1}.$$

Case II. Small Trap.

1. For *annular space*, $a_1 = 0.95$, $a_2 = 1.35$, $l = 19.05$. Hence

$$F_1 = 1812 \quad \text{cm}^3 \cdot \text{sec}^{-1}.$$
$$\frac{1}{F_1} = 5.518 \cdot 10^{-4}.$$

2. For the *inside tube*, $a = 0.794$, $l = 71.2$ cm,

$$F_2 = 687.3 \quad \text{cm}^3 \cdot \text{sec}^{-1}.$$
$$\frac{1}{F_2} = 14.55 \cdot 10^{-4}.$$

3. For the *side tube*, $a = 0.794$, $l = 8$, $K = 0.172$,

$$F_3 = 3968 \quad \text{cm}^3 \cdot \text{sec}^{-1}.$$
$$\frac{1}{F_3} = 2.520 \cdot 10^{-4}.$$

Hence $1/F = 1/F_1 + 1/F_2 + 1/F_3 = 22.59 \cdot 10^{-4}$, and

$$F = 442.7 \quad \text{cm}^3 \cdot \text{sec}^{-1}.$$

In this case, also, the major part of the resistance is contributed by the long length of the inside tube. Since $1/F$ varies as l/a^3 it is obvious that, whenever it is necessary to use a long length of tube, the diameter should be made as large as practicable.

It should be observed that at the temperature of liquid air ($T = 90$ approximately) the conductance for any gas will be $\sqrt{90/298} = 0.55$ times that for the same gas at 25° C. (See pages 65–67.)

Knudsen's equations for flow have been tested not only by Knudsen himself, but also by W. Gaede[12] and W. Klose.[13] Gaede measured the rate of flow of hydrogen through a narrow slit between two plates. The observed deviations from Knudsen's deductions were due, presumably, to formation of a film of adsorbed gas on the walls, which would lead to a decrease in the value of the coefficient of slip. (See equation 1.12.)

Klose determined rates of flow at low and intermediate pressures through cylindrical tubes. He used not only straight tubes, but also tubes bent into the shape of right angles as well as large-bore taps. He compared the observed results with those calculated (a) on the basis of Poiseuille's law with correction for slip (discussed in section 1) and (b) on the basis of Knudsen's semi-empirical relations discussed in section 3. His conclusions were as follows:

At very low pressures, where L is greater than a, Knudsen's equations for molecular flow represent the observations very satisfactorily. The value of F depends *only on the total length of path* and on the values of a for different sections. *The introduction of bends or wide-bore taps has no effect.* At normal pressures, where L is very much less than a, Poiseuille's law applies very accurately. For intermediate pressures, observations on rates of flow of nitrogen through cylindrical tubes (85 to 92 cm in length and values of a ranging from 0.1 to 0.35 cm) were in better agreement with Knudsen's relations (discussed in the following section) than with those in which a correction for slip is introduced.

Klose also observed the minimum in the value of F at low pressures, as predicted by Knudsen's theory. With increase in pressure above the range of application of Knudsen's theory of molecular flow, the values of F exhibited a gradual increase.[14]

From the above equations for F it follows that for different gases F varies inversely as $\sqrt{\rho_1}$, that is, inversely as $\sqrt{M}$. This indicates a method for the separation of gases of different molecular weights which has been applied very successfully in certain cases. For instance, by means of porous walls G. Hertz[15] and his associates have effected a partial separation of the isotopes of helium, carbon, and nitrogen, while A. Farkas[16] has been able to separate completely the isotopes of hydrogen (H_2 and D_2).

---

[12] *Ann. Physik,* **41,** 289 (1913).

[13] *Physik. Z.,* **31,** 503 (1930); *Ann. Physik,* **11,** 73 (1931).

[14] See discussion in the following section.

As shown in a subsequent section, the capillaries in porous diaphragms correspond to values of the radius ranging from 1 to $5 \cdot 10^{-5}$ cm. Consequently flow of molecular type occurs through such diaphragms at pressures of 10^{-2} to 10^{-1} atmosphere.

It is also evident that such porous walls should be especially useful for removing traces of lighter gases from a gas of heavier molecular weight.

3. FLOW AT INTERMEDIATE PRESSURES

Equation 1.14 was deduced on the basis of Maxwell's theory of slip. M. Knudsen[17] approached the problem from a more empirical point of view and as the result of a series of measurements he deduced the following relation for flow

$$F = \alpha_1 P_{\mu ba} + \alpha_2 \left(\frac{1 + c_1 P_{\mu ba}}{1 + c_2 P_{\mu ba}} \right) \quad \text{cm}^3 \cdot \text{sec}^{-1}, \tag{1}$$

where

$$P_{\mu ba} = \text{average pressure in } \textit{microbars},$$

$$\alpha_1 = \frac{\pi}{8\eta} \cdot \frac{a^4}{l} = \frac{0.3926}{\eta} \frac{a^4}{l} \quad \text{cm}^3 \cdot \text{sec}^{-1} \cdot \text{microbar}^{-1}, \tag{1.2}$$

$$\alpha_2 = \frac{2}{3} \cdot \frac{a}{l} A v_a = 30{,}476 \frac{a^3}{l} \sqrt{\frac{T}{M}} \quad \text{cm}^3 \cdot \text{sec}^{-1}, \tag{2.8}$$

$$c_1 = 2a \frac{\sqrt{\rho_1}}{\eta}, \tag{2a}$$

and

$$c_2 = 2.47a \frac{\sqrt{\rho_1}}{\eta}. \tag{3a}$$

---

[15] *Z. Physik*, **79**, 108 (1932); H. Harmsen, *Z. Physik*, **82**, 589 (1933), and H. Harmsen, G. Hertz, and W. Schutze, *Z. Physik*, **90**, 703(1934). Also see R. M. Barrer, *Diffusion in and through Solids*, Macmillan and Company, Cambridge, England, 1941 (designated RB), for a more detailed discussion of these investigations.

[16] *Light and Heavy Hydrogen*, Cambridge University Press, 1935, p. 120.

[17] *Ann. Physik*, **28**, 75 (1909).

Substituting for η and ρ_1, we obtain the relations

$$c_1 P_{\mu ba} = 2.507 \frac{a}{L_a'} = 2.507 \frac{aP_{\mu ba}}{L_{1m}} \tag{2b}$$

$$c_2 P_{\mu ba} = 3.095 \frac{a}{L_a'} = 3.095 \frac{aP_{\mu ba}}{L_{1m}} \tag{3b}$$

where L_a' = mean free path (in centimeters) at $P_{\mu ba}$ and L_{1m} = mean free path (in centimeters) at 1 microbar.

Since $P_{\mu ba} = \frac{4}{3}P_{\mu a}$, where $P_{\mu a}$ = average pressure in *microns*, and $L_{1m} = \frac{4}{3}L_1$, where L_1 = mean free path in cm at 1 micron, equation 1 can be expressed in terms of $P_{\mu a}$, the *average pressure in microns*, as follows:

$$F = \frac{0.5236}{\eta} \cdot \frac{a^4}{l} P_{\mu a} + 3.048 \cdot 10^4 Z \frac{a^3}{l} \sqrt{\frac{T}{M}} \quad \text{cm}^3 \cdot \text{sec}^{-1}, \tag{4}$$

where

$$Z = \frac{1 + 2.507 aP_{\mu a}/L_1}{1 + 3.095 aP_{\mu a}/L_1}. \tag{5}$$

For $P_{\mu a}$ very small compared to L_1/a, $Z = 1$, and equation 4 becomes identical with equation 2.8. For $P_{\mu a}$ very large compared to L_1/a, $Z = 0.81$, and equation 4 becomes practically identical with 1.3*a*. Thus equation 1 or 4 represents the conductance as the sum of two parallel conductances—one corresponding to Poiseuille flow, and the other to Knudsen flow.

It will be observed that equation 2.8 expresses the value of F_t for a *very long tube* ($l/a > 100$ approximately), since this is also the condition under which the expression used for α_1 (equation 1) is valid.[18]

In terms of d_i, the diameter of the capillary in inches, and l_i, the length in inches, equation 4 becomes

$$F = \frac{0.5362}{\eta} \frac{d_i^4}{l_i} P_{\mu a} + 2.458 \cdot 10^4 Z_i \frac{d_i^3}{l_i} \sqrt{\frac{T}{M}} \quad \text{cm}^3 \cdot \text{sec}^{-1}, \tag{6}$$

where

$$Z_i = \frac{1 + 3.184 d_i P_{\mu a}/L_1}{1 + 3.931 d_i P_{\mu a}/L_1} \tag{7}$$

and L_1 = mean free path *in centimeters* at 1 micron.

---

[18] An interesting application of equation 4 to the flow of gas in the mass spectrometer has been published by R. E. Honig, *J. Applied Phys.*, **16**, 646 (1945). It should be noted that Fig. 3 in this paper applies to a capillary of diameter 0.066 mm (not cm).

For air at 25° C ($\eta = 1.845 \cdot 10^{-4}$),

$$F = 2.838 \frac{a^4}{l} P_{\mu a} + 97.75 Z \frac{a^3}{l} \quad \textit{liters} \cdot \mathrm{sec}^{-1} \tag{8}$$

$$= 2.906 \frac{d_i^4}{l_i} P_{\mu a} + 78.81 Z \frac{d_i^3}{l_i} \quad \textit{liters} \cdot \mathrm{sec}^{-1}. \tag{9}$$

A very convenient expression for F may be derived in terms of a/L_a, as follows:

Substituting from the relation

$$\eta = 0.5 \rho v_a L,$$

equation 1 becomes

$$F = \frac{v_a A}{4(l/a)} \left[\frac{\pi}{8} \cdot \frac{a}{L_a} + \frac{8}{3} \left(\frac{1 + 2.507a/L_a}{1 + 3.095a/L_a} \right) \right], \tag{10}$$

in which $a/L_a = aP_{\mu a}/L_1$, the pressure is expressed in microns, and L_1 = mean free path at 1 micron.

Differentiating the expression in the large brackets with respect to a/L_a, it is readily shown that F is a minimum[19] for

$$\frac{a}{L_a} = \frac{1}{3.095} = 0.323.$$

Since $\frac{3}{8} \cdot \pi/8 = 0.1472$, equation 8 can be expressed in the very simple form

$$F = F_t \left(0.1472 \frac{a}{L_a} + Z \right), \tag{11}$$

where Z is expressed by equation 5, and

$$F_t = 30.48 \frac{a^3}{l} \sqrt{\frac{T}{M}} \quad \text{liters} \cdot \mathrm{sec}^{-1}$$

$$= 24.58 \frac{d_i^3}{l_i} \sqrt{\frac{T}{M}} \quad \text{liters} \cdot \mathrm{sec}^{-1}.$$

Table 8 gives values of $0.1472a/L_a$, of Z, and of F/F_t for a range of values of $a/L_a = aP_{\mu a}/L_1$.

It will be observed that, for a/L_a greater than about 100, the Poiseuille term is the predominant one, while for a/L_a less than about 1, the Knudsen term becomes important.

---

[19] This is in agreement with Knudsen's deduction, when account is taken of the fact that he made use of the relation $\eta = 0.3097 \rho v_a L$.

TABLE 8

RATIO OF CONDUCTANCE OF CYLINDRICAL TUBE (F) TO THAT FOR MOLECULAR FLOW (F_t) AS A FUNCTION OF a/L_a

a/L_a	$0.1472\ (a/L_a)$	Z	F/F_t
10^4	1472.0	0.810	1472.81
10^3	147.2	0.810	148.01
10^2	14.72	0.810	15.53
10	1.472	0.816	2.288
5	0.736	0.822	1.558
1	0.147	0.857	1.004
0.5	0.074	0.885	0.959
0.323	0.047	0.905	0.952 (minim.)
0.2	0.029	0.933	0.962
0.1	0.015	0.955	0.970
0.05	0.007	0.974	0.981
0.01	0.002	0.995	0.997
0	0	1.000	1.000

These conclusions may also be expressed as follows: Replacing L_a by $L_1/P_{\mu a}$, where $P_{\mu a}$ is the *average pressure* along the tube, *in microns*, the data in the above table show that, for *values of* $aP_{\mu a}$ *greater than 100* L_1, the flow is *almost completely viscous*, while for values of $aP_{\mu a}$ *less than* L_1, *the flow is over 95 per cent molecular*. Figure 4 shows a semi-log plot of F/F_t as a function of $aP_{\mu a}/L_1$.

For instance, for air at 25° C, $L_1 = 5.09$ cm. Hence, the Poiseuille law is applicable for values of the average pressure above $509/a$ microns, while the relations for molecular flow are applicable in the range below $5.09/a$ microns. Furthermore, the minimum value of F occurs at $P_{\mu a} = 1.644/a$ microns, and it should be carefully noted that, in these relations, a = *radius* of tube in centimeters.

As an illustration of the application of the data in Table 8, it is of special interest to calculate the rate of leak of air through a "pinhole" in an evacuated device at atmospheric pressure and 25° C.

In this case, $P_{\mu 2} = 7.6 \cdot 10^5$, $P_{\mu 1} = 0$, and $P_{\mu a} = 3.8 \cdot 10^5$. For air at 25° C, $L_1 = 5.09$ cm.

Now let us assume two sizes of holes:

1. $l = 0.1$ cm, $a = 5 \cdot 10^{-5}$ cm (0.25 mil diameter),
2. $l = 0.1$ cm, $a = 5 \cdot 10^{-4}$ cm (2.5 mil diameter).

Hence we derive the following results:

1. $a/L_a = 3.73$, $F/F_t = 1.4$, and $Q = FP_{\mu 2} = 3.75$ micron · liters per *hour*.
2. $a/L_a = 37.3$, $F/F_t = 6.3$, and $Q = 4.48$ micron · liters per *second*.

As will be observed from the values of F/F_t, the ratio of viscous to molecular flow is greater for the larger-diameter capillary. Also, case 1 serves to emphasize the fact that, even for a very fine hole, the rate of leak may be quite considerable.

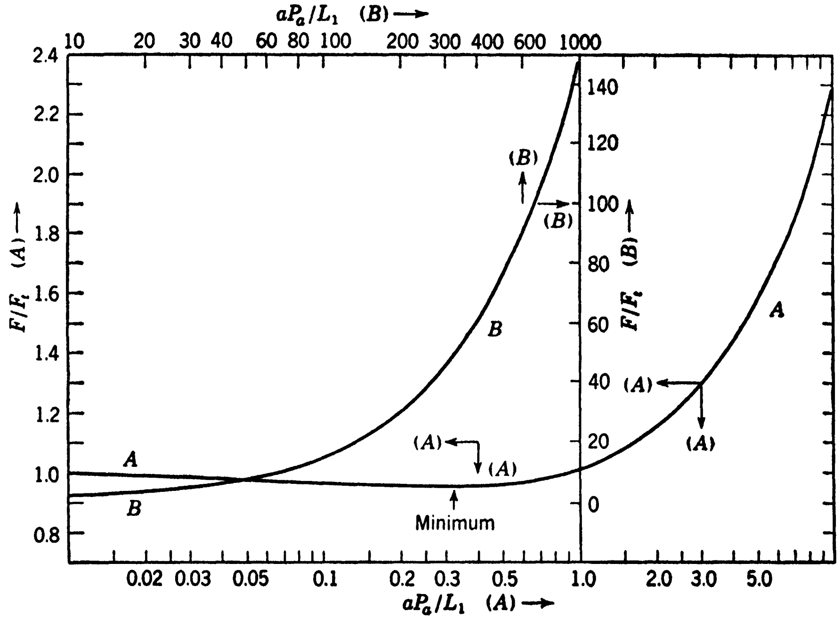

FIG. 4. Plot of ratio F/F_t versus aP_a/L_1 for cylindrical tube where P_a = average pressure in microns, a = radius of tube (centimeters), and L_1 = mean free path (centimeters) at 1 micron. F = conductance for P_a, F_t = conductance for "molecular" flow. For curve A use scales (A), and for curve B, scales (B), as indicated by directions of arrows.

For air at 25° C, equation 11 can be written in the form

$$F = F_t\left(0.0290aP_{\mu a} + \frac{1 + 0.493aP_{\mu a}}{1 + 0.608aP_{\mu a}}\right) \text{ liters}\cdot\text{sec}^{-1}, \qquad (12)$$

where F_t is expressed in liters · sec^{-1}, as above.

Also, the rate of flow,

$$Q_{\mu l} = F\,(P_{\mu 2} - P_{\mu 1}) \quad \text{micron}\cdot\text{liters}\cdot\text{sec}^{-1}. \qquad (13)$$

From the last two equations it follows that, in the range of molecular flow, Q varies linearly with the value of $(P_{\mu 2} - P_{\mu 1})$, while in the range of viscous flow Q varies with the value of $(P_{\mu 2}^2 - P_{\mu 1}^2)$. Figure 5 shows a plot log Q versus log $P_{\mu 2}$ for a capillary 100 cm long with 0.51-cm

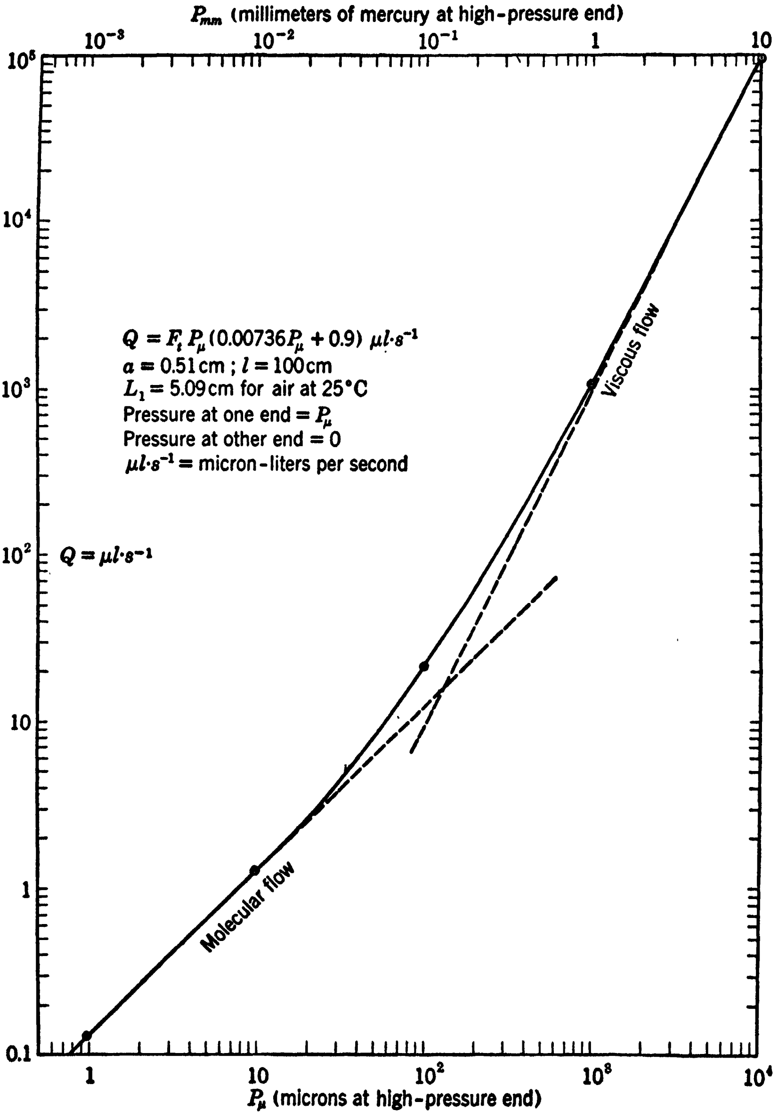

FIG. 5. Rate of flow of air at 25° C in micron · liters/sec as a function of pressure P_μ at inlet and $P = 0$ at other end.

radius. At low pressures, the slope is unity. With increase in pressure the slope increases, and at the higher pressures it becomes 2. The plot shows the transition region of pressures in which the rate of flow changes character. At very low pressures (less than 1μ), $F_t = 0.163$ liter · sec^{-1}. The value $Z = 0.9$ in the parentheses is used as an average over the range of pressures in the transition region.

In terms of d_i = diameter in inches, l_f = length in feet, and cu ft · min^{-1}, equation 12 takes the form

$$F = 13.92\frac{d_i^3}{l_f}\left(0.0368d_iP_{\mu a} + \frac{1 + 0.626d_iP_{\mu a}}{1 + 0.772d_iP_{\mu a}}\right) \quad \text{cu ft} \cdot \text{min}^{-1} \qquad (14)$$

and

$$Q_{\mu c} = F(P_{\mu 2} - P_{\mu 1}) \quad \text{micron} \cdot \text{cu ft} \cdot \text{min}^{-1}.$$

It will be observed that in equations 8 and 12,

$$2.838 = 0.1472 \times \frac{97.75}{5.09}$$

$$0.0290 = \frac{0.1472}{5.09}.$$

In the case of an orifice in a very thin wall, the relation for F_0 is the same as at low pressures for d less than L_a, where d corresponds to the diameter of the circular orifice or longest dimension of the non-circular orifice.

In equations 10 and 11 and in Table 8, F is expressed as a function of F_t (the conductance for molecular flow) and a/L_a; it is also possible to derive an expression for F as a function of the conductance for Poiseuille, or viscous, flow and L_a/a.

In a very significant paper by G. P. Brown, A. DiNardo, G. K. Cheng, and T. K. Sherwood[20] the relation deduced for the conductance is of the form (see equation 1.13),

$$F = F_P\left[1 + 4\left(\frac{2}{f} - 1\right)\frac{L_a}{a}\right], \qquad (15)$$

where

$$F_P = \text{conductance for Poiseuille flow}$$
$$= \frac{1.33\pi a^4 P_{\mu a}}{8\eta l} = \frac{0.5236}{\eta}\frac{a^4}{l}P_{\mu a} \quad \text{cm}^3 \cdot \text{sec}^{-1},$$

---

[20] *J. Applied Phys.*, **17**, 802 (1946). See also two papers by W. P. Dryer, in *Chem. Eng.*, **54**, November and December, 1947, in which the relations derived in the first three sections of this chapter, as well as in section 5, have been presented in a form convenient for use by engineers in designing vacuum systems.

and f denotes Maxwell's constant corresponding to the fraction of the gas molecules striking the walls that is diffusely reflected.

From a comparison with equation 4 it follows that we should obtain the relation

$$4F_P\left(\frac{2}{f} - 1\right)\frac{L_a}{a} = \frac{2a}{3l} \cdot \pi a^2 v_a \cdot Z, \tag{16}$$

where Z is defined by equation 5.

For $l/a > 100$, and $Z = 1$ (region of molecular flow), this leads to the value $f = 0.74$. A comparison of values of F actually observed by previous investigators with those calculated by means of the last equation leads to the value $f = 0.77$. For higher pressures the calculated value of f is found to be 0.84. The above-mentioned authors have shown that for the flow of air in iron and copper pipes values of F in agreement with those observed may be obtained by assuming $f = 0.90$. The original paper also contains a chart from which F may be calculated for a range of values of L_a/a.

4. FLOW OF GASES THROUGH POROUS DIAPHRAGMS

In terms of A_a, the average pressure in atmospheres, equation 3.4 has the form

$$F = \frac{3.978 \cdot 10^5}{\eta} \frac{a^4}{l} A_a + 3.048 \cdot 10^4 Z \frac{a^3}{l}\sqrt{\frac{T}{M}} \quad \text{cm}^3 \cdot \text{sec}^{-1}. \tag{1}$$

This equation has been applied by H. Adzumi[21] in interpreting his observations and those of others on the *rate of flow of gases through porous walls.*

According to Adzumi a porous diaphragm may be regarded as a network of capillaries which are connected both in series and in parallel. Hence, a^4/l and a^3/l in the above equation should be replaced by the equivalent "conductances,"

$$\alpha = \sum \frac{1}{\sum l_i/r_i^4} \quad \text{and} \quad \beta = \sum \frac{1}{\sum l_i/r_i^3} \cdot$$

Furthermore, Adzumi assumes for Z an average value of 0.9. Consequently, equation 1 may be replaced by the equation

$$F = \frac{3.978 \cdot 10^5}{\eta} \cdot \alpha A_a + 2.743 \cdot 10^4 \beta \sqrt{\frac{T}{M}} \tag{2}$$

$$= cA_a + b, \tag{3}$$

---

[21] *Bull. Chem. Soc. Japan,* **12**, 304 (1937). The topic is also discussed comprehensively in RB, p. 65.

where $c = 3.798 \cdot 10^5\alpha/\eta \quad \text{cm}^3 \cdot \text{atm}^{-1} \cdot \text{sec}^{-1}$,

$$b = 2.743 \cdot 10^4\beta\sqrt{T/M} \quad \text{cm}^3 \cdot \text{sec}^{-1}.$$

Let d denote the thickness (in centimeters) and S the area (in square centimeters) of the porous plate, and let

$$\alpha_0 = \frac{\alpha d}{S}; \quad \beta_0 = \frac{\beta d}{S}. \tag{4}$$

If all pores in the plate have a uniform radius, R, and N is the number of pores per unit area, then

$$\alpha_0 = NR^4 \quad \text{and} \quad \beta_0 = NR^3.$$

Consequently,

$$R = \frac{\alpha_0}{\beta_0} \quad \text{and} \quad N = \frac{\beta_0{}^4}{\alpha_0{}^3}. \tag{5}$$

That is,

$$R = \frac{2.743c\eta}{37.98b}\sqrt{\frac{T}{M}} \tag{6}$$

and

$$N = \frac{10^{-4}}{2.743} \cdot \frac{bd}{SR^3}\sqrt{\frac{M}{T}}. \tag{7}$$

Adzumi has applied these relations to observations made by J. Sameshima[22] on the rates of flow of seven gases through an unglazed earthenware plate, at 25° C and at the following pressures: $A_2 = 1.0, 1.5, 2.0, 2.5$ atm, and $A_1 = 0$, so that $A_a = 0.5, 0.75, 1.0$, and 1.25 atm, respectively. The gases used included CH_4, NH_3, C_2H_2, C_2H_4, air, O_2, and CO_2. For all these gases over the whole range of pressures, Adzumi deduced the relation

$$F = \frac{7.282 \cdot 10^{-6}}{\eta}A_a + \frac{0.1636}{\sqrt{M}} \quad \text{cm}^3 \cdot \text{sec}^{-1}. \tag{8}$$

For instance, for air ($\eta = 1.845 \cdot 10^{-4}$ and $M = 29$) the last equation becomes

$$F = 3.945 \cdot 10^{-2}A_a + 0.03038,$$

which leads to the conclusion that, for $A_a = 0.5$ atm,

$$F = 0.01972 + 0.03038 = 0.05010.$$

---

[22] *Bull. Chem. Soc. Japan*, **1**, 5 (1926).

That is, for $A_2 = 1$ and $A_1 = 0$ atm, the rate of flow is 0.0501 cm^3/sec, measured at atmospheric pressure.

Adzumi also investigated the rate of flow of *air at 20° C*, through a number of other types of porous plates. Table 9 gives a brief description and values d and S for the plates used.

TABLE 9

DIMENSIONS OF POROUS PLATES USED FOR DETERMINATION OF RATES OF FLOW OF AIR AT 20° C

		d (cm)	S (cm^2)
I	Porous plate used by Sameshima	0.15	0.28
II	Compact plate used in organic preparations	.27	2.22
III	Rough plate used in organic preparations	.41	2.22
IV	Mantel of a Daniell cell (white)	.2	0.27

Table 10 gives observed values (for air) of c and b in equation 3, and also derived values of α, β, R, and N.

TABLE 10

VALUES OF CONSTANTS IN EQUATION 3 CALCULATED FROM RATES OF FLOW

Plate	10^2c	10^2b	$10^{11}\alpha$	$10^7\beta$	10^5R	$10^{-5}N$
I	3.945	3.038	1.83	3.45	5.3	12.
II	0.9705	1.430	0.45	1.64	2.77	2.4
III	1.790	1.500	0.83	1.72	4.84	2.8
IV	2.372	5.948	1.10	6.82	1.61	960.

The values deduced for N and R are, of course, to be regarded merely as indicating the magnitudes of these numbers.

Of the four samples of porous plate discussed by Adzumi, II has the lowest conductance. For $A_2 = 1$ and $A_1 = 0$, the rate of flow through this plate is 0.019 $cm^3 \cdot sec^{-1}$, measured at 1 atm. At $A_2 = 0.1$ and $A_1 = 0$, the rate of flow is 0.00148 $cm^3 \cdot sec^{-1}$, measured at 1 atm, of which about 97.3 per cent is of the free-molecule type of flow.

In terms of the gas "permeability," per unit area, of a porous plate, designated by P_G, it will be observed that

$$P_G = \frac{2AV}{St(A_2 - A_1)(A_2 + A_1)}, \tag{9}$$

where S = area of plate and AV = quantity of gas flowing through the plate in time t, for a pressure difference $A_2 - A_1$. Hence

$$P_G = \frac{2F}{S(A_2 + A_1)} = \frac{F}{SA_a}, \tag{10}$$

where F = conductance, and A_a = average pressure.

These observations and conclusions regarding the flow of gases through porous diaphragms have been applied in this laboratory to the development of calibrated leaks.

5. RATE OF EXHAUST THROUGH A TUBE OR ORIFICE

In vacuum work the problem often occurs of determining the effect on rate of exhaust of a given admittance F between the volume, V, that is being exhausted, and the pump. Since we shall consider, in a subsequent section, the subject of high-vacuum, high-speed pumps, we shall assume in the following discussion that the speed of the pumps is sufficiently high to maintain the pressure $P = 0$ at the pump inlet. That is, we assume that the whole drop in pressure occurs in the conductance F.

Let P designate the pressure (in *microbars*) in the volume V at any instant during the exhaust. Then, the rate of exhaust, that is, the volume of gas in cubic centimeters (measured at 1 microbar) removed per second is given by the relation

$$-V\frac{dP}{dt} = FP. \tag{1}$$

For the whole range of pressures, from atmospheric to very low pressure, F varies with P in the manner shown in equations 3.1, 3.8, and 3.9. For the purpose of solving the differential equation given above, we shall assume the validity of the approximate relation, derived from equation 3.11,

$$F = 0.0736\frac{a}{c}F_tP + F_t, \tag{2}$$

where $P = 2P_a$, and c = mean free path at 1 microbar.

As is evident from the data in Table 8, the error involved in using the assumption $Z = 1$ does not exceed 10 per cent in the range $10 > a/L_a >$ 0.5 microbar, and is less than this in the higher-pressure and very low-pressure regions.

Introducing equation 2 into 1, the latter assumes the form

$$-\frac{dP}{dt} = bP^2 + kP, \tag{3}$$

where

$$b = 0.0736\frac{aF_t}{cV} \tag{4}$$

and

$$k = \frac{F_t}{V}. \tag{5}$$

Hence

$$-\frac{dP}{P} + \frac{dP}{(P + k/b)} = k\,dt.$$

Integrating the last equation, we obtain the result

$$\ln\left(\frac{P_1}{P_2}\right) - \ln\left(\frac{P_1 + k/b}{P_2 + k/b}\right) = k(t_2 - t_1), \tag{6}$$

where P_1 = pressure at t_1, P_2 = pressure at t_2, and t_2 is greater than t_1, so that $P_1 > P_2$. The symbol ln is used to indicate logarithms to base ϵ.

Converting to ordinary logs, equation 6 becomes

$$\log\left(\frac{P_1}{P_2}\right) - \log\left(\frac{P_1 + k/b}{P_2 + k/b}\right) = \frac{k}{2.303}(t_2 - t_1). \tag{7}$$

There are two limiting cases for which equation 6 or 7 assumes a simpler form.

Case I. P_2 is very much greater than k/b. This is valid, in general, for $P_2 \geqslant 100$ microbars (75 microns).

Since

$$\ln\left(P + \frac{k}{b}\right) - \ln P \doteq \ln\left(1 + \frac{k}{bP}\right) = \frac{k}{bP},$$

equation 6 becomes

$$\frac{1}{b}\left(\frac{1}{P_2} - \frac{1}{P_1}\right) = t_2 - t_1. \tag{8}$$

That is, $1/P$ *varies linearly with* t.

Case II. P is very much less than k/b. This is valid in general in the range $P_1 \leqslant 1$ microbar. Equation 7 then becomes

$$\log\left(\frac{P_1}{P_2}\right) = \frac{k}{2.303}(t_2 - t_1)$$

or

$$t_2 - t_1 = \frac{2.303}{k}\log\left(\frac{P_1}{P_2}\right) \tag{9}$$

$$= \frac{2.303V}{F_t}\log\left(\frac{P_1}{P_2}\right). \tag{10}$$

For $P_1/P_2 = 10$,

$$t_2 - t_1 = \Delta t_0 = \frac{2.303V}{F_t}. \tag{11}$$

We shall designate Δt_0 the interval of time required to reduce the pressure in V to *one-tenth* its instantaneous value, as the *time constant* of the conductance $F = F_t$ for the volume V. Evidently Δt_0 varies linearly with V.

Although it is customary in such an equation as 9 to designate, as the time constant, that value of $(t_2 - t_1)$ which reduces the pressure to $1/\epsilon$th (36.79 per cent) of its value at any given instant, the definition given in equation 11 is evidently much more convenient for practical applications in high-vacuum technique. It is obvious that, if we plot P against t on semi-log paper, Δt_0 may be obtained directly from the straight-line plot. Furthermore $2\Delta t_0$ is the period required to reduce the pressure to 1 per cent, $3\Delta t_0$, the period to reduce the pressure to 0.1 per cent of its value at any instant, and so forth.

For the range of pressures intermediate between cases I and II, equation 7 must be used.

We shall now consider two illustrations of the application of the above relations. In both we shall assume air at 25° C, for which $c = 6.78$ cm at 1 microbar.

Case I. $V = 5000\ \text{cm}^3$, $l = 100$ cm, $a = 0.5$. For this tube, as shown in section 2, $F_t = 122.2\ \text{cm}^3 \cdot \text{sec}^{-1}$. Hence

$$b = 1.326 \cdot 10^{-4}$$

$$k = 2.444 \cdot 10^{-2}$$

$$\frac{2.303}{k} = 94.2\ \text{sec} = \Delta t_0$$

$$\frac{k}{b} = 184.2\ \text{microbar} = 138\mu.$$

Table 11 gives values of $t_2 - t_1$ and of the total time (in seconds) for the reduction of pressure in the system. The values of P_1 and P_2 are given in *microbars*.

It will be observed that the interval of time required to reduce the pressure from 10^6 microbar (= 750 mm) to 1 microbar (= 0.75 micron) is just slightly greater than that required to reduce the pressure from 1 to 0.01 microbar.

Case II. $V = 100$ liters, $l = 20$, $a = 10$. Hence $l/a = 2$, $K = 0.5136$, and $F_t = KF_0 = 1883\ \text{liters} \cdot \text{sec}^{-1}$.

TABLE 11

RATE OF EXHAUST OF AIR THROUGH A TUBE FOR WHICH $l = 100$ CM AND $a = 0.05$ CM

P_1	P_2	$t_2 - t_1$	Total Time
10^6	10^5	0.0678	
10^5	10^4	0.678	0.746
10^4	10^3	6.16	6.91
10^3	10^2	35.8	42.7
10^2	10	78.6	121.3
10	1	92.3	213.6
1	0.1	94.2	307.8
0.1	0.01	94.2	402.0

In this case, the interval of time required to reduce the pressure to that at which molecular flow occurs is so extremely low that the only value of interest is that of Δt_0. From the preceding relations it follows that

$$\Delta t_0 = \frac{2.303V}{KF_0} = \frac{2.303 \cdot 100}{1883}$$
$$= 0.123 \text{ sec.}$$

A comparison of equations 8 and 11 shows that the interval of time required to reduce the pressure in a system from atmospheric to that at which molecular flow begins is relatively short when compared with the interval required for further reduction of the pressure to the order of 10^{-3} microbar (or micron). This follows from the fact that, in the viscous-flow range, the conductance varies as a^4, whereas in the molecular-flow range it varies as a^3. Hence, for large values of a, the first period is negligible in comparison with the second. This may be illustrated quantitatively by the following example.

From equation 8 it follows that, for $P_2 = 0.1P_1$,

$$t_2 - t_1 = \frac{9}{bP_1} = \frac{122.3cV}{P_1 a F_t}.$$

Hence it follows from equation 11 that

$$\frac{t_2 - t_1}{\Delta t_0} = \frac{53.1c}{P_1 a}. \qquad (12)$$

For air at 25° C, $c = 6.78$ cm at 1 microbar. Let us assume $P_1 = 10^4$ microbars. Then the ratio

$$\frac{t_2 - t_1}{\Delta t_0} = \frac{3.60 \cdot 10^{-2}}{a}.$$

For $a = 0.5$, the ratio has the value 0.072 (which is in agreement with the value 6.78/94.2 shown in Table 11); for $a = 10$, the ratio has the value 0.0036. That is, for the reduction of the pressure to one-tenth its value at any instant, the time required in the viscous-flow range of pressures is 0.36 per cent of that required in the molecular-flow range.

In section 2, Table 6 gives values of F for a range of sizes of tubes and orifices. The last column in this table gives values of $2303/F_t$, that is of Δt_0 for $V = 1000\ \text{cm}^3$. (F_t and V should be given in the *same* units of volume.)

Since $1/F_t$ corresponds to a resistance, and the total resistance of two or more resistances in series is given by the relation

$$\frac{1}{F} = \frac{1}{F_1} + \frac{1}{F_2} + \cdots, \tag{13}$$

it follows that $\Delta t_0 =$ time constant for the total resistance

$$= (\Delta t_0)_1 + (\Delta t_0)_2 +. \tag{14}$$

That is, the time constant of a series of tubes is equal to the sum of the time constants for each element of the series. For instance, the time constant of a tube in series with a stopcock and another tube is equal to the sum of the time constants for each of the sections.

It is also important to observe that, whereas Δt_0 is a constant which has the same value *independently of the unit of pressure* (whether microbars, microns, or millimeters of mercury), the value of b depends upon the unit of pressure. Let b_{mm} denote the value for P_{mm}, and $b_{\mu b}$ the value for $P_{\mu b}$. Then, it follows that

$$b_{mm} = 133b_{\mu b} \tag{15}$$

and

$$\frac{k}{b_{mm}} = \frac{1}{1333}\frac{k}{b_{\mu b}}. \tag{16}$$

It should be noted that in deducing equation 9 it was assumed that the values of P_1 and P_2 are large compared with that of the ultimate pressure P_s observed at the low-pressure end of the tube (of conductance F_t). If, however, this condition is not satisfied, then P_1 and P_2 in equation 9 should be replaced by $P_1 - P_s$ and $P_2 - P_s$, respectively. Obviously P_s should be expressed in the same units as P_1 and P_2.[23]

---

[23] See remarks in Chapter 3, section 2.

Note added during final proofreading: In connection with the topics discussed in this chapter, see also C. E. Norman, *Ind. Eng. Chem.*, **40**, 783 (1948).

CHAPTER 3

MECHANICAL PUMPS

1. HISTORICAL REVIEW

Before the advent of the carbon-filament lamp (1879), interest in the properties of gases at low pressures was manifested by relatively few investigators. Hittorf in Germany and Crookes in England made important observations on electric discharges in gases at pressures ranging as low as a fraction of a millimeter of mercury, and the Geissler discharge tube was a familiar showpiece in lectures on physics. To obtain the pressures required for such electric discharge tubes and other experiments at low pressures, piston pumps were generally used, which reduced the pressure to about 0.25 mm of mercury. For still lower pressures recourse was had to the hand-operated Toepler pump.

With the introduction of incandescent-filament lamps and the consequent need for vacuum pumping equipment, rotary oil pumps were adopted, by which vacua of the order of 10^{-1} to 10^{-2} mm could be obtained. These pumps, towards the development of which W. Gaede made important contributions, exhausted into a "rough" vacuum of about 1 to 2 cm of mercury which, in turn, was obtained by means of a large rotary oil pump, operating against atmospheric pressure. Incidentally, it should be mentioned that, in order to obtain the much lower pressures required for efficient operation and long life of lamps, "getters" were applied to the filaments. After seal-off these materials were flashed off the filament and "cleaned-up" the residual gases.[1]

In 1905 Gaede introduced his rotary mercury pump, and a little later the rotary oil pump was applied widely in the manufacture of incandescent lamps, as mentioned above. Although with the mercury pump, backed up by the oil pump, it was possible to attain pressures as low as 10^{-1} micron, the speed obtained was quite low. A radically new departure in the design of vacuum pumps was represented by the invention by Gaede, in 1913, of the "molecular" pump, by which much lower pressures could be obtained with much higher speeds of exhaust. In fact, this type of pump was used for two or three years in the Research

---

[1] See Chapter 10 for discussion of this topic.

Laboratory of the General Electric Company in the commercial production of Coolidge X-ray tubes.

A still more important advance in vacuum technique occurred in 1915 when Gaede published an account of his "diffusion" pump, which was the direct incentive for the Langmuir "condensation" pump in 1916. By means of these mercury-vapor pumps it was possible to obtain pressures as low as 10^{-4} micron and thus meet the demands of the rapidly expanding radio and communication techniques for electronic devices, which, as well known, require extremely low pressures for efficient operation. In this manner vacuum technology, which had hitherto found commercial application only in the incandescent-filament lamp industry, now entered into a completely new field which, since about 1920, has developed into one of importance, not only for communication and broadcasting, but also for industrial control operations, television, radar, and many other applications.

It is hardly necessary to state that during the Second World War these developments yielded extremely important contributions towards the successful outcome of the struggle.

In 1928, C. R. Burch, of the Metropolitan-Vickers Electrical Company of England, found that certain high-boiling petroleum derivatives could be used effectively in condensation pumps to replace the mercury. This led K. C. D. Hickman and his associates at the Eastman Kodak Company Research Laboratories (and subsequently in the laboratory of the Distillation Products, Inc.) to investigate the practical possibilities of synthetic phthalates and sebacates for use in vapor pumps. Since these compounds and certain petroleum distillation products possess very low vapor pressures (less than about 10^{-6} mm) at room temperatures, it is possible to eliminate a cooling trap between the system to be exhausted and pump and thus utilize pumps of very high speeds.

Such pumps have been utilized by the Distillation Products, Inc., for "molecular" distillation and the fractionation of natural organic oils for the isolation of vitamins. Other applications, such as the vacuum furnace distillation of metals and the dehydration of penicillin and plasma, have been developed extensively by the National Research Corporation.

During the Second World War oil-vapor pumps of extremely high speed were utilized extensively in a variety of important industrial operations.

As a result there has been developed, since about 1940, a new industry —*vacuum technology*. The production of vacua of the order of 10^{-3} micron and even lower has been transformed from a laboratory curiosity to an industrial operation carried out on a scale that would, at one time, have been considered utterly fantastic. In the near future the vacuum engineer and vacuum technologist will take their place in industrial activities along with the engineers and technologists trained in the older fields.

The following three chapters will deal with the most essential element in this new technique—the vacuum pump. In subsequent chapters a number of other topics will be discussed which are of importance in vacuum technique.

2. GENERAL REMARKS ON OPERATION OF PUMPS[2]

In comparing vacuum pumps it is necessary to consider the following factors, which are the main characteristics of a pump:

1. Exhaust Pressure. This is the pressure against which the pump may be operated. In general, the higher the degree of vacuum desired on the "fine" or intake side of the pump, the smaller the exhaust pressure should be. The low exhaust pressure is then obtained by means of another (so-called "rough") pump, in series with the high-vacuum pump, which in turn exhausts into the atmosphere. Two or more rough pumps may be used in series in order to obtain a sufficiently low exhaust pressure for the fine pump.

2. Degree of Vacuum Attainable. "This is the lower limit of pressure which may be attained in a closed vessel connected to the pump. With most types of pump the degree of vacuum attainable depends to a large extent on the exhaust pressure used. This is usually due to leakage through the pump." For the vapor pumps, there is theoretically no lower limit to the pressure which may be attained (except that set by the pressure of the vapor itself); for the Gaede molecular pump the limiting pressure bears a constant ratio to the exhaust pressure.

3. Speed of the Pump.[3] Let P_s denote the lower limit of pressure attainable with a given pump. Then S, the *speed of the pump*, is defined, like F in Chapter 2, section 5, by the relation

$$-\frac{dP}{dt} = \frac{S}{C}(P - P_s), \tag{1}$$

where C is the volume to be exhausted.

By integration, there is obtained from this, a relation, similar to equation II.5.9,

$$\log\left(\frac{P_1 - P_s}{P_2 - P_s}\right) = \frac{S}{2.303C}(t_2 - t_1). \tag{2}$$

---

[2] See discussion by I. Langmuir, *Gen. Elec. Rev.*, **19**, 1060 (1916).

[3] Methods for the determination of vacuum pump speeds are discussed in section 7.

Like F, S corresponds to a conductance and is usually expressed in $\mathrm{cm}^3 \cdot \mathrm{sec}^{-1}$, liters $\cdot$ sec^{-1}, or cu ft $\cdot$ min^{-1}.

For S independent of P, a plot of log $(P - P_s)$ versus t gives a straight line, the slope of which is

$$\frac{\Delta \log (P - P_s)}{\Delta t} = \frac{S}{2.303C}. \tag{3}$$

Hence, the interval of time (in seconds) required to reduce the value of $(P - P_s)$ to *one-tenth* its value at any initial instant is given by

$$\Delta t_0 = \frac{2.303C}{S} \text{ sec}, \tag{4}$$

where C and S are measured in the same units of volume.

Equation 2 is actually equivalent to the relation

$$P_t - P_s = (P_0 - P_s)e^{-(S/C)t}, \tag{2a}$$

where P_0 and P_t are the values of P at $t = 0$ and t, and e is the base of the natural system of logarithms. Hence, S may also be defined as that value of C in which the pump will reduce the pressure difference to $1/e$th (36.79 per cent) of its instantaneous value, in 1 sec.

In terms of this notation we can also express equation 1 in the form

$$-\frac{dP}{dt} = \frac{EP}{C}, \tag{5a}$$

where

$$E = S(1 - P_s/P). \tag{5b}$$

Thus E corresponds to the *actual speed of exhaust* at any instant. At the beginning of the exhaust, P is very large compared to P_s, and hence the value of E is practically identical with that of S. However, as the value of P approaches that of P_s, E decreases and finally becomes equal to zero for $P = P_s$. Thus a plot of log P versus t will be linear at the beginning with a slope given by equation 3. But, as P approaches P_s, the plot will become more and more convex towards the axis of time and will finally become horizontal.

The *speed of exhaust observed* for any system depends not only on S_p, the intrinsic speed of the pump, and on the value of P_s, but also on the resistance to flow of gases of the connecting tubes, etc., between the pump and the volume that is being exhausted.

Let F denote the conductance of these connections, let us assume that $P_s = 0$, and let P and P_p denote the simultaneous values, at any instant, of the pressure in the volume C and at the opening to the pump, respectively. Then, Q, *the rate of flow* of gas at any instant, expressed, for example, in micron · liters per second or millimeters · cubic feet per minute, is given by the relation

$$Q = F(P - P_p) = S_pP_p = SP,$$

where S is the actually observed speed of pumping.

That is: $P = Q/S$; $P_p = Q/S_p$; $P - P_p = Q/F$; and, therefore,

$$\frac{1}{S} = \frac{1}{S_p} + \frac{1}{F}. \tag{6a}$$

This is one of the most important relations in vacuum technique. It signifies that $1/S$ and $1/S_p$ are to be regarded as "resistances," in the same sense as $1/F$. The last equation may also be expressed in the following forms:

$$S = S_p\left(\frac{1}{1 + S_p/F}\right). \tag{6b}$$

$$S_p = S\left(\frac{1}{1 - S/F}\right). \tag{6c}$$

$$S = F\left(\frac{1}{1 + F/S_p}\right). \tag{6d}$$

Thus S is always smaller than S_p, and the value of the ratio S/S_p actually obtained depends on that of F/S_p. More generally, let $F/S_p = n$. Then

$$\frac{S}{S_p} = \frac{n}{n + 1} \tag{7a}$$

and

$$\frac{F}{S} = n + 1. \tag{7b}$$

The application of these relations is illustrated by the data in Table 1, in which n is assigned a series of increasing values.

TABLE 1

RATIO BETWEEN ACTUAL SPEED OF EXHAUST AND INTRINSIC SPEED OF PUMP AS A FUNCTION OF CONDUCTANCE OF CONNECTIONS

$n = F/S_p$	S/S_p	S/F
0.1	0.091	0.909
1.0	.500	.5
5.0	.833	.167

That is, as the value of F is increased, the value of S approaches, more and more, that of S_p. *In order to utilize to the greatest extent the speed available from a given pump, the connections between the pump and the rest of the system should be made as large as practicable.*

B. B. Dayton, of the Distillation Products, Inc., has drawn the writer's attention to the fact that, for large values of the ratio F/S_p (5 or higher), equation 6*a* yields values of S/S_p which are too low. The reason for this is stated by him to be the following:

> When the speed S_p of a diffusion pump has been measured by allowing air to diffuse into the mouth of the pump from all directions in a test dome whose diameter is considerably greater than that of the pump mouth, and when this speed is more than 10 per cent of the theoretical admittance of the mouth (11.67 liters·sec^{-1}·cm^{-2}), then the measured value of S_p includes an "end correction" similar to that applying to short tubes. Therefore, when a pump is joined to a short tube of about the same diameter, the net speed (S) will not be given correctly by formula 6*a* since the end correction is then included twice.

The procedure for calculating an approximate value of S, recommended by Dayton, is as follows:

We shall assume that the mouth of the pump, of radius a (centimeters), is joined to the volume to be exhausted by a short length (l) of tubing of the same radius. Using the relation

$$S_p = 36.66Ka^2,$$

where K is Clausing's factor,[4] it is now possible, from the data in Table 2.3 or from the plot of K as a function of l/a in Fig. 2.2, to determine a length l_p equivalent in speed to that of the pump.

Now, let us assume further that the net speed desired for the added tubing and pump is fS_p (where f is less than 1). Hence we can now use the relation

$$fS_p = 36.66Ka^2$$

to determine the equivalent length l_e of the pump and tubing. The length of tubing to be used as a connection is then given by $l = l_e - l_p$.

For example, given a pump for which $S_p = 275$ liters · sec^{-1} and $a = 5$ cm, it follows that

$$K = \frac{275}{36.66 \times 25} = 0.30.$$

From the plot in Fig. 2.2, the corresponding value of l_p/a is found to be 5.5 and hence $l_p = 27.5$ cm. For $f = 0.8$,

$$K = \frac{220}{36.66 \times 25} = 0.24,$$

---

[4] See Chapter 2, section 2.

and the corresponding value of $l_e = 37.5$. Hence, the value of $l = 10$ cm, approximately. This is the length of tubing of radius 5 cm to be used as connection between the pump and the volume to be exhausted in order that the net speed of the system shall not be less than 80 per cent of the intrinsic speed of the pump.

In general, vacuum pumps serve one of two purposes. The first is that of producing as high a vacuum as possible in a device that will be sealed off the pump once this condition is secured. The second purpose is that of continuously maintaining an extremely low pressure in a system.

Since devices such as X-ray tubes and vacuum tubes in general are to be sealed off the pump, the most important requisite of the pump is that it shall produce such a low pressure that traces of residual gases do not affect the electrical characteristics of the device. These devices are connected to the pump through constrictions, liquid-air traps, stopcocks, and so forth. Under these conditions, the resultant conductance of the connections may vary from 100 $\text{cm}^3 \cdot \text{sec}^{-1}$ to 1000 $\text{cm}^3 \cdot \text{sec}^{-1}$. Since the value of S_p for most vapor-stream pumps is at least equal to or greater than 1000 $\text{cm}^3 \cdot \text{sec}^{-1}$, the speed of exhaust is limited to a large extent by the resistance of the connections, as shown by the above equations; consequently, increasing the value of S_p is of no particular advantage.

On the other hand, in the electron microscope, in the electron diffraction camera, and in distillation operations, where it is important to maintain as low a pressure as possible against low rates of leak, it is necessary that F be very much greater than S_p and also that S_p be sufficiently large to take care of the rate at which gas may leak into the system from outside, or of the rate at which gas may be evolved in the system itself.

As illustrations of the application of these remarks we shall consider two cases.

Case I. A certain device is connected to a pump through a tube ($l = 25, a = 0.5$) in series with a wide-bore stopcock ($l = 3.2, a = 0.51$). According to Tables 2.6 and 2.7 the values of $1/F$ for each of these parts (for air at 25° C) are $2.044 \cdot 10^{-3}$ and $3.817 \cdot 10^{-4}$ ($\text{cm}^{-3} \cdot \text{sec}$), respectively. The device is sealed on by means of a constriction ($l = 15$, $a = 0.3$), for which $1/F = 5.679 \cdot 10^{-3}$. Therefore the total resistance is $8.105 \cdot 10^{-3}$ corresponding to $F_0 = 123.4\ \text{cm}^3 \cdot \text{sec}^{-1}$.

Since S_p is, in general, much greater than this value of F, we can use equations 7 to investigate the effect of varying S_p. Let us assume that we have two pumps available, for one of which $S_p = S_{PA} = 2F_0$, and for the other, $S_{PB} = 10F_0$. For pump A, $S/F_0 = 2/3$; for pump B, $S/F_0 = 10/11$. That is, increasing the speed of the pump fivefold has increased the effective speed of exhaust from $0.667F_0$ to $0.909F_0$, or only about 36 per cent. Even if we used a pump having an extremely high value of S_p, it would not be possible to increase the effective speed beyond that of F_0.

Case II. Assuming that we have available a pump for which the value of S_p is known, the minimum value of F may be determined, by means of equation 6, for which S will be equal to or exceed a given value S_0. We shall designate this value by F_0, where

$$\frac{1}{F_0} \leqslant \left(\frac{1}{S_0} - \frac{1}{S_p}\right).$$

Let us assume $S_p = 200$ liters · sec^{-1}, and $S_0 = 100$ liters · sec^{-1}. Then F_0 must be equal to or greater than 200 liters · sec^{-1}. For air at 25° C, flowing through a tube,

$$F_0 = 36.66a^2K \quad \text{liters} \cdot \text{sec}^{-1},$$

where K is given by Table 2.3. Hence,

$$a^2K = \frac{200}{36.66} = 5.456.$$

It will be found that the following combinations of l and a will satisfy this condition:

a	K	l/a	l
5 cm	0.218	9.0	45 cm
4	.341	4.4	17.6
3	.606	1.35	4.05

Cases often occur in which gas is evolved from the walls or other parts of the system at such a rate that the lower limit of pressure which the pump can produce is not attained. This may also occur if the rate of leakage of gas into the system, through seals or joints, has an appreciable value.

Let Q denote, as before, the rate at which gas is evolved or leaks into the system. A stationary condition is then attained at which the rate of gas evolution is equal to that at which this gas is removed by the pump. Let S_0 denote the conductance of pump and connecting tube. At the stationary state, the pressure P_s is given by the relation

$$Q = S_0P_s. \tag{8}$$

Thus, the value of Q may be determined from a knowledge of S_0 together with an observation on the value of P_s. For instance, Langmuir gives the following illustration:[5]

---

[5] *Gen. Elec. Rev.*, **19**, 1060 (1916).

Measurements of pressure by various forms of supersensitive vacuum gauges have shown that the rate of evolution of water vapor from glass surfaces at room temperature is such that pressures below 0.2 microbar could not be attained even when using a molecular pump ($S_p = 870$ cm$^3 \cdot$ sec^{-1}) continuously for an hour. In this case we can calculate by equation 8 that Q must have been 170 microbar · cm^3 per second. This corresponds to 0.00017 cm$^3 \cdot$ sec^{-1} of gas at atmospheric pressure, or 0.62 cm^3 of water vapor per hour. In this case the surface of glass was about 1800 cm^2.

3. DESIGN OF HIGH-VACUUM SYSTEM[6]

The considerations discussed in the previous section are directly applicable to the problem of designing a high-vacuum exhaust system. Such a system consists, in general, of the following components:

1. The device, of volume C (liters), to be exhausted and maintained at a pressure P_0 (mm).
2. Connections of conductance F_1 (liter · sec^{-1}) to a "vapor" pump.
3. A vapor pump which has the speed S_p at the pressure P_0 and is capable of operating against a backing pressure as high as P_f (mm).
4. Connections of conductance F_2 (liter · sec^{-1}) between the vapor pump and the fore pump.
5. A fore pump, capable of operating at a reasonable speed, S_f (liter · sec^{-1}), at the pressure P_f.

Let us assume that gas is leaking into the system at a rate of Q (mm · liter · sec^{-1}). Hence,

$$Q \doteq S_p' P_0, \tag{1}$$

where S_p' is the speed actually obtained, and

$$\frac{1}{S_p'} = \frac{1}{S_p} + \frac{1}{F_1}. \tag{2}$$

Therefore,

$$S_p = \frac{Q}{P_0}\left(\frac{F_1}{F_1 - C/P_0}\right) \tag{3a}$$

$$= f_1 \frac{Q}{P_0}, \tag{3b}$$

---

[6] The writer wishes to acknowledge his indebtedness to a publication, by the same title, by Dr. C. M. Van Atta, which is issued by Kinney Manufacturing Company, Boston, Mass. The reader should also consult the very interesting paper, "Vacuum Pumping Equipment and Systems," by H. M. Sullivan, *Rev. Sci. Instruments*, **19**, 1 (1948), for a description of the different types of pumps which are available today, and which are discussed in this chapter and also Chapters 4 and 5.

where f_1 is a value greater than unity and corresponds to the value of S_p/S in Table 1.

For the fore pump we obtain, in a similar manner, the relations

$$S_f = f_2 \frac{Q}{P_f}, \tag{4}$$

where

$$f_2 = \frac{F_2}{F_2 - Q/P_f}. \tag{5}$$

Since Q/P_f is much less than Q/P_0, F_2 may be made considerably smaller than F_1. Like f_1, the factor f_2 is greater than unity.

In order to take care of possible contingencies it is advisable to choose values of S_p and S_f which will compensate adequately for even larger values of f_1 and f_2 than those calculated by means of equations 3 and 5.

As an illustration of the application of these relations, let us consider the following case:

$$Q = 10^{-3}\ \text{mm} \cdot \text{liter} \cdot \text{sec}^{-1} \quad (1\ \text{micron} \cdot \text{liter} \cdot \text{sec}^{-1}),$$
$$P_0 = 10^{-5}\ \text{mm}, \quad \text{and} \quad P_f = 10^{-2}\ \text{mm}.$$

Then

$$S_p = f_1 \cdot \frac{10^{-3}}{10^{-5}} = 100 f_1 \quad \text{liter} \cdot \text{sec}^{-1},$$
$$S_f = f_2 \cdot \frac{10^{-3}}{10^{-2}} = 0.1 f_2 \quad \text{liter} \cdot \text{sec}^{-1}.$$

Let us assume the values $f_1 = f_2 = 5$. Then, the pumps chosen should have the values $S_p = 500$ liter · sec^{-1} and $S_f = 0.5$ liter · sec^{-1}.

These are, however, not the only considerations that have to be taken into account. We must also consider the period required to pump the system from 760 to $P_f = 10^{-2}$ mm. This is given by the relation

$$t = \frac{2.303C}{f_2 S_f} \log \frac{760}{P_f}, \tag{6}$$

where S_f now denotes the *average* value of the speed over the range of pressures.

Assuming $C = 100$ liters, and the values for f_2, S_f, and P_f given above, we obtain the result

$$t = \frac{230.3 \times 4.88}{0.5} = 2830 \quad \text{sec}$$
$$= 47.2 \quad \text{min}.$$

If this is too long an interval, we should choose a larger value of S_f than 0.5 liter/sec. Obviously these conclusions indicate lower limits for the values of S_p and S_f, and the actual choice of pumps will have to be governed to a large extent by the sizes available from the manufacturer.

Equation 6 assumes that it is possible to assign an average value of S_f over the whole range of pressures. If this value varies greatly with pressure, then equation 6 must be replaced by a series of the form:

$$t = 2.303C\left\{\frac{1}{S_1}\log\frac{760}{P_1} + \frac{1}{S_2}\log\frac{P_1}{P_2} + \cdots + \frac{1}{S_n}\log\frac{P_{n-1}}{P_n}\right\}, \qquad (7)$$

where S_1 is the speed of exhaust for the small range 760 to P_1, S_2 is the speed for the range P_1 to P_2, and so forth. This relation is, in effect, analogous to that given previously for the speed of exhaust through a capillary tube.

For the period of exhaust by the vapor pump, we have, in the above case, the relation

$$t_1 = \frac{2.30C}{S_p}\log\frac{P}{P_0}$$

$$= \frac{2.30 \times 100 \times 3}{500} = 1.38 \quad \text{sec.}$$

Thus the rate of exhaust of the system is governed to a very large extent by the speed of the fore pump, rate of leak, and capacity of the system.

In connection with this topic it is also of interest to make some remarks about the rating of mechanical pumps. A figure frequently mentioned in manufacturers' descriptions is the *free air displacement*, designated by D. By this is meant the volume of air that the pump passes per unit time, at atmospheric pressure. Now, if we let S_1 denote the speed at 1 micron (in the same units of volume and time as D), then $r = S_1/D$ has been designated the "merit factor" of the pump.[7] It is evident that, the larger the value of r, the greater the pumping speed in the range of 1 micron, for a given value of D.

4. EARLIER TYPES OF MECHANICAL PUMPS

The early forms of exhaust pumps were of the piston type. Since they have been superseded in modern practice, and since they are described in many elementary textbooks,[8] no detailed description of them need be made here.

---

[7] Suggested in *Cenco News Chats*, February, 1937.

The use of a water-jet suction pump is a familiar practice in laboratory work, especially in filtering operations. The *Sprengel* mercury pump operates on the same principle, and G. W. A. Kahlbaum described a modification capable of exhausting to 0.003 micron.[9]

1. Geissler-Toepler Pump.[10] The principle of this pump is fundamentally the same as that applied by Torricelli in his famous experiment. In this type (Fig. 1) mercury forces the piston and also opens and closes certain ports, so that no valves are needed except one rough glass valve (*G*) to prevent the mercury from entering the vessel *E* which is being exhausted. The essential parts of the pump are made of glass, and the air from *E* is exhausted by alternately raising and lowering the mercury reservoir *R* which is connected to the tube of barometric length below *B*. At each upward "stroke," the gas in *B* is closed from *E* and forced through the tube *F* into the atmosphere at *M*. Then, on the downward stroke, the pressure in *E* is lowered by expansion of the gas into *B*. E. Bessel-

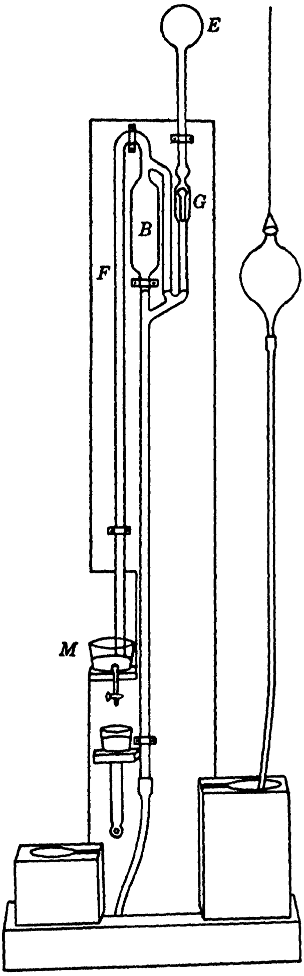

FIG. 1. Toepler pump.

---

[8] Some of these pumps are the following: (1) Geryk Vacuum Pump, see E. H. Barton, *An Introduction to the Mechanics of Fluids*, p. 197, Longmans, Green & Company, 1915; see also *Encyclopædia Britannica*, 14th edition, Vol. 22, p. 126. (2) Gaede's Piston Pump, E. H. Barton, *loc. cit.*, p. 188, W. Gaede, *Physik. Z.*, **14**, 1238 (1913). A description of early types of mechanical pumps and of the Gaede and Siegbahn types, described in section 6, is given by R. Neumann, *Electronic Engineering*, Vol. 20, January and February, 1948. These articles also include a comprehensive bibliography.

[9] See older treatises on physics. Kahlbaum's pump is described in *Wied. Ann.*, **53**, 199 (1894), also in *Ann. Physik*, **10**, 623 (1903).

[10] E. H. Barton, *loc. cit.*, from whose book Fig. 1 is taken. See also *Encyclopædia Britannica*, 14th edition, Vol. 22, p. 926.

Hagen[11] has described a modified form of Toepler pump with which he claims to have obtained pressures of residual gas as low as 0.012 micron.[12] Both the Sprengel and Toepler pumps have rendered very useful service in high-vacuum investigations, and there is no doubt that with care it is possible by their use to obtain pressures as low as 0.02 to 0.01 micron.

The great disadvantages of these pumps are, however, twofold. First, they require constant personal attention during the exhaust, and second, the speed of exhaust is extremely slow, since it depends upon the rate at which the mercury can be raised and lowered alternately. It is of interest to note in this connection the results obtained by Scheel and Heuse[13] in their investigation of the degree of vacuum attainable with different types of pump. They used a 6-liter bulb and measured the speed of exhaust by means of a very sensitive McLeod gauge. In the experiments with a Toepler pump, each stroke actually required 2 minutes, and 2 more minutes were allowed between strokes for equalization of pressure. Table 2 shows the pressures at the end of different intervals of time.

The last column gives the "speed of exhaust" as calculated by equation 2.5*a*. Compared with the speed of even 100 cm^3/sec obtained by a Gaede rotary mercury or an ordinary oil pump, the speeds in Table 2 are manifestly very low. Considering, furthermore, that, in the case where gas is continually evolved from the walls, the minimum attainable pressure is given by the ratio S/Q, where Q denotes the rate of gas evolution, it is seen that in actual practice it would be very difficult to obtain pressures below about 0.01 micron by means of a Toepler pump.

Similar results were obtained by Scheel and Heuse in investigating the rate of exhaust of a 6-liter bulb by means of a Sprengel pump (improved by L. Zehnder[14]).

2. Gaede Rotary Mercury Pump. Obviously the process of exhausting even a relatively small volume by means of a Toepler pump is an extremely tedious operation. The invention by Kaufmann[15] of a rotary mercury pump in 1905 was therefore a welcome development in this field. However, it was very soon superseded by a rotary mercury pump, designed by W. Gaede[16] at about the same time, which was used

---

[11] *Wied. Ann.*, **12**, 425 (1881).

[12] Other forms of Toepler pump are described by A. Stock, *Ber. deut. chem. Ges.*, **38**, 2182 (1905), and E. Grimsehl, *Physik. Z.*, **8**, 762 (1907).

[13] *Z. Instrumentenk.*, **29**, 47 (1909).

[14] *Ann. Physik*, **10**, 623 (1903).

[15] *Encyclopædia Britannica*, 14th edition, Vol. 22, p. 927.

[16] *Verhandl. deut. physik. Ges.*, **7**, 287 (1905); *Physik. Z.*, **6**, 758 (1905). *Encyclopædia Britannica*, 14th edition, Vol. 22, p. 930.

TABLE 2

SPEED OF EXHAUST WITH TOEPLER PUMP

t (min)	P_{mm}	$E = \frac{2.3V}{60t} \log \frac{P_1}{P_2}$
0	0.0645	0.40
2	.0399	.38
24	.0254	
48	.0107	.35
60	.00709	
108	.00141	.35
120	.00093	
180	.00024	.39
192	.00015	
240	.000053	.28
252	.000038	
264	.000032	.06
300	.000025	

extensively for a long time in the commercial exhaust of incandescent lamps and of Roentgen tubes. The pump consists of an iron casing (with glass front) partially filled with mercury, in which a porcelain drum is made to rotate. A *rough pump* producing a vacuum of 10 to 20 mm is used as *fore pump.* Figure 2 shows a vertical section of the pump, and Fig. 3 a front view. The iron case is shown at g, and g' is a heavy glass plate through which pass the tubes R and r which connect to the vessel to be exhausted and to the fore pump, respectively. The porcelain drum t is built up of two (or more) sections as shown in Fig. 2 and rotates on the axis a. As the drum rotates in the direction of the arrow (see Fig. 3), the compartment W_1 is at first increased in volume and thus sucks in the gas at the opening f_1, from the vessel to be exhausted. During the second part of the revolution, the opening f_1 becomes covered with mercury, as shown at f_2, and the gas is then forced out under pressure from the compartment W_2 into the space between the walls Z_1 and t_1 and into the rough pump connection at r.

The speed of exhaust observed with a volume of 6250 cm^3 varied from about 95 $cm^3 \cdot sec^{-1}$ at $P_\mu = 30$ to about 7 $cm^3 \cdot sec^{-1}$ at $P_\mu = 0.07$.

3. Gaede Rotary Oil Pump.[17] Figure 4 shows the construction of a pump of this type designed by Gaede primarily for the purpose of functioning as a fore pump to the rotary mercury pump just described. The pump consists of a steel cylinder A which rotates eccentrically inside a steel casing G. The projections at s are held tightly against the

---

[17] *Encyclopædia Britannica,* 14th edition, Vol. 22, p. 929. Also see G. Meyer, *Verhandl. deut. physik. Ges.,* 10, 753 (1907).

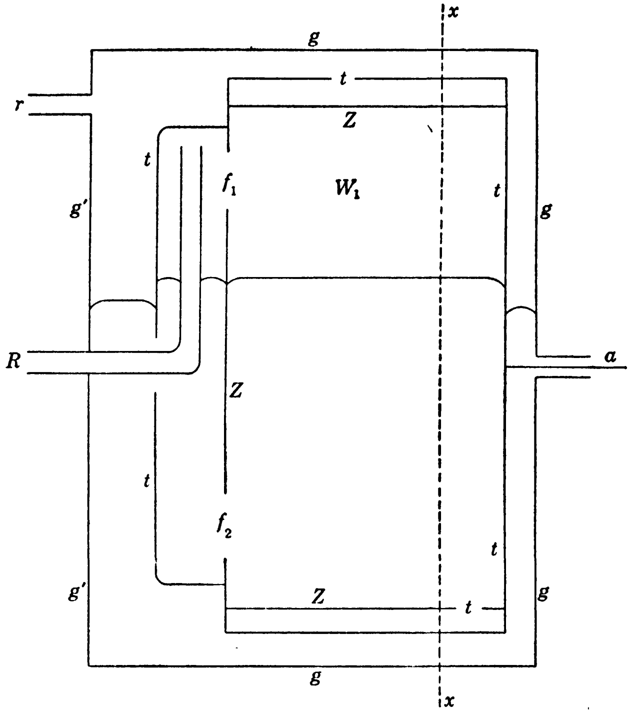

FIG. 2. Gaede rotary mercury pump. Vertical section.

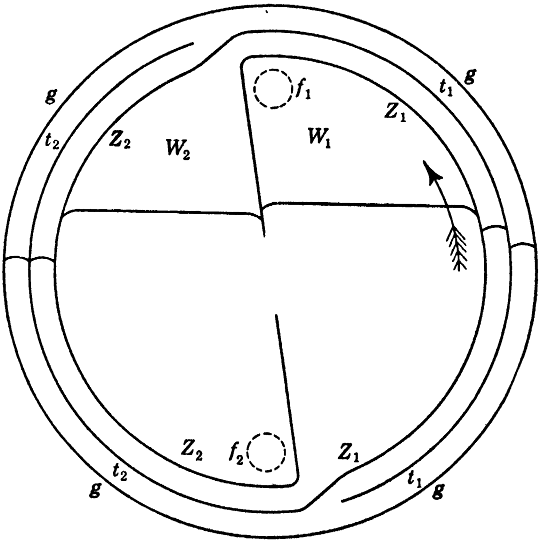

FIG. 3. Gaede rotary mercury pump. Section perpendicular to axis of rotation, through plane shown at x in Fig. 2.

inner wall by means of springs, so that as the cylinder rotates the air is sucked in at *C* and forced out through the valve *D* into the oil chamber *O* and from there into the atmosphere at *J*. The oil serves as an automatic lubricant and also helps to prevent air from leaking back into the fine-pump side by forming a film between the rotating and stationary members.

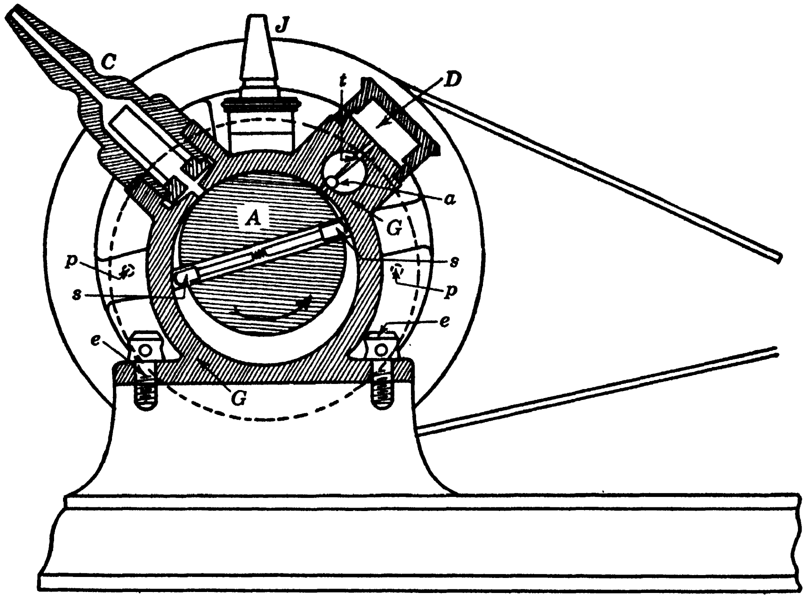

FIG. 4. Gaede rotary oil pump. Front view.

With a "rough" vacuum of about 10 mm mercury, such a pump could reduce the pressure to about 1 micron, with a speed of exhaust of 100–150 $\mathrm{cm}^3 \cdot \mathrm{sec}^{-1}$.

5. COMMERCIAL TYPES OF ROTARY OIL PUMPS

At the present time rotary oil pumps are available in considerable variety. In the following discussion are described briefly some of the types produced by the more important manufacturing organizations in the United States which have been found to be satisfactory for use in high-vacuum technique, both with and without the addition of vapor pumps.

Cenco High-Vacuum Pumps. (Central Scientific Company, Chicago, Ill.) Figure 5 is an illustration of the "Cenco Hypervac 20" equipped with motor drive.

A diagram of the mode of operation is shown in Fig. 6. Essentially, it is a two-stage oil-seal mechanical pump, in which the second stage (shown at the left) acts as a backing pump for the first stage. During the initial period of exhaust, when the pressure in *C* exceeds atmospheric, the valve *F* opens until the pressure is reduced below atmospheric. With pumps of this type it is possible to obtain vacua of the order of 0.1 micron at speeds varying (according to capacity and speed of rotor) from 1.5 to 10 liters/sec at 1 micron.

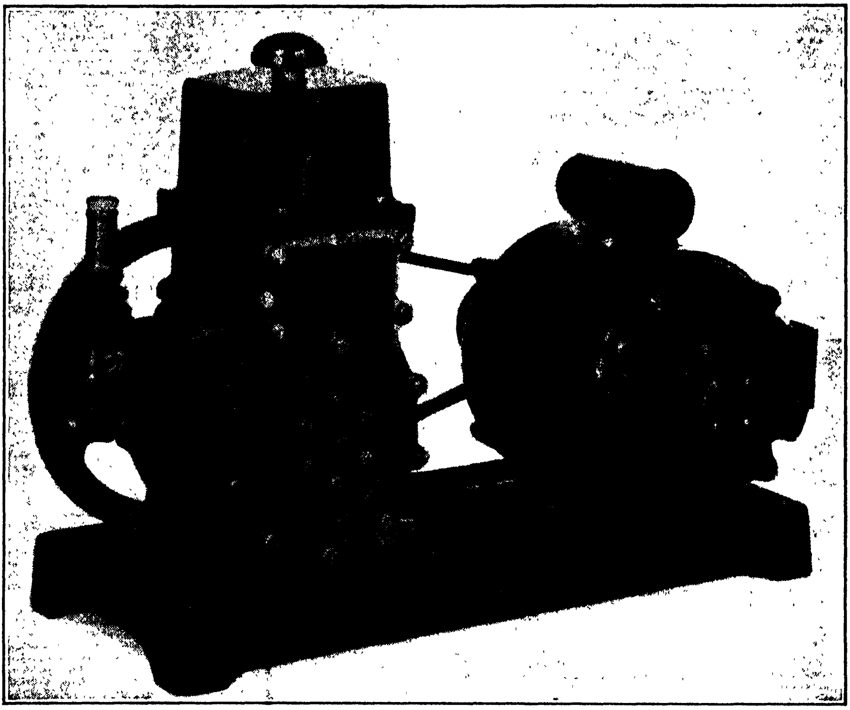

FIG. 5. Cenco Hypervac pump, type 20.

Table 3 gives characteristic data (taken from a more detailed tabulation in the catalogue) for the different types of pumps made by the same company. S_1 designates the speed at 1 micron.

Figure 7 shows plots of log S versus log P_μ for these different types.

Kinney Pumps. (Kinney Manufacturing Company, Boston, Mass.) The operating mechanism of this pump is shown in Figs. 8 and 9. In Fig. 8, the plunger is shown in a position in which gas is being removed from the system; in Fig. 9 the plunger is shown in the position for expulsion of gas. The model CVD (compound high vacuum) is illus-

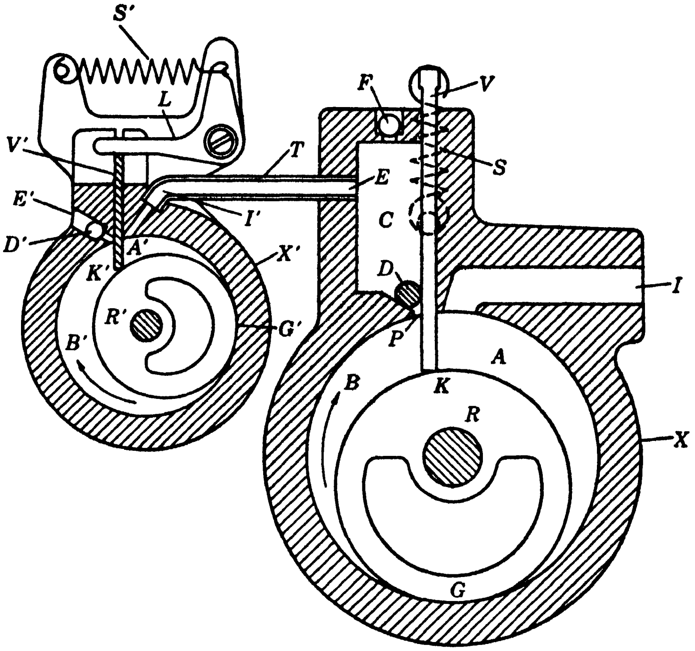

FIG. 6. Schematic diagram of working principle of Cenco Hypervac pumps. *I*, *I'*, intake; *E*, *E'*, exhaust; *D*, *D'*, exhaust valve; *C*, interstage; *F*, interstage exhaust valve; *V*, *V'*, vane; S, S,' vane spring; *L*, vane lever; *R*, *R'*, rotor; *X*, *X'*, stator; *A*, *A'*, intake chamber; *B*, *B'*, exhaust chamber; *P*, exhaust port; *K*, *K'*, contact line of vane with rotor; *G*, *G'*, contact line of rotor with stator; *T*, connecting tube.

TABLE 3

CHARACTERISTIC DATA FOR CENCO PUMPS

		Megavac		Hypervac	
Type	Hyvac	A	B	20	100
Guaranteed vacuum (P_μ)	0.3	0.1	0.1	0.1	0.1
D ($\text{cm}^3 \cdot \text{sec}^{-1}$)	170	510	940	3300	16,000
D ($\text{liter} \cdot \text{min}^{-1}$)	10	31	57	198	960
S_1 ($\text{cm}^3 \cdot \text{sec}^{-1}$)	79	210	375	1390	11,500
$100r$	46	41	40	42	72

trated in Fig. 10. With this pump, pressures as low as 0.2 to 0.1 micron can be obtained.

Figure 11 shows plots of speed (in cu ft $\cdot$ min^{-1})[18] versus log *P*.

---

[18] 1 cu ft/min = 471.95 cm^3/sec
= 28.32 liters/min.
1 liter/sec = 2.119 cu ft/min.

Values of the displacement, D (cu ft/min) are 15.2 and 46.0 for CVD556 and CVD8610, respectively. Hence the value of r, the figure of merit, is about 50 per cent for each of these pumps.

Stokes Microvac Pumps. (F. J. Stokes Machine Company, Philadelphia, Pa.) Figure 12 shows a cross section of this type of rotary oil pump, and the external appearance of model 212E-8 is shown in Fig. 13, which also shows the oil clarifier at the left. The value of D for this model is given as 115 cu ft/min, and Fig. 14 shows the variation with pressure in the value of r for one of the most recent models. Thus, at 10 microns the speed is 57.5 cu ft · min^{-1} or 27.14 liters · sec^{-1}.

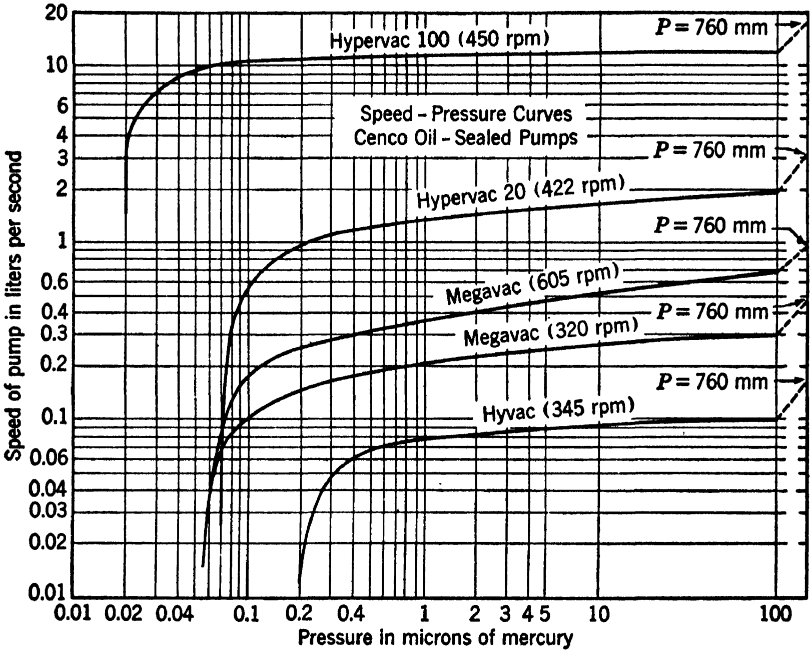

FIG. 7. Log-log plots of speed versus pressure for Cenco pumps.

As indicated in the last figure, the minimum pressure claimed for the pump is about 2.5 microns.

Welch Duo-Seal Pumps. (W. M. Welch Scientific Company, Chicago, Ill.) A diagrammatic sketch of the method of operation of this design is shown in Fig. 15. The rotor is mounted eccentrically with reference to the stator and is provided with two metal vanes which move in and out of their slots as the rotor revolves and which press constantly against the inner wall. Thus a crescent-shaped air space is swept out twice during each revolution. The inlet and outlet ports are sealed

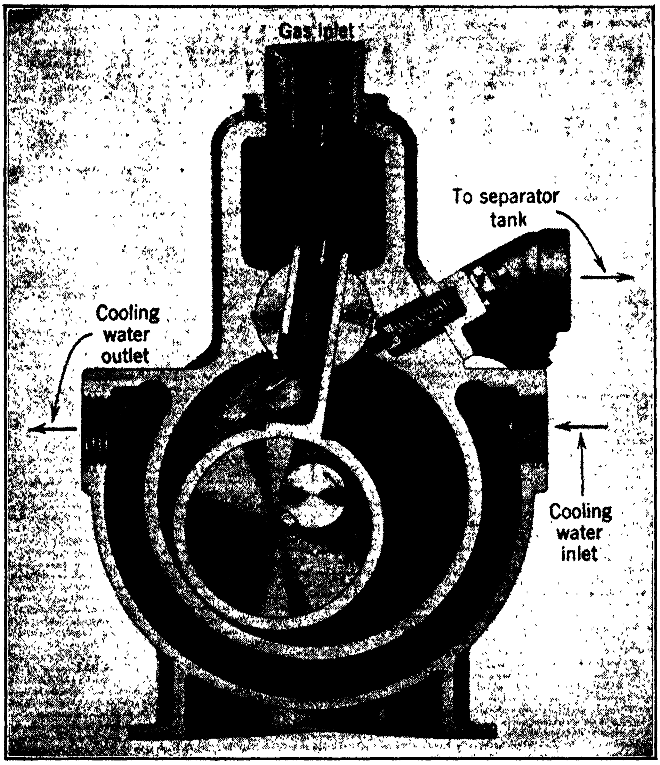

FIG. 8. Illustrating principle of operation of Kinney rotary oil pump. Period I.

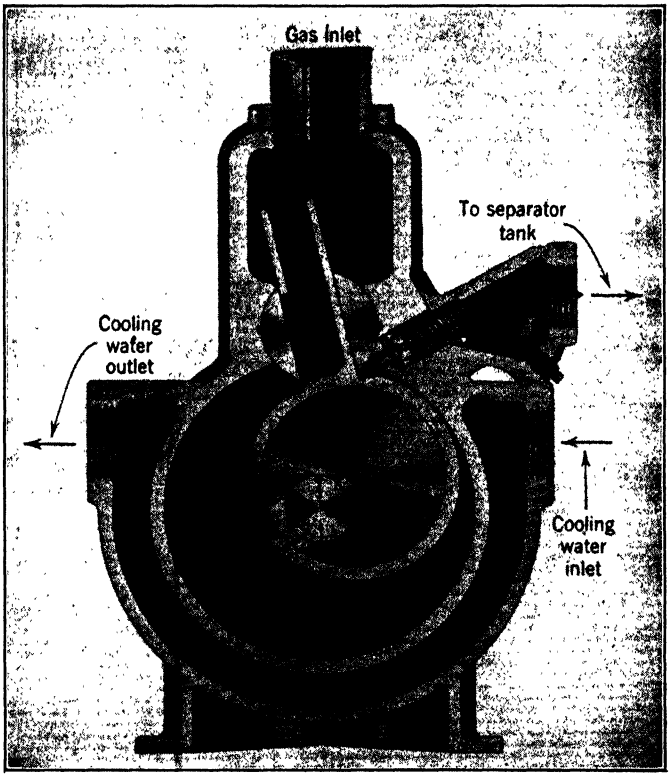

FIG. 9. Illustrating principle of operation of Kinney rotary oil pump. Period II.

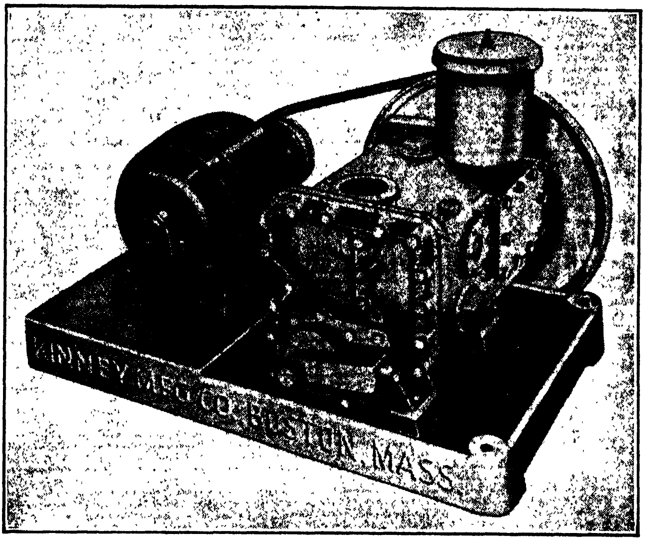

FIG. 10. External appearance of Kinney rotary oil pump.

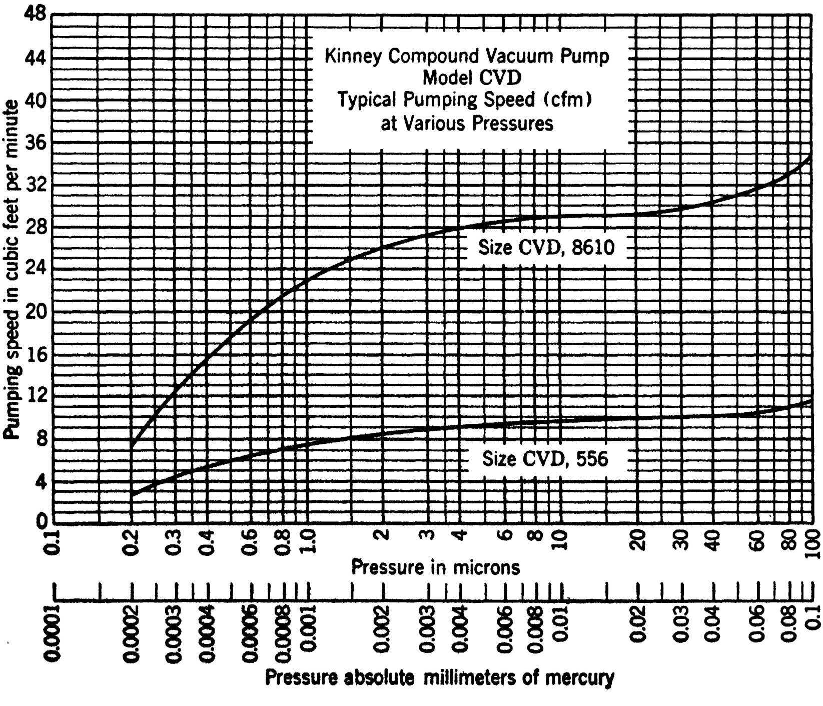

FIG. 11. Semi-log plots of speed versus pressure for two sizes of Kinney pump.

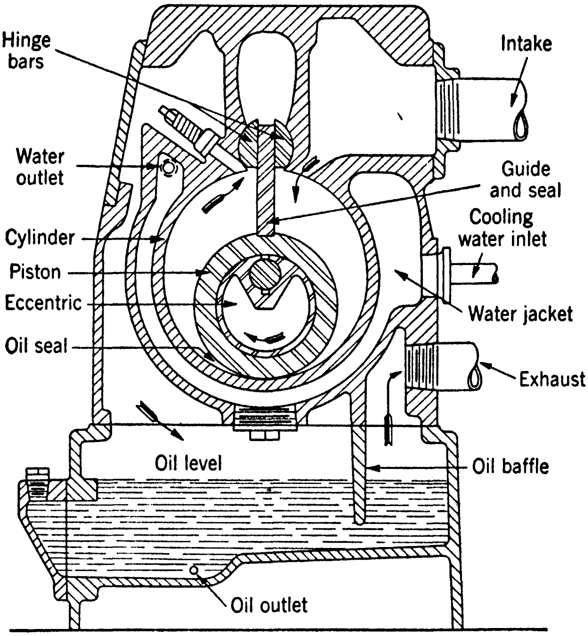

FIG. 12. Illustrating operation of Stokes rotary oil pump.

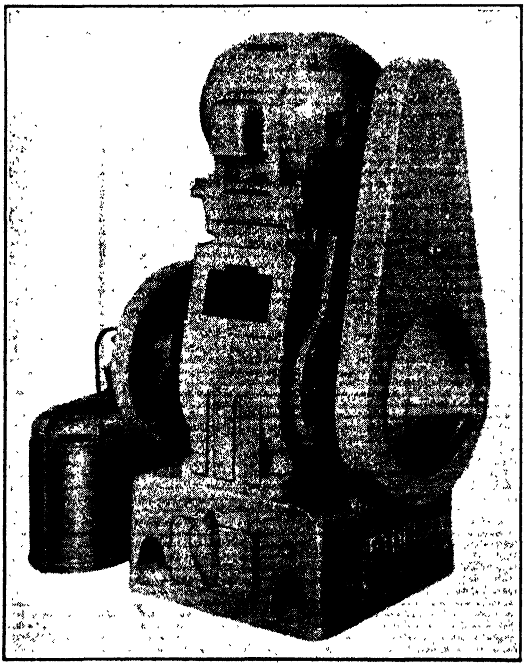

FIG. 13. External appearance of Stokes Microvac pump.

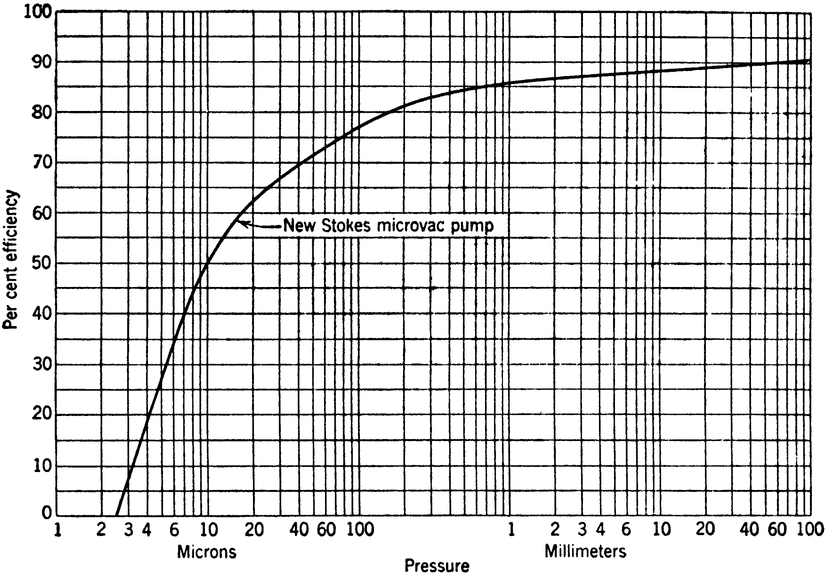

FIG. 14. Semi-log plot of exhaust efficiency versus pressure for Stokes Microvac pump.

from each other by a thin film of oil. Figure 16 shows the outer appearance of the two-stage pump (Catalogue No. 1405), and Fig. 17 shows a

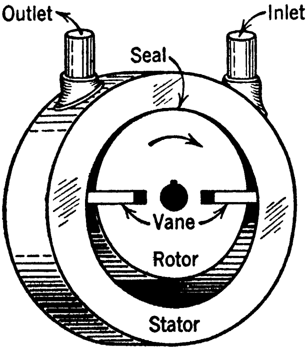

FIG. 15. Diagrammatic sketch of principle of operation of Welch Duo-seal pump.

plot of log S versus log P_{mm} for this pump with which it is possible to obtain a pressure of about 0.05 micron.

The value of D (liters per minute) for this pump is given in the catalogue as 33.4.

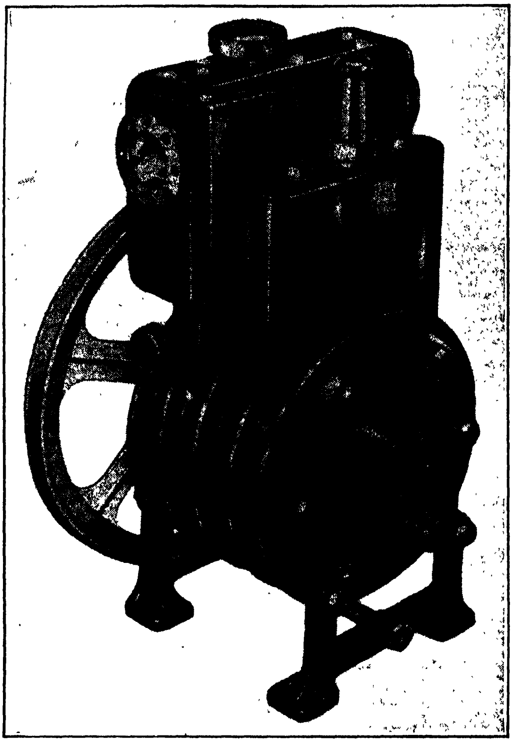

FIG. 16. External appearance of Welch Duo-seal pump.

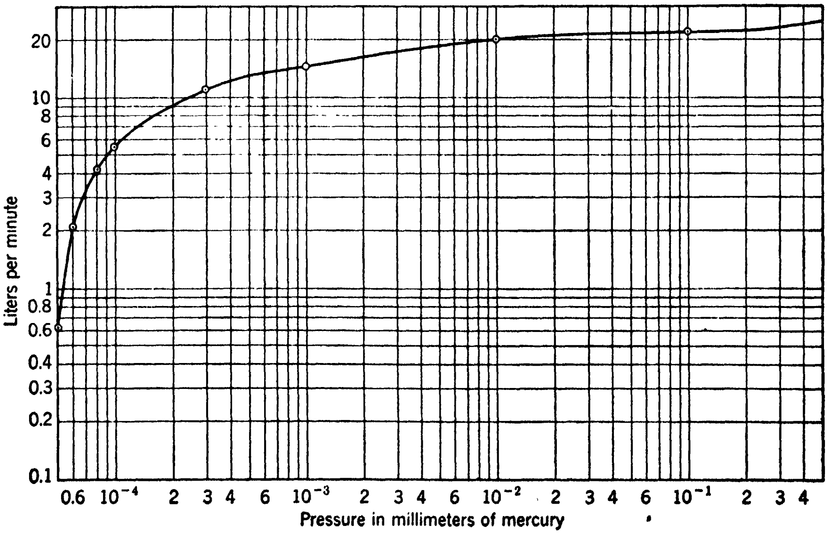

FIG. 17. Log-log plot of speed versus pressure for Welch pump.

6. MOLECULAR PUMPS

The Gaede molecular pump undoubtedly marked a distinct advance in the design of pumps for the production of high vacua. The difference between this pump and the types previously constructed has been well described by Gaede himself in the paper which he published in 1913.[19]

> All high-vacuum pumps known up to the present consist of an exhaust arrangement which, according to the original idea of Otto von Guericke, separates a definite volume of gas from the vessel to be exhausted, and then gives it up to a fore vacuum or the atmosphere. It is absolutely essential in these pumps to separate the rough side from the higher vacuum side as much as possible. This is accomplished in the mechanical pumps by tight-fitting pistons and valves, and in the case of mercury and oil pumps by means of the liquids themselves. On the other hand, in the case of the molecular pump there is no separation, whether piston or fluid, between the high vacuum and fore vacuum.

The gas is dragged along from the vessel to be exhausted into the fore vacuum by means of a cylinder rotating with high velocity inside a hermetically sealed casing. The pump thus represents a logical development and application of the laws of flow of gases at very low pressures as investigated by Knudsen, Smoluchowski, and Gaede himself.

The fundamental principle of the pump may be illustrated by means of Fig. 18. The cylinder A rotates on an axis a (in the direction of the arrow) inside the air-tight stator B, and drags the gas from the opening n towards the opening m, so that a pressure difference is built up in the manometer M, as shown by the mercury levels at o and p. Between m and n there is a slot in the case B as shown in the diagram, while at every other point A and B are very close together. Now, at ordinary pressures the viscosity is independent of the pressure. Under these conditions, as Gaede shows, the difference in pressure at o and p depends only on the speed of rotation u of the cylinder, the coefficient of viscosity of the gas η, the length of the slot l, and h, the depth measured radially, according to the following relation:

$$P_1 - P_2 = \frac{6lu\eta}{h^2}, \tag{1}$$

where P_1 is the pressure on the high side.

---

[19] W. Gaede, "The Molecular Air Pump," *Ann. Physik*, **41**, 337–380 (1913). This paper contains a complete discussion of the theory and construction of the pump. Briefer descriptions may also be found in the following: W. Gaede, *Physik. Z.*, **13**, 864–870 (1912), and *Verhandl. deut. physik. Ges.*, **14**, 775–787 (1912); K. Goes, *Physik. Z.*, **13**, 1105 (1912), and **14**, 170–172 (1913); *Electrician (London)*, **70**, 48–50 (1912); K. Jellinek, *Lehrbuch d. physikal. Chemie*, I, 1, pp. 330–333, 1914; M. L. Dunoyer, *Les idées modernes sur la constitution de la matière*, pp. 215–271, 1913.

At *low pressures*, however, the number of collisions between gas molecules becomes relatively small compared with the number of collisions between the gas molecules and the walls. Under these conditions the molecules therefore tend to take up the same direction of motion as the surface against which they strike, if that surface is in motion. This conclusion is based upon the investigations of Knudsen on the laws of molecular flow, which have been discussed in Chapter 2. The relation previously deduced is therefore found to be no longer applicable, and, instead of the pressure difference remaining constant at constant speed of rotation, the *pressure ratio is now constant* and independent of the pressure in the fore vacuum. Gaede shows that, at very low pressures,

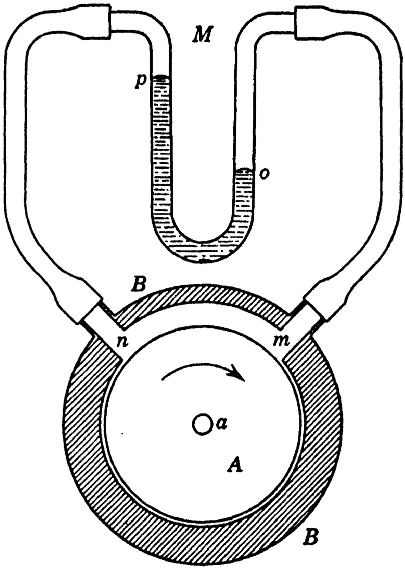

FIG. 18. Diagram illustrating principle of operation of Gaede molecular pump.

$$\frac{P_1}{P_2} = \epsilon^{bu}, \tag{2}$$

where b is a constant whose value depends upon the nature of the gas and the dimensions of the slot in the casing B of the pump, so that, at constant speed of rotation u, the ratio between the pressures on the two sides of the pump is constant.

The construction of the actual pump based on these principles is illustrated in Figs. 19 and 20. The rotating cylinder A has twelve parallel slots around the circumference, into which project the extensions *C* from the outer casing. If *A* rotates clockwise, the pressure at *m* is greater than that at *n*, and, in order to increase this pressure, different sections are connected in series. The distance between the outer edge of the cylinder *A* and the inside of the shell *B* is about 0.01 cm. The overall radius of *A* is 5 cm, and the depth of the slots varies from 0.15 cm in the outer section to 0.6 cm in the inner ones. With the cylinder rotating clockwise as indicated, the vessel to be exhausted is connected at *S*, while the opening *T* is connected to an ordinary mercury or oil pump capable of exhausting to a pressure of less than 0.05 mm Hg. Since the speed of rotation of the cylinder is very high (about 8000 rpm) oil cups are provided at *F*, and the shaft *N* is so designed that the oil in the spiral slot is driven outward by the centrifugal action. The slots in

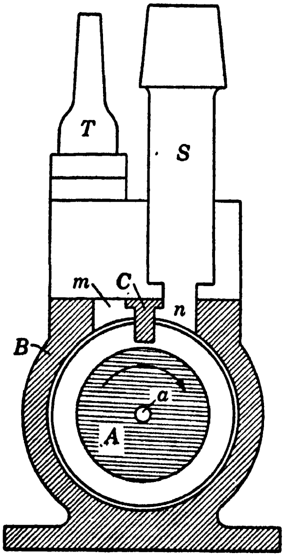

FIG. 19. Construction of Gaede molecular pump. Front view.

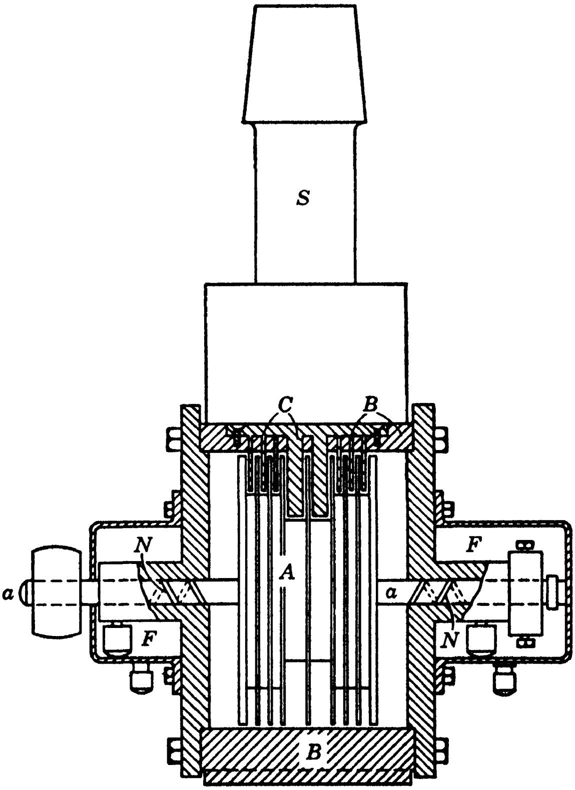

FIG. 20. Construction of Gaede molecular pump. Side view.

the rotor are so arranged that the lowest pressure is in the center, and the pressure increases uniformly outward until the ends, where it is equal to that produced by the rough pump, into which the outlet T exhausts.

The effect of variation in the speed of rotation and in the fore-pump pressure on the degree of vacuum produced by the molecular pump is shown in Table 4.

TABLE 4

EFFECT OF SPEED OF ROTATION ON DEGREE OF VACUUM OBTAINED WITH GAEDE MOLECULAR PUMP

Speed of Rotation (rpm)	Rough-Pump Pressure P_{mm}	Pressure on Fine Side P_{mm}
12,000	0.05	0.0000003
12,000	1	0.000005
12,000	10	0.00003
12,000	20	0.0003
6,000	0.05	0.00002
2,500	0.05	0.0003
8,200	0.1	Not measurable
8,200	1	0.00002
8,200	10	0.0005
6,200	0.1	0.00001
6,200	1.0	0.00005
4,000	1.1	0.00003
4,000	1	0.0003

The pressures on the fine side were measured with an extremely sensitive McLeod gauge, except that the first result given in the table was estimated. The writer's own experiments[20] with the Gaede molecular pump at 8000 rpm showed that with a rough-pump pressure of 20 mm the fine-side pressure was 0.0004 mm, so that the ratio of the pressures was 50,000—a result in accord with figures given by Gaede.

The speed of the pump as defined by equation 2.1 was found by Gaede to vary with the magnitude of the rough-pump pressure. The curve A in Fig. 21 shows that the maximum speed was about 1400 cm^3/sec with a fore vacuum of 0.01 mm. For comparison, curve B also shows the speed characteristic for the Gaede rotary mercury pump, which had a speed of about 130 cm^3/sec at the maximum.

A modified form of the molecular pump, designed by F. Holweck,[21] is illustrated in Fig. 22. The details of the design are given in the title of the figure. With a given fore-vacuum pressure (P_1) and given speed of revolution, the fine-vacuum pressure (P_2) depends upon the clearance between the rotating cylinder and the casing. With a clearance of 0.025 mm (1 mil) and a pressure P_1 ranging from 0.01 to 70 mm., the ratio P_1/P_2 obtained was about $7 \cdot 10^7$. With a clearance twice as great, the maximum value of P_1/P_2 for the range 0.01 to 20 mm was about $2 \cdot 10^7$.

---

[20] S. Dushman, *Phys. Rev.*, **5**, 224 (1915).

[21] *Compt. rend.*, **177**, 43 (1923). See also LD, pp. 36–38 (from which Fig. 22 is taken), and *Encyclopædia Britannica*, 14th edition, Vol. 22, p. 931.

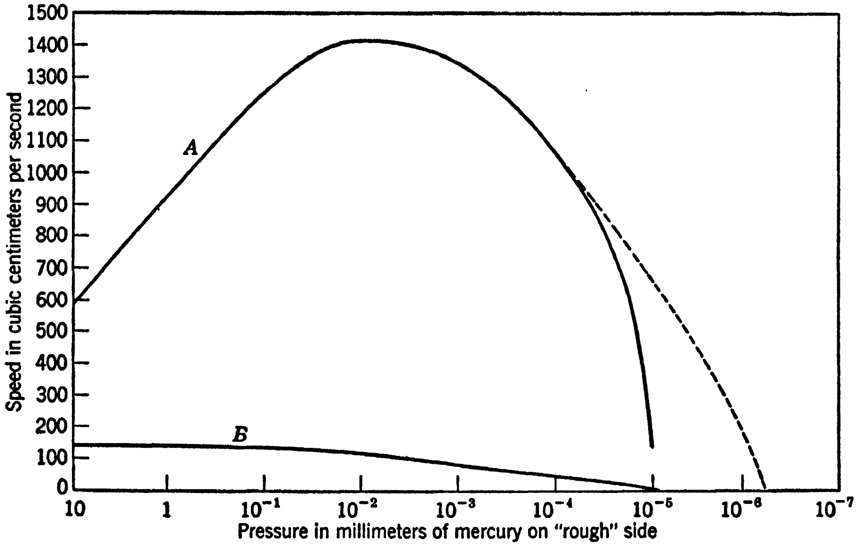

Fig. 21. Plot (curve *A*) showing effect on speed of molecular pump of variation in fore-pump pressure. Curve *B* shows speed characteristic of rotary Gaede mercury pump.

S. von Friesen[22] has described a single-disk molecular pump devised by S. Siegbahn, about 1927, for use with X-ray spectrometers. The following description of the construction is quoted from von Friesen's publication.

> Figure 23 shows a schematic section through an early pump. A circular steel disk (1) rotates inside a metal container consisting of the two shields (3). The clearance between the sides of the disk and the shields is a few hundredths of a millimeter. Spiral grooves have been cut in the shields, deep at the periphery and gradually decreasing in depth towards the center. At the outer end the cross section

[22] *Rev. Sci. Instruments*, **11**, 362 (1940). Also a description of the most recent design has been published by M. Siegbahn in *Archives for Mathematics, Astronomy and Physics* (*Royal Swedish Academy*), Vol. 30 B, No. 2 (1943).

is square and about 10 × 10 mm. Near the axis it is only about 10 × 1 mm. The disk rotates at 4000–10,000 rpm. It is mounted on ball bearings. With specially selected bearings it has been found possible to increase the speed of rotation to more than 20,000 rpm. A rubber gasket provides the vacuum-tight joint between the shields on the high-vacuum side, i.e., at the periphery. There are paper gaskets on the low-vacuum side. A long journal bearing for the shaft (6) provides means of connection between the pulley (7) and the shaft (2) of the disk with the maintenance of a fore vacuum inside. There is a flexible coupling (5) between (6) and (2). At the periphery, a conical ground joint (4) provides the connection to the apparatus which is to be evacuated. There is also a needle valve (9). The sense of rotation is such that molecules which strike the disk acquire a velocity component down the spiral groove towards the axis. There they are pumped out through the channels (8) by means of a fore pump. All bearings are situated in the region of fore vacuum, which permits the use of ordinary lubricants.

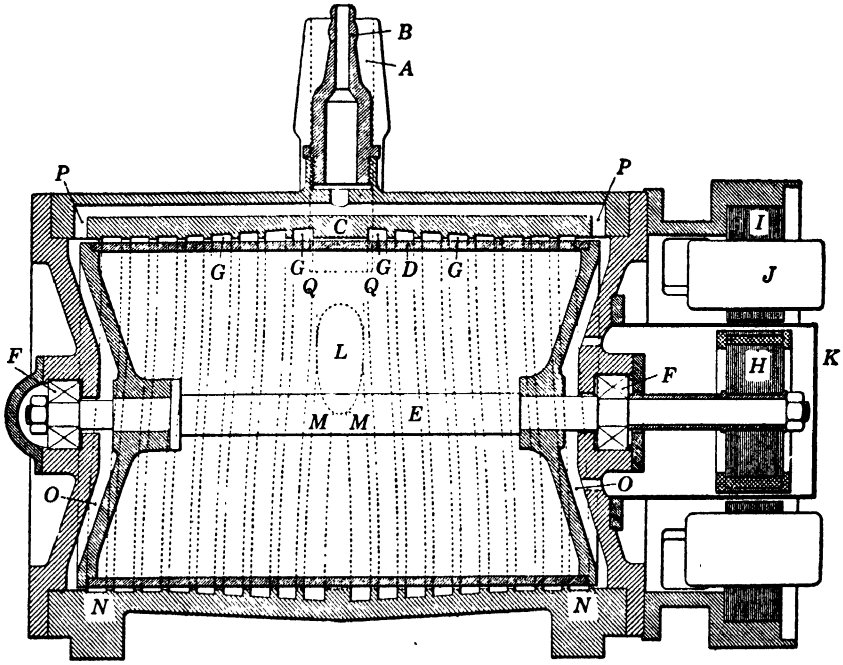

FIG. 22. Construction of Holweck molecular pump. *A*, low-pressure end of pump; *B*, high-pressure end leading to fore pump; *C*, pump body, of bronze; *D*, drum of Duralumin; *E*, axle; *F*, *F*, ball bearings; *G*, *G*, spiral channels, left- and right-handed, decreasing in depth; *H*, rotor of the driving motor; *I*, stator of motor; *J*, field coils of stator; *K*, gas-tight hood, of Constantan, enclosing the rotor in the fore vacuum; *L*, opening of intake tube; *M*, *M*, ends of the grooves; *N*, *N*, other ends of the grooves coming out into the spaces *O*, joined to the fore vacuum through the channels *P*; *Q*, *Q*, seating of wire gauze cage. The distance between the drum and the pump body and the depth of the *N* ends of the grooves are exaggerated.

Figure 24 shows the construction of a larger pump. There are three spiral grooves (I, II, III) in each shield, instead of one, each of them starting at the periphery and ending near the center. The pump may thus be described as three separate pumps connected in parallel inside a common case. The individual grooves have been made wider and deeper. The width is 22 mm. The depth varies between 22 and 1 mm.

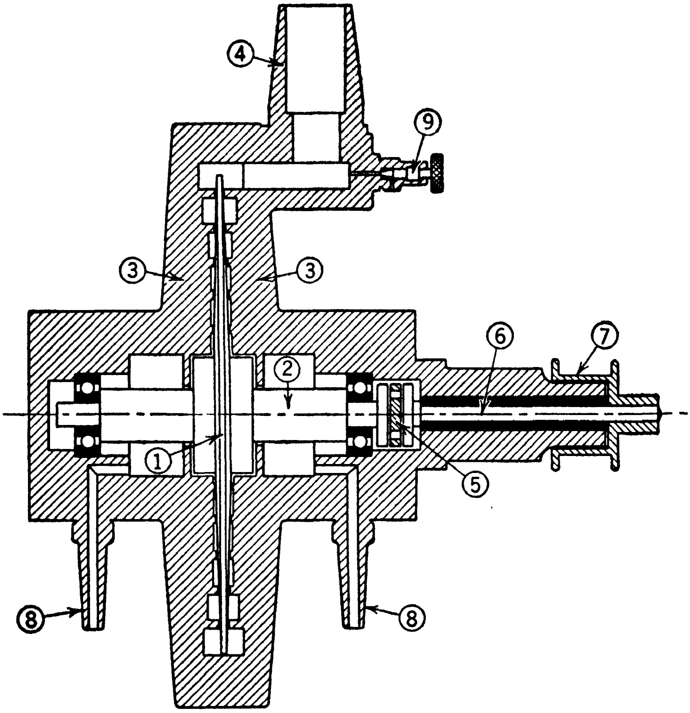

FIG. 23. Schematic diagram of a molecular pump of the ordinary Siegbahn type. Diameter of disk 22 cm.

The high-vacuum ends are joined by means of the pieces (4) to wide metal tubes (9) which have a common outlet (10). This outlet has been provided with a flange for the use of a rubber gasket seal between the pump and the apparatus to be evacuated. A new feature in this design is the use of ball bearings to support the pulley (7) and the addition of another flexible coupling (5) at the outer end of the axis.

It is stated that the pump will operate even against a pressure of several millimeters, and the pumping speed at 3700 rpm is 73 liters/sec at 10^{-3} mm. "The highest vacuum obtained is $6 \cdot 10^{-7}$ mm, as measured by means of an ionization gauge. No refrigerant or drying agent was used." This lower limit is apparently set by the vapor pressure of Apiezon grease, which according to G. Seydel[23] is about $5 \cdot 10^{-7}$ mm.

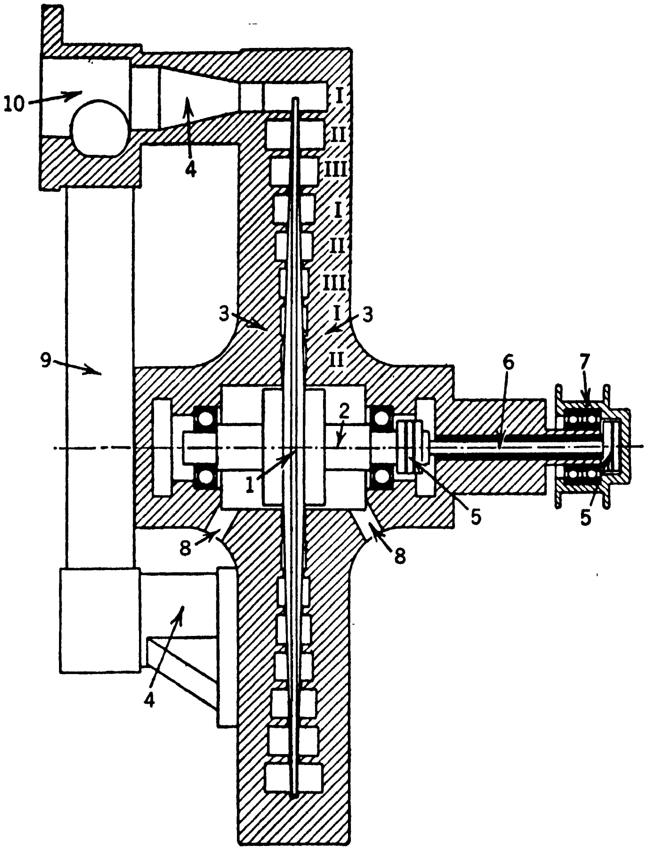

FIG. 24. Schematic diagram of a Siegbahn molecular pump with high pumping speed. Diameter of disk 54 cm.

The advantage of these pumps over diffusion pumps [according to von Friesen] is three-fold. In the first place, the time required to get them into operation is less than that required for other pumps. In the second place, they pump all kinds of gases and vapors which means that *no liquid-air traps or similar devices are required.*[24] This, in turn, means that the full speed of the pump can be utilized at all times. Thirdly, *molecular pumps have the property of pumping heavy gases faster than light ones*[24] in contrast to the diffusion pumps which behave in the opposite way. This fact constitutes a very important advantage in cyclotron work where it is essential to maintain a certain pressure of deuterium (or helium, or hydrogen) in the tank with the amount of *impurities not exceeding* a certain upper limit.

---

[23] *Z. tech. Physik*, **16**, 107 (1935).

[24] Italicized by the writer.

According to S. Eklund,[25] the fine-pump pressure (P) obtainable with a pump of the Siegbahn design is expressed as a function of the fore-pump pressure (p) by the empirical relation

$$P = P_0 + cp,$$

where P_0 is the limiting pressure and c is a pressure-ratio constant the value of which is of the order of 10^{-6} (for P and p in millimeters of mercury). Furthermore the speed of exhaust increases linearly with speed of rotation, and, for pumps with disk diameters between 22.5 and 27.5 cm, the highest speeds (about 14 liters/sec) were obtained at about 9000 rpm.

With a disk diameter of 54 cm, speeds of 60–80 liters/sec were obtained at about 8300 rpm, independently of the high-vacuum pressure (which ranged from 10^{-2} mm Hg to $2 \cdot 10^{-6}$ mm Hg).

It should be added that, according to personal reports to the writer, both Holweck and Siegbahn molecular pumps are in general use in Europe for laboratory purposes, whereas in this country mercury-vapor and oil-vapor pumps (especially the latter, where liquid air is not readily available) are customarily used.

7. DETERMINATION OF SPEED OF PUMP

In this section we shall describe a number of procedures which may be used to determine the value of S_p, the intrinsic speed of a pump, as defined by equation 2.1.

1. Constant-Pressure Method. G. W. C. Kaye[26] has described a simple method which is illustrated in Fig. 25. Into a large bulb[27] which is connected directly to the pump and also has a gauge attached, as indicated, air is admitted through a needle valve.[28] The rate at which the air is admitted is measured by the rate at which a mercury pellet travels along the calibrated capillary.

---

[25] *Archives for Mathematics, Astronomy and Physics* (*Royal Swedish Academy*), Vol. 27A, No. 21 (1940); Vol. 29A, No. 4 (1942). The writer is indebted to Dr. Eklund for sending him reprints of these papers.

[26] *High Vacua*, p. 162; FM, p. 59.

[27] It is very important that gas should be able to diffuse into the pump inlet from all directions. Therefore the *leak should be connected* to a tube of larger diameter than that of the pump inlet. This point is discussed at further length at the end of this section.

[28] JY, p. 23, gives an illustration of such a needle valve. An improved form of this type of valve has been described by P. Alexander, *J. Sci. Instruments*, **21**, 216 (1944). Also G. C. Eltenton, *ibid*, **16**, 27, (1939), has described a "greaseless" leak, the value of which may be varied by moving a wire of gradually changing diameter along the axis of a closely fitting capillary.

Let $Q_{\mu l}$ denote the rate, in *micron · liters · sec*$^{-1}$, at which air is entering the bulb, and let P_μ denote the pressure as measured by the gauge. When the rate of motion of the pellet is constant,

$$Q_{\mu l} = SP_\mu, \tag{1}$$

where S is the speed of the system (in liters · sec^{-1}) including the connection between the bulb and the pump. If F denotes the conductance of this connection, which may be calculated from the dimensions, then

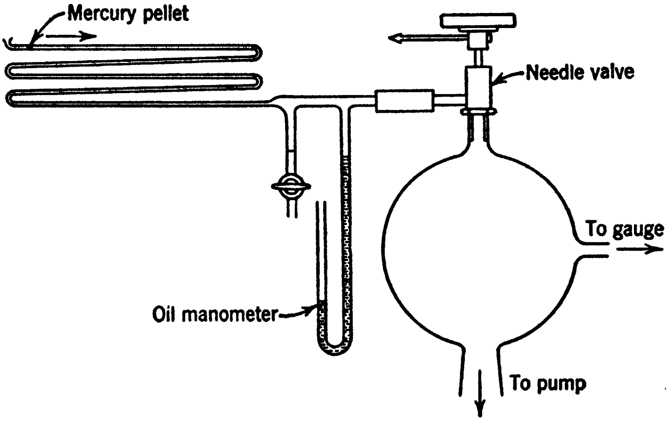

FIG. 25. Apparatus for measuring speed of pump (Kaye).

$$\frac{1}{S_p} = \frac{1}{F} = \frac{1}{S}$$

and

$$S_p = \frac{S}{1 - S/F}. \tag{2}$$

Since, in general, S_p, the intrinsic speed of the pump, varies with the fine-pump pressure, P, a series of determinations should be made at different values of $Q_{\mu l}$, and in this manner a plot is obtained of S_p as a function of P.

Instead of measuring the rate of flow of gas by means of the rate of motion of the moving pellet, a customary procedure is to observe the rate of rise of oil in an oil manometer of known cross section, the closed end of which is connected to the vacuum system through an adjustable throttle valve, as shown in Fig. 26.

The theory of the method has been described by J. R. Downing[29] as follows:

Let V_0 = initial total free volume, and let P_0 = pressure when the oil is at the same height in both sides of the manometer. Also, let A_1 and A_2 denote the cross-sectional areas in the two sides.

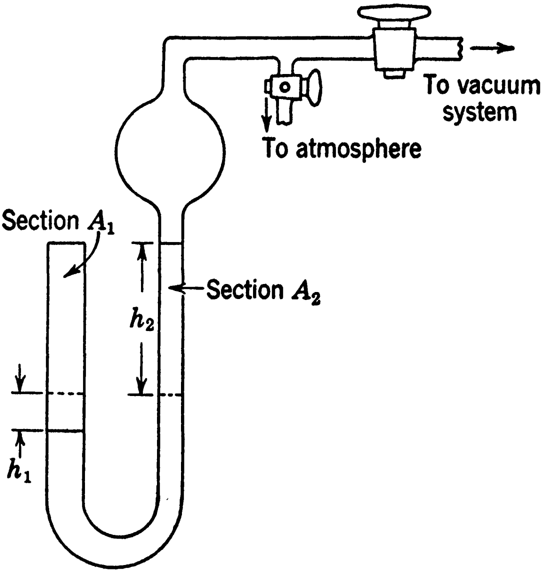

FIG. 26. Constant-pressure method for measuring speed of pump (Downing).

At any subsequent time, t, the oil in the left-hand side will have been lowered a height h_1, and the oil in the right-hand side will have been raised a height h_2. Consequently, the volume of oil displaced is given by

$$L = \int_0^{h_2} A_2 dh = \int_0^{h_1} A_1 dh.$$

Also,

$$V = V_0 - L,$$

$$^{30}P = P_0 - (h_1 + h_2),$$

and

$$PV = P_0V_0 - V_0(h_1 + h_2) - P_0L + (h_1 + h_2)L.$$

---

[29] Personal communication from the National Research Corporation.

[30] It is evident that, in this and the following equations, P and P_0 should be expressed in terms of the equivalent height of oil.

Therefore, the volume of air at unit pressure which enters the system, per unit time, is

$$\frac{P_0V_0 - PV}{P_0t} = \frac{L}{t}\left[1 + \frac{(h_1 + h_2)}{P_0}\left(\frac{V_0}{L} - 1\right)\right]. \tag{3}$$

As Downing points out, the most common error is caused by neglecting the term $V_0(h_1 + h_2)/(LP_0)$. As he has also shown, the effect caused by dynamic head (viscosity effect) may be neglected in comparison with that due to static head, which is given by equation 3.

A variation of the constant-pressure method described by H. C. Howard[31] is specially adapted for measuring speeds of exhaust up to 20 liters · $\sec^{-1}$. The following quotation from the publication contains a description of the arrangement used, which is shown in Fig. 27.

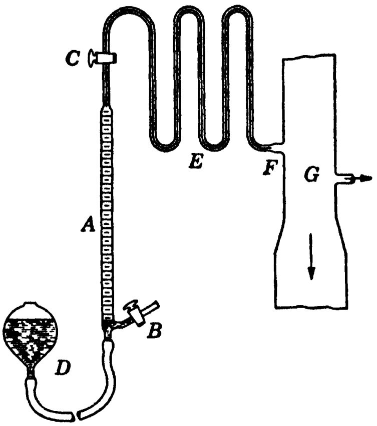

FIG. 27. Alternative constant-pressure method for measuring speed of pump (Howard).

> *A* is an ordinary gas burette of 50-cc capacity, calibrated to 0.1 cc, *B* a stopcock of 3-mm bore, and *C* of 1 mm with the edge of the bore slightly nicked so as to permit adjustment of any desired leak. *D* is a mercury leveling bulb. The capillary *E* is sealed to the system at some convenient place as *F*. The pressure in the system at the point *G* is measured by a McLeod gauge.
>
> To make a determination stopcock *C* is closed and the level of the mercury in the burette is lowered until there is free communication to the atmosphere through stopcock *B*. Stopcock *C* is then cautiously opened until the pressure at *G* reaches approximately the desired value, which in our work was 1 micron. When the pressure in the system has become constant, usually in about 30 minutes, the level of the mercury in the burette is raised until communication with the atmosphere is cut off; stopcock *B* is closed and the volume of air in the burette, the time, and the atmospheric pressure recorded. As the air is evacuated by the pump from the burette, the pressure is kept approximately atmospheric by adjusting the height of the leveling bulb. At the end of a convenient period of time, say 15 minutes, the pressure in the burette is adjusted to atmospheric and the burette reading and time recorded.

A relatively "quick method," which is a modification of the previously mentioned one, has been described by G. C. Eltenton.[32]

In determinations of pumping speeds made in this laboratory, the writer has found it very convenient to use "calibrated leaks" made of partly sintered porcelain rods.[33] These rods are coated with glass on the sides, so that flow can take place only through the ends, and are sealed into glass tubes, as shown in L in Fig. 28. They are calibrated by means of the arrangement shown in the figure.

---

[31] *Rev. Sci. Instruments*, **6**, 327 (1935).

[32] *J. Sci. Instruments*, **15**, 415 (1938); also JY, p. 59.

The leak is inserted between a bulb A containing dried gas at a pressure P_A, as indicated by the attached manometer, and the bulb B, which is connected to a pump through a stopcock. By means of a McLeod gauge connected to this bulb the rate can be measured at which gas passes through the leak L.

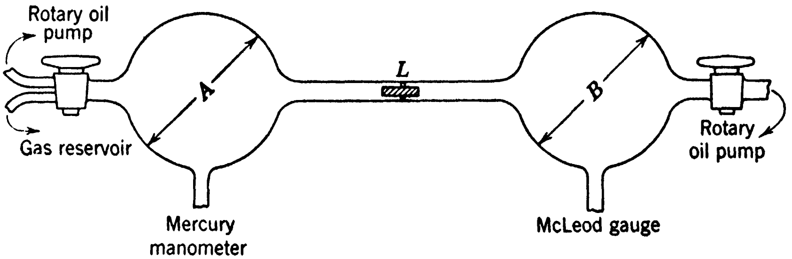

FIG. 28. Illustrating method of calibrating leak for use in measuring speeds of pumps.

Let V denote the total volume (in liters) of the bulb B and gauge. Then

$$
\begin{aligned}
Q_{\mu l} &= \text{rate at which gas enters bulb } B \text{ (in micron} \cdot \text{liters} \cdot \text{sec}^{-1}\text{)} \\
&= V\frac{dP}{dt},
\end{aligned}
$$

where P = pressure as read by the McLeod gauge at any instant, t seconds, after the start of the experiment.

As shown in Chapter 2, it follows from equation 3.1 that

$$\frac{Q_{\mu l}}{P} = A + cP, \tag{5}$$

where A represents the "free molecule" flow, and cP the Poiseuille flow at pressure P. Hence

$$A = \frac{a}{\sqrt{M}} \tag{6}$$

---

[33] A description of the preparation and characteristics of these leaks will be published in the near future.

and

$$c = \frac{b}{\eta}, \tag{7}$$

where a and b are constants characteristic of each individual leak.

Experimentally it has been found possible to control temperature and time of sintering of the rods so that the value of $Q_{\mu l}$ for air (at atmospheric pressure and room temperature) can be varied from 100 to 0.2 micron · liters per minute or less.

A procedure very similar to that involving the use of a calibrated leak is that in which a capillary of known conductance, F (which may be deduced from its dimensions), is used in series with a needle valve or other form of leak. If the conductance F is connected at one end to the pump, and the higher pressure as measured by a McLeod gauge is $P_{\mu 1}$, while the pressure at the pump as measured by an ionization gauge is $P_{\mu 2}$, then, at equilibrium between rate of inflow and rate of outflow,

$$SP_{\mu 2} = F(P_{\mu 1} - P_{\mu 2}). \tag{8}$$

2. The Constant-Volume Method is essentially an application of equation 2.4. It involves a series of measurements of the pressure in a large volume C during the exhaust by the pump whose speed is to be determined.

For example, let us assume $C = 10$ liters and $S = 0.5$ liter · sec^{-1}. Then, for P large compared to P_s,

$$\Delta t = \frac{23.03}{0.5} \cdot \Delta \log P. \tag{9}$$

For $\Delta \log P = 1$, that is, for a decrease in pressure to one-tenth its initial value, $\Delta t = 46$ sec. Since S varies with P, the most reliable method for deriving values of S is to plot $\log P$ versus t and then calculate the values of the slope of this curve at a series of decreasing values of P.

As pointed out in section 2, this method actually yields values of E, the speed of exhaust, where, according to equation 2.5b,

$$E = S\left(1 - \frac{P_s}{P}\right),$$

and P_s = ultimate pressure attained by the pump.

The greatest source of error involved in such a series of measurements is due to gas evolution from glass or metal surfaces, which, obviously, would make the observed value of E or S less than the actual value for the pump itself.

P. Alexander[34] has described a method which, he states, eliminates difficulties inherent in both the constant volume and constant pressure methods. The interval of time is measured which is required to reduce the pressure in a given volume from an initial pressure P_1 to a final value P_2, where the values of these pressures are of the order of magnitude of normal atmospheric pressure. The known volume is connected in this case to the pump through a needle valve, and the speed is then determined from these data by observing the values of P_2 and of the pressure at the pump inlet.

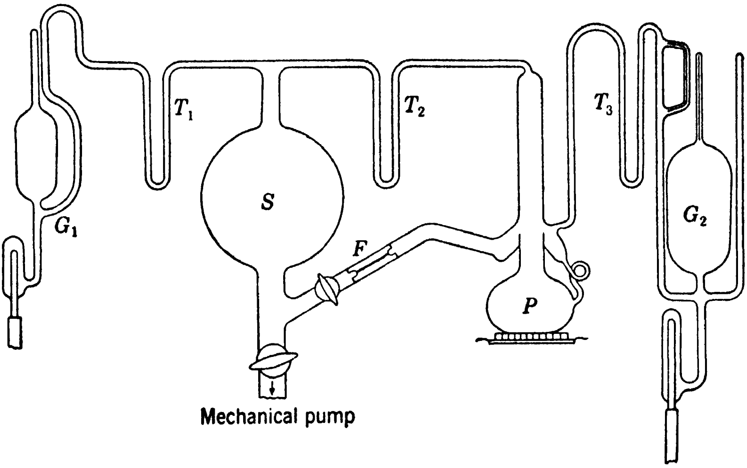

FIG. 29. Illustrating circulatory method for measuring speed of pump.

3. Circulatory Method. This method has been used in this laboratory by J. H. Payne[35] and also by M. Matricon[36] and K. C. D. Hickman and C. R. Sanford.[37] A diagram of the arrangement used by the last two is shown in Fig. 29, taken from their publication.

A calibrated "leak" of conductance F is inserted between the pump P and a reservoir S. The reservoir is connected through a large-bore stopcock to a mechanical pump which can exhaust to 0.1 micron. The McLeod gauges G_2 and G_1 indicate respectively the pressure P_2 in the jet chamber and the pressure P_1 in the reservoir S. "Traps T_1, T_2, and T_3 are included for the condensation of volatiles by liquid air or solid carbon dioxide. The condensation pump circulates the gas round and round against any chosen backing pressure, producing a reduction of pressure between the calibrated leak and the jet." The speed is determined by means of equation 8 above.

---

[34] *J. Sci. Instruments*, **21**, 216 (1944).
[35] *J. Franklin Inst.*, **211**, 689 (1931).
[36] *J. phys. radium*, **3**, 127 (1932).
[37] *Rev. Sci. Instruments*, **1**, 140 (1930).

Summarizing the different methods for measuring speed of pumps, the writer is of the opinion, as a result of personal experience, that the constant-pressure method, involving the use of a calibrated leak such as that described above, is extremely convenient. By varying the pressure at the inlet end of the leak (which can be measured with a manometer or coarse McLeod gauge) it is possible to obtain, in a relatively short period, values of the speed for a series of values of the equilibrium pressure at the pump inlet.

In connection with the application of equation 8, B. B. Dayton has pointed out that considerable variation in the measurement of S may result from failure to realize the effect of location of the gauge (used for measuring the pressure P_2 at the pump) with respect to the gas inlet. The following remarks are based largely on Dayton's[38] excellent discussion of the procedure to be used for accurate determination of pump speeds.

When gas enters a chamber from a narrow tube under conditions of molecular flow there is considerable beaming. The amount of this beaming has been calculated by P. Clausing[39] for a short tube with a length equal to its diameter. The full curve (see Fig. 30) shows the distribution calculated; the dotted curve shows the cosine-law distribution predicted for free molecular flow through a hole in a thin plate. These calculations have been checked experimentally by A. Ellett.[40] Dayton also mentions that M. Korsunsky and S. Vekshinsky[41]

> calculated the distribution to be expected when silver is evaporated on to a glass plate through narrow tubes under conditions of molecular flow. The calculations were then checked by evaporating silver through a narrow quartz tube using several different source temperatures and distances to the plate. In all cases the plate showed a central spot of high density and a rapid decrease in density away from the center, as measured by a microphotometer, in good agreement with the calculations. This distribution was compared with the normal spherical distribution from a point source consisting of a spherical silver drop on a tungsten wire.

Consequently, as Dayton points out,

> If the air is beamed away from the mouth of the gauge, the pressure recorded will be lower than normal; on the other hand if the mouth of the gauge is located directly

---

[38] Paper presented at High Vacuum Symposium, Oct. 30–31, 1947, Cambridge, Mass. See *Ind. Eng. Chem.*, **40**, 795 (1948).

[39] *Z. Physik*, **66**, 471 (1930).

[40] *Phys. Rev.*, **37**, 1699 (1931).

[41] *J. Phys. U.S.S.R.*, **9**, 399 (1945).

opposite the air inlet so that the air is beamed directly into the mouth of the gauge, the pressure reading will be higher than normal, and the measured pump speed will be less than the true speed. . . . This effect has been verified by experiments in our laboratories in which the measured speed is nearly one-half the true speed.

In order to overcome errors due to these effects, Dayton makes the following recommendation.

We believe that the proper procedure is to build a test dome of diameter equal to, or preferably larger than, that of the pump casing, and height at least equal to the diameter. The air is then introduced from a point high on the side of the dome so that the molecules are scattered into a random distribution about the top of the dome. The molecules can then diffuse through the mouth of the pump from all directions in a way which approximates the actual flow in most applications.

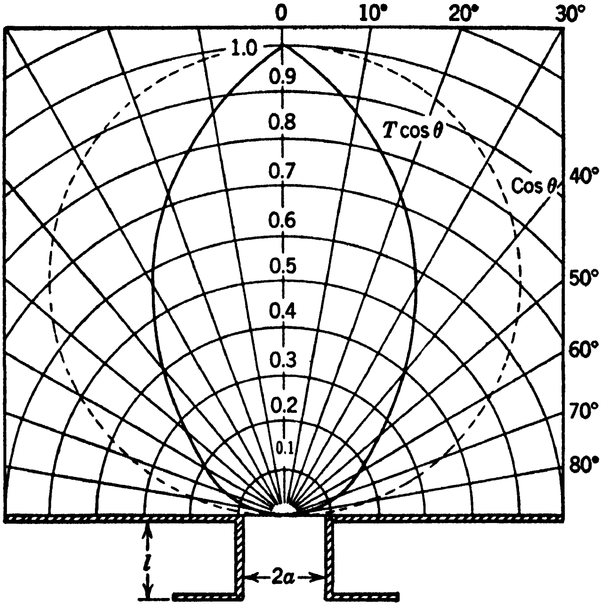

FIG. 30. Spatial distribution for free molecule flow through a short tube under conditions where L, the mean free path, is greater than $2a$, the diameter, and $l = 2a$. $T \cos \theta$, the full curve, shows the calculated distribution (T = function of θ), and the dotted curve shows the expected cosine law distribution. (Clausing.) The significance of the values on the vertical scale is illustrated by the following example: for 40°, $\cos \theta = 0.766$ and $T \cos \theta = 0.4$.

In fact data obtained by Dayton show that

the true speed as measured with a dome may be 50 per cent of the pseudo-speed as measured with a blank-off plate with air beamed directly into the jet of an unbaffled pump, while even with a baffle located in the top of the pump casing the speed with a dome may be 25 per cent less than the value obtained with a plate.

Because a number of investigators have failed to take these precautions, the values observed by them for pump speeds are probably considerably higher than the true speeds. Furthermore, from these observed values of S, values of the Ho coefficient[42] are deduced which are much too high. According to Dayton, values of this coefficient in excess of 45 to 50 per cent are to be regarded with suspicion.[43]

For this reason also Dayton has recommended that the plane of the mouth of the gauge should be placed perpendicular to that of the pump.

An alternative suggestion for eliminating directional effects on ionization gauges is to mount the electrodes of the gauge directly *inside* the test dome, as has been done by J. Blears[44] and as is shown in Fig. 5.27.

It should also be mentioned in this connection that, in Part II of his paper, Dayton has also treated very comprehensively the methods of measuring the gas flow which have been discussed above.

---

[42] The Ho coefficient is defined as the ratio between the observed speed and the theoretical value for the rate of flow of gas through the annular area between the nozzle and the walls. This is discussed in the following chapter.

[43] As an illustration Dayton cites the measurements by Copley and his associates on the speeds of the mercury vapor jet pump shown in Fig. 4.25.

[44] *Proc. Roy. Soc. London*, A, **188**, 62 (1946). See discussion in Chapter 5.

CHAPTER 4

STEAM-JET EJECTORS AND MERCURY-VAPOR PUMPS

1. STEAM-JET EJECTORS[1]

The first application of the principle of the steam-jet ejector to the production of a low pressure appears to have been made by M. Leblanc,[2] who, according to Dunoyer, showed that it is possible by means of such an ejector to obtain a pressure as low as 1 mm of mercury.

The diagrammatic sketch in Fig. 1, which is taken from a bulletin[3] published by one of the manufacturers, shows the standard terminology for the different parts of a steam ejector. The operating principle is described in this bulletin as follows:

> The steam-jet ejector operates on a mass-velocity principle. The propelling steam expands through a divergent nozzle, converting its pressure energy into velocity energy, and the mass of high-velocity steam is discharged from the nozzle in a directed flow through an air chamber and into a convergent-divergent diffuser. As the steam passes through the air chamber, it comes in contact with, and entrains, a definite mass of the vapors (or gases) to be evacuated. It imparts to this mass a portion of its own velocity by being decelerated, and the resultant total mass at the resultant velocity enters the diffuser where its velocity energy is, in greater part, converted into pressure, thus permitting the resultant mass to be discharged at a pressure considerably higher than the pressure in the air chamber. The entrained mass is thus compressed from a low absolute pressure to some higher absolute pressure.

In entering the nozzle from the steam chest the steam expands at the throat to a pressure P_t which is about 55 per cent of the pressure in the chest, and in the nozzle there is a further isentropic expansion to the value P_k which is the same as that at the suction opening. As shown in Fig. 1, the steam jet diverges in the region near the nozzle, in which the gas or vapor entering from the system to be evacuated is entrained in the steam. The mixture of gas or vapor and steam filling the cross-section of the diffuser is then compressed isentropically until it reaches the pressure P_D at the discharge opening. The relation between the kinetic energy of the steam just beyond the throat, and the pressures P_k and P_D, is of the form:[4]

---

[1] The writer is greatly indebted to P. Freneau and Dr. J. R. Shields of Elliott Company, Jeannette, Pa., for reading over the first draft of this section and for extremely helpful comments and suggestions. Where information or data obtained from this source are given in this section it is designated by the notation (FS).

[2] LD, pp. 41–42.

[3] *Bulletin* G-10, Elliott Company, Jeannette, Pa.

$$\frac{v^2}{2} = \frac{\gamma}{(\gamma - 1)} \frac{P_k}{\rho_k} \left[\left(\frac{P_D}{P_k} \right)^{\frac{(\gamma-1)}{\gamma}} - 1 \right], \tag{1}$$

where γ = ratio of specific heat at constant pressure to specific heat at constant volume = 1.32 for steam; ρ_k = density in gm · cm^{-3} at pressure P_k; P_D and P_k denote the pressures in microbars; and v = velocity of jet in cm · sec^{-1}.

Usually single-stage ejectors are operated at about the value of the ratio $P_D/P_k = 7.5$ (FS). Assuming that $P_D = 10^6$ microbars (750 mm Hg), the corresponding value of $P_k = 1.333 \cdot 10^5$ microbars (100 mm Hg), and $\rho_k = 8.97 \cdot 10^{-5}$ g · cm^{-3}. Also, $(7.5)^{(\gamma-1)/\gamma} = (7.5)^{0.2424} = 1.629$. Hence $v = 8.782 \cdot 10^4$ cm · sec^{-1}.

At the pressure P_k and density ρ_k, the velocity of sound as derived from equation 4.18, Chapter 1, is $u = 4.43 \cdot 10^4$ cm · sec^{-1}. Thus the velocity of the steam in the jet exceeds that of sound, and the value of v/u (which is known as the *Mach number*), in the above case, is 1.983.

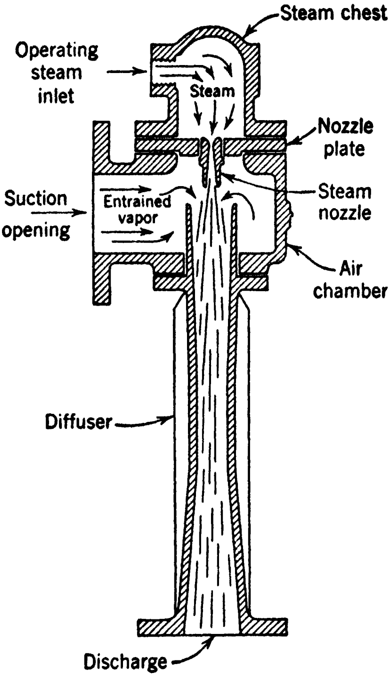

FIG. 1. Illustrating terminology for parts of steam-jet ejector.

In general, the value of the Mach number for single-stage ejectors, discharging against atmospheric back pressure, ranges as high as 3. In booster stages, that is in those stages where the back pressure is less than atmospheric, particularly in the first stages of a four- or five-stage ejector (of which illustrations are given in the following discussion), the Mach number may be as high as 9 to 11, depending on the initial steam pressure and the air-chamber pressure (FS).

Owing to this high velocity of the steam there is practically no diffusion of steam or entrained gas laterally and there is no back diffusion of entrained gas from the discharge opening. It is because of this phenomenon that it is possible by means of a steam ejector to obtain pressures as low as 100 microns or even less.[5]

---

[4] *Steam and Gas Turbines*, Vol. II, p. 972, by A. Stodola, translated by L. C. Loewenstein, McGraw-Hill Book Company, 1927.

Since the expansion of the steam in the nozzle is isentropic, the temperature in the jet, at the mouth, decreases to such a low value that the vapor pressure of water at that temperature is equal to that of P_k.

In this connection the following comments by Freneau and Shields are of importance.

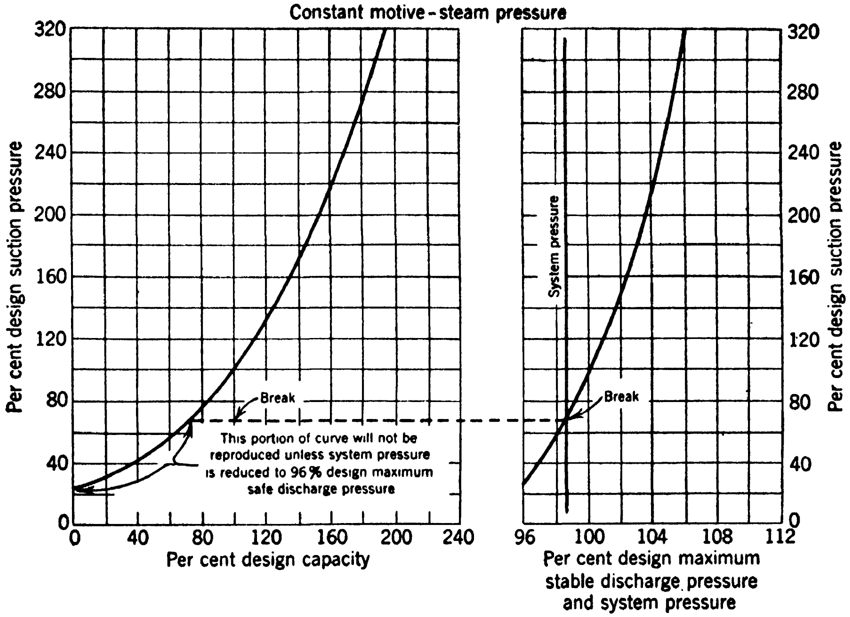

FIG. 2. Typical ejector performance curve for constant motive steam pressure, showing stable range and break point, for suction and discharge pressures expressed as percentage of design value (Freneau).

It is interesting to note that in the case of ejectors operating below approximately 4 mm mercury absolute, the isentropic expansion traverses the liquid phase into the solid-phase region, with temperatures well below freezing, so that in the case of five and some four stage ejectors it is necessary to add auxiliary heat input in order to prevent both the nozzle and diffuser from freezing.

Figure 2 taken from a paper by Freneau[6] illustrates a typical plot of the characteristics of a steam-jet air evacuator.

The right-hand chart shows the maximum discharge pressure against which the unit can operate without breaking, and the left-hand, the capacity vs. absolute suction pressure relation for stable operation. If the actual discharge pressure is at all times less than the maximum safe discharge value, the left-hand section of the chart can be used to determine the time-pressure curve of evacuation. . . .

---

[5] The writer is indebted to L. S. Stinson of Elliott Company for this explanation.

[6] *Power*, March 1947, p. 76, from which the passage quoted is taken.

Ejector capacity is almost always given in pounds per hour; in other words, a rate of removal. The ejector plot in the left chart of Fig. 2 is, therefore, absolute pressure vs. *rate of pumping*.

The plots in Fig. 3 (FS) show typical performance curves of ejector stages. Curves *A* correspond to ejector operation on design steam rate; curves *B*, to ejector operation on less than design steam rate; and curves *C*, to operation on more than design steam rate.

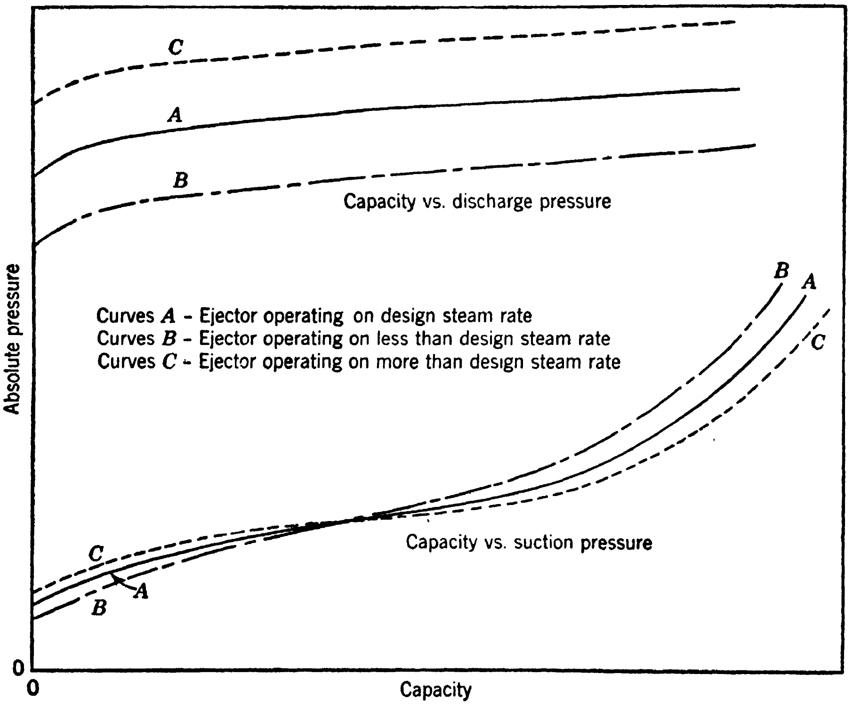

FIG. 3. Typical performance curves of ejector stage (Freneau and Shields).

According to Freneau and Shields,

When ejectors are compared to mechanical-type pumps, it must be remembered that because of its inherent characteristics, the suction pressure of an ejector cannot be varied by throttling the steam supply without a corresponding decrease in diffuser throat area or in back pressure. The former is very difficult to accomplish practically, so that it is not possible to throttle an ejector stage without decreasing the discharge pressure. Since the minimum back pressure is usually fixed for a given design, provisions for variable capacity must be made, if necessary, by artificially loading the stage with steam or air (preferably the former), or using a number of stages in parallel that are cut in or out as required. The latter method, while initially expensive, does permit steam saving during part-load operation. In the condensing type of ejector, it is possible to save steam by throttling if colder than design water temperature is available as during winter operation.

As an illustration of the operation of booster-stage ejectors and single-stage ejectors, there are given in Table 1 experimental results obtained by R. Royds and E. Johnson[7] with a number of different designs of nozzles and diffusers. It will be observed that the value of P_k increased considerably when air was allowed to enter at the suction end.

It should be noted that

$$1 \text{ lb dry air (at } 70° \text{ F)} = 13.34 \quad \text{atm} \cdot \text{cu ft}$$

and

$$\begin{aligned} 1 \text{ lb dry air (at } 70° \text{ F) per hour} &= 77.69 \quad \text{mm} \cdot \text{liters} \cdot \text{sec}^{-1} \\ &= 165.0 \quad \text{mm} \cdot \text{cu ft} \cdot \text{min}^{-1}. \end{aligned}$$

TABLE 1

EXPERIMENTAL DATA FOR OPERATION OF STEAM EJECTORS

Number of experiment	1	2	3	4	5	6
Steam pressure (lb/in.^{2})	50	60	100	100	140	140
Steam temperature (° F)	388	393	400	402	402	395
Temperature at nozzle outlet (° F)	273	290	314	316	345	335
Inlet pressure, P_k (mm Hg)	4.32	6.86	16.8	53.1	17.78	56.9
Outlet pressure, P_D (mm Hg)	151.7	266.4	402.0	485.1	690.8	717.0
Ratio P_D/P_k	35.13	38.85	24.0	9.14	38.86	12.6
Air supply (lb/hr)	0	0	0	11.25	0	11.3
Steam flow (lb/hr)	—	56.5	101	101	144	143.5

In the operation of an ejector "the shape and size of the diffuser is the major determining factor in ejector performance" (FS).[8]

As mentioned previously, it is necessary, in order to obtain low pressures, to operate an ejector stage in series with one or more booster stages, and Fig. 4[9] shows a sectional view of a two-stage non-condensing type of ejector. Figure 5[10] shows a diagrammatic sketch of a three-stage condensing steam-jet evacuator.

---

[7] *Proc. Inst. Mech. Eng.*, **145**, 193 (1941).

[8] A brief discussion of the design of jet evacuators is contained in a publication by A. E. Kroll, *Chem. Eng. Progress*, February 1947, p. 21.

[9] *Bulletin* G-10, Elliott Company.

The number of stages actually employed to obtain a desired low pressure depends upon the capacity required. Thus it is possible with a five-stage ejector to maintain 50 microns absolute pressure with quite high capacity.

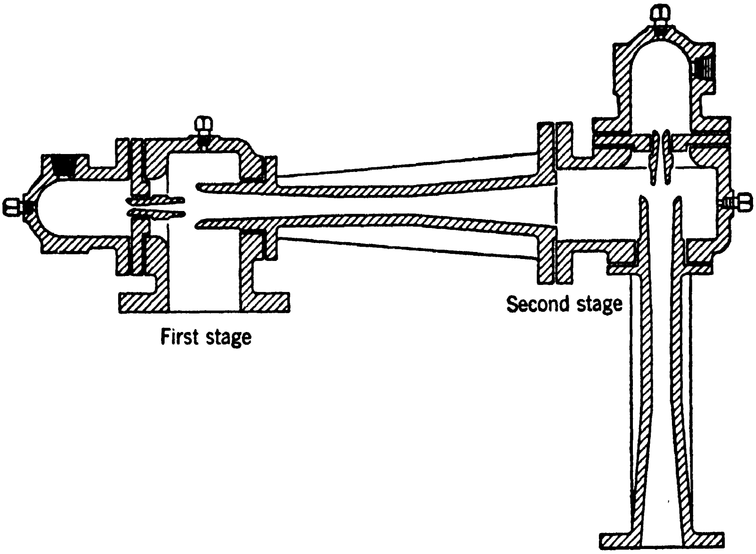

FIG. 4. Sectional view of two-stage non-condensing type of ejector.

For this reason the ejector pump has found extensive application in the chemical industry for large-scale fractional distillation, in refrigeration, and in metallurgical processes. For instance, L. S. Stinson has described[11] such a system of ejector pumps used for the production of magnesium in a vacuum furnace by the reaction between magnesia and ferrosilicon.[12]

Plots of speed vs. pressure for a two-, four-, and five-stage commercial steam ejector are shown in a paper by R. S. Morse.[13] He states that, "In most industrial plants, particularly with pressures involving condensible vapors, steam ejector systems are recommended under most conditions for all total gas pressures above 500 microns." At this pressure, a representative ejector would operate at a speed of about 5.5 lb per hour of vapor. Assuming a molecular weight of 100, this would correspond to a speed of about 20 atm · cu ft/hr or 30,000 cu ft/hr at 0.5 mm.

---

[10] *Bulletin* S-EH, Schulte and Koerting Company, Philadelphia.

[11] *Powerfax,* Winter 1944, published by Elliott Company.

[12] This is also described in the same number of *Powerfax* by G. D. Bagley. Also see discussion at Symposium on Vacuum Technique held at Cambridge, Mass., Oct. 30–31, 1947.

[13] *Ind. Eng. Chem.,* **39**, 1064 (1947).

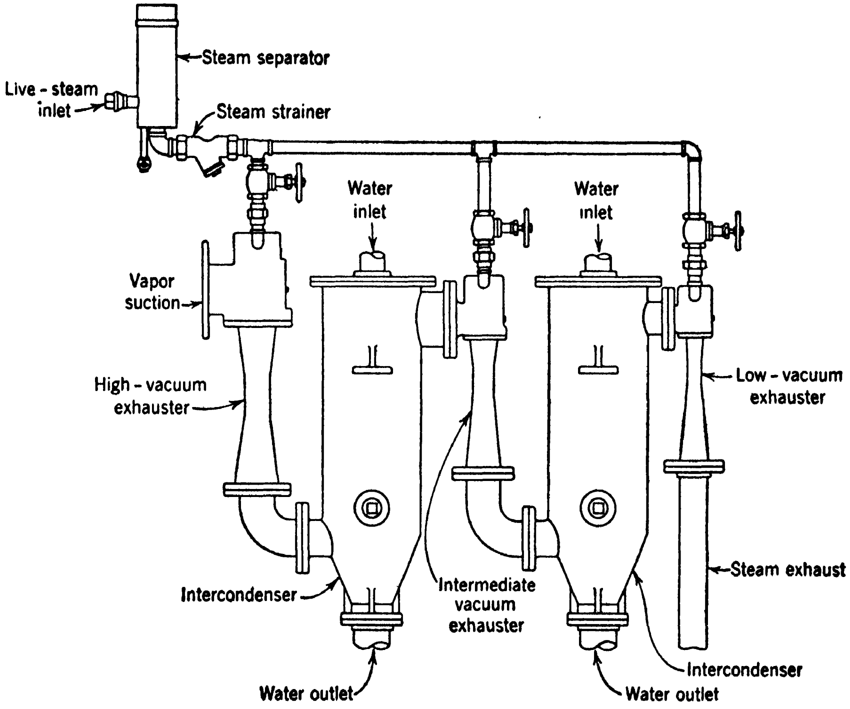

FIG. 5. Diagrammatic sketch of a three-stage condensing steam-jet vacuum pump.

The possibility of using different organic vapors in ejectors, instead of steam, has also been investigated.[14]

As will be evident from the discussion of vapor pumps in this and the following chapter, the principles of operation of the steam-jet ejector have also been applied in the design of vapor pumps, especially those that operate against rather high fore-pump pressures.

---

[14] For illustration see the paper by L. T. Work and V. W. Haedrich, "Performance of Ejectors as a Function of Molecular Weights of Vapors," in *J. Ind. Eng. Chem.*, **31**, 464 (1939).

2. DIFFUSION OF GASES IN A VAPOR STREAM

In 1915, W. Gaede[15] published a description of a high-vacuum pump which involves no mechanical motion but depends for its operation on *diffusion* of residual gases, through a slit or fine opening, into a high-velocity stream of mercury vapor traveling in front of the opening. The theory of operation of this pump is best explained by means of the following illustrations and considerations which are discussed by Gaede.

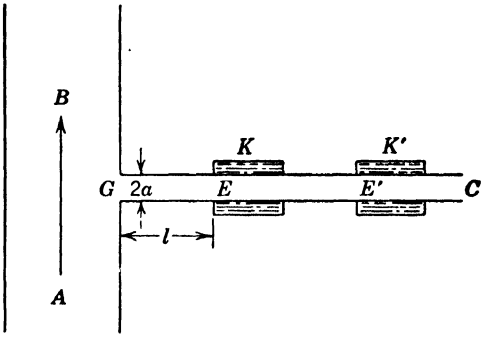

FIG. 6. Illustrating removal of gas by diffusion into a stream of vapor.

In Fig. 6, *AB* represents a stream of mercury vapor passing in the direction of the arrow in front of the opening *G* of a tube which connects at *C* with the volume to be exhausted. At *K* and *K'* the side tube is cooled by water, with the result that any mercury vapor passing into the tube is condensed at *E* and *E'*. The residual pressure of the vapor at these points is thus reduced to less than 10^{-3} mm. The vapor stream in the vertical tube entrains any molecules of air that get into the stream, and consequently there is a constant *diffusion* of gas from *C* towards *G*, due to the concentration gradient established along the tube.

Let u denote the velocity of the mercury vapor *in the direction GE*, and let n denote the concentration of gas molecules at any point x along this length, where $x = 0$ at E, and G corresponds to $x = -l$.

The rate at which gas passes from E to G is given by $-D(dn/dx)$, where *D is the diffusion constant of the gas in the mercury vapor.* The rate at which gas molecules are returned from G to E because of the velocity u of the vapor is nu. In the stationary state these rates must be equal, and consequently

---

[15] *Ann. Physik,* **46,** 357 (1915), also *Z. tech. Physik,* **4,** 337 (1923). The latter presents a summary of the earlier paper and also discusses the relation of Gaede's diffusion pump to Langmuir's condensation pump, which is described in section 4.

$$nu + \frac{D\,dn}{dx} = 0.$$

Since n is proportional to the pressure P of the gas, the last equation becomes

$$Pu + \frac{D\,dP}{dx} = 0, \tag{1}$$

where dP/dx is the pressure gradient along the tube in the gas, which is equal to and opposite to the pressure gradient in the mercury vapor.

Integrating equation 1 over the total length l between E and G, we obtain the relation[16]

$$\ln \beta = \ln \frac{P_G}{P_E} = -\frac{ul}{D}, \tag{2}$$

where P_E and P_G denote the pressures of gas at E and G, respectively, and β designates the value of the ratio P_G/P_E.

The last equation can be expressed in a form which does not involve u as follows: By definition, u = volume of mercury vapor per unit time per unit area. Hence,

$$u = \frac{P_{\mu b}F}{\pi a^2}$$

$$= P_{\mu b} \cdot \frac{2}{3} \cdot \frac{a}{l} v_a{}', \tag{3}$$

where $P_{\mu b}$ = pressure of mercury vapor at G, in microbars.

F = conductance for mercury vapor of tube of radius a.

$v_a{}'$ = average velocity of mercury atoms at $T°$ K

$$= 1028\sqrt{T} \quad \text{cm} \cdot \text{sec}^{-1}. \tag{4}$$

T = temperature corresponding to pressure $P_{\mu b}$.

Furthermore, since the diffusion constant, D, *for the gas*, varies inversely as the pressure of mercury vapor, we have the relation

---

[16] For a more comprehensive discussion of the derivation of this equation see K. F. Herzfeld and H. M. Smallwood, *Taylor's Treatise on Physical Chemistry*, 2nd edition, pp. 215–217. G. Hertz, *Physik. Z.*, **23**, 433 (1922), has shown that by using a stream of water vapor it is possible to obtain, because of the difference in rates of diffusion, a separation of pure helium from a mixture containing 70 per cent neon.

$$D = \frac{D_0}{P_{\mu b}}, \tag{5}$$

where D_0 = value at 1 microbar.

Hence, equation 2 can be written in the form

$$\ln \frac{P_G}{P_E} = -\frac{2}{3} \frac{av_a' \cdot P_{\mu b}}{D_0}, \tag{6}$$

that is,

$$\log \beta = -\frac{2}{6.91} \frac{av_a' \cdot P_{\mu b}}{D_0}. \tag{7}$$

As an illustration of the application of the last equation let us consider the case in which the temperature of the mercury vapor at G is 100° C ($T = 373$). Hence $v_a' = 1.985 \cdot 10^4$ cm $\cdot$ sec^{-1}, and $P_{\mu b} = 1333 \cdot 0.27 = 360$. At this temperature, for air in mercury vapor, $D = 0.2$ at 760 mm of mercury. Hence, $D_0 = 2.026 \cdot 10^5$, and, for $a = 0.1$ cm, $\beta = 0.79$.

In a special series of experiments, Gaede obtained results in agreement with equation 7.

The quantity of gas that would normally flow through the tube from E to G is proportional to $P_E - P_G$. However, in consequence of the streaming of mercury vapor from G to E, a back pressure of magnitude ΔP is set up, which, as shown by Gaede, is given by the relation

$$\Delta P_{\mu b} = P_E(1 - \beta). \tag{8}$$

where P_E (as well as P_G) is expressed in microbars.

Hence, the quantity of gas passing into the opening at G, per unit time, is given by

$$Q = (P_E - P_G - \Delta P)F_t, \tag{9}$$

where F_t is the conductance, *for the gas*, of the tube between E and G.

Since P_G is maintained at practically zero by the stream of mercury vapor, it follows that the speed of exhaust is given by

$$S = F_t \cdot \epsilon^{-ul/D} \tag{10}$$

$$= \frac{2}{3} v_a \cdot \frac{\pi a^3}{l} \cdot \epsilon^{-b/D_0}, \tag{11}$$

where v_a = average velocity of gas molecules in the side tube, and

$$b = \tfrac{2}{3} a v_a' P_{\mu b}. \tag{12}$$

Figure 7 shows a plot of $S(\mathrm{cm}^3 \cdot \mathrm{sec}^{-1})$ versus $a(\mathrm{cm})$ as deduced by Gaede by means of the above relations. It will be observed that, since a enters into the exponential term of equation 11, the value of S must pass through a maximum with increase in a, and then decrease exponentially.

From the discussion, in Chapter 2, of the laws of flow of gases, it follows that equation 11 is valid only for those pressures at which a is of the same order of magnitude as or less than the mean free path of the gas molecules. Thus, if a is replaced by a number of fine capillaries in parallel, the pressure at which the arrangement will function as a pump is increased.

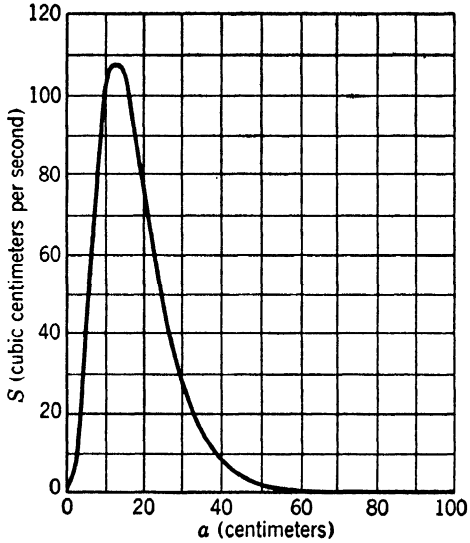

FIG. 7. Speed of exhaust by diffusion through a capillary.

As a first approximation we can omit the exponential terms in equation 11 and thus obtain a relation, for the speed of exhaust, of the form

$$S = \frac{2}{3} v_a \frac{\pi a^3}{l}, \tag{13}$$

which is identical with the value of the conductance, F_t, for a cylindrical tube of radius a and length l, under the condition l/a very large.

However, under these circumstances, F_t has a very low value. If, on the other hand, we attempt to reduce l and increase a, then equation 11 is no longer valid.

As a result of these considerations Gaede was led to the development of the theory of diffusion of gas molecules through a fine opening or narrow slit which is traversed by the vapor of a readily condensible liquid.

Let us consider the case of a circular opening of area A in a thin wall which separates the space G (containing gas) from the space B which is filled with the vapor. Gas molecules pass through the opening from G into B, while the vapor molecules pass through the opening in the opposite direction and are condensed on an adjacent surface. A fraction, α, of the gas molecules approaching the opening collide with the vapor molecules from the space B and are removed by the stream of vapor, passing in front of the opening, as fast as they enter. Under these conditions the speed of exhaust of the gas is given by the relation

$$S = \frac{\alpha A v_a}{4}. \tag{14}$$

Gaede has shown that α is a function of a/L, where a = radius of circular opening (or width of slit) and L = mean free path of gas. A plot of α as a function of $2a/L$ shows that α increases from 0 for $a = 0$ to slightly less than 1 for $a/L = 0.5$, and increases very slowly, for larger values of a/L, to the limiting value 1.

From the last equation it follows that the speed of exhaust varies inversely as the square root of the molecular weight of the gas and is independent of the pressure. In this respect, therefore, a "diffusion" pump represents a radical departure from the mechanical pumps described in the previous chapter.

In deducing equation 14 it has been assumed that the stream of vapor removes the incoming molecules of gas completely. As Gaede points out, this is not necessarily a valid assumption. The vapor can remove only a limited fraction of the gas molecules which collide with those of the vapor. That is, the vapor has a limited "extracting power."[17] It is evident that this factor, which we will designate by k, must increase with the velocity of the vapor stream and with decrease in the value of a. Hence the factor α in equation 14 should be replaced by $k\alpha$.

The speed is also reduced as a result of back diffusion of gas from the fore pump. Just below the orifice the pressure of gas, P_0, is maintained at an extremely low value because gas is removed very rapidly by the stream of vapor. Since this pressure is lower than P_f, the pressure at the opening to the fore pump, there is a back diffusion of gas, and from equation 2 it follows that

$$\beta = \frac{P_0}{P_f} = \epsilon^{-ul/D} \tag{15}$$

---

[17] This translation of the German term "Aufnahmefähigkeit" has been suggested by T. L. Ho, *Physics*, **2**, 386 (1932).

where l denotes the average distance which the vapor travels before it is condensed.

Consequently, the net speed of exhaust through the orifice is given by

$$S = 0.25Av_a\left(k\alpha - \frac{\beta P_f}{P}\right), \tag{16}$$

where P denotes the pressure in the volume that is being exhausted.[18]

If the value of β is not negligible, then it is possible for the speed of exhaust to become equal to zero at a pressure

$$P_s = \frac{P_f\beta}{k\alpha}, \tag{17}$$

which, therefore, represents the lower limit of pressure attainable on the high-vacuum side. In fact, at low velocities of the vapor, β may be greater than $k\alpha P/P_f$, and S then becomes *negative*. Gas diffuses from the fore pump into the high-vacuum side.

It is of interest to determine the manner in which β varies with the pressure of mercury vapor. Let us consider the case, discussed previously, of air, with mercury vapor at $T = 373$, for which the values of both v_a' and D_0 are given above. The value of D_0 varies approximately at $T^{3/2}$, that of v_a' varies as $\sqrt{T}$.

Table 2 gives values of P_f/P_0 calculated by means of equation 7 for a series of temperatures at which the corresponding pressures of mercury vapor are given by P_{mm}, and for two values of a.

TABLE 2

VALUES OF P_f/P_0 FOR A SERIES OF PRESSURES OF MERCURY VAPOR

T	P_{mm}	$a = 0.1$	$a = 1.0$
355	0.1	2.50	$9.45 \cdot 10^3$
373	0.27	10.50	$1.62 \cdot 10^{10}$
385	0.505	70.70	$3.16 \cdot 10^{18}$
400	1.04	$4.65 \cdot 10^3$	

Thus β decreases rapidly with increase in T and with a sufficiently high velocity of the vapor,

$$S = \frac{k\alpha A}{\sqrt{2\pi\rho_1}}. \tag{18}$$

---

[18] P must obviously be *higher* than P_0 in order that gas may diffuse through the orifice.

That is, for air at 25° C

$$S = 6.281 \cdot 10^4 \frac{k\alpha A}{\sqrt{M}} \quad \text{cm}^3 \cdot \text{sec}^{-1} \tag{19}$$

$$= 11.67\, k\alpha A \quad \text{liter} \cdot \text{sec}^{-1} \text{ for air.} \tag{20}$$

3. THE GAEDE DIFFUSION PUMP

A simple illustration of the manner in which the above considerations have been applied by Gaede towards the development of a high-vacuum vapor pump is given in Fig. 8. A blast of steam is blown through the tube *AB*, in which is fixed a porous diaphragm *C*. The vessel to be exhausted is attached at *E*. Water vapor diffuses through the capillaries in the diaphragm into the trap *D*, where it is condensed by some refrigerating agent, while air diffuses through the diaphragm in the opposite direction into the tube *AB*, from where it is drawn away rapidly by the blast of steam. The result is that the pressure in *E* decreases and finally reaches a very low value.

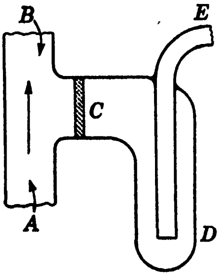

FIG. 8. Illustrating method of operation of Gaede diffusion pump.

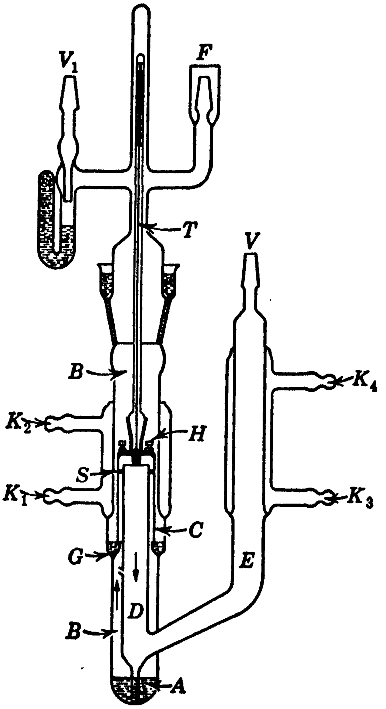

FIG. 9. Original Gaede diffusion pump.

The actual construction of the Gaede "diffusion" pump is shown in Fig. 9. The porous diaphragm used in the construction shown in Fig. 8 is replaced by a steel cylinder *C* with a narrow slit *S* whose width can be altered by means of the set screws *H*. The cylinder is set in the mercury trough *G*, which forms a seal between the low- and high-pressure sides. The mercury at *A* is heated, and the stream of vapor passes over the slit in the steel cylinder in the directions indicated by the arrows. The air or other gas from the system to be exhausted (connected at *F*) diffuses into this mercury stream at *S*, and then passes out through *E* into the fore pump, which is connected at *V*. Any mercury vapor passing out through *S* is condensed on the glass in the immediate neighborhood by means of the water cooling jacket K_1K_2. The opening V_1 connects with the fore pump or other source of rough vacuum and is used for exhausting the system until the pressure gets low enough for the operation of the diffusion pump to become effective. As soon as this stage is reached the mercury in the trap automatically closes this opening and the exhaust then continues by means of the diffusion pump.

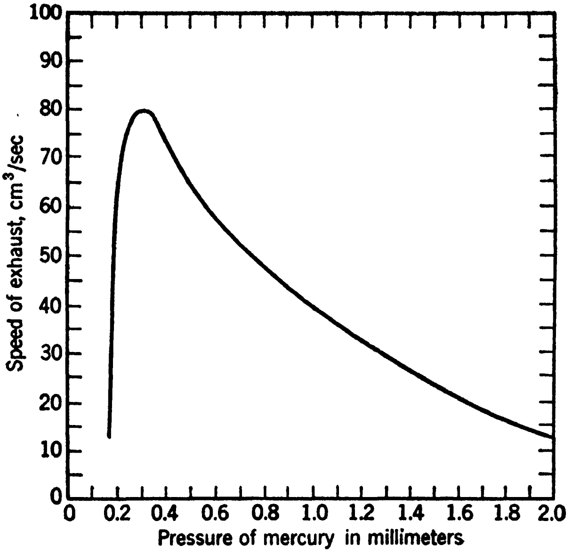

FIG. 10. Effect of variation in mercury-vapor pressure on speed of Gaede diffusion pump.

Since the maximum speed of the pump is attained when the width of the slit *S* is of the same order of magnitude as the mean free path of the gas molecules in the mercury vapor, the pressure of the mercury vapor has to be maintained fairly constant. For this purpose, a thermometer *T* is placed inside the tube *B*.

The effect of varying the temperature (and consequently the pressure of mercury vapor) on the speed of exhaust is shown by the plot in Fig. 10. In this experiment the slit width was 0.012 cm, corresponding to $A = 0.13$ cm^2. The maximum speed of 80 cm$^3 \cdot$ sec^{-1} was obtained at a temperature of the mercury vapor of 100° C. This corresponds to 615 cm$^3 \cdot$ sec$^{-1} \cdot$ cm^{-2} (as compared with $S = 11{,}670$ cm$^3 \cdot$ sec$^{-1} \cdot$ cm^{-2} given in Table 2.2). It follows that in this case $k = 0.053$. The values for k observed by Gaede in other experiments varied from 0.04 to 0.14.

The value of L_A, the mean free path of gas molecules in mercury vapor, may be calculated by means of equation 8.33, Chapter 1. Assuming that the concentration of molecules of air is small compared to that of the mercury vapor, and that the temperature of the air is 25° C,

$$L_A = \frac{1.961 \cdot 10^{-5} T_B}{P_{mm}\sqrt{1 + 4.835 \cdot 10^{-4} T_B}}, \qquad (1)$$

where P_{mm} = vapor pressure of the mercury at the temperature T_B. For $T_B = 373$ and $P_{mm} = 0.273$, $L_A = 2.47 \cdot 10^{-2}$ cm, whereas, as observed above, $2a = 1.2 \cdot 10^{-2}$.

The great advantage of the diffusion pump over the mechanical types of pump consists in the fact that there is theoretically no limit, except that imposed by equation 2.16, to the degree of vacuum that can be attained by its operation. With the Gaede rotary pump and all mechanical pumps the speed of exhaust decreases with decrease in pressure. With the Gaede molecular pump the minimum pressure attainable depends upon the pressure in the fore vacuum since the ratio of the pressures is constant for the pump. Thus, in all these pumps, the pressure attainable in the exhaust system has a fixed lower limit. Although the diffusion pump has no such limitation, it does have the double disadvantage of low exhaust speed and the necessity of carefully regulating the temperature of the mercury vapor.

4. THE LANGMUIR CONDENSATION PUMPS

Both these disadvantages are eliminated in the design of vapor pump developed by Langmuir,[19] in which some of the features of the ejector pump are incorporated. An analysis of the action of this pump shows, according to Langmuir, that in its action two separate processes are involved.

1. The process by which the gas is drawn into the blast of vapor.
2. The action of the blast in carrying the admixed gas along into a condensing chamber from which it cannot return to the vessel being exhausted.

The ejector pump fails at low pressure because, at these pressures,

---

[19] *Gen. Elec. Rev.*, **19**, 1060 (1916), also *J. Franklin Inst.*, **182**, 719 (1916).

"according to the kinetic theory of gases, the molecules in a jet of gas, passing out into a high vacuum, must spread laterally, so that there is no tendency for gas molecules to be *drawn* into such a blast."

These considerations and the results of his previous investigations on the mechanism of condensation of gas molecules on solid surfaces led Langmuir to the conclusion that the mercury atoms could readily be prevented from returning in the direction from which the gas molecules are diffusing by simply cooling the walls of the tube near the mercury-vapor outlet. Under these conditions the mercury atoms ought to be rapidly condensed as they strike the walls. At the same time the gas molecules diffusing in from the system to be exhausted would collide with the high-speed mercury atoms at the jet and thus acquire from them a velocity component which would remove them rapidly from the space around the jet opening. The whole action of the pump constructed on the basis of this reasoning thus rests on the fundamental principle *that the mercury vapor, after having imparted its momentum to the gas molecules, is rapidly condensed as it leaves the jet* and the temperature is maintained so low that the mercury does not re-evaporate to any measurable extent. Langmuir therefore suggested that pumps based on this principle should be designated as "condensation" pumps.

Thus the difference between the operation of the condensation pump and that of the ejector pump is due fundamentally to the fact that in the ejector pump the gas or vapor is entrained by the jet traveling, as shown in section 1, at supersonic speed, whereas in the condensation pump the gas molecules acquire a forward momentum as a result of collisions with mercury atoms, which are then removed by condensation on the walls.

However, from the fact, mentioned in section 1, that it is possible by means of vapor ejector pumps to obtain fairly low pressures (10 to 100 microns or even lower), it may be concluded that the mechanism of evacuation in the condensation pump is similar in many respects to that in the ejector pump. That this conclusion is justified will be evident from the subsequent discussion in this chapter (see especially section 7) and from the fact that higher speeds of pumping may be obtained by suitable design of the nozzle through which the mercury vapor enters the condensing chamber.

An early type of glass pump constructed on the condensation principle is shown in Fig. 11, and the following description is given by Langmuir.

> In this pump, mercury vapor from the flask *A* is carried through the thermally insulated tube *B* to the nozzle *L*. The vessel to be exhausted is connected to *R*. The gas from this vessel passes through the trap *G* and the tube *F* into the annular space *E*. At *P* this gas comes into contact with the mercury-vapor blast issuing

from the nozzle *L* and is thus forced outward and downward against the walls of the tube *C* and is finally driven down into the space *D* from which it escapes into the rough-pump connection *N*. The mercury which condenses on the sides of the water-cooled tube *C* passes back through the tube *M* into the boiler *A*.

In order that the pump may function properly it is essential that the end of the nozzle *L* shall be located below the level at which the water stands in the condenser *J*. In other words, the overflow tube *K* must be placed at a somewhat higher level than the lower end of the nozzle as is indicated in the figure. The other dimensions of the pump are of relative unimportance. The distance between *L* and *D* must be sufficiently great so that no perceptible quantity of gas can diffuse back against the blast of mercury vapor, and so that a large enough condensing area is furnished.

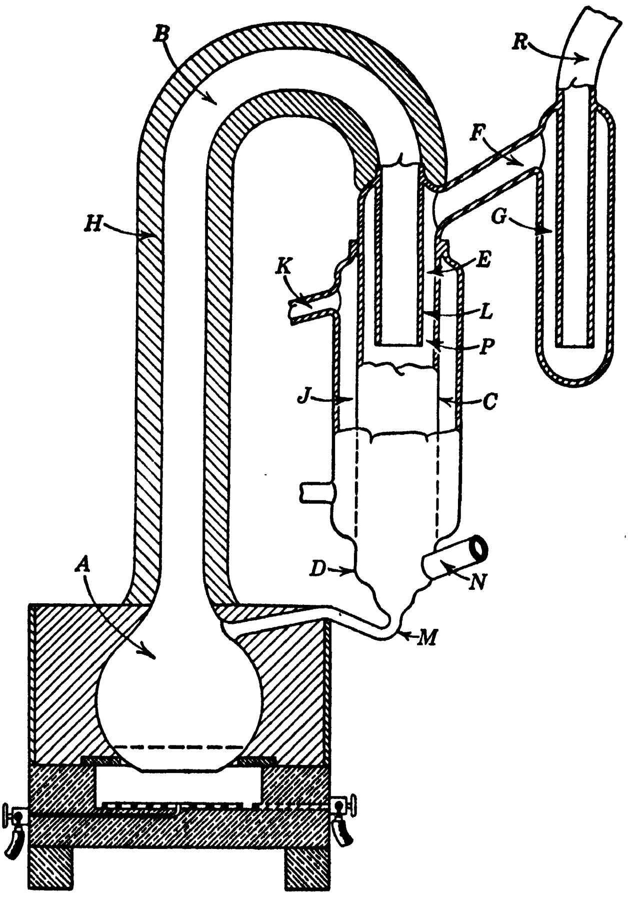

FIG. 11. Langmuir condensation pump, glass form.

The pump may be made in any suitable size. Some have been constructed in which the tube *B* and the nozzle *L* were one and a quarter inches in diameter while in other pumps this tube was only one-quarter of an inch in diameter and the length of the whole pump was only about four inches. The larger the pump the greater is the speed of exhaustion that may be obtained.

In the operation of the pump the mercury boiler *A* is heated by either gas or electric heating so that the mercury evaporates at a moderate rate. A thermometer placed in contact with the tube *B*, under the heat insulation, usually reads between 100 and 120 degrees C when the pump is operating satisfactorily. Under these conditions the mercury in the boiler *A* evaporates quietly from its surface. No bubbles are formed so there is never any tendency to bumping.

Unlike Gaede's diffusion pump, there is nothing critical about the adjustment of the temperature. With an electrically heated pump in which the nozzle *L* was ⅞ in. in diameter, the pump began to operate satisfactorily when the heating unit delivered 220 watts. The speed of exhaustion remains practically unchanged when the heating current is increased even to a point where about 550 watts is applied.

The back pressure against which the pump will operate depends, however, upon the amount and velocity of the mercury vapor escaping from the nozzle. Thus in the case above cited, with 220 watts, the pump would not operate with a back pressure exceeding about 50 microbars, whereas with 550 watts back pressures as high as 800 microbars did not affect the operation of the pump.

The speed of a pump of this construction has been found to be about 1700 $\mathrm{cm}^3 \cdot \mathrm{sec}^{-1}$ with 265-watt input and a maximum fore-pump pressure of 0.3 mm of mercury.

As with the Gaede pump, there is no definite lower limit to which the pressure may be reduced. Such a lower limit could arise only through diffusion of gas from the fore pump (*N* in Fig. 11) against the blast of mercury vapor passing down from *L*. According to equation 3.1 above, the mean free path of a molecule of air in mercury vapor at a pressure of 1 mm is $7.2 \cdot 10^{-3}$ cm. The probability that a molecule will move a distance x/L_A *without* suffering a collision is ϵ^{-x/L_A}. Table 3 gives a few values of x/L_A and the corresponding values of the exponential function.

TABLE 3

PROBABILITY OF COLLISION AS A FUNCTION OF THE RATIO BETWEEN DISTANCE TRAVERSED AND MEAN FREE PATH

x/L_A	ϵ^{-x/L_A}	x/L_A	ϵ^{-x/L_A}
0.5	0.607	4.0	0.018
1.0	.368	5.0	.0067
2.0	.135	7.5	.00055
3.0	.050	10.0	.000045

Thus, for $L_A = 7.2 \cdot 10^{-3}$, the probability that a molecule will travel a distance $x = 7.2 \cdot 10^{-2}$ cm without a collision is 0.000045, and the probability that it will move freely a distance of several centimeters is infinitesimally small.

For most practical purposes a glass pump has many disadvantages. Langmuir therefore applied the same principles to the construction of a metal pump. According to Langmuir,

> One type of pump which has proved relatively simple in construction and efficient in operation is shown diagrammatically in Fig. 12. A metal cylinder *A* is provided with two openings *B* and *C*, of which *B* is connected to the backing pump and *C* is connected to the vessel to be exhausted. Inside of the cylinder is a funnel-shaped tube *F* which rests on the bottom of the cylinder *A*. Suspended from the top of the cylinder is a cup *E* inverted over the upper end of *F*. A water jacket *J* surrounds the walls of the cylinder *A* from the level of *B* to a point somewhat above the lower edge of the cup *E*.
>
> Mercury is placed in the cylinder as indicated at *D*. By applying heat to the bottom of the cylinder the mercury is caused to evaporate. The vapor passes up through *F* and is deflected by *E* and is thus directed downward and outward against the water-cooled walls of *A*. The gas entering at *C* passes down between *A* and *E* and at *P* meets the mercury-vapor blast and is thus forced down along the walls of *A*

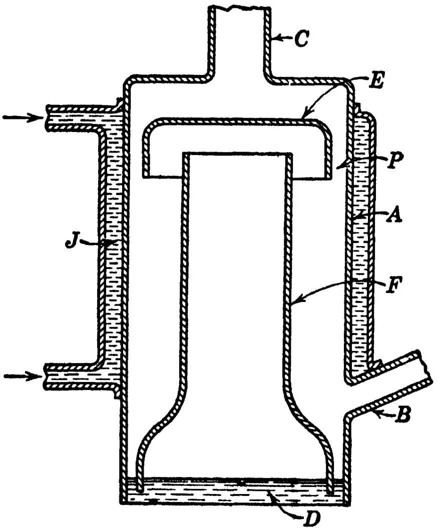

FIG. 12. Diagram of construction of condensation pump, metal form.

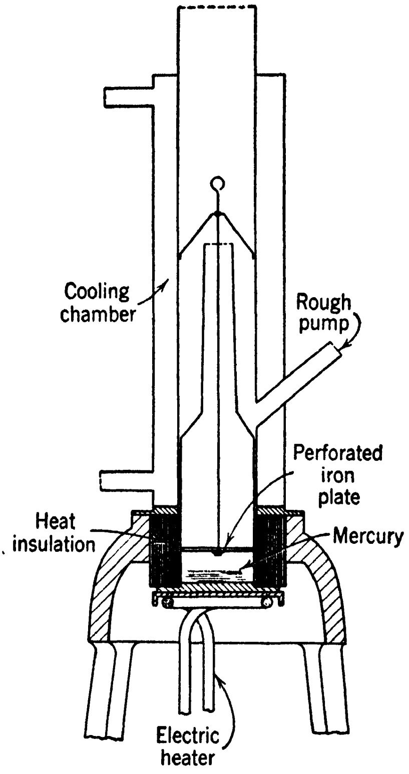

FIG. 13. Construction of single-stage condensation pump, metal form.

and out of the tube *B*. The mercury which condenses on the walls of *A* falls down along the lower part of the funnel *F* and returns again to *D* through small openings provided where the funnel rests upon the bottom of the cylinder.

Figure 13 shows an early form of single-stage metal pump constructed in this laboratory. The demountable design was intended for ease in cleaning the inside of the pump. With 35 cm^3 of mercury and 250-watt input, the speed obtained was 6 liters · sec^{-1} against a fore pressure of 0.1 mm.

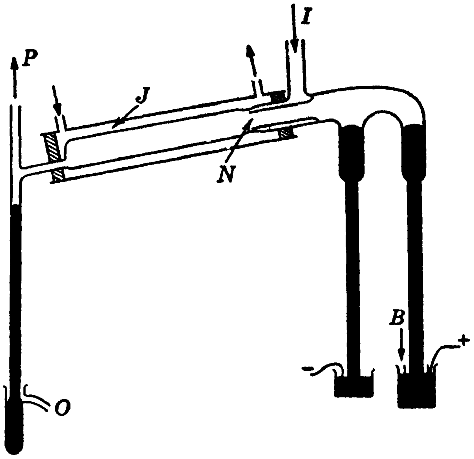

FIG. 14. Condensation pump, arc type.

One of the earliest forms of mercury condensation pumps is that described by H. B. Williams.[20] A construction used by L. T. Jones and N. O. Russell[21] is illustrated in Fig. 14. The advantage of this form is that it "permits using the pump as a mercury still at the same time that it is being used for exhaustion purposes. Two barometer columns introduce the mercury into the arc, the arc being started by blowing in one neck of the Woulff bottle, as shown at *B*. The mercury vapor is driven through the nozzle *N* and condenses in the chamber surrounded by the water jacket *J*. The condensed clean mercury is then drawn off at *O*." With a current of 10–15 amp, a speed of exhaust of 400 cm^3 · sec^{-1} was obtained.

Simple constructions of condensation pumps have also been described by W. C. Baker[22] and by J. E. Shrader and R. G. Sherwood.[23] Full details of Sherwood's construction, with all necessary dimensions, are given in the original paper. The speed of the pump was observed to be a maximum at about 400–500 watts input. Pressures as low as $2 \cdot 10^{-5}$ micron were obtained after the precaution had been taken of heating all the glass parts to a temperature of 500° C for a long period.

---

[20] *Phys. Rev.*, **7**, 583 (1916).
[21] *Phys. Rev.*, **10**, 301 (1917).
[22] *Phys. Rev.*, **10**, 642 (1917).
[23] *Phys. Rev.*, **12**, 70 (1918).

An interesting form of mercury-vapor pump, designed by W. W. Crawford,[24] is shown in Figs. 15 and 16.

The mercury vapor generated in the boiler B at a pressure of 10 mm of mercury or more, escapes through the narrow throat T (Fig. 15), ahead of the point of entrainment. The vapor expands in the diverging nozzle N, and the issuing jet passes through the tube E, which it fills, and condenses in D, mostly, where it is found at the upper end. A slight amount of vapor escapes into the chamber A and condenses there. The condensed vapor drains back through the tubes a and b, to the boiler.

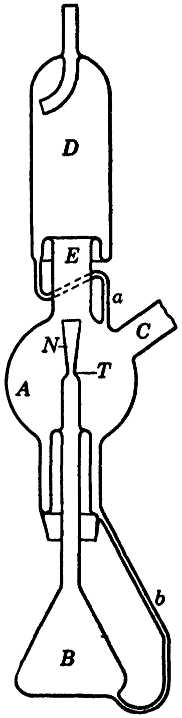

FIG. 15. Crawford's design of glass condensation pump, vertical form.

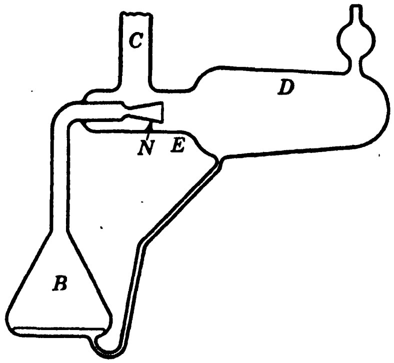

FIG. 16. Crawford's design of glass condensation pump, horizontal form.

The vessel to be exhausted is connected at C, while D connects with the rough pump. The speed of the pump in series with 10 cm of tubing, 1.9 in diameter, was observed to be around 1300 cm^3/sec at a boiler pressure of 10 mm of mercury.

As will be observed, the introduction of a jet, designed along the same lines as the nozzle in an ejector, made it possible to operate this pump at a much higher boiler pressure. In a subsequent section the further application of these considerations will be discussed in greater detail.

[24] *Phys. Rev.*, **10**, 557 (1917).

5. MULTISTAGE PUMPS

Since the single-stage pump described above requires a relatively low fore-pump pressure, a number of designs were developed in which one or more stages are added, which operate more on the principle of the ejector.

Thus Gaede[25] described a three-stage pump made entirely of steel, which could be operated against a pressure of 20 mm at a speed of 60 liters · sec^{-1} for air and 100 liters · sec^{-1} for hydrogen.

As in the case of the single-stage pumps, a large number of different designs of two- and three-stage mercury-vapor pumps have been described in the literature. In fact it may be stated that each laboratory has developed its own particular modification which it believes to be a distinct improvement over all other types. This remark applies especially to the designs of pumps made of Pyrex (Corning G 702 P) or Nonex, which can be operated at higher temperatures of the mercury boiler than are possible with pumps made of lead or lime glass.

A two-stage pump made of Pyrex has been described by E. K. Kurth, and Fig. 17 shows a variation of this construction designed by W. A. Ruggles in this laboratory. It has the great advantage that the glass blowing is not very difficult.

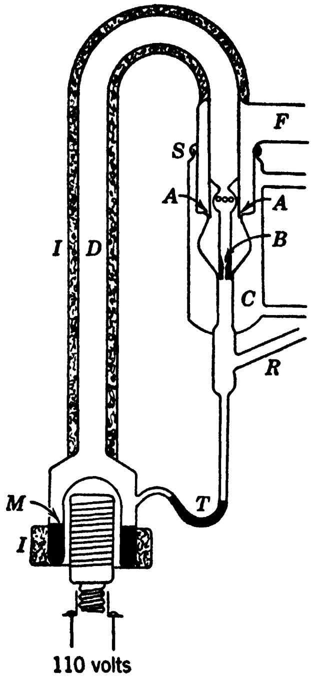

FIG. 17. Design of Kurth-Ruggles two-stage mercury-vapor pump, glass form.

The mercury boiler shown at M is heated by a standard radiant heater unit as shown, and the blast of mercury passes up the tube D which is covered with some heat-insulating material I. The mercury passing through the small holes past the opening A is condensed on the adjacent parts of the walls by the cooling water in the jacket C, and thus functions there on the condensation pump principle, while the higher-pressure stage occurs at the opening to the nozzle B. The rough pump is connected to R, and the vessel to be exhausted, at F. Tape, S, is wound around the top of the water jacket C and thus provides a flexible joint there.

---

[25] *Z. tech. Physik*, **4**, 337 (1923). This pump has also been described by the writer in *J. Franklin Inst.*, **211**, 689 (1931).

The speed obtained with this pump, when used in series with a liquid-air trap, is about 700 $cm^3 \cdot sec^{-1}$, and pressures as low as $5 \cdot 10^{-5}$ micron have been attained, as measured by an ionization gauge.

Two-stage mercury-vapor pumps have also been described by M. Volmer,[26] C. A. Kraus,[27] and H. F. Stimson.[28] The last two consist essentially of two Langmuir pumps in series. The speed attained with Stimson's design is reported to be 250 $cm^3 \cdot sec^{-1}$.

Two designs of all-metal mercury-vapor pumps have been described by I. Backhurst and G. W. C. Kaye,[29] in which the first stage utilizes the principle of the ejector. The speed obtained in the second, more compact design varies from 1000 to 7000 $cm^3 \cdot sec^{-1}$, "depending on the pressure in the vessel being exhausted and also on the value of the back pressure against which the pump is working. . . . The pump will readily produce a vacuum of the order of 10^{-5} mm or less when working against a back pressure of 1 mm of mercury."

A two-stage metal pump, designed by the Philips Lamp Company, of Eindhoven, Holland, around 1926, has a speed of 1700 $cm^3 \cdot sec^{-1}$ at a fore-pump pressure as high as 4.9 cm.

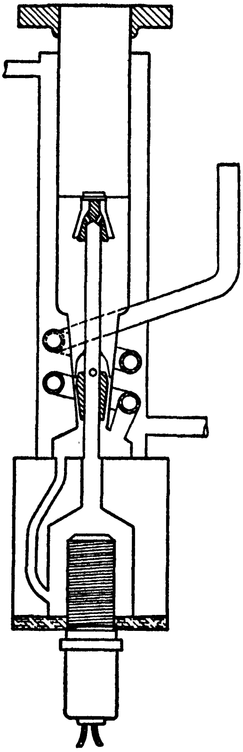

FIG. 18. Design of two-stage mercury-vapor pump of metal.

About 1930 a considerable amount of work was carried on in this laboratory by J. H. Payne in cooperation with the Incandescent Lamp Division of the General Electric Company in order to determine the most suitable design for a high-speed, high-vacuum, multistage metal pump.[30] Figure 18 shows a design of two-stage pump having the following characteristics: Volume of mercury, 70 cm^3; power input, 550 watts; fore-pump pressure, 1 to 2 mm; minimum pressure, about $3 \cdot 10^{-4}$ micron; speed, 12 to 15 liters $\cdot$ sec^{-1}.

A three-stage pump of similar design, used in exhaust of high-power transmitting tubes, gives the same degree of vacuum at a speed of 60 liters · $\sec^{-1}$.

---

[26] *Ber. deut. chem. Ges.*, **52**, 804 (1919); *Z. angew. Chem.*, **34**, 149 (1921), also Gaede, *loc. cit.*

[27] *J. Am. Chem. Soc.*, **39**, 2183 (1917).

[28] *J. Wash. Acad. Sci.*, **7**, 477 (1917).

[29] *Phil. Mag.*, **47**, 918, 1016 (1924).

[30] This work has been discussed in *J. Franklin Inst.*, **211**, 689 (1931).

6. PERFORMANCE CHARACTERISTICS OF MERCURY-VAPOR PUMPS AS INFLUENCED BY DIFFERENT FACTORS

The speed of exhaust of a given vapor pump and minimum pressure attained in the performance are dependent on a number of factors, such as fore-pump pressure, temperature of cooling water, and power input in the heater.

Table 4 gives the results of some observations, made by the writer, with an early form of metal single-stage pump, on the variation in ultimate pressure with energy input in the heater. The fore-pump pressure was 0.0146 mm, and the pressure on the high-vacuum side was measured with an ionization gauge. The amount of mercury used in the pump was 626 g, and the normal power input was 300 watts, with a flow of 1000 $\text{cm}^3 \cdot \text{min}^{-1}$ of water.

TABLE 4

MINIMUM PRESSURE OBTAINED WITH MERCURY-VAPOR PUMP AS A FUNCTION OF WATTS IN HEATER

Watts in Heater	P_μ
130	0.20
150	.25
170	.03
180	.017
200	.010
220	.005
240	.0019
280	.0015
300	.0015

Similar results were obtained on multistage pumps by C. T. DeGroat of the Electronics Division of the General Electric Company.[31] In his observations, made with a number of pumps, the speed of exhaust is found to be independent of fore-pump pressure as long as this pressure is below a certain critical value. Immediately above this value, the speed decreases rapidly. Also the same observer found that the minimum high-vacuum pressure is independent of fore-pump pressure over the same range as the speed.

---

[31] Personal communication.

A comprehensive paper on the topic has been published by M. Matricon.[32] A diagrammatic sketch of the single-stage mercury-vapor pump used in his investigation is shown in Fig. 19. The dimensions are given in millimeters.

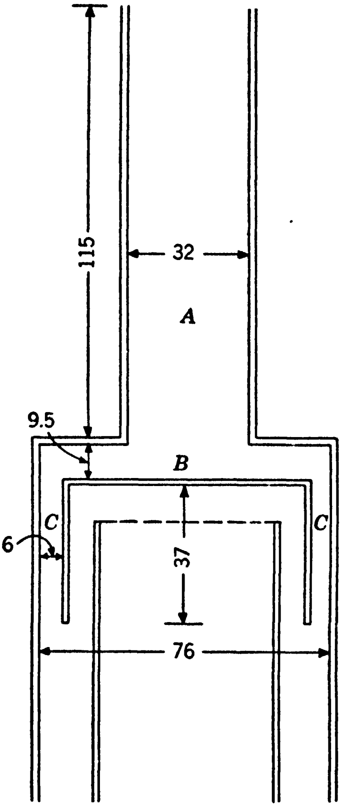

FIG. 19. Dimensions (in millimeters) of single-stage vapor pump of metal used by Matricon.

Figure 20 taken from this paper shows plots of S (liters · sec^{-1}) versus log P_f (the fore-pump pressure in millimeters of mercury). With high power input in the heater β is extremely small, because of the large value of u in equation 2.15, and therefore the pump begins to function at a relatively high fore-pump pressure (see curve 1). As the power input is decreased, the results shown in curves 2, 3, and 4 are obtained. These observations were made with a sufficient flow of water to maintain the temperature of the condenser wall at 17.5° C. On decreasing the rate of flow, so that the temperature of the wall rose to 30° C, curve 5 was obtained, in spite of the fact that the power input was the same as in 1.

Figure 21 gives log-log plots of P_{mm} (fine-pump pressure) versus P_f (in millimeters of mercury) for argon and hydrogen at three different values of the watt input. The data for both gases were practically the same in the low-pressure range and differed only slightly in the range $P_{mm} = 10^{-4}$ to 10^{-3}. It will be observed that, below $P_f = 10^{-1}$ mm, $P_f/P_{mm} = 500$ approximately.

Though these observations show that the limiting pressure obtained was the same (for constant value of P_f) for both argon and hydrogen, it is to be expected, from theoretical considerations, that the value of P_0 (fine-pump pressure) obtained would be higher for a lighter gas than for a heavier one.

---

[32] *J. Phys.*, 3, 127 (1932).

According to equation 2.15,

$$\log P_f - \log P_0 = \frac{ul}{2.303D}. \tag{1}$$

For constant temperature of the vapor, u and l are constant. On the other hand, at constant pressures, D varies approximately inversely[33] as $M^{1/2}$. Let $(P_0)_A$ denote the value of P_0 for argon and $(P_0)_H$ that for hydrogen. Then it follows from equation 1 that

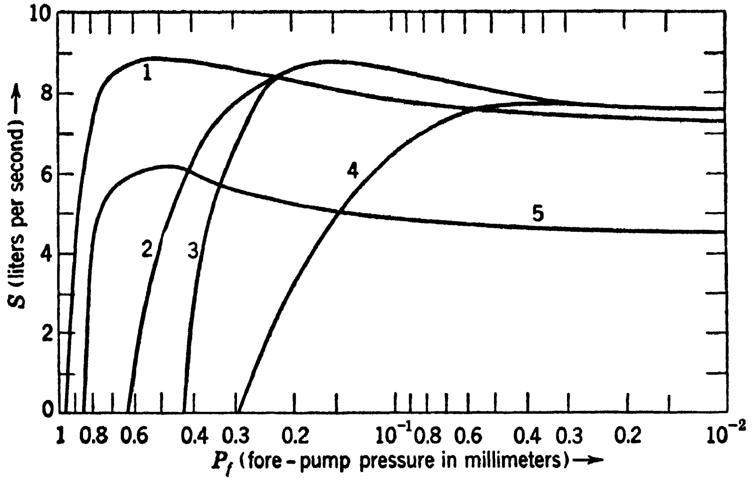

FIG. 20. Semi-log plots of speed of pump versus fore-pump pressure (Matricon).

$$\log P_f - \log (P_0)_A = C\sqrt{39.9}$$

and

$$\log P_f - \log (P_0)_H = C\sqrt{2},$$

where C is a constant involving u and l.

Let us assume that, in the case of argon, the value $(P_0)_A = 10^{-6}$ mm for $P_f = 10^{-1}$ mm. Therefore $C\sqrt{39.9} = 5$, that is, $C = 0.792$, and we obtain the result $(P_0)_H = 7.59 \cdot 10^{-3}$ mm.

The ratio P_0/P_f is usually so small for all gases that this effect of molecular weight is not often observed. It may, however, happen (as the writer has actually observed) that, though a pump gives a good vacuum with air or argon, it is no longer as effective with hydrogen.

---

[33] This statement is approximately valid since the molecular weight of the vapor is in general considerably higher than that of the gas which is being eliminated. Matricon, *loc. cit.*, has discussed this question at considerable length.

Since P_0/P_f decreases with increase in the velocity (u) of the vapor, the obvious remedy for such a situation is increasing the heater watts.

One very important factor with regard to any pump is the relation between speed of exhaust and pressure P *in the system* ($P > P_0$). In

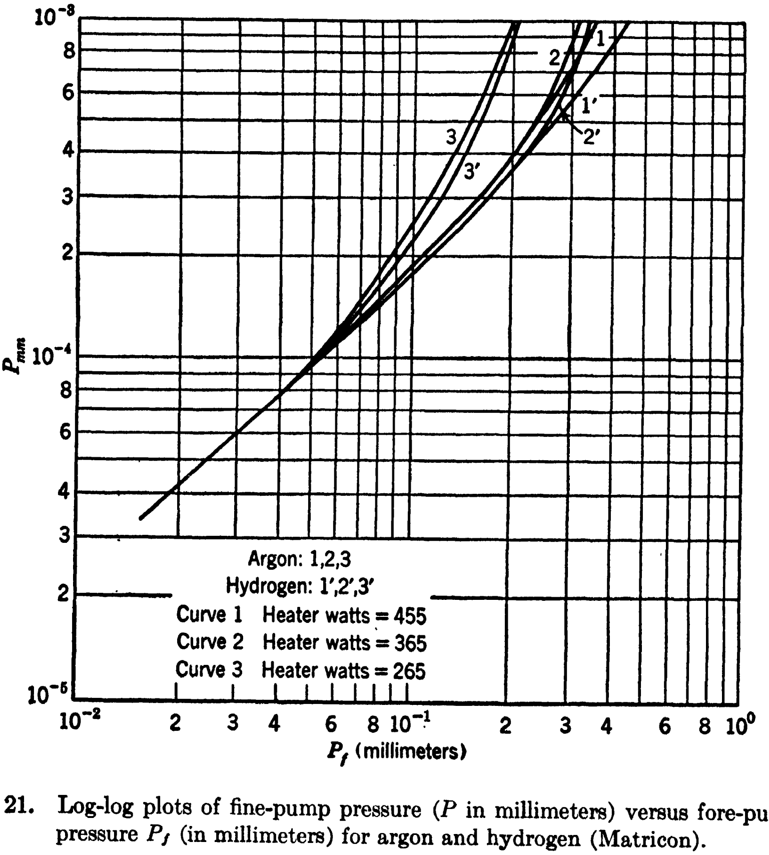

FIG. 21. Log-log plots of fine-pump pressure (P in millimeters) versus fore-pump pressure P_f (in millimeters) for argon and hydrogen (Matricon).

order to discuss this problem it is necessary to refer once more to equation 2.16, which, in view of equation 2.15, can be written in the form

$$S = \frac{Av_a}{4}\left(B - \frac{P_0}{P}\right). \qquad (2)$$

In this expression, the factor ($Av_a/4$) corresponds to the conductance of the orifice through which the gas diffuses into the stream of vapor. It may, therefore, be designated by F_0, a quantity that can be calculated for any given design of nozzle and gives the theoretically maximum value of S. The quantity B depends upon the temperature of the vapor (mercury in this case) at the nozzle. Thus, if we let

$$BF_0 = S_m,$$

then equation 2 can be written in the form

$$S = S_m - \frac{F_0 P_0}{P}. \tag{3}$$

This relation indicates that at very low pressures the speed should decrease with P and that the difference between the maximum value and that actually observed should vary inversely as the pressure. Evidently, for $P_0/P = B$, the value of S is zero.

Before considering the manner in which the value of the factor B in equation 2 varies with the design of nozzle used in a pump, it is well to point out that, in any experimental determination of the value of B from direct measurements of S for a given pump, it is necessary to introduce certain corrections. In pumps used in practice the value of S which is actually measured for the given area of orifice at the nozzle must be corrected for the effect of resistance to flow due to the length of tube above the orifice. (The discussion at the end of the previous chapter should be considered in this connection.) Denoting the admittance in series with the orifice by F, and the intrinsic speed at the nozzle by S_p, the observed value of the speed is given by the relation, deduced in Chapter 3,

$$\frac{1}{S} = \frac{1}{S_p} + \frac{1}{F}.$$

As an illustration of the application of this relation it is of interest to calculate the values of S, S_p, and B for the pump, the dimensions of which are given in Fig. 19, and which was used by Matricon in making the observations plotted in Figs. 20 and 21.[34]

From the dimensions given in Fig. 19 we obtain the following values of the conductances for air at 25° C ($\text{cm}^3 \cdot \text{sec}^{-1}$).

Section A, $F_A = 2.35 \cdot 10^4$, $1/F_A = 4.36 \cdot 10^{-5}$.

Section B, $F_B = 2.56 \cdot 10^5$, $1/F_B = 0.39 \cdot 10^{-5}$.

Annular section C, $F_C = 6.67 \cdot 10^4$, $1/F_C = 1.5 \cdot 10^{-5}$.

Hence,

$$\frac{1}{F} = \frac{1}{F_A} + \frac{1}{F_B} + \frac{1}{F_C} = 6.90 \cdot 10^{-5}.$$

---

[34] *Loc. cit.* The value of F_B in the following calculation is that given by Matricon. The other values were calculated by the writer from the relations given in Chapter 2.

Now the observed speed of the pump was $7.8 \cdot 10^3$, corresponding to $1/S = 12.82 \cdot 10^{-5}$. Hence the intrinsic speed of the pump is given by the relation

$$\frac{1}{S_p} = (12.82 - 6.90)10^{-5} = 5.92 \cdot 10^{-5},$$

that is, $S_p = 16{,}890 \text{ cm}^3 \cdot \text{sec}^{-1}$.

Since the area of the slit across which diffusion occurs is 13.2 cm^2, $Av_a/4 = 1.54 \cdot 10^5$. Hence

$$B = \frac{1.69 \cdot 10^4}{1.54 \cdot 10^5} = 0.11.$$

It will be observed that the resistance of the cylindrical section A constitutes about two-thirds of the total resistance, $1/F$. By decreasing the length of this section, the value of $1/F$ would have been decreased, thus yielding higher values of both S and B. This result serves to emphasize once more *the importance of making all connections between the pump and system as short as possible* if full advantage is to be taken of the maximum potential speed of a given design of pump.

Since the cross section of A is 8.04 cm^2, the speed *per unit area* of opening is approximately 1000 $\text{cm}^3 \cdot \text{sec}^{-1} \cdot \text{cm}^{-2}$ compared to 11,670 $\text{cm}^3 \cdot \text{sec}^{-1} \cdot \text{cm}^{-2}$, which is the theoretical speed. Thus the ratio between actually observed and calculated speed for the pump is about 0.085. The same result has also been obtained in this laboratory on metal pumps. In general, the ratio between the observed speed and that calculated for an opening of equal area from the relation $S = 11{,}670A$ varies, for mercury-vapor pumps, between 0.07 and 0.1.

7. EFFECT OF DESIGN OF NOZZLES

Attention was drawn in section 3 to the construction of a pump in which a specially designed jet was incorporated. A number of investigators have followed out this suggestion at further length.

A high-speed pump made of glass, with metal nozzle, has been described by I. Estermann and H. T. Byck.[35] Figure 22 shows the construction of the pump, while Fig. 23 shows the details of the metal nozzle insert.

> In order to determine the dimensions affording maximum pumping speed the first nozzle was constructed in such a way that the width of the diffusion area could be successively increased by turning down the outer part of the nozzle on a lathe, and

---

[35] *Rev. Sci. Instruments*, **3**, 482 (1932).

at the same time the bottom face of the inner part of the nozzle was cut back to maintain approximately the same relative length.

The results obtained for different values of the clearance are shown in Table 5. The second column gives the value of the annular area between the nozzle and the wall.

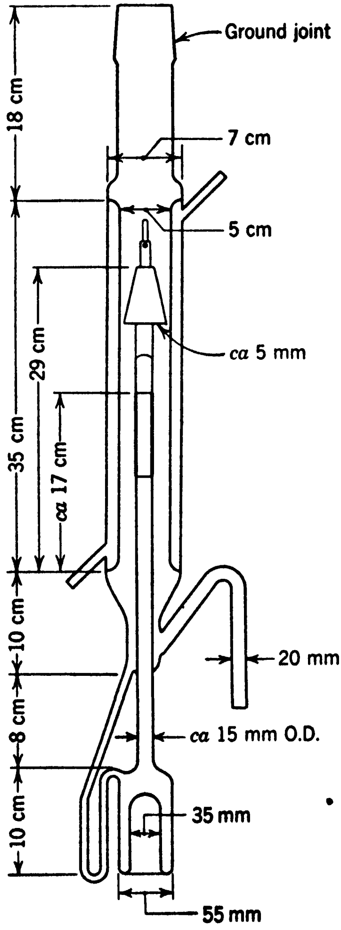

FIG. 22. Glass-metal mercury-vapor pump (Estermann and Byck).

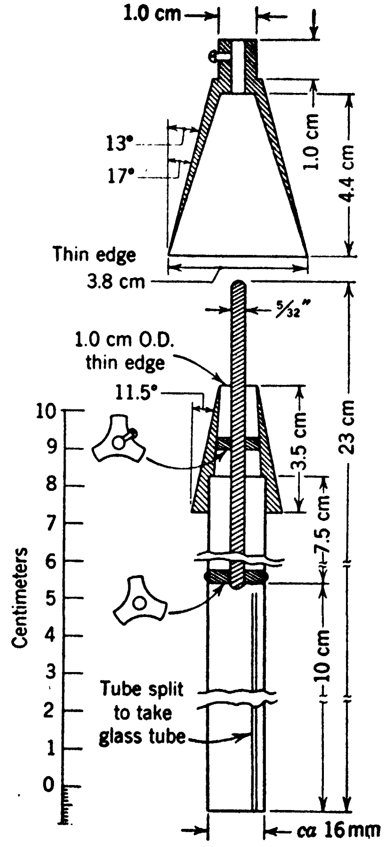

FIG. 23. Details of metal nozzle for pump shown in Fig. 22.

As will be observed, the maximum speed was reached for a clearance of about 5 mm. Theoretically the value of S for air is 11.67 liters $\cdot$ sec^{-1} $\cdot$ cm^{-2}. The maximum value actually obtained was

TABLE 5

EFFECT OF NOZZLE DESIGN ON SPEED OF PUMP (ESTERMANN AND BYCK)

Clearance (cm)	Region Area of Diffusion (cm^2)	S (liters · sec^{-1})	S/area
0.1	1.5	3.0	2.0
.2	2.9	5.0	1.72
.33	4.7	8.5	1.81
.55	7.4	13.0	1.76
.63	8.4	9.5	1.13
.71	9.2	8.4	0.91

1.8 liters · sec^{-1} · cm^{-2}. Since the speed was measured at 30 cm above the nozzle, and $a = 2.5$ cm, the observed speed should be corrected for the "resistance" of this length of tube. From the relations given in Chapter 2, it follows that F (for the tube) = 39.42 liters · sec^{-1}. Hence the observed value $S = 13$ liters · sec^{-1} corresponds to a corrected value of $S = 19.5$ liters · sec^{-1}, and the intrinsic speed per cm^2 is 2.6 liters · sec^{-1}, or about 23 per cent of the theoretical value.

T. L. Ho[36] has discussed the influence of number and design of nozzles on the value of B in equation 6.2, which he designates as the "speed factor." He has pointed out that the magnitude of k (see equation 2.16), the extracting power of the vapor for gas, "depends largely on the shape of the nozzle and the intensity of distribution of the vapor below the slit."

In order to determine the correct magnitude of the speed factor it is necessary, as has been discussed above in the case of the pump used by Matricon, to correct the observed speed of the pump for the resistance of the volume between the inlet to the pump and the region near the slit. The factor B is then obtained as the ratio between the corrected speed, S_c, and the conductance of the annular orifice through which the gas diffuses into the vapor stream from the high-vacuum side.

An examination by Ho of a number of different designs of nozzles used with mercury-vapor pumps, illustrated (with important dimensions) in Fig. 24, yielded the results shown in Table 6.

Evidently the speed factor is increased by using a divergent jet instead of a straight one. Other factors, such as size of chamber and the extent to which the nozzle is thrust into the chamber, affect the value of the speed factor. This is accounted for by Ho on the basis of the effects produced on the values of α and k. By varying the area, a maximum value is obtained for the product $k\alpha$, which has been mentioned in equation 2.16 above.

---

[36] *Physics*, **2**, 386 (1932). See remarks in footnote 17 above.

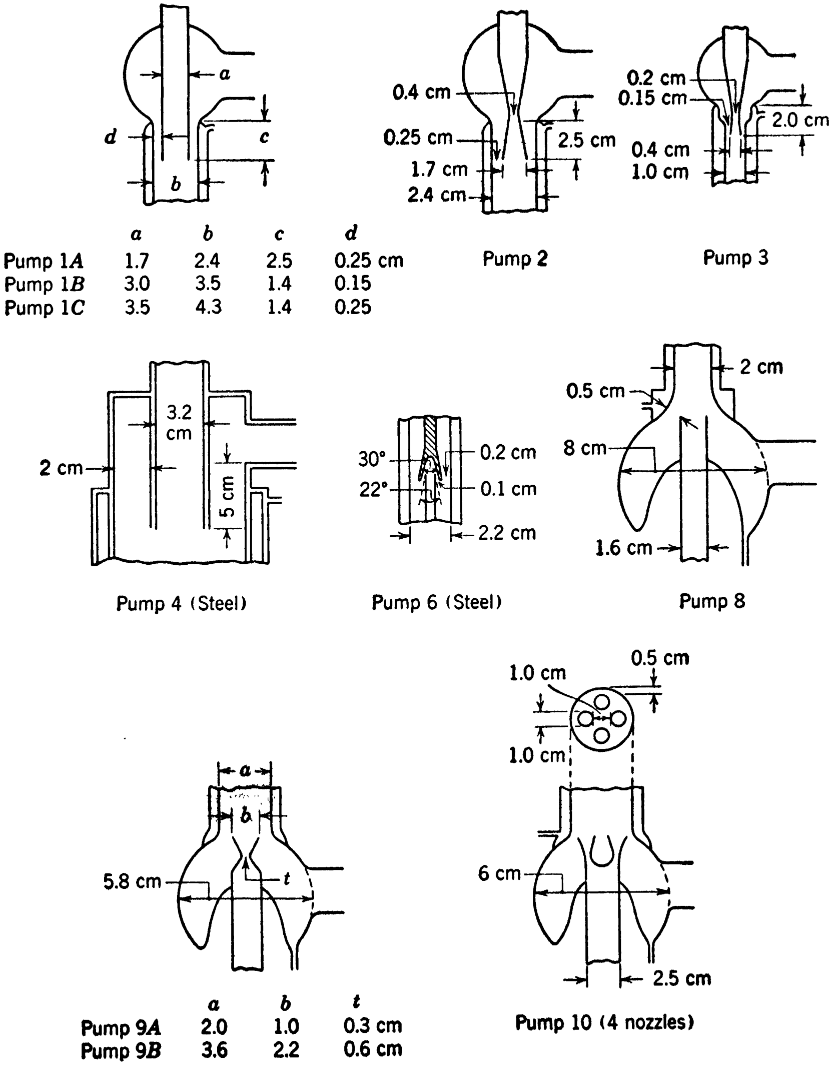

	a	b	c	d
Pump 1A	1.7	2.4	2.5	0.25 cm
Pump 1B	3.0	3.5	1.4	0.15
Pump 1C	3.5	4.3	1.4	0.25

	a	b	t
Pump 9A	2.0	1.0	0.3 cm
Pump 9B	3.6	2.2	0.6 cm

FIG. 24. Designs of nozzles for mercury-vapor pumps investigated by Ho.

One conclusion drawn by Ho which is of interest in connection with the subject of oil-vapor pumps (discussed in the following chapter) is the following:

TABLE 6

EFFECT OF NOZZLE DESIGN ON SPEED FACTOR (Ho)

Pump	Form	Slit area (cm^2)	Watts Input	Speed ($liters \cdot sec^{-1}$)	Speed Factor
1A	Straight nozzle Small chamber	1.54	115	1.01	0.056
1B	Small chamber	1.48	140	3.5	0.20
1C	Small chamber	2.9	140	5.7	0.17
2	Divergent nozzle Small chamber	1.54	115	1.57	0.086
3	Small chamber	0.27	110	0.57	0.18
6	Small steel	1.26	300	1.16	0.079
8	Small steel, upward	2.5	60	3.2	0.11
9A	Upward	2.4	60	4.0	0.14
9B	Upward	6.4	140	14.5	0.20
10	4 nozzles, upward	9.5	140	28.0	0.26
11	4 nozzles	9.5	140	33.0	0.30
12	7 nozzles	22.8	200	55.0	0.21
13	19 nozzles	155.0	700	320.0	0.18

The speeds [according to Ho] were specified as (1) at the position along the inlet tube and close to the nozzle chamber, (2) constant at pressures from 10^{-3} to 10^{-5} mm Hg, (3) against a fore pressure of below 0.1 mm Hg, (4) the water cooling was at room temperature and the temperature difference between the inlet and the outlet water was about 2° C.

"The speed of the pump filled with *n*-butyl phthalate is higher than that of the same pump with mercury." This is accounted for by the lower vapor pressure of the former, which causes an increase in the value of α.

A study of the speed of divergent-nozzle pumps has been made by M. J. Copley, O. C. Simpson, H. M. Tenney, and T. E. Phipps.[37] The following description of the experimental arrangement, tests, and results obtained is quoted from their paper:

Six diffusion pumps with divergent nozzles have been constructed and their speeds measured as a function of the annular area between the end of the nozzle and the condenser wall. Figure 25 shows the construction of nozzle and nozzle chamber. The dimensions of the nozzle were calculated from simple turbine theory[38] to fit the following assumed conditions: working substance, mercury vapor; pressure at throat, 10 mm of Hg;[39] pressure at mouth, 10^{-3} mm of Hg. The same nozzle dimensions were employed throughout the series (Pumps 1–6, Table 7): namely, an inner diameter of 0.3 cm at the throat; an inner diameter of 2.4 cm and an outer diameter of 2.6 cm at the mouth; a length along the axis of 11.8 cm; and an angle of divergence of 10°. The clearance *a*, which is the width of the annular space between the end of the nozzle and the condenser wall, was varied in the series from 0.6 to 1.6 cm.

---

[37] *Rev. Sci. Instruments,* **6**, 265 (1935).

[38] Crawford, *Phys. Rev.,* **10**, 557 (1917).

[39] This corresponds to a temperature of about 184° C.

Speeds were measured in all cases at the entrance to the nozzle chamber (*B*, Fig. 25). The speed was measured in the usual manner: air was admitted at a measured rate from the atmospheric into the high-vacuum side of the pump at *L* (Fig. 25); a McLeod gauge connected to the entrance of the nozzle chamber at *B* measured the pressure for different rates of admission of air.

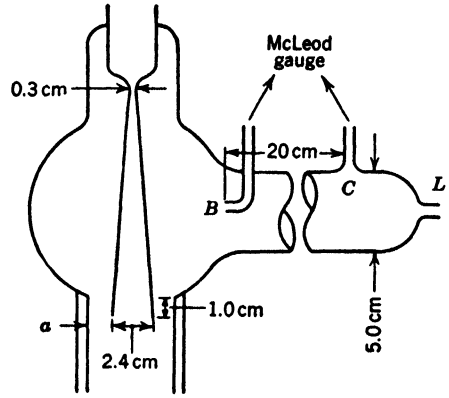

FIG. 25. Design of nozzle and nozzle chamber (Copley et alii).

Table 7 shows the results obtained on six pumps with divergent nozzles, one pump with straight nozzle, using mercury, and two pumps with divergent nozzles using one of the esters. The design of the last is shown in Fig. 5.6.

The observations show that, while the speed increased with annular area, the speed factor passed through a maximum for pump 2. Comparison of these results with those obtained by Ho for multiple-nozzle pumps shows that the speed factors of the latter are lower than those of the single-long-nozzle series. The single test on pump 7 shows that a long straight nozzle is not as efficient as a divergent nozzle. The authors state,

> The above observations appear to establish a superiority of speed factor for pumps with long divergent nozzles over the straight nozzle type and over short divergent nozzle types, whether of single or multiple nozzle design.
>
> The speed factors obtained for pumps 8 and 9 with butyl phthalate are seen to be in excellent agreement with those in the series of smaller pumps *at the same annular width.*

It is furthermore stated that, with pump 4, an ultimate vacuum of less than 10^{-7} mm of mercury was obtained, as measured by an ionization gauge.

TABLE 7

DATA UPON SPEED OF PUMPS WITH LONG DIVERGENT NOZZLES*

Pump No.	Annular Width (mm)	Annular Area (cm^2)	Boiler Pressure Head (mm)	Speed at B ($l \cdot \text{sec}^{-1}$)	Speed at C ($l \cdot \text{sec}^{-1}$)	Ideal Speed at Annulus ($l \cdot \text{sec}^{-1}$)	Speed Factor
1	6.0	6.03	9–15	35		70	0.50
2	7.0	7.26	9–15	50	35	85	.59
3	10.0	11.3	9–15	66		132	.50
4	12.0	14.3	15–20	74	39	167	.44
5	14.0	17.6	20–25	77		206	.37
6	16.0	21.1	20–25	99		247	.40
7	7.0	7.26	1	26		85	.31
8	9.0	24.0	70	143		281	.51
9	12.0	33.2	70	175		388	.45

* Pumps 1 to 6: all glass; long divergent nozzle; mercury.

Pump 7: all glass; straight nozzle; mercury.

Pumps 8 and 9: composite metal-glass; long divergent nozzle; n-dibutyl phthalate.

The vapor pressure of mercury is 1 mm at 126° C and 20 mm at 206° C.

Figures 26 and 27 show sketches, drawn to scale, of two variations of the Copley pump which are due to W. B. Nottingham. In actual experience in this laboratory these pumps have been found to yield excellent results with respect to both speed and ultimate vacuum.

8. ROLE OF DIFFUSION AND CONDENSATION IN VAPOR-STREAM PUMPS

As stated in section 4, Langmuir has stressed the part played in his design of pump by condensation of mercury on the cooled surface near the gas inlet. On the other hand, in the paper published in 1923,[40] Gaede maintained that Langmuir's construction is nothing more than a diffusion pump. One of his principal arguments was that the shortest distance (d) between the nozzle L (Fig. 11) and the condensation surface must be less than L, the mean free path of the molecules. However, as was pointed out in the previous section, at the pressures of mercury vapor used in the condensation pump, L is of the order of 10^{-2} cm, which is considerably less than d. Furthermore the argument was advanced in that connection that this condition is essential in order to prevent the back diffusion of gas into the high-vacuum chamber. But Gaede contended that a considerable number of mercury molecules which leave the nozzle also possess components of velocity in a direction opposite to that of the main stream, and that consequently there exists a high probability that gas molecules will be scattered in the same direction.

---

[40] *Z. tech. Physik*, 4, 337 (1923).

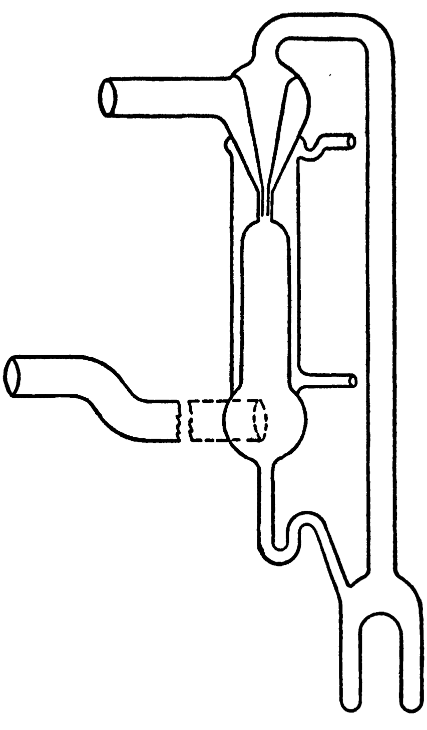

FIG. 26. Convergent nozzle type of vapor pump. (Nottingham.)

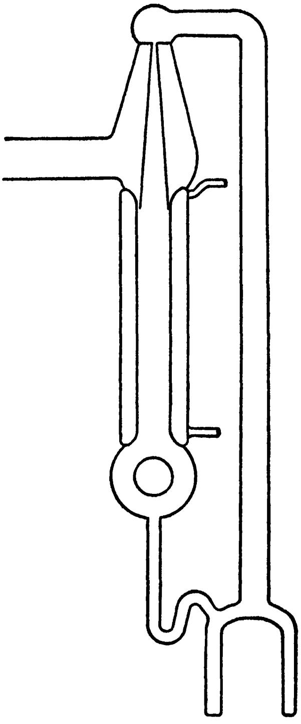

FIG. 27. Divergent nozzle type of vapor pump. (Nottingham.)

Because of the existence of this differences of opinion it has seemed to the writer that the term "vapor-stream" pumps, suggested by E. N. daC. Andrade,[41] is probably a very satisfactory designation.

---

[41] *Encyclopædia Britannica*, 14th edition, Vol. 22, p. 930. The shorter designation "vapor pump" has been used by the writer.

Moreover, this seems justifiable in view of the theoretical investigation published by W. Molthan,[42] and the more recent work carried out by P. Alexander[43] on the design of a very high-speed mercury-vapor pump.

Molthan concludes in his paper that the velocity of the vapor (in a straight nozzle) cannot exceed that of sound and is therefore of the same magnitude as the molecular velocities.[44] In the following discussion we shall assume that the vapor is flowing out of a nozzle, such as L in Fig. 11, in a *downward* direction, and shall therefore describe the motion of molecules which are scattered back into the chamber E as moving upward.

If the vapor enters a space in which the gas pressure is appreciable, it will have the *form of a jet*, in which practically all the vapor molecules are directed downward. There is a slight lateral expansion of the jet as the distance from the nozzle opening increases, and eddies are formed at the boundary between the jet and gas. The gas flows into the jet by suction, as pointed out by Langmuir.

A high vacuum cannot be reached in this manner whenever the gas pressure becomes less than that of the vapor, since molecules of the vapor are scattered in all directions and push the gas molecules backward.

If, however, the vapor enters a vacuum with a velocity equal to that of sound, as in the vapor-stream pumps, the stream must spread out in the manner shown in Fig. 28, reproduced from Molthan's paper. In this diagram "the dotted line is always at right angles to the stream line and its length between two stream lines is proportional to the mean free path within the angular range under consideration. In this manner, it is found that the mean free path of the gas molecules at the place of entrance into the vapor stream in the direction of a is about 75 times longer than the mean free path at b in the range of the main vapor stream." This conclusion depends upon the assumption that L[45] is greater than the diameter of the nozzle opening — a condition that is obviously fulfilled in all vapor-stream pumps. It will be observed that, on the basis of Molthan's conclusion, the value of L for molecules of air in the diffusion slit in the case of mercury vapor at 1 mm pressure would be $75 \cdot 7.2 \cdot 10^{-3} = 0.54$ cm, which is of the same order of magnitude as the width of the slit.

"In the diffusion pump," as Molthan states, "the bulk of the vapor flows downward while only a slight amount of vapor is flowing back and upward, so that the gas can diffuse into the part of the vapor which flows downward."

---

[42] *Z. tech. Physik,* **7**, 377, 452 (1926); **8**, 80 (1927).

[43] *J. Sci. Instruments,* **23**, 11 (1946).

[44] See the discussion in section 1 of this chapter.

[45] L = mean free path.

Furthermore, according to Molthan, it is possible to use the same pump first as ejector, and then as diffuser. At higher pressures, where L is small compared to the width (d) of the suction slit, the pump may function as a vapor-jet pump until a pressure is reached at which L is comparable with d, and then the pump begins to act as a diffusion pump. This is especially true of two-stage pumps and those with a larger number of stages.

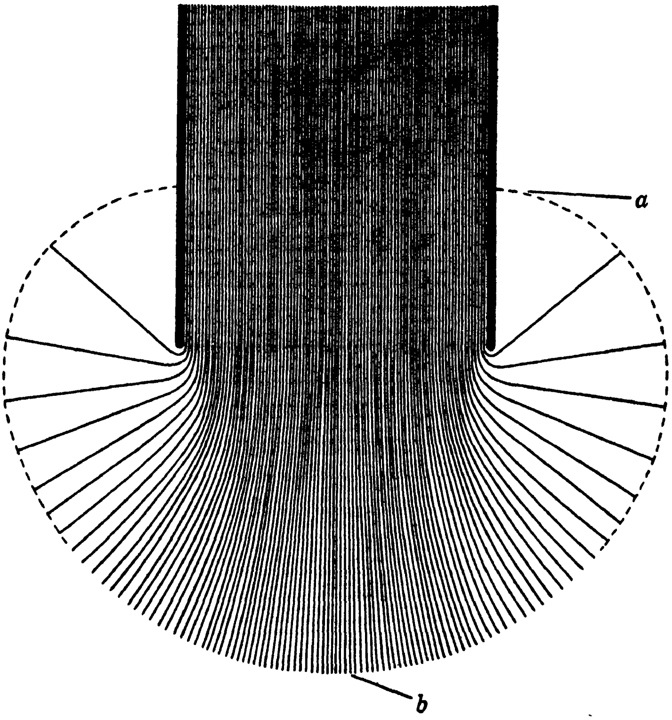

FIG. 28. Scattering of mercury-vapor stream at the mouth of straight nozzle (Molthan). The distance between two stream lines is proportional to the mean free path.

The investigation by Alexander undoubtedly represents a very important contribution towards the elucidation of the mechanism of operation of vapor pumps.

He has shown that on the basis of theoretical considerations the pumping effect of a vapor pump cannot be explained by Gaede's theory of diffusion. In view of the fact that for air at room temperature the speed of effusion through an opening is 11.67 liters · $\sec^{-1}$ · cm^{-2}, it is simply impossible to obtain any appreciable speeds of exhaust through a slit which must be made very fine in order to maintain a value of L/d of approximately unity at fore-pump pressures of the order of 0.1 mm.

Accordingly Alexander has investigated more carefully the nature of the processes that occur at the nozzle of a vapor pump, by which the streaming vapor removes the gas molecules entering the space around the nozzle. From experiments with a specially designed nozzle he found that the *velocity of the mercury-vapor stream varied*, with different rates of heating of the mercury in the boiler, *from 1.2 to 3.4 times the value of the most probable velocity of mercury molecules at the temperature of the vapor.*[46] With the value of the ratio equal to 1.2, it may be deduced from the Maxwell-Boltzmann distribution law "that 44 out of 1000 molecules of mercury will escape the vapor stream into the space above it."

In order to determine the manner in which the mercury-vapor stream spreads out after passing through the gap of the nozzle, special experiments were carried out in which determinations were made of the weights of cadimum vapor condensed on small glass sheets placed in different directions from that of the vapor stream.

These observations show, according to Alexander,

> that the vapor stream remains quite compact for a considerable distance from the nozzle: the density of the vapor diminishes rapidly with the angle in all directions; very little vapor spreads in a direction at right angles to the streaming direction.

The conclusions drawn are as follows:

> Due to the high, downward-directed momentum of the mercury molecules the gas molecules entering the vapor stream from the mouth of the pump will receive higher velocities than those which correspond to the temperature of the gas. Therefore the streaming velocity of the gas below the nozzle will be higher than above it, and the density of the gas in this region will be lower. Further, below the nozzle, the vapor gets less dense and its driving effect on the gas diminishes and finally ceases. The streaming velocity of the gas decreases accordingly and its density increases. Thus the density of the gas will be at a minimum in a region just below the nozzle, and will gradually increase below this region, reaching a maximum further below, nearer to the backing outlet. The mercury stream has to be dense enough to prevent the gas from streaming backwards from the high-density region to the region of lowest density. The wider the throat of the pump the lower the density of the vapor will

---

[46] It will be observed from this statement and the considerations advanced by Alexander in the following discussion that according to Alexander the operation of the vapor pump is quite similar in many respects to that of the steam ejector.

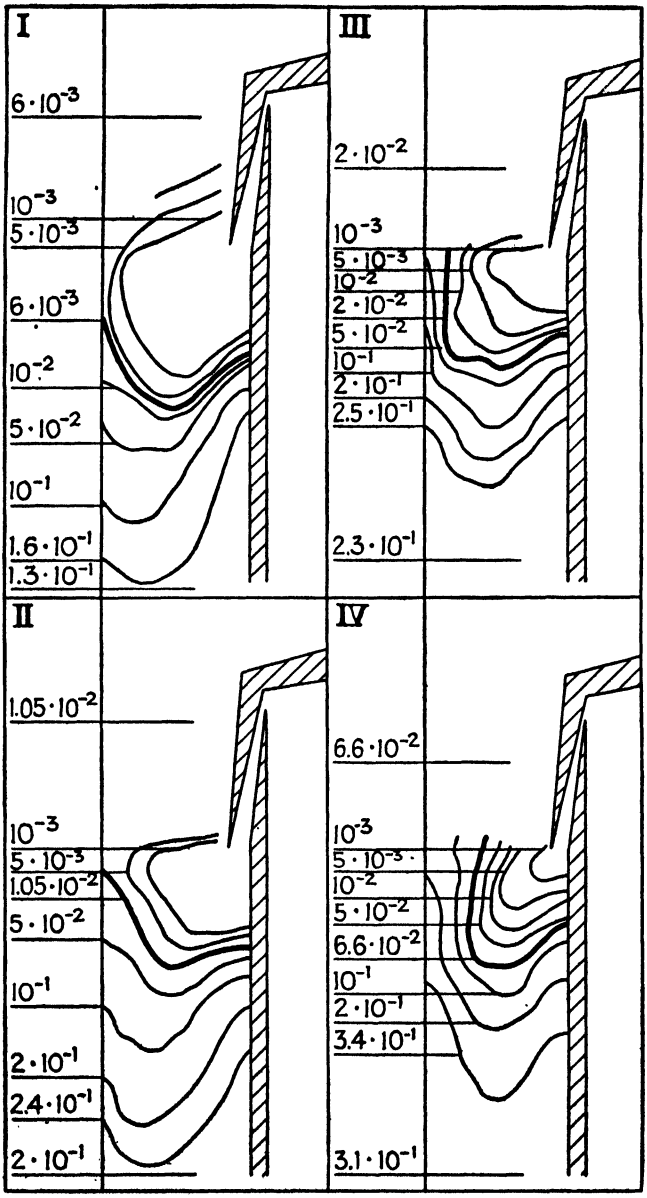

FIG. 29. Isobars showing distribution of pressures (P_{mm}) at different points below the nozzle of a mercury-vapor pump (Alexander). The thick line is the isobar with a value equal to the pressure at the opening of the pump.

be, and it will be lowest along the wall. Evidently, at a certain width of the throat the vapor stream along the wall will not be dense enough to "seal off" the compressed gas, and the gas will spread backwards along the wall into the low-pressure space.

The graphs in Fig. 29 show the experimental confirmation of this idea. They represent that part of the half cross-section of the pumping space which lies between the mouth of the pump and the backing outlet.

The pressure readings obtained at different points below the nozzle are shown as isobars, with the pressure marked in the left-hand column of each diagram. The thick line is the isobar with a value equal to the pressure at the opening of the pump.

The pressure at the inlet P_{mm}, the backing pressure bP_{mm}, and the speed of the pump S (liters · sec^{-1}) in each set of readings were as follows:

Diagram	I	II	III	IV
P_{mm}	$6 \cdot 10^{-3}$	$1.05 \cdot 10^{-2}$	$2 \cdot 10^{-2}$	$6.6 \cdot 10^{-2}$
bP_{mm}	0.13	0.2	0.23	0.31
S	135	130	83	34

Plots of the speed of the pump versus pressure showed a gradual increase with increase in pressure P to a maximum, followed by a rather steep drop with further increase in pressure. At the maximum,

the sealing effect of the vapor starts to break down and air streams backward along the wall. The critical value of the working pressure where this decline sets in is higher if the heat input and the mass of circulating mercury is larger.

Alexander continues,

Summing up the results obtained, the pumping effect of the vapor stream can be described as follows.

(1) The high-velocity vapor stream directed in the pumping direction sweeps away the gas from the space in front of the nozzle, thereby creating a region in which the molecular density of the gas is a minimum. The gas swept away is driven by the vapor stream in the direction of the backing outlet at a higher velocity than that which the gas would obtain by streaming along any pressure gradient.

(2) Farther away from the nozzle the vapor loses its density by expansion and condensation on the wall, and the gas loses its streaming velocity. Thereby a region is created in which the density of the gas reaches a maximum.

(3) The condition of efficient working of the pump is that on any line parallel to the pumping direction such a point of minimum and maximum gas density should exist. This condition is never perfectly fulfilled above a certain limit of the working pressure, which limit depends on the density and velocity of the vapor stream and on the design of the pump.

(4) Provided that condition (3) is fulfilled, the speed of the pump is directly proportional to the area of the throat.

A pump designed on the basis of this theory is described as follows:

A high pumping speed will be reached if (1) the area of the throat is as large as possible, (2) the nozzle is directed straight into the pumping direction, (3) the density of the vapor along the outer wall is as high as possible, and (4) both walls enclosing the pumping space are cooled. In order to extend the range of pressures within which the pump works efficiently, three parameters have to be controllable, namely, the heat input, the width of the throat and the gap of the nozzle.

Conditions (1) and (2) seem to be contradictory to condition (3), because a large area of the throat and a straight downwards directed nozzle mean lower density of the vapor along the wall. This difficulty is largely overcome by shaping the outer wall so that it is not parallel to the pumping direction. In Fig. 30 the line *th* is the width of the throat, *N* the nozzle, and the arrow shows the pumping direction. The line *d* can be regarded as the boundary within which the densest part of the vapor is concentrated, and the density along the wall at the point *P* depends on the length of this line. By constructing the water-cooled wall *W* in such a way as indicated by the broken line, the length of *d* can be considerably reduced without reducing *th*. The consequent reduction of area will not impede the flow of gas as the pressure of the gas in this region is comparatively high.

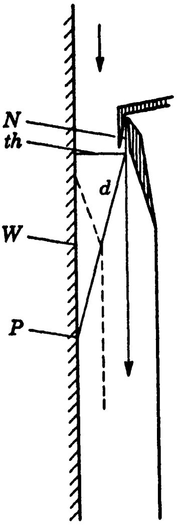

Fig. 30. Illustrating principle of new mercury-vapor pump (Alexander).

Figure 31 shows the schematic cross-section of the pump. The boiler-head is essentially the same as in the prototype pump, but the nozzle is directed straight downwards. *wj* is the outer water-jacket and *iwj* is the inner water-jacket surrounding, but not touching, the central tube. The central tube is telescopic, so that the nozzle can be lowered or raised in such a way that the nozzle orifice can be in any position between the points *t* and *b*. The tube forming the main body of the pump is 17.5 cm in diameter, and it widens conically at the top end to 27.5 cm. The second boiler tube and nozzle in the lower part of the pump forms a "second stage" which has no direct influence on the pumping principle and therefore it has not been discussed in this paper. Its main function is that it enables a higher backing pressure to be used and so the use of a smaller backing pump is possible.

Depending on the position of the boiler-head the width of the throat varies between 1.5 and 5 cm, and its area between 86 and 353 cm^2. The gap of the nozzle varies between 1 and 3 mm. The mercury is heated by an electric heater, and the heat input can have any value up to 12 kw. At working pressures above $5 \cdot 10^{-2}$ mm, 12 kw heat input and the smallest throat give the best pumping speeds, while at the lowest pressures only 2.7 kw heat input is needed and the largest throat should be used. It is a simple matter to control the position of the nozzle from outside through a gland so that the optimum adjustment may always be used.

In Fig. 32 graph I shows the maximum pumping speeds between the working pressures of 10^{-4} and 10^{-1} mm, obtainable by using the optimum adjustments for each pressure range. Graph II shows the highest pumping speeds of the prototype pump. Not only the absolute pumping speed but also the efficiency of this pump is much higher than that of the prototype pump. While the former gives at 10^{-3} mm pressure a pumping speed of 85 *l*/sec for each kilowatt of heat input, the new pump gives 280 *l*/sec. At 10^{-2} mm the pumping speed of the prototype pump for each square centimeter of throat area is 1.2 *l*/sec, the new pump's corresponding figure is 2.8 *l*/sec.

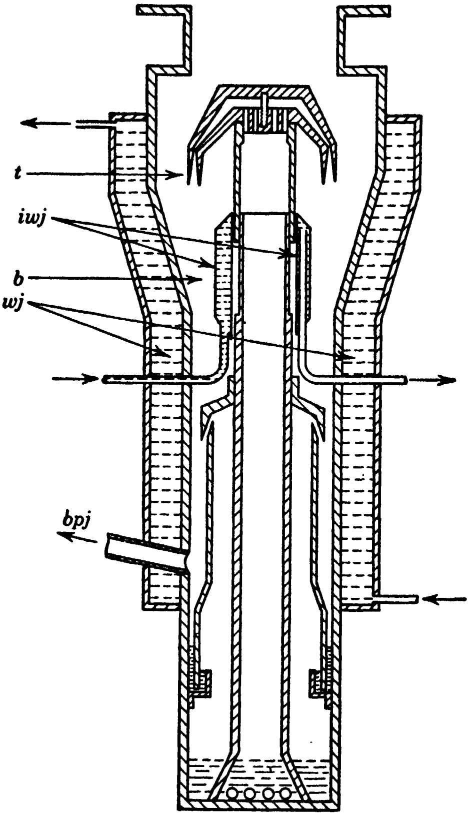

FIG. 31. Schematic cross-section of specially designed mercury-vapor pump (Alexander).

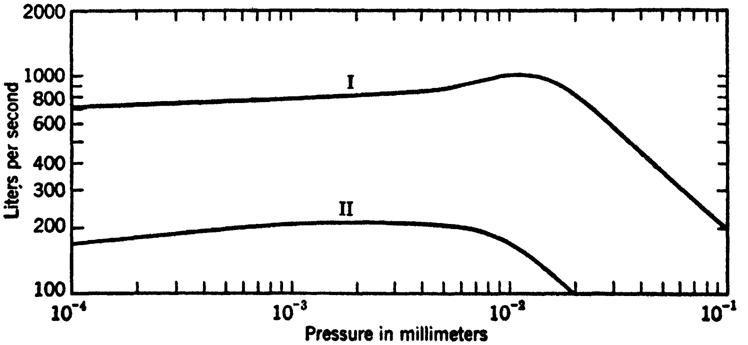

FIG. 32. Log-log plots of speed versus fine pressure for mercury-vapor pump shown in Fig. 31 (I), compared with "prototype pump" (II).

The backing pump used was the same as that used with the prototype pump. It has been found that the pumping speed is, within wide limits, independent of the backing pressure, especially at lower working pressures. Below a pressure of $1.5 \cdot 10^{-2}$ mm the pumping speed is constant up to a backing pressure of 2.5 mm.

These observations and conclusions are evidently in agreement with the views expressed originally by Langmuir regarding the mechanism of operation of the vapor pump and the importance of the condensation effect. As, furthermore, Alexander points out, his observations are in distinct disagreement with Gaede's contention that all vapor pumps function as diffusion pumps, and these conclusions are further confirmed by the observations shown in Table 8 on the performance of the new pump. In this table, H denotes the heat input in watts, *th* the width of the throat in centimeters (see Fig. 30), and A is the area of the throat in square centimeters, so that S/A is the speed in liters $\cdot$ sec$^{-1} \cdot$ cm^{-2} at the pressures indicated in the table.

TABLE 8

PERFORMANCE OF MERCURY-VAPOR PUMP (ALEXANDER)

		S/A			
H	*th*	10^{-4} mm	10^{-3} mm	2×10^{-3} mm	10^{-2} mm
12,000	1.50	0.9	1.4	—	3.2
12,000	3.30	0.9	1.4	—	2.6
12,000	5.00	0.9	1.4	—	2.5
9,250	2.25	1.3	1.7	—	3.3
9,250	3.10	1.3	1.7	—	2.9
9,250	5.00	1.3	1.7	—	2.8
2,700	1.50	2.0	2.2	2.5	—
2,700	3.30	2.0	2.0	1.9	—
2,700	5.00	2.0	1.9	1.6	—

Finally the author states that a second pump has been constructed which has a speed of about 1400 liters $\cdot$ sec^{-1} in the pressure range 10^{-4} to 10^{-2} mm, with a maximum speed of 4 liters $\cdot$ sec$^{-1} \cdot$ cm^{-2} of throat area.

The lowest pressures mentioned in the paper are in the range of 10^{-4} mm, and an extrapolation of the plots of S versus P indicates that the speed decreases at still lower pressures. This is probably due to back diffusion of gas through the throat, in accordance with equation 2.16, which increases with increase in the width of the throat.

One fact of interest in connection with high-speed mercury-vapor pumps is that thermal efficiency, that is S per kilowatt energy input, increases with S. For instance, a mercury-vapor pump having a speed of 10 liters $\cdot$ sec^{-1} may require about 500 watts at a fore-pump pressure of 1 to 2 mm; and pumps are available which have a speed of 50 liters $\cdot$ sec^{-1} with the same energy input. In the case of the mercury-vapor pumps designed by Alexander, the *speed per kilowatt input* varies from 85 to 400 liters $\cdot$ sec^{-1}/kw with increase in speed. This is no doubt largely due to the fact that radiation and conduction losses per unit volume of pump decrease with increase in size. The same observation also applies to oil-vapor pumps, as will be evident from the discussion in the following chapter.

9. DESIGN OF COOLING TRAP AND SUBSTITUTES FOR LIQUID AIR

In the discussion in the preceding sections, the speeds mentioned refer to the values observed at the pump inlet. However, since it is usually necessary, in particular applications, to keep mercury vapor out of the system to be exhausted, some provision must be made for this purpose. If a pressure of the order of 10^{-3} micron is to be maintained in a system, mercury, which has a vapor pressure of 0.185 micron at 0° C, must be prevented from diffusing into the system. This may be accomplished by means of gold foil, sodium, or potassium with which the mercury reacts to form an amalgam.[47] However, the more usual method involves the use of a trap which is cooled by either solid carbon dioxide in acetone or by liquid air. As shown in Chapter 11, Table 13, the vapor pressure of mercury at $-78.6°$ C, the temperature of sublimation of solid carbon dioxide, is about $3 \cdot 10^{-6}$ micron, and hence this temperature should be sufficiently low to achieve a satisfactory removal of mercury. But it is important to observe that, at this temperature, the vapor pressure of ice is as high as 0.5 micron, and, while the mercury-vapor pump does remove water vapor, the rate at which this vapor is eliminated from the system is not as high as when the trap is cooled in liquid air.

As mentioned previously, the insertion of such a trap decreases the effective speed of pumping, and therefore it is important to use a trap which shall have the maximum practicable conductivity. Furthermore, this trap must be designed to present a maximum of condensation surface for any mercury vapor that diffuses into it from the pump.

As shown in Chapter 2, section 2, the maximum conductivity for the conventional[48] construction of trap is obtained by making the outside diameter as large as practical, and making the inside diameter of the inner tube 0.62 of that of the inside diameter of the outer tube. In order to obtain as large a surface as possible for condensation of mercury, the length must not be decreased to an abnormally low value.

---

[47] See subsequent discussion in this section.

[48] By "conventional" is meant the type illustrated in Fig. 2.3, which is immersed in a Dewar flask containing the refrigerant.

Another, less conventional, design[49] is shown in Fig. 33. Though this has a higher conductivity for gas flow, it leaves one surface exposed to room temperature. This, of course, can be taken care of by heat insulation.

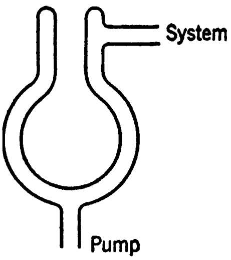

FIG. 33. Alternative design of liquid-air trap of glass.

The effect of the added resistance due to the trap obviously becomes more pronounced, the greater the intrinsic speed of the pump, and therefore the use of baffles has been proposed. As will be pointed out in the next chapter this suggestion has found extensive application in connection with oil-vapor pumps.

An elaborate development of this idea has been described by D. L. Northrup, C. M. Van Atta, and L. C. Van Atta.[50] A gear pump is used to circulate butyl alcohol which is cooled by Dry Ice, in a coil surrounding a cylindrical tube and welded to it for good thermal conductivity. This tube, which is as wide as the opening to the mercury-vapor pump, is located between the pump and the system to be exhausted, and inserted in it is a "winding staircase" of baffle elements which may be welded to the walls. By means of this arrangement the temperature of the trap may be maintained in the range −50° to −78.6° C.

For continuous operation a standard refrigerating equipment is recommended in which "Freon" is circulated by means of a compressor unit through an expansion coil of copper tubing.

According to the above-mentioned investigators,

> the vapor trap and refrigerant unit described above have been used in conjunction with a 130-liter per second mercury diffusion pump in evacuating a porcelain-tube accelerating tube. In this evacuated volume of 450 liters with a measured rate of leak of $5 \cdot 10^{-6}$ liter per second at 1 millimeter, the equilibrium pressure after 24 hours of pumping was $1 \cdot 10^{-5}$ mm Hg without liquid air and $6 \cdot 10^{-7}$ mm Hg with liquid air added to a re-entrant trap in the main volume.

---

[49] A metal construction of this type is shown in *Bulletin* 10, "High Vacuum Apparatus," by Central Scientific Company. T. H. Johnson, *J. Franklin Inst.*, **205**, 99 (1928), has described a modification of the design shown in Fig. 33, which not only has high conductance (about 10 liters · $\sec^{-1}$) and large surface area for the condensation of mercury but also reduces to a minimum the probability for back-diffusion of mercury into the system.

[50] *Rev. Sci. Instruments*, **11**, 207 (1940).

In the commercial dehydration of products such as penicillin cold traps have been utilized extensively, and the design of a large rotary condenser type of cold trap is shown in an interesting paper by R. S. Morse,[51] which discusses the subject "high-vacuum technology." The refrigerant is circulated around a chamber in which the ice is collected and then removed by means of scraper blades.

As substitutes for liquid air a number of investigators have suggested the use of traps which contain sodium or potassium, which react with mercury vapor to form amalgams some of which possess extremely low vapor pressures at room temperature.

F. E. Poindexter[52] and A. L. Hughes and Poindexter[53] reported that, by use of potassium, pressures of mercury vapor as low as 10^{-8} mm were obtained, as measured by an ionization gauge. Poindexter calculated that the vapor pressure of a 1 : 1 sodium amalgam at 20° C is about $3 \cdot 10^{-8}$ mm, and he concluded that "a trap containing 10 g of sodium should hold the mercury vapor beyond the trap down to 10^{-8} mm for over two years."[54]

The chief objection to the use of the alkali metals to replace liquid air is that the trap has to be reactivated by distilling into it fresh alkali metal each time the system is opened to the atmosphere.

In a paper by K. W. Hunten, G. A. Woonton, and E. C. Longhurst[55] the development of a specially designed trap is reported "which is self reactivating even after admission of moist air and which, therefore, can be used with systems which are repeatedly brought to atmospheric pressure by the admission of dried or even undried air." Alloys of sodium and potassium containing 3 to 5 per cent potassium, which are liquid at room temperature, are much more satisfactory than either potassium or sodium alone. According to the authors the effectiveness of these alloys "is presumably due to the ability of the small amount of liquid solution present to wander about among the crystals of sodium and transport mercury from the surface to the interior of the mass." Furthermore, "Over a period of twenty-two days, a vacuum system protected by this type of trap was pumped repeatedly from atmospheric pressure to $5 \cdot 10^{-7}$ mm Hg; during this time the trap required no attention."

[51] *J. Ind. Eng. Chem.*, **39**, 1064 (1947).

[52] *J. Optical Soc. Am.*, **9**, 629 (1924), also *Phys. Rev.*, **28**, 208 (1926).

[53] *Phil. Mag.*, **50**, 423 (1925).

[54] See Chapter 11, section 4, for discussion of the vapor-pressure data for amalgams of sodium and potassium.

[55] *Rev. Sci. Instruments*, **18**, 842 (1947). The writer is indebted to Dr. Hunten for a copy of the paper before publication. Detailed information on the method used for introducing the alkali metals into the trap is given in the original publication.

In this connection mention should also be made of the application by G. W. Lobb and J. Bell[56] of liquid amalgams of Na-Bi and Li-Bi in a high-vacuum cut-off. Amalgams containing about 0.2 per cent sodium, lithium, and bismuth have vapor pressures of about $5 \cdot 10^{-8}$ mm at room temperatures and have proved satisfactory for sealing off a part of a vacuum system from the pump. The freezing points are about −44° C (compared with −39.6° C for mercury).

---

[56] *J. Sci. Instruments*, **12**, 14 (1935).

CHAPTER 5

VAPOR PUMPS USING ORGANIC LIQUIDS

1. INVESTIGATION OF SUITABLE LIQUIDS

In 1928 C. R. Burch,[1] of the Metropolitan-Vickers Electrical Company, Ltd., England, observed that mercury could be replaced in condensation pumps by certain high-boiling-point petroleum distillates. One such product is described by him as having a vapor pressure of 1 microbar at 118° C and capable of being heated to a temperature corresponding to a vapor pressure of 100 microbars. Using this liquid in a condensation pump, Burch was able to obtain a vacuum of 10^{-4} microbar without the customary liquid-air trap. As a result of this work many metal pumps have been designed by the Metropolitan-Vickers Company in which these petroleum hydrocarbons known as Apiezon A and Apiezon B replace mercury.

These observations were followed up in this country by K. C. D. Hickman[2] and his associates, who have carried out a great deal of experimental work both on "molecular distillation" and on the development of vapor pumps in which organic liquids replace mercury.

The contributions made by this group of investigators, with respect to high-vacuum technique, have been along two directions: first, the synthesis of pure organic compounds which can be used satisfactorily in a vapor pump; and, second, development of designs of pumps which will operate efficiently in producing the desired degree of vacuum.

It should be observed in this connection that there exists a fundamental difference between mercury and organic liquids: whereas all gases and vapors are insoluble in mercury, the organic oils dissolve all kinds of gases and vapors, forming not only true solutions but also different types of metastable compounds. Hence, the oils have to be constantly purged, and, as will be shown in the subsequent discussion, this objective has been regarded by Hickman and his collaborators as fundamental in the development of both oils and pumps.

---

[1] *Nature*, **122**, 729 (1928); *Proc. Roy. Soc. London*, **A**, **123**, 271 (1929).

[2] Formerly of the Eastman Kodak Laboratories, later Director of Research of the Distillation Products, Inc., Rochester, N. Y.

Figure 1 shows a relatively simple form of glass pump designed for use with di-*n*-butyl phthalate or butyl benzyl phthalate. The system to be exhausted is connected at *A* and the fore pump at *B*. A gauge for measuring low pressure is connected at *C*. Only a mild form of cooling is required, and, with tubes 1.5 cm in diameter or less, "copper wire coiled and looped about the stem will produce excellent cooling."

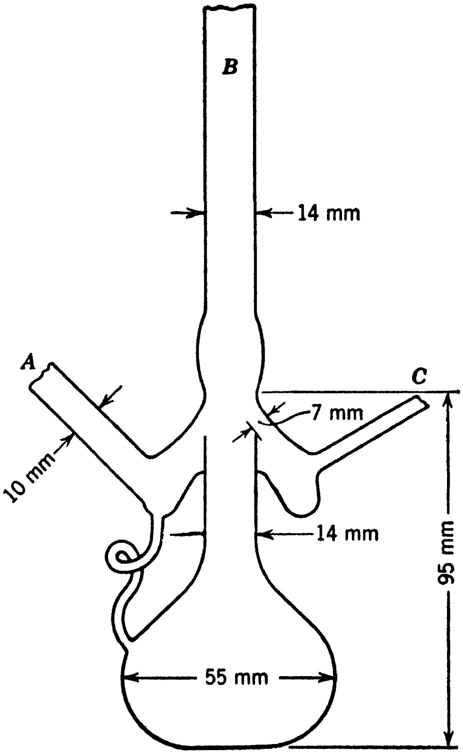

FIG. 1. Simple form of glass pump for use with oil vapors (Hickman).

With this construction and the phthalates mentioned above, it was found possible to obtain pressures as low as 10^{-6} mm at speeds as high as 9.5 liters · sec^{-1}, against a fore-pump pressure of approximately 0.1 mm.

Experience with the earlier types of Apiezon and butyl phthalate pumps led to the recognition that in the presence, in these liquids, of even extremely small traces of more volatile constituents the vacuum would be spoiled by diffusion of these impurities into the high-vacuum side. This led to an investigation by Hickman[3] of a design of pump in which "the oil constituents will be separated in the proper order by a mechanism which will preserve continuous fractionation and purging." It was shown that a pump having an extra compartment to segregate the impurities yields higher vacua than are usually obtainable with a given liquid. The ultimate pressure obtained at the high-vacuum end of the pump is equal to the saturation vapor pressure of the purified liquid. Normally only slight cooling is required in order to prevent the actual wandering of oil into the high vacuum. Baffles also assist materially in this respect, as will be mentioned more fully in a subsequent section.

---

[3] *J. Franklin Inst.*, **221**, 215, 383 (1936).

For use in pumps of the fractionating design, Hickman and his associates have produced a number of esters which have shown satisfactory characteristics. Table 1 gives a partial list of these liquids[4] with their chemical formulas, molecular weights (M), densities (ρ), and molecular diameters (δ). The last were calculated from the densities by means of equation 8.44 in Chapter 1, that is, the relation

$$\delta = 1.329 \cdot 10^{-8} \left(\frac{M}{\rho}\right)^{1/3}.$$

The phthalates are esters of phthalic acid, $C_6H_4(COOH)_2$, which is a derivative of benzene, C_6H_6, while the sebacates are esters of the straight-chain hydrocarbon derivative sebacic acid, which has the formula $HOOC \cdot (CH_2)_8 \cdot COOH$.

TABLE 1

COMPOSITION AND PROPERTIES OF ESTERS (HICKMAN)

Name	Formula	M	ρ	$10^8\delta$	Trade Designation
n-dibutyl phthalate	$C_6H_4(COOC_4H_9)_2$	278.1	1.0465	8.54	
i · diamyl phthalate	$C_6H_4(COOC_5H_{11})_2$	306.2	1.0190	8.90	Amoil
Di-2 ethyl hexyl phthalate	$C_6H_4(COOC_8H_{17})_2$	390.3	0.9796	9.78	Octoil
n-dibutyl sebacate	$C_8H_{16}(COOC_4H_9)_2$	314.3	0.933	9.25	
i · diamyl sebacate	$C_8H_{16}(COOC_5H_{11})_2$	343.3	0.9251	9.55	Amoil-S
Di-2-ethyl hexyl sebacate	$C_8H_{16}(COOC_8H_{17})_2$	426.3	0.9103	10.32	Octoil-S

Direct determinations of the vapor pressures of the butyl and octyl phthalates have been made by K. C. D. Hickman, J. C. Hecker, and

---

[4] From catalogue of Distillation Products, Inc. See also *J. Franklin Inst.*, **221**, 383 (1936), for similar data on a number of other phthalates.

N. D. Embree,[5] using different forms of hypsometers. F. H. Verhoek and A. L. Marshall[6] have determined vapor pressures for butyl phthalate and dibenzyl sebacate as well as for some other organic liquids not only by means of the static methods used by Hickman and his associates but also from the loss in weight on evaporation according to the procedures developed by Knudsen and Langmuir.

Both sets of investigators observed that their experimental data could be represented very satisfactorily by a relation of the form

$$\log P = A - \frac{B}{T}. \tag{1}$$

where A and B are constants for each liquid. It should be observed that the latent heat of evaporation L, in calories per mole, is given by the relation

$$L = 4.574B. \tag{2}$$

Equation 1 signifies that a plot of log P versus $1/T$ should yield a straight line. Such plots for a number of the phthalates have been shown for the range 0.1 to 10 mm in the paper by Hickman.[7]

More recently, data on the vapor pressures of some of these esters and other oils used in vapor pumps have been obtained in the research laboratories of both the Metropolitan-Vickers Electrical Company, Ltd.,[8] and the Distillation Products, Inc.[9]

A summary of vapor-pressure data obtained from these sources is given in Table 2. In the case of the data from reference (3), values of the constants were derived from large-scale plots of log P versus $1/T$. The values[10] of P_μ at 25° C were either calculated from the values of A and B or obtained by extrapolation.

The abbreviations used to designate the esters investigated by Verhoek and Marshall are as follows:

Tri-*m*-cresyl phosphate	*m*-Cr
Tri-*p*-cresyl phosphate	*p*-Cr
Dibenzyl sebacate	b-S

---

[5] *J. Ind. Eng. Chem., Anal. Ed.*, **9**, 264 (1937).

[6] *J. Am. Chem. Soc.*, **61**, 2737 (1939). See description in Chapter 6.

[7] *J. Franklin Inst.*, **221**, 383 (1936).

[8] The writer wishes to acknowledge his indebtedness to Sir Arthur P. Fleming, Director of the Research Department of the Metropolitan-Vickers Electrical Company, for permission to use the data given in a report by Dr. G. Burrows.

[9] These values were kindly communicated to the writer by Dr. B. B. Dayton of the Research Laboratory of Distillation Products, Inc. Also see footnote to Table 2.

[10] These values correspond to the "ultimate vacua" obtained with vapor pumps using these oils.

Two samples of the first-named ester, from two different sources, were investigated.

TABLE 2

VAPOR-PRESSURE DATA FOR OILS USED IN VAPOR PUMPS*

				Degrees C for P_μ =							P_μ at
Ester	Ref.	A	B	10^3	10^2	10	1	10^{-1}	10^{-2}	10^{-3}	25° C
Butyl phthalate	1	14.215	4680	144	110	81	56	34	15	−1	$3.3 \cdot 10^{-2}$
	2	15.589	5120	134	104	78	55	35	18	2	$2.5 \cdot 10^{-2}$
	3	14.05	4625	145	111	81	57	37	20	4	$2.0 \cdot 10^{-2}$
	4	14.50	4780	143	109	81	57	35	17	0	$2.9 \cdot 10^{-2}$
Amoil	4	13.60	4610	162	124	93	66	43	22	5	$1.3 \cdot 10^{-2}$
Octoil	1	15.116	5590	188	153	123	97	74	54	35	$2.3 \cdot 10^{-4}$
	3	14.15	5205	194	155	123	95	72	53	35	$2.2 \cdot 10^{-4}$
	4	13.00	4870	214	170	133	102	75	52	31	$4.6 \cdot 10^{-4}$
Amoil-S	4	14.40	5190	182	146	114	87	64	43	25	$1 \cdot 10^{-3}$
Octoil-S	3	14.26	5514	215	177	142	114	89	68	50	$2 \cdot 10^{-5}$
	5	16.54	6434	205	171	141	116	94	74	56	$9 \cdot 10^{-6}$
m-Cr(1)	2	15.886	6088	199	165	136	110	87	67	50	$3 \cdot 10^{-5}$
m-Cr(2)	2	13.982	5373	207	175	141	111	86	63	43	$9 \cdot 10^{-5}$
p-Cr	2	15.223	5926	212	175	144	116	92	71	52	$2 \cdot 10^{-5}$
b-S	2	15.775	6320	222	186	155	128	104	82	64	$4 \cdot 10^{-6}$
Arochlor	3			161	123	93	67	45	27	10	$8 \cdot 10^{-3}$
Apiezon A	3			186	144	110	82	58	37	20	$2 \cdot 10^{-3}$
Apiezon B	3			206	162	127	97	73	50	31	$4 \cdot 10^{-4}$
Litton oil	3			209	167	132	103	77	57	38	$1.4 \cdot 10^{-4}$
171 Dist.	3			213	171	135	106	81	60	42	$9 \cdot 10^{-5}$

* References:

1. Hickman, Hecker, and Embree (1937), *loc. cit.*
2. Verhoek and Marshall (1939), *loc. cit.*
3. Metropolitan-Vickers (1946), personal communication.
4. Values of constants deduced by S. F. Kapff and R. B. Jacobs of Distillation Products, Inc.
5. Values of constants deduced from plot sent to the writer by Dayton of Distillation Products, Inc.

The oils for which the data are given in the lowest five rows of Table 2 are obtained from distillation of petroleum oils, and the data were taken from the large-scale plots. Arochlor is a chlorinated hydrocarbon.

Litton oil[11] is described as a straight-chain hydrocarbon of the general formula C_nH_{2n}, while "171 Dist." is obtained as a distillate from Apiezon B. The values for A correspond to values of P_μ.

Recently considerable work has been carried out both in this and other laboratories on the use of silicone oils in vapor pumps. These investigations are discussed in section 6 of this chapter.

In his 1936 publication, Hickman reported the results of his investigation on the behavior of these esters in vapor pumps and on suitable designs of pumps for utilizing these oils. Particular attention was given to the necessity, pointed out by C. R. Burch in 1932, of eliminating, from the oil, products which are more volatile and which result from thermal decomposition. The degree of vacuum attainable with different oils was measured by means of an ionization gauge, and, although the interpretation of the observed ion currents in terms of absolute pressures is probably questionable, these data did provide a measure of the relative pressures under similar conditions.[12]

The most promising of a large number of synthetic esters were investigated more thoroughly with regard to their thermal stability and general suitability in vapor pumps furnished with fractionating compartments.

Hickman states

> The rate of conditioning is of great practical importance. It is the factor which determines the period necessary to secure a high vacuum in an assembly which has previously been at atmospheric pressure. . . . The rate of conditioning is almost instantaneous with a mercury condensation pump. With oil pumps, it is more rapid with a saturated compound having little affinity for air than for an unsaturated compound, and in this respect, the phthalate esters are particularly useful. . . . The rate of conditioning of the three phthalates, butyl, amyl, and hexyl, is such that their optimum vacuums are reached in 10 to 30 minutes.

While benzyl and octyl phthalates give higher vacuum they require longer periods for the first conditioning.

A further characteristic investigated by Hickman was the "degree of maltreatment" that could be tolerated.

> The degree of maltreatment, adopted as standard in the experiments on hot exposure, was the admission of air at atmospheric pressure for exactly two minutes to the pump, previously boiling under vacuum, the heating current being maintained during the exposure. . . . Butyl, amyl, and hexyl phthalates showed no indications whatsoever of harm by this treatment.

---

[11] Marketed by Litton Engineering Laboratories, Redwood City, Calif.

[12] The relation between ion-current measurements and absolute pressures is discussed in Chapter 6, section 7.

Finally it is of interest to quote the conclusions reached by Hickman with regard to the choice of a satisfactory oil for fractionating pumps.[13]

> The highest (unmeasurable) vacuums recorded in this work were secured by using Apiezon A, amyl phthalate, or hexyl phthalate with a trap cooled by Dry Ice. When a mixture of ice and salt was used to replace the solid carbon dioxide, an equally high vacuum was obtained with hexyl phthalate. The vacuums given by Apiezon A and amyl phthalate trapped with ice and salt were nearly as good.

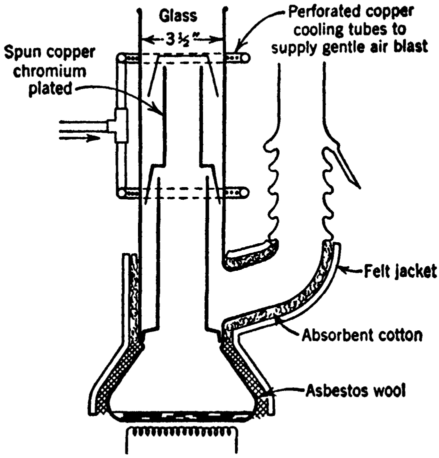
Glass
3½"
Perforated copper cooling tubes to supply gentle air blast
Spun copper chromium plated
Felt jacket
Absorbent cotton
Asbestos wool

FIG. 2. Design of fractionating vapor pump (Hickman).

> The highest vacuum obtained without a cooled trap at a room temperature of 25° C was secured with octyl phthalate. Only slightly inferior were heptyl and benzyl phthalates. Heptyl phthalate proved to be the fastest in operation and most resistant to maltreatment. Either heptyl or benzyl phthalates employed in a three-compartment pump or other pump with fractionating features provide a ready source of vacuum of the order 10^{-6} to 10^{-7} mm without the use of an absorbent or refrigerated trap.
>
> Equally low pressures can be obtained with hexyl phthalate and a trap cooled with ice, or with amyl phthalate and ice and salt.

Figure 2[14] shows a design of pump with fractionating features. Hickman observes with respect to this pump that

> The points to note are: A short wide vapor supply, cooling restricted to the upper portions of the jacket, and an abnormally large side arm leading to the mechanical pump. The side arm is provided with catchment lobes and its junction with the main portion is heavily lagged. The heat input is adjusted until there is perceptible refluxing in the arm, but the outflow of vapor is not allowed to exert sufficient back pressure to interfere with the jet performance.

[13] *J. Franklin Inst.*, **221**, 383 (1936).

[14] *J. Franklin Inst.*, **221**, 232 (1936).

Both hexyl phthalate and the Apiezon oils gave good performance in this design.

One important fact about these oils, to which Hickman has drawn attention, is that

> *the vapors are powerfully adsorbed to glass and metal surfaces,*[15] the degree of molecular crowding varying with every slight alteration of temperature. The walls of a 500-cc flask in equilibrium with a butyl phthalate vacuum at 25° C will evolve many thousands of volumes of gas on gentle warming. If the pressure is read immediately after cooling, it will be found to be less than that in the rest of the system owing to readsorption of the vapor by the walls. An ionization gauge that has been freshly torched and bombarded exerts a powerful "getter" action and may record a pressure a hundred times lower than that in the rest of the apparatus.

As will be observed from the data in Table 2, the vapor pressures at room temperature of the oils listed there are much lower than that of mercury at this temperature ($1 \cdot 10^{-2}$ to $1 \cdot 10^{-5}$ micron as compared with 1.8 microns for mercury). This fact gives rise to at least two advantages possessed by oil-vapor pumps as compared with those using mercury vapor. First, it is necessary to insert, between the system and a mercury-vapor pump, a trap cooled to a sufficiently low temperature to prevent the diffusion of mercury vapor into the system. In oil-vapor pumps, especially those using higher-molecular-weight oils, the trap may be eliminated for a large number of applications. Usually, cooling the connection between pump and system with a blast of air, or the insertion of a baffle (see subsequent section), is sufficient to prevent even the slight amount of diffusion of oil vapor that might occur otherwise. Consequently it is possible to make full use of the maximum intrinsic speed of the pump. The second advantage is that water cooling can be eliminated and replaced by a cold air blast, which makes it possible to operate the pump as a portable unit at locations where connections to the water supply and drains are not available. However, as will be pointed out in a subsequent section, these advantages are partly balanced by certain characteristics of the behavior of oils.

Note on the Mean Free Paths in Oil Vapors. The mean free path of a molecule of nitrogen or oxygen (A) in the vapor of the oil (B) at a temperature T_B, corresponding to a vapor pressure of 0.1 mm, can be calculated from equation I.8.33. That is,

$$L_A^* = \frac{1}{\pi n_B \delta_{AB}{}^2} \sqrt{\frac{1}{1 + 30T_B/(M_B T_A)}},$$

---

[15] Italics due to the writer. This characteristic is of special importance in using an ionization gauge to measure pressures in a system evacuated by an oil-vapor pump.

where $n_B = 9.656 \cdot 10^{17}/T_B$, from equation I.3.4*b*; $n_A \ll n_B$; and T_A = temperature of gas A.

Thus, for Octoil-S, $\delta_B = 10.32 \cdot 10^{-8}$, according to Table 1, and, since $\delta_A = 3.1 \cdot 10^{-8}$, $\delta_{AB} = 6.71 \cdot 10^{-8}$.

At 0.1 mm pressure, $T_B = 438$. Hence, for $T_A = 298$, $L_A = 3.06 \cdot 10^{-2}$ cm. At the same pressure, the mean free path of the molecules of Octoil-S, in the pure vapor, according to equation I.8.20*b*, is $9.59 \cdot 10^{-3}$ cm.

These results are of interest in connection with the design of nozzles for use in the pumps, since, as pointed out in the discussion of mercury-vapor pumps, the width of the diffusion slit for optimum operation of the pump should be of the same order as the value of L for the gas being exhausted.

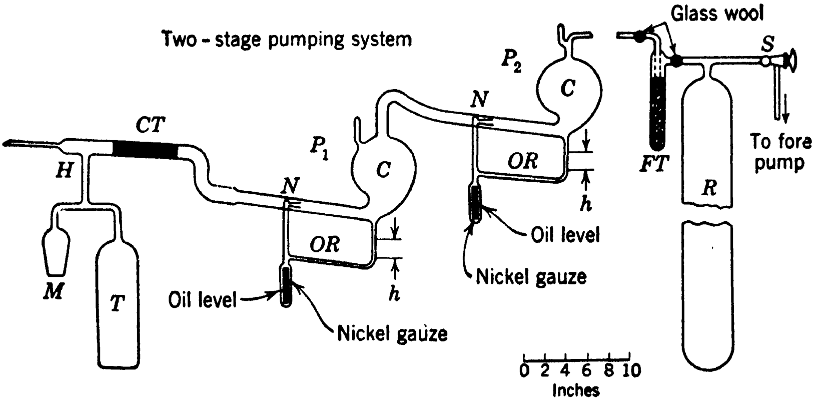

FIG. 3. Two-stage glass oil-charcoal pump system (Becker and Jaycox).

2. NON-FRACTIONATING OIL-VAPOR PUMPS

One of the earliest developments demonstrating the advantages of continuous rectification during the operation of oil pumps was due to J. A. Becker and E. K. Jaycox.[16] An arrangement of two pumps, in series with a trap containing activated charcoal, was used, as shown in Fig. 3.

The following description of the system is given by the authors:

> It consists of two air-cooled diffusion pumps, P_1 and P_2, connected in series: a simple charcoal trap, CT; a header, H, the tube to be exhausted, T; an ionization manometer, M, to measure the pressure; a fore trap, FT; a reservoir, R; a stopcock, S; and a fore pump.

---

[16] *Rev. Sci. Instruments*, **2**, 773 (1931).

> The diffusion pumps P_1 and P_2 are identical. Each consists of a boiler, the lower half of which contains the oil, an aspirator nozzle, *N*; a condensing chamber, *C*, and tubing, *OR*, through which the oil is returned to the boiler. A small cylinder of nickel gauze inserted in each boiler prevents violent bubbling. The shape of the boiler is such that it can be heated by a small electric oven placed around it. To conserve the boiler heat and to prevent excessive condensation of oil on the tubing leading to the aspirator nozzle, the boiler oven and this tubing are wrapped with asbestos cloth [not shown in Fig. 3]. No artificial cooling of the condensation chamber is necessary.... The charcoal trap, *CT*, consists of a nickel mesh cylinder filled with commercial activated charcoal.... This charcoal trap takes the place of the conventional liquid-air trap.
>
> The fore trap, *FT*, can be filled with hydrolo, alumina, charcoal or some other good absorbent material. Its function is to prevent the more volatile oil vapors of the fore pump from mixing with the low-vapor-pressure oil in the diffusion pump.

The height, *h*, of oil in the tube *OR* is used to indicate the maximum temperature to which the liquid in the pump may be heated.

The oils used in this work were Apiezon A and B and also *n*-butyl phthalate, butyl benzyl phthalate, and dibenzyl phthalate, which had also been investigated by Hickman and C. R. Sanford.[17]

The exhaust procedure is described as follows: After the pressure in the system has been decreased to that produced by the fore pump, the traps, *CT* and *FT*, the tube *T* and the manometer *M* are baked out. When the temperature of the charcoal trap has reached about 400° C, the diffusion pumps are started. A bake-out period of 20 minutes at 400° C is ordinarily sufficient for the charcoal trap, and a few minutes for the fore trap.

The authors state,

> When larger tubes which require a prolonged baking of from one to several hours are to be exhausted, it is advantageous to continue the baking of the charcoal until the tube has been well outgassed. The charcoal should be kept hot until five or ten minutes before the tube is cooled.

In the writer's experience it is virtually impossible to obtain pressures below 10^{-3} micron until all parts of an exhaust system have been heated to a temperature of 200–300° C.

Becker and Jaycox state that they were able to obtain pressures as low as $2 \cdot 10^{-5}$ micron. (Under ordinary operating conditions the pressure obtained is about ten times greater.) They also observed that the pressure increased whenever the ionization gauge was turned on. In fact, unless the electrodes in the latter had been outgassed very thoroughly it was not possible to obtain the best vacuum.

The main conclusion drawn from this investigation was that it is possible by means of an oil-vapor pump to obtain just as low pressures as can be obtained by means of mercury-vapor pumps.

---

[17] *Rev. Sci. Instruments*, 1, 140 (1930).

In connection with their investigation on the design of a high-speed mercury-vapor pump I. Estermann and H. T. Byck[18] also developed a pump for use with organic liquids. The design which was found to be satisfactory for mercury vapor could also be adapted for organic liquids,

> if [as these investigators state] such changes in dimensions were made as were dictated by the different physical properties of the organic compounds. Their steep vapor-pressure curves call for a short wide connecting tube (which must be protected against cooling) between boiler and nozzle. The ease of condensation permits a short cooling surface, and the lower vapor pressure at room temperature permits a larger clearance between nozzle and condensing wall.

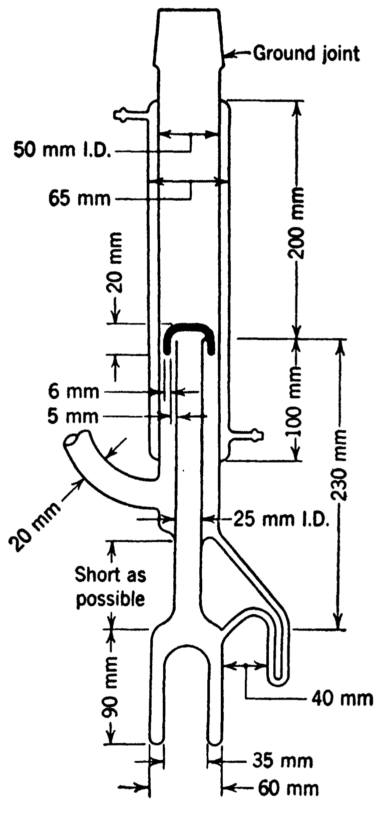

FIG. 4(*a*). Vapor pump for butyl phthalate (Estermann and Byck).

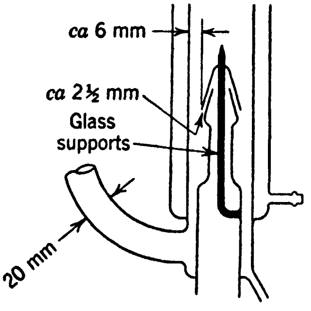

FIG. 4(*b*). Design of annular jet for butyl phthalate pump.

A pump designed for use with butyl phthalate is shown in Fig. 4(*a*). With a fore-pump pressure of less than 0.1 mm Hg, a vacuum of less than 10^{-6} mm (measured with a McLeod gauge) was obtained and a speed of 15 liters/sec. "By replacing the coaxial cylindrical jet by a jet of the annular type [Fig. 4(*b*)] the pumping capacity could be increased about 50 per cent."

Pumps of this type could be operated very satisfactorily with Apiezon oil, but then the fore-pump pressure had to be lowered to about 0.07 mm Hg.

---

[18] *Rev. Sci. Instruments,* **3,** 482 (1932).

Comparing the dimensions of the pump in Fig. 4(*a*) with those of the mercury-vapor pump shown in Fig. 4.22, it will be seen that, for the same size of opening at the top of the pump, the pump with oil gave higher values for the speed of exhaust than the one with mercury.

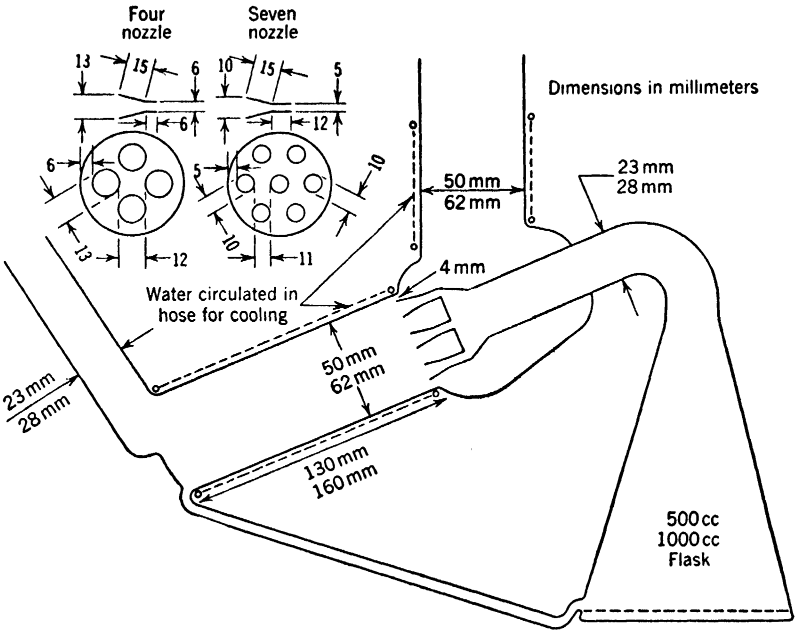

FIG. 5. Design and important dimensions of a four- or seven-nozzle oil-vapor pump (Zabel). In the main drawing the upper number is the dimension for the four-nozzle and the lower number the dimension for the seven-nozzle pump. The dimensions of the nozzles and their arrangement are shown separately for each pump.

A high-speed oil-vapor pump designed by R. M. Zabel[19] is illustrated in Fig. 5. In view of Ho's demonstration of the advantages of multi-nozzle vapor jets in mercury pumps, two pumps were tested, one with four and the other with seven nozzles. At a fine-pump pressure of 0.05 micron, the speeds obtained (liters · sec^{-1}) for air were 41 and 76, respectively, with a backing pressure of 20 microns. With suitable design of heating element and insulation, about 200 watts was required for operation of the small pump and about 300 watts for the larger pump.

[19] *Rev. Sci. Instruments*, **6**, 54 (1935).

Mention has been made in the previous chapter of a divergent nozzle construction of a metal-glass pump designed by Copley, Simpson, Tenney, and Phipps,[20] for use with butyl phthalate. This pump is illustrated in Fig. 6, and speed data are given in Table 4.6.

A two-stage pump has also been described by H. W. Edwards[21] in which conical baffles were found to be "particularly effective in preventing oil vapor from entering the chamber to be evacuated and at the same time in offering a minimum of impedance to the flow of gas through the pump."

A multiple-nozzle type of metal pump has been described by I. Amdur.[22] When operated with Apiezon B at a maximum fore-pump pressure of 30 microns, the speed obtained for hydrogen was 250 liters $\cdot$ sec^{-1} at 0.1 micron. The heat input was 630 watts.

3. FRACTIONATING TYPES OF OIL-VAPOR PUMPS

Mention has been made in the previous section of a fractionating type of pump designed by Hickman in 1936, which is shown in Fig. 2. Vertical, all-metal constructions, based on the self-fractionating principle, were also designed by A. E. Lockenvitz,[23] L. Malter and N. Marcuvitz,[24] and C. Sykes and F. E. Bancroft.[25]

Figure 7 shows the construction used by Malter and Marcuvitz. The 1-in. scale at the lower left-hand corner gives an idea of the outside dimensions, and the original paper gives details of dimensions of cones and clearances.

As these investigators point out,

> The vertical arrangement of stages is old. The actual geometry of the upper two stages, i.e., cone flares, wall clearance, outlet holes from outer cylinder *A* to cones, etc., was obtained from a three-stage pump designed by Hickman. Our modifications reside in the first or bottom stage and in the introduction of fractionating cylinders *B* and *C*.

The function of these cylinders is described as follows:

> During operation the condensate of the vapor issuing from the separate stages collects in the region surrounding the lower end of cylinder *B*. It is prevented from immediately entering into the region between *B* and *C* by the small size of the apertures in

---

[20] *Rev. Sci. Instruments*, **6**, 265 (1935).

[21] *Rev. Sci. Instruments*, **6**, 145 (1935).

[22] *Rev. Sci. Instruments*, **7**, 395 (1936).

[23] *Rev. Sci. Instruments*, **8**, 322 (1937).

[24] *Rev. Sci. Instruments*, **9**, 92 (1938).

[25] *Chem. Abst.*, **32**, 4393 (1938). See drawings of this pump and of the other two in the paper by K. C. D. Hickman, *J. Applied Phys.*, **11**, 303 (1940).

cylinder *B*. As a consequence, the lowest boiling-point fractions are boiled off before the remaining fluid passes into the region between *B* and *C*. In the same way further low boiling-point fractions are boiled off in the regions between cylinders *B* and *C* with the result that the fluid which finally works its way through the two sets of apertures into the interior of cylinder *B* is composed of the highest boiling-point fractions, or in other words, the fractions of lowest vapor pressure.

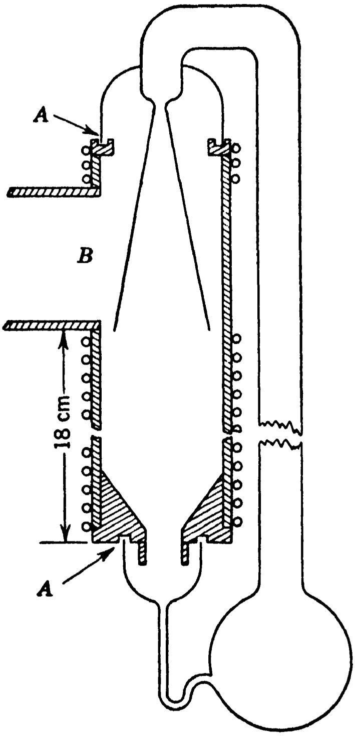

FIG. 6. Design of composite metal-glass pumps 8 and 9 (see Table 4.6) for use with oils (Copley et alii). The glass-to-metal joints are shown at *AA*.

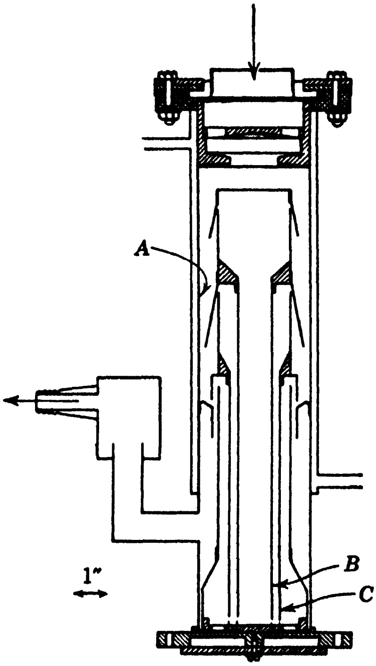

FIG. 7. Vertical, all-metal vapor pump of fractionating type (Malter and Marcuvitz).

Table 3 shows the ultimate pressures (as measured by an ionization gauge connected to the pump) obtained by these investigators, with and without the two inner fractionating cylinders.

With 450 watts the pump operated against a fore pressure of 150 microns, and with 600 watts the fore pressure could be increased to 0.5 mm.

It was found necessary in this design to insert a baffle at the top of

TABLE 3

EFFECT OF FRACTIONATING CHAMBER ON ULTIMATE VACUUM

	Octoil	"Burned" Octoil	Apiezon B
Fractionating cylinders in	$8 \cdot 10^{-8}$ mm	$2.0 \cdot 10^{-7}$ mm	$2.4 \cdot 10^{-7}$ mm
Fractionating cylinders removed	$4 \cdot 10^{-7}$	$9.0 \cdot 10^{-7}$	$1.0 \cdot 10^{-6}$

the pump, as shown in the figure. Using Octoil-S, "the speed without this baffle varied between 70 and 80 liters · sec^{-1}, over a pressure range of 10^{-3} to 10^{-6} mm of Hg. The insertion of the baffle reduced this to between 35 and 40 liters · sec^{-1}." It should also be mentioned that, according to the authors, "It appears that octoil will stand punishment which will completely ruin Apiezon B."

Following this work, Hickman[26] devised a glass-and-metal fractionating pump of horizontal construction.[27]

Figure 8[28] shows a photograph of a water-cooled, three-stage fractionating pump made of Pyrex, and the same design has also been constructed for air cooling. A novel feature of this construction is the insertion of the heating coils in the liquid. In consequence of this, and of the fact that the boilers are covered with insulating material, optimum efficiency is obtained for the transfer of heat to the oil. The high-vacuum connection is at the left, through an opening of 1⅙-in. inside diameter. The fore pump is connected at the right through an opening ⅞ in. in inside diameter. The total length is 25 in., and the height 13 in.

The small boiler at the left functions as a sink for non-volatiles produced during the operation of the pump. Special connecting tubes are provided between this reservoir and the space adjacent to the high vacuum as well as to the oil in the other boilers.

The pump requires 200 g of Octoil-S and operates at a fore pressure as high as 0.10 mm, with a power input varying from 90 to 250 watts. The speed is stated to be 25 liters · sec^{-1} at 10^{-4} mm, and the ultimate vacuum, $5 \cdot 10^{-8}$ mm at 25° C. Values of the speed at a series of heating currents and fine pressures are shown in Fig. 9.

---

[26] *J. Applied Phys.* **11,** 303 (1940): Catalogue, type GF-25W.

[27] In his paper Hickman gives reasons for favoring horizontal rather than vertical construction. Two of the main advantages of the horizontal type are due, as pointed out by JY, p. 13, to the fact that the jet diameter is independent of the boiler area and that the heat input to the separate boilers can be regulated precisely. However, it should be observed that the larger sizes of metal pumps developed by the different manufacturers are of the vertical type.

[28] Catalogue type GF-25A.

A line drawing of an air-cooled two-stage pump of the same type is shown in Fig. 10.[29] At the maximum heater current of 1.8 amp, this has a speed of 26 liters · sec^{-1} at about 10^{-5} mm and yields an ultimate vacuum, with Octoil or Octoil-S, of $7 \cdot 10^{-7}$ mm at 25° C.

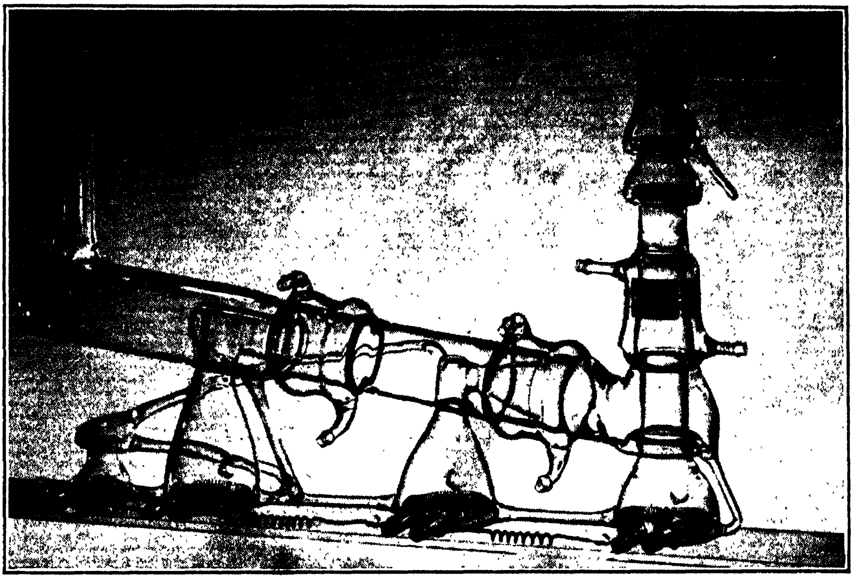

FIG. 8. Water-cooled, three-stage fractionating pump (Distillation Products, Inc.).

For vacuum systems such as the electron microscope, cyclotrons, vacuum spectrographs, lens coating, and metal evaporation outfits, high-speed three-stage pumps have been developed such as shown in Fig. 11.[30] While the illustration shows a glass container with aluminum insert of slits, a similar design has also been incorporated in an all-metal pump which has welded on the outer surface copper coils through which water is circulated for cooling. With an opening at the top, 3⅞ in. in inside diameter, the speed obtained for air is 220 liters · sec^{-1} at 10^{-4} mm pressure. The ultimate vacuum, with Octoil or Amoil-S, is about $5 \cdot 10^{-6}$ mm at 25° C, with a fore-pump pressure of 0.10 mm. At the rated speed, the value of the Ho coefficient is about 31 per cent. Pumps of this design provided with larger openings have been built by the Distillation Products for speeds as high as 15,000 liters · sec^{-1}.

To provide the low fore-pump pressure (10^{-3} mm or less) required by

---

[29] Catalogue type GF-20A.

[30] Catalogue type GM-220AB.

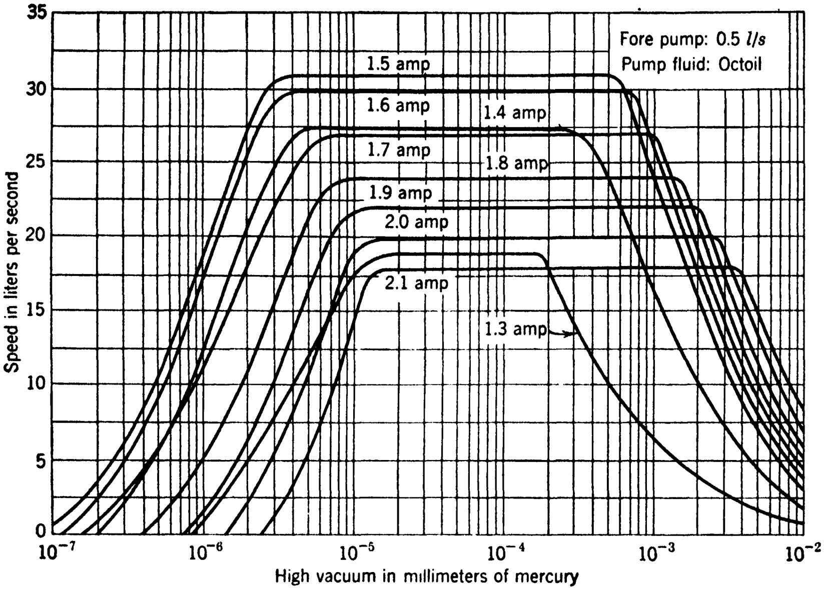

FIG. 9. Semi-log plots of speed versus pressure obtained with pump shown in Fig. 8, at a series of heating currents.

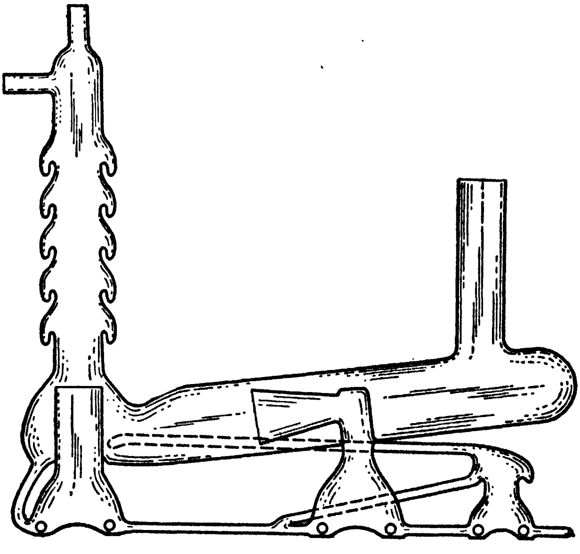

FIG. 10. Diagrammatic sketch of an air-cooled two-stage fractionating pump (Distillation Products, Inc.).

vapor pumps used for obtaining very low pressures, the same organization has also constructed a series of so-called booster pumps, which operate with butyl phthalate or butyl sebacate at the higher fore-pump pressures (up to 500 microns) such as are obtained from high-speed mechanical pumps. Figure 12 shows an X-ray photograph of a small booster type,[31] which has overall dimensions of $7\frac{5}{16}$ in. by $3\frac{7}{8}$ in. and a speed of 10 liters · sec^{-1}. With octoil an ultimate vacuum of $1 \cdot 10^{-3}$ micron is obtainable.

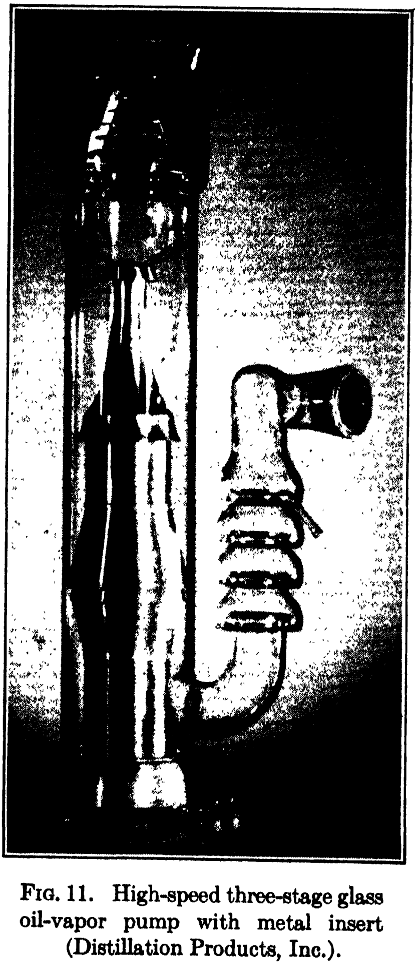

Fig. 11. High-speed three-stage glass oil-vapor pump with metal insert (Distillation Products, Inc.).

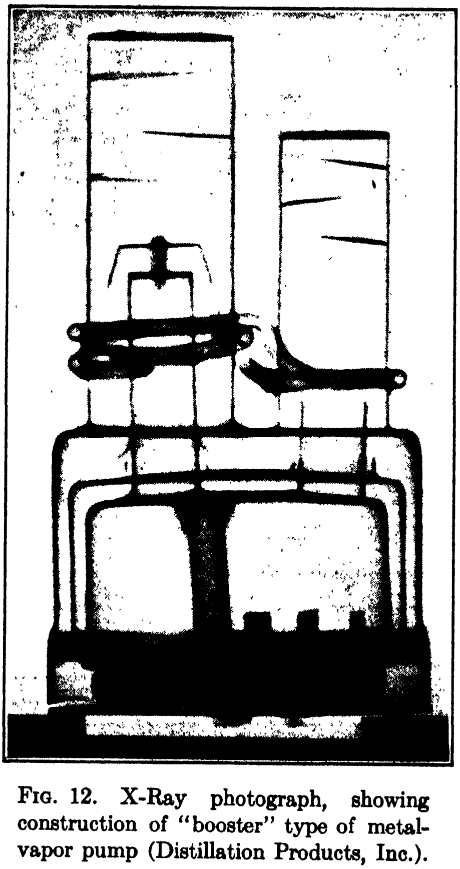

Fig. 12. X-Ray photograph, showing construction of "booster" type of metal-vapor pump (Distillation Products, Inc.).

---

[31] Catalogue type VMF-10.

Figure 13 is a side elevation of a pump developed by Hickman and G. Kuipers which operates as an oil ejector booster pump.[32]

A boiler, *A*, is closed at one end but has a removable flange at the other. Vapor leaves from the vapor dome through a pipe, *B*, and is expanded through a jet, *D*, into a water-cooled diffuser *E*. The boiler and vapor pipe are heavily lagged as at *J*. Gas is taken into the system through the large flange, *C*, and is removed by the fore pump at *K* after cleaning by the baffle system, *F*. Condensed pump fluid returns to the boiler through the line, *H*, with a working head, *G*. The most usual pressures are from 6 in. to 30 in. absolute. . . . It is usual with the higher working pressures to keep the height of the apparatus small, placing a motor-operated return pump in the bend of the pipe, *H*. Heating of the fluid is generally done by electrical immersion elements placed in the boiler but not shown in the diagram. Suitable operating fluids in our order of preference are petroleum oils, narrow cuts of light lubricating fractions; chlorinated hydrocarbons, ethyl or propyl phthalate. The more volatile silicone pump oils will be admirable when their cost is materially reduced.

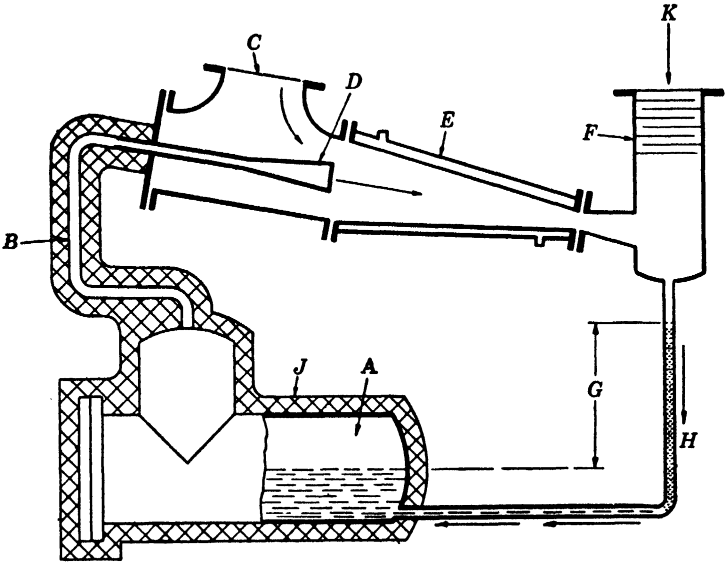

FIG. 13. Side elevation of high-speed oil-vapor ejector pump (Distillation Products).

The speed of the pump is stated to be 350 liters · sec^{-1} at 100 microns and decreases to below about 100 liters · sec^{-1} at 10 microns and also at 1 mm.

---

[32] Catalogue type KB-300. The writer is indebted to Dr. Hickman for the drawing and also for a personal communication describing the pump. The passages quoted are from this communication which has been supplemented by material published by the Distillation Products, Inc., regarding speed and ultimate pressure.

The pump is especially useful in those operations, such as vacuum smelting, dehydration, and distillation, where a pressure of the order of 20–100 microns must be maintained in systems where gas is continuously evolved. . . . The KB-300 is also effectively applied as a backing pump for exceptionally high-speed diffusion pumps such as the MC-7000 and MC-15000, or with installations of several parallel high-speed MC-500 pumps.

Plots of the speeds of the different types of pumps built by the Distillation Products are shown in Fig. 14. The dotted plot designated S4 shows the speed of the KB-300 as a fore pump, and the plot designated RP shows the speed of a standard mechanical rotary pump, such as would be used to supply the fore pressure of a KB or MB pump.

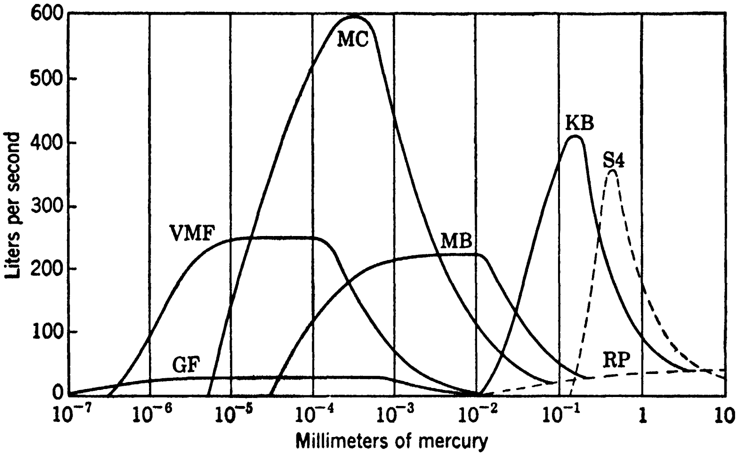

FIG. 14. Semi-log plots of speed versus pressure for a number of vapor pumps designed by Distillation Products, Inc.

The design of a three-stage all-metal pump, built by the National Research Corporation,[33] is shown in Fig. 15.[34] This has a 2-in. opening, operates either with Narcoil or mercury, and is water-cooled. Values of the speed,[35] at 10^{-4} mm (measured by a McLeod gauge), in the vacuum system, obtained at a heat input of 200 watts, as a function of fore pressure, are shown in Fig. 16. It is of interest to note that for this pump as well as for other types of construction for which published data are available, the speed obtained with a given design of pump is greater with oil than with mercury. The observation that above a certain critical fore pressure the speed decreases rapidly to zero is characteristic of both oil- and mercury-vapor pumps.

---

[33] Cambridge, Mass.

[34] H-2 pump, type 111.

[35] 1 cu ft · min^{-1} = 0.472 liter · sec^{-1}.

With pumps provided with 6-, 10-, and 16-in.-diameter inlet openings,[36] the speeds obtained at 10^{-4} mm, with Narcoil 10, are 1250 cu ft · min^{-1} (590 liters · sec^{-1}), 3000 cu ft · min^{-1} (1416 liters · sec^{-1}), and 9000 cu ft · min^{-1}, respectively. The maximum fore pressures are 200, 450, and 250 microns, respectively. The ultimate vacuum obtained in these pumps is about $1 \cdot 10^{-3}$ micron.

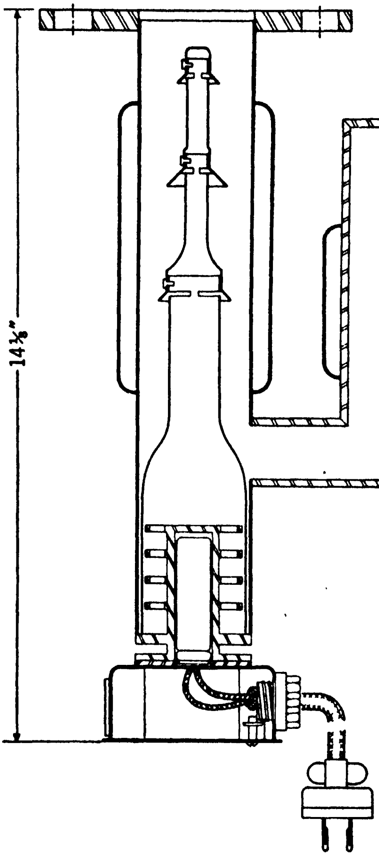

FIG. 15. Design of three-stage all-metal oil-vapor pump (National Research Corporation).

A booster pump built by the same organization is illustrated in

---

[36] H-6, H-10, and H-16 pumps, respectively.

Fig. 17.[37] It is a two-stage metal pump, water-cooled, and has a 6-in. inlet opening. With 6 kilowatt input and Narcoil, the speed is 1200 cu ft · min^{-1} (566 liters · sec^{-1}) at 7 to 1.5 microns and the pump operates at a maximum fore pressure of 500 microns.

The Eimac vacuum pump, built by Eitel-McCullough,[38] is of glass and has a metal insert of a three-stage jet assembly. The pump is fastened to the system and also to the fore pump by means of detachable collars and gaskets. Without a baffle, the speed is about 70 liters · sec^{-1}, the range $3 \cdot 10^{-6}$ to 10^{-3} mm, approximately. With the baffle insert, the speed is reduced to about half the value.

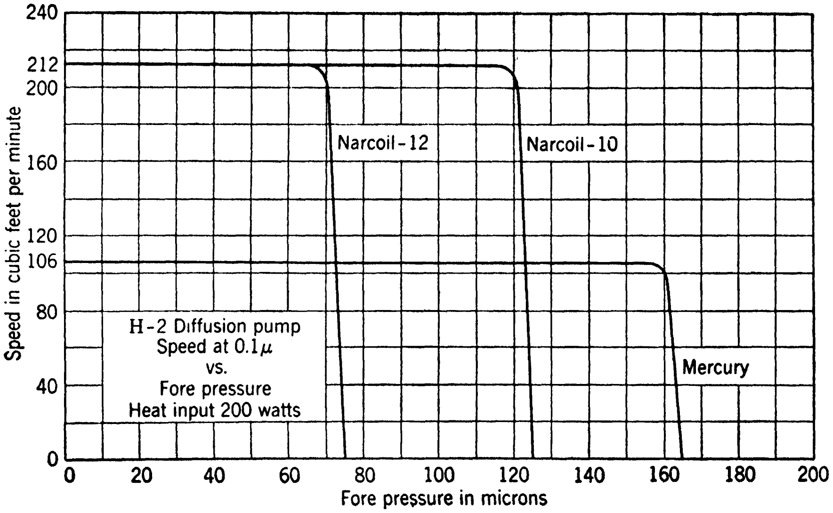

FIG. 16. Plots of speed versus fore-pump pressure for pump shown in Fig. 15.

The Metropolitan-Vickers Electrical Company of England has also built a series of vapor pumps, which use oil distillates such as Apiezon A and B. Sectional views of two of these, designated type O3B and Metrovac 8-in., are shown in Figs. 18 and 19, respectively. These are all-metal, water-cooled and provided with a baffle at the inlet. The corresponding performance curves are shown in Figs. 20 and 21 respectively.[39]

---

[37] Type 107 B-6 pump.

[38] San Bruno, Cal.

[39] Further information on pumps built in England is contained in a publication by R. Witty, *J. Sci. Instruments*, **22**, 201 (1945). See also R. Neumann, *Electronic Engineering*, Vol. 20, March, April, and May, 1948, for description of the different types of mercury-vapor and oil-vapor pumps developed in England and Holland. These articles also include a comprehensive list of references.

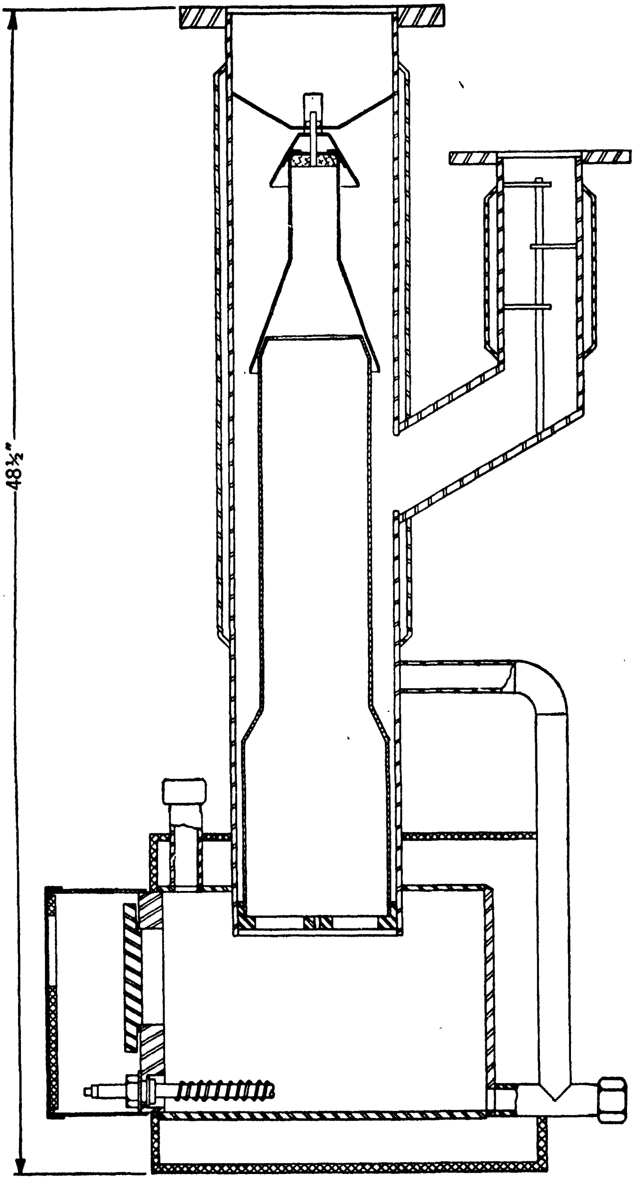

FIG. 17. Two-stage metal oil-vapor pump (National Research Corporation).

R. Jaeckel[40] has described a three-stage metal fractionating pump, made in Germany, which operates with Apiezon B at a speed of 20 liters · $\sec^{-1}$ and gives an ultimate vacuum of about $5 \cdot 10^{-3}$ micron. Jaeckel and H. J. Schroeder[41] have also described an oil-vapor pump which has a speed greater than 1000 liters · $\sec^{-1}$ for air at 20° C, with a fore-pump pressure of $6 \cdot 10^{-4}$ mm. The pump requires only 1500 watts. The inlet area is 400 cm^2, so that speed is 1 liter · $\sec^{-1}$ per watt, whereas in other pumps the efficiency is only about a half this value. As fore pump another oil-vapor is used which has a speed of 250 liters · $\sec^{-1}$.

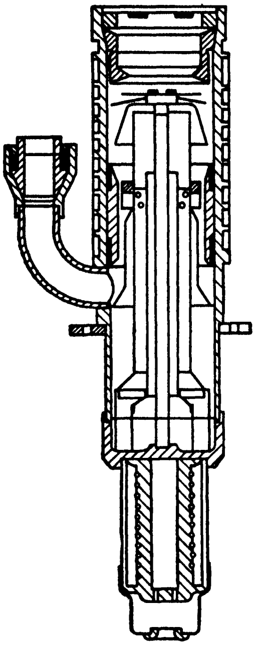

FIG. 18. Metrovac type 03B oil-vapor pump.

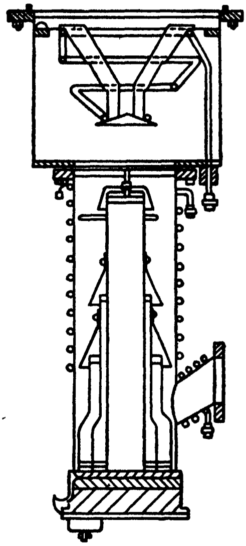

FIG. 19. Metrovac 8-in.-diameter oil-vapor pump.

4. JET DESIGN AND BAFFLES

As has been stated in the previous chapter, the design of jets is of extreme importance in affecting the magnitude of the speed factor (or

---

[40] *Z. tech. Physik,* **23**, 177 (1942).

[41] *Z. tech. Physik,* **24**, 69 (1943).

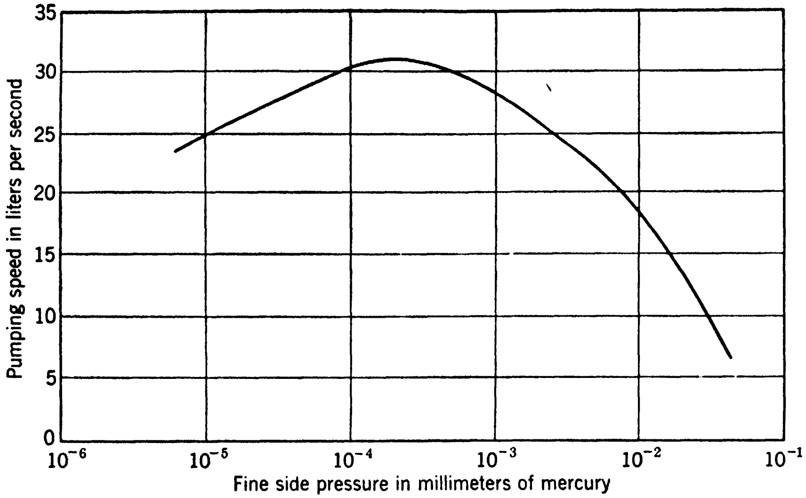

FIG. 20. Semi-log plot of speed versus fine side pressure (at 600 watts) for pump shown in Fig. 18.

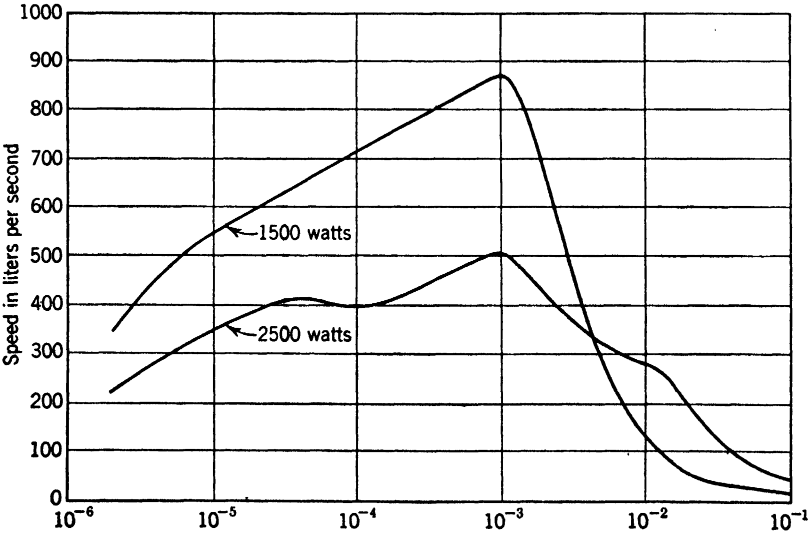

FIG. 21. Semi-log plot of speed versus fine side pressure for pump shown in Fig. 19.

Ho coefficient). This has been illustrated in section 2 in the discussion of the observations by Estermann and Byck on the effect of nozzle design on the speed of an oil-vapor pump.

J. Holtsmark, W. Ramm, and S. Westin[42] have made similar observations on the relation between pumping speed and size of diffusion jet for three different types of deflectors, such as are used in the Metropolitan-Vickers pumps described above. The three types are shown in Fig. 22, and the speed (in liters · $\sec^{-1}$ at 1 micron air) for each type (differing in the value of α, the angle of deflection) as a function of the width of the annular distance, δ, is shown in Fig. 23. At about 11 mm the pump stalled, and, as will be observed, a sloping deflector gave a higher speed than the cylindrical one. In all the tests the form of the triangular ring B (shown in Fig. 22) was maintained constant. According to the above investigators, "the critical fore vacuum of the pump has been measured and found to decrease from 5 to $3.5 \cdot 10^{-2}$ mm Hg when the pumping speed was increased from 20 to the maximum value, about 80 liters · $\sec^{-1}$."

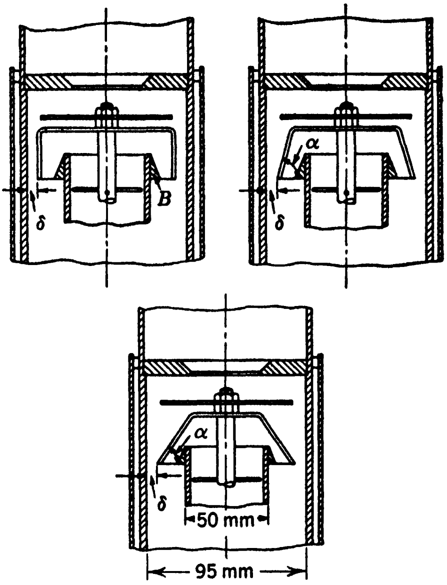

FIG. 22. Designs of jets for oil-vapor pump, used in investigation by Holtsmark et alii.

---

[42] *Rev. Sci. Instruments*, **8**, 90 (1937).

Hickman[43] has discussed this topic at considerable length. "Langmuir," he states,

> has shown that the air . . . handled by the pump collects as a layer against the walls before being driven down to the exit and expelled. Now it is apparent in Fig. 24 (*a*) that air which is entrained near the jet may be rejected again laterally where the operating vapors curve upward. The high concentration of air which has been left by vapors condensed at the wall is in especially favorable position to pass back. The passing back is favored by high fore-pressures which bend the operating stream backwards. It is also favored by too thorough condensation of the operating fluid.

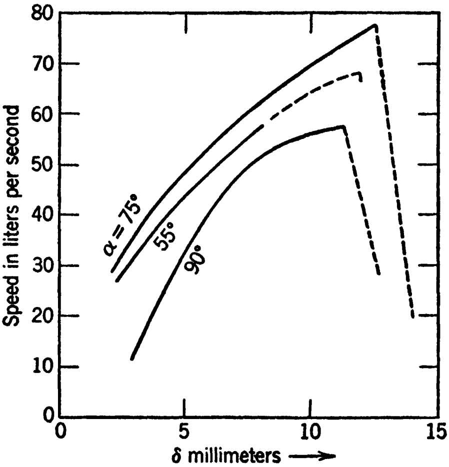

FIG. 23. Illustrating effect, on speed of pump, of jet designs shown in Fig. 22.

The molecules of this fluid, although exhibiting random motion, have a forward impressed velocity which we observe is not entirely lost on collision with condensate if this is maintained at a sufficiently high temperature. Incomplete condensation is needed to provide dilution and entrainment of the gas concentrated near the walls and also to preserve the downward passage of the gas stream. Where a water-cooled metal pump casing of high conductivity is employed, the jets must be redesigned to supply more vapor. The region that does need to be kept cold is just above the jet, at *A* in the figure. Region *B* should be kept warm, and *C* relatively hot. This is all achieved with air cooling or cooling by a spiral of tubing supplied at the top with a slow stream of cold water.

We have repeatedly confirmed the advantage of matching the cooling to the design of jet. We may define speed as the net profit of passage forward over passage back, and ultimate vacuum as the position of equilibrium between pumping speed and rate of contamination or leakage. Both speed and ultimate vacuum may benefit from moderate cooling. Thus a three-jet glass fractionating pump, filled with Octoil, gave an ultimate vacuum $1.6 \cdot 10^{-7}$ when air-cooled; $2.1 \cdot 10^{-7}$ mm water-cooled. A glass-metal pump of capacity 220 liters/sec had a speed of 120 liters/sec when the glass envelope was replaced by water-cooled metal.

---

[43] *J. Applied Phys.* **11**, 303 (1940).

The Ho coefficient and the permissible width of annulus between jet and walls are increased by lowering the fore vacuum and improving the design of jet. Perhaps the most convenient way to obtain a low fore-pressure for any given jet is to place another jet in advance. Two jets in tandem have long been in use, but only recently has the advantage of a third or even fourth jet been appreciated. Thus when the fore-pressure for the high-vacuum jet has been reduced to 10^{-3} mm or less, the mean free path of the gas in random or sideways motion below the jet is more than an inch and clearances of 1–3 in. can be used without diminishing the admission coefficient. Expansion of the vapors after the manner of Crawford[44] should be used to the extent that the operating fluid will boil under compression without cracking. But most important of all, the jet should be directed straight downward with provision for expansion of the vapors toward the center of the pump.

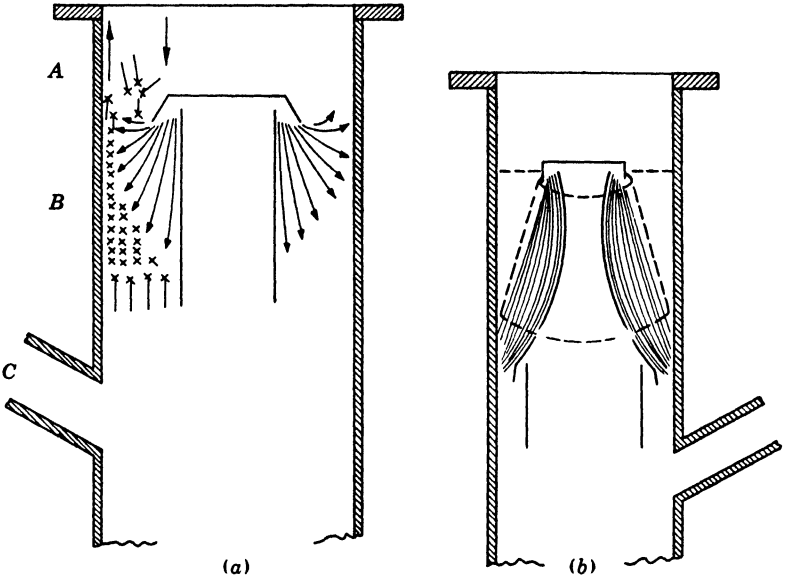

FIG. 24. Design of Embree jet (*b*) compared with straight-sided jet (*a*).

As the result of an investigation by N. Embree a jet design was evolved, shown in Fig. 24(*b*), in which there is provision for expansion of the vapors towards the center, as shown in the figure. By means of this construction, as compared with that shown in (*a*), the Ho coefficient of the pump is raised to as much as 30 per cent, whereas in the more usual designs of nozzles this coefficient, as mentioned previously, is between 2 and 20 per cent. In explanation of this, Hickman makes the following remark:

---

[44] See Figs. 4.15 and 4.16.

> It is evident that the high speed coefficient of the present pump is more apparent than real. The collecting zone with the Embree jet is not measured by the area of the annulus between the jet gap and the walls but by the area of the cones indicated by the dotted lines in Fig. 24(*b*). The speed of the pump is thus the summation of the mechanical admittance to the jet region and the diffusive admittance through the cone of actuating vapors themselves.

Evidently each region in a multijet pump transmits the *same quantity* of gas, but, as the pressure increases, the volume decreases. That is, the *micron · liters remain constant*, and consequently each jet in series should, as Hickman points out, have slightly greater micron · liter capacity. He states that, by adjusting the dimensions and clearances of the different jets in series in accordance with this conclusion, speed factors as high as 50 per cent have been obtained in the pumps of larger sizes.

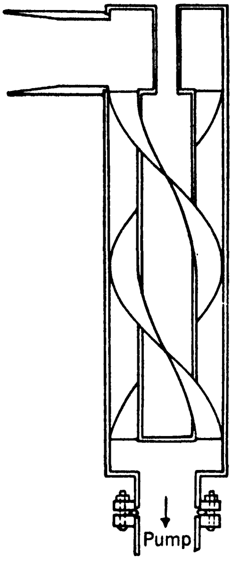

FIG. 25. Low-resistance cooling baffle for use with oil-vapor pumps (More et alii).

Although, as has been stated in the previous sections, it is possible with the different esters and oils mentioned above to obtain pressures below 10^{-7} mm without the use of *extremely* cold traps (such as are required for mercury-vapor pumps), it has been found advantageous to prevent, as far as possible, any transport of the oil vapors towards the high-vacuum side. In the pump designed by Malter baffles are introduced for this purpose, even though such inserts cut down the speed to about 50 per cent.

K. R. More, R. F. Humphreys, and W. W. Watson[45] have suggested the insertion between the pump and system of a metal cooling chamber such as shown in Fig. 25. The inner container for Dry Ice is surrounded by two helical ramps located diametrically opposite each other. These are soldered to the surface of the inner cylinder and fit snugly into the annular space between the inner and outer cylinders.

"It is evident," these investigators state, "that such a trap offers but little resistance to the flow of air downwards while at the same time effectively preventing the passage of oil vapor upwards."

---

[45] *Rev. Sci. Instruments*, **8**, 263 (1937).

According to R. S. Morse,[46] who has investigated a number of different types, baffles may be either hot or cooled. "When, for example," he states, "a grid structure, filament, or right angle bend, is introduced between the pump and system and kept hot enough to decompose all impinging oil vapor, no oil reaches the system. Regardless of the type of organic oil employed, the resulting end decomposition products are volatile gases and impure carbon. The gases are, of course, easily pumped from the system and the residual carbon has a negligible vapor pressure." A suggested design is illustrated in Fig. 26(*a*). "A series of electrically heated plates is introduced between the pump and the apparatus under exhaustion as shown." Under these conditions the ultimate pressure attainable may be increased as much as tenfold, depending upon the pumping speed available and rate of gas evolution.

Although baffles of this type may prove advantageous under certain conditions, it would seem that better results could be obtained by mechanical baffles of suitable design, with a certain amount of simultaneous cooling.

"One of the most simple forms of efficient cooled mechanical baffles" is shown in Fig. 26(*b*). It is claimed that "with such an arrangement the effective pumping speed is reduced by a factor slightly greater than 2," and at the same time oil vapor is completely prevented from entering the high-vacuum system.

A mechanical baffle of conical type has also been found effective, especially with horizontal pumps.

The efficiency of such baffles has been demonstrated by observations on the electron emissivity of a tungsten-filament cathode. After the pump is "conditioned" there is no observed decrease in emission due to back diffusion of oil vapors. In some experiments which the writer has carried out with the three-stage glass fractionating pump, a cold blast at the right-angled bend in the tubing connecting the ionization gauge to the pump has been found sufficient to prevent any decrease in emission or carbonization of a tungsten filament.[47]

As mentioned above (in section 2), Becker and Jaycox demonstrated that very low pressures could be obtained with an oil-vapor pump by use of a trap containing activated charcoal. P. A. Anderson[48] has described a specially designed charcoal trap for this purpose which can be outgassed much more rapidly than the conventional trap consisting of a Pyrex tube wound with a resistor. Standard activated charcoal is

[46] *Rev. Sci. Instruments*, **11**, 277 (1940), and K.C.D. Hickman, *loc. cit.*

[47] The writer has used this as a test for the presence of hydrocarbon vapor by operating the aged filament at 2000–2200° K for a period of at least 25 hours.

[48] *Rev. Sci. Instruments*, **8**, 493 (1937).

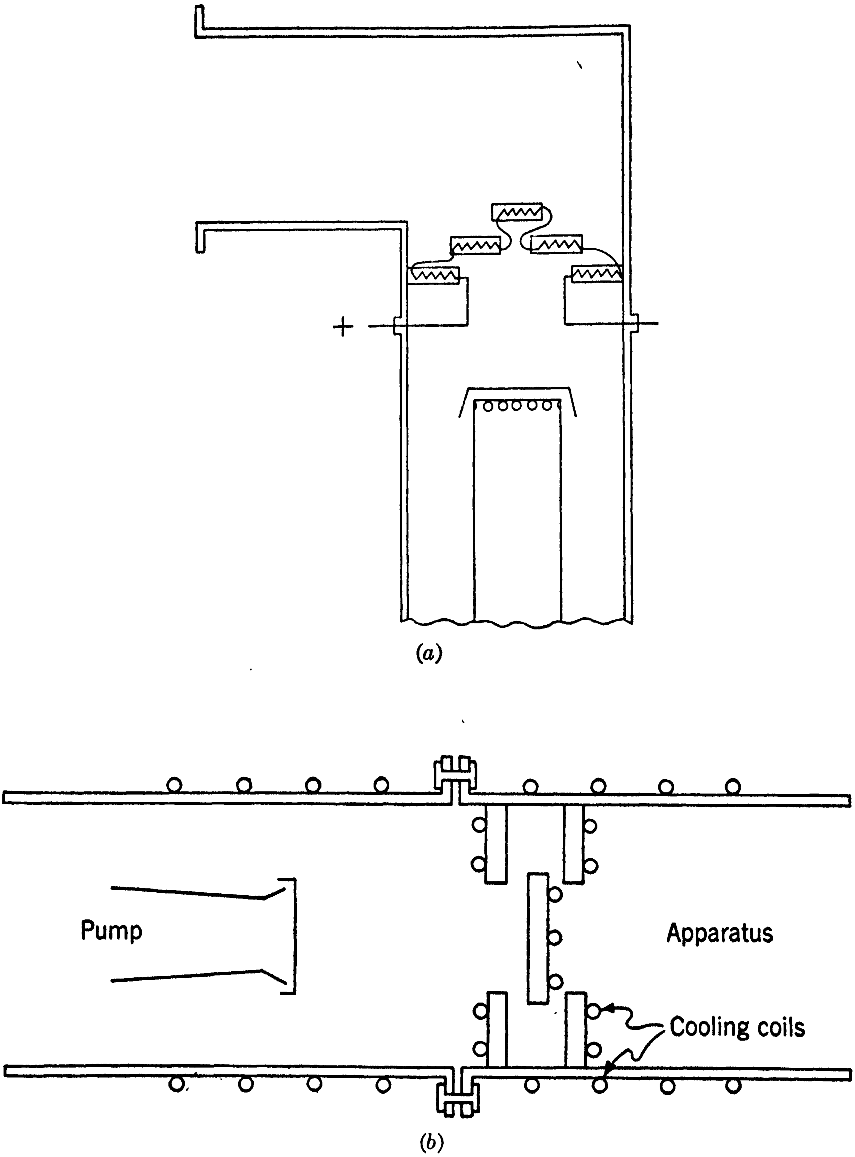

(a)

(b)

FIG. 26. Hot (a) and cold (b) baffles for use with oil-vapor pumps (Morse).

packed between graphite electrodes and plugs of Pyrex wool. By passage of current, the temperature during outgassing is raised to 800–900° C (instead of about 550° C as with the more usual type of trap), and consequently the charcoal exhibits high absorptive capacity even while hot. Using two such traps in series with an oil-vapor pump Anderson was able to obtain as good a vacuum as with a mercury-vapor pump and liquid-air trap.[49]

5. STABILITY OF OILS. ULTIMATE VACUUM OF OIL-VAPOR PUMPS

The question regarding the stability of the organic liquids on heating is obviously of great importance. As mentioned previously, Hickman and his associates have observed that the high-boiling-point phthalates and sebacates developed by them are extremely stable at the temperatures used in their pumps. Any tarry products that may be formed during the operation of the pump are eliminated by a small compartment which connects with both the vacuum and the oil chambers.

The stability of the oils with respect to oxidation is also of importance since accidents may occur, during the operation of the pump, which lead to a sudden inrush of air. Hickman has developed for this purpose a test for "degree of maltreatment" which was mentioned previously.

This problem has been investigated very fully by R. Jaeckel.[50] A special comparison was made between the behavior of Apiezon B and Octoil in glass and metal pumps of different designs. The pressures were measured by means of both an ionization gauge and the "Molvakumeter" devised by W. Gaede.[51]

The degree of vacuum attained was of the same order for both liquids and varied from 10^{-5} mm to 10^{-6} mm, depending upon the particular arrangement and type of diffusion pumps used. As is to be expected, the pressures indicated by the ionization gauge are higher, in general, than those indicated by Gaede's gauge, owing to the fact that the calibration of the ionization gauge varies[52] with the nature of the vapor.

Observations were made on the time intervals required to attain good vacuum after air at different pressures was allowed to leak into the system, also on the effects of moisture and of large leaks produced suddenly.

The conclusions drawn are as follows: (1) although the organic liquids are sensitive to oxidation and thermal dissociation, the recovery after maltreatment is fairly rapid because of the fractionating chamber; (2) the pure hydrocarbons (Apiezons) are relatively more insensitive in these respects than Octoil and Octoil-S. The last conclusion, however, is not confirmed by the experience of a number of workers in this country. For instance, in connection with an investigation of equipment satisfactory for the factory exhaust of vacuum tubes, C. T. DeGroat[53] has concluded that the esters are much superior in performance to other types of oils.

---

[49] See section 12, Chapter 10.

[50] *Z. tech. Physik*, **23**, 177 (1942).

[51] *Z. tech. Physik*. **15**, 664 (1934). See Fig. 6.32.

[52] See discussion of this topic in Chapter 6, section 7.

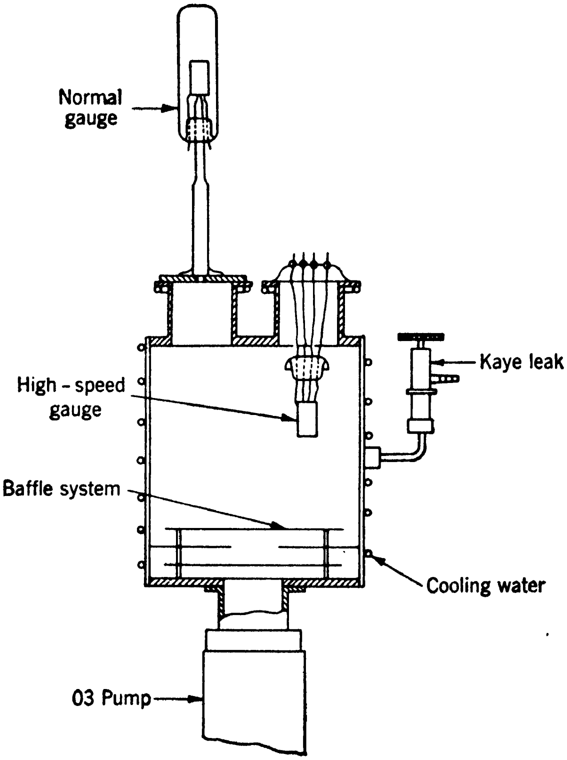

FIG. 27. Experimental arrangement used by Blears for measuring "ultimate" pressures obtained with oil-vapor pumps.

One interesting conclusion drawn by Jaeckel was to the effect that, though all organic liquids are dissociated at high temperatures and suffer oxidation, thermal dissociation is favored by metal surfaces. Thus glass pumps give lower ultimate pressures than metal pumps.

---

[53] Engineer, Electronics Division, General Electric Company, Schenectady, N. Y., to whom the writer is indebted for a personal communication on this subject as well as on other problems of vacuum technique.

A series of interesting observations on the ultimate pressures of oil-vapor pumps has been reported by J. Blears.[54] The experimental arrangement used is shown in Fig. 27 and is described as follows.

> A 10-liter steel bell jar was evacuated by a standard pumping plant consisting of a rotary pump and two oil-diffusion pumps in cascade (Metrovac D.R. 1, 02, and 03). The diffusion pump fillings were Apiezon "A" and "B" oils respectively. The internal baffles of the 03 pump had been removed and replaced by a large internal baffle in the bell jar itself. Two ionization gauges having identical electrode systems were used to measure the pressure, one being mounted on a tubulation in the normal manner, and the other being removed from its glass envelope and mounted directly inside the bell jar. These gauges have been called the "normal" and the "high-speed" gauges respectively.

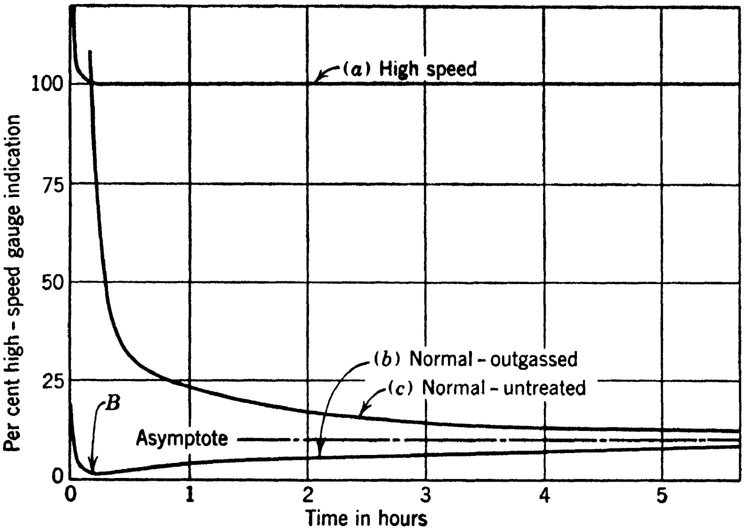

FIG. 28. Relative indications of "normal" and "high-speed" ionization gauges (Blears).

After the pumps were started, readings were taken on both gauges till the indicated pressures reached approximately constant values, as shown in Fig. 28. It should be noted that, in this and the following diagrams, the pressures indicated are in terms of equivalent nitrogen pressures. As will be observed the ultimate pressure indicated by the normal gauge was only a few per cent of that indicated by the high-speed gauge. Experiments in which different gases were admitted led to the conclusion that the difference in pressures was due to sorption of oil vapor in the normal gauge. That the readings on both gauges were proportional to the pressure in the bell jar was shown by the fact that plots of log P versus temperature of cooling water for each gauge were found to lie on parallel straight lines.[55]

---

[54] *Nature*, **154**, 20 (1944); *Proc. Roy. Soc. London*, A, **188**, 62 (1947). The writer is indebted to Sir Arthur Fleming, Director of the Research Department of the Metropolitan-Vickers Electrical Company, Ltd., for sending him a preliminary report on the results of this investigation.

A consideration of the sorption, evaporation, and decomposition processes in the two gauges leads Blears to the conclusion that the correct ultimate pressure obtained with a given oil is that indicated by the high-speed gauge, which, according to this investigator,

> is defined ideally as a gauge in which every molecule absorbed is immediately replaced and where every molecule produced by reactions is immediately removed, so that the pressure in the interelectrode space is always equal to the pressure in the rest of the vacuum system.

Table 4 gives data thus observed for the ultimate pressures obtained with a number of oils, after the pumps had been operated for 16 to 24 hours.

TABLE 4

ULTIMATE PRESSURES PRODUCED BY DIFFUSION-PUMP OILS (EXPRESSED IN TERMS OF EQUIVALENT NITROGEN PRESSURES AT 20° C)

P in mm $\cdot 10^{-6}$

Oil	Measured Values		Values Quoted in the Literature
	Standard	Fractionating	
Octoil-S	6.4	2.9	0.01–1.0
Litton oil	14.0	6.6	1.0
Apiezon B	17.0	9.2	0.1–5.0
Apiezon A	45.0	19.0	10.0
Dibutyl phthalate	225	—	100
Arochlor 1254	310	260	100

As was to be expected, the pressures obtained with a pump of fractionating type (Metro 03 was used in all cases) were lower than those obtained with the standard or non-fractionating type. The important conclusion from these observations is that the ultimate pressures obtained with oil-vapor pumps are considerably higher than those previously reported in the literature.

One very important feature about these measurements which must be given further consideration, however, is the interpretation to be assigned to the "equivalent nitrogen pressure" indications. As will be pointed out in Chapter 6, section 7, in the discussion of the calibration of an ionization gauge for different vapors, the equivalent nitrogen pressures of organic vapors are considerably higher than the absolute pressures (5 to 10 times larger). Consequently there may not be such a great difference between the pressures obtained by Blears and those quoted in the literature.

---

[55] See Fig. 6.69.

6. USE OF SILICONE OILS

During the past few years a great deal of interest has been aroused in the possible application of silicone oils in vapor pumps. Considerable work on this topic has been carried on both in this laboratory and other laboratories.

The most important liquids of this group are the cyclic and linear methyl polysiloxanes. These may be regarded as composed of the following units: $(CH_3)_2SiO$, which is designated a D unit, to indicate its "difunctional" nature, and which forms a repeating unit in the polymer; $(CH_3)SiO_{3/2}$, which is designated a T unit, to indicate its "trifunctional" nature; and $(CH_3)_3SiO_{1/2}$, designated an M unit, to indicate that it is a terminating "monofunctional" unit in the polymer.

Thus MD_9M corresponds to the chemical formula

$$[(CH_3)_3SiO_{1/2}][(CH_3)_2SiO]_9[(CH_3)_3SiO_{1/2}],$$

and TM_3 to the formula

$$[(CH_3)SiO_{3/2}][(CH_3)_2SiO]_3.$$

Liquids of the composition $D_n (n > 1)$ constitute cyclic compounds.

The vapor pressures and viscosities of these polymers have been investigated in detail by D. F. Wilcock[56] in this laboratory, and the following remarks regarding the relations he has observed between vapor pressure and composition are based on this work.

Denoting the total number of silicon atoms in the polymer by x, the following relations were obtained for the vapor pressure in *microns:* for $x > 5$:

For linear methyl polysiloxanes,

$$\log P_\mu = 9.28 - \frac{1030}{T} + x\left(0.443 - \frac{360}{T}\right). \tag{1}$$

For cyclic methyl polysiloxanes,

$$\log P_\mu = 10.07 - \frac{1190}{T} + x\left(0.265 - \frac{294}{T}\right). \tag{2}$$

---

[56] *J. Am. Chem. Soc.*, **68**, 691 (1946).

Thus, with increase in length of chain, the vapor pressure for any given temperature decreases. This is illustrated in Table 5 by the values of P_μ calculated for the series of linear polymers ranging from $x = 13$ to $x = 18$, corresponding to $MD_{x-2}M$. In calculating these values the relations used were of the form

$$\log P_\mu = A - \frac{B}{T}, \tag{3}$$

with the values of A and B calculated for given values of x by means of equations 1 and 2.

The second and third columns give the values of the constants A and B in equation 3 used for calculating the data in the other columns.

TABLE 5

VAPOR PRESSURES OF LINEAR SILICONE POLYMERS

x	A	B	P_μ at 25° C	Temperature in degrees C for $P_\mu =$ 10^4	10^2	1	10^{-2}	10^{-4}
12	14.60	5350	$4.4 \cdot 10^{-4}$	232	152	93	49	15
13	15.04	5710	$7.6 \cdot 10^{-5}$	244	165	107	62	27
14	15.48	6070	$1.3 \cdot 10^{-5}$	256	177	119	74	39
15	15.93	6430	$2.2 \cdot 10^{-6}$	266	189	131	86	50
16	16.37	6790	$3.8 \cdot 10^{-7}$	276	200	142	97	60
17	16.81	7150	$6.5 \cdot 10^{-8}$	285	210	152	107	70
18	17.25	7510	$1.2 \cdot 10^{-8}$	294	219	162	117	80

These data show that silicone polymers in which the number of silicon atoms exceeds 12 possess sufficiently low vapor pressures at room temperatures for use in vapor pumps. Actual experiments carried out by R. A. Boyle[57] have led to the conclusion that by fractional distillation of silicones products may be obtained having the approximate composition of a mixture of MD_9M and $MD_{10}M$ ($x = 11$ to 12) and producing a vacuum of about 10^{-3} micron or better in a Distillation Products VMF 5 pump. In this investigation it has also been demonstrated that these oils are apparently superior to the hydrocarbon and ester types of liquids in resistance to both cracking and oxidation at high temperatures.[58]

---

[57] Chemical Engineering Division, General Electric Company.

[58] It should be noted, however, that when these silicones decompose on metal surfaces they yield a layer of an insulating material (presumably a suboxide of silicon) which can be removed only by heating to above 400–500° C. As will be more fully discussed in Chapter 6, section 7, this insulating deposit formed, in the course of time, on the positive-ion collector of an ionization gauge gives rise to gradually decreasing positive-ion readings, and thus renders the gauge useless as a pressure indicator.

These conclusions regarding the stability of silicones are in agreement with observations published by G. P. Brown[59] on the comparative performances in a non-fractionating metal pump of the commercial

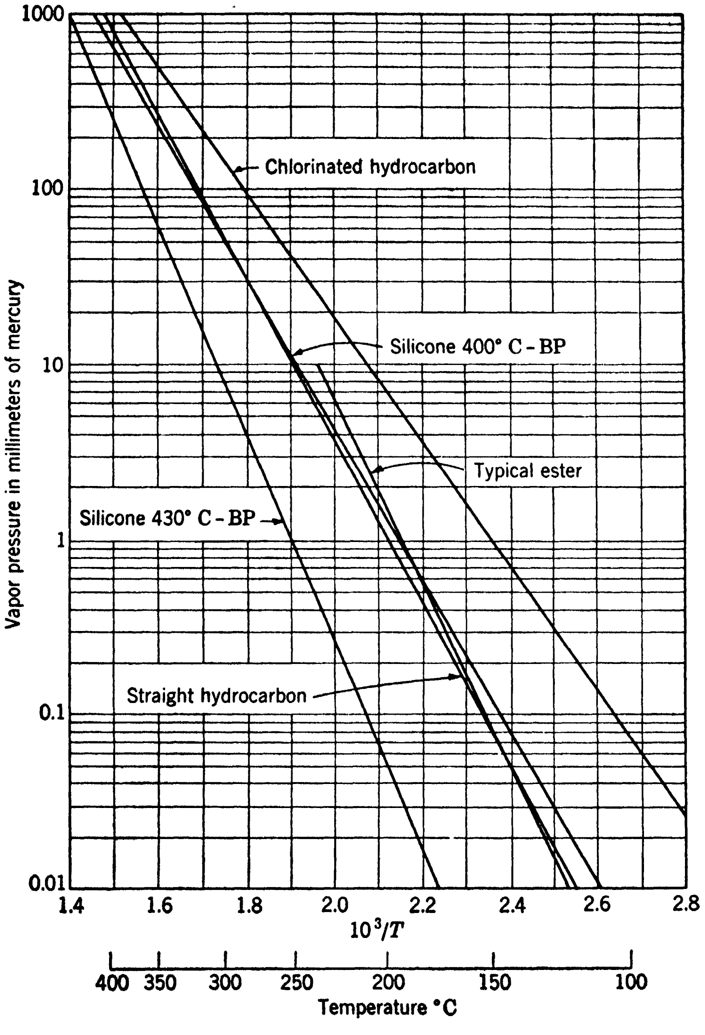

FIG. 29. Plots of log of vapor pressure (P_{mm}) versus $1/T$ for silicones and other oils used in oil-vapor pumps (Brown).

products Litton C, Octoil, Narcoil, and two silicones with boiling points of 400° C and 430° C. From the plots of log P_{mm} versus $1/T$ shown in

---

[59] *Rev. Sci. Instruments*, **16**, 316 (1945).

Fig. 29 the values of A and B for the higher-boiling-point liquid are found to be 14.24 (for P_μ) and 5880 respectively. This leads to the results: $P_\mu = 3.3 \cdot 10^{-6}$ at 25° C and $P_\mu = 1$ at 140° C, which correspond according to the data in Table 5 to those of a linear methyl polysiloxane for which x has the value 16 or 17. The silicone boiling at 400° C corresponds roughly to a linear polymer for which x has the value 13 or 14.

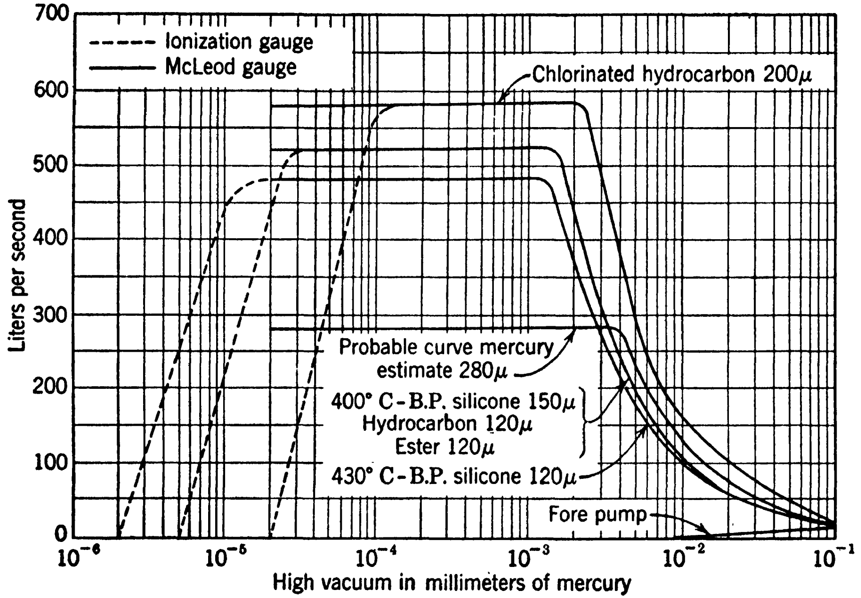

FIG. 30. Speed versus log P_{mm} for various pump oils in a typical 6-in. metal pump. Data for fore pressures in microns indicated for each curve (Brown).

Figure 30 shows semi-log plots of speed versus pressure for the different oils as well as for mercury, in the same design of pump. The values of the fore pressures (microns) are indicated on each curve. According to the author, "Extrapolated vapor pressure, temperature data, and test results show the high-boiling-point silicone to produce the highest vacuum as indicated by an untrapped ionization gauge. The silicone was further found to be nearly completely resistant to oxidation when exposed to air while hot." In other respects the different oils showed only minor differences. It is of interest to note that in these experiments the lowest speed was obtained with mercury vapor.

In connection with the use of oil-vapor pumps in technological applications R. S. Morse[60] has made the following interesting statement:

---

[60] *Ind. Eng. Chem.*, **39**, 1064 (1947).

Recent trends have demonstrated the possibility of improving the fore-pressure characteristics of pumps through the use of high boiler pressure and improved jet design. It is now apparent that the limit on gas handling capacity of a diffusion pump below 10^{-4} mm is in reality only a function of the "pumping speed" of the entrance of the mouth of the pump.

Oil diffusion pumps, 32 inches in diameter with a capacity of 30,000 cubic feet per minute[61] at 10^{-5} mm, have been built in great numbers. . . .

With newer ejector type oil diffusion pumps greater speeds are now possible in the higher micron range. With minor exceptions the use of mercury in diffusion pumps in this country is now limited to laboratory apparatus or electronics applications where fore-pressure operation above 1 mm is essential.

Both chlorinated compounds, such as the so-called Arochlor series, and refined hydrocarbon pump oils have been used with success in many large installations during the war, particularly because of greater stability in the presence of water vapor and because of lower cost. The use of silicone type oils has recently been advanced, and the resulting improved stability after exposure to air at high temperature is a useful factor.[62] Because of contamination problems at the extremely low pressures employed, the electronics industry in many instances still prefers the organic esters.

[61] The maximum theoretical speed for molecular flow through an orifice of 1-in radius with air at 25° C is 500 cu ft/min. This corresponds to 256 × 500 = 128,000 cu ft/min for an orifice 32 in. in diameter.

[62] See discussion by G. P. Brown, *loc. cit.*

CHAPTER 6

MANOMETERS FOR LOW GAS PRESSURES[1]

1. APPLICATION OF ELECTRICAL DISCHARGE IN GAS AT LOW PRESSURES

The breakdown voltage in a gas between two electrodes (preferably plane surfaces) located a fixed distance apart is a function of the pressure. As the pressure is decreased from atmospheric, the voltage required to initiate a discharge decreases, reaching a minimum value at a pressure of about a millimeter of mercury or less, depending upon the geometrical arrangement, shape and area, of the electrodes and upon the nature of the gas. As the pressure is then decreased still further, the breakdown voltage increases rapidly until it exceeds that of the available voltage source. With a discharge tube of given design and high-voltage source it is therefore possible to obtain in this manner a semi-quantitative indication of pressure, especially the value at which the discharge ceases.

The appearance of the discharge has been used by a number of observers as a criterion of the order of magnitude of the pressure. A more detailed discussion of these observations has been reported by H. Stintzing[2] and is also given by J. Yarwood.[3]

---

[1] The writer has made considerable use of the article entitled "High-Vacuum Gauges" by M. Pirani and R. Neumann, *Electronic Engineering* (England), December, 1944, January, February, and March, 1945, which contains a very comprehensive list of references. The topic is also discussed in FM, pp. 71–102.

Extensive lists of references are given in the following publications:

G. Mönch, *Vakuum Technik im Laboratorium,* Weimer, 1937. Published by J. W. Edwards, Ann Arbor, Mich., by authority of Alien Property Custodian.

H. Klumb and H. Schwarz, *Z. Physik,* **122**, 418 (1944).

The reader should also consult, in this connection, the articles by W. E. Barr and V. J. Anhorn, "Vacuum Gages" in *Instruments,* **19**, 666, 734 (1946). The first paper contains detailed information on the design and construction of McLeod gauges; the second deals with some of the other types of gauges most frequently used in vacuum technique, such as the Pirani, thermocouple, and Knudsen gauges.

A condensation of the contents of this chapter has been published by the writer in *Instruments,* **20**, 234 (1947).

[2] *Z. physik. Chem.*, **108**, 70 (1914); Pirani and Neumann, *loc. cit.*; Mönch, *op. cit.*, p. 54.

[3] JY, pp. 19–21.

G. Burrows[4] has described a discharge tube suitable for metal systems. The construction is shown in Fig. 1. The tube is operated from a spark coil providing a spark in air about 3/8 to 1/2 in. long. According to the author,

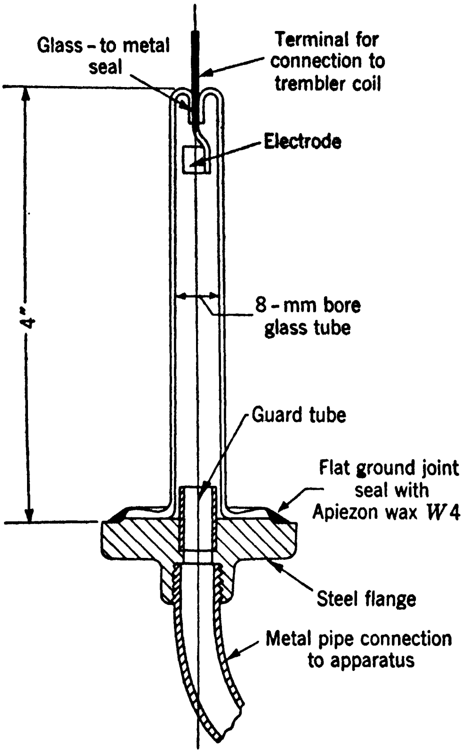
Glass - to metal seal
Terminal for connection to trembler coil
Electrode
4"
8 - mm bore glass tube
Guard tube
Flat ground joint seal with Apiezon wax *W*4
Steel flange
Metal pipe connection to apparatus

Fig. 1. Discharge tube for estimation of pressure (Burrows).

The following approximate relationships exist between the discharge as observed in a discharge tube of the type shown and the corresponding air pressure:

1/2-cm-diameter column of glow discharge = 10 mm Hg
First visible striations = 1.5 mm
Striations pitched 1 cm apart = 0.5 mm
Green fluorescence on inside walls = 0.01 mm
Black-out in dark (under vacuum conditions) = 0.001 mm or less

The discharge tube also enables an estimation to be made of the kind of gas or vapor present, thus

APPEARANCE	KIND OF GAS
Red or pink	Air
Greenish gray	Decomposed oil
Faint (transparent) blue	Water vapor

---

[4] *J. Sci. Instruments*, **20**, 21 (1943).

The gas discharge as an indicator of low pressures has also been applied in a device designated the *skanascope.*[5] One type of design consists of a cylindrical metal tube which is connected to the vacuum system and along the axis of which is located a metal rod. With a given maximum a-c voltage applied between the rod and cylinder a discharge is initiated at a certain pressure P_i. As the pressure is reduced the current in the discharge decreases and drops abruptly to practically zero at a certain pressure, P_f. The discharge excites a fluorescent screen inserted in one end of the metal cylinder, and the intensity of the luminescence serves as an indicator of the degree of vacuum. Thus, for air, the values of P_i and P_f, corresponding to initiation of the discharge and to cessation, are 600 microns and 30 microns, respectively. The values of these critical pressures vary with the composition of the gas.

By changing the arrangement of the electrodes and replacing the fluorescent screen by a fluorescent tube in series with the discharge it is possible to decrease the value of P_f for air to 5 microns.

A high-frequency spark coil is an essential device in experimental work on high vacuum. In practice a spot at which a leak is suspected may be detected more readily by wetting it with carbon tetrachloride or other volatile organic liquid. The presence of a leak is then indicated by the change in color of the glow produced by the spark coil.

For the measurement of low pressures the different types of gauges may be classified, according to the basic principles involved, as follows:

1. Manometers which use mercury or some very non-volatile liquid.
2. Manometers which operate on the same principle as the Bourdon gauge, that is, the pressure produces a deformation in a thin wall.
3. Viscosity manometers.
4. Radiometer type of manometers, which measure the rate of transfer of momentum from a hot to a cold surface.
5. Conductivity type of manometers, involving the effect of pressure on the rate of heat transfer.
6. Ionization gauges.

2. MERCURY (AND OTHER LIQUID) MANOMETERS

Numerous attempts have been made to increase the sensitivity which may be obtained in reading the height of a barometric column or U-tube manometer.

Rayleigh Gauge.[6] The essential parts of the Rayleigh gauge (Fig. 2*a*) are two glass bulbs, one of which communicates with a good vacuum by a tube *C*, and the other with the system in which the pressure is to be measured. Two glass pointers are sealed into the bulbs, and the bulbs are attached to a T-connection which forms the upper end of a barometric column. Mercury can be raised and lowered in the bulbs by means of a reservoir connected to the barometric column and the level thus brought up so as to be flush with the ends of the pointers. Any difference in pressure on the mercury in the two bulbs is then measured by gradually tilting the framework on which the bulbs are fastened and observing the deflection on a mirror which is located on top of the bulbs. According to Rayleigh this gauge can be used to read pressures between 1.5 mm and $1 \cdot 10^{-3}$ mm of mercury.

---

[5] Developed by the Skaneateles Manufacturing Company, Syracuse, N. Y.

[6] *Phil. Trans.*, A, **196**, 208 (1901); *Z. physik. Chem.*, **37**, 713 (1901).

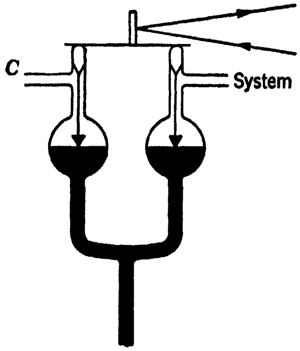

FIG. 2*a*. Rayleigh form of differential manometer.

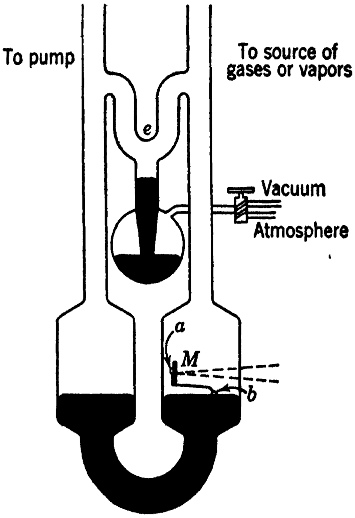

FIG. 2*b*. Optical-lever manometer (Shrader and Ryder).

A modified form of this gauge was used by K. Scheel and W. Heuse[7] for measuring the vapor pressure of water at temperatures below 0° C, and similar manometers have been constructed by M. Thiesen[8] and E. Hering.[9] An ingenious modification of Rayleigh's method has been used by C. F. Mündel[10] for measuring vapor pressures at very low temperatures; and a very sensitive optical method for measuring slight differences in level of two mercury surfaces, developed by K. Prytz,[11] has been used extensively by different investigators in connection with Rayleigh's method.[12]

---

[7] *Z. Instrumentenk.*, **29**, 344–349 (1909). K. Jellinek, *Lehrbuch d. physik. Chem.*, I, 1, p. 321. *Ann. Physik*, **29**, 723 (1909).

[8] *Z. Instrumentenk.*, **6**, 89 (1886), and **24**, 276 (1904).

[9] *Ann. Physik*, (4), **21**, 319 (1906).

[10] *Z. physik. Chem.*, **85**, 435 (1913).

In the *optical-lever manometer*, described by J. E. Shrader and H. M. Ryder,[13] the same object is attained by a very simple construction. The following description is quoted from the original paper:

> A mercury U-tube manometer (Fig. 2*b*) is formed in the usual manner, except that the surfaces of the mercury are so arranged as to be of relatively large area. Above one of the surfaces, within the tube, is arranged an optical lever as shown in the illustration. This lever is supported by two knife edges, *a*, which rest on loops of wire, which in turn are sealed into the glass walls of the tube; a glass bead *b*, fused to the end of the lever arm, acts as a float on the mercury surface, and in this way transmits the motion of the mercury surface to the lever arm. A mirror *M* attached at the position shown acts in the usual manner to reflect a beam of light from a lamp to a scale, if the gauge is to be arranged as an indicating instrument. If the gauge is to be used for recording variations in pressure, the scale may be replaced by a photographic device such as is used in oscillographic work.
>
> The cross connection *e* provides an easy means of evacuating the whole system with one pump located as shown. With this stopcock or mercury cutoff open, a zero reading can be easily obtained, after which this connection may be closed and the gases or vapors introduced for measurement. This system provides also for the measurement of small variations in pressure, with an original pressure of any desired value, this value in no way affecting the absolute sensibility of the gauge.

A sensitivity of 10^{-3} mm of mercury is claimed for the gauge, and it certainly ought to prove useful where the McLeod gauge is inapplicable.

A more elaborate modification of the optical-lever manometer has been described by E. K. Carver,[14] by which pressures as low as 10^{-4} mm may be measured, and a simple form, which may be used in the ranges 10 to $5 \cdot 10^{-2}$ mm, or 1 to $5 \cdot 10^{-3}$ mm, has been constructed by M. L. Hamlin.[15] K. Newbury and C. L. Utterback[16] have measured the vapor pressures of waxes and greases by observing the deflection of a mirror attached to an iron float on top of the mercury. The sensitivity obtained is of the order of 10^{-3} mm.

Instead of an iron float, M. C. Johnson and G. O. Harrison[17] have suspended "a glass float on the top of the mercury surface by means of flattened platinum wires which wrap around a roller of glass rod about 1 mm diameter. The mirror is fastened to this roller and two more flattened platinum wires also wrap round the rod and suspend it from a stout copper wire soldered to a brass ring which can slide loosely into the manometer tube." It is stated that with this construction pressure differences between 0.5 and $2 \cdot 10^{-4}$ mm of mercury can be measured.

---

[11] *Ann. Physik,* (4), **16**, 735 (1905).

[12] C. F. Mündel, *loc. cit.*, and M. Knudsen, *Ann. Physik,* (4), **33**, 1435 (1910).

[13] *Phys. Rev.*, **13**, 321 (1919).

[14] *J. Am. Chem. Soc.*, **45**, 59 (1923).

[15] *J. Am. Chem. Soc.*, **47**, 709 (1925).

[16] *Rev. Sci. Instruments*, **3**, 593 (1932).

[17] *J. Sci. Instruments*, **6**, 305 (1929).

A form of U-tube manometer sensitive to $5 \cdot 10^{-3}$ mm has been described by T. G. Pearson.[18]

A tilting differential mercury manometer for *recording* pressures between 0.01 and 5 mm, developed in several different forms by K. C. D. Hickman[19] should be of interest in certain continuous operations at moderately low pressures.

In this manometer the mercury may be replaced by an organic liquid of extremely low vapor pressure, and G. Burrows[20] has described such a manometer in which Apiezon oil is used. Though the sensitivity, as compared with a mercury manometer, is thereby increased to as much as fifteenfold there are two serious objections to an oil manometer. The first arises because of the solubility of the gas in the oil, and the second is due to the sluggishness of operation resulting from the high viscosity of the liquid and its tendency to stick to the glass walls.

In order to measure pressure differences of the order of 10^{-2} mm, in two mercury columns, H. Klumb and Th. Haase[21] fasten a fine tungsten wire, about 100 cm long, along the axis of each leg of a U-tube manometer. The difference in pressure in the two sides effects a corresponding difference in the resistances of the two wires, which is determined by a Wheatstone bridge method. At pressures down to 1 mm, the difference in resistance is proportional to the pressure difference. At lower pressures (below about 0.1 mm) the indications are complicated by heat-conduction losses from the wires in the gas. However, by putting a layer of a low-vapor-pressure oil (such as *n*-dibutyl phthalate) on the surface of the mercury and using very short lengths of wire so that the wire is wholly covered by oil, the change in resistance is found to be proportional to the pressure difference, and it is claimed that pressures as low as 0.01 mm may be measured.

[18] *Z. physik. Chem.*, **A**, **156**, 86 (1931). FM, p. 84.

[19] *J. Optical Soc. Am.*, **18**, 305 (1929). Mention should be made, in this connection, of the Dubrovin gauge, made by W. M. Welch Scientific Company. This consists of a glass tube, about half-filled with mercury, connected to the system. Floating on the mercury is a metal tube closed at the top by a flat disk, used as an indicator, and loosely closed at the other end, which is immersed in the mercury, by a glass ball. The interior of the metal tube is evacuated, and, therefore, the tube will float high on the mercury when the pressure is reduced and low when the pressure is high. The gauge may be used to measure pressures ranging from 0.1 mm to 20 mm of mercury.

[20] *J. Sci. Instruments*, **20**, 21 (1943).

[21] *Z. tech. Physik*, **13**, 372 (1932).

For measuring small pressure differences of mercury at a distance from the system, A. Simon and F. Fehér[22] have made use of a special electronic circuit in which the capacity is determined between the upper part of the mercury column and a piece of tinfoil wrapped around the outside of the glass tube.

Mention should also be made of the application by J. J. Manley[23] of the Michelson interferometer to determine pressures ranging from 10^{-4} to 20 mm.

McLeod Gauge. The principle of the McLeod gauge, first described by H. McLeod,[24] consists in compressing a given volume V, of the gas whose pressure P is to be measured, to a much smaller volume v and observing the resultant pressure p, which in accordance with Boyle's law is given by the relation

$$p = \frac{PV}{v}. \tag{1}$$

One of the simplest forms of McLeod gauge is shown in Fig. 3*a*. The bulb, B, to which is attached a capillary tube *aa*, is connected to the low-pressure system as indicated and also to the barometric column below. In order to avoid errors due to the effect of capillarity, a tube, *bb*, of the same diameter as *aa*, is sealed on as a by-path to the larger tube E. To operate the gauge the reservoir R is raised, thus forcing the mercury up in the barometric column T until the gas in the bulb and capillary is shut off from the remainder of the system at C. As the mercury is raised further, the gas in B is compressed until finally the mercury in the capillary *bb* is level with the top of the inside of the capillary *aa* (corresponding to the point 0 on the scale). The pressure on the gas in the capillary is then equal to the sum of the pressure in the system and that of the mercury column of length h, which is also the length of the capillary *aa* that contains the compressed gas.

Figure 3*b* shows a very common design of gauge in which the reservoir illustrated in Fig. 3*a* is replaced by a wide tube with a wooden (or glass) plunger which serves to raise the mercury, as shown in the figure on the right-hand side.[25]

Let V denote the volume (in cubic centimeters) of the capillary and of the bulb B down to the level C at which the gas in the bulb becomes trapped when the mercury is raised. Let P_{mm} denote the pressure in the system. Also, let b denote the volume (in cubic centimeters) of the capillary *per millimeter* length.

---

[22] *Z. Elektrochem.*, **35**, 162 (1929). The original paper contains a comprehensive list of references to other methods available for telemetering of pressure differences.

[23] *Proc. Phys. Soc.*, **40**, 57 (1927–1928).

[24] *Phil. Mag.*, **48**, 110 (1874).

[25] Detailed drawings of a number of designs of McLeod gauges are shown by W. E. Barr and V. J. Anhorn, in *Instruments*, **19**, 666 (1946).

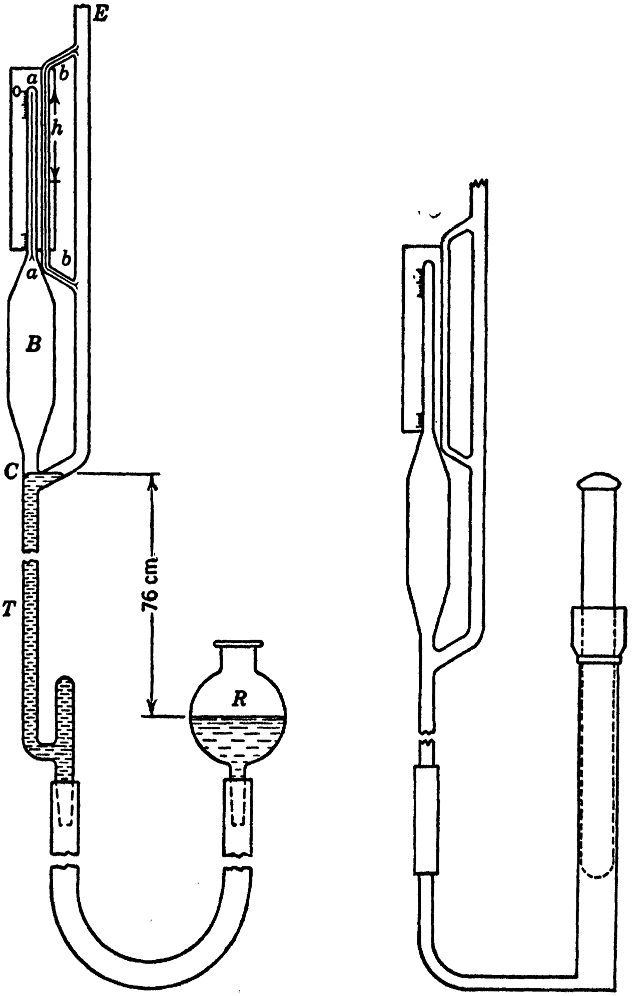

(*a*). Form with reservoir that can be raised or lowered.

(*b*). Form with plunger.

FIG. 3. McLeod gauge.

$$\text{Volume of gas trapped} = v = bh \quad (\text{cm}^3).$$

$$\text{Pressure in capillary} = P_{mm} + h,$$

Hence

$$(P_{mm} + h)bh = P_{mm}V,$$

or

$$P_{mm} = \frac{bh^2}{V - bh}. \tag{2}$$

For gauges in which a plunger or reservoir is used to raise the mercury in the capillary, the value usually chosen for V is between 75 and 100 cm^3, and the diameter of the capillary is between 0.7 and 2.5 mm.

Let d = diameter of capillary in millimeters; then $b = 7.854 \cdot 10^{-4}d^2$ cm^3 per millimeter length, and

$$P_{mm} = \frac{7.854 \cdot 10^{-4}d^2h^2}{V - 7.854 \cdot 10^{-4}d^2h}.$$

For a capillary 150 mm in length (an upper limit for the length),

$$P_{mm} = \frac{17.67d^2}{V - 0.1179d^2};$$

for $d = 3$ mm, and $V = 100$,

$$P_{mm} = \frac{159.1}{100 - 1.06} = 1.607.$$

Thus, if we use a capillary 3 mm or less in bore and a bulb of 100 cm^3 volume the error resulting from the omission of the term bh in the denominator of equation 2 is less than 1 per cent.

For gauges designed for measuring maximum pressures of 1 mm or less, the more simple relation is valid, of the form

$$P_{mm} = \left(\frac{b}{V}\right)h^2 = Kh^2, \tag{3}$$

where K is known as the "gauge constant," expressed in millimeters of mercury per millimeter length.

Expressing h and d in *millimeters*, and V in *cubic centimeters*, the values of K for gauges such as are used in ordinary laboratory practice are shown in Table 1. The values given in the last column, that is, 10^6K, evidently correspond to the *pressures in microns* for $h = 10$ mm.

It will be observed that $P_{\mu b} = 1333Kh^2$.

To avoid the error which arises when the value of h is small, it is often preferable to compress the gas in the capillary aa to a *definite* volume v, and then observe the height h_1 (in millimeters) of the mercury above

TABLE 1

VALUES OF THE McLEOD GAUGE CONSTANT FOR TYPICAL DIMENSIONS OF BULB AND CAPILLARY

d (mm)	V (cm^3)	10^5K
1	100	0.785
1	60	1.309
1.5	100	1.767
1.5	60	2.945
2.5	100	4.909

this level in the side capillary. In that case, since

$$P_{mm} = \frac{vh_1}{V}, \tag{4}$$

it is seen that h_1 is directly proportional to P_{mm}, and the magnitude of this quantity can be determined by means of a cathetometer. This method, however, is not as sensitive at low pressures as that described above.

Also, if the range of pressures to be measured is large, the single capillary *aa* may be replaced by two or more capillaries of different bores, the coarser one being sealed directly to V, and the finer one on top of this, and so on. The serious objection to this construction is the inaccuracy involved in the readings at the junctions between the capillaries.

It is evident that the sensitivity of the gauge can be made extremely high by increasing the ratio V/v, that is, V/b. However, in the case of gauges of the construction described above, practical considerations limit the magnitude of V because of the weight of mercury to be raised. Furthermore, in capillaries of very small bore (0.5–0.7 mm), the mercury tends to stick badly as the level is raised and the column breaks as the level is lowered, thus leaving a portion hanging in the capillary.

The causes of these phenomena and methods of overcoming the resulting errors in measurements have been investigated in considerable detail,[26] especially by P. Rosenberg[27] and G. Haase.[28] Haase concludes that the principal causes are as follows: (1) slight oxidation of the mercury when exposed to air, (2) condition of the inside surface of the capillary which is due to chemical attack by water vapor or chemically corrosive vapors. Capillary tubing which has been exposed to the atmosphere for a long period should not be used for the construction of a McLeod gauge.

---

[26] C. Hagen, *Physik. Z.*, **27**, 47 (1926), *Z. tech. Physik*, **8**, 599 (1927).

[27] *Rev. Sci. Instruments*, **9**, 258 (1938).

[28] *Z. tech. Physik*, **24**, 27, 53 (1943).

One method for the treatment of capillary tubing, for which satisfactory results have been claimed and which is described by Haase, is the following:

> A wire having a diameter about ⅝ that of the inside diameter of the capillary is dipped into an abrasive material, such as alumina, and is then drawn carefully through the capillary. By turning the wire and successive draws through the capillary, the inner wall becomes polished until it is no longer transparent. With suitable illumination the position of the mercury meniscus can be observed quite well.

Although heating the capillary to the softening point restores the transparency it is likely to deform the tubing; consequently as short a length as possible should be heated in forming the closed end. Obviously this treatment should be applied to the capillary before it is sealed to the bulb.

Haase has also observed that, after the capillary has been sealed off at the end and attached to the bulb, treatment with hydrofluoric acid or the vapor of the acid accomplishes the same result as the treatment with an abrasive.

Another very essential precaution is to use mercury that has been vacuum-distilled, and, if the gauge is to be used in connection with an oil-vapor pump or where water vapor is likely to be present, a liquid-air trap should be inserted between the gauge and the rest of the system.

By careful attention to these details Haase states that he has been able to construct an accurate gauge having the dimensions $V = 1400$ cm^3 and $d = 0.7$ mm, for which

$$P_{mm} = 3 \cdot 10^{-7} h^2,$$

where h is expressed in millimeters. For $h = 180$, $P_{mm} = 10^{-2}$.

In the construction of such a gauge, the mercury reservoir is connected by means of stopcocks to the rough vacuum and the atmosphere. The mercury is raised by opening the stopcock to the atmosphere and lowered by opening the other stopcock to the vacuum. Both the reservoir and the upper bulb should be supported solidly in plaster of paris and provision made for a box around the bottom of the reservoir to contain the mercury that would be spilled in case of breakage.

This design is illustrated in Fig. 4, which shows the construction of a very sensitive gauge described by P. Rosenberg.[29] The volume of bulb A is 1300 cm^3, and that of B about 2500 cm^3. B contains about 60 lb of mercury. Both bulbs are thick walled and supported by plaster of paris blocks P and Q. With capillaries of 0.63-mm internal diameter, the value of b/V (which Rosenberg designates the compression ratio) is $2.4 \cdot 10^{-7}$. In the construction of the capillaries, the method described above (which consists in roughening the inside walls of the capillaries) was used to prevent sticking and breaking of mercury threads while the mercury is in motion.

---

[29] *Rev. Sci. Instruments*, **10**, 131 (1939).

In this laboratory a gauge constructed in the manner just described and having a ratio b/V of $6.89 \cdot 10^{-7}$ has been found to work very satisfactorily even without roughening the inside of the capillary (probably because of the larger diameter of the capillary).

It is evident that the McLeod gauge does not indicate the pressure of mercury vapor and condensible vapors such as those of oil, water, and ammonia.

The vapor pressures of water at 15°, 20°, and 25° C are 12.79, 17.54, and 23.76 mm Hg, respectively. Hence, in the presence of water vapor condensation will occur in the capillary as h is decreased and therefore the value of h will no longer correspond to the real pressure in the system. It is of interest to note in this connection the observations made by M. H. Armbruster[30] that condensation occurs in the capillary at a lower pressure than that corresponding to the vapor pressure for the temperatures at which the reading is taken.[31] This can be avoided by heating the capillary to a slightly higher temperature, so that the condensation will occur at a pressure above that of the gases in the system.[32]

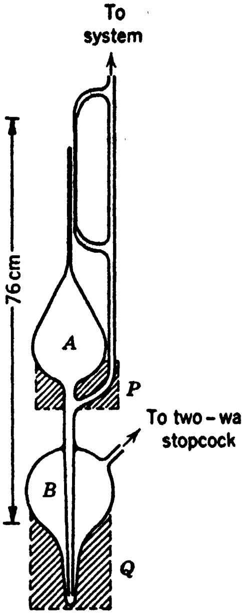

FIG. 4. Construction of a very sensitive McLeod gauge.

Even for measuring the pressure of carbon dioxide the gauge is not reliable. In using it to measure very low pressures, such as those produced by a Gaede molecular or Langmuir condensation pump, a liquid-air trap should be inserted between the gauge and the remainder of the system in order to prevent diffusion of mercury or other vapor into the vessel to be exhausted.

---

[30] *J. Am. Chem. Soc.*, **68**, 1342 (1946).

[31] Similar observations have been recorded, as Miss Armbruster notes, by J. C. W. Frazer, W. A. Patrick, and H. E. Smith, *J. Phys. Chem.*, **31**, 897 (1927), and A. S. Coolidge, *J. Am. Chem. Soc.*, **49**, 708 (1927).

[32] For a discussion of the procedure for measuring the pressure of water vapor see E. W. Flosdorf, *Ind. Eng. Chem., Anal. Ed.*, **17**, 198 (1945).

Regarding the accuracy of the gauge for indicating the pressure of the so-called permanent gases (hydrogen, helium, argon, oxygen, nitrogen, and carbon monoxide) a careful investigation carried out by Scheel and Heuse[33] showed that if the bulb and tubing are carefully dried (to eliminate the presence of a film of water) the results obtained for air are certainly reliable down to pressures of 0.01 mm of mercury and are probably just as accurate at lower pressures.

Rayleigh[34] found, by means of his differential manometer, that in the range of pressures 0.001 mm to 1.5 mm Boyle's law holds accurately for nitrogen, hydrogen, and oxygen; and Scheel and Heuse[35] observed the same result with their membrane manometer. A very careful investigation on this point was carried out by W. Gaede[36] in connection with his work on the laws of flow of gases at low pressures. He found that, with nitrogen and hydrogen, when care is taken to dry the walls thoroughly, the McLeod gauge is quite accurate down to very low pressures (below 0.0001 mm), whereas, with oxygen, errors are likely to arise because of the formation of an oxide scum on the surface of the mercury which causes the surface to wet the glass in the capillary. However, this scum may be removed by heating the capillary carefully and the mercury then becomes quite clean again.

For "condensible" gases, such as carbon dioxide, ammonia, sulfur dioxide, and most hydrocarbons, a correction must be applied to the observed readings for adsorption on the walls.[37]

If a reservoir is used with a rubber-tube connection to the barometric column, the tubing should be thoroughly cleaned and dried to remove any loose particles and also to prevent as much as possible the injurious effect of the sulfur present in rubber. Only the cleanest mercury should be used, and all glass parts of the gauge should be dried thoroughly before filling with mercury. A new McLeod gauge will give erroneous observations at the beginning until all the condensible vapors adhering to the walls have been removed by gentle heating with simultaneous exhaustion.[38]

The best procedure for calibrating the gauge is as follows: A length of capillary tubing of the desired diameter is first inspected under a microscope for uniformity of bore.[39] A drop of mercury sufficient to fill about one-third or one-fourth of the total length is then introduced into the capillary and the corresponding length measured, using a metal scale on which lengths can be measured to at least 0.5 mm (under a microscope).[40] Three or four determinations of this nature are made for different points along the capillary, and the weight of mercury used is determined to within at least $1 \cdot 10^{-3}$ g. The volume V should also be obtained by weighing the bulb and capillary when filled with mercury or water to the level of the shut-off cross section.

---

[33] *Ber. deut. physik. Ges.*, **6**, 785 (1908); **7**, 1 (1909).

[34] *Phil. Trans.*, **A**, **196**, 208 (1901).

[35] *Loc. cit.*

[36] *Ann. Physik*, **41**, 289 (1913).

[37] M. Francis, *Trans. Faraday Soc.*, **31**, 1325 (1935).

[38] See LD, p. 71, for illustration of this behavior of a fresh gauge.

[39] Specially selected capillary tubing of uniform bore is now available commercially.

A very important feature in connection with the construction of a McLeod gauge is the sealing off of the top of the capillary in such a manner as to leave the inside as flat as possible, without any rounded end to the bore. The method to be used in the sealing operation in order to secure this objective has been described in detail by R. J. Clark,[41] and in the same connection there is a discussion of the precautions to be taken in calibration.

There are described in the literature,[42] and in catalogues of firms selling physical apparatus, a number of variations in the construction of McLeod gauges.

A. H. Pfund[43] has combined the McLeod gauge with a hot-wire gauge (see section 6 of this chapter) in order to extend the range of the former to still lower values. A very small filament made of fine tungsten wire is sealed into the capillary at the top. Down to a certain pressure the gauge is used as described above. At lower pressures, at which the observed value of h becomes only a millimeter or so, the filament is heated to a very faint red, and the resistance at constant current is found to vary linearly with the pressure. In this range the gauge must be calibrated separately for each gas. As an illustration of the increased sensitivity thus obtained, Pfund gives the following data:

The limit of the "unaided" gauge was $5.26 \cdot 10^{-5}$ mm for $h = 1$ mm, whereas, by using the hot wire, the range was extended to $1.7 \cdot 10^{-7}$ mm. Since a portable galvanometer was used as indicating instrument for measuring the resistance, the range could be extended to still lower values by using a sensitive wall galvanometer.

For pressures in the range such as 0–1000 microns and higher, and for factory purposes, "swivel" types of gauges are available such as that shown in Fig. 5, which is taken from a publication by E. W. Flosdorf.[44] The gauge is connected to the system by a rubber-tube connection at P, and is mounted on a framework so that turning it cuts off a definite volume of the gas in the system at pressure P and causes this volume to be compressed to a smaller volume at a higher pressure.

---

[40] See LD, p. 68, for method of correction required for the form of the meniscus.

[41] *J. Sci. Instruments*, **5**, 126 (1928).

[42] See especially the paper by M. Pirani and R. Neumann cited in reference 1.

[43] *Phys. Rev.*, **18**, 78 (1921).

[44] *Ind. Eng. Chem., Anal. Ed.*, **17**, 198 (1945).

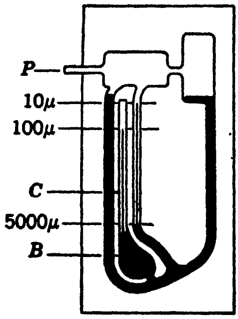

FIG. 5. Swivel form of McLeod gauge.

A similar design, devised by M. Bruner,[45] and designated the *vacustat*[46] is described by Yarwood.[47] The Gaede vacuscope,[48] resembles the last two gauges in its compactness.

It consists of a central expanded part to which are sealed, on one side, one arm in the form of a U-tube, and another arm, on the other side, which functions as a McLeod gauge. When in the horizontal position the gauge is evacuated, and when tilted to one of the two other positions, which are in the vertical plane and 180° apart, it can measure pressures as low as 10^{-2} mm or as high as 80 mm.

H. Moser[49] has described a more elaborate variation of the vacustat which has three ranges: 760 to 1 mm; 1 to 10^{-2} mm, and 10^{-2} to 10^{-4} mm.

3. MECHANICAL MANOMETERS[50]

A number of attempts have been made to construct low-pressure manometers which depend upon the measurement of the mechanical deformation suffered by a thin wall or diaphragm under pressure. At ordinary pressures this principle has been utilized in the construction of the Bourdon spiral. E. Ladenburg and E. Lehmann,[51] and subsequently F. M. G. Johnson and D. McIntosh,[52] have described a low-pressure gauge consisting of a flat tapered glass tube bent in the form of a spiral. The walls are usually very thin, so that the device may be sensitive to small pressure differences. A glass mirror is attached to the end of the spiral and the spiral is sealed into another chamber in which the pressure may be varied. The system whose pressure is to be measured is connected to the spiral. In using the instrument, the pressure outside the spiral is varied until it is equal to that in the spiral, as indicated by the mirror, and the pressure outside is then measured by an ordinary mercury manometer. The device has been used for measuring the pressure of corrosive gases like chlorine and ammonium chloride vapor. A similar type of manometer has also been used by C. G. Jackson for measuring the dissociation pressure of cupric bromide.[53] These gauges, however, are not sensitive to pressures below about 100 microns. A quartz spiral gauge operated on the same principle and devised by M. Bodenstein and W. Dux[54] is shown in Fig. 6. As described by Farkas and Melville,[55] this gauge "consisted of a long thin spiral of flattened silica tubing carrying a mirror at the end to detect the extent of 'unwinding' of the spiral."[56]

---

[45] *Helv. Chim. Acta,* **13**, 915 (1930). An earlier form similar to this in many respects was described by H. J. Reiff, *Z. Instrumentenk.*, **34**, 97 (1914).

[46] Made by W. Edwards and Company, England.

[47] JY, p. 39.

[48] Described by FM, p. 93.

[49] *Physik. Z.*, **36**, 1 (1935).

[50] A very comprehensive list of references on this type of manometer has been given by C. Kenty, *Rev. Sci. Instruments*, **11**, 377 (1940), in connection with the description of a manometer with thin quartz wall designed for pressures ranging from a few centimeters of mercury to 50 atmospheres.

[51] *Verhandl. deut. physik. Ges.*, **8**, 20 (1906).

[52] *J. Am. Chem. Soc.*, **31**, 1138 (1909); *Z. physik. Chem.*, **61**, 457 (1908).

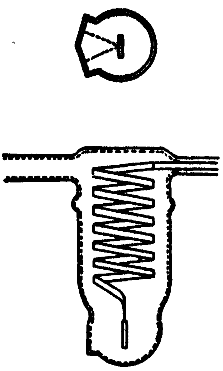

FIG. 6. Quartz spiral gauge.

Two methods of mounting the spirals are used: in one, a long light pointer is sealed to the closed end at 90° to the axis of the coil and the deflection is noted of the end of this pointer; in the other, a suspension, to which a galvanometer mirror is fastened, is attached to the end of the spiral and the spiral is mounted with its axis vertical and the open end (connecting to the system) at the bottom. In both methods the spiral is enclosed in a glass tube opened at one end, so that the pressure inside the spiral may be balanced, if desired, by an external pressure. It is stated that the most sensitive form of this gauge (that constructed according to the second method) is capable of measuring pressures of the order of 2 mm of mercury.

A form of Bourdon gauge, described by S. G. Foord,[57] is shown in Fig. 7. It consists of a collapsed thin bulb B to which is attached a short butt *D*. *D* is surrounded by a rigidly supported ring *C*, which limits its traverse to about ±0.5 mm. "By this means," as the author states,

---

[53] For further details regarding this type of manometer, refer to K. Jellinek, *Lehrb. physik. Chem.*, I, 1, p. 638, also to the references given in footnotes 51 and 52.

[54] *Z. physik. Chem.*, 85, 297 (1913).

[55] FM, p. 86.

[56] An extensive account of similar manometers made of glass or quartz has been given by B. P. Harteck, *Wien-Harms Handbuch der experimental Physik*, Vol. III, 2, p. 254, 1929.

[57] *J. Sci. Instruments*, 11, 126 (1934).

> a gauge which would fracture at about 200 mm of mercury may be made to withstand a pressure difference of ±1 atmosphere. To compensate for the loss of sensitivity in using such a comparatively strong bulb, the deflection is multiplied by means of a simple all-glass lever system as shown, the lateral motion of the butt being transmitted by a flexible link *E* to the pointer proper *F*, which is rendered free to bend about its point of support by drawing out its lower extremity to a fine rod.

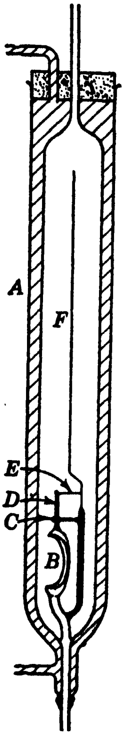

FIG. 7. Thin-wall type of gauge (Foord). The extent of deformation of the thin wall, *B*, is observed by the deflection of the end of the pointer *F*.

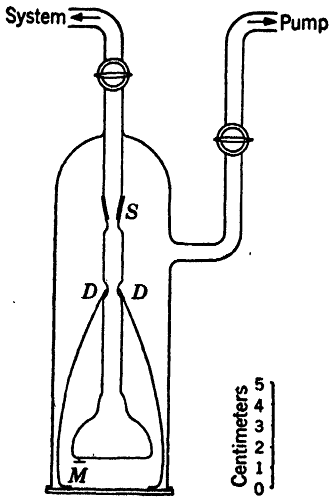

FIG. 8. Thin glass-wall manometer for direct reading (Grigorovici). The extent of the deformation is observed by means of the small mirror *M*.

A water jacket *A* is provided, and the gauge is best operated in a vertical position. According to the author, A gauge of this type has been constructed which gives a deflection of 0.54 mm per mm of mercury, using a pointer 20 cm in length, and there is no doubt that more sensitive gauges could be made if required, especially if not called upon to withstand such a large maximum difference of pressure.

It is this requirement, of course, that puts limitations on the use of a gauge of this type. Furthermore, it obviously requires a considerable number of trials to make a bulb such as *B* which will be both thin-walled and not too fragile.

A glass membrane manometer designed by R. Grigorovici[58] is shown in Fig. 8. It consists of an evacuated glass tube, which is closed at one end by a glass plate (cemented to the tube), and inside of which is a glass membrane. This membrane is prepared by softening a thin glass bulb to the point at which one side will collapse to form a flat surface, as shown. Two wires *DD* support the membrane against the cover plate, and the deflection of the membrane is measured by means of a small mirror, *M*, fastened at the edge, and a telescope and scale. A ground joint *S* is provided so that the membrane can be readily replaced. The gauge may be used in the range 0.1 to 5.0 mm of mercury.

The membrane manometer used by K. Scheel and W. Heuse[59] for measuring the vapor pressure of ice at very low temperatures consisted of a very shallow cylindrical glass box separated into two compartments (parallel to the flat sides) by a thin copper membrane. One compartment was connected to the system; the other was connected directly to a high-vacuum pump. The deformation of the membrane, due to the slight difference in pressure on the two sides, was then measured by noting the number of interference rings produced by the pressure of the membrane against a glass plate.

The instrument was found capable of measuring pressures down to about 0.001 mm of mercury, but difficulties were encountered in using it because of the continual gas evolution from the walls of the device.

The deflection of the membrane may, obviously, be measured by means of an optical system similar to that used in the mercury manometer devised by Shrader and Ryder, that is, by attaching a pointer to the membrane and letting this pointer deflect a mirror. Such a manometer (sensitive to 10^{-4} mm Hg) has been described by E. A. Stewardson.[60] In this case a thin diaphragm of mica or glass was used. This type of manometer has been applied to a considerable extent, especially where it was necessary to measure pressures of gases that react chemically with mercury.[61]

---

[58] *Z. tech. Physik,* **20,** 102 (1939).

[59] *Z. Instrumentenk.,* **29,** 14 (1909); *Ber. deut. physik. Ges.,* **11,** 1 (1909).

[60] *J. Sci. Instruments,* **7,** 217 (1930).

The deflection of the membrane can also be measured by observing the change in capacity with respect to a stationary membrane. This is the method used by K. Sommermeyer.[62] An accuracy of 0.01 mm is claimed for this particular gauge.

Although the manometer designed by W. H. Rodebush and C. E. Coons[63] is not of the same type as the other gauges described above, it has this feature in common with them, that it *measures absolute pressure directly* and is therefore independent of the molecular weight of the gas or vapor. Figure 9 shows an improved form of the gauge, made by V. Deitz,[64] for measuring the vapor pressure of potassium chloride and cesium iodide.

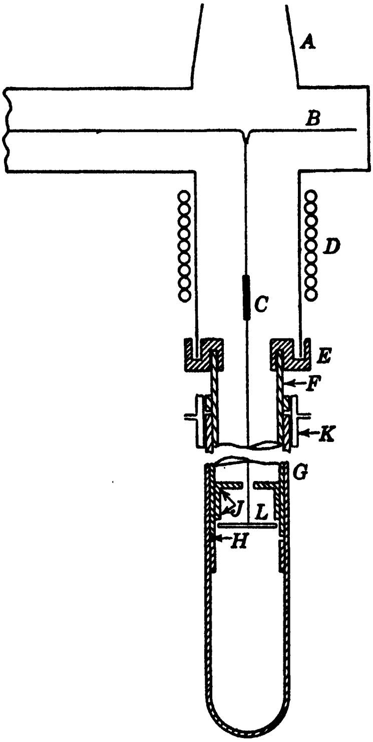

FIG. 9. Manometer for determination of absolute vapor pressures (Deitz).

As Farkas and Melville[65] state,

> The only disadvantage of this absolute manometer is that gas or vapor has to be continuously applied to the measuring chamber owing to leakage past the silica disk.

The following description of the gauge is given by Deitz:

> *L* is a disk of fused quartz about 2.5 cm in diameter, the upper surface of which is ground to seat on the ground end of the quartz tube *J*. *C* is a small needle of soft iron, enclosed in glass, and *B* is a cantilever arm made from a quartz fiber by which the system is suspended. *B* is about 10 in. long from the point of suspension to the point of support, which is a quartz to Pyrex seal to the rest of the apparatus. The arm *B* extends outwards for about 2 in. past the suspension support and is pulled out to a fine point, the extreme tip being about a millimeter from a plane window. A microscope was then used to measure the position of the arm and hence give the

---

[61] See R. Seeliger, *Z. tech. Physik*, **1**, 20 (1920), and G. Kornfeld and E. Klingler, *Z. physik. Chem.*, **B**, **4**, 37 (1929).

[62] *Z. physik. Chem.*, **A**, **155**, 208 (1931).

[63] *J. Am. Chem. Soc.*, **49**, 1953 (1927).

[64] *J. Chem. Phys.*, **4**, 575 (1936).

[65] FM, p. 93.

vertical position of the quartz disk. *D* is a coil through which a current is passed to bring an electromagnetic traction on *C*, thus pulling the disk upward to seat on *J*.

The ground seat, *J*, is sealed within a transparent quartz tube, *F*, 12-mm bore, the top of which is sealed to the remainder of the apparatus by a DeKhotinsky joint at *E*, in the manner shown. Surrounding the quartz tube *F* is another transparent quartz tube, *G*, 14 in. long, which is closed at the bottom. A short length of quartz tube of the same diameter as *F* is sealed within *G*. The seal is made at the bottom, the top end having been previously ground to make a seat with the bottom of the inner tube *F* at *H*. The salt crystals are placed at the bottom of the outside tube *G*. This is then slipped into place and sealed at *K* by means of a water-cooled picein joint. The long suspension is lowered into place through the opening of the ground joint at *A*. The female part of the joint carries a test tube sealed concentrically within, which serves as a liquid air cooled surface.

In operation the pressure is measured by noting the value of the current at which the disk just drops from its seat on the end of the tube.

At the null point the apparatus functions as an electromagnetic balance. The forces upwards consist of the tension in the quartz cantilever support, the magnetic pull of the solenoid, and the force due to the pressure of the vapor on the quartz lid, equal to the pressure times the area. The force downward is the force of gravity. As the pressure increases, the pull necessary from the solenoid decreases.

For calibration the procedure used was as follows:

The quartz disk was replaced by an aluminum pan and sufficient weights added to make the total weight equal the weight of the quartz disk. The necessary current was then passed through the solenoid to bring the pointed end of the cantilever arm *B* to the null-point position, previously observed with the quartz disk seated in place. By removing weights from the pan and observing the corresponding decrease in the solenoid current, a calibration was obtained.

The calibration curve was observed to be linear, and the slope gave the decrease in current per unit increase in total pressure on the disk.

The pressures measured ranged from about 1 to 30 microns.

A somewhat similar method for the determination of the *vapor pressures of oils* has been described by Hickman, Hecker, and Embree,[66] and a modified design of their apparatus, used by Verhoek and Marshall,[67] is shown in Fig. 10.

The sample to be investigated is located in the bulb *B*, which is maintained at the desired temperature. The vapor emitted through the orifice, *O*, exerts a pressure on the disk *D*, and the magnitude of the pressure is measured by turning the entire apparatus through an angle θ that is just sufficient to close the orifice.

Let W = weight in grams of the assembled pendulum, and A = area of orifice. Then

---

[66] *Ind. Eng. Chem., Anal. Ed.*, **9**, 264 (1937).

[67] *J. Am. Chem. Soc.*, **61**, 2737 (1939). The results obtained in this investigation as well as the preceding one have been discussed in Chapter 5, especially Table 5.2.

$$P_\mu = \frac{W \sin \theta}{0.00136A},$$

where the factor in the denominator converts the pressure from grams per square centimeter into microns. (In the device described, $W = 0.787$ g, and $A = 7.716$ cm^2.)

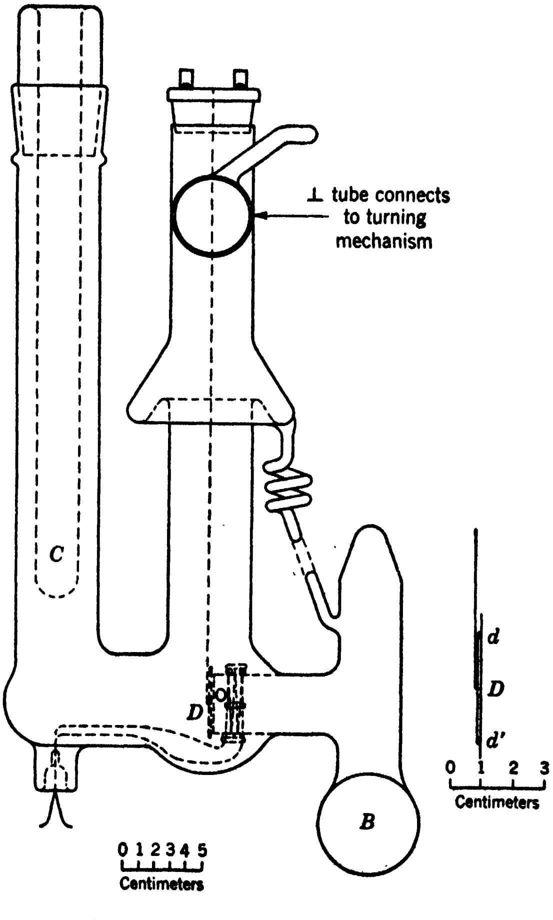

FIG. 10. Manometer for determination of absolute vapor pressures (Verhoek and Marshall).

In order to eliminate possible back pressure on the disk D and prevent the disk from adhering to the glass by the surface tension of any liquid formed, a condensing tube, C, filled with liquid air is used and a platinum resistance heater is located around the glass tube at O.

Further details of construction quoted from the original paper are as follows:

> To measure θ, the turning motion was carried through a worm gear to a disk 15.0 cm in diameter divided on its circumference into 216 divisions, each of which corresponded to a deflection of one minute of arc. Consecutive readings at a given temperature could easily be reproduced to within one minute of arc. The pendulum consists of a Duralumin disk D, 0.013 cm thick, suspended by means of Duralumin wire, 0.05 cm in diameter, from a shaft riding in jeweled bearings. The circular corrugation (dd', Fig. 10) in the disk serves to stiffen and hold it perfectly flat.

In connection with a discussion of methods for the determination of absolute vapor pressures, it is also of interest to mention the method devised by M. Volmer, S. Heller, and K. Neumann[68] and applied by Neumann and E. Volker[69] to measure vapor pressures of potassium and mercury in the range 10^{-2} to 10^{-5} mm.

The material to be investigated is placed in a small glass vessel consisting of two bulbs joined by a short piece of rather wide tubing and provided with a tubulation at the center and with two very small holes in the bulbs which are opposite to each other. The vessel is suspended at the center, and the surrounding glass container is evacuated. The vapor streaming out of the two holes causes the suspended vessel to be rotated through an angle which is proportional to the pressure.

4. VISCOSITY MANOMETERS

As shown in Chapter 1, section 8, the rate of transfer of momentum from a surface moving with velocity u in the plane of the surface, to a stationary surface parallel to it at distance d, is given, at low pressures, by the relation

$$B = \frac{\eta u}{d + 2\zeta}. \tag{I.8.35}$$

In this equation ζ is the coefficient of slip, which is proportional to the mean free path L and, consequently, is inversely proportional to the pressure.

Hence, the last equation can be written in the form

$$B = \frac{\eta u}{d + 2bL} \tag{1a}$$

---

[68] *Z. physik. Chem.*, *Bodenstein-Festschrift*, p. 863, 1931.

[69] *Z. physik. Chem.*, **A**, **161**, 33 (1932).

or

$$B = \frac{\eta u}{d + c/P}, \tag{1b}$$

where b and c are constants which vary with the nature of the gas and that of the surface. In general, the constant b has a value of the order of unity.

At very low pressures, where $L \gg d$, equation 1a becomes

$$B = \frac{\eta u}{2bL},$$

and, substituting from the relation

$$\eta = 0.5\rho v_a L,$$

we obtain the relation

$$B = K_1 \rho v_a u \tag{2}$$

$$= K_2 P \sqrt{\frac{M}{R_0 T}} \cdot u, \tag{3}$$

where K_1 and K_2 are constants.

A relation of the same form as these equations may be derived from considerations similar to those used in deriving the laws of molecular flow.

The number of molecules crossing unit area per unit time is given by

$$\nu = \tfrac{1}{4} n v_a.$$

If the molecules are leaving a surface having a velocity u, the momentum transferred per molecule is mu. Hence,

$$B = \nu m u$$

$$= P \sqrt{\frac{M}{2\pi R_0 T}} \cdot u. \tag{4a}$$

Thus we can write, in general,

$$B = KuP \sqrt{\frac{M}{T}}, \tag{4b}$$

where K is a constant.

As will be observed, the coefficient η/d, which is independent of P at normal pressures, is replaced at low pressures by the coefficient $P\sqrt{M/T}$, which varies linearly with the pressure.

In applying the above considerations to the construction of a gauge, two different methods have been used. In the first of these, which is applied in what we may designate for reference as the "decrement" type of gauge, a surface is set in oscillation and the rate of decrease of the amplitude of oscillation is taken as a measure of the pressure. Physically, the damping may be explained as due to the gradual equalization of energy between the moving surface and the molecules of gas striking it.

In the second method, a surface is set in *continuous* rotation and the amount of twist imparted to an adjacent surface is used to measure the pressure. The molecules striking the moving surface acquire a momentum in the direction of motion which they tend in turn to impart to the other surface. If that surface is suspended and free to turn about an axis which is perpendicular to the direction of motion of the rotating surface, it will be twisted around until the force due to the incident molecules is just balanced by the torsion of the suspension. We may, therefore, designate this as the "static" type of viscosity gauge, to emphasize the fact that observations with this method are taken under stationary conditions.

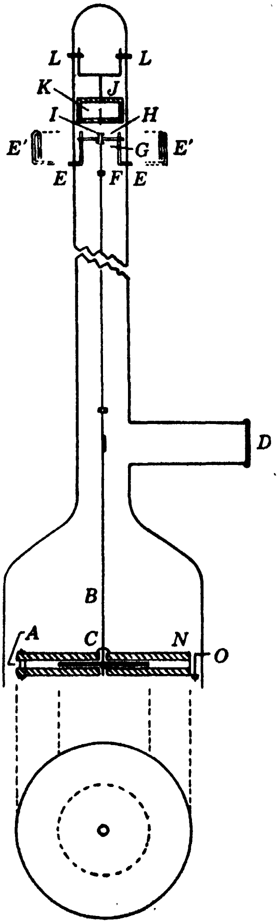

FIG. 11. Decrement type of viscosity gauge (Hogg).

Decrement Type of Viscosity Gauge. A gauge based on this principle was first suggested by W. Sutherland[70] and subsequently a very careful investigation on the same subject was carried out by J. L. Hogg.[71] The construction used by Hogg, which was essentially the same as that used by Maxwell, and by A. Kundt and E. Warburg, in their determinations of the coefficient of viscosity, is shown in Fig. 11. A thin glass disk is suspended by means of a wire between two fixed horizontal plates N. The wire carries a mirror which may be viewed through a plate-glass window D by means of a telescope and scale. At the top, the wire is supported by clamps and is connected to a soft-iron armature J which is supported by the swivel head K. Turning this armature by means of an external magnet sets the center disk in oscillation, and the rate of decrease of the amplitude of these oscillations is then observed by means of the telescope pointed at the window D.

---

[70] *Phil. Mag.*, **43**, 83 (1897).

[71] *Proc. Am. Acad. Arts Sci.*, **42**, 115 (1906), and **45**, 3 (1909). *Contributions from the Jefferson Physical Lab.*, 1906, No. 4, and 1909, No. 4.

Let θ denote the angles of twist at any instant. Then the motion of the suspended disk is expressed by a differential equation of the form

$$I\frac{d^2\theta}{dt^2} + R\frac{d\theta}{dt} + K\theta = 0, \tag{5}$$

where I = moment of inertia of disk (ml^2).
R = coefficient of damping (ml^2t^{-1}).
K = coefficient of restoring force (ml^2t^{-2}).

The dimensions of each of these coefficients is given in parentheses. Hence the dimensions of each term in the equation are ml^2t^{-2}.

The solution of this equation is of the form

$$\theta = \theta_0\epsilon^{-Rt/2I}\cos 2\pi\nu(t - t_0), \tag{6}$$

where t_0 may be set equal to zero, and ν is the frequency of oscillation, which is given by

$$2\pi\nu = \left(\frac{1}{IK} - \frac{R_2}{4I^2}\right)^{1/2}. \tag{7}$$

That is, the maximum amplitude of θ, denoted by A, decreases exponentially with the time. The solution expressed by equation 6 is valid if the damping factor is not too great. In fact, there exists a critical relation,

$$R^2 \leqslant \frac{4I}{K},$$

which must be satisfied for the occurrence of oscillations.

Let $\tau = 1/\nu$ denote the *period* of a complete oscillation. If A_1 and A_2 denote two successive values of the maximum amplitude A, it follows from equation 6 that

$$\frac{A_2}{A_1} = \epsilon^{-R\tau/2I} = \epsilon^{-\lambda}, \tag{8}$$

where λ is known as the *logarithmic decrement*.

Let $t_{0.5}$ designate the time required for the maximum amplitude to decrease to half its initial value. Then

$$t_{0.5} = \frac{\ln 2}{R/(2I)} = \frac{\tau \ln 2}{\lambda}. \tag{9}$$

At normal pressures, R is proportional to the product of η/d and l^4, where l is a length proportional to the radius of the disk, and d is the distance between the disk and stationary plate. Thus, at these pressures, λ is independent of the pressure. However, at lower pressures, it follows, as shown above, that R must vary linearly with the product $\rho v_a l^4$. Consequently, λ should vary linearly with the pressure.

This statement, however, requires some modification. Let λ_0 denote the value of the decrement at normal pressures, and μ the decrement of the suspension itself.

From equation 1*b* and the above considerations regarding the variation with pressure in the value of R, it follows that, in the intermediate range of pressures for which L, the mean free path, is not very large compared to d,

$$\frac{\lambda_0 - \mu}{\lambda - \mu} = 1 + \frac{C}{Pd}; \tag{10a}$$

that is,

$$\left(\frac{\lambda_0 - \mu}{\lambda - \mu} - 1\right) P = \frac{C}{d}, \tag{10b}$$

where C is a constant.

This is the relation used by Hogg in connection with his gauge. It is evident that this gauge is not suitable for measuring very low pressures, since the value of λ then becomes comparable with that of μ and therefore the determination of P involves large experimental errors.

A contribution to the theory of this type of gauge has also been published by P. E. Shaw.[72] He has recorded measurements down to $0.35 \cdot 10^{-3}$ mm of mercury.

Quartz Fiber Gauges. This method was first suggested by I. Langmuir[73] for measuring the pressure of residual gas in a sealed-off incandescent lamp, and it has been used by the writer in some investigations. Following Langmuir's suggestion, a gauge of this type was described by F. Haber and F. Kerschbaum[74] in a paper in which the theory of its operation was also discussed in detail.

While these investigators used the gauge to measure the pressures of vapors of water, iodine, and mercury, A. Henglein[75] used the same type of gauge to measure the dissociation pressure of chlorine at high temperatures, and D. H. Scott[76] applied it to measure vapor pressures of cesium and rubidium.

---

[72] *Proc. Phys. Soc. London*, **29**, 171 (1917).

[73] *J. Am. Chem. Soc.*, **35**, 105 (1913).

[74] *Z. Elektrochem.*, **20**, 296 (1914).

[75] *Z. anorg. allgem. Chem.*, **123**, 145 (1922).

The construction of the gauge described by Haber and Kerschbaum is shown in Fig. 12*a*. It consists of a fine quartz fiber (diameter ranging from 0.01 to 0.005 cm) sealed into the top of a glass tube. The fiber is set in oscillation by tapping the glass bulb gently, and the rate of decrease of the amplitude of vibration is observed by means of a telescope and lamp, as shown in Fig. 12*b*.

Theoretical considerations, which are discussed more fully below, lead to the following relation for the determination of the pressure.

Let $t_{0.5}$ denote the interval of time required for the maximum amplitude to decrease to half value. Then,

$$P\sqrt{M} = \frac{B}{t_{0.5}} - C, \tag{11}$$

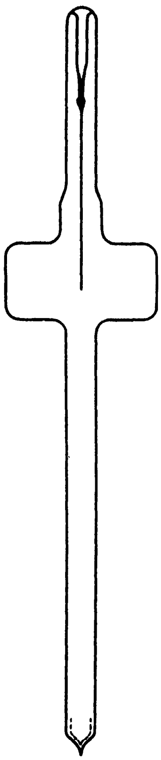

FIG. 12*a*. Quartz fiber gauge.

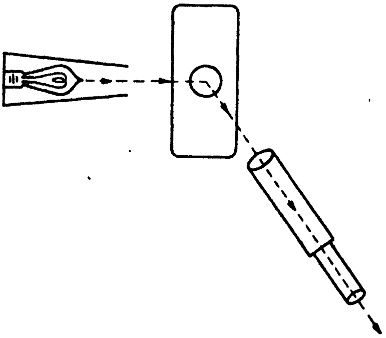

FIG. 12*b*. Optical arrangement for quartz fiber gauge.

where B and C are constants characteristic of the fiber. The physical significance of these constants will be evident from the discussion of the theory of operation of the gauge.

In the case of a mixture of two or more gases, the sum of the terms $P_i\sqrt{M_i}$ for each gas must be used instead of $P\sqrt{M}$, where P_i is the partial pressure of the gas of molecular weight M_i.

It is evident from the form of the last equation that B/C corresponds to the value t_0 at which the amplitude would decrease to half value in a perfect vacuum. For calibration, it is necessary to obtain only two points, corresponding to the two constants B and C. One of these may be determined by observing the value t_0 in a very good vacuum; the other point may be obtained by calibrating against a McLeod gauge with some gas of definite composition.

---

[76] *Phil. Mag.*, **47**, 32 (1924).

The following data are given by Haber and Kerschbaum for a quartz fiber 7.0 cm long and 0.013 cm in diameter. Air was used for calibration.

P_{mm}	$P_{mm}\sqrt{M}$	$t_{0.5}$ (seconds)	B
0.00302	0.01625	74	1.22
.00494	.02654	46	1.23
.00775	.0417	31	1.30
.0117	.0630	22	1.39
.01880	.101	12	1.23
.0260	.140	10	1.40
$C = 0.0003$			Avg. 1.28

Some measurements with air taken by H. A. Huthsteiner in this laboratory, using a fiber 3.8 cm long and 0.0045 cm diameter, are given for comparison.

P_{mm}	$t_{0.5}$ (seconds)
0.00058	105
.00342	31
.0080	16
.0190	6.5

Plotting P_{mm} against $1/t_{0.5}$ gives a straight line whose equation is $P_{mm} = 0.130/t_{0.5} - 6.55 \cdot 10^{-4}$. For air, $\sqrt{M} = 5.38$. Hence, for this particular fiber

$$P_{mm}\sqrt{M} = \frac{0.705}{t_{0.5}} - 0.00353.$$

Since $t_0 = 200$ in this case, it is evident that this fiber could not be used for measuring pressures below about 0.0001 mm of air. It also follows from the form of the above relation that the heavier the gas the lower the range of pressures over which the gauge may be used.

The optical arrangement suggested by Haber and Kerschbaum (Fig. 12b) may be varied in practice by fastening a scale to the back of the gauge and placing the lamp in such a position that the light beam passes practically parallel to this scale. The scale and tip of the quartz fiber are then sighted by means of a cathetometer.

These investigators used tubes which were more or less flattened on two sides, but ordinary cylindrical-walled tubes are more convenient and almost as satisfactory. As observed by Haber and Kerschbaum, care should be taken to tap the glass in such a manner that the fiber vibrates in the plane at right angles to the line of sight from the cathetometer. With a little experience, this can readily be accomplished. In view of the simplicity of construction and relative ease of manipulation, the quartz-fiber gauge ought to find a useful field of application in low-pressure technique, where the pressures to be measured are not below about 0.05 micron.

The difficulty encountered in getting the fiber to vibrate in a definite plane led A. S. Coolidge[77] to devise a bifilar form of gauge, in which two quartz fibers are fastened to the support 1 cm apart and fused together at the free ends, forming a V.

In this laboratory Mrs. M. R. Andrews[78] replaced the vibration element by a strip of 0.1 mm molybdenum about 10 cm long by 2 mm wide. This was welded to a strip of 10 mil nickel which was in turn welded to two leads in the stem of a bulb. The gauge was used to measure vapor pressures of naphthalene as low as $0.034 \cdot 10^{-3}$ mm.

A form of the decrement gauge used by E. Bolton King[79] is shown in Fig. 13. The construction is described as follows:

> The essential part consists of a silica fiber *A*, between 3 and 4 μ in diameter and 4 cm long, which is fixed by a small amount of gold to the silica frame *B*, the tension, which thus does not vary with changes in temperature, being about half that required for breaking. At the center of this fiber, and at right angles to it, are fixed two 10 μ fibers 2.5 cm long, one on either side of the suspension. The ends of these remote from the frame are fused into a sphere about 50 μ in diameter, while the other ends are fixed together by a minute amount of iron, which, when activated by an electromagnet outside the case, also serves to start the oscillations of the cross-piece, the damping of which is measured. If the external case is of glass, the frame is held in the cylindrical socket *D* by the spring *E*, while if it is of silica the frame is fused directly to it. Two flat windows, *G* and *F*, are fused to the case, the former for observing and the latter for illuminating the tip of the cross-piece.

The gauge is exhausted through the opening *H*.

The lower limit of the gauge for a light gas such as oxygen is stated to be $2 \cdot 10^{-6}$ mm.

A considerable increase in the sensitivity of this type of gauge was obtained by E. Brüche[80] by the development of a quartz "surface" manometer. The details of construction of this gauge, shown in Fig. 14, are as follows: To the supporting rod *T* are fastened two flat quartz fibers 75 mm long and 0.8 by 0.1 mm in cross section. These are attached to a quartz membrane 25 by 25 mm in area and 0.04 mm thick.

---

[77] *J. Am. Chem. Soc.*, **45**, 1637 (1923).

[78] *J. Phys. Chem.*, **30**, 1497 (1926).

[79] *Proc. Phys. Soc. London*, **38**, 80 (1925).

[80] *Physik. Z.*, **26**, 717 (1925); *Ann. Physik*, **79**, 695 (1926).

This membrane has fastened to it, at the bottom, a very thin-walled small quartz tube in which is sealed a piece of iron wire, E, 7 mm long and 0.5 mm in diameter. Below this is a pointer, S, which is used to indicate the amplitude of vibration by means of a telescope, M. A fork, G, limits the extent of the vibration. A 4-cm-diameter tube encloses the vibrating system, which is supported on the glass framework, F.

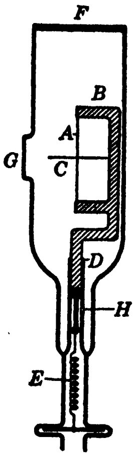

FIG. 13. Decrement type of viscosity gauge (King).

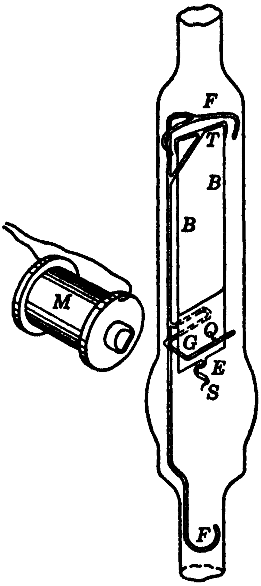

FIG. 14. Quartz membrane manometer.

Brüche confirmed, by measurements with hydrogen, air, and the inert gases, the validity of equation 11 over the range $5 \cdot 10^{-4}$ mm to $2 \cdot 10^{-2}$ mm, and concluded from his experience that this type of gauge should find extensive application in high-vacuum technique and for the measurement of very low pressures of chemically active vapors.

More recently, the theory and applicability of this type of gauge have been discussed very comprehensively in two papers by G. Wetterer.[81] The following remarks are based largely on the contents of the second of these papers.

As mentioned above, the motion of the quartz membrane and supporting wires is represented by equation 5, in which θ denotes the angular displacement with respect to a vertical axis. The coefficient of damping, R, is the sum of two coefficients, R_a, which represents the damping due to the gas molecules, and R_i, which corresponds to the intrinsic damping of the system in vacuo.

---

[81] *Z. tech. Physik*, **20**, 281 (1939); *Wiss. Veröffentl. Siemens-Werken*, **19**, 68 (1940).

Consequently, we can write equation 9 in the form

$$t_{0.5} = \frac{2I \cdot \ln 2}{R_a + R_i}$$

$$= \frac{1.3863I}{R_a + R_i}. \tag{12}$$

As stated above, R_a is proportional to the product of ρv_a and a quantity which has the dimension of l^4. In order to calculate the magnitudes of R_a and I, the moment of inertia, Wetterer assumes that the system of quartz fibers and membrane can be replaced by a duplex fiber and two rectangles as shown in Fig. 15. Using the designations for the dimensions given in this figure, Wetterer derived the following relations:

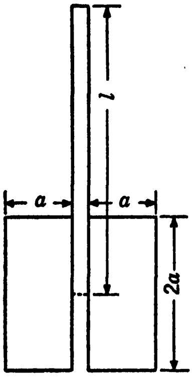

FIG. 15. Illustrating theory of membrane manometer.

$$R = \frac{4P\sqrt{M}}{\sqrt{3R_0T}}\left(\frac{Dl^3}{3} + 2l^2a^2 + \frac{2}{3}a^4\right) + R_i, \tag{13}$$

$$I = \frac{m_1l^2}{3} + \frac{m_2}{2}\left(l^2 + \frac{a^2}{3}\right), \tag{14}$$

where D = width of fiber (centimeters).
m_1 = mass of each fiber (grams).
m_2 = mass of membrane (grams)
$= 4a^2d \cdot s$.
d = thickness of membrane.
s = density of quartz.

Substituting these relations in equation 12, it follows that

$$t_{0.5} = \frac{K_1}{K_2P\sqrt{M} + R_i}, \tag{15}$$

where K_1, K_2, and R_i are constants which depend upon the dimensions and density of the quartz fibers and membrane. This equation can obviously be rewritten in the form given in equation 11.

For fine wires having negligible mass compared with that of the

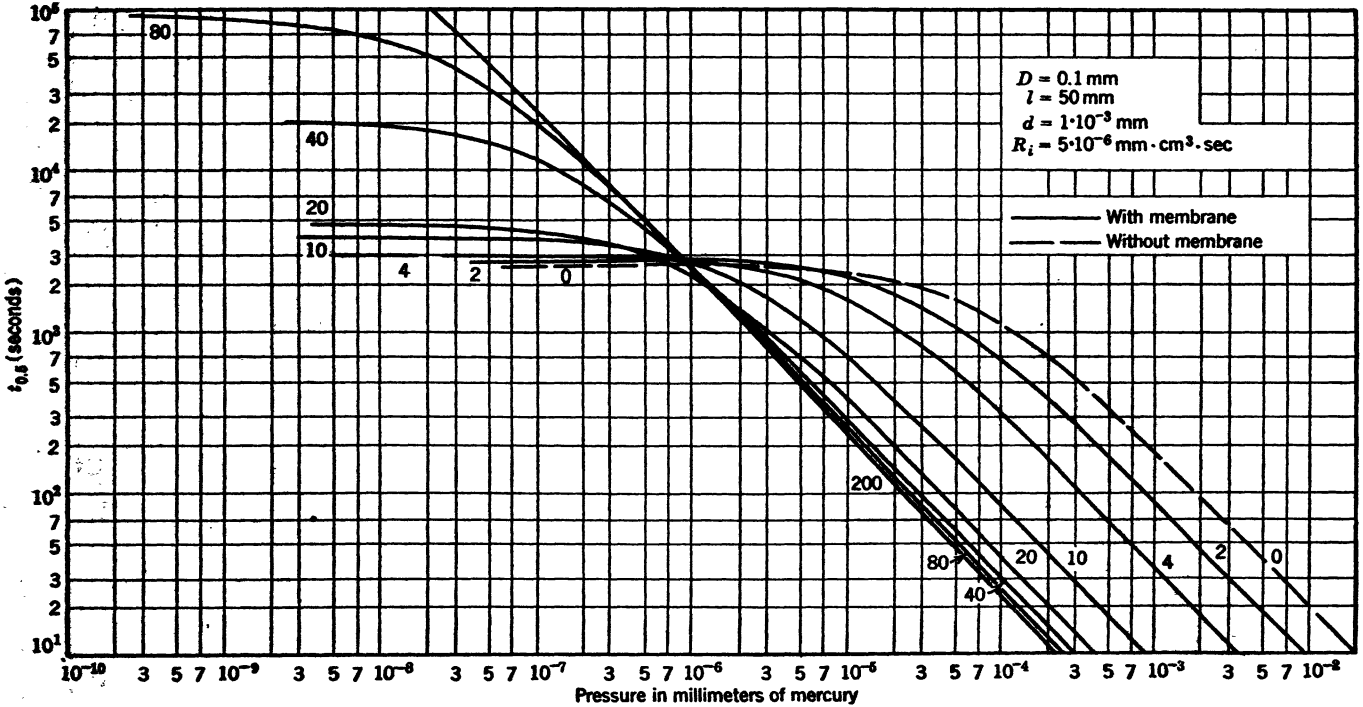

FIG. 16. Calibration curves for a vibrating membrane manometer (Wetterer) for a series of values of $2a$ (the length of side of a square membrane) in millimeters.

membrane, equation 15 takes the form

$$t_{0.5} = \frac{K_3 d}{P\sqrt{M} + K_4}, \tag{16}$$

where K_3 and K_4 are constants. Thus the value of $t_{0.5}$ varies directly with d, the thickness of the membrane. At higher pressures, the value of K_4 is negligible compared to $P\sqrt{M}$, and the last equation then reduces to

$$P = \frac{k_3 d}{t_{0.5}\sqrt{M}}, \tag{17}$$

that is, $\log P = \log (K_3 d) - \log (t_{0.5}) - 0.5 \log M$, and consequently the plot of P versus $t_{0.5}$ on log-log scales should be linear with a 45° slope.

Figure 16 shows such plots for a series of membranes for which a varies from 1 to 100 mm. As will be observed the plots show a 45° slope at higher pressure and become flatter at lower pressures. The flatter region of each curve indicates the lower limit of pressure for practical purpose. The larger the value of a, the lower the pressure at which such a gauge may be operated.

For practical use, Wetterer has also developed an attachment which makes it possible to project the indicator of the quartz membrane on a matt screen.

Since values of $t_{0.5}$ greater than 10^4 seconds are obviously impractical it would seem that the lower limit of pressure which could be measured by this type of gauge is about 10^{-4} micron.

A very interesting application of the considerations discussed above has been described by J. W. Beams, J. L. Young III, and J. W. Moore,[82] in connection with their investigations on the production of high centrifugal fields by spinning small steel spherical rotors at extremely high speeds in a vacuum. They made the following observation. When the rotor, after being brought up to speed, is allowed to spin freely with driving power off, the speed decelerates at a rate that depends on the pressure in accordance with the relation

$$P_{\mu b}\sqrt{\frac{M}{2\pi R_0 T}} = \frac{r\rho}{5t}\ln\frac{f_0}{f}, \tag{18}$$

where r = radius of spherical rotor,
ρ = density of the steel ($=7.8$ g/cm^3),

---

[82] *J. Applied Phys.*, **17**, 886 (1946).

f_0 = revolutions per second initially,
f = revolutions per second at time t (seconds),

and M, R_0, and T have the usual signification.

"With a 1.59-mm rotor spinning freely at about 120,000 rps, with a pressure of about 10^{-5} mm Hg, it required roughly 2 hours to lose 1 per cent of its speed." The pressure actually measured with an ionization gauge was between 10^{-5} and $2 \cdot 10^{-5}$ mm of Hg.

Rotating Disk or Molecular Gauges. The molecular gauge suggested by I. Langmuir[83] represents a direct application of equation 4*b*. The construction and results obtained with a gauge built on this principle have been described by Dushman.[84] It consists of a glass bulb *B* (Fig. 17*a*) in which are contained a rotating disk *A* and, suspended above it, another disk *C*. The disk *A* is made of thin aluminum and is attached to a steel or tungsten shaft *H* mounted on jewel bearings and carrying a magnetic needle *NS*. Where the gauge is to be used for measuring the pressure of corrosive gases like chlorine, the shaft and disk may be made of platinum. The disk *C* is of very thin mica, about 0.0025 cm thick and 3 cm in diameter. A small mirror *M*, about 0.5 cm square, is attached to the mica disk by a framework of thin aluminum. This framework carries a hook with square notch which fits into another hook similarly shaped, so that there is no tendency for one hook to turn on the other.

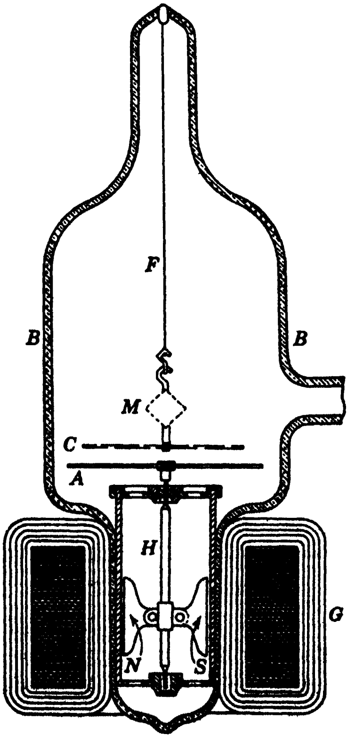

FIG. 17*a*. Molecular gauge.

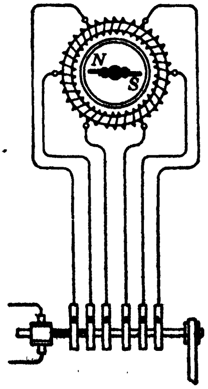

FIG. 17*b*. Rotating commutator for use with molecular gauge.

---

[83] *Phys. Rev.*, 1, 337 (1913).
[84] *Phys. Rev.*, 5, 212 (1915).

The upper hook is attached to a quartz fiber, F, about $2 \cdot 10^{-3}$ cm diameter and 15 cm long.

The lower disk can be rotated by means of a rotating magnetic field produced outside the bulb. This field is more conveniently obtained by a Gramme ring, GG, supplied at six points with current from a commutating device rotated by a motor (Fig. 17*b*). In this way the speed of the motor determines absolutely the speed of the disk, and the speed of the latter may thus be varied from a few revolutions per minute up to 10,000 or more.

By applying equation 4*b* it can be shown that the angle of torque (α) on the upper disk is given by the equation

$$\alpha = \frac{K\tau^2 r^4}{I} \cdot P\omega \sqrt{\frac{M}{T}}, \tag{19}$$

where τ = period of oscillation.
r = radius of rotating disk.
I = moment of inertia of disk.
ω = angular velocity of rotation.
K = constant, which depends upon the nature of the gas and the accommodation coefficients for transfer of momentum.

Hence, for any one gauge, the torque on the upper disk is proportional to the product of the speed of rotation of the aluminum disk and the quantity $P\sqrt{M/T}$. The sensitivity of the gauge can thus be increased by increasing the speed of rotation; also, by illuminating the mirror and using an arrangement similar to that used for galvanometers, it is possible to use the gauge to measure pressures of the order 10^{-3} to 10^{-4} micron.

The gauge actually used for measuring very low pressures showed a deflection of 1100 mm per microbar of air, at 1000 rpm, with the scale 50 cm from the mirror. Up to a pressure at which the mean free path of the gas molecules becomes comparable with the distance between the two disks, the deflections, at constant speed of rotation, were found to be proportional to the pressure as observed by a McLeod gauge.

At extremely low pressures (below about $3 \cdot 10^{-4}$ micron) the indications of the gauge were found to be inaccurate because of two sources of error. First, the rotation of the magnetic field produced by the Gramme ring tends to induce eddy currents in the metal framework that holds the mirror; and second, there is a tendency for the upper disk to start swinging, especially at very high speeds of rotation of the aluminum disk. As the damping at low pressures is very feeble, it is exceedingly difficult to stop this oscillation when once started.

Working independently of Langmuir, and about the same time, A.

Timiriazeff[85] also suggested the application of equation 4*b* to the construction of a low-pressure gauge. Since he was primarily interested in determining the laws of slip for different gases, his actual design is not suitable for a very sensitive gauge. Instead of a rotating disk with a stationary disk situated symmetrically above it, Timiriazeff used a rotating cylinder with a stationary cylinder placed symmetrically inside it and suspended by a phosphor-bronze wire.

Though no subsequent investigators (as far as the writer is aware) have attempted to use this type of construction for a vacuum gauge, there is no doubt that, by application of technique available at the present time, such a gauge could be constructed very much more readily and would prove extremely useful for the measurement of low pressures.

A gauge based on the same principle has been described by H. Riegger.[86]

5. RADIOMETER TYPE OF GAUGES

Crookes' Radiometer. One of the first instruments to be used for detecting low gas pressures was the radiometer devised by Sir William Crookes in 1873. The instrument, which is described in most textbooks, consists of a glass bulb in which a small vane or fly is mounted on a vertical axis. The vane has four arms of aluminum wire on which are attached four small plates of thin mica, coated on one side with lamp black. These plates are set so that their planes are parallel to the axis. If a source of light or heat is brought near the bulb, and the rarefaction is just right, the fly rotates, but at very low pressures the rotation practically ceases.

The theory of the device was apparently not very well understood for a long time, and attempts to use it as a gauge for low pressures yielded very unsatisfactory results. Dewar[87] has stated the case for this instrument as follows:

> The radiometer may be used as an efficient instrument of research for the detection of small gas pressures. For quantitative measurements the torsion balance or bifilar suspension must be employed.

Some years ago W. E. Ruder, of this laboratory, developed a method of using the radiometer for the measurement of the residual gas pressure in incandescent lamps. The following account was prepared by him at the request of the writer:

---

[85] *Ann. Physik*, **40**, 971 (1913).

[86] *Z. tech. Physik*, **1**, 16 (1920); *Sci. Abst.*, **24**, 153 (1921).

[87] *Proc. Roy. Soc. London*, **A**, **79**, 529 (1907).

> It was found that when exhausted to the degree required in an incandescent lamp the radiometer could not be made to revolve, even in the brightest sunlight. In order to get a measure of the vacuum, the radiometer vanes were revolved rapidly by shaking the lamp, and the time required to come to a complete stop was therefore a measure of the resistance offered to the vanes by the gas, together with the frictional resistance of the bearings. The latter quantity was found to be so small in most cases that a direct comparison of the rates of decay of speed of the vanes gave a satisfactory measure of the degree of evacuation. In this manner a complete set of curves was obtained which showed the change in vacuum in an incandescent lamp during its whole life and under a variety of conditions of exhaust. The chief objections to this method of measuring vacua were the difficulty in calibrating the radiometer and the difference in frictional resistance offered by different radiometers. For *comparative* results, however, the method was entirely satisfactory.

As a result of his investigations of the laws of heat transfer in gases at low pressures, Knudsen arrived at a clear explanation of the radiometer action and furthermore developed, along the same lines, an accurate gauge for the measurement of extremely low pressures.

According to Knudsen, a mechanical force is exerted between two surfaces maintained at different temperatures in a gas at low pressure. This is due to the fact that the molecules striking the hotter surface rebound with a higher average kinetic energy than those that strike the colder surface. In the case of the radiometer the blackened surfaces absorb heat from the source of light, and the molecules rebounding from the vanes are therefore at a higher temperature than those striking the walls of the bulb. Consequently a momentum is imparted to the vanes which tends to make them rotate.[88]

Knudsen Gauge. The principle of this gauge[89] may be explained by referring to the lower part of Fig. 18. Let us consider two parallel strips A and B placed at a distance apart which is *less* than the mean free path of the molecules. Let A be at the same temperature T_0 as the residual gas, while B is maintained at a higher temperature T_1. On the side away from B, A will be bombarded by molecules having a root-mean-square velocity v_0, corresponding to the temperature T_0, as given by the equation

$$v_0 = \sqrt{\frac{3R_0T_0}{M}}.$$

These molecules will, of course, rebound from A with the same velocity.

---

[88] The theory of the radiometer, especially at medium pressures, has been dealt with rather fully by G. D. West, *Proc. Phys. Soc.* (*London*), **25**, 324 (1912–1913); **28**, 259 (1915–1916); **31**, 278 (1918–1919); **32**, 166, 222 (1919–1920). More recent discussion of the same topic is given at the end of this section.

[89] *Ann. Physik*, **32**, 809 (1910).

However, on the side towards B, A will be bombarded by molecules coming from B and having a higher velocity v_1 corresponding to the temperature T_1. Consequently A will receive momentum at a greater rate on the side towards B than on the opposite side, and will therefore be repelled from B.

In deriving the relation between the pressure of the gas and the force exerted on the surface A, we shall follow the simple derivation given by G. W. Todd.[90]

If the distance between the surfaces A and B is *less than the mean free path,* the force F is given by the *rate at which momentum is transferred* per unit area from B to A, that is,

$$\begin{aligned} F &= \tfrac{1}{6}nv_0(mv_1 - mv_0) \\ &= \frac{1}{6}\frac{P_{\mu b}}{kT_0}\cdot 3k(\sqrt{T_1T_0} - T_0) \\ &= \frac{1}{2}P_{\mu b}\left(\sqrt{\frac{T_1}{T_0}} - 1\right). \qquad (1) \end{aligned}$$

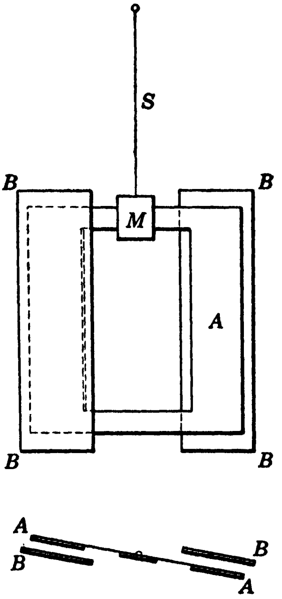

FIG. 18. Diagrammatic sketch of Knudsen type of gauge.

For small differences of temperatures, and for the purpose of pressure measurements, this equation may be written in the form

$$P_{\mu b} = 4F\left(\frac{T_0}{T_1 - T_0}\right) \qquad (2)$$

Thus, for constant value of $(T_1 - T_0)/T_0$, the force is proportional to the pressure and is *independent of the molecular weight of the gas.*

In order to measure this force of repulsion, Knudsen uses the arrangement shown diagrammatically in the upper part of Fig. 18. The strip A is replaced by a rectangular vane, cut out in the center and suspended by means of a fiber S. Two strips BB which can be heated are placed symmetrically on opposite sides of this vane, and the force of repulsion is then balanced by the torsion of the fiber. By means of the mirror, M, the deflection can then be measured in the same manner as in galvanometers.

---

[90] *Phil. Mag.*, **38**, 381 (1919). See also derivation by A. E. Lockenvitz, *Rev. Sci. Instruments*, **9**, 417 (1938).

For this arrangement, equation 2 assumes the form

$$P_{\mu b} = \frac{4\pi^2 ID}{rA\tau^2 d} \cdot \frac{T}{T_1 - T}, \tag{3}$$

where I = moment of inertia of the moving vane.
r = mean radius of the moving vane.
A = area of the vane A opposite each strip B.
τ = period of vibration of the vane.
D = scale deflection.
d = scale distance.

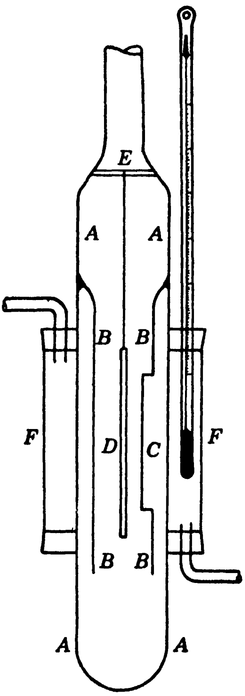

FIG. 19. Simple construction of Knudsen gauge.

Since all these quantities can be measured directly, it follows that the device can be used as an *absolute manometer,* without the necessity of calibrating against any other gauge. It is also evident that the indications of this gauge must be independent of the nature of the gas to be measured.

In his first paper on this subject, Knudsen mentioned several different forms of construction which might be used in making a gauge on the foregoing principle but gave very few constructional details. One form which appears to be very simple in construction is shown in Fig. 19.

In AA, a glass tube about 1.4 cm in diameter, is sealed a narrow tube BB which has a rectangular piece cut out at C, 0.41 cm wide by 2.95 cm long. A piece of mica D is suspended in front of this opening by means of a fiber fastened at E. The tube AA can be heated by means of an external water jacket FF. As the temperature of the water in FF is raised, the mica plate is repelled by the "hot" molecules traveling through the opening C, and the amount of deflection can be observed by means of a microscope.

Variations of this construction were described by Knudsen in a later paper.[91] E. v. Angerer[92] described a Knudsen manometer which consisted of a silvered mica vane between two electrically heated platinum strips. He stated that pressures as low as $8 \cdot 10^{-7}$ mm of mercury could be measured with it.

---

[91] *Ann. Physik,* **44,** 525 (1914).
[92] *Ann. Physik,* **41,** 1 (1913).

The same type of design has also been used by J. W. Woodrow[93] and by J. E. Shrader and R. G. Sherwood.[94]

Woodrow's Modification of Knudsen Gauge. The following description of Woodrow's form of Knudsen gauge is quoted from the original publication:

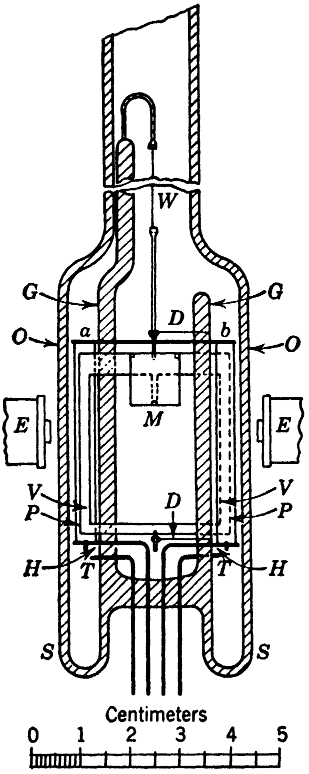

FIG. 20a. Woodrow's modification of Knudsen gauge.

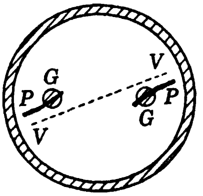

FIG. 20b. Cross-sectional view through the middle of the gauge shown in Fig. 20a.

> Several different gauges were constructed varying in sensitivity so as to be used at different pressures. A typical gauge is shown in Figs. 20a and 20b, and the electrical circuits are given in Fig. 21. The glass rods *GG* served as supports for the metallic parts of the gauge. All the internal electrical connections and adjustments, with the exception of the final leveling, were made before the outer glass walls *OO* were sealed on at *SS*. The suspension *W* was a phosphor-bronze ribbon 50 mm in length which had been obtained from W. G. Pye and Co. and was listed by them as No. 0000. The movable vane *VV* consisted of a rectangular frame of aluminum 0.076 mm in thickness, the dimensions of the outer rectangle being 30 by 36 mm and the inner 26 by 30 mm. The heating plates *PP* were platinum strips 4 mm wide, 40 mm long, and 0.025 mm thick. The deflections of the movable vane were obtained in the usual way by the reflection of a beam of light from the mirror *M*. Figure 20b is a cross-sectional view through the middle of Fig. 20a.
>
> All of the platinum connections were made by electric welding, as that was found much more satisfactory than the use of any kind of solder, especially when heated. After a little practice, it was possible to weld the thin platinum heating vanes to the heavy platinum wire so as to make a perfectly continuous contact throughout its

---

[93] *Phys. Rev.*, **4**, 491 (1914).

[94] *Phys. Rev.*, **12**, 70 (1918).

width. The phosphor-bronze suspension was connected at both ends by threading through three small holes drilled into the flattened extremities of the platinum and aluminum wires respectively. The small loops *DD* were so placed that they supported the movable vane *V* except when the gauge was leveled for taking readings. This made the gauge readily portable and, by placing it in the inverted position when connected to the molecular pump, the danger of the breaking of the suspension by vibration was eliminated. One gauge of medium sensitivity was constructed so as to be sufficiently steady to be used when connected directly to the molecular pump. Large glass tubing was employed in all the connecting portions of the apparatus.

A small electromagnet, shown at *E* in Fig. 20*a*, was employed in bringing the moving vane to rest. This was found to be quite necessary in working with the most sensitive gauges, since in a very good vacuum the damping is so small that the vane will not settle down sufficiently for the taking of readings for some time after an accidental disturbance has set it vibrating. It should be noted that the electromagnet must have either an air core or one of good, soft Norway iron, for otherwise the residual magnetism will produce a false zero if the aluminum vane is at all magnetic, as was the case with the samples of metal investigated in this laboratory. Under these conditions it is obvious that the electromagnet should be used only for damping and that the exciting current should be shut off while making observations.

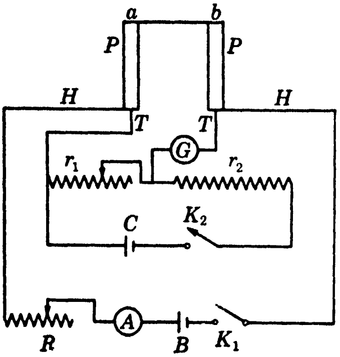

FIG. 21. Electrical circuit for determining the temperature of the heating strips in gauge shown in Figs. 20*a* and *b*.

Several methods were tried for determining the temperature of the heating strips, and that shown in diagram in Fig. 21 was finally settled upon as giving the most satisfactory results. The potentiometer leads *TT* were connected by electric welding to the very extremities of the platinum heating vanes *PP*. The heating current was regulated by the variable resistance *R* and its value was read on the ammeter *A*. The resistance r_2 was kept constant at 10,000 ohms and r_1 varied to obtain a balance of the sensitive galvanometer *G*. The potentiometer battery *C* consisted of a carefully calibrated Weston Standard Cell. This arrangement gave an accurate method of measuring the resistance of the platinum strips *PP*, plus the heavy platinum wire *ab*, the total cold resistance being 0.17 ohm. This cold resistance was determined by plotting the curve connecting resistance and heating current under a constant low pressure and extrapolating backward to the intersection with the axis of resistance. If the resistance is measured for small currents, the value at zero current, that is the cold resistance, can be determined very accurately. The temperature coefficient of resistance of the platinum, which contained a small amount of iridium, was carefully determined and was found to give a linear relation within the range of temperatures employed. The value of the coefficient was $2.35 \cdot 10^{-3}$ ohm per degree C. With this system one can determine the mean temperature of the heating strips with sufficient accuracy, the error for temperature difference of about 50° C being less than 4 per cent.

Woodrow also observed that in order to avoid electrostatic effects it was necessary to silver-coat the outside of the glass walls, which were then grounded. Similarly the moving system was connected through the suspension to that terminal of the heating strips that was grounded.

With the gauge whose dimensions are given above, the period of a complete oscillation was 10 sec and the calculated moment of inertia of the moving vane was 0.074 $g \cdot cm^2$. This gives, for the pressure, the relations

$$P_{\mu b} = 2.9 \cdot 10^{-5} \frac{T}{T_1 - T} d,$$

$$P_{mm} = 2.2 \cdot 10^{-8} \frac{T}{T_1 - T} d,$$

where d is the deflection in millimeters on a scale at a distance of 1 meter from the mirror.

Thus, with a temperature difference of 100° C, the gauge could be used to read pressures as low as $3 \cdot 10^{-8}$ mm of mercury.

Shrader and Sherwood's Modification of Knudsen Gauge. The construction used by Shrader and Sherwood differed in a few details from that used by Woodrow. In view of the importance of the Knudsen gauge for low-pressure measurements, the description of this modification is worth quoting.

The gauge is shown in Fig. 22. It is enclosed in a hard glass tube 2 in. in diameter and 9 in. long. The heating strip *aa* is of platinum, 0.018 mm thick and 7.5 mm wide with a total length of 18 cm. It is folded at the top forming a cross piece and two parallel sides. The ends are brazed to 20-mil tungsten leading-in wires at the bottom. Fifteen-mil tungsten wires *b* sealed into the glass-rod support serve as a spring support for the platinum strip. This allows accurate adjustment of the strip and sufficient tension is secured to keep the strip taut during heating. One of these wires is carried up the glass-rod support, sealed into it at *c*, leaving a free end *d* to serve for electrical connection of the moving vane to the heating strip. Connection is made by the wire pressing under tension against the tungsten wire *e* to which the suspension of the vane is fastened. Potential leads of fine platinum wires *ff* are welded to the strip about 1 cm from the ends and are brazed to tungsten sealing-in wires.

The movable rectangular vane *g* is made of aluminum 0.0076 cm thick. A standard size adopted is 3.2 cm by 4 cm outside dimensions, the width of the vane being 0.5 cm. Because of liability of warping during heat treatment the vane is stiffened by an aluminum wire passing through slits at the top and a hole at the bottom into which the wire is hooked and fastened firmly. For portability, two copper wires *h* are sealed into the glass-rod support while the free ends form loops around the rod, these forming guides for the vane. The mirror is fastened at the bottom of the vane by leaving a small projection of the aluminum at the lower edge and cutting out small tongues from the material of the vane on either side. The mirror is laid in place and the projection and the two tongues are pressed closely over it, holding it securely.

Silver mirrors were tried, but failed to withstand the heat treatment to which the gauge and system were subjected. Mirrors made by coating microscope cover glass with china decorators' platinum solution, followed by baking at 500°, solved this difficulty.

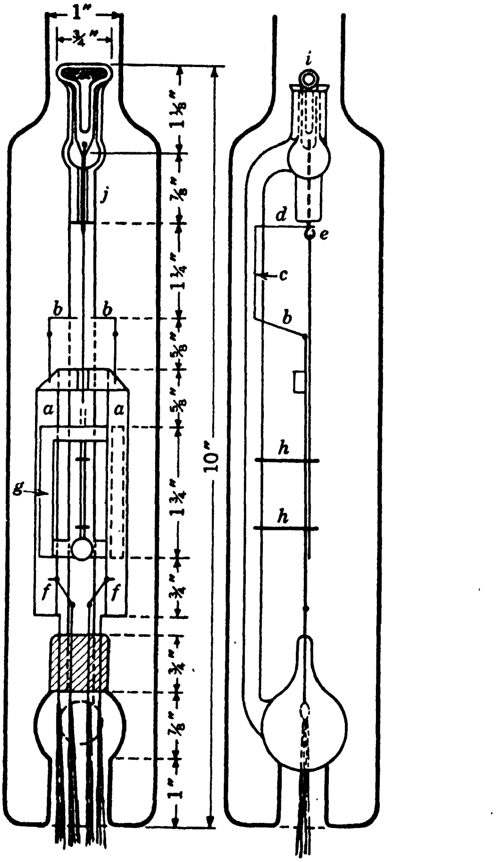

FIG. 22. Shrader and Sherwood's modification of Knudsen gauge.

The distance between the heating strip and the vane is adjusted from outside the case by magnetic control on a piece of soft iron *i* sealed into a glass stem to which the suspension is fastened.

The suspension is 0.0005-in. tungsten wire. This is fastened to small aluminum hooks around which the wire is wrapped several times after which the hooks are pressed firmly together. This method is not difficult and holds the wire securely. A hook on the end of a tungsten wire sealed into a glass stem, the free end passing through a capillary rod *j* on the glass support, serves to hold the suspension.

A gauge such as has been described, using a 0.0005-in. tungsten suspension from 6 to 7 cm long, has such a sensibility that a scale deflection of 1 mm at a meter's distance with a temperature difference of 150° C between the heating strip and the movable vane indicates pressures of $1 \cdot 10^{-8}$ to $5 \cdot 10^{-8}$ mm Hg. One gauge of other dimensions than those given above would indicate a pressure of $5 \cdot 10^{-9}$ mm Hg under the same conditions.

The temperature of the heated strips was measured by substantially the same electrical method as that used by Woodrow.

L. F. Richardson[95] has described a construction of Knudsen gauge in which the force of repulsion is balanced by means of a magnetic field, and H. Riegger,[96] a commercial form made in Germany at that time.

In connection with his investigations on the theory of the radiometer E. Fredlund[97] constructed several forms of the Knudsen gauge which are quite elaborate. In all these constructions the movable vane is a thin circular metal disk located in the center between two large metal plates that are maintained at a constant difference in temperature. Two magnet needles are attached to the suspension of the disk and the force on the disk is balanced by passing current through two coils located in planes parallel to that of the disk. Thus the magnitude of the current required to obtain zero deflection is a direct measure of the pressure.

The theoretical implications of the work of Fredlund and other investigators are discussed at the end of this section.

As Jesse W. M. DuMond and W. M. Pickels, Jr.,[98] have pointed out, the reason for the infrequent use of the Knudsen gauge, "in spite of its manifold advantages, lies in the elaborate designs and precautions described by the above-named workers," who really regarded the gauge itself "as the object of a research problem rather than a tool."

Figure 23 shows a line drawing of the gauge designed by these investigators. The movable vane (1) consists of a rectangular frame of 2.5-mil aluminum to which is fastened an axle (2) of 32-mil aluminum. This axle carries an ordinary galvanometer mirror (5), attached to a 0.5-mil tungsten wire, which is fastened to an aluminum wire held by means of a set screw (8) in the hole in the bottom of the steel taper plug (9). A vacuum-tight seal is obtained by means of laboratory wax or stopcock grease. The heaters (14) are helices of Chromel resistance wire, and the current leads are provided by means of the insulated vacuum tight plugs fastened by the nuts (18). The cylindrical brass envelope (20) of the gauge with its window and water jackets (21) is slipped over the brass disks (11) and (12) and sealed at (12) by means of solder or Apiezon wax. Two Helmholtz coils outside the case are used to obtain magnetic damping.

[95] *Proc. Phys. Soc. London,* **31,** 270 (1918–1919).

[96] *Z. tech. Physik,* **1,** 66 (1920).

[97] *Ann. Physik,* **13,** 802 (1932); **14,** 617 (1932); **30,** 99 (1937).

[98] *Rev. Sci. Instruments,* **6,** 362 (1935).

The investigators state,

> instead of maintaining the gauge heater at constant temperature for all gas pressures in the gauge we let the heater assume whatever temperature the combined effect of radiation loss and gas conduction loss impose with a constant wattage input to the heater.

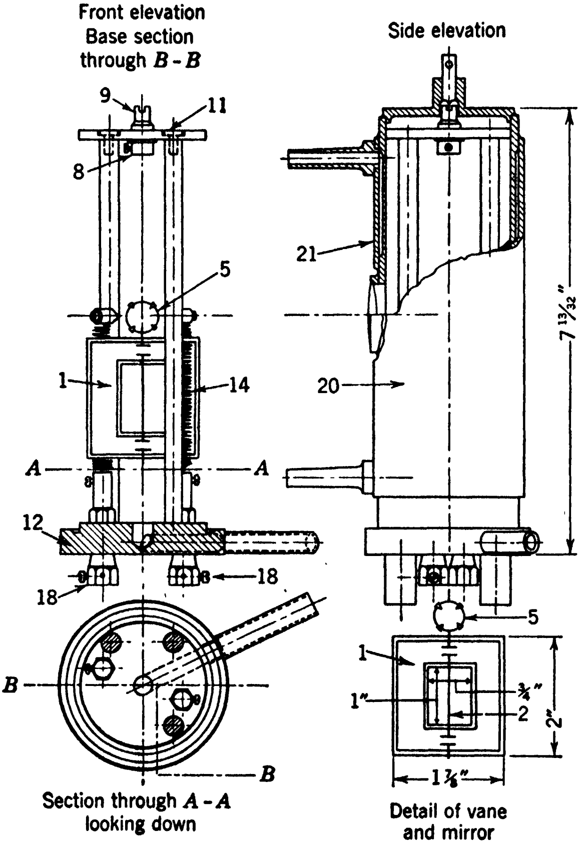
Front elevation Base section through *B* - *B*

Side elevation

Section through *A* - *A* looking down

Detail of vane and mirror

FIG. 23. Construction of DuMond and Pickels form of Knudsen gauge.

Under these conditions, the relation between deflection of the mirror (D) and pressure is not linear, but has the form

$$D = \frac{CP}{1 + BP}, \tag{4}$$

where C and B are two constants derived from a calibration of the gauge against a McLeod gauge (with liquid-air trap inserted between the

McLeod and the Knudsen gauge). The deflection is observed by means of a small lamp and galvanometer screen. By varying the wattage in the heater coils two scales are obtained for the pressure readings. On the more sensitive of these, pressures as low as 10^{-7} mm can be detected.

A more rugged form of Knudsen gauge and, consequently, one that is not as sensitive as that devised by DuMond and Pickels has been described by A. E. Lockenvitz.[99] The details of construction are shown in Fig. 24. As will be observed it consists, essentially, of a very thin aluminum leaf swinging freely from its upper edge between two surfaces maintained at constant temperatures. The author states,

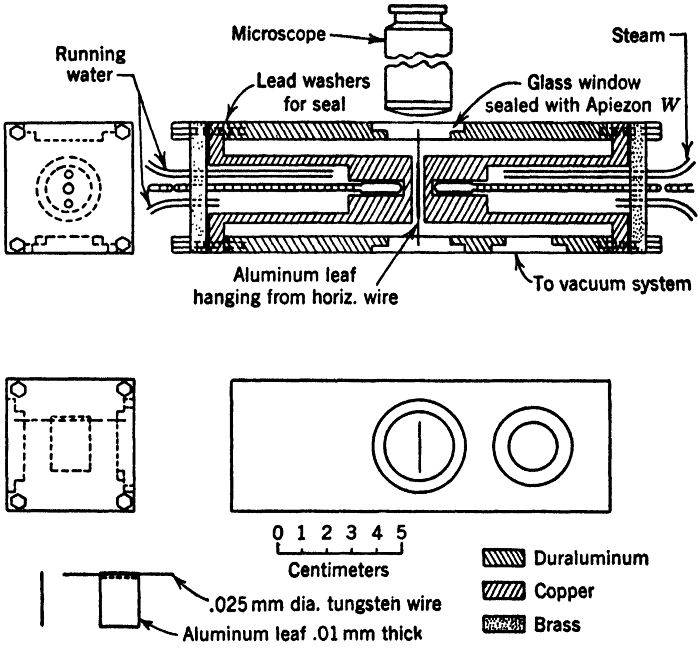
Microscope
Steam
Running water
Lead washers for seal
Glass window sealed with Apiezon *W*
Aluminum leaf hanging from horiz. wire
To vacuum system
0 1 2 3 4 5
Centimeters
.025 mm dia. tungsten wire
Aluminum leaf .01 mm thick
▨ Duraluminum
▨ Copper
▨ Brass

FIG. 24. Construction of Knudsen gauge by Lockenvitz.

> The hot and cold plates, which are machined out of copper, are sealed to the body by means of lead washers. The glass windows for observing the deflection of the leaf are sealed in with Apiezon W wax. The 0.01 mm thick aluminum leaf is hung from a fine wire by folding the top edge of the leaf over about 0.5 mm. A microscope is fastened to the body of the gauge and is focussed on one bottom corner of the aluminum leaf so that a deflection of 0.005 mm can easily be read on the scale in the micrometer eyepiece.

The pressure is directly proportional to the deflection.

[99] *Rev. Sci. Instruments*, **9**, 417 (1938).

The lower limit of the gauge is stated to be about $0.75 \cdot 10^{-2}$ micron.

> However by using a thinner or a larger leaf, or both, the lower limits could easily be extended to the region of 10^{-3} microbar. In that case it might be advisable to construct the gauge out of glass, since gases given off by the large metal surfaces would be troublesome.

It will be observed that all such gauges in which an Apiezon wax or low-melting-point solder is used obviously cannot be given a heat treatment in order to eliminate adsorbed gases. Hence they must be maintained on the exhaust system for quite a long period before the pressure indications actually correspond to pressures in the rest of the system.

In contrast to the forms described above is the "simple Knudsen gauge" described by A. L. Hughes,[100] which is shown in Fig. 25. It consists of a Pyrex tube, 2.5 cm in diameter and 15 cm long. The heater, Pt, is made of a platinum strip 10 cm long, 1.3 cm wide, and 1.10^{-4} cm (0.04 mil) thick, and is connected to two 50-mil tungsten leads. The movable strip, A, is made of aluminum leaf, 12 cm long, 0.4 cm wide, and $5 \cdot 10^{-5}$ cm (0.02 mil) thick. The strip is fastened to a 50-mil tungsten lead which is sealed in a ground-glass joint. The joint is sealed on the *outside*, as shown, by a suitable wax of very low vapor pressure. The author states that

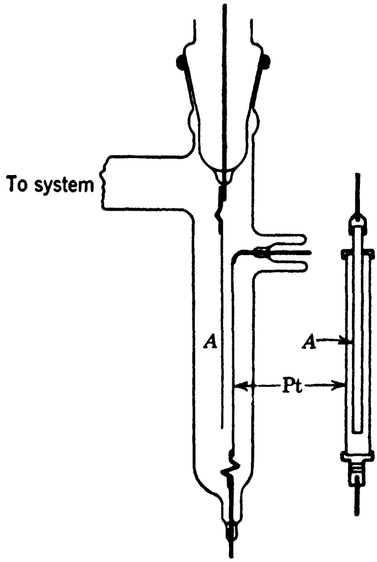

FIG. 25. Simple form of Knudsen gauge by Hughes.

> the aluminum leaf is connected electrically to the heater to ensure that no electrostatic effects causing undesirable delections of the leaf can occur. The motion of the tip of the free end of the leaf is measured by means of a reading microscope with 100 divisions in its scale. Seventeen divisions correspond to 1 mm.
>
> Current to raise the temperature of this heater is provided by a storage battery and measured by an ammeter.

The sensitivity increases with increase in heating current as shown in Table 2.

---

[100] *Rev. Sci. Instruments*, **8**, 409 (1937).

TABLE 2

VARIATION IN SENSITIVITY OF KNUDSEN GAUGE WITH HEATING CURRENT (HUGHES)

Heating Current (amp)	1 Scale Division Equals	10^{-3} Micron Equals
0.2	304. · 10^{-4} micron	0.033 scale division
0.5	46.5	0.22
1.0	12.4	0.81
1.5	6.5	1.54
2.0	4.37	2.28
2.5	3.16	3.17

Calibration curves for the low-pressure and high-pressure ranges are shown in Figs. 26*a* and 26*b*, respectively.

Obviously, the ground-glass joint could be replaced by a permanent seal and the aluminum foil by one of a higher-melting-point metal to permit baking out the gauge at 400 to 500° C.

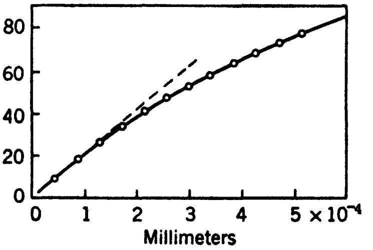

FIG. 26*a*. Calibration for the low-pressure range of gauge shown in Fig. 25, heating current 0.5 amp. *Ordinates*, eyepiece scale divisions. Abscissas = 10^{-4} mm.

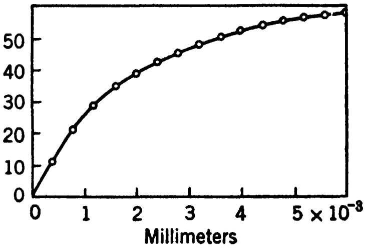

FIG. 26*b*. Calibration for the high-pressure range of gauge shown in Fig. 25, heating current 0.2 amp. *Ordinates*, eyepiece scale divisions. Abscissas = 10^{-3} mm.

A construction radically different from that of all the Knudsen gauges mentioned above has been described by H. Klumb and H. Schwarz.[101] Instead of a vane in a plane parallel to that of the heated surface, a cylindrical arrangement of vanes is used, as shown in Figs. 27*a* and 27*b*. This system *R* is suspended in the annular space between the outer glass tube *G* and inner tube *H* (see Fig. 27*b*), and a spiral heater is inserted in *H*. The molecules striking the glass surface *H* acquire a correspondingly higher kinetic energy, and, when these molecules strike the vertical vanes of the system R, R acquires a rotational moment which is observed by the deflection of the mirror M attached to the suspension. (See Fig. 28.) The whole assembly, including the tungsten wire suspension and cooling chamber for the glass walls opposite R, is shown in Fig. 29. The dimensions (in millimeters) are indicated in the figure.

---

[101] *Z. Physik*, **122**, 418 (1944).

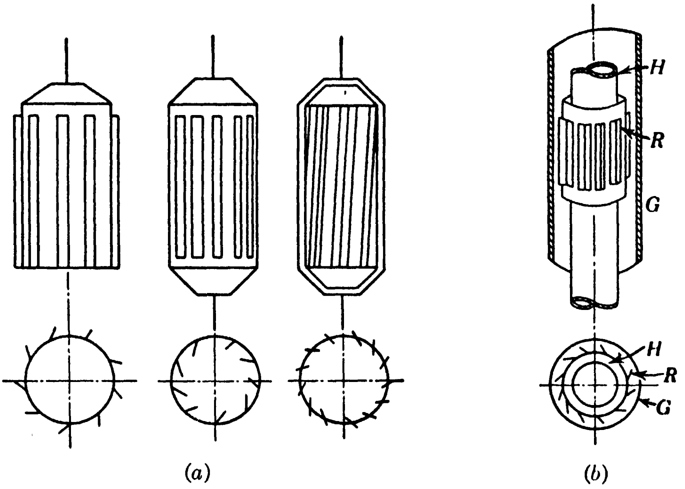

FIG. 27. Klumb-Schwarz modification of Knudsen gauge. (a) Showing cylindrical arrangement of vanes. (b) Assembly of vanes and heated inner cylinder.

Instead of observing the deflection directly, a compensating magnetic field (produced by the action of the solenoids W_1W_2 on the iron armature D) may be used, as shown in Fig. 30.

Let θ denote the angular deflection. Then the pressure is given by the relation

$$C_0\theta = P, \quad \text{or} \quad \theta = E_0P, \tag{5}$$

where C_0 is designated the "reduction factor," and E_0 the "gauge sensitivity." Furthermore,

$$E_0 = K\left(\sqrt{\frac{T_1}{T_0}} - 1\right), \tag{6}$$

where T_1 is the temperature of the hot surface, T_0 that of the cold surface, and K is a constant dependent upon the geometrical arrangement of surfaces, their dimensions, and also upon the magnitude of the accommodation coefficient for the gas used. (See discussion below.)

Figure 31 gives plots of data obtained under different conditions.

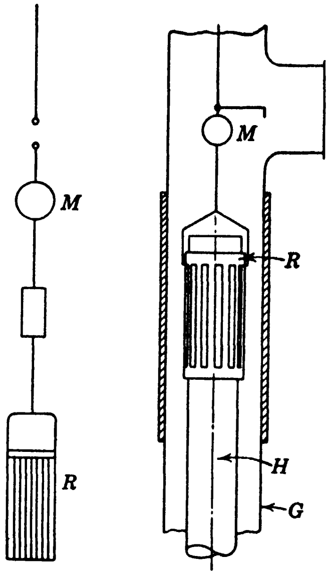

FIG. 28. Illustrating assembly of vanes and suspension for Klumb-Schwarz form of gauge.

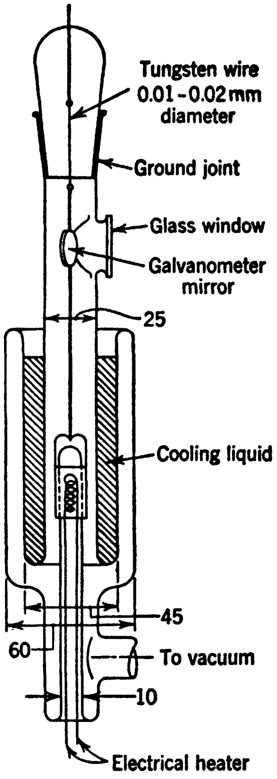

FIG. 29. Diagrammatic sketch of Klumb-Schwarz construction of gauge. Tube dimensions are given in millimeters.

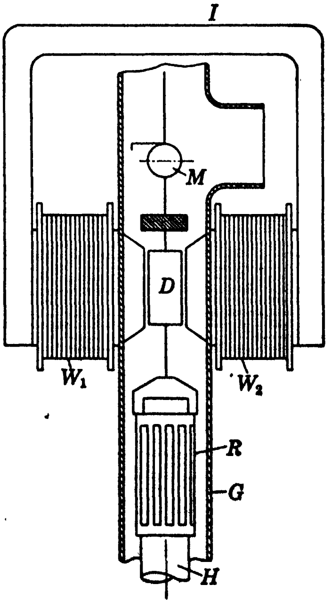

FIG. 30. Alternative arrangement for gauge shown in Fig. 29, involving use of a magnetic field.

The continuous curves were obtained for air with a gauge having a tungsten wire suspension 0.02 mm diameter and a cold temperature of 13° C (cooling water). The dotted curves were obtained for air, with a tungsten suspension 0.01 mm in diameter and an external temperature

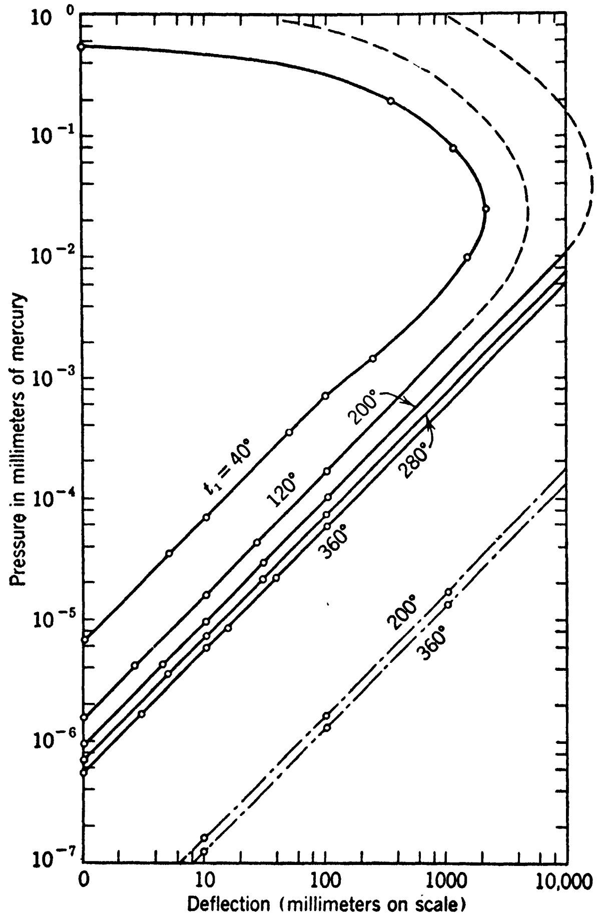

Fig. 31. Log-log plot of deflection versus pressure for Klumb-Schwarz gauge.

of −180° C (liquid air). The temperatures of the heated surface (t_1) are given in degrees Centigrade, and the pressures in millimeters of mercury. The abscissas denote the deflections in scale divisions.

In accordance with equation 5 the plots on log-log scales should be linear with a slope of 45°. As shown in Fig. 31 the data for pressures below about 10 microns are in agreement with the theoretical deductions. Furthermore, it was observed that, in accordance with equation 6, E_0 varied linearly with the value of $\sqrt{T_1/T_0}$, independently of the nature of the gas used.

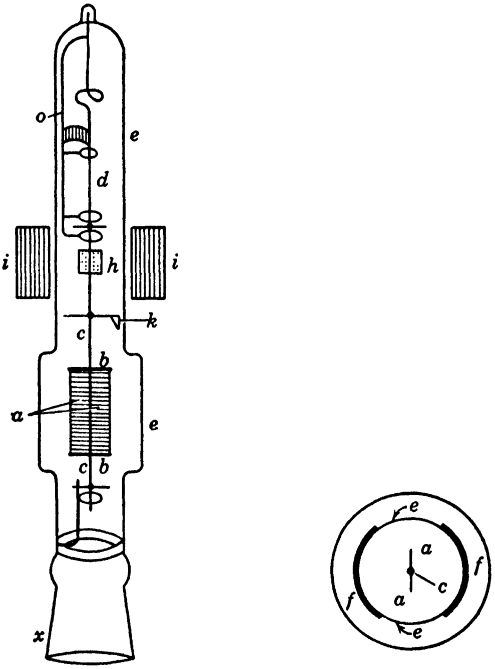

(a) (b)

FIG. 32. " Molvakumeter " (Gaede).

The *Molvakumeter* devised by W. Gaede[102] is of interest because it incorporates features of both the viscosity type of gauge and the Knudsen type. Figure 32*a* gives a diagrammatic sketch of the construction used. A thin aluminum vane, *a* (1 mg weight), is fastened by means of a fine glass fiber *b* to another glass fiber *c*, which carries a pointer, *k*. This, in turn, is attached above to the fine quartz fiber *d*. Protection against too great a deflection and breakage in manipulation are provided, as shown in the figure, by supports attached to the wire *o*. The vane *a* is inside the tube *e*, which is connected with the vacuum system by means of the ground-glass opening *x*, and outside the region *e* are located two heating surfaces *f* arranged as shown in Fig. 32*b*.

---

[102] *Z. tech. Physik*, **15**, 664 (1934).

The vane is set in oscillation by means of the very thin magnetized plate h and a current pulse in the coil i. Let τ_0 denote the period of oscillation when the heating surfaces f are not operating, and τ the period when these are operated. Then, the pressure

$$P = A\left(\frac{1}{\tau^2} - \frac{1}{\tau_0^2}\right), \tag{7}$$

where A is an empirically determined constant. According to Gaede, the turning moment is proportional to the square of the radius of the foil a and inversely proportional to the radius of the tube e.

The maximum amplitude of the oscillations will decrease in the period t from α_0 to α_n. Since this is a pure viscosity effect,

$$P\sqrt{M} = B\frac{\log(\alpha_0/\alpha_n)}{t}. \tag{8}$$

Hence by combining these two equations both P and M can be determined. These equations are applicable only for pressures lower than about 10^{-4} mm mercury, at which pressures, L, the mean free path, is large compared to the distance from the glass wall, e, to the aluminum foil a.

Gaede has also described an optical arrangement for observing pressures higher than 10^{-4} mm. In the particular instrument used by him the values observed were as follows: $\tau_0 = 0.5$ min and $\tau = 0.25$ min at $P_{mm} = 10^{-5}$. From 20 successive oscillations the value of τ could thus be determined with an accuracy of 1 per cent, and P to within 10^{-7} mm.

Theory of the Radiometer Type of Gauge. At the beginning of this section, a simple derivation was given for the relation between the pressure and the force exerted on a surface by a parallel plane surface at higher temperature. As stated above, equation 1 is valid only at pressures so low that the mean free path, L, of the molecules is greater than the distance between the cold and hot surfaces. It is only under these conditions that the molecules can transfer momentum directly from the hot to the cold surface. At higher pressures, the "hot" molecules must lose part of their energy by collisions with cold molecules before reaching the cold surface. Hence it would be expected that the force exerted on the cold surface, which is known as the radiometer pressure and which we shall designate by F, will be lower at higher pressures, in spite of the fact that the concentration of molecules is higher.

A number of investigators have made measurements on the variation in the magnitude of F with pressure. The results obtained by E. Brüche and W. Littwin[103] with a number of different gases are of particular interest. In their experiments they used a gauge in which the thin vane for measuring F was located symmetrically between a hot surface and a cold surface. Figure 33 shows the variation in relative value of F with pressures in millimeters (plotted on log scale) for different values of the distance (d), in millimeters, between each surface and the vane. At any given pressure, the value of F is decreased by increase in d, because of the decrease in the ratio L/d. Furthermore all the curves show that F attains a maximum value, F_m, for a certain pressure, P_m.

---

[103] *Z. Physik*, **52**, 318 (1928).

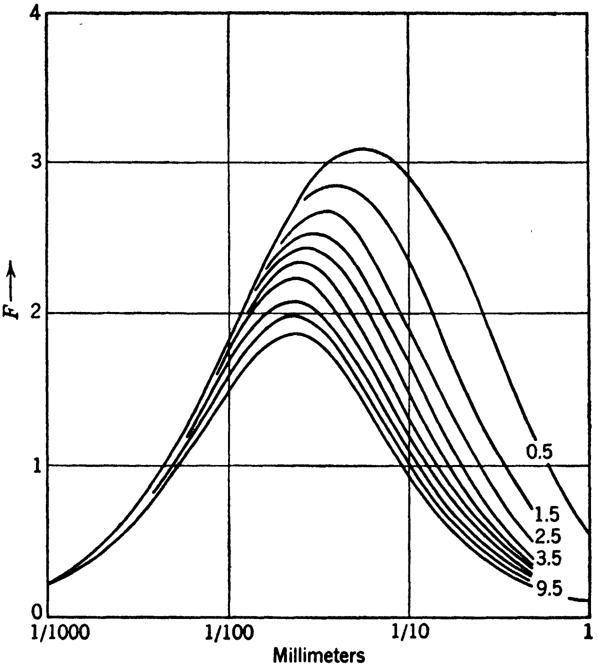

FIG. 33. The values of the force F (in arbitrary units) on the movable vane in a Knudsen gauge, plotted against $\log P_{mm}$, for a series of values of the distance between the heated surface and the vane. From observations by Brüche and Littwin.

From their observations Brüche and Littwin concluded that for any gas and given value of d these could be best represented by a relation of the form

$$F = \frac{1}{a/P + P/b}, \tag{9}$$

where a and b are two empirically determined constants. At very low pressures, this assumes the form, similar to equation 1,

$$F = \frac{P}{a}, \tag{10}$$

and at high pressures the relation becomes

$$F = \frac{b}{P}. \tag{11}$$

Thus the variation in F with P is represented on linear scales by a curve such as AMB which is shown in Fig. 34. At very low pressures, F increases linearly with P until the pressure attains a value corresponding approximately to the point A (6 to 7 microns). With further increase in P, F deviates more and more from the linear plot and reaches a maximum value at M (about 50 microns). Beyond this point F decreases slowly and approaches asymptotically the values given by the hyperbola $F = b/P$.

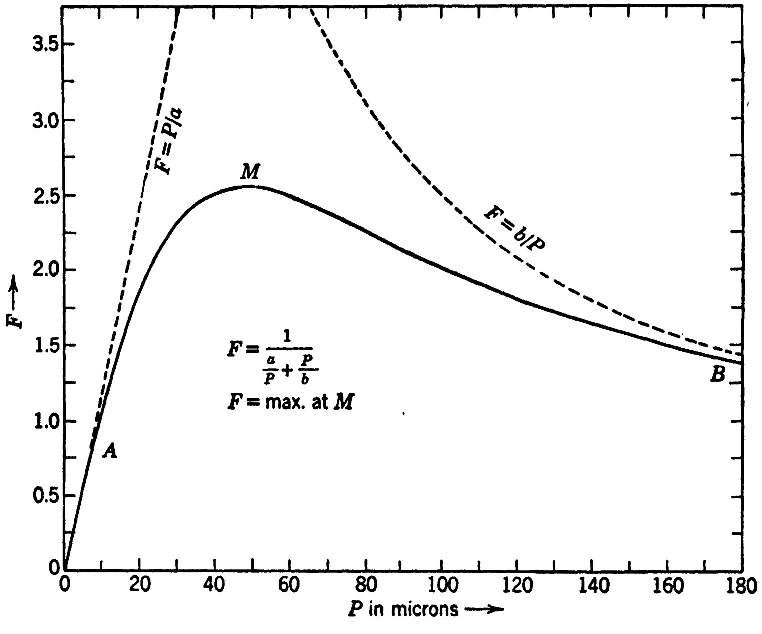

FIG. 34. The force F on the movable vane in a Knudsen gauge, plotted versus P_μ, illustrating the application of equation 9.

For constant value of d, and different gases, it was observed that the values of F_m (the maximum value of F), and of the pressure at which this maximum occurs, vary in approximately the same manner as those of L.[104] Thus, if AMB represents the plot for helium, the plots for other gases would lie below it, and that for carbon dioxide would be below that for argon or oxygen.

E. Fredlund[105] found that, in general, the linear relation (equation 10) between F and P is valid for values of L/d which are greater than about 13. For instance, $d = 0.485$ cm corresponds to the following maximum values of P_μ for different gases: H_2, 1.3; N_2, 0.73; O_2, 0.8; and A, 0.8. On the other hand, for $d = 0.095$ cm, the maximum values of P_μ for the applicability of the linear relations were as follows: H_2, 5.75; N_2, 3.25; O_2, 3.65.

It follows that the relation between F and P is a function of the ratio L/d, which approaches that given by the linear relation for L/d very large and deviates from the linear relation more and more as L/d becomes smaller (at increased pressures).

A factor that has not been taken into account in deriving equation 1 above is the *accommodation coefficient*, designated in Chapter 1, section 10, by α. If this coefficient has a value less than unity, then equation 1 has to be replaced by the relation

$$F = \frac{KP}{2}\left(\sqrt{\frac{T_1}{T_0}} - 1\right), \qquad (12)$$

where K is a function of the values of α for each surface the value of which lies between 0 and 1. Hence equation 1 cannot be used to deduce a calibration for a Knudsen gauge from moments of inertia, etc., unless some definite value is assumed for the factor K. This point has been discussed at length by Fredlund, who reaches the conclusion that in most cases the factor K is only slightly less than 1.

6. HEAT CONDUCTIVITY MANOMETERS

Energy is dissipated from a heated surface in a gas in two ways: (1) by radiation:

$$E_R = 5.67 \cdot 10^{-12}(\epsilon_1 T_1^4 - \epsilon_0 T_0^4) \quad \text{watts} \cdot \text{cm}^{-2}, \qquad (1)$$

where ϵ_1 is the radiant emissivity and T_1 the temperature of the heated surface, and ϵ_0 and T_0 refer to the cold surface; and (2) by conduction through the gas.

(*a*) At *normal pressure* the conductivity, λ, is independent of the pressure, and the loss is given by the relation (see Chapter 1, section 10)

---

[104] See Tables 1.6 and 1.7 for values of L at 1 micron and 25° C.

[105] *Ann. Physik*, **13**, 802 (1932); **14**, 617 (1932); **30**, 99 (1937).

$$E_c = 4.186\lambda(dT/dx) \quad \text{watts} \cdot \text{cm}^{-2}, \tag{2}$$

where λ is expressed in $\text{cal} \cdot \text{cm}^{-2} \cdot \text{sec}^{-1}$ per unit temperature gradient, at the surface, and dT/dx is the gradient in $\text{deg} \cdot \text{cm}^{-1}$.

(*b*) At *low pressures*, where the distance between hot and cold surfaces is less than the mean free path, the loss by conduction is given by the relation (see equation I.10.6)

$$E_K = \frac{4}{3}\frac{\alpha}{2-\alpha}\Lambda_M P_\mu \sqrt{\frac{273.2}{T_0}}(T_1 - T_0) \quad \text{watts} \cdot \text{cm}^{-2}, \tag{3}$$

where Λ_M = molecular heat conductivity in $\text{watts} \cdot \text{cm}^{-2}$ at 0° C, and
α = accommodation coefficient.

Hence, for given values of T_1 and T_0, the energy loss by conduction in a gas at low pressures, increases linearly with the pressure. Evidently the sensitivity of the conductivity method for the determination of pressure depends upon the relation between the two quantities E_R and E_K.

Let us calculate the values of E_R and E_K for hydrogen ($\lambda_0 = 41.3 \cdot 10^{-5}$, $\Lambda_M = 45.54 \cdot 10^{-6}$), assuming $\epsilon_1 = \epsilon_2 = \alpha = 1$. Table 3 gives the values of E_R and E_K for a series of values of T_1 and T_0. The first two rows in the table give, for comparison, values of E_c. The last column gives the value of the conduction loss per micron. Thus for $T_1 = 373$, $T_0 = 273$, $E_K = E_R$ for $P_\mu = 12.92$.

TABLE 3

HEAT LOSS FROM PLANE SURFACE IN HYDROGEN

[watts/cm²]

Pressure	dT/dx	T_1	T_0	E_R	E_c	E_K per micron
1 atm	100	373	273	7.83	17.3	—
1 atm	50	323	273	3.02	8.7	—
1 micron	—	373	273	7.83	—	0.606
1 micron	—	323	273	3.02	—	0.303
1 micron	—	323	90	5.25	—	7.78

It follows that, at $T_1 = 373$, $T_0 = 273$, and $P_\mu = 10^{-2}$, the loss by temperature radiation from a "perfect" radiator is about 100 times that due to conduction by the gas. Hence, in order to reduce the effect of the term E_R and to increase the relative effect of E_K, at low pressures, the surfaces used should have as low an emissivity as can be obtained, while it is advantageous to decrease T_0 to as low a value as convenient. For tungsten and platinum (outgassed at high temperature) the value of ϵ varies from about 0.03 at 0° C to about 0.10 at 500° C.

Gauges depending for their indication of pressure on the conductivity of the gas are, in general, operated under conditions in which the energy input is maintained practically constant. Hence the temperature of the heated surface decreases with increase in pressure, and the different types of conductivity gauges involve different methods for determining the change in temperature. In the thermocouple type, the temperature is determined by means of a thermocouple spot-welded at the center of a heated wire; in the resistance type, the change in temperature is determined, as the name implies, by measuring the change in resistance, and, finally, since the length of a wire varies with temperature, this leads to a third method of measuring the temperature.

Thermocouple Gauges. The earliest application of this type of gauge was made by W. Voege,[106] who used a small thermocouple attached to a wire heated by constant alternating current. W. Rohn[107] adopted the novel idea of heating the thermocouple in the gas by an external source of radiation (an incandescent lamp maintained at constant voltage), while E. Rumpf[108] surrounded the thermocouple with a heated spiral.

A customary construction of gauge is that used by Th. Haase, G. Klages, and H. Klumb.[109] Figure 35, taken from their paper, shows the arrangement, which consists of a ribbon or wire, H, heated by current (alternating or direct), and a thermocouple, T, the junction of which is spot-welded at the center of H. In this case H was a Constantan ribbon, 0.72 mm wide, 0.05 mm thick, and 49 mm long, connected to the inner leads a_1 amd a_2 sealed in the glass tube R, which in turn was connected to the system in which the pressure was to be determined. An iron-Constantan couple was used, and an annular space was provided, as shown in the figure, for ice water or other liquid by means of which the temperature of the glass walls could be maintained at constant temperature (T_0).

Figure 36 shows plots of the deflections of an indicating instrument connected to the leads of the thermocouples, as a function of the pressure of air. The three plots were obtained under the following conditions:

CURVE	INPUT (watts)	TEMPERATURE (°C)
a	0.014	48
b	.226	314
c	.98	508

---

[106] *Physik. Z.*, **7**, 498 (1906).
[107] *Z. Elektrochem.*, **20**, 539 (1914).
[108] *Z. tech. Physik*, **7**, 224 (1926).
[109] *Physik. Z.*, **37**, 440 (1936).

As shown by these plots, the range for air was from 1 mm down to a pressure between 10^{-3} and 10^{-4} mm. Observations with hydrogen and carbon dioxide showed that the change in temperature with pressure decreases with increase in molecular weight of the gas. This conclusion is in agreement with that obtained from an inspection of the relative values of Λ_M.

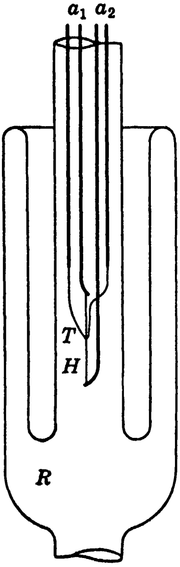

FIG. 35. Thermocouple gauge (Haase, Klages, and Klumb).

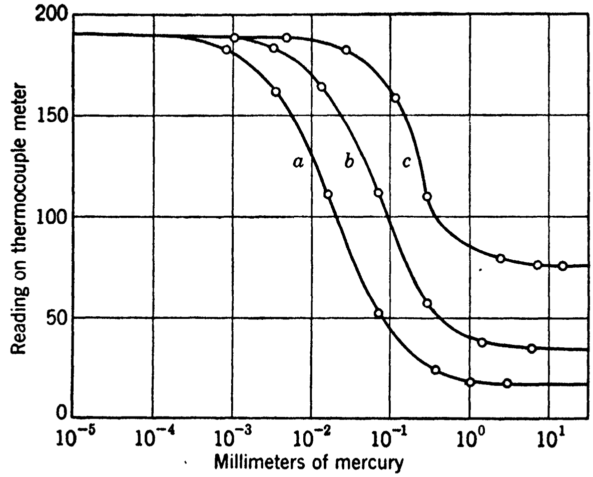

FIG. 36. Plots of readings on thermocouple meter versus log P_{mm} (for air), at three values of the heating current, with gauge shown in Fig. 35.

W. J. H. Moll and H. C. Burger,[110] with a similar design of gauge, in which a more sensitive thermocouple was used, obtained an operating range from about 10^{-1} to 10^{-4} mm. C. Weisz and H. Westmeyer[111] were able to extend the range down to about 10^{-5} mm, by using a very thin wire (0.04 mm diameter).

The construction used by W. Bartholomeyczyk[112] is very simple. A four-lead glass stem is used. The heater, which is a 0.01 mm platinum wire, is fastened to the two outer leads, and at the center of the heater there is fastened the junction of the thermocouple, consisting of 0.01-mm iron (or copper) and Constantan wires. These are connected to the two inner leads of the stem. The range of operation is given as 10 to 0.1 mm.

---

[110] *Z. tech. Physik*, **21**, 199 (1940).

[111] *Z. Instrumentenk.*, **60**, 53 (1940).

[112] *Z. tech. Physik*, **22**, 25 (1941).

The construction of a thermocouple gauge developed in this laboratory by N. T. Gordon is illustrated in Fig. 37*a*. It consists of a platinum-iridium ribbon 3.66 cm by 0.0234 by 0.0078 cm, to the center of which is welded a thermocouple of Nichrome-advance ribbon (0.01 cm by 0.00125 cm), all mounted on a four-lead stem in a tubular bulb similar to that used for the UX-199 radiotron. Figure 37*b* shows the circuit used. A constant current of approximately 0.030 to 0.050 amp, depending on the range of pressures to be measured, is passed through the platinum ribbon, and a sensitive microammeter is used to read the thermocouple emf. The heater filament operates at a temperature varying from 100° C to 200° C.

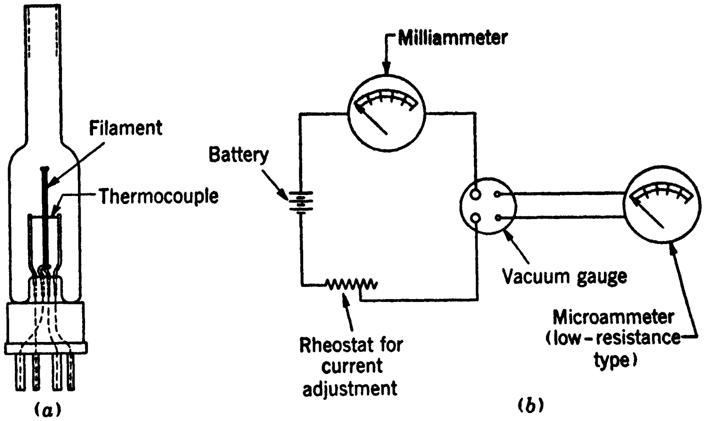
Filament
Thermocouple
(a)
Milliammeter
Battery
Vacuum gauge
Rheostat for current adjustment
Microammeter (low-resistance type)
(b)

FIG. 37. Thermocouple gauge and auxiliary circuit.

Figure 38 shows plots of log P_μ versus microammeter readings, obtained by means of this gauge, for hydrogen, nitrogen, and xenon. In these observations the walls of the tube were at room temperature ($T_0 \approx 300$). As will be observed the gauge is most sensitive, under these conditions, for the range 10^{-2} to about 10^{-1} mm.[113]

For all-metal vacuum systems, R. T. Webber and C. T. Lane[114] have designed a thermocouple gauge which consists of Chromel and Alumel wires arranged on a support in the form of an X, welded at the center. Constant current is supplied to the lower arms of the X by a battery and resistance, and the temperature of the junction is measured by a galvanometer in series with a high resistance, connected to the upper arms of the X. The calibration curves resemble those shown in Fig. 38.

---

[113] A similar type of gauge has been described by G. C. Dunlap and J. G. Trump, *Rev. Sci. Instruments*, **8**, 37 (1937).

[114] *Rev. Sci. Instruments*, **17**, 308 (1946).

Resistance Gauges (Pirani-Hale Type). The fact that the heat conductivity of a gas at low pressures decreases linearly with the pressure was applied by E. Warburg, G. Leithauser, and E. Johansen[115] to the construction of a gauge in which the variation in temperature of a bolometer strip was determined from the change in resistance.

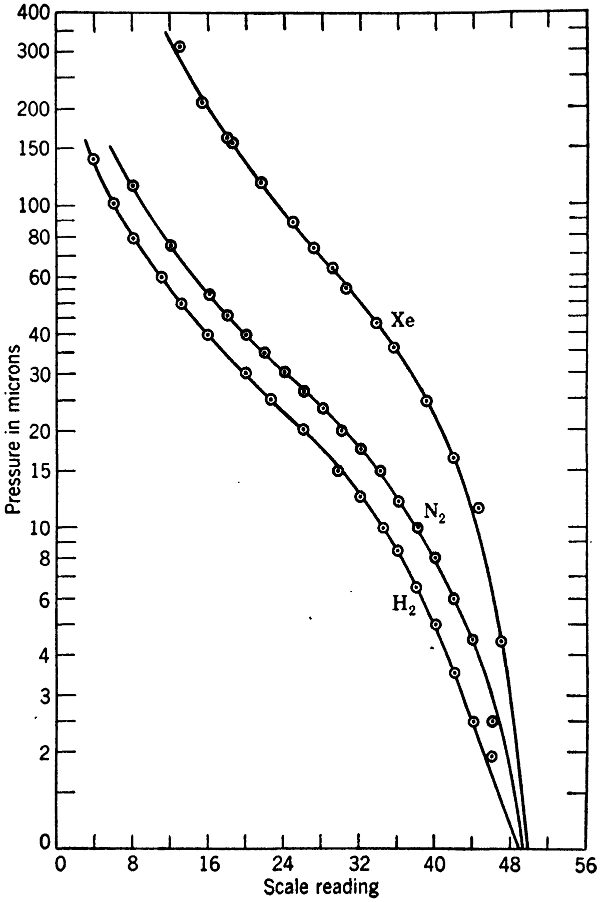

FIG. 38. Calibration plots for gauge shown in Fig. 37.

M. Pirani[116] pointed out that, in order to construct a gauge based on the relation between the heat conducted from a wire and the pressure, three different schemes could be used.

---

[115] *Ann. Physik,* **24,** 25 (1907).

[116] *Verhandl. deut. physik. Ges.,* **8,** 686 (1906).

1. The voltage on the wire is maintained constant, and the change in current is observed as a function of the pressure.

2. The resistance (and consequently the temperature) of the wire is maintained constant, and the energy input required for this is observed as a function of the pressure.

3. The current is maintained constant, and the change in resistance is observed as a function of the pressure.

The first scheme was tried using an ordinary 110-volt tantalum lamp. Better results, however, were obtained when the tantalum wire was clamped tightly to the anchor wires in order to keep constant the heat loss through the supports. With the improved instrument the two other methods were tried, using a Wheatstone bridge arrangement to measure the resistance of the wire, and the third one was finally recommended as the most sensitive for making pressure measurements.

While the principle of the Pirani gauge is thus extremely simple, the sensitivity actually obtained by Pirani was not very great, the lower limit of accuracy being around 0.1 micron.

An improved form of this gauge, constructed by C. F. Hale,[117] is illustrated in Fig. 39. The following description is quoted from Hale's paper:

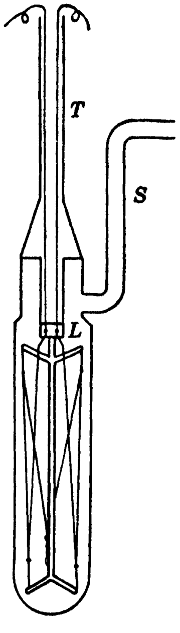

FIG. 39. Hale's improved form of Pirani gauge.

> A piece of pure platinum wire, 0.028 mm in diameter and 450 mm long, is mounted upon a glass stem carrying two radial glass supports near the top and three at the bottom. The wire is anchored to these radial supports by means of short pieces of platinum wire 0.052 mm in diameter. The anchor is fused into the radial supports at one end, and the other end is made fast to the manometer wire either by an arc weld or by a tiny glass bead. The leading-in wires at *L*, to which the ends of the manometer wire are welded, are of platinum, 0.31 mm in diameter. All of the platinum wire employed in making the manometer was drawn from the same lot of larger wire and was assumed to be of uniform purity. The temperature coefficient of the manometer wire was found to be 0.00376 per cent per degree. The platinum leading-in wires are joined to heavy copper leads (1.1-mm diameter) by welded joints, and these joints are fused into the stem as in electric lamps. The stem is sealed into a tubular bulb 3.2 cm in diameter and 11.4 cm long. This size of bulb is easily obtained, since it is the size regularly used for 50-watt tubular lamps, such as

---

[117] *Trans. Am. Electrochem. Soc.*, **20**, **243** (1911).

are commonly employed for galvanometer illumination. At S is a tube by which the manometer is connected with the system whose pressure is being studied. The upper end of the stem T is considerably elongated to permit the complete immersion of the manometer in a constant temperature bath, whose temperature was approximately 0° C. This stem tube is made of sufficient length to leave 15 cm of it above the level of the bath, a provision which we found to be necessary in order to avoid the condensation of atmospheric moisture upon the top of the tube and the leading-in wires during humid weather. For electrical insulation this tube is packed with purified dry asbestos wool.

A diagram of the electrical connections is shown in Fig. 40. A Wheatstone bridge arrangement was used for measuring the resistance changes; and, in order to increase the sensitivity of the gauge, an exact duplicate was exhausted as carefully as possible to an extremely low pressure, sealed off, and inserted in one arm of the bridge as a compensator. Both the compensator C and manometer I were kept immersed in the constant-temperature bath. R_1 was a Manganin wire resistance of 925.6 ohms, and R_2, a decade plug box containing 10,000 ohms. The strength of the current, as indicated by the milliammeter A, was maintained constant at $9.25 \cdot 10^{-3}$ amp by means of the battery and resistance R_3. This current was sufficient to raise the temperature of the wire in the manometer and compensator to about 125° at the lowest pressures.

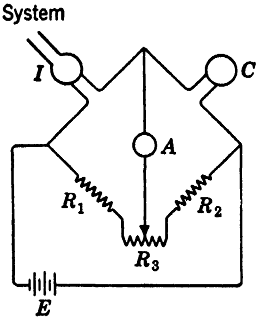

FIG. 40. Electrical circuit for Pirani gauge.

In calibrating the gauge against a McLeod gauge care had to be taken to keep mercury vapor out by means of a liquid-air trap inserted between the manometer and the remainder of the system.

The indications of the manometer are dependent upon the thermal conductivity of the gas used. Hale's measurements showed that the lower limit of sensitivity for a gauge of this construction is about 10^{-5} mm.

Subsequently further measurements with a Pirani gauge were carried out by Misamichi So[118] and N. R. Campbell.[119]

The construction of gauge used by Misamichi So differed in a few slight details from that of Hale. It was found that the sensitivity of the gauge is higher the lower the temperature of the surrounding bath. At 0° C, and with a heating current of 0.03 amp for a platinum wire 0.076

---

[118] *Proc. Phys. Math. Soc. Japan*, 3rd Ser., **1**, 152 (1919).

[119] *Proc. Phys. Soc. London*, **33**, 287 (1921).

mm in diameter, the sensitivity, as measured by $(dR/dP)(1/R)$, was observed to be $1.38 \cdot 10^{-3}$ per $1 \cdot 10^{-4}$ mm of mercury. Furthermore, varying the heating current from 0.03 to 0.05 amp was found to produce no change in sensitivity.

Instead of measuring the change in resistance, Campbell measures the potential which must be supplied to the Wheatstone bridge to keep the resistance (and therefore the temperature) of the wire constant. Three Manganin resistances are chosen so that the bridge is balanced when the manometric wire is at a convenient temperature, say 100° C. A voltmeter is connected to the terminals of the bridge, and the potential across the whole bridge is varied by means of a rheostat in the battery circuit until a balance is obtained.

If V_0 is the potential required for a balance when $P = 0$, and V is the potential at any pressure P, it is found that

$$\frac{V^2 - V_0^2}{V_0^2} = k \cdot f(P), \tag{4}$$

where k is a constant for any given gauge and $f(P)$ is a function of the pressure. The function is actually found to be approximately proportional to P. For pressures ranging as high as 0.15 mm, as pointed out by Campbell, this method of using the Pirani gauge is specially adapted where it is desirable to measure pressures greater than about 1 micron. For such pressures the method used by Hale does not give a linear relation between change in resistance and pressure.

Of interest in this connection is the investigation by H. Murmann[120] on the variation in sensitivity with variation in the radius of wire (r), current (I), and temperature difference ($T_1 - T_0$).

Let us consider the case of a metal filament at temperature T_1 in a tube the walls of which are at temperature T_0. The energy loss per unit area is given by the relation

$$\frac{I^2\rho_0}{2\pi^2 r^3}\{1 + \alpha(T_1 - T_0)\} = \sigma_1 T_1^4 - \sigma_0 T_0^4 + KP(T_1 - T_0), \tag{5}$$

where ρ_0 denotes the specific resistivity at T_0, α is the temperature coefficient of resistance, K denotes a constant the value of which is determined from equation 3, and σ_1, σ_0 are radiation constants defined by means of equation 1.

For *constant watt input* and in good vacuum ($P = 0$), the value of $T_1 - T_0$ is constant (for a given filament material) for constant values of I^2/r^3. That is, in a vacuum, the temperature is a function of $I/r^{3/2}$.

---

[120] *Z. Physik*, **86**, 14 (1933).

As the pressure is increased at *constant value of* I^2/r^3, $T_1 - T_0$ must decrease. This is illustrated by the plots in Fig. 41 taken on a wire (90% Pt + 10% Ir), having a diameter of $5.1 \cdot 10^{-3}$ cm (2 mil). The

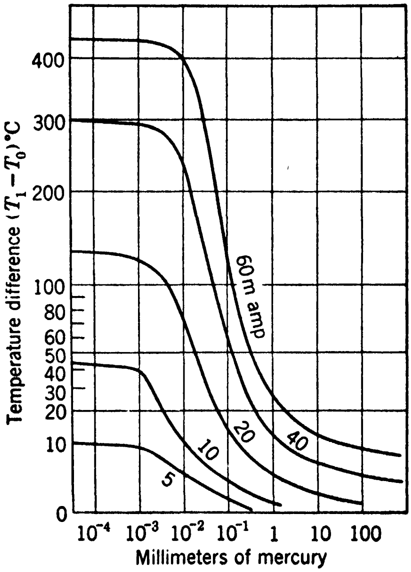

FIG. 41. Log-log plots of temperature difference (between wire and walls of Pirani gauge) versus pressure, for a series of values of the heating current.

currents are given in milliamperes and the pressures in millimeters. Evidently the value of the ratio

$$S = \frac{\Delta(T_1 - T_0)}{(T_1 - T_0)} \cdot \frac{P}{\Delta P}$$

varies with P. From the plots, Murmann finds that, at $P_{mm} = 10^{-4}$, the maximum value of S is obtained for $I = 22.3$ ma. On the other hand, as P is increased, the value of I for maximum value of S must be increased.

These conclusions are in agreement with the observations made by F. Knauer and O. Stern[121] in using a hot-wire manometer to determine the intensity of a molecular beam of a light gas.

An investigation on the design of a sensitive form of Pirani gauge was carried out by L. F. Stanley.[122] Two identical tubes were placed, as in

---

[121] *Z. Physik*, **53**, 766 (1929).

[122] *Proc. Phys. Soc., London*, **41**, 194 (1928–1929).

Hale's arrangement, in the opposite arms of a Callendar-Griffith's bridge. The heated element in each tube was a loop of 0.001-in. platinum wire 10 cm in length, together with a compensating loop of the same wire, 2 cm in length. Constant current was supplied to the filaments. In using the gauge "the short loop of the manometer was placed in the arm of the bridge containing the longer loop of the compensator, and vice versa."

It was observed that, with the walls at constant temperature, the sensitivity (measured as dR/dP, where R is the resistance, in bridge units) was greater for a filament temperature of 100° C than for a temperature of 30° C. Increasing the temperature beyond 100° C seemed to have little effect on the sensitivity. Variation of the temperature of the glass walls from 100° C to about −180° C showed that, the lower the temperature, the greater the sensitivity of the arrangement to variations of pressure. Pressures in the range $2 \cdot 10^{-3}$ mm to $4 \cdot 10^{-6}$ mm could be measured very satisfactorily.

In this laboratory H. C. Thompson and E. F. Hennelly developed a simple form of direct-reading gauge which has proved very convenient in practice. The measuring tube and compensator each consists of a glass tube 1 in. in diameter and approximately 3 in. long in which four, or more, standard 25-watt, 115-volt tungsten-filament coils are welded to supports, the total resistance being about 15 ohms at room temperature. The resistances R_1 and R_2 (see Fig. 40) are about 14 ohms each, and the resistance R_3 about 2 ohms, which can be adjusted to obtain zero current in the ammeter A. A dry-cell battery supplies the constant source of potential.

Figure 42 shows plots of the current (in milliamperes) versus P_μ for a typical outfit. In order to prevent confusion three scales for pressure have been used. These scales are displaced along the axis of abscissas, so that the origin in each case is at $P_\mu = 0$. Curves A, B, B', and C refer to dry air at three different battery voltages; curves D and E refer to hydrogen and argon, respectively. It will be observed that, for pressures below about 40 microns, the plots are linear and practically independent of battery voltage.

By use of a sensitive milliammeter and care in construction of the tube and compensator, pressures as low as 10^{-3} micron may be measured by this arrangement. Ordinarily, however, where it is desired to use a relatively cheap type of indicating instrument, the lower limit of sensitivity is between 10^{-2} and 10^{-1} micron.

It should be added that Pirani gauges consisting of two tubes (one as compensator) and of a case containing the requisite electrical circuits are available from a number of manufacturers, and they have found wide application in vacuum technique.

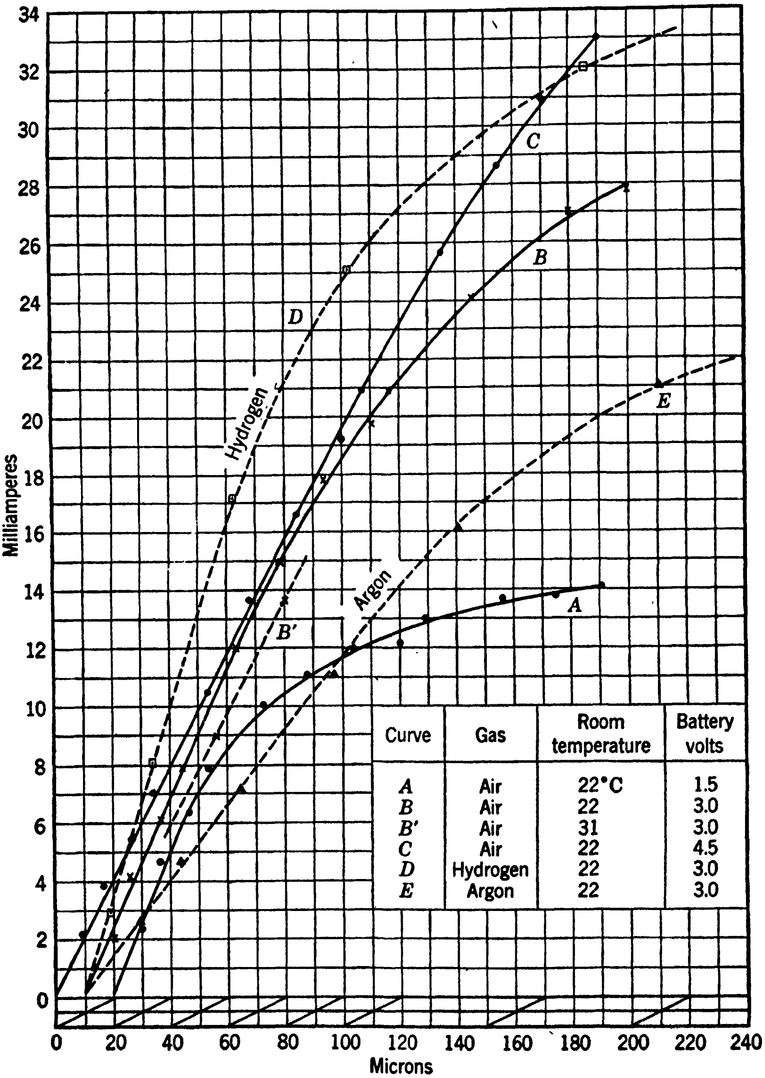

Curve	Gas	Room temperature	Battery volts
A	Air	22°C	1.5
B	Air	22	3.0
B'	Air	31	3.0
C	Air	22	4.5
D	Hydrogen	22	3.0
E	Argon	22	3.0

FIG. 42. Calibration plots for Pirani gauge.

The problem of designing a very sensitive gauge for measuring the intensity of a molecular beam of gas has been considered by A. Ellett and R. M. Zabel.[123]

---

[123] *Phys. Rev.*, **37**, 1102, 1112 (1931).

If in equation 5 above we assume $\sigma_1 = \sigma_0$, and that the energy loss by conduction is negligible compared to that by radiation, then, at constant watt input,

$$\frac{dT}{dP} = \frac{C(T - T_0)}{T^3}, \tag{6}$$

where C is a constant. The expression on the right-hand side of this equation has a maximum value for $T = \frac{3}{2}T_0$, and substituting this value in the last equation we obtain the relation

$$\left(\frac{dT}{dP}\right)_{\text{max.}} = \frac{C'}{T_0^2}, \tag{7}$$

where C' is another constant.

Hence the value of the maximum temperature change for a given change in pressure varies inversely as the square of the absolute temperature of the walls of the tube in which the heater is sealed. Since the resistance, R, varies linearly with T, it also follows that

$$\frac{dR}{R_0 dP} = \frac{C''(T - T_0)}{T^3}, \tag{8}$$

where C'' is a constant, and hence the change in resistance with pressure has the same maximum as dT/dP.

From these relations the following conclusions are drawn by the investigators:

1. In a bridge circuit, of which the hot wire constitutes one arm, which is operated at constant watt input, the galvanometer deflection should be proportional to the pressure.

2. The sensitivity of the gauge is proportional to the square root of the area of the wire.

3. For maximum sensitivity the wire should be as long as convenient, and the diameter should be adjusted so that its resistance is of the same order of magnitude as that of the galvanometer.

The construction of a gauge which is described as sensitive to pressures of less than 10^{-5} micron is shown in Fig. 43. The wire used had a diameter of 0.001 in. The writers state,

> The sensitivity attained by the use of nickel wire is in all cases greater than that for tungsten. Nickel wire has the additional advantage that it may be flattened more easily than tungsten which greatly increases the sensitivity. . . . Immersing the walls of the gauge in liquid oxygen approximately multiplied the sensitivity of the gauge by 2 when the galvanometer resistance is high and by 7 when the galvanometer resistance is low.

The authors conclude that a compensating gauge is not as satisfactory as one gauge immersed in a constant-temperature bath.

For reading pressures as low as $2 \cdot 10^{-3}$ micron, A. L. Reimann[124] has used a manometer constructed as follows: To a four-lead stem in a tubular bulb were attached two independent stabilized tungsten spiral filaments, each of 0.047 mm diameter wire, of 28 cm length, wound into a spiral 0.9 mm in diameter and 6 cm in length. Each filament was flashed in a vacuum at 20 volts for 10 minutes prior to use. This tube was clamped to a similar evacuated and sealed-off tube and both were immersed in a water-bath at room temperature. The filaments in each bulb were connected up to form opposite arms of a Wheatstone bridge, across whose ends a P.D. of 2 volts was maintained. The bridge was balanced with a good vacuum in the manometer by adjusting a very small variable resistance inserted in one arm, and the "out-of-balance" current in a microammeter was then taken as a measure of the pressure. By inserting a resistance in series with the microammeter the manometer could be made less sensitive.

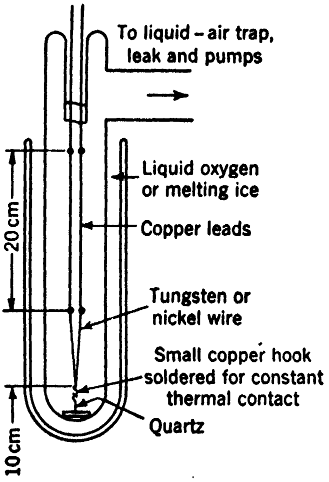
To liquid-air trap, leak and pumps
Liquid oxygen or melting ice
Copper leads
Tungsten or nickel wire
Small copper hook soldered for constant thermal contact
Quartz
20cm
10cm

FIG. 43. Construction of ultra-sensitive Pirani gauge (Ellett and Zabel).

This gauge was used by Reimann to investigate rates and extent of clean-up of hydrogen by magnesium.[125]

A similar arrangement of two manometers has been described by W. Hunsmann.[126] Each manometer consists of a cylindrical bulb having a 0.2-mm nickel wire along the axis. In order to obtain reproducible results, even at higher pressures, the filament is attached at one end to the lead-in wire by a steel spring which is short-circuited by means of a copper wire.

Instead of using two tubes in the two arms of a Wheatstone bridge, E. J. Scott[127] has suggested measuring the resistance of the wire by feeding the voltage drop across it onto the grid of a triode tube. This allows the pressure to be read directly on the calibrated scale of a galvanometer contained in the plate circuit. Although the scale reading is a simple function of the pressure, the relation is by no means linear over the entire range.

---

[124] *Phil. Mag.*, **16**, 673 (1933).

[125] See Chapter 10, section 2.

[126] *Z. Elektrochem.*, **44**, 540 (1938).

[127] *Rev. Sci. Instruments*, **10**, 349 (1939).

Figure 44 shows the electrical circuit. The hot wire constitutes the resistance R_1,

which consists of the filaments of three 6-watt lamps connected in series to give about 700 ohms. The resistance R_2 is made up of a 20,000-ohm fixed resistor and a 2000-ohm variable resistor. The two resistances, R_1 and R_2, constitute a simple potentiometer, or bleeder. The resistance R_3 is a load resistance of 10,000 ohms. This serves to give the triode a more nearly linear characteristic for values of the grid voltage near cut-off. . . . The voltage $E_2 + E_3$ across the resistances $R_2 + R_3$ is the plate voltage of the tube. The voltage E_1 across the Pirani resistance R_1 is the grid voltage of the tube.

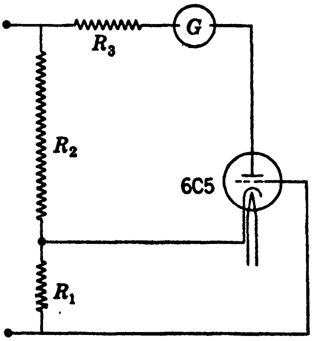

FIG. 44. Electrical circuit for automatic gauge (Scott).

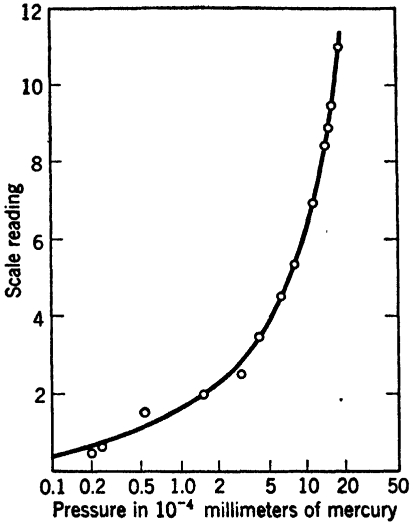

FIG. 45. Calibration curve for Pirani gauge circuit shown in Fig. 44.

The resistance R_2 is adjusted to give a certain plate current for a known pressure, and as the pressure changes both E_1 and E_2 will vary in opposite directions while $E_1 + E_2$ remains constant. With decrease in pressure, R_1 and, consequently, E_1 increases, which makes the grid more negative and decreases the plate current. The author states that the arrangement "affords a simple, rapid, and reliable means of measuring pressures between 10^{-2} and 1 micron." Figure 45 shows the calibration curve obtained, presumably, with air.

The observation that certain *semi-conductors* possess a high (negative) temperature coefficient of resistance has been applied by E. Weise[128] to the construction of a Pirani gauge. In the earlier form the resistance consisted of a small thin-walled tube of magnesium-titanium spinel. A tube 1 mm in diameter, 30 mm long, and with a wall thickness of 0.1 mm, has a resistance of 15,000 ohms. In the more recent form this resistance is in the form of a thin film, 20 microns thick and 10 cm^2 in area. The thin film is attached to two supporting spirals of tungsten wire[129] as shown in Fig. 46.

---

[128] *Z. tech. Physik*, **18**, 467 (1937); **24**, 66 (1943).

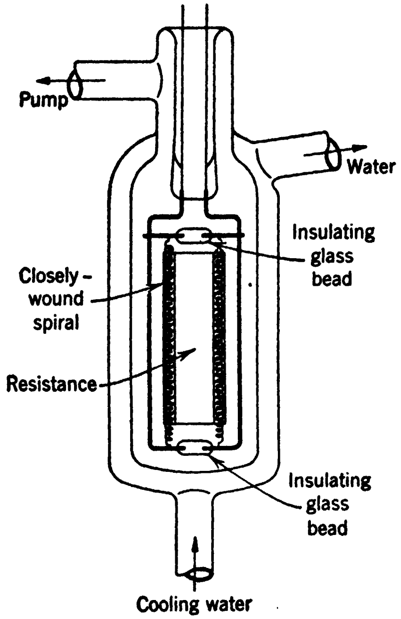

FIG. 46. Pirani gauge involving use of a semi-conductor as heated element.

For high accuracy a bridge circuit is used, and water at constant temperature (city water) is circulated through the outer jacket. For ordinary tests, the resistor is connected to another series resistor, and the current indicated at constant voltage across the high resistance is a function of the pressure. The values chosen for the constant voltage and series resistor depend upon the desired pressure range. Figure 47 shows calibration curves for air and hydrogen for a resistor under conditions in which the pressure was varied from 1 mm to 10^{-3} mm. The author states that, by varying the voltage and series resistor, it is possible

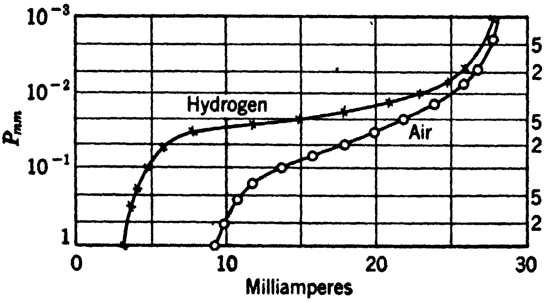

FIG. 47. Calibration curves for air and hydrogen with gauge shown in Fig. 46.

---

[129] No description is given in the original paper of the method used for producing such thin films of the semi-conducting material.

to vary the range of sensitivity from atmospheric pressure down to 10^{-6} mm.

In the original paper there is also described a relay circuit for using the gauge for maintaining constant, low gas pressure in a system.

A semi-conductor, having a high negative temperature coefficient of resistance, has also been utilized by J. A. Becker, C. B. Green, and G. L. Pearson in the development of the *thermistor manometer*.[130] The thermistor element consists of a small bead of a semi-conducting material which is fastened to two leads and sealed into a small bulb. Two elements are used, with characteristics matched so that they can be operated in adjacent arms of a Wheatstone bridge, as shown in Fig. 48. One element (V-550A) is sealed off in good vacuum and gettered. This serves as a temperature compensator for the other element (V-550B), which is connected to the system in which the pressure is to be determined. Typical characteristics of an element at 25° C and 10^{-3} micron are as follows:

Resistance at zero power	approximately 50,000 ohms
Voltage at 0.5 ma	approximately 2 volts
Voltage at 3.0 ma	approximately 1 volt

The suggested circuit constants are as follows:

Current, each thermistor in high vacuum	approximately 3 ma
Voltage across bridge (ac or dc)	approximately 9 volts
Bridge ratio arms	approximately 2,000 ohms
Bridge balance potentiometer	approximately 1,000 ohms
Meter resistance	approximately 10,000 ohms

The bridge is balanced under conditions of good vacuum in the manometer, and the off-balance current then becomes a measure of the pressure. The exact calibration varies with the nature of the gas, and Fig. 48 shows two such calibration curves, plotted on log-log scales, obtained on a thermistor manometer by A. H. Young in this laboratory, by means of a McLeod gauge. The ordinates correspond to milliamperes through a 10,000-ohm resistance.

The fact that these plots are practically linear over the range of pressures from 1 to about 1000 microns gives this type of gauge an advantage over the thermocouple type of gauge and should make it extremely useful in vacuum technique.

---

[130] The writer wishes to acknowledge his appreciation of the kindness of Dr. Becker in sending him the description and samples of thermistors in advance of publication. A paper on the properties and applications of thermistors was presented at the A.I.E.E. meeting, June 24–28, 1946. See *Trans. A.I.E.E.*, **65**, 711 (1946), also *Bell Sys. Tech. J.*, **26**, 170 (1947).

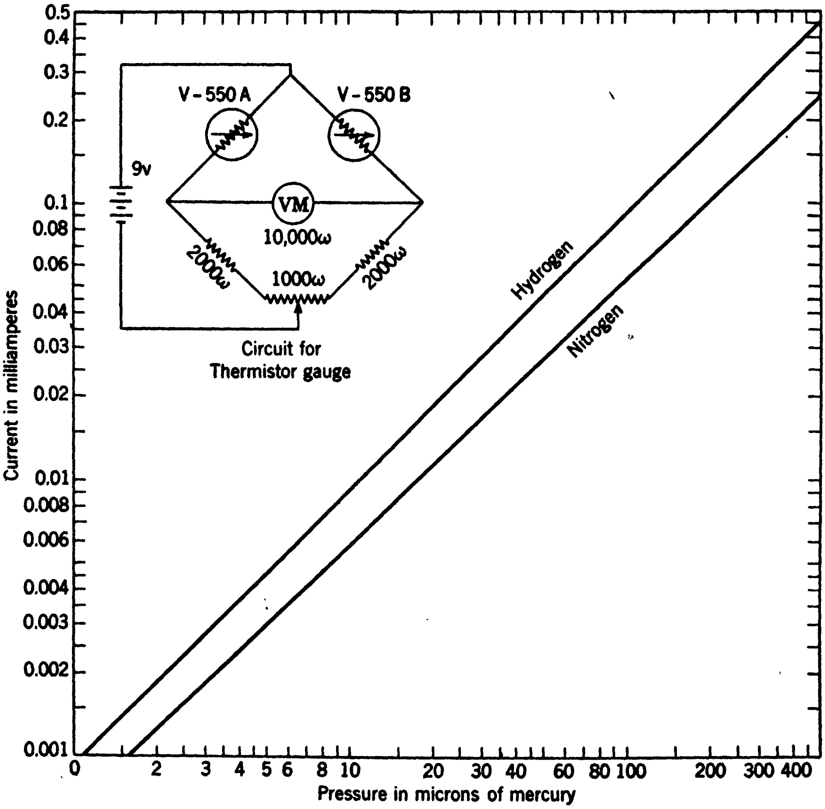

FIG. 48. Diagram of circuit and calibration plots for hydrogen and nitrogen with thermistor gauge.

Gauges Which Involve Linear Expansion of Metal Wire or Strip. Since the linear expansion of a heated wire is a function of the temperature it is evident that such observations may also be applied to measure the pressure of a gas in which the wire is located.

A manometer based on this principle has been described by H. Murmann.[131] Two very thin platinum-iridium wires are each fastened at both ends to a framework and connected in the center to a spiral which can be used to indicate the expansion of the wires when heated. The lower limit of sensitivity is apparently about 10^{-3} mm.

[131] *Z. tech. Physik*, **14**, 538 (1933).

Much more practical are gauges in which bimetallic strips are used. H. Klumb and Th. Haase[132] have described three different forms of such a gauge.

Let a_1 denote the thickness and E_1 the modulus of elasticity of one of the metals, and a_2 and E_2 denote the corresponding values for the second metal. Then, according to W. A. Michelson,[133]

$$\frac{a_1}{a_2} = \sqrt{\frac{E_1}{E_2}}. \tag{9}$$

Furthermore, if l denotes the total length, and d the total thickness, of the strip, then the deflection, y, for a temperature rise of $t - t_0$ degrees C is given by the relation

$$y = 10^{-4}k \cdot \frac{l^2}{d} (t - t_0), \tag{10}$$

where k denotes the "specific" deflection for $l = 100$ mm, and $d = 1$ mm. The value of k is proportional to the difference in coefficients of linear expansion and varies from 0.1 to 0.14 mm for industrially available bimetallic strips.

Figure 49 shows the construction of a gauge in which the deflection is observed by means of a microscope. The sketch at the right shows further details. The bimetallic strip has the dimensions 1 mm by 0.1 mm by 35 mm. To this is fastened a glass fiber about 70 mm long which carries a weight of about 100 mg. At 0.1 volt, the heating current in the strip is about 250 milliamp.

Figure 50 shows calibration curves for three gases in the range 10 to 10^{-5} mm. With the microscope used, 1-mm deflection was equal to 30 scale divisions.

In another design of the gauge the band is in the form of a spiral having 14 turns and 6-mm outside diameter. To the lower end of this spiral is attached a galvanometer mirror, and the deflections are observed optically. The zero position of the mirror is adjusted by means of the torsion head, at the top of the greased joint, and the heating current is applied at the upper and lower terminals.

The plot of angular deflection of the mirror as a function of pressure exhibits a curve quite similar in its characteristics to that shown in the previous figure.

In the third form, compensation is provided for variations in external temperature by means of a second heated spiral made of bimetallic strip.

---

[132] *Physik. Z.*, **37**, 27 (1936).

[133] *Physik. Z.*, **9**, 18 (1908).

W. Seeman[134] has pointed out that a similar design of low-pressure gauge utilizing a compensation spiral has been developed by Brown, Boveri and Company, Switzerland.

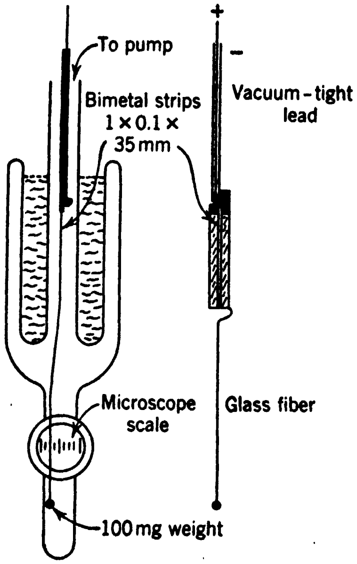

FIG. 49. Bimetallic strip manometer with microscope scale for reading deflection (Klumb and Haase).

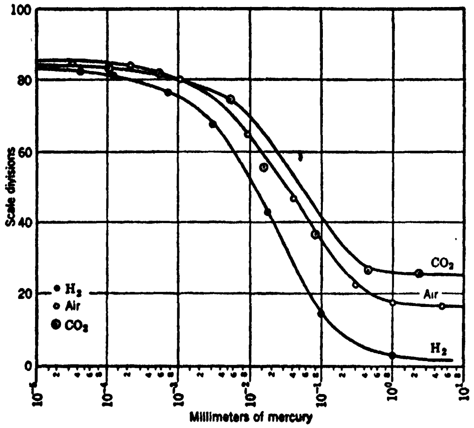

FIG. 50. Calibration curves for manometer shown in Fig. 49, for three gases, with cooling liquid at 0° C.

7. IONIZATION GAUGES

Design. The kinetic energy acquired by an electron in passing through a potential difference of V volts corresponds to Ve, where e is the charge of the electron. When this energy exceeds a certain critical value, corresponding to the voltage V_i, there is a definite probability, which varies with V and with the nature of the gas, that collisions between electrons and molecules will result in the formation of positive ions. The relatively high-velocity electron, on colliding with a gas molecule, drives an electron out of the molecule, leaving it positively charged. The values of V_i for different monatomic vapors and gases vary from 3.88 volts for cesium to 24.58 volts for helium, which has the highest ionizing potential. For oxygen, nitrogen, hydrogen, and other diatomic gases, the values of V_i range around 15 volts.

---

[134] *Physik. Z.*, **37**, 446 (1936).

For a constant value of the accelerating voltage, in excess of V_i, the number of positive ions formed per electron should vary linearly with the pressure, at least at low pressures, since any one electron could not possibly make more than one collision in passing from the cathode to the anode.[135] Consequently a determination of the rate of production of positive ions for a given electron current should yield a measure of the pressure. This leads to the following definition for the *sensitivity*, S, of a gauge of this type:

Let i_p and i_e denote the positive ion and electron currents respectively (both expressed in the same units), at a given pressure P. Then

$$S = \frac{i_p}{Pi_e} \tag{1}$$

or

$$P = \frac{1}{S}\frac{i_p}{i_e}. \tag{2}$$

Thus $S = m \cdot 10^{-3}$ per micron signifies that the sensitivity is m microamperes per milliampere per micron.

It will be observed that

$$S \text{ per microbar} = 0.75S \text{ per micron.}$$

In 1916, O. E. Buckley[136] published the following description of the construction of an ionization gauge:

> The manometer consists of three electrodes sealed in a glass bulb which serve as cathode, anode, and collector of positive ions. The cathode may be any source of pure electron discharge such as a Wehnelt cathode or a heated tungsten or other metallic filament. The exact forms of the electrodes are not of great importance. The collector is preferably situated between the other two electrodes and is of such form as not to entirely block the electron current to the anode. A milliammeter is used to measure the current to the anode and a sensitive galvanometer to measure the current from the collector which is maintained negative with respect to the cathode so as to pick up only the positive ions.
>
> Currents [he continues] from 0.2 to 2.0 milliamperes were used with from 100 to 250 volts between cathode and anode. The collector was held at 10 volts negative with respect to the cathode. The resulting current to the collector at a pressure of 10^{-3} mm was about one-thousandth the current to the anode and at lower pressures was proportionately less.

---

[135] It should be observed that, for low-velocity electrons such as are obtained in the ionization gauge, the mean free path for electrons is $4\sqrt{2}$ times the mean free path for the molecules, while for ions the mean free path is $\sqrt{2}$ times that for the molecules. See J. D. Cobine, *Gaseous Conductors*, McGraw-Hill Book Company, 1941.

[136] *Proc. Natl. Acad. Sci. U.S.*, **2**, 683 (1916).

Evidently, the lower limit of pressure that can be measured with such a gauge depends upon the sensitivity of the indicating instrument in the collector circuit, and this may be considered the most important feature of the ionization gauge from the point of view of laboratory vacuum technique. Certain disadvantageous features about the use of the gauge will be discussed in a subsequent section.

Any standard construction of three-electrode device, such as used in commercial radio tubes, may be utilized as an ionization gauge. Two different types of circuits have been suggested: (*a*) the "internal control" type, in which the middle electrode (grid of a triode) functions as positive-ion collector; and (*b*) the "external control" type, in which the outer electrode (plate of a triode) functions as positive-ion collector. These are illustrated in Figs. 51(*a*) and (*b*), respectively.

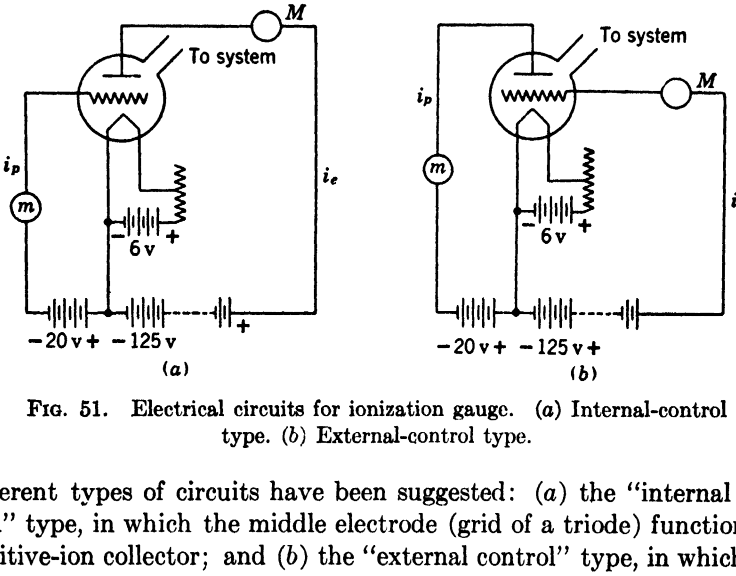

FIG. 51. Electrical circuits for ionization gauge. (*a*) Internal-control type. (*b*) External-control type.

The meters *m* and *M* indicate the positive-ion and electron currents, respectively.

The potentials used may be varied from about 100 to 300 volts on the anode and from −2 to −25 volts on the ion collector. Also, instead of using an A battery to supply current to the filament and connecting the zero potential lead of the B battery to the midpoint of a high resistance across the filament, it is more customary to use an a-c step-down transformer and then connect the zero potential lead to the secondary winding, as shown in Fig. 52.

It is also customary to use the gauge with the external-control type of circuit since it is more sensitive under these conditions.

A design of gauge used by S. Dushman and C. G. Found[137] in their investigation is shown in Fig. 53. The cathode and anode were made of two tungsten filaments, each wound in the form of a double spiral and mounted coaxially on a four-lead stem sealed into the upper end of a glass tube about 4 cm in diameter and 12 cm long. The inner spiral (the cathode) was made of 5 turns of 0.125-mm wire wound on a 0.125-mm mandrel. The outer spiral was made of 3 turns of 0.125-mm wire wound on a 3.65-mm mandrel. The positive-ion collector surrounding the spirals was a molybdenum cylinder about 12 mm in diameter and 12 mm long, supported on a two-lead stem sealed in at the lower end of the tube. As will be observed from the figure, the external-control type of circuit was used, since this provides a longer electrical leakage path between the ion collector and the other electrodes.

---

[137] *Phys. Rev.*, **17**, 7 (1921).

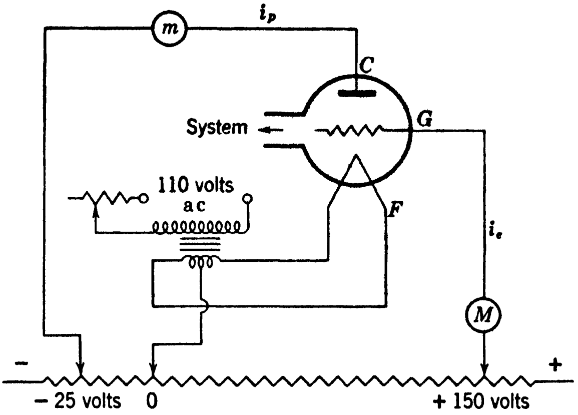

FIG. 52. Electrical circuit for ionization gauge involving use of filament transformer. *C* denotes the positive-ion collector, *G* the electron collector, and *F* the filament.

The best conditions for operation of the gauge were found to be as follows:

(*a*) For very low pressures (below about 1 micron): V_g (voltage on electron collector) = 250, V_c (voltage on positive-ion collector) = −20, and i_e = 20 milliamperes. Under these conditions $S = 5 \cdot 10^{-3}$ per micron for argon, which corresponds to 5 microamperes per milliampere per micron.

(*b*) For higher pressures (1 to 10 microns): V_g = 125, V_c = −20, i_e = 0.5 milliamperes. In this case, $S = 4.6 \cdot 10^{-3}$ per micron for argon.

Before using the gauge for any measurements it is absolutely necessary to bake out the tube to as high a temperature as practicable (450° C for Pyrex or Nonex), and to eliminate all occluded gases from the electrodes and leads. For the filaments this is accomplished by direct passage of current, and for the collector, high-frequency heating is most convenient. To clean the leads supporting the spirals, one spiral is used as hot cathode to bombard the other.

Where a grid instead of the outer spiral is the anode, electron bombardment should be used. During the series of measurements of pressure it is advisable to maintain the filament at a temperature approximately that required for the desired emission, and the anode voltage should be applied *only for the relatively short interval* required to adjust the cathode current for the emission at which it is desired to measure the ion current. This is necessary wherever there is likely to be voltage clean-up of the gas. (See discussion in Chapter 10.)

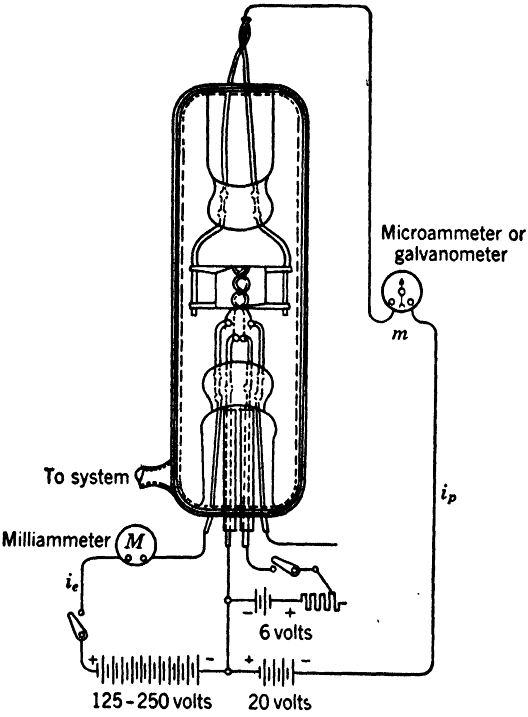

FIG. 53. Construction of ionization gauge and electrical circuits (Dushman and Found).

Since the ionization gauge indicates the *total pressure* ("condensible" and "non-condensible" gases), extra care should be taken to eliminate completely, by means of a liquid-air trap, mercury, water-vapor, etc., from the gauge. The positive-ion current, at constant pressure, is a function of the nature of the gas used, of V_g, and of the electron current, and it also depends upon whether an external or internal type of control circuit is used. It is therefore of interest to discuss briefly some of the observations made by Found and Dushman on the characteristics of the gauge shown in Fig. 53.

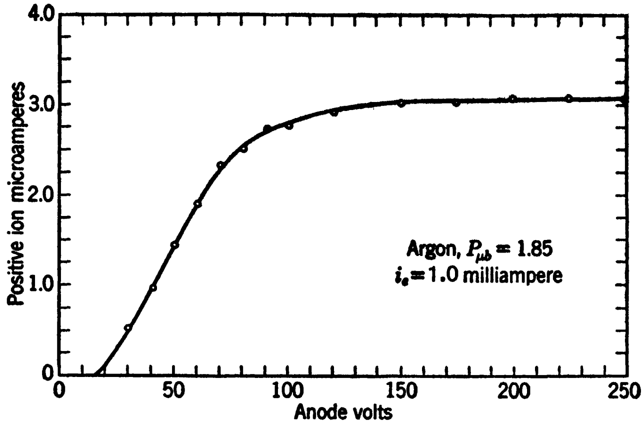

FIG. 54. Positive-ion current versus anode voltage at constant electron current and constant pressure, for gauge shown in Fig. 53. Internal-control type of circuit.

With the external-control connection, it was observed that, other conditions remaining constant, a variation in V_c from 0 to -22 volts resulted in only a small change in the ion current (about 10 per cent). However, it appeared advisable to use the higher negative voltage in order to prevent electrons from reaching the collector.

Figure 57 shows the relation between i_p (positive-ion current in microamperes) and V_g for a constant pressure of 1.85 microbars of argon and $i_e = 0.5$ milliampere.

The effect of varying i_e at the same pressure and at the value $V_g = 250$ is shown in Fig. 55. It will be observed that there was a slight deviation from proportionality at the higher values of i_e.

Using the internal-control connection at the same pressure and same value of V_g, the plot shown in Fig. 56 was obtained. The variation in i_p with V_g, at this pressure and $i_e = 1.0$ milliampere, is shown in Fig. 54.

As will be observed, S is greater for the external- than for the internal-control type of circuit. (This statement is valid for practically all the different types of construction of ionization gauge.) At 1.85 microbars

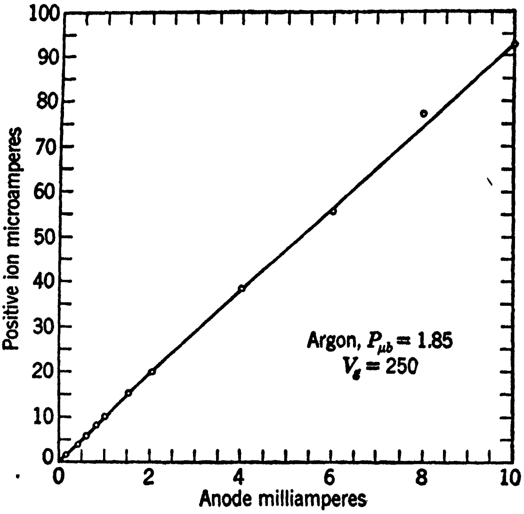

FIG. 55. Positive-ion current versus electron current at constant pressure and constant anode voltage, for gauge shown in Fig. 53. External-control type of circuit.

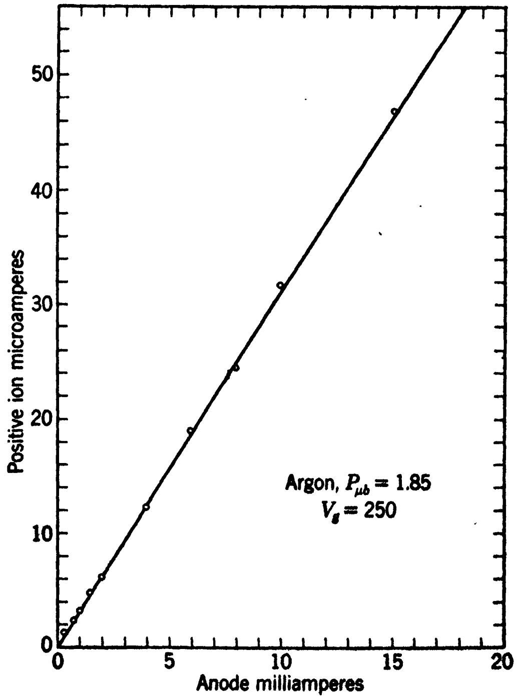

FIG. 56. Positive-ion current versus electron current at constant pressure and constant anode voltage, for gauge shown in Fig. 53. Internal-control type of circuit.

(1.39 microns) argon, $S = 6.85 \cdot 10^{-3}$ per micron for the former, and is about one-third of this value for the latter. On the other hand, the proportionality between i_p and i_e is observed to be valid for higher pressures with the internal control than with the external control. Furthermore, at constant pressure, i_p/i_e is practically constant over the range 125–250 volts on the anode for the internal control while it is sensitive to variations in V_g when the external control is used.

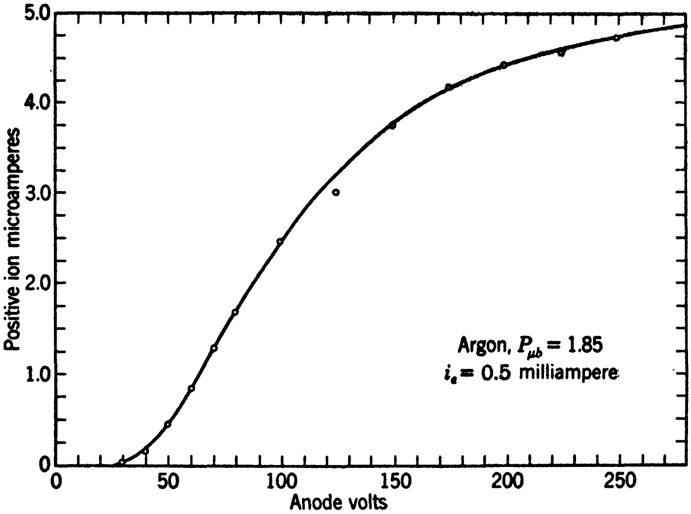

FIG. 57. Positive-ion current versus anode volts at constant pressure and constant electron current, for gauge shown in Fig. 53. External-control type of circuit.

In order to obtain a calibration of the ionization gauge at pressures too low to measure with a McLeod gauge, a method was used based on Knudsen's laws of flow. Between a large bulb (A) connected to a McLeod gauge and the ionization gauge which was connected to another large bulb, B, there was inserted a "resistance" made of a long length of capillary tubing, the conductance of which, F, could be calculated by means of Knudsen's equations. Let C denote the total volume of bulb B and the gauge. Then the pressure, P, in the gauge at any instant is determined by the relation

$$C\frac{dP}{dt} = F(P_A - P),$$

where P_A = pressure in bulb A. Since, under the conditions chosen, P was negligible compared to P_A, the rate of flow could be assumed to be practically constant, and therefore the rate of increase in i_p (at constant value of i_e) as measured by the ionization gauge should be constant and proportional to the rate of increase in pressure calculated from the above relation. The observations confirmed this expected proportionality and showed that, for $i_e = 20$ milliamperes and $V_g = 250$, $S = 5.07 \cdot 10^{-3}$ per micron of argon, down to the lowest pressure. (The variation in S with the nature of the gas is discussed in a subsequent section.)

The constancy of S over the range 10^{-3} to 10^{-5} mm was also confirmed by Misamichi So.[138]

In experiments with vacuum tubes it was discovered by H. Barkhausen and K. Kurz[139] that *high-frequency oscillations* could be maintained in a circuit of the Lecher wire type connected to the grid and plate. The mechanism of generation of these oscillations was investigated by E. W. B. Gill and J. H. Morrell.[140] These oscillations occur even in the absence of the Lecher wires and cause reversals of the positive-ion current that normally flows to the collector. The writer has observed that in a very good vacuum (below about 10^{-6} mm) the microammeter may suddenly indicate that, in spite of its negative potential, the collector is actually receiving electrons.

Apparently the occurrence of this phenomenon depends upon the geometrical design of the ionization gauge, and E. K. Jaycox and H. W. Weinhart[141] have described a construction which is free of this highly undesirable feature. Figure 58 shows working drawings of this gauge. The filament, or cathode, which may be either 0.004 in. thoriated-tungsten, or heavy oxide-coated, is mounted in the shape of a W with three connections, one at each end and one in the center. This is located in the central plane of a nickel wire grid, and the collector is in the form of two parallel nickel plates, connected electrically and located "one on either side of the filament-grid structure." For $V_g = 120$, $V_c = -6$, and $i_e = 20$ milliamperes, a calibration on the pump, against a McLeod gauge, yielded the approximate value $S = 12.5 \cdot 10^{-3}$ per micron. At a pressure of $1 \cdot 10^{-8}$ mm, i_p was found to vary linearly with variation in the value of i_e from 0 to 40 milliamperes, yielding the result $S = 10 \cdot 10^{-3}$ per micron. The value of i_p for a given value of P was observed to vary approximately linearly with anode potential for values of V above about 120, as shown in Fig. 59, so that, for 240 volts, the value of S obtained was about $37.6 \cdot 10^{-3}$ per micron. Hence, with a galvanometer reading as low as $1 \cdot 10^{-9}$ ampere, pressures of the order of 10^{-6} micron could be measured readily. Presumably the residual gas in these observations was nitrogen, although the authors have not so stated in their original paper.

---

[138] *Proc. Phys. Math. Soc. Japan*, I, 76 (1919).

[139] *Physik. Z.*, **21**, 1 (1920).

[140] *Phil. Mag.*, **44**, 161 (1922).

[141] *Rev. Sci. Instruments*, **2**, 401 (1931).

An ionization gauge for the detection of molecular rays has been described by M. J. Copley, T. E. Phipps, and J. Glasser.[142] It consists

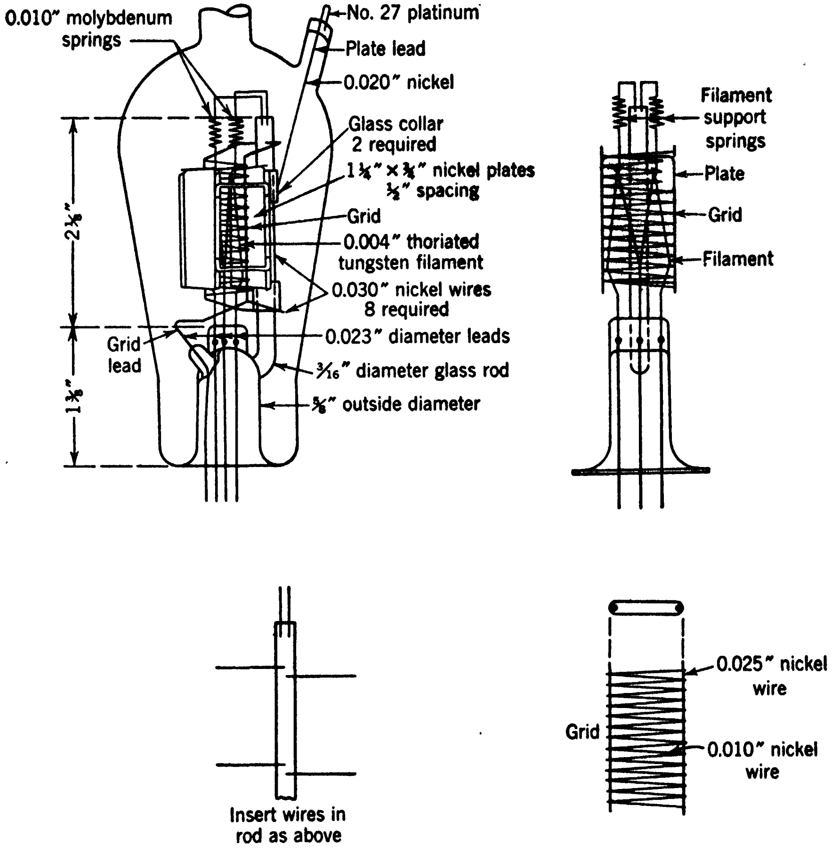

FIG. 58. Working drawings of ionization gauge (Jaycox and Weinhart).

of a 2-mil thoriated-tungsten filament, 1.5 cm long, along the axis of a double helix of 10-mil molybdenum or tungsten, which function as cathode and anode, respectively, while the collector is a thin layer of metal distilled on the walls of the cylindrical tube by evaporation from the anode (which is heated to a very high temperature for the purpose). A flush seal through the glass forms a connection to this deposit. The two inside electrodes can be degassed very readily by heating them to between 2000° and 2500° K, and the metallic deposit is degassed at the same time by the radiation from the helical electrode. The total volume of the gauge is 3 cm^3, and its sensitivity is $9.5 \cdot 10^{-3}$ per micron of argon at all electron current values up to 20 milliamperes.

---

[142] *Rev. Sci. Instruments*, **6**, 371 (1935).

The construction of a gauge for atomic beam measurements has also been described by R. D. Huntoon and A. Ellett.[143] All electrodes had two leads sealed in, which permitted ready outgassing. It was observed that instability could be avoided by making the collector negative by 2 volts and the grid potential not greater than 70 volts. The emission was limited to about 2 milliamperes. With this design, the possibilities of producing Barkhausen oscillations were greatly reduced. According to the authors, with an amplifier and galvanometer in the collector circuit, beam pressure changes of the order of 10^{-8} micron could be detected.

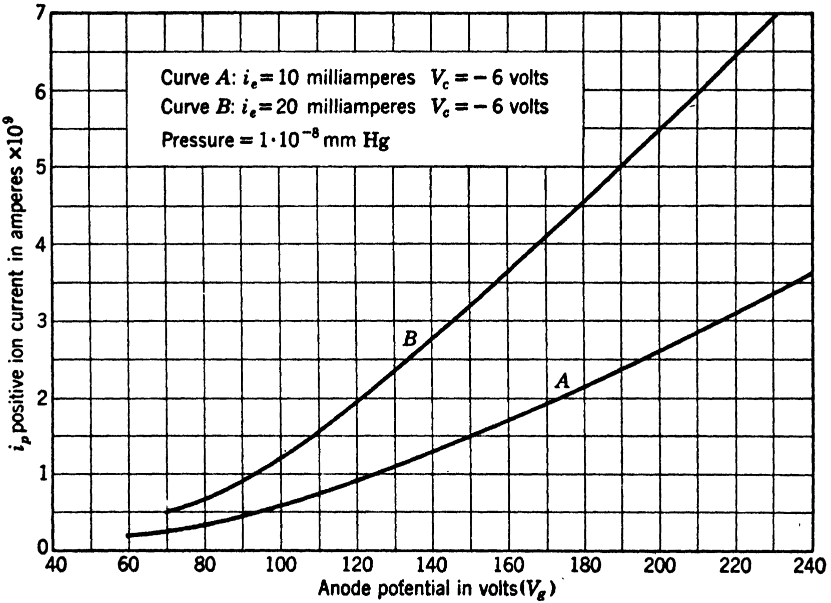

FIG. 59. Plot of positive-ion current versus anode volts at constant pressure and constant electron current for gauge shown in Fig. 58.

A construction which was devised by R. S. Morse and R. M. Bowie[144] and which is widely used by workers in vacuum technique is illustrated in Fig. 60. Here, also, the electron collector is a filament, and the positive-ion collector consists of a platinum film deposited on a portion of the inner wall. "Electrical contact," as the authors state, "is made to this extremely thin, slightly translucent film by means of a fine wire entirely embedded in the glass. The external plate contact is in the form of a metallized ring about the center of the bulb." This construction thus introduced an extremely long leakage path between the inner electrodes and the positive-ion collector. Conditions for operation are as follows:

---

[143] *Phys. Rev.*, **49**, 381 (1936).

[144] *Rev. Sci. Instruments*, **11**, 91 (1940). This gauge is made by Distillation Products, Inc., Rochester, N. Y., and is designated Type VG-1.

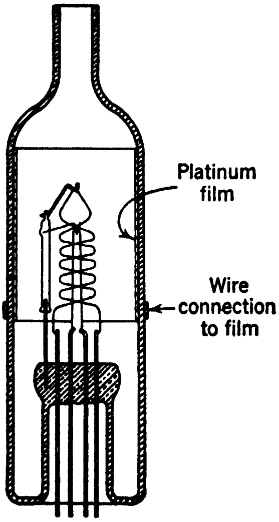

FIG. 60. Ionization gauge (Morse and Bowie).

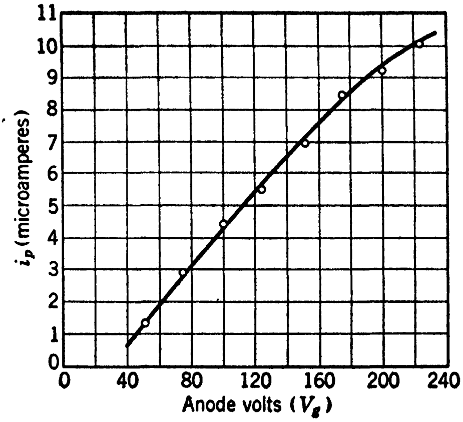

FIG. 61. Plot of positive-ion current versus anode volts at constant pressure and constant electron current, for gauge shown in Fig. 60.

$V_g = 150$, $V_c = -25$, $i_e = 5 \cdot 10^{-3}$ ampere, and the filament current (approximately 2.75 amperes at 3.50 volts) is adjusted to yield the desired emission.

The variation in i_p with V_g, for constant values of i_e and P, is shown in Fig. 61. According to Morse and Bowie, they observed the value $S = 40 \cdot 10^{-3}$ per micron for nitrogen. (See, however, Table 5.)

As has been mentioned previously any standard type of triode radiotron may be used as a gauge, and in the literature there are a considerable number of references to the application of other constructions of gauges than those described above.

Thus, L. N. Ridenour[145] has reported very satisfactory results with a Western Electric D79510 gauge tube. This has a "combined" oxide-coated filament, and it is stated that "this tube appears to stand operation in a poor vacuum better than filaments of other types tried."

Indeed, many users of ionization gauges prefer oxide-coated cathodes just because of the fact that a sudden inrush of air, as the result of a leak, is not as likely to burn out this type of filament as one of tungsten, or, at least, it is possible to switch off the current supply before any permanent damage has been done to the cathode.

An oxide-coated cathode is also used in the gauge developed by C. M. Fogel,[146] shown in Fig. 62. The plates *A* and *D* are of nickel, plate *A* serving as electron collector and *D* as ion collector. The oxide-coated filament *B*, supported by the hook *E*, is placed midway between the plates. A nickel shield, *C*, is placed between *B* and *D* at a short distance above the surface of the press, in order to reduce leakage between cathode and ion collector. The degassing of the plates is carried out by electron bombardment. The potentials used are $V_B = 0$, $V_A = 200$, and $V_D = -13$ volts, and the electron current is set at 20 milliamperes. Under these conditions, the sensitivity of the gauge is stated to be 100 microamperes per micron, presumably for air. While the sensitivity does not vary linearly with V_A, it does increase about 11 per cent with increase from 200 to 250 volts, and it decreases about the same percentage in passing from 200 to 150 volts.

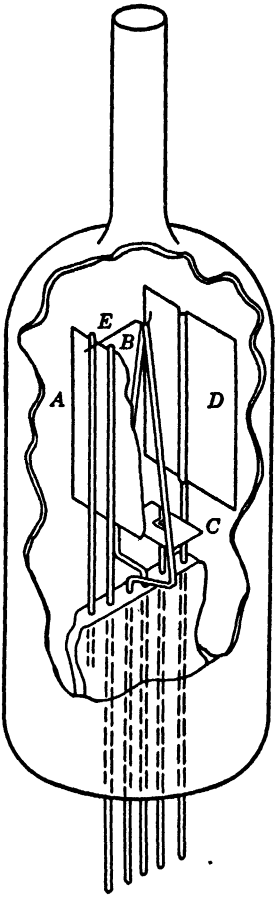

FIG. 62. Ionization gauge (Fogel).

One of the greatest disadvantages of the hot-cathode type of ion gauge is that the cathode is likely to be poisoned or even destroyed by chemically active gases such as oxygen and hydrocarbon vapors. In many vacuum-technique operations it is necessary to introduce air from time to time in order to seal on a fresh tube. Then the ion gauge has to be re-exhausted, and the gases adsorbed by the electrodes in the presence of air have to be eliminated. It is often necessary under these conditions to reactivate the cathode, and this may prove especially difficult for an oxide-coated cathode.

---

[145] *Rev. Sci. Instruments,* **12,** 134 (1941).

[146] *Proc. Inst. Radio Engnrs.,* **34,** 302 (1946).

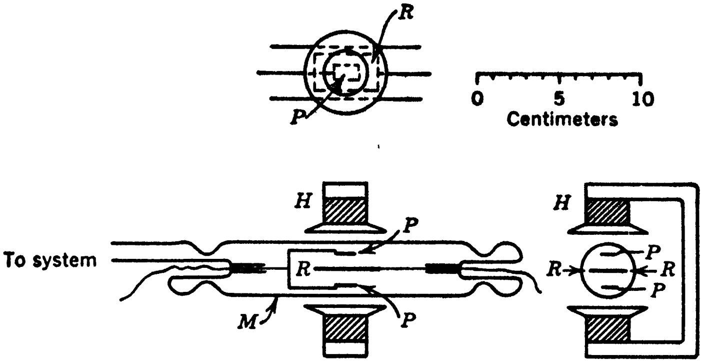

FIG. 63. Cold-cathode ionization gauge (Penning).

In order to overcome these difficulties the *Philips ionization manometer* developed by F. M. Penning[147] has received considerable acceptance by workers in the field of high-vacuum technique.

In this gauge, the electrons emitted from a *cold cathode* of zirconium, thorium, or other type of active surface are deflected by means of a magnetic field so that the total length of path covered in reaching the anode is many hundreds of times the direct distance between the two electrodes. As a result the ionization produced per electron at any given pressure is considerably greater than would be obtained in the absence of a magnetic field. The magnitude of the total discharge current, which is the sum of the positive-ion current to the cathode and the electron current from the same electrode, is used as a measure of the pressure of gas present.

Figure 63 shows the construction of the gauge. The manometer tube, *M*, contains a ring-shaped cathode *R* located between the anode plates *P*. The magnetic field (about 370 oersteds) is applied by means of the permanent magnet *H*. A microammeter (to measure the current) and 1 megohm resistance are connected in series with the manometer across a d-c source of about 2000 volts.

---

[147] *Physica*, **4**, 71 (1937); JY, p. 48.

For approximate measurement of the pressure, the microammeter may be replaced by a glow tube provided with a cathode having the form of a metal rod (Philips tube 4662). The length (l) of the glow along this rod is proportional to the current.

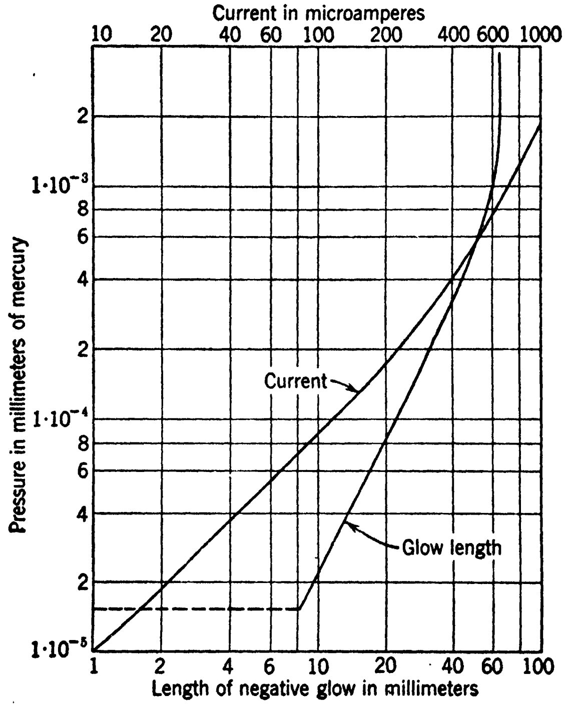

FIG. 64. Typical calibration curves of gauge shown in Fig. 63. Either the glow length or the discharge current may be used as a measure of the pressure.

Figure 64, taken from Penning's paper, gives a calibration curve for the manometer, which is applicable to hydrogen, carbon monoxide, argon, and air. As shown, the gauge is sensitive to pressures as low as about 10^{-2} micron.

An all-metal construction of the Philips gauge has been designed by the Distillation Products; it is provided with a control cabinet containing a half-wave rectifier with a filter circuit for supplying the high-voltage direct current. A high and low selector switch makes it possible to read either low or higher pressures.[148]

---

[148] A circuit diagram and calibration curve for a Philips gauge are also shown in the paper by H. A. Thomas, T. W. Williams, and J. A. Hipple, *Rev. Sci. Instruments*, 17, 368 (1946).

A novel type of cold-cathode gauge was developed by J. R. Downing and G. Mellen[149] in the laboratories of the National Research Corporation, Cambridge, Mass., and designated the "Alphatron," to indicate that the ionization is produced by alpha particles. Figure 65 shows a sketch of the ionization chamber and electrical circuit. A d-c poten-

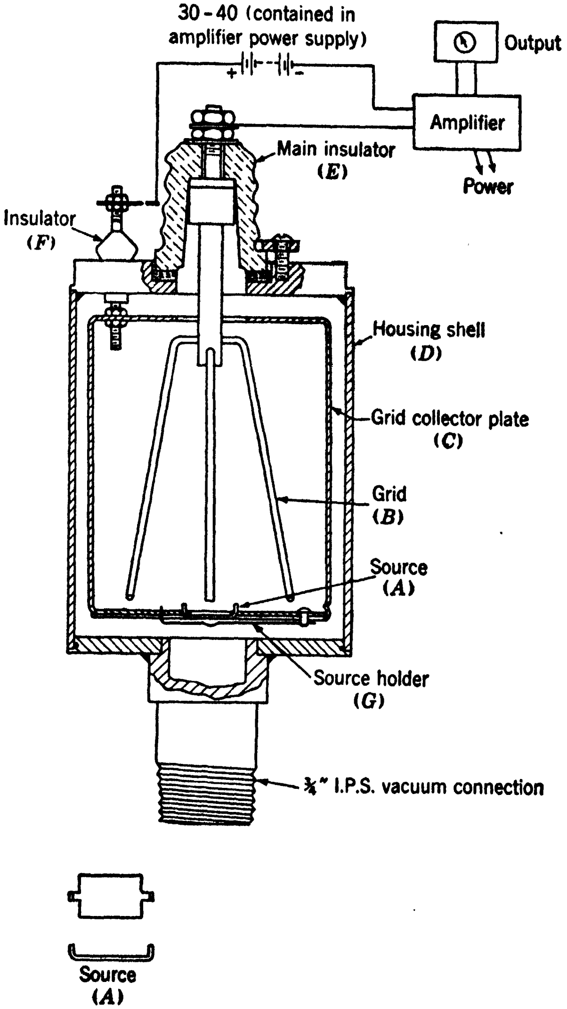

FIG. 65. Diagram of ionization chamber of Alphatron gauge.

---

[149] *Rev. Sci. Instruments*, **17**, 218 (1946), also *Electronics*, April, 1946, p. 142.

tial of 30 to 40 volts is applied between the two grids (*B*) and (*C*), and the very small ionization current, produced by the alpha particles from the radium source *A*, is greatly amplified so that it can be read on a standard type of microammeter. The d-c voltage as well as the power for operating the amplifier set is obtained from the regular a-c, 60-cycle, 110-volt supply.

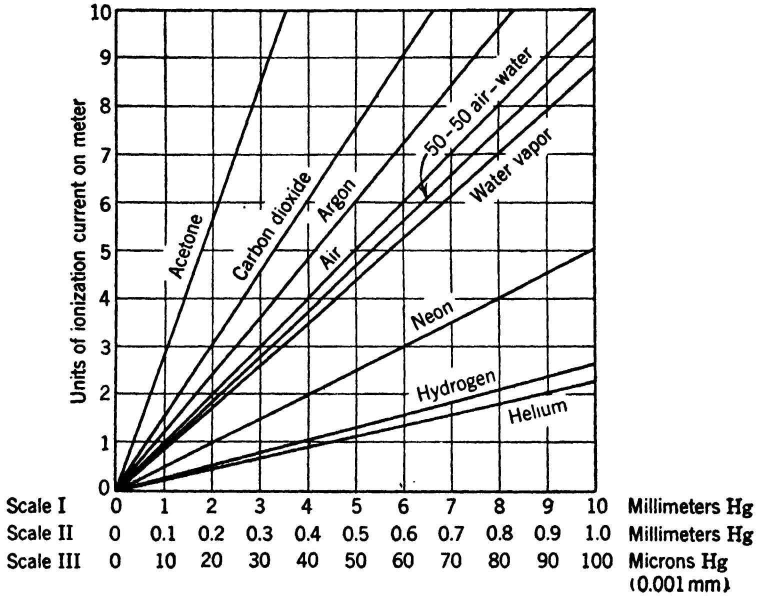

FIG. 66. Calibration plots for Alphatron gauge.

In the operating instructions for the gauge, it is stated that

> the radium source is so constructed that a small quantity (0.2 milligram) of radium in equilibrium with its disintegration products, radon, radium A, radium B, and so forth, radiates alpha particles at a constant rate. . . . Since radon, the first disintegration product of radium, is a gas, the walls must be sealed to prevent the loss of radon gas so that the succeeding products may be held in the source and their alpha activity utilized.

Calibration plots are shown in Fig. 66 for a number of gases over three ranges of pressure. For air at 100 microns, the actual ionization current is approximately $2 \cdot 10^{-11}$ ampere and varies linearly with pressure up to about 25 mm of mercury. Comparing the values of relative ionization for the gases, air (nitrogen), neon, helium, and hydrogen, with those given subsequently in Table 5, for the calibration of the hot-cathode gauge, it is evident that the two sets of data are quite different. This result is, of course, to be expected since the ionizing sources are so radically different.

One obvious advantage of this gauge is that there is no filament to burn out and no possibility of chemical reaction between the gas and the cathode. On the other hand, there are certain precautions (discussed very fully in the operating instructions) which have to be carefully attended to in using the gauge, in order to avoid any possible physiological effects arising from the radium emanation.

The ionization varies linearly with pressure up to several millimeters of mercury but not at much higher pressures. Actually plots of ionization versus pressure show a maximum value at about 150 mm for air, and at about 500 mm for hydrogen.

Calibration of Hot-Cathode Gauge for Different Gases. The sensitivity of any given design of gauge depends upon the nature of the gas used. In their early investigation on the calibration of an ionization gauge, Found and Dushman[150] concluded that the sensitivity S varies directly with the number of electrons in the molecule. On the basis of the knowledge of the arrangement and number of electrons in the atoms of different gases such a conclusion seemed quite incomprehensible, and a subsequent investigation was carried out by N. B. Reynolds.[151]

More recently, A. H. Young and the writer[152] repeated this work, with gauges similar in design to some of those used by Reynolds and also including the type VG-1 described above. A summary of the results obtained in both these investigations is given in Tables 4, 5, and 6. In these tables, S signifies, as stated previously, the value of the ratio i_p/i_e per micron.

Table 4 gives the values of S (per micron) obtained by Reynolds for four gases and for mercury vapor, with seven gauges of the design originally described by Found and Dushman (see Fig. 53). Data were also obtained for two FP-62 tubes, which are triodes of the UV-200 construction. The oval flat plate was used as ion collector, the grid as anode, and the hairpin filament as cathode.

The measurements were carried out under the two sets of conditions: (a) higher pressures, $i_e = 0.5$ milliampere, $V_g = 125$; and (b) lower pressures, $i_e = 20$ milliampere, $V_g = 250$.

In order to compare observations on the same gas with different gauges, the values of r (= ratio of S for the gas to S for argon) are also given in the table. As will be observed the values of r for any one gas,

---

[150] *Phys. Rev.*, **23**, 734 (1924).

[151] *Physics*, **1**, 182 (1931).

[152] *Phys. Rev.*, **68**, 278 (1945).

TABLE 4

CALIBRATION OF IONIZATION GAUGE (REYNOLDS)

		10^3S					$r = S/S_A$			
Gauge	i_e	He	Ne	A	Hg	N_2	He	Ne	Hg	N_2
1	0.5		0.88	6.93	12			0.127	1.73	
2			.75	5.87				.128		
3				5.33		3.73				0.70
4			.67	4.80		3.20		.140		.67
5			.56	4.53		2.53		.124		.56
6		0.40	.53	4.53		2.93	0.09	.117		.65
7		.40	.27	3.73			.11	.072		.61
Average:				5.10			.10	.118	1.73	.64
FP-62	0.5	0.61	1.07	5.60		4.53	0.11	0.191		0.81
Ditto			1.15			5.33				
1	20.0		1.27	5.33	13.3			0.238	2.5	
3				5.86		4.40				0.75
4			1.20	4.93		4.00		.246		.81
5			1.13	5.13		3.33		.220		.65
6		0.65	1.40	5.00		3.67	0.13	.280		.73
7		.61	1.00	4.67		3.40	.13	.214		.73
Average:				5.15			.13	.24		.73

TABLE 5

CALIBRATION OF IONIZATION GAUGE (DUSHMAN AND YOUNG)

(i_e = 1.0 ma)

Gas	FP-62(1)		FP-62(2)		VG-1		Average Value	
	10^3S	r	10^3S	r	10^3S	r	r	$r(P_i)$
He	0.77	0.140	0.70	0.133	2.88	0.127	0.133	0.14
Ne	1.08	0.196	1.08	0.205	4.65	0.206	0.202	0.21
A	5.50	1.0	5.27	1.0	22.6	1.0	1.0	1.00
Kr	8.9	1.62	8.4	1.59	32.9	1.46	1.56	
Xe	12.0	2.16	13.0	2.46	50.9	2.25	2.29	
Hg	15.0	2.73	14.5	2.75	72.0	3.18	2.89	1.90
H_2	2.14	0.39	2.10	0.40	8.65	0.38	0.39	0.34
N_2	4.90	0.89	4.40	0.83	18.2	0.81	0.84	0.90

obtained with different gauges, do not differ greatly except in the data for neon at 0.5 milliampere.

The results obtained by Young and Dushman are given in Table 5. Comparing these with those given in Table 4, the agreement is found to be reasonably fair, except for mercury, for which the more recent data are to be considered more reliable. Of greatest interest is the fact that the values of r for the different gases seem to be independent, to a large extent, of the design of gauge used. That is, for any one gauge it is only necessary to obtain a calibration with one gas (argon is best), and

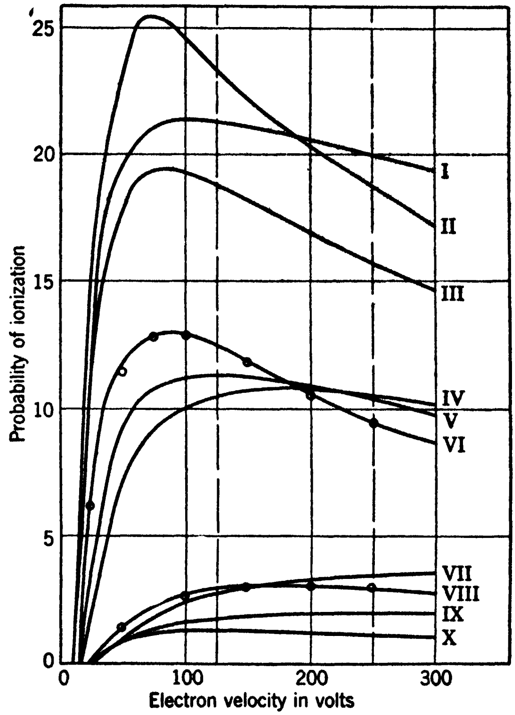

FIG. 67. Probability of ionization (ions per electron per centimeter path at 1-mm pressure) as function of electron velocity.

then, by means of the average values of r, the values of S for the other gases may be deduced. Whether this conclusion is valid for all possible variations in design is questionable, since the observations have been made on only two or three designs of gauge which are fairly similar.

In his investigation Reynolds compared his results for the values of S with the results derived by means of a graphical integration based on the probability of ionization (P_i) of different gases as a function of electron velocity. The observations recorded in the literature on the values of P_i as a function of electron velocity are shown in Fig. 67, taken from Reynolds' paper. The different curves were obtained from the following sources: I, mercury—K. T. Compton and C. C. Van

Voorhis;[153] II, mercury—W. Bleakney;[154] III, mercury—P. T. Smith;[155] IV, nitrogen—Compton and Van Voorhis; V, argon—Compton and Van Voorhis; VI, argon—Smith; VII, neon—Compton and Van Voorhis; VIII, neon—Smith; IX, helium—Compton and Van Voorhis; X, helium—Smith. The circles represent results obtained by Bleakney for argon and neon.[156]

Assuming a linear potential distribution between the electrodes, Reynolds calculated from these curves, and the known distances between the electrodes, the total probability of ionization per electron between the ionizing potential and the maximum anode voltage, V_g. Multiplying this value by i_e gave the calculated value i_p at 1 mm pressure. He found that i_p (the observed value) was equal to 3.9 times that calculated, a factor which could readily be accounted for on the basis of theoretical considerations.

It will be observed that the values of P_i shown in Fig. 67 are in the same order, for the different gases, as the values of r given in Tables 4 and 5. The writer finds that these values are in rather remarkable agreement with the relative values for P_i observed for 100-volt electrons by I. Langmuir and H. A. Jones.[157] These relative values are given in the last column of Table 5.

TABLE 6

RELATIVE SENSITIVITIES OF IONIZATION GAUGE COMPARED WITH IONIZATION PROBABILITIES

Gas	V_i	$r(L \text{ and } J)$	$r(Y \text{ and } D)$	$r(R)$
He	24.58	0.14	0.13	0.10–0.13
Ne	21.56	0.21	0.20	0.12–0.24
A	15.76	1.00	1.00	1.00
Kr	14.00		1.56	
Xe	12.13		2.29	
Hg	10.43	1.90	2.89	1.73–2.50
H_2		0.34	0.39	
N_2		0.90	0.84	0.73–0.81

Table 6 shows that, for the rare gases and mercury, the values of r, as observed by Langmuir and Jones, Young and Dushman, and Reynolds, increase with decrease in V_i. On the whole there appears to be a fair agreement between the values of r for any one gas obtained in these three investigations. Similar observations on the relation between the values of P_i and those of V_i have been made by a number of investigators. A natural assumption is that log r should decrease linearly with increase in V_i.

---

[153] *Phys. Rev.*, **26**, 436 (1925); **27**, 724 (1926).

[154] *Phys. Rev.*, **34**, 157 (1929); **35**, 139, 1180 (1930); **36**, 1303 (1930).

[155] *Phys. Rev.*, **36**, 293 (1930); **37**, 809 (1931). Also a curve for helium is given by P. T. Smith, *Phys. Rev.*, **39**, 270 (1932).

[156] Similar plots, including a few more recent observations, are given in the review by R. B. Brode, *Rev. Modern Phys.*, **5**, 257 (1933).

[157] *Phys. Rev.*, **31**, 357 (1928), Table VIII.

For the gases neon, argon, krypton, and xenon a plot of log r (or log S for the same gauge) versus V_i is approximately linear. However, the values for helium, mercury, hydrogen, and nitrogen do not fall on this plot. In the case of hydrogen and nitrogen the values for V_i obtained by C. G. Found[158] are 15.1 and 15.8 volts, respectively.

For cadmium, $V_i = 8.95$ volts, and it was to be expected, on the assumption that log r increases with decrease in V_i, that r for cadmium would be greater than r for mercury. However, the value of S actually observed, in this laboratory, by H. Huthsteimer, using a VG-1 gauge, was 44 microamperes per milliampere per micron, corresponding to $r = 2$. A calibration carried out with the same type of gauge for iodine vapor yielded the results $S = 100 \cdot 10^{-3}$ per micron and $r = 4.4$.

As is evident from Fig. 68, the values of S per micron (for a standard gauge) versus N_e, the *total number of electrons per molecule*, for the different monatomic and diatomic vapors and gases lie on a fairly satisfactory straight line. Although these observations thus confirm the conclusion deduced some years ago by Found and the writer, they are still just as difficult to explain.

A comprehensive discussion of the theory of the ionization gauge has been published by N. Margulis.[159] He finds that the observations on the values of P_i made by K. T. Compton and Van Voorhis[160] may be adequately represented by a relation of the form

$$P_i(V_g) = \alpha(V_g - V_i)\epsilon^{-(V_g-V_i)/\beta}, \tag{3}$$

where P_i is the probability of ionization as a function of accelerating voltage (V_g), and α and β are constants, characteristic of each gas, for which the values are deduced from the experimental data. On the assumption that the electrodes are in the form of concentric cylinders, that the internal-control type of circuit is used, and that the distribution of potential between the electrodes is linear, the relation derived for the gauge constant is of the form

$$S = \frac{BP}{V_g}[\beta - (V_g - V_i + \beta)\epsilon^{-(V_g-V_i)/\beta}], \tag{4}$$

---

[158] *Phys. Rev.*, **16**, 41 (1920).

[159] *Physik. Z. Sowjetunion*, **5**, 407 (1934).

[160] *Loc. cit.*

where B is a constant for the given design of tube and for any given gas.

For external-control type of circuit, the relation for S has the same form except that the constant B is different.

A comparison of calculated with observed values of S for a given construction of gauge shows good agreement in the case of the internal-control and less favorable accord in the case of the external-control type of circuit. It is evident that the above equations do not lead to any simple relation between r and V_i.

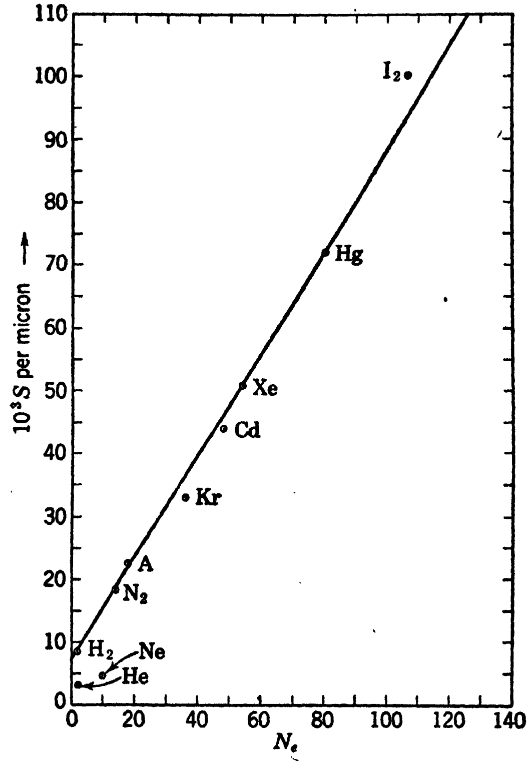

FIG. 68. Plot of sensitivity of ionization gauge versus number of electrons in molecule, for different gases and vapors. 10^3S per micron = microamperes per milliampere per micron.

In this connection it is of interest to compare with the above data some observations on the values of S made by H. Simon[161] with a Telefunken "R. E. 11" triode. With the external-control type of circuit, the values of S per micron (observed) and values of r calculated from the values of S were as follows:

---

[161] *Z. tech. Physik,* **5**, 221 (1924); also A. Goetz, *Physik und Technik des Hochvakuums,* Braunschweig, 1926, p. 197.

	A	N_2	H_2
10^3S	1.88	1.44	0.58
r	1	0.77	0.31

Although obtained with quite a different design of triode, the values of r for nitrogen and hydrogen are in fair agreement with those given in Tables 5 and 6. The actual values of S obtained by Simon are obviously much lower than those recorded in Table 5.

Also deserving of comment are the plots for P_i as a function of anode voltage which have been published by A. Boburieth[162] in a review of characteristics of ionization gauges. According to these plots, the maximum values of P_i occur for hydrogen, nitrogen, and mercury at about 200 volts, whereas, according to the plots in Fig. 67, the maximum values are observed at anode potentials ranging between 75 and 150 volts. Since the author does not state the source of his plots, some question may be raised regarding their reliability. However, the actually observed value of S for argon is stated to be about $62.5 \cdot 10^{-3}$ per micron with an anode potential of 250 volts, whereas the maximum value given in Table 5 is $22.6 \cdot 10^{-3}$ for 150 volts on the anode.

The gauge used in this case consisted of a V-shaped tungsten filament inside a cylindrical anode made of tungsten in the form of a spiral with only a few turns, while the collector consisted of a molybdenum box of rectangular cross section outside the anode. Gauges of similar design, tried out in this laboratory, have not proved to be as sensitive as the VG-1 construction described above.

When the ionization gauge is used to measure the pressure of gases or vapors which can react chemically or electrochemically (as ions) with the cathode or the other metal elements, the interpretation of the positive-ion currents observed becomes quite difficult. In the presence of water vapor, carbon monoxide, carbon dioxide, and halogen gases, the cathode is attacked very rapidly, even at pressures below 10^{-2} micron, and calibration of the gauge becomes almost impossible. In the presence of hydrocarbon vapors tungsten reacts to form carbides (W_2C and WC), thus affecting both the resistance and electron emissivity. Even at pressures of 10^{-2} micron, these reactions occur at a fairly rapid rate and ultimately lead to burn-out of the cathode.

In his investigations on the ultimate pressures obtainable with oil-vapor pumps, Hickman assumed that, for a given ratio of positive ion to electron current, the real vapor pressure relative to that of nitrogen, for the same value of i_e, is $28.0/M$, where M denotes the molecular weight of the liquid used. Thus, for the different esters, the positive-ion currents (for constant values of i_e and anode V) would be 11 to 13 times those observed at the same absolute pressure for nitrogen.[163]

---

[162] *Le Vide*, **1**, 61 (1946).

Actually, the molecules of the vapor are decomposed by the hot cathode into hydrogen, carbon monoxide, carbon dioxide, and hydrocarbon compounds of lower molecular weight. Obviously these molecules contribute towards the observed positive-ion current, and the magnitude of this additional current must depend upon the rate at which the decomposition products are removed from the immediate neighborhood of the electrodes. These conclusions are strikingly illustrated by observations made by J. Blears,[164] which have been discussed in Chapter 5, in his investigation on the ultimate pressures obtained in vapor pumps, and also by results obtained in this laboratory, which are discussed below.

In Fig. 69, taken from Blears' paper, are given pressure-temperature plots for several oils. "For comparison purposes," as Blears states, "a curve for mercury has been added (the 20° C value for this material was measured with the ionization gauge, but the slope is taken from the standard tables)." All these pressures are expressed in terms of the calibration of the gauge for nitrogen.

Assuming that these plots correspond to the vapor pressures of the different liquids in the temperature range obtained by means of the cooling water, it is possible to conclude that the equivalent nitrogen pressure is anywhere from 20 to 200 times that of the actual vapor pressure as deduced from the data in Table 5.2.[165]

In order to investigate this matter at further length a series of observations was made in this laboratory by H. Huthsteiner. The arrangement used in this investigation was the following.

A standard gauge, to the lower end of which was connected an appendix containing a few cubic centimeters of the oil, was immersed in an oil bath maintained at constant temperature. The upper end of the gauge was connected through a short length of wide tubing to a large-diameter trap and this, in turn, to a high-speed oil-vapor pump. In some of the experiments the trap was replaced by a U-tube containing activated charcoal. Thus any decomposition products or volatile constituents in the oil under investigation were removed continuously. The filament current and plate voltage were applied only during the very short interval of time (less than a minute) required to adjust the circuit for the desired value of i_e and to read the corresponding value of i_p.

---

[163] This assumption was deduced from the statement made in 1922 by Found and Dushman regarding the calibration of an ionization gauge for different gases.

[164] *Proc. Roy. Soc. London*, A, 188, 62 (1947).

[165] In correspondence with the writer Dr. Blears has advanced valid reasons against drawing such a conclusion.

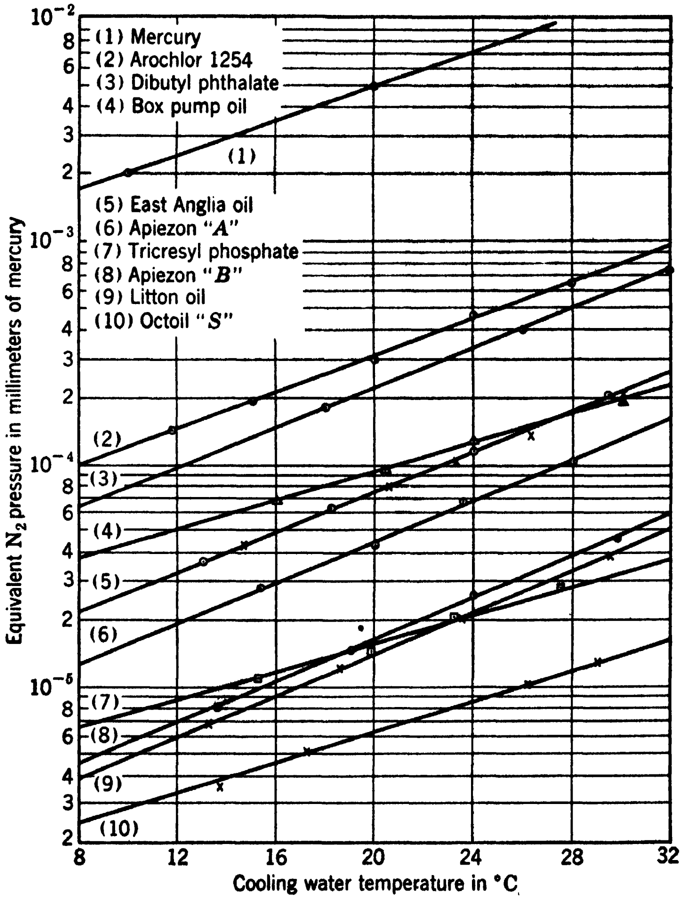

FIG. 69. Ultimate pressures of typical fluids as measured with "high-speed" ionization gauge (Blears).

In this manner a series of calibrations of the gauge were obtained for different temperatures of the bath, corresponding to vapor pressures of the oil ranging from about 0.1 to 1.0 micron. The values of the vapor pressures were obtained from the data in Table 5.2.

Before starting a series of measurements, the oil in the appendix was evacuated for an hour or longer at a temperature above the maximum used in the calibration. The voltages on the anode and collector were the same as those used in the calibration with nitrogen, for which the sensitivity, under these conditions, was 18.3 microamperes per milliampere per micron.

In the case of Octoil-S a plot of log i_p (at constant value of i_e) versus $1/T$ was observed to lie parallel to the plot of log P_μ versus $1/T$ (using the data obtained from Metropolitan-Vickers)[166] which corresponds to a value for S of $91 \cdot 10^{-3}$ per micron. This value was obtained for $i_e =$ 0.1 ma. For higher values of i_e, the value of S tended to increase, especially at pressures of about 1 micron.

With Amoil-S the initial values of S were around $130 \cdot 10^{-3}$ per micron. However, this value increased with time, even when the oil was maintained at constant temperature. Evidently this oil is adsorbed by the collector and grid, and hence the resulting positive-ion current is much greater than that corresponding to the equilibrium vapor pressure.

In the experiments with butyl sebacate a similar increase was observed from an initial value for S of about $120 \cdot 10^{-3}$ to $300 \cdot 10^{-3}$ per micron and higher.

Some observations made with silicone oil were of special interest. The initial value of S was about $50 \cdot 10^{-3}$ per micron. However, with the oil at a temperature of about 80° C and with the gauge operated continuously the sensitivity decreased in the course of several hours to about $10 \cdot 10^{-3}$, owing, evidently, to the formation of an insulating layer (presumably SiO) on the collector. This could be removed by heating the electrode with high frequency, after which the gauge exhibited normal sensitivity for quite a period (the length of which decreased with increase in the vapor pressure of the oil in the gauge).

On the other hand, in observations on naphthalene, a comparison of the values obtained for the ratio i_p/i_e at a series of temperatures with values of the vapor pressure published by Mrs. M. R. Andrews[167] yielded an average value for S of about $15.5 \cdot 10^{-3}$ per micron.

All these observations lead to the obvious conclusion that, in using an ionization gauge to measure vapor pressures of organic liquids and solids, considerable caution must be used in the interpretation of the observed data.

In connection with the interpretation of ionization gauge measurements at pressures below about 10^{-4} micron, some very significant observations have been drawn to the attention of the writer by W. B. Nottingham. In attempting to evacuate electronic devices to extremely low pressures (see discussion in Chapter 10, section 12), it has been observed by Nottingham and also by Apker, in this laboratory, that it is practically impossible to measure pressures below about 10^{-5} micron, although the thermionic and photoelectric emission characteristics indicate pressure of residual gas much below 10^{-5} micron. Nottingham has suggested (and obtained experimental evidence in confirmation of this suggestion) that the soft X-rays, produced by the incidence of 150 to 250 volt electrons on the anode, liberate photoelectrons from the ion collector. Since these electrons *emitted* from the ion collector cannot be distinguished on the current meter from the positive ions *incident* on the collector there must exist a lower limit to the value of i_p, with decrease in pressure, which corresponds to pure photoelectric emission. This lower limit of computed pressure is apparently about 10^{-5} micron. Therefore, in order to measure still lower pressures, Nottingham has proposed a design of gauge in which it will be possible to separate the two effects. Since the experimental work is still incomplete no further results can be reported at this time.

---

[166] See reference 3, Table 5.2.

[167] *J. Phys. Chem.*, **27**, 270 (1933).

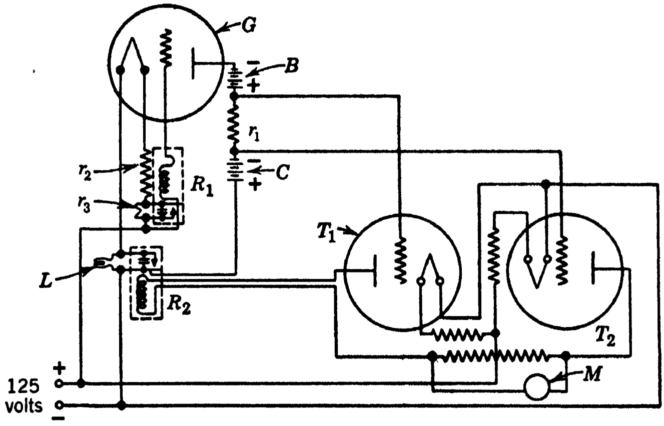

FIG. 70. Circuit for direct-reading ionization gauge (Found and Reynolds).

Control Circuits for Ionization Gauge. The desirability of maintaining a constant value of i_e in a series of pressure measurements has led to the development of a considerable variety of electrical circuits which employ control devices of different types.

C. G. Found and N. B. Reynolds[168] used a circuit which is shown in Fig. 70. The filament of the particular gauge, G, required about 1 ampere heating current. The authors state,

---

[168] *J. Optical Soc. Am. and Rev. Sci. Instruments*, **13**, 217 (1926).

This is supplied from 125 volt line through a resistance r_2 in the positive arm. The accelerating voltage to the grid is supplied from the same source, the positive terminal being connected to the grid through the coil of a relay or Kearsley stabilizer, R_1,[169] across the contacts. The relay is adjusted so that when the electron current to the grid increases above 10 ma, the contacts open, throwing the resistance r_3 in series with the filament, thus decreasing its temperature and maintaining the electron current in the gauge constant at 10 ma. The plate is used as collector and is held 27 volts negative by means of the batteries B and C. In order to amplify the positive-ion currents, a resistance r_1 is placed in series with the collector and the voltage drop across this is amplified by means of a push-pull amplifier circuit using UV-201A radiotrons, T_1 and T_2. The current, indicated by the meter M, is proportional to the positive-ion current to the plate in the gauge G, and is therefore proportional to the pressure.

A mechanical relay control of the filament current has also been proposed by E. K. Jaycox and H. W. Weinhart.[170] W. P. Overbeck and F. A. Meyer[171] have suggested the application of a saturable-core transformer to the control circuit of a gauge, while J. B. Hoag and N. M. Smith[172] have described a control circuit which uses a thyratron.

Because of difficulties inherent in all these circuits, L. N. Ridenour and C. W. Lampson[173] proposed a circuit in which the power supplied to the filament is controlled by the grid voltage in two triodes which are used with a transformer to produce full-wave rectification. This grid voltage is controlled in turn by the electron current in the gauge. The circuit thus uses radiotrons exclusively, and the source of energy is 110-volt alternating current.

J. B. H. Kuper[174] has described a circuit for a-c operation of the gauge in which batteries are completely eliminated.

A modified construction of gauge, which is very interesting, is described by C. G. Montgomery and D. D. Montgomery.[175] They state,

> Instead of using a single grid and accelerating the whole emission of the filament, it is possible to employ a gauge with two grids, and accelerate only those electrons which have passed the first grid. The number of such electrons can be regulated by the potential of the first grid, and is then largely independent of the emission of the filament and the filament current. It is then possible to control the potential of the first grid in such a way as to make this independence practically complete.

A standard type "47" vacuum tube is used for the gauge, and the sensitivity obtained has a value $S = 3.33 \cdot 10^{-2}$ per micron.

---

[169] W. K. Kearsley, *J. Radiol.*, July, 1921.

[170] *Rev. Sci. Instruments*, **2**, 401 (1931).

[171] *Rev. Sci. Instruments*, **5**, 287 (1934).

[172] *Rev. Sci. Instruments*, **7**, 497 (1937).

[173] *Rev. Sci. Instruments*, **8**, 162 (1937).

[174] *Rev. Sci. Instruments*, **8**, 394 (1934).

[175] *Rev. Sci. Instruments*, **9**, 58 (1938).

A control circuit has also been described by R. M. Bowie,[176] in which high sensitivity and stability are achieved by means of a balanced amplifier, negative feedback, and a gas tube voltage regulator.

A radical type of control and indicating circuit has been described by L. N. Ridenour,[177] in which the grid control circuit is the same as that proposed previously by Ridenour and Lampson. The circuit is stated to have the following features:

> (1) No meters whatever are required; the plate current of the gauge tube is indicated by a 6E5 tube,[178] both during normal operation and during the outgassing operation. (2) The grid current in the gauge is held constant at any desired value, regardless of changes in line voltage, gas pressure, or the nature of gas in the vacuum system. (3) Outgassing of the grid of the gauge tube may be done by throwing one switch. (4) The grid current is controlled automatically during outgassing. (5) Any type of tube may be used as gauge tube proper, without changes in the control and indicating circuit.

The actual circuit is quite a complex affair to anyone but an electronic expert, and the interested reader should consult the original paper for complete details.

An emission-regulating circuit has also been described by R. B. Nelson and A. K. Wing, Jr.[179] Both Ridenour and Nelson[180] have introduced modifications in the control circuit which make it possible to use the arrangement either as a gauge or as a leak detector (see discussion in section 9 of this chapter).

J. M. Lafferty of this laboratory has developed a circuit which has proved very satisfactory in operation. Though it does not possess the emission-regulating feature of some of the more complicated circuits, it is very simple to construct and operate. He states:[181]

> The circuit shown in Fig. 71 may be divided into three parts, (1) the regulated power supply, (2) the balanced bridge d-c amplifier, and (3) the ionization gauge.
>
> The d-c power supply voltage is held nearly constant by means of the voltage regulator tubes V_2 and V_3. The various voltages required are tapped off from the potentiometer network R_2 through R_7. The potentiometer R_6, R_7 supplies a 25-volt negative bias for the ionization gauge plate, R_2 and R_3 provide 150 volts for the grid. The potentiometer R_4, R_5 across V_3 gives 0.2 volt for calibrating the amplifier. A total potential of 255 volts across the two VR tubes (V_2 and V_3) is supplied to the amplifier tube V_4. R_1 is adjusted so that a total current of 60 ma flows through it.
>
> The amplifier is a bridge-type vacuum-tube voltmeter. This type of circuit has

---

[176] *Rev. Sci. Instruments*, **11**, 265 (1940).

[177] *Rev. Sci. Instruments*, **12**, 134 (1941).

[178] This is also known as a "magic eye" tube since it contains a fluorescent screen on which a pattern is produced.

[179] *Rev. Sci. Instruments*, **13**, 215 (1942).

[180] *Rev. Sci. Instruments*, **16**, 55 (1945).

[181] Personal communication.

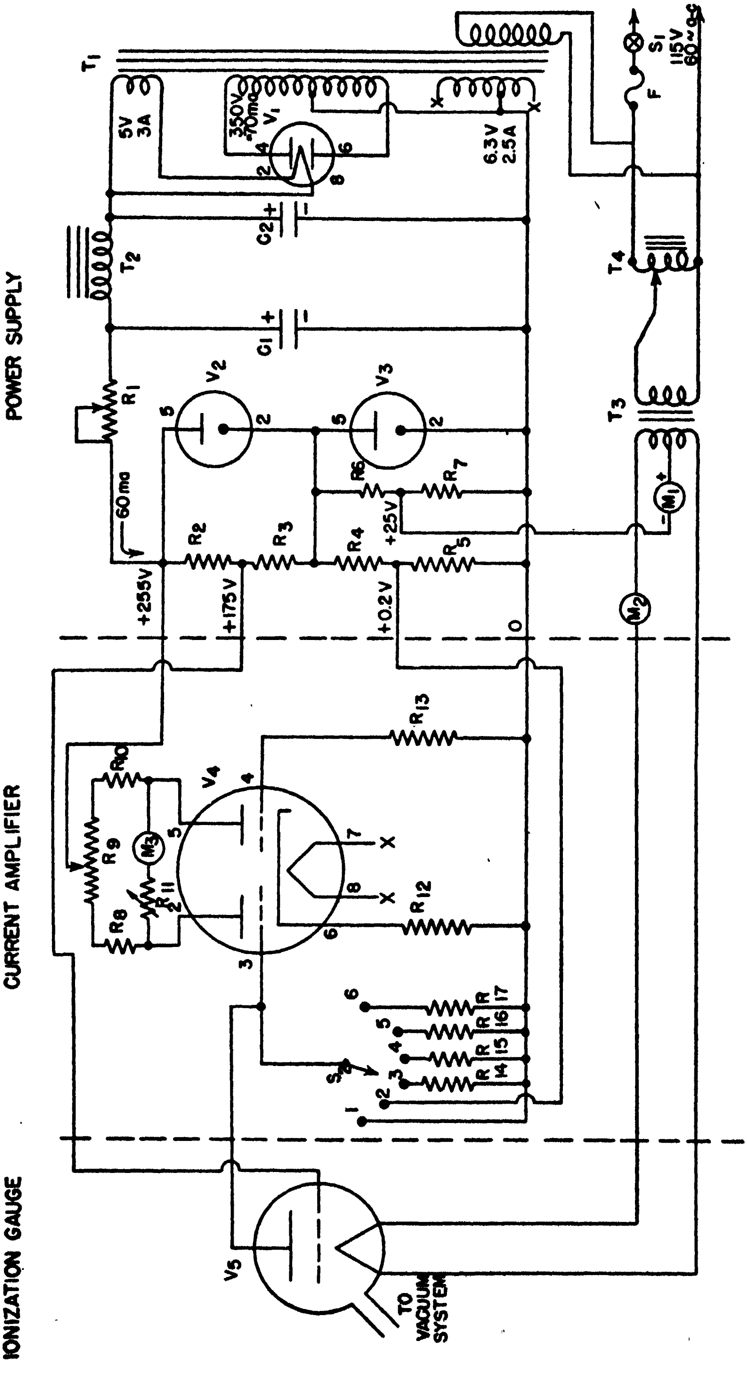
POWER SUPPLY
CURRENT AMPLIFIER
IONIZATION GAUGE
T1
5V 3A
350V 70ma
V1
6.3V 2.5A
S1
F
115V 60~
T2
C2
C1
R1
V2
V3
60ma
R2
R3
R4
R5
R6
R7
+25V
+255V
+175V
+0.2V
0
M1
M2
T3
T4
R13
R10
R9
M3
R8
R11
V4
R12
R14
R15
R16
R17
S2
V5
TO VACUUM SYSTEM

C_1	30 μfd ELECTROLYTIC 450 VOLTS
C_2	"
R_1	3,000 OHMS, 5 WATTS
R_2	2,250 OHMS, 5 WATTS
R_3	2,500 OHMS, 2 WATTS
R_4	4,000 OHMS, 2 WATTS
R_5	950 OHMS, 2 WATTS
R_6	20,000 OHMS, 2 WATTS
R_7	38 OHMS, 2 WATTS
R_8	10,000 OHMS, 2 WATTS
R_9	5,000 OHMS, 4 WATTS, WIRE WOUND
R_{10}	10,000 OHMS, 2 WATTS
R_{11}	25,000 OHMS, 4 WATTS, WIRE WOUND
R_{12}	2,000 OHMS, 2 WATTS
R_{13}	2 MEGOHMS, 1 WATT
R_{14}	2,000 OHMS, 1 WATT, WIRE WOUND PRECISION
R_{15}	20,000 OHMS 1 WATT, WIRE WOUND PRECISION
R_{16}	200,000 OHMS, 1 WATT, WIRE WOUND PRECISION
R_{17}	2 MEGOHMS, 2 WATTS, WIRE WOUND PRECISION

T_1	POWER TRANSFORMER, (THORDARSON T-13R12 OR EQUIVALENT)
T_2	CHOKE, 10h @ 110 ma, (THORDARSON T-57C54 OR EQUIVALENT)
T_3	FILAMENT TRANSFORMER, 5 VOLTS @ 4 AMPS (THORDARSON T-63F99 OR EQUIVALENT)
T_4	1 AMP VARIAC TYPE 200-B
V_1	5U4-G
V_2	VR-150-30
V_3	VR-105-30
V_4	6SC7
V_5	IONIZATION GAUGE D.P.I. TYPE VG-1 OR EQUIVALENT
F	3 AMP FUSE
S_1	TOGGLE SWITCH
S_2	6 POINT TAP SWITCH
M_1	0-10 ma d-c
M_2	0-5 amp a-c
M_3	0-50 μ amp d-c

FIG. 71. Circuits for ionization gauge (Lafferty).

the advantage of being quite stable against variations in plate and filament voltage. Both arms of the bridge are affected nearly the same by these variations and bridge balance is maintained. Further stabilization is obtained by means of negative feedback through the common self-biasing resistor R_{12}. Resistors R_8 and R_{10} form two arms of the bridge circuit and the triodes form the other two arms. Positive-ion current from the gauge flowing through any one of the resistors R_{14}–R_{17} produces a voltage drop which is applied to the grid of the left-hand triode. This produces an unbalancing of the bridge resulting in a current flow through the microammeter M_3. This current is indicative of the pressure in V_5.

The procedure for operating the circuit is as follows: S_1 is turned on and the circuit allowed to warm up for about 3 minutes. With the Variac turned down so that the ionization gauge filament is off, and the selector switch S_2 set at tap 1, the bridge is balanced by adjusting R_9 until the current through M_3 is zero. The amplifier is next calibrated by turning the selector switch to position 2. This applies 0.2 volt to the amplifier. By varying R_{11}, the current through M_3 is adjusted to give a full-scale deflection of 50 microamperes. The sensitivity of the amplifier is now such that a full-scale deflection of M_3 would be obtained on application of 100, 10, 1, or 0.1 microampere to the amplifier input with the selector switch on positions 3, 4, 5, and 6 respectively. The Variac is now turned up until the ionization gauge filament gives 5 milliamperes of electron emission as measured by M_1. The selector switch is turned to the proper tap and the pressure is read on M_3. If the ionization gauge has a sensitivity of 20 microamperes per micron, a full-scale deflection of M_3 on taps 3, 4, 5, and 6 corresponds to pressures of $5 \cdot 10^{-3}$, $5 \cdot 10^{-4}$, $5 \cdot 10^{-5}$, and $5 \cdot 10^{-6}$ mm of mercury respectively.

When the tap switch is set on the most sensitive position there may be a slight zero shift of M_3 due to the flow of positive-ion grid current from the amplifier tube V_4 through R_{17}. This may be corrected by turning the Variac down and readjusting the zero by means of R_9 with the tap switch set at position 6.

By placing a No. 3002 Sola constant voltage transformer in the 115 volt line, the zero shift and changes in the sensitivity of the amplifier are negligible for a ±20 per cent change in line voltage.

A commercially available control system for the ionization gauge, in which the electron current is maintained constant, has been described by H. E. Van Valkenburg,[182] and E. A. Hamacher[183] has described a circuit for an automatic ionization gauge and audiofrequency monitor for use with a cyclotron.

A control system developed by R. G. Picard, P. C. Smith and S. M. Zollers[184] makes use of both a thermocouple and cold-cathode discharge tube (similar to that devised by Penning). Figure 72 shows the circuit diagram, which is described as follows:

"The two pole–three position switch S-1, which controls the a-c power to the circuit through protective fuse F-1, is optional. In the No. 1 position, all power is "off." In the No. 2 position, power is supplied to a thermocouple gauge, V-3, and its associated components, T-1, R-1, V-2, and M-1. In the No. 3 position, power is supplied to the discharge gauge, V-1, and its associated circuit components, T-2, R-2, 3 and 4, C-1, V-4, and M-2, as well as the thermocouple gauge circuit. . . . Since neither gauge, V-1 nor V-3, is affected by atmospheric gases at pressures from 760 mm down to the lowest attainable by the system, input power may be fed continuously to the circuit or controlled by a simple "on-off" switch.

---

[182] *Gen. Elec. Rev.*, **49**, 38 (1946).

[183] *Rev. Sci. Instruments*, **17**, 281 (1946).

[184] *Rev. Sci. Instruments*, **17**, 125 (1946).

The power for the thermocouple is supplied by the transformer T-1 and regulated by R-1. The thermocurrent output from the junction is measured by the galvanometer M-1, which has a full-scale sensitivity of 7.5 millivolts. An amperite regulator V-2 (capable of supplying 15 to 25 per cent more current than required by the thermocouple) is used to overcome the effect of line voltage regulation.

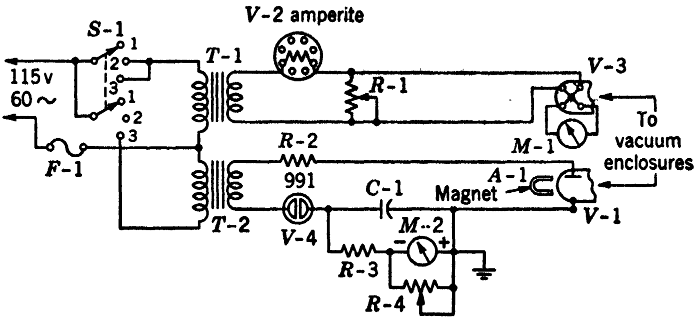

Fig. 72. Control circuit for use with thermocouple and cold-cathode discharge tube (Picard et alii).

Voltage for the diode is supplied by the secondary of T-2 and the current in the circuit is limited by R-2 to a maximum of 3 milliamperes. At atmospheric pressure, no current flows in the circuit. As the pressure surrounding the gauge elements is reduced to about 200 microns, a discharge occurs in the gas and an alternating current flows through V-1, V-4, and C-1. V-4 is a type 991 neon tube which fires as a result of the alternating current, causing both of its elements to glow. As the pressure is further reduced, V-1 begins to rectify the applied alternating current and continues to act as a unidirectional conductor to the end point of its ability to indicate pressure. As V-1 starts to rectify, one element of V-4 commences to lose its glow intensity, and, at a pressure of 25 microns, this element is completely without illumination. At the low point of the effective range of V-1, V-4 is without illumination except for a very small discharge which plays back and forth between its elements. V-4 acts as a simple, quick indicator of current flow and relative pressure.

Capacitor C-1 by-passes alternating current around the d-c milliammeter (1 milliampere full-scale deflection). R-3 acts as a current-limiting resistor for M-2, and R-4 is an adjustable shunt which is set during calibration to limit the current in M-2 to a full-scale reading. Meter M-2 reads the discharge current developed in V-1, and the readings can be translated into accurate terms of pressure by calibration against a McLeod gauge.

One element of the discharge gauge consists of the metal shell of the tube. A permanent magnet, *A*-1, serves to increase the ionization considerably and makes it possible to use the gauge to measure pressures as low as 0.1 micron.

Figure 73 shows the calibration of the two gauges over a range of pressures.

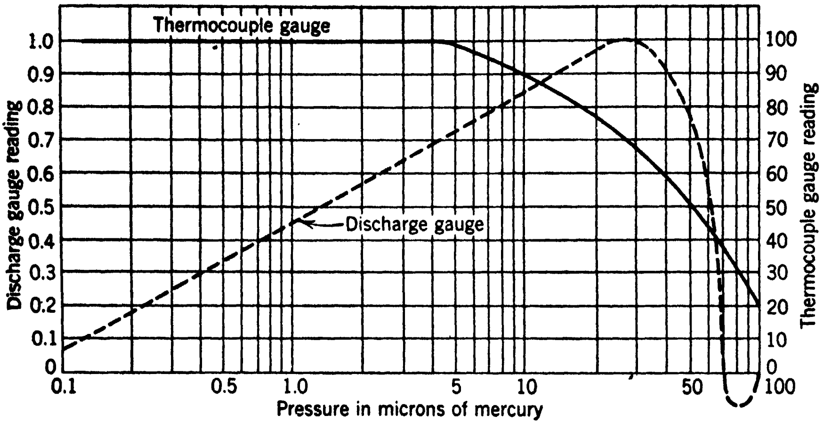

FIG. 73. Calibration curves for combination of gauges used in circuit shown in Fig. 72.

For general use, the meters and circuits have been incorporated in a single unit from which cables extend to the gauges and also to the source of alternating current. Furthermore there is described in the publication a circuit "whereby the current from the gauges may be used to control equipment so that the pressure in the vacuum system may be used to operate other devices."

8. GENERAL REMARKS ON GAUGES

In the different problems encountered in high-vacuum technique the question usually arises as to what one or two of the assortment of gauges described in the previous sections would be most satisfactory. Even if some of the designs described are obviously either impractical or very limited in their application, there still remains a considerable variety from which a choice may be made. One of the most important factors that must be considered is the range of pressures to be measured. Another factor is the nature of the gas or gases present in the system. Is it necessary to eliminate condensible vapors from the gauge? How does the sensitivity of the gauge depend upon the nature of the gases or vapors?

Figure 74 shows the approximate range of pressures of the gauges described in this chapter. The full line indicates the usual range, and the dashed portions to the left indicate sensitivities which have been, or may be, attained by specially designed constructions.

The two bottom rows give values of $n/(3.24)$, where n denotes the number of molecules per cm^3 at 25° C, and values of L, the mean free path (in centimeters) for air at 25° C.

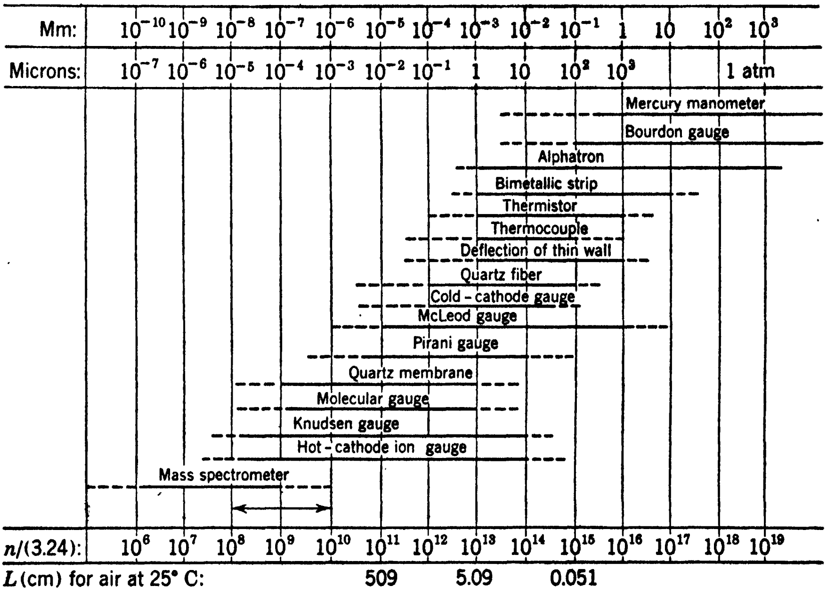

FIG. 74. Chart showing ranges of pressures for different types of gauges.

By means of this chart it should be possible to choose two or more types of gauges that meet the requirements of any special conditions in vacuum technical operations.

The advantages and disadvantages of the principal types of gauges for use with oil-vapor pumps have been stated in a paper by J. W. DuMond and W. M. Pickels.[185] Their discussion, which is limited to the McLeod, Pirani, ionization, and Knudsen types of gauges, is summarized in the following remarks.

---

[185] *Rev. Sci. Instruments*, **6**, 362 (1935).

The McLeod gauge has the following disadvantages: (1) It does not give continuous readings of the pressure. (2) It is insensitive to condensible vapors. (3) In order to eliminate mercury from the rest of the system it is necessary to insert a liquid air trap. "Such traps," it is stated, "are never completely effective over long periods. (4) The readings are never very dependable below 10^{-4} or 10^{-5} mm Hg pressure."

The ionization gauge has a very wide range of pressures but possesses the following disadvantages: (1) It requires considerable auxiliary electrical equipment. (2) Its sensitivity varies for different gases and vapors. (3) The filament emission may be "poisoned" in the presence of certain gases. (4) The filament is susceptible to burn-out if exposed to air while hot. (5) "Ion-bombardment destroys the filament more or less rapidly with continued use." (6) The electrodes must be outgassed very thoroughly before the gauge can be used to give reliable indications, especially at extremely low pressures. (7) The hot filament decomposes certain gases (especially hydrocarbons).

To these disadvantages may be added those due to chemical and electrical "clean-up" effects. As will be discussed more fully in Chapter 10, the gradual decrease in pressure in an electrical discharge tube is a well-known phenomenon, which is observed with cold as well as with hot cathodes. Such clean-up occurs with all gases and obviously must be taken into account in the interpretation of observations made by means of an ionization gauge. In fact, H. Schwarz[186] has made the following statement: "Everyone who measures pressures under 10^{-4} mm with the ionization gauge must regard his measurements with more or less skepticism."

However, in view of the experience of the writer, the situation is not quite as bad as this statement would imply. If the plate voltage or current to the filament is applied only during the *very short interval* necessary to observe both the electron and positive-ion currents, then the amount of clean-up is reduced to a minimum. That is, *the gauge should not be operated continuously* when it is desired to determine the pressure in a sealed-off system. With a circuit such as that devised by Ridenour or Nelson which has been described in the previous section, a pressure determination may be made in a few seconds and it will be found that under these conditions the reduction in pressure is negligible.

As DuMond and Pickels point out, the Pirani or hot-wire gauge has two main disadvantages: (1) "It is very difficult with it to maintain a stable 'zero' point of pressure and it cannot therefore be used with confidence to measure pressures much below 10^{-4} mm Hg." (2) As the pressure is decreased below about 10^{-3} mm Hg, the loss of heat by conduction becomes negligibly small as compared with the radiation loss. It is stated:

---

[186] *Z. Physik*, **122**, 437 (1943).

> No modification in the geometrical design of the gauge can improve the ratio of energy loss by gas conduction to energy loss by radiation since at these low pressures the molecules of gas travel in straight lines between the wire and the walls just as the photons of radiation do.
>
> Now this is the chief reason for the superiority of the Knudsen gauge. At these pressures the energy transported by molecules of gas is small compared to the energy transported by photons of radiation, but the *momentum* transported by molecules is huge compared to the momentum transported by photons on account of the comparatively enormous mass of the molecules. The Pirani gauge measures the molecular *energy* transport while the Knudsen gauge measures the momentum transport, hence its superiority.

The main advantages of the Knudsen type are the following: (1) It requires no auxiliary electrical circuits such as are used with the ionization gauge. (2) The deflections of the mirror are proportional to the pressure and correspond to absolute pressures, independently of the nature of the gas.

On the other hand, the use of a suspension involves difficulties similar to those met with in any sensitive galvanometer, especially when dealing with extremely low pressures. Such difficulties will arise whenever the gauge is subjected to external causes of vibration. Moreover, in a gauge such as that designed by DuMond and Pickels it is very difficult to outgas the parts, and any wax or grease joints are likely to be sources of constant gas evolution.

The fact is that each of the different types of gauges described in the previous sections possesses both advantages and disadvantages. The experimenter must decide upon the objective of any set of measurements and then choose that gauge or those gauges which will give him the desired information most conveniently and to the desired degree of accuracy. Many times information of order of magnitude of the pressure is sufficient; at other times a continuous record of variation in pressure may be desired, without any reference to the nature of the gases present.

For instance, in the evacuation of electronic devices the factor of significance is the ratio i_p/i_e, irrespective of the nature of the ions. An ionization gauge gives this information directly, and, though the necessity for using auxiliary electrical circuits may appear a disadvantage, the actual fact is that such gauges have found extensive application in factory practice as well as in the laboratory.

The same statement applies to a Pirani gauge. In industrial applications of vacuum technique as well as in purely scientific investigations the hot-wire gauge is widely used, along with the thermocouple and McLeod gauges.

9. LEAK DETECTORS

To the experimenter interested in exhaust problems, one of the greatest difficulties results from the presence of leaks. Leaks may occur from a variety of causes, and the increasing complexity of tube design has multiplied the number of these causes to a great extent.

The time-honored method of detecting leaks in glass systems is by means of a Tesla spark-coil; a leak at any point is indicated by a characteristic pink color of the discharge, due to the presence of nitrogen in the system. (Occasionally, if the spark is too intense, the spark-coil itself will produce a fine hole!) If ether, carbon tetrachloride, or acetone is poured on the suspected spot, the presence of a leak will be indicated by the characteristic color of the glow due to the presence in the system of the vapors of these compounds.

The spark-coil test is, of course, useless for leaks in metal parts. Furthermore, this test is not very sensitive. In order to maintain a discharge the pressure in the system must be of the order of a few microns, and this pressure implies, even with a fairly moderate speed of exhaust, a high rate of leak of air into the system.

For any exhaust system operating under optimum conditions, there will be established a stationary pressure, P_s, which corresponds to equilibrium between rate of leak of gas into the system and rate of exhaust. This leakage of gas in the system may also arise, in "tight" systems, from evolution of gas at some part of the system which has not been baked out well, or it may be due to back diffusion from the pump.

The pressure is measured by some form of low-pressure gauge attached to the system, and any abnormal leak will be observed by the gauge as an increase in pressure above the value P_s. Under these conditions the location of the leak may be found by isolating parts of the system, if possible, or by coating suspected places with a suitable wax. J. B. H. Kuper[187] has observed that the best location for the gauge is immediately above the fore pump, and he has used for this purpose an ordinary 40-watt light bulb, as a Pirani gauge, with a duplicate bulb sealed off at 1 micron as compensator. The bridge circuit is fed from the a-c mains, and an audioamplifier and loud speaker are used to indicate gas evolution or leakage.

[187] *Rev. Sci. Instruments*, **8**, 131 (1937).

Since the Pirani gauge is most sensitive for hydrogen, a method used in many laboratories is to insert such a gauge in the position suggested by Kuper and pass a jet, through which a fine stream of hydrogen is flowing, over suspected points on the vacuum system. The fact that hydrogen diffuses through a hole more rapidly than air, combined with the much greater thermal conductivity of hydrogen, causes a marked change in the indication of the gauge when the jet strikes a leak. Obviously, a thermocouple or thermistor gauge may be used instead of the Pirani, although the Pirani is more sensitive.

The application of this method, using *a very sensitive Pirani gauge*, has been investigated by F. W. Reuter and C. Kenty in the Lamp Development Laboratory of the General Electric Company.[188] The method of measuring a leak, as described by these investigators, is to close off the main pump with a mercury cut-off and measure the rate of increase in pressure in the system as a function of the time, first with air flowing through the leak, and then with hydrogen. It is evident that with extremely small leaks the interval of time required to reach a decision regarding the actual occurrence of a leak must become quite large. Furthermore, it is always necessary to distinguish between rate of evolution of gas in the system itself and increase in pressure due to a leak: the rate of evolution will, in general, decrease with time and should ultimately become extremely small, whereas with a leak the pressure should increase linearly with time. Actually Reuter and Kenty were able to detect leaks of the order of magnitude of $1 \cdot 10^{-5}$ micron · liter per hour.

However, especially in production, it is usually essential to detect a "leaker" in as short a time as possible; consequently other methods have been applied, which, though much less sensitive, are still both sensitive and speedy enough to detect a very high percentage of leaks.

The effect of gases like oxygen and halogen compounds on the electron emission from a tungsten or oxide-coated filament has been applied to detection of leaks. For instance, Ridenour[189] has observed that "a very small air leak" is sufficient to increase the current required by a "combined oxide" filament of a Western Electric (D79510) gauge tube for the standard emission value from 1.4–1.6 to 1.8–2.0 amperes.

While testing for leaks by noting the response on an ion gauge caused by different liquids, J. H. Manley, L. J. Haworth, and E. A. Luebke[190] observed a decrease in emission resulting from entrance of the vapor at the leak. This observation led E. J. Lawton[191] of this laboratory to develop a method of leak testing which depends upon *the effect of oxygen on the emission from a tungsten filament.*

---

[188] Located at Nela Park, Cleveland. The remarks in this paragraph are based on a personal communication.

[189] *Rev. Sci. Instruments*, **12**, 134 (1944).

[190] *Rev. Sci. Instruments*, **10**, 389 (1939).

As had been observed many years previously by I. Langmuir, an adsorbed layer of oxygen on tungsten decreases the emission to a tremendous extent. Thus if a diode containing a heated tungsten filament as cathode is inserted in a vacuum system as near as possible to the device under test and a jet of oxygen is passed over a leak in some part of the device, the emission will suddenly decrease because of the effect of the increased concentration of oxygen in the diode.

Hydrogen can be used in the same manner as oxygen; it usually causes a decrease in emission because the atomic hydrogen formed at the incandescent filament (see discussion in Chapter 10 on chemical clean-up) reduces some of the oxides present and the water vapor then affects the emission in the same manner as oxygen.

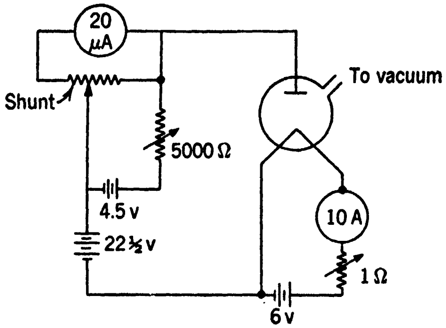

FIG. 75. Battery-operated leak detector involving effect of oxygen on emission from tungsten (Lawton).

The following description of the leak detector based on this principle, and simple circuit used in this laboratory by W. A. Ruggles, is given in a paper by R. B. Nelson.[192]

> The leak detector consists of a diode with a pure tungsten filament and a closely spaced plate. A potential of approximately 22 volts is used to draw saturated emission from the filament, which is heated by a storage battery. The emission current is measured by a microammeter supplied with a bucking voltage so that a sensitive meter may be used and small changes in the emission observed. Figure 75 shows the circuit diagram. With this apparatus, a leak of 10^{-3} cc of air per hour has been readily detected.

---

[191] *Rev. Sci. Instruments,* **11**, 134 (1940).

[192] *Rev. Sci. Instruments,* **16**, 55 (1945).

A leak of this magnitude corresponds to about 0.76 micron · liter per hour. Actually L. R. Koller of this laboratory has observed that it is possible to detect by this method rates of leak which are as low as 0.01 micron · liter per hour.

Since the battery-operated detector presents certain practical disadvantages, Nelson developed an a-c operated detector which is shown in Fig. 76. The description of the circuit is as follows:

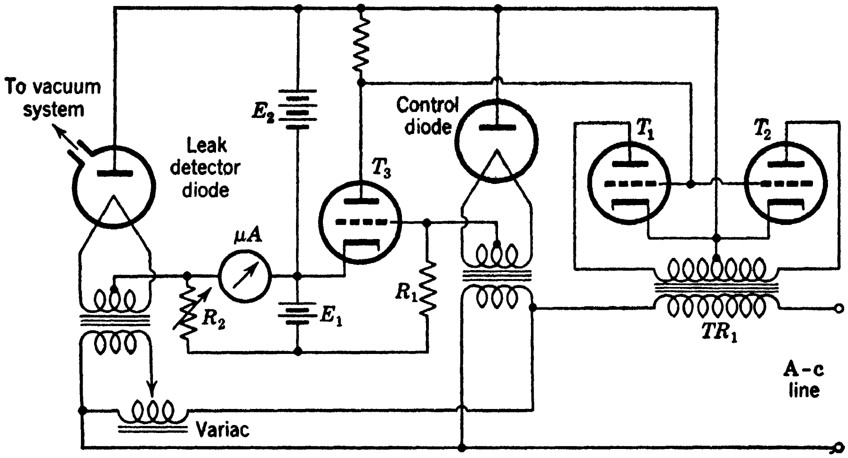

FIG. 76. Essential elements of a-c operated leak detector based on the same principle as the circuit in Fig. 75 (R. B. Nelson).

A control diode similar to the leak detector, but highly evacuated and sealed off, has its filament heated by the same source of a-c power as the leak detector filament. The saturated thermionic emission current of the "control diode" is fed back to regulate the a-c voltage which heats both filaments, thus compensating for line voltage changes in such a way as to keep constant emission in the control diode. Since we regulate the thermionic emission—the same rapidly changing function of filament power which we want to measure in the leak detector diode—the emission of the leak detector can be held quite constant as the line voltage varies.

The feedback circuit by which the emission current of the control diode regulates the a-c voltage is similar to the emission-regulating circuit for an ionization gauge described by Ridenour and Lampson.[193] A transformer TR_1 has its primary in series with the a-c line which heats the filaments. Across the secondary in full-wave connection are two triodes T_1 and T_2. As the grid voltage of the triodes is raised, lowering their plate resistance, the impedance of the transformer primary is likewise lowered. This causes a decreased voltage drop across the primary and hence increased voltage on the filaments of the diodes.

The emission current of the control diode, passing through resistor R_1, produces the grid voltage of the d-c amplifier tube T_3, a high-μ triode. The cathode of this tube is held at a steady positive potential E_1, so that the tube is cut off until the voltage drop in R_1 is almost equal to E_1. Further increase in grid voltage causes T_3 to conduct, producing a negative bias on the grids of T_1 and T_2.

---

[193] L. N. Ridenour and C. W. Lampson, *Rev. Sci. Instruments*, 8, 162 (1937).

The control circuit thus regulates the emission current of the control diode to a value about equal to E_1/R_1. Since the leak-detector diode may not have an identical filament, its filament transformer runs from a Variac by which the emission may be adjusted. The steady emission is balanced out from the microammeter by current through R_2 so that a sensitive meter may be used and small changes in emission detected.

Experience has shown that the leak detector must be run for about 15 minutes before the emission becomes sufficiently stable to look for leaks.

As mentioned previously, Nelson has combined the circuit for the leak detector with that required to operate an ionization gauge, and a description of the combined circuit is given in the original publication. The whole system is arranged in a box provided on the panel with two indicating instruments and control switches, which can be plugged into the standard 115–127 volt 60-cycle a-c supply.

An interesting method for the detection of leaks described by H. Nelson[194] involves the use of a *hydrogen ionization gauge*, which is shown in Fig. 77. According to Nelson's description,

Part *A* is an evacuated and sealed-off ionization-gauge tube with a piece of palladium tubing *P* forming part of the envelope. Part *B* is made from Nonex glass tubing, ring-sealed onto the glass envelope of the ionization-gauge tube. *C* is a coil of platinum-clad molybdenum wire which serves to heat the palladium tubing.

When this device is sealed to a vacuum system, it may be used for detecting and locating air leaks in a manner similar to that in which a conventional ionization gauge is used but with several important advantages. The palladium tubing is heated to a temperature of about 800° C at which it is exceedingly permeable to hydrogen but to no other gases or vapors. If a jet of hydrogen, illuminating, or forming gas is then used to probe the system for leaks, hydrogen will enter the vacuum system at the point of leakage, pass through the walls of the palladium tubing, and give an increased pressure reading in the ionization-gauge unit. After the leak has been located and the hydrogen jet removed, the hydrogen is pumped out from the ionization-gauge tube through the walls of the hot palladium tubing. Since a far higher vacuum may be maintained in the sealed-off ionization-gauge tube with aid of getter than normally exists in a vacuum system, it follows that far smaller leaks can be detected by the technique described above than by the conventional technique in which the ionization-gauge tube is directly connected to the vacuum system.

For detecting and locating air leaks in vacuum-tube envelopes the arrangement shown diagrammatically in Fig. 78 is used.

With *T* immersed in liquid air and with all stopcocks open, the system is pumped to a pressure of about 10^{-4} mm of mercury. (The use of a mercury- or oil-diffusion pump is not required.) The palladium tubing of the hydrogen gauge is then heated to about 800° C, a hydrogen hood is lowered over the tube under test, and the ion current of the sealed-off ionization gauge is watched for indication of a leak. If an increase in the ion current indicates the presence of a leak, the hydrogen hood is raised and suspected points on the tube are probed by a fine hydrogen jet until a further increase in the ion current indicates the exact location of the leak. When a leak is too small to be located by the above method, increased sensitivity may be obtained by closing the stopcock S_2 before applying hydrogen to the tube under test. To obtain maximum sensitivity, hydrogen may be allowed to diffuse through the leak in the tube under test with stopcocks S_1 and S_2 both closed for a period of one or more minutes, after which stopcock S_1 is opened to allow the accumulated hydrogen to give indication of leakage.

---

[194] *Rev. Sci. Instruments*, **16**, 273 (1945).

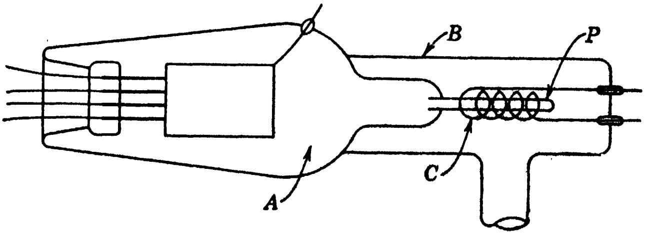

FIG. 77. Leak-detector tube involving use of palladium tube and ionization gauge (H. Nelson).

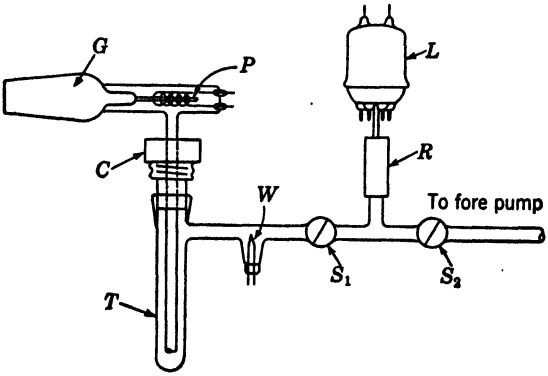

FIG. 78. Arrangement for use on exhaust system of leak detector shown in Fig. 77. C = compression rubber port; G = hydrogen gauge; L = tube under test; P = palladium; R = rubber port; S_1, S_2 = stopcocks; T = liquid-air trap; and W = tungsten filament.

Nelson has drawn attention to the fact that lack of sensitivity may be observed because of adsorption of oxygen on the palladium or because of the presence of oil vapors in the space surrounding the tube. To avoid the latter difficulty it is recommended that the hydrogen gauge should be removed before the trap is allowed to reach room temperature.

With regard to the sensitivity of the detector, the following statement is made.

> During the period that the leak detector has been in use, leaks of widely different magnitude have been located. Leaks large enough to cause a vacuum tube to lose completely its vacuum in less than 24 hours after seal-off can usually be located in less than 2 or 3 minutes after the tube is put on the detector. Leaks of smaller magnitude require more time for their location but they can usually be found if they are large enough to cause a tube to lose its vacuum completely in less than two weeks after seal-off or if the rate of flow of hydrogen through the leak is greater than about $1 \cdot 10^{-4}$ micron · liter per second. [This corresponds to about 0.36 micron · liter per hour.]

An ionization gauge with helium has been found by the writer to be a very useful and convenient leak detector in factory practice. As pointed out in section 7, the sensitivity of the ionization gauge for helium is about one-sixth that for nitrogen (or air). If a gauge is connected to the exhaust system at some point between the origin of the leak and the vapor pump, it will indicate a pressure (in microns) of air, which is determined by the relation

$$Q = SP_0, \tag{1}$$

where Q = rate of leak of air in, for instance, micron · liters · sec^{-1}, and S = speed of exhaust in liters · sec^{-1}. The value of P_0 will obviously be higher than the ultimate pressure obtainable for a "tight" system. If, now, helium at atmospheric pressure is directed by means of a fine jet at the point where the leak is present, then the values of both Q and S are increased in the ratio $\sqrt{29/4}$ and therefore the absolute value of P_0 is not affected. However, since this pressure is due to helium instead of air, the ion current is considerably smaller.

If Q is very small, so that the stationary value of P_0 is only slightly higher than it would be if no leak were present, the magnitude of P_0 may be increased, at constant value of Q, by closing the main stopcock to the pump and letting the evacuation take place through a smaller-diameter tube which is connected in parallel with the stopcock between the gauge and pump.

Actual tests have shown that it is possible by means of this procedure to demonstrate the presence of leaks which correspond to about 0.2 micron · liter per hour. One advantage of this method is that a number of tubes may be connected to the same pumping system at the same time and it is then possible by means of the ionization gauge and a helium jet to determine which particular tube or tubes leak. Another advantage is the fact that no time-lag is involved. The change in the value of the positive-ion current on replacing the air by helium occurs practically instantaneously.

It should also be mentioned that replacing the helium by vapor of a volatile organic liquid such as ether or acetone causes an *increase* in the ion current over that observed with air. This observation is evidently in agreement with the results, mentioned in section 7, which have been obtained by Blears, and also in this laboratory, on the magnitudes of the positive-ion currents in the presence of organic vapors.

A summary of vacuum testing methods in use before 1943, quoted from the paper by R. B. Jacobs and H. F. Zuhr,[195] is given in Table 7.

In the first three methods the probe fluids were chosen to insure maximum sensitivity of the gauge indications. With increase in "tightness" of vacuum systems it became possible to replace the hot-wire gauge by one of the ionization type (method 4). The authors state,

> To obtain the ultimate sensitivity of these methods the dynamic method was discarded and one of the following methods adopted: (1) the "backing space" technique, or (2) the apparent change in rate of pressure build-up when probe gas displaces air flowing through the leak. Both methods achieve the improved sensitivity at the expense of an increase in testing time.
>
> Backing space is the name given to the process of multiplying the effect of the probe gas by permitting the diffusion pump to compress the gas into a dead volume. This is achieved by shutting the valve in the foreline leading to the mechanical pump. The method further requires judgment in the analysis of the signal indicated on the gauge controls.

Furthermore the operation of this method requires highly trained personnel. In methods 7 and 8 the system has to be outgassed for a prolonged period.

The *most sensitive method for the detection of leaks*, and one which also gives an indication in a minimum of time, was developed during World War II.[196] It involves the *use of a mass spectrometer with helium*,[197] and the principle by which it operates may be described briefly as follows:

When a beam of positive ions, accelerated by a potential V, is passed through a magnetic field of strength H, the ions are sorted out, according to their values of e/m, where m is the mass of the ion, and e the charge.

---

[195] *J. Applied Phys.*, **18**, 34 (1947). The original rates of leak, expressed in micron · cubic feet per hour, have been converted into micron · liters per minute (μl/m) by means of the conversion factor, 1 μcf/h = 0.472 μl/m.

[196] Jacobs and Zuhr, *loc. cit.*

[197] A. O. Nier, C. M. Stevens, A. Hustrulid, and T. A. Abbott, *J. Applied Phys.*, **18**, 30 (1947).

TABLE 7

RÉSUMÉ OF VACUUM TESTING METHODS IN USE PRIOR TO 1943 (JACOBS AND ZUHR)

Leak Detector	Operating Range, microns	Size of Leak Discernible	Commonly Used Probes	Remarks
1. Tesla coil	50–1000	μl/m		Useful only on glass systems
2. Discharge tube	100–1000		Acetone, methanol, CO_2, H_2	Residual gases confusing
3. Hot-wire gauge	<100	4.7–470	Acetone, methanol H_2	Affected by pressure changes and residual vapor
4. Ionization gauge	<0.5	0.47–47	Gaseous hydrocarbons, H_2, O_2	Affected by pressure changes and residual vapor
5. Hot wire with backing space	<100	24–47	Gaseous hydrocarbons, H_2, O_2	Time-consuming
6. Ionization gauge with backing space	<0.5	0.5–47	Gaseous hydrocarbons, H_2, O_2	Time-consuming
7. Hot wire with pressure build-up	<50	0.5–47	Gaseous hydrocarbons, H_2, O_2; masking with vacuum putty	Extensive outgassing required
8. Ionization gauge with pressure build-up	<0.5	0.5–47	Gaseous hydrocarbons, H_2, O_2; masking with vacuum putty	Extensive outgassing required

The radius of curvature, R, of the path of any given type of *singly charged* ion is determined by the relation

$$R = 143.9 \frac{\sqrt{MV}}{H}, \tag{2}$$

where R is expressed in centimeters, V in volts, H in gauss, and M is the molar mass of the ion in grams.

For example, for $R = 4.0$ cm and $H = 1500$ gauss, the values of V for helium ($M = 4.003$) and nitrogen ($M = 14.008$, since N^+ is formed), are found to be 434 volts and 124 volts, respectively. Thus, for a given value of the radius of curvature, the ions reaching a collector may be differentiated by varying the value of V, and the magnitude of the ion current at any given voltage setting will depend on the concentration of the ions in the beam, that is, on the rate at which the corresponding molecules leak into the spectrometer.

For the detection of leaks helium has been chosen as testing gas for the following reasons:

1. Because of the low value of M, the rate of diffusion through a leak is greater than that of any other gas except hydrogen.

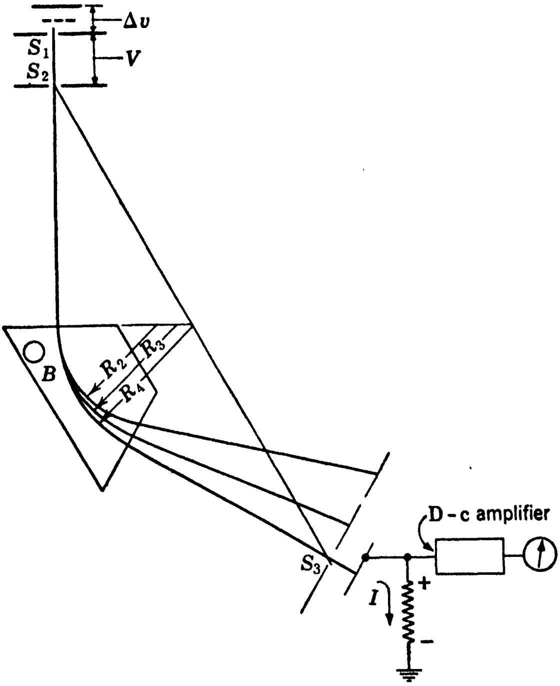

FIG. 79. Sixty-degree mass spectrometer. The ions are repelled through the slit S_1 by a small positive voltage Δv, and are accelerated between S_1 and S_2 by the potential V. Helium ions sorted according to the value of R, the radius of curvature, enter the slit S_3 and are discharged on the collector plate, causing a positive current, I, to flow through the high resistance to ground..

2. Helium occurs in the atmosphere to the extent of only 1 part in 200,000 parts of air.

3. There is no possibility that an ion due to any other gas will give an indication that can be mistaken for helium.

The application of the mass spectrometer to the detection of leaks has been described in two papers, one by W. G. Worcester and E. G. Doughty,[198] and the other by H. A. Thomas, T. W. Williams, and J. A. Hipple.[199]

---

[198] *Trans. Am. Inst. Elect. Engrs.*, **65**, 946 (1946).

[199] *Rev. Sci. Instruments*, **17**, 368 (1946); *Westinghouse Engineer*, **6**, 108 (1946).

The type of spectrometer developed by the first-named investigators is best illustrated by Figs. 79 and 80. The positive ions, produced by ionization of gas molecules by means of electrons emitted from a hot tungsten filament, are accelerated by means of a potential of about 270 volts applied to the slits S_1 and S_2 (see Fig. 79) and deflected through an angle of 60° by the field of about 900 gauss due to a permanent magnet with trapezoidal pole pieces, which is inside the spectrometer tube.[200] For a given type of ion, the radii of curvature corresponding to different values of the accelerating voltage are represented by R_2, R_3, and R_4. With the values of V and H given above, the value of R for helium ions is 5.25 cm, and, if the slit S_3 is set for this value of R, only helium ions will reach the collector, whereas all other types of ions will be deflected either to the right or left of the slit.

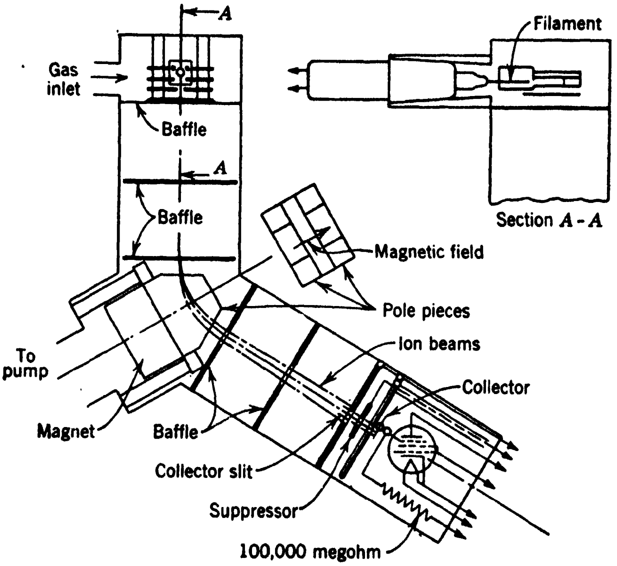

FIG. 80. Diagram of mass spectrometer.

The spectrometer tube the details of which are shown in Fig. 80 is of metal, and the first stage of the amplifier in the output circuit of the ion collector is mounted in the tube, "in order to keep the high resistance and the grid connections dry to minimize leakage currents, to keep the leads as short as possible from collector plate to the grid of the first tube, and to provide electrostatic shielding for the input stage." The other stages of the amplifier are mounted on the top part of the control panel, as indicated in the block diagram in Fig. 81.

---

[200] This design of spectrometer was based on that described by A.O.C. Nier, *Rev. Sci. Instruments*, **11**, 212 (1940).

Both the primary emission from the tungsten filament and the emission in the ion gauge connected to the exhaust system are maintained at fixed values by individual control circuits. The control circuit for the ion gauge is so arranged as to operate a relay whenever the pressure in the system exceeds a predetermined value.

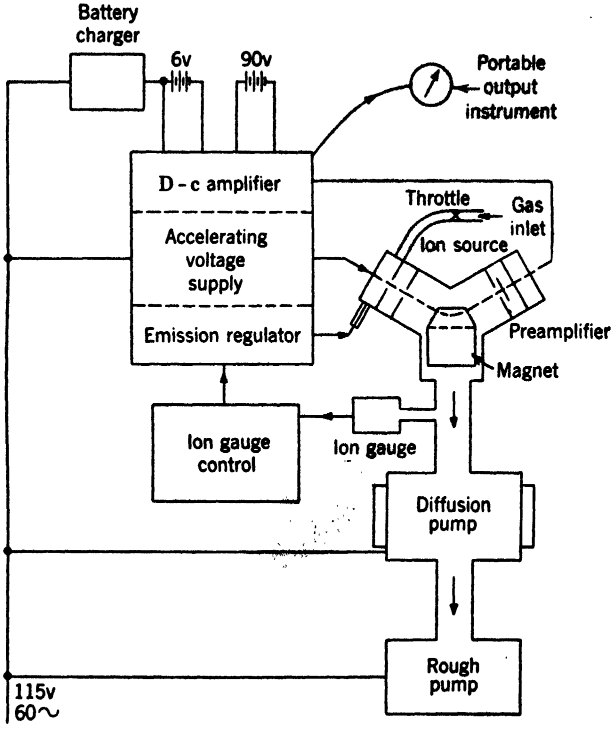

FIG. 81. Block diagram of circuits for leak detector.

In the description of the pumping system it is stated that

> the vacuum in the leak detector is maintained by an oil diffusion pump with a cylindrical Dry Ice trap. The speed of this combination is about 30 liters per second. The diffusion pump requires about 3 cc per second of tap water for cooling. By means of a thermal switch the diffusion pump heater is shut off if the flow of cooling water is not sufficient. Normal heater operation requires about 350 watts from a 110-volt power line. The fore vacuum is obtained with a small mechanical vacuum pump.

Figure 82 shows a rear view of the assembled leak detector.

A relatively simple arrangement for testing tubes for leaks is shown in Fig. 83. The test objects are first exhausted by the mechanical roughing pump (shown at the left), and when the pressure, as indicated, for instance, by a thermocouple gauge connected to the test manifold is sufficiently low the throttle valve to the spectrometer tube is opened. A fine jet of helium is passed over suspected parts in each of the tubes, and the presence of a leak is indicated on the portable output meter shown in Fig. 81 by a peak in the current at about 240 to 250 volts as the accelerating voltage is varied from 200 to 300 volts (see Fig. 84). According to the authors,

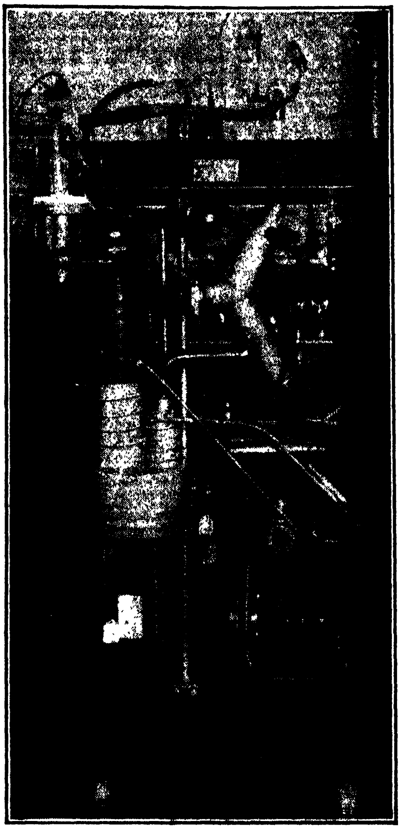

FIG. 82. Photograph showing rear view of commercial form of G.E. leak detector, using "VMF" 100 vacuum pump. Door open.

The sensitivity of the leak detector is such that it will detect the helium in normal air (1 part helium in 200,000 parts air). Under these conditions the partial pressure of helium in the leak detector is only $5 \cdot 10^{-11}$ mm Hg, measured at the ion gauge tube. The quantity of helium flowing through the spectrometer tube is about $1.5 \cdot 10^{-9}$ mm · liter per second.

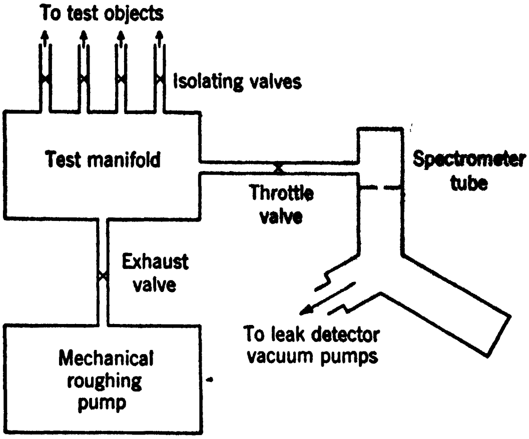

FIG. 83. Simple leak test manifold.

This corresponds to about $5.4 \cdot 10^{-3}$ micron · liter per hour, and the sensitivity claimed for this detector is about 100 times that claimed for the other types of detectors described above. In his own experience the writer has found that leaks of the order of 0.05 micron · liter per hour can be quite readily detected by the instrument in a few minutes.

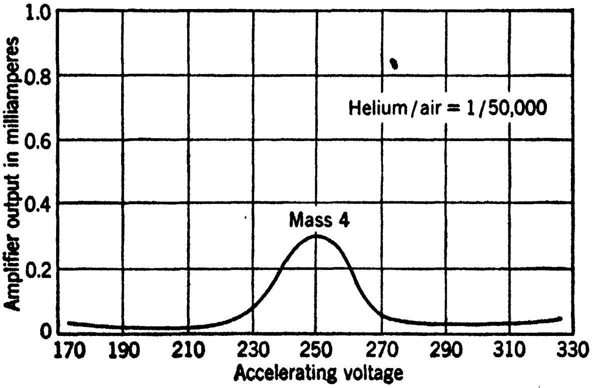

FIG. 84. Typical helium spectrum from leak detector.

The mass spectrometer used by Thomas, Williams, and Hipple[201] is different in design. The beam is deflected through 180° and is prefocused for helium. An external Alnico magnet produces a field of about 1540 gauss and the helium ions are accelerated by about 350 volts, corresponding to a value for R of 3.5 cm. A Philips ion gauge, such as described in section 7, is used for monitoring the pressure in the spectrometer tube. The magnetic field required for this purpose is obtained from the same magnet as that used to deflect the positive-ion beam. A diagram of the vacuum system used for the leak detector is shown in Fig. 85. The authors state that "the instrument can detect as little as 1 part of helium in 400,000 parts of air at an operating pressure of 0.3 micron of mercury."

---

[201] *Loc. cit.*

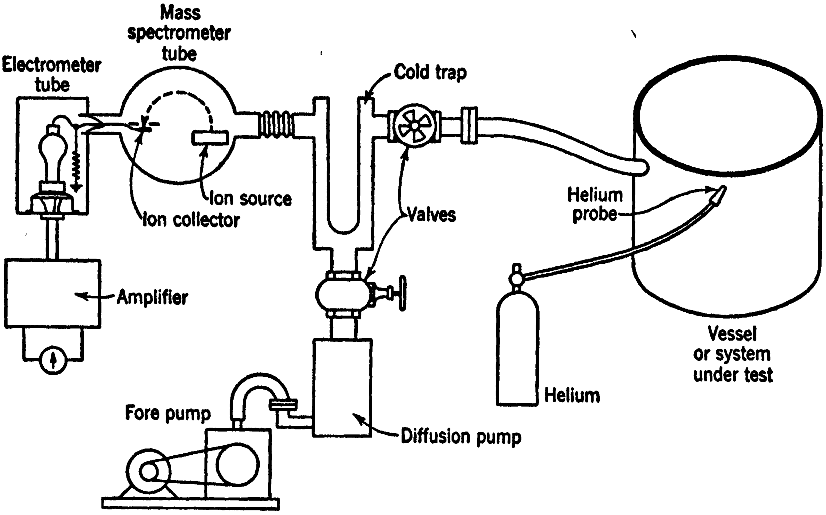

FIG. 85. Schematic diagram of vacuum system for leak detector (Thomas et alii).

According to Jacobs and Zuhr,[202] the values of the inherent sensitivity (ratio of probe gas to air detectable) for the differential Pirani gauge and the mass spectrometer are 1/3000 and 1/100,000, respectively. They also give the following data for the smallest leak detectable in vessels of volume V having a pressure build-up of 200 microns per hour:

V		Smallest Leak Detectable	
cubic feet	liters	micron · cu ft/hr	micron · liters/hr
<1	<28.3	<0.01	<0.283
10	283	0.02	0.57
100	2,832	0.2	5.7
1000	28,316	2.0	57.

---

[202] *Loc. cit.*

Thus, for V between 1 and 10 cu ft, the smallest leak detectable varies from 0.01 to 0.02 micron · cu ft/hr, and similarly for the other ranges of values of V.

Quite different in principle from all the other methods of leak detection described above is that involved in the *positive-ion detector for halogen compounds* which has been described by W. C. White and J. S. Hickey.[203]

Some of the earliest investigators in the field of thermionic emission, such as O. W. Richardson, had observed that platinum, even in air, at a temperature of a red heat, emits positive ions, and that the rate of ion emission increases with temperatures according to a relation similar to that observed for electron emission from incandescent cathodes.[204] This positive-ion emission is most probably due to the presence in the anode of salts of the alkali metals, although this may not be the correct interpretation of the mechanism of operation of the device described below.

It was observed by C. W. Rice of the General Electric Company that this emission, at any given anode temperature, of positive ions in air is increased very markedly when vapors of compounds containing a halogen strike the electrode surface. This observation forms the basis of the detector developed and described by White and Hickey.

A diagrammatic sketch of the device and simple circuit used for its operation are shown in Fig. 86*a*. The detector consists of a platinum cylinder, P, which is heated by an insulated platinum filament, F, the low voltage required for this purpose being supplied by the transformer, T. A metal cylinder, C, concentric with P, is connected through a microammeter (μA) to the negative end of a d-c source of voltage (50–500 volts) while P is connected through the midpoint of the secondary of T to the positive end of the voltage source.

In using the device for detection of leaks, air or any other suitable gas containing a halogen vapor is introduced into the system at a positive pressure. This positive pressure forces the air containing the halogen out through the leak where it may be picked up by the device and is indicated by the meter in the detector circuit, as shown in Fig. 86*b*. Or the detector may be sealed on the vacuum system in series with the pump (preferably between the rough and the fine pumps). Air containing a halogen vapor is forced under pressure through a very small jet and directed at any suspected spot in the system, and then is picked up by the detector.

---

[203] *Electronics,* **21,** 100 (1948).

[204] See discussion in Chapter 10, section 8, also references to literature given there.

In using the detector, the temperature of the anode should be between 850° and 950° C. At lower temperatures, the positive-ion emission is too small, and at higher temperatures the emission becomes unstable. Typical halogen compounds, which are fairly volatile at room temperatures and therefore applicable in using the positive-ion detector, are "Freon," carbon tetrachloride, and chloroform.

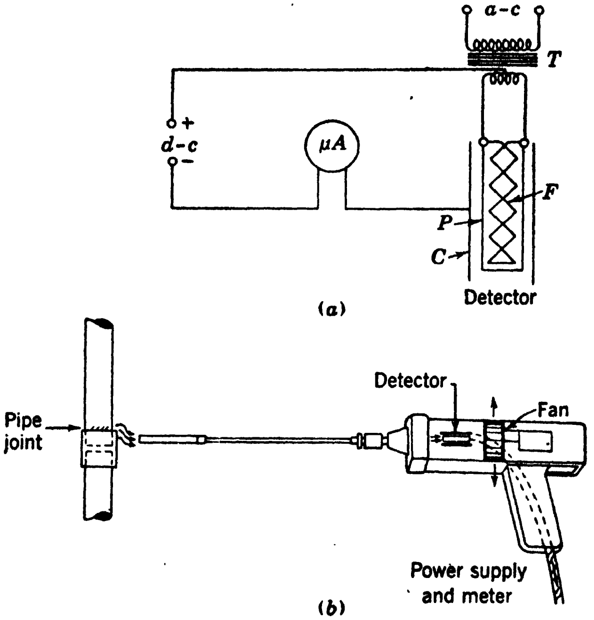

FIG. 86. (*a*) Diagrammatic sketch of design of thermionic detector for vapors of halogen compounds and electric circuits used in its operation. (*b*) Illustrating the application of the detector for location of leaks in a vacuum system.

Instead of a microammeter, as shown in Fig. 86*a*, an amplifier may be utilized, and under these conditions, according to White and Hickey, "the limit of sensitivity to small leaks is of the same order of magnitude as that obtained with the mass spectrometer." In practice, the "thermionic halogen vapor detector," as it has been designated, has found application in the production testing of refrigeration units, the mercury-arc rectifier, and a large number of similar leak-location problems.

CHAPTER 7

SORPTION OF GASES AND VAPORS BY SOLIDS

1. ADSORPTION, ABSORPTION, OCCLUSION, AND SORPTION[1]

One of the most important problems in high-vacuum technique is the removing of gases and vapors which are present both on the surface and in the interior of glass walls and metal parts. The fact that charcoal and finely divided metals, after thorough evacuation, can take up considerable volumes of different gases and vapors has found applications in a great number of industrial processes.

There are at least three mechanisms by which a gas or vapor may be taken up by a solid. The solid may actually react with the gas or vapor chemically. For example, phosphorus pentoxide (P_2O_5) removes water vapor by combining with it chemically to form phosphoric acid (H_3PO_4). This and similar types of "clean-up" by chemical reaction will be discussed in Chapter 10.

There are, however, two physical mechanisms by which gas or vapor disappears in the presence of an evacuated solid. The gas may condense as a layer (having a thickness of one or more molecules) *on the surface;* this is known as *adsorption.* The gas may also enter into the *interior of the solid* in much the same manner as gas dissolving in a liquid; this is known as *absorption*. In many cases the gas taken up by the solid may be present in both conditions, or it is difficult to determine the exact nature of the mechanism involved. Consequently, the term *sorption*, introduced by J. W. McBain in 1909, is often used as a "non-generic" term, which includes both adsorption and absorption. Since the terms absorption and *occlusion* describe essentially the same phenomena, the latter term has been generally discarded.

---

[1] In connection with this and the following chapter the writer has made use of the following reference books. The abbreviations used for them are indicated in parentheses.

1. S. Brunauer, *The Adsorption of Gases and Vapors*, Vol. I, *Physical Adsorption*, Princeton University Press, Princeton, N.J., 1943 (SB).
2. J. W. McBain, *The Sorption of Gases and Vapours by Solids*, George Routledge and Sons, London, England, 1932 (McB).
3. S. J. Gregg, *The Adsorption of Gases by Solids*, Methuen's Monographs on Chemical Subjects, D. Van Nostrand Company, New York, 1934 (JG).

The last volume contains a rather compact but excellent summary of the topic. Reference 2 contains a great deal of detailed information on charcoal and silica gel, as well as other adsorbents. Reference 1 deals more with the theoretical aspects and with specific adsorbents only as they illustrate the theoretical deductions.

Since the topic of adsorption is also of great importance in the interpretation of the effects of catalysts in chemical reactions, numerous references to the subject are to be found in the literature on rates of chemical reactions, surface chemistry, and colloids.

Data and references on the adsorption of gases are given in *International Critical Tables*, Vol. 3, pp. 250–251, McGraw-Hill Book Company, New York, 1928.

The solid which takes up the gas is known as an *adsorbent;* the gas or vapor removed from the gas phase is known as *adsorbate.*

The process of removing gas from an adsorbent is ordinarily designated *desorption.*

Materials differ widely with respect to their capacity for adsorbing gases and vapors. Table 1, taken from H. Freundlich's book,[2] compares the behavior of charcoal, meerschaum, and glass powder.

TABLE 1

RELATIVE ADSORPTION OF GASES BY THREE ADSORBENTS

Adsorbent	Gas	Volume Adsorbed at P_{mm} = 100 (cm^3/g at 0° C and 760 mm)
Wood charcoal	CO_2	24.9
	NH_3	95.1
	SO_2	73.6
	CH_3Cl	57.7
Meerschaum	NH_3	84.5
	SO_2	24.3
	CH_3Cl	27.1
Glass powder	CO_2	1
	NH_3	9
	SO_2	6

As will be discussed more fully in the following sections, the sorptive capacity of any one adsorbent depends largely upon the extent of surface per unit mass. Since adsorption at low pressures is undoubtedly limited to a layer one molecule thick (*monolayer*), the amount actually adsorbed per unit mass of any adsorbent is much greater for porous substances such as charcoal, silica gel, and finely divided oxides and metals than for plane surfaces such as glass, mica, and smooth metal surfaces.

Whereas absorption or true solution of gases in metals increases with increase in temperature, adsorption increases with decrease in temperature, and, in general, the adsorption is greater at any given temperature for those gases that are more readily condensible or have the higher boiling points.

---

[2] *Kapillarchemie*, p. 97, Leipzig, 1909.

This is illustrated by the data in Table 2,[3] taken from a paper by W. Hene.[4]

TABLE 2

ADSORPTION OF GASES BY CHARCOAL
(Volume per gram adsorbent, temperature 15° C)

Gas	Volume Adsorbed, cm³	Boiling Point, ° C	Critical Temperature*
$COCl_2$	440	+8.3° C	182° C
SO_2	380	−10.0	157.2
CH_3Cl	277	−23.7	143.1
NH_3	181	−33.35	132.4
H_2S	99	−61.8	100.4
HCl	72	−83.7	51.4
N_2O	54	−89.5	36.5
C_2H_2	49	−88.5	36
CO_2	48	−78.5	31.1
CH_4	16	−161.5	−82.5
CO	9	−192	−139
O_2	8	−183	−118.8
N_2	8	−195.8	−147.1
H_2	5	−252.8	−239.9

* Values given in *Handbook of Physics and Chemistry*, 1945 edition.

Similar observations have been made by other investigators. For instance, I. Langmuir's[5] data on the adsorption of gases on mica and glass surfaces at low temperatures show that the order in which the different gases are adsorbed on these surfaces is methane, carbon monoxide, nitrogen, argon, and oxygen — the first being adsorbed to the greatest extent. The order of the boiling points is methane, oxygen, argon, carbon monoxide, and nitrogen, the last having the lowest boiling point.

In the present chapter, and in the following ones, the observations on sorption of gases and vapors by solids will be discussed from the point of view of their importance in high-vacuum technique. This necessarily means the omission of many of the topics which are discussed comprehensively in the three reference works mentioned above. The literature available on the subject is so extensive that it has been extremely difficult to confine the discussion in this book to a reasonable limit. However, in view of the ready availability of the reference works cited and numerous papers published in English and American journals, it is hoped that the summary presented here will prove both useful and stimulating.

---

[3] SB, p. 12; McB, p. 102.

[4] Dissertation, Hamburg, 1921.

[5] *J. Am. Chem. Soc.*, **40**, 1361 (1918).

2. SOME TYPICAL ADSORPTION ISOTHERMS

In order to investigate the sorption of a gas or vapor by a given adsorbent, a definite weight or area of the adsorbent is first of all desorbed at as high a temperature as practicable, in a good vacuum, in order to remove all adsorbed or absorbed gases. Then, while the adsorbent is maintained at a constant, known temperature, a definite volume of the adsorbate is introduced into the system and the decrease in pressure is noted when equilibrium is attained.[6]

It is observed that there exists, in most cases, a definite relation between the volume (v in cubic centimeters) adsorbed per unit mass (or unit area) of adsorbent and the pressure (P), which can be expressed in the form

$$v = f(P,T),$$

where f is an algebraic function of the variables P and T. A plot of v versus P, *at constant temperature*, is known as an *adsorption isotherm.* From the isotherms at a series of temperatures, it is possible to plot *adsorption isosteres*, which give the variation of the equilibrium pressure with temperature for a *constant amount of gas absorbed.* The isosteres are thus analogous to vapor-pressure curves of liquids, and as in the case of the latter, the *heat of adsorption* (Q_S) is given by the relation

$$Q_S = -R_0 \frac{d \ln P}{d(1/T)}, \tag{1}$$

where R_0 is the gas constant per mole.

From the isotherms it is also possible to plot *isobars*, which indicate the amounts adsorbed, at a series of temperatures, for a given *constant pressure.* Illustrations of both isosteres and isobars are given in the subsequent discussion.

In the following section the form of the adsorption isotherm is discussed for those cases in which the adsorbed gas forms a monolayer or, at most, a layer only a few molecules thick. Adsorption isosteres and heat of adsorption are discussed in subsequent sections.

The data on the amount of adsorption are usually expressed in terms of v_0, the volume in cubic centimeters at 0° C and 760 mm (S.T.P.) per gram of adsorbent, or per square centimeter of smooth surface (glass, mica, metals). Some observers record their data in terms of v_{20}, the volume per gram (or per unit area) at 20° C and 760 mm. Other investigators have given the amounts adsorbed in terms of x, the mass in *milligram per gram* of adsorbent, or in terms of N_M, the number of *moles per gram*. Tables 3 and 4 give the values of conversion factors which will be found useful in comparing data from different sources. The fifth column in Table 4 gives the number of molecules required to form a layer one molecule thick (unimolecular layer or monolayer), while v_{20} and v_0 give the values of the corresponding volumes in cubic centimeters at 760 mm and 20° C and 0° C, respectively.

---

[6] For description of the methods used in obtaining sorption data see references in footnote 1.

TABLE 3

CONVERSION FACTORS FOR AMOUNT ADSORBED

$v_{20} = v_0 \times 293.2/273.2 = 1.074 v_0.$
$v_0 = 0.9317 v_{20}.$
$Q_{\mu l} =$ number of micron · liters at $t°$ C $= 760v$,
where $v =$ volume in cm^3 at 1 atm and $t°$ C.
$N_M = v_0/22{,}415 =$ number of moles/g,
$= v_{20}/24{,}050.$
$10^6 N_M =$ number of micromoles/g.
$x = 10^3 N_M M =$ mg/g,
$= v_0 M/(22.415) = v_{20} M/(24.050).$
$n_S =$ number of molecules adsorbed per gram,
$= 6.023 \cdot 10^{23} N_M,$
$= 2.687 \cdot 10^{19} v_0,$
$= 2.504 \cdot 10^{19} v_{20}.$
$v_t = 1.3158 \cdot 10^{-3} Q_{\mu l}$ (at $t°$ C).

TABLE 4

NUMBER OF MOLECULES PER MONOLAYER AND EQUIVALENT VOLUMES

Gas	M	$M/(22.415)$	$M/(24.050)$	$10^{-14} N_S$*	$10^5 v_{20}$	$10^5 v_0$†
H_2	2.016	0.0900	0.08381	15.22	6.08	5.67
He	4.003	0.1790	0.1664	24.16	9.65	8.99
A	39.94	1.7820	1.661	8.54	3.41	3.18
N_2	28.02	1.250	1.165	8.10	3.24	3.02
O_2	32.00	1.428	1.330	8.71	3.48	3.24
CO	28.01	1.250	1.165	8.07	3.23	3.00
CO_2	44.01	1.963	1.830	5.34	2.13	1.99
CH_4	16.03	0.7152	0.6664	5.23	2.09	1.95
NH_3	17.03	0.7597	0.7078	4.56	1.82	1.70
H_2O	18.02	0.8041	0.7492	5.27	2.11	1.96

* Values of N_S taken from Table 1.6. Values for CO, CH_4, and NH_3 were calculated from the values of η_0, $1.659 \cdot 10^{-4}$, $1.022 \cdot 10^{-4}$, and $0.92 \cdot 10^{-4}$, respectively.

† To deduce the values at 25° C, multiply the values given in this column by 1.091.

Figure 1 shows adsorption isotherms for nitrogen on activated coconut charcoal, as observed by I. Homfray.[7] Values of v_0 are plotted against P, the pressure in millimeters, for the range −78° C to 100° C.

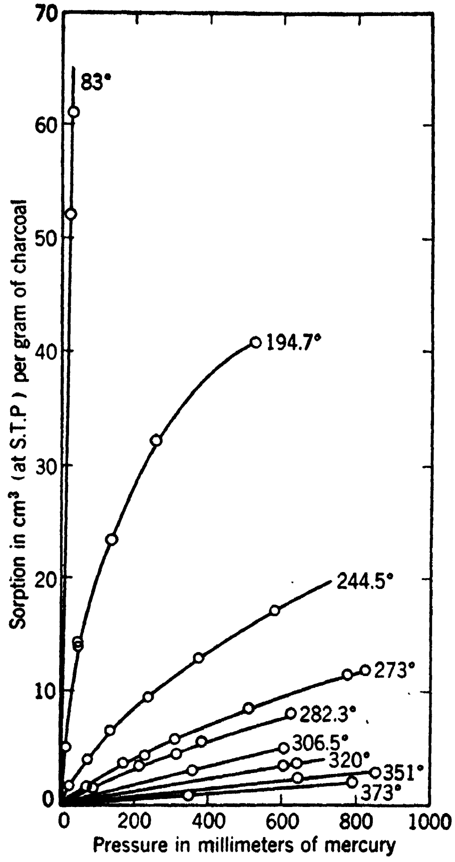

FIG. 1. Isotherms for the sorption of nitrogen by coconut charcoal (Homfray).

Figure 2 shows isotherms at low pressures for carbon dioxide on wood charcoal, as observed by A. Magnus and H. Kratz.[8] Figure 3 gives the isotherms over a higher range of pressures. The ordinates give micromoles ($10^6 N_M$) per gram of adsorbent, and the corresponding values of v_0 are indicated on the right-hand scale. ($v_0 =$ 0.02242 × micromoles.)

[7] *Z. physik. Chem.*, **74**, 129 (1910); McB, p. 101, Fig. 28.

[8] *Z. anorg. Chem.*, **184**, 241 (1929).

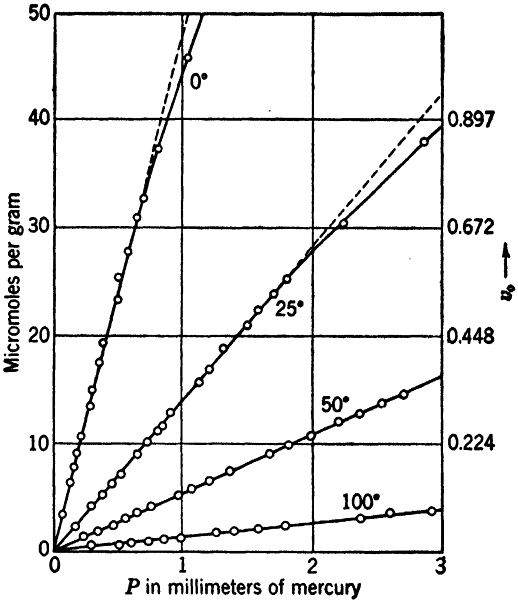

FIG. 2. Isotherms for the sorption at low pressures of carbon dioxide by wood charcoal (Magnus and Kratz).

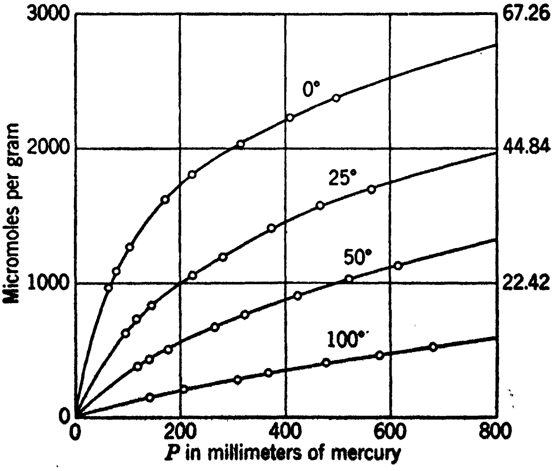

FIG. 3. Isotherms for the sorption at higher pressures of carbon dioxide by wood charcoal (Magnus and Kratz).

Figure 4, taken from a more recent paper by M. H. Armbruster,[9] gives low-temperature adsorption isotherms for carbon monoxide, nitrogen, and argon on smooth silver (area = 8002 cm^2), while Fig. 5 shows plots of observations made by W. G. Frankenburg[10] on the adsorption of hydrogen on tungsten powder. From the latter set of measurements, it was concluded that the "true saturation value" for the particular sample of powder used was 6.60 · 10^{-6} mole hydrogen per gram (instead of 3.60 · 10^{-6} as would follow from the isotherm for −195° C). Table 5 gives the adsorbed amounts in percentage of this value as a function of the equilibrium pressures at various temperatures.

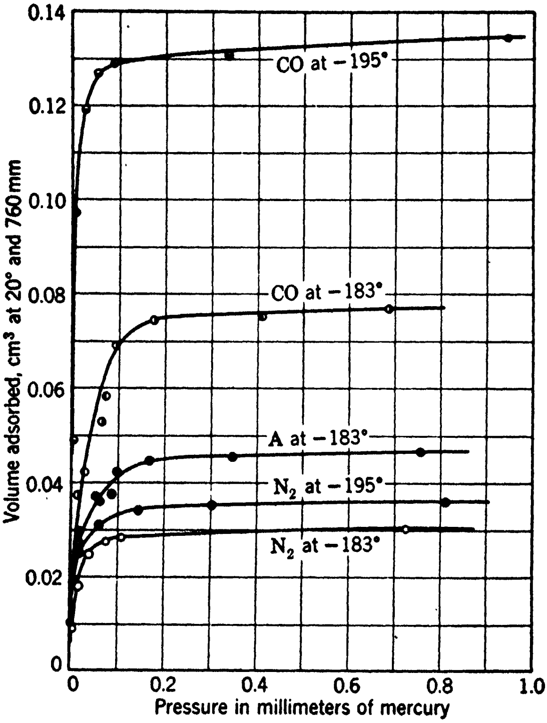

FIG. 4. Isotherms for the adsorption of carbon monoxide, argon, and nitrogen on smooth silver at −183° C and −195° C (Armbruster).

It will be observed that in all cases the amount adsorbed at any given temperature increases more or less rapidly with increase in pres-

---

[9] *J. Am. Chem. Soc.*, 64, 2545 (1942).

[10] *J. Am. Chem. Soc.*, 66, 1827 (1944).

TABLE 5

ADSORPTION OF HYDROGEN BY TUNGSTEN POWDER, EXPRESSED AS PERCENTAGE OF SATURATION VALUE

Equilibrium	Temperatures, ° C							
P_{mm}	0	100	200	300	400	500	600	700
$1 \cdot 10^{-6}$			4.4	0.8				
$1 \cdot 10^{-4}$	21.0	15.5	7.5	3.3	0.9			
$1 \cdot 10^{-3}$	23.5	17.5	10.0	4.6	1.8	0.6		
$1 \cdot 10^{-2}$	25.5	19.0	12.0	6.5	3.1	1.2	0.4	0.15
$1 \cdot 10^{-1}$	29.5	23.5	16.0	10.0	5.6	2.4	0.9	0.5
1	33.0	27.5	20.5	14.0	9.5	5.0	2.4	1.5
10	38.0	32.5	26.5	20.0	16.0	10.5	7.0	4.5

sure at very low pressures, then increases less rapidly at higher pressures and finally tends to reach a limiting value at still higher pressures. Furthermore, for the same equilibrium pressure, the amount adsorbed decreases with increase in temperature. These isotherms are qualitatively characteristic of almost all observations on adsorption over a range of pressures and temperatures at which the amount adsorbed does not exceed that corresponding to approximately a unimolecular layer. For cases of multimolecular adsorption the isotherms do not tend to flatten with increase in pressure but exhibit a more or less continuous increase in pressure up to a value P_S, which corresponds to the saturation vapor pressure of the adsorbate at the given temperature.

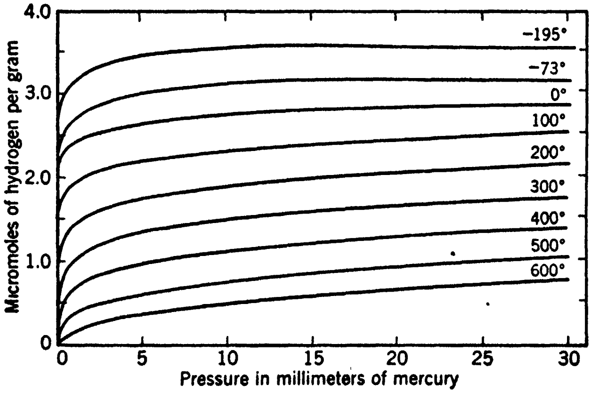

FIG. 5. Isotherms for the adsorption of hydrogen on tungsten powder (Frankenburg).

Although in the above discussion it has been implied that the amount adsorbed is a continuous function of the equilibrium pressure, there is much evidence for the conclusion that the adsorption isotherm is "composed of a series of intersecting curves or loops, so small that to a first approximation one continuous curve could be drawn right through them, with the experimental points lying distributed somewhat irregularly about it."[11]

Such discontinuities were first observed by A. J. Allmand and R. Chaplin[12] in measurements on the sorption of carbon tetrachloride by charcoal. Subsequent observations by Allmand and L. J. Burrage[13] on the sorption of both water and carbon tetrachloride by charcoal confirmed the earlier results.[14]

Similar evidence of discontinuities has been obtained by A. F. Benton and T. A. White[15] on quite a different type of system—hydrogen on Ni at −191°, and hydrogen on copper at −183°. Otherwise, their existence does not seem to have been noted by other workers. Up to the present, no satisfactory explanation of the phenomenon has been forthcoming.[16]

3. PARABOLIC AND HYPERBOLIC EQUATIONS FOR ADSORPTION ISOTHERM

A number of algebraic expressions have been deduced by different investigators to describe the variation (at constant temperature) in amount adsorbed with the pressure. A review of these different relations is given in the following remarks.

Parabolic Adsorption Isotherm. In 1909 H. Freundlich[17] proposed the semiempirical relation

$$v = kP^{1/n}, \tag{1}$$

where k and n are constants that depend upon the nature of both adsorbent and adsorbate and also upon the temperature. This relation is usually expressed in the form

$$\log v = \log k + \frac{1}{n} \log P, \tag{2}$$

so that a plot of log v versus log P should yield a straight line, the slope of which gives the value of n in accordance with the relation

---

[11] JG, p. 5.

[12] *Proc. Roy. Soc. London*, A, **129**, 235 (1930).

[13] *J. Phys. Chem.*, **35**, 1692 (1931).

[14] See also A. J. Allmand, L. J. Burrage, and R. Chaplin, *Trans. Faraday Soc.*, **28**, 218 (1932).

[15] *J. Am. Chem. Soc.*, **52**, 2325 (1930); **53**, 2807, 3301 (1931).

[16] JG, p. 7.

[17] *Kapillarchemie*, Vol. I, pp. 153–172, Leipzig, 1930.

$$\frac{d\,(\log v)}{d\,(\log P)} = \frac{1}{n}. \tag{3}$$

In all cases n is greater than or equal to unity. Figure 6 shows plots of $\log N_M$ versus $\log P$ for the isotherms plotted in Fig. 5. Table 6, taken from the paper by Frankenburg (see Table 5), gives values, for a series of temperatures, of the slope $(d \log P/d \log N_M)$ for two tungsten powders. The values given in the second and third columns were obtained for total amounts adsorbed greater than 0.8 per cent of the saturation value; the values in the last column were obtained for adsorptions less than 0.8 per cent of saturation. (The values plotted in Figs. 5 and 6 are for powder 9798.)

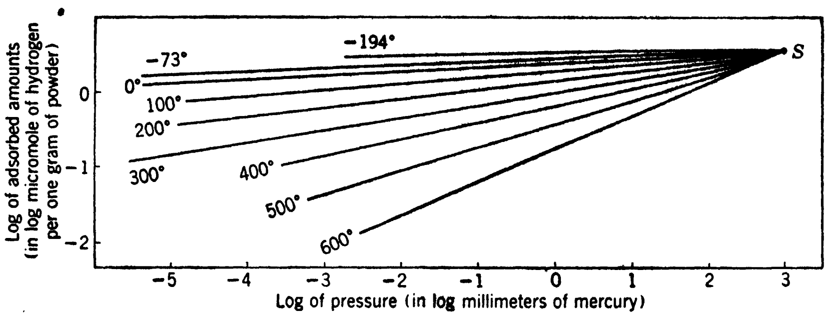

FIG. 6. Log-log plots of isotherms shown in Fig. 5.

TABLE 6

VALUES OF n FOR ADSORPTION OF HYDROGEN BY TUNGSTEN POWDER

Temperature, °C	Powder 9798	Powder 9799	
−194	(67.4)	Not measured	
−73	24.1	Not measured	
0	16.85	16.41	
100	10.88	10.74	
200	7.80	7.36	
300	5.80	5.40	
400	4.04	4.30	2.02
500	3.08	3.04	2.04
600	2.30	2.32	1.98
650	2.09	2.23	2.00
700	1.85	1.85	2.06
750	1.71	1.73	2.03

Another illustration of the application of equation 1 is shown in the plots in Fig. 7, of observations on the adsorption of nitrogen on different surfaces of steel, which were made at low temperatures and quite low pressures by M. H. Armbruster and J. B. Austin.[18] The steel used was in the form of strips, and the total areas were 11,130 cm^2 and 24,680 cm^2, for samples 2 and 3, respectively. In the plots the amounts adsorbed are expressed in terms of atm · cm^3 at 20° C. As the investigators point out,

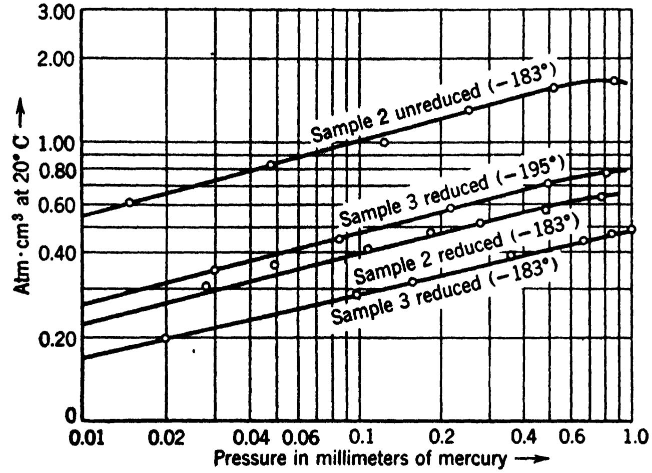

FIG. 7. Log-log plots of volume versus pressure for the adsorption of nitrogen on steel (Armbruster and Austin).

> These data yield a straight line over the 200 fold pressure range, 0.001 to 0.20 mm; moreover, the several lines are substantially parallel, with a slope corresponding to a value of n of about 4. A similar plot of the data for argon yields an analogous set of parallel straight lines with a slope corresponding to a value of n of about 3.

As Brunauer points out,[19]

> In general a large number of the experimental results in the field of van der Waals adsorption[20] (and even in chemisorption) can be expressed by means of the Freundlich equation in the middle pressure range. A still larger number cannot be expressed satisfactorily. Where the equation is obeyed, it can be used as an interpolation formula.

---

[18] *J. Am. Chem. Soc.* **66**, 159 (1944).

[19] SB, p. 57.

[20] The terminology indicates that the forces between gas molecules and atoms on the surface of the adsorbent are of the same nature as those leading to deviations from the ideal-gas laws for gases at high pressures. Heats of evaporation and of adsorption constitute a measure of the magnitudes of these forces. (See section 7.)

As an example of this Brunauer cites the observations of K. Peters and K. Weil[21] on the adsorption of argon, krypton, and xenon on charcoal. The adsorption isotherms for different temperatures are shown in Fig. 8, while Fig. 9 shows the plots of log v_0 (cm^3, S.T.P.) versus log P_{mm}. The values of k and $1/n$ for the three gases are given in Table 7 (where $k = \text{cm}^3/(\text{mm})^{1/n}$).

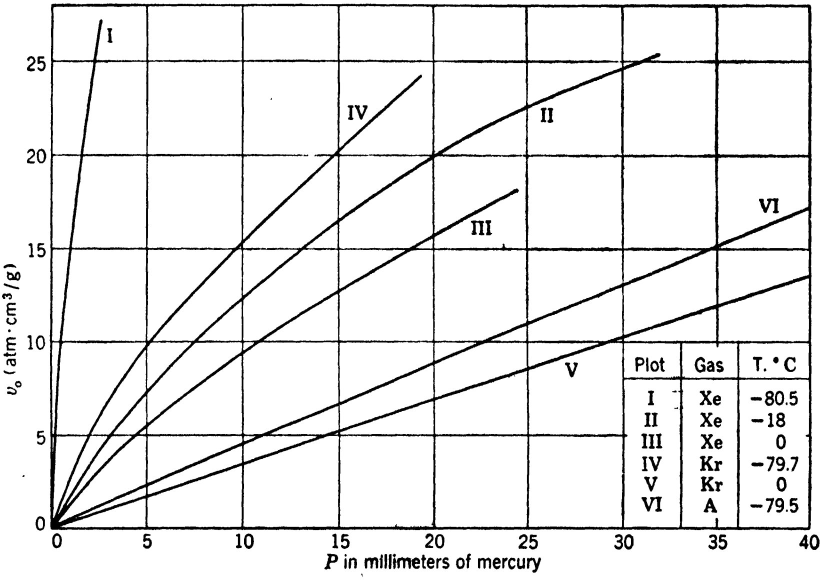

FIG. 8. Isotherms for adsorption of argon, krypton, and xenon on charcoal (Peters and Weil).

TABLE 7

ADSORPTION CONSTANTS OF RARE GASES (PER GRAM CHARCOAL)

	T = 193		T = 255.2		T = 273.2	
Gas	k	$1/n$	k	$1/n$	k	$1/n$
Argon	0.500	0.950	(0.0764)	(1.0)	(0.0581)	1.0
Krypton	2.927	.711	(0.497)	(0.885)	0.340	1.0
Xenon	15.99	.574	2.458	0.692	1.583	0.77

As will be observed, the value of k for any one gas decreases with increase in temperature, while the value of $1/n$ increases and ultimately reaches the value unity. For different gases, the values of k increase in general, and those of $1/n$ decrease, with rise in boiling point, as shown by the data in Table 8[22] (where $k = \text{cm}^3/(\text{mm})^{1/n}$).

---

[21] *Z. physik. Chem.*, **A**, **148**, 1 (1930).

A similar conclusion has been drawn by Langmuir,[23] as mentioned previously, from his observations on the adsorption of a number of

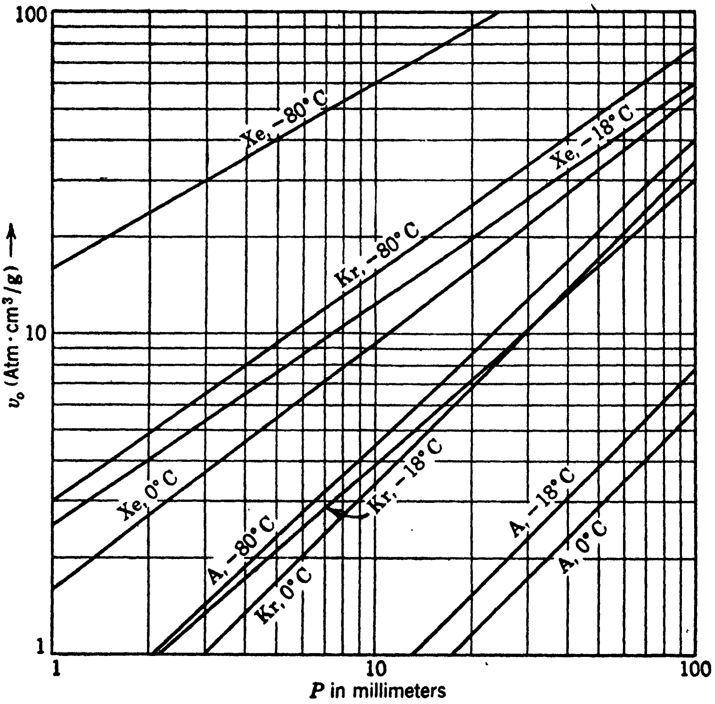

FIG. 9. Log-log plots of isotherms shown in Fig. 8.

TABLE 8

ADSORPTION CONSTANTS OF GASES ON COCONUT CHARCOAL
(1 g of adsorbent at 0° C)

Gas	k	$1/n$	Boiling Point, °C
N_2	0.26	0.87	−195.8
CO	0.56	.76	−191.6
A	0.22	.88	−185.7
CH_4	2.69	.56	−161.5
C_2H_4	23.7	.23	−103.9
CO_2	8.25	.53	− 78.5

---

[22] H. Freundlich, *op. cit.*, p. 170.
[23] *J. Am. Chem. Soc.*, **40**, 1361 (1918).

gases on mica and glass surfaces at low temperatures. If the gases are arranged in order, according to the amounts required to saturate the surface, it is found that this order is the same as that of the boiling points.

For $n = 1$, the amount adsorbed varies directly as the pressure. A similar relation has been observed to apply to the solubility of gases in liquids; it is known as *Henry's law.*[24] As will be shown in the subsequent discussion there is considerable evidence that for many cases of adsorption the linear relation between v and P applies at very low pressures. Figure 2 shows that, in the sorption of carbon dioxide by coconut charcoal at 0° C and higher temperatures, Henry's law is valid in the range of a few millimeters pressure. Table 9 gives average values of the ratio $10^6 N_M/P_{mm}$ (micromoles/g/mm) and the upper values of P_{mm} at which the ratio begins to decrease below the value in the table (as shown in Fig. 3).

TABLE 9

Application of Henry's Law to Adsorption of Carbon Dioxide on Charcoal

$t°$ C	$10^6 N_M/P_{mm}$*	Approximate Upper Limit of P_{mm}
0	47.11	0.7
25	14.13	1.7
50	5.445	3.0
100	1.389	11.8

* Values given by Magnus and Kratz, *loc. cit.*

Similar illustrations of the applicability of Henry's law have been observed by H. H. Lowry and S. O. Morgan[25] in the adsorption of nitrogen on graphite at 56.7° C and 100° C. Other isotherms of the same nature have been mentioned by S. J. Gregg.[26] In general, however, the amount adsorbed increases fairly rapidly with pressures at low pressures and then flattens off gradually at higher pressures. This is especially true when charcoal and fine metallic powders are the adsorbents. On the other hand, with the gels of silica and similar oxides, the isotherm tends to resemble the form demanded by Henry's law.

Hyperbolic Adsorption Isotherm. While the parabolic equation is to a large extent empirical in origin, I. Langmuir developed a conception of adsorption phenomena which led not only to the formulation of an extremely important relation for the adsorption isotherm but also to a logical interpretation of the nature of the forces existing at the surfaces of solids and liquids.

---

[24] Proposed by William Henry (1803–1805).

[25] *J. Phys. Chem.*, **29**, 1105 (1925).

[26] JG, p. 3.

Because of the fundamental importance of Langmuir's views, we quote at length from the original paper,[27] in which these new ideas were set forth in detail:

> During the year 1914, in connection with studies of electron emission and chemical reactions at low pressures, I became much interested in the phenomena of adsorption, and developed a theory which has been strikingly verified by a large number of experiments carried out since that time. According to this theory there is an abrupt change in properties in passing through the surface of any solid or liquid. The atoms forming the surface of a solid are held to the underlying atoms by forces similar to those acting between the atoms inside the solid. From Bragg's work on crystal structure and from many other considerations we know that these forces are of the type that have usually been classed as chemical. In the surface layer, because of the asymmetry of the conditions, the arrangement of the atoms must always be slightly different from that in the interior. These atoms will be unsaturated chemically and thus they are surrounded by an intense field of force.
>
> From other considerations, I was led to believe that when gas molecules impinge against any solid or liquid surface they do not in general rebound elastically, but condense on the surface, being held by the field of force of the surface atoms. These molecules may subsequently evaporate from the surface. The length of time that elapses between the condensation of a molecule and its subsequent evaporation depends on the intensity of the surface forces. Adsorption is the direct result of this time lag. If the surface forces are relatively intense, evaporation will take place at only a negligible rate, so that the surface of the solid becomes completely covered with a layer of molecules. In cases of true adsorption this layer will usually be not more than one molecule deep, for as soon as the surface becomes covered by a single layer the surface forces are chemically saturated. Where, on the other hand, the surface forces are weak the evaporation may occur so soon after condensation that only a small fraction of the surface becomes covered by a single layer of adsorbed molecules. In agreement with the chemical nature of the surface forces, the range of these forces has been found to be extremely small, of the order of 10^{-8} cm. That is, the effective range of the forces is usually much less than the diameter of the molecules. The molecules thus usually orient themselves in definite ways in the surface layer since they are held to the surface by forces acting between the surface and particular atoms or groups of atoms in the adsorbed molecule.

On the basis of this conception of the nature of the forces acting in adsorption, it follows that the material adsorbed on the surface will rarely exceed that contained in one layer of molecules (a *monolayer*), and the relation developed by Langmuir for the adsorption isotherm forms a logical consequence. He remarks,

---

[27] *J. Am. Chem. Soc.*, **40**, 1361 (1918). A review of the theory and further experimental evidence for the adsorption of gases on metals as monatomic films are also given in the extremely important paper, "Surface Chemistry," *Chem. Revs.*, **13**, 147 (1933).

The plane faces of a crystal must consist of atoms forming a regular plane lattice structure. The atoms in the cleavage surface of crystals like mica are those which have the weakest stray fields of force of any of the atoms in the crystal. It is probable that in mica the hydrogen atoms cover most, if not all, of the surface, since hydrogen atoms when chemically saturated by such elements as oxygen possess only weak residual valence. In the case of glass, and other oxygen compounds like quartz or calcite, the surface probably consists of a lattice of oxygen atoms. The surface of crystals thus resembles to some extent a checkerboard. When molecules of gas are adsorbed by such a surface these molecules take up definite positions with respect to the surface lattice and thus tend to form a new lattice above the old. A unit area of any crystal surface, therefore, has a definite number of "elementary spaces,"[28] each capable of holding one adsorbed molecule or atom. In general, these elementary spaces will not all be exactly alike. There will frequently be cases where there are two or three different kinds of spaces. For example, in a mica crystal it may be that both oxygen and hydrogen atoms, arranged in a regular lattice, form the surface in such a way that different elementary spaces are surrounded by different numbers or arrangements of atoms. In Fig. 10 is given a conceivable arrangement of oxygen and hydrogen atoms in a surface lattice:

H O H H O H
H H O H H O
O H H O H H
H O H H O H
H H O H H O
O H H O H H

FIG. 10. Probable arrangement of oxygen and hydrogen atoms in a surface lattice of mica (Langmuir).

If the adsorbed molecules take up positions over the centers of the square formed by four of the surface atoms, it is seen from this diagram that there are two kinds of elementary spaces, those represented by $\begin{matrix}H & O\\ H & H\end{matrix}$ and those represented by $\begin{matrix}H & O\\ O & H\end{matrix}$. For each of the latter there are two of the former kind of space. In case the adsorbed atoms arrange themselves directly above the surface atoms, there would still be two kinds of elementary spaces. From considerations of this kind we see that a crystal surface may have spaces of only one kind, or may have two, three, or more different kinds of spaces representing definite simple fractions of the surface.

Each kind of elementary space will, in general, have a different tendency to adsorb gases. As the pressure of gas is increased the adsorption will then tend to take place in steps, the different kinds of spaces being successively filled by the adsorbed molecules. The quantities of gas adsorbed in the different steps should in general bear simple stoichiometric ratios to each other. For example, suppose adsorption takes place more readily in the spaces represented by $\begin{matrix}H & O\\ O & H\end{matrix}$ in Fig. 10 than in the spaces $\begin{matrix}H & O\\ H & H\end{matrix}$. Then the first step in the adsorption will be to saturate the $\begin{matrix}H & O\\ O & H\end{matrix}$ spaces and in the second step the $\begin{matrix}H & O\\ H & H\end{matrix}$ spaces will be saturated. Since there are twice as many of the second kind as of the former, the second step will represent just twice as much gas as the first step. When different gases are adsorbed alternately by the same crystal surface the maximum amounts of gas adsorbed will often be related in a simple stoichiometric manner. Thus, if each elementary space holds one adsorbed molecule, equal volumes of different gases will be adsorbed. It may, however, happen that two or three molecules of one gas can occupy a space previously occupied by a single molecule of another gas. In this case the maximum volumes adsorbed will bear the relation 1 : 2 or 1 : 3. Where more than one molecule can occupy a single elementary space the forces holding the successive molecules will usually differ. Thus the first molecule may be held by a strong force, but when the space is shared by a second molecule the force holding each of the two may be much weaker. This will lead to a tendency for the adsorption to occur in steps just as though there were several kinds of elementary spaces. On the other hand, it may sometimes happen that the forces holding each of two molecules may be greater than the force holding a single one. Adsorption would then not occur in steps, but according to laws quite different from those where only one molecule occupies an elementary space.

---

[28] Subsequently designated by Langmuir as "sites."

The molecules of many gases will be so large that they cannot occupy adjacent elementary spaces on the crystal surface. This may cause one-half or a third of the elementary spaces to be occupied, in which case stoichiometric relations might still exist. It may happen more often that molecules are only slightly too large for the elementary spaces so that they occupy adjacent spaces only by crowding each other. Phenomena of this kind are very familiar to organic chemists, under the name "steric hindrance." This crowding of the molecules may, in many cases, completely obliterate the stoichiometric relations that would otherwise occur. The effect of steric hindrance will be to make it difficult to saturate the surface with any adsorbed substance. The exact fraction of the elementary spaces which may be filled will depend on a large number of factors such as the shape and elastic properties of the molecules and their mobility on the surface.

With amorphous substances like glass, the surface atoms are probably not arranged in a regular lattice formation. There will, therefore, be an indefinite number of different kinds of elementary spaces. We should not expect the adsorption to occur in steps representing stoichiometric proportions of gas. The number of elementary spaces may, however, be quite definitely determinable so that the maximum amounts of different gases adsorbed may still stand in stoichiometric relations.

At any given pressure $P_{\mu b}$, the number of molecules striking unit area per second is given by the relation

$$\nu = \frac{P_{\mu b}}{\sqrt{2\pi mkT}} = \frac{3.513 \cdot 10^{22} P_{mm}}{\sqrt{MT}} = cP, \tag{4}$$

where the value of c depends on the unit of pressure.

Let α = fraction of molecules incident on surface that condense, and let μ = number of *adatoms*[29] evaporating per square centimeter per second.

[29] A designation introduced subsequently by J. A. Becker and Langmuir for *adsorbed atoms* or *molecules*.

At equilibrium,

$$\alpha\nu = \mu. \tag{5}$$

Let σ_1 = total number of "elementary spaces," or *sites*, available for adsorption, and let σ = number of adatoms per square centimeter at pressure P.

Assuming that a single adatom can occupy one site, then the fraction of surface covered at equilibrium is given by

$$\theta = \frac{\sigma}{\sigma_1}. \tag{6}$$

Let us assume also that (1) "the adsorption sites are all identical and (2) the potential energy of an adatom in a site is independent of the presence of adatoms in other sites; in other words, the adatoms in separate sites exert no forces on one another."[30] Then

$$\mu = \mu_1\theta, \tag{7}$$

where μ_1 is the rate of evaporation for a completely covered surface. Also,

$$\alpha\nu = \alpha_0\nu(1 - \theta), \tag{8}$$

where α_0 is a coefficient of the order unity. Hence, at equilibrium,

$$\mu_1\theta = \alpha_0\nu(1 - \theta) \tag{9}$$

or

$$\frac{\theta}{1 - \theta} = \frac{\alpha_0\nu}{\mu_1}$$

while

$$\frac{1}{1 - \theta} = \frac{\mu_1 + \alpha_0\nu}{\mu_0}.$$

It follows that

$$\theta = \frac{\alpha_0\nu}{\mu_1 + \alpha_0\nu} \tag{10}$$

is the equation for the adsorption isotherm.

Let

$$b = \frac{\alpha_0 c}{\mu_1}, \tag{11}$$

where c is defined by equation 4.

---

[30] I. Langmuir, *J. Chem. Soc.*, **1940**, 511; the Seventeenth Faraday Lecture, entitled "Monolayers on Solids."

Since μ_1 is a function of the temperature, it follows that b is a constant for any given temperature.

Then equation 10 takes the form

$$\theta = \frac{bP}{1 + bP} \tag{12a}$$

$$= b\left(\frac{1}{P} + b\right)^{-1} \tag{12b}$$

This is the equation of a rectangular hyperbola, hence the designation "hyperbolic" isotherm.

From 12a it follows that

$$\theta = bP(1 - \theta). \tag{13}$$

It is more convenient to write the equation for the isotherm in terms of v, the volume adsorbed, or x, the amount adsorbed. Let v_s and x_s denote the maximum values, when the surface is completely covered. Then

$$\theta = \frac{v}{v_s}\left(= \frac{x}{x_s}\right), \tag{14}$$

and equation 13 becomes

$$v = \frac{v_s bP}{1 + bP}, \tag{15}$$

which may also be written in the form[31]

$$P = \frac{v}{b(v_s - v)}. \tag{16}$$

In order to test the validity of the hyperbolic equations for any series of adsorption data, it is convenient to write equation 15 in the form

$$\frac{P}{v} = \frac{1}{bv_s} + \frac{P}{v_s} \tag{17a}$$

or

$$\frac{1}{v} = \frac{1}{bv_s} \cdot \frac{1}{P} + \frac{1}{v_s}. \tag{17b}$$

That is, a plot of P/v versus P should yield a straight line, the slope of which corresponds to $1/v_s$, while the intercept on the ordinate axis for $P = 0$ is equal to $1/(bv_s)$.

---

[31] This is the expression used, for instance, by W. G. Frankenburg, *J. Am. Chem. Soc.*, **66**, 1838 (1944).

As an illustration of this conclusion, Fig. 11 shows such plots, from the paper by M. H. Armbruster, of the isotherms shown in Fig. 4 above.

It also follows from the last equation that a plot of $1/v$ versus $1/P$ should yield a straight line, which is another method of expressing the equation for a rectangular hyperbola.

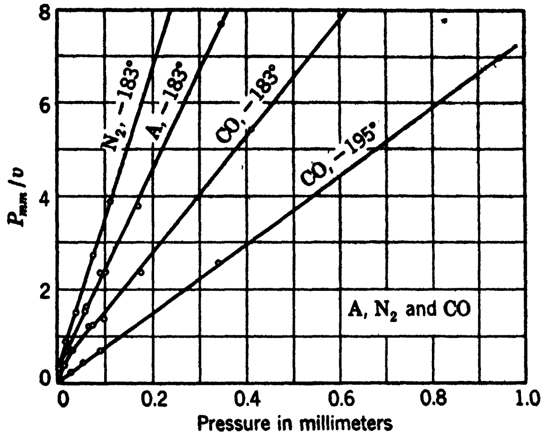

FIG. 11. Isotherms shown in Fig. 4 plotted as P_{mm}/v versus P_{mm}.

Equation 16 shows that a straight line should also be obtained by plotting v/P versus v. In that case, the intercept on the ordinate axis for $v = 0$ is equal to bv_s, while the slope is equal to $-b$.

It is evident that for very low pressures, where $bP \ll 1$ and θ *is extremely small* (v very much less than v_s),

$$v = v_s bP. \tag{18}$$

That is, the amount adsorbed is proportional to P, and the adsorption therefore obeys Henry's law.

It will be noted that, in the above equations, b has the reciprocal dimension of the pressure, while v and v_s must be expressed in the same units of volume or mass.

As a further illustration of the application of the hyperbolic equation, Table 10 gives equilibrium values of v and $P_{\mu b}$ observed by Langmuir[32] for the adsorption of nitrogen on mica at 90° K.

These values are plotted in curve A, Fig. 12, which is the corresponding isotherm. From the linear plot, B, of $P_{\mu b}/v$ versus $P_{\mu b}$, and the other linear plot, C, of $v/P_{\mu b}$ versus v, the values $v_s = 38.9 \cdot 10^{-3}$ cm^3 and

---

[32] *Loc. cit.*, Table VII, p. 1383.

$b = 0.156$ microbar^{-1} were deduced by Langmuir in the manner indicated above.

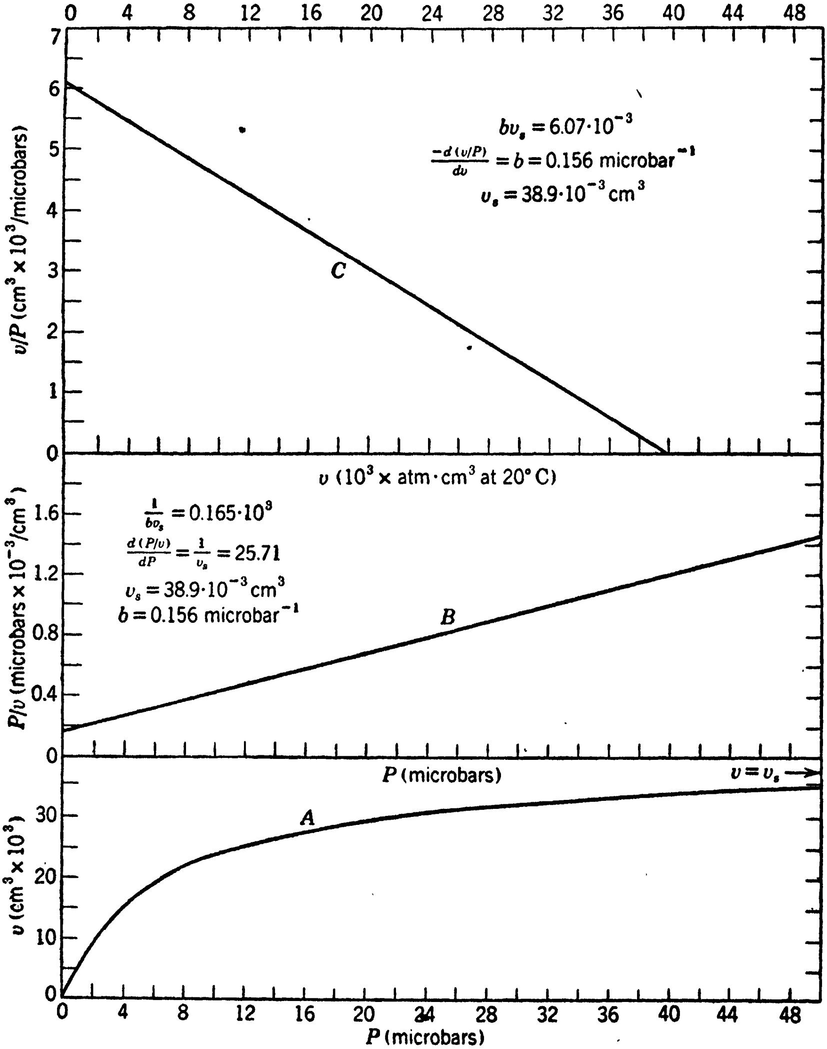

FIG. 12. Adsorption data for nitrogen on mica at −183° C plotted (A) v in atm · cm^3 versus $P_{\mu b}$, (B) $P_{\mu b}/v$ versus $P_{\mu b}$, and (C) $v/P_{\mu b}$ versus v.

He also showed that the hyperbolic equation was in good agreement with similar measurements of the adsorption of methane, carbon monoxide, argon, oxygen, and carbon dioxide on mica at 90° K and 155° K and on glass surfaces at 90° K.

TABLE 10

Adsorption of N_2 on Mica at 90° K

$P_{\mu b}$	$10^3 v_{20}$	$10^{-3}P_{\mu b}/v_{20}$	$P_{\mu b}$	$10^3 v_{20}$	$10^{-3}P_{\mu b}/v_{20}$
34.0	33.0	1.028	6.1	19.0	0.321
23.8	30.8	0.773	5.0	17.0	.294
17.3	28.2	0.614	4.0	15.1	.265
13.0	25.5	0.510	3.4	13.4	.254
9.5	23.9	0.398	2.8	12.0	.233
7.4	21.6	0.343			

In subsequent sections more detailed discussion will be given of these results as well as of the observations on the sorption of several gases by coconut charcoal made by I. Homfray,[33] A. Titoff,[34] and L. B. Richardson,[35] all of which, as has been shown by H. Zeise,[36] may be represented very satisfactorily by the hyperbolic equation.

The hyperbolic equation has been derived on the basis of thermodynamical considerations by M. Volmer,[37] and by statistical mechanics methods by R. H. Fowler[38] and a number of other investigators, the most recent of whom are K. J. Laidler, S. Glasstone, and H. Eyring.[39]

It is of interest to quote the summary of Fowler's derivation as given by Brunauer.[40]

> Fowler emphasizes the fact that the original kinetic derivation is apt to obscure the essentially thermodynamic character of the [Langmuir] equation and may lead to the erroneous belief that the form of the equation depends on the mechanism of condensation and evaporation of the adsorbed molecules. As a matter of fact, it depends only on the entire set of states, adsorbed and gaseous, that are accessible to the molecules at equilibrium. The statistical derivation is based on three assumptions: (1) the molecules of the gas are adsorbed without dissociation to definite points of attachment on the surface of the adsorbent; (2) each point of attachment can accommodate one and only one adsorbed molecule; and (3) the energies of the states of any adsorbed molecules are independent of the presence or absence of any other adsorbed molecules on neighboring points of attachment. These assumptions are similar to those of Langmuir. The first assumption, although not stated, is implied in the kinetic derivation. When dissociation occurs, the form of the Langmuir equation is different from equation 15.[41] The second assumption corresponds to Langmuir's assumption of unimolecularity, embodied in equation 8. The third corresponds to the assumption of no interaction between adsorbed molecules.

---

[33] *Z. physik. Chem.*, **74**, 129 (1910).

[34] *Z. physik. Chem.*, **74**, 641 (1910).

[35] *J. Am. Chem. Soc.*, **39**, 1829 (1917).

[36] *Z. physik. Chem.*, **A**, **136**, 385 (1928), **A**, **138**, 289 (1928).

[37] *Z. physik, Chem.*. 253 **115**, (1925).

[38] *Proc. Cambridge Phil. Soc.*, **31**, 260 (1935); **32**, 144 (1936).

[39] *J. Chem. Phys.*, **8**, 659 (1940).

[40] SB, pp. 66–67.

[41] See subsequent discussion.

This, as mentioned already, leads to equation 15.

Langmuir also showed that the same considerations as those used in deriving the hyperbolic equation lead to modifications of this equation in special cases.

One such case is that in which the surface contains several kinds of elementary spaces or sites. Let v_1, v_2, etc., denote the maximum values of the adsorptions for each of these varieties of sites. Then the expression for the isotherm is

$$\frac{v}{P} = \frac{v_1 b_1}{1 + b_1 P} + \frac{v_2 b_2}{1 + b_2 P} + , \tag{19}$$

where b_1, b_2, etc., refer to the different types of sites, and

$$v_1 + v_2 + \cdots = v_s. \tag{20}$$

Another very important case is that in which the molecules are adsorbed as atoms. Langmuir writes,

> In the cases considered above, molecules of adsorbed substance have acted as indivisible units; that is, when a molecule evaporated from the surface it contained the same atoms as when it was first adsorbed. There is good evidence that the forces which hold adsorbed substances act primarily on the individual atoms rather than on the molecules. When these forces are sufficiently strong, it may happen that the atoms leaving the surface become paired in a different manner from that in the original molecules.
>
> For example, consider the adsorption of a diatomic gas such as oxygen on a metallic surface. Let us assume that the atoms are individually held to the metal, each atom occupying one elementary space. The rate of evaporation of the atoms is negligibly small, but occasionally adjacent atoms combine together and thus nearly saturate each other chemically, so that their rate of evaporation becomes much greater. The atoms thus leave the surface only in pairs as molecules. Starting with a bare surface, if a small amount of gas is adsorbed, the adjacent atoms will nearly always be the atoms which condensed together when a molecule was adsorbed. But from time to time two molecules will happen to be adsorbed in adjacent spaces. One atom of one molecule and one of the other may then evaporate from the surface as a new molecule, leaving two isolated atoms which cannot combine together as a molecule and are therefore compelled to remain on the surface. When a stationary state has been reached there will be a haphazard distribution of atoms over the surface. The problem may then be treated as follows:
>
> Let θ be the fraction of the surface covered by adsorbed atoms, while $(1 - \theta)$ is the fraction which is bare. In order that a given molecule approaching the surface may condense (and be retained for an appreciable time) on the surface, two particular elementary spaces must be vacant. The chance of one of these spaces being vacant is $(1 - \theta)$; that both shall be vacant is $(1 - \theta)^2$. The rate of condensation is thus equal to $\alpha_0 \nu (1 - \theta)^2$. Evaporation only occurs when adsorbed atoms are in adjacent spaces. The chance that an atom shall be in a given space is θ. Therefore, the chance that atoms shall be in adjacent spaces is proportional to θ^2. The rate of evaporation of molecules from the surface is therefore equal to $\mu_1 \theta^2$, where, as before,

μ_1 is the rate of evaporation from a completely covered surface. For equilibrium we then have the condition

$$\alpha_0\nu(1 - \theta)^2 = \mu_1\theta^2. \tag{21}$$

This leads to the relations

$$\theta = \frac{\sqrt{bP}}{1 + \sqrt{bP}} \tag{22}$$

and

$$v = \frac{v_s\sqrt{bP}}{1 + \sqrt{bP}}. \tag{23}$$

> Thus [as Langmuir states], in this case, even at relatively low pressures, the total amount of adsorbed gas varies in proportion to the square root of the pressure. If three instead of two elementary spaces are occupied by the atoms of each molecule, then the square root relation expressed by equation 23 becomes a cube root relation.

Hence the last equation may be expressed in the more general form

$$v = \frac{v_s(bP)^{1/n}}{1 + (bP)^{1/n}} \tag{24}$$

where $n \geqslant 1$, and this can also be written

$$\theta^n = bP(1 - \theta)^n. \tag{25}$$

For small values of θ, this evidently becomes identical in form with the Freundlich equation 1.

By analogy with the hyperbolic equation (for which $n = 1$), it is evident that, for the purpose of testing the validity of equation 24, it may be expressed in the two alternative forms:

$$\frac{P^{1/n}}{v} = \frac{1}{c_1} + \frac{P^{1/n}}{c_2} \tag{26}$$

or

$$\frac{v}{P^{1/n}} = k_1 - k_2v, \tag{27}$$

where n, and the constants c_1, c_2, k_1, and k_2, are determined from the slopes and intercepts on the axis of ordinates, for the linear plots.

While the hyperbolic equation has been shown by a number of investigators to be in good agreement with the observations on adsorption, difficulties have arisen in reconciling the actually derived values of the constants v_s and b with the physical significance attached to them by Langmuir.

As an illustration, Table 11 shows the values of the constants b and v_s/A (where A = total area of surface), as deduced by Langmuir from the adsorption isotherms observed by him. From these isotherms, the number of molecules per square centimeter at saturation have been calculated by means of the relation

$$\sigma_1 = 2.504 \cdot 10^{19} \frac{v_s}{A}. \qquad (28)^{42}$$

On the other hand, the total number of molecules per square centimeter required to form a completely covered unimolecular layer is given by the relation (see Chapter 1, equation 8.43)

$$N_s = 1.1547\delta^{-2}, \qquad (29)$$

where δ, the molecular diameter, has been deduced from the values of the coefficient of viscosity. These values for a number of gases are given in Table 4 above.

Therefore, the ratio

$$\frac{\sigma_1}{N_s} = \alpha \qquad (30)^{43}$$

gives the fraction of the total surface covered. As will be observed from Table 11, the values of this ratio deduced from Langmuir's observations are considerably less than unity for all the cases investigated except for methane at 90° K and for carbon dioxide at 155° K.

Similar conclusions have been deduced by Armbruster and Austin[44] from their observations on the adsorption of gases on smooth surfaces of steel, some of which are plotted in Fig. 7 above. The ratio of the value of v_s, as derived from the Langmuir equation, to the value of v_s for nitrogen at $-183°$ (which would correspond to a complete monolayer) exceeds unity in only a relatively few cases. A large number of investigations have led to the conclusion that in general the observed value of v_s corresponds to a complete monolayer only at very low temperatures and that, at higher temperatures, the amount adsorbed corresponds to an incomplete monolayer.[45]

However, as may be observed from the data in Table 11, the values of v_s (or α) for the different gases vary over a much greater range, for

---

[42] The number of molecules per cubic centimeter at 760 mm and 20° C is $2.504 \cdot 10^{19}$.

[43] The values given in Table 11 are different from those derived by Langmuir because of the difference in values of N_s used in the calculation.

[44] *J. Am. Chem. Soc.*, **66**, 159 (1944).

[45] Another illustration of this conclusion is given by Armbruster and Austin, *J. Am. Chem. Soc.*, **60**, 467 (1938), based on their observations on the adsorption of gases on plane surfaces of mica.

TABLE 11*

VALUES OF ADSORPTION CONSTANTS IN HYPERBOLIC EQUATION DEDUCED BY LANGMUIR FROM ISOTHERMS

Gas	b (microbar^{-1})	$10^7 v_s/A$	$10^{-15}\sigma_1$	α	$10^5 \tau_1$†
		A. Adsorption on Mica at 90° K			
N_2	0.085	56.5	0.142	0.175	2.29
	.156	67.6	.169	0.209	5.08
CH_4	.107	169.	.423	0.809	6.51
	.168	214.	.536	1.02	13.00
CO	.65	100.	.251	0.391	30.96
A	.065	52.2	.130	0.153	1.91
O_2	.080	34.8	.087	0.10	1.42
		B. Adsorption on Mica at 155° K			
N_2	0.0176	20.5	0.0513	0.063	0.225
CH_4	.009	43.5	.109	.208	0.181
CO	.0069	34.8	.087	.136	0.146
A	.024	19.5	.049	.057	0.350
O_2	.043	8.2	.021	.024	0.241
CO_2	.071	113.0	.283	.530	6.32
	.085	99.0	.248	.465	6.64
		C. Adsorption on Glass at 90° K			
N_2	0.088	69.0	0.173	0.213	2.92
CH_4	.064	114.0	.286	.545	2.63
CO	.083	82.4	.206	.322	3.28
A	.051	60.0	.150	.176	1.76
O_2	.079	43.0	.108	.123	1.74

* This corresponds to Tables XVIII, XIX and XX, *loc. cit.* The notation used is different from that of Langmuir. The following table compares the two sets of symbols.

TABLE 11		LANGMUIR
b	corresponds to	a
v_s	corresponds to	b
α	corresponds to	β

† The significance of this constant is discussed in section 6 below.

the same adsorbent, than can be accounted for on the basis of the values of N_S.

An illustration of a similar nature, quoted by Brunauer,[46] is found in the data obtained by E. C. Markham and A. F. Benton[47] on the adsorption of oxygen, carbon monoxide, and carbon dioxide on silica. Figure

---

[46] SB, p. 76.

[47] *J. Am. Chem. Soc.*, **53**, 497 (1931).

13[48] shows plots of $1/v_0$ versus $1/P_{mm}$ for the three gases. Curve 1 applies to oxygen at 0° C, curve 2 to carbon monoxide at 0° C, and curve 3 to carbon dioxide at 100° C.

The values of v_s are 397 cm^3 for oxygen at 0° C, 322.6 cm^3 for carbon monoxide at 0° C, and 426.4 cm^3 for carbon dioxide at 100° C. For carbon monoxide at 100° C a value as low as 60.2 cm^3 was observed.

In explanation of the low values of α (see Table 11) observed in his measurements Langmuir suggested that "the adsorption of most of these gases does not occur over the whole surface, but only where the arrangement of the surface atoms is such as to give particularly strong stray fields of force." The adsorption thus takes place according to equation 19, and it is only the volume of gas necessary to cover a fraction of the surface, corresponding to v_1, that is measured as v_s, while v_2, v_3, etc., are negligibly small.

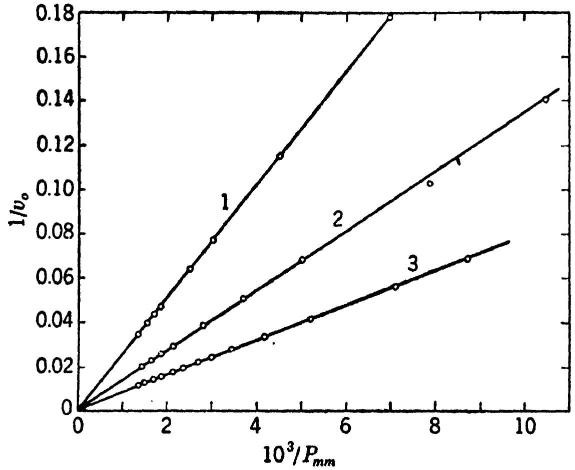

FIG. 13. Plots of $1/v_0$ versus $1/P_{mm}$ for the adsorption on silica of oxygen at 0° C (curve 1), carbon monoxide at 0° C (curve 2) and carbon dioxide at 100° C (curve 3). v_0 in cm^3 (S.T.P.) per gram.

"That an apparently homogeneous surface will in reality be extremely unhomogeneous in respect to its absorbing power" has been emphasized by E. K. Rideal,[49] from whose book the following remarks are of interest.

> A gas but feebly adsorbed such as argon will adhere only to those portions of the surface where the adsorbing forces are strong, whilst carbon monoxide which is

---

[48] SB, Fig. 39, p. 77. v_0 is given in cubic centimeters per gram.

[49] *An Introduction to Surface Chemistry*, Cambridge University Press, p. 141, 1926.

relatively strongly adsorbed will adhere to all parts of the surface. Thus the saturation value of a gas or the availability of a surface will vary in accordance with the system chosen. We find for example that the saturation capacities of a metal such as copper varies with the nature of the gas. For ethylene and hydrogen the ratio of the saturation capacities of 0° C on active reduced copper is 2.3 : 1; for copper which has been sintered at 450° C the ratio is found to be 5.9 : 1. Whilst the total adsorption per gram of metal has fallen only some 20 per cent for ethylene the adsorption for hydrogen has been seriously diminished. With carbon monoxide, ethylene, and hydrogen on copper the ratio of the saturation capacities is of the order 3 : 2.3 : 1. Evidently parts of the copper are accessible to carbon monoxide which do not retain either ethylene or hydrogen.

Similar explanations must exist for a large number of observations in connection with catalytic investigations.

There seems to be no question, however, that

when the adsorption takes place in a unimolecular layer (or part of a layer), the data can often be fitted satisfactorily by means of the simple Langmuir equation. This usually happens when one deals with a relatively homogeneous surface, or surface element.[50]

As will be discussed more fully in the following section, difficulties have also been encountered in the interpretation of the values deduced for the constant b. Consequently, a number of investigators have concluded that, in spite of the formal agreement with adsorption data, the equation should be written in the form[51]

$$v = \frac{c_1 c_2 P}{1 + c_2 P}, \tag{31}$$

where c_1 and c_2 are empirical constants whose physical significance may be disregarded.

On the whole, the generally accepted view of the hyperbolic equation for the adsorption isotherm is expressed by S. J. Gregg:[52]

Summarizing, it may be said that for plane adsorbents, and also to a large extent for porous adsorbents provided the pressure is not too high, the Langmuir formula would appear to give a fairly satisfactory representation of the experimental adsorption results. Whilst it is true that the constants in the equation still remain empirical in nature and their values are incapable of deduction in any fundamental way from the mechanism postulated by Langmuir, yet the latter is generally agreed, from other considerations, to be very probable. And as for Langmuir's most important conception of all—the monomolecular adsorption layer—this is now supported by a great deal of experimental evidence for the range of low and medium concentrations, and may be taken as the generally accepted view.

---

[50] SB, p. 82, Brunauer draws attention to the work of A. Antropoff (*Z. Elektrochem.*, **39**, 616 [1933]; **42**, 544 [1936]), who observed that the adsorption isotherms of nitrogen on charcoal up to 200 atm pressure obey the hyperbolic equation.

[51] For instance, H. Zeise, *Z. physik. Chem.*; **A**, **136**, 385, (1928); **A**, **138**, 289 (1928).

[52] JG, p. 66.

4. OTHER EXPRESSIONS FOR THE ADSORPTION ISOTHERM

In a very comprehensive paper, published in 1940,[53] Langmuir has shown that, by application of statistical considerations similar to those used by Fowler and others, it is possible to deduce other expressions for the adsorption isotherm by introducing different assumptions.

As Langmuir points out, assumptions 2 and 3, mentioned by Fowler, cannot be generally valid. The maximum number of adatoms that can condense per unit area of a surface must depend, obviously, on the ratio between the diameter (d) of the atom or molecule and the distance (d_s) between the centers of the sites or possible points of attachment.

Let σ again denote the number (per unit area) of sites occupied by adatoms, and σ_s the *total* number of sites per unit area. The maximum number of sites available for condensation of adatoms (σ_1) will not necessarily be identical with σ_s; $\sigma_1 = \sigma_s$ only if d/d_s is less than 1. For d/d_s greater than 1, σ_1 will be less than σ_s, and Langmuir introduces the parameter

$$\gamma = \frac{\sigma_s}{\sigma_1}. \tag{1}$$

For $d/d_s > 1$, each adatom on the surface will form the center of a region from which other adatoms are excluded. The adatoms therefore give rise to an *exclusion pattern.* For instance, for $d/d_s = 1.25$, $\gamma = 2$ and the number of sites in the exclusion pattern is $E = 5$, while, for $d/d_s = \sqrt{2}$, $\gamma = 4$ and $E = 9$.

If we denote the number of sites per unit area that lie within the exclusion patterns of adatoms by σ_E, then the number of *free sites* per unit area is

$$\sigma_f = \sigma_s - \sigma_E. \tag{2}$$

Now, if we consider assumption 3 in Fowler's discussion, there is a great deal of experimental evidence, as mentioned already, for the conclusion that forces of repulsion between adatoms become more and more effective the more crowded the adatoms. The many investigations on the behavior of thin films on liquids[54] and solids lead to the conclusion that the "equation of state" for unimolecular layers (or *monolayers*) must contain repulsive and attractive force terms similar to those used in the van der Waals equation for gases and vapors at higher pressures and low temperatures.

---

[53] *J. Chem. Soc.*, **1940**, 511.

[54] See especially N. K. Adam, *The Physics and Chemistry of Surfaces*, Clarendon Press, Oxford, 1938.

As is well known, this equation can be written in the form

$$P = \frac{R_0T}{V - b_0} - \frac{a_0}{V^2}, \tag{3}$$

where the constant b_0 (usually designated b) is a measure of the repulsion between molecules, and a_0 (commonly designated a) is a measure of the attractive or cohesive forces between molecules.

For a monolayer in which the energy of each adatom is independent of the presence of other adatoms, that is, for an ideal two-dimensional gas, it has been shown by Langmuir[55] that

$$F = \sigma kT, \tag{4}$$

where F is analogous to the pressure in the ideal gas law

$$P = nkT.$$

In both equations k denotes the Boltzmann gas constant; but in the first equation σ denotes the number of *adatoms per square centimeter*, while in the second equation, n denotes the number of molecules per cubic centimeter.

Langmuir and also M. Volmer[56] have shown that, for crowded surfaces, the equation of state should have the form

$$F(a' - a_0') = kT, \tag{5}$$

where $a' = 1/\sigma$ and $a' - a_0'$ corresponds to the factor $(V - b_0)$ in the van der Waals equation (3).

"To compare the many equations of state that can be derived on the basis of different postulates regarding the forces of interaction," Langmuir has proposed the expression for the equation of state in the form

$$F = \frac{\sigma_1 kT\theta}{Y(\theta)}, \tag{6}$$

"where $Y(\theta)$ is a function of θ which must approach unity at low values of θ and approach zero when θ becomes nearly unity."

Corresponding to a given equation of state, there exists another function, denoted by $Z(\theta)$, to characterize the adsorption isotherm which, according to Langmuir, may be expressed in the form

---

[55] *J. Am. Chem. Soc.*, **54**, 2817 (1932).

[56] *Z. physik. Chem.*, **115**, 253 (1925).

$$P = \frac{B\theta}{Z(\theta)}, \tag{7}$$

where B is a function of the temperature, analogous to b in equations 3.12 and 3.15.

The manner in which the expression for $Z(\theta)$ may be derived in any particular case is best understood by quoting the following remarks from Langmuir's paper.

> Let us make the problem of the adsorption isotherm definite by assuming that the presence of an adatom in a given site has no effect on the adsorption in sites that lie outside of its exclusion pattern. . . . Consider a gas of pressure P in equilibrium with an adsorbed film of gas on the surface of a crystal. Select a particular atom of gas and follow its history as it moves back and forth between the gas and the surface phases. Since this atom, when it condenses on the surface, can go only into free sites, the total probability that it is on the surface at any given time is proportional to σ_f. There is an equal probability that any other atom in the system will be found on the surface, and since the number of such atoms is proportional to the pressure, the adsorption isotherm can be written
>
> $$\sigma = BP\sigma_f, \tag{8}$$
>
> where B is an undetermined constant which depends on the temperature.

For the special case in which $d/d_s < 1$, we have $E = 1$, $\sigma_E = \sigma$, and $\sigma_1 = \sigma_s$. Hence the last equation becomes

$$\frac{\sigma}{\sigma_1} = BP\frac{(\sigma_s - \sigma_E)}{\sigma_1} = BP\left(1 - \frac{\sigma}{\sigma_1}\right);$$

that is,

$$\theta = BP(1 - \theta),$$

which is the hyperbolic equation discussed above.

For the general case, where γ is greater than unity, the expression for the isotherm becomes more complicated. In this connection Langmuir has made use of conclusions derived by L. Tonks[57] for the form of the equation of state and of the corresponding function $Z(\theta)$ for adsorption on a square lattice.

For instance, for a square lattice and adatoms for which $d/d_s < 1.42$, $\gamma = 2$, and $E = 5$, Tonks has deduced the following relation for the isotherm.

$$\theta = BP(1 - 2.5\theta + 1.5\theta^2 + 0.75\theta^3 + \cdots), \tag{9}$$

which is valid for the range $0 \leqslant \theta \leqslant 0.5$.

---

[57] *Phys. Rev.*, **50**, 955 (1936), and *J. Chem. Phys.*, **8**, 477 (1940).

"With still larger adatoms," as Langmuir points out, "of diameters from $1.42d_s$ to $2d_s$, we have $E = 9$ and $\gamma = 4$." Tonks has shown that, for θ very small, the expression for the corresponding isotherm is

$$\theta = BP(1 - 2.25\theta + \theta^2 + \cdots), \tag{10}$$

and Langmuir finds that, over the whole range of values of θ, a good approximation is given by an equation of the form

$$\theta = BP(1 - \theta)^n, \tag{11}$$

where $n = 2.25$.

Expressed in terms of v and v_s, this relation has the form

$$v = bv_sP\left(1 - \frac{v}{v_s}\right)^n. \tag{12}$$

Taking logarithms of both sides, we obtain the relation

$$\ln\left(\frac{v}{P}\right) = \ln\,(bv_s) + n\ln\left(1 - \frac{v}{v_s}\right),$$

which for small values of v/v_s can be written

$$\log\left(\frac{v}{P}\right) = A - Cv, \tag{13}$$

where A and C are empirically determined constants.

That is, a plot of $\log\,(v/P)$ versus v should yield a straight line, the slope of which is given by $C = n/(2.303v_s)$, and the intercept for $v = 0$ is $A = \log\,(bv_s)$.

Equation 13 is the adsorption relation proposed by A. M. Williams[58] and also by D. C. Henry.[59] Equation 11 can evidently be derived by means of the same reasoning as the hyperbolic equation if it is assumed that an adatom requires n *adjacent sites for attachment, rather than one.*

For θ less than approximately 0.30, equation 11 can be written in the form

$$\ln\left(\frac{\theta}{P}\right) = \ln B - n\theta, \tag{14}$$

which corresponds to equation 13.

A modification of equation 12 derived by F. J. Wilkins[60] on the basis of thermodynamic and statistical arguments has the form

---

[58] *Proc. Roy. Soc. London*, **A**, **96**, 287, 298 (1919–1920).

[59] *Phil. Mag.*, (6), **44**, 689 (1922).

[60] *Proc. Roy. Soc. London*, **A**, **164**, 496 (1938).

$$\ln\left(\frac{v}{P}\right) = \ln\,(bv_s) - k_1\left(\frac{v}{v_s}\right) - k_2\left(\frac{v}{v_s}\right)^2, \tag{15}$$

where b, k_1, and k_2 are three empirically determined constants.

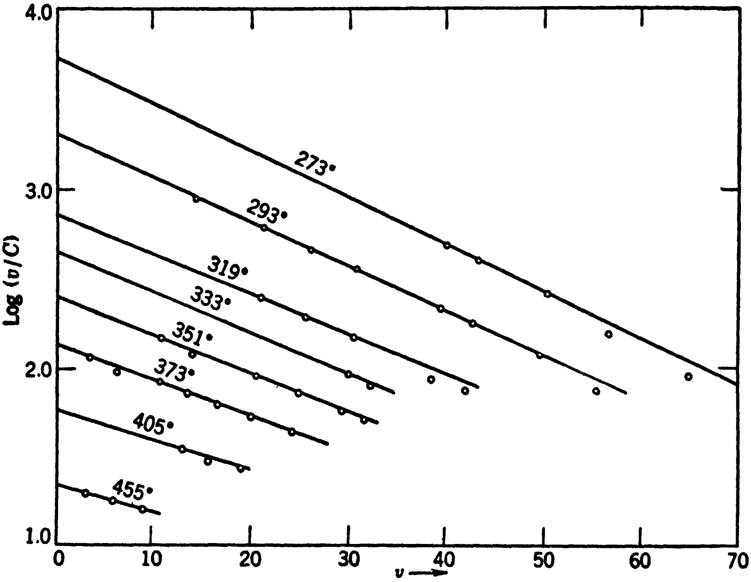

Fig. 14. Data for the sorption of ethylene by charcoal plotted according to Henry-Williams adsorption equation. C denotes the concentration of the gas, which is proportional to the pressure.

Figure 14[61] shows the adsorption isotherms plotted by Williams for data obtained by I. Homfray[62] on the sorption of ethylene by charcoal.

Another variation of the hyperbolic adsorption isotherm, proposed by A. Magnus,[63] is based on the assumption "that the adsorbed molecules on the surface behave like a two-dimensional imperfect gas, obeying an equation of state analogous to the van der Waals equation."[64] The equation can be written in the form

$$v = \frac{k_1k_2P - k_3v^2}{1 + k_1P - (k_3/k_2)v^2}, \tag{16}$$

---

[61] Williams, *loc. cit.;* SB, Fig. 43, p. 86.

[62] *Loc. cit.* (See Table 8.4 for observed data.)

[63] *Z. physik. Chem.*, A, **142**, 401 (1929).

[64] SB, p. 89.

where k_1, k_2, and k_3 are empirical constants. By rearranging terms the last equation can be expressed in the form

$$P = \frac{v}{k_1 k_2}\left(\frac{1}{1 - v/k_2} + k_3 v\right). \tag{17}$$

For $k_3 = 0$, which corresponds to the case of a film obeying the equation of state (see equation 4 for an ideal two-dimensional gas), the last equation becomes identical with the hyperbolic expression, with $k_2 = v_s$, and $k_1 = b$.

In terms of θ, equation 17 assumes the form

$$\theta = \frac{bP(1 - \theta)}{1 + c\theta(1 - \theta)}, \tag{18}$$

where c is a constant which becomes equal to zero for $k_3 = 0$.

According to Brunauer,[65] "the Magnus equation apparently works fairly well for charcoal, but not for metals and silica gel, or alumina." The explanation suggested is that only for charcoal is the adsorption of the monolayer type.

In a paper on the adsorption of gases (such as argon, nitrogen, and carbon monoxide), on smooth surfaces of steel, at liquid-air temperatures, Marion H. Armbruster and J. B. Austin[66] have stated that, while their observations satisfy the hyperbolic equation over a considerable range of pressures, marked deviations are observed in the lowest pressure range. "These deviations," according to the authors, "are all of the same kind—the volume adsorbed at a given pressure in the low range being greater than that calculated by extrapolation of the data in the high pressure range."[67]

The authors mention that similar deviations from the hyperbolic equation have been observed by other investigators[68] and that these deviations occur in the range of pressures for which the parabolic equation applies. They have therefore proposed an expression for the isotherm which represents a combination of the hyperbolic and parabolic equations of the form

---

[65] SB, p. 92.

[66] *J. Am. Chem. Soc.*, **66**, 159 (1944).

[67] The same observation has also been made by Armbruster in papers on the sorption of water vapor on steel surfaces at 20° C (*J. Am. Chem. Soc.*, **68**, 1347, [1946]). Above 0.4 mm, the sorption isotherm could be represented very satisfactorily by the Langmuir equation, but below this pressure the sorption exceeded that predicted by the equation. Of further interest is the conclusion that for some of the isotherms the values deduced for v_s corresponded to 2 or 3 times the values of v_s for a complete monolayer.

[68] R. M. Barrer, *Proc. Roy. Soc. London*, **A**, **161**, 476 (1937); Wilkins, *ibid.*, **A**, **164**, 510 (1938).

$$v = v_s\left(\frac{bP}{1 + bP}\right)^{1/n}, \tag{19}$$

where n is greater than 1.

Expressed in terms of θ, this equation takes the form

$$\theta^n = bP(1 - \theta^n). \tag{20}$$

Equation 19 is a generalized form of the equation

$$v = \sqrt{\frac{k_1k_2P}{1 + k_1P}}, \tag{21}$$

which was found by H. Zeise[69] to be in satisfactory agreement with data on the adsorption of gases and vapors on glass. The same equation has also been found by E. Mueller and K. Schwabe[70] to fit the data on the adsorption of hydrogen on platinum.

Armbruster and Austin observed that their data on the adsorption of gases on steel could be represented by equation 19 with the values $n = 3$ for nitrogen, $n = 4$ for argon, and n varying between 4 and 5 for carbon monoxide. To account for these values of n it is suggested that in these cases the rate of evaporation of adatoms must be assumed to vary as θ^n, and that the actual value of the exponent is "a measure of the departure of the behavior of the sorbed film from that of an ideal two-dimensional gas."

For small values of θ, equations 19 and 20 approximate to the Freundlich relation, that is

$$\theta = KP^{1/n}$$

or

$$v = kP^{1/n}. \tag{3.1}$$

In the previous section it was observed that the equation

$$\theta^n = bP(1 - \theta)^n \tag{3.25}$$

also approximates the Freundlich relation for small values of θ. However, since $(1 - \theta^n)$ is always greater (for the same value of θ) than $(1 - \theta)^n$, it follows that equation 19 or 20 will approximate more closely to the parabolic relation for larger values of θ than the last equation.

A summary of the different expressions for the adsorption isotherms deduced for the case of adsorption as a unimolecular layer is given in Table 12, while Table 13 contains values of a number of functions of θ which serve to illustrate the more generalized expressions mentioned in Table 12. These values of $Z(\theta)$ have been used to plot the curves shown in Fig. 15 which give θ as a function of P. All but one of these curves have been plotted in such a manner as to make the values of θ approach the plot of $\theta = BP$ for $\theta = 0$. (That is, it is postulated that for low values of θ Henry's law becomes valid.)

---

[69] *Z. physik. Chem.*, **136**, 385 (1928).

[70] *Z. Elektrochem.*, **35**, 165 (1929).

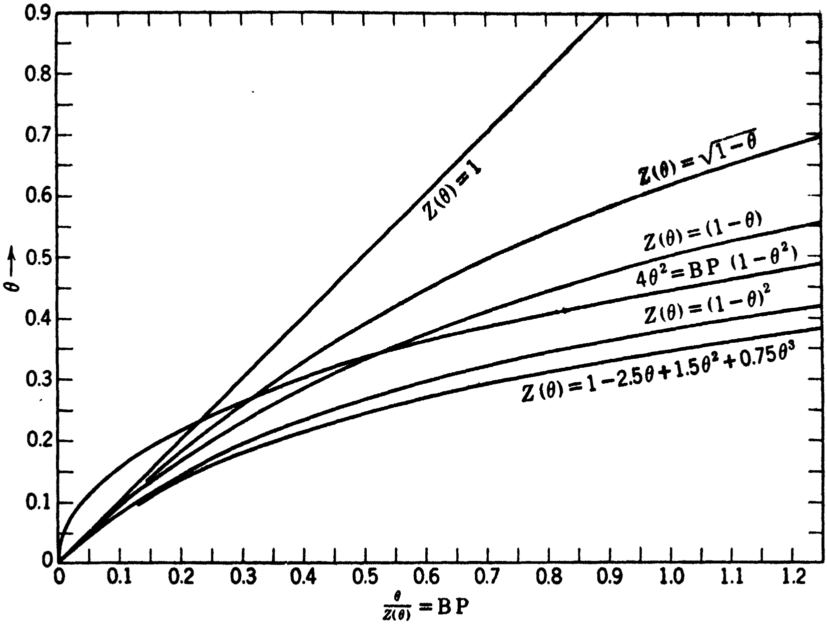

FIG. 15. Plots of θ versus $\theta/Z(\theta)$, illustrating the different equations for the adsorption isotherm. The expression for $Z(\theta)$ is given for each curve.

In the case of the curve for the equation

$$4\theta^2 = BP(1 - \theta^2) \tag{22}$$

the factor 4 has been introduced in order to make the value of θ for $BP = 0.53$ agree with that of θ for the same value of BP as given by the hyperbolic isotherm, $\theta = BP(1 - \theta)$. It will be observed, that while the two curves are in approximate agreement for a range of values of pressures in the neighborhood of $BP = 0.5$, the plot of equation 22 gives much higher values of θ in the range of low pressures than the hyperbolic equation.

TABLE 12

EQUATIONS FOR ADSORPTION ISOTHERMS

Author	In Terms of v	In Terms of θ
Langmuir	$v = \dfrac{v_s bP}{1 + bP}$	$\theta = bP(1 - \theta)$
Henry's law	$v = kP$	$\theta = bP$
Williams-Henry	$v = bv_sP(1 - v/v_s)^n$ $\log (v/P) = A - Bv$	$\theta = bP(1 - \theta)^n$ $\log (\theta/P) = K - n\theta$
Magnus	$P = \dfrac{v}{k_1k_2}\left(\dfrac{1}{1 - v/k_2} + k_3v\right)$	$\theta = \dfrac{bP(1 - \theta)}{1 + c\theta(1 - \theta)}$
Tonks	$v = bv_sPZ(v/v_s)$ For form of $Z(\theta)$ see discussion	$\theta = bPZ(\theta)$
Langmuir	$v = \dfrac{v_s(bP)^{1/n}}{1 + (bP)^{1/n}}$	$\theta^n = bP(1 - \theta)^n$
Zeise	$v = v_s\left(\dfrac{1 + bP}{bP}\right)^{1/n}$	$\theta^n = bP(1 - \theta^n)$
Freundlich	$v = kP^{1/n}$	$\theta^n = bP$

5. MULTIMOLECULAR ADSORPTION

Brunauer-Emmett-Teller Equation. While the type of isotherm discussed in the previous sections has been most successfully interpreted on the assumption of unimolecular adsorption, there are other types of sorption isotherms which are attributed to multimolecular adsorption. In Fig. 16[71] is shown a series of isotherms which were observed for nitrogen and argon on an aluminum oxide promoted iron catalyst. In fact this type of sorption is characteristic, in general, of vapor adsorption at pressures approaching saturation values.

On the basis of assumptions similar to those used by Langmuir, S. Brunauer, P. H. Emmett, and E. Teller deduced an equation for multimolecular adsorption which may be expressed in the form[72]

$$\frac{P}{v(P_0 - P)} = \frac{1}{v_m c} + \frac{(c - 1)}{v_m c} \cdot \frac{P}{P_0}, \tag{1}$$

---

[71] SB, p. 162, Fig. 72.

[72] See SB, pp. 151–155, for derivation; also *J. Am. Chem. Soc.*, **60**, 309 (1938).

TABLE 13

VALUES OF FUNCTIONS OF θ

θ	$\frac{\theta}{\sqrt{1-\theta}}$	$\frac{\theta}{1-\theta}$	$\frac{\theta}{(1-\theta)^2}$	$\frac{\theta}{Z(\theta)}$*	$\frac{\theta^2}{1-\theta^2}$	θ^2	$\frac{\theta}{(1-\theta)^3}$	$\frac{\theta^3}{1-\theta^3}$
0	0	0	0	0	0	0		
0.05	0.0513	0.0526	0.0554	0.0569	0.0025	0.0025	0.0583	0.0001
0.10	0.1054	0.1111	0.1234	0.1306	0.0101	0.0100	0.1372	0.001
0.15	0.1628	0.1765	0.2076	0.2266	0.0230	0.0225	0.2442	0.0034
0.20	0.2237	0.2500	0.3125	0.3532	0.0417	0.0400	0.3905	0.0081
0.25	0.2887	0.3333	0.4444	0.5202	0.0667	0.0625	0.6054	0.0159
0.30	0.3586	0.4285	0.6122	0.7402	0.0989	0.0900	0.8746	0.0278
0.35	0.4342	0.5386	0.8285	1.027	0.1396	0.1225	1.275	0.0448
0.40	0.5165	0.6667	1.111	1.389	0.1904	0.1600	1.852	0.0684
0.45	0.6067	0.8181	1.488	1.825	0.2539	0.2025	2.704	0.1027
0.50	0.7071	1.0000	2.000	2.286	0.3333	0.2500	4.000	0.1429
0.60	0.9488	1.5000	3.750		0.5624	0.3600	9.376	0.2755
0.70	1.277	2.333	7.777		0.9607	0.4900	25.92	0.5220
0.80	1.788	4.000	20.00		1.778	0.6400	100	1.049
0.90	2.845	9.000	90.00		4.263	0.8100	900	2.689
1.00	∞	∞	∞		∞	1.0	∞	∞

* $Z(\theta) = 1 - 2.5\theta + 1.5\theta^2 + 0.75\theta^3$.

where v_m and c are constants at any temperature, and P_0 is the saturation pressure of the gas at the given temperature.

Thus, for an adsorption isotherm which obeys this relation, a plot of the expression $Pv^{-1}(P_0 - P)^{-1}$ versus P/P_0 should yield a straight line for which the intercept is $1/(v_mc)$ and the slope is $(c - 1)/(v_mc)$.

In deriving equation 1 it was assumed that the adsorption occurs by formation of a unimolecular layer as a first stage, and that this is followed by condensation of the gas to form an infinite number of layers. If the adsorption occurs on the walls of capillaries and n denotes the maximum number of layers that can be adsorbed between the walls, then the last equation must be replaced by the relation

$$v = \frac{v_mcx}{1 - x} \cdot \frac{1 - (n + 1)x^n + nx^{n+1}}{1 + (c - 1)x - cx^{n+1}}, \qquad (2)$$

where $x = P/P_0$.

Figure 17[73] shows the adsorption isotherm of nitrogen on an iron catalyst at 77.4° K and the plots for a series of values of n, using values of v_m and c deduced from a straight-line plot. As will be observed, the four isotherms are identical up to $P/P_0 = 0.35$ and diverge only at relatively higher values.

---

[73] SB, p. 160, Fig. 71.

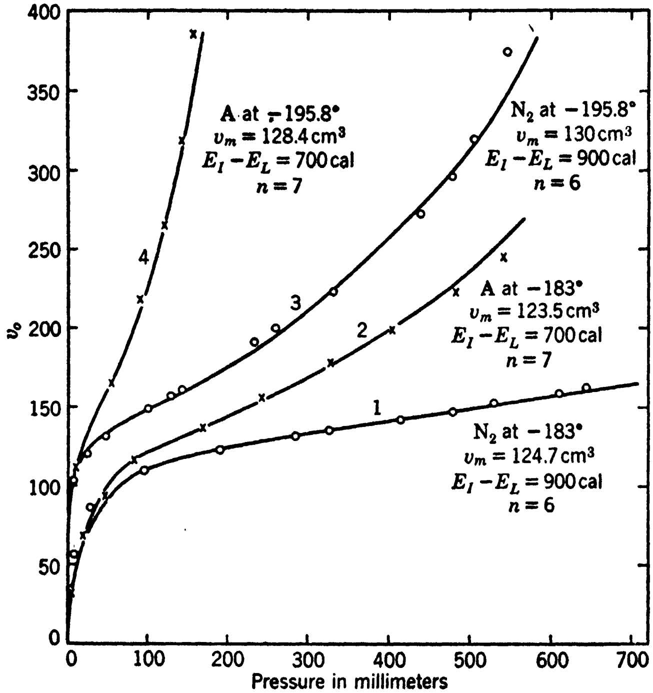

FIG. 16. Adsorption isotherms for nitrogen and argon on a promoted iron catalyst observed for −183° C. The isotherms for −195.8° C were calculated from those for −183° C by means of the BET equation 2 (Brunauer).

The last equation evidently has two limiting cases: (1) $n - \infty$, for which equation 1 should be valid; (2) $n = 1$, corresponding to *unimolecular* adsorption. In this case, this equation assumes the hyperbolic form

$$\frac{P}{v} = \frac{P_0}{cv_m} + \frac{P}{v_m}, \tag{3}$$

which is derived from equation 1 by assuming that P is very much less than P_0, and that $(c - 1)$ is approximately equal to c. That this last assumption is justified follows from a comparison of the last equation with equation 3.17a or 3.17b. It is seen that c/P_0 corresponds to the constant b, while v_m corresponds to v_s. Thus, in the plot shown in Fig. 17, v_m is the value indicated at the point B in the plot of v_0 versus P/P_0.

Since $c = bP_0$, it must correspond to a pure number, and a consideration of the manner in which this number enters into the derivation of equation 2 shows that, to a first approximation,

$$c = \epsilon^{(E_I - E_L)/R_0T}, \tag{4}$$

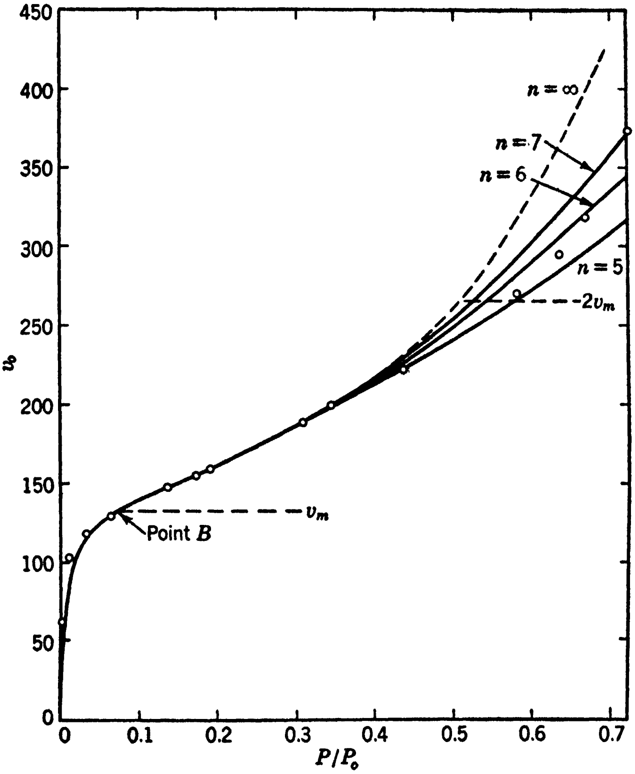

Fig. 17. Adsorption isotherm for nitrogen on an iron catalyst at −195.8° C plotted according to the BET equation 2 for a series of values of n. The observed data are indicated by circles (Brunauer).

where E_I = energy of adsorption of monolayer, and E_L = energy of condensation of the adsorbed vapor or gas.[74] In each case the energy is expressed in calories per gram-molecular weight (that is, per mole).

In Fig. 16 the values of $E_I - E_L$ are indicated for each adsorption isotherm, and it is of interest to note that, for $T = 77.4$ (−195.8° C),

---

[74] This conclusion will become more evident from the discussion in the following section.

$$c = \epsilon^{700/(R_0T)} = 95.6.$$

Figure 18[75] shows adsorption isotherms of nitrogen on six different adsorbents at 90.1° K plotted according to equation 1. The values of the constants v_m (cm^3/g) and $(E_I - E_L)$ (calories per mole) are shown in Table 14, given by Brunauer.[76]

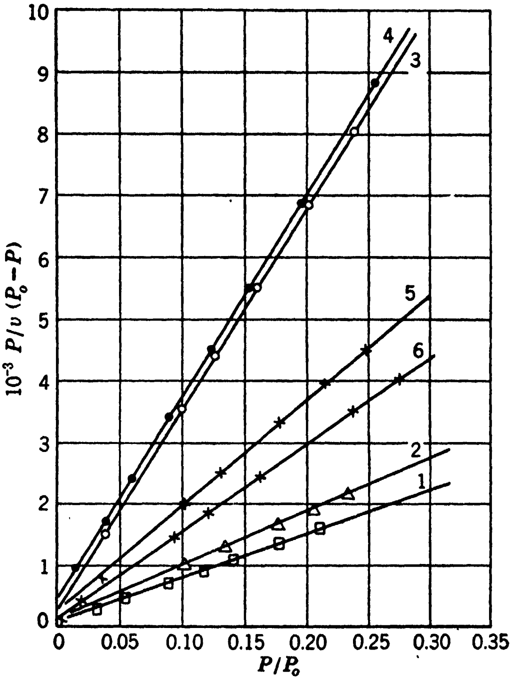

FIG. 18. Adsorption isotherms at 90.1° K for nitrogen on six different adsorbents (given in Table 14) plotted according to equation 1 (Brunauer).

While the theoretical values of v_m were derived from the linear plots by the method indicated above, the experimental values of v_m were obtained from the actually observed values at the points B of the curves. As will be observed, the agreement between the two sets of values is very satisfactory.

The advantages and disadvantages of the theory have been stated by Brunauer[77] in the following remarks:

---

[75] SB, p. 156, Fig. 69; P. H. Emmett, *J. Ind. Eng. Chem.*, **37**, 639 (1945).

[76] SB, p. 157, Table XIV.

[77] SB, pp. 177–178.

TABLE 14

VALUES OF v_m (B.E.T. EQUATION) AND OF HEAT OF ADSORPTION OF NITROGEN AT 90.1° K DEDUCED FROM THE ISOTHERMS

Adsorbent	Plot in Fig. 18	v_m (theoretical)	v_m (experimental)	$E_I - E_L$
Unpromoted Fe catalyst 973 II	1	0.29	0.27	774
Fe_2O_3-Al catalyst 424	2	2.23	2.09	774
Fe-Al_2O_3-K_2O catalyst 958	3	0.56	0.55	854
Fused Cu catalyst	4	0.05	0.05	776
Cr_2O_3 gel	5	53.3	50.5	738
Silica gel	6	116.2	127.0	794

The multimolecular adsorption theory is the first attempt to arrive at a unified theory of physical adsorption. It describes the entire course of an adsorption isotherm, including unimolecular adsorption, multimolecular adsorption, and capillary condensation, whereas previous theories have dealt only with one or another of these adsorption regions. At the same time it supplies an isotherm equation that can describe all the five different isotherm types, whereas previous equations have dealt only with one type of isotherm at a time, and no equations have been offered at all for three of the five isotherm types.

The theory has several limitations. At low pressures it reduces to the Langmuir equation, consequently all the criticism that has been levelled against the Langmuir theory can be directed equally well against the multimolecular adsorption theory in the low-pressure region of the adsorption isotherm. The most active parts of the surfaces of most adsorbents are strongly heterogeneous, with strongly varying heats of adsorption, therefore the Langmuir equation is not obeyed. For most adsorbents the theory breaks down in the region from zero pressure to $P/P_0 = 0.05$, and for some adsorbents to as high as 0.10. It may be restated that in this region the only theory that can deal successfully with physical adsorption is the potential theory.

The multimolecular adsorption theory is at its best in the middle adsorption region, i.e., in the region preceding and following the building up of a unimolecular layer. There are several reasons for this. In the first place the less active parts of the surfaces of most adsorbents are roughly homogeneous, therefore an average value of E_1 can be used without introducing a serious error. In the second place the heterogeneity of the surface does not show up any more in the second adsorbed layer, and so E_L becomes a very good approximation to the heat of adsorption in that layer. Finally, since most adsorbents have capillaries that are at least several molecular diameters wide, the difficulties due to capillary condensation do not yet begin to appear in this region. Thus the two-constant equation (1) is obeyed very closely for many adsorbents to at least $P/P_0 = 0.35$, and sometimes to 0.50. This fact enables one to evaluate accurately the surface area of the adsorbent.[78]

Undoubtedly there is considerable evidence of a very satisfactory nature for concluding that, in the presence of vapors at or near their saturation pressures, it is possible for the adsorbed material to exist in the form of a multimolecular layer. However, it is also well to mention in this connection the arguments advanced by Langmuir in his 1918 paper against assuming the general existence of such adsorbed film. He states,

---

[78] See section 9 of this chapter for discussion of this topic.

> There appear to be three main reasons which have led these investigators to conclude that adsorbed films are relatively thick. In most cases the experiments have been carried out with porous materials such as charcoal, so that it has not been possible to determine with certainty the effective adsorbing surface. Other workers have employed metal foil or other surfaces of known area, but in order to get sufficiently large surfaces have packed so much foil, etc., into small vessels that enormous numbers of capillary spaces were formed. They then employed saturated or nearly saturated vapors bringing about actual condensation of liquid in the capillary spaces. The third cause of error has consisted in the use of substances which actually dissolve the vapor thought to be adsorbed. The so-called adsorption of water vapor by glass is an example of this kind.

In concluding the discussion of the Brunauer-Emmett-Teller equation it is of interest to observe that a simplified derivation of this equation has been given by A. G. Foster.[79] He states,

> It should be emphasized that the new theory, unlike the older "potential" theories[80] of multilayer adsorption put forward by Eucken and Polanyi, does not postulate the existence of long-range adsorption forces, but is consistent with Langmuir's views on the short range of these forces. Adsorption beyond the first layer takes place under the influence of the cohesive forces of the molecules of the adsorbed substance acting as in the liquid state, so that a fraction of the surface must always be covered with a layer more than one molecule thick except at very low pressures, or above the critical temperature, or in pores too narrow to admit a second layer. Although the new theory gives a satisfactory explanation of S-shaped isothermals without assuming that capillary condensation occurs, it should be regarded as complementary to, rather than as superseding, the capillary theory.

In a second paper[81] Foster has shown that the saturation values for unimolecular adsorption calculated from the corrected data at lower pressures (by allowing for multilayer adsorption) agree with those derived by the "point *B*" method of Emmett and his collaborators from the data at higher pressures.

It should be added that G. Pickett[82] and R. B. Anderson[83] have suggested modifications of the Brunauer-Emmett-Teller equation which extend its applicability to higher values of P/P_0.

---

[79] *J. Chem. Soc.*, November, 1945, p. 769.

[80] This is discussed in the following section.

[81] *J. Chem. Soc.*, November, 1945, p. 773.

[82] *J. Am. Chem. Soc.*, **67**, 1958 (1945).

[83] *J. Am. Chem. Soc.*, **68**, 686 (1946).

Application of the Potential Theory. In 1914 A. Eucken[84] and M. Polanyi[85] developed a theory according to which adsorption is due to strong attractive forces exerted by the adsorbent upon the gas in its neighborhood. As Brunauer describes the assumptions involved,[86]

> The forces of attraction reaching out from the surface are so great that many adsorbed layers can form on the surface. These layers are under compression, partly because of the attractive force of the surface, partly because each layer is compressed by all the layers adsorbed on top of it. The compression is the greatest on the first adsorbed layer, less on the second, and so on until the density decreases to that of the surrounding gas.
>
> The adsorption potential at a point near the adsorbent is defined (by Polanyi) as the work done by adsorption forces in bringing in molecules from the gas phase to that point.

For gas pressures much below the critical value, this potential is given by the relation

$$\epsilon_i = R_0 T \ln\left(\frac{P_0}{P_x}\right), \tag{5}$$

where P_0 is saturation pressure, and P_x the pressure in the gas phase at the point at which the *weight* of adsorbed vapor per unit area is given by x. At this point, the *volume*, ϕ_i, of the adsorbed vapor per unit area is given by the relation

$$\phi_i = \frac{x}{\delta_T}, \tag{6}$$

where δ_T is the density of the liquid at temperature T.

At the surface of the adsorbent, $\phi = 0$, and ϵ_i has its maximum value, ϵ_0. As we pass outwards, towards the gas, ϵ_i decreases and ϕ_i increases until, at the boundary of the adsorbed layers, the density drops abruptly to that of the gas, $\epsilon_i = 0$, and ϕ reaches a maximum value. Thus the different layers parallel to the surface of the adsorbent form a series of equipotential surfaces at each of which ϵ_i and ϕ_i have definite values.

> The potential theory assumes that the adsorption potential does not change with temperature,
>
> $$\frac{d\epsilon_i}{dT} = 0,$$
>
> from which it follows that
>
> $$\frac{d\phi_i}{dT} = 0.$$

---

[84] *Verhandl. deut. physik. Ges.*, **16**, 345 (1914).

[85] *Verhandl. deut. physik. Ges.*, **16**, 1012 (1914).

[86] SB, p. 96. This reference as well as Chapter XVII in McB should be consulted for detailed discussion of the topic.

This means that the curve representing the potential distribution in the adsorption space, i.e., $\epsilon = f(\phi)$, is the same for all temperatures. For this reason the curve is called the *characteristic curve.*

Since ϵ and ϕ can be expressed in principle as functions of the pressure, the temperature, and the amount of gas adsorbed, the equation $\epsilon = f(\phi)$ can be regarded as equivalent to an isotherm equation.[87]

In practice such a plot of ϵ versus ϕ is usually derived from one experimentally determined isotherm, and all other isotherms are then calculated from this curve.

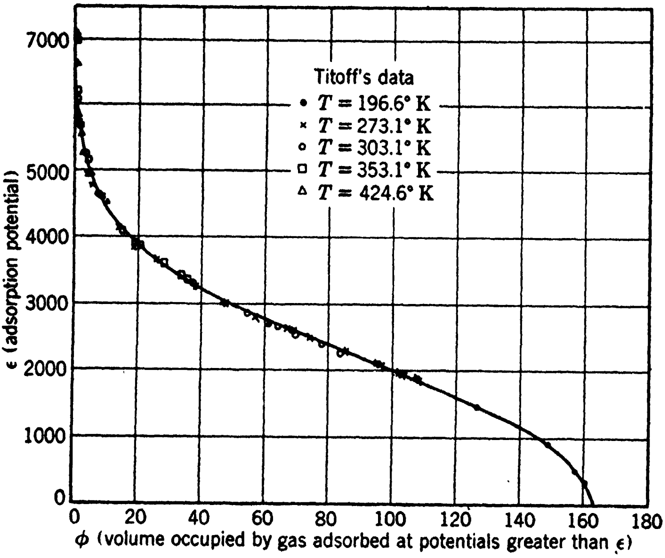

FIG. 19. Characteristic curve calculated, on the basis of the potential theory, from Titoff's data for the adsorption of carbon dioxide on charcoal, where ϵ is expressed in calories per mole (Lowry and Olmstead).

The first calculations were made by Polanyi.[88] The method was improved subsequently by L. Berenyi[89] and by H. H. Lowry and P. S. Olmstead.[90] Figure 19 shows a characteristic curve calculated by Lowry and Olmstead from A. Titoff's data on the adsorption of carbon dioxide on charcoal.

---

[87] SB, p. 99. The quotations in this section and remarks are based on the comprehensive discussion of this topic by Brunauer in Chapter V.

[88] *Loc. cit.*

[89] *Z. physik. Chem.* **94**, 628 (1920), **105**, 55 (1923).

[90] *J. Phys. Chem.*, **31**, 1601 (1927). SB, p. 108.

As Brunauer states, the work of these investigators

> proves conclusively that with the help of the theory one can calculate from one experimental isotherm all others at different temperatures. Polanyi[91] also investigated, together with Berenyi, the relation between the characteristic curves of different gases obtained on the same adsorbent. They found empirically the following relation between the maximum adsorption potential ϵ_0 and the van der Waals constant a of the gas
>
> $$\epsilon_0 = k\sqrt{a}. \tag{7}$$
>
> Table 15 shows that this equation holds quite well for all gases investigated, except hydrogen.

This table is of interest not only because it gives quantitative values of the adsorption potential[92] but also because it shows the "non-specific nature of van der Waals adsorption." The last two columns in the table (which have been added by the writer) give values of E_L (latent heat of vaporization in calories per mole) and of the boiling point.

TABLE 15*

RELATION BETWEEN ϵ_0 (ADSORPTION POTENTIAL) AND a (VAN DER WAALS' CONSTANT) FOR ADSORPTION BY CHARCOAL

Adsorbed Gas	ϵ_0 in Calories	$10^3\sqrt{a}$	$10^{-3}\epsilon_0/\sqrt{a}$	E_L	t_B
C_2H_4	7100	94.1	75	3343	−103.8° C
CO_2	6100	84.7	72	6847	−78.5
CH_4	5230	60.8	86	2215	−161.5
CO	4840	53.0	91	1415	−192.0
O_2	4450	51.9	86	1629	−182.95
N_2	4320	51.8	83	1334	−195.78
A	4100	51.0	80	1502	−185.66
H_2	~3100	20.6	150	217.7	−252.74

* The value of E_L for C_2H_4 was calculated from that for CH_4 by assuming the validity of Trouton's law. All the other values of E_L and values of t_B were taken from Table 19, section 7 of this chapter.

In summarizing this topic, Brunauer makes the following remarks:

> Polanyi's theory is eminently successful in accounting for the temperature dependence of physical adsorption. The calculations of Berenyi and of Lowry and Olmstead prove definitely that the adsorbed substance behaves very much like a compressed gas, and at lower temperatures like a liquid. The deviations of the experimental data from the theory are partly due to experimental error, although slight systematic

---

[91] *Z. Elektrochem.*, **26**, 370 (1920).

[92] Note that this is expressed in terms of calories per mole. See SB, p. 111. The constant a, is identical with the constant a_0 in equation 4.3.

deviations were also found. This is understandable, since one would not expect the adsorbed gas to obey *exactly* the three-dimensional equation of state. It is indeed surprising how far-reaching the agreement actually is.

The potential theory applies to both unimolecular and multimolecular adsorption. It is the only theory of physical adsorption that can handle quantitatively adsorption on a strongly heterogeneous surface. Since the theory does not attempt to formulate an isotherm equation, the scope of information obtainable from it is limited. One cannot determine with its help the extent of the surface of the adsorbent or the pore size distribution; indeed, one cannot even tell whether the adsorption is unimolecular or multimolecular."

Equations of Patrick and Palmer. For the adsorption isotherms of sulfur dioxide, ammonia, bromine, and butane on silica gel, W. A. Patrick[93] and his collaborators found that the observations were in agreement with the empirical equation

$$\log v_l = \log k + \frac{1}{n} \log \left(\frac{P\sigma_t}{P_0}\right), \tag{8}$$

where v_l = volume of adsorbed *liquid.*
P_0 = saturation pressure of gas.
σ_t = surface tension.
k and n are empirical constants.

W. G. Palmer and R. E. D. Clark[94] observed that the adsorption of various organic vapors on vitreous silica could be represented as straight lines by plotting log ϵ, the logarithm of the Polanyi potential, against v, the volume adsorbed. That is,

$$\log \log \left(\frac{P_0}{P}\right) = k_1 - k_2 v, \tag{9}$$

where k_1 and k_2 are two empirical constants.

This equation has been applied by M. H. Armbruster[95] in plotting her observations on the adsorption of carbon monoxide, argon, and nitrogen at very low temperatures on surfaces of smooth silver. It should be stated, however, that plots of P/v against P also gave good straight lines.

6. TEMPERATURE VARIATION OF ADSORPTION

For a given equilibrium pressure, the amount sorbed always decreases with increase in temperature, as shown by the adsorption isotherms for a series of temperatures. As mentioned previously the *isostere* represents the variation in pressure with temperature for a constant amount sorbed.

---

[93] SB, pp. 121–126; *J. Phys. Chem.*, **29**, 336, 421, 601 (1925).

[94] *Proc. Roy. Soc. London*, A, **149**, 360 (1935); Palmer, *ibid.*, A, **160**, 254 (1937).

[95] *J. Am. Chem. Soc.*, **64**, 2545 (1942).

Referring to the parabolic equation (3.1), it is observed that the constant k decreases and the exponent $(1/n)$ increases with increase in temperature. In fact, for small amounts sorbed, the exponent approaches the value unity; that is, the sorption varies linearly with pressure (Henry's law). These generalizations are illustrated by the data in Table 9 above.

In their investigations on the sorption of various gases by coconut charcoal, both I. Homfray[96] and A. Titoff[97] observed the empirical relation that *for a given pressure* the logarithm of the amount sorbed per gram of charcoal decreases linearly with increase in temperature. That is,

$$\frac{d \ln (x/m)}{dT} = -K, \qquad (1)$$

where K is a constant.

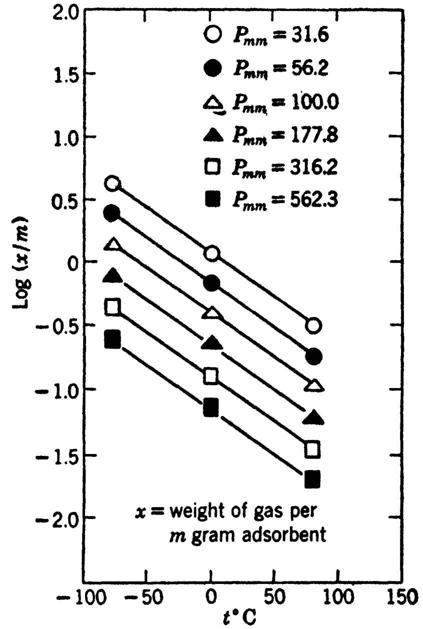

FIG. 20. Isobars for the sorption of hydrogen by charcoal at three temperatures (McBain).

Figure 20[98] shows a plot of the isobars for the adsorption of hydrogen on charcoal, for a series of pressures, as derived by Titoff from the isotherms.

On the other hand, B. Iliin[99] has deduced a relation for the isobar of the form

$$\log x = A - k\sqrt{T}. \qquad (2)$$

One of the best-known relations for the isostere is that deduced by A. M. Williams, which has the form

$$\log\left(\frac{vT}{P}\right) = \frac{k_1}{T} + k_2. \qquad (3)$$

---

[96] *Z. physik. Chem.*, **74**, 129 (1910).

[97] *Z. physik. Chem.*, **74**, 641 (1910).

[98] McB, p. 98, Fig. 26.

[99] *Z. physik. Chem.*, **107**, 145 (1923); *Phil. Mag.*, **48**, 193 (1924).

Figure 21[100] shows adsorption isosteres for ammonia on charcoal plotted by A. M. Williams in accordance with this equation, for a series of values of v_0, the volume adsorbed.

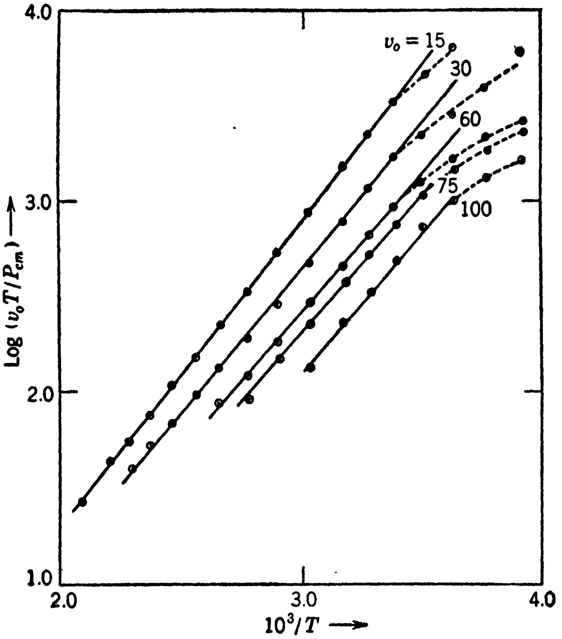

FIG. 21. Adsorption isosteres for ammonia on charcoal plotted according to equation 3 for a series of values of v_0, the volume adsorbed (cm^3, S.T.P.) per gram charcoal at pressure P_{cm} and $T°$ K (Williams).

Turning to the consideration of the hyperbolic equation for the isotherm, of the form

$$v = \frac{v_s bP}{1 + bP}, \tag{3.15}$$

it is of interest to discuss the manner in which both v_s and b vary with T for constant value of v.

E. Hückel[101] pointed out that, since v_s corresponds, theoretically, to a complete monolayer, the value of this constant should be practically independent of T. However, all the experimental evidence has shown that it is not, and several investigators have discussed the problem at length.[102]

---

[100] *Proc. Roy. Soc. London*, **96**, 287 (1919–1920), SB, p. 88.

[101] *Adsorption und Kapillarkondensation*, 1928.

As mentioned previously H. Zeise has shown that the hyperbolic equation (3.15) represents very satisfactorily the data obtained by I. F. Homfray,[103] A. Titoff[103] and L. B. Richardson[104] for the sorption of a number of gases by coconut charcoal. For any one gas the values of v_s are observed to decrease linearly with increase in temperature, while for the variation of b with temperature Zeise has deduced an empirical relation of the form

$$\log b = a_1 - a_2 \log T, \tag{4}$$

where a_1 and a_2 are constants. However, as will be discussed below, such a relation can possess no theoretically valid support.[105]

In section 3, in discussing Langmuir's observations on the sorption of a number of gases by mica and glass (see Table 11), it was observed that, except for the case of methane, the values of α (the fraction of the maximum available surface covered with a monolayer) were found to be considerably less than unity. Furthermore, for any given gas, α was observed to decrease to a marked extent with increase in temperature.

Similar results have been obtained by F. J. Wilkins[106] for the adsorption of nitrogen, argon, and oxygen on platinum. Table 16 gives the values observed for σ_1 and α.[107] From the linear plots of log α for each of the gases nitrogen and argon versus $1/T$, it follows that α may be expressed as a function of T by means of the relation

$$\alpha = c\epsilon^{\beta/T}. \tag{5}$$

From the plots of log α versus $1/T$, the values derived for β are approximately 406 and 491 for nitrogen and argon, respectively.

A similar decrease (with increase in temperature) in the values of α has been observed by M. H. Armbruster[108] for the adsorption of gases at low temperatures on silver. Table 17 gives values of σ_1 and of α obtained for four gases.

---

[102] Principally the following: H. Zeise, *Z. physik. Chem.*, **138**, 289 (1928); F. J. Wilkins and A. F. H. Ward, *Z. physik. Chem.*, **144**, 259 (1929); R. S. Bradley, *Phil. Mag.*, **11**, 690 (1931); F. J. Wilkins, *Proc. Roy. Soc. London*, A, **164**, 510 (1938).

[103] *Loc. cit.* See footnotes 96 and 97.

[104] *J. Am. Chem. Soc.*, **39**, 1829 (1917).

[105] Values of v_s and b for the different gases are given in Table 8.6.

[106] *Proc. Roy. Soc. London*, A, **164**, 510 (1938).

[107] The values given in Table 16 were calculated by means of the values of N_S given in Table 1.6.

[108] *J. Am. Chem. Soc.*, **64**, 2545 (1942).

TABLE 16

VALUES OF σ_1 AND OF α FOR THE ADSORPTION OF NITROGEN, ARGON, AND OXYGEN ON PLATINUM (WILKINS)

T	$10^3/T$	Nitrogen		Argon		Oxygen	
		$10^{-14}\sigma_1$	α	$10^{-14}\sigma_1$	α	$10^{-14}\sigma_1$	α
77.3	12.94			7.83	0.917		
83.5	11.98	2.77	0.342				
90.5	11.05	1.99	.245	2.59	.303	3.25	0.373
112.2	8.91	0.663	.0816	1.39	.162		
170.4	5.87	0.253	.0312	0.235	.0275	0.572	.0657

If the temperature coefficient of v_s (and therefore that of $1/\alpha$) corresponds to that of an ideal gas,[109] $-d\alpha/(\alpha\, dT)$ should be equal to $1/T$ (i.e., 0.011 for $T = 90°$ K). The actually observed values approach this theoretical value in only one case and are considerably different in all the others.

TABLE 17

VALUES OF σ_1 AND OF α FOR ADSORPTION ON SILVER

Gas	Temperature, °C	$10^{-14}\sigma_1$	α	$-d\alpha/(\alpha\, dT)$
A	−183	1.53	0.20	
N_2	−195	1.12	.17	
	−183	0.96	.15	0.0098
CO	−195	4.28	.65	
	−183	2.42	.37	.0359
O_2 (pumped)	−195	7.22	.94	
O_2 (pumped	−183	1.42	.18	.0674
O_2 (baked)	−195	5.60	.78	
O_2 (baked)	−183	3.09	.40	.0406
	− 78.5	2.30	.29	.0024

On the other hand, for the adsorption of the same gases on "smooth surfaces" of steel, over the same range of temperatures, Armbruster and Austin observed apparent values of α which ranged from 0.15 for one isotherm to greater than 5 in another case and averaged about unity at the two lowest temperatures. At −78° C, the values of α for carbon dioxide varied from 0.44 to 0.60. In order to account for values of α greater than 1, the investigators assumed that the specific surface must have been about 4 times that of the geometric area.

---

[109] This suggestion was made by Wilkins and A. F. H. Ward, *Z. physik. Chem.*, A, **144**, 259 (1929).

Let us consider now the effect of variation in temperature on the value of the constant b as exhibited by Langmuir's data in Table 11 and those derived by Zeise from the adsorption data for gases on charcoal.

From equations 3.4 and 3.11 it follows that, for $P_{\mu b}$,

$$b = \frac{N_A}{\sqrt{2\pi M R_0 T}} \cdot \frac{\alpha_0}{\mu_1}, \tag{6}$$

where we shall assume that $\alpha_0 = 1$, independently of T.

Since μ_1 denotes the rate of evaporation of adatoms, it is reasonable to assume (as in the evaporation of solids and liquids) that μ_1 is an exponential function of T of the form

$$\mu_1 = \mu_0 \epsilon^{-Q/(R_0 T)}, \tag{7}$$

where Q corresponds to the heat of vaporization in *calories per mole*.

Hence,

$$\ln b = \ln b_0 - \frac{1}{2} \ln T + \frac{Q}{R_0 T} \tag{8a}$$

or

$$\log b = \log b_0 - \frac{1}{2} \log T + \frac{Q}{4.574T}. \tag{8b}$$

Consequently, a plot of log $(b\sqrt{T})$ versus $1/T$ should yield a straight line, the slope of which corresponds to the value of $Q/4.574$.

Since Langmuir made his observations for adsorption on mica at only two temperatures, and the values of b vary widely for the same temperature with methane and nitrogen, it is impossible to use these data to derive values of Q.

For the values of c_2 (which, according to equation 3.31, correspond to b) Zeise deduced the empirical relation given in equation 4. However, for a number of the observations on adsorption plots of log c_2 versus $1/T$ are fairly linear with slopes corresponding to the approximate values of Q shown in Table 18. (The variation in log T may be neglected.)

TABLE 18

VALUES OF Q FROM VALUES OF c_2 COMPARED WITH OBSERVED VALUES OF HEAT OF ADSORPTION

Investigator	Gas	Q	Q_S
Titoff	N_2	2540	3684
Titoff	NH_3	3810	7200
Richardson	NH_3	4570	7200
Richardson	CO_2	3550	6100
Homfray	A	2675	3636
Homfray	CO	2400	3416

The last column gives values of Q_S, the heats of sorption (see discussion in the following section) for the gases on charcoal at −185° C, as measured by J. Dewar and, independently, by P. A. Favre.[110]

Though the values of Q given in the table should be regarded as very approximate, the fact that they are of the same magnitude as those given in the last column is in agreement with the physical interpretation of the constant b involved in equations 6 and 7.

In his discussion of the significance of the constant b in the hyperbolic equation, Langmuir introduced the concept of *average life* of adatoms.

If we divide μ_1 by σ_1, the number of adatoms per square centimeter corresponding to v_s, we obtain the value of the average probability per second for the evaporation of adatoms. The reciprocal, that is,

$$\tau_1 = \frac{\sigma_1}{\mu_1}, \tag{9}$$

is designated the *average life* of an adsorbed molecule on the surface.

From this definition and equation 6 it follows that

$$\tau_1 = \sigma_1 b\sqrt{2\pi M R_0 T} \cdot \frac{1}{N_A} \tag{10a}$$

$$= 22{,}860\sigma_1 b\sqrt{MT} \cdot \frac{1}{N_A} \tag{10b}$$

$$= \frac{\sigma_1 b\sqrt{MT}}{2.635 \cdot 10^{19}},$$

where b is expressed in microbar^{-1}.

This was the relation used in deriving the values of τ_1 given in Table 11. That these values are considerably greater than the corresponding values for the liquefied gas is evident from the following considerations:

Let τ_L = average life of a molecule on the surface of the liquid. Then,

$$\tau_L = \frac{N_S}{\mu_L}, \tag{11}$$

where N_S = number of molecules per cm^2 (see Table 4) and μ_L = rate of evaporation in molecules · cm^{-2} sec^{-1}.

As shown in Chapter 1, at the vapor pressure $P_{\mu b}$,

$$\mu_L = 2.635 \cdot 10^{19} \frac{P_{\mu b}}{\sqrt{MT}}. \tag{12}$$

---

[110] The values of Q_S obtained by these investigators are taken from McB, pp. 406–407. The values of Q should also be compared with those of L in Table 19.

Hence,

$$\frac{\tau_1}{\tau_L} = \frac{\sigma_1 b P_{\mu b}}{N_S} = \alpha b P_{\mu b}. \tag{13}$$

For instance, for oxygen and carbon monoxide the values of $P_{\mu b}$ at 90° K are $1 \cdot 10^6$ and $3 \cdot 10^6$, respectively. The corresponding values of N_S are $8.7 \cdot 10^{14}$ and $8.0 \cdot 10^{14}$, respectively. From the values of σ_1 and b given in Table 11, it follows that the values of τ_1/τ_L for oxygen and carbon monoxide adsorbed on surfaces of mica or glass are 8100 and 614,000 respectively.[111]

From these and similar results obtained by other investigators it must be concluded that adatoms are held at the surface of an adsorbent by much stronger forces than those that are effective in the liquid state between similar molecules.

It is evident that this must be so; otherwise it would be impossible to form the first layer, and in some experiments by R. W. Wood[112] and M. Knudsen[113] this phenomenon has actually been observed.

In Wood's experiments a stream of cadmium vapor in a well-exhausted bulb was allowed to strike a glass surface at different temperatures. No visible deposit was observed unless the glass was held at a temperature below about −90° C. On the other hand, once a deposit was started by cooling the glass at that spot with liquid air, the deposition of cadmium continued even after the deposit was warmed to room temperature.

From these and similar observations Wood concluded that, whereas cadmium atoms condense on a cadmium surface at any temperature, they condense on glass only if the temperature is below about −90° C. At higher temperatures all the atoms are reflected.

Similar observations were made by Knudsen and also by J. Weyssenhoff.[114] Knudsen experimented with mercury vapor and observed that at temperatures above −130° C most of the molecules impinging on a glass surface were apparently reflected. With other vapors a similar "critical temperature" was observed above which no condensation occurred. With NH_4Cl, this critical change occurred at −183° C, with copper at temperatures varying between 350° and 575° C, while with zinc, cadmium, and magnesium the critical range extended between

---

[111] For a more comprehensive discussion see the original paper by Langmuir, *J. Am. Chem. Soc.*, **40**, 1361 (1918), also his more recent paper in *J. Chem. Soc.*, **1940**, 511.

[112] *Phil. Mag.*, **30**, 300 (1915); **32**, 364 (1916).

[113] *Ann. Physik*, **50**, 472 (1916).

[114] *Ann. Physik*, **58**, 505 (1919).

−183° and −78° C. All these observations held true only for a glass surface. On the other hand, mercury atoms condensed on a mercury surface at all temperatures. This same observation had been made by Knudsen in a previous investigation,[115] and in fact he had applied equation 12 to determine the vapor pressure of mercury at extremely low temperatures from the rate of evaporation. As has been pointed out in a previous connection, the application of this equation involves the assumption that there is no reflection of atoms of the vapor striking the surface from which evaporation is occurring.

Weyssenhoff carried out some experiments in order to determine the amount of reflection of mercury atoms striking surfaces of gold and iron. Although no absolute determinations of the amount of reflection were obtained, he concluded from his experiments that, at −100° C, the reflection from gold is 5 to 10 times less than that from iron.

These observations were interpreted by these investigators as indicating that at some temperature the accommodation coefficient for condensation changes very rapidly from zero to unity. Langmuir, however, repeated Wood's experiments[116] and concluded from his observations that this deduction was not justifiable.

In his experiments, Langmuir used cadmium vapor in a well-exhausted bulb and investigated the effect of cooling a portion of the glass surface to different temperatures. He found that "traces of residual gas may prevent the growth of the deposit, particularly in those places which have been most effectively cooled. This is probably due to the adsorption of the gas by the cooled metal deposit." By using a side tube containing charcoal immersed in liquid air this effect was eliminated.

> If all the cadmium [he states] is distilled to the lower half of the bulb and this is then heated to 220° in an oil bath while the upper half is at room temperature, a fog-like deposit is formed on the upper part of the bulb in about 15 seconds. This deposit is very different from that obtained by cooling the bulb in liquid air. Microscopic examination shows that it consists of myriads of small crystals. According to the condensation-evaporation theory, the formation of this fog is readily understood. Each atom of cadmium, striking the glass at room temperature, remains on the surface for a certain length of time before evaporating off. If the pressure is very low, the chance is small that another atom will be deposited, adjacent to the first, before this has had time to evaporate. But at higher pressures this frequently happens. Now if two atoms are placed side by side on a surface of glass, a larger amount of work must be done to evaporate one of these atoms than if the atoms were not in contact. Not only does the attractive force between the cadmium atom and the glass have to be overcome, but also that between the two cadmium atoms. Therefore, the rate of evaporation of atoms from pairs will be much less than that of single atoms. Groups of three and four atoms will be still more stable. Groups of

---

[115] *Ann. Physik,* **48**, 1113 (1915).

[116] *Proc. Natl. Acad. Sci. U.S.*, **3**, 141 (1917).

two, three, four atoms, etc., will thus serve as nuclei on which crystals can grow. The tendency to form groups of two atoms increases with the square of the pressure, while groups of three form at a rate proportional to the cube of the pressure. Therefore the tendency for a foggy deposit to be formed increases rapidly as the pressure is raised or the temperature of the condensing surface is lowered.

On the other hand, according to the reflection theory, there seems to be no satisfactory way of explaining why the foggy deposit should form under these conditions.

Experiments show clearly that, when a beam of cadmium vapor at very low pressure strikes a given glass surface at room temperature, no foggy deposit is formed, although when the same quantity of camium is made to impinge against the surface in a shorter time (and therefore at higher pressure) a foggy deposit remains. This fact constitutes strong proof of the condensation-evaporation theory.

A deposit of cadmium of extraordinarily small thickness will serve as a nucleus for the condensation of more cadmium at room temperature. Let all the cadmium be distilled to the lower half of the bulb. Now heat the lower half to 60° C. Apply a wad of cotton, wet with liquid air, to a portion of the upper half for 1 minute, and then allow the bulb to warm up to room temperature. Now heat the lower half of the bulb to 170° C. In about 30 seconds a deposit of cadmium appears which rapidly grows to a silver-like mirror. This deposit only occurs where the bulb was previously cooled by liquid air.

Langmuir calculated from the vapor-pressure data for cadmium that

a deposit which forms in 1 minute with the vapor from cadmium at 60° contains only enough cadmium atoms to cover 3/1000 of the surface of the glass. Yet this deposit serves as an effective nucleus for the formation of a visible deposit.

At lower temperatures where the vapor pressure is much smaller the probability that the atoms striking the glass will fall into positions adjacent to atoms already on the surface becomes very much smaller and the atoms evaporate before new ones arrive; consequently there is no apparent condensation. Langmuir stated the difference between his point of view and that of Wood and the others quite clearly:

When an atom strikes a surface and rebounds elastically from it, we are justified in speaking of this process as a reflection. Even if the collision is only partially elastic, we may still use this term. The idea that should be expressed in the word "reflection" is that the atom leaves the surface by a process which is the direct result of the collision of the atom against the surface.

On the other hand, according to the condensation-evaporation theory, there is no direct connection between the condensation and subsequent evaporation. The chance that a given atom on a surface will evaporate in a given time is not dependent on the length of time that has elapsed since the condensation of that atom. Atoms striking a surface have a certain average "life" on the surface, depending on the temperature of the surface and the intensity of the forces holding the atom. According to the "reflection" theory, the life of an atom on the surface is simply the duration of a collision, a time practically independent of temperature and of the magnitude of the surface forces.

The above experiments prove [as stated by Langmuir] that the range of atomic forces is very small and that they act only between atoms practically in contact with each other. Thus a surface covered by a single layer of cadmium atoms behaves, as far as condensation and evaporation are concerned, like a surface of massive cadmium.

In this manner it is possible therefore to account very well for the apparent reflection of cadmium and mercury from glass surfaces, and it is seen that these observations are not at all in contradiction to Langmuir's theory.

From their experiments, M. Volmer and I. Estermann[117] concluded that, for liquid mercury, the accommodation coefficient (that is, the ratio designated α_0 in the derivation of the hyperbolic equation for the sorption isotherm) for condensation is unity, while for the solid it is slightly smaller. They also observed that for other substances, such as sulfur, phosphorus, and benzophenone, the value of the accommodation coefficient varied from 0.2 to 0.5. On the whole they expressed views in accord with Langmuir in concluding that the first stage in the condensation of molecules on a crystalline surface consists in adsorption.

In concluding this section it is of interest to mention the relations that must exist between the temperature coefficients of the different terms in the hyperbolic equation for the adsorption isotherm.

Differentiating the terms in equation 3.15 with respect to T, we obtain the two relations:

(1) For $dv/dT = 0$, that is, for *constant adsorption,*

$$\frac{d \ln P}{dT} = -\frac{dv_s}{(v_s - v)\,dT} - \frac{d \ln b}{dT}; \qquad (14)$$

(2) For $dP/dT = 0$, that is, for *constant pressure,*

$$\frac{d \ln v}{dT} = \frac{d \ln v_s}{dT} + \left(\frac{v_s - 1}{v_s}\right)\frac{d \ln b}{dT}. \qquad (15)$$

Assuming that

$$\ln b = \ln b_0 + \frac{Q}{R_0 T} \qquad (16)^{118}$$

and that, therefore,

$$\frac{d \ln b}{dT} = -\frac{Q}{R_0 T^2}, \qquad (17)$$

and knowing that, if v_s changes with T, dv_s/dT is always negative, it follows from the last equations that (1) for constant amount adsorbed, P must increase with increase in T; (2) for constant pressure, v must decrease with increase in T.

---

[117] *Z. Physik,* 7, 1, 13 (1921).

[118] For the purpose of this argument we may neglect the factor $1/\sqrt{T}$ in equation 6.

These conclusions are, of course, also evident from an inspection of a series of isotherms at different temperatures.

7. HEAT OF SORPTION

As mentioned previously, heat is evolved when a gas is sorbed and taken up when the sorbed gas is removed. The Clapeyron equation may therefore be applied to the isostere to determine the heat of sorption in the same manner as the heat of vaporization may be determined from a vapor-pressure curve. The isosteric heat of sorption is thus determined by means of the relation

$$Q_S = -R_0 \frac{d \ln P}{d(1/T)} \tag{1a}$$

$$= \frac{4.574 \, (\log P_2 - \log P_1)}{1/T_1 - 1/T_2}, \tag{1b}$$

where Q_S is expressed in calories per mole, and P_1 and P_2 are equilibrium pressures at temperatures T_1 and T_2, respectively, for a given amount adsorbed.

The fact that heat must be supplied to a surface to desorb it "has found application," as McBain observes,[119] "in the production of low temperatures, as, for example, reaching 6° abs by pumping off hydrogen sorbed at the temperature of liquid air or liquid hydrogen.[120]

The determination of the value of Q_S derives its importance from the fact that it is a measure of the interaction energy between the adsorbed molecules and the surface atoms. As mentioned in section 5, it is possible from the value of the constant c in the Brunauer-Emmett-Teller equation to derive the value of $E_I - E_L$, where E_I is the energy of formation of the first adsorbed layer of molecules and E_L is the energy of condensation of the molecules to form the liquid. Furthermore, as was pointed out in the previous section, it is possible under certain conditions for E_L to exceed E_I.

Since we shall have occasion to compare the values of heats of sorption with those of the heats of condensation, L, of the gases, Table 19

---

[119] McB, p. 400.

[120] F. Simon, *Physik. Z.*, **27**, 790 (1926). See also D. H. Andrews, R. K. Witt, and E. Crigler, *Refrig. Eng.*, **19**, 177 (1930).

TABLE 19

HEATS OF CONDENSATION OF GASES

Gas	$t°$ C	Cal · g^{-1}	M	L* (cal · mole^{-1})	L_S (cal · mole^{-1})
He	−268.6	6.0	4.003	24.0	590
H_2	−252.8	108.0	2.016	217.7	
N_2	−195.6	47.6	28.02	1334	1860
CO	−192	50.5	28.01	1415	2090
A	−186	37.6	39.94	1502	2800
O_2	−182.9	50.9	32.00	1629	2060
CH_4	−159	138.2	16.03	2215	2700
N_2O	−30	67.9	44.02	2989	
CO_2	−60	87.3	44.01	3842	
	−78.5	138.0	44.01	6074	
NH_3	−33.4	327.5	17.03	5565	
SO_2	−10.1	95.0	64.06	6085	
H_2O	0	596.7	18.02	10750	

* *International Critical Tables*, Vol. 5, pp. 135–139.

gives values of the heat of sorption, in the third column, and, for comparison, values of L for a number of the gases which have been used in investigations on sorption.

The last column gives the observed heats of sublimation, L_S, of the crystals.[121]

The heats of sorption (in calories per mole) may be calculated from the isosteres by means of equation 1*b* or by plotting log P, for constant amount adsorbed, against $1/T$, but they have also been determined by calorimetric methods.[122] Table 20, taken from a review of this topic by H. R. Kruyt and J. G. Modderman,[123] illustrates the kind of agreement obtained by the two methods. The data were obtained by Titoff for carbon dioxide on charcoal at 0° C and 30° C.

On porous, non-metallic adsorbents such as charcoal and silica gel, the differential heat of sorption is very close to, or somewhat greater than, the latent heat of condensation for the adsorbate, indicating that the forces between surface atoms of the adsorbent and molecules of the adsorbate are of the same nature as the van der Waals forces which are effective in bringing about condensation of a vapor. On the other hand, in sorption by metals, the values of Q_S are usually of the same order as chemical heats of reaction. Hence the designation *chemisorption* for this type of sorption.

In the system oxygen-charcoal both van der Waals sorption and

---

[121] SB, p. 193.

[122] These are described in SB, Chapter III, and McB, Chapter XIV.

[123] *Chem. Revs.*, 7, 259 (1930); SB, p. 223.

TABLE 20

Heat of Adsorption for Carbon Dioxide on Charcoal

v_0	Q_S	Q (calorimetric)
1.82	8130	7727
4.02	7705	7280
10.3	6966	
19.72	6548	6831
28.87	6292	6720
34.07	6452	6585
38.14	6383	
41.4	6495	
44.9	6428	6540

chemisorption occur, as illustrated by Fig. 22, taken from a paper by F. G. Keyes and M. J. Marshall.[124] From an initial value of 72,000 cal per mole, the heat of sorption decreases rapidly with increase in amount sorbed to about 4000 cal per mole for very large amounts sorbed.

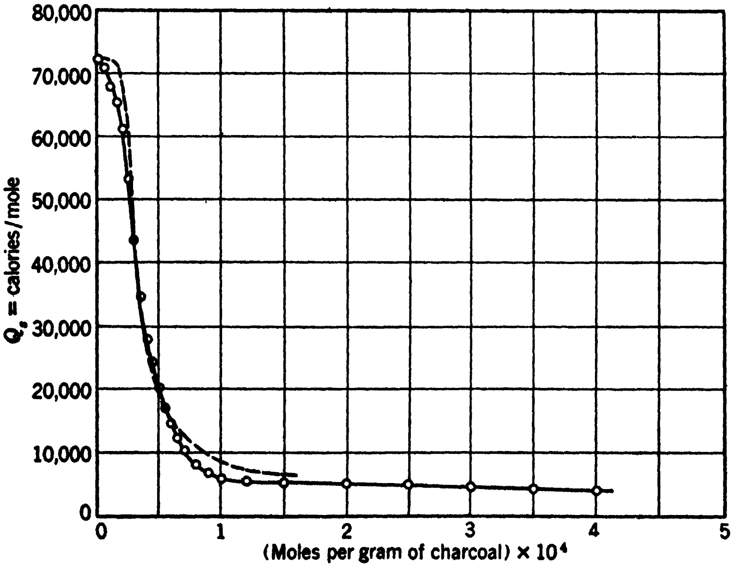

Fig. 22. Heat of adsorption for oxygen on charcoal, as a function of amount adsorbed (Keyes and Marshall).

This decrease in Q_S with increase in amount adsorbed is characteristic of a large number of cases of adsorption. It is, in fact, illustrated by the data in Table 20, on the sorption of carbon dioxide by charcoal, and is further shown in the data given in Table 21, taken from E. Hückel,[125] giving the so-called "differential" and "integral" heats of adsorption. The first column gives the amounts of gas adsorbed, and the second, the ratio between the increase in heat of sorption (calories per gram of charcoal) per mole increase in gas adsorbed. The ratio

---

[124] *J. Am. Chem. Soc.*, **49**, 156 (1927); SB, p. 228, Fig. 83.

$$q_d = \frac{\Delta q}{\Delta a} \tag{2}$$

is known as the differential heat of sorption. The third column gives the integral or total heat of sorption for the corresponding value of a, in terms of calories per gram of adsorbent, while the last column gives the value in terms of calories per mole of gas adsorbed, where $q_i/a = Q_S$.

TABLE 21

DIFFERENTIAL AND INTEGRAL HEATS OF ADSORPTION FOR CARBON DIOXIDE ON CHARCOAL

10^5a 10^5 Moles/g of charcoal	q_d Cal/mole	q_i Cal/g of charcoal	q_i/a Cal/mole
	Nitrogen		
1.157	8,350	0.097	8,350
10.91	4,650	0.509	4,660
18.7	4,075	0.865	4,620
32.5	4,720	1.52	4,660
45.2	4,550	2.09	4,620
58.3	4,770	2.72	4,650
	Ammonia		
24.2	11,270	2.7	11,270
134.6	8,540	12.2	9,030
269.5	8,060	23.1	8,550
403	7,830	33.5	8,300
516	7,880	42.1	8,140
568	8,380	46.3	8,150
591	8,650	48.4	8,180
606	8,710	49.8	8,200

In general, the heats of sorption for the *same gas* on different adsorbents are roughly the same. Also the heats of sorption for different gases increase, in general, with increase in boiling point. For instance, as Brunauer points out,

---

[125] *Adsorption und Kapillarkondensation*, pp. 22–35, Leipzig, 1928; quoted in SB, p. 219, Table XXVI.

> Helium, boiling at 4.2° K, has a heat of adsorption of about 140 calories per mole; hydrogen, boiling at 20.4° K, has a heat of adsorption of about 1500 calories per mole, and the four gases, argon, nitrogen, oxygen, and carbon monoxide, boiling in the temperature range 77.3–90.1° K, have heats of adsorption of about 3000–4000 calories per mole.
>
> For ammonia, carbon dioxide, and nitrous oxide Favre obtained heats of adsorption of 7200, 7300, and 7400 calories per mole, respectively. For ethylene, acetylene, carbon dioxide, and nitrous oxide Gregg obtained values of 6600, 8100, 6900, and 7200 calories per mole, respectively. These heats of adsorption were obtained on charcoal. The boiling points of the five gases lie between 169° and 240° K.[126]

Similarly, for a number of organic vapors which have their boiling points in the range 300–350° K, the observed heats of adsorption on charcoal fall between 12,000 and 15,500 calories per mole.[127]

For the adsorption of nitrogen, argon, and carbon monoxide on smooth surfaces of steel and silver, Armbruster and Austin[128] have deduced, from the observed adsorption isotherms at −183° C and −195° C, the values of adsorption heats shown in Table 22. The last column gives values which these investigators have deduced from data of F. J. Wilkins.[129]

TABLE 22

VALUES OF HEAT OF ADSORPTION ON METAL SURFACES
(CALORIES PER MOLE)

	Fe			
	Unreduced	Reduced	Ag	Pt
A	3280	3200	3500	3280
N_2	3280	3120	3600	3385
CO		3400	3170	3600

It will be observed that the range of values is the same as that given above by Brunauer for the same gases.

Comparison of the values for heats of sorption obtained by different investigators with those for the corresponding latent heats of vaporization and sublimation (see Table 19) leads to the conclusion that the forces between adsorbed molecules and the surface atoms of the adsorbent are of the same nature as the van der Waals forces of cohesion. Actually, it has been found possible to calculate the magnitudes of these forces from theoretical considerations and deduce from these conclusions approximate values of heats of sorption.

---

[126] SB, pp. 240–241.

[127] SB, p. 241. A very comprehensive survey of data on heats of adsorption has been given by H. R. Kruyt and J. G. Modderman in *International Critical Tables*, Vol. V, pp. 139–141. The values of Q, given in joules, can be converted into calories by multiplying by the factor 0.2392. Also calories per mole = 22,400 × (calories per cm^3).

[128] *J. Am. Chem. Soc.*, **66**, 159 (1944).

[129] *Proc. Roy. Soc., London*, **A**, **164**, 496 (1938).

For example, for the adsorption of argon and carbon dioxide on ionic crystals (such as those of the alkali halides) the experimental and theoretical heats of sorption are found to be in very fair agreement. Similar results have been obtained for the heats of sorption of hydrogen, argon, and nitrogen on graphite.[130] The most elaborate calculation of this nature has been carried out by W. J. C. Orr[131] on the adsorption of argon, nitrogen, and oxygen on crystals of potassium chloride and cesium iodide. For each of these gases the maximum values of the heats of sorption (which range from 2000 to 3000 calories per mole) are observed for the completed monolayers ($\theta = 1$), with more or less rapid decreases for $\theta > 1$.

It is of interest to note as shown in Table 23,[132] the relation observed by Orr between the number of layers and the values of P/P_0, where P_0 denotes the saturation vapor pressure of the bulk gas phase.

TABLE 23

RELATION BETWEEN THICKNESS OF ADSORBED LAYER AND "RELATIVE" PRESSURE

		P/P_0				Bulk
No. of "layers":		1	2	3	4	Condensed
Gas	T					Phase
Argon	79.35	0.25	0.69	0.90	0.96	Solid*
Argon	86.89	.22	.63	.80	.90	Liquid
Oxygen	79.32	.20	.65	.80	.85	Liquid
Nitrogen	73.57	.012	.44	.70	.85	Liquid

* Melting point of argon = 83.9° K.

As Orr points out,

> The similarity between oxygen and argon and the contrast in their behavior to that of nitrogen is here very clearly brought out, the relatively very low value of P/P_0 at one monolayer, in the case of nitrogen, being indicative of the much stronger interaction of these molecules with the surface. It is also significant to note that P/P_0 for nitrogen reaches values similar to those of oxygen and argon when about three

---

[130] See SB, p. 215.

[131] *Trans. Faraday Soc.*, **35**, 1247 (1939).

[132] *Proc. Roy. Soc. London*, **A**, **173**, 349 (1939).

or four apparent layers are adsorbed, thus illustrating the very rapid falling off in the influence of the surface field. The fact that the vapor pressure does not reach exactly the saturation vapor pressure in about four layers, as would be expected from the known range of molecular forces, but tends asymptotically towards it, is undoubtedly to be explained by a lowering of the vapor pressure of the bulk phase due to capillary effects occurring in wide cracks or holes in the crystal surface.[133] Although rapid condensation in bulk does not set in till about four or five layers have condensed, the heat of adsorption, in the case of argon, falls to the sublimation heat of the solid very close to the completion of a second layer, while, in the case of oxygen and nitrogen, it falls to the heat of vaporization of the liquid when between two and three layers have been condensed.

The conclusions stated in this quotation with regard to both the range of the attractive forces and the limitation on the number of monolayers that can form on the surface of an adsorbent are extremely significant and in agreement with conclusions which Langmuir expressed in his earliest papers.

8. RATE OF SORPTION

Some of the earliest experiments on rate of sorption were made by Blythswood and H. S. Allen.[134] They observed that the rate of sorption of air by charcoal at the temperature of liquid air could be represented quite accurately by the first-order reaction equation

$$\frac{dx}{dt} = k(A - x), \tag{1}$$

where x = amount adsorbed at time t.
A = total amount adsorbed when equilibrium was attained.
k = constant.

Integrating equation 1 we obtain the relation

$$\log (A - x) = \log A - 0.4343kt. \tag{2}$$

That is, a plot of $\log (A - x)$ versus t should yield a straight line, for which the intercept at $t = 0$ is $\log A$, and the slope

$$-\frac{\Delta \log (A - x)}{\Delta t} = 0.4343k.$$

An equation similar to equation 1 was deduced by Langmuir[135] for the rate of adsorption of molecules to form a monolayer.

---

[133] This refers to the well-known fact that the vapor pressure of a liquid in a capillary is lower than that of the bulk phase, and the lowering in vapor pressure is a function of the radius of the capillary bore.

[134] *Phil. Mag.* **10**, 497 (1905).

[135] *J. Am. Chem. Soc.*, **40**, 1361 (1918).

Let θ' denote the fraction of the surface covered at any instant of time t, for the case in which the fraction at equilibrium is θ. Then it follows from considerations similar to those used in deriving equation 3.9 that

$$\sigma_1 \frac{d\theta'}{dt} = \alpha_0\nu - (\mu_1 + \alpha_0\nu)\theta'. \tag{3}$$

Introducing the relation for θ given by equation 3.10, we obtain the differential equation

$$\frac{\sigma_1}{\mu_1}\frac{d\theta'}{dt} = \left(1 + \frac{\alpha_0\nu}{\mu_1}\right)(\theta - \theta'), \tag{4}$$

which is obviously similar in form to equation 1.

Introducing the relation $\tau_1 = \sigma_1/\mu_1$ given in equation 6.9, equation 4 leads to the integral relation

$$\tau_1 \log\left(\frac{\theta}{\theta - \theta'}\right) = \frac{(1 + \alpha_0\nu/\mu_1)t}{2.303}. \tag{5}$$

For $\theta - \theta' = \frac{1}{2}\theta$, that is, for the equilibrium to proceed halfway to its final value, the time required is given by the relation

$$t_{0.5} = \frac{0.6932\tau_1}{1 + \alpha_0\nu/\mu_1} \tag{6a}$$

$$= \frac{0.6932\tau_1}{1 + bP_{\mu b}}; \tag{6b}$$

and, for $\theta - \theta' = \frac{1}{10}\theta$,

$$t_{0.9} = \frac{2.303\tau_1}{1 + bP_{\mu b}}. \tag{7}$$

Since, as shown in Table 11, τ_1 for adsorption on mica and glass is of the order of 10^{-5} to 10^{-4} sec, it is evident that for these adsorbents equilibrium is attained in considerably less than a second.

Rates of sorption at constant pressure for ammonia, carbon dioxide, sulfur dioxide, and nitrous oxide by glass surfaces have been investigated by D. H. Bangham and F. P. Burt.[136] They derived the empirical expression

$$\frac{d \log s}{d \log t} = \frac{1}{n}, \tag{8}$$

where s = amount adsorbed, and n is a constant.

---

[136] *Proc. Roy. Soc. London*, **A**, **105**, 481 (1924). See also McB, p. 48.

Since this relation would indicate an infinite amount of sorption at infinite time, the expression used for longer periods is

$$\log \frac{\sigma}{\sigma - s} = kt^{1/n}, \tag{9}$$

where σ is the estimated saturation value. For $n = 1$, this evidently becomes identical with equation 2, while for small values of s and t the last equation becomes identical with equation 8.

The rate of sorption of hydrogen by charcoal at the temperature of liquid air has been specially investigated by J. B. Firth[137] and J. W. McBain.[138] Both investigators observed that equilibrium is attained only after a lapse of many hours. Most of the gas is apparently condensed practically instantaneously on the surface. This is followed by a gradual diffusion of the hydrogen into the charcoal, the rate of which, as shown by McBain, is in agreement with the laws of diffusion.

The rate of occlusion of gases by chabasite and other members of the zeolite group of minerals has been investigated by R. M. Barrer and D. A. Ibbitson.[139] In these minerals, as will be discussed in greater detail in the following chapter, the rate of diffusion of molecules along pores, or very fine channels, is the controlling factor, as shown by the fact that the rate of occlusion depends upon the relative diameters of the molecules and the pores, as well as on the external pressure and temperature.

These and similar observations will be discussed more fully in connection with the remarks on specific adsorbents in the next chapter. As Brunauer[140] observes,

> In general, it seems safe to conclude that in van der Waals adsorption the gas molecules are adsorbed as rapidly as they can reach the surface. The slow effects are either due to chemisorption, chemical reaction, solution, or to the inability of the molecules to get in contact with the surface of the adsorbent.

A problem of interest in connection with the slow rate of sorption which follows the practically instantaneous adsorption as a unimolecular layer is the time required for molecules to cover the surface of a pore or very narrow channel. If the rate of re-evaporation of adsorbed molecules is very small, then, as shown by P. Clausing,[141] the time t necessary to cover the surface of the pore with molecules is

---

[137] *Z. physik. Chem.*, **86**, 294 (1914).

[138] *Z. physik. Chem.*, **68**, 471 (1909).

[139] *Trans. Faraday Soc.*, **40**, 195 (1944).

[140] SB, p. 8.

[141] *Ann. Physik*, **7**, 489, 521 (1930). This reference is mentioned in the publication by O. Beeck, A. E. Smith, and A. Wheeler, on catalytic activity, crystal structure, and adsorptive properties of evaporated metal films, *Proc. Roy. Soc. London*, **A**, **177**, 62 (1940–1941).

$$t = \frac{3l^2}{8a^2 S\nu}, \tag{10}$$

where l = length, a = radius of pore, S = cross-sectional area of a molecule, and ν = rate at which molecules strike a surface at the pressure P.

For instance, let us assume that $l = 0.1$ cm, $a = 10^{-5}$ cm, $P_\mu = 1$, and that the gas is nitrogen at $T = 80$. Then

$$\nu = 7.41 \cdot 10^{17}\ \text{sec}^{-1}\ \text{cm}^{-2},$$

$$S = 16.2 \cdot 10^{-16}\ \text{cm}^2,$$

and

$$t = 8.68 \text{ hours.}$$

Since ν varies linearly with P, t for 10 microns would be 52.1 min. Thus, for long pores of very small diameter, the time required to saturate the walls of these pores may be quite long.

9. SURFACE OF ADSORBENTS

As mentioned in a previous section the heat of adsorption for any given gas is approximately the same for different adsorbents. Thus the only other important factor by which the adsorption on different adsorbents can be influenced is the extent of surface per unit mass of adsorbent.

The different methods by which the surface area can be determined have been described very comprehensively by Brunauer[142] and by McBain.[143] In the following discussion three of these methods will be described briefly.

The method developed by F. P. Bowden and E. K. Rideal[144] and by Bowden and E. A. O'Connor[145] is applicable only to metals, and is described by Brunauer as follows:

> When a metal is made the cathode in a dilute acid and current is passed through the solution, the potential changes due to accumulation of hydrogen on the electrode. This phenomenon is called polarization. Bowden and Rideal noted that the change in potential was proportional to the amount of hydrogen deposited on the electrode,
>
> $$-\frac{\Delta E}{\Delta V} = K, \tag{1}$$

---

[142] SB, Chapter IX, especially p. 282 for quotation.

[143] McB, Chapter X, p. 325.

[144] *Proc. Roy. Soc. London*, A, **120**, 59, 80 (1928).

[145] *Proc. Roy. Soc. London*, A, **128**, 317 (1930).

where E is the potential, and V the amount of hydrogen on the surface of the cathode. They also made the important discovery that K was not dependent on the nature of the metal but only on its surface area. All liquid metals investigated (mercury, amalgamated silver, platinized mercury, liquid gallium, liquid Wood's metal) required about $6 \cdot 10^{-7}$ coulomb of electricity per square centimeter surface to produce a change of 100 millivolts in the electrode potential. It seemed therefore safe to assume for all metals that

$$-E = \frac{KV}{A} + \text{constant}, \tag{2}$$

where A is the surface area accessible to hydrogen ions and K/A is a constant for all metals. A will be referred to as the *true* surface of the metal.

In the electrolytic method of surface determination one measures the quantity of electricity necessary to produce a change of 100 millivolts in the electrode potential. When this value is divided by $6 \cdot 10^{-7}$ coulomb one obtains the ratio between the true surface of the metal and its apparent surface.

Table 24[146] gives values of this ratio for a number of cases, as observed by the above-mentioned investigators.

TABLE 24

THE RATIO BETWEEN TRUE SURFACE AND THE APPARENT SURFACE OR THAT OF A LIQUID AS FOUND BY THE METHOD OF ELECTROLYTIC POLARIZATION

Surface	*Ratio*
Platinum, bright foil	2.2
Platinum, bright foil, cleaned in acid and heated in a flame	3.3
Platinum, platinized	1830
Gallium, solidifying undisturbed	1.7
Nickel, polished, new	75
Nickel, polished, old	9.7
Nickel, activated by alternate oxidation and reduction, new	46
Nickel, activated by alternate oxidation and reduction, old	29
Nickel, activated, then annealed, new	10.8
Nickel, activated, then annealed, old	7.7
Nickel, repolished and electroplated, new	12
Nickel, repolished and electroplated, old	9.5
Nickel, rolled, new	5.8
Nickel, rolled, old	3.5
Wood's metal, solidifying undisturbed	1.4
Wood's metal, sandpapered	6.3
Wood's metal, corroded by etching with nitric acid	800–1000
Silver, freshly etched with dilute nitric acid	51
Silver, etched with dilute nitric acid, after 20 hours	37
Silver, finely sandpapered	16
Silver, amalgamated, after 1 hour	1.2
Silver, amalgamated, after 20 hours	1.3
Silver, amalgamated, after 150 hours	1.8
Arc carbon rod	328–366

---

[146] McB, p. 341.

A more generally applicable method of measuring the surface area of an adsorbent has been developed by S. Brunauer and P. H. Emmett[147] on the basis of their theory of multimolecular adsorption. As shown in section 5, their equation for the isotherm leads to a determination of a constant v_m, which theoretically corresponds to the volume of gas required to form a unimolecular layer. From a knowledge of the molecular cross sections it is thus possible to derive a value for the surface area of the adsorbent.

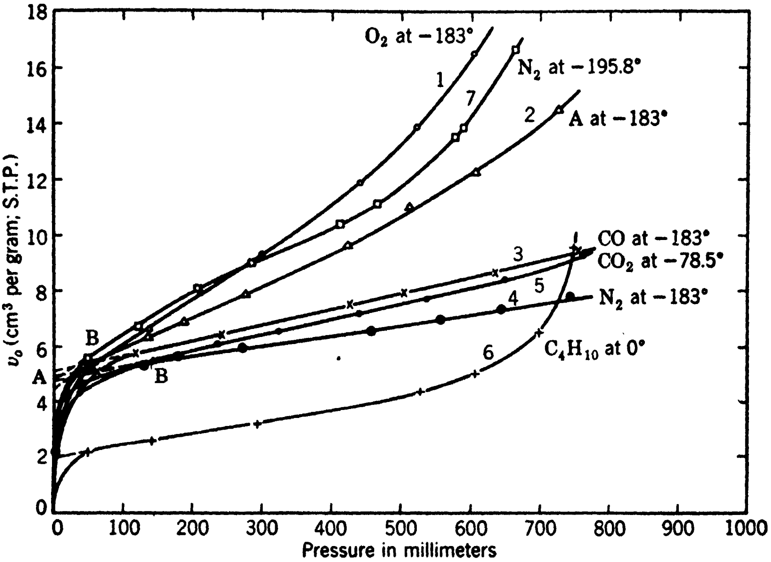

FIG. 23. Determination of the surface area of an iron catalyst by the gas adsorption method. The value of v_m at the point B is regarded as that corresponding to the volume (cm^3, S.T.P.) of a monolayer (Brunauer).

Instead of attempting to determine v_m, Brunauer and his collaborators have also used the isotherms directly for a determination of surface area. This is illustrated by the adsorption isotherms shown in Fig. 23[148] for six different gases on an iron catalyst. As Brunauer points out,

> The isotherms are S-shaped with three distinct regions: the low-pressure region is concave to the pressure axis, the high-pressure region is convex, and between the two there is a linear portion. ... It will be noted that the five smaller molecules of approximately equal size (N_2, O_2, A, CO, and CO_2) show approximately equal

---

[147] For a review of the subject, see also the publication by P. H. Emmett, *Ind. Eng. Chem.*, **37**, 639 (1945).

[148] SB, p. 286, Fig. 100; *J. Am. Chem. Soc.*, **59**, 1553 (1937).

adsorptions around 50 mm pressure, but at higher pressures the isotherms diverge widely. At first it was believed that the extrapolation of the intermediate straight-line portion to zero pressure (Point A) corresponded to the volume of gas necessary to cover the surface with a unimolecular adsorbed layer,[149] but later the beginning of the straight portion (Point B) was chosen as the most likely point to correspond to the monolayer.[150]

Granted that Point B corresponds to the number of molecules in a complete monolayer, the surface area of the adsorbent can then be calculated as follows:

Assuming that the adsorbed molecules have the same packing on the surface as the molecules of the solidified gas have in their plane of closest packing, we obtain for the area covered by a molecule,

$$\text{Area } (S) = \frac{4\sqrt{3}}{2}\left(\frac{M}{4\sqrt{2}N_A\rho_s}\right)^{2/3} \text{ cm}^2, \tag{3}$$

where N_A is the Avogadro constant, and ρ_s is the density of the solidified gas.

Hence,

$$S = 1.091\left(\frac{M}{N_A\rho_s}\right)^{2/3} \text{ cm}^2 \tag{4}$$

$$= 1.530 \cdot 10^{-16}(M/\rho_s)^{2/3} \text{ cm}^2. \tag{5}$$

The coefficient 1.091 has been designated the "packing factor," and, as shown by H. K. Livingston,[151] its value varies with the type of packing.

For closest packing,

$$S = \frac{\sqrt{3}}{2}\delta^2 = 0.866\delta^2, \tag{6}$$

where δ = molecular diameter. Hence, we obtain from equation 5 the relations

$$\delta = 1.074\sqrt{S}$$

$$= 1.329 \cdot 10^{-8}\left(\frac{M}{\rho_s}\right)^{1/3} \tag{7}$$

and

$$S = 1.103\frac{\pi\delta^2}{4}. \tag{8}$$

---

[149] S. Brunauer and P. H. Emmett, *J. Am. Chem. Soc.*, **57**, 1754 (1935).

[150] P. H. Emmett and S. Brunauer, *J. Am. Chem. Soc.*, **59**, 1553 (1937).

[151] *J. Am. Chem. Soc.*, **66**, 569 (1944).

That is, the cross-sectional area is 1.103 times the projected area of the molecule if it is regarded as a sphere of diameter δ.

The *number of molecules which can be adsorbed per square centimeter* to form a monolayer is given by $N = 1/S$, and the *volume* of gas at S.T.P. is given by

$$\begin{aligned} v_0 &= \frac{10^{-19}N}{2.687} = 3.722 \cdot 10^{-20}N \\ &= 3.722 \cdot \frac{10^{-20}}{S}, \end{aligned} \tag{9}$$

where S is the area per molecule calculated by means of equation 5 either from the density of the solid (giving S_s) or from that of the liquid (giving S_l).

Table 25 gives values of S and $1/S$, as deduced from the values of ρ_s and ρ_l in rows 1 and 4.[152] The temperatures corresponding to these values of the density are given in rows 2 and 5. Row 3 gives the values of the lattice constant, a, in centimeters.

Corresponding values of S_s and S_l, and their reciprocals, are given in rows 6 to 9 inclusive. For comparison there are also given in row 10 values of $N_S{}^0$ derived on the basis of kinetic theory relations from η_0, the coefficient of viscosity at 0° C.[153]

Rows 11 and 12 give the values of v_0, the volume adsorbed per square centimeter corresponding to a monolayer as calculated from values of $1/S_s$ and of $N_S{}^0$, respectively. The values in row 11 marked with an asterisk were derived from the values of $1/S_l$.[154]

Finally, the last row in Table 25 gives values of $1/S_b$, as derived from values of the van der Waals constant b_0, which are given in the standard

---

[152] All the values of the density, with the exception of that for sulfur dioxide, are taken from the paper by Emmett and Brunauer, *J. Am. Chem. Soc.*, **59**, 1553 (1937). The value of ρ_l for sulfur dioxide is taken from standard tables.

[153] Some of the values are taken from Table 1.6. For the following gases the values of η_0 used for the calculation of $N_S{}^0$ are taken from the summary by A. E. Schuil, *Phil. Mag.*, **28**, 679 (1939).

Gas:	N_2O	NO	SO_2	CH_4	NH_3	CO
$10^5\eta_0$:	13.88	17.77	11.58	10.22	9.16	16.59

[154] It is of interest to observe that Langmuir, *J. Am. Chem. Soc.*, **40**, 1361 (1918), used the following values of $1/S$:

Gas:	N_2	O_4	A	CO	CO_2	NH_3
$10^{-14}/S$:	6.6	7.7	7.7	6.6	6.1	6.3

Also Brunauer (*loc. cit.*) gives for H_2O the value $S = 11.5 \cdot 10^{-16}$ cm^2; that is, $1/S = 8.70 \cdot 10^{14}$.

TABLE 25

Molecular Areas and Number of Molecules per Square Centimeter

	Gas:	N_2	O_2	A	CO	CO_2	CH_4	NH_3	H_2O	N_2O	NO	SO_2
1) ρ_s	$g \cdot cm^{-3}$	1.026	1.426	1.65	—	1.565	—	—	—	—	—	—
2) t	°C	−252.5	−252.5	−253	−252.5	−80	−253	−80	—	—	—	—
3) $10^8 a$	cm	—	—	—	5.63	—	5.89	5.19	—	5.77	—	—
4) ρ_l	$g \cdot cm^{-3}$	0.808	1.14	1.374	0.763	1.179	0.392	0.688	1.00	1.199	1.269	0.642
5) t	°C	−195.8	−183	−183	−183	−56.6	−140	−36	3.98	−80	−150	−50
6) $10^{16} S_s$	cm^2	13.8	12.1	12.8	13.7	14.1	15.0	11.7	—	14.4	—	—
7) $10^{16} S_l$	cm^2	16.2	14.1	14.4	16.8	17.0	18.1	12.9	10.51	16.8	12.5	3.29
8) $10^{-14}/S_s$	cm^{-2}	7.25	8.26	7.81	7.30	7.09	6.67	8.55	—	6.94	—	—
9) $10^{-14}/S_l$	cm^{-2}	6.17	7.09	6.94	5.95	5.88	5.53	7.75	9.52	5.95	8.00	3.04
10) $10^{-14} N_S{}^g$	cm^{-2}	8.10	8.71	8.54	8.07	5.35	5.23	4.56	5.27	5.36	10.23	3.73
11) $10^5 (v_0)_s$	cm^3	2.70	3.07	2.91	2.72	2.64	2.48	3.18	3.54*	2.58	2.98*	1.13*
12) $10^5 (v_0)_N$	cm^3	3.02	3.24	3.18	3.00	1.99	1.95	1.70	1.96	2.00	3.81	1.39
13) $10^{-14}/S_b$	cm^{-2}	11.69	13.42	13.31	11.54	11.04	11.01	12.12	13.80	10.78	14.65	9.16

* Derived from the values of $1/S_l$.

tables. The relation used is

$$\frac{1}{S_b} = \frac{1.695 \cdot 10^{13}}{{b_0}^{2/3}}. \tag{10}$$

For example, for argon, $b_0 = 1.437 \cdot 10^{-3}$. Hence $S_b = 7.51 \cdot 10^{-16}$, $1/S_b = 13.31 \cdot 10^{14}$, and $\delta = 2.95 \cdot 10^{-8}$.

From the values of v_m, the volume (S.T.P.), adsorbed per gram, as determined from the point B in Fig. 23, it is possible to calculate the effective surface area, A_m, in *square meters per gram*, of the adsorbent, by means of the relation

$$A_m = 2.687 \cdot 10^{15} v_m S. \tag{11}$$

Thus, for nitrogen at −195° C, $S = 16.2 \cdot 10^{-16}$ cm². Hence,

$$A_m = 4.352 v_m.$$

Table 26 gives values of A_m, thus deduced from the observed values of v_m, for the iron catalyst used in determining the plots in the above figure.

TABLE 26

SURFACE AREA OF IRON CATALYST

Gas	Temperature of Isotherm, ° C	Boiling Point of Gas, ° C	Point B, cm³ at 0° C and 760 mm	Calculated Area, sq m/g	
				Solid Packing	Liquid Packing
N_2	−183	−195.8	5.5	0.444	0.548
N_2	−195.8		5.5	.444	.522
CO	−183	−191.6	5.7	.457	.561
A	−183	−185.7	5.8	.435	.489
O_2	−183	−183.0	5.5	.390	.454
CO_2	−78.5	−78.5	5.95	.491	.593
C_4H_{10}	0	−0.3	2.2	.411	.411

The adsorption method has been used by Brunauer and Emmett as well as other investigators to determine surface areas of a variety of adsorbents. Table 27 taken from Brunauer[155] shows that "the method is applicable through a 100,000fold variation in specific surface, from unreduced Fe_3O_4 to Darco G."

---

[155] *J. Am. Chem. Soc.*, **59**, 1553 (1937); SB, p. 298. See also determinations (by means of this method) of surface area for "pigments, carbon blacks, cements and miscellaneous finely divided or porous materials," by P. H. Emmett and T. DeWitt, *Ind. Eng. Chem., Anal. Ed.*, **13**, 28 (1941). Using the same technique, W. R. Smith, F. S. Thornhill, and R. I. Bray, *Ind. Eng. Chem.*, **33**, 1303 (1941), have obtained values for the surface area of carbon black ranging from 15 to 64 m²/g. A com-

Assuming that the adsorbent is constituted of microscopic (or ultramicroscopic) spheres of diameter d (in cm), a relation for A ($= \text{cm}^2/\text{g}$) in terms of d and the density, ρ (g/cm^3), is obtained as follows:

Let n = number of particles per gram.

$$A = n\pi d^2,$$

$$1 = n\rho \frac{\pi}{6} d^3.$$

Hence

$$A = \frac{6}{d\rho}\cdot \tag{12}$$

For example, the density of activated charcoal[156] varies over a considerable range. Assuming that $\rho = 2$ and $A = 4 \cdot 10^6\ \text{cm}^2/\text{g}$, it follows from the last equation that $d = 7.5 \cdot 10^{-7}$ cm.

For the measurement of relatively small surfaces, such as those of oxide-coated cathodes, L. A. Wooten and J. R. C. Brown[157] have developed a method which represents an extension of that of Emmett and Brunauer. Instead of using nitrogen at temperatures such that P_0 is of the order of 1 atmosphere, these investivators have used butane at $-116°$ C ($P_0 = 0.17$ mm), and ethylene at $-183°$ C ($P_0 = 0.0305$ mm) and at $-195.8°$ C ($P_0 = 7.3 \cdot 10^{-4}$ mm). For ethylene, $S = 17.55 \cdot 10^{-16}\ \text{cm}^2$, and for butane, $S = 32.0 \cdot 10^{-16}\ \text{cm}^2$. At these low pressures, it is possible to measure accurately the much smaller quantities of gas adsorbed by small areas. The adsorption isotherms obtained by plotting v adsorbed versus P/P_0 resemble those obtained, for large areas, with nitrogen at $-195.8°$ C, and it is possible by application of equation 5.1 to calculate v_m. In this manner, Wooten and Brown found that, for oxide-coated cathodes, the surface areas are approximately 10 cm^2 per milligram of coating. Areas as low as 10 cm^2 could be measured by this method.

Krypton has been used in a similar manner by R. A. Beebe, J. B.

---

prehensive review of values obtained for the surface area of colloidal carbons is given in *Columbian Colloidal Carbons*, Vol. III, 1942, published by Columbian Carbon Company Research Laboratories. It is of interest to note that, although the calculated diameters (see equation 12 above) show good agreement in many cases with electron microscope observations, there is poor agreement in other cases.

[156] The value of ρ for charcoal is discussed in McB, pp. 79–92.

[157] *J. Am. Chem. Soc.*, **65**, 113 (1943).

TABLE 27

SPECIFIC SURFACE AREAS OF VARIOUS ADSORBENTS

Adsorbent	Specific surface, sq m/g
1. Fe_3O_4 catalyst (unreduced)	0.02
2. Fe catalyst 973, sample I, unpromoted	0.55
3. Fe catalyst 973, sample II, unpromoted	1.24
4. Fe catalyst 954, 10.2% Al_2O_3	11.03
5. Fe catalyst 424, 1.03% Al_2O_3, 0.19% ZrO_2	9.44
6. Fe catalyst 931, 1.3% Al_2O_3, 1.59% K_2O	4.78
7. Fe catalyst 958, 0.35% Al_2O_3 0.08% K_2O	2.50
8. Fe catalyst 930, 1.07% K_2O	0.56
9. Fused copper catalyst	0.23
10. Commercial copper catalyst	0.42
11. Pumice	0.38
12. Ni on pumice, 91.8% pumice	1.27
13. NiO on pumice, 89.8% pumice	4.28
14. Cr_2O_3 gel	228
15. Cr_2O_3 "glowed"	28.3
16. KCl (finer than 200 mesh)	0.24
17. $CuSO_4{\cdot}5H_2O$ (40–100 mesh)	0.16
18. $CuSO_4$ anhydrous	6.23
19. Cecil soil, 9418	32.3
20. Cecil soil colloid, 9418	58.6
21. Barnes soil, 10,308	44.2
22. Barnes soil colloid, 10,308	101.2
23. Glaucosil	82
24. Silica gel I (non-electrodialyzed)	584
25. Silica gel II (electrodialyzed)	614
26. Dried bacteria	0.17
27. Dried bacteria (pulverized)	3.41
28. Granular Darco B	576
29. Granular Darco G	2123
30. Activated charcoal	775
31. Lampblack	28
32. Acetylene black	64
33. Grade 3 rubber black	135
34. Carbolac 1 color black	947
35. Graphite	30.47
36. Cuprene	20.7
37. Paper	1.59
38. Cement	1.08
39. TiO_2	7.88
40. $BaSO_4$	4.30
41. $ZrSiO_4$	2.76
42. Lithopone	34.8
43. Lithopone, calcined	1.37
44. Lithopone, calcined and ground	3.43
45. Porous glass	125.2

Beckwith, and J. M. Honig.[158] The saturation pressure of this gas at the temperature of liquid nitrogen is about 2 mm. By comparing adsorption isotherms for nitrogen and krypton on the same sample of TiO_2, it was concluded that the cross-sectional area for krypton is $(19.5 \pm 0.4) \cdot 10^{-16}$ cm². From adsorption isotherms for krypton with other materials in the range of values of P/P_0 below about 0.3, surface areas as low as $1.6 \cdot 10^{-2}$ square meter per gram were obtained, as shown in the second column of Table 28. The third column gives, for comparison, values obtained with nitrogen.

TABLE 28

SURFACE AREAS OF ADSORBENTS

Adsorbent	Square Meters per Gram	
	Krypton	Nitrogen
Marble	$1.69 \cdot 10^{-2}$	
Quartz	$3.70 \cdot 10^{-2}$	
Glass wool	$5.94 \cdot 10^{-1}$	
Cork	$7.10 \cdot 10^{-1}$	
Cotton	$8.01 \cdot 10^{-1}$	
Anatase	13.92	13.92
Porous glass	110.	121.

The B.E.T. method for measuring surface area depends upon an experimental determination of the point B on the isotherm (corresponding to the completion of a monolayer) and on calculated values of the number of molecules required to form a complete monolayer per unit area; the method described by W. D. Harkins and G. Jura[159] does not require any assumption regarding the cross-sectional area of the adsorbate molecule.

These investigators observed that if log (P/P_0) is plotted against $1/v^2$, where v denotes the amount of gas adsorbed per unit mass of adsorbent, a straight line is obtained, and the area per unit mass is proportional to the square root of the slope. That is, in the relation

$$\log\left(\frac{P}{P_0}\right) = B - \frac{c}{v^2}, \tag{13}$$

$$A_m = k\sqrt{c}. \tag{14}$$

where A_m = area in square meters per gram, and k is a constant for any given adsorbate and approximately independent of the nature of the adsorbent. The values obtained are: for water vapor at 25° C, $k = 3.83$; for nitrogen at $-195.8°$, $k = 4.06$; for n-butane at 0° C, $k = 13.6$; and for n-heptane at 25°, $k = 16.9$.

---

[158] *J. Am. Chem. Soc.*, **67**, 1554 (1945).

[159] *J. Am. Chem. Soc.*, **66**, 1362 and 1366 (1944); also discussed by P. H. Emmett, *Ind. Eng. Chem.*, **37**, 639 (1945), *J. Am. Chem. Soc.*, **68**, 1784 (1946), and H. K. Livingston, *J. Chem. Phys.*, **12**, 466 (1944).

Figure 24, from the publication by Harkins and Jura, shows adsorption isotherms of nitrogen at $-195.8°$ C on some porous solids. Using

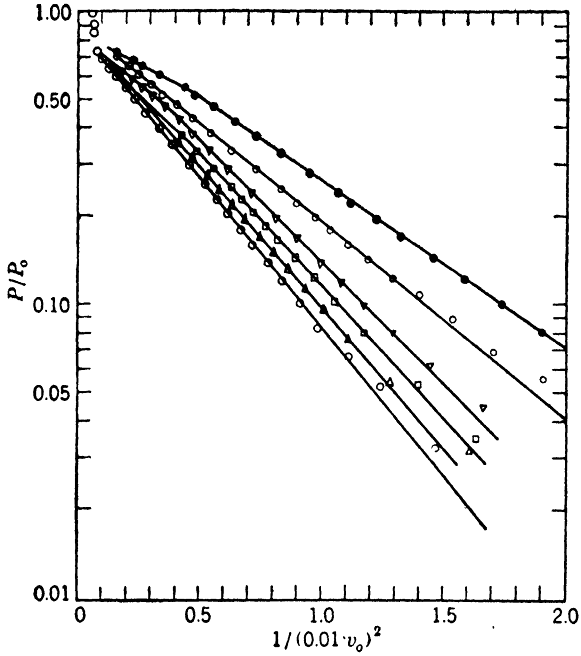

FIG. 24. Nitrogen isotherms on porous solids. The area A_m, square meters per gram, is given by the relation $A_m = 4.06\sqrt{c}$, where c is defined by equation 13 as the slope of the linear portion of the plot, and v_0 denotes the volume adsorbed (cm^3, S.T.P.) per gram of adsorbent (Harkins and Jura).

the value $k = 4.06$, the areas calculated from the observed values of c, beginning at the uppermost plot, are 321, 365, 395, 409, 438, and 455 square meters per gram.

Harkins and Jura have shown that the areas calculated for several adsorbents by the B.E.T. method are in very satisfactory agreement (within 20 per cent) with the values obtained by equations 13 and 14.

It is of interest to mention that, from a plot of log (P/P_0) versus $1/v^2$, Beebe and his associates found, from their adsorption data discussed above, that, for krypton, $k = 4.20$ at the temperature of liquid nitrogen.

In the methods for measuring surface area of adsorbents proposed by E. N. Harvey[160] and by S. S. Kistler, E. A. Fischer, and I. R. Freeman,[161] it is assumed that the S-shaped adsorption isotherm is a combination of unimolecular physical adsorption and capillary condensation. "Even though," as Emmett remarks, "it appears to be fundamentally incorrect thus to neglect multilayer adsorption," the results obtained so far by these investigators are in fair accord with those obtained by the other two methods discussed above. For a discussion of the considerations and mathematical relations underlying these methods, the reader should consult either the original papers or the review by Emmett. For some of the other methods for determining surface area, such as those used by earlier investigators and those involving a determination of the heat of wetting, the reader will find comprehensive treatments in the works by Brunauer and McBain.

> If physical adsorption [as Brunauer states[162]] were completely non-specific, the nature of the adsorbent surface would be entirely immaterial and only the extent of the surface area would matter. Whether one measures the adsorption on an ionic crystal like sodium chloride, on a semi-conductor like graphite, or on a metallic conductor like iron, the adsorption per unit surface would then be the same. . . . Of course, this does not happen. The isotherms do not coincide, because even the slight differences in the heats of adsorption bring a certain amount of specificity into van der Waals adsorption.

However, occasionally such non-specificity has been observed, and Brunauer cites some observations by V. R. Deitz and L. F. Gleysteen[163] which show that, for twelve different bone chars, the adsorption per unit area plotted against relative pressure (P/P_0) fall on practically the identical curve.

An illustration of high degree of specificity is shown by the isotherms of water on the four ionic adsorbents, ThO_2, Al_2O_3, WO_3, and ZrO_2, at 99.4° C.[164] At any given pressure, the amounts adsorbed per cubic centimeter of adsorbent are much greater for ThO_2 than for ZrO_2 and for the other two adsorbents, in the order in which they have been given.

[160] *J. Am. Chem. Soc.*, **65**, 2343 (1943).

[161] *J. Am. Chem. Soc.*, **65**, 1909 (1943).

[162] SB, pp. 330.

[163] *J. Research Natl. Bur. Standards*, **29**, 191 (1942), RP 1496.

[164] J. N. Pearce and M. J. Rice, *J. Phys. Chem.*, **33**, 692 (1929).

CHAPTER 8

SORPTION OF GASES BY "ACTIVE" CHARCOAL, SILICATES (INCLUDING GLASSES), AND CELLULOSE

1. PREPARATION AND STRUCTURE OF ACTIVATED CHARCOAL

The capacity of charcoal for sorption of gases depends both on the nature of the source used in the preparation and on the type of heat treatment. H. Baerwald[1] showed that by heating charcoal above 500° C its adsorptive power is increased considerably; also that charcoal from coconut shell is a much better adsorbent than that from the soft part of the nut or from wood. F. Bergter[2] measured the rate of adsorption of nitrogen, oxygen, and air on coconut charcoal at about 18° C, and before World War I a number of other investigators, including Sir James Dewar, M. W. Travers,[3] J. W. McBain,[4] I. F. Homfray,[5] A. Titoff,[6] G. Claude,[7] and others carried out important investigations on the sorption of different gases by charcoal, the results of which will be mentioned subsequently. However, the incidence of the war in 1914 and the necessity of developing a highly efficient adsorbent for use in gas masks provided a tremendous stimulus to further investigations in this field. As a result there was evolved a technique for the production of a highly activated form of charcoal, and, furthermore, comprehensive studies were carried out on the relation between the structure of the adsorbent and its adsorptive capacity.

The procedure used by McBain and others in preparing coconut charcoal was as follows: The soft part was heated in a muffle furnace for several hours at just below a red heat, until no more evolution of vapor could be observed. Then the temperature was raised to a dull red heat for 30 sec. Before use as an adsorbent the charcoal would be heated to 440° C for several hours, in vacuo.

---

[1] *Ann. Physik,* **23**, 84 (1907).

[2] *Ann. Physik,* **37**, 472 (1912).

[3] *Proc. Roy. Soc. London,* **A, 78**, 9 (1907).

[4] *Phil. Mag.,* **18**, 916 (1909).

[5] *Z. physik. Chem.,* **74**, 129 (1910).

[6] *Z. physik. Chem.,* **74**, 641 (1910).

[7] *Compt. rend.,* **158**, 861 (1914).

H. B. Lemon[8] observed in 1915 that different samples of charcoal made from the same source (coconut shell) showed very wide variations in sorptive power. It was found that this was due to variations in heat treatment, and that increased activation could be produced by repeated evacuations at 650° C, each evacuation being followed by sorption of air at the temperature of liquid air. On the other hand, a decrease in sorptive capacity resulted from heating the charcoal to as high as 800° C to 900° C during evacuation.

The theory was advanced that the successive sorptions of air oxidize non-volatile hydrocarbons present in the charcoal. As a result, an air process of activation was evolved which, as described by F. M. Dorsey,[9] consisted essentially of the following operations: (1) initial distillation of cracked coconut hulls to a temperature of 850° C to 900° C, and (2) "air treating" this carbonized material, screened 6 to 14 mesh, at 350° C to 400° C, for a certain length of time.

The essential characteristics of an active charcoal, according to Lamb, Wilson, and Chaney,[9] are (1) high and fine-grained porosity, (2) the presence of amorphous base carbon, (3) freedom from adsorbed hydrocarbons.

To secure these objects it is necessary to use dense woods, carry out the distillation at relatively low temperatures, and then oxidize the hydrocarbons without injuring the carbon base to any measurable extent. "The permissible range of temperatures for the latter operation is a relatively narrow one, only about 50 to 75°." For air oxidation this lies between 350° C and 450° C. Subsequently a steam process of activation was adopted, and for this reaction the optimum temperature is between 800° C and 1000° C. Other methods of activation have been used in Europe. All these processes yield charcoal which is much more active than that obtained by the simple distillation process used at one time.

From a study of the slope of the vapor pressure curves of liquids adsorbed upon such charcoal, the indications are that the pores have, if a cylindrical form be assumed, an average diameter of about $5 \cdot 10^{-7}$ cm. On this basis, 1 cm^3 of active charcoal would contain about 1000 sq m of surface.

---

[8] *Phys. Rev.*, **14**, 281 (1919).

[9] The results of the investigations on this subject carried out by the Chemical Warfare Service, U. S. Army, have been published mainly in the following papers:

A. B. Lamb, R. E. Wilson, and N. K. Chaney, *J. Ind. Eng. Chem.*, **11**, 420 (1919), on gas mask absorbents.

F. M. Dorsey, *J. Ind. Eng. Chem.*, **11**, 281 (1919), on the development of activated charcoal.

N. K. Chaney, *Trans. Am. Electrochem. Soc.*, **36**, 91 (1919). The writer is indebted to these publications for the information on the properties and preparation of activated charcoal.

The density of activated charcoal from coconut shells is about 0.4. Hence 1 g would contain about 2500 sq m of surface. Assuming that the clean-up by charcoal is due to a condensation of gas molecules on the surface, and that the diameter of a hydrogen molecule is about $2 \cdot 10^{-8}$ cm, it would require approximately 2000 cm^3 (measured at 0° C and 760 mm) to cover the surface of 1 g of charcoal. Compared with this the adsorptions obtained by Homfray, Titoff, and Firth, even at atmospheric pressure, are very low, which may be accounted for partly by the smaller porosity of the charcoal used by them.

It is of interest in this connection to mention a theory regarding the structure of charcoal which has been advanced by N. K. Chaney.[10] According to this theory,

> elementary carbon (other than diamond and graphite) exists in two modifications, "active" and "inactive" or *alpha* and *beta*. All "primary" amorphous carbon consists essentially of a stabilized complex of hydrocarbons, adsorbed on a base of "active" or *alpha* carbon. The active modification is formed whenever carbon is deposited at relatively low temperatures by chemical or thermal decomposition of carbon-bearing materials; in general below 500° C to 600° C. The inactive modification results from similar decomposition at higher temperatures, in general above 600° C to 700° C. The temperature at which molecular carbon is set free is apparently the controlling factor in determining whether it is of the active or inactive variety.

The active form is characterized by a very high specific adsorptive capacity for gases. Chaney distinguishes between the true adsorptive capacity characteristic of the active form and a capillary capacity by virtue of which gas is taken up in pores formed by the loosely bound structure which results from carbonization of any carbon-bearing material, and he differentiates these as follows: On saturating an adsorbent and then noting the rate at which the gas is removed, it is observed that the portion adsorbed in capillary spaces is given off readily while that adsorbed specifically is given off very slowly.

> The weight of gas retained, after rapid weight loss has ceased, called the "retentivity" of the adsorbent, is a measure, therefore, of the proportion of active carbon present, in a given weight of adsorbent. This test applied to pre-war charcoals shows that their adsorptive capacity is almost wholly capillary and dependent upon the physical structure left by distillation in the primary carbon. In general even this capacity is extremely small compared with present standards.

The observation made by McBain that the sorption of hydrogen by ordinary charcoal at low temperatures occurs in two stages finds an explanation from this point of view. The major portion of the gas is taken up very rapidly, while a residual portion requires quite an interval of time to condense.

---

[10] *Loc. cit.*

The problem in preparing active charcoal, according to Chaney, therefore consists in devising some method that will get rid of the hydrocarbons adsorbed specifically by the active carbon at the instant of formation. This adsorbed gas forms quite stable complexes with the carbon base and constitutes the product which he designates as primary carbon, "because it is the original product first occurring in low-temperature distillation of carboniferous material." The methods of preparing active charcoal by oxidation with steam and other schemes therefore have for their purpose the removal of these adsorbed hydrocarbons.

In discussing the mechanism of the capillary and specific adsorptions, Chaney remarks:

> The simplest theoretical assumption is that capillary adsorption is the filling of actual cells with liquid due to lowered surface tension, and dependent upon the size of capillaries, i.e., the physical structure of the absorbent only. The specific capacity has been assumed to represent a field of force—probably due to unsaturated valences—which is independent of a grosser physical structure of the absorbent, i.e., it represents adsorption on a plane surface.

In view of his theory, discussed in the previous chapter, that true adsorption consists in the formation of a monolayer, Langmuir has pointed out[11] that

> truly porous bodies, such as charcoal, probably consist of atoms combined together in branching chains of great complexity. The fibers of cellulose from which charcoal is usually formed consist of practically endless groups of atoms
>
> 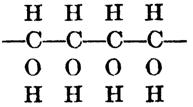
>
> $$\begin{array}{c} \mathrm{H}\quad\mathrm{H}\quad\mathrm{H}\quad\mathrm{H} \\ -\mathrm{C}-\mathrm{C}-\mathrm{C}-\mathrm{C}- \\ \mathrm{O}\quad\mathrm{O}\quad\mathrm{O}\quad\mathrm{O} \\ \mathrm{H}\quad\mathrm{H}\quad\mathrm{H}\quad\mathrm{H} \end{array}$$
>
> held together by primary valences in the direction of their length and by secondary valence in the transverse directions. When the hydrogen and oxygen atoms are driven out by heat, the carbon atoms for the most part remain in their chains, but a certain number of cross linkages occur between these chains. *The porosity of the charcoal thus undoubtedly extends down to atomic dimensions.* The unsaturated state of the remaining carbon atoms explains the practical impossibility of removing the last traces of oxygen and hydrogen from any form of amorphous carbon.
>
> Hence it is evident that, with a structure of this kind, it is meaningless to talk about the surface on which the adsorption can take place.

On plane surfaces the maximum adsorption would correspond to a layer one molecule deep; but in the case of charcoal, there is no definite surface that can be covered by a unimolecular layer. The atoms of carbon would be separated by spaces which might hold one or more molecules of the gas, and, on the other hand, these spaces might be too small to hold even one molecule.

---

[11] *J. Am. Chem. Soc.*, **38**, 2221 (1916).

It will be observed that Chaney agrees with Langmuir in concluding that the specific absorptive capacity of activated charcoal is a measure of the amount of gas condensed as a unimolecular layer.

H. Briggs,[12] as a result of his investigations on the adsorption of gas on charcoal and silica gel, concludes that, while the chemical characteristics of a material affect its properties as a gas-adsorbent, there are, with any given material, two factors which also influence the adsorptive power: "(*a*) the degree of canalization of the substance, i.e., its porosity on the microscopic or ultramicroscopic scale, and (*b*) the degree of porosity on the molar scale." From the measurements on the size of the pores made by Lamb, Wilson, and Chaney,[13] which have already been mentioned, Briggs infers that "the greater part of the internal gaseous space of an efficient adsorbent consists of passages which are not greatly larger than the gas molecules." According to his view, Chaney's assumption of the existence of two allotropic forms in active charcoal is not sufficiently supported by the experimental evidence, and he concludes that the efficiency of activated charcoal is due to the presence of the molar interstices.

H. H. Sheldon[14] has shown that, although ordinarily nitrogen is more readily adsorbed on charcoal than hydrogen, it is possible by suitable treatment to produce a charcoal in which the relative adsorptive capacities for the two gases are reversed. He has also observed that evacuation of charcoal at 600° C followed by adsorption of oxygen at low temperatures, and this again by re-evacuation at the higher temperature, leads to considerable improvement in the adsorptive capacity of charcoal.

J. C. Philip, S. Dunnill, and O. Workman[15] have made similar observations with wood charcoal. The greater the facilities for the access of air to the material during heating, the greater the resulting increase that was obtained in the sorptive power. They also observed that the increased activity was accompanied by a decrease in bulk density, indicating, according to Briggs, an increasing degree of "molar" porosity.

These observations are in accord with results obtained in this laboratory. A given sample of charcoal shows marked improvements as a clean-up reagent in high-vacuum work after it has been evacuated and saturated with gas several times in succession.

It should be mentioned in this connection that A. Magnus and H. Kratz[16] have developed a method for the purification of charcoal by which a material free from oxides may be obtained. B. Bruns and A. Frumkin[17] have also described a method for obtaining ash-free charcoal in which very pure sucrose is used as starting material. The charcoal obtained by charring the sucrose in a silica dish is activated by heating for 4 to 5 hours at 1100° C, in a current of carbon dioxide.

---

[12] *Proc. Roy. Soc. London*, A, **100**, 88 (1921–1922).

[13] *Loc. cit.*

[14] *Phys. Rev.*, **16**, 165 (1920).

[15] *Trans. Chem. Soc. London*, **117**, 362 (1920).

[16] *Z. anorg. Chem.*, **184**, 241 (1929).

In general, a preliminary sorption of the gas followed by desorption at relatively high temperatures, ranging from 500° C to 800° C, improves the sorptive capacity for the particular gas. This is probably due to elimination of other gases that may be present in a sorbed condition in the adsorbent.

The effect of activation on a number of charcoals is shown by the data in Table 1, which were obtained by M. E. Barker.[18] The most important result is that shown in the second column, viz., the increase in surface. Furthermore, true density and pore space are increased by activation.

TABLE 1

EFFECT OF THE ACTIVATION OF CHARCOAL ON PORE SPACE

Charcoal	Adsorption of CCl_4, mg per g	Granule Density, g/cc	True Density, g/cc	Volume, cc/g	Charcoal Substance, cc/g	Pore Space, cc/g	Pore Space Filled by Adsorbed CCl_4	
							cc/g	%
Primary coconut	47	0.96	1.46	1.04	0.685	0.355	0.032	9.1
Activated coconut	630	0.84	2.15	1.19	0.465	0.725	0.420	58
Primary ironwood	30	0.89	1.46	1.123	0.685	0.438	0.020	4.6
Activated ironwood	1160	0.72	2.15	1.39	0.465	0.925	0.774	83.6
Primary lignite	30	1.09	1.43	0.92	0.70	0.220	0.020	9.1
Activated lignite	640	0.89	2.15	1.12	0.465	0.655	0.426	65
Extremely activated lignite	2715	0.31	2.15	3.23	0.465	2.765	1.81	65

Barker[19] has also discussed at length the relation between the effect of nature of source and type of treatment on the sorptive capacity. Specific mention is made of observations made by H. Briggs[20] on the sorption by various charcoals of nitrogen and hydrogen, which are shown in Table 2. The table gives the volumes (cm^3, S.T.P.) per gram charcoal adsorbed at 1 atm pressure.

---

[17] *Z. physik. Chem.*, A, **141**, 141 (1929).

[18] *J. Ind. Eng. Chem.*, **22**, 926 (1930).

[19] See remarks, McB, Chapter IV, p. 58. (The notation McB is explained in footnote 1, Chapter 7.)

[20] *Proc. Roy. Soc. London*, A, **100**, 58 (1921). McB, p. 79.

TABLE 2

VALUES OF v_0 FOR ADSORPTION OF NITROGEN AND HYDROGEN BY CHARCOAL AT LIQUID-AIR TEMPERATURE AND ATMOSPHERIC PRESSURE

Substance	N_2	H_2
Coconut charcoal (activated by steaming)	247	127
Birch charcoal (activated)	202	123
German impregnated charcoal 1918	303	63.8
Briquetted coal, charcoal, and dusts	206	96.7
Cleveland (U. S.) activated anthracite	89.7	56.3
Colloidal silica (Briggs)	376	51.6

2. SORPTION DATA AT HIGHER PRESSURES

Most of the investigations on the sorption of gases by charcoal have been concerned with sorption at pressures above 1 mm, and there are relatively few published data on sorption at the lower pressures. Though such data are discussed in the next section, it is of importance to review those obtained at higher pressures.

The adsorption data obtained by K. Peters and K. Weil[21] have been mentioned at the beginning of the previous chapter in connection with the application of the Freundlich or parabolic equation for the isotherms.

From the values given in Table 7.1 for the constants k and $1/n$, we deduce the values given in Table 3 for the sorptions at the temperatures for which the isotherms were observed. In this and the following tables, the values under v_0 correspond to the volume (cm^3 per gram charcoal) measured at 0° C and 760 mm (S.T.P.).

TABLE 3

SORPTION OF RARE GASES BY CHARCOAL AT LOW TEMPERATURES

		v_0 at P_{mm} =	
Gas	$t°$ C	1	10
Argon	−80.2	0.5	4.37
	−18.0	0.076	0.764
	0	0.058	0.581
Krypton	−79.7	2.93	15.03
	−18.0	0.497	3.81
	0.0	0.340	3.40
Xenon	−80.5	15.99	59.98
	−18.0	2.458	12.10
	0	1.583	9.32

---

[21] *Z. physik. Chem.*, **A**, **148**, 1 (1930).

As will be observed, the sorption at any given temperature increases with increase in boiling point of the liquefied gas.

Data on the sorption of the more common gases by charcoal have been published by Miss I. F. Homfray,[22] A. Titoff,[23] and L. B. Richardson.[24] Tables 4 and 5 give a survey of the observations made by the first two of these investigators. From the plots of the values of P_{mm}/v_0, given in the third column of each set of data, against P_{mm} it is possible, as shown in the previous chapter, to deduce values of the adsorption constants v_s and b in the hyperbolic equation

$$v_0 = \frac{v_s b P_{mm}}{1 + bP_{mm}}. \tag{1}$$

These are given in Table 6. The values marked by an asterisk for the corresponding temperatures are based on the values, calculated by H. Zeise,[25] of the constants c_1 and c_2 in the relation

$$x = \frac{c_1 c_2 P}{1 + c_2 P}, \tag{2}$$

where x = milligrams per gram, at pressure P in centimeters. For the other sets of data the values of the sorption constants have been calculated by the writer from the most satisfactory plots of P_{mm}/v_0 versus P_{mm}.

From these values of the sorption constants the values of v_0 have been deduced as shown in the last two columns of Table 6 for $P_{mm} = 1$ and $P_{mm} = 10$, respectively.

It will be observed that for hydrogen at −79° C and 0° C, and for argon at −190° C, the data are in approximate agreement with Henry's law.

For those sorption data which could not be at all fitted by the hyperbolic equation, values of v_0 for the two pressures have been obtained by an approximate interpolation. It should also be stated that in general the observed values of P_{mm}/v_0 at pressures below 10 mm are lower than those deduced from the linear plots for the higher pressures. Hence, the values of v_0 for this range of pressures are actually greater than those given in the last two columns.

However, the values of v_0 serve to provide a comparison between the behavior of different gases at the same pressure, and they also indicate

---

[22] *Z. physik. Chem.*, **74**, 129 (1910).

[23] *Z. physik. Chem.*, **74**, 641 (1910).

[24] *J. Am. Chem. Soc.*, **39**, 1829 (1917).

[25] *Z. physik. Chem.*, A, **136**, 385 (1928); A, **138**, 289 (1928).

TABLE 4

SORPTION DATA FOR ACTIVATED CHARCOAL (HOMFRAY)

P_{mm}	v_0	P_{mm}/v_0
Helium, −190° C		
120	0.337	356
171	0.466	367
235	0.809	290
427.6	1.167	366
705.0	1.839	383
Argon, −190° C		
4.6	15.9	0.289
17.0	66.4	0.256
379	77.7	0.488
410	93.5	0.439
−128° C		
4.0	3.82	1.047
6.0	5.12	1.170
12.8	9.92	1.283
13.4	13.05	1.028
19.4	15.91	1.220
27.0	19.23	1.404
36	25.08	1.435
97	48.8	1.99
228	57.8	3 95
360	64.3	5.59
790	76.9	10.27
−78.5° C		
8	1.28	6.27
19	3.77	5.04
24	5.09	4.71
54.2	10.02	5.41
98.4	15.56	6.46
129	18.81	6.85
218	24.84	8.78
295	29.14	10.13
564	39.88	14.15
758	47.47	15.96
−37° C		
309.6	11.98	25.85
417	14.41	28.94
568.4	17.23	32.98
815	22.15	36.81

P_{mm}	v_0	P_{mm}/v_0
Nitrogen −190° C		
13	52.4	0.248
22	61.8	0.348
33	80.7.	0.409
343	90.4	3.796
−78.5° C		
14	5.06	2.77
46	14.27	3.15
135	23.61	5.72
253	32.56	7.77
518	40.83	12.69
0° C		
72	1.53	47.10
173	3.61	47.92
229	4.39	52.22
312	5.94	52.55
510	8.57	59.53
Carbon Monoxide −78.5° C		
6	6.2	0.96
30	17.3	1.74
40	20.9	1.91
72	27.7	2.60
117	34.1	3.43
148	34.3	4.32
187	40.5	4.62
228	46.7	4.88
442	53.1	8.32
−33.7° C		
101	9.2	11.0
188	14.5	13.0
320	19.6	16.4
430	22.6	19.0
540	25.6	21.1
670	28.3	23.6
0° C		
73	2.53	28.9
180	5.57	32.3

P_{mm}	v_0	P_{mm}/v_0
Carbon Monoxide, 0° C		
309	8.47	36.5
540	12.85	42.0
713	17.43	40.9
882	17.64	50.0
20° C		
123	2.36	52.1
300	5.20	57.8
495	7.83	63.2
856	11.81	72.5
Carbon Dioxide 0° C		
60	21.2	2.83
87	26.4	3.30
123	32.2	3.82
179	38.6	4.65
242	38.1	6.35
20° C		
20	4.86	4.12
29	6.58	4.41
63	12.8	4.91
85	15.7	5.43
128	21.0	6.09
186	26.1	7.11
288	31.9	9.04
374	38.2	9.79
500	44.3	11.30
Ethylene, 0° C		
70	39.5	1.77
93	42.8	2.17
168	49.9	3.37
319	56.5.	5.65
616	64.5	9.56
20° C		
15	10.4	1.45
32	20.8	1.54
52	25.6	2.03
79	30.5	2.59

TABLE 4 (*Continued*)

P_{mm}	v_0	P_{mm}/v_0	P_{mm}	v_0	P_{mm}/v_0	P_{mm}	v_0	P_{mm}/v_0
	Ethylene, 20° C			Methane, −18° C			Methane, 0° C	
171	39.2	4.37	70	12.5	5.60	358	22.3	16.1
220	42.4	5.19	103	15.8	6.51	451	25.3	17.8
388	49.1	7.90	151	19.6	7.71	578	28.4	20.4
685	55.2	12.41	190	22.9	8.31	702	31.0	22.5
			242	26.1	9.29			
	Methane, −33° C		311	29.4	10.6		20° C	
36	12.6	2.85	393	32.4	12.1	40	2.7	14.1
53	16.0	3.31	484	35.4	13.7	69	4.3	16.0
76	19.9	3.82				127	7.2	17.7
102	23.2	4.40		0° C		248	11.9	20.9
132	26.5	4.98	67	7.4	9.1	355	15.0	23.7
171	29.9	5.72	134	12.3	10.8	497	18.4	26.9
215	33.1	6.50	191	15.2	12.6	640	21.3	30.0
270	36.2	7.43	274	19.1	14.3	795	24.2	32.9

the variation with temperature. Comparing the data obtained by Homfray with those obtained by Titoff, it is seen that, for the same gas at any given temperature and pressure, the values of v_0 deduced from Homfray's data are somewhat larger than those deduced from Titoff's data. Richardson's values of v_0 tend to be lower than those observed by Titoff. These results indicate the variations to be expected from different samples of charcoal.

More recent data on the sorption of the more common gases by charcoal, at very low temperatures, have been obtained by S. Brunauer and P. H. Emmett.[26] Figure 1 taken from their paper shows the actual isotherms, while Fig. 2[27] gives plots according to the hyperbolic equation. Table 7 gives values of v_s derived from these plots by Brunauer and Emmett and the corresponding values of the surface area per gram for both solid and liquid packing.

From these values of v_s and the plots in Fig. 2, values have been calculated by the writer for b, bv_s, and v_0 for 1 mm and 10 mm, which are given at the end of Table 6 below. It will be observed that the values of the sorption obtained by the more recent investigators do not differ radically from those obtained, under similar conditions of temperature and pressure, by the earlier investigators.

It will be observed from the data given in Table 7 that the values of the surface area deduced from the different isotherms are in very good agreement. In fact, as Brunauer and Emmett point out, "If the

---

[26] *J. Am. Chem. Soc.*, **59**, 2682 (1937).

[27] SB, p. 41. (See footnote 1, Chapter 7, for meaning of SB.)

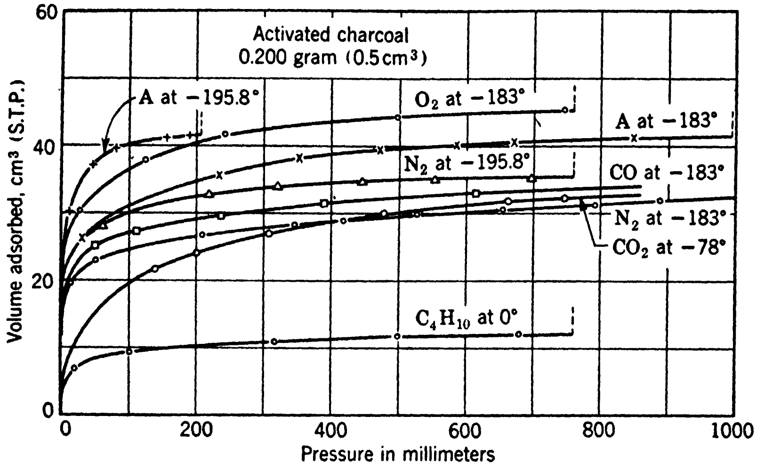

FIG. 1. Low-temperature adsorption isotherms on charcoal (Brunauer and Emmett).

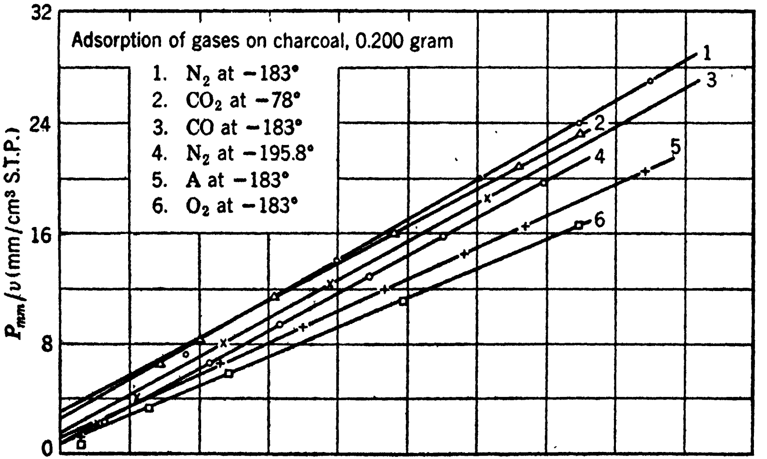

FIG. 2. Adsorption isotherms on charcoal (from Fig. 1) plotted according to the hyperbolic equation (Brunauer).

TABLE 5

SORPTION DATA FOR ACTIVATED CHARCOAL (TITOFF)*

P_{mm}	v_0	P_{mm}/v_0
Hydrogen, −78.5° C		
7.9	0.059	134.8
19.0	0.148	128.4
67.5	0.531	127.1
141.9	1.121	126.3
236.9	1.892	125.2
347.9	2.787	124.4
471.8	3.607	130.7
561.9	4.276	131.6
721.6	5.414	133.3
0° C		
17.4	0.039	452.5
39.3	0.098	400.0
66.9	0.149	446.4
119.4	0.270	442.5
206.9	0.451	456.6
322.8	0.698	462.9
427.5	0.914	467.3
537.3	1.139	471.7
642.1	1.343	478.5
744.2	1.554	478.5
Nitrogen, −78.5° C		
1.5	0.145	10.35
4.6	0.894	5.15
12.5	3.468	3.60
66.4	12.04	5.52
149.5	20.03	7.47
271.4	27.94	9.27
388.4	33.43	11.62
542.9	38.39	14.15
740.6	43.51	17.02
0° C		
4.3	0.111	38.75
12.1	0.298	40.61
39.3	0.987	39.82
129.8	3.043	42.67
229.4	5.082	45.09
340.1	7.047	48.26
562.3	10.31	54.54
774.6	13.05	59.36
Nitrogen, 30° C		
8.6	0.082	104.9
20.3	0.227	89.4
64.5	0.766	84.2
144.6	1.718	81.2
239.6	2.764	86.7
347.6	3.875	89.7
455.4	4.959	91.8
650.0	6.646	97.8
752.3	7.490	100.4
Ammonia, −23.5° C		
0.3	5.496	0.055
2.9	17.17	0.169
16.3	44.97	0.362
112.2	119.3	0.941
770.2	151.3	5.09
−23.5° C		
2.5	8.34	0.30
26.6	62.99	0.42
389.1	147.3	2.64
536.0	151.8	3.53
790.6	157.5	5.02
0° C		
2.9	5.41	0.536
28.8	30.16	0.955
78.7	60.39	1.30
161.0	90.29	1.78
319.2	115.7	2.76
490.0	127.1	3.86
636.4	132.4	4.81
746.7	135.9	5.49
0° C		
2.6	5.54	0.47
29.1	30.58	0.95
77.5	60.98	1.27
245.6	107.8	2.28
466.0	126.3	3.69
764.5	135.4	5.65
Ammonia, 30° C		
1.2	2.62	0.46
20.5	8.64	2.37
62.0	19.81	3.13
151.3	40.43	3.74
269.1	60.02	4.49
408.2	79.97	5.11
679.0	97.63	6.96
785.4	103.5	7.59
Carbon Dioxide, −76.5° C		
0.3	15.26	0.020
1.8	41.51	0.043
41.3	86.74	0.476
168.6	104.1	1.615
483.1	111.5	4.343
691.0	114.1	6.056
0° C		
0.5	0.849	0.589
3.2	3.460	0.925
10.9	8.506	1.28
25.4	15.15	1.68
83.0	27.78	2.99
173.5	39.90	4.35
315.9	50.24	6.29
457.2	56.82	8.05
589.1	61.37	9.60
703.2	64.53	10.90
755.1	65.85	11.29
30° C		
1.3	0.507	2.56
5.3	1.823	2.91
14.7	4.016	3.56
50.7	10.29	4.93
138.5	19.72	7.03
283.3	28.87	9.81
398.9	34.07	11.70
498.1	38.14	13.06
621.8	41.45	15.01
758.6	44.93	16.89

* For NH_3 two sets of data are given for each of the two temperatures.

TABLE 6

SORPTION CONSTANTS FOR CHARCOAL

Source	Gas	°C	v_s	$b(\text{mm}^{-1})$	bv_s	v_0 for P_{mm} =	
						1	10
Homfray	He	−190			$2.78 \cdot 10^{-3}$	$2.78 \cdot 10^{-3}$	$2.78 \cdot 10^{-2}$
Homfray	A	−190			3.63	3.63	36.3
		−128*	84.6	$1.11 \cdot 10^{-2}$	$9.39 \cdot 10^{-1}$	0.93	8.46
		−78.5*	65.1	$3.16 \cdot 10^{-3}$	$2.06 \cdot 10^{-1}$	0.21	2.00
		−37*	51.9	$9.04 \cdot 10^{-4}$	$4.70 \cdot 10^{-2}$	0.047	0.465
		0*	41.7	$4.2 \cdot 10^{-4}$	$1.75 \cdot 10^{-2}$	0.0175	0.174
Homfray	N_2	−190	93.0	$1.0 \cdot 10^{-1}$	9.30	8.45	46.5
		−78.5	41.1	$9.7 \cdot 10^{-3}$	$4.00 \cdot 10^{-1}$	0.396	3.65
		0	10.6	$3.1 \cdot 10^{-3}$	$3.28 \cdot 10^{-2}$	0.033	0.318
Homfray	CO	−78.5*	60.5	$1.33 \cdot 10^{-2}$	$8.04 \cdot 10^{-1}$	0.794	7.10
		−33.7*	43.0	$2.74 \cdot 10^{-3}$	$1.18 \cdot 10^{-1}$	0.118	1.15
		0*	35.8	$1.01 \cdot 10^{-3}$	$3.62 \cdot 10^{-2}$	0.036	0.359
		20	33.9	$6.05 \cdot 10^{-4}$	$2.06 \cdot 10^{-2}$	0.0021	0.021
Homfray	CO_2	0	69.0	$7.25 \cdot 10^{-3}$	$5.0 \cdot 10^{-1}$	0.497	4.67
		20	56.6	$4.53 \cdot 10^{-3}$	$2.56 \cdot 10^{-1}$	0.255	2.45
Homfray	CH_4	−33	56.5	$6.68 \cdot 10^{-3}$	$3.77 \cdot 10^{-1}$	0.374	3.53
		−18	44.8	$5.58 \cdot 10^{-3}$	$2.50 \cdot 10^{-1}$	0.249	2.37
		0	50	$2.30 \cdot 10^{-3}$	$1.15 \cdot 10^{-1}$	0.115	1.12
		20	40	$1.71 \cdot 10^{-3}$	$7.0 \cdot 10^{-2}$	0.070	0.689
Homfray	C_2H_4	0	67.8	$1.48 \cdot 10^{-2}$	1.00	0.985	8.71
		20	56.6	$1.51 \cdot 10^{-2}$	$8.33 \cdot 10^{-1}$	0.821	7.23
Richardson	CO_2	−64*	110.5	$1.19 \cdot 10^{-2}$	1.29	1.275	11.53
		−43*	102.8	$8.2 \cdot 10^{-3}$	$8.43 \cdot 10^{-1}$	0.837	7.79
		0*	83.7	$3.6 \cdot 10^{-3}$	$3.03 \cdot 10^{-1}$	0.303	2.92
		30	71.4	$1.65 \cdot 10^{-3}$	$1.18 \cdot 10^{-1}$	0.118	1.16
		70*	51.8	$9.6 \cdot 10^{-4}$	$4.97 \cdot 10^{-2}$	0.050	0.493
Richardson	NH_3	−20*	167.2	$1.01 \cdot 10^{-2}$	1.69	1.673	15.35
		0*	153.2	$7.02 \cdot 10^{-3}$	1.075	1.068	10.05
		30	143.1	$2.85 \cdot 10^{-3}$	$4.11 \cdot 10^{-1}$	0.410	4.00
		85*	114.0	$6.41 \cdot 10^{-4}$	$7.31 \cdot 10^{-2}$	0.073	0.725
Titoff	H_2	−79			$7.69 \cdot 10^{-3}$	$7.7 \cdot 10^{-3}$	$7.7 \cdot 10^{-2}$
		0			$2.15 \cdot 10^{-3}$	$2.2 \cdot 10^{-3}$	$2.2 \cdot 10^{-2}$

TABLE 6 (*Continued*)

Source	Gas	° C	v_s	$b(\text{mm}^{-1})$	bv_s	v_0 for P_{mm} =	
						1	10
Titoff	N_2	−79*	57.7	$3.89 \cdot 10^{-3}$	$2.22 \cdot 10^{-1}$	0.221	2.14
		0*	38.0	$6.71 \cdot 10^{-4}$	$2.55 \cdot 10^{-2}$	0.026	0.253
		30*	35.8	$3.52 \cdot 10^{-4}$	$1.26 \cdot 10^{-2}$	0.013	0.126
		80*	21.9	$2.16 \cdot 10^{-4}$	$4.74 \cdot 10^{-3}$	0.005	0.047
Titoff	CO_2	−76.5	118	—	—	(25)	(50)
		0	74	—	—	1.5	8.0
		30	51	—	—	0.4	3.3
Titoff	NH_3	−23.5*	168.5	$2.14 \cdot 10^{-2}$	3.61	3.54	29.74
		0*	151.2	$1.01 \cdot 10^{-2}$	1.53	1.52	13.90
		30*	130.9	$4.06 \cdot 10^{-3}$	$5.31 \cdot 10^{-1}$	0.529	5.10
		151.3*	22.9	$1.15 \cdot 10^{-3}$	$2.64 \cdot 10^{-2}$	0.026	0.26
Brunauer and Emmett	N_2	−183	173	$1.20 \cdot 10^{-2}$	2.09	2.06	18.60
		−195.8	181.5	$3.94 \cdot 10^{-2}$	7.15	6.87	51.25
	O_2	−183	234.6	$3.23 \cdot 10^{-2}$	7.58	7.35	57.25
	A	−183	215.5	$2.37 \cdot 10^{-2}$	5.10	4.88	41.25
	CO	−183	179.5	$3.03 \cdot 10^{-2}$	5.45	5.30	41.8
	CO_2	−78	185.5	$1.17 \cdot 10^{-2}$	2.17	2.15	19.45

* Based on values calculated by means of the constants in Zeise's equation.

surface area of the charcoal used in these experiments is taken as 845 sq m/g, the *maximum* deviation from this value is less than 6 per cent."

In the range 1 to 10 mm, oxygen is adsorbed by charcoal at −183° C in about three or four times as great an amount as nitrogen, and the

TABLE 7

SURFACE AREA OF ACTIVATED CHARCOAL DERIVED BY B.E.T. METHOD

Gas	Temperature, ° C	v_s	Square Meters per Gram	
			Solid Packing	Liquid Packing
N_2	−195.8	181.5	677	795
N_2	−183	173.0	646	795
A	−195.8	215.5	746	804
A	−183	215.5	746	839
O_2	−183	234.6	767	894
CO	−183	179.5	665	820
CO	−78	185.5	707	853

adsorbing power for air is about three times that for nitrogen. According to H. B. Lemon and K. Blodgett,[28]

> oxygen which boils at −182.95° C is adsorbed and expelled so much more readily than nitrogen, which boils at −195.8° C, that Dewar, after finding that the gas adsorbed by charcoal from air was 57 per cent oxygen, recommended "that one of the most rapid means of extracting a high percentage of oxygen from atmospheric air is to adsorb it in charcoal at low temperatures and then to expel it either rapidly or slowly by heating the mass of charcoal to the ordinary temperature."[29]

Lemon and Blodgett found that in a mixture the two gases are not adsorbed independently, and that "there is a nearly linear relation between the logarithm of the equilibrium pressure and the per cent of oxygen in the mixture." Table 8 shows the values of the final pressure obtained under the same conditions from mixtures of the two gases.

TABLE 8

SORPTION BY CHARCOAL OF MIXTURES OF OXYGEN AND NITROGEN AT LIQUID-AIR TEMPERATURE

% Oxygen	% Nitrogen	Final Pressure, mm
100		0.0797
75	25	0.240
50	50	0.924
35	65	2.14
20	80	4.89
10	90	8.86
	100	18.6

The sorption of oxygen by pure sugar charcoal has been investigated by A. Lendle.[30] In agreement with a number of previous investigators he has observed that the attainment of equilibrium requires considerable periods of time. H. S. Taylor[31] has interpreted this slow sorption as due to an activation process.

Table 9 gives sorption data at 0° C and 25° C obtained by Lendle, using charcoal which had been degassed for 150 minutes at 780° C. The values given were obtained at the end of 90 minutes. Simultaneously with the values of v_0, observations were made in a calorimeter on the integral molar heat of sorption, Q_S.

---

[28] *Phys. Rev.*, **14**, 394 (1919).

[29] It is of interest to observe in this connection that the selective sorption of different gases by charcoal may be used for the purification of gases. Thus, where it is desirable to obtain pure helium, charcoal in liquid air may be used to remove other gases such as nitrogen, oxygen, and even hydrogen. Similarly hydrogen may be freed of traces of nitrogen and oxygen. See, for instance, R. E. Wilson, *Phys. Rev.*, **16**, 8 (1920).

[30] *Z. physik. Chem.*, **A**, **172**, 77 (1935).

[31] *J. Am. Chem. Soc.*, **53**, 578 (1931).

TABLE 9

SORPTION OF OXYGEN BY SUGAR CHARCOAL

0° C			25° C		
P_{mm}	v_0	Q_S	P_{mm}	v_0	Q_S
$7.71 \cdot 10^{-3}$	0.303	67,760	$6.52 \cdot 10^{-3}$	0.248	79,400
$4.3 \cdot 10^{-2}$	0.474	51,856	0.1554	0.858	63,060
0.540	1.215	39,000	0.5664	1.195	54,860
3.020	2.121	32,640	4.658	2.608	43,200
7.732	3.725	25,660	6.116	2.760	39,340
10.29	4.764	19,300	9.40	4.015	36,900
20.8	8.460	16,010	18.20	6.019	31,430
39.7	13.93	13,170	70.90	10.46	20,770
62.2	20.18	10,727	94.1	17.99	13,510
82.0	25.45	10,230	113.8	18.97	13,200

Comparing these values with those observed by Titoff and Homfray for nitrogen at 0° C (see Tables 4 and 5), it is obvious that the sorption of oxygen by charcoal is considerably higher, especially at very low pressures.

At −80° C, equilibrium is established very rapidly, but as the temperature is increased the rate at which equilibrium is reached decreases.

As will be observed, the heat of adsorption decreases from about 80,000 cal/mole initially to about 10,000 cal/mole, corresponding to the fact that the type of sorption changes from chemisorption to purely physical adsorption.

An important feature of the sorption of oxygen by charcoal, for which the change in value of Q_S is an explanation, is that, unlike most other cases of sorption, it is not reversible. When charcoal which has taken up oxygen is heated, only a portion of the gas is recovered as oxygen, the remainder being re-evolved as carbon monoxide and dioxide. It has been shown by H. H. Lowry and G. A. Hulett[32] that, while some of the oxygen is adsorbed on the surface and may be recovered by heating, the remainder is attached to carbon atoms by valence forces. It is these chemically bound oxygen molecules which can be removed from the surface only in the form of carbon monoxide and carbon dioxide by heating the charcoal above 200° C.

The sorption of *water vapor* by charcoal exhibits a behavior quite different from that observed for the less readily condensible gases. Figure 3[33] shows an isotherm for sugar charcoal at 0° C as determined by A. S. Coolidge.[34] At pressures below about 1.5 mm, the amount adsorbed is very small and obeys Henry's law. Between 1.5 and 2.5 mm, the sorption increases very rapidly, and this is followed by very slowly increasing sorption until the saturation vapor pressure of water at 0° C

---

[32] *J. Am. Chem. Soc.*, **42**, 1408 (1920). This paper contains also a large number of references to previous literature on this topic.

[33] 1 mg H_2O = $3.37 \cdot 10^{19}$ molecules.

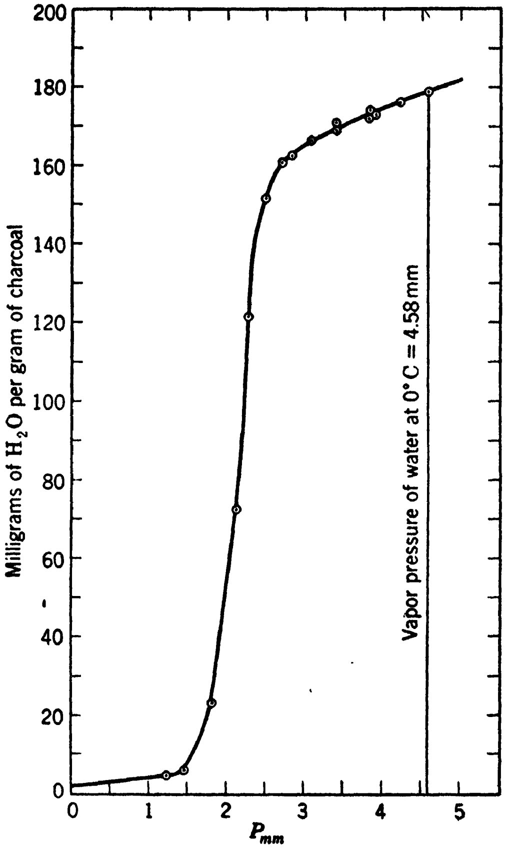

FIG. 3. Adsorption isotherm for water vapor on sugar charcoal at 0° C (Coolidge).

(4.58 mm) is reached. A series of isosteres for different values of the amount sorbed is shown in Fig. 4.

Figure 5 shows a series of isotherms at 0° C and 100° C for charcoal prepared by different methods. The amounts adsorbed, in milligrams, are plotted against relative pressures, P/P_0, where P_0 denotes the vapor pressure for water at the given temperature. The lower of the two isotherms designated C represents the same data as shown in Fig. 3, while the upper isotherm *C* represents the sorption data at 100° C. The charcoal used for determining these two isotherms was prepared from "pure cane sugar recrystallized from conductivity water with the aid of

---

[34] *J. Am. Chem. Soc.*, **49**, 708 (1927).

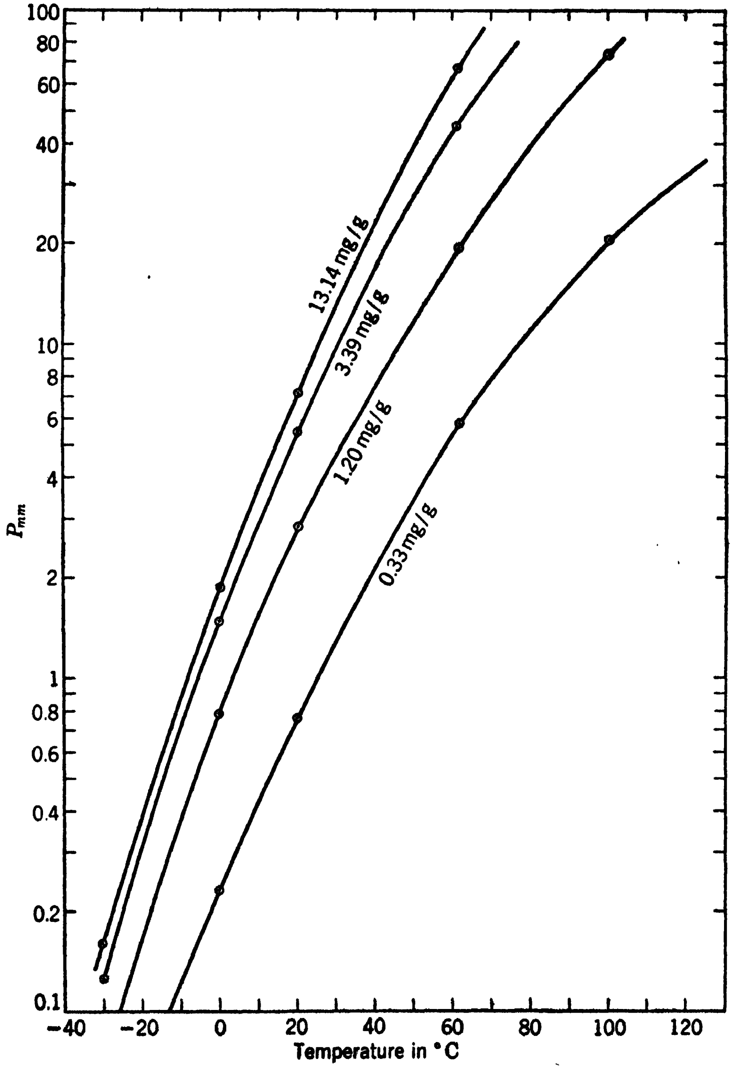

FIG. 4. Isosteres for the adsorption of water vapor on sugar charcoal (Coolidge).

alcohol, and charred in a platinum basin at about 1000° C, in a vacuum." The isotherms *AA* were obtained with untreated coconut charcoal; those designated *BB* were obtained with the same charcoal after treatment with hydrofluoric acid to remove mineral ash. In each case, the upper curve *A* (or *B*) corresponds to determinations at 100° C, and the lower curve *A* (or *B*) corresponds to determinations at 0° C.

As is evident from these isotherms, the adsorption on purified charcoal is extremely low for values of P/P_0 less than about 0.3. Coolidge explains this by the hydrophobic nature of carbon; that is, carbon is difficultly wet by water. On the other hand, he points out that silica, silicates (including glass), and inorganic compounds in general, are hydrophilic. "Therefore," he states,

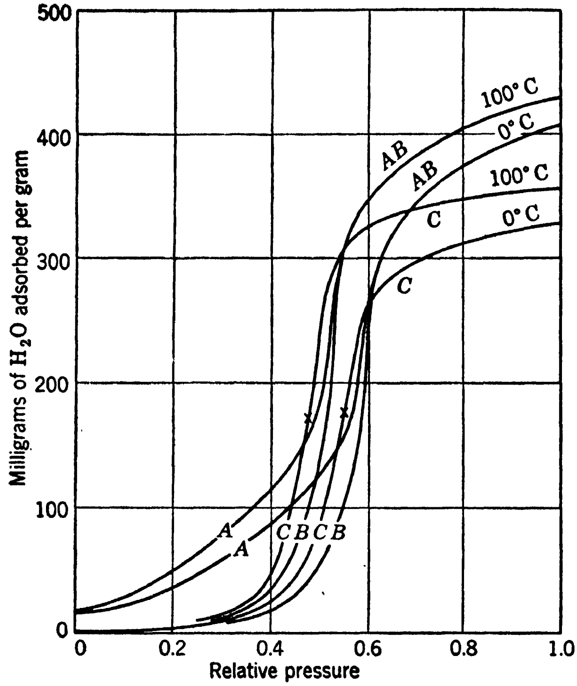

FIG. 5. Isotherms at 0° and 100° C for the sorption of water vapor by sugar charcoal and coconut charcoal (Coolidge).

> it is not surprising that small amounts of hydrophilic impurities, probably siliceous, should exercise a profound influence upon the adsorption of water by carbon at low concentrations, and should be able to cause a serious irreversible retention. At higher concentrations, where the determining factor is the volume of capillary space available, the effect would not be noticed.

A series of isotherms for different temperatures, obtained with the sugar charcoal, is plotted in Fig. 6. In this figure, the amounts adsorbed, in milligrams per gram, are plotted against relative pressure. From the plots of the isosteres the following values of the molal heat of adsorption were derived:

Temperature, °C:	−15	10	40	80	128	187
Molal heat:	11,100	10,000	9300	8300	7200	5200

At the lower temperatures the molal heat of adsorption is about the same as the latent heat of evaporation of liquid water.

From the data given by Coolidge it would seem that about 10 mg H_2O per gram of charcoal corresponded to a complete monolayer, while the maximum amount adsorbed was about 180 mg/g. According to the data in Table 7.25, a monolayer of H_2O corresponds to $2.8 \cdot 10^{-5}$ mg/cm^2. It would therefore follow that the adsorbing area of the charcoal used by Coolidge was about 350 sq m/g, and that the maximum amount adsorbed corresponded to about 18 monolayers. This is in qualitative accord with the observation by Lowry and Hulett[35] that, in the sorption of water by charcoal, the adsorbed water corresponded to a layer about 13 molecules thick. From this they concluded that "water vapor is not adsorbed, but is held by capillary action."

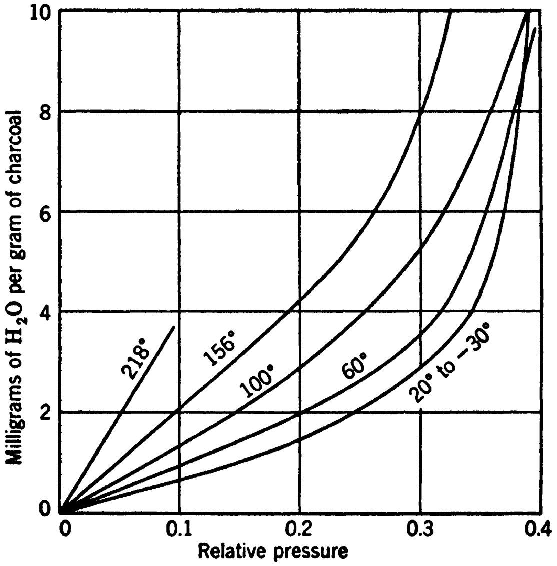

FIG. 6. Isotherms at a series of temperatures for sorption of water vapor by sugar charcoal (Coolidge).

---

[35] *J. Am. Chem. Soc.*, **42**, 1393 (1920).

The sorption of water vapor by activated charcoals has also been investigated by A. J. Allmand and his associates,[36] both in the presence and in the absence of other gases.

They observed that, after absorption of water, the charcoal retains a certain amount (2.3 to 10 mg/g) on desorption. This hysteresis effect is illustrated by the data in Table 10 for sorption and desorption at 25° C, in which the charcoal had been previously outgassed at 800° C. At 25° C the saturation vapor pressure of water is 23.756 mm.

TABLE 10

SORPTION AND DESORPTION OF WATER FOR CHARCOAL AT 25° C

Sorption		Desorption	
P_{mm}	Mg H_2O per g	P_{mm}	Mg H_2O per g
3.64	10.6	18.68	731.4
9.24	23.8	17.35	659.4
12.79	44.9	16.75	571.6
15.41	84.0	15.97	438.8
18.15	222.2		
18.40	345.9		
19.42	593.0		
23.70	780.2		

For different temperatures of outgassing, the amount adsorbed, at the saturation pressure for 25° C, varied from 285 to 851 mg H_2O per gram, but in all cases a similar difference was observed between the sorption and desorption data.

The adsorption of water vapor on carbon black has been investigated by P. H. Emmett and R. B. Anderson.[37] Two commercial varieties of carbon black were used. Figure 7 shows results obtained for one of these. The specific areas for the original sample and that for the sample degassed at 1000° C, as determined by the adsorption isotherm with nitrogen at −195° C, exhibited hardly any change. But the adsorption of water vapor was decreased considerably by the degassing treatment. In the figure, data indicated by circles were obtained by volumetric measurements; those indicated by squares were obtained gravimetrically. Solid circles and squares are desorption points.

---

[36] P. G. T. Hand and D. O. Shiels, *J. Phys. Chem.*, **32**, 441 (1929); A. J. Allmand, R. Chaplin, and D. O. Shiels, *J. Phys. Chem.*, **33**, 1151 (1929); A. J. Allmand and P. G. T. Hand, *J. Phys. Chem.*, **33**, 1161 (1929); A. J. Allmand, P. G. T. Hand, J. E. Manning, and D. O. Shiels, *J. Phys. Chem.*, **33**, 1682 (1929); A. J. Allmand, P. G. T. Hand, and J. E. Manning, *J. Phys. Chem.*, **33**, 1694 (1929).

[37] *J. Am. Chem. Soc.*, **67**, 1492 (1945).

Similar results were obtained with the other sample of carbon black. From these observations it is evident that in these cases the heat treatment, though producing little or no change in specific area of the adsorbent, did affect its adsorption capacity for water vapor.

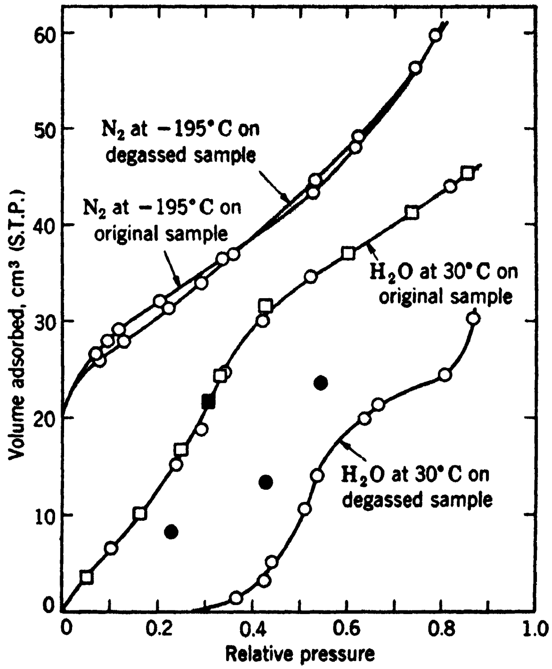

Fig. 7. Adsorption of nitrogen at −195° C and water vapor at 30° C on a sample of carbon black (Grade 6 Speron) before and after degassing at 1000° C. Data indicated by circles were obtained by volumetric method; those indicated by squares were obtained gravimetrically. Solid circles and squares are desorption points. (Emmett and Anderson.)

The sorption of hydrogen by coconut charcoal at the *temperature of liquid air* has been investigated by J. W. McBain[38] and J. B. Firth.[39] In both cases it was observed that equilibrium is attained only after a lapse of many hours. According to McBain most of the gas is condensed instantaneously on the surface (true adsorption) and this is followed by a gradual diffusion of the hydrogen into the charcoal at a rate which obeys the regular law of diffusion. This last stage corresponds to (interstitial) solution of the gas between the carbon atoms, and McBain concludes that this solubility is proportional to the square root of the pressure, indicating that the dissolved gas is in the atomic condition. Furthermore, McBain concludes that the *solubility* of hydrogen at liquid-air temperature is at least 100 times that observed at room temperature.

---

[38] *Z. physik. Chem.*, **68**, 471 (1909); *Phil. Mag.*, **18**, 916 (1909).

[39] *Z. physik. Chem.*, **86**, 294 (1914).

J. B. Firth has shown that his equilibrium sorption data are in good agreement with a relation of the form

$$v_0 = kP^{1/4}. \tag{3}$$

For P in millimeters and v_0 in cubic centimeters at S.T.P. per gram, k has the average value 20 $\text{cm}^3/(\text{mm})^{1/4}$. Assuming the validity of this relation[40] down to very low pressures, the corresponding equilibrium values are found to be those given in Table 11.

TABLE 11

SORPTION DATA FOR HYDROGEN BY CHARCOAL AT LIQUID-AIR TEMPERATURE

P_{mm}	v_0	P_{mm}	v_0
500	94.6	10^{-1}	11.2
100	63.1	10^{-2}	6.3
10	35.5	10^{-3}	3.55
1	20	10^{-4}	2.00

A number of investigators have compared the sorptive capacity of graphite with that of coconut charcoal. In the case of carbon dioxide, A. Magnus and H. Kratz[41] have observed that the amount adsorbed on graphite at any given temperature and pressure is about 1/700 of that adsorbed on charcoal.

Similar observations have been made by H. H. Lowry and S. O. Morgan[42] on the sorption of carbon dioxide, nitrogen, and hydrogen by graphitic carbon. Even at the temperature of liquid air, the hydrogen adsorption is only about 1/10 of that observed for active charcoal.

3. SORPTION DATA AT LOW PRESSURES

Observations on the sorption of gases by charcoal at low pressures have been published by J. Dewar,[43] G. Claude,[44] and H. Rowe.[45]

---

[40] The isotherms plotted by Firth are certainly not in agreement with the hyperbolic equation.

[41] *Z. anorg. Chem.*, **184**, 241 (1929).

[42] *J. Phys. Chem.*, **29**, 1105 (1925).

[43] *Proc. Roy. Inst. Gt. Brit.*, **18**, 751 (1907); SB, p. 37.

[44] *Compt. rend.*, **158**, 861 (1914).

[45] *Phil. Mag.*, **1**, 109, 1042 (1926).

Some of the data obtained by Rowe for sorption at room temperature are shown in Table 12.

TABLE 12

SORPTION BY CHARCOAL AT ROOM TEMPERATURE (ROWE)

CO_2 at 15° C		N_2 at 15° C		O_2 at 22° C	
P_μ	q^*	P_μ	q^*	P_μ	q^*
0.326	5.165	3.231	0.1313	0.136	2.299
1.164	25.21	5.727	0.2212	0.298	9.204
4.250	56.10	10.88	0.3145	0.608	22.48
9.989	75.48	20.76	0.7782	1.011	39.50
17.85	92.70	45.10	1.734	1.830	76.35
42.78	131.2	99.64	5.066	5.921	203.2
73.02	150.5	117.0	6.642	74.49	670.1

$^*q$ = cm³ at 1 mm of mercury and 15° C,
$v_0 = 1.206 \cdot 10^{-3}q$ = cm³ at 760 mm and 0° C.

For carbon dioxide above 1.75 microns, for nitrogen above 30 microns, and for oxygen above 4 microns, the data are represented by the Henry-Williams equation of the form

$$\log\left(\frac{q}{P}\right) = A_0 - A_1 q. \tag{4}$$

From the data published by Rowe, it follows that, for $P_{mm} = 10^{-2}$ and $P_{mm} = 10^{-1}$, the volumes adsorbed at *room temperature* (measured in terms of *cubic centimeters at S.T.P.*), per gram, are as follows:

	$P_{mm} = 10^{-2}$ mm	$P_{mm} = 10^{-1}$ mm
CO_2	0.090	0.199
N_2	0.00036	0.006
O_2	0.360	0.900

Table 13 gives the sorption data obtained by Rowe at −183° C (liquid oxygen). For nitrogen and carbon monoxide the observations at pressures above about 10^{-3} mm are in good agreement with the hyperbolic equation. The values for v_s, b, and bv_s deduced from the data are shown at the bottom of the table. For hydrogen, two series of observations were made, and in both series it was observed that to a first approximation v varies *linearly* with P (which is different from the result observed by Firth), especially at pressures above $5 \cdot 10^{-3}$ mm. From these data we deduce the equilibrium values (cm³/g at S.T.P.) at 10^{-2} mm and 10^{-1} mm, which are given in Table 15.

As will be observed, the values of P_{mm}/v_0 for the low-pressure range

TABLE 13

SORPTION BY ACTIVATED CHARCOAL AT −183° C (H. ROWE)

Nitrogen			Carbon Monoxide			Hydrogen		
P_{mm}	v_0	$10^4 P_{mm}/v_0$	P_{mm}	v_0	$10^5 P_{mm}/v_0$	P_{mm}	v_0	P_{mm}/v_0
$3.0 \cdot 10^{-5}$	0.223	1.35	$2.4 \cdot 10^{-5}$	0.339	7.08	$7.00 \cdot 10^{-4}$	0.0046	0.152
6.4	0.336	1.91	9.8	2.475	3.96	9.44	.0073	.129
$1.16 \cdot 10^{-4}$	1.095	1.06	$1.87 \cdot 10^{-4}$	4.007	4.67	$1.51 \cdot 10^{-3}$	.0122	.124
2.67	2.539	1.05	6.77	17.96	3.77	2.57	.0231	.111
4.69	4.318	1.09	$1.20 \cdot 10^{-3}$	30.01	4.00	3.40	.0304	.112
8.15	8.832	0.92	1.46	35.33	4.13	4.25	.0403	.105
$1.32 \cdot 10^{-3}$	13.54	.97	2.08	47.78	4.35	5.83	.0563	.104
1.99	22.14	.90	3.08	57.17	5.39	8.07	.0781	.103
4.38	39.11	1.12	5.17	67.53	7.66	12.21	.126	.097
6.66	44.16	1.51	11.80	81.88	14.41	15.72	.170	.093
9.72	49.21	1.98	20.75	91.82	22.60	19.36	.212	.091
13.11	54.48	2.40	40.24	100.96	39.87	$22.81 \cdot 10^{-3}$	.255	.090
18.60	60.73	3.06	55.68	104.75	53.16			
22.58	65.78	3.44	$83.01 \cdot 10^{-3}$	111.23	74.64			
31.09	70.82	4.39						
46.06	75.13	6.14						
55.99	77.33	7.25						
70.30	79.77	8.82						
$79.75 \cdot 10^{-3}$	81.31	9.80						

Nitrogen:

$v_s = 88.9$ cm³/g.
$b = 132.3$ mm⁻¹.
$bv_s = 11{,}765$ cm³ · mm⁻¹/g.

Carbon Monoxide:

$v_s = 114.7$ cm³/g.
$b = 218.1$ mm⁻¹.
$bv_s = 25{,}000$ cm³ · mm⁻¹/g.

Hydrogen:

$$\text{Ave} = 0.100 \frac{\text{mm}}{\text{cm}^3} \cdot \text{g}.$$

Second series:

$$\text{Ave} = 0.051 \frac{\text{mm}}{\text{cm}^3} \cdot \text{g}.$$

$v_0 = $ cm³ (S.T.P.)/g.

are greater than those deduced from the values of v_s and b given at the bottom of the tables. However, in view of possible experimental errors involved in the determination of both P_{mm} and v_0 in the low-pressure range, the values of the constants in the hyperbolic equation were actually deduced by the writer from the determinations in the higher-pressure range.

Table 14 gives sorption data for nitrogen, hydrogen, and neon obtained by Claude. In the case of helium, the volume sorbed at 27 mm and $-195.5°$ C was 0.21 cm^3/g.

From the plot of P_{mm}/v_0 versus P_{mm} for hydrogen, the values of v_s and b shown at the bottom of the table were deduced. These were used to calculate values of v_0 for the range $P_{mm} = 10^{-2}$ to 1, which are given in Table 15. In the case of neon, $v_0 = 0.222P_{mm}$, and, since the data for nitrogen could not be fitted by a hyperbolic type of equation, the values given in Table 15 were obtained by interpolation.

For comparison, Table 16 gives values observed by Dewar for the pressures corresponding to different amounts of sorption of hydrogen and nitrogen by 25 g of charcoal at the temperature of liquid air.

All these observations agree in the conclusion that nitrogen (or air) is sorbed by charcoal at liquid-air temperature to a considerably larger extent than hydrogen.

In this laboratory, H. Huthsteiner has measured the adsorption of nitrogen and hydrogen by activated charcoal at $-195.8°$ C. The charcoal was heated during exhaust to about 500° C, and after the McLeod gauge indicated an extremely low residual pressure the charcoal tube was immersed in liquid nitrogen and successive known amounts of the gas were admitted. In less than 5 minutes equilibrium was attained and the pressure noted.

For hydrogen, over the range 0 to 250 microns, the volume adsorbed per gram of charcoal (S.T.P.) was found to be in agreement with the relation

$$v_0 = 1.6 \cdot 10^{-2} P_\mu.$$

For nitrogen, the following data were obtained:

P_μ:	1	2	3	4	5
v_0:	4	16	30	45	60

A comparison with the data in Table 13 shows the effect of the lower temperature in increased amounts adsorbed.

For application of data such as those given in Table 15, in vacuum technique, in the manner discussed in the following section, it should be observed that 1 $\text{atm} \cdot \text{cm}^3 = 760$ $\text{micron} \cdot \text{liters}$, that is, 1 $\text{micron} \cdot \text{liter}$ corresponds to $v_0 = 1.316 \cdot 10^{-3}$.

TABLE 14

SORPTION BY ACTIVATED CHARCOAL AT VERY LOW TEMPERATURES (CLAUDE)

Nitrogen (−182.5° C)			Hydrogen (−195.5° C)			Neon (−195.5° C)		
P_{mm}	v_0	P_{mm}/v_0	P_{mm}	v_0	P_{mm}/v_0	P_{mm}	v_0	P_{mm}/v_0
0.004	9.35	$4.28 \cdot 10^{-4}$	0.006	0.105	0.057	0.45	0.105	4.29
0.010	18.70	5.35	0.0115	0.21	.055	0.88	0.21	4.19
0.032	37.4	8.56	0.0205	0.42	.049	1.30	0.32	4.06
0.088	46.6	$1.89 \cdot 10^{-3}$	0.036	0.84	.043	1.74	0.42	4.14
0.385	56	6.88	0.083	2.05	.040	3.5	0.84	4.17
1.107	65.3	$1.35 \cdot 10^{-2}$	0.176	3.71	.047	5.3	1.22	4.34
11.50	93	0.124	0.475	8.40	.054	7.2	1.63	4.42
33.2	103	0.322	1.06	14	.076	11.3	2.44	4.63
90	112	0.804	3.50	28	.125	15.5	3.25	4.77
247	121	2.04	8.7	42	.207	19.4	4.06	4.78
			20.6	56	.368	30.5	6.18	4.94
			43.7	63	.694	40.5	8.01	5.06

Nitrogen: $v_s = 125$ cm³/g.

Hydrogen: $v_s = 64.7$ cm³/g.
$b = 0.281 \text{ mm}^{-1}$.

Neon: Ave = 4.50

TABLE 15

SORPTION BY ACTIVATED CHARCOAL AT LOW PRESSURES AND VERY LOW TEMPERATURES

Investigator	$t°$ C	Gas	v_0 for P_{mm} = 10^{-2}	10^{-1}	1	
Rowe	−183	H_2	0.10	1.00	10.00	First series
			0.196	1.96	19.60	Second series
	−183	N_2	50.65	82.7	88.3	
	−183	CO	78.6	109.6	114.0	
Claude	−195.5	H_2	0.181	1.77	14.2	
	−182.5	N_2	18.7	47	65	
	−195.5	Ne	0.002	0.022	0.22	

TABLE 16

VALUES OF PRESSURE FOR DIFFERENT AMOUNTS OF SORPTION OBSERVED AT T = 90 (DEWAR)

	Equilibrium Pressure, mm	
Volume per 25 g	For hydrogen	For nitrogen
0	0.00003	0.00005
5	.0228	—
10	.0455	—
15	.0645	—
20	.0861	—
25	.1105	—
30	.1339	.00031
35	.1623	—
40	.1870	—
130	—	.0010
500	—	.00314
1000	—	.01756
1500	—	.02920
2500	—	.06172

4. USE OF CHARCOAL AT LOW TEMPERATURES IN HIGH-VACUUM SYSTEMS

From the sorption data given in the previous section it is possible to calculate the reduction in pressure that should be obtained by means of charcoal at very low temperature connected to the system.

Let V = volume, in cm^3, of system.
w = weight of charcoal in g.
P_{mm1} = initial pressure.
P_{mm2} = equilibrium pressure after immersing charcoal tube in low-temperature bath.
v = volume adsorbed (cm^3 at S.T.P.).

Evidently,

$$\frac{VP_{mm1}}{760} = \frac{VP_{mm2}}{760} + v \tag{1}$$

I. For $v = \dfrac{wbv_s P_{mm2}}{1 + bP_{mm2}}$ and $P_{mm1} \gg P_{mm2}$,

$$\frac{1}{P_{mm2}} = \frac{760wbv_s}{VP_{mm1}} - b. \tag{2}$$

II. For $v = kwP_{mm}$,

$$P_{mm2} = \frac{VP_{mm1}}{760}\left(\frac{1}{V/760 + kw}\right). \tag{3}$$

Let us assume that $V = 1000$ cm^3, $P_{mm1} = 100 \cdot 10^{-3}$, $w = 1$, and $t = -183°$ C. Using the values of the constants v_s and b obtained by Rowe (see Table 13), it is found that, for nitrogen, $P_{mm2} = 0.012 \cdot 10^{-3}$, while for hydrogen, $P_{mm2} = 1.16 \cdot 10^{-2}$, for $k = 10.0$.

J. W. Woodrow[46] measured, with a Knudsen gauge (see Chapter 6), the amount of clean-up of different gases by charcoal at liquid-air temperatures. Neither the volume of the apparatus nor weight of charcoal is given. The charcoal was heated under simultaneous evacuation until the pressure fell to $1.5 \cdot 10^{-6}$ mm of mercury ($2 \cdot 10^{-3}$ microbar), and hydrogen, oxygen, or nitrogen was then introduced at an initial pressure of about 0.65 microbar. The rate of clean-up in each case as followed with the gauge is shown in Table 17.

TABLE 17

RATE OF CLEAN-UP BY CHARCOAL AT ABOUT −190° C
(PRESSURE IN MICROBARS)

Time	Hydrogen	Oxygen	Nitrogen
0	0.647	0.667	0.600
5 sec		.387	
10 sec		.227	
1 min	.613	.0027	.020
5 min	.547	.002	
20 min	.387		
1 hr	.253		.007
3 hr	.180	.002	
10 hr	.180	.002	.007

Miss M. Daly and the writer also carried out some experiments, in this laboratory, on the adsorption of gases by charcoal at low temperatures. Specially activated products, supplied by F. M. Dorsey, were used in this work. Pressures were determined by means of the ionization gauge, and the rate of clean-up of residual gases present after sealing off the pump was observed. The gauge and tube containing 5 g charcoal with a large bulb (total volume = 3000 cm^3) were well exhausted on the condensation pump, with simultaneous heating of the charcoal for over an hour to 360° C. After this system was sealed off the pump, the pressure was measured, and then liquid air put on the charcoal. The pressures (in microbars) before cooling the charcoal, and after, were as follows:

---

[46] *Phys. Rev.*, **4**, 491 (1914).

V	Initial Pressure	Final Pressure
3000 cm^3	0.022	0.0004
3000 cm^3	.036	.0004
3000 cm^3	.92	.0006

It may be noted that the sensitivity of the galvanometer used with the ionization gauge was such that 0.0004 microbar was about the lowest pressure that could actually be measured.

In carrying out experiments with hydrogen, the same apparatus was used, except that another side tube was sealed on in which was contained a small thin-walled glass pellet (volume 3 cm^3) filled with hydrogen at a known pressure. After the gauge, charcoal tube, and bulb were exhausted, this system was sealed off, the hydrogen pellet broken by shaking, and the residual pressure observed after immersing the charcoal tube in liquid air. Five grams of activated charcoal were used as in the previous experiments. The residual gas pressure was also measured before breaking the pellet. Table 18 shows some of the results obtained.

In general it required about an hour to attain equilibrium. In accord with McBain's observations it was found that the initial condensation was followed by a slow diffusion of gas into the charcoal.

TABLE 18

CLEAN-UP OF HYDROGEN BY ACTIVATED CHARCOAL AT −190° C (PRESSURES IN MICROBARS)

V	Pressure after Sealing off	Initial Pressure of Hydrogen	Final Pressure at Room Temperature	Pressure at Liquid-Air Temperature
3025	0.0180	0.31	0.014	0.0004
100	.104	8.64	0.02	.0004
3025	.022	8.33	2.0	.15
100	.28	17.7	0.24	.0016

A certain fraction of this clean-up was no doubt due to the action of the gauge itself. As mentioned in Chapter 6 and also in Chapter 10, an electrical clean-up occurs in all hot-cathode devices. Furthermore, in the presence of a heated filament atomic hydrogen is formed which is cleaned up at the temperature of liquid air. A blank experiment carried out without the use of charcoal gave the following results:

$V = 340$; pressure after seal off = 1.60 microbars.

On breaking the hydrogen pellet, the pressure rose to 7 microbars, then fell, owing to clean-up by the gauge, to 2 microbars. Liquid air was put on the side tube, and the pressure fell in the course of 6 hours to 0.16 microbar. On removal of the liquid air, the pressure came back to 1.2 microbars.

In the measurements with charcoal the gauge filaments were lighted only during the time necessary to take a pressure reading, so that any error due to clean-up in the gauge was certainly not very large.

It is evident from these observations that with a charcoal tube immersed in liquid air it is possible to adsorb appreciable volumes of hydrogen and obtain residual gas pressures of less than 0.0001 micron.

O. Winkler[47] has investigated the clean-up of nitrogen and hydrogen, at a temperature of −183° C, by charcoal and silica gel. He observed that sorption and desorption curves did not coincide, but that the volume sorbed for a given value of P increased in successive runs. The limits actually observed for *nitrogen* on charcoal are shown as curves 1 and 2 in Fig. 8, while Rowe's data (see Table 13) are plotted as curve 3. In the case of *hydrogen,* the sorption and desorption were found to be completely identical for a given sample of charcoal. For different samples the isotherms were observed to lie between the two limiting plots 4 and 5, whereas Rowe's observations lie on plots 6 and 4. Winkler also observed, in agreement with Firth and McBain, that for the attainment of equilibrium in both sorption and desorption of hydrogen a period of as much as 1 to 3 hours was required.

Some extremely interesting observations on the sorption by carbon dust have been made by R. H. Savage[48] in this laboratory.

The dust, formed by the wear of graphite rods rubbing against a rotating base in vacuum, has been found to adsorb hydrogen, nitrogen, oxygen, carbon monoxide, carbon dioxide, and methane *irreversibly* at room temperature. The hydrogen clean-up, 2 cc/g of dust, is 10^5 times the adsorption shown by representative activated charcoals at room temperature, and pressures of the order of 10 microns.

---

[47] *Z. tech. Physik,* **14,** 319 (1933).

[48] *J. Applied Phys.,* **19,** 1 (1948). The quotation is from a paper by Savage and J. R. C. Brown, *J. Am. Chem. Soc.,* **70,** 2362 (1948).

The total surface of the dust, as determined, in accordance with the B.E.T. method, by adsorption of nitrogen at −195° C, was found to be about 400 m^2/g, whereas the *chemically active* specific surface of the dust, as indicated by the hydrogen clean-up, was about 5 m^2/g.

The authors have interpreted these observations on the assumption that the dust consists of ultramicroscopic plates of graphite which are about 20 angstroms thick and about 3500 angstroms in diameter and that the hydrogen is adsorbed on "unsaturated carbon valences at points of cleavage at right angles to the main (001) cleavage plane."

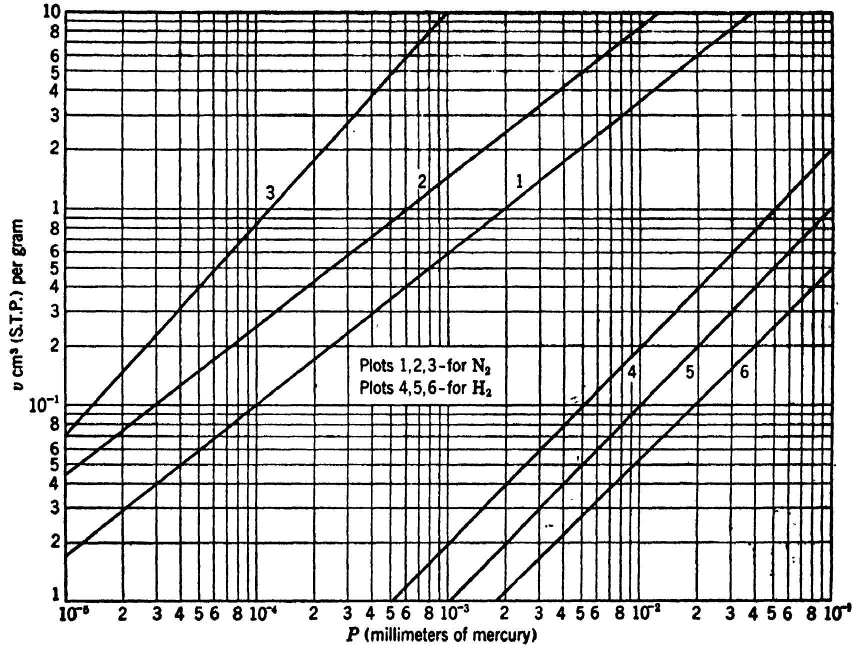

FIG. 8. Log-log plots of isotherms for adsorption of nitrogen and hydrogen by activated charcoal at −183° C and low pressures. Plots 1 and 2 for nitrogen and 4 and 5 for hydrogen represent limits observed by Winkler. Plot 3 for nitrogen and 4 and 6 for hydrogen were obtained by Rowe.

As will be observed, the value of the total specific area of the graphite dust given above is approximately one half of the values given in Table 7, whereas, according to observations made in Chapter 7, footnote 155, the surface area of colloidal carbon black ranges from 15 to 64 m^2/g.

5. SORPTION BY SILICA GEL AND SILICATES[49]

Although charcoal is the best general adsorbent for high-vacuum technique, other adsorbents which have been used in special technical applications should be mentioned.

Silica gel, which is a "partially dehydrated jelly of silicic acid," and certain complex silicates, known as zeolites, are of interest mainly in the sorption of water vapor and certain organic vapors.

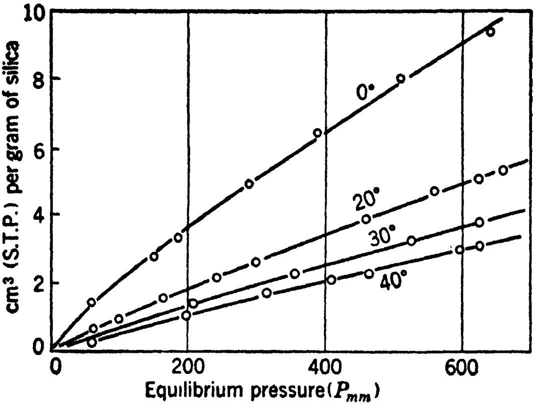

FIG. 9. Isotherms for the sorption of carbon dioxide by silica gel (Patrick, Preston, and Owens).

According to S. J. Gregg,[50]

> The characteristics of adsorption on silica gel differ somewhat from those of charcoal, particularly with respect to the Freundlich isotherm, for in the case of many gases, e.g., sulfur dioxide, nitrogen peroxide, butane—the Freundlich equation holds fairly accurately. Moreover, deviations from Henry's law even seem to be much less than for charcoal.

Figure 9[51] shows isotherms for the sorption of *carbon dioxide by silica gel* as determined by W. A. Patrick, W. C. Preston, and A. E. Owens.[52] As will be observed the sorption per gram of silica gel is considerably less than that obtained per gram of charcoal. Similar observations have been made by A. Magnus and R. Kieffer[53] and by A. Magnus and

---

[49] The remarks in this section are largely based upon the comprehensive discussion by McBain, McB, Chapters V and VI.

[50] JG, p. 11. (See footnote 1, Chapter 7, for reference.)

[51] McB, p. 196, Fig. 69.

[52] *J. Phys. Chem.*, **29**, 421 (1925).

[53] *Z. anorg. allgem. Chem.*, **179**, 215 (1929).

H. Kratz.[54] Table 19 compares the sorptions at 0° C and at two different pressures observed by these two sets of investigators with the values deduced from Homfray's observations.

TABLE 19

COMPARISON OF SORPTION OF CO_2 BY SILICA GEL AND BY CHARCOAL

	cm^3/g at	
	$P_{mm} = 1$	$P_{mm} = 10$
CO_2 on silica gel (M and K)	0.163	1.63
CO_2 on charcoal (M and K)	1.06	~5
CO_2 on charcoal (Homfray)	0.5	4.66

As will be observed from Fig. 9 the sorption of carbon dioxide by silica gel obeys Henry's law up to 10 mm pressure at 0° C, and up to much higher pressures at higher temperatures.

For the adsorption of *argon* on silica gel, Henry's law is obeyed to several hundred millimeters' pressure. At 0° C, the actually observed amount, according to the results obtained by W. Kälberer and C. Schuster,[55] is approximately $0.1 \cdot 10^{-6}$ mole/g per mm ($= 2.24 \cdot 10^{-3}$ $atm \cdot cm^3 \cdot g^{-1} \cdot mm^{-1}$), whereas, according to I. Homfray, the sorption of argon at 0° C by charcoal is about $1.75 \cdot 10^{-2}$ $atm \cdot cm^3 g^{-1} mm^{-1}$. (See Table 6.)

Similarly, in respect to the other common gases, the sorption by silica gel is less than that obtained for the sorption by charcoal.[56]

Figure 10, taken from the publication by A. S. Coolidge,[57] shows the relative adsorption of water vapor by a number of different adsorbents, including charcoal and silica gel. The remarkably high sorption by chabasite and the sorption by glass are discussed below.

One especially interesting characteristic of silica gel and of similar gels prepared from TiO_2, Al_2O_3, SnO_2, and other oxides is also illustrated in Fig. 10. This is the phenomenon of hysteresis in sorption and desorption isotherms.

The hysteresis in the sorption of water vapor by silica gel has been investigated very fully by L. M. Pidgeon[58] and K. S. Rao.[59] A typical plot of the sorption data at 20° C, obtained by Pidgeon, is shown in

---

[54] *Z. anorg. allgem. Chem.*, **184**, 241 (1929).

[55] *Z. physik. Chem.*, **A**, **141**, 270 (1929).

[56] Sorption data for oxygen on silica gel at −49° C to −69° C are given by A. Magnus and K. Gräbling, *Z. physik. Chem.*, **A**, **145**, 27 (1929).

[57] *J. Am. Chem. Soc.*, **49**, 708 (1927).

[58] *Can. J. Research*, **10**, 713 (1934).

[59] *J. Phys. Chem.*, **45**, 513 (1941).

Fig. 11. The arrows indicate the order in which the observations were made. Pidgeon also concluded from his observations "that the hysteresis loop which appears during water sorption by silica gel has a real existence and is not due to the failure to eliminate air and other gases from the system"—an explanation which had been suggested by previous investigators. Rao also confirmed the existence of such a hysteresis loop at values of x/m above 15 per cent, where x/m = weight of H_2O per unit weight of gel.

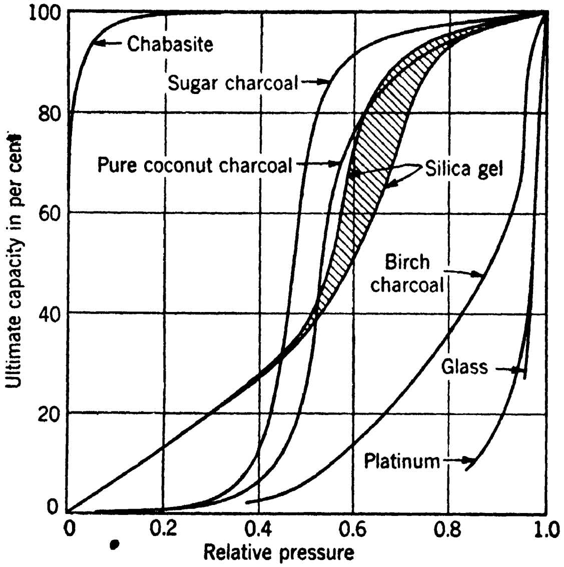

Fig. 10. Isotherms for the relative sorption of water vapor by different adsorbents, illustrating the hysteresis phenomenon observed with silica gel (Coolidge).

The effective area of silica gel as determined by Brunauer and Emmett (see Table 7.27) is about 600 sq m/g, that is, approximately 75 per cent of that of active charcoal.

Chabasite, a mineral belonging to the class of zeolites, has the formula $CaAl_2Si_4O_{12} \cdot 6H_2O$. These minerals are of special interest because of two significant characteristics. The first of these, as described by Gregg,[60] is that "unlike ordinary crystals containing water of crystallization they can be dehydrated without any change in the form of their crystal lattice." As a result, molecules of different gases can occupy the spaces left vacant by the removal of water, and the zeolites are therefore good absorbents. This is, however, true only for certain gases

[60] JG, p. 12.

and involves the second characteristic of chabasite and the zeolites in general, viz., that these minerals exhibit a phenomenon known as *persorption.*

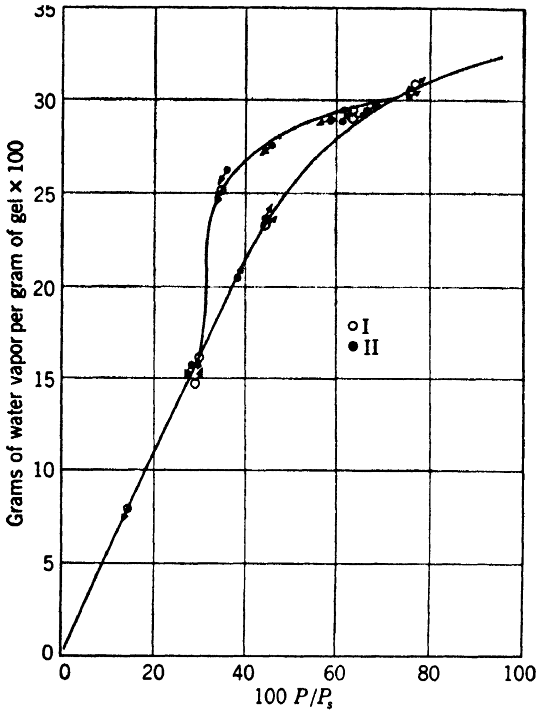

FIG. 11. Sorption and desorption curves for water vapor and silica gel at 20° C. Sorption plotted versus relative pressure, P/P_s, where P_s = saturation pressure of

According to Brunauer,[61]

> Persorption may be defined as adsorption in pores that are only slightly wider than the diameter of the adsorbate molecules. By using molecules of different diameters and noting the extent to which adsorption under given experimental conditions decreases as the size of the molecule increases one can study the structure of the finest pores of the adsorbent.

The amount of gas taken up by chabasite (or any of the other zeolites) varies, at constant temperature and pressure, with the degree of dehydration. Table 20 presents a summary of observations made by A. B. Lamb and J. C. Woodhouse[62] on the sorption by chabasite, at 0° C and 1 atm pressure, of three gases. The first column for each gas gives the temperature (°C) at which the mineral was heated with simultaneous evacuation; the second column gives the percentage dehydration; and the third column, the amount occluded, v_0 (in cm^3, S.T.P.) per gram of anhydrous mineral. From these observations it is concluded that maximum occlusion of hydrogen, oxygen, and carbon dioxide at 0° C occurs when 97.8, 96.9, and 92.9 per cent respectively of the original water has been removed by suitable heat treatment. A similar maximum sorption was observed for carbon dioxide at the same percentage dehydration, at 34.5° C, 61.2° C, and 100° C. (The maximum values of amount adsorbed are indicated in Table 20 by asterisks.)

---

[61] SB, p. 366.

[62] *J. Am. Chem. Soc.*, **58**, 2637 (1936).

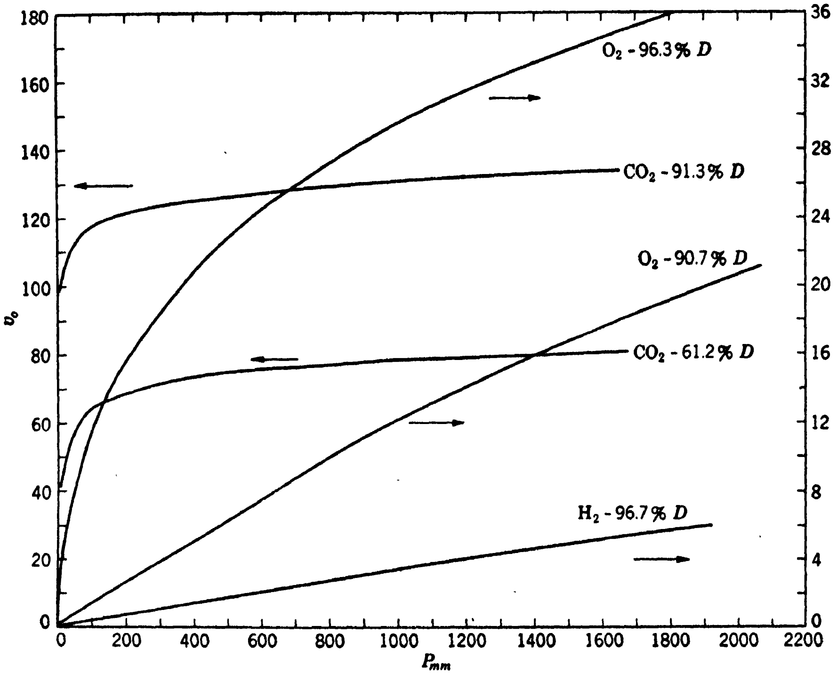

FIG. 12. Typical isotherms at 0° C for the sorption of hydrogen, carbon dioxide, and oxygen by dehydrated chabasite. Per cent dehydration (D) is given for each isotherm. Scale for v_0 is indicated by an arrow. (Lamb and Woodhouse.)

This variation in amount of adsorption with extent of dehydration is explained on the assumption that the pore sizes and extent of corresponding inner surface change with percentage of dehydration. In fact, as shown in the bottom row in Table 20, the specific sorption of dehydrated chabasite approaches closely that of charcoal.

Figure 12 shows typical isotherms at 0° C for hydrogen, oxygen, and carbon dioxide, as observed in this investigation, for different percentages of dehydration (D).

TABLE 20

SORPTION OF HYDROGEN, OXYGEN, AND CARBON DIOXIDE BY DEHYDRATED CHABASITE AT 0° C AND 760 MM

(LAMB & WOODHOUSE)

Hydrogen			Oxygen			Carbon Dioxide		
t° C	Per Cent D	v_0	t° C	Per Cent D	v_0	t° C	Per Cent D	v_0
180	61.4	0.1	250	40.0	1	120	33.2	33
255	78.4	0.5	306	74.0	5.8	180	61.2	77
380	91.3	1.0	390	90.7	9.7	250	77.0	103
630	96.3	2.6	460	94.5	15.2	390	90.7	128
634	96.7	2.75*	575	95.5	21.3	380	91.3	130*
640	97.5	2.7	635	96.3	27.0*	512	93.8	118
			635	96.7	23.2	608	95.7	119
			730	97.8	18.0	635	96.3	115
Sorption by charcoal at 0° C and 760 mm:		1.5			20			87

As shown by a number of investigators, by use of X-ray methods, three types of zeolite framework have been recognized: (1) three-dimensional networks (chabasite, analcite); (2) fibrous structures (natrolite, etc.); (3) plate-like structures (heulandite).

> These frameworks [as R. M. Barrer[63] states] are anionic Si-O-Al networks, containing interstitial and exchangeable cations, and also neutral molecules of water, which are replaceable in some instances by molecules of ammonia, iodine, mercury, or gases.

In the publication from which this statement is quoted are given data on the sorption isotherms for hydrogen, nitrogen, and argon by dehydrated chabasite and analcite[64] at temperatures ranging from −184° C to 110° C. The saturation amounts observed at the lowest temperature, per gram of *original* chabasite, were as follows:

Hydrogen approximately	280 cm^3 (S.T.P.)
Argon approximately	250 cm^3 (S.T.P.)
Nitrogen approximately	164 cm^3 (S.T.P.)

---

[63] *Proc. Roy. Soc. London*, **A**, **167**, 392 (1938).

[64] "The dehydration of chabasite was carried out *in vacuo* at progressively increasing temperatures for several days. The temperature was finally raised to 480° C for 1 day." In the case of analcite ($Na_8Al_8Si_{12}O_{48} \cdot 12H_2O$) dehydration in vacuo was carried out at 330° C for 3 days.

Since the original chabasite contains 21.34 per cent, by weight, of H_2O, this would correspond to 266 cm^3 water vapor (S.T.P.) per gram of original chabasite, or 338 cm^3 per gram of *completely dehydrated* chabasite. According to Table 7.25, the number of argon atoms per square centimeter required to form a complete monolayer is $7.81 \cdot 10^{14}$. Hence the specific adsorption area for completely dehydrated chabasite is calculated to be about 1164 sq m/g, which, as will be observed from Table 7.27, exceeds that deduced for activated charcoal (775 sq m/g). Using the value, given above, for nitrogen ($1/S = 7.25 \cdot 10^{14}$) the adsorption area is calculated as about 608 sq m/g of dehydrated chabasite.

For analcite the volume of water vapor is 0.078 cm^3 (S.T.P.) per gram of original material, which obviously corresponds to a much smaller specific area, and, according to Barrer's observations, the saturation values are considerably less than those for chabasite. In both cases, the sorption isotherms for the above gases, at temperatures higher than that of liquid air, show characteristics similar to those obtained with other adsorbents.

However, as mentioned previously, while chabasite is an excellent adsorbent for vapors or gases constituted of smaller molecules, such as water, oxygen, nitrogen, hydrogen, vapors or gases constituted of larger molecules are not adsorbed at all, or only with difficulty. Thus O. Schmidt[65] observed that, at 20° C and 760 mm pressure, the volumes of gas (S.T.P.) adsorbed per gram of chabasite are as follows:

H_2	A	O_2	N_2	CO	CH_4	CO_2	NH_3	H_2O	
3.3	28.1	34.3	52.2	74.5	80.4	282.0	567.0	702.0	cm^3

From these and similar observations for the larger molecules of organic compounds, he concluded that the pore diameter for chabasite is about $3.5 \cdot 10^{-8}$ cm.

This characteristic behavior of chabasite, which has been designated above by the term "persorption," has been investigated more extensively by R. M. Barrer and D. A. Ibbitson.[66]

They have determined both occlusion isotherms and rates of occlusion of hydrocarbons by active chabasite and analcite over a range of temperatures. The isotherms resemble those obtained by Lamb and Woodhouse, which have been described above. Figure 13 shows typical isotherms obtained for four normal-chain hydrocarbons. Table 21 gives a summary of saturation values, as observed by the above investigators, for a number of gases in both chabasite and analcite, and, for comparison, the diameter or length in angstrom units (1 A = 10^{-8} cm).

---

[65] *Z. physik. Chem.*, **133**, 263 (1928), also McB, pp. 166–176, which contains a comprehensive discussion of this topic.

[66] *Trans. Faraday Soc.*, **40**, 195 (1944).

As will be observed the saturation values in this table for hydrogen and argon are less than those given by Barrer in the previous publication. Consequently the specific areas deduced from these values would be of the order of 600 sq m/g. The decrease in the saturation value with increase in the length of the molecule is the most important conclusion to be deduced from the data in the table.

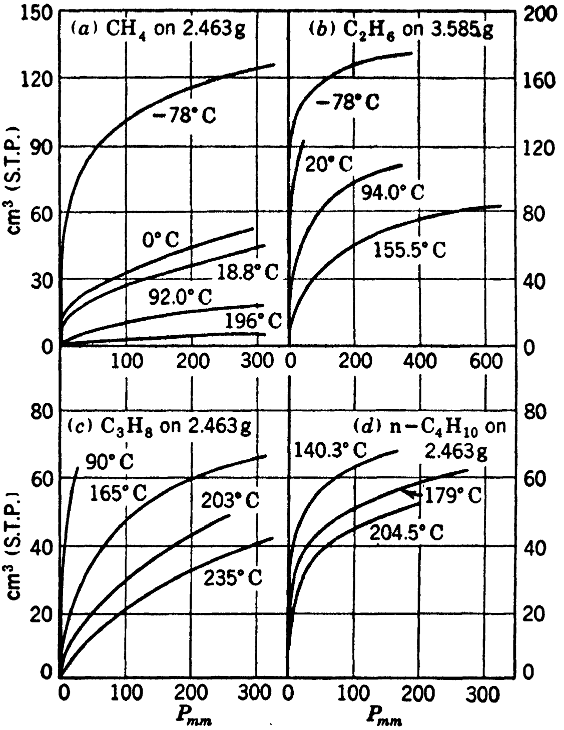

FIG. 13. Isotherms for sorption by chabasite of four normal-chain hydrocarbons (Barrer and Ibbitson).

Of special interest are the results obtained by Barrer and Ibbitson[67] for rates of occlusion of hydrocarbons. If Q_0, Q_t, and Q_∞ denote the amounts occluded at $t = 0$, t, and $t = \infty$, respectively, then it was observed that, for values of y less than about 0.2,

$$y = \frac{Q_t - Q_0}{Q_\infty - Q_0} = k\sqrt{t}, \tag{1}$$

---

[67] *Trans. Faraday Soc.*, **40**, 206 (1944).

TABLE 21

SATURATION VALUES FOR SORPTION BY CHABASITE AND ANALCITE

Gas	Diameter or Length	cm³/g (S.T.P.) Chabasite	cm³/g (S.T.P.) Analcite
H_2O	2.76	266	97
NH_3	3.60	193	72
H_2	3.74	186	69
A	3.84	181	67
O_2	3.83	181	67
N_2	4.08	170	63
CH_4	4.00	173	64
C_2H_6	5.54	125	46.4
C_3H_8	6.52	106	39.5
n-C_4H_{10}	7.78	89	33.1
n-C_5H_{12}	9.04	77	28.5
n-C_6H_{14}	10.34	67	25.0
n-C_7H_{16}	11.56	59	22.2

where k is a constant the value of which depends upon the particle size and the coefficient of diffusion D. It was also observed that k decreased with increase in y. This is interpreted as follows:

Let θ denote the fraction of interstitial sites on which occlusion takes place. Then D_θ, the diffusion constant corresponding to a given value of θ, is related to D_0, the value for $\theta = 0$, by the equation

$$D_\theta = D_0(1 - \theta), \tag{2}$$

and, since the constant k varies linearly with $\sqrt{D_\theta}$, the value of this constant must decrease with increase in the value of θ, that is, with increase in the value of y.

It was also observed that k increases with increase in temperature, and, from a plot of log k versus $1/T$, a value for the energy of activation could be deduced.

For the effect of pressure, it was observed that the rate of sorption follows a "hyperbolic" relation of the form

$$\frac{dQ}{dt} = \frac{k_1 P}{1 + k_2 P}. \tag{3}$$

That is, with increase in pressure, the rate increases at first, practically linearly with P, then, as P is increased still more, the increase in rate becomes less and less, until finally the rate attains a constant value.

A comparison of rates of occlusion for different hydrocarbons under given conditions of temperature and pressure shows that the rate decreases with increase in the number of carbon atoms in the hydrocarbon chain and also becomes extremely small for branched-chain hydrocarbons. This result is interpreted by Barrer and Ibbitson as follows:

> The rate of sorption depends upon the cross section of the solute molecules. In Fig. 14 the cross sections are shown to scale for CH_4 (or C_2H_6); for a *n*-hydrocarbon (propane); and for a branched-chain hydrocarbon (isobutane). These represent classes of solute which enter the zeolitic lattice respectively with great rapidity, slowly and with an energy of activation, or not at all. Since the cross-sectional diameters[68] are, in order, 4.00, 4.89, and 5.58 A, one sees that the narrowest cross section of the interstitial channel in both chabasite and active analcite must lie between 4.89 and 5.58 A. . . . The three types of molecule given in Fig. 14 may then be used as yardsticks to measure the narrowest cross section of any zeolite channel, or in a zeolite thus "calibrated" one may fix within narrow limits the cross sections of other molecules.

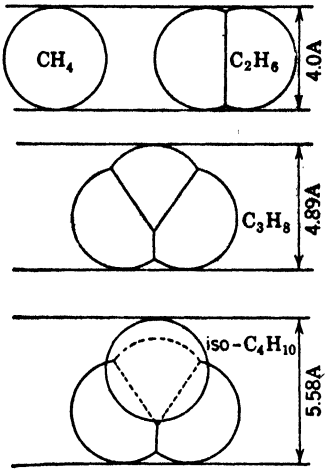

FIG. 14. The dimensions (in angstrom units) of representative molecules respectively very rapidly occluded (CH_4 and C_2H_6), occluded by activated diffusion (C_3H_8), and excluded (*iso*-C_4H_{10}) (Barrer and Ibbitson).

Confirming observations obtained by other investigators, Barrer and Ibbitson also observed that the rate of sorption was greatly affected by the conditions of dehydration of the original mineral and the fineness of subdivision of the mineral.

As will be noted, Barrer and Ibbitson refer to "solute molecules" rather than occluded or adsorbed molecules. The reasons for this designation are discussed by them in the following remarks:

> McBain [they state] used the term persorption to describe the uptake of gases by porous solids such as charcoal and silica gel, in which the pore systems are quite irregular. In zeolites on the other hand the occluded molecules form a regularly disposed, frequently mobile, interstitial component of the dehydrated crystal lattice and the sorption process is better described as solid solution.

The term "interstitial" is used to indicate that the solute molecules occupy interstices left by the removal of H_2O from the original lattice structure, and these investigators conclude that "zeolitic solid solution is very similar to the solutions of H_2 in Pd. It differs from the latter in that there is in zeolitic solution no *specific* interaction between solute and solid such as characterizes hydrogen-metal systems."[69] Thus sorption of gases by dehydrated zeolitic minerals is a purely physical interaction.[70]

---

[68] According to L. Pauling, *The Nature of the Chemical Bond*, p. 189, Cornell University Press, 1940.

The adsorption characteristics of chabasite for such polar gases and vapors as water vapor, oxygen, and carbon dioxide might find a useful application in vacuum technique.

The sorption of water vapor by other silicates and quartz is a topic that has received considerable attention. For instance, R. W. Bunsen observed in 1885 that, even at 500° C, silicates retain appreciable amounts of water vapor. L. J. Briggs[71] measured the sorption of water vapor by quartz powder. Fifty grams were used, having a superficial area of 20 sq m. The amounts adsorbed at different pressures of water vapor at 30° C are indicated in Table 22.

TABLE 22

SORPTION OF WATER VAPOR BY QUARTZ POWDER

P_{mm}	Mg H_2O Adsorbed	Number of Monolayers
0.2	0.5	0.9
10.7	2.9*	5.1
19.6	4.6	8.1
26.1	9.0	15.9
31.4	26.7	47.0

* Value obtained with samples dried to constant weight at 110° C.

The saturation vapor pressure at 30° C is 31.82 mm. Assuming, as deduced in Table 7.27, that a monolayer of water corresponds to $3.5 \cdot 10^{-5}$ cm³ per cm², that is, $2.84 \cdot 10^{-5}$ mg H_2O per cm², it follows that the number of monolayers adsorbed at each pressure were those given in the last column of Table 22. It should be observed that the value marked with an asterisk was obtained with samples which had previously been dried to constant weight at 110° C.

Similar results have been obtained by J. R. Katz[72] for the sorption of water vapor by pulverized synthetic quartz and anorthite

---

[69] These systems are discussed in Chapter 9.

[70] A further contribution to the study of the zeolites is given in a publication by Barrer, *Trans. Faraday Soc.*, **40**, 555 (1944), on sorption by two other zeolites, gmelinite and mordenite.

[71] *J. Phys. Chem.*, **9**, 617 (1905).

[72] *Proc. Amsterdam Acad.*, **15**, 445 (1912). The quotation is from Langmuir's paper, *J. Am. Chem. Soc.*, **38**, 2283 (1916).

($CaO \cdot Al_2O_3 \cdot 2SiO_2$). "The amount of water taken up reaches a fairly definite limit when the vapor pressure of the water is about 0.7 of the saturated vapor. The quantities of water adsorbed per square centimeter of surface under these conditions were $1.3 \cdot 10^{-6}$ g for quartz and $6.2 \cdot 10^{-6}$ g for anorthite." These correspond to 46 and 177 monolayers, respectively.

W. G. Palmer and R. E. D. Clark[73] have concluded that in the sorption of certain organic vapors by vitreous silica ($A_m = 0.469$ sq m/g) the films consist of two complete monolayers when the relative pressure is 0.5 to 0.6. (Relative pressure $= P/P_0$, where $P_0 =$ saturation vapor pressure.) In a subsequent investigation,[74] W. G. Palmer has shown that at saturation pressure the films are probably as many as four molecules thick.

6. EVOLUTION AND SORPTION OF GASES BY GLASS[75]

Observations on Evolution of Gases. The problem of completely removing adsorbed or absorbed water vapor from the walls of glass vessels is one of the most important in high-vacuum technique. Since glass is related to the silicates it is not surprising that its behavior with respect to water vapor is similar to that of quartz and the silicates, which were discussed in the previous section.

Thus Bunsen (1885) observed that a glass surface that had previously been dried thoroughly at 20° C evolved 22.3 mg from an area of 2.11 sq m, which corresponds to a layer of adsorbed water about 37 molecules thick. According to L. J. Briggs,[76]

> E. Warburg and T. Ihmori[77] found that measurable amounts of water vapor were condensed upon the surface of freshly blown glass bulbs and of bulbs which had not been thoroughly washed. After washing or boiling these glass surfaces and then thoroughly drying, no adsorption of water vapor could be detected.

There is no doubt that wherever the layer of adsorbed vapor is apparently more than one or two molecules in thickness we are not dealing with true adsorption phenomena. According to Langmuir, the sorption by glass is to be regarded as a process of solution of the water in the glass, in much the same manner as in the sorption of moisture by sodium silicate and the gels. It is also quite possible that in very fine powders the moisture may be actually condensed as a liquid in fine capillary spaces between the grains. The presence of such relatively large amounts of water vapor on glass surfaces (and even metal surfaces, as will be mentioned in Chapter 9) means that, in experimenting at very low pressures, special care must be taken to remove water vapor by heating all parts to as high temperatures as possible with simultaneous absorption of the vapor in a liquid air trap or phosphorus pentoxide.

---

[73] *Proc. Roy. Soc. London*, **A**, **149**, 360 (1935).

[74] *Proc. Roy. Soc. London*, **A**, **160**, 254 (1937).

[75] A comprehensive review of this topic is given in the treatise entitled *The Properties of Glass*, by G. W. Morey (pp. 89–101), published by Reinhold Publishing Corporation, New York, 1938.

[76] *J. Phys. Chem.*, **9**, 617 (1905).

[77] *Wied. Ann.*, **27**, 481 (1886); **31**, 1006 (1887).

The evolution of water vapor and other gases from glass was investigated very extensively by I. Langmuir. His earlier work on the evolution of gas from the walls of bulbs, such as were used for incandescent lamps about that time, has been described by him in the following remarks:[78]

> On heating bulbs of 40-watt lamps for 3 hours to a temperature of 200° C, after having dried out the bulbs at room temperature for 24 hours by exposing in a good vacuum to a tube immersed in liquid air, the following average quantities of gas were given off:
>
> 200 cu mm water vapor
> 5 cu mm carbon dioxide
> 2 cu mm nitrogen
>
> These are the quantities of gas, liberated by the heating, expressed in cubic millimeters at room temperature and atmospheric pressure.
>
> By raising the temperature of the bulbs from 200° C to 350° C an additional quantity of water vapor was obtained, so that the total now became
>
> 300 cu mm water vapor
> 20 cu mm carbon dioxide
> 4 cu mm nitrogen
>
> A subsequent heating of the bulbs to 500° C caused the total amount of gas evolved to increase to
>
> 450 cu mm water vapor
> 30 cu mm carbon dioxide
> 5 cu mm nitrogen
>
> At each temperature the gas stopped coming off the glass after a half hour of heating, only to begin again whenever the temperature was raised to a higher value than that to which the bulb had been previously heated.
>
> It therefore seems that, even by heating the bulb to 500° C, not all of the water vapor can be removed, but it does seem probable that after this treatment the amount of water vapor that can come off a bulb at ordinary temperatures must be extremely small.
>
> The internal surface of this bulb was about 200 sq cm. The number of molecules of gas given off per sq cm was thus $56 \cdot 10^{15}$ molecules of H_2O; $37 \cdot 10^{15}$ molecules

---

[78] *Trans. Am. Inst. Elec. Eng.*, **32**, 1921 (1913), and *J. Am. Chem. Soc.*, **38**, 2221 (1916).

of CO_2, and $0.6 \cdot 10^{15}$ molecules of N_2. If we calculate the number of molecules of each of the gases necessary to cover a *square centimeter one molecule deep* (taking the molecules to be cubical in shape) we find $1.0 \cdot 10^{15}$ for H_2O; $0.77 \cdot 10^{15}$ for CO_2, and $0.67 \cdot 10^{15}$ for N_2. Thus the quantities of gas obtained from this bulb correspond to: a layer of water 55 molecules deep, a layer of carbon dioxide 4.8 molecules deep, and a layer of nitrogen 0.9 molecule deep.[79]

On the other hand Langmuir has observed[80] that microscope cover glasses (2.5 cm in diameter and 0.14 mm thick) previously heated to the softening point and then heated in vacuo gave off amounts corresponding to the following numbers of layers of molecules: 4.5 for water vapor, 1.05 for carbon dioxide, and 0.9 for nitrogen.[81] It will be observed that, for the last two gases, the amounts adsorbed corresponded to monolayers.

Langmuir also investigated the optimum conditions for the evolution of water vapor from glass. It was observed that certain lamps made of sodium magnesium borosilicate glass (G-702-P), and consisting of high-wattage filaments in very small bulbs, blackened very rapidly if they were baked out at 550–600° C during exhaust, while lamps baked out at 400–500° C did not blacken so rapidly. The effect was ascribed to water vapor evolved from the glass during the life of the lamp, and experiments were therefore undertaken to try to remedy this condition.

The following description of the experiments is taken from Langmuir's patent specifications.[82]

> Three lots of lamps were made with the same structural details and operating characteristics; the first lot was exhausted at approximately 450° C, the second lot at 550° C, and the third lot at 550° C, at first, and then at 400° C. The average life of the first lot was approximately 575 hours, of the second lot 300 hours, and of the third lot over 900 hours, the conditions of operation with all three lots being the same.

The explanation given of this result is as follows:

> Apparently the treatment at 400° C to 500° C liberates the water vapor only from a comparatively thin surface layer of the glass. If, however, the exhaust is continued at 400° C to 500° C, no more water vapor will be drawn out of the deeper layers, and that which remains in the surface layer will be liberated.

The main conclusion arrived at by Langmuir is that, in order to remove water vapor efficiently from the walls of glass vessels, the *heating during*

---

[79] These values are to be compared with those given in Table 7.25 for the number of molecules ($1/S_1$) required to form a monolayer. These are $0.95 \cdot 10^{15}$ for water vapor, $0.71 \cdot 10^{15}$ for carbon dioxide, and $0.73 \cdot 10^{15}$ for nitrogen.

[80] *J. Am. Chem. Soc.*, **40**, 1361 (1918).

[81] These values are of course, based on Langmuir's values for the number of molecules required to form a monolayer.

[82] Patent 1,273,629, July 23, 1918.

exhaust should be carried out in two or more stages of gradually decreasing temperatures. He found that ½-hour treatment at each of the above temperature ranges was sufficient, and he made the interesting observation, which is in accord with that made by Sherwood (see below), that, whereas the gas evolution at temperatures below 500° C practically

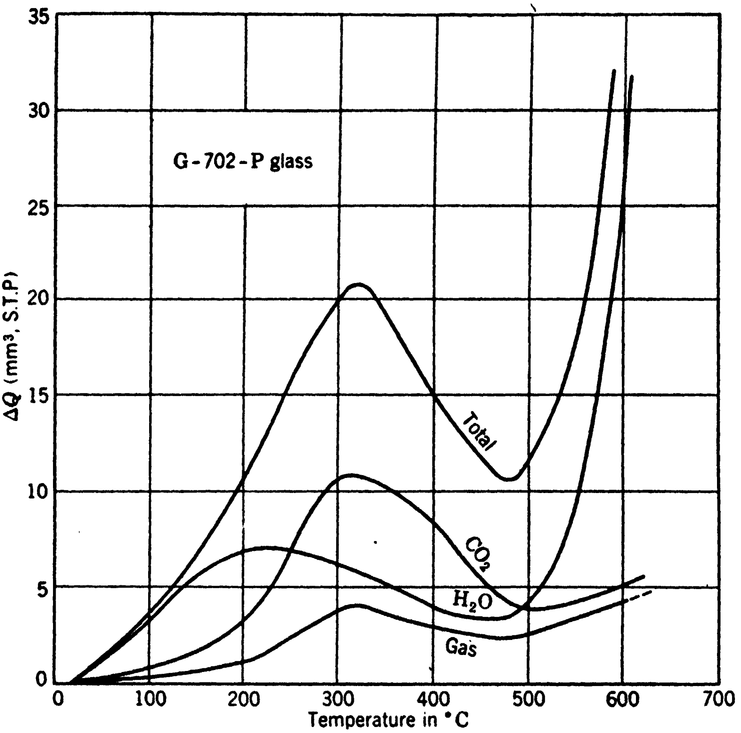

FIG. 15. Evolution of gas from Corning G-702-P glass, showing amount, ΔQ (mm^3 STP), liberated at a series of increasing temperatures (Sherwood). In this and the two subsequent figures, "gas" refers to the non-condensible volume (consisting of hydrogen, nitrogen, oxygen, and carbon monoxide).

ceases at the end of ½ hour, the evolution of water vapor at higher temperatures continues indefinitely no matter how long the heating period. Apparently the glass actually suffers a chemical decomposition at higher temperatures.

An extensive series of investigations on the gases and vapors evolved from glass was carried out by R. G. Sherwood[83] and J. E. Shrader.[84]

---

[83] *J. Am. Chem. Soc.*, **40**, 1645 (1918); *Phys. Rev.*, **12**, 448 (1918).

[84] *Phys. Rev.*, **13**, 434 (1919). See also abstract of a paper by D. Ulrey, *Phys. Rev.*, **14**, 160 (1919), which discusses the same subject.

Sherwood measured the amounts of water vapor, carbon dioxide, and gases non-condensible in liquid air liberated from different kinds of glass at various temperatures. Figure 15 shows the results obtained with Corning G-702-P glass—a high-melting-point glass used extensively in the manufacture of the gas-filled type of incandescent lamp. The samples of glass used in these measurements had a total area of about 350 cm^2, and the curves show the amounts of gas liberated at different temperatures. The period of heating at each temperature was 3 hours. Figures 16 and 17 show similar data with samples of soda glass and lead glass, respectively. It will be observed that in all samples the gas evolution first reaches a maximum which is at about 300° C for G-702-P, 150° C for soda glass, and 175° C for lead glass, then decreases, and again rises rapidly at a temperature which is above the softening point of the glass. Sherwood concluded that the products removed below 300° C are adsorbed gases, while at higher temperatures there is an actual

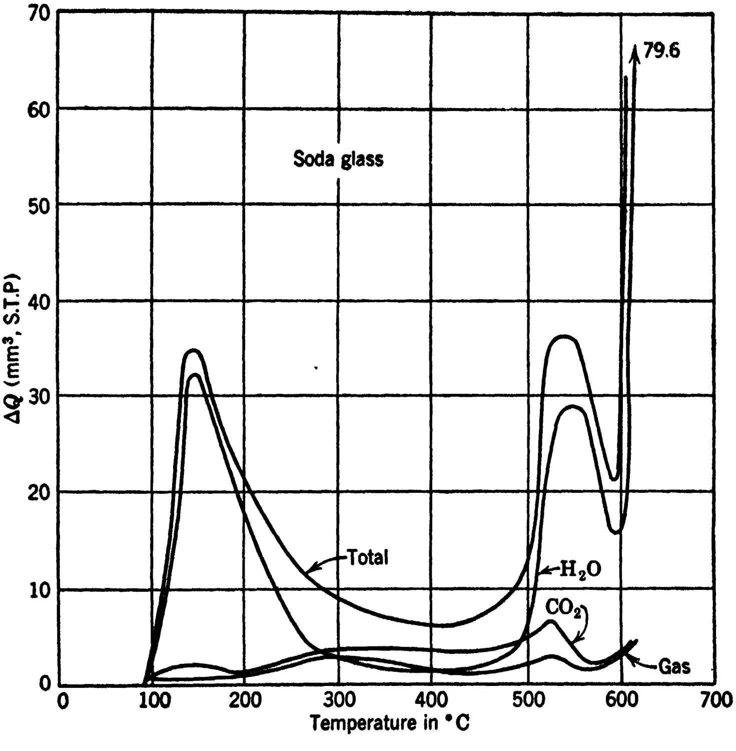

FIG. 16. Evolution of gas from soda glass (Sherwood).

decomposition of the glass itself. In other experiments, it was observed that at the higher temperatures the gas evolution continued even after the samples were heated for 24 hours and longer. By previously annealing the glass at very high temperatures, the subsequent gas evolution in vacuum was decreased considerably, a result in accord with certain observations made by Langmuir and mentioned before.

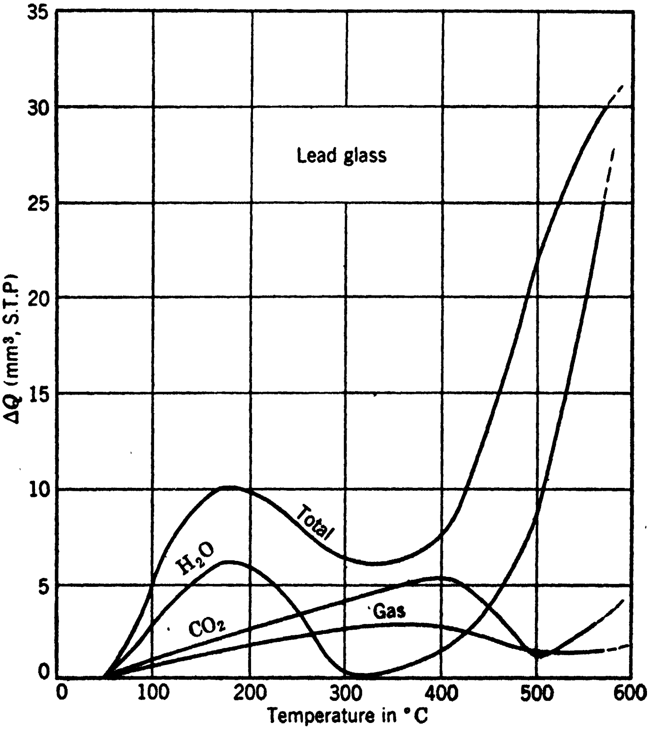

FIG. 17. Evolution of gas from ordinary lead glass (Sherwood).

Similar results have been obtained in this laboratory by Mrs. M. Andrews and J. Pangburn in investigating the gases evolved from lamp bulbs. Analyzing Sherwood's data, we find that, for instance, in the case of soda glass, the total gas evolved up to 200° C was about 50 mm^3, or about 0.15 mm^3/cm^2, most of which was H_2O; this would correspond to a layer of gas about four molecules deep. Sherwood concluded that the gases which are removed fairly rapidly at lower temperature are genuine adsorption products, as they correspond to quantities represented by a layer of gas that does not exceed one or two molecules in thickness. As the temperature of the glass is raised to the softening point, the gas evolved consists practically wholly of water vapor, and undoubtedly this arises, as mentioned above, from the chemical decomposition of the glass.

Investigations by C. A. Kidner and H. A. Huthsteiner, in this laboratory, on the rate of evolution of water vapor and non-condensible gases from glass bulbs have shown that, at the highest temperatures at which the exhausted bulb can be heated, most of the adsorbed gas is evolved in the first 2 or 3 minutes. Preheating in dry air is also beneficial in removing most of this adsorbed gas. The preheating at ordinary pressure possesses the advantage that the glass can be heated to much higher temperatures, as there is no danger of the bulb's sucking inward.

Some interesting measurements were carried out by Sherwood on the adsorption of water vapor and other gases by dry surfaces of glass. Dry air could be removed very rapidly at ordinary temperature, whereas for either moist air or air mixed with carbon dioxide, the rate of leakage at ordinary temperature was very slow. However, on heating to a high temperature practically all this adsorbed gas could be removed in a few minutes. It is interesting to observe that, in one experiment, after a pressure of about 10^{-4} mm H_2O had been reached by evacuation, the bulb (of about 9000 cm^3 capacity) was sealed off and after standing 10 hours the pressure rose to 0.0095 mm, owing to the gas leakage from the walls, but did not materially increase subsequently. This gas most probably was adsorbed air since it could not be condensed in liquid air. The writer's experience has shown that invariably there is a slight increase in pressure after the bulb is sealed off. Part of this increase is due to gases adsorbed on the glass near the constriction, which is heated to a high temperature during sealing off, and a portion is due to gradual leakage from the walls. Even with the utmost precaution in baking out at high temperature and low exhaust pressure, there is always a slight increase in pressure in the sealed-off device.

In an investigation on the minimum pressure attainable with a Gaede molecular pump, Dushman observed[85] that unless care was taken to torch[86] the tubing connecting the gauge to the pump it was impossible to

[85] *Phys. Rev.*, **5**, 212 (1915).

[86] In *Rev. Sci. Instruments*, **18**, 856 (1947), J. Rothstein has drawn attention to the use of silver chloride as a temperature indicator for hand torching in high-vacuum work. Some silver chloride is fused to the glass to form a thin layer. "When solid, the silver chloride has a dull, opaque, whitish matte appearance, which becomes successively dark, shiny, and transparent when fusion occurs" at 455° C.

It is of interest to mention in this connection that in the production of vacuum incandescent tungsten lamps certain organic compounds were frequently coated on the button of the glass stem supporting the filament to indicate by the change in get below about 0.025 micron, because of the slow evolution of water vapor at ordinary temperature. When, however, the tubing was baked out at 330° C, the pressure could be reduced to $5 \cdot 10^{-4}$ micron. Similar results have been reported by Shrader. The volume of the system exhausted in his experiments was about 2 liters. The effect of heat treatment on the vacuum obtainable after pumping until equilibrium was reached at that temperature is shown by the following results:

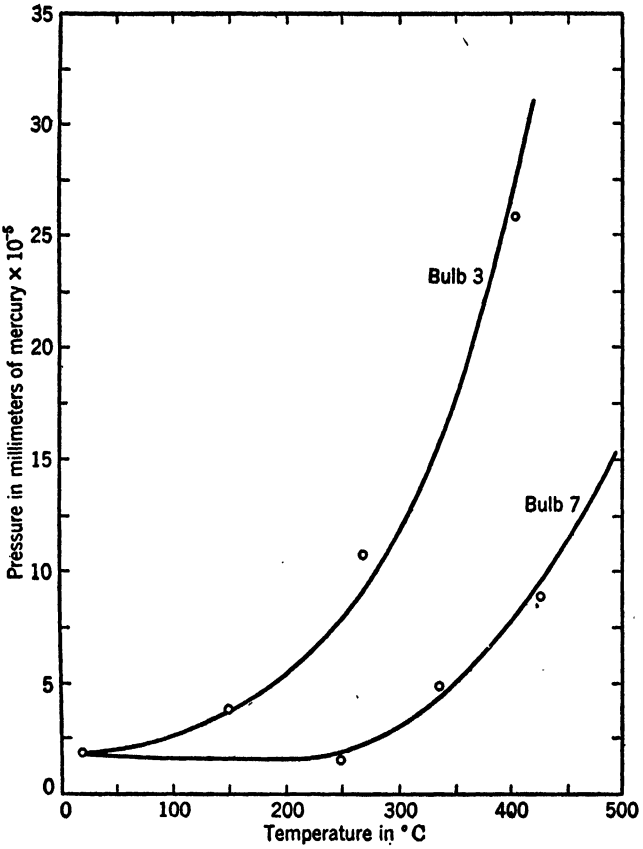

FIG. 18. Increase in pressure in sealed-off, well-evacuated bulb after reheating at a series of increasing temperatures (Shrader).

---

color the maximum temperature attained inside the bulb during bake-out on the pump. The composition of the coating used varied with the range of temperatures to be indicated.

Temperature, °C:	20	100	200	300	500
P_{mm}:	$1 \cdot 10^{-5}$	$1.9 \cdot 10^{-6}$	$1.7 \cdot 10^{-7}$	$1.2 \cdot 10^{-7}$	$2.4 \cdot 10^{-8}$

Shrader also observed that not only does the vacuum in sealed vessels gradually deteriorate with time, at first rapidly and then more slowly, but also that "subsequent heating even at temperatures lower than the heat-treating temperature (on the pump) results in increase of pressure due to further liberation of gases and vapors from the glass." Figure 18 shows the effect of heating a sealed-off system consisting of a 1500 cm^3 bulb and gauge of 500 cm^3 capacity for 1 hour at increasing successive temperatures. In each case the bulbs had previously been heated at 500° C on the pump.

A comprehensive investigation has been carried out by J. E. Harris and E. E. Schumacher[87] on the relation between chemical composition of glasses and the gas evolution on heating to 400–500° C. Table 23 gives a list of the types of glass used and their chemical composition in per cent by weight of each constituent.

TABLE 23

CHEMICAL ANALYSES OF THE GLASSES USED FOR DETERMINATION OF AMOUNT AND COMPOSITION OF GASES EVOLVED (HARRIS AND SCHUMACHER)

	1	2	3	4	5	6
SiO_2	69.93	69.40	64.64	61.50	72.05	65.47
Al_2O_3	1.54	0.78	0.20	0.57	2.21	2.99
Fe_2O_3	0.19	0.14	0.04	0.11	0.05	0.51
PbO	1.44	Trace	21.66	22.55	6.11	20.20
CaO	3.17	5.15	0.02	0.21	0.06	0.22
MgO	0.03	4.09	0.02	0.36	0.09	0.13
Na_2O	21.02	16.67	9.10	8.14	4.23	6.40
K_2O	0.10	0.20	3.20	3.76	1.12	3.59
P_2O_5	0.08	0.16	0.75	0.34	Trace	Trace
Sb_2O_3	0.05	0.10	—	Trace	—	—
MnO_2	0.09	0.19	—	0.19	0.01	0.073
B_2O_3	2.36	3.12	0.37	2.27	14.07	—

The B_2O_3 was determined by difference. Glasses 3 and 5 contained traces of fluorine, and glass 6 contained 0.013 per cent sulfur trioxide as well as a trace of barium oxide. Glasses 1 and 2 are soda-lime glasses; 3, 4, and 6 are soda-lead glasses; and 5 is a borosilicate of lead and soda.

The procedure for determining the gas evolution is described by the authors as follows:

> For the purpose of determining the amount of gases given up by the various types of glass, the glass was first cleaned with chromic acid, and washed thoroughly with

---

[87] *J. Ind. Eng. Chem.*, **15**, 174 (1923).

water. It was then placed in the sample container, made of the same glass as that being tested—and the pump operated for several hours in order to dry the sample thoroughly. The pump—a mercury-vapor pump in conjunction with two oil pumps—was operated until the pressure within the apparatus after being trapped off from the pump remained constant at about 1 · 10^{-6} mm for a period of at least 2 hr. The glass was then heated to a temperature as close to the softening range as it was possible to go without causing the container to collapse; it was kept at this temperature until the gas pressure became constant, when the volumes of the gases were determined in the manner outlined above. The period required for completely driving off the gases ranged from 65 to 80 hr.

The temperature to which the glasses were heated was 500° C for sample 5, and 400° C for all the other samples. The amount and composition of the gas evolved in each case are shown in Table 24.

TABLE 24

AMOUNT* AND COMPOSITION OF GASES EVOLVED DURING HEAT TREATMENT IN VACUUM (HARRIS AND SCHUMACHER)

Sample	% Total Alkali	Composition of Gas, %			Atm · cm^3 · 10^4 per cm^2 area	Atm · cm^3 · 10^4 per cm^3 glass
1	21.12	H_2O	88.5		46.6	726
		CO_2	10.5		5.5	86
		P.G.†	1.0		0.5	8
				Total	52.6	820
2	16.87	H_2O	92.6		30.0	508
		CO_2	6.3		2.0	34
		P.G.	1.1		0.4	6
				Total	32.4	548
3	12.30	H_2O	96.4		23.7	506
		CO_2	2.2		0.5	11
		P.G.	1.4		0.4	8
				Total	24.6	525
4	11.90	H_2O	97.2		25.4	568
		CO_2	1.4		0.4	8
		P.G.	1.4		0.4	8
				Total	26.2	584
5	5.35	H_2O	33.3		0.6	12
		CO_2	44.5		0.9	16
		P.G.	22.2		0.4	8
				Total	1.9	36
6	9.99	H_2O	49.6		1.0	19
		CO_2	49.6		1.0	19
		P.G.	0.8		0.02	0.3
				Total	2.02	38.3

* 10^{-3} atm · cm^3 = 0.76 μ · liter.

† P.G. = Non-condensible at − 190° C.

For both carbon dioxide and water vapor, the volume of gas (S.T.P.) required for a monolayer is about $2 \cdot 10^{-5}$ cm^3/cm^2 while for oxygen, nitrogen, and carbon monoxide it is about $3 \cdot 10^{-5}$ cm^3/cm^2 (as shown in Table 7.25). The data in Table 24 indicate that the non-condensible gas must have been present as an adsorbed layer approximately one molecule thick.

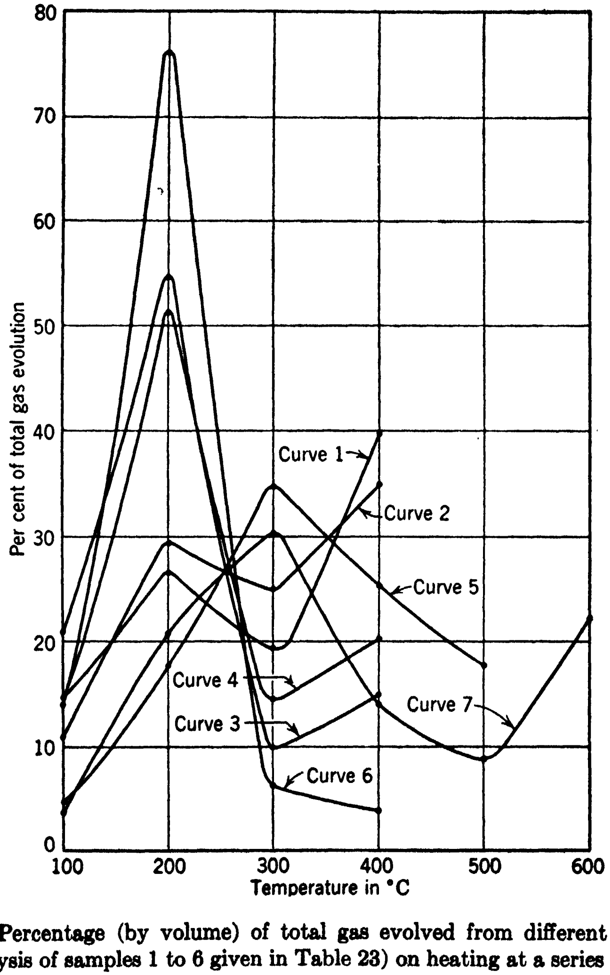

FIG. 19. Percentage (by volume) of total gas evolved from different samples of glass (analysis of samples 1 to 6 given in Table 23) on heating at a series of temperatures. Curve 7 is for a sample of Pyrex. (Harris and Schumacher.)

Although it would appear from the table that the gas content decreases with decreasing alkali content, there are other factors that affect the gas content. For instance, glass 6 had been subjected to a heat treatment of between 1500° C and 1600° C for a period of 1 hour.

Arranged in order of increasing temperature at which the glass begins to soften, glasses 3, 4, and 6 would be lowest, 5 highest, and 1 and 2 would be intermediate.[88] Thus the fact that glass 5 "undoubtedly received a higher heat treatment in the melting process, because of its higher melting point and greater viscosity, than did the other glasses that were tested," would account for its low gas content.

A further set of experiments was carried out in which the pressures of the gases evolved were measured at intervals of 100° C, from 100° C to the softening point of the glass. The results of these experiments are shown in Fig. 19. The numbers on the curves refer to the corresponding numbers of the glass samples. (See Table 23.) A run made with Pyrex glass is shown as curve 7. This is a borosilicate glass that is "practically free from alkali and heavy metals."

> It is seen [the investigators state] that the *adsorbed*[89] gases for the lime and lead glasses are practically all given up at a temperature of 200° C, while 300° C is required in the case of the borosilicate glasses. The *absorbed* gases begin to come off at the softening points of the various glasses, 400° C for the lead and lime glasses, and 600° C for the borosilicate glasses. ... In this connection it should be stated that the amount of absorbed gases found in the above experiments represents only that portion of the dissolved gases which lies nearest the surface of the glass. Owing to the great viscosity of the glass at the temperatures used, the rate of diffusion of the gas would be altogether too slow to permit any considerable portion to reach the surface.

To obtain further data on the volumes *adsorbed*, "the glasses were heated to a temperature high enough to drive off all the adsorbed gases, as indicated by the curves in Fig. 19 (200° C for curves 1, 2, 3, and 4, and 300° for 5) and the amount of carbon dioxide and permanent gases determined." The results are shown in Table 25.

TABLE 25

AMOUNTS* OF CO_2 AND NON-CONDENSIBLE GASES ADSORBED BY DIFFERENT SAMPLES OF GLASS (HARRIS AND SCHUMACHER)

Glass No.	Volume in 10^{-5} cm^3/cm^2 of Adsorbed CO_2	Volume in 10^{-5} cm^3/cm^2 of Adsorbed Non-Condensible Gas
1	19.3	1.300
2	10.4	1.800
3	7.5	2.650
4	7.5	2.350
5	4.5	0.480
6	6.5	0.009

* 10^{-4} atm · cm^3 = 0.076 μ · liter.

---

[88] Personal communication from Dr. L. Navias of this laboratory.

[89] Italicized by the writer.

The authors summarized the results of their investigation as follows:

1. Glasses whose compositions run high in alkali give off more gas during their heat treatment than do those of lower alkali content.
2. A definite relation appears to exist between the amount of water vapor held by a glass and its alkali content.
3. A relation, although not as pronounced as that mentioned above, appears to exist between the amount of carbon dioxide held by a glass and its alkali content.
4. Adsorbed carbon dioxide seems to be held to glass primarily by primary valence forces.
5. Adsorbed permanent gases seem to be held to glass primarily by secondary valence forces.
6. Glass relatively free from adsorbed gas can be produced by means of heating the glass during its melting process to a sufficiently high temperature.

More recent results obtained by C. H. Cartwright on three types of glass are shown in Figs. 20, 21, and 22.[90]

The samples used are described as follows:

1. Glass 0080, Corning brand, clear lime bulb glass.
2. Glass 7740, Pyrex brand, heat-resistant clear chemical glass.
3. Glass 7910, Vycor brand, 96 per cent silica, ultra violet-transmitting glass.[91]

Figure 20 shows the amounts of gas[92] (in $mm \cdot cm^3/100$ cm^2 of surface at 25° C) evolved from glasses 0080 and 7740 as a function of the temperature.

Only one glass sample was used in obtaining each curve and that sample was heated for 1 hour at each of the temperatures indicated. The curves show a maximum at 150° C and increased evolution at the strain point. This is in agreement with the work of Sherwood and of Harris and Schumacher.

The rate curves shown in Fig. 21 were calculated from the results obtained in 008—run 1. As will be observed, these curves show that on baking out at constant temperature most of the gas is evolved very quickly.

Figure 22 compares the gas evolution from glass 0080 and glass 7910. The comparatively small gas evolution from 7910 is no doubt due to the fact that this glass is fined at high temperatures.

One further important observation made in this investigation was that "heating the lime glass to 500° C at atmospheric pressure re-

---

[90] The writer wishes to express his indebtedness for this information to Dr. J. T. Littleton, Director of the Research Laboratory of the Corning Glass Works, and Dr. B. J. Todd, who prepared the summary and the plots shown in the three figures mentioned above.

[91] According to L. Navias and R. L. Green, *J. Am. Ceram. Soc.*, **29**, 267 (1946), this glass contains 3 per cent B_2O_3 and a "very low" content of Na_2O.

[92] $1 \text{ mm} \cdot \text{cm}^3 = 1\ \mu \cdot \text{liter}$,
$1 \text{ mm} \cdot \text{cm}^3/10^2 \text{ cm}^2 = 0.01\ \mu \cdot \text{liter/cm}^2$.

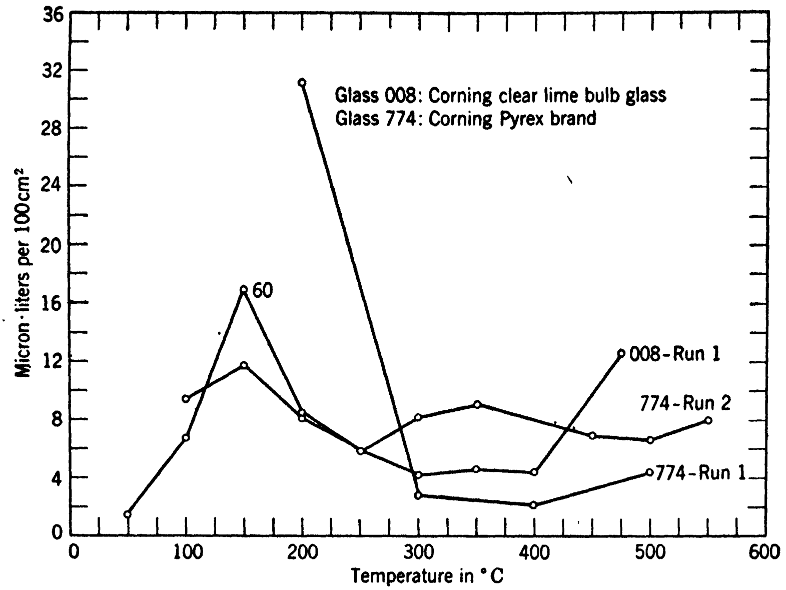

FIG. 20. Amounts of gas evolved from two samples of glass as a function of the temperature (Cartwright).

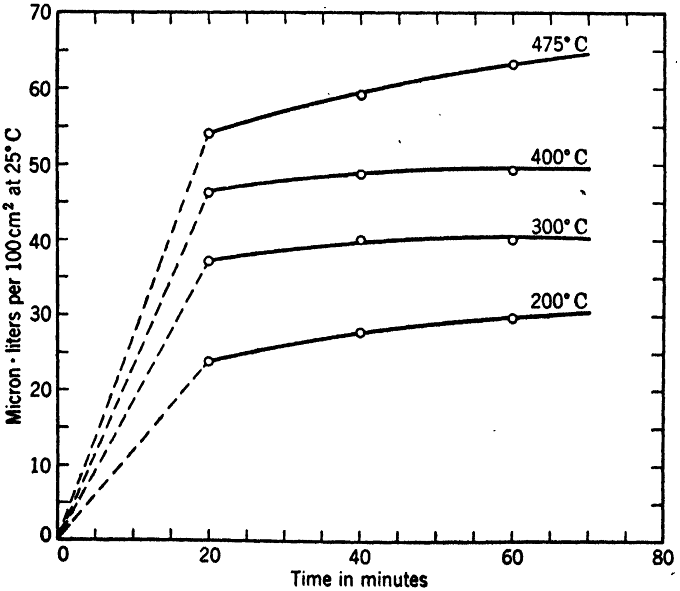

FIG. 21. Rate curves derived from plot in Fig. 20 for glass 008 (Cartwright).

moves 80–90 per cent of the gas that would otherwise be evolved in the bake out." This observation has been confirmed repeatedly by similar observations in this laboratory.

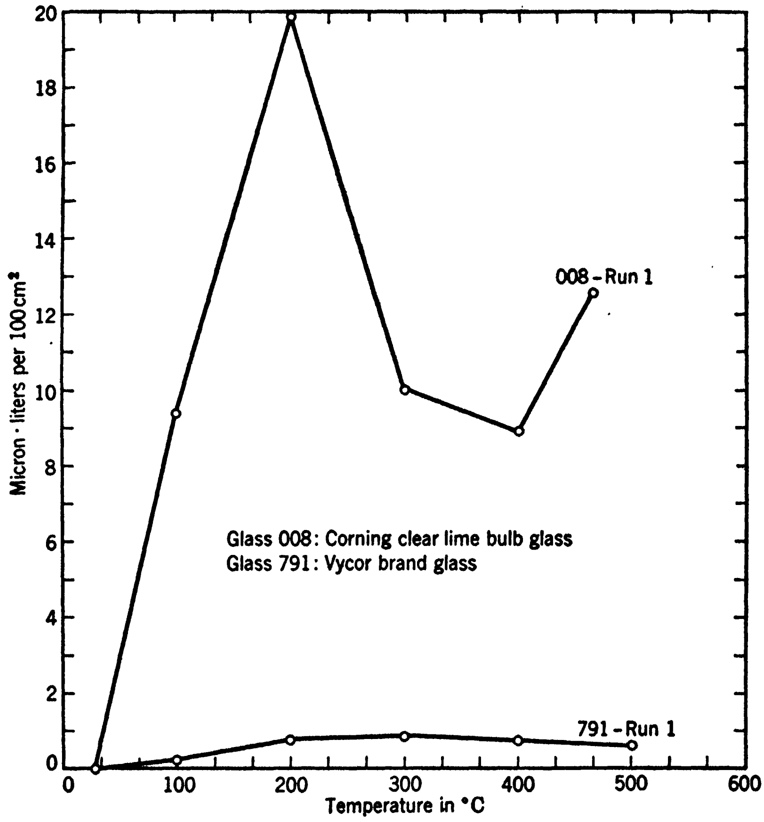

FIG. 22. Comparison of gas evolution as a function of the temperature for a Corning brand lime glass (008) and Vycor brand glass (791) (Cartwright).

G. W. Morey[93] states that

> the volatile substances found in solution in glass are all components of the original batch: water, in combination as hydroxides or hydrated salts, or as "wet" batch; carbon dioxide in combination as carbonates; oxygen, in combination as nitrate or introduced mechanically as entrapped air; sulfur dioxide introduced as sodium sulfate; and nitrogen, from entrapped air. During the melting of the glass, these substances are given off in large quantities; that which remains in the glass is only a small proportion of that introduced into the batch.

---

[93] *Op. cit.*

As shown by P. Niggli,[94] the amount of gas in solution in the glass depends on the temperature of treatment, the pressure of each gas in the atmosphere above the melt, and the composition of the glass.

E. W. Washburn, F. F. Footitt, and E. N. Bunting[95] found that glass molten in vacuum gave off amounts of different gases which are shown in Table 26.

TABLE 26

AMOUNT AND COMPOSITION OF DISSOLVED GASES IN FINISHED GLASS

Glass	Weight Per Cent				Volume in cm³ (S.T.P.) per 100 g			
	O_2	CO_2	N_2	Total	O_2	CO_2	N_2	Total
Barium flint 1	0.035	0.011		0.046	24.5	8.8		33.3
Barium flint 2	.015	.0045		.020	10.5	3.6		14.1
Light flint	.0045	.014	0.0025	.21	3.2	11.2	2.0	16.4
Borosilicate	.0036	.0035	.0031	.010	2.5	2.8	2.5	7.8
Water at 0° C					5.15	179.2	2.24	

The last four columns give the volumes in cubic centimeters at 0° C and 760 mm pressure, per 100 g of glass. The solubilities in water at 0° C are given for comparison at the bottom of the table. It is evident that the amounts of gases dissolved in molten glass are considerable. Compared with the volumes of gases actually evolved from glass vessels in high-vacuum exhaust, even at the highest temperatures practicable, the volumes observed for molten glass are much larger. This probably accounts to some extent for the observed increases in pressure in sealed-off glass vessels.

R. H. Dalton[96] devised an apparatus for analyzing the gases evolved from glass at 1400° C. Table 27 gives the amount and composition of the gas from several commercial glasses, and from one experimental glass, No. 8, containing an unusually large amount of arsenic. The third column gives the volume in cubic centimeters (S.T.P.) per gram of glass.

Table 28 summarizes observations made by C. Hahner, G. Q. Voigt, and A. N. Finn[97] on different glasses at the temperatures shown in the

---

[94] *J. Am. Chem. Soc.*, **35**, 1693 (1913).

[95] *Univ. Illinois Eng. Expt. Sta. Bull.* 118 (1920).

[96] *J. Am. Ceram. Soc.*, 16, 425 (1933); *J. Am. Chem. Soc.*, **57**, 2150 (1935). G. W. Morey, *op. cit.*, p. 100.

[97] *J. Research Natl. Bur. Standards*, **19**, 95 (1937).

TABLE 27

VOLUME AND COMPOSITION OF GASES EVOLVED FROM GLASS AT 1400° C (DALTON)

No.	Glass Type	v_0	Percentage Composition of Gases*				
			H_2O	SO_2	CO_2	O_2	R
1	Barium (optical)	0.71	23		38.5	38.5	0.1
2	Soda-lime (milk bottle)	0.93	51	33.5	3	11.5	0.1
3	Borosilicate (heat-resistant)	0.40	91.5		5	3.5	
4	Soda-lime (bulb)	0.90	44	35.5	5.75	14.5	
5	Borosilicate (heat-resistant)	0.36	90.5	0.3	3.5	6	
6	Borosilicate (bulb)	0.74	94	2.5	3	3.25	
7	Lead (sign tubing)	0.70	36	8	0.7	56.5	
8	Soda-lime (experimental)	1.41	28	10	8	63	
9	Borosilicate (heat-resistant)	0.44	93	2	4	4	

* The values given are, in each case, the average values of two sets of determinations given in the original paper. The symbol R refers to nitrogen and other noncondensible gases.

second column. The first group includes optical glasses; the second group, commercial glasses. The last column, headed As, refers to the total percentages of As_2O_3 and As_2O_5. (The original table gives the separate values for each of these oxides.) The term R_2O_3 refers to oxides of aluminum, iron, etc. The light barium crown C also contained 0.5 per cent Sb_2O_3. The last sample was analyzed only for SO_3.

In Tables 23, 27, and 28 the compositions have been given for a number of types of glass, in connection with the amount and composition of gases evolved on heating to high temperatures. It is therefore of interest to note the data in Table 29, for the chemical composition (per cent by weight) of glasses used in high-vacuum devices, taken from a paper by R. W. Douglas[98] dealing with the thermal, mechanical and electrical properties of these glasses.

The customary classification and applications are described as follows:

A, B, and C are *soft soda glasses,* used in lamp and radio tubes, also in tubing for neon sign lights.

D, E, F, and G are *hard borosilicate glasses,* used in high-wattage lamps and vacuum tubes, also in vapor stream pumps and in chemical apparatus.

H and I are *lead glasses,* used in vacuum seals of lamps and tubes.

J and K are *extra hard* glasses, used in mercury-vapor discharge lamps.

L refers to a special glass used in sodium-vapor lamps because of its resistance to chemical attack by sodium.

---

[98] *J. Sci. Instruments,* **22,** 81 (1945).

TABLE 28

VOLUME* AND COMPOSITION OF GASES FROM GLASSES AND COMPOSITIONS OF THE GLASSES

	t° C	Volume per 100 g of Glass			Percentage Composition of Glass							
		H_2O	$O_2 + R$†	$CO_2 + SO_2$	SiO_2	Na_2O	K_2O	CaO	ZnO	BaO	B_2O_3	As
Borosilicate crown A	1325	49	0.2	<0.1	65.6	7.91	12.8	—	1.8	—	11.4	0.43
Borosilicate crown B	1345	29	0	0	65.6	7.9	12.8	—	1.8	—	11.4	.5
Light barium crown A	1350	20	1.0	0	47.1	1.9	7.7	2.1	8.5	27.9	4.3	.54
	1325	31	0.8	0								
Light barium crown B	1345	21	1.2	0.7	46.6	0.5	7.1	—	7.8	33.7	3.7	.6
Light barium crown C	1345	17	1.1	<0.1	46.9	0.5	7.1	—	7.8	33.2	3.7	.2
Light crown A	1300	33	1.7	4.0	71.0	15.4	—	13.1	—	—	—	.32
Light crown B	1350	38	5.4	4.1	71.0	15.4	—	13.1	—	—	—	.5
					SiO_2	Na_2O	K_2O	CaO	MgO	SO_3	R_2O_3	
Window glass A	1345	16	10.2	43.1	72.1	13.5	—	10.0	3.3	0.35	0.7	
Window glass B	1345	28	17.1	17.0	72.6	15.0	—	8.0	3.6	.47	0.7	
Window glass C	1345	22	32.5	26.6	73.1	12.4	0.1	13.3	0.3	.44	1.0	
Window glass D	1345	26	22.2	51.2	70.9	12.2	.1	11.2	4.4	.41	0.9	
Window glass E	1345	32	7.9	40.2	71.5	15.0	.2	10.6	1.8	.45	.9	
Window glass F	1345	26	3.3	40.4	72.3	15.1	.3	10.0	1.0	.50	.6	
Soda-lime tubing	1345	23	3.0	14.0	—	—	—	—	—	.19	—	

* Volume in cm^3 (S.T.P.).

† The symbol R refers to other non-condensible gases.

TABLE 29

Chemical Composition of Glasses Used in High-Vacuum Devices

Type	SiO_2	Al_2O_3	B_2O_3	PbO	CaO	MgO	Na_2O	K_2O	BaO
A	70.5	1.8	—	—	6.7	3.4	16.7	0.8	—
B	69.0	4.0	—	—	5.8	1.6	17.5	1.9	—
C	69.3	3.1	1.2	—	5.6	3.4	16.8	0.6	—
D	80.1	3.0	12.0	—	0.2	—	3.9	0.3	—
E	80.6	2.7	12.2	—	—	—	4.2	—	—
F	71.0	7.4	13.7	—	0.3	—	5.3	2.4	—
G	71.6	5.7	11.0	—	3.6	0.6	3.5	3.9	—
H	56.5	1.5	—	29.0	0.2	0.6	5.6	6.6	—
I	57.0	1.5	—	29.4	0.2	0.4	4.1	7.3	—
J	54.5	21.1	7.4	—	13.5	—	—	—	3.5
K	58.7	22.4	3.0	—	5.9	8.4	1.1	0.2	—
L	22.6	23.7	37.0	—	10.0	—	6.5	0.2	—

Adsorption on Glass. The observations made by Langmuir on adsorption, at liquid-air temperatures, of carbon monoxide, argon, oxygen, methane, and nitrogen, on well-desorbed surfaces of glass have been summarized in Table 7.11. As will be observed, the values of α, the fraction of the surface covered with a monolayer, ranged from 0.123 for oxygen to 0.545 for methane.

H. Zeise[99] repeated Langmuir's experiments, using much larger surfaces of glass microscope covers, which were heated in vacuum for 2½ hours at 420° C, and for an hour longer at 420° C to 450° C. The adsorption isotherms were observed at very low pressures (in the range of 10^{-2} mm and lower) at 90° K. Zeise found that though the results could not be represented satisfactorily by the hyperbolic equation, they did satisfy a relation of the form

$$q = \sqrt{\frac{k_1 k_2 P}{1 + k_2 P}}, \tag{1}$$

where q = number of moles per unit area.

Hence, the volume adsorbed per square centimeter at saturation, v_s, is given by the relation

$$v_s = 22{,}415\sqrt{k_1} \quad \text{cm}^3 \text{ (S.T.P.)}, \tag{2}$$

---

[99] *Z. physik. Chem.*, **136**, 385 (1928). See discussion of this work in Chapter 7.

and α, the fraction of the surface covered, by the relation

$$\alpha = 22{,}415 \frac{\sqrt{k_1}}{(v_0)_s} \tag{3}$$

where $(v_0)_s$ is the volume corresponding to a layer one molecule thick. (See row 11, Table 7.25.)

Table 30 gives the values of k_1 observed by Zeise from which have been calculated the values of v_s and α.

TABLE 30

ADSORPTION ON PLANE GLASS SURFACES AT 90° K (ZEISE)

Gas	$10^{19}k_1$	$10^5 v_s$	$10^5 (v_0)_s$	α
CH_4	7.59	1.953	2.48	0.79
	7.21	1.903		.77
	7.86	1.987		.80
N_2	1.70	0.924	2.70	.34
	1.88	0.972		.36
O_2	1.24	0.789	3.07	.26
	0.63	0.561		.18
H_2		(0.35)	(5)	(.07)

The adsorption data for hydrogen were not sufficiently reliable to obtain a satisfactory value for k_1, but by comparison with the observations for oxygen it may be concluded that v_s was approximately the value given in parentheses. As shown in the last column, the values deduced for α are less than unity and are of the same order as those observed by Langmuir.

F. Durau[100] investigated the adsorption on carefully dried and evacuated glass powder. Even after treatment in vacuum at 570° C, the powder continued to give off gas at higher temperatures (up to 1060° C). At each temperature an equilibrium was reached at which the gas evolution was practically zero. After the high-temperature treatment the powder did not adsorb nitrogen, hydrogen, or dry air at 18° C. It was observed that carbon dioxide was adsorbed, but only to the extent of 16.4 per cent of the surface at 1 atm pressure. The surface area of the powder was determined from measurements of the adsorption of dyes.[101]

The sorption of water vapor by glass has been investigated by I. R. McHaffie and S. Lehner[102] by a method which, as Brunauer describes it, consists simply in measuring at different temperatures the pressure of a known amount of vapor enclosed in a vessel of known volume and known surface area. At the lower temperatures part of the vapor must be in the liquid form, at the higher temperature all must be in the gaseous state.

---

[100] *Z. Physik*, **37**, 419 (1926).

[101] See description of this method in SB, p. 277; McB, p. 334.

[102] *J. Chem. Soc.*, **127**, 1559 (1925); *J. Phys. Chem.*, **31**, 719 (1927); see SB, p. 320; McB, p. 225, for detailed discussion.

At these higher temperatures the pressure decreases linearly with decrease in temperature; at the lower temperatures, the pressure will correspond to that of the saturation vapor pressure of the liquid. When adsorption occurs, the transition in the plot of P versus T from the high-temperature to the low-temperature range will not be sharp, but gradual.

From their observations, McHaffie and Lehner arrived at the following conclusion: For values of P/P_0 less than about 0.7, the number of molecular layers adsorbed is one or less; but as P is increased and approaches P_0 the number of layers increases rapidly and approaches a value of the order of 100.

J. C. W. Frazer, W. A. Patrick, and H. E. Smith[103] have, however, criticized this conclusion because of the fact that McHaffie and Lehner had used glass washed with chromic acid. This undoubtedly increased the effective surface area manyfold. For instance, P. H. Emmett[104] found by the method of nitrogen adsorption that washing small glass spheres with chromic acid increased their surface by 40 per cent. Similar observations have been made by H. S. Frank[105] in the case of Pyrex glass treated with chromic acid cleaning solution. But, even if the actual quantitative data obtained by McHaffie and Lehner are in error, it may be concluded from their observations and from those made by J. H. Frazer[106] that, for relatively large values of P/P_0, the adsorbed layers of water are many molecular diameters thick.

The low-pressure adsorption of water vapor on glass, at 25° C, has been measured by H. S. Frank.[107] As mentioned above, the Pyrex surface was treated with chromic acid and then washed with distilled water and evacuated at ordinary temperature. Water vapor was then let in at low pressure, and the equilibrium pressure was determined as well as the amount adsorbed. The observations are summarized in Table 31. The volume in cubic centimeters (S.T.P.) per square centimeter is denoted by v_0.

The last column gives the thickness of the adsorbed layer in molecular diameters. That is,[108]

---

[103] *J. Phys. Chem.*, **31**, 897 (1927).

[104] See E. O. Kraemer, *Advances in Colloid Science*, Chapter I, Interscience Publishers, New York, 1942.

[105] *J. Phys. Chem.*, **33**, 970 (1929).

[106] *Phys. Rev.*, **33**, 970 (1929).

[107] *Loc. cit.*

$$n = 10^5 \frac{v_0}{3.54}. \tag{4}$$

Assuming that the effective surface was greater than that calculated from the geometrical dimensions, these results are entirely compatible with the conclusion that the adsorbed water formed a layer that did not exceed about one molecule in thickness.

TABLE 31

ADSORPTION OF WATER VAPOR BY GLASS AT 25° C

P_μ	$10^5 v_0$	n
5.2	1.157	0.327
13.4	2.201	0.622
46.2	4.340	1.226
64.8	5.231	1.478
87.0	5.969	1.686

Of interest are some observations made by J. J. Manley[109] on what he has designated as primary and secondary adsorption skins. As has been observed repeatedly, in a sealed-off system which has previously been evacuated thoroughly, a small gas evolution continues for months. The rate of this evolution decreases with time and finally reaches an extremely low value. Such a system was left undisturbed for 3 years. Then tin foil was put on the outside of the bulb and connected to one pole of an induction coil. Current was passed through the glass for 5 minutes, and this procedure was repeated ten times. The bulb was filled with a bright glow during discharge, and at the end of the experiment the volume of gas evolved corresponded to a layer approximately 20 molecules thick.

From this observation Manley concludes that

> in addition to the skin removable by pumping and termed a *secondary* skin, the glass possesses a *primary* and far more permanent one. . . . From my experiments it appears (1) that a nude surface, when brought into contact with a gas, first acquires a true, permanent and primary skin which under all conditions is retained even in the presence of high vacua; and (2) that the completed primary skin adsorbs a quantity of its parent gas in much the same way as solids in general do. According to this view the skin which I have termed secondary is not a true skin, but a certain mass of gas which varies with temperature, pressure, etc., condensed upon and commingled with the molecular groups forming the true and primary skin.

---

[108] The values of n thus deduced are less than those given by Frank because of the different value of molecular cross section used by the writer.

[109] *Proc. Phys. Soc. London*, **36**, 288 (1924).

The method used by Manley in denuding the glass surface is closely allied to that of electrical clean-up of gases, which is discussed in Chapter 10.

Finally, observations made by H. C. Hamaker, H. Bruining, and A. H. W. Aten, Jr.,[110] on a very probable cause of slumping of oxide cathodes in vacuum tubes should be mentioned. According to these investigators there is a slow evolution of hydrogen chloride from glass heated to 400° C, due to the reaction

$$2NaCl + SiO_2 + H_2O \rightarrow 2HCl + Na_2SiO_3.$$

The hydrogen chloride reacts with the carbonates or oxides on the cathode to form the corresponding chlorides.

> When the cathode is subsequently heated these chlorides evaporate and condense on the grid and the anode. Under electron bombardment these chlorides decompose, thereby producing chlorine atoms or positive chlorine ions which poison the cathode emission in a very pronounced way.

The sodium chloride is introduced in the manufacture of glass as a slight impurity in the sodium carbonate. The reaction between the salt and water vapor occurs "on a production scale" at red to dull-red temperatures. But at 400° C hydrogen chloride is evolved at a sufficient rate to produce the poisoning effect mentioned above. However, if the temperature of the glass during bake-out on the pump is not raised to much above 200° C, the rate of reaction is decreased enormously. The authors have observed that, in order to prevent the deleterious effects of hydrogen chloride on the cathode, "a large patch of barium carbonate somewhere in the bulb proved effective" as well as "evaporation of some of the barium getter before baking-out or rinsing the interior of the bulb with caustic potash solution before sealing-in."

7. DIFFUSION OF GASES THROUGH QUARTZ AND GLASSES[111]

It has been observed that thin-walled vessels of quartz or glass are permeable to helium, hydrogen, and a few other gases, especially at higher temperatures.

Let q denote the *volume in cubic centimeters* (S.T.P.) flowing through the wall, *per square centimeter per second.* Since q varies linearly with the pressure of the gas,[112] and inversely as the wall thickness, d, we can express these relations in the form

---

[110] *Philips Research Repts.*, 2, 171 (1947).

[111] The discussion in this section is based largely on the comprehensive review of the topic by R. M. Barrer, *Diffusion In and Through Solids*, pp. 117–143, The Macmillan Company, New York, 1941. This reference is designated RB. See also discussion of diffusion of gases in metals in Chapter 9, section 10.

$$q = \frac{KP}{d}, \tag{1}$$

where K is designated the *permeability.* In the literature on this topic P is usually expressed in centimeters of mercury (as P_{cm}), and d in millimeters. Hence K denotes *the volume in cubic centimeters* ($S.T.P.$) *per second per square centimeter, per millimeter thickness, per centimeter pressure.*

The value of K increases rapidly with increase in T, and it has been observed that it is possible to express K as a function of T by means of the relation

$$K = K_0 \epsilon^{-E/R_0T}, \tag{2}$$

where E is the activation energy for the reaction, expressed in calories per mole. The last equation can be written in the form

$$\log K = A - \frac{B}{T}, \tag{3}$$

where

$$A = \log K_0$$

and

$$B = \frac{E}{4.574}. \tag{4}$$

Instead of expressing the rate of flow in atm · cm³/sec, which is a magnitude of the order of 10^{-8} to 10^{-10} or less, it is more convenient from a practical point of view to express the rate in terms of $Q_{\mu l}$ *micron · liters* (at 0° C) *per hour per square centimeter, per millimeter thickness,* for $P_{cm} = 76$. Hence

$$Q_{\mu l} = 3600 \cdot 760 \cdot 76K = 2.08 \cdot 10^8 K. \tag{5}$$

For the rate in micron · liters at 25° C, the value obtained by means of the last equation should be multiplied by the factor $298/273 = 1.091$.

From equations 4 and 5 it follows that

$$\log Q_{\mu l} = 8.318 + A - \frac{B}{T}, \tag{6}$$

---

[112] In this discussion it is assumed that $P = 0$ on one side of the wall through which diffusion occurs. Otherwise P in the following equations should be replaced by ΔP, the pressure difference.

by means of which it is possible to derive the value of T corresponding to any given value of $Q_{\mu l}$.

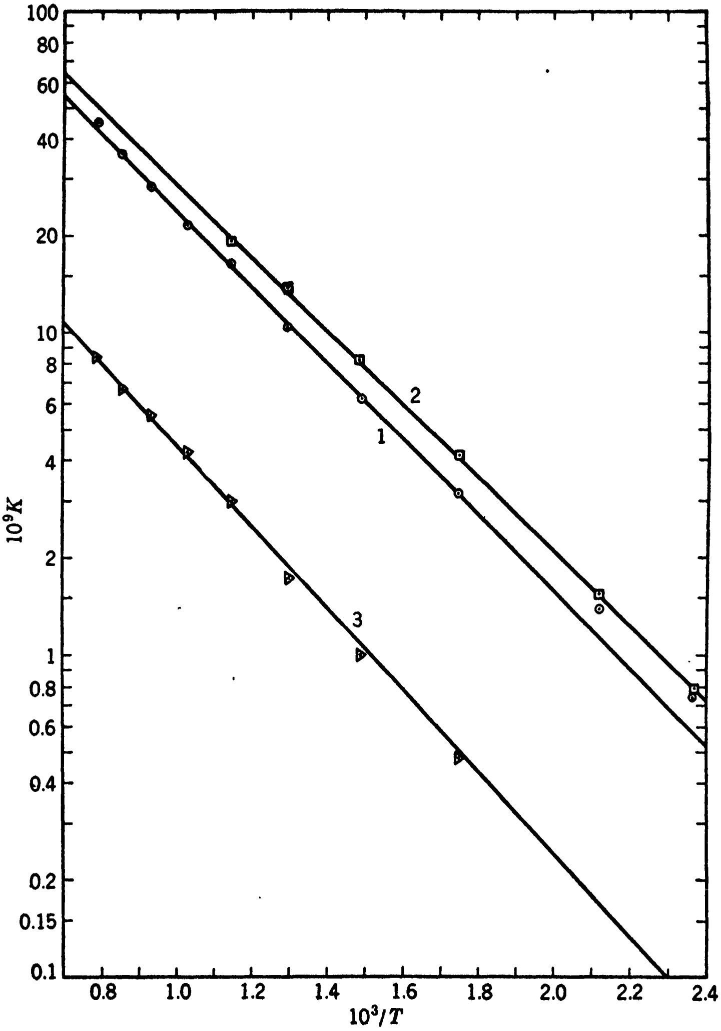

FIG. 23. Semi-log plots of permeability versus $1/T$ for helium in quartz, according to three different publications. (Numbers on plots correspond to references to Tables 32 and 33.)

As an illustration of the method used in deriving values of A, B, E and $Q_{\mu l}$ from observed values of K we shall use the data given in Table 32 for the permeability of helium in quartz, which are taken from Barrer's treatise.

TABLE 32

VALUES OF THE PERMEABILITY (10^9K) FOR $He\text{-}SiO_2$

t° C	$10^3/T$	Ref. 1*	Ref. 2*	Ref. 3*
150	2.364	0.73	0.78	—
200	2.114	1.39	1.52	—
300	1.745	3.15	4.13	0.48
400	1.486	6.15	8.25	0.99
500	1.294	10.4	13.8	1.72
600	1.145	16.4	19.3	3.00
700	1.028	21.9	—	4.25
800	0.922	28.5	—	5.50
900	0.853	36.2	—	6.72
1000	0.786	45.4	—	8.42

* See references below Table 33.

Figure 23 shows corresponding plots of log K versus $10^3/T$. From these plots are derived the values of the constants A, B, and E, from which in turn are derived the values of the temperature in degrees Centigrade for $Q_{\mu l} = 0.1$ and 1.0 (micron · liter/hr). Values thus calculated are shown in Table 33.

TABLE 33

PERMEABILITIES OF QUARTZ AND PYREX

System	Ref.	$9 + A$	B	E	$8.318 + A$	t° C for $Q_{\mu l}$ =	
						1.0	0.1
$He\text{-}SiO_2$ (150–1000° C)	1	2.570	1186	5,429	1.888	355	134
	2	2.609	1147	5,247	1.927	322	119
	3	1.912	1266	5,793	1.229	757	295
$He\text{-}SiO_2$ (−200–150° C)	2	2.363	1042	4,771	1.681	347	116
	2	2.349	1059	4,846	1.667	362	124
$Ne\text{-}SiO_2$	1	1.864	2094	9,583	1.182	—	686
$H_2\text{-}SiO_2$	3	2.417	1888	8,640	1.735	815	417
	4	2.373	1694	7,756	1.691	729	356
	5	2.125	1778	8,141	1.443	959	455
$N_2\text{-}SiO_2$	3	4.086	4820	22,060	3.404	1143	821
	5	4.778	5508	25,210	4.096	1072	808
He-Pyrex	6	1.580	1170	5,356	0.898	—	314
Air-porcelain	7	4.280	7800	35,700	3.598	—	1440

References for Tables 32 and 33

1. L. S. T'sai and T. Hogness, *J. Phys. Chem.*, **36**, 2595 (1932).
2. E. O. Braaten and G. Clark, *J. Am. Chem. Soc.*, **57**, 2714 (1935).
3. R. M. Barrer, *J. Chem. Soc.*, **1934**, 378.
4. G. A. Williams and J. B. Ferguson, *J. Am. Chem. Soc.*, **44**, 2160 (1922); **46**, 635 (1924).
5. J. Johnston and R. Burt, *J. Optical Soc. Am.*, **6**, 734 (1922).
6. W. D. Urry, *J. Am. Chem. Soc.*, **54**, 3887 (1932).
7. W. F. Roeser, *Bur. Standards J. Research*, **7**, 485 (1931) (RP 354).

Barrer has deduced values for E which are somewhat higher than those given in Table 33. This is probably due to the fact, which is evident from an inspection of the plots in Fig. 23, that a certain amount of personal judgment is involved in drawing the "best" straight line through the set of points for a given temperature.

Urry's observation that Pyrex is permeable to hydrogen has not been confirmed by Williams and Ferguson.

Barrer has observed permeation of air, oxygen, and argon in quartz. For argon the rate was extremely slow and was accelerated by treatment of the surface with hydrofluoric acid.

In order to show the selectivity of the permeability of silica towards a number of gases, Barrer has used the observations upon which the constants given in Table 33 are based to calculate the permeabilities of a number of gases at 900° C.[113] Values of K and derived values of $Q_{\mu l}$ are given in Table 34.

TABLE 34

VALUES OF THE PERMEABILITIES OF DIFFERENT GASES IN FUSED QUARTZ AT 900° C

Gas	10^9K	$Q_{\mu l}$
He	36.2	7.52
H_2	6.4	1.33
Ne	1.18	0.245
N_2	0.95	0.198
A	0.58	0.120

Barrer has also compared the permeability of different materials for the same gas (helium) at around 300° C. These values and derived values of $Q_{\mu l}$ are given in Table 35.

C. C. Van Voorhis[114] investigated the permeability of a number of glasses to helium. He observed that acidic oxides such as boric oxide or

---

[113] Values for helium and neon are also given by E. L. Jossem, *Rev. Sci. Instruments*, **11**, 164 (1940).

[114] *Phys. Rev.*, **23**, 557 (1927); RB, p. 129.

TABLE 35

PERMEABILITIES OF DIFFERENT GLASSES AND QUARTZ FOR HELIUM AT ABOUT 300° C

Material	Temperature, ° C	$10^9 K$	$Q_{\mu l}$
SiO_2	300	3.15	0.655
Pyrex	300	0.38	.079
Soda-glass	283	0.0098	.00204
Lead-glass	283	0.0037	.00077

silica increased the permeability, while basic oxides decreased it approximately in proportion to their amount.

The results obtained by Roeser on the passage of air through porcelain varied for different samples, and his values of log K versus $1/T$ do not give a satisfactory linear plot. Hence, the values for the permeability constants given in the last row of Table 33 should be considered as only approximate.

According to A. S. Russell and J. J. Stokes, Jr.,[115] the diffusion of hydrogen through Vycor glass, in the range 700° C to 975° C, is about the same as that of hydrogen through quartz, in the same range of temperatures. The rate of diffusion of oxygen was observed to be about one-twelfth that of hydrogen.

The mechanism of diffusion in glasses and silica has been discussed comprehensively by Barrer.[116] He states,

> The diffusing gases can migrate according to two mechanisms. Helium, hydrogen, and neon can pass through the "lattice" of fused silica at high temperatures. The heavy gases, oxygen, nitrogen, and argon, migrate mainly through slip planes. At low temperatures, helium, hydrogen, and neon also show slip-plane diffusion. There is evidence that migration proceeds from the adsorbed layer, not directly from the gas phase.

Barrer has shown that the values observed for the energy of activation can be accounted for on the basis of the known laws of interaction of the rare gases, nitrogen, and hydrogen with glass and quartz.

A similar opinion regarding the mechanism of diffusion in glass is favored by W. A. Weyl.[117] He states,

> As in chemical reactions the molecule jumps from place to place and the kinetics of this process can be treated from the point of view of reaction rates. The activation energy of the chemical process corresponds to the energy required to jump over an energy hill; that is, to squeeze through the electric fields of its neighbors. If the

---

[115] *J. Am. Chem. Soc.*, **69**, 1316 (1947).

[116] *J. Chem. Soc.*, **1934**, 378; also J. H. Simons and W. R. Ham, *J. Chem. Phys.*, **7**, 899 (1939).

[117] *Research*, **1**, 50 (1947).

constituents of the solid exert strong forces upon the diffusing units, the activation energy is high and the process is slow. The chemical concept accounts for the fact that hydrogen diffuses much more slowly through the oxygen network of a glass than does helium because of the smaller "chemical affinity" for the oxygen ions.

Furthermore, it is possible on this basis to interpret the observations made by P. L. Smith and N. W. Taylor[118] on the diffusion of a gas through glasses of the same composition but different heat treatment. According to Weyl, "A glass which has been chilled from a high temperature can be considered an unstable modification having a higher energy content. The higher chemical affinity of such a chilled glass increases the activation energy of the diffusing units and slows down the diffusion rate." It has also been observed that, "with the exception of lead-containing glass, all showed a marked decrease in the diffusion after chilling.

The experiments indicate that chilling exerts two antagonistic effects upon the diffusion of gases through a glass:

a. The more spacious network of the rapidly chilled glass (lower density) enables gas atoms or molecules to flow faster than through the more "compacted" well-annealed glass.

b. The chemical forces of a chilled glass are stronger, or the valence forces of the ions are less "saturated," than those of the annealed glass. The stronger forces delay diffusion by increasing the activation energy, or raise the energy barriers over which the diffusing atoms have to pass.

For soda-lime silicate and borosilcate glasses the second factor apparently dominates the diffusion process and as a result the diffusion is faster in the annealed glass than in the chilled one.

Finally, it is important to note that the permeability is actually proportional to the diffusion constant of the gas in the material and to the solubility of the gas, in accordance with the relation

$$K = Dc\frac{\Delta P}{d}, \tag{7}$$

where D = diffusion constant.

c = solubility.

$\frac{\Delta P}{d}$ = pressure gradient across the thickness.

The solubility of hydrogen and helium in fused silica is approximately 0.01 cm^3 (S.T.P.) per cm^3 at 1 atm and temperatures above about 700° C. Substituting this value in the above equation, it is possible, from the observed values of K, to derive values of D. Thus, for helium in fused silica, the value of D at 500° C lies between 10^{-7} and 10^{-8} $\mathrm{cm}^2 \cdot \mathrm{sec}^{-1}$.

---

[118] *J. Am. Ceramic Soc.*, **23**, 139 (1940).

Since the value of c may be assumed to be constant over a considerable range of temperature, it follows that in the relation

$$D = D_0 \epsilon^{-E/R_0 T} \tag{8}$$

the values of E are approximately the same as those derived from the temperature variation in K.

8. SORPTION AND DESORPTION PHENOMENA IN CELLULOSE[119]

Occasionally the problem arises in vacuum technique of evacuating a device in which cellulose materials such as cotton, paper, or wood are present. The principal difficulty encountered in that connection is due to the fact that water vapor as well as carbon dioxide and many organic compounds (especially those containing a hydroxyl or —OH group) are strongly adsorbed by cellulose. It has therefore seemed to the writer that a brief review of some of the most salient observations might prove of interest.

Cellulose[120] has the chemical composition $C_6H_{10}O_5$. Its avidity for water is shown in the formation of a hydrate, $(C_6H_{10}O_5)_2H_2O$. When heated to a temperature above about 130° C in vacuum, cellulose begins to decompose at an appreciable rate with consequent loss of mechanical and electrical strength. It is therefore impractical, in general, to evacuate cellulose materials at temperatures in excess of the above value.

Like silica gel and other adsorbents mentioned in the previous sections, the sorption and desorption isotherms for water and cellulose present a "hysteresis" loop. Figure 24 shows plots of observations made by E. Filby and O. Maass[121] on standard cellulose at 20° C, in which percentage moisture is plotted against percentage relative humidity.

Table 36, taken from a publication by S. E. Sheppard and P. T. Newsome,[122] gives typical data for the sorption by cotton cellulose at 23° C. Before these observations, the samples had been evacuated and dried at 105° C. The three sets of data refer to results published by different investigators.

---

[119] For discussion of earlier work on this topic see McB, Chapter XII, p. 358.

[120] For a discussion of the chemical and physical characteristics of cellulose and its derivatives, the reader should consult the treatise *Cellulose and Cellulose Derivatives* by E. Ott, High Polymers, Vol. 5, Interscience Publishers, 1943. This contains a chapter, "Sorption of Water and Other Vapors by Cellulose," by E. I. Valko. *The Chemistry of Cellulose* by E. Heuser, John Wiley and Sons, New York, 1944, contains a chapter on the reactions of cellulose with water.

[121] *Can. J. Research* **B13**, 1 (1935).

[122] *J. Ind. Eng. Chem.*, **26**, 285 (1934).

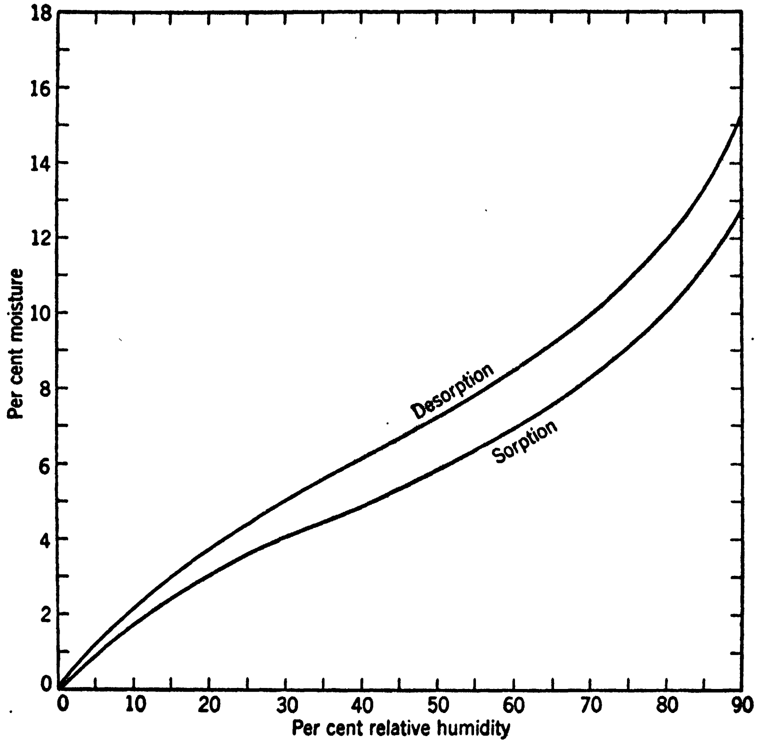

Fig. 24. Sorption and desorption isotherm for water vapor and standard cellulose at 20° C (Filby and Maass).

TABLE 36

Sorption of Water Vapor by Cellulose Cotton at 23° C

Relative Humidity	P_{mm}, of H_2O vapor	Sorption Milligrams H_2O per Gram Cotton		
0.05	1.054	14.4	10.4	12.5
0.10	2.107	20.4	17.1	19.0
0.15	3.161	24.4	21.6	23.2
0.20	4.214	28.4	25.8	26.4
0.25	5.268	33.4	29.8	29.6
0.30	6.321	37.4	33.6	32.8
0.40	8.428	45.8	40.8	39.4
0.50	10.54	54.4	48.1	46.0
0.60	12.64	63.8	56.9	53.3
0.70	14.75	75.8	66.5	62.0
0.80	16.86	93.8	81.5	71.6
0.90	18.96	125.6	115.4	84.0
1.00	21.07			

Of special significance in connection with vacuum technique are the observations made by S. M. Neale and W. A. Stringfellow.[123] They determined the amounts taken up by cotton *at low pressures*, for a series of temperatures. Table 37 summarizes their results, which were obtained with samples of yarn that had been evacuated at 90° C for several hours. A definite amount of water was then admitted to the cotton, the temperature raised to the desired value, and the pressure read periodically until a steady value was obtained. "Steady readings were obtained within an hour or two after a change of temperature." The system was re-evacuated with the cotton at 90° C before the next admission of water.

TABLE 37

EQUILIBRIUM PRESSURES FOR DIFFERENT AMOUNTS OF WATER ADSORBED BY COTTON AT A SERIES OF TEMPERATURES

Water adsorbed, mg/g	Pressure in Microns						
	20° C	30	40	50	60	70	80
0.120	(1.08)	2.00	4.33	9.00	19.9	39.0	77.0
0.234	1.65	3.60	8.5	19.2	40.8	81	157
0.517	4.06	10.3	23.4	51	107.5	219	440
0.795	7.65	17.8	40.8	88	185	380	725
1.060	11.9	27.8	62.5	139	306	586	—
1.595	20.15	47.0	111.4	250	510	(880)	
Vapor pressure of water, mm:	17.54	31.82	55.32	92.5	149.4	233.7	355.1

The last line gives the vapor pressure of water, at each temperature, in millimeters of mercury, from which the equilibrium pressure may be derived in terms of relative humidity. For instance, an equilibrium pressure of 250 microns at 50° C corresponds to $250 \cdot 10^{-3} \cdot 100/92.5 = 0.27$ per cent relative humidity.

Figure 25 shows plots of these data, and from them we conclude that, if a device is sealed off under such conditions that the pressure of water vapor at 30° C is 17.8 microns, the amount of water retained in the cotton is 0.795 mg/g.

Neale and Stringfellow also showed that, for the isosteres (curves for constant amount adsorbed), values of $\log P$ plotted against $1/T$ yield straight lines with the same slope, independent of the amount sorbed, corresponding to a heat of adsorption, $Q = 15{,}700$ cal/mole.[124] That is,

---

[123] *Trans. Faraday Soc.*, **37**, 525 (1941).

[124] The values of the heat of evaporation of water at 40° C and 100° C are 10,332 and 9712 cal/mole, respectively.

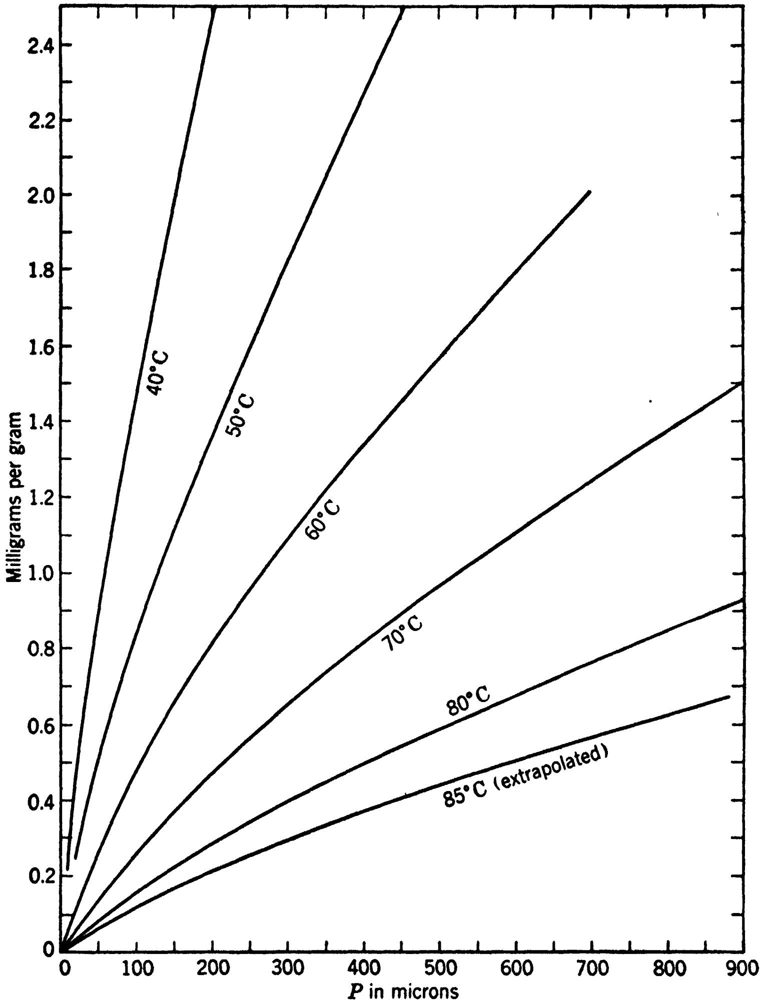

Fig. 25. Sorption isotherms for water vapor by cotton at a series of temperatures (Neale and Stringfellow).

for *constant amount adsorbed*,

$$\log P_t = \log P_{70} + \frac{15{,}700}{4.574}\left(\frac{1}{343} - \frac{1}{T}\right),$$

where the value of P at 70° C, for the given amount of sorption, is obtained from the plot in Fig. 25, and P_t is the equilibrium pressure at t° C.

Extrapolating, by means of the last equation, to higher temperatures, we obtain the sorption isotherm for 85° C, plotted in Fig. 25, and the isotherms for higher temperatures shown in Fig. 26. Assuming that for small amounts of water adsorbed there is a linear variation with pressure, it follows that for a vapor pressure of 1 mm at, for instance, 140° C, the amount of water retained by the cotton would be 0.05 mg/g.

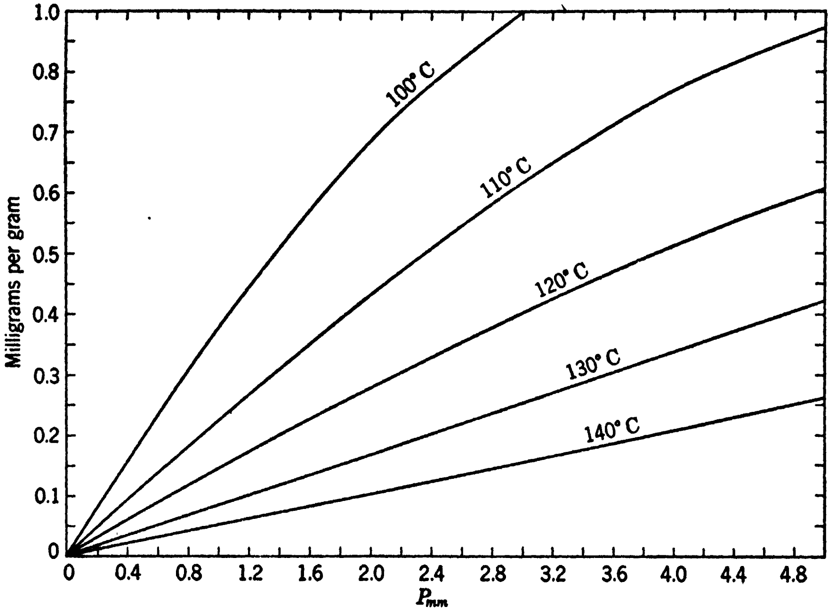

FIG. 26. Sorption isotherms for water vapor by cotton, extrapolated to higher temperatures from the isotherms in Fig. 25.

It is interesting to compare these sorption data for cotton, extrapolated from observations at temperatures below 100° C, with observations made by C. C. Houtz and D. A. McLean[125] on the sorption of water vapor by paper, at temperatures ranging from 100° C to 150° C.

The samples were weighed in the dry condition after being heated at 100° C, in vacuum, for at least 8 hours. Figure 27 shows the isotherms, obtained with linen rag paper, in which the amount sorbed (mg per 100 g paper) is plotted against the pressure of water vapor.

Observations, made under similar conditions, with wood pulp gave somewhat higher values for the amount sorbed. Table 38 gives data obtained at relatively low vapor pressures for the two samples of paper and, for comparison, values taken from the plots in Fig. 26 for cotton.

[125] *J. Phys. Chem.*, **43**, 309 (1939).

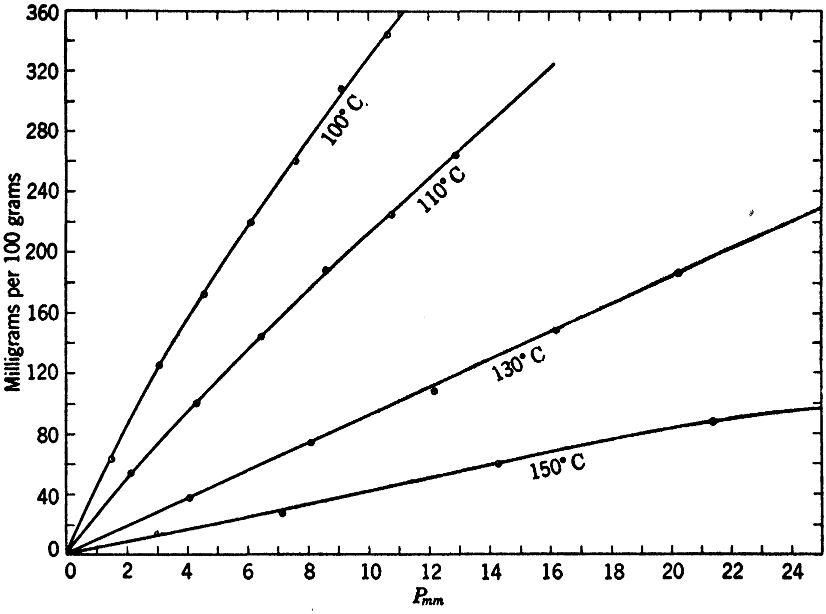

FIG. 27. Isotherms for sorption of water vapor by linen rag paper (Houtz and McLean).

TABLE 38

SORPTION OF WATER BY PAPER AND COTTON IN THE RANGE 100–150° C

t° C	P_{mm}	Milligrams per Gram		
		Linen Rag	Wood Pulp	Cotton
100	1.52	0.63	0.92	0.55
	3.04	1.25	1.60	.91
110	2.15	0.54	0.77	.46
	4.30	1.00	1.32	.80
120	2.98	—	0.72	.40
	5.96	—	1.20	—
130	4.05	0.38	0.56	.34
140	4.05	—	—	.21
150	7.14	0.28	0.40	—

Houtz and McLean found that their isotherms could be represented by the Freundlich relation

$$\log \alpha = \log A + \frac{1}{n} \log P, \tag{1}$$

where α = milligrams of H_2O per gram of paper adsorbed at pressure P, and A and $1/n$ are constants. The values of $1/n$ varied from 0.99 to 0.767, depending on the temperature and on whether linen or wood paper was used.

In a subsequent publication[126] the same investigators observed that by heating the paper at 150° C during evacuation the sorption was reduced to a reproducible minimum which varied from 85 to 70 per cent of the amount sorbed under similar conditions of temperature and pressure by the same material heated at 100° C. Similar variations were obtained in the values of $1/n$ as in the earlier series of measurements.

Also a similar relation was observed for the isosteres as that observed by Neale and Stringfellow. From these linear plots of $\log P$ versus $1/T$ for constant values of α, it was concluded that the heat of adsorption Q (in calories per mole H_2O) decreased with α as follows:

α	Q
0.25	15,800
0.50	15,300
1.00	14,800
2.00	14,300
3.50	14,000

It will be observed that the highest value observed for Q in this investigation is in remarkable agreement with the value 15,700 deduced by Neale and Stringfellow.

The results obtained in these investigations are typical of those obtained by other observers.[127]

In an investigation carried out in this laboratory by A. H. Young and the writer, on the rate and extent of desorption of samples of fiber and wood pulp, the following results were obtained:

For samples evacuated at both room temperature and 140° C, the rate of decrease in weight (w) was observed to follow the first-order equation

$$-\frac{dw}{dt} = k(w - w_0), \tag{2}$$

where w_0 = weight at $t = \infty$, and k denotes the "rate constant." That is, a plot of $\log (w - w_0)$ versus t yields a straight line, the slope of which is proportional to k. At room temperature, the total time required to remove 90 per cent of the adsorbed water from an approximately 1-g sample of fiber was of the order of 8 hours, thus indicating that the rate of desorption was governed by the rate of diffusion of water vapor through the pores or capillaries.

---

[126] *J. Phys. Chem.*, **45**, 111 (1941).

[127] See for instance the discussion and references given by E. I. Valko, *op. cit.*

The percentage loss by weight during evacuation for a typical sample was as follows:

At 27° C	about 2.5 per cent
Between 27° C and 140° C	about 2.5 per cent
At 140° C	about 1.2 per cent
Total =	6.2 per cent

This percentage corresponds to that sorbed by cotton, at room temperature, in an atmosphere of 60 per cent relative humidity.

In the case of wood pulp, the observed rate of desorption, for the same size sample as that of fiber or paper, was much faster; and of a total loss in weight, on evacuation, of approximately 5 per cent, 4.5 per cent was obtained at room temperature.

When desorbed samples of fiber and wood pulp were exposed to an atmosphere containing 30 per cent relative humidity at room temperature, it was observed that the rates of sorption were so slow that even after several hours the gain in weight was only about 2 per cent. Even after 24 hours, the amount of water adsorbed was less than that given off during desorption.

Of special importance in the evacuation of cellulose is the fact that the material undergoes thermal decomposition at a noticeable rate at 100° C and at a much higher rate as the temperature is increased above 100° C. The following discussion is based on the data published by E. J. Murphy.[128]

The gases evolved during thermal decomposition of cellulose and their relative proportions are given by the approximate molar ratios: $10\,H_2O : 2\,CO_2 : 1\,CO$. As Murphy has stated,

> It is difficult to determine when paper is dry. As the drying process progresses, the rate at which water vapor comes off steadily decreases, but water vapor continues to come off, however long the drying is continued. Raising the temperature increases the rate of drying, but it also increases the rate of thermal decomposition. Water vapor coming from the thermal decomposition of cellulose is not distinguishable directly from water vapor coming from the adsorbed state. Thus the fact that water vapor continues to come off after protracted drying at any temperature above about 100° C does not mean that the paper can be dried further: It is not feasible to reach a condition where no more water vapor is evolved by paper.
>
> Dryness, or the lowest possible concentration of adsorbed water, can be recognized when water vapor comes off in association with CO_2 and CO in proportions appropriate to the temperature of the paper. At temperatures of the order of 130° C, paper which is yielding 2 or 3 molecules of water in association with about 1 molecule of CO_2 and 1 of CO (or some proportions of this order) would be accounted dry. The degree of dryness could not be increased at this temperature without changing the composition of the paper. Thus the composition of the gas evolved can be used to determine an "end point" in the drying operation.

---

[128] *Trans. Am. Electrochem. Soc.*, **83**, 161 (1943).

A plot of the rate of gas evolution versus $1/T$ on semi-log paper yields a straight line. For *kraft paper*, the relation between rate of gas evolution in *cubic millimeters* (at normal temperature and pressure) *per hour per gram* (denoted by q) is given by the relation, deduced from the plot,

$$\log q = 18.24 - \frac{7424}{T},$$

corresponding to the activation energy, $Q = 33{,}950$ cal/mole.

Assuming that 70 per cent by volume is H_2O, this rate corresponds in mass to

$$\begin{aligned} m &= 8.050 \cdot 10^{-4} \cdot 0.7q \text{ mg } H_2O/\text{hr/g} \\ &= 5.635 \cdot 10^{-4} q \text{ mg } H_2O/\text{hr/g}. \end{aligned}$$

Hence

$$\log m = 14.751 - \frac{7424}{T}.$$

From the last equation we obtain the values for m, in *milligrams water per hour per gram of paper*, given in Table 39.

TABLE 39

RATE OF EVOLUTION OF WATER FROM PAPER, FOR A SERIES OF TEMPERATURES (MURPHY)

$t°$ C	10^6m	$t°$ C	10^4m
80	0.537	120	0.741
90	2.00	130	2.14
100	7.08	140	6.03
110	24.0		

For linen paper, the rate of decomposition, according to Murphy, is about 55 per cent of that for kraft paper.

It has also been observed by Murphy that paper reacts slowly with oxygen even at as low a temperature as 80° C. After exposing paper at 135° C to air at atmospheric pressure for 1 hour the subsequent rate of evolution of gas in vacuum was increased considerably.

The original report also contains a discussion of the effect of increased temperatures of desorption on the mechanical properties of paper.

CHAPTER 9

GASES AND METALS

1. INTRODUCTORY REMARKS

In his early work on the reactions of tungsten and molybdenum with different gases at low pressures and the further investigations on thermionic emission, Langmuir recognized the importance of eliminating from these metals all traces of residual gases. Subsequent developments in the production of electronic devices have served to emphasize this conclusion. In addition, recent investigations have also demonstrated that the mechanical and other physical characteristics of metals may be seriously affected by the presence in them of occluded or dissolved gases.

Hence, a knowledge of the manner in which metals may take up gases and of the conditions under which these gases may be removed is of extreme importance in vacuum technique.

In this chapter this subject will be discussed under the following headings:

I. Sorption of gases by metals.
II. Diffusion of gases through metals.
III. Degassing of metals.

Naturally there is available a vast literature on the subject, some of which can be summarized only briefly within the limitations of the present volume. However, treatises by C. J. Smithells[1] and R. M. Barrer,[2] together with those by Brunauer and McBain referred to in Chapters 7 and 8, should prove extremely valuable for further details on many of the topics discussed in this chapter.

2. PHYSICAL ADSORPTION AND CHEMISORPTION

In Chapter 7 many illustrations have been mentioned of physical adsorption on metals, in the form both of smooth surfaces and of fine powders. Such examples of adsorption are characterized by the fact that the isotherms may be represented, at least at low pressures, by one of the equations that apply to adsorption in the form of monolayers. Furthermore, the observations that such adsorption is approximately non-specific with respect to the nature of the adsorbent and decreases at constant pressure with increase in temperature, and that the temperature coefficient of the sorption corresponds to a low heat of adsorption, lead to the conclusion that such adsorption phenomena are due to the action of so-called van der Waals forces.

---

[1] C. J. Smithells, *Gases and Metals*, Chapman and Hall, London, 1937. (Ref. CS.)

[2] R. M. Barrer, *Diffusion In and Through Solids*, Chapters IV and V, Cambridge University Press, 1941. (Ref. RB.)

As another illustration of pure physical adsorption, the observations of F. Durau and C. H. Teckentrup,[3] on the sorption of different gases by finely divided iron powder, may be cited. This adsorbent was obtained by filing vacuum-fused electrolytic iron in vacuum; the isotherms were observed at 18° C, and for the pressure range 50 to 750 mm, for the following gases: A, H_2, N_2, CO, N_2O, CH_4, C_2H_6, C_3H_8, C_2H_4, C_3H_6, and CH_3Cl. With these gases equilibrium was established very rapidly, and the isotherms were observed to be completely reversible. From an estimate of the gross surface area of the powder, the conclusion was drawn that the amount of adsorbed gas did not exceed that of a complete monolayer.

On the other hand, in the case of O_2, CO_2, C_2N_2, NO, SO_2, and HCl (over the same range of pressures and at 18° C), the rate of adsorption was found to be much lower, and, even after desorption at less than 10^{-2} mm, relatively large amounts of the sorbed gases were retained by the powder. From this observation it was concluded that these gases were chemisorbed to a certain extent.

In general, finely divided metals take up gases in large amounts. The sorption of hydrogen and carbon monoxide by pyrophoric iron, nickel, and cobalt has been investigated by N. Nikitin.[4] Hydrogen is absorbed in considerable amounts by these powders at the temperature of liquid air. At higher temperatures (−80° C and room temperature) iron powder does not absorb hydrogen, but as the temperature is increased to 380° C and higher the amount absorbed increases rapidly. This is due to the fact that at the lower temperatures physical adsorption takes place, which decreases with increase in temperature, whereas at the higher temperatures, as discussed more fully in a subsequent section, the hydrogen goes into solution and the amount dissolved varies as $\sqrt{P}$ and increases with the temperature.

In true physical adsorption the amount sorbed increases with decrease in temperature, as stated in the previous chapters. However, it has been observed that frequently the sorption, after decreasing with increase in temperature to a minimum value, exhibits a reversal in this respect with still further increase in temperature until a maximum value is attained, after which further increase in temperature results in decreased absorption once more.

---

[3] *Ann. Physik,* **12**, 927 (1932).

[4] *Z. anorg. Chem,* **154**, 130 (1926).

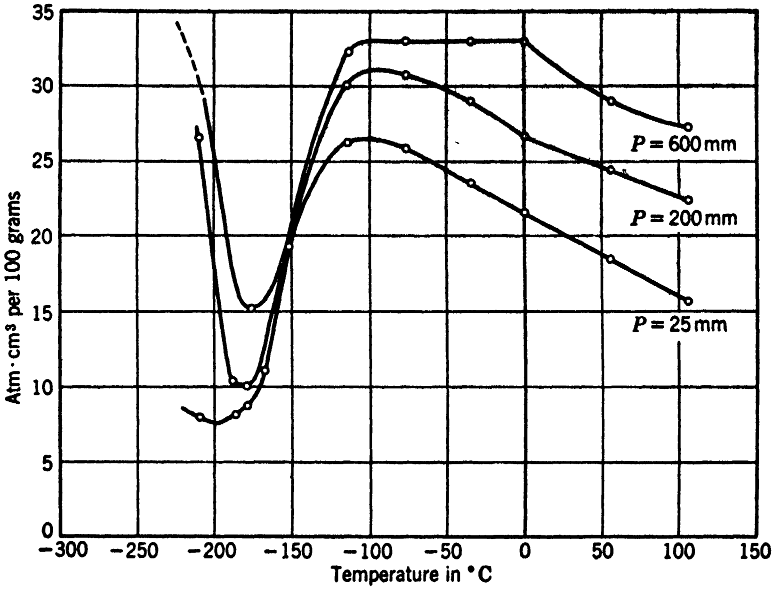

FIG. 1. Isobars for the adsorption of hydrogen on nickel powder at three different pressures (Benton and White).

Figure 1 shows isobars for hydrogen on nickel powder, which were observed by A. F. Benton and T. A. White.[5] Whereas equilibrium was reached almost instantaneously at −180° C, about 1 to 2 hours was required at −100° C, and as will be observed the amount absorbed at −100° C was over 3 times that absorbed at −180° C.

Similar observations have been made by Benton and White[6] on the sorption of hydrogen by nickel and copper (see Fig. 2) and by H. S. Taylor and P. V. McKinney[7] on the sorption of carbon monoxide by palladium. As indicated in Fig. 2, the sorption of hydrogen by nickel is a maximum at 0° C. There are many examples of sorption in which the physical adsorption at low temperatures is succeeded by a much greater amount of sorption at higher temperatures, and the rate of this sorption is usually very slow. This second stage has been designated *activated adsorption*[8] and also *chemisorption*, since the corresponding energy evolved is of the same order of magnitude as that evolved in chemical reactions.[9]

---

[5] *J. Am. Chem. Soc.*, **52**, 2325 (1930); CS, p. 32, Fig. 22.

[6] *J. Am. Chem. Soc.*, **54**, 1373 (1932).

[7] *J. Am. Chem. Soc.*, **53**, 3604 (1931).

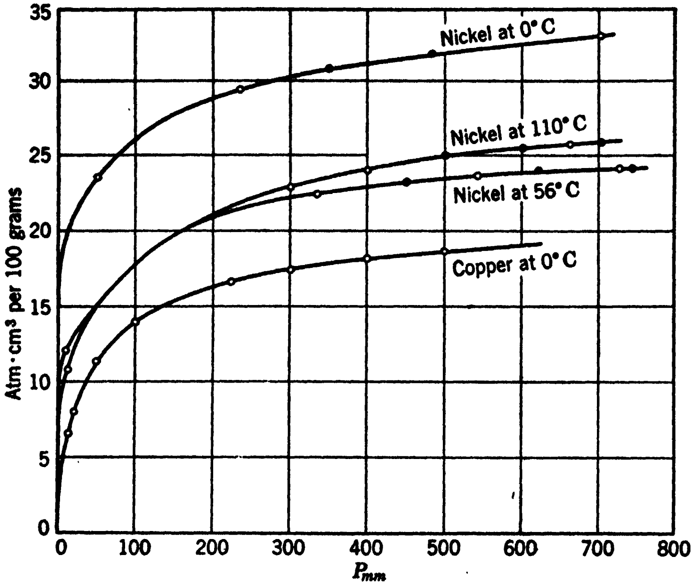

FIG. 2. Adsorption isotherms for hydrogen on nickel and copper, illustrating chemisorption (Benton and White).

As would be expected, on the basis of this interpretation, activated adsorption has not been observed for the rare gases, for nitrogen on copper, or for hydrogen on gold and silver. "It would appear, therefore," as Smithells states,[10]

> that this type of adsorption depends on a chemical attraction between the metal surface and the gas, and is most strongly marked in such systems as oxygen-silver, carbon monoxide-nickel, and hydrogen with copper, nickel, or iron. . . . Although it cannot actually be chemical combination, since no new phase is formed, it is probably a necessary preliminary to chemical action which may occur at still higher

---

[8] H. S. Taylor, *J. Am. Chem. Soc.*, **53**, 578 (1931).

[9] See CS, p. 48, for a summary of values of heats of activated adsorption, which range from 4000 to over 100,000 cal/g-mole of gas.

[10] CS, p. 30.

temperatures. In the systems just mentioned, for example, definite compounds Ag_2O, $Ni(CO)_4$, NiH_2, etc., between gas and metal are known.

Smithells states,[11]

> Whilst the process of physical adsorption is perfectly reversible with respect to changes in temperature and pressure, this is not the case with activated adsorption. So far as pressure changes are concerned, the isotherms usually show reversibility, although this is not always so. . . .
>
> Activated adsorption is never reversible with respect to changes in temperature. If the equilibrium value is found by admitting gas to the adsorbent at a temperature T_1, and it is then heated, still in contact with the gas, to a higher temperature T_2, on again cooling to T_1 the equilibrium value is higher than before. . . . It is significant that the gas adsorbed as the result of thermal activation cannot be removed by evacuation at T_1, but only at higher temperatures. This is, of course, in accordance with the usual practice of baking during evacuation to remove gas adsorbed on glass and metal parts of vacuum apparatus.

An illustration of activated adsorption which is of importance in the exhaust of vacuum tubes is found in the investigations of K. H. Kingdon[12] and Langmuir on the effect of adsorbed oxygen on the thermionic emission from tungsten filaments. At low temperatures and low pressures oxygen is adsorbed and decreases the emission to values that range from 10^{-2} to 10^{-5} of that from pure tungsten. It is only on heating the filament in vacuum to about 1700° C or higher that the adsorbed layer is removed with a resulting restoration of the emission to its original value. According to Langmuir,

> An oxygen film on tungsten at 1500° K does not evaporate in less than a year. . . . The fact that a monatomic film of oxygen on tungsten does not react with hydrogen at 1500° K is a striking indication that the oxygen is in a condition far different from that of gaseous oxygen.

J. K. Roberts[13] has also obtained evidence for the activated adsorption of hydrogen on a clean tungsten surface. Desorption is observed only at temperatures above 400° C.

Characteristic of the isotherms due to chemisorption are the very large sorption values observed at low pressures, and the comparatively small increase in sorption with increase in pressure, over a large range of pressures.

Observations on the rate of sorption due to chemical forces lead to the conclusion that this rate is actually dependent upon a rate of diffusion of the gas into the adsorbent, in which it "dissolves."

---

[11] This quotation and that in the next paragraph are from CS, pp. 38–39.

[12] *Phys. Rev.*, **24**, 510 (1924). See also Langmuir and D. S. Villars, *J. Am. Chem. Soc.*, **53**, 486 (1931) and Langmuir, *Chem. Revs.*, **13**, 147 (1933), for discussion of this topic. The remarks quoted are taken from this extremely important paper.

[13] *Proc. Roy. Soc. London*, **A**, **152**, 445 (1935).

The phenomena of chemisorption are of special interest in connection with the interpretation of the behavior of many catalysts. Since the discussion of this topic is beyond the scope of this chapter, the reader is referred for further details to the treatises mentioned above and to a number of papers published by H. S. Taylor and his associates.

3. GENERAL REMARKS ON SORPTION OF GASES BY METALS[14]

Gases (with the exception of the rare gases) may react with metals to form compounds or solutions of the gas in the solid or liquid metal. As far as has been observed, the gases of Group 0 do not dissolve in any metal either in the liquid or solid state.

There are four different types of interaction between *hydrogen* and metals.

1. With the alkali and alkaline-earth metals (Groups IA and IIA) hydrides are formed, such as NaH and CaH_2, which are ionic in behavior, with hydrogen as the negative ion.
2. With elements such as C, Si, S, Se, As, and other metals of Groups IVB, VB, and VIB, covalent hydrides are formed, such as H_2S, AsH_3, and SiH_4.
3. With a number of metals such as Cu, Ag, Cr, Mo, W, Fe, Co, Ni, Al, and Pt, hydrogen forms true solutions, as indicated by (*a*) the observation that the solubility varies as $\sqrt{P}$, and (*b*) the increase in solubility with increase in temperature. We shall designate these metals as *Group A*.
4. With elements of Group IIIA (Ce, La, etc.), Group IVA (Ti, Zr, Th, Hf), and Group VA (V, Cb, Ta) hydrogen forms pseudo-hydrides. While the solubility varies as $\sqrt{P}$ for certain ranges of values of P, it decreases with increase in temperature. Under certain conditions palladium behaves with respect to hydrogen in the same manner. These metals will be designated in the following discussion as *Group B*.

Hydrogen is not absorbed by Au, Zn, Cd, In, or Tl.

In the case of *oxygen* it is often difficult to distinguish between solution of oxygen and solution of oxides. However, the formation of true solutions has been determined in Ag, Cu, Co, and a few other metals.

Nitrogen dissolves only in those metals which form nitrides at higher temperatures, e.g., Al (molten), Zr, Ta, Mn, and Fe.

Carbon monoxide behaves in a similar manner. Thus it is absorbed by Ni and Fe, each of which is capable of forming a carbonyl.

---

[14] See the "summary of the reactivity of gases towards metals," RB, p. 146; also D. P. Smith, *J. Phys. Chem.*, **23**, 186 (1919).

The observations on the solubility of sulfur dioxide in molten copper are discussed in a subsequent section.

In discussing the sorption of gases by metals, the solubility (or gas content) may be expressed in terms of a variety of units. These units and conversion factors in terms of other units are as follows:

$$v_0 = \text{cm}^3 \text{ (S.T.P.) per 1 g metal.}$$

$$s = \text{cm}^3 \text{ (S.T.P.) per 100 g metal} = 100\, v_0.$$

$$\begin{aligned} V_g &= \text{volume of gas (S.T.P.) per 1 volume of metal.} \\ &= v_0\rho = 10^{-2}s\rho, \text{ where } \rho = \text{density of metal.} \end{aligned} \tag{1}$$

$$\begin{aligned} x = \text{mg per 100 g} &= 4.461 \cdot v_0 M \\ &= 4.461 \cdot 10^{-2} sM, \end{aligned} \tag{2}$$

where M = molecular weight of gas. Hence

$$s = 22.42x/M \tag{3}$$

$$p_w = \text{per cent by weight} = 10^{-3}x = 4.461 \times 10^{-5} sM. \tag{4}$$

Gas:	H_2	O_2	N_2 or CO	H_2O	CO_2
$c_M = 4.461 \times 10^{-2}M$:	8.995×10^{-2}	1.428	1.250	0.8041	1.963
$1/c_M = 22.42/M$:	11.12	0.700	0.800	1.244	0.5093

$$s = \frac{10^3}{c_M} p_w. \tag{5}$$

$$\begin{aligned} \mu m &= \text{number of } \textit{micromoles} \text{ per 100 g} \\ &= 44.61s. \end{aligned} \tag{6}$$

$$s = 2.242 \cdot 10^{-2}\, \mu m. \tag{7}$$

For a *diatomic* gas in a metal of atomic mass A,

$$\begin{aligned} r &= \text{number of atoms per atom of metal,} \\ &= 2 \cdot 10^{-5} \frac{Ax}{M} = 8.922 \cdot 10^{-7} As \end{aligned} \tag{8}$$

$$= 8.922 \cdot 10^{-5} V_g \frac{A}{\rho}. \tag{9}$$

4. SOLUBILITY OF HYDROGEN IN METALS OF GROUP A

Typical metals of this group are iron and nickel. The values of s are quite small, as compared with those for metals of Group B. Consequently, the magnitude of r is of the order of 10^{-4} (1 atom of hydrogen for 10^4 atoms of metal). As mentioned above, the value of s increases at constant temperature as $\sqrt{P}$, from which it follows that the hydrogen is *absorbed as atoms.* At constant pressure, the solubility increases with increase in temperature, indicating that *energy is absorbed* in the process of sorption. The solubility can thus be expressed, as a function of pressure and temperature, by a relation of the form

$$s = s_0\sqrt{P}\epsilon^{-Q_S/(2R_0T)}, \tag{1}$$

where s_0 is a constant.

The factor 2 in the denominator of the exponential takes into account the fact that the hydrogen enters the metal lattice as atoms, and Q_S therefore denotes the heat absorbed in calories *per gram-mole* hydrogen.

The last equation may be expressed in terms of ordinary logs in the form

$$\log s = \log s_0 + 0.5 \log P - \frac{Q_S}{9.148T}, \tag{2}$$

and evidently the value of Q_S may be derived from the slope of the linear plot of log s (at constant pressure) versus $1/T$.

A large number of investigators have worked on this topic, and a list of these, together with reference numbers, is given in List I.[15]

List I. References on Solubility of Hydrogen in Metals of Group A

IRON

1. A. Sieverts, *Z. Metallkunde,* **21**, 37 (1929).
2. E. Martin, *Arch. Eisenhüttenw.,* **3**, 407 (1929/30).
3. A. Sieverts and H. Hagen, *Z. physik. Chem.,* **A**, **155**, 314 (1931).
4. L. Luckemeyer-Hasse and H. Schenck, *Arch. Eisenhüttenw.,* **6**, 209 (1932/33).
5. F. Pihlstrand, *C.A.,* **31**, 8471 (1937).
6. W. Baukloh and R. Müller, *Arch. Eisenhüttenw.,* **11**, 509 (1937/38).
7. K. Iwasé and M. Fukusima, *Science Repts., Tôhoku Imp. Univ.,* **27**, 162 (1938–1939).
8. A. Sieverts, G. Zapf, and H. Moritz, *Z. physik. Chem.,* **A**, **183**, 19 (1938/39).
9. J. H. Andrew, H. Lee, and A. G. Quarrell, *J. Iron Steel Inst. London,* **146**, No. II, p. 181 (1942).
10. M. H. Armbruster, *J. Am. Chem. Soc.,* **65**, 1043 (1943).

NICKEL

See references 1, 4, 10, and 11.

11. J. Smittenberg, *Rec. trav. chim.,* **53**, 1065 (1934).

---

[15] A very comprehensive bibliography on the solubility of gases in metals is given by O. Kubaschewski, *Z. Elektrochem.,* **44**, 152 (1938).

COBALT

See references 1 and 12.

12. A. Sieverts and H. Hagen, *Z. physik. Chem.*, **A, 169**, 237 (1934).

COPPER

See references 1 and 13.

13. P. Roentgen and F. Moeller, *Metallwirtschaft*, **13**, 81, 97 (1934).

ALUMINUM

See references 1, 13, and 14–17.

14. J. Czochralski, *Z. Metallkunde*, **14**, 277 (1922).
15. K. Iwasé, *Science Repts., Tôhoku Imp. Univ.*, **15**, 531 (1926).
16. P. Roentgen and H. Braun, *Metallwirtschaft*, **11**, 459, 471 (1932).
17. L. L. Bircumshaw, *Trans. Faraday Soc.*, **31**, 1439 (1935).

MANGANESE

See references 4, 6, and 18.

18. A. Sieverts and H. Moritz, *Z. physik. Chem.*, A, **180**, 249 (1937).

SILVER

19. E. W. R. Steacie and F. M. G. Johnson, *Proc. Roy. Soc. London*, **A, 117**, 662 (1928).

MOLYBDENUM

See references 2 and 20.

20. A. Sieverts and K. Brüning, *Arch. Eisenhüttenw.*, **7**, 641 (1933–1934).

CHROMIUM

See references 2 and 4.

MISCELLANEOUS ALLOYS

21. L. Kirschfeld and A. Sieverts, *Z. Elektrochem.*, **36**, 123 (1930).
22. A. Sieverts and K. Brüning, *Z. physik. Chem.*, **A, 168**, 411 (1934).
23. A. Sieverts and H. Hagen, *Z. physik. Chem.*, **A, 174**, 247 (1935).

Solubility of Hydrogen in Iron ($A = 55.85$, $\rho = 7.88$). Table 1 gives values of s, x, μm, V_g, and r obtained by Sieverts (1), for the range 400° C to 1650° C, at 1 atm. The last column gives more recent values obtained by Sieverts, Zapf, and Moritz (8).

Figure 3, taken from reference 8, shows a plot (a) of the solubility data at 1 atm over the range of 400° C to 1200° C. The insert (b) shows data obtained with both increasing and decreasing temperatures (above 1250° C). The plots also show data obtained by other investigators.

As is well known, iron exhibits three critical temperatures for the solid, corresponding to the phase transformations shown in Table 2.[16] In this table are indicated the associated lattice structure and range of stability for each phase. The last column in Table 1 and the plot in Fig. 3 show that at each critical temperature and at the melting point (1535° C) there is a change in solubility. At the $\alpha-\gamma$ transition and at the melting point the solubility increases considerably.

---

[16] *Metals Handbook*, 1939 Edition, p. 427.

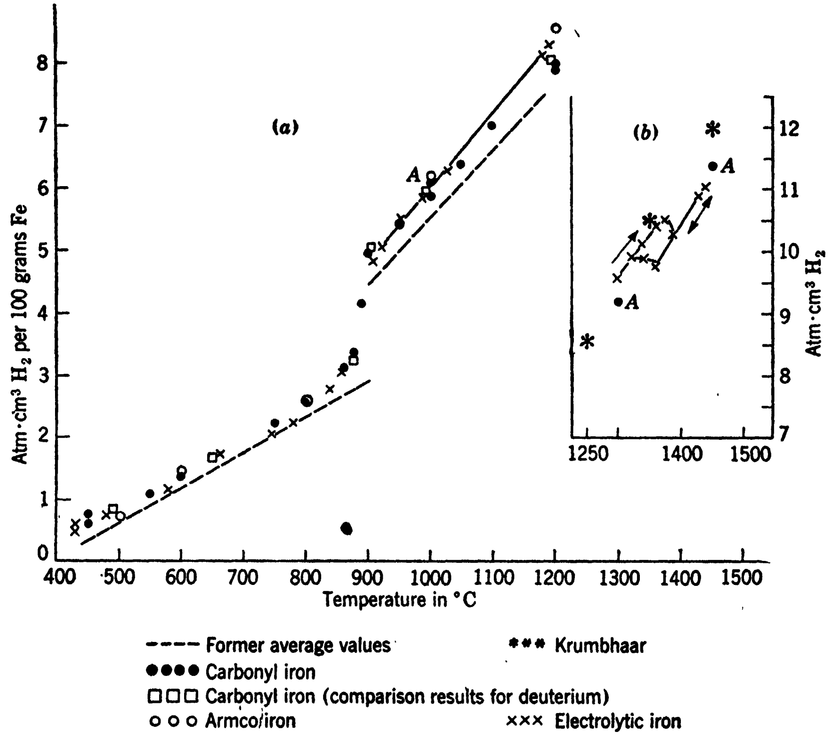

FIG. 3. Solubility of hydrogen (at 1 atmosphere) in iron, as a function of the temperature (Sieverts and Hagen).

Even at the melting point, the value of V_g is approximately 1, while that of r for the δ phase, just below the melting point, is $6.64 \cdot 10^{-4}$, or about 1 hydrogen atom per 1500 iron atoms.

The greater value of s for the γ than for the α phase is accounted for by Luckemeyer-Hasse and Schenck (4) as due to the fact that the hydrogen atom (which as mentioned subsequently is actually present as a proton) can be more readily located in an interstitial site in the looser face-centered structure than in the more closely packed body-centered structure.

This topic has also been investigated by Miss M. Armbruster (10). She determined the values of s for the three temperatures, 400, 500, and

TABLE 1

SOLUBILITY OF HYDROGEN IN IRON AT 1 ATM*
(SIEVERTS ET ALII)

t° C	s	$100x$	μm	V_g	$10^4 r$	$s(8)$	
400	0.35	3.15	15.6	0.0276	0.175		
500	0.75	6.75	33.5	0.0590	0.374	0.6	
600	1.20	10.80	53.5	0.0945	0.597		
700	1.85	16.65	82.5	0.146	0.922	1.8	
800	2.45	22.05	109.2	0.193	1.22		
900	4.05	36.45	182	0.319	2.02	3.0 (α)	4.7 (γ)
1000	5.50	49.50	245	0.433	2.74		
1100	6.60	59.40	294	0.519	3.29	7.0	
1200	7.95	71.55	355	0.626	3.96	8.2	
1300	9.50	85.50	424	0.748	4.73	10.1	
1400	11.20	100.8	500	0.881	5.58	10.5 (γ)	10.1 (δ)
1500	12.75	114.8	569	1.00	6.36		
1535 (s)	13.32	119.9	594	1.05	6.64	14 (δ)	
(l)	26.64	239.8	1188	2.10	13.28	25 (l)	
1550	27.75	249.8	1238	2.18	13.82	26	
1650	30.97	278.7	1381	2.44	15.43		

* Values of μm, V_g, and r calculated by the writer.

TABLE 2

ALLOTROPIC FORMS AND TRANSFORMATION POINTS FOR IRON

Phase Designation	Lattice Structure	Range of Stability in Degrees Centigrade
Alpha (α)	Body-centered cubic	to 906
Gamma (γ)	Face-centered cubic	906–1403
Delta (δ)	Body-centered cubic	1403–1537
Liquid		Above 1537

600° C, and for the range 18.9 to 629 mm at 600° C. Figure 4, taken from her publication, shows that the $\sqrt{P}$ law is valid down to very low pressures. It was found that all the observations at the three temperatures are in agreement with the relation

$$\log(\mu m) = 1.946 + 0.5 \log P_{mm} - \frac{1454}{T}, \tag{3}$$

where the solubility is measured in *micromoles per 100 g* iron. That this equation is valid for all temperatures up to 900° C is shown by the data in Table 3, taken from Miss Armbruster's publication, in which a comparison has been made of values calculated by means of the above equation (data for carbonyl iron in the first row) with those observed by previous investigators.

The second-last column gives values of the heat of solution, in *calories per gram-mole hydrogen* as derived from each set of observations. From equation 3 it follows that

$$Q_S = 9.148 \times 1454 = 13{,}300.$$

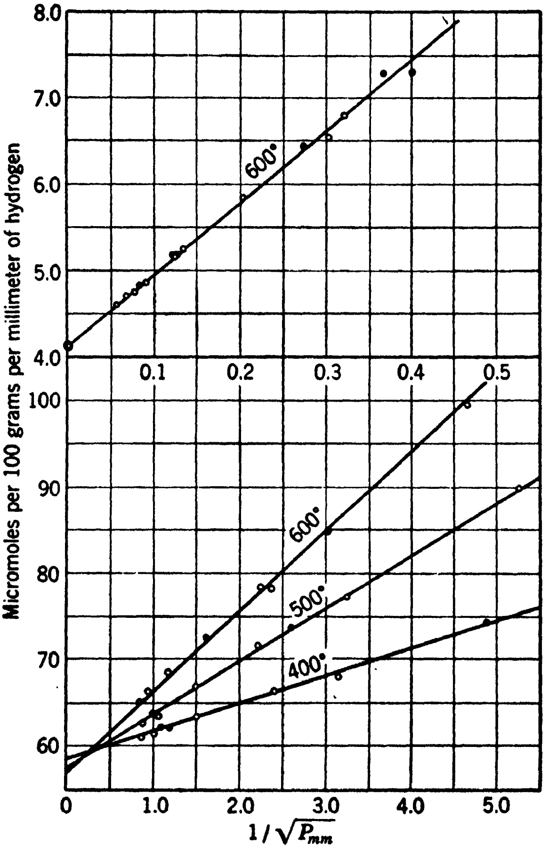

FIG. 4. Plot of solubility data for hydrogen in iron. Ordinates denote values of micromoles per 100 g iron per mm pressure. Abscissas give values of $1/\sqrt{P_{mm}}$. Upper section shows plot at 600° C and higher pressure range; lower section shows plots at 600° C, 500° C and 400° C for lower pressure range. Open and closed circles designate measurements with increasing and decreasing pressure, respectively; double circle is value of intercept as determined by a blank measurement with argon. (Armbruster.)

According to Sieverts, Zapf, and Moritz (8), the solubility of deuterium (D_2) in both armco- and carbonyl-iron is *lower* than that of ordinary hydrogen. The difference in the value of *s* was observed to vary from 0.1 to 0.9 over the range 600° C to 1450° C.

TABLE 3

COMPARISON OF SOLUBILITY DETERMINATIONS OF HYDROGEN AT 1 ATM IN DIFFERENT SAMPLES OF IRON (ARMBRUSTER)

Solubility in Micromoles per 100 g

Form of Sample	Temperatures, ° C							Q_S	Ref.
	300°	400°	500°	600°	700°	800°	900°		
Carbonyl sheet	7.06	16.8	32.0	52.6	78.0	107	140	13,300	10
Wire 2 mm	—	15.2	29.4	50.4	73.4	96.8	138	13,900	5
Wire and powder	—	15.6	26.8	53.5	80.3	106	134	13,700	8
Chips	4.4	8.9	29.0	51.3	78.0	105	129	13,800	4
Sheet 0.3 mm	—	8.0	26.3	53.1	78.1	103	125	12,300	2
Tubing	18.5	29.9	44.6	59.8	80.3	110	138	11,300	9
Electrolytic sheet	—	27.6	51.3	81.2	113	169	223	13,500	6
Electrolytic block	—	11.2	33.4	57.1	91	125	163	14,500	6
Reduced iron	—	13.4	44.6	78.0	110	145	195	13,000	6
Electrolytic	—	—	22.3	44.6	71.4	96.8	125	14,400	7
Reduced	—	8.9	31.2	62.4	84.7	114	143	11,400	7

Solubility of Hydrogen in Nickel ($A = 58.69$, $\rho = 8.9$). The earliest work on the solubility of hydrogen in nickel was carried out by Sieverts and his associates (1907–1911). The measurements were repeated by Smittenberg (11), using a much more refined technique. To secure a large surface, 12,000 m of wire, about 0.02 mm diameter (total weight = 42g, and total surface = 8430 cm^2) was used. This was made of vacuum-fused metal. Before exposing to hydrogen, the wire was heated in vacuum in steps of increasing temperature up to 900° C. The gas evolved during this treatment consisted almost entirely of carbon monoxide.

> After a 24-hours' evacuation at 900°, the temperature was gradually lowered to 600° and the flushing-out (with hydrogen) repeated several times at this temperature. Only after this treatment was it possible to obtain accurate and reproducible results for the amount of hydrogen sorbed by the nickel at different pressures and temperatures.

It was shown that, for 300° C and 600° C, the isotherms obeyed the $\sqrt{P}$ law. Furthermore, the isobar at 0.1 mm was found to be in good agreement with Sieverts' data when they were recalculated for the much lower pressure used by Smittenberg. Table 4 gives the values of s and μm at 1 atm based on the data obtained by Sieverts and Smittenberg.

The noteworthy features about these data are (1) the fact that the solubility of hydrogen in nickel is greater than that in iron, especially at

TABLE 4

SOLUBILITY OF HYDROGEN AT 1 ATM IN NICKEL*
(SIEVERTS AND SMITTENBERG)

$t°$ C:	200	300	400	500	600	700	800	900	1000	1100	1200	1300	1400	1452	1500	1600
s:	1.70	2.35	3.15	4.10	5.25	6.50	7.75	9.10	9.80	12.15	14.25	14.7	16.2	(m.p.)	41.6	43.1
μm:	76	105	141	183	234	290	346	406	437	542	636	656	723		1860	1920
V_g:	0.151	0.209	0.280	0.365	0.467	0.578	0.689	0.809	0.873	1.08	1.27	1.31	1.44		3.70	3.84
10^4r:	0.89	1.23	1.65	2.15	2.75	3.40	4.06	4.76	5.13	6.36	7.46	7.70	8.48		21.8	22.6

* Values of μm, V_g, and r calculated by the writer.

the lower temperatures, and (2) the considerable increase in solubility at the melting point.

More recently, solubility determinations were carried out by Miss Armbruster (10) on a sample of 99.5 per cent nickel in the form of strip 0.14 mm thick (weight = 337.7 g). The observations were made at 400°, 500°, and 600°, over the pressure range 0.001 to 1.8 mm. It was found that the results obtained could be represented by the relation, similar to that obtained for iron,

$$\log \mu m = 1.732 + 0.5 \log P_{mm} - \frac{645}{T}. \tag{4}$$

Table 5 (10) presents a comparison of the values of μm, calculated by means of this equation for 1 atm pressure, with those of previous investigators.

TABLE 5

COMPARISON OF THE DETERMINATIONS OF THE SOLUBILITY OF HYDROGEN AT 1 ATM IN DIFFERENT SAMPLES OF NICKEL (ARMBRUSTER)

Solubility in Micromoles per 100 g

	Temperatures, ° C								
Form of Sample	300°	400°	500°	600°	700°	800°	900°	Q_S	Ref.
Sheet	111	164	218	271	323	373	419	5900	10
Wire	135	183	244	297	349	393	436	5300	(11)
Wire and chips	105	161	186	245	301	356	411	6100	(1)
	89	112	145	192	251	312	381	4300 (300–500°) 9000 (500–900°)	(4)

The value derived by Miss Armbruster is Q_S = 5900 cals/g-mole H_2.

Solubility of Hydrogen in Alloys of Iron and Nickel. Figure 5 (10) shows plots (according to Miss Armbruster) of log (μm) versus $1/T$, at $P_{mm} = 760$, for nickel, iron, and a number of iron-nickel alloys.

According to the data in Tables 3 and 4, the values of μm at 400° C and 1 atm are 17 for iron and 164 for nickel. (Values of s are 0.38 and 3.68, respectively.) The plots for the iron-nickel alloys lie between those for the two metals, and for each alloy the solubility can be expressed by an equation similar to equations 3 and 4. From the slopes of these plots it is seen that the value of Q_S decreases with increase in nickel content, as would be expected from a comparison of the values for the pure metals.

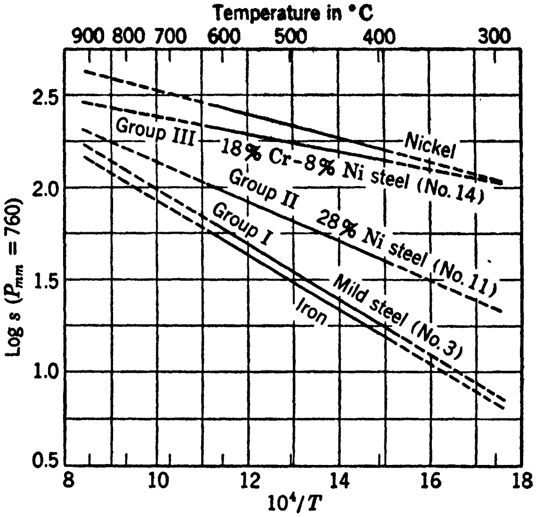

FIG. 5. Log of solubility of hydrogen at 1 atmosphere in iron, nickel, and a typical steel from each of the three groups, plotted versus $1/T$. From the slopes of the straight lines, values of the heat of solution (Q_S) are derived. (Armbruster.)

The alloys tested by Miss Armbruster could be divided into three groups: (I), the ferritic type, for which the values of s observed are substantially the same as for pure iron; (II), which comprised a 28 per cent steel and a 13 per cent Mn steel; and (III), the austenitic type, which comprised two stainless steels, Cr 18, Ni 8; and Cr 13, C 0.3; as well as nickel itself.

Similar observations on the effects of alloying elements have been made by other investigators. Figure 6 (9) shows an isobar at 1 atm for a 5 per cent nickel alloy compared with that for vacuum-melted iron.

Lückemeyer and Schenck (4) have determined the solubility of hydrogen in Fe-Cr-Ni alloys of different compositions. The values of s

range from slightly above that for iron (most cases) to slightly lower than this. The same investigators also observed (in agreement with Miss Armbruster's observations) that, in Fe-Ni alloys ranging from 3.3 per cent Ni to 8.48 per cent Ni, *s* increases with increase in nickel content.

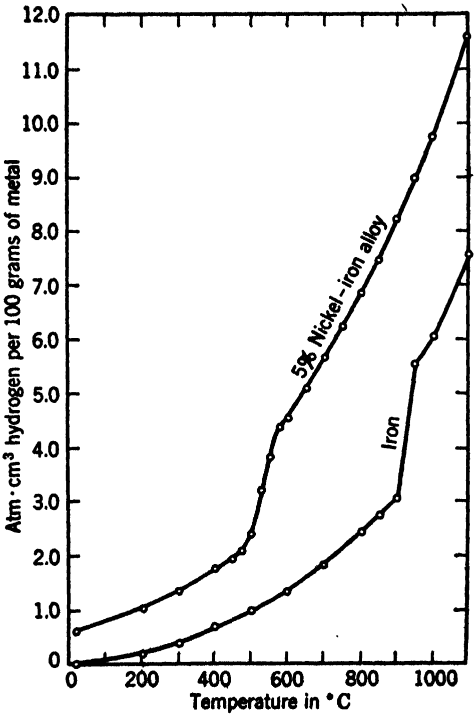

FIG. 6. Plots of solubility data for hydrogen at 1 atmosphere in a 5 per cent nickel-iron alloy and in vacuum-melted iron, as a function of the temperature (Andrew, Lee, and Quarrell).

Solubility of Hydrogen in Cobalt ($A = 58.94$, $\rho = 8.8$). The values of the solubility at 1 atm as observed by Sieverts and Hagen (12) are given in Table 6.

As is evident from a comparison of the data in Tables 6 and 1, the solubility of hydrogen in cobalt is less than that in iron. From a plot of log s versus $1/T$, the value derived for the heat of absorption is $Q_S = 14{,}550$ cal/g-mole H_2.

Solubility of Hydrogen in Copper ($A = 63.57$, $\rho = 8.95$). The values obtained by Sieverts (1) are given in Table 7. These are slightly higher than the values obtained subsequently by Roentgen and Moeller (13).

TABLE 6

SOLUBILITY OF HYDROGEN AT 1 ATM IN COBALT*
(SIEVERTS AND HAGEN)

t° C:	600	700	800	900	1000	1100	1150	1200
x:	0.08	0.110	0.167	0.227	0.298	0.390	0.437	0.490
s:	0.89	1.22	1.85	2.52	3.21	4.33	4.85	5.44
10^4r:	0.47	0.65	0.98	1.34	1.76	2.30	2.58	2.89
V_g:	0.08	0.108	0.164	0.223	0.293	0.383	0.430	0.481

* Values of s, r, and V_g calculated by the writer.

Below the melting point, the solubility of hydrogen is less in copper than in iron, but at the melting point the solubility increases to almost three times that for the solid, and, as the temperature is increased higher, s approaches closely that for hydrogen in iron at the same temperature.

TABLE 7

SOLUBILITY OF HYDROGEN AT 1 ATM IN COPPER*
(SIEVERTS)

t° C:	400	500	600	700	800	900	1000
s:	0.06	0.16	0.30	0.49	0.72	1.08	1.58
V_g:	0.0054	0.0143	0.0268	0.0439	0.0644	0.0967	0.141
10^4r:	0.053	0.0908	0.170	0.278	0.409	0.613	0.896

t° C:	1083 (m.p.)		1100	1200	1300	1400	1500
s:	2.10 (s)	6.00 (l)	6.3	8.1	10.0	11.8	13.6
V_g:	0.188	0.537	0.564	0.725	0.893	1.05	1.22
10^4r:	1.19	3.40	3.58	4.60	5.67	6.70	7.71

* Values of V_g and r calculated by the writer.

The heat of absorption, deduced from the plot of log s versus $1/T$, is $Q_S = 18{,}300$ cal/g-mole H_2.

Roentgen and Moeller state that the addition of small percentages of aluminum to copper decreases the solubility of hydrogen proportionally. Figure 7 (1) shows the effect of alloying with other metals on the solubility of hydrogen in *molten* copper. (Note that $s = 11.12x$.)

N. P. Allen[17] has observed that the solubility of hydrogen in molten copper is decreased considerably when oxygen is also present in solution. Thus, for 0.05 per cent by weight of oxygen (0.35 cm^3/100 g), the value of s for hydrogen is decreased to 0.45 cm^3 (S.T.P.) per 100 g.

---

[17] *J. Inst. Metals*, **43**, 81 (1930).

The solubility of hydrogen in *fused* copper and copper-tin alloys (bronzes) has been investigated by M. B. Bever and C. F. Floe.[18] Their results are summarized in Table 8.

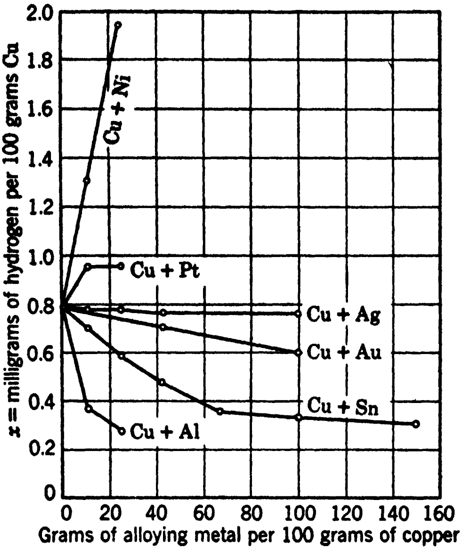

FIG. 7. Effect of alloying metals on the solubility of hydrogen in molten copper (Sieverts).

TABLE 8

SOLUBILITY OF H_2 AT 1 ATM IN COPPER, COPPER-TIN ALLOYS, AND TIN (BEVER AND FLOE)

s = cm³ (S.T.P.) per 100 g metal

		Bronzes Containing p Atomic Per Cent Sn					
t° C	Pure Cu	p = 3.3	6.5	12.9	26.4	39.3	100
1000	—	—	3.09	2.11	0.53	0.50	0.04
1100	5.73	4.80	4.11	2.97	0.94	0.76	.09
1200	7.33	6.28	5.35	3.94	1.50	1.15	.205
1300	9.37	7.81	6.85	5.10	—	1.61	.355
% Sn by wt:		5.9	11.5	21.7	40.2	54.8	100

The values of s for pure copper are in good agreement with those observed by Roentgen and Moeller, which, as stated previously, are slightly lower than those given in Table 7. The last column in Table 8 gives values of s for fused tin, and, as will be observed, the solubility values for the bronzes decrease with increase in percentage of tin.

---

[18] *Trans. A.I.M.E.*, **156**, 149 (1944).

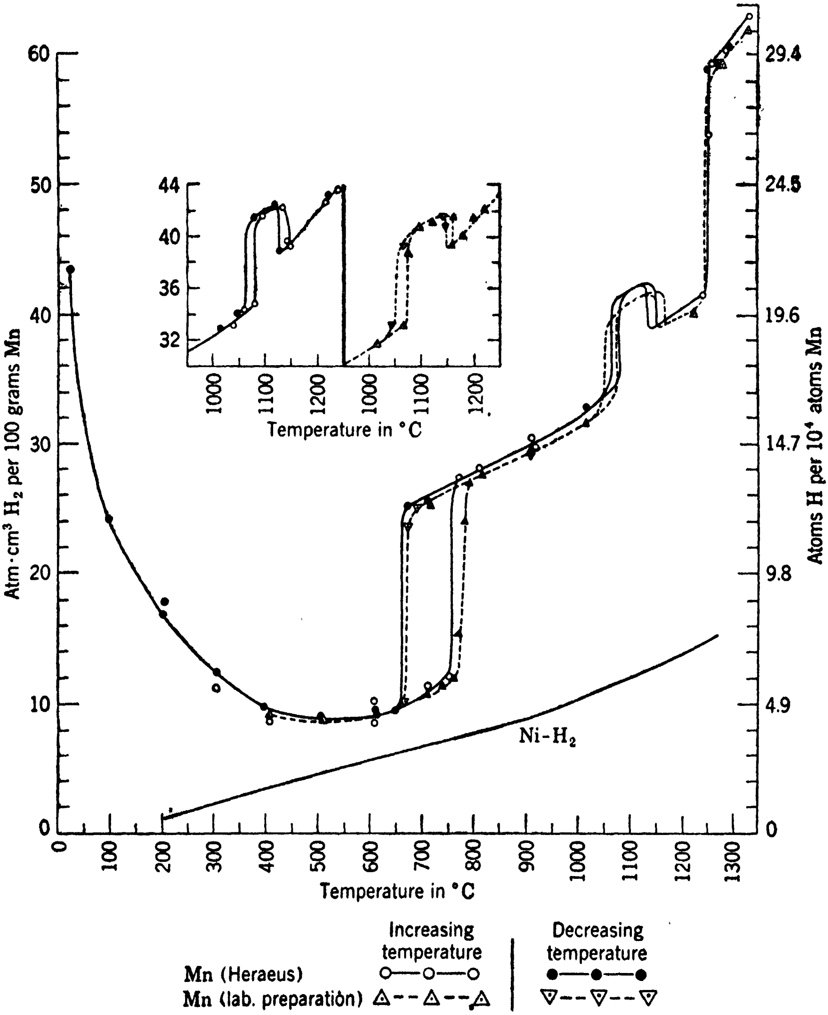

FIG. 8. Isobars (at 1 atmosphere) for solubility of hydrogen in two samples of pure manganese at various temperatures. Inset shows plots for the range 1000° C to 1250° C. (Sieverts and Moritz.)

According to Bever and Floe, "the investigation points definitely to hydrogen as a major source of porosity in bronze castings." These results also indicate that caution must be exercised in the use of bronze solders in a hydrogen atmosphere for devices that are to be evacuated.

For tin, $A = 118.70$ and $\rho = 7.28$. Hence, at 1300° C, $r = 3.76 \cdot 10^{-5}$ and $V_g = 0.0258$.

Solubility of Hydrogen in Manganese ($A = 54.93$, $\rho = 7.2$). Figure 8 (18) shows the isobar at 760 mm as obtained by Sieverts and Moritz (18) for very pure metal. As for the other metals discussed above, the $\sqrt{P}$ law was found to apply to the Mn-H_2 system, as shown by isotherms at 192° C, 608° C, and 912° C.

Comparing the isobar at 1 atm for this system with that for Ni-H_2 (see the lowest curve in Fig. 8), it is evident that the solubility of hydrogen in pure manganese is much greater than that observed for nickel.

An interesting and new feature, observed only in this system, is the occurrence of a *minimum* in the solubility at about 550° C. The character of the isobar is accounted for by the fact that manganese has four crystal modifications as follows:

α-manganese, cubic, 58 atoms per elementary cube.
β-manganese, cubic, 20 atoms per elementary cube.
β'-manganese, cubic face-centered.
γ-manganese, tetragonal face-centered.

Table 9 gives the solubility data at temperatures below and above each of the transition temperatures and at the melting point (1242° C).

TABLE 9

SOLUBILITY OF HYDROGEN AT 1 ATM IN MANGANESE
(SIEVERTS AND MORITZ)

s = cm³ (S.T.P.) per 100 g metal

Transition Point	°C	Pure Mn		Technical Mn	
		Heraeus	S.M.	97.8% Mn	96.4% Mn
A_1	600	9	9	7.5	0.5
	800	27	27	23	13.0
A_2	1050	34	33	30	19.5
	1100	42	41	35.5	(23)
A_3	1125	42.5	41.5	—	—
	1165	40	39.5		
M.p.	1242	cryst. 44	44	37	—
		liquid 59	59	52	—
	1320	62	63	(58)	

Data are given for two samples of "pure" metal, one obtained from Heraeus and the other prepared by the investigators (SM), and also for two samples of "technical" manganese.

The solubility in the α form *decreases* with increase in temperature; that in the β and β' forms *increases* with increase in temperature.

Evidently the presence of impurities in the metal decreases the solubility of hydrogen, in agreement with the fact that the solubility data obtained by Luckemeyer-Hasse and Schenck are still lower than those given in Table 9.

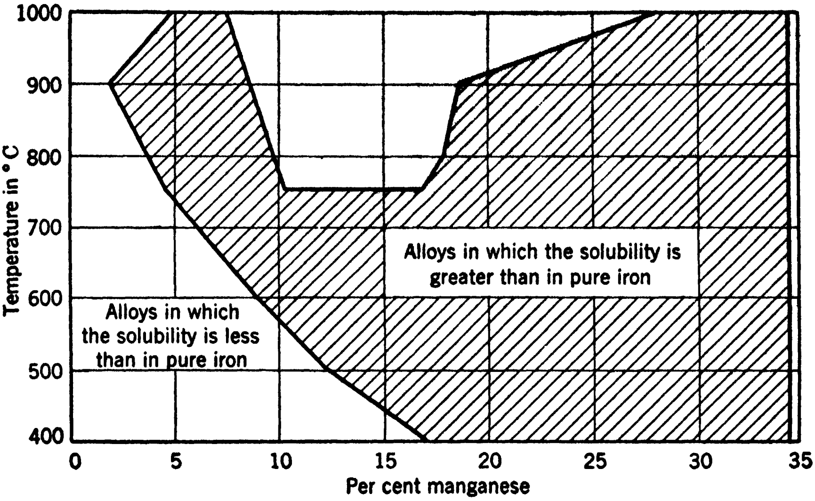

FIG. 9. Composition of iron-manganese alloys in which the solubility of hydrogen is *less* than that in pure iron (clear region) and alloys in which the solubility is *greater* than that in pure iron (shaded region) (Baukloh and Müller).

The value $s = 40$ corresponds to the values $V_g = 2.88$ and $r = 19.6 \cdot 10^{-4}$.

The solubility of hydrogen in iron-manganese alloys has been determined by Baukloh and Müller (6). Figure 9 taken from their publication presents a comparison of the solubility data for different percentages of manganese in iron over the ranges of temperatures 400° C to 1000° C. The shaded area corresponds to compositions of alloys in which hydrogen is more soluble than in pure iron; the unshaded area corresponds to alloy compositions in which hydrogen is less soluble.

As will be observed, there is a range of compositions (between 10 and 20 per cent manganese) in which the solubility decreases at temperatures above 750° C, owing to the transformation from an α to an ϵ phase, in which hydrogen is much less soluble than in α-iron.

Solubility of Hydrogen in Chromium and Molybdenum. (For Cr, $A = 52.01$, $\rho = 7.1$; for Mo, $A = 95.95$, $\rho = 10.2$.) An isobar at 1 atm for the solubility of hydrogen in *chromium* is shown by E. Martin (2). Since the original data are not given, approximate values of s were taken from the plot. These appear along with values of V_0 and r, in Table 10.

TABLE 10

SOLUBILITY OF HYDROGEN AT 1 ATM IN CHROMIUM (MARTIN)

s = cm^3 (S.T.P.) per 100 g

$t°$ C:	600	800	900	1000	1100
s:	0.5	1.0	2.0	3.0	4.2
V_0:	0.035	0.07	0.14	0.42	0.3
$10^4 r$:	0.23	0.46	0.92	1.4	2.0

Thus the solubility data for chromium lie between those for cobalt and copper.

The solubility of hydrogen in *molybdenum* has been investigated by Martin (2) and by Sieverts and Brüning (20). The values obtained by the latter two, which are somewhat lower than those quoted by Martin, are given in Table 11. The solubility values are considerably lower than those for hydrogen in cobalt. A plot of log x versus $1/T$ yields values that are too scattered for an accurate determination of Q_S. From the data in italics in the table (which agrees with a smooth curve in the original paper), the value deduced is $Q_S = 14{,}000$ cal/mole H_2.

TABLE 11

SOLUBILITY OF HYDROGEN AT $P_{mm} = 753$ IN MOLYBDENUM
(SIEVERTS AND BRÜNING)

$t°$ C:	420	617	763*	791	983*	995	998	1095*
x:	0.015	0.017	*0.023*	0.022	0.029	0.051	*0.044*	*0.056*
s:	0.167	0.189	0.255	0.244	0.322	0.566	0.488	0.622
$10^4 r$:	0.14	0.16	0.22	0.21	0.28	0.49	0.42	0.53

* Values obtained with molybdenum powder; the other values were obtained with wire.

For alloys of molybdenum and iron, the solubility of hydrogen increases almost linearly with the iron content up to 52 per cent iron.[19] For smaller molybdenum content, the solubility is only slightly less than that in pure iron. The plots of log *s* versus $1/T$ for the series up to 52 per cent iron are practically parallel. Actually these linear plots, which are much better than those for molybdenum, give the same value for Q_S as that deduced above.

---

[19] Plots of s versus molybdenum content for different temperatures are shown in CS, pp. 185–186.

Solubility of Hydrogen in Aluminum ($A = 26.97$, $\rho = 2.70$). The gas is practically insoluble in the solid metal, but is soluble to a small extent in the molten metal (m.p., 659° C). Determinations of *s* have been made by Bircumshaw (17), Roentgen and Moeller (13), and Roentgen and Braun (16). These three sets of data are in approximate agreement. The solubilities measured by Iwasé (15) are so much greater than those obtained by the other investigators that they should be disregarded.

More recently the subject has been investigated by W. D. Robertson[20] and by G. J. Azarian and E. Epremian.[21]

Epremian confirmed the validity of the $\sqrt{P}$ law over the range $P = 40$ to $P = 760$ mm of mercury. Their values of *s* (cm³/100 g at 1 atm) are given in the second and third columns, Table 12, along with the values obtained by the other investigators, including Czochralski (14).

TABLE 12

SOLUBILITY OF HYDROGEN AT 1 ATM IN MOLTEN ALUMINUM

t° C	Azarian and Epremian		Ref. 17		Ref. 13 Ref. 16		Ref. 14	
	s	V_g	*s*	V_g	t° C	*s*	t° C	*s*
700	0.15*		0.23	0.006	690	0.27	1200	~2.5
800	0.493	0.013	0.89	.024	866	1.45	1500	~5.5
900	1.480	.040	1.87	.051	1096	5.00	Ref. 15	
940	1.867	.050			1233	8.02	800	~10
1000	3.0*		3.86	.104			900	~17

* Extrapolated from a plot of log *s* versus $1/T$.

From the plot of log *s* versus $1/T$, Bircumshaw deduced the value $Q_S = 43{,}400$ cal/g-mole H_2, whereas Azarian and Epremian deduced the value $Q_S = 50{,}800$.

According to Roentgen and Moeller, copper alloyed with the aluminum reduces the value of *s* by an amount that varies linearly with the percentage of copper, so that for about 30 atomic per cent of aluminum s is negligibly small.[22]

---

[20] Thesis, M.I.T., 1942.

[21] Thesis, M.I.T., 1943, a copy of which was kindly given the writer by Mr. Epremian.

It has also been reported[23] that silicon, manganese, and nickel reduce the solubility, while addition of magnesium increases the solubility of hydrogen in aluminum.

Smithells[24] has stated that "Hydrogen accounts for about 80 per cent of the gas which can be extracted from commercial aluminum by vacuum treatment, although it cannot all be present in solution." Rapid cooling of the fused metal probably leaves some of the excess gas occluded in small pores.

Solubility of Hydrogen in Platinum and Silver. (For Pt, $A = 195.23$, $\rho = 21.45$; for Ag, $A = 107.88$, $\rho = 10.50$.) The data on platinum, given in Table 13, were obtained by Sieverts (1).

TABLE 13

SOLUBILITY OF HYDROGEN AT 1 ATM IN PLATINUM (SIEVERTS)

$t°$ C:	409	827	1033	1136	1239	1342
s:	0.067	0.10	0.233	0.40	0.61	0.93
V_g:	.014	.022	.050	.086	0.131	0.201
10^4r:	.12	.18	.41	.70	1.07	1.64

For the range 1000° C to 1350° C, $Q_S = 34{,}500$.

Table 14 gives data on the solubility of hydrogen in silver obtained by Steacie and Johnson (19). From the values of V_g, at 80 cm pressure, given in their publication, values of s and 10^4r were calculated for atmospheric pressure.

TABLE 14

SOLUBILITY OF HYDROGEN IN SILVER
(STEACIE AND JOHNSON)

			Solubility at 1 atm		
$t°$ C	$V_g(P_{cm} = 80)$	$\sqrt{P_{cm}}/V_g$	s	V_g	10^4r
400	0.006	1500	0.055	0.0058	0.054
500	.012	750	.110	.0116	.107
600	.019	470	.176	.0185	.170
700	.025	358	.232	.0244	.224
800	.036	248	.334	.0351	.322
900	.046	195	.427	.0448	.411

---

[22] Plots of the data for a series of temperatures are shown in CS, p. 182.

[23] J. Erickson, *Light Metal Age*, July, 1944, p. 19.

[24] CS, p. 161.

The values in the third column in Table 14 are average values. From the plot of log *s* versus $1/T$, the value derived for the heat of absorption is $Q_S = 11{,}900$ cal/g-mole H_2. A comparison with the data for the other metals shows that the solubility of hydrogen at 1 atm in silver is about one-tenth that (at the same pressure) in cobalt.

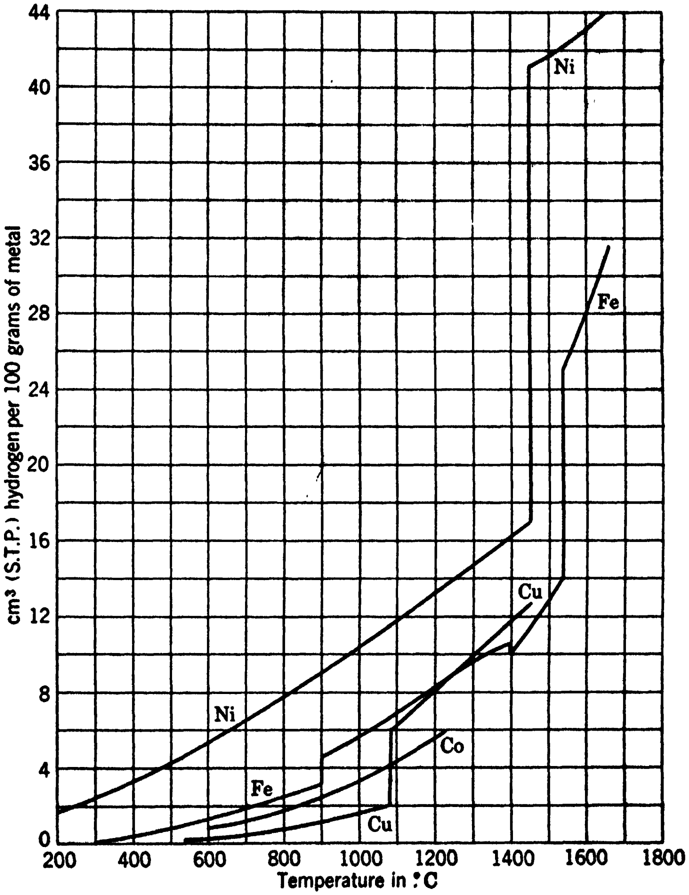

FIG. 10. Comparison of isobars for the solubility of hydrogen at 1 atmosphere in nickel, iron, cobalt, and copper.

Table 15 presents a summary of the solubility data for the metals of Group A (with the exception of Mn), and Fig. 10 shows the isobars at 1 atm for Ni, Fe, Co, and Cu. The plot for Cr would be located between those for Co and Cu, and that for Al below that for Cu.

TABLE 15

SOLUBILITY (cm^3/100 G) OF HYDROGEN AT 1 ATM, IN METALS OF GROUP A

$t°$ C	Ni	Fe	Co	Cr	Cu	Al	Ag	Mo	Pt
200	1.70								
300	2.35	0.16							
400	3.15	0.35			0.06		0.055	0.165	0.065
500	4.10	0.75			0.16		.110	.175	
600	5.25	1.20	0.89	0.5	0.30		.176	.185	0.075
700	6.50	1.85	1.22		0.49	0.15	.232	.21	
800	7.75	2.45	1.85	1.0	0.72	0.49	.334	.25	0.095
900	9.10	3.0 (α) 4.7 (γ)	2.52	2.0	1.08	1.48	.427	.29	0.135
1000	9.80	5.50	3.21	3.0	1.58	3.0		.50	0.20
1100	12.15	7.00	4.33	4.2	6.3 (l)			.62	0.35
1200	14.25	8.25	5.44		8.1				0.52
1300	14.7	10.1			10.0				0.77
1400	16.2	10.5 (γ) 10.1 (δ)			11.8				1.15
1500	41.6 (l)				13.6				
1535		14 (δ) 25 (l)							
1600	43.1	28							
1650		31							
$10^{-3}Q_S$	5.9	13.3	15.55		18.30	50.80	11.90	14.00	34.50
$V_g(800)$	0.69	0.19	0.164	0.071	0.066	0.024	0.036	0.025	0.020
$10^4 r(800)$	4.06	1.22	0.98	0.46	0.41	0.214	0.33	0.214	0.165
M.p. (°C)	1452	1535	1480	1615	1083	659	961	2620	1755

5. SOLUBILITY OF HYDROGEN IN METALS OF GROUP B

Solubility values, in terms of cm^3 (S.T.P.) *per gram* ($= 10^{-2}s$), are shown in Table 16.[25] Figure 11 shows plots of the isobars at 1 atm pressure. As with metals of Group A, s varies as $\sqrt{P}$, leading to the conclusion that, in both cases, hydrogen enters the lattice structure as atoms, or rather as protons.

There are, however, the following striking differences between the values of s for the two groups:

(*a*) The solubility of hydrogen in metals of Group B is 10^3 to 10^4 times that of the solubility in metals of Group A. This is indicated by a comparison of values of V_g and r. In Table 16, the values of these quantities are given for room temperature. These correspond to "hydrides" of the composition MH_r, where M denotes a metal of this group, and *r is not an integer.*

---

[25] For some of the metals, the values given by CS, p. 161, were used.

TABLE 16

SORPTION OF HYDROGEN BY METALS OF GROUP B

$10^{-2}s$ = cm³ (S.T.P.) per g, at 1 atm pressure

Temperature, °C	Ti	V	Zr	Cb	La	Ce	Ta	Th	Pd
20	407.4	150	235.5	55.0	223	215	46	148	(60)
300		65	—	44.4	192	184	33	—	(3.3)
400	387.7	38	—	36.8	182	176	25	—	2.3
500	366.0	19	—	22.7	172	168	14	—	1.9
600	334.7	10	184	9.88	163	160	7	91	1.8
700	183.9	6.4	176	5.11	153	152	4.2	88	1.70
800	140.9	4.4	165	3.30	143	145	2.5	81	1.62
900	98.2	3.2	138	2.17	134	138	1.8	77	1.57
1000	66.1	2.5	78	1.63	123	130	1.4	26	1.55
1100	45.9	2.1	47	—	111	113	1.1	19	1.54
1200	—	—	32	—	41	53	1.0	17.5	—
A	47.90	50.95	91.22	92.91	138.92	140.13	180.88	232.12	106.7
ρ	4.52	5.87	6.4	8.4	6.15	6.90	16.62	11.2	11.40
V_g	1800	900	1525	460	1490	1450	765	1660	700
r	1.75	0.72	1.92	0.47	2.76	2.69	0.78	3.07	0.59
ρ_{HM}	3.91	5.30	5.67	—	5.83	5.7	15.10	—	10.76

(*b*) The solubility *decreases* with increase in temperature. That is, *heat is evolved* when hydrogen enters into solution, and hence the reaction involved in the formation of any one of the hydrides is exothermic, as in the formation of the chemically well-defined hydrides of the alkali and alkaline-earth metals. The magnitude of Q, obtained from a plot of $\log s$ versus $1/T$, corresponds to the heat of formation of the "hydride."

(*c*) The density of the saturated solution indicated by ρ_{HM} in the lowest row of the table, is uniformly *less* than that of the metal itself (designated by ρ). The values of ρ given in the second row at the bottom of Table 16 are taken from the standard handbook and are not the same, in general, as those given by A. Sieverts and A. Gotta.[26]

---

[26] *Z. anorg. Chem.*, **172**, 1 (1928); **187**, 155 (1930).

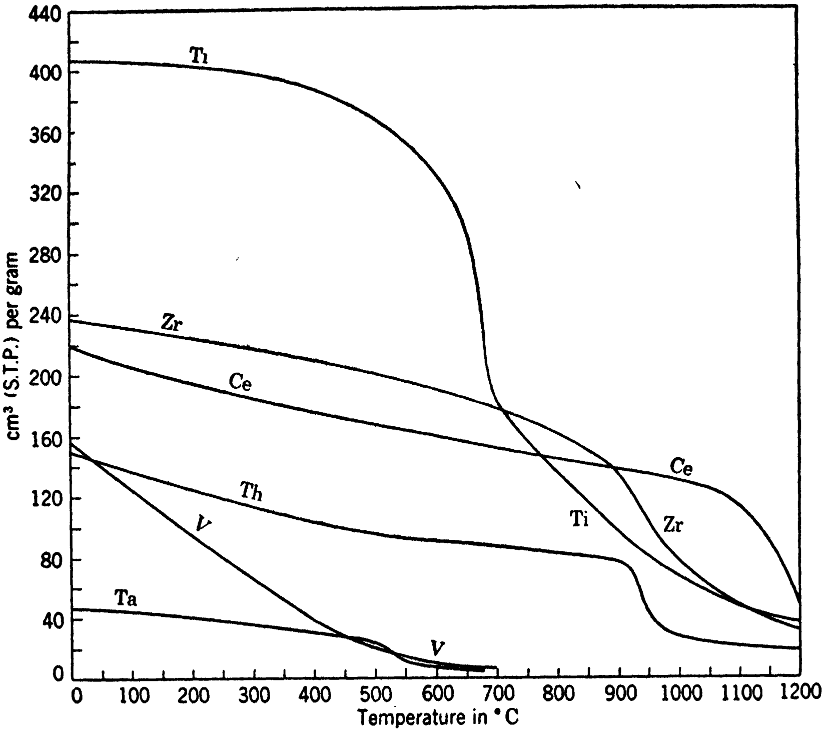

FIG. 11. Plots of the data for the solubility of hydrogen at 1 atmosphere (cm^3, S.T.P., per g metal) in metals of Group B at various temperatures.

A bibliography of references to the literature on the solubility data for hydrogen in metals of Group B is given in List II.[27]

List II. References on Solubility of Hydrogen in Metals of Group B

1. (Ta, W) A. Sieverts and E. Bergner, *Ber. deut. chem. Ges.*, **44**, 2394 (1911); also see reference 17 below.
2. (Ce) A. Sieverts and G. Müller-Goldegg, *Z. anorg. Chem.*, **131**, 65 (1923).
3. (Ce, La, Ce-Mg) A. Sieverts and E. Roell, *Z. anorg. Chem.*, **146**, 149 (1925).
4. (Pr, Nd) A. Sieverts and E. Roell, *Z. anorg. Chem.*, **150**, 261 (1926).
5. (Zr, Th) A. Sieverts and E. Roell, *Z. anorg. Chem.*, **153**, 289 (1926). Also see reference 18 below.
6. (V, Ti) H. Huber, L. Kirschfeld, and A. Sieverts, *Ber. deut. chem. Ges.*, **59B**, 2891 (1926).
7. (La, Ce, Pr) A. Sieverts and A. Gotta, *Z. anorg. Chem.*, **172**, 1 (1928).
8. (Ti) L. Kirschfeld and A. Sieverts, *Z. physik. Chem.*, **A**, **145**, 227 (1929).

---

[27] For a comprehensive bibliography on the solubility of gases in these metals see O. Kubaschewski, *Z. Elektrochem.*, **44**, 152 (1938).

9. A. Sieverts, *Z. Metallkunde*, **21**, 37 (1929)—summary of previous results.
10. (Cb) H. Hagen and A. Sieverts, *Z. anorg. Chem.*, **185**, 225 (1930).
11. (Zr, Ta) A. Sieverts and A. Gotta, *Z. anorg. Chem.*, **187**, 155 (1930).
12. (V) L. Kirschfeld and A. Sieverts, *Z. Elektrochem.*, **36**, 123 (1930).
13. (Ti) A. Sieverts and A. Gotta, *Z. anorg. Chem.*, **199**, 384 (1931).
14. (Pd) H. Brüning and A. Sieverts, *Z. physik. Chem.*, **A**, **163**, 409 (1932).
15. (Pd) L. J. Gillespie and F. P. Hall, *J. Am. Chem. Soc.*, **48**, 1207 (1926).
16. (Pd) L. J. Gillespie and L. S. Galstaun, *J. Am. Chem. Soc.*, **58**, 2565 (1936).
17. (Ta) A. Sieverts and H. Brüning, *Z. physik. Chem.*, **A**, **174**, 365 (1935).
18. (Zr) M. N. A. Hall, S. L. H. Martin, and A. L. G. Rees, *Trans. Faraday Soc.*, **41**, 306 (1945). This paper contains an extensive list of references to previous publications.

We shall now consider, in more detail, the solubility data for each of the metals mentioned in Table 16 and the interpretation of the phenomena involved.

Palladium. Of all the metals for which data are given in Table 16, *palladium* has received the most attention.[28] Whether in the form of foil, sponge, or palladium "black," the metal takes up as much as 900 volumes of hydrogen at normal pressure and temperature. The actual amount varies with method of preparation as well as with the nature of the previous heat and exhaust treatment. The sorption at the temperature of liquid air is about ten times that observed at room temperature and much greater than that observed for charcoal at the same low temperature.

Figure 12 shows plots of the isotherms as calculated by J. R. Lacher (see subsequent remarks) compared with the actual data (indicated by circles) obtained by Gillespie and Galstaun (16). The abscissas give values of the variable $\theta = r/0.59$ (used by Lacher in his interpretation of the observations). As will be observed, each isotherm exhibits a horizontal portion for which the pressure of hydrogen is constant over a range of values of r. At room temperature the maximum value of r for the horizontal portion is about 0.6. With increase in temperature the range of values of r for which P is constant decreases, and finally, at 295° C and 19.87 atm, there remains only a point of inflection at $r = 0.27$. Table 17 gives the values of P associated with the horizontal portions at a series of temperatures.

According to Gillespie and Galstaun, these dissociation pressure data are represented very satisfactorily by the relation

$$\log P_{atm} = 4.6018 - \frac{1877.82}{T}, \tag{1}$$

where T = absolute temperature.

---

[28] For review of the earlier literature see McB., p. 288 et seq.

This leads to a value for the heat of formation of the alloy of

$$\begin{aligned} Q &= 1877.82 \times 4.574 \\ &= 8588 \text{ cal/mole } H_2. \end{aligned}$$

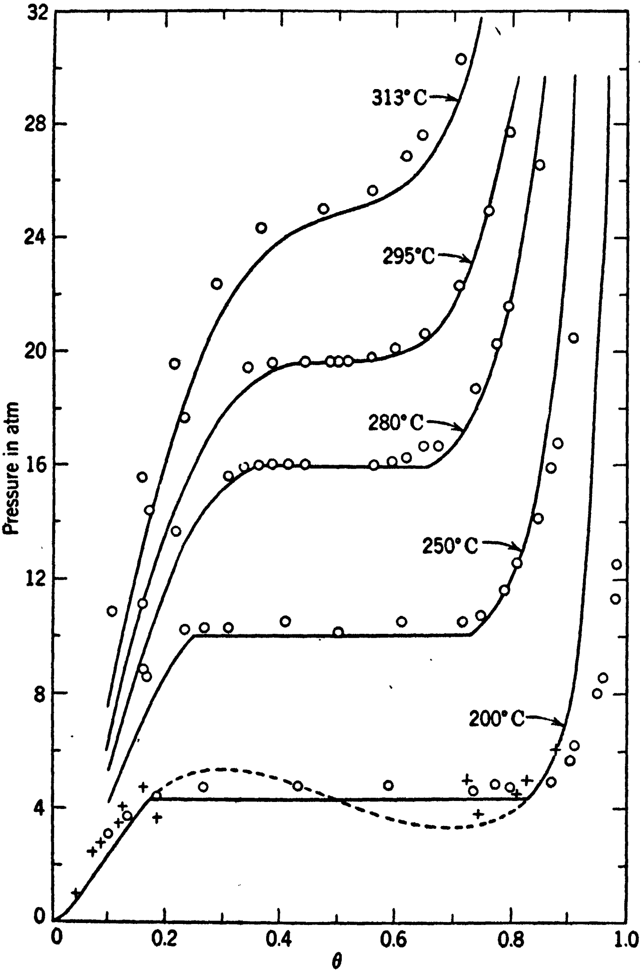

FIG. 12. Pressure-solubility isotherms for system hydrogen-palladium at a series of temperatures. $\theta = r/0.59$, where r = number of hydrogen atoms per atom of palladium. The observed values are indicated by circles; the plots are those calculated according to theory. (Lacher.)

Above 300° C, the solubility of hydrogen in palladium decreases with increase in temperature as shown in Table 16. It is of interest to note

TABLE 17

DISSOCIATION PRESSURES OF PdH_r ALLOYS

Temperature, °C	P_{atm}	P_{mm}
295	19.77	
250	10.28	
200	4.295	
150	1.455	
135	1.0	760
100		223.4
80		145.9
50		46.8
30		19.3
0		4.0

that the solubility of deuterium (D_2) is somewhat less than that of ordinary hydrogen.

Solubility values for hydrogen and deuterium in palladium at 760 mm and for the temperature range 300° C to 1200° C have been determined by A. Sieverts and G. Zapf[29] and Sieverts and W. Danz.[30] These data are given in Table 18.

TABLE 18*

VALUES OF (SOLUBILITY) s FOR H_2 AND D_2 AT 1 ATM, IN PALLADIUM

t° C	$10^{-2}s_H$	$10^{-2}s_D$	s_D/s_H
300	1.64	1.10	0.67
400	1.26	0.938	.74
500	—	0.831	—
600	0.927	0.758	.82
700	—	0.742	—
800	0.84	0.729	.87
900	—	0.719	—
1000	0.785	0.715	.91
1100		0.695	
1200	0.712		

* These values for hydrogen are evidently lower than those given for palladium in Table 16. The latter were taken from CS, p. 161.

For the temperature range 600° C to 1200° C, and pressures up to 1 atm, both hydrogen and deuterium obey the $\sqrt{P}$ law.

A number of investigators have suggested explanations for these observations on the palladium-hydrogen system, but the most satisfactory interpretation is that given by J. R. Lacher.[31]

---

[29] *Z. physik. Chem.*, **A**, **174**, 359 (1935).

[30] *Z. physik. Chem.*, **B**, **34**, 158 (1936).

[31] *Proc. Roy. Soc. London*, **A**, **161** 525 (1937).

As will be observed from the shape of the isotherms in Fig. 12, there is a region of values of r for which the pressure remains constant. According to Lacher, "When r is less than r_α or greater than r_β,[32] the pressure increases with increasing concentration." While equilibrium is established very rapidly in the regions of $r < r_\alpha$ and $r > r_\beta$, hysteresis effects have been observed for the region $r_\alpha < r < r_\beta$, which indicate that equilibrium is established much more slowly in this range of compositions. Also there is X-ray evidence for the conclusion that, in this region of constant pressure, the hydrogen-palladium system consists of "two coexistent expanded palladium lattices."

Furthermore,

> at the critical temperature r is 0.270. The value of r_α, at which the second phase appears, decreases as the temperature decreases; the value of r_β, at which the first phase disappears, increases.

The fact that the observed maximum value of r is about 0.6 is explained by Lacher on the basis of the electron configuration of the palladium atom as follows:

> Palladium is a transition metal and has two bands of allowed electron states, namely the *s* and *d* bands. These bands overlap. The *s* band can accommodate two electrons per atom and the *d* band ten. Palladium furnishes only ten, with the result that the two bands are not completely filled. Gold has one more electron than palladium, and when Pd is alloyed with Au, measurements of the susceptibility and electrical resistance can be explained by assuming that the extra electron goes into the *d* band which is filled up when between 0.55 and 0.60 electrons per atom have been added.[33] Similarly, when palladium is alloyed with hydrogen, its paramagnetic susceptibility decreases and becomes zero when between 0.53 and 0.66 hydrogen atom per palladium atom have been added. This suggests that the dissolved hydrogen is almost completely ionized and that the electrons go into the *d* shell. It suggests further that a definite process of hydrogen absorption will reach completion when $r = 0.6$ approximately.

In order to account for the observed isotherms, Lacher assumes the following mechanism for the process of solution of hydrogen in palladium:

Let M_s denote the number of hydrogen atoms per unit volume which enter into solution. These will be present in the metal as protons (nuclei of hydrogen atoms, that is, ionized atoms) and electrons. Let N_s denote the number of available energy "holes" into which these protons may enter. "In order to explain the occurrence of critical phenomena, we must assume further that the energy of absorption depends on the number of holes filled, increasing as the number of holes filled increases." This assumption is similar to the one introduced to account for critical temperatures (or Curie points) in order-disorder phenomena.

---

[32] The significance of the subscripts α and β will appear from the subsequent discussion.

[33] This is discussed more fully in the book entitled *The Theory of the Properties of Metals and Alloys*, by N. F. Mott and H. Jones, p. 189 et seq., The Clarendon Press, Oxford, 1936.

The problem thus becomes similar to problems in that group of phenomena. Assuming that "the rate of increase in absorption energy is directly proportional to the fraction of holes filled" (that is, to $\theta = M_s/N_s$), and solving the problem by the methods of statistical mechanics, Lacher deduces a relation between θ, P, and T of the form

$$\log P_{mm} = 7.4826 + \frac{2 \log \theta}{1 - \theta} - \frac{891.2 + 1973.4\theta}{T}. \tag{2}$$

From the value of the coefficient of $1/T$, it follows that the exothermic heat of solution, in calories per gram-mole of hydrogen, is

$$\begin{aligned} Q &= 4080 + 9028\theta \\ &= 8594 \quad \text{for} \quad \theta = 0.5, \end{aligned}$$

which is in good agreement with the value $Q = 8588$ derived from the measurements made by Gillespie and Galstaun. It is also in agreement with the observation that the energy evolution varies linearly with the concentration of hydrogen at lower temperatures.

The isotherms calculated by means of equation 2 are practically identical with those observed by Gillespie and Galstaun (16) and also by Sieverts and Brüning (14).

We shall quote from Lacher's paper, once more, with regard to the physical interpretation of the equations which he has deduced.

> When we add hydrogen to palladium, the pressure will increase continuously (according to the $\sqrt{P}$ law at first) until $M_s/N_s = \theta_\alpha$. In the region $0 \leqslant \theta \leqslant \theta_\alpha$, the hydrogen is distributed uniformly among the available holes, and there is only one solid phase—the α-phase. As more hydrogen is added, the pressure remains constant until $\theta = \theta_\beta$. In the region $\theta_\alpha < \theta < \theta_\beta$ the hydrogen cannot be uniformly distributed among the available holes. Instead, there are regions where the density is θ_α and others where it is θ_β—the α- and β-phases co-exist. It is in this concentration range that X-ray analysis shows the co-existence of two expanded palladium lattices. When one adds hydrogen, the β-phase increases at the expense of the α-phase until the system becomes homogeneous again at $\theta = \theta_\beta$. This, again, is what is found by X-ray analysis. When θ is slightly greater than θ_α, the intensity of the lines due to the α-phase is greater than those due to the β-phase. When hydrogen is added, the intensity of the lines due to the α-phase falls off while simultaneously the intensity due to the β-phase lines increases. When still more hydrogen is added, the equilibrium pressure increases again, and in the region $\theta_\beta \leqslant \theta \leqslant 1$ only the pure β-phase exists. As the temperature is raised, both θ_α and θ_β approach each other,

until at the critical temperature $\theta_\alpha = \theta_\beta = \frac{1}{2}$. Above this temperature only one phase can exist.

On the basis of this theory of the coexistence of two phases, it is possible, as Lacher shows, to interpret the hysteresis effects mentioned above.

For temperatures above 600° C, the solubility (cm$_3$/100 g Pd) of hydrogen (s_{H}) and deuterium (s_{D}) can be represented by the following equations:

$$s_{\mathrm{H}} = 48\epsilon^{1150/R_0T}\sqrt{P_{atm}},$$

$$s_{\mathrm{D}} = 60\epsilon^{410/R_0T}\sqrt{P_{atm}};$$

that is,

$$\log s_{\mathrm{H}} = 0.241 + 0.5 \log P_{mm} + \frac{251.4}{T}, \tag{3}$$

$$\log s_{\mathrm{D}} = 0.338 + 0.5 \log P_{mm} + \frac{89.6}{T}. \tag{4}$$

The solubility of hydrogen in a number of alloys of palladium has been investigated. Since a comprehensive discussion of the results obtained has been given by Smithells,[34] only some of the more salient features need be mentioned about these observations.

In alloys with platinum the solubility of hydrogen is lower, and the decrease in solubility increases with increase in percentage of platinum. In alloys with silver, the solubility at constant temperature increases with increase in content of silver to a maximum value at about 40 per cent silver, and then decreases to a very low value for 70 per cent silver. The maximum values of the solubilities decrease with increase in temperature. Alloys of palladium with gold show similar characteristics with regard to solubility at lower temperatures (below about 400° C), but at higher temperatures the value of the solubility decreases continuously, with increase in percentage of gold, to a very low value for 80 per cent gold.

In boron-palladium alloys, at temperatures above 160° C, the solubility of hydrogen reaches a maximum value of about 1300 cm^3/100 g for 6.9 atomic per cent of boron. For both smaller and larger contents of boron, the value of s is lower, decreasing at all temperatures to a very low value for 20 atomic per cent of boron. With increase in temperature, the solubility decreases in the same manner as for pure palladium.

We shall now proceed to discuss, in more detail, some of the other metals of Group B.

---

[34] CS, pp. 187–191; also RB, pp. 158–160, and reference 9 in List II.

Titanium (references 6, 8, 9, 13). Only the hydrides of lithium, sodium, and calcium have higher hydrogen content. Above 800° C, the solubility follows the $\sqrt{P}$ law. Sorption begins at 375° C and occurs at a rapid rate above 400° C. Figure 13 shows isotherms at four different temperatures. The shape of the 600° C isotherm is accounted for, as for palladium, by the presence of two phases. G. Hägg[35] has demonstrated by X-ray investigation that the solid solutions consist of an α phase up to 35 atomic per cent, and a β phase for 50 atomic per cent of hydrogen and higher. The α phase is a closely packed hexagonal lattice; the β phase, a face-centered cubic lattice.

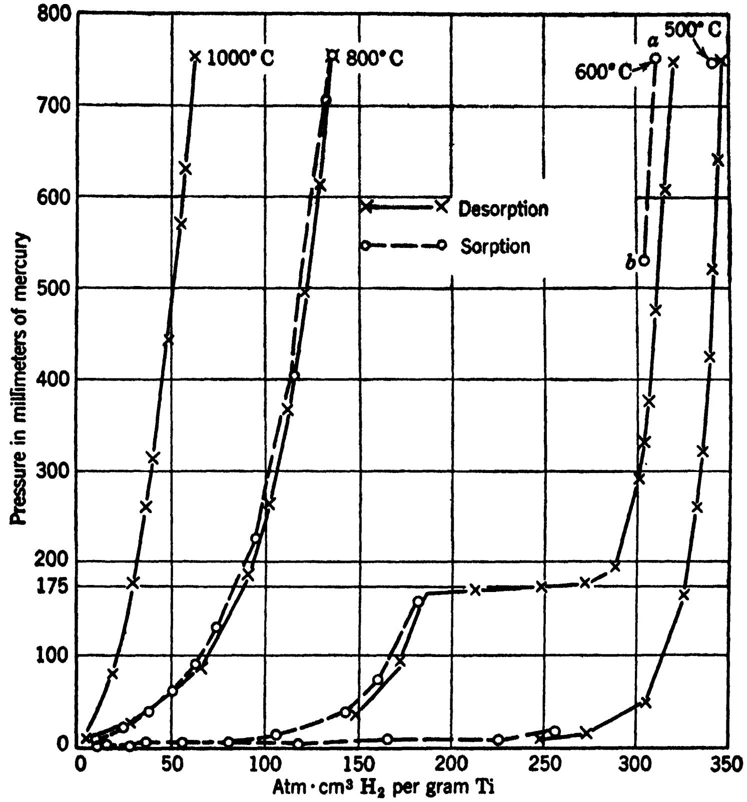

FIG. 13. Isotherms at four different temperatures for the system hydrogen-titanium (Sieverts).

---

[35] *Z. physik. Chem.*, **B**, **11**, 433 (1931).

The maximum content of hydrogen in the solid solution corresponds to the formula $TiH_{1.75}$, and, as mentioned in the last row in Table 16, the density of the "hydride" is 3.91 as compared with $\rho = 4.52$ for titanium. The decrease in density varies linearly with the hydrogen content, and this fact indicates that the entrance of hydrogen atoms into interstitial sites in the metal lattice effects an expansion of the lattice. According to Hägg, the average value for the radius of the hydrogen atom is $0.44 \cdot 10^{-8}$ cm. It is of interest to note that this value is *less* than the Bohr radius of the orbit of the electron ($0.5292 \cdot 10^{-8}$ cm) in the normal state of the hydrogen atom.

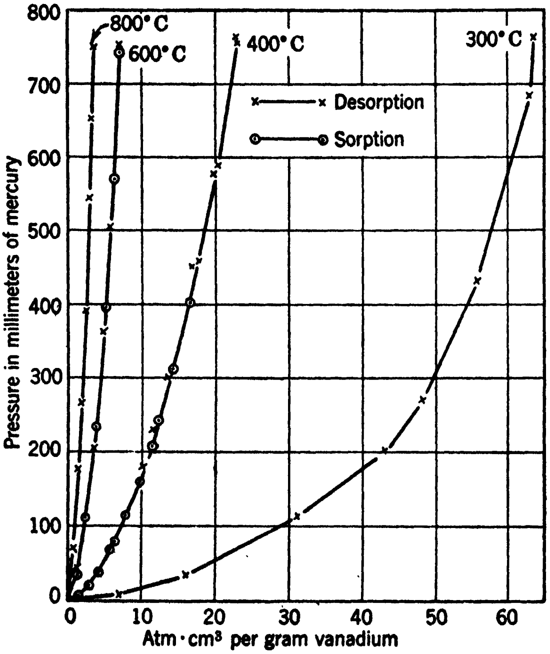

FIG. 14. Isotherms at four different temperatures for the system hydrogen-vanadium (Kirschfeld and Sieverts).

It is important to observe that in titanium, as in the other metals of Group B, maximum sorption is obtained only after the metal has been heated in vacuum for a prolonged period at a very high temperature. The metal thus degassed absorbs hydrogen very rapidly at a moderately high temperature. The sorption under these conditions is completely reversible. Sorption at lower temperatures is usually effected by cooling the metal, which has been saturated at the higher temperatures, in hydrogen.

Vanadium (references 6, 12). The maximum hydrogen content corresponds to the chemical composition $VH_{0.72}$, and the density of this solid solution is 5.30 as compared with 5.87 for the metal. Figure 14 shows isotherms for solutions of hydrogen in vanadium. As indicated on the curves the isotherms are reversible, and all of them follow the $\sqrt{P}$ law.

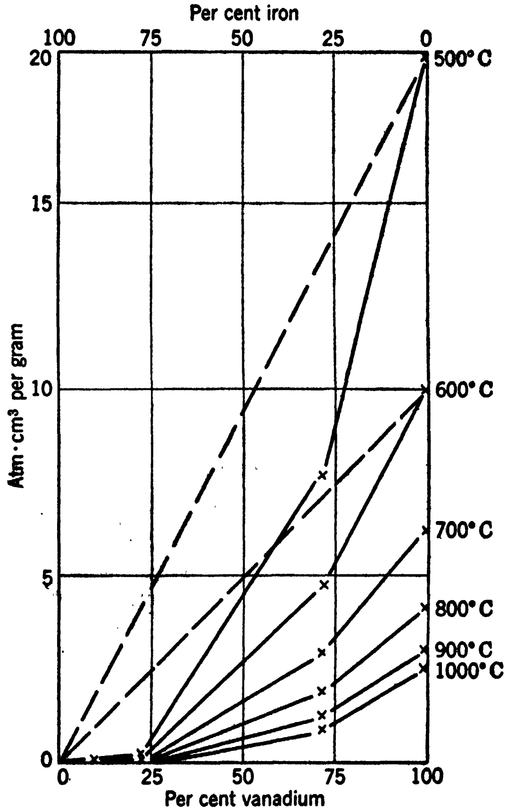

FIG. 15. Isobars at 1 atmosphere and a series of temperatures for the sorption of hydrogen in iron-vanadium alloys (Kirschfeld and Sieverts).

Kirschfeld and Sieverts also investigated the solubility of hydrogen in three ferrovanadium alloys. Isobars for these alloys at a series of temperatures are shown in Fig. 15.

Zirconium (references 5, 11, 18). Sieverts and Roell (5) gave the metal a preliminary treatment at 800° C to 1100° C in vacuum, and rapid absorption of hydrogen at atmospheric pressure was observed above 700° C. Above 1000° C, the isotherms follow the $\sqrt{P}$ law.

The maximum hydrogen content corresponds to the composition $ZrH_{1.92}$, and the density of this composition is 5.67 as compared with 6.4 for pure zirconium.

Hägg[36] has concluded, from X-ray investigations, that, beginning with an α phase (close-packed hexagonal lattice) at 5 atomic per cent hydrogen, a γ phase of similar structure but more expanded lattice dimensions is observed for a solution containing 33 atomic per cent hydrogen. At higher temperatures a β phase (face-centered cubic lattice) is observed at about 20 atomic per cent hydrogen. At 50 atomic per cent, a δ phase (face-centered cubic lattice) is observed, and at the highest concentration an ϵ phase is formed in which the metal atoms form a face-centered tetragonal lattice.

More recent observations on the solubility of hydrogen in zirconium have been published by Hall, Martin, and Rees (18). Figure 16 shows isotherms for a compact sample of the metal containing 0.023 atom oxygen per atom zirconium. The inset shows the initial portions of the isotherms on an expanded pressure scale. The ordinates give the solubility in cm³ H_2 (S.T.P.) per gram of metal.

Isotherms obtained for ductile zirconium wire and zirconium powder exhibit similar characteristics, although the values for the solubility at the same temperature and pressure may differ by a few per cent. The authors ascribe these variations to contamination by oxygen and nitrogen. From observations on metal containing different amounts of oxygen up to about 1 atom oxygen per atom zirconium, the tentative conclusion is drawn that "with zirconium-oxygen solid solutions the volume of hydrogen sorbed at saturation is decreased by a volume equivalent to that of oxygen present."

The isobar at 760 mm for zirconium containing 0.058 atom oxygen or less is substantially the same as that observed by Sieverts and Roell (5), and the volume of hydrogen dissolved at 20° C (on cooling from 400° C to 825° C) was observed to be about 240 cm³ (S.T.P.) per gram.

Columbium (reference 10). The isotherms for 300° C and 400° C do not follow the $\sqrt{P}$ law. This law applies approximately to isotherms at 500° C and higher. On heating the metal to 1100° C in a good vacuum and letting it cool to room temperature, sorption of hydrogen occurs very rapidly. On repeated sorption and desorption, the amount going into solution decreases (aging phenomenon). The maximum solubility corresponds to $r = 0.47$, which is the lowest value observed for any of the metals of Group B.

---

[36] *Loc. cit.*

Cerium (references 2, 3, 7, 9), **Lanthanum** (3, 7), **Praseodymium** (4), and **Neodymium** (4). The isobars for the first three metals are almost identical; that for neodymium is somewhat lower. All these metals form hydrides for which the values of r range around 2.7. As will be

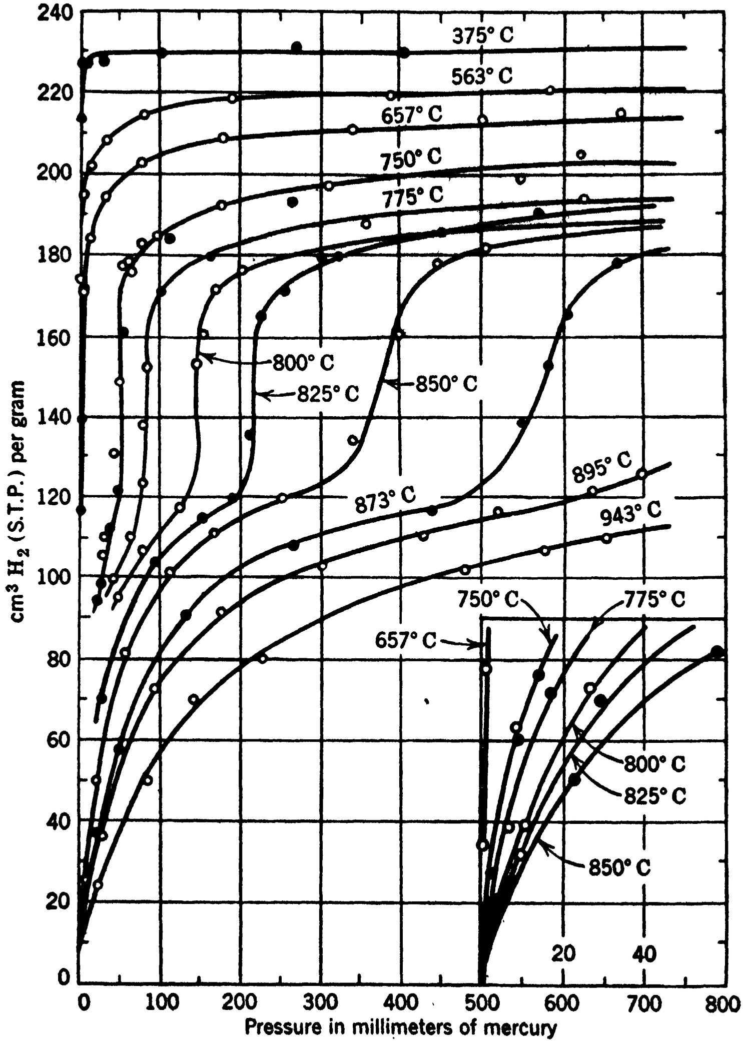

FIG. 16. Isotherms at various temperatures for the sorption of hydrogen by compact sample of zirconium containing 0.023 atom oxygen per atom zirconium. Whole series on same sample of 0.04093 g, with duplicate sets of points for 750° C. *Inset.* Initial portion of isotherms at lower pressures. (Hall, Martin, and Rees.)

observed from the data in Table 16 and Fig. 11, the solubility of hydrogen in cerium and lanthanum, as well as zirconium, decreases only slowly with increase in temperature. Even at 1000° C, the solubility in lanthanum and cerium is only about half of that observed at room temperature.

The isotherms resemble to a certain extent those observed for the hydrogen-palladium system. At higher pressures, they exhibit a steep increase in pressure with increase in solubility of hydrogen, of the same nature as that observed with the hydrogen-palladium systems for the β phase.

The following data are given to illustrate the relatively large sorptions observed at low pressures:

METAL	P_{mm}	$t°$ C	cm³/g
LaCe[37]	1.0	600	140
	0.2	800	3.2
Ce	0.2	800	3.24
	0.5	600	135.6

Tantalum (references 1, 11, 17). M. Pirani[38] observed that this metal when heated in hydrogen could occlude about 740 times its volume of the gas. On subsequent heating in vacuum about 550 volumes were given off, and the rest of the gas could be removed only at the melting point of the metal. Pirani also observed that the sorbed hydrogen makes a tantalum filament quite brittle and increases its electrical resistivity—observations that will be referred to in a subsequent section.

A more careful investigation by Sieverts and Bergner (1) showed that a wire heated in a vacuum to 1200° C absorbs hydrogen slowly at temperatures above 500° C. However, once the wire is saturated with gas at higher temperatures, it absorbs very much more readily at lower temperatures. The same investigators also observed that the sorption follows the $\sqrt{P}$ law. The values of v_0 (cm^3/g) obtained by these investigators at a series of temperatures are shown in Table 19.

As observed with titanium and zirconium, the alloys with hydrogen form three phases. Up to about 12 atomic per cent hydrogen the structure is body-centered cubic (α phase); between 31 and 35 atomic per cent hydrogen, the structure is that of a closely packed hexagonal lattice (β phase), and between 48 and 52 atomic per cent a γ phase is formed, which has the structure of a slightly deformed body-centered cubic lattice.

---

[37] Alloys of lanthanum and cerium are designated "misch metal."

[38] *Z. Elektrochem.*, **11**, 555 (1905).

TABLE 19

SORPTION (CM^3/G) OF HYDROGEN AT 1 ATM BY TANTALUM
(SIEVERTS AND BERGNER)

° C	v_0	° C	v_0
100	44.5	730	3.71
183	41.9	830	2.25
263	36.4	930	1.66
314	33.0	1030	1.32
474	17.5	1130	1.07
530	11.9	1230	0.89
630	5.69		

Thorium (reference 5). The metal powder used by Sieverts and Roell was 96 per cent pure. After a preliminary heating at 800° C to 1100° C in vacuum, sorption of hydrogen was observed to occur at 400° C. At 475° C the rate of sorption was quite rapid.

The sorption and desorption isotherms did not coincide at any temperature. This is illustrated by the observations recorded in Table 20. The metal was first heated in vacuum to 1100° C, and cooled. Hydrogen was then admitted and the metal heated to 530° C.

TABLE 20

SORPTION AND DESORPTION DATA FOR HYDROGEN IN THORIUM

t° C	P_{mm}	cm^3/g	t° C	P_{mm}	cm^3/g
530	760	95.6	800	754	82.4
	Cooled in H_2			Cooled in H_2	
25	754	136.6	25	752	141.0
800	754	86.4	1100	756	27.5
	298	84.0		288	23.6
	167	79.8		0	19.6
	69.7	42.6		467	(29.5)
	27.8	25.9		757	(40.3)
	2.1	17.6			

As for the other metals of Group B, the maximum solubility of hydrogen in thorium does not correspond to a stoichiometric composition, since r has the value 3.07.

Summarizing the data given in Table 16 and the isobars shown in Fig. 11 it is of interest to compare the relation between these isobars and the positions of the metals in the periodic arrangement. According to the periodic arrangement the metals of Group B fall in the following three groups: (*a*) Ti, Zr, Th; (*b*) La, Ce, Pr, Nd; (*c*) V, Cb, Ta.

In each group, the solubility decreases with increase in atomic number of the metal; and while the solubility is highest for titanium, it is lowest for tantalum.

As has been mentioned previously, *heat is evolved* in the formation of these solid solutions. The values of these heats of formation, Q, in calories per g-mole H_2 are given in Table 21; for comparison, there are also given values for the hydrides of the alkali and alkaline-earth metals. The numbers in parentheses give the references in List II.

TABLE 21

HEATS OF FORMATION OF HYDROGEN ALLOYS AND HYDRIDES

Hydrogen Alloys	Q (cal/mole H_2)	Hydrides	Q (cal/mole H_2)
$PdH_{0.59}$	8,588	LiH	43,000
$TiH_{1.75}$	36,000 (13)	NaH	26,280
$ZrH_{1.92}$	40,500 (11)	KH	28,200
$LaH_{2.8}$	40,090 (7)	CaH_2	48,880
$CeH_{2.7}$	42,260 (7)	SrH_2	42,060
$PrH_{2.8}$	39,520 (7)	BaH_2	40,860

As will be observed, the values of Q for the "hydrides" of the metals of Group B are comparable with those for the hydrides of the alkali and alkaline-earth metals.

(However, the similarity between the two classes of hydrides does not extend beyond the fact that values of the heats of solution are of the same order of magnitude as the heats of formation of the chemically defined hydrides. On heating, the latter dissociate, and for each temperature there exists a definite dissociation pressure of hydrogen which can be expressed as a function of the temperature by a relation similar to that used for expressing the vapor pressure of a solid or liquid. Consequently these observations are discussed in Chapter 11 along with the observations on the dissociation of nitrides and oxides.)

Because of the high values of the solubility of hydrogen, as well as other gases, in titanium, zirconium, and thorium, these metals have been utilized in the production of electronic tubes as "getters," since they improve the vacuum in a sealed-off device. (This topic is discussed at greater length in the following chapter.)

One other characteristic of the metals of Group B must also be mentioned in this connection. All of them, including alloys which contain fairly appreciable percentages of other metals, exhibit an *increase in the electrical resistivity* when hydrogen is taken up.

Denoting the ratio of the resistivity of the hydride to that of the pure metal by Z, it was shown by Sieverts and Brüning[39] that in the case of *tantalum*

$$Z - 1 = Kr, \tag{5}$$

where r has the same significance as in Table 16, and $K = 1.6$ for 500° C and 600° C for all values of r. (For 400° C, $K = 1.8$.) That is, the resistivity increases linearly with the concentration of hydrogen.

From observations on palladium wires, the same investigators[40] found that equation 5 is valid only for lower concentrations of hydrogen, because of the phase changes which occur at higher concentrations. The maximum value of Z, observed for $r = 0.5$, was about 1.5, independently of the temperature in the range 160° C to 310° C.

Hagen and Sieverts[41] obtained similar results with palladium at higher temperatures and higher pressures of hydrogen, as well as with Pd-Ag and Pd-Au alloys.[42]

The fact that drawn tantalum wire becomes brittle when heated in hydrogen is well known. This is no doubt the result of the straining of the lattice structure due to hydrogen absorption. Other metals, e.g. copper, are also embrittled by hydrogen.

In general, dissolved gases affect the mechanical properties of metals,[43] and a large number of investigations published in metallurgical journals have dealt with this topic.

6. DERIVATION OF RELATIONS FOR THE SOLUBILITY OF HYDROGEN IN METALS

By applying the methods of statistical mechanics, R. H. Fowler and J. C. Smithells[44] have been able to deduce relations for the solubility of hydrogen which apply to each of the two groups A and B.

The plots shown in Fig. 17, taken from their paper, serve to emphasize the radical differences between the two groups. The ordinates give the values of $\log_e s$, where $s = 10^2 v_0 = \text{cm}^3$ (S.T.P.) per 100 g; and the abscissas give values of $10^4/T$. Thus the slopes of the lines are proportional to the heats of solution. As will be observed, these slopes for metals of Group A are in the opposite direction to those for metals of Group B, which corresponds, as mentioned previously, to the fact that heat is absorbed in metals of Group A when hydrogen goes into solution, and heat is evolved in metals of Group B.

---

[39] *Z. physik. Chem.*, A, **174**, 365 (1935).

[40] *Z. physik. Chem.*, A, **163**, 409 (1932).

[41] *Z. physik. Chem.*, A, **165**, 1 (1933).

[42] *Z. physik. Chem.*, A, **174**, 247 (1935).

[43] A brief résumé is given by CS, pp. 191–198.

[44] *Proc. Roy. Soc. London*, A, **160**, 37 (1937). See also RB, pp. 152–155.

Fowler and Smithells assume that in metals of Group A the protons move quite freely throughout the lattice, because of their low concentration, whereas in metals of Group B the protons become "localized" as a result of their high concentration, which brings into play binding forces between protons and metal atoms.

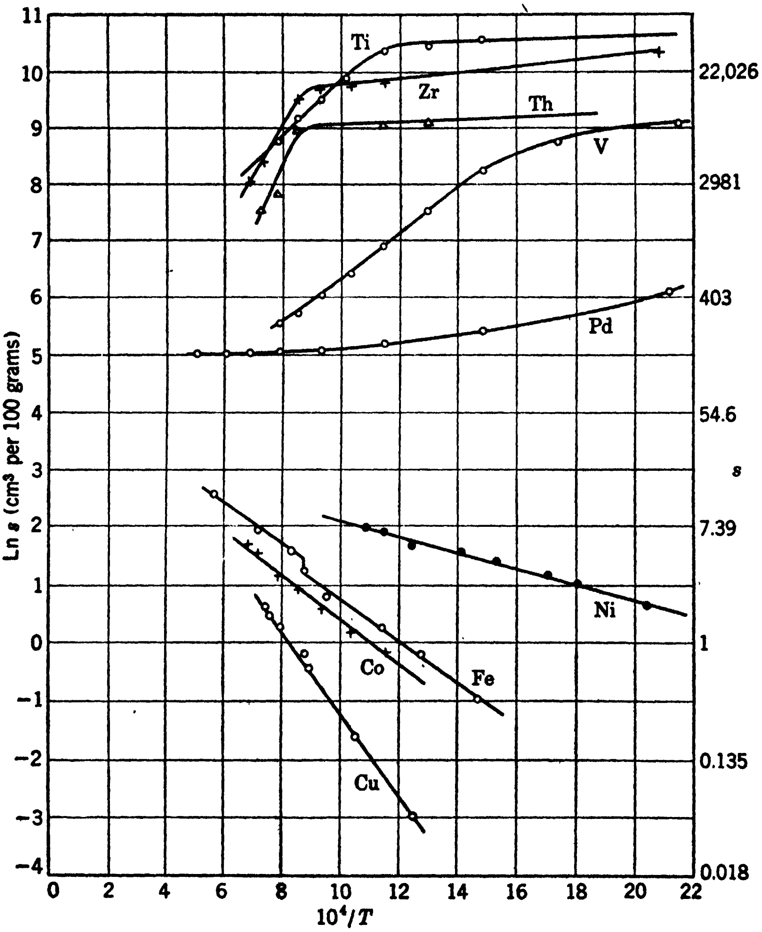

FIG. 17. Plots of ln s versus $1/T$ for metals of Groups A and B. The values of s (cm^3, S.T.P., per 100 g) are indicated for corresponding values of ln s. (Fowler and Smithells.)

For *metals of Group A*, the relation deduced for s is

$$\log s = 2.774 + 0.5 \log P_{mm} - 0.25 \log T - \log \rho - \frac{Q_S}{9.148T}, \quad (1)$$

where ordinary logs are used, ρ = density, and Q_S = heat of solution in calories per gram-mole of hydrogen. (Values for Q_S are given in one of the lower rows of Table 15.)

For *metals of Group B*, the relation deduced is

$$\log \left(\frac{s}{s_0 - s}\right) = 0.242 + 0.5 \log P_{mm} - 1.75 \log T + \frac{Q}{9.148T}, \quad (2)$$

where s_0 = solubility at saturation, at room temperature, and Q = heat evolved in calories per gram-mole of hydrogen.

Many of the values of Q_S and Q derived by Fowler and Smithells (designated by FS) are quite different from those given in Tables 15 and 21, as shown by the data in Table 22.

TABLE 22

HEATS OF SOLUTION OF HYDROGEN IN METALS

	Q_S (cal/mole H_2)			Q (cal/mole H_2)	
Metal	Table 15	FS	Metal	Table 20	FS
Cu	18,300	14,100	Ti	36,000	10,000
Co	15,500	7,300	Zr	40,500	17,500
Fe	13,300	7,000	Th	—	22,500
Ni	5,900	5,600	V	—	7,700
Al	43,400	45,500	Pd	8,588	2,040
Pt	34,500	85,400			
Mo	14,000	3,500			
Ag	11,900	11,600			

Applying equation 1 to the solubility data for nickel and iron and using the values of Q_S given in Table 15, the calculated values for s are found to be about 10 times those observed.

Similar results are obtained by application of equation 2 to vanadium, for instance, by using the value for Q given in Table 21 and the value of s_0 given in Table 16.

7. SOLUBILITY OF HYDROGEN IN PALLADIUM-LIKE METALS AND PALLADIUM BLACK

Although none of the other metals of the palladium and platinum group (the "noble" metals) behave like palladium with respect to hydrogen, they do absorb hydrogen to a very noticeable extent even at room temperature, when in a *finely divided state*. Table 23 gives absorption data at 1 atm observed by E. Müller and K. Schwabe.[45] The metals were obtained in powder form by reduction of the oxides, and were then saturated with nitrogen and evacuated at 18° C.

TABLE 23

SORPTION DATA FOR HYDROGEN BY "NOBLE" METALS AT 18° C AND 1 ATM

Metal:	Ru	Rh	Pd	Os	Ir	Pt
v_0:	124	101	79	74	49	35
V_g:	1520	1240	910	1660	1100	760
A:	101.7	102.9	106.7	190.2	193.1	195.2
ρ:	12.2	12.5	11.4	22.48	22.42	21.45
r:	1.12	0.93	0.75	1.26	1.0	0.61

It will be observed that the hydrogen absorbed corresponded to a value of the order of 1 atom H per atom of metal. The values given in the table were the highest sorptions observed. Temperature of reduction and duration of treatment in hydrogen affected the sorption to a considerable extent.

With the exception of palladium (for which the value of the amount absorbed is even higher than that recorded in Table 16), it was observed that the sorption capacity depended upon the extent of the surface. This indicates that the sorption in these metals is due either to physical adsorption or, probably, chemisorption. Müller and Schwabe have used as an argument in favor of this conclusion the data obtained by L. Mond, W. Ramsay, and J. Shields[46] on the sorption of hydrogen at room temperature by platinum foil which had been "activated" by heat treatment in hydrogen. These data are given in Table 24.

TABLE 24

SORPTION (v_0) AT ROOM TEMPERATURE FOR HYDROGEN BY ACTIVATED PT-FOIL

Series I			Series II		
P_{mm}	v_0	P_{mm}/v_0^2	P_{mm}	v_0	P_{mm}/v_0^2
11.1	1.877	3.150	22.4	1.888	6.284
30.9	1.941	8.204	59.5	1.937	15.85
176.5	2.000	44.11	125.7	1.963	32.60
371.4	2.015	91.47	264.5	2.012	65.31
767.0	2.030	186.1	416.9	2.085	95.85
			767.0	2.085	176.4

---

[45] *Z. Elektrochem.*, **35**, 165 (1929).

[46] *Phil. Trans. Roy. Soc. London*, **A**, **191**, 105 (1898).

Müller and Schwabe found that the two series of observations recorded in Table 24 could be represented by the Zeise equation (see Chapter 8),

$$v_0 = \sqrt{\frac{k_1 k_2 P}{1 + k_2 P}} = \text{cm}^3/\text{g}. \qquad (1)$$

In accordance with this relation, a plot of P/v_0^2 against P is found to be linear.

Isobars for some of the metals under discussion have also been determined by A. Gutbier and W. Schieferdecker.[47] From the plots of these observations at 1 atm the interpolated values have been obtained which are given in Table 25.

TABLE 25

SORPTION (v_0) AT 1 ATM FOR HYDROGEN BY PD-LIKE METALS

t° C	Pd	Ir (black)	Ir (powder)	Ir (460° C)	Ru (black)	Os (black)
20	70	5.61	1.10	0.58	1.20	3.15
60	64	4.90	0.85	.47	0.90	2.57
100	59	4.45	.80	.43	.78	2.24
140	52	4.05	.74	.40	.66	2.06
150	32.8	3.95	.73	.38	.62	2.02
160	11.4	3.80	.71	.37	.60	2.00
180	5.7	3.60	.69	.35	.55	1.94
190	4.6	3.55	.67	.33	.52	1.92

The fourth column gives the results for a Heräus gray powder, and the next column gives results for the same powder after being heated to 460° C. As will be observed the values of v_0 decrease approximately linearly with the temperature.

By heating the powders to temperatures not exceeding 350° C, the sorption at lower temperatures was increased. It was also observed that the sorption of carbon monoxide by iridium was about the same as that of hydrogen.

A. F. Benton[48] observed that "platinum black" at 25° C and 1 atm absorbed 36.7 volumes of hydrogen, 37.8 volumes of carbon monoxide, and 20.4 of oxygen. The sorption of hydrogen per gram was about 1.68 cm³ at 760 mm and about 1.38 cm³ at 1 mm.

The sorption by *palladium black* at liquid-air temperature is about ten times that observed at room temperature and exceeds that observed for charcoal. The data obtained by S. Valentiner[49] for the sorption of hydrogen by palladium black at three temperatures are shown in Table 26.

---

[47] *Z. anorg. Chem.*, **184**, 305 (1929).

[48] *J. Am. Chem. Soc.*, **48**, 1850 (1926).

[49] *Ber. deut. physik. Ges.*, **13**, 1003 (1911).

TABLE 26

Sorption of Hydrogen by Palladium Black (Valentiner)

$t = 20°$ C		$t = -20°$ C		$t = -190°$ C	
P_{mm}	v_0	P_{mm}	v_0	P_{mm}	v_0
0.001	0.10	0.014	0.27	0.0005	2.05
.005	.26	.031	.33	.0015	2.11
.037	.40	.056	.37	.001	3.06
.110	.52	.087	.41	.001	9.1
.190	.59	.184	.49	.002	33.0
.315	.70	.30	.55	.005	40.0
.52	.82	.52	.61	.012	47.2
.76	.92	.88	.67	.025	63.0

Since 1 cm^3 (S.T.P.) is equal to 760 micron · liters (at 0° C) these sorptions, especially at room temperature and lower temperatures, and at pressures as low as 0.5 micron, are remarkably high. Consequently experiments were carried out by the writer and his associates, during 1918, on the possibility of utilizing palladium as an adsorbent for the evacuation of small radio vacuum tubes.

The method of preparation has been described by C. Hoitsema.[50] With slight variations this method was used by the writer as follows:

The palladium in the form of sheet or wire is dissolved in aqua regia and evaporated on a water bath till acid vapors have disappeared; the solution is then diluted and warmed, and concentrated solution of sodium carbonate is added to neutralize free acid. A slight amount of acetic acid is then added, the solution is warmed, and a warm concentrated solution of sodium formate is added. The palladium comes down as a black flocculent precipitate which settles rapidly at the bottom of the beaker. The supernatant liquid is decanted, and the precipitate washed with distilled water till the wash water shows no traces of chlorides. The palladium "black" is then washed with alcohol and transferred to a U-tube, where it is dried by blowing air over it and then evacuated on a rough pump. The U-tube ought to have side tubes through which gas can be passed and constrictions at which it can be sealed off later. After the rough evacuation (with slight warming of the U-tube), hydrogen is passed over the palladium black for some time, and while the gas is still passing through the tube the tube is sealed off at the constrictions. This leaves the palladium black in equilibrium with hydrogen, and it can be kept active for a long time.

---

[50] A very comprehensive review of the earlier observations made by this investigator and others on the sorption characteristics of palladium and the other metals of this group is given in McB, pp. 286–305.

For use in exhaust work, the U-tube is opened and a sample transferred to a tube such as is used in sorption by charcoal. It is well to cover the top of the palladium black with glass wool in order to prevent it from being drawn into the rest of the apparatus when vacuum is applied.

A number of experiments were carried out in this laboratory by A. G. Huntley, Miss M. Daly, and the writer. While the behavior of palladium black was found to be extremely erratic, the results obtained, as illustrated by the following experiment, showed that it is possible to obtain samples possessing very high absorbing power.

An ionization gauge with an appendix containing about 1 g of palladium black was well exhausted on a condensation pump and sealed off at a residual gas pressure of about 0.2 micron (the gas consisting probably of nitrogen and hydrogen). On immersion of the appendix in liquid air, the pressure decreased to 0.003 micron with the gauge filament lighted. On turning off the filament for some time, and then lighting it for an instant, the pressure was observed to have decreased still further to 0.0004 micron. Apparently, there is a continual slight evolution of gas from the walls of the gauge and filament leads even after the metal parts have been bombarded for a long time. In other experiments pressures as low as 0.0001 micron were obtained in a sealed-off gauge with a palladium tube immersed in liquid air.

A number of experiments were carried out using palladium black for absorbing the residual gases in a small hot-cathode diode exhausted on an oil pump only. An ordinary lamp exhaust system was used giving an exhaust pressure of about 1 micron. A few *milligrams* of palladium black were placed in a diode (about 100 cm^3 volume) which contained a 6-volt 2.5-ampere tungsten filament and a cylindrical molybdenum anode about ¼ in. in diameter by ⅞ in. in length. The tube was exhausted on the oil pump, with simultaneous heating in an oven for 30 minutes at 360° C, and sealed off. The metal cylinder was then bombarded to a white heat by making the filament cathode. The gases evolved were absorbed rapidly by the palladium black, in spite of its being above room temperature, and finally the vacuum became so good that excellent space-charge characteristics were obtained. Special experiments showed that in order to obtain this condition the pressure must be at least as low as 0.05 micron. Thus even with a few milligrams of palladium black at room temperature it was possible to clean up appreciable quantities of gas. Similar results were obtained repeatedly.

In fact a large number of small diodes and triodes were exhausted in this manner, with the regular exhaust system used in lamp factories, and without a mercury-vapor pump or liquid air.

As subsequent investigation showed that the same results could be obtained with the very much cheaper activated charcoal, and, furthermore, as some samples of palladium black absolutely failed for some undetermined reason to act as absorbents, this method was used for only a short time. The results, however, suggest interesting possibilities in the production of high vacua by means of palladium black, and further investigation ought to be carried out to determine definitely the conditions under which it can be made active. It has been shown by E. B. Maxted[51] that hydrogen sulfide inhibits the absorbing efficiency of palladium black. Similar facts have been known for a long time about various metallic catalysts, and probably the same causes influence the behavior of palladium black.

8. SOLUBILITY OF NITROGEN IN METALS

According to Smithells,[52]

> Nitrogen is only soluble in those metals which are capable of forming nitrides.... Nitrogen has been shown to be insoluble, within the limits of the experimental method in cobalt, copper, silver, and gold. Those metals which, like iron and molybdenum absorb nitrogen show the same kind of changes in lattice structure, mechanical and electrical properties as are shown when the hydride-forming elements absorb hydrogen.

When iron and other nitride-forming metals are heated in nitrogen, the amount of nitrogen which actually enters into solution is of the order of 1 per cent or less by weight, and there is no tendency to form a nitride. The methods of formation of the nitrides are discussed in Chapter 12.

The most reliable data on the solubility of *nitrogen in iron* are those obtained by A. Sieverts[53] and by A. Sieverts, G. Zapf, and H. Moritz.[54] Table 27 gives the values of s (cm^3/100 g) at approximately 1 atm pressure, as observed on a sample of Armco iron. (The actual pressures in millimeters are indicated in parentheses.) The data for the temperatures 750–900° C are those published in 1931; the other data are those given in the second paper. Figure 18, taken from this paper, shows the isobar at 1 atm. As shown by this plot, the value of s exhibits a considerable increase at the α-γ transition, a decrease at the γ-δ transition, and, again, quite an increase at the melting point.

---

[51] *J. Chem. Soc.*, **115**, 1050 (1919).

[52] CS, p. 170.

[53] *Z. physik. Chem.*, A, **155**, 299 (1931).

[54] *Z. physik. Chem.*, A, **183**, 19 (1938–1939).

The solubility obeys the $\sqrt{P}$ law, which signifies that the nitrogen dissolves in iron as *atoms*.

TABLE 27

SOLUBILITY (CM³/100 G) OF NITROGEN AT 1 ATM IN IRON

°C:	750	890	900							
s:	0.32	1.60	20.							
°C:	1200	1300	1400	1450	1390					
$(P_{mm} = 754)s$:	19.2	18.2	13.9	9.3	17.2					
°C:	1300	1390	1400	1420	1460	1390	1070	920	840	805
$(P_{mm} = 758)s$:	16.8	16.6	10.6	8.1	8.5	16.6	19.0	9.3	4.6	1.1
°C:	1310	1380	1440	1500	1540	1460				
$(P_{mm} = 744)s$:	17.4	17.1	8.8	9.7	24.6	10.5				
°C:	1540	1560	1560							
$(P_{mm} = 760)s$:	24.6	26.7	27.9							

For $s = 25$, $V_g = 1.57$ and $10^4 r = 10$, also $x = 1.25s$.

Comparing the solubility of nitrogen with that of hydrogen in iron, it is seen that hydrogen is more soluble in α-iron, but above 900° C the solubilities are of the same order of magnitude.

The solubility of nitrogen in *molten iron* has been investigated by J. Chipman and D. W. Murphy.[55] At about 740 mm pressure, the solubility is 0.039 per cent (by weight) just above the melting point, and 0.04 per cent at 1760° C. This corresponds to a value $s = 32$ cm³/100 g iron. It was observed that in this case also s varies as $\sqrt{P}$.

These investigators also observed that the rate of solution of nitrogen in molten iron is given by the simple relation

$$\frac{ds}{dt} = k(s_0 - s), \tag{1}$$

where s_0 is the saturation solubility. Small concentrations of aluminum or silicon in the iron caused the rate of solution to increase ten- to twenty-fold.

The solubility data are in agreement with the observation that, on degassing iron, the volume of gas evolved rarely exceeds about 20 cm³/100 g. The rate of gas evolution is very low at 800° C on account of the low rate of diffusion of the dissolved gas but increases rapidly with the temperature.

---

[55] *Trans. A.I.M.E.*, **116**, 179 (1935).

While carbon monoxide is probably soluble in iron to some extent, no solubility data are available. The observed evolution of carbon monoxide and dioxide on degassing iron may be accounted for (as in the case of nickel) by diffusion of carbon and reduction of oxides in the metal.

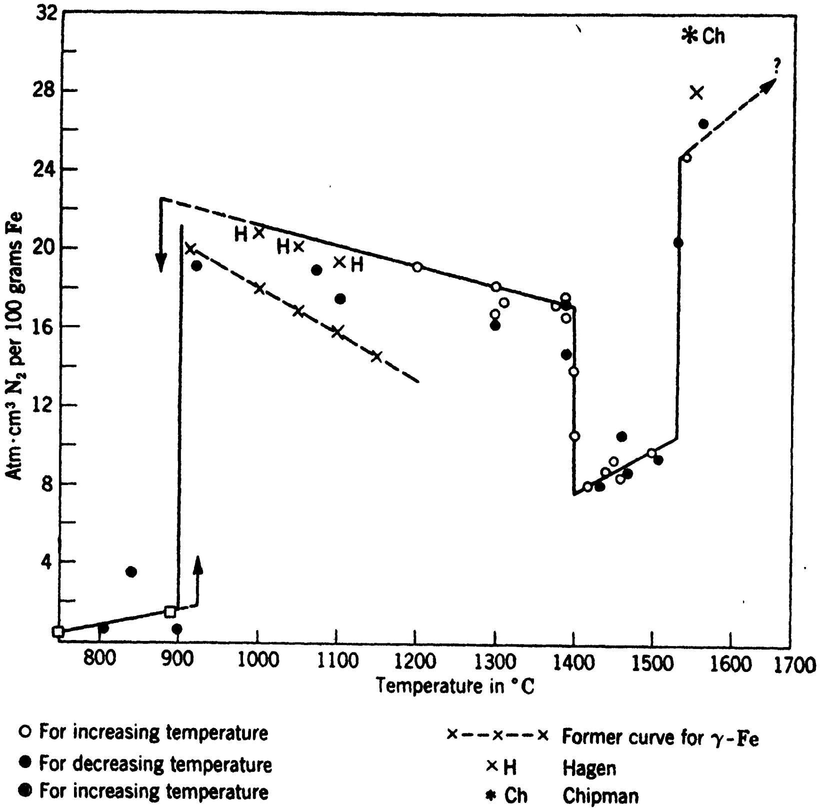

FIG. 18. Isobar for the solubility of nitrogen at 1 atmosphere in Armco iron. Data obtained by other investigators are also shown. (Sieverts, Zapf, and Moritz.)

The solubility of *nitrogen in molybdenum* has been investigated in the range 936° C to 1168° C by A. Sieverts and H. Brüning,[56] and in the range 1200° C to 2400° C by F. J. Norton and A. L. Marshall.[57] Table 28 gives the solubility data observed by the first-mentioned investigators, for molybdenum wire. The solubility follows the $\sqrt{P}$ law at all temperatures.

---

[56] *Arch. Eisenhüttenw.* **7**, 641 (1933).

[57] *Trans. A.I.M.E.*, **156**, 351 (1944), and personal communication.

TABLE 28

SOLUBILITY OF NITROGEN AT 753 MM IN MOLYBDENUM WIRE

$t°$ C	s = cm^3/100 g	x = mg/100 g*	10^3r*
936	58.8	73.51	50.4
1020	29.1	36.34	24.9
1045	24.7	30.90	21.2
1081	20.1	25.11	17.2
1118	16.5	20.65	14.2
1142	15.1	18.88	12.9
1168	13.0	16.27	11.2

* $x = 1.25s$; $10^4r = 0.686x$.

On the other hand, molybdenum sheet absorbed much smaller amounts, 1.59 mg/100 g at 1127° C and 3.69 mg/100 g at 829° C. These results are in agreement with those obtained by E. Martin.[58]

Table 29 gives the solubility data obtained by Norton and Marshall for nitrogen in *molybdenum* and *tungsten.*

TABLE 29

SOLUBILITY OF NITROGEN AT 1 ATM IN MOLYBDENUM AND TUNGSTEN

	Molybdenum			Tungsten		
°C	mg/100 g	cm^3/100 g	V_g	mg/100 g	cm^3/100 g	V_g
2400	20.	16.	1.65	0.38	0.304	0.059
2000	10.5	8.4	0.87	.11	.088	.017
1600	4.3	3.44	.35	.019	.015	.003
1200	1.05	0.84	.09	.0013	.001	.0002
Heat of Solution: (cal/mole N_2)		38,500			74,700	

It is difficult to understand the reason for the radical differences between the two sets of observations, both with respect to order of magnitude of s and also with respect to the variation with temperature. It should be stated that Sieverts and Brüning also investigated the solubility of nitrogen in molybdenum-iron alloys. At 1100° C and 1150° C the solubility increases with addition of molybdenum, from that in pure iron (about 4 cm^3/100 g) to about 16 cm^3/100 g at 10 atomic per cent molybdenum. Further increase in molybdenum content causes the solubility to decrease to a minimum at 40 atomic per cent molybdenum, after which the solubility increases until it reaches that for pure molybdenum.

---

[58] *Arch. Eisenhüttenw.*, **3**, 407 (1929–1930).

Nitrogen is soluble in *molten* aluminum, and the solubility increases with the temperature. At the melting point, $s = 1\ \mathrm{cm}^3/100\ \mathrm{g}$.

According to the observations of J. H. DeBoer and J. D. Fast,[59] *zirconium* heated in nitrogen takes up 1 atom of nitrogen to 11 of zirconium, forming a solid solution of the nitride ZrN.

The electrical resistivity of this solution is greater than that of the metal; also, instead of a sharp transition from the α to the β phase at 865° C, the transition range is extended over several hundred degrees.

Oxygen is absorbed in a similar manner by zirconium, to the extent of 1 atom of oxygen to 9 atoms of zirconium, and the effect on the electrical resistance is the same as that of nitrogen.

The investigators state that "oxygen as well as nitrogen dissolves homogeneously in metallic zirconium. When a zirconium rod which is covered with a thick white oxide layer is heated in vacuo, the metallic luster reappears. The oxide has dissolved in the metal, and a homogeneous phase has apparently once more been formed." Along with the increase in electric resistivity there is a rise in the melting point and the lattice becomes expanded.

With many of the metals, nitrogen reacts to form nitrides. The thermodynamic properties of these compounds are discussed in Chapter 12.

9. SOLUBILITY OF OXYGEN AND OTHER GASES

The difficulty in the experimental determination of the solubility of oxygen in metals has been stated by J. C. Smithells[60] as follows:

> Oxygen is soluble to some extent in most metals, but except in the case of the noble metals, an oxide phase also appears when the limit of solid solubility is exceeded. The solid solubility of oxygen in the common metals is usually considered as small in comparison with the total amount of oxygen which may be present in the metal. Many molten metals are capable of dissolving large quantities of oxygen (or of their own oxides, which amounts to the same thing), but on freezing the excess oxygen is precipitated as oxide. The solubility of oxygen in the solid metals is of the same order as that of hydrogen. It is, however, much more difficult to determine accurately.

The system oxygen-copper has been investigated by F. N. Rhines and C. H. Mathewson.[61] The melting points of the metal and Cu_2O are 1083° C and 1235° C, respectively. The eutectic melts at 1065° C. Table 30 gives solubility data observed below this temperature, according to Rhines and Mathewson, and also the data observed by A. Phillips

---

[59] *Rec. trav. chim.* **55**, 459 (1936).

[60] CS, p. 175.

[61] *Trans. A.I.M.E.*, **111**, 337 (1934).

TABLE 30

SOLID SOLUBILITY OF OXYGEN IN COPPER

	Rhines and Mathewson		Phillips and Skinner	
t° C	cm^3/100 g	Weight Per Cent	t° C	Weight Per Cent
600	5.0	0.0071	700	0.0022
800	6.6	.0094	850	.0025–.0029
950	7.0	.0100	900	.0027–.0035
1050	10.9	.0156	950	.0034–.0046
			1000	.0044–.0055
			1050	.0072–.0077

and E. N. Skinner,[62] who used samples of copper from different sources; the table shows the range of values observed for the solubilities. The main reason for the difference between the two sets of data seems to be actual experimental difficulties in the analytical determination of such small percentages of dissolved gas. The values of the solubility limit reported by Rhines and Mathewson were obtained by exposing copper sheets "to free access of air at a definite temperature in a Hevi Duty muffle furnace for periods varying between one day and three weeks." Data on the dissociation pressures of the oxides of copper are given in Table 12.5.

The observations on the solubility of *oxygen in iron* have been summarized by Smithells as follows:[63]

> The solubility of oxygen in *liquid iron* increases from 147 cm^3/100 g (0.21 per cent oxygen by weight) at the melting point to 387 cm^3/100 g (0.552 per cent by weight) at 1734° C. Oxygen is probably more soluble in γ than in α or δ iron, and estimates of the solubility in the range between 800° C and 1000° C vary from 24 to 28 cm^3/100 g.

C. H. Herty, Jr., and J. M. Gaines[64] have shown that oxygen must dissolve in liquid iron as FeO, and it probably dissolves in the solid metal in the same form. This view is in accord with the observations on the solubility of oxygen in copper and also in cobalt.

The saturation solubility data obtained by A. U. Seybolt and C. H. Mathewson[65] for *oxygen in cobalt* are shown in Table 31. These results were observed, as in the case of copper, by heating the metal "in an oxygen atmosphere at the temperature chosen, for a sufficient time to obtain equilibrium by diffusion of oxygen through it."

[62] *Trans. A.I.M.E.*, **143**, 301 (1941).

[63] CS, p. 177.

[64] *Trans. A.I.M.E.*, **80**, 142, *Iron and Steel* (1928).

[65] *Trans. A.I.M.E.*, **117**, 156 (1935).

TABLE 31

SOLID SOLUBILITY OF OXYGEN IN COBALT

° C	mg/100 g	Atomic Per Cent CoO	$cm^3/100$ g
600	6	0.0221	4.2
700	9	.0332	6.3
810	16	.0588	11.2
875	10	.0369	7.0
945	7	.0258	4.9
1000	8	.0295	5.6
1200	13	.0479	9.1

Figure 19 taken from the original paper shows a plot of 1/T versus log (oxygen content). The abrupt decrease in solubility at about 875° C (the point indicated by two concentric circles) leads to the conclusion that a crystallographic transformation of cobalt in the cobalt-oxygen system occurs at this temperature. In pure cobalt this transformation occurs at 850° C.

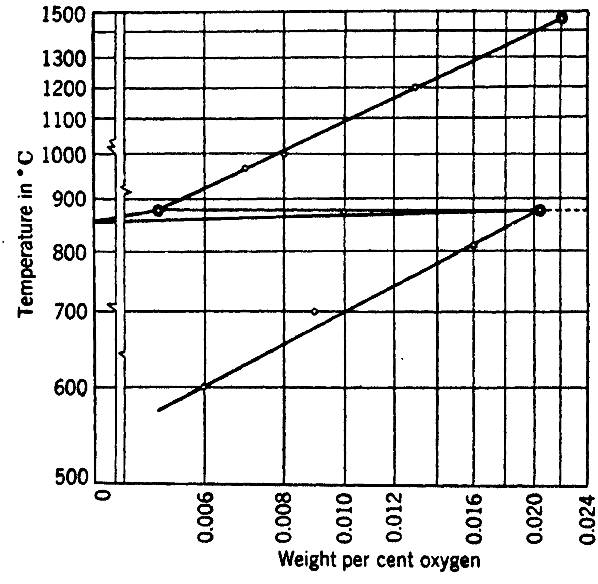

FIG. 19. Phase diagram for cobalt-cobaltous oxide system in which 1/T is plotted against log of percentage by weight of CoO, but temperature is shown in degrees Centrigrade and the weight per cent oxygen is given. At the point indicated by two concentric circles (875° C) there is an abrupt decrease in solubility. (Seybolt and Mathewson.)

For the upper range of temperatures the linear plot yields the value $Q_S = 8650$ cal per mole oxygen, for the heat of solution.

In the case of *nickel*, the observation has been recorded by P. D. Merica and R. G. Waltenberg[66] that "Nickel melted in the presence of oxygen yields an oxide (NiO) with which it forms a eutectic. This eutectic contains about 0.24 per cent oxygen, corresponding to 1.1 per cent NiO, and melts at 1438° C."

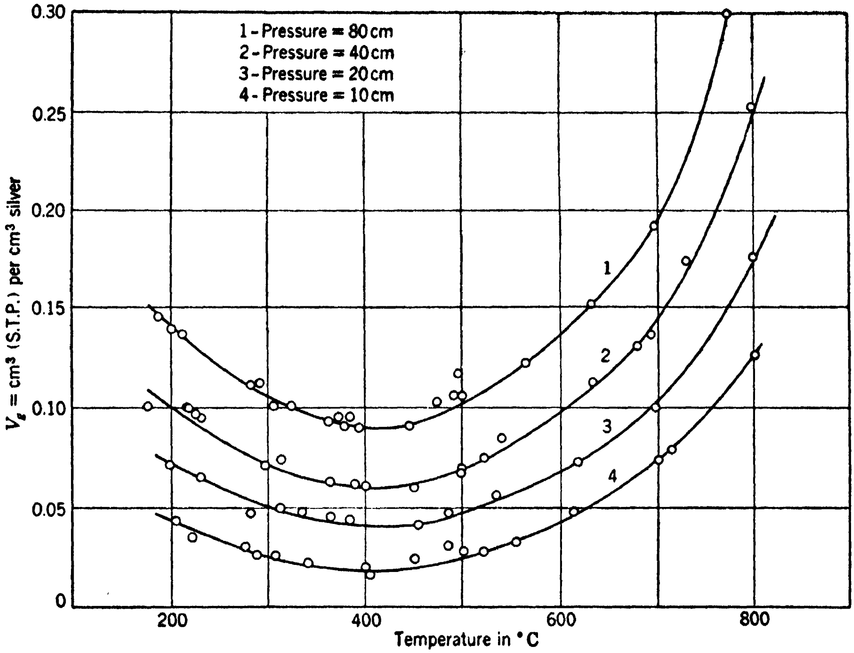

FIG. 20. Isobars at four pressures for the solubility of oxygen in silver (Steacie and Johnson).

In Chapter 12 the related topics are discussed of rates of oxidation and of dissociation pressures of the oxides of the metals.

The system *silver-oxygen* has been investigated by E. W. R. Steacie and F. M. G. Johnson[67] and also by J. H. Simons.[68] The solubility of oxygen in solid silver and rate of solution are proportional to $\sqrt{P}$. Table 32 gives the data obtained by Steacie and Johnson for a pressure of 800 mm. The third row gives values of $s/\sqrt{P_{mm}}$, and Fig. 20 shows plots of four isobars giving values of $V_g\ (=v_0 p)$ as a function of the temperature at constant pressure.

---

[66] *Technol. Paper, Natl. Bur. Standards*, **19**, No. 281, p. 155 (1924–1925).

[67] *Proc. Roy. Soc. London*, **A**, **112**, 542 (1926).

[68] *J. Phys. Chem.*, **36**, 652 (1932).

TABLE 32

SOLUBILITY (CM^3 PER 100 G) OF OXYGEN AT 800 MM IN SILVER

$t°$ C:	200	300	400	500	600	700	800
s:	1.3	0.924	0.828	0.905	1.26	1.84	3.37
$10^2 s/\sqrt{P_{mm}}$:	4.78	3.27	2.93	3.20	4.45	6.50	11.92

The most interesting feature about these data is the occurrence of a minimum at about 400° C. Steacie and Johnson have accounted for this minimum on the assumption that, below 400° C, the dissolved oxygen exists in the form of Ag_2O, and above this temperature as oxygen atoms, since Ag_2O is a relatively unstable compound.

Simons has argued that the minimum is due to a balance between (1) increase in solubility of Ag_2O in silver with increase in temperature, and (2) increase in dissociation pressure of the oxide with increase in temperature. The dissociation pressures of Ag_2O for a series of temperatures are given in Table 12.3, and from these data it will be observed that at 400° C the dissociation pressure is about 115 atm.

According to Simons the solubility of Ag_2O in silver is given by the relation

$$\log z = 0.0034(t - 300), \tag{1}$$

where z = g Ag_2O per 1000 g Ag, and t = °C.

The solubility of oxygen in *molten silver* was investigated by A. Sieverts and J. Hagenacker,[69] and Table 33 gives the results of their determinations. The third row gives the values of the ratio of oxygen atoms to silver atoms. As will be observed there is about a 40-fold increase in the solubility at the melting point.

TABLE 33

SOLUBILITY OF OXYGEN AT 1 ATM IN MOLTEN SILVER

$t°$ C:	923	960.5	973	1024	1075	1125
mg/100 g		m.p.	305	295	277	264
O: 10^4 Ag			206	199	187	178
Vol. O_2: vol. Ag			22.4	21.5	20.4	19.4
s	5.43		213.5	205.6	193.9	184.9

At 1075° C, 1 volume of molten silver in air (oxygen pressure about 150 mm) dissolves about 9 volumes oxygen. As in the case of the solid metal s varies as $\sqrt{P}$.

---

[69] *Z. physik. Chem.*, **68**, 115 (1909).

The liberation of oxygen from silver during solidification has been studied by N. P. Allen[70] with the view of eliminating blow-holes in the cast metal. He has made some interesting calculations on the internal pressures developed in molten silver in consequence of oxygen liberation and in the reduction of Cu_2O in molten copper by hydrogen. By applying external pressure of sufficient magnitude, or by means of a deoxidant, sound castings can be obtained. Allen has also observed that the melting point of silver is lowered by oxygen in accordance with the equation

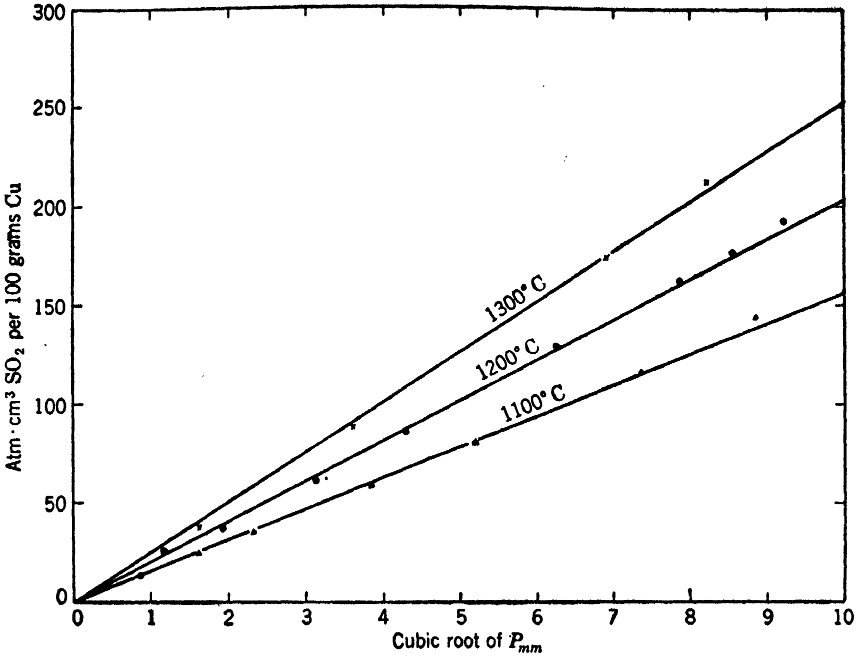

FIG. 21. Solubility of sulfur dioxide in molten copper at three temperatures plotted versus cube root of P_{mm} (Floe and Chipman).

$$t_m = 961 - 22.31\sqrt{P_{atm}}, \qquad (2)$$

where t_m = melting point in degrees centigrade.

The solubility of *sulfur dioxide in molten copper* has been a very interesting topic of investigation on account of both its technical importance and its theoretical significance. The earlier workers on this problem, A. Sieverts and W. Krumbhaar,[71] and Sieverts and E. Bergner,[72] concluded that the solubility varies as $\sqrt[3]{P}$.

[70] *J. Inst. Metals*, **49**, 317 (1932).

[71] *Z. physik. Chem.*, **74**, 295 (1910).

[72] *Z. physik. Chem.*, **82**, 257 (1913).

However, such a relation could not be reconciled with any logical interpretation. It is therefore of interest that the most recent work, carried out by C. F. Floe and J. Chipman,[73] has cleared up the problem, in a very satisfactory manner.

In *pure* molten copper, from which sulfur and oxygen are completely eliminated, s varies as $\sqrt[3]{P}$. In the presence of an *excess of sulfur*, s varies as $\sqrt{P}$, and in both cases the linear plots pass through the origin. Excess of oxygen decreases the solubility. Figure 21 shows plots of s (cm^3/100 g) versus $\sqrt[3]{P_{mm}}$.

Assuming that when SO_2 passes into solution the reaction is

$$6\text{Cu}\ (l) + \text{SO}_2\ (g) = \text{Cu}_2\text{S (in Cu)} + 2\text{Cu}_2\text{O}$$

there should exist an equilibrium constant

$$K = \frac{(\text{Cu}_2\text{S})(\text{Cu}_2\text{O})^2}{(\text{Cu})^6 P(\text{SO}_2)},$$

that is,

$$K' = \frac{(\%\,\text{S}) \times (\%\,\text{O})^2}{P(\text{SO}_2)}$$
$$= \frac{(\%\,\text{SO}_2)^3}{P(\text{SO}_2)},$$

since the percentage concentrations of sulfur and oxygen are the same and proportional to s.

The values of K' for P_{mm} (SO_2) derived by Floe and Chipman for the three temperatures at which observations were made are as follows:

	1100° C	1200° C	1300° C
$K' =$	$1.1 \cdot 10^{-5}$	$2.4 \cdot 10^{-5}$	$4.4 \cdot 10^{-5}$

The observation that, for each temperature, the value of the constant K' exhibits a slight linear increase with pressure is interpreted by the investigators as due either to "deviations from the laws of dilute solutions or increased reaction with the fused-silica tube."

From the linear plot of log K' versus $1/T$ the conclusion is drawn that, for the reaction

$$\text{SO}_2\ (g) = \text{S (in Cu)} + 2\text{O (in Cu)},$$

$$\Delta F = \text{increase in free energy}$$
$$= 30{,}700 + 0.38T.$$

That is, the heat of reaction is 30,700 cal per mole SO_2.

---

[73] *Trans. A.I.M.E.*, **143**, 287 (1941); **147**, 28 (1942).

The solubility of oxygen and nitrogen in tantalum and the effect on the electrical resistance of the metal have been investigated in this laboratory by Mrs. M. R. Andrews, and the topic is discussed in Chapter 10 in the section dealing with chemical clean-up.

The solubility of oxygen and of "oxide gases," such as SO_2, CO, CO_2, and H_2O, in metals and the chemical reactions involved have been discussed by H. Lepp in a series of papers.[74] In general, it can be stated that these gases react with metals in much the same manner as sulfur dioxide with copper, and at any temperature and pressure of gas an equilibrium state is established between oxidizing gas, metal, oxide, and reduction product.

For an adequate discussion of this topic we must therefore consider these reactions (as has been done in Chapter 12) from the thermodynamic point of view, that is, on the basis of free-energy data.

10. DIFFUSION OF GASES THROUGH METALS

As Steacie and Johnson have stated,[75]

> The phenomena of absorption of gases by metals, and diffusion of gases through metals, must be fundamentally connected. It is virtually impossible to conceive of a mechanism for diffusion other than that of solution on the high-pressure side of the metal and subsequent giving up of the gas on the low-pressure side which is supersaturated. Apparently, then, solution must precede diffusion. This conclusion is substantiated by the fact that there is no known case of a gas diffusing through a metal in which it is not apparently soluble.

It follows that, even where the solubility of a gas in a metal has not been determined, the fact that diffusion of this gas occurs through a certain metal is a valid reason for assuming that the gas is soluble to some extent in the metal.

That diffusion occurs by a motion of the atoms (or protons in the case of hydrogen) along interstitial sites follows from the observation that the rate of diffusion follows the $\sqrt{P}$ law, and also that the rare gases and polyatomic molecules do not diffuse (at least noticeably) through metals. That in general diffusion of gases occurs through the crystal lattice and not along grain boundaries was shown by an experiment reported by C. A. Edwards[76] in which he found

> that no difference could be detected between the rate at which hydrogen diffused through a single crystal of iron, and through the same material after it had been recrystallized into a mass of small crystals.

Evidently, rates of sorption and desorption of gases must depend on rates of diffusion of the gases through the metals, that is, on the nature of the concentration gradients at the two surfaces of the sample, and on the values of the diffusion constants.

---

[74] *Metal Ind.*, **47**, 315 (1935); **53**, 27, 59, 79, 103, 131 (1938).

[75] *Proc. Roy. Soc. London*, **A**, **112**, 542 (1926).

[76] *Trans. A.I.M.E.*, **117**, 13 (1935).

Let D = diffusion constant ($\text{cm}^2 \cdot \text{sec}^{-1}$) and C = concentration at any point inside the metal, in cm^3 (S.T.P.) per cm^3 metal.

Then the amount (in atm · cm^3 or equivalent micron · liters) passing through the area A per unit time is given by the relation

$$q = -DA\frac{dC}{dx}, \tag{1}$$

where dC/dx is the concentration gradient at the point x.

In the *stationary state* this gradient is constant throughout the thickness, d, of the metal sheet. For C we can substitute the values of V_g (the volume of gas per volume of metal) at the high-pressure and low-pressure surfaces, and the last equation assumes the form

$$q = \frac{DAK}{d}(V_{g1} - V_{g2}), \tag{2}$$

where, for a diatomic gas (such as H_2, O_2, N_2, etc.),

$$V_{g1} = K\sqrt{P_{mm1}} \quad \text{and} \quad V_{g2} = K\sqrt{P_{mm2}}, \tag{3}$$

and P_{mm1} and P_{mm2} denote the pressures at the two surfaces.

Hence, equation 2 assumes the form

$$q = \frac{DAK}{d}(\sqrt{P_{mm1}} - \sqrt{P_{mm2}}). \tag{4}$$

For a cylindrical tube of length l, inside diameter a, and outside diameter b,

$$q = DfK(\sqrt{P_{mm1}} - \sqrt{P_{mm2}}), \tag{5}$$

where

$$f = \frac{2\pi l}{\ln(b/a)} = \frac{2.73l}{\log(b/a)} \tag{6}$$

$$= \frac{\pi l a}{d} \quad \text{for} \quad 2d \ll a \qquad (2d = b - a).$$

Since we shall consider diffusion through flat surfaces, and also assume $\sqrt{P_{mm2}} = 0$, the equation for diffusion becomes

$$q = DK\frac{A}{d}\sqrt{P}, \tag{7}$$

where P is the pressure at the surface into which the gas penetrates.

At constant pressure the rate of diffusion increases exponentially with the temperature, and, from theoretical considerations, O. W. Richardson, J. Nicol, and T. Parnell[77] derived the relation,

$$q = q_0\sqrt{T}\epsilon^{-b_0/T}, \tag{8}$$

where q_0 and b_0 are constants for a given gas-metal system.

As shown by Smithells, this equation can be replaced for all practical purposes by a relation which does not involve the $\sqrt{T}$ factor, and taking into account equation 7 it is possible to express the rate at which gas diffuses in *atm · cm*^{3} *per cm*^{2} *per sec* by the relation

$$q = \frac{k_0}{d}\sqrt{P_{mm}}\,\epsilon^{-b_0/T}, \tag{9}$$

where k_0 is a characteristic of the gas-metal system, which involves the two constants designated above by D and K. In the following discussion d is expressed in *millimeters* and P in *millimeters of mercury.*[78]

In terms of *micron · liters* ($Q_{\mu l}$) at 0° C, *per minute*,

$$Q_{\mu l} = 760 \times 60q = 45{,}600q. \tag{10}$$

The constant b_0 is defined by the relation

$$b_0 = \frac{E_0}{2R_0}, \tag{11}$$

where E_0 = heat of diffusion in g-calories *per mole*, and $E_0/2$ = heat of diffusion in g-calories per *g-atom*.

In terms of micron liters at $T = 298$,

$$\begin{aligned} Q_{\mu l}' &= 760 \times 60\,q \times \frac{298}{273} \\ &= 1.091Q_{\mu l}. \end{aligned} \tag{12}$$

For $P_{mm} = 760$, and $d = 1$ *mm*,

$$q = k_0\sqrt{760}\epsilon^{-b_0/T};$$

---

[77] *Phil. Mag.*, **8**, 1 (1904).

[78] These are the units used by Smithells, and q is identical with the quantity designated D in his treatise. The constant k_0 is identical with the constant designated K by Smithells and also with the constant P_0 used by Barrer (RB, p. 168).

that is,

$$\log q = \log k_0 + 1.4404 - \frac{b_0}{2.303T}$$

$$= \log k_0 + 1.4404 - \frac{E_0}{9.148T}, \tag{13}$$

and

$$\begin{aligned} \log Q_{\mu l} &= \text{micron} \cdot \text{liters (at } 0^\circ \text{ C) per cm}^2\text{, } \textit{per min}, \\ &\ \text{per mm thickness, at } P_{mm} = 760 \\ &= \log k_0 + 6.0994 - B/T \qquad (14) \\ &= C - B/T, \end{aligned}$$

where

$$\left. \begin{aligned} C &= \log k_0 + 6.0994 \\ B &= E_0/9.148 \end{aligned} \right\} \tag{15}$$

Values of k and E_0 are given for a number of gas-metal systems by Smithells.[79] From these, values of C and B were calculated which are given in Table 34. These constants were then used to calculate values of t (°C) for which $Q_{\mu l}$ has values ranging from 0.1 to 100. In some cases, for which the value of t thus calculated would exceed that of fusion, values of t are given for lower values of $Q_{\mu l}$, which are indicated in parentheses following the value of t. The second column in the table gives the reference number for the source of the original data, as shown in the bibliography, List III, which follows:

List III. References on Rates of Diffusion of Gases through Metals

1. V. Lombard, *Compt. rend.*, **177**, 116 (1923).
2. H. G. Deming and B. C. Hendricks, *J. Am. Chem. Soc.*, **45**, 2857 (1923).
3. W. R. Ham, *J. Chem. Phys.*, **1**, 476 (1933); *Phys. Rev.*, **45**, 741 (1934).
4. G. Borelius and S. Lindblom, *Ann. Physik*, **82**, 201 (1926–1927); G. Borelius, *Ann. Physik*, **83**, 121 (1927).
5. C. J. Smithells and C. E. Ransley, *Proc. Roy. Soc. London*, **A**, **150**, 172 (1935); **152**, 706 (1936).
6. O. W. Richardson, J. Nicol, and T. Parnell, *Phil. Mag.*, **8**, 1 (1904).
7. R. Jouan, *J. phys. radium*, **7**, 101 (1936).
7. R. M. Barrer, *Trans. Faraday Soc.*, **36**, 1235 (1940).
9. V. Lombard and C. Eichner, *Compt. rend.*, **194**, 1929 (1932); *Bull. soc. chim. France*, **53**, 1176 (1933); *Compt. rend.*, **196**, 1998 (1933).
10. E. O. Braaten and G. F. Clark, *Proc. Roy. Soc. London*, **A**, **153**, 504 (1935–1936).
11. H. M. Ryder, *Elec. J.*, **17**, 161 (1920).

---

[79] CS, p. 95, Table 9; also by Smithells and C. E. Ransley, *Proc. Roy. Soc. London*, **A**, **150**, 172 (1935), in Table V, p. 182.

12. F. M. G. Johnson and P. Larose, *J. Am. Chem. Soc.*, **46**, 1377 (1924); **49**, 312 (1927).

13. L. Spencer, *J. Chem. Soc.*, **123**, 2124 (1923).

TABLE 34

CONSTANTS FOR RATES OF DIFFUSION OF GASES THROUGH METALS AND VALUES OF t° C FOR $Q_{\mu l}$ = MICRON · LITERS (0° C) PER CM^2 PER MIN PER MM THICKNESS AT 1 ATM PRESSURE

System	Ref.	C	B	t° C for $Q_{\mu l}$ =			
				0.1	1.0	10.	100.
H_2-Ni	1	4.4611	3371	344	483	701	1097
	2	4.0288	3031	330	479	727	1221
	3	4.1206	2929	299	438	666	1108
	4	4.2455	3017	302	438	657	1071
	5	4.2578	2898	278	408	616	1010
H_2-Pt	6	4.2486	4285	544	736	1016	1732
	3	4.1713	3936	488	671	968	1539
	7	5.010	4220	429	571	779	1130
H_2-Pd	9,1	5.783	2318	69	128	212	340
	8	4.5765	2296	139	229	369	618
H_2-Cu	5	3.4611	3629	541	775	1041 (5)	
	10	3.2755	4307	734	1042		
H_2-Fe	5	3.3116	2100	214	361	735	1029 (50)
	4	3.3035	2055	204	349	619	1303
	11	3.480	2405	264	418	697	1352
H_2-Al	5	5.723	6735	$Q_{\mu l} = 1.03 \cdot 10^{-3}$ for 500° C $= 1.02 \cdot 10^{-2}$ for 600° C			
H_2-Mo	5	4.0679	4417	598	813	1167	1862
N_2-Mo	5	5.0185	9837	1362	1687	2174	2444 (25)
N_2-Fe	11	3.7526	5204	822	1114	1431 (5)	
CO-Fe	11	3.2133	4066	692	993	1344 (5)	
O_2-Ag	12	4.413	4941	640	846		
	13	4.673	4941	598	784	940 (4)	
	13	5.121	4941	534	692	926 (4)	

The values of t given in Table 34 were derived by means of the relation

$$T = t + 273 = \frac{B}{C - \log Q_{\mu l}}. \tag{16}$$

In order to derive t for $Q_{\mu l}' = 1.091\ Q_{\mu l}$ = rate in micron · liters at 25° C,

$$T = t + 273 = \frac{B}{C + 0.0380 - \log Q_{\mu l}'}. \tag{17}$$

A table of selected values of the constants k and b_0 in equation 9 is shown in a publication by E. L. Jossem.[80] This table also gives values of q for the different gas-metal systems for $T = 1200°$ K. Figure 22 shows a simple arrangement, recommended in this paper, for introducing hydrogen through a heated palladium tube into a system. The rate of penetration is controlled by the temperature of operation of the tungsten winding H.

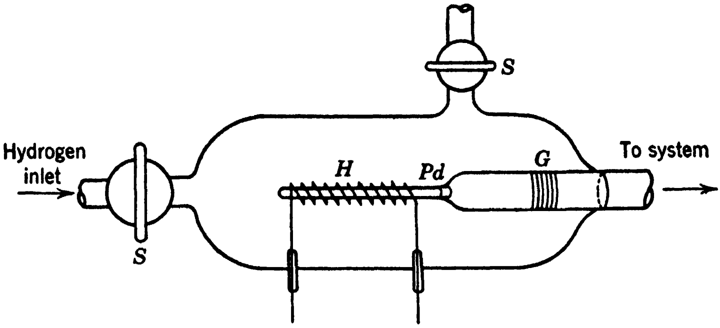

FIG. 22. A constant, controllable arrangement for the diffusion of hydrogen through palladium. H = heater coil, Pd = palladium tube, G = graded seal, and S = stopcock. (Jossem.)

The fact that hydrogen diffuses through palladium much more readily than through any other metal is utilized for the introduction of the pure gas into an evacuated system. Even at room temperature, the rate of diffusion may be fairly rapid, as has been observed by the writer, especially if the palladium happens to be in a well-activated condition.

The $\sqrt{P}$ relation for rate of diffusion is valid, in general, only at higher pressures (around atmospheric pressure and higher). At low pressures the rate decreases below the value predicted by this relation, and Smithells and Ransley[81] have deduced a modification of the relation which is based on the view that diffusion must be preceded by adsorption on the surface. They state,

> Since at any instant diffusion can only occur through those parts of the surface which are covered by adsorbed gas, the *effective* area of the metal is $A\theta$, where A is the total area of the surface and θ the fraction of the surface covered.

---

[80] *Rev. Sci. Instruments*, **11**, 164 (1940). This contains additional references to those given in List III above.

[81] List III, reference 5.

According to the Langmuir adsorption equation,

$$\theta = \frac{cP}{1 + cP},$$

where c is a constant for any particular gas-metal system. Hence, the rate of diffusion should be given, at constant temperature (and for $d = 1$ mm), by

$$q = k\sqrt{P}\left(\frac{cP}{1 + cP}\right), \tag{18}$$

where

$$k = k_0\epsilon^{-b_0/T}. \tag{19}$$

This conclusion has been confirmed by the observations made by Smithells and Ransley for a number of gas-metal systems, and also by Braaten and Clark.[82] Illustrations of the validity of equation 18 will be given in the subsequent discussion.

There are two other sets of observations which are interpreted most satisfactorily by the adsorption theory.

> Nitrogen will diffuse [as Smithells and Ransley observe] through iron, chromium, and molybdenum, with which, under suitable conditions, it can form nitrides, but not through copper and nickel, towards which it is chemically inert. We are therefore led to the conclusion that not only must adsorption occur as a preliminary to diffusion, but that activated adsorption with dissociation of the adsorbed molecules is necessary, and that purely physical adsorption with weak binding forces will not result in diffusion. This hypothesis explains the specific nature of diffusion.

In these respects diffusion of gases through metals is thus of quite a different nature from diffusion of gases through glasses, quartz, and similar materials. In such materials, as observed in Chapter 8, the rate of diffusion varies *linearly* with the pressure, thus indicating that diffusion in these cases is a *molecular*, and not an atomic, process.

The other set of observations which supports the adsorption theory includes those made on the *effects of surface treatment*. This is illustrated by the data in Table 35, taken from the publication by Smithells and Ransley, which give the results of observations on the rate of diffusion of hydrogen through nickel and iron. They state:

> Etching the surface with acid had a far more marked effect, increasing the rate of diffusion by 10 times. The increased adsorption is also shown by the much larger value of c in equation 18 found for etched surfaces.

---

[82] List III, reference 10.

TABLE 35

EFFECT OF SURFACE TREATMENT OF METALS ON RATE OF DIFFUSION OF HYDROGEN

Metal	Treatment	$t°$ C	P_{mm}	q
Nickel	Polished	750	0.042	$1.39 \cdot 10^{-6}$
	Oxidized and reduced	750	.042	2.70
	Polished	750	.091	2.91
	Oxidized and reduced	750	.091	4.23
Iron	Polished	400	.77	$0.47 \cdot 10^{-7}$
	Etched	400	.77	4.4
	Polished	590	.073	1.28
	Oxidized and reduced at 600° C	590	.073	0.76
	Oxidized and reduced at 800° C	590	.073	1.54

Such observations also probably account for the wide variation in the values of the diffusion constants and derived values of rates of diffusion in Table 34.

While, in general, q (or $Q_{\mu l}$) varies with the pressure in accordance with equation 18 above, the rate of diffusion may become independent of the pressure if a compound is formed between the gas and the metal. Smithells and Ransley have shown that at 900° C and higher temperatures the rate of diffusion of oxygen through nickel is practically constant at pressures above 0.25 mm, because the diffusion is limited by rate of formation of NiO.

As will be observed from the data in Table 34, there is a very wide difference between the rates of diffusion obtained by at least two investigators for hydrogen through palladium. Smithells[83] states that this metal "appears to be particularly affected by preliminary treatment, and its capricious behavior has been noted by a number of workers."

The rate of diffusion for hydrogen in palladium is considerably greater than that observed for other gas-metal systems. Figure 23, from the paper by Smithells and Ransley, shows plots of observations reported by Lombard, which illustrate the application of equation 18. For the pressure in millimeters, c has the value 0.054 for 780° K and 0.01 for 645° K. For $P_{mm} = 400$, the plots show $q = 10 \cdot 10^{-3}$ at 780° K and $q = 2.2 \cdot 10^{-3}$ at 645° K. (In Fig. 23 and subsequent figures, $10^n q$ signifies that the *unit of ordinates* is 10^{-n} atm · cm^3 per cm^2 per sec per mm thickness. Also, in the equations for the plots, $P = P_{mm}$.)

The data plotted in Fig. 23 lead to the values $C = 5.783$ and $B = 2318$, which are given in Table 34. On the other hand, the observations of Lombard and Eichner[84] lead to the values $C = 4.014$ and $B = 1063$, and the constants given by Smithells and Ransley lead to the values $C = 4.712$ and $B = 918$. For a so called "inactive" palladium, Barrer[85] deduced constants which correspond to $C = 4.577$ and $B = 2296$. Table 36 gives values of $Q_{\mu l}$ for a series of temperatures as derived by means of these four sets of values of C and B.

---

[83] CS, p. 113.

[84] List III, reference 9.

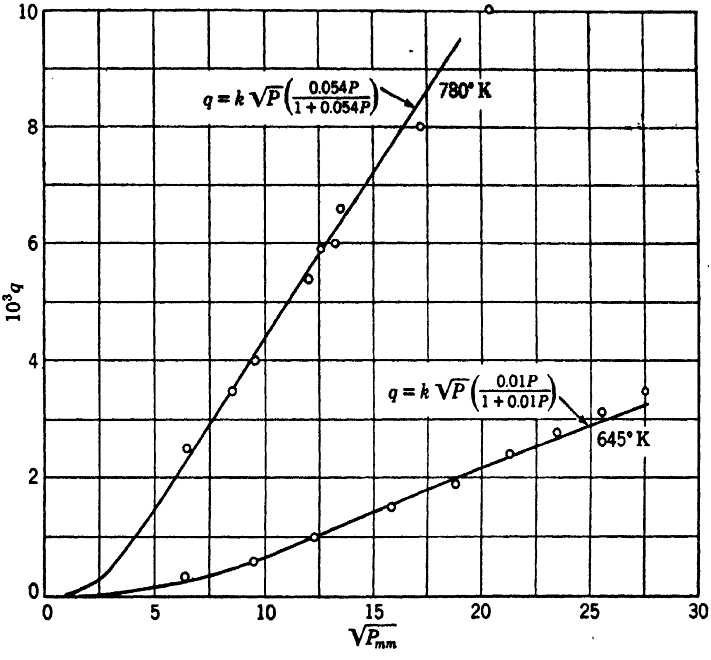

Fig. 23. Rate of diffusion (q) of hydrogen through palladium plotted versus $\sqrt{P_{mm}}$, illustrating application of equation 18. In the equations for each plot, P corresponds to P_{mm}. (Smithells and Ransley.)

TABLE 36

Values of $Q_{\mu l}$ for H_2-Pd System

T	$C = 4.712$ $B = 918$	$C = 4.104$ $B = 1063$	$C = 5.783$ $B = 2318$	$C = 4.577$ $B = 2296$
600	1521	216	83	6
700	2518	386	294	20
800	3664	597	767	51
900	4920	838	1611	106
1000	6223	1100	2917	191

---

[85] List III, reference 8.

Figure 24 gives a plot of observations made by Smithells and Ransley on the diffusion of hydrogen through copper at 723° K. These observations are satisfactorily represented by equation 18 with the value $c = 0.1 \text{ mm}^{-1}$. As shown in Table 34 the rates of diffusion observed in this investigation are much higher than those observed by Braaten and Clark.

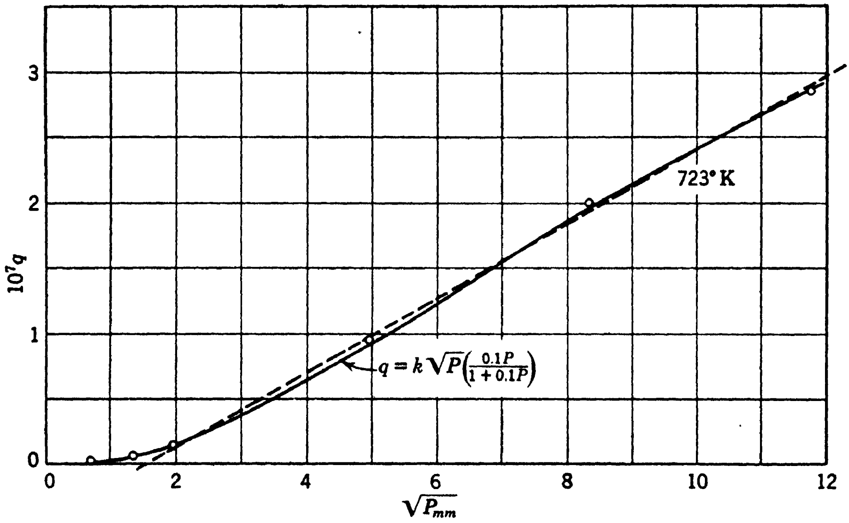

FIG. 24. Rate of diffusion (q) of hydrogen through copper plotted versus $\sqrt{P_{mm}}$. In the equation for the plot, P corresponds to P_{mm}. (Smithells and Ransley.)

Plots drawn by Smithells and Ransley of observations made by Borelius and Lindblom, on the diffusion of hydrogen through iron, at 571° K and 633° K, are shown in Fig. 25, while Fig. 26 shows similar plots for 805° K and 975° K. Evidently all the plots are in agreement with equation 18, with the value of c increasing with increase in T from 0.01 mm^{-1} at 571° K to 0.1 mm^{-1} at 975° K.

The effect of surface treatment on the diffusion of hydrogen through aluminum has been investigated by Smithells and Ransley. It was found that, by means of a special treatment for removal of the oxide film, the rate of diffusion could be increased about sixfold. But gradual poisoning of the surface by oxygen then caused the rate to decrease gradually. The constants in Table 34 were deduced from the plot for 558° C shown in Fig. 27.[86]

Finally, it is interesting to compare the rates of diffusion of gases

---

[86] *Proc. Roy. Soc. London*, **A**, **152**, 706 (1936).

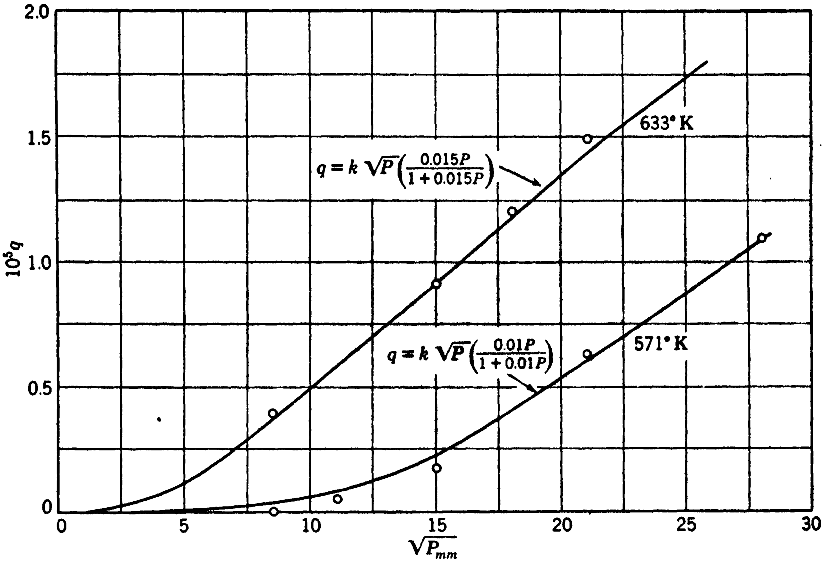

FIG. 25. Rate of diffusion (q) of hydrogen through iron, at lower temperatures, plotted versus $\sqrt{P_{mm}}$. In the equations for the two plots, P corresponds to P_{mm}. (Borelius and Lindblom.)

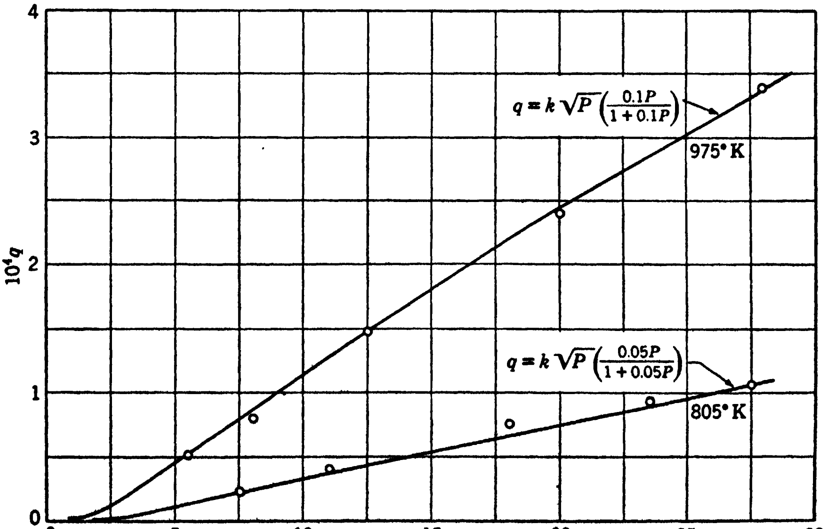

FIG. 26. Rate of diffusion (q) of hydrogen through iron, at higher temperatures, plotted versus $\sqrt{P_{mm}}$. In the equation for the two plots, P corresponds to P_{mm}. (Borelius and Lindblom.)

through quartz with those observed for metals. A comparison of the data in Table 8.33 and those in Table 34 (allowing for the difference in the definition of $Q_{\mu l}$) shows that for hydrogen or nitrogen, at 1 atm, the rate of diffusion, for the same temperature and value of d, is much higher through metals than through quartz.

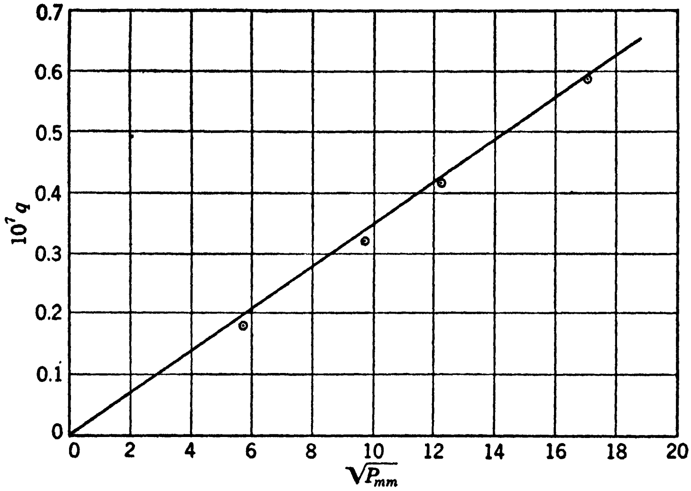

FIG. 27. Rate of diffusion (q) of hydrogen through aluminum at 558° C plotted versus $\sqrt{P_{mm}}$ (Smithells and Ransley).

11. RATES OF SORPTION AND DESORPTION. CALCULATION OF DIFFUSION CONSTANTS

The rates at which these processes occur will, in general, depend upon rates of diffusion of gases into or out of plates or wires of metals in which the gases are soluble. These rates may therefore be deduced as particular solutions of Fick's law, which for diffusion in one direction is of the form[87]

$$\frac{\partial C}{\partial t} = \frac{\partial}{\partial x}\left(D \frac{\partial C}{\partial x}\right), \tag{1}$$

where C denotes the concentration (in grams per cubic centimeter) at time t, at a point distant x from the origin, and D is the diffusion constant in $\text{cm}^2 \cdot \text{sec}^{-1}$.

---

[87] Solutions of this equation and that for diffusion in a wire are discussed by Barrer (RB, Chapter 1), and in a number of mathematical treatises on Fourier's series and Bessel functions.

This equation is applicable, for instance, to the desorption of gas from a thin plate. Let $2a$ denote the thickness of a sheet of metal for which the width and length are each very large compared to $2a$.

Let C_0 denote the concentration of dissolved gas, uniform throughout the range $x = 0$ to $x = 2a$, at $t = 0$. Then the fraction, f, of the total gas content which has diffused to the two surfaces at any time, t, is given by the relation

$$f = 1 - \frac{8}{\pi^2}\left(\epsilon^{-z} + \frac{\epsilon^{-9z}}{9} + \frac{\epsilon^{-25z}}{25} + \cdots\right), \tag{2}$$

where

$$z = \frac{\pi^2}{4} \cdot \frac{Dt}{a^2}.$$

From this equation, it follows that plots of f versus t/a^2 should be similar for different samples, independently of the value of D. This conclusion, we shall find, is valid for all cases of diffusion.

In connection with the determination of oxygen in steel by the Ledebur method (see the following section), T. E. Brower, B. M. Larsen, and W. E. Shenk[88] used a very thin ribbon of the metal, crumpled up and packed into an Invar metal container. Hydrogen was passed over the metal heated to 1100° C, and the H_2O formed as a result of the diffusion outward of the dissolved oxygen was collected and weighed.

As is evident, the series in the parentheses in equation 2 converges rapidly. This is seen from the following values:

z:	0.20	0.25	0.30
ϵ^{-z}:	.8187	.7788	.7408
$\epsilon^{-9z}/(9\epsilon^{-z})$:	.0225	.0150	.0102
Dt/a^2:	.0811	.1014	.1216

For values of $Dt/a^2 > 0.0892$, the second term in parentheses in equation 2 is less than 2 per cent of the first term. Hence, to a first approximation, equation 2 can be written in the form

$$\log(1 - f) = \log\left(\frac{8}{\pi^2}\right) - \frac{\pi^2}{4 \times 2.303} \cdot \frac{Dt}{a^2}. \tag{3}$$

That is, under these conditions a plot of $\log(1 - f)$ versus t/a^2 becomes linear, with a slope

$$\frac{\Delta \log(1 - f)}{\Delta(t/a^2)} = \frac{-\pi^2 D}{9.212}, \tag{4}$$

from which the value of D may be deduced.

---

[88] *Trans. A.I.M.E.*, **113**, 61 (1934).

By application of this method, the value deduced for the coefficient of diffusion of oxygen in steel at 1100° C was $D = 1 \cdot 10^{-9}$ cm$^2 \cdot$ sec^{-1}, which appears reasonable when compared with the value $D = 7.5 \cdot 10^{-10}$ cm $\cdot$ sec^{-1} deduced by other investigators for 1000° C.

The preceding remarks may be illustrated by the following example. Let $a = 10^{-2}$ cm ($= 4 \cdot 10^{-3}$ in.). Then, for $D = 1 \cdot 10^{-9}$ cm$^2 \cdot$ sec^{-1}, and $Dt/a^2 = 0.0811$, $t = 2.25$ hours, and $f = 0.321$. To degas the plate to 10 per cent of its initial gas content ($f = 0.90$), the time required would be about 23.6 hours.

For the case in which the concentration gradient is uniform over a film of thickness l, equation 1 assumes the simple form

$$\begin{aligned}\frac{dC}{dt} &= \frac{D(C_0 - C)}{l} \\ &= k(C_0 - C). \qquad (5)\end{aligned}$$

This relation for rate of absorption (and a similar one for rate of desorption) is observed quite frequently. Assuming that the different gases are adsorbed to the same extent on the surface of the metal, the values observed for k are in the same ratio as those of D.

J. A. M. van Liempt[89] has used a relation for calculating values of D from rates of degassing, which for a metal plate of width very large compared with the thickness $2a$, has the form

$$\frac{C}{C_0} = 1 - \frac{2}{\sqrt{\pi}} \int_0^y \epsilon^{-\beta^2} d\beta, \qquad (6)$$

where $y = \dfrac{x}{2\sqrt{Dt}}$; the integral is the "error function"; C_0 = initial concentration of gas, uniform throughout the thickness; and C = concentration at distance x from the central plane, at time t.

Equation 6 is identical with that deduced for the rate of diffusion of gas into a semi-infinite solid for the condition $C = C_0$ at the boundary ($x = 0$) for all values of t, and the initial condition $C = 0$ for all values of $x > 0$.

A discussion of the rather involved method used by van Liempt in applying this relation to rates of degassing is given by Barrer.[90]

It is of interest to note that from equation 6 it may be deduced that the rate at which gas diffuses into the solid, per unit area of surface, is given by

---

[89] *Rec. travaux chim.*, **57**, 871 (1938).

[90] RB, pp. 215–217.

$$\frac{dQ}{dt} = C_0 \sqrt{\frac{D}{\pi t}}, \tag{7}$$

and hence, the *total amount* which has diffused into the solid per unit area of surface at time t is

$$Q = 2C_0 \sqrt{\frac{Dt}{\pi}}. \tag{8}$$

For the sorption and desorption of gas in the case of a *wire* heated by the passage of current, where diffusion is radial, equation 1 is replaced by the equation

$$\frac{\partial C}{\partial t} = \frac{D}{r} \cdot \frac{\partial}{\partial r}\left(r \frac{\partial C}{\partial r}\right). \tag{9}$$

The solution of this equation, as applied to the rate of degassing of a wire of radius r, has been given by G. Euringer.[91]

For *large values* of Dt/r^2 (D in $\text{cm}^2 \cdot \text{sec}^{-1}$, t in sec, and r in cm), the solution has the form

$$\log G = \log \frac{2C_0 D}{r} - \frac{2.519Dt}{r^2}, \tag{10}$$

where G = rate of evolution of gas in atm · cm^3 per cm^2 per sec, and C_0 = initial concentration of gas in cm^3 (S.T.P.) per cm^3 (that is, $C_0 = V_g$ for $t = 0$).

Since it may be assumed that, at constant temperature, D is a constant, it follows from the last equation that a plot of log G versus t should yield a straight line (at least for sufficiently large values of t), the slope of which is given by $-2.519D/r^2$. Such a plot, obtained by Smithells and Ransley,[92] is shown in Fig. 28. This is a plot of the natural logarithm of G versus t (G = rate of evolution of carbon monoxide) during the degassing of a nickel wire 1 mm in diameter at 950° C.

The absolute values of D for carbon monoxide in nickel thus derived were

$$\begin{aligned} D &= 4.0 \cdot 10^{-8}\ \text{cm}^2 \cdot \text{sec}^{-1} \quad \text{at } 950^\circ\ \text{C} \\ &= 14.0 \cdot 10^{-8}\ \text{cm}^2 \cdot \text{sec}^{-1} \quad \text{at } 1050^\circ\ \text{C}. \end{aligned}$$

The same investigators obtained, for the rate of diffusion of carbon monoxide through nickel at 900° C and *1 mm pressure*, the average value $q_1 = 2.05 \cdot 10^{-10}$ cm^3 (S.T.P.) per sec per cm^2 per mm thickness. From the values given in Table 34 for the constants C and B ($C = 4.2578$, $B = 2898$ for H_2-Ni; $C = 3.2133$, $B = 4066$ for CO-Fe) we derive the following values for $t = 900°$ C:

---

[91] *Z. Physik*, **96**, 37 (1935).

[92] *Proc. Roy. Soc. London*, **A**, **155**, 195 (1936), Fig. 4.

$$\text{CO-Fe,} \quad q_1 = 4.45 \cdot 10^{-7},$$

$$H_2\text{-Ni,} \quad q_1 = 4.87 \cdot 10^{-5}.$$

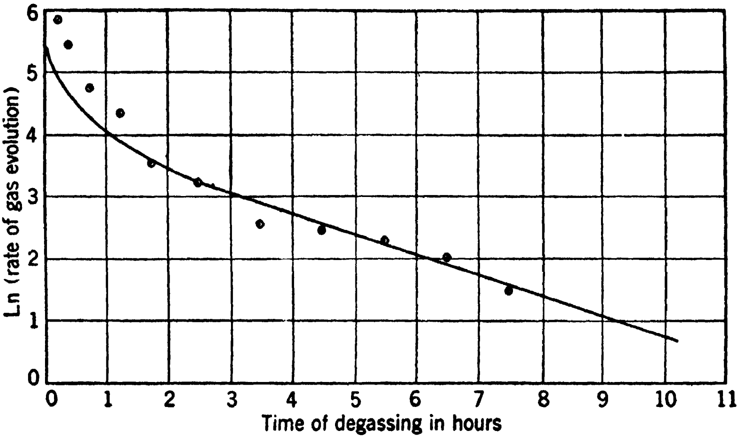

FIG. 28. Plot of natural log of rate of degassing versus time in hours. The full line shows the theoretical curve; the linear portion of the plot follows the relation $\log G = A - Bt$, where G denotes the rate of evolution of carbon monoxide from a nickel wire at 950° C. (Smithells and Ransley.)

The value of q_1 for carbon monoxide in nickel is thus considerably smaller than those for carbon monoxide in iron and hydrogen in nickel. From a comparison of this value for carbon monoxide in nickel with the rate of evolution of carbon monoxide corresponding to the values of G observed by them, Smithells and Ransley concluded that the gas could not be present in the nickel as carbon monoxide.

"The most reasonable explanation," according to them, "of the desorption of carbon monoxide from nickel is derived from a reaction between dissolved oxygen and carbon, probably present in the metal as nickel oxide and nickel carbide." This explanation was confirmed by determinations of rates of diffusion of oxygen and carbon through nickel. Table 37 gives the values of D (cm$^2 \cdot$ sec^{-1}) obtained for these elements in nickel by Smithells and Ransley, and, for comparison, values obtained for steel by a group of English investigators.

TABLE 37

VALUES OF DIFFUSION CONSTANTS FOR CARBON AND OXYGEN IN NICKEL AND STEEL

Metal	$t°$ C	10^8D for Carbon	$10^{10}D$ for Oxygen
Nickel	900	1.8	1.5
	950	3.7	6.8
	1000	7.2	23.6
	1050	13.3	78.0
Steel	900	3.8	—
	950	8.7	—
	1000	20.0	7.5

At saturation, nickel contains about 1.1 per cent (by weight) NiO and 0.4 per cent carbon. These were the values of C_0 used in calculating the above values of D.

As Smithells and Ransley point out, "Commercial nickel always contains a small percentage of carbon, usually of the order of 0.03 per cent, which is much in excess of that required to account for the carbon monoxide desorbed."

From observations on the rate of evolution of hydrogen from a nickel wire, Euringer[93] obtained the following values of D ($\text{cm}^2 \cdot \text{sec}^{-1}$) for the system H_2-Ni:

$t°$ C:	165	125	85
10^8D:	10.5	3.4	0.86

These results can be represented by the relation

$$D = 2.04 \cdot 10^{-3}\epsilon^{-8700/R_0T}.$$

Barrer[94] has quoted the following results, obtained by A. Bramley and his associates, on the diffusion of nitrogen in steel:

$t°$ C:	800	850	900	950	1000	1050	1100
10^8D:	1.2	3.0	6.0	10.8	13.5	25.0	40.0

These results are in agreement with the relation

$$D = 1.07 \cdot 10^{-1}\epsilon^{-34,000/R_0T}.$$

Thus the values of D for any gas-metal system can be represented as a function of T by a relation similar to that used for q (or $Q_{\mu l}$) above, that is, by a relation of the form

$$\log D = C' - \frac{B'}{T}. \tag{11}$$

---

[93] *Loc. cit.*

[94] RB, p. 224.

Table 38 gives values of B' derived from the values of D given in Table 37 and, for comparison, the values of B given in Table 34. The values for N_2-Mo and N_2-W were deduced by F. J. Norton and A. L. Marshall[95] from observations on the rate of gas evolution from samples which had been saturated previously with nitrogen.

That the values of B' need not necessarily agree with those of B follows from the fact that according to equation 10.1 the variation with temperature of q includes the variations of both D and C.

TABLE 38

VALUES OF B' FOR DIFFUSION CONSTANTS COMPARED WITH THOSE OF B FOR PERMEABILITY

System	B'	B (Table 34)
H_2-Ni	1,900	2898–3371
CO-Ni	8,100	
C-Ni	8,950	
O_2-Ni	17,150	
N_2-Fe	7,430	5204
N_2-Mo	5,816	9837
N_2-W	11,040	

12. EARLIER INVESTIGATIONS ON DEGASSING OF METALS

In the preceding sections it has been shown that gases are adsorbed on the surface and are also present in the interior of metal parts either in a state of solution or in the form of chemical compounds. Gases may also be present in microscopic blow-holes or pores. The surface of certain metals, especially copper and iron, may be covered with a film of oxide which has a thickness varying from 10^{-4} to 10^{-6} cm.

If such metal parts are not previously degassed they will gradually evolve gas in an evacuated volume, especially if they are heated to even a slight extent, because of increased rate of diffusion from the inside towards the surface. Consequently, one of the most important problems in vacuum technique is the elimination of all sorbed gases from metal parts.

As will be pointed out at greater length in a subsequent chapter, metal parts may be preheated in pure, dry hydrogen whenever the nature of the metal permits it. A preliminary heating in vacuum by means of high frequency is extremely worth while, since, after such a treatment, metals may be stored for at least a few days in a dry atmosphere at

---

[95] *Trans. Am. Inst. Met. Eng.*, **156**, 351 (1944).

100° C to 200° C without reabsorption of more than an almost negligible amount of gas.[96]

The literature on the amount and composition of the gases which are evolved from metals when degassed in vacuum at higher temperatures, is very extensive. In this section and those that follow only the more important investigations can be reviewed.[97]

In connection with his investigations on the causes of blackening of evacuated tungsten-filament lamps, Langmuir developed a method for analyzing the small amounts of gas contained in metals and glass.[98] He observed[99] that, when care is taken to denude the glass walls of occluded water vapor and carbon dioxide, the amount of gas evolved from a tungsten filament does not exceed ten times the volume of the metal. Most of the gas is eliminated at a temperature of 1500° C, and it consists of about 70 to 80 per cent by volume of carbon monoxide, the remainder being mostly hydrogen and carbon dioxide.

During the course of this investigation the amounts and composition of the gases evolved from other metals used in the construction of incandescent-filament lamps were determined. The metals were in the form of filaments having a total volume of about 30 cu mm, so that they could be heated by passing current through them. Different samples of so-called "untreated" nickel wires gave off amounts of gas varying from 5 to 15 cu mm (S.T.P.), consisting of about 75 to 90 per cent carbon monoxide and 20 to 10 per cent carbon dioxide with small amounts of hydrogen. Similar filaments of Monel metal, copper and copper-coated nickel-iron alloy (used for leads in lead-glass stems) evolved amounts of gas varying from 3 to 20 cu mm of gas. The composition of the gas was found to be about the same as that evolved from nickel wires. It will be observed that in all these cases the volume of gas did not exceed that of the metal, but, since 1 cu mm (S.T.P.) corresponds to about 0.83 micron · liter at room temperature, it is evidently important to eliminate this gas before sealing off an evacuated device containing parts made of these metals.

H. M. Ryder,[100] by a modification of Langmuir's method of analysis, determined the nature and composition of the gases evolved on heating untreated commercial copper in vacuum. It was observed that the gases removed, in order of decreasing amounts, were carbon dioxide, carbon monoxide, water vapor, and nitrogen. The total amount of gas evolved at temperatures below 750° C was about 0.153 cm^3 per cm^3 of metal.

---

[96] See subsequent remarks in this section.

[97] The following remarks are taken from the writer's review of this topic in *J. Franklin Inst.*, **211**, pp. 728–736 (1931).

[98] *J. Am. Chem. Soc.*, **35**, 105 (1912). Also see section 17 in this chapter.

[99] *Trans. Am. Inst. Elec. Eng.*, **32**, 1921 (1913).

[100] *J. Am. Chem. Soc.*, **40**, 1656 (1918); *J. Franklin Inst.*, **187**, 508 (1919).

The gases in steel were investigated by G. Alleman and C. J. Darlington.[101] Some typical results obtained in this work are shown in Table 39.

TABLE 39

AMOUNT AND COMPOSITION OF GAS EVOLVED FROM STEEL

Volume of Gas per Gram of Metal, cm^3	Volume of Gas per cm^3 of Metal, cm^3	Maximum Temperature, °C	Composition of Gas in Volume Per Cent				
			CO_2	O_2	CO	H_2	N_2
(1) 25.2	197	1468	0.13	2.08	59.8	18.18	19.81
(2) 18.6	146	1500	1.20	0	79.8	11.65	7.35
(3) 8.5	67	1100	0.68	1.57	26.15	43.40	28.20

The analyses of the three metal samples were as follows:

SAMPLE	(1) AND (2)	(3)
Per cent carbon	1.049	0.084
Per cent silicon	0.153	.005
Per cent phosphorus	.045	.094
Per cent sulfur	.028	.082
Per cent manganese	.405	.536

Table 40 shows results of an analysis of the gases obtained from a Bessemer steel (0.1 per cent carbon) at different temperatures. The total amount of gas evolved was 28.1 cm^3 per gram or 220 cm^3 per cm^3 of metal.

It will be observed that the hydrogen and carbon dioxide were evolved at 1250° C and lower, whereas the removal of nitrogen and oxygen required much higher temperatures. At the highest temperatures the metals were in a fused condition. Another interesting feature of these results is the relatively large total volume of gas evolved as compared with the results for tungsten, nickel, and copper already mentioned.

By 1929 the large-scale production of vacuum-fused metals had attained considerable importance, especially in Germany, and a paper

---

[101] *J. Franklin Inst.*, **185**, 161, 333, 461 (1918). This paper contains a comprehensive review of previous investigations on gases in ferrous alloys.

TABLE 40

COMPOSITION IN VOLUME PER CENT OF GAS EVOLVED FROM BESSEMER STEEL AT A SERIES OF TEMPERATURES

Gas	At 1000° C	At 1250° C	At 1500° C	At 1675° C
CO_2	1.08	0.62	0.00	0.00
O_2	2.4	3.07	4.28	6.25
CO	48.9	56.10	18.75	8.42
H_2	21.16	15.08	4.20	1.10
N_2	26.46	25.13	72.77	84.23

by W. Rohn[102] deals with the technique and properties of vacuum-fused metals. According to this paper, the volume of gas obtained in this process is about 16 to 120 times that of the metal. The gas consists mostly of hydrogen and carbon monoxide and is ascribed to chemical reactions which have not been completed during reduction of the oxide and proceed to completion during the process of vacuum fusion. Thus carbon monoxide and dioxide are due to a reaction between carbon in the metal and residual oxides, while hydrogen is due to reaction between water vapor and the metals. (We shall find that this explanation of the origin of these gases is confirmed by many investigators.)

Rohn's observations on a chrome-nickel alloy showed that *most of the gas is evolved after the metal is fused,* and that this gas contains a relatively large proportion of carbon monoxide with smaller percentages of nitrogen, oxygen, and hydrogen. However, most of the hydrogen is evolved at temperatures below 1000° C.

As Rohn has pointed out, metals and alloys fused in vacuum are softer and more ductile than the same materials fused in air. For instance, copper containing a small amount of Cu_2O, does not exhibit embrittlement after fusion in vacuum, and furthermore the electrical conductivity is higher (by about 1 or 2 per cent) than that of ordinary commercial copper.

Naturally, the problem of developing a technique for the fusion of metals in vacuum and subsequent analysis of the gas evolved has received considerable attention. Some of the laboratory methods which have been developed during recent years will be described in a subsequent section. In a comprehensive review of the methods used previously, W. Hessenbruch[103] has also given data on the amount and composition of gases evolved from heated samples of different metals. Tables 41 and 42 show results observed for copper and nickel, respectively.

---

[102] *Z. Metallkunde,* **21**, 12 (1929).

[103] *Z. Metallkunde,* **21**, 46 (1929).

TABLE 41

AMOUNT AND COMPOSITION OF GAS IN COPPER TREATED AT 1250° C

Sample	Volume of Gas per 100 g Metal, cm³	Volume of Gas per cm³ Metal, cm³	Composition of Gas in Volume Per Cent			
			SO_2	H_2	CO	N_2
Refined Cu (1)	2.72	0.24	58.2	7.90	19.50	14.40
Refined Cu (2)	1.46	0.13	85.7	7.43		6.87
Refined Cu (3)	1.79	0.16	33.9	28.55	37.55	
Refined Cu (4)	0.73	0.07	61.1	11.11	22.22	5.57
Electrolytic Cu	7.97	0.71	10.9	39.52	49.70	

TABLE 42

AMOUNT AND COMPOSITION OF GAS IN NICKEL TREATED AT 1470° C

Sample	Volume of Gas per 100 g Metal, cm³	Volume of Gas per cm³ Metal, cm³	Composition of Gas in Volume Per Cent			
			CO_2	CO	H_2	N_2
Cube Ni	482	42.9	2.30	90.0	3.50	4.20
"Mond" Ni	113	10.1	2.92	72.4	24.70	
Electrolytic Ni	7.88	0.7	0.00	21.1	78.9	

The SO_2 obtained in the case of copper is evidently due to the reaction

$$Cu_2S + 2Cu_2O = SO_2 + 6Cu,$$

which has been discussed in Section 9 in connection with the determinations of the solubility of SO_2 in molten copper.[104]

In the case of electrolytic nickel, the large amount of hydrogen must be due to gas occluded by the metal during deposition.

Tables 43 and 44, taken from the same source as the previous two tables, show results obtained on samples of commercial aluminum evacuated at 1200° C and iron evacuated at 1550° C (both metals being in the fused condition). The analysis of the metal gives percentage by weight of the different constituents. The total volume of gas in $cm^3/100\ cm^3$ and in cm^3/kg, in Table 44, were derived by means of the conversion factors in Table 45.

A. Villachon and G. Chaudron[105] investigated the evolution of gases from metals in a vacuum furnace in which the pressure could be maintained at 0.02 mm at about 1700° C and at 0.002 mm at 1000° C. The fusion was carried out in magnesite crucibles. Then the samples were rolled to thin sheets, the nickel sheets being heated in quartz tubes to

---

[104] See also the remarks by E. H. Schulz, *Z. Metallkunde*, **21**, 7 (1929).

[105] *Rev. Mét.* **27**, 368 (1930).

TABLE 43

AMOUNT AND COMPOSITION OF GAS IN ALUMINUM EVACUATED AT 1200° C

Sample No.	Analysis of Metal			Total Volume of Gas		Composition of Gas in Volume Per Cent			
	Al	Si	Fe	cm^3/kg	$cm^3/100\ cm^3$	H_2	CO	CO_2	N_2
1	97.61	1.24	1.15	46.1	12.5	71.60	11.90	5.65	10.85
2	99.52	0.22	0.26	39.4	10.6	74.70	11.16	—	14.20
3	98.40	.45	1.15	87.8	23.7	83.26	8.54	3.98	4.22
4	98.62	.98	0.40	63.8	17.2	84.31	12.08	2.98	0.63
5	99.50	.24	0.26	70.3	19.0	71.70	15.38	2.56	10.36
6	99.01	.08	0.65	172.0	46.4	88.13	8.48	3.39	—
7	99.01	.06	0.65	124.5	33.6	77.33	17.20	5.47	—

TABLE 44

AMOUNT AND COMPOSITION OF GAS IN IRON EVACUATED AT 1550° C

Sample	Analysis of Metal				Total Volume of Gas		Gas Composition Per Cent by Weight		
	C	Si	Mn	S	cm^3/kg	$cm^3/100\ cm^3$	O_2	H_2	N_2
Electrolytic	0.02	0.02	0.02	0.0028	211.6	166.5	0.010	0.0010	0.0037
Armco	.02	—	.05	—	540.4	425.3	.062	.0007	.0035
Swedish	.04	—	—	—	1221.6	961.6	.152	.0012	.0029

TABLE 45

CONVERSION FACTORS FOR GAS ANALYSIS

0.10 Per Cent by Weight	= cm^3/kg	= $cm^3/100\ cm^3$ Fe
Hydrogen	11,200	8,853.0
Oxygen	700	553.4
Nitrogen	800	632.4
Carbon monoxide	800	632.4
Carbon dioxide	509	402.4

800° C and the copper sheets and iron sheets being heated in Pyrex tubes to 600° C. The gas evolved was found to be composed of hydrogen and carbon monoxide, and the total amount was approximately equal in volume to that of the metal. This would correspond to about 11 cm^3 per 100 g of metal.

The oxide film on the surface of aluminum hinders the elimination of gas, and Chaudron[106] used an electric discharge to clean the surface. The surface was made the cathode in a high-voltage (130 kv) low current discharge (of a few milliamperes). The improvement obtained in removal of gas was certainly remarkable. Whereas, by heating the molten metal in a pressure of 10 microns, 20.0 cm^3 gas was obtained per 100 g of metal, as much as 192 cm^3 per 100 g aluminum was extracted by use of the gas discharge.

For many purposes, a knowledge of the exact composition of the gas is not nearly as important as information about the total volume that can be removed by heating to a temperature just below fusion. On the basis of such data it is possible to compare the results obtained by different procedures for the preliminary treatment of metal parts. In order to obtain such data, Mrs. M. R. Andrews,[107] working in this laboratory, developed the arrangement shown diagrammatically in Fig. 29.

Samples of the metals to be investigated were heated in a molybdenum cup (M) contained in a 7-in. bulb. The evolved gases were removed by means of a mercury pump into a reservoir to which was connected a McLeod gauge. Thus the total amount of gas could be measured. By means of a liquid-air trap below the reservoir a determination could also be made of the amount of gas not condensible at about −190° C, which includes hydrogen, nitrogen, and carbon monoxide, while the condensible gas was mostly carbon dioxide.

The procedure adopted for making an analysis consisted in placing the sample in the tube B. The whole system was baked at 450° C for 1 hour, and the molybdenum cup was heated with the high frequency to degas it. The sample was then shaken into the cup by tapping the tube *B* gently, and the reservoir for collecting evolved gas was closed off from the final pump. The high frequency was applied again, the temperature of the cup being determined by an optical pyrometer, and the heating continued until the gas evolution had become negligible at the maximum temperature.

---

[106] *Aluminum*, **19**, 594 (1937); O. Kubaschewski, *Z. Elektrochem.*, **44**, 152 (1938).

[107] *J. Franklin Inst.*, **211**, 689 (1931).

The molybdenum cup was fastened on a pivot so that it could be emptied after the gas determination. The mica shield was inserted to prevent cracking of the seal. In this manner several samples could be inserted in tube *B* and a gas determination made on each, without opening the connection to the evacuating system.

Table 46 shows some typical results obtained by this method. Since the densities of both copper and nickel are approximately the same (8.9), 100 cm^3 per kg metal corresponds to 0.89 volume of gas per volume of metal. Thus the data show that the volume of gas rarely exceeded that of the metal and by treatment at high temperature in vacuum the gas content could be reduced to less than 10 per cent of the volume of the metal.

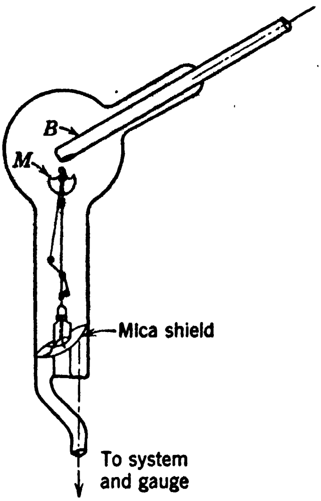

FIG. 29. Arrangement for heating up samples in molybdenum cup for determination of gases evolved from metals (Andrews).

An interesting point observed during this investigation, which was confirmed during the course of the work described in the next section, was that vacuum-fired samples exposed to a dry atmosphere take up extremely small amounts of gas unless touched with the fingers.

The effect of grease on the surface of samples to be tested for gas content has been emphasized by K. Steinhäuser.[108] He has shown that insufficient care in removing grease from the surface of aluminum leads to erratic results in the subsequent determinations of gases evolved on heating the samples in vacuum. The procedure recommended for preliminary treatment is as follows: After the samples are cleaned with a suitable volatile solvent (ether, alcohol, or benzene) they are heated to 350° C in a gas flame. Samples of aluminum treated in this manner, then heated to 1050° C in vacuum and allowed to solidify in vacuum, evolved consistently about 0.5 cm^3 per 100 g of metal (1.35 cm^3 per

---

[108] *Z. Metallkunde*, **26**, 136 (1934).

TABLE 46

AMOUNTS OF NON-CONDENSIBLE AND CONDENSIBLE GAS EVOLVED BY HEATING SAMPLES OF METALS IN VACUUM

Material	Non-Condensible Gas in cm³/kg	Condensible Gas in cm³/kg
Ni wire, 0.030 in., H_2-annealed	49.0	3.1
	76.0	3.9
Ni strip, 8 mil	60.2	8.2
Ni strip, vacuum-treated (1 hr @ 1000° C)	40.5	5.5
Mo sheet	52.9	8.3
Mo sheet, treated in H_2 (15 min @ 1150° C)	10.8	4.0
Mo sheet, heated in vacuum (1 hr @ 1050° C)	9.8	3.7
Ni, H_2-annealed, diamond drawn	96.0	6.5
Cu, pure, deoxidized	12.1	2.5
	6.3	2.1
	2.5	1.6
Cu, heated to 1600° C in vacuum	22.0	—
	6.3	3.6
Cu, boiled in vacuum in Mo cup	5.4	3.3

100 cm³ aluminum). The gas was composed of about 70 per cent by volume hydrogen and 30 per cent methane. (Since methane could have come only from carbon introduced during the heating in a gas flame, the question arises whether even better results could not have been obtained by heating the samples to about 400° C in dry nitrogen.)

In this laboratory, A. L. Marshall[109] obtained the data for copper shown in Table 47. The "surface gas" corresponds to that evolved at temperatures of 1000° C and lower; the major portion of the "interior gas" was evolved during volatilization of the metal. The gas evolved consisted largely of carbon monoxide with smaller amounts of hydrogen and carbon dioxide, except in the case of electrolytic copper where most of the surface gas was found to consist of hydrogen.

TABLE 47

VOLUME OF GAS EVOLVED FROM COPPER HEATED IN VACUUM

	Volume of Gas, cm³/100 cm³		Total Volume
Nature of Sample	Surface Gas	Interior Gas	cm³/kg
1. Electrolytic	0.51	7.1	8.57
2. Commercial	.67	4.0	5.22
3. Vacuum-fused	.91	3.68	5.13
4. Vacuum-fused	.69	5.2	6.58

---

[109] Reported by the writer, *J. Franklin Inst.*, **211**, 735 (1931).

A summary of the range of values, obtained in the different investigations reviewed in this section, for the amount of gas evolved, is given in Table 48. The results on steel given in Table 39 are omitted from this summary since they are obviously very much higher than any values obtained subsequently.

TABLE 48

SUMMARY OF GAS-EVOLUTION DATA

Table	Metal	Cm³ per kg Metal	Cm³ per 100 cm³ Metal
41	Copper	7–80	6–72
42	Nickel	79–4800	70–4300
43	Aluminum	40–172	11–46
44	Iron	11–110	9–87
46	Nickel	46–102	41–92
46	Copper	4–22	3.6–20

The conclusion that can be drawn from this summary is that the total volume of gas evolved rarely exceeds that of the metal.

13. INVESTIGATION ON DEGASSING OF METALS BY NORTON AND MARSHALL

A very comprehensive series of determinations of the amounts and composition of the gases evolved from molybdenum, tungsten, iron, nickel, and graphite was carried out by F. J. Norton and A. L. Marshall.[110]

The analytical method used, which is described fully in the original paper, was a modification of the methods used by Langmuir and Ryder.[111] Because of their importance in vacuum-tube technique, the results obtained are reviewed in the following sections at some length.

Degassing of Molybdenum. The samples, thoroughly cleaned by a chemical procedure described in the paper, were heated to successively higher temperatures and the gas evolved at each stage was collected and analyzed. The following quotation from the original paper describes the initial observations.

> Hydrogen comes off most readily at the lower temperatures, as Alleman and Darlington[112] found with ferrous alloys. The amount of this is relatively small.
>
> The next gas to appear is carbon monoxide, which comes off readily at 1000° C and lower. It persists, in small amounts, to the higher temperatures.

---

[110] *Trans. Am. Inst. Mining Met. Engrs.*, **156**, 351 (1944).

[111] See section 17 for description of this method.

[112] *Loc. cit.*, footnote 101.

> Nitrogen is more difficult to remove and requires a temperature of 1200° and up before it comes off.

In view of these observations, all subsequent degassing experiments were carried out at 1760° C. The total volume of gas evolved varied from 0.86 to 8.2 cm^3 (S.T.P.) per kg. The composition of the gas showed the following variations in percentage by volume:

N_2: 22–98 (most frequently, over 60 per cent)
CO: 0–76 (most frequently, 15–36 per cent)
CO_2: 0–9 (most frequently, 3–6 per cent)
H_2: 0–17 (most frequently, 0 per cent)

The volume and composition of the gas evolved were found to be affected by the method of cleaning in the preparation of the sample for vacuum treatment. According to the authors,

> One of the most striking things found in this investigation of molybdenum was that a sample once degassed stays degassed, if proper precautions are taken. The most important requirement is to avoid handling the sample. . . . If precautions are taken, and the sample is handled with tweezers and kept wrapped in condenser paper, the surface contamination is reduced to a minimum.

Degassed samples were exposed to air and then degassed again. The volume of gas obtained in that case was found to correspond to an approximately unimolecular layer (physically adsorbed). This observation on the effect of storing degassed samples, which, as mentioned previously, was also observed by Mrs. Andrews, is evidently of extreme importance in high-vacuum technique, where it is frequently necessary or convenient to degas metal parts in one operation and then store them for subsequent use.

Another series of experiments showed that "samples of moybdenum fired in a tube hydrogen furnace at atmospheric pressure and 2000° C gave off less gas on subsequent degassing than was present in unfired samples." A subsequent degassing at 1760° C for ½ to 1 hour was sufficient for complete removal of residual occluded gases. (All the degassing at high temperature was carried out by means of high-frequency heating.) It was observed that *the volume of this residual gas decreased with increase in purity of the hydrogen used,* as is illustrated by the observations recorded in Table 49.

The "percentage of total gas removed" was calculated by assuming 4.5 cm^3 per kg as the normal amount of gas in a sample that had been given a similar cleaning treatment before heating in vacuum.

The effect, on the volume of gas evolved, of using extremely pure hydrogen such as is obtained by diffusion through heated palladium is very significant, and still more important is the observation that degas-

TABLE 49

EFFECT OF TREATMENT OF MOLYBDENUM ON GAS CONTENT

Method	Gas Left in Mo, cm^3/kg Average	Gas Left in Mo, cm^3/kg Lowest	Average Percentage of Total Gas Removed
Hydrogen firing, tube furnace at 1 atm	1.15	0.86	74.8
Arsem vacuum furnace	0.95	.58	75.9
Tungsten vacuum furnace	.82	.44	81.5
Purified line hydrogen, 1 atm	.47	.39	89.6
Line hydrogen diffused through heated palladium	.16	.07	96.4

sing may be accomplished by heating samples in purified hydrogen instead of in a vacuum furnace.

As has, however, been mentioned previously, hydrogen firing is not always a safe procedure because of so-called embrittlement effects.

Observations made by Norton and Marshall on rates of degassing have been discussed in section 11 of this chapter.

Degassing of Tungsten and Nickel. To degas tungsten at a rate comparable with that observed for molybdenum at 1800° C, it was found necessary to heat the metal to 2300–2430° C. The amount of gas evolved from tungsten was observed to be about 15 to 25 per cent of that evolved from a similar sample of molybdenum and averaged about 0.3 cm^3 per kg. The average composition of the gas was about 67 per cent nitrogen, 30 per cent carbon monoxide, and 3 per cent hydrogen.

Since nickel has the same vapor pressure at 1030° C as molybdenum at 1760° C (about 3 microns), this fixed an upper limit to the temperature at which the nickel could be heated for any length of time in vacuum. A sample of vacuum-melted nickel heated to 1090° C for about 7 hours gave off 2.8 cm^3 per kg, while, from a sample of "Electro" nickel heated to 1100° C for 15 hours and then to 1200° C for 4 hours, 19.3 cm^3 per kg was obtained. In this case the gas evolved consisted of 60 to 90 per cent carbon dioxide, 2 to 40 per cent hydrogen, and 6 to 11 per cent nitrogen.

Degassing of Iron. Norton and Marshall describe the different types of iron investigated as follows:

1. Ordinary low-carbon stamping steel.
2. Svea iron. This is described[113] as a special type of exceptionally pure Swedish iron made by a secret process to approach a chemically pure iron.
3. Cast steel. A manganese molybdenum steel with the following analysis: carbon, 0.24 per cent; silicon, 0.34; sulfur, 0.010; phosphorus, 0.017; manganese, 1.29; molybdenum, 0.49.

---

[113] H. C. Todd, *Radio Engineering*, **12**, 18 (1932).

4. Bain cast steel of analysis: carbon, 0.17 per cent; silicon, 0.37; sulfur, 0.010; phosphorus, 0.019; manganese, 0.47; chromium, 1.74; molybdenum, 0.69.

5. "New iron" made by the General Reduction Corporation, Detroit. . . . The composition was: carbon, 0.05; silicon, 0.008; sulfur, 0.006; phosphorus, 0.008; manganese, 0.18 per cent.

The samples were heated in vacuum to as high as 1370° C. The total amounts of gas (cm^3 per kg) evolved from each of the samples, desginated by the numbers given above, were as follows:

1, 700; 2, 288; 2, 230; 3, 174; 4, 155; 5, 82; 5, 70.

The last sample, which was "New iron," previously fused by high-frequency heating, evidently evolved the lowest amount of gas. The gas evolved from the different samples of iron consisted mainly of nitrogen and carbon monoxide, with smaller amounts of carbon dioxide and hydrogen.

Degassing of Graphite. Samples such as are used for anodes in Tungar rectifiers were given a preliminary firing in a hydrogen furnace at 1500° C and then heated in an Arsem vacuum furnace at 1800° C.

> At 2150° C [according to Norton and Marshall] it is possible to degas graphite so that subsequent heating at a higher temperature gives no further gas. It is very interesting to note that the gas evolved in the range 1700° C to 2200° C is predominantly nitrogen. A piece of graphite, which has been degassed completely, on subsequent exposure to air, absorbs oxygen, and some of this is so firmly bound that it is only desorbed as carbon monoxide on subsequent heating to 2150° C.

The volume evolved varied from 1.5 to 12.3 cm^3 per kg, and consisted mainly of hydrogen, carbon monoxide, and nitrogen with a much smaller percentage of carbon dioxide.

Table 50 presents a summary of the results obtained in this investigation. The second and third columns give the range of values observed for the amount of gas evolved in the different sets of experiments.

TABLE 50

RANGE OF VALUES FOR TOTAL GAS EVOLVED FROM MATERIALS INVESTIGATED BY NORTON AND MARSHALL

Material	Total Gas Evolved in cm^3 (S.T.P.)	
	per kg	per 100 cm^3
Tungsten	0.2–0.4	0.4–0.8
Molybdenum	1–10	1–10
Nickel	3–20	3–18
Iron (and steel)	70–700	55–550
Graphite, processed at 1800° C	1.5–12	0.33–2.7
Graphite, unprocessed	270 and higher	60 and higher

Only with iron and unprocessed graphite did the volume of gas evolved exceed that of the metal. Tungsten, since it is sintered in hydrogen at a temperature of about 3655° K (melting point), contains the smallest amount of gas per unit volume, and molybdenum has about three to five times as much.

The important conclusions that may be drawn from the results obtained by Norton and Marshall are the following:

1. A preliminary firing in *very pure hydrogen* at as high a temperature as possible yields a much more gas-free metal and should be used whenever hydrogen produces no deleterious effects on the mechanical or electrical properties of the metal.
2. Since the rate of evolution of gas increases rapidly with increase in temperature, the sample should be evacuated at as high a temperature as practicable.
3. The total amount of gas evolved per unit mass or unit volume depends to a great extent on the nature of the preliminary treatment such as method of cleaning, purity of hydrogen used for annealing or for the elimination of oxides, and even on the metallurgical procedures followed in the production of the sample.

14. DETERMINATION OF OXYGEN CONTENT OF METALS FROM COMPOSITION OF GASES EVOLVED

According to Smithells,[114] "the total quantity of gas that can be extracted from commercial metals by heating *in vacuo* is usually between 1 and 20 cm^3 per 100 g of metal. With copper and aluminum the gas is largely hydrogen, but carbon monoxide is the chief constituent in iron and nickel." That the carbon monoxide is due to a reaction between carbon (usually present as carbide) and oxygen (or oxides) in the metal has been demonstrated by several investigators, including Smithells and Ransley, as noted in section 11.

In an excellent review dealing with the application of nickel in the radio-tube industry, E. M. Wise[115] has pointed out the importance of the oxygen content in the metal on account of its bad effect on the life of oxide-coated cathodes. The fact that iron contains about 10 to 50 times as much oxygen as nickel does is due to the inherent difference in ease of oxidation (as will be pointed out in more detail in Chapter 12).

Furthermore, as Wise states,

> Nickel is melted by special methods which insure a minimum oxygen content, and finally an addition of about 0.1 per cent of magnesium is made which may further

---

[114] CS, p. 204.

[115] *Proc. Inst. Radio Engrs.*, **25**, 714 (1937).

lower the available oxygen and which confers several other desirable properties on the nickel. The methods employed in annealing nickel are such as to reduce the oxygen content further.

Since, as will be shown in a subsequent chapter, many metal oxides possess extremely low dissociation pressures even at 1500–1800° C, the "vacuum-fusion method" is frequently used for the purpose of determining the oxygen in the form of carbon monoxide. This procedure, developed by H. C. Vacher and L. Jordan,[116] consists in fusing the metal in vacuum in a graphite crucible.[117] Improvements in the method have been described by L. Reeve;[118] results obtained by him on the temperature of reduction of oxides by carbon are shown in Table 51.

TABLE 51

DEGREE OF REDUCTION OF OXIDES BY CARBON

Oxide	Temperature of Reduction, °C	Percentage Yield of Oxygen Collected as Carbon Monoxide
FeO, iron oxide	1000–1050	97.3
MnO, manganous oxide	1150	86.9
SiO_2, silica	1300	100.0
Al_2O_3, alumina	1550–1600	75.0

"Very slow reduction was observed at temperatures about 50° C below those quoted in the table."

It should be observed, that, in terms of volume at S.T.P.,

$$1 \text{ per cent by weight of oxygen (O)} = 14 \text{ cm}^3 \text{ CO per g.}$$
$$1 \text{ per cent by weight of carbon (C)} = 18.67 \text{ cm}^3 \text{ CO per g.}$$

Thus, from a measurement of the carbon monoxide evolution at different temperatures, it is possible to determine the nature and amount of each oxide present in the metal. As an illustration of the application of the vacuum-fusion method, Reeve gives the analytical results shown in Table 52 of a bare weld wire which contained 0.021 per cent carbon, 0.09 per cent manganese, and 0.014 per cent silicon.

It is of interest to note that, as observed previously by other investigators, the greater part of the hydrogen in steel is evolved at about 1150° C and comparatively smaller amounts are evolved at 1300° C and higher.

---

[116] *J. Research Natl. Bur. Standards*, **7**, 375 (1931).

[117] This method is discussed at greater length in section 17.

[118] *Trans. Am. Inst. Mining Met. Engrs.*, **113**, 82 (1934).

TABLE 52

PERCENTAGE BY WEIGHT OF OXYGEN, NITROGEN, AND HYDROGEN EVOLVED FROM BARE WELD IRON AT DIFFERENT TEMPERATURES

Temperature, °C	Oxygen as	Per Cent	Per Cent N_2	Per Cent H_2
1050	FeO	0.282	0.159	0.00025
1300	SiO_2	.0003	.0077	
1500	Al_2O_3	.022	.0141	

A second method for the determination of oxygen in metals is that originally suggested by A. Ledebur, in which *carefully purified hydrogen* is passed over the metal at a high temperature and the oxygen is collected and weighed as H_2O. The method has been described very fully by B. M. Larsen and T. E. Brower,[119] and an improved techique has been described by the same investigators and W. E. Shenk.[120]

Wise[121] has given, in Table 53, a summary of oxygen determinations, made by the last-mentioned investigators, on samples of iron, and also data for several heats of commercial "A" nickel.

TABLE 53

PERCENTAGE OF OXYGEN AS FeO IN SAMPLES OF DIFFERENT METALS

Description of Metal Used	Per Cent Oxygen as FeO	Equivalent O as CO, cm³ per kg
Ingot iron (low-carbon, high-purity)	0.040–0.060	560–840
Electrolytic iron	.018– .024	250–340
Pure iron, vacuum-melted	.003– .006	42– 84
Ingot iron heated in H_2 at 1500° C	.002	28
Low- and medium-carbon milled steels	.012– .033	168–462
Commercial "A" Nickel (four samples)	.001– .002	14– 28
Iron-aluminum alloy, 0.25% Al*	.002	28
Iron-aluminum alloy, 0.50% Al*	Trace	—
Carbonyl iron, pressed from powder and rolled into sheet*	.012	168

* Values not given in Wise's table but taken from the paper by Larsen, Brower, and Shenk.

Comparing the gas evolution from iron with that from nickel it is evident that nickel is much more suitable for vacuum devices than iron. With regard to other impurities Wise has made the following comments:

---

[119] *Trans. A.I.M.E.*, **100**, 196 (1932).

[120] *Trans. A.I.M.E.*, **113**, 61 (1934). These publications give references to the extensive literature on this topic.

[121] *Loc. cit.*

Phosphorus and sulfur while not gaseous at room temperature volatilize rather easily and in some respects behave like gases. The phosphorus content of nickel is very low, about 0.003 per cent, while that of iron may range from 0.018 to about 0.065 per cent. Phosphorus seems to be tolerated by thoriated cathodes but experiments indicate that it is detrimental to oxide-coated cathodes.

Sulfur in all tube parts is definitely detrimental, and this element is carefully controlled in nickel, the amount present being normally 0.005 per cent or less. The sulfur content of irons is usually 0.025 to 0.45 per cent. Some methods of steel manufacture lead to values as high as 0.060 per cent sulfur.

Sulfur is extremely detrimental to oxide-coated cathodes, and the use of material containing appreciable quantities of this element in plates and other tube parts is known to be extremely undesirable.

The problem of the source of nitrogen in iron and its alloys has been discussed by Reeve. In view of the observations on the dissociation pressures of the nitrides, which are discussed in Chapter 12 (also see comments at the end of section 8 of this chapter), he has suggested that the nitrogen evolved at 1300° C is associated with silicon and that at 1570° C with aluminum.

The topic discussed in this section is intimately related to the problems, dealt with in Chapter 12, of the conditions for the reduction of oxides by carbon and hydrogen, and the reader is therefore referred to that chapter for further discussion of the subject.

15. EMBRITTLEMENT OF METALS BY HYDROGEN

In section 13 attention was drawn to the observation made by Norton and Marshall on the beneficial effect in reducing the gas content in metals of a preliminary heating in extremely pure hydrogen. However, it was also mentioned that in the case of tantalum such a treatment leads to injurious effects on the mechanical properties. Similar effects are also observed in the case of copper.

As stated in section 5, a tantalum filament, heated in hydrogen to a high temperature and then cooled in the gas to room temperature, takes up about 740 times its volume of hydrogen. It was first observed by M. Pirani[122] that such a filament, although originally quite ductile, becomes very brittle when saturated with hydrogen. It can be crushed easily, because of the formation of very small crystals. Also the electrical resistance increases about 100 per cent. However, if the filament is raised to a very high temperature in a good vacuum, the ductibility as well as the original resistance is restored. Pirani observed that in order to achieve this result the temperature must be high enough to sinter the filament and that the gas is not completely eliminated unless the pressure

[122] *Z. Elektrochem.*, **11**, 555 (1905).

is maintained at as low a value as possible (much less than 100 microns). In fact, Pirani concluded that the only method of eliminating the gas completely was to fuse the metal and maintaining it in that condition for a long time in a very good vacuum.

Pirani also observed that a tantalum filament is oxidized to Ta_2O_5 when heated to a high temperature in a stream of hydrogen, even when the gas has been passed over freshly reduced copper turnings (heated in an oven to 500–600° C) in order to remove oxygen and water vapor. Only by passing the gas over heated calcium or molten sodium was it found possible to purify it to such an extent as to prevent surface oxidation of the tantalum filament.

Indeed, tantalum filaments heated to a high temperature may be used to remove residual traces of water vapor and other oxidizing gases from hydrogen. In this respect tantalum may be used instead of chromium powder, which is also an efficient reagent for the purification of hydrogen. (The reason for this characteristic behavior of both tantalum and chromium will be evident from the discussion in Chapter 12 of the equilibria between the oxides and hydrogen.)

The so-called "embrittlement" of copper which results from treatment of the metal in a hydrogen atmosphere is an interesting phenomenon, similar to that observed in the case of tantalum, which has received a great deal of attention from metallurgists. The following summary is based upon the comprehensive discussion of this topic by L. L. Wyman.[123]

Wyman has shown that annealing copper alternately in an oxidizing and reducing atmosphere is specially effective in causing embrittlement. During the oxidizing cycle, oxygen diffuses into the metal and brings about formation of Cu_2O; during the reducing cycle, hydrogen diffuses into the metal and the water vapor formed causes ruptures along grain boundaries.

Wyman's investigation led to the following conclusions:

1. Neither pure copper when oxidized or deoxidized nor rough-pitch copper up to 0.06 per cent oxygen is embrittled by hydrogen at temperatures of 400° C or below, at 4 hours.

2(*a*). The rate of oxygen penetration into "pure" copper decreases markedly below 800° C.

(*b*) The rate of hydrogen penetration into oxygen-bearing copper decreases markedly below 700° C. Consequently, up to about 800° C, the coppers containing no oxygen are superior to tough-pitch coppers for resistance to the embrittling action of oxidation-reduction cycles.

The elimination of oxygen by purifying process or by means of deoxidation of the copper is advantageous in increasing the resistance to the embrittling action of reducing gases.

---

[123] *Trans. A.I.M.E.*, **104**, 141 (1933); **111**, 305 (1934) and **137**, 291 (1940); *General Elec. Rev.*, **37**, 120 (1934).

F. N. Rhines and W. A. Anderson[124] have observed embrittlement not only when Cu_2O is present but also when readily oxidizable alloying elements are present in the copper. The explanation is the same as that suggested by Wyman.

> Hydrogen [they state] diffuses through copper much faster than the water vapor can escape by diffusion and a pressure sufficient to rupture the material is built up. The cracks and holes apparently occur at the grain boundaries, because of inherent weakness there, because of more favorable conditions for nuclear formation there, because the oxide is more plentiful there, or because hydrogen enters more readily at the grain boundaries.

While Rhines and Anderson conclude that hydrogen is the only gas that will produce embrittlement of the type discussed above, other investigators have observed the same phenomenon with illuminating gas. This, however, involves no contradiction with the previous statement, since this gas contains hydrogen as well as methane and both gases react with oxides.

In a review entitled "The Influence of Gas-Metal Diffusion in Fabricating Processes,"[125] Rhines has emphasized the important fact that hydrogen may diffuse into metals as a result of a reaction between the heated metal and water vapor, or as a result of chemical action, as in pickling or electrolysis. This leads to embrittlement in the case of other metals such as iron and its alloys and in nickels.

As has been pointed out in section 5, the densities of the "hydrides" of palladium and of other metals of Group B are all lower than those of the pure metals. That is, the lattice expands as a result of the presence of hydrogen atoms (or rather protons) in interstitial sites. While the solutions of hydrogen in metals of Group A, such as iron and nickel, exhibit considerably less expansion, there is, nevertheless, a slight expansion which is probably effective, as Rhines points out, in producing stresses which ultimately lead to cracking, flaking, and similar phenomena.

> Electroplates [Rhines states], particularly those of iron, nickel, and chromium, if formed under conditions where a considerable quantity of hydrogen is released, are often very brittle and give trouble in buffing. . . .
>
> When ferrous materials are subjected to stress at elevated temperatures, the presence of dissolved hydrogen promotes the development of cracks. Thus hot formed products contaminated with hydrogen are slowly cooled to avoid the development of shatter cracks. Flakes in wrought steel are believed to result from the development of fine cracks in the metal when it is worked without first being freed of hydrogen by sufficiently prolonged heating.

---

[124] *Trans. A. I. M. E.*, **143**, 312 (1941).

[125] *Trans. A.I.M.E.*, **156**, 335 (1944).

> Some other metals are similarly sensitive to hydrogen embrittlement. Electrolytic nickel, as produced, contains a considerable quantity of hydrogen, which is partly retained through subsequent melting and casting operations if special precautions are not taken. When such nickel is rolled or forged, cracks develop. It is found possible to eliminate the major part of the hydrogen in melting by oxidation or by a carbon boil.

In order to recover ductility in samples of ferrous alloys which have been pickled, the usual procedure consists in allowing the samples to stand in the air for some time or baking them at a low temperature in order to let the hydrogen diffuse out.[126]

H. H. Uhlig[127] has observed that low-carbon manganese-iron alloys, treated at 1000° C in hydrogen and quenched, are embrittled by retained hydrogen, whereas the alloys treated in vacuum at 1000° C and quenched in vacuum are ductile, since the hydrogen is eliminated in the vacuum treatment. The important conclusion drawn from his investigation is that *the alloys are brittle only if hydrogen is retained.* Thus, if a treatment in hydrogen at high temperature is followed by a *rapid* quench, the alloy is brittle. If, however, the quench is sufficiently slow to permit the hydrogen to diffuse out as the alloy cools, then the ductility is retained.

In agreement with Wyman, Rhines has emphasized the part played by oxides in the metal. He states:

> Many commercial metals and alloys contain oxygen either in solid solution or in the form of an oxide. When such materials are heated in the presence of hydrogen, carbon monoxide, or similar reducing gases, the hydrogen or carbon may diffuse into the metal and there reduce the oxides or react with the oxygen to form insoluble water vapor or one of the gaseous oxides of carbon. If this occurs when the products of reaction are confined, a considerable pressure may be generated and blisters or cracks will form.
>
> Repeated cycles [he continues] of oxidizing and reducing conditions promote the disintegration of materials that are not particularly sensitive to either conditions alone. Apparently minute cracks which are caused by grain-boundary oxidation and which would grow only slowly under constant oxidation are freed of the obstructing filling of oxide during the reduction phases, and so admit gas more readily on subsequent oxidation.

Such a "water cycle," as it has been designated, also occurs in evacuated devices if precautions are not taken to eliminate water vapor as completely as possible. The phenomenon was first observed by Langmuir in connection with his investigations on the causes of blackening in vacuum tungsten-filament lamps. If these lamps are not exhausted with sufficient care to remove all traces of water vapor or possible sources of evolution of the vapor, the vapor is dissociated at the incandescent filament with formation of oxygen and hydrogen. In contact with the filament at temperatures of about 1500° C and higher, atomic hydrogen is formed, which is an even more effective reducing agent than molecular hydrogen. The cycle which then occurs is as follows: The oxygen forms WO_2 and WO_3 which volatilize and condense on the glass walls. The atomic hydrogen reduces the oxides to tungsten, and the resulting water vapor then goes through the same cycle as before, thus causing a very rapid blackening of the glass bulb. Similar reaction may also occur with other metals. In a hot-cathode device, it results not only in rapid distintegration of the cathode but also in a considerable decrease in electron emissivity, because of the "poisoning" effect of oxygen.

---

[126] See remarks in section 17 in connection with the discussion of the determination of hydrogen in iron alloys.

[127] *Trans. Am. Inst. Mining Met. Engrs.*, **158** (*Iron and Steel*), 183 (1944).

To the vacuum-tube engineer interested in the fabrication of devices having metal containers, or to the designer of vacuum systems made of metal for large-scale operations, the degassing characteristics of the metals used are obviously of primary importance. It is for this reason that the rather lengthy discussion has been given in this and the preceding sections of topics which, at first glance, may appear to be more pertinent to metallurgy than to vacuum technique. Also, for the same reason, it has been considered worth while to add the remarks made in the following section, which deals with a closely allied topic.

16. OBSERVATIONS ON GASES IN CAST METALS

During the refining or melting operations, metals are quite likely to take up large volumes of gas. This is due primarily to the fact, emphasized in section 4, that the solubility of gases, especially that of hydrogen, in metals of Group A increases with the temperature and is greater in the fused metal than in the solid. That the increase in solubility at the melting point is considerable is shown by the data in Table 54, which are taken from the tables in section 4, indicated in the first column. As usual, s = cm^3 (S.T.P.) per 100 g metal.

TABLE 54

INCREASE IN SOLUBILITY (AT 1 ATM) OF HYDROGEN IN METALS AT MELTING POINT

Table 1	Iron	t° C:	1500	1535 (m.p.)	1550	1650
		s:	12.75		27.75	30.97
Table 4	Nickel	t° C:	1400	1452 (m.p.)	1500	1600
		s:	16.52		41.6	43.1
Table 7	Copper	t° C:	1000	1083 (m.p.)	1100	1200
		s:	1.58	2.10 (solid) 6.10 (liquid)	6.3	8.1

For hydrogen in aluminum, s is negligible for the solid but increases rapidly with the temperature above the melting point. For oxygen in silver at 1 atm, s increases from 5.4 at 923° C to 213.5 at 973° C (melting point = 960.5° C).

On solidification the large excess of gas held in solution is liberated and is likely to be trapped in the metal, as it crystallizes, in the form of minute cavities or blow-holes, which result in unsound castings.

As observed in the discussion of the data in Table 33 on the solubility of oxygen in molten silver, N. P. Allen[128] has shown that the trapped gases exert enormous pressures.

In general the gas that most frequently causes defects in the casting of metals such as iron, nickel, copper, or aluminum is hydrogen. This may come from decomposition by the fused metal of water vapor or hydrocarbon vapor present in furnace gases, or from reaction with moisture in the sand molds.

In a melt which contains, in addition to hydrogen, a small amount of dissolved oxygen, the gases recombine on solidification to form steam and this gives rise to what has been designated "reaction unsoundness" or "steam unsoundness." This was first observed by N. P. Allen in his investigation on gases in molten copper. He concluded that, as a result of the reaction between hydrogen and oxygen, "the blow-holes are much smaller, more numerous, and tend to congregate in those parts of the crystal grain last to solidify and in the crystal boundaries."[129]

This type of porosity is observed when the oxygen content exceeds a certain critical value, and according to observations by Allen and A. C. Street[130] this critical oxygen content is apparently connected with the solid solubility of the oxygen in the metal.

It should be observed that, in a paper by Allen and T. Hewitt,[131] it was shown that the behavior of the system consisting of molten copper in equilibrium with hydrogen, oxygen, and steam is "consistent with the ordinary mass-action laws, and that from the data obtained the dissociation pressure of cuprous oxide could be calculated."[132]

A review of the investigations carried out by himself and previous workers on gases in molten and solid copper has been given by O. W. Ellis.[133] Many of the observations reported in this paper, such as those on the solubility in copper of carbon dioxide and water vapor, are, however, not confirmed by other investigators.

---

[128] *J. Inst. Metals*, **49**, 317 (1932).

[129] *J. Inst. Metals*, **43**, 81 (1930).

[130] *J. Inst. Metals*, **51**, 233 (1933). This investigation reports observations on "the effects of hydrogen and oxygen on the unsoundness of copper-nickel alloys."

[131] *J. Inst. Metals*, **51**, 257 (1933).

[132] This is discussed in Chapter 12.

[133] *Trans. Am. Inst., Mining Met. Engrs.*, **106**, 487 (1933).

The results obtained by Allen and his associates, as well as methods for the degassing of metals, have been discussed fully by J. C. Chaston.[134] The different methods which have been proposed for the degassing of metals are summarized by Chaston as follows:

1. Vacuum fusion.[135]
2. Presolidification.[136]
3. Bubbling a stream of nitrogen through the molten metal before casting.[137]
4. Use of oxidizing fluxes.[138]

The relative merits of the first three methods were also discussed in an earlier paper by W. E. Prytherch.[139] In a series of experiments on the effects of oxygen, hydrogen, and sulfur dioxide on the soundness of ingots he observed that the nature of the unsoundness due to dissolved gases "depends on the conditions of temperature, on rate of solidification, and possibly on shape of ingot obtained during casting." Furthermore he concluded that, "Under conditions of the experiments [carried out in this investigation] it has been found that the method of removing gases from copper by oxidation of the metal and its subsequent removal is extremely slow and incomplete."

Molten aluminum can absorb ten times as much hydrogen as corresponds to equilibrium solubility, and according to Claus and his associates[140] this gas is due to a reaction between the metal and water vapor. This dissolved excess gas is likely to be emitted during solidification with intense frothing, and as a remedy it is recommended that the metal should be kept for some time at a temperature just above the melting point in a furnace atmosphere as free as possible from water vapor. They have also used the third method mentioned above, but in the case of aluminum they have obtained good results by using chlorine or mixtures of this gas and nitrogen instead of pure nitrogen.

The second method, as described by Chaston, "consists simply in allowing the melt to cool slowly in a crucible so as to expel most of the dissolved hydrogen and then to remelt the metal as rapidly as possible."

---

[134] *Metal Treatment*, **11**, 212, 213 (1944–1945). Chaston also gives the following references on degassing of metals: D. R. Tullis, *J. Inst. Metals*, **40**, 55 (1928); W. Rosenhain, J. D. Grogan, and T. H. Schofield, *J. Inst. Metals*, **44**, 305 (1930); J. D. Grogan and T. H. Schofield, *J. Inst. Metals*, **49**, 301 (1932); D. Hanson and I. G. Slater, *J. Inst. Metals*, **46**, 187, 216 (1931).

[135] W. J. P. Rohn, *J. Inst. Metals*, **42**, 203 (1929). See also remarks in section 12.

[136] S. L. Archbutt, *J. Inst. Metals*, **33**, 227 (1925).

[137] W. Claus, S. Briesemeister, and E. Kalähne, *Z. Metallkunde*, **21**, 268 (1929).

[138] W. T. Pell-Walpole, *J. Inst. Metals*, **70**, 127 (1944).

[139] *J. Inst. Metals*, **43**, 73 (1930).

[140] See footnote 137.

Undoubtedly the most effective method of degassing metals is fusion in vacuum. Evidence for this statement has been presented in the previous sections of this chapter, and the most recent confirmation is given in a publication by R. S. Morse.[141] The gas content of vacuum-melted copper obtained in the laboratory of the National Research Corporation, as compared with oxygen-free commercial metal, is stated to be as follows:

GAS	VACUUM-MELTED per cent by weight	OXYGEN-FREE COMMERCIAL
Hydrogen	0.00001	0.00012
Oxygen	.00039	.00045
Other gases	.00002	.00040
Sulfur	.00006	.00230

It should be noted that, according to the conversion factors in Table 45, the hydrogen content of the vacuum-melted metal corresponds to 1.12 atm · cm^3 per kilogram, and the oxygen content to 2.73 atm · cm^3 per kilogram.

The application of the methods, discussed above, to the degassing of aluminum has also been discussed by J. L. Erickson.[142]

Of special interest in this connection are the observations reported by H. H. Johnson, L. H. Arner, and H. A. Schwartz[143] on the slow evolution of gases from cast steel at *room temperature.* The gas consists of carbon monoxide, nitrogen, and hydrogen, and the rate of evolution increases both with increase in temperature and with decrease in the partial pressure of the evolved gases in the surrounding atmosphere. Furthermore the rate varies with time in the same manner as that of a first-order reaction, so that after a period of several hundred hours the volume of gas evolved reaches a constant value which is of the order of a few cubic centimeters per 100 g of metal.

Since 1 atm · cm^3 corresponds to approximately 760 micron · liters it is evident that such a rate of gas evolution would make a material practically useless for application in the fabrication of vacuum devices.

One important conclusion that can be drawn from the discussion in this section is that in attempting to use cast metals in vacuum devices extremely great care should be exercised to make certain that the castings are vacuum tight. Though certain palliative procedures may be used for "vacuum-proofing" a porous container, they are obviously not always reliable and care should be taken, if it is necessary to use a casting, to check its soundness by preliminary tests.

---

[141] *Ind. Eng. Chem.*, **30**, 1064 (1947). Furnaces for the vacuum fusion of metals have been described in the following publications: A. U. Seybolt, *Metals Progress*, **50**, 1102 (1946), and A. R. Kaufmann and E. Gordon, *Metals Progress*, **52**, 387 (1947).

[142] *Light Metal Age*, **2**, No. 4, 19 (1944).

[143] *Trans. Am. Soc. Metals*, **37**, 309 (1946).

17. ANALYSIS OF GASES IN METALS[144]

The so-called "low-pressure" method for the determination of gases in metals, glass, etc., was first developed by I. Langmuir.[145] It was further refined by H. M. Ryder,[146] and it has been modified in certain details and utilized extensively by subsequent investigators—C. H. Prescott, Jr.,[147] R. H. Dalton,[148] Norton and Marshall,[149] and others.

In its simplest form, the apparatus used consists of a McLeod gauge for measuring the pressure of the gas (in a known total volume) and a Toepler pump for transferring the gas into other parts of the system in which each of the constituents can be determined by suitable chemical reactions. Mercury cut-offs are used to separate each individual reaction, and solid carbon dioxide and liquid air are used to condense out the different products.

Without entering into a detailed description of the arrangements used by the different investigators mentioned above, the general principles involved may be illustrated by means of the system shown in Fig. 30, which was developed by J. J. Naughton of this laboratory for the determination of gases in metals.

The equipment used consists of two parts: (1) the gas extraction and measurement section, and (2) the gas analysis section.

The *extraction section* (shown at the right in Fig. 30) consists, according to Naughton's description,

> of a quartz tube furnace, F_1, which contains the graphite crucible, C, and suitable shields. The gases are extracted by melting the metal in this furnace.[150] They are quickly swept away by a mercury-diffusion pump and concentrated by a Toepler pump, T, in a known volume, A. The pressure of gas in this known volume, measured with a McLeod gauge, M_1, gives the quantity of gas in the metal sample.

---

[144] An excellent review of methods of "micro-gas analysis" is given in FM, pp. 174–201.

[145] *J. Am. Chem. Soc.*, **34**, 1310 (1912).

[146] *J. Am. Chem. Soc.*, **40**, 1656 (1918).

[147] *J. Am. Chem. Soc.*, **50**, 3237 (1928).

[148] *J. Am. Chem. Soc.*, **57**, 2150 (1935).

[149] *Trans. Am. Inst. Mining Met. Engrs.*, **102**, 287 (1932); **104**, 136 (1933).

[150] The heating is carried out by means of an induction furnace.

The *gas analysis section* is a circulatory system comprising a known volume, *B*, in which the gas being analyzed can be concentrated and measured.[151] A McLeod gauge, M_2, which is part of *B*, is provided for making this measurement. A furnace containing a tube filled with copper oxide, F_2, a freeze-out trap, *Tr*, and a mercury-diffusion pump, *P*, for circulating the gas arc the other essential parts of the system.

For analysis, a portion of the gas extracted from a metal is admitted to the known volume. Its pressure is measured and it is then circulated over frozen acetone to remove water vapor. After removal has been effected the remaining gas is concentrated in the known volume, *B*, and its pressure measured. The difference between the pressure before and after the removal of a component gives the pressure of the component gas in the mixture. Carbon dioxide is removed by passing through the freeze-out trap surrounded by liquid nitrogen. Hydrogen is first oxidized to water vapor by passing through the copper oxide furnace, and the water is removed as before. Similarly, the carbon monoxide is oxidized to carbon dioxide which is

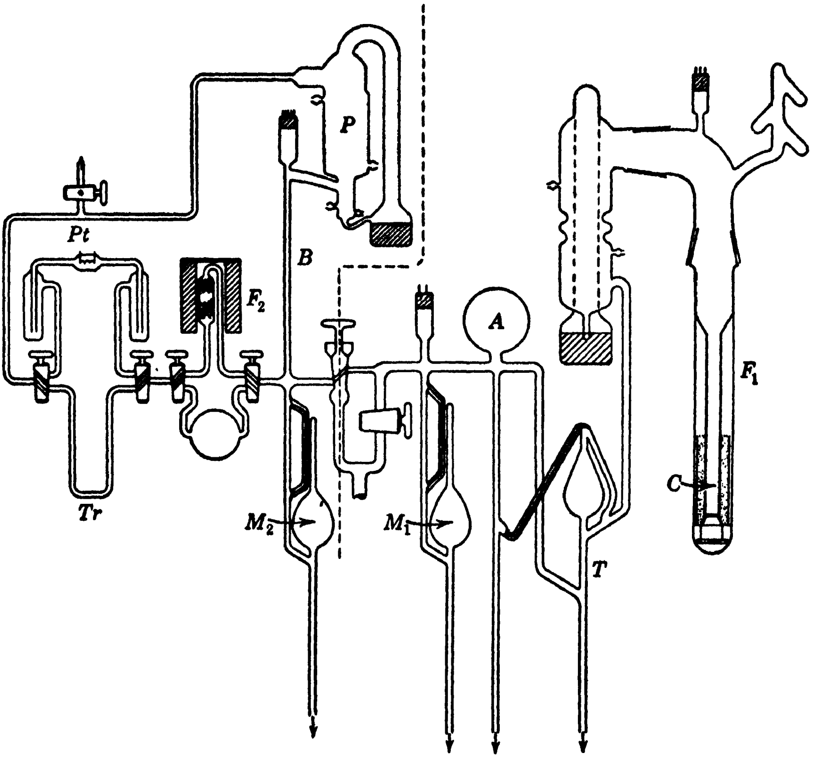

FIG. 30. System for determination of amount and composition of gas evolved from metals (Naughton).

---

[151] In order to increase the accuracy of the determination of this volume, Naughton and Uhlig have used a modified design of mercury-vapor pump which is described in *Ind. Eng. Chem., Anal. Ed.,* **15**, 750 (1943).

> then removed as already noted. These are the gases usually found in the gas extracted from a metal. At times methane is also a component of the gas mixture. This gas is removed by admitting a known amount of pure oxygen and burning the mixture over a hot platinum filament, Pt. Traps are provided before and after this filament to prevent oxidation of mercury vapor and consequent error.
>
> With this gas analysis equipment [Naughton states] it is possible to analyze a sample of gas whose total volume is as small as 0.005 cm^3 (S.T.P.).

One further precaution that has to be taken in connection with the use of the equipment is that good thermal contact is maintained between the metal and the crucible. This is sometimes accomplished by means of a metal flux, such as iron, in which carbon is readily soluble.

In the case of iron-manganese alloys the manganese evaporates at relatively low temperatures[152] and the deposit adsorbs considerable amounts of hydrogen. Hence in a determination of hydrogen in such alloys by the vacuum extraction method, Naughton has used tin as a flux[153] in order to extract the gas at a temperature at which evaporation of manganese is negligible.

The determination of hydrogen in ferrous materials by vacuum extraction at 800° C has been investigated by V. C. F. Holm and J. G. Thompson.[154] They observed that as much as 90 per cent of the hydrogen introduced into iron alloys by cathodic charging or by heating in hydrogen at high temperatures is evolved from the metal during a few days' storage at room temperature. The final values for the hydrogen content are, in general, of the same order as the solubility of the gas at room temperature.

A great many investigators have dealt with the problem of oxygen determination, and the topic has been discussed at length in a paper by J. G. Thompson, H. C. Vacher, and H. A. Bright.[155]

A method for the analysis of gases which was first described by N. R. Campbell[156] and has been applied successfully by many subsequent investigators is designated by Farkas and Melville[157] as "low-temperature distillation."

---

[152] See vapor-pressure data in Table 11.2.

[153] *Trans. Am. Inst. Mining Met. Engrs.*, **162**, 385 (1945). This is one of a number of papers given at a symposium on the determination of hydrogen in steel and published in the same volume of the *Transactions*, pp. 353–412.

[154] *J. Research Natl. Bur. Standards*, **26**, 245 (1941), also J. G. Thompson, *Trans. Am. Inst. Mining Met. Engrs.*, **162**, 369 (1945).

[155] *J. Research Natl. Bur. Standards*, **18**, 259 (1937). This and the previous paper contain further references to the literature on these topics. See also remarks in Section 14.

[156] *Proc. Phys. Soc.*, **33**, 287 (1920–1921).

[157] FM, p. 187.

The principle of the method can be illustrated by the technique, developed in this laboratory by F. J. Norton for the determination of H_2O and CO_2 in the gases evolved in the evacuation of devices containing cellulose materials.

The gas to be analyzed is collected in a known volume, V liters, which includes the volume of the gauge and that of an appendix. Thus, if the pressure is P_μ, the total quantity is $P_\mu V$ micron · liters. On immersing the appendix in liquid air the H_2O and CO_2 are frozen out and the residual pressure $P_{\mu 0}$ corresponds to the amount of non-condensible constituents (N_2, O_2, CO, and H_2). On removing the liquid air and letting the temperature of the appendix rise at a measurable rate (−195° C to 25° C in 20 minutes), the CO_2 begins to evaporate, and, as the temperature increases, the pressure versus temperature plot obtained (shown in curve AA', Fig. 31) corresponds to the vapor-pressure curve of CO_2. (According to the data in Tables 11.14 (*a*) and (*b*) the vapor pressure of solid CO_2 is 0.5μ at −169° C and increases to 10μ at −158° C.) After all the CO_2 has evaporated, the pressure indicated is $P_{\mu 1}$. As the temperature increases beyond that corresponding to this pressure there is only a negligible increase in pressure (as shown by the approximately horizontal portion $A'B$ in Fig. 31) until a temperature is reached at which the vapor pressure of H_2O becomes significant. (As shown in Table 11.13, the vapor pressure is 0.4μ at −80° C and increases to about 100μ at −40° C.) Thus a plot of pressure versus temperature is obtained, such as BB' in Fig. 31.

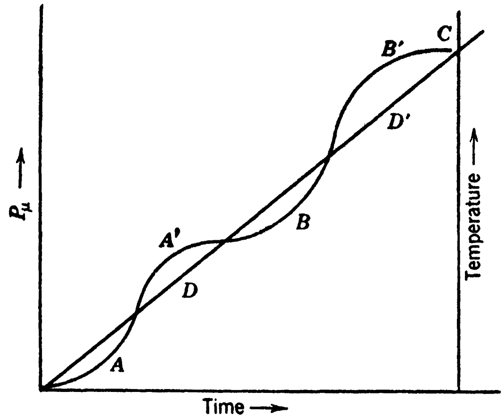

FIG. 31. Illustrating method of "low-temperature distillation" for analysis of gases evolved. *A* thermocouple gauge gives the record (*AA′ BB′ C*) of the vapor pressure and amount of each constituent; the linear plot *DD′* shows the variation in temperature with time. (Norton.)

The approximately horizontal portion, $B'C$, indicates the pressure $P_{\mu 2}$ obtained on complete evaporation of the water vapor. Thus the composition of the gas (by volume) is as follows:

$$\text{Non-condensible gas: } \frac{100\, P_{\mu 0}}{P_{\mu 0} + P_{\mu 1} + P_{\mu 2}} \text{ per cent,}$$

$$\text{Carbon dioxide: } \frac{100\, P_{\mu 1}}{P_{\mu 0} + P_{\mu 1} + P_{\mu 2}} \text{ per cent,}$$

$$\text{Water vapor: } \frac{100\, P_{\mu 2}}{P_{\mu 0} + P_{\mu 1} + P_{\mu 2}} \text{ per cent.}$$

The technique as developed by Norton consists in connecting a photoelectric recorder to a thermocouple which measures the temperature of the appendix and a second recorder to a thermocouple gauge which measures the pressure in the system. This procedure yields two simultaneous records, as shown in Fig. 31, in which $AA'BB'C$ gives a record of pressure versus time, while the linear plot, DD, gives the record of temperatures versus time.

As Norton has pointed out, the same procedure can be used for the analysis of gases that are evolved during exhaust. A trap to which a thermocouple is attached is inserted between the system and the pump, and, during pumping, liquid air is applied to the trap for a definite period. The liquid air is then removed and the trap warmed slowly. The temperature and pressure recorders are started. As the temperature rises to a value at which a particular gas begins to evaporate, a peak will be observed on the pressure recorder, and the position of this peak as well as its height will indicate both the nature of the gas and its relative amount. In this manner a succession of peaks is observed from which the nature of the constituents and their relative amounts may be determined.

Farkas and Melville have described the application of the method to the analysis of a mixture of paraffin hydrocarbons and also refer to the refinement of the method used by J. J. Sebastian and H. C. Howard.[158]

C. Kenty and F. W. Reuter, Jr.,[159] have also used a modification of the same method for the analysis of gases evolved during exhaust. After identification of the condensible gases by their condensation points, a known amount of oxygen is added to the non-condensible residue. The mixture is compressed into a small volume and ignited by a heated platinum filament. The H_2O and CO_2 formed are then determined as described above. Any residual oxygen is determined by noting the decrease in pressure in the presence of a heated tungsten filament, and the residue is then assumed to be nitrogen.

---

[158] *Ind. Eng. Chem., Anal. Ed.*, **6**, 172 (1934).

[159] *Rev. Sci. Instruments*, **18**, 918 (1947).

Non-condensible gas can also be analyzed by comparing the absolute pressure reading, as read by a McLeod gauge, with the indication on a thermocouple (or Pirani) gauge which has been calibrated for the different possible constituent gases and mixtures of these gases. This method is similar to that used by R. G. Dickinson and A. C. G. Mitchell[160] for the analysis of hydrogen-nitrogen mixtures.

Kenty and Reuter have also taken the speed of exhaust through a standard capillary as an additional criterion for the analysis of the evolved gas. This depends upon the fact that speed of exhaust varies inversely as $\sqrt{M}$.

From the vapor-pressure data in Tables 11.15 (*a*) and (*b*) it is evident that the method of fractional distillation can be applied, under certain conditions, to the determination of small traces of oxygen, nitrogen, and hydrogen in krypton and xenon.[161]

---

[160] *Proc. Natl. Acad. Sci.*, **12**, 692 (1926).

[161] This has been used by C. Kenty, *Rev. Sci. Instruments*, **17**, 158 (1946), for the determination of a small amount of impurity in xenon.

Note added during final proofreading: A description of a furnace and procedure for the vacuum-melting and casting of copper has been published by R. A. Stauffer, K. Fox, and W. O. Di Pietro, *Ind. Eng. Chem.*, **40**, 820 (1948).

CHAPTER 10

CHEMICAL AND ELECTRICAL CLEAN-UP OF GASES AT LOW PRESSURES

1. GENERAL REMARKS

During the last decade of the nineteenth century when commercial production of carbon-filament lamps was initiated, it was recognized that the degree of vacuum attainable by means of the pumps available at that time was not sufficiently good for long-life operation of the lamps. In order to improve the vacuum in a sealed-off lamp, Malignani, in 1894, introduced the use of a suspension, in a viscous liquid, of red phosphorus which was painted on the inside of the exhaust tube of the lamp. After the tubulation from the pump was closed off the filament was flashed at a higher voltage than normal and the result was a considerable decrease in pressure of residual gases. Subsequently other chemicals were introduced with the same purpose, and these came to be designated as "getters," that is, clean-up reagents for residual gases.

As will be evident from the discussion in the following sections, the mechanism of clean-up by getters is different from that involved in the use of coconut charcoal, palladium black, and similar adsorbents mentioned in Chapter 8.

In 1907 F. Soddy proposed the volatilization of calcium as a method for reducing the pressure in a sealed-off tube below that obtained by the use of a pump. During the course of his early investigations on the vacuum tungsten-filament lamps Langmuir observed that the pressure of residual gases in a lamp was decreased as a result of chemical reactions between the tungsten and residual gases, that is, evaporated tungsten functioned as a getter.

The greatest impetus to further investigations on getters came as a result of the increasing applications of vacuum technique for the industrial production of hot-cathode, high-vacuum devices. Even though it is possible by means of vapor pumps to obtain pressures sufficiently low for the operation of such electronic devices, the use of getters not only permits a reduction of the time of exhaust but also serves to maintain, in the sealed-off tube, the degree of vacuum necessary for efficient operation and long life. Thus the getters not only "get" the residual gases, but also "keep" them in much the same manner as, for instance, sodium retains the oxygen with which it has combined to form the oxide. In fact, the present-day large-scale production of the vast numbers of electronic devices would be well-nigh impossible if it were not for the aid rendered by getters.

In hot-cathode devices the residual gases may act deleteriously in two ways. First, if the mean free path for an electron is of the same order of magnitude as, or less than, the distance between anode and cathode, gas molecules are ionized by collision with electrons, and, since one positive ion can neutralize the space-charge effect[1] due to hundreds of electrons, it requires only a relatively small concentration of ions to eliminate the control of the space current by means of the anode or grid voltage.

Second, the electron emission from the cathode is decreased, in general, either by formation of adsorbed unimolecular layers of the gas on the surface or by positive-ion bombardment of the emitting surface and consequent removal (by sputtering) of the material that is active in the emission of electrons.[2] For instance, the electron emission from thoriated tungsten is extremely sensitive to traces of residual oxygen. At a pressure of $1 \cdot 10^{-3}$ micron, the rate of incidence of oxygen molecules is $3.6 \cdot 10^{14}$ molecules $\text{cm}^{-2} \cdot \text{sec}^{-1}$. Since the number of molecules required to form a monolayer is $8.7 \cdot 10^{14}$ cm^{-2}, such an adsorbed layer would be obtained in about 2 sec. Hence, in order to obtain a life of several thousand hours the residual pressure of oxygen must be less than about 10^{-9} micron.

The mechanism by means of which the residual pressure is reduced by a getter is often quite complex and not always understood thoroughly. In some cases the action is purely chemical; the getter, such as barium, combines chemically with residual hydrogen, oxygen, nitrogen, and so forth. This reaction may occur as a result of collisions between barium atoms obtained by evaporation of the metal and molecules of the residual gases. Or the gas molecules may combine with the metal deposit by two successive processes: adsorption, followed by diffusion into the inner layers. In this manner the metal can combine with a much greater amount of gas than that required to form a monolayer. Thus the gettering action may be one of two types or a combination of them. These two types have been described by L. F. Ehrke and C. M. Slack[3] as follows:

---

[1] See discussion in section 8.

[2] A detailed discussion of the effects of gases on emission is given by A. L. Reimann, *Thermionic Emission*, John Wiley & Sons, New York, 1934. See also review by S. Dushman, *Rev. Modern Phys.*, **2**, 381 (1930).

1. *Dispersal* gettering in which clean-up takes place while the getter is being dispersed or volatilized in the presence of the gas to be cleaned up.
2. *Contact* gettering, in which a previously vaporized getter acts to clean up any gas which may be introduced into its presence. This term is also applied to the getter action which may continue after volatilization ceases in case of dispersal gettering.

Still another type of clean-up occurs when voltage is applied between the anode and hot cathode. This has been designated *voltage clean-up*,[4] and it is due to interaction between electrons emitted from the cathode and the molecules in the gas. The latter may be dissociated to form atoms that are extremely active chemically. Such dissociation may also be produced, as in the case of hydrogen, by contact of the hydrogen with a tungsten filament operated at temperatures above 2000° K. Furthermore, as a result of collisions between electrons and molecules, excited molecules and positive ions are formed, as mentioned previously. Under the action of the applied voltage the ions are driven with high velocities into the negatively charged walls and electrodes. The retention by the latter of the gas thus cleaned up depends in a very complex manner on the temperature, on the nature of getter deposit and of electrodes, and on the pressure of gas.

PART A. CHEMICAL CLEAN-UP

2. CLEAN-UP OF GASES BY EVAPORATED METALS[5]

The use of calcium for the production of high vacua was first proposed, as mentioned previously, by F. Soddy.[6] He found that in a gas at reasonably low pressure the heating of calcium to a temperature at which it begins to volatilize would cause the pressure to decrease rapidly to a point at which the gas is "non-conducting." For heating the calcium Soddy recommended either a small quartz-tube furnace wound with platinum wire, or an inductive method of heating (analogous to that available from a high-frequency equipment). No data were given by Soddy about the degree of vacuum actually attained or the rate of clean-up. As an indicator of the degree of vacuum, he used a spectrum tube and described his results as follows:

---

[3] *J. Applied Phys.*, **11**, 129 (1940).

[4] This topic is discussed below in section 6 and subsequent sections.

[5] An extremely comprehensive review of the subject entitled "Gettering and Getters" has been published in *Light Metals*, January, 1944, p. 34, and February, p. 77. The first part reviews the scientific investigations; the second part reviews the patent literature, methods of attaching the getters in production of tubes, and chemical methods of obtaining the getters.

Another reference, of which the writer was unable to obtain a copy, is a small book by Martin Littman, entitled *Getterstoffe und ihre Anwendung in der Hochvakuumtechnik*, published by C. F. Winter'sche Verlagsbuchhandlung, Leipzig, 1938. According to a review in *Z. Elektrochem.*, **45**, 431 (1939), the contents deal largely with fabrication problems.

[6] *Proc. Roy. Soc. London*, A, **78**, 429 (1907).

> If the apparatus (consisting of a large vessel in which is contained the quartz-tube furnace), charged with a small piece of calcium, and furnished with a Plücker spectrum tube, is exhausted by a Fleuss pump and the furnace heated, gases consisting of compounds of hydrogen, carbon, and oxygen are given out by the calcium. If the connection with the pump is then shut off and the heating continued, absorption of the remaining gases accompanied by volatilization of the calcium takes place, and the vacuum rises almost instantly to a point at which no discharge can be passed through the spectrum tube. By a non-conducting vacuum is to be understood one of greater resistance than an alternative spark gap in air of 2 to 3 cm.

Soddy observed that CO, CO_2, H_2O, C_2N_2, SO_2, NH_3, and oxides of nitrogen are all readily cleaned up. The absorption of hydrogen is not so great. He states:

> There is no doubt that a low initial pressure, not exceeding a few millimeters of mercury, is as essential a condition in causing calcium to combine with gases as a high temperature. For rapid and continuous absorption, volatilization is essential. The film of volatilized metal continues, even in the cold, to absorb, although more slowly, than the vapor itself.

Argon, helium, and the other rare gases are, of course, not cleaned up by calcium, so that this method has proved useful for the purification of the rare gases. J. H. Clough[7] found that for this purpose the best results are obtained by means of a discharge tube containing a solid calcium anode and robust tungsten filament as cathode. The two electrodes are placed fairly close to each other, and on lighting the filament it is possible to start an arc in the rare gases at very low voltages. Under the action of the arc, the calcium at the anode is gradually volatilized and the chemically active gases are absorbed.

Clough also observed that titanium and magnesium are very effective as clean-up metals when used in the above manner. There is some evidence, according to G. M. J. Mackay,[8] that the reaction here is not altogether a purely chemical one. "Apparently the arc activates the gaseous impurities so that they combine more readily with the chemical agents (calcium, etc.), in the bulb."

In order to obtain some data on the practical value of the calcium reaction in cleaning up residual gases, C. A. Kidner and the writer carried out some experiments with hydrogen. This gas was chosen because it is the most difficult to clean up and also because it is a very frequent constituent of residual gases present in high-vacuum devices.

---

[7] Patent Specification 1,246,054 (1917).

[8] Patent Specification 1,208,597 (1917).

Calcium in the form of wire was laid inside a tungsten spiral, so that it could be heated by passing current through the spiral. By varying the filament current, the rate of volatilization could be controlled and the rate of clean-up measured under different conditions. The pressure was measured by a McLeod gauge, and the volume of the system containing hydrogen was 2500 cm^3. In one experiment, the pressure was decreased from 200 to 3 microns (approximately) in almost 30 minutes. At the end of this period practically all the calcium had been volatilized and it covered the sides of the bulb. It was observed that the rate of clean-up increases with the rate of evaporation of the calcium and is apparently proportional to the pressure of hydrogen.

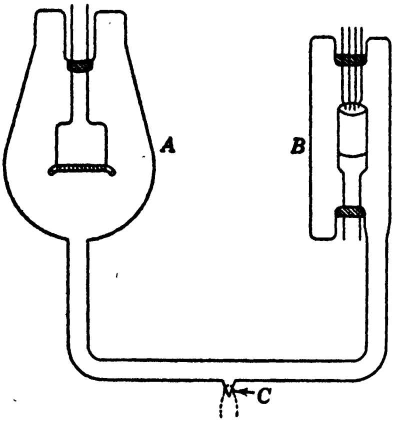

FIG. 1. Arrangement of bulb and gauge for tests on clean-up by getters (Andrews).

Similar experiments were tried with magnesium, but no noticeable clean-up was observed. Soddy found that strontium and barium act like calcium, but as calcium can now be obtained commercially in very pure form it is much more convenient for practical application. Soddy also observed that the presence of CaH_2 in the calcium makes the metal much more difficult to volatilize.

Some experiments, carried out in 1921 at higher pressures (7.5 to 75 microns) by C. A. Kidner and the writer showed that the calcium deposit on the glass does not adsorb either hydrogen or oxygen to any marked extent. Even active hydrogen (formed by heating a tungsten filament to a high temperature in the hydrogen) is only slightly adsorbed by the cold calcium deposit. On the other hand, in some earlier experiments in which an ionization gauge was used, it was observed that with a low initial pressure of hydrogen the calcium deposit cleaned up the gas gradually. Thus, in one case, the pressure in a sealed-off system of about 500-cm^3 capacity decreased from 1.5 to 0.5 micron during the volatilization of the calcium (which occurred in a few minutes), and subsequently the deposit continued to adsorb gas until at the end of 2 hours the pressure had decreased to about 0.0005 micron.

Subsequently, Mrs. M. R. Andrews and J. Bacon, in this laboratory, made a systematic investigation on the behavior of different getters in sealed-off tubes.[9] A 40-watt lamp bulb *A* (see Fig. 1) containing the getter was connected to an ionization gauge (*B*). The anode and leads of the gauge were of molybdenum and the filaments of tungsten, and all metal parts were thoroughly degassed while on the pump. A liquid-air trap was used between pump and getter system, and the getter was volatilized slowly before seal-off. Figure 2 shows results obtained with magnesium flashed by different methods. Plot 1 shows the variation in pressure with time for a bulb without getter, exhausted under the same conditions as the bulbs with getter. The next two lower plots (2 and 3) were obtained with magnesium flashed from a tungsten spiral without previous degassing. Plot 4 represents results for a sample of magnesium degassed by operating the spiral at a red heat for about 15 minutes before the metal was vaporized. The three lowest plots were obtained with magnesium in molybdenum envelopes, which were thoroughly degassed before flashing.

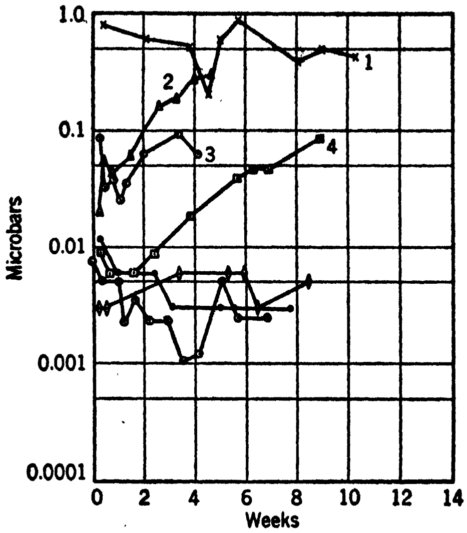

FIG. 2. Clean-up over a long period by magnesium getter in arrangement shown in Fig. 1. Plot 1, blank, without getter; plots 2 and 3, with getter not degassed; plot 4, with degassed getter. Lowest three plots with getter in molybdenum envelope, well degassed before flashing.

---

[9] *J. Franklin Inst.*, **211**, 689 (1931).

The same difference between ordinary metal and degassed metal is illustrated in the plots in Fig. 3, for calcium. The two upper plots were obtained with metal which had been degassed for 15 minutes in the tungsten spiral; the three lower plots were obtained with metal which was vaporized for a period of 2 hours.

The behavior of sodium, illustrated in Fig. 4, is very interesting. The three upper plots were obtained with pellets consisting of NaCl + Ca in a metal case. On flashing these at high temperatures sodium is formed and condenses on the bulb wall. The lowest two plots were obtained with metal formed on the bulb wall by electrolysis of the glass in the usual manner. Evidently the latter procedure produces a much more gas-free metal and the resulting vacuum was much better (0.0001 to 0.001 microbar) than with any of the other getters.

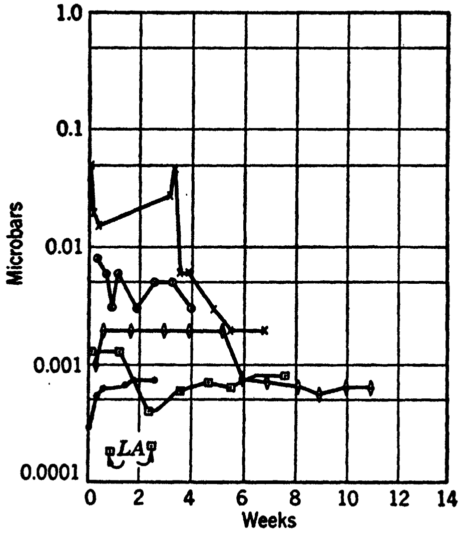

FIG. 3. Clean-up over a long period by calcium getter in arrangement shown in Fig. 1. Two upper plots obtained with metal degassed for 15 minutes before flashing; three lower plots, with metal vaporized for 2 hours.

The order in which getters may be rated as clean-up reagents for most gases corresponds roughly to the chemical activity. Thus cesium is the most active metal, but its relatively high vapor pressure and ready tendency to produce positive ions prevent its general use. Sodium ranks as a clean-up reagent, although, even in that case, the fact that the metal has an appreciable vapor pressure at 200° C is an objection. Of the alkaline-earth metals, barium is the most efficient, but it is difficult to use because it is readily oxidizable. This difficulty has been overcome to some extent by using it in the form of an alloy with aluminum.[10] On the other hand, calcium is not so readily oxidizable and is almost as efficient as barium. Magnesium cleans up oxygen to a pressure sufficiently low for the operation of thoriated filaments but is not as active as the other getters for hydrogen and nitrogen. However, its freedom from oxidation in air and the relative ease with which it can be fastened to the anode have led to its general use (until recently) in the manufacture of radio tubes.

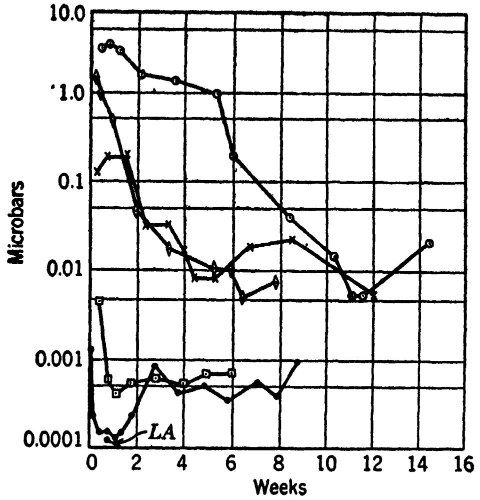

FIG. 4. Clean-up over a long period by sodium getter in arrangement shown in Fig. 1. Three upper plots obtained by means of pellets of NaCl + Ca; two lower plots with sodium produced by electrolysis of the glass. The point *LA* was obtained with bulb at liquid-air temperature.

A. L. Reimann[11] has investigated the clean-up of gases by evaporation of magnesium, calcium, and barium. The apparatus used by him for observing clean-up of hydrogen by magnesium is shown in Fig. 5. It consisted of a bulb *B* containing the magnesium and, connected to this by wide tubing, a Pirani manometer *M*. In *B* were sealed an oxide-coated filament *F*, a nickel mesh anode *A*, and a nickel disk *D*, which was well degassed and to which was welded a piece of very pure magnesium ribbon.

The disk was so arranged that by tilting the apparatus it could be made to take up position 1 or 2. This made it possible to heat the anode by high frequency without at the same time dispersing the magnesium when the disk was in position 2. The Pirani gauge contained two independent stabilized tungsten spiral filaments which were flashed in vacuum before use.[12]

---

[10] See discussion in section 3.

[11] *Phil. Mag.*, **16**, 673 (1933); **18**, 1117 (1934).

A palladium tube, *Pd*, was used to introduce hydrogen into the well-evacuated system.

The most significant conclusions from Reimann's observations on the clean-up of hydrogen by magnesium are as follows:

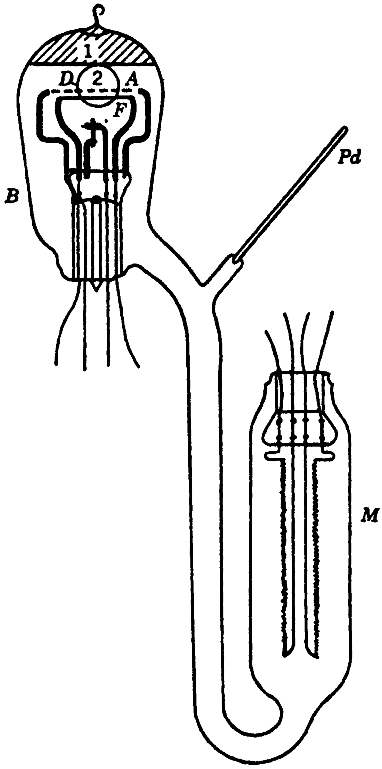

FIG. 5. Apparatus used by Reimann for investigating clean-up of hydrogen by magnesium: *B*, bulb containing magnesium; *M*, Pirani gauge; *F*, oxide-coated filament; *A*, nickel mesh anode; *D*, degassed nickel disk.

1. A clean magnesium surface takes up very large amounts of hydrogen. In one experiment the gettered deposit contained about one-sixth as many atoms of hydrogen as of magnesium.
2. The process of clean-up is one of "contact gettering," and the hydrogen diffuses inwards rapidly.
3. Hydrogen is also cleaned up during the slow evaporation of the magnesium. "The evidence is that this is also contact gettering."
4. Atomic hydrogen and hydrogen ions, produced by passing current between the electrodes in bulb *B*, in a low pressure of the gas, are cleaned up much more rapidly than the molecular form.
5. A considerable portion of the gas thus absorbed is re-evolved when the ionizing discharge is stopped.
6. The hydrogen cleaned up by contact gettering may also be reliberated from the deposit if it is bombarded with electrons or with ionized carbon monoxide.

Using an arrangement similar to that described above, Reimann also carried out a series of experiments on the clean-up of other gases as well as hydrogen, by magnesium, calcium, and barium. One interesting fact brought out in this work and confirmed by other investigators is the difference in efficiency of gettering between ordinary bright barium and "black" barium. The former is obtained by slow evaporation of the metal in good vacuum; the latter, by rapid evaporation in the presence of a relatively high pressure of nitrogen. The black form is much superior in gettering power, probably because it is in a much finer state of division than the barium which forms as a bright deposit. As summarized in the review in *Light Metals,*

---

[12] This and subsequent quotations, unless otherwise indicated, are taken from the review, in *Light Metals*, cited in footnote 5.

> Reimann's general conclusions are:
>
> (1) Both speed and capacity in the contact gettering of a given gas generally increase in the order: magnesium, calcium, bright barium (deposited under good vacuum condition), and black barium (deposited under relatively gassy conditions).
>
> (2) In most cases of contact gettering the getter takes up much more gas than would cover its apparent surface with a monomolecular layer before showing signs of "fatigue." The gas may either combine chemically with the getter or be adsorbed on its surface. Adsorption is usually followed by diffusion into the interior of the getter deposit.
>
> (3) In general, a rise in temperature accelerates the absorption of further gas, probably by promoting diffusion.
>
> (4) A gas which has been absorbed by a getter without forming a chemical compound with it may be reliberated (*a*) by virtue of its "vapor pressure," which increases strongly with both concentration and temperature, (*b*) by being displaced by another gas which combines with the getter, (*c*) by impinging electrons (even quite slow ones), or (*d*) by positive ions.
>
> (5) Electric-discharge gettering may be regarded as the contact gettering of particles which are a direct or indirect product of the discharge, and which differ from the ordinary molecules of the gas. Examples of such particles are positive ions, metastable molecules, and single atoms. In some cases the products of the discharge form with the getter a stable chemical compound, where none would be formed by mere contact gettering of the ordinary molecules.

A very comprehensive investigation has been carried out by L. F. Ehrke and C. M. Slack[13] on the relative gettering efficiencies of a number of metals for different gases, in the absence of any electric discharge. A detailed description is given in the original paper of the methods adopted in each case for obtaining quantitative determinations of the amount of getter evaporated and of the quantity of gas cleaned up.

One very important conclusion confirmed by this investigation is that regarding "the superior gettering powers of the diffuse layers produced by vaporizing the getter in the presence of a gas, as compared to those of the bright getter deposits produced in a high vacuum." In order to obtain such diffuse deposits free of adsorbed gas, the vaporization was carried out in 1–3 mm of argon. "In the case of barium," the investigators state, "such a layer is black and the exposed side resembles a layer of lampblack when viewed by the naked eye. Magnesium and aluminum treated in this way yielded layers of varying shades of gray."

---

[13] *J. Applied Phys.*, **11**, 129 (1940).

From the chemical formula of the compound formed the theoretical efficiency of a getter may be readily calculated thus:

Let MX_n represent the formula where M represents the atomic weight of the metal, and X that of the non-metallic element (the molecular weight of which is assumed to be X_2). Then,

$$M \text{ gram} = \frac{n}{2} \times \frac{22{,}415 \times 298}{273} \quad \text{atm} \cdot \text{cm}^3 \text{ of gas at } 25^\circ \text{ C.}$$

Hence

$$1 \text{ mg} = n \times \frac{9296}{M} \quad \text{micron} \cdot \text{liters at } 25^\circ \text{ C.}$$

Table 1 gives values of the ratio, $\mu \cdot$ liters per mg, for a number of metals used as getters and for the three gases hydrogen, nitrogen, and oxygen.

TABLE 1

VOLUME OF GAS PER UNIT MASS OF METAL FOR FORMATION OF CHEMICAL COMPOUND

			$\mu \cdot$ liters/mg for		
Metal	M	$9296/M$	Oxide	Nitride	Hydride
Magnesium	24.32	382.2	382.2	254.8	764.4
Aluminum	26.97	344.6	516.9	344.6	—
Silicon	28.06	331.3	662.6	—	1325.2
Calcium	40.08	231.9	231.9	154.6	463.8
Titanium	47.90	194.1	388.2	194.1	(388.2)
Strontium	87.63	106.1	106.1	70.8	212.3
Zirconium	91.22	101.9	203.8	101.9	(203.8)
Barium	137.36	67.67	67.7	45.1	135.4
Lanthanum	138.92	66.91	100.4	—	(200.8)
Cerium	140.13	66.36	132.7	66.4	(265.4)
Thorium	232.12	40.05	80.1	40.1	(120.2)
Uranium	238.07	39.04	53.6	—	—

The figures in parentheses are based on the assumption that the hydrides obey stoichiometric relations, which, as discussed in the previous chapter, is not actually true for many of these metals.

A summary of the results observed by Ehrke and Slack is given in Table 2. The theoretical values in the last column are taken from the previous table. The superiority of gettering by diffuse deposits is evident, as is also the fact that barium and misch metal were the most active.

TABLE 2

VOLUME OF GAS CLEANED UP PER UNIT MASS OF METAL (EHRKE AND SLACK)

Getter	Gas	Micron · liters per mg Cleaned up		
		Bright Deposit	Diffuse Deposit	Theoretical Value
Aluminum	O_2 N_2, H_2, CO_2	7.5 None	38.6 None	516.9
Magnesium	O_2 CO_2 N_2, H_2	20 None None at room temperature	202 Slight None at room temperature	382.2
Thorium	O_2 H_2	7.45 19.45	33.15 53.7	80.1 120.2
Uranium	O_2 H_2	10.56 8.9	9.26 21.5	53.6
Misch metal	O_2 H_2 N_2 CO_2	21.2 46.1 3.18 2.2	50.9 63.9 16.1 44.8	100–133 200–265 66
Barium	O_2 H_2 N_2 CO_2	15.2 87.5 9.5 5.21	45 73.0 36.1 59.5	67.7 135.4 45.1

With regard to the nature of each of the getters the following remarks are of interest. Both the *aluminum* and *magnesium* were in the form of wire twisted around the turns of a tungsten coil. Difficulty was experienced in degassing these metals without causing some evaporation. With neither getter was it possible to clean up nitrogen, hydrogen, or carbon dioxide, either at room temperature or by heating the deposit to 200° C or even higher. The clean-up of oxygen by diffuse magnesium appeared to be permanent since no gas evolution occurred even on heating the deposit to 265° C.

No clean-up was observed in the case of hydrogen and nitrogen. However, a deposited layer of magnesium will clean up the gas in the presence of an electrical discharge. This is in accord with Reimann's observations, and the conclusion drawn is that "It is probable that the use of magnesium in radio tubes and similar devices has been successful largely because of the presence of ionization in such devices."

Barium was found to be the best clean-up reagent. It was obtained from two commercial products: Batalum and "KIC" getter, which are described in the following section. "The batalum getter," according to Ehrke and Slack, "was found to exert a very powerful clean-up action when vaporized in the presence of air. On the other hand, when flashed in a high vacuum after careful degassing, its gettering powers were much diminished." For this reason the experiments were carried out by evaporating the getter in the presence of argon, to yield a diffuse deposit. The quantitative determinations mentioned in Table 2 were made with the KIC getter, and they refer to the amounts cleaned up at room temperature. Heating the deposits to 200° C caused additional clean-up, but further heating to 300° C caused evolution of nitrogen and hydrogen which had been taken up at the lower temperature. In the presence of mercury vapor barium is ineffective as a getter.

As is evident from the data in Table 2, *misch metal* was found to have about the same gettering power as barium. The active constituents in this alloy are chiefly cerium and lanthanum. Small slugs of the metal were inserted into tungsten coils and evaporated by passing current through the coil.

The *thorium* and *uranium,* in the form of small pieces of wire, were used in the same manner as the misch metal, and both diffuse and bright deposits were obtained by evaporation. Though these metals proved to be effective getters for hydrogen and oxygen, they are rather inconvenient to use on account of the high temperature required for flashing,[14] and the presence of oxides on the surface.

Ehrke and Slack also carried out some experiments with zirconium, which will be discussed in a subsequent section dealing with the use of this metal as a getter.

From their observations these investigators concluded that the clean-up by the deposits formed as a result of evaporation of the metals is of the "contact gettering" type. This is in accord with the statement that normally the area covered by the deposit was about 75 cm^2. Now to form a monolayer of oxygen or hydrogen about $2.5 \cdot 10^{-2}$ micron · liter · cm^{-2} is required, and, though no indication is given in the paper regarding actual quantity of metal per square centimeter of deposit, it may be assumed that the amounts of gas cleaned up were of the same order of magnitude as that required to form monolayers.

In agreement with the observations mentioned above, J. E. De Graaf and H. C. Hamaker[15] found that the efficiency of a barium getter can be improved considerably by evaporating the metal in 5 mm of argon. They state,

---

[14] This is in accord with the vapor-pressure data for these metals given in Table 11.2.

[15] *Physica,* 9, 297 (1942).

> With nitrogen, carbon monoxide, or carbon dioxide good results can be obtained, but the pressure must be lower (about 0.4 mm) since otherwise too much of the gas is adsorbed during evaporation. . . . A satisfactory black barium layer can also be produced by means of gas evolved from the getter pellet during evaporation; for instance, if we add some barium nitride or carbonate to the barium metal, nitrogen or carbon dioxide will be developed upon heating so that the introduction of special gases into the apparatus can be dispensed with.

Nickel-clad barium was used in this investigation. The gas content varied widely for different samples, but a sample which gave satisfactory results evolved a total volume of 678 mm^3 (S.T.P.) from 80 mg of metal. The percentage composition of the gas evolved was as follows: H_2, 57.5; N_2, 38.3; CO, 3.5; and CO_2, 0.7. Since this amount of gas would react with about 10 per cent of the barium, it has been suggested that the getter should be degassed before evaporation of the metal. However, De Graaf and Hamaker have found that "rapid evaporation without pumping will frequently lead to much better results."

One important factor stressed in this work is the effect of temperature on the clean-up by the barium deposit. They state,

> If the glass bulb is cooled with liquid air during barium evaporation the activity of the deposit increases, whereas by heating to 200° C its capacity is diminished. This decrease is specially pronounced with a glass underlayer which is probably due to a reaction of the barium with some constituents of the glass. An evolution of gas from the glass, followed by adsorption, seems less likely considering that the bulb was previously degassed at 450° C. But even when the barium is condensed on a metal surface, thoroughly outgassed by high-frequency induction, its activity is found to decrease upon heating to 200° C. These observations suggest recrystallization leading to a coarser structure and a reduced adsorption.
>
> On the other hand [they continue], the activity of a deposit will be increased if the tube is constantly kept at a higher temperature.

That is, a deposit heated and cooled to room temperature has a lower activity than one that has not been treated at higher temperature; *but if the adsorption is also carried out at higher temperature, the activity is increased.* The observations lead to the conclusion that the rate of decrease of pressure can be represented at any temperature by a relation of the form

$$-\frac{VdP}{dt} = bA(1-\theta)\epsilon^{-Q/R_0T}, \tag{1}$$

where V = volume; A = area of barium deposit, θ = fraction of surface already covered with adsorbed gas, b = constant, and Q = energy of activation.

For a fresh black barium layer, the values of Q observed varied from 900 cal/mole for nitrogen to 1300 cal/mole for hydrogen. With less active surfaces (produced by heat treatment or evaporation under unfavorable conditions) the values of Q observed were as high as 9000 cal/mole for both hydrogen and nitrogen.

The sorption of nitrogen takes place with formation of Ba_3N_2, as shown by the evolution of ammonia when the deposit is moistened after sorption of the gas. "The sorption," it is stated, "roughly takes place in two stages: a rapid stage by which about 16 mg or 20 per cent of the barium available react, followed by a slow sorption by which an additional 40 mg or 50 per cent of the metal are converted into nitride."

Hydrogen is adsorbed with formation of BaH_2, and "the deposit changes into a transparent layer." Even after all the metal has reacted, hydrogen sorption continues. This has been interpreted as a solution of hydrogen in the hydride.

Of special interest is the following observation by the same investigators. "When a barium layer," they state, "is left in contact with dry O_2, CO, or CO_2 for a considerable time, it still retains its black appearance so that with these gases we have a reaction or adsorption on the surface only and no diffusion through the resulting layer." This result is evidently at variance with that obtained by Ehrke and Slack.

In conclusion De Graaf and Hamaker state that, for optimum getter action by barium, the temperature of the deposit should not exceed 150° C, if the pressure is to remain at less than 10^{-5} mm Hg.

3. TECHNICAL GETTERS[16]

For use in the commercial production of electronic devices, the getter should, in general, be in a form which can be volatilized by high-frequency heating. The criteria for the choice of a satisfactory getter have been described by E. A. Lederer and D. H. Wamsley[17] as follows:

> It is required that the getter material shall be chemically inert during the assembly of the vacuum device. After mechanical exhaustion it should become highly active chemically. The transformation from the inactive to the active state is carried out by the application of heat. The technique is as follows:
>
> (*a*) A change in the chemical modification; example: phosphorus.
>
> (*b*) Evaporation of active metals, protected by oxide films; example: magnesium.
>
> (*c*) Vaporization of active material from an alloy which is inert at room temperature; example: Ba-Al alloy.

---

[16] This section is based to a large extent on the review, mentioned previously, in *Light Metals*, February, 1944, p. 77. This gives a review of the patent literature and data on the composition, sizes, etc., of commercially available getters.

[17] *RCA Rev.*, July, 1937, p. 117.

(*d*) Active material protected by metal case; example: copper-clad barium.

(*e*) Production of active material inside the vacuum device by means of a chemical reaction; example: the cesium dichromate and silicon reaction to form cesium metal.

Also, for mass production of all-metal tubes, the requirements to be fulfilled are stated to be as follows:

1. The getter deposit should consist mainly of barium metal.
2. Complete control with respect to time and quantity of getter flash is essential.
3. Complete control over place of deposition of getter flash is essential.
4. It is preferable to flash getter while metal envelope is cold after completion of degassing and exhaust.
5. Low vapor pressure of getter deposit at highest temperatures encountered during final processing and operation of tubes is essential.

The fact that the efficient getters are all metals which are more or less readily oxidizable on exposure to air has led to the development of alloys of these metals with less oxidizable metals, such as Ba-Al, Mg-Al, and so forth, and also to combinations such as copper-clad or nickel-clad barium cited above. Calcium or barium coated with magnesium has also been proposed.

KIC getter wire[18] is manufactured [according to Ehrke and Slack] by filling an 0.080 in. iron tube with liquid barium in vacuum, drawing down the composite wire thus formed to 0.020 in. or 0.030 in. and then grinding one side flat to a thickness of about 0.003 in. of iron over the barium core. This wire may be heated by the passage of current through it or, if suitably disposed, by high-frequency heating. The getter is degassed by heating to about 750° C and the barium diffuses through the thin side of the wire when the temperature reaches about 850° C.

These investigators also found that a length of 1 cm of getter wire of 0.02-in. diameter mounted on 0.020-in. nickel leads yielded, on the average, 2.35 mg barium under the flashing conditions used.

Batalum getter, developed by Lederer and Wamsley,[19] functions in much the same manner as the silicon-cesium dichromate getter for the production of cesium in photocells. The first form of this getter consisted of a mixture of barium and strontium carbonates, coated or sprayed on a tantalum wire. At 800–1100° C the carbonates dissociate to form the oxides, and at about 1200° C the oxides react with the tantalum to form metallic barium. More recently Lederer[20] has found it advantageous to replace the carbonates by barium berylliate which is obtained by means of the reaction.

$$BaCO_3 + BeO = BaBeO_2 + CO_2.$$

---

[18] Made by the Kemet Laboratories, Cleveland, Ohio.

[19] *Loc. cit.*

[20] *RCA Rev.*, January, 1940, p. 310.

The mixture of carbonate and beryllium oxide is fired in hydrogen at about 1065° C and then refired in air at 1250–1275° C. The proportions normally used are BaO:BeO = 1:2.4. The average yield of barium obtained by flashing the berylliate getter is about 60 per cent, which is higher than the yield of 40 per cent reported in the earlier paper for the carbonate coating.

Lederer and Wamsley state that,

> Calcium, lithium, and magnesium may be formed from their carbonates by the same technique, but they do not compare with barium and strontium for gettering rate and stability of compound formed.

Table 11.2 gives data on the vapor pressures of barium and the other metals mentioned for use as getters.

Other methods which have been utilized for the preparation of pure barium and other alkaline-earth metals involve the use of aluminum,[21] and silicon.[22]

4. CLEAN-UP BY ZIRCONIUM AND TITANIUM

In the previous chapter mention has been made of the observations on the sorption of hydrogen and other gases by zirconium, titanium, and the rare-earth metals.

Hydrogen is taken up very rapidly by metallic zirconium. According to J. H. de Boer and J. D. Fast[23] the sorption begins when the zirconium is heated to about 400° C and is completed at 500° C. As the temperature is increased, the metal gives up hydrogen, but at 850° C the hydrogen is again taken up during the transition from α to β zirconium. With further increase in temperature above 880° C, hydrogen is evolved. The sorption and desorption are reversible with decrease in temperature.

> A significant phenomenon [as the investigators state] is the fact that when the hydrogen pressure has decreased (at a given temperature) to a constant value, and then the heating is suddenly interrupted, the pressure decreases abruptly during the short interval of cooling. During the very rapid passage from the higher temperature to room temperature, therefore, a large amount of hydrogen is quickly taken up. This behavior was only observed for initial temperatures above 1200° K.

It would appear that preliminary heating to a high temperature is a necessary condition for the sorption of hydrogen at lower temperatures.

As shown in Table 9.16, the solubility of hydrogen in zirconium at room temperature is about 1500 volumes (measured at 1 atm) per volume of metal. This solubility decreases only about 10 per cent with increase in temperature to 500° C, and then decreases much more rapidly with further increase in temperature.

---

[21] M. Guntz, *Compt. rend.*, **143**, 339 (1906); P. S. Danner, *J. Am. Chem. Soc.*, **46**, 2382 (1924).

[22] C. Matignon, *Compt. rend.*, **156**, 1378 (1913). Both methods are described fully in the review in *Light Metals* cited in footnote 5.

[23] *Rec. trav. chim.*, **55**, 350 (1936).

The results of an investigation on the sorption of oxygen and nitrogen by zirconium are reported by the same investigators in a second paper.[24] They state,

> Oxygen as well as nitrogen dissolves homogeneously in metallic zirconium. When a zirconium rod, which is covered with a thick white oxide layer, is heated *in vacuo* the metallic luster reappears.

The solubility of the above gases in both zirconium and titanium at high temperatures is considerable. This is of advantage in using these metals as clean-up agents, since the film of oxide formed by exposure to air disappears when the metal is heated, and it is therefore possible for further clean-up of gas to occur in the sealed-off tube containing a filament of zirconium or titanium.

According to J. D. Fast,[25] who has investigated comprehensively the getter action of zirconium, the chemical activity of the elements in the fourth group of the periodic system increases in the order titanium, zirconium, hafnium, thorium. However, thorium does not dissolve nitrogen and oxygen to any appreciable extent, and most attention has been given to the use of zirconium. Fast states,

> The gas pressures with which the saturated solutions of oxygen or nitrogen in zirconium remain in equilibrium are too low for direct measurement. Even at a temperature of 1500° C, the saturation is in any case less than 10^{-8} atmosphere, whilst for oxygen and nitrogen contents far below the saturation limit, the equilibrium pressures are of course much lower still. The result of this is that, when zirconium is heated to a high temperature in a closed space in an atmosphere of oxygen, nitrogen, or mixtures of these gases, the gas is absorbed, with the exception of immeasurably small quantities, provided there is a sufficiently large surplus of metal. A better high vacuum is produced than can be obtained with the best high-vacuum pumps.

For the absorption of hydrogen the most favorable temperature is stated to be 300–400° C, and for the absorption of all other gases (except, of course, those of the rare-gas group) about 1400° C, although the reaction occurs in the range 1000–1600° C.

Ehrke and Slack[26] have reported the following results obtained by use of a zirconium ribbon which could be heated to the desired temperature by passing current through it. Nitrogen was only slightly cleaned up at 1527° C. Clean-up of oxygen set in at about 885° C, and the rate increased with temperature to a high value at 1142° C. On further heating to 1452° C there was a slight evolution of gas. Clean-up of hydrogen set in at 760° C and increased with increase in temperature to as high as 1400° C. These observations are evidently at variance with those reported by Fast.

---

[24] *Rec. trav. chim.*, **55**, 459 (1936).

[25] *Foote Prints*, **10**, No. 2, p. 1 (1927).

[26] *Loc. cit.*

S. Hukagawa and J. Nambo[27] have reported on the sorption of gases by finely divided zirconium powder. The powder was mixed with a binder and sprayed on a molybdenum ribbon, which was then heated to 1100° C in a vacuum furnace in order to produce an adherent coating of the powder. By passing current through a filament of the coated ribbon it was possible to determine by means of a Pirani gauge the amount of gas cleaned up. The optimum temperatures for sorption of different gases were found to be as follows:

Gas:	N_2	O_2	CO	H_2
Optimum temperature (°C):	600	200–800	500	550

It was observed that in order to obtain appreciable sorption it was necessary to degas the filament well by heating it on the exhaust system for several hours at 1100° C.

More recently, W. G. Guldner and L. A. Wooten have reported[27a] results obtained in an investigation on the getter action of zirconium in the form of metal powder as well as that of ductile strip.

The zirconium powder, of which one sample had a specific area of 0.83 square meter per gram, was applied to molybdenum anodes of a standard type by the spray method. Nitrocellulose dissolved in amyl acetate or colloidal silicic acid (for high-voltage tubes) was used as a binder for the powder. In some of the experiments zirconium hydride (containing 1.9 per cent by weight hydrogen) was used.

After the anodes were outgassed at a temperature of 1000° C or higher, zirconium powder reacted with oxygen at 400° C, with nitrogen, carbon monoxide, and carbon dioxide at 500° to 800° C, and with hydrogen at 350° C. The volumes sorbed (in micron · liters per milligram) at the different temperatures were observed to be as follows:

Oxygen	at 400° C	1.99
Nitrogen	at 500° C	1.00
Nitrogen	at 800° C	1.46
Carbon monoxide	at 500° C	0.43
Carbon monoxide	at 800° C	3.65
Carbon dioxide	at 500° C	0.57
Carbon dioxide	at 800° C	3.04
Hydrogen	at 350° C	13.33

---

[27] *Electrotech. J.* (*Japan*), **5**, 27 (1941). See *C.A.*, **35**, 7844 (1941).

[27a] At the Phosphor Symposium of the Electrochemical Society, held at Columbus, Ohio, April 17, 1948. The authors kindly sent a copy of their paper to the writer, from which the passages quoted are taken.

"These are the amounts sorbed before the residual pressure over the zirconium exceeds 1μ." By means of X-ray diffraction patterns it was shown that the oxide, nitride, and carbide are formed in these reactions.

The optimum temperatures for clean-up of the gases were found to be above 400° C for oxygen, 300° C for hydrogen, and above 800° C for the other three gases.

> In the range 200 to 350° C, water vapor is cleaned up at about the same rate as oxygen . . . In agreement with Hall, Martin and Rees, it has been found that the sorption characteristics, both as to rate and capacity, are affected by the purity of the zirconium used.

The advantages of zirconium as a getter are stated to be as follows:

> 1. Relatively large amounts of gas may be sorbed by zirconium at elevated temperature to pressures of less than 10^{-5} mm Hg. X-ray and electron diffraction analysis indicates that the gases can diffuse into the metal, thus leaving a pure metal surface for reaction with additional gas.
> 2. Zirconium powder applied to a molybdenum anode with a silica binder and preheated at 1300° C in vacuum can be operated at a temperature of 800° C in vacuum without evolution of gas.
> 3. With the exception of hydrogen, zirconium forms very stable solid solutions or compounds with the gases studied.

Finally, zirconium possesses an advantage over barium and magnesium getters since mercury vapor does not interfere with its getter action.

5. REACTIONS BETWEEN GASES AT LOW PRESSURES AND INCANDESCENT FILAMENTS

In a series of investigations on the reactions between different gases and heated tungsten filaments, I. Langmuir made a number of observations of great significance in connection with high-vacuum technique.[28]

Clean-up of Oxygen.[29] At temperatures above about 1250° K and at pressures below about 75 microns, the oxide WO_3 distils as fast as formed, leaving the surface clean. The rate of clean-up of oxygen at any given temperature (T) of the filament is found to be proportional to the pressure, that is, proportional to the rate at which oxygen molecules strike the tungsten surface. However, only a fraction, β, of the molecules incident on the surface react with the tungsten.

Let V = volume of the system, in cm^3,
P_μ = pressure at any instant,
A = area of filament, in cm^2,

---

[28] The earlier work on this subject has been reviewed by Langmuir in *J. Am. Chem. Soc.*, **37**, 1139 (1915).

[29] *J. Am. Chem. Soc.*, **35**, 105 (1913).

and we shall assume that the molecules possess a velocity corresponding to 25° C.

Then the rate of clean-up is given by

$$-n_1 V \frac{dP_\mu}{dt} = \nu_1 \beta A P_\mu, \tag{1}$$

where n_1 = number of molecules per cm^3 at 1 micron and 25° C
= $3.240 \cdot 10^{13}$.
ν_1 = number of molecules incident on a surface per sec per cm^2 at 1 micron and 25° C
= $3.60 \cdot 10^{17}$.

Hence equation 1 becomes

$$-\frac{dP_\mu}{dt} = \frac{1.111 \cdot 10^4 \beta A P_\mu}{V}. \tag{2}$$

It follows that the pressure decreases with time t (in seconds) in accordance with the relation

$$\log P_{\mu 0} - \log P_\mu = \frac{1.111 \cdot 10^4 \beta A t}{2.303 V}, \tag{3}$$

where $P_{\mu 0}$ = pressure at $t = 0$.

Hence the interval of time, Δt_0, required to reduce the pressure to 0.1 of its initial value is

$$\Delta t_0 = \frac{2.073 \cdot 10^{-4} V}{\beta A}. \tag{4}$$

The values of β actually observed by Langmuir for a series of temperatures are shown in Table 3.

TABLE 3

VALUES OF THE "ACCOMMODATION" COEFFICIENT FOR THE CLEAN-UP OF OXYGEN BY TUNGSTEN*

T(°K)	β	T(°K)	β
1070	0.00033	2020	0.049
1270	.0011	2290	.095
1470	.0053	2520	.12
1570	.0094	2770	.15
1770	.0255		

* Values given in *J. Am. Chem. Soc.*, **37**, 1139 (1915).

Thus, for $A = 0.1$, $V = 1000$, and $T = 1470$, it follows from equation 4 that $\Delta t_0 = 6.52$ minutes, and at $T = 2290$, $\Delta t_0 = 21.8$ seconds.

For the range $T = 1070$ to $T = 1770$, the values of β can be represented as a function of T by a relation of the form

$$\log \beta = A - \frac{B}{T},$$

where the activation energy, $Q = 2.303R_0B$, is about 26,500 calories per mole oxygen.

Clean-up of Nitrogen by Tungsten.[30] At pressures below about 75 microns and at filament temperatures ranging from 2500° K to 2800° K the rate of clean-up is constant down to pressures as low as 2 or 3 microns. At these temperatures the tungsten evaporates at an appreciable rate. As Langmuir states,

> A comparison of the amount of nitrogen cleaned up with the loss of weight of the filament showed that the ratio was the same as that in a compound of the formula WN_2. This ratio still held if the temperature of the filament was raised several hundred degrees, where the rate of clean-up was over four hundred times more rapid. Measurements showed that the rate of loss in weight of the filament in low-pressure nitrogen was the same as in vacuum, so it was evident that the nitrogen did not attack the filament.

It is evident that in this case $\beta = 1$, and the true reaction velocity is identical with that of the rate of evaporation of tungsten. On the basis of the revised data published by H. A. Jones and I. Langmuir,[31] the rate of evaporation of tungsten, as a function of T, is given by the relation

$$\log G\ (\text{gram} \cdot \text{cm}^{-2} \cdot \text{sec}^{-1}) = 9.28 - 0.5 \log T - \frac{40{,}650}{T}.$$

Since 1 gram tungsten combines with 121.9 cm^3 of nitrogen (S.T.P.) to form WN_2, the rate of clean-up (q) in terms of cm^3 (S.T.P.) per sec per cm^2 of tungsten surface is given by

$$\log q = 11.366 - 0.5 \log T - \frac{40{,}650}{T}.$$

Thus at $T = 2800$, $q = 7.9 \cdot 10^{-4}$ cm^3 per cm^2 per minute = 0.659 micron · liter (25° C) per cm^2 per minute.

At lower pressures the rate of clean-up is no longer constant because the tungsten atoms can travel directly to the walls without colliding with nitrogen molecules. However, *on cooling the bulb containing the filament*

---

[30] *J. Am. Chem. Soc.*, **35**, 931 (1913); **37**, 1139 (1915).

[31] *Gen. Elec. Rev.*, **30**, 310, 354 (1927).

in liquid air, it is found that the tungsten atoms combine with nitrogen molecules adsorbed on the glass, with the result that the rate of clean-up maintains a constant value down to materially lower pressures than observed for the bulb at room temperature.

This observation has been applied by Langmuir,[32] and subsequently by the writer, to improve the vacuum in a sealed-off bulb containing a hot cathode, so that emission data could be obtained from a surface as free as possible of adsorbed gases.

Some experiments carried out in this laboratory by H. Huthsteiner and C. A. Kidner to determine the degree of vacuum attainable by this method yielded the following typical results. Using a hairpin filament about 0.0076 cm in diameter and 7.5 cm long, with nickel leads heavy enough (0.1-cm diameter) not to become excessively heated, it was possible by increasing the temperature of the filament to 2700° K to obtain a clean-up from about 0.02 microbar to 0.0015 microbar, the pressure being measured by an ionization gauge attached to the bulb. An appendix sealed onto the system, consisting of the gauge and bulb, was then immersed in liquid air, and on the filament being heated to 2700° K the pressure was observed to decrease to 0.001 microbar (0.00075 micron).

In another experiment in which the bulb containing the tungsten filament was wholly immersed in liquid air during evaporation of the tungsten, the pressure was decreased from about 0.1 microbar to 0.005 microbar. Taking into account the fact that during these experiments the ionization gauge itself was not immersed in liquid air, there is no doubt that the degree of vacuum attainable in Langmuir's experiments must have been better than 0.0005 microbar and most probably nearer 0.0001 microbar.

Clean-up of Carbon Monoxide by Tungsten. With the bulb at room temperature, according to Langmuir,[33]

> carbon monoxide was observed to behave exactly like nitrogen. In fact, with the filament at a given temperature, the curves obtained first with nitrogen and then with carbon monoxide proved to be identical. This proved that each atom of tungsten combined with one molecule of CO, presumably to form a compound WCO.

With the bulb immersed in liquid air, the observations were similar to those made with nitrogen under the same conditions.

Clean-up of Nitrogen by Molybdenum. In this case the results obtained have been summarized by Langmuir as follows:[34]

---

[32] *Phys. Rev.*, **2**, 450 (1913); *Physik. Z.*, **15**, 516 (1914).

[33] *J. Am. Chem. Soc.*, **37**, 1139 (1915).

[34] *J. Am. Chem. Soc.*, **41**, 167 (1919).

1. At temperatures above 2000° K and in pressures of nitrogen below about 0.03 mm, molybdenum evaporates at the same rate as in vacuum. Molybdenum, like tungsten, is therefore not attacked by nitrogen at any temperature.
2. However, the amount of nitrogen cleaned up is always much less than that required to form MoN_2.
3. The rate of clean-up is independent of the pressure of the nitrogen between 0.75 micron and 30 microns.
4. The rate of clean-up increases considerably if the bulb is cooled in liquid air or solid carbon dioxide, and decreases if the bulb is heated.
5. The rate of clean-up increases with the temperature much more slowly than the rate of evaporation of molybdenum.

If we introduce a coefficient β, defined in the same manner as above, for the clean-up of oxygen by tungsten, then the values of β actually observed ranged from 0.4 to 0.01. One interesting observation is that

with very minute pressures of water vapor such as result even in the presence of drying agents, from failure to bake out the bulb, no clean-up of nitrogen occurs. Under these same conditions, however, molybdenum will clean up carbon monoxide, and tungsten will clean up nitrogen or carbon monoxide. In each of these cases β is unity.

From the fact [Langmuir states] that β is independent of the pressures but varies with the bulb temperature and filament temperature it is necessary to conclude that the reaction takes place in the space around the filament, that each collision between molybdenum atoms and nitrogen molecules results in combination, but that at least two products are formed. These probably are: a first-order compound of the formula NMoN and a second-order compound MoN_2. The proportion of these two depends on the relative velocity of the molecules at the moment of collision and also on the internal energy of the nitrogen molecules. The first compound is very stable and cannot be decomposed on the bulb by heating to 360° C. The second compound, on the other hand, is so unstable that it decomposes practically completely on striking the bulb.

In these experiments [Langmuir states in an earlier paper[35]] the molybdenum deposit which collected on the bulb had very remarkable properties. It adsorbed large quantities of nitrogen, but not hydrogen, if cooled by liquid air. But, at room temperature and above, it could slowly dissolve large quantities of hydrogen which it would slowly give up again at 300° C. Although it contained a large amount of nitrogen, none of this gas could be driven off by heating it at 360°; but if it was heated in nitrogen at 250° C, it apparently combined with the nitrogen, for this gas was absorbed and was not liberated by heating at 360° C in a vacuum.

Dissociation of Hydrogen, Chlorine, and Oxygen. When a wire of tungsten, palladium, or platinum is heated to a temperature above about 1500° K, in *hydrogen* at a low pressure, some of the molecules striking the filament are dissociated into atoms. At temperatures above 2000° K, this dissociation of the gas in contact with the filament causes the absorption of a very large quantity of heat. The atomic hydrogen produced diffuses out and recombines at the walls to form molecules with liberation of heat. This explains the observation that the energy loss from a tungsten wire heated in hydrogen is many times greater than it should be on the assumption that the heat loss is due exclusively to thermal conduction by the gas. According to most recent determinations, the heat of dissociation of molecular hydrogen is 102,700 calories per mole. Thus the energy liberated in recombination of atoms is considerable, and this fact has been applied by Langmuir to the development of atomic hydrogen welding.

---

[35] *J. Am. Chem. Soc.*, **37**, 1139 (1915).

In a series of papers Langmuir[36] has discussed the mechanism of dissociation and calculated the degree of dissociation (α) as a function of the temperature and pressure. Table 4 gives values of this quantity for a series of temperatures and two pressures.

TABLE 4

DEGREE OF DISSOCIATION (α) OF HYDROGEN FOR THE RANGE $T = 1600°$ K to $T = 3000°$ K

T	$P_{mm} = 760$	$P_{mm} = 1$	T	$P_{mm} = 760$	$P_{mm} = 1$
1600	0.00020	0.0055	2400	0.0216	0.447
1800	.00093	.025	2600	.044	.692
2000	.0033	.087	2800	.081	.86
2200	.0092	.224	3000	.13	.94

> This atomic hydrogen [Langmuir states] has remarkable properties. It is readily adsorbed by glass surfaces at room temperatures, although more strongly at liquid-air temperatures; but only a very small amount (a few cubic millimeters) can be so retained because the atoms evidently react together to form molecular hydrogen as soon as they come in contact, even at liquid-air temperatures. The atomic hydrogen reacts instantly at room temperature with oxygen, phosphorus, and many reducible substances such as WO_3, PtO_2, etc.

Thus the clean-up of hydrogen in the presence of an incandescent tungsten filament is due to dissociation of molecules into atoms, which is followed by an adsorption of the atoms on the glass walls.

In some experiments carried on in this laboratory about 1915, G. M. J. Mackay observed that fused P_2O_5 is capable of cleaning up very large amounts of atomic hydrogen, and this accounted for H. Huthsteiner's observation that a trace of P_2O_5 sublimed into a bulb containing a tungsten filament cleans up residual gases, especially hydrogen, to a very low pressure when the filament is heated to a high temperature. It was observed by these investigators that, with the filament at 2300° K, the pressure of hydrogen in a volume of 850 cm^3 could be reduced from 150 to 1 micron in 2 minutes. At 2700° K, the pressure was reduced from 1005 to 4 microns in about 3 minutes. That the clean-up was due to P_2O_5 vapor was shown by the further observation that only a slight decrease in pressure occurred when the bulb was immersed in liquid air.

---

[36] *J. Am. Chem. Soc.*, **37**, 417 (1915), and subsequent papers.

Of special interest in this connection is the reaction with water vapor. It was observed very early in the production of vacuum incandescent tungsten-filament lamps that lamps exhausted at low temperatures (say 100–200° C) blacken rapidly during life.[37] Langmuir has remarked that

a lamp made up with a side tube containing a little water which is kept cooled by a freezing mixture of solid carbon dioxide and acetone ($-78.5°$ C) will blacken very rapidly when running at normal efficiency, although the vapor pressure of water at this temperature is only about $4 \cdot 10^{-4}$ mm.

The explanation [Langmuir states] of the behavior of water vapor seems to be as follows:

The water vapor coming into contact with the filament is decomposed, the oxygen combining with the tungsten and the hydrogen being evolved. The oxide distils to the bulb, where it is subsequently reduced to metallic tungsten by atomic hydrogen given off by the filament, water vapor being simultaneously produced. The action can thus repeat itself indefinitely with a limited quantity of water vapor.

Several experiments indicated that the amount of tungsten that was carried from the filament to the bulb was often many times greater than the chemical equivalent of the hydrogen produced, so the deposit on the bulb could not well be formed by the simple attack of the filament by water vapor.

Another experiment demonstrated that even the yellow oxide, WO_3, could be reduced at room temperature by atomic hydrogen. A filament was heated in a well-exhausted bulb containing a low pressure of oxygen; this gave an invisible deposit of the yellow oxide on the bulb. The remaining oxygen was pumped out and dry hydrogen was admitted. The filament was now lighted to a temperature (2000° K) so low that it could not possibly produce blackening under ordinary conditions. In a short time the bulb became distinctly dark, thus indicating a reduction of the oxide by the active hydrogen. Further treatment in hydrogen failed to produce any further darkening, showing that the oxide could only be reduced superficially.

Even in the absence of water vapor, the "water-vapor cycle" may occur in the presence of a low pressure of hydrogen if traces of oxides are present on the filament leads.

Chlorine molecules in contact with a heated tungsten filament are dissociated into atoms in the same manner as hydrogen molecules. Langmuir has described the following typical observations made with chlorine in the presence of a heated tungsten filament:

By heating a tungsten filament for a short time to 3000° K in a high vacuum a sufficient quantity volatilizes to form a black deposit on the bulb. If, now, a low pressure of chlorine be admitted to the bulb, this does not perceptibly attack the deposit on the bulb nor the filament, even if the bulb is heated to 200° C. However, if the filament is now heated to a high temperature, while the bulb is kept cool, the tungsten deposit on the bulb soon disappears. The chlorine has evidently been activated or dissociated by the filament and the atoms formed travel at these low pressures directly from the filament to the bulb without having any chance to recombine on the way.

---

[37] I. Langmuir, *Trans. A.I.E.E.*, 32, 1893 (1913).

The experiment is more striking if two filaments be placed side by side in the same bulb containing a very low pressure of chlorine. If one of the filaments be heated to a high temperature it is found that the other one, which remains cold, is gradually eaten away on the side facing the hot filament until it finally disappears completely. The hot one does not lose at all in weight, but may even become heavier by having tungsten deposited on it by the decomposition of the chloride formed by the attack of the cold filament.

Langmuir also obtained evidence, in connection with his investigations on thermionic emission, that oxygen molecules incident on a tungsten filament at very high temperatures are dissociated into atoms. Only, since the heat of dissociation of molecular oxygen is higher than that of hydrogen (about 117,000 cal per mole),[38] the degree of dissociation at any given temperature and pressure is considerably less than that of hydrogen under the same conditions. Thus the degree of dissociation of oxygen at 1 atm pressure is 1 per cent between 2500° K and 2600° K, and about 6 per cent at 3000° K.

The observations on the dissociation of chlorine and oxygen at the surface of an incandescent filament account for the operation of the so-called "regenerative" getters[39] used formerly in the commercial production of vacuum lamps. Such getters as tungsten oxychloride and potassium thallium chloride were introduced into the lamp at some point where the temperature would be sufficiently high to obtain a low pressure of chlorine. The atomic chlorine would then combine with the tungsten deposit on the glass walls and thus maintain a clear glass surface for a much longer time than in the absence of these getters.

Other materials, such as barium chlorate, were used to produce, by dissociation of the compound, a low pressure of oxygen, which would then prevent blackening by a mechanism similar to that involved in the case of chlorine compounds.

Reactions between Incandescent Tungsten and Hydrocarbon Vapors. Hydrocarbon vapors are decomposed by tungsten, at temperatures above about 1500° K, into carbon and hydrogen, the carbon being taken up by the tungsten to form carbides.[40]

---

[38] H. L. Johnston and M. K. Walker, *J. Am. Chem. Soc.*, **55**, 187 (1933).

[39] J. W. Howell and H. Schroeder, *History of the Incandescent Lamp*, The Maqua Company, Schenectady, N. Y., 1927, p. 131.

[40] M. R. Andrews and S. Dushman, *J. Franklin Inst.*, **192**, 545 (1921).

Mrs. M. R. Andrews investigated the reaction between the vapor of naphthalene ($C_{10}H_8$) and incandescent tungsten.[41] At 18° C, the vapor pressure of the naphthalene is about 63.5 microns according to Mrs. Andrews' observations, so that the reaction could be studied at relatively low vapor pressures.

Chemical analysis of the filaments carbonized at a temperature of 1600° K or higher and determination of the hydrogen evolved showed that the first stage in the reaction is the formation of the carbide W_2C. The conductance (at room temperature) of the filament decreases linearly with increase in carbon content until the whole filament is converted into W_2C (3.16 per cent carbon by weight). The conductance of W_2C is about 7 per cent of that of pure tungsten. By further treatment in hydrocarbon vapor, the carbon content continues to increase and the conductivity increases linearly with carbon content until the composition corresponding to WC is attained (6.12 per cent carbon). The conductance of the WC is 40 per cent of that of pure tungsten.

Other hydrocarbons, such as benzene, toluene, acetylene, methane, and illuminating gas, react with incandescent tungsten in the same manner. The reaction is of importance in the production of electronic devices using thoriated-tungsten-filament cathodes (0.5 to 1.5 per cent ThO_2 in the tungsten). As a result of a preliminary flashing in hydrocarbon vapors it is possible to activate the filaments more readily and obtain longer life.

The thermal dissociation (at low pressures) of methane by a platinum filament covered with alkaline-earth oxides has been investigated by G. M. Schwab and E. Pietsch.[42] The reaction was found to be of the first order with respect to pressure of methane, and a calculation of the ratio β of the rate at which the methane molecules are dissociated compared with the rate of incidence on the filament showed that β increases exponentially with the temperature in accordance with the equation (similar to that deduced for the reaction between oxygen and tungsten)

$$\log \beta = 4.55 - \frac{12{,}000}{T}.$$

This result leads to a value $Q = 54{,}900$ cal/mole for the activation energy of the dissociation. Values of β actually observed varied from $1.05 \cdot 10^{-4}$ for $T = 1373$ to $14.3 \cdot 10^{-4}$ for $T = 1551$. As will be observed, these values are very much lower than those obtained by Langmuir for the clean-up of oxygen by tungsten (see Table 3).

[41] *J. Phys. Chem.*, **27**, 270 (1923).

[42] *Z. Elektrochem.*, **32**, 430 (1926).

By surrounding the filament with a wire mesh cylinder and making the cylinder positive with respect to the filament as an electron emitter (see the section on clean-up in hot-cathode devices), it was possible to determine the effect on the dissociation of collisions between electrons and the molecules of methane. An increase in rate of dissociation was observed for electron energies in excess of 15 to 16 volts, which probably corresponds to the ionizing potential of methane. This result was interpreted by the investigators as indicating a dissociation into free hydrogen atoms in accordance with the equation

$$CH_4 \rightarrow C + 4H.$$

Reaction between Carbon and Oxygen. Experiments carried out by Langmuir[43] showed that, as compared with the oxidation of tungsten,

> the phenomena involved in the oxidation of carbon are very complex. These experiments [he states] seem to show that, when oxygen acts on carbon at, say, 1200° K, part of the oxygen reacts to form carbon dioxide, but another part forms an adsorption layer of some sort on the surface which retards the velocity of the reaction. . . . At higher temperatures the rate of formation of this adsorption layer increases rapidly. When a sufficient quantity has accumulated this compound begins to decompose, forming carbon monoxide, the higher the temperature the more rapid being the formation of this gas.

This adsorbed layer can be heated for half an hour at 2200° K, in the highest vacuum, without being completely decomposed. With carbon dioxide no reaction could be observed at 1220° K, but at 1700° K and higher carbon monoxide was formed, and, since the total volume remained constant, Langmuir concluded that the reaction is

$$CO_2 + C = CO \text{ (gas)} + CO \text{ (adsorbed on carbon)}.$$

On the other hand, this adsorbed compound was not formed on heating a carbon filament in carbon monoxide to even as high as 2400° K.

Because of the scientific interest in this problem and also because of its application in industry, the kinetics of the reactions between oxygen and carbon at high temperatures has been much studied by a number of investigators, notably by L. Meyer[44] and V. Sihvonen,[45] both of whom used the carbon-filament technique. In view of the more recent observations made, by means of the same technique, by R. F. Strickland-Constable[46] there is a question with regard to the interpretation of the results obtained by Meyer. Strickland-Constable has suggested that these results could be explained by the presence of a glow discharge, which would occur because of electron emission from the negative end of the filament and an appreciable positive potential at the other end.

---

[43] *J. Am. Chem. Soc.*, **37**, 1139 (1915).

[44] *Trans. Faraday Soc.*, **34**, 1056 (1938).

[45] *Trans. Faraday Soc.*, **34**, 1062 (1938).

[46] *Trans. Faraday Soc.*, **40**, 333 (1944).

On the whole the observations made by Strickland-Constable are in agreement with those obtained by Langmuir and Sihvonen. In the temperature range 900–2000° C, carbon monoxide is the primary product, and over the range of pressures from 0.02 to 0.5 mm the reaction is of the first order. Strickland-Constable states,

> The rate of reaction rises from 900° C to 1100° C and is constant between 1600° C and 2000° C. Between these two ranges there is a zone in which the rate is very sensitive to the immediate past history of the filament. If the preceding experiments were at higher temperatures, the reaction rate is abnormally high, and if at a lower temperature, the rate is abnormally low. . . . [Also] evidence was obtained which was not in agreement with the view that oxygen is sorbed in appreciable quantities by a freshly outgassed filament at high temperatures.

Reaction of Gases with Incandescent Tantalum. Observations on these reactions have been reported by Mrs. M. R. Andrews.[47] Before investigating the rate and extent of clean-up of different gases, "the tantalum filament was given a preliminary degassing in vacuum at 2400–2500° K, until the cold resistance had decreased to a constant value and no more gas was evolved."

It was shown that *nitrogen*, at least in low concentrations, enters the tantalum in the form of a solution. At any given temperature, there is a definite relation, which can be attained either by sorption or desorption, between concentration of gas in metal (c) and gas pressure (P) of the form

$$c = k\sqrt{P},$$

which is similar to that mentioned in Chapter 9 for the solubility of hydrogen in tantalum and other metals.

Up to concentrations of about 100 volumes of nitrogen (S.T.P.) per volume of metal, the variation in equilibrium pressure with temperature, for constant amount of gas sorbed, is shown by the two plots in Fig. 6. As will be observed, the equilibrium pressure for constant amount dissolved decreases with decrease in temperature; and from the plots, the heat of solution is found to be 102,000 cal/mole of nitrogen.

Assuming, as shown on the plots, that for $T = 2000$ and an equilibrium pressure of 2 microns the volume of gas sorbed per volume of metal is 80, it is of interest to calculate the equilibrium conditions for a 10-mil-diameter filament 10 cm long and $T = 2000$. Since the volume of metal is $5.07 \cdot 10^{-3}$ cm^3, and 1 cm^3 gas (S.T.P.) = 829 micron · liters at 25° C, an absorption of 1 volume gas per 1 volume of metal would correspond to 4.2 micron · liters, and the corresponding equilibrium pressure would be given by the relation

---

[47] *J. Am. Chem. Soc.*, **54**, 1845 (1932).

$$P_\mu = \frac{(4.2)^2 \times 2}{6400} = 5.5 \cdot 10^{-3}.$$

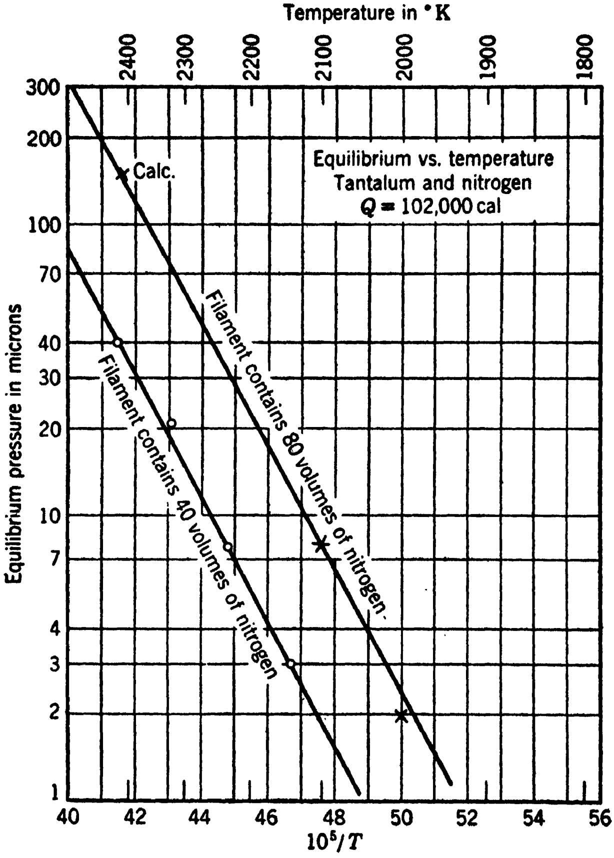

FIG. 6. Log of equilibrium pressure of nitrogen versus $1/T$ for tantalum, for two concentrations of nitrogen (Andrews).

This example illustrates the application which can be made of such data as those shown in Fig. 6 in order to calculate the amount of clean-up that may be obtained under given experimental conditions.

At higher concentrations of nitrogen evidence was obtained for the conclusion that absorption can take place (accompanied by decrease in pressure) leading to the formation of TaN. This would require about 1000 volumes of nitrogen per volume of metal.

According to Mrs. Andrews' observations,

> *Oxygen* is absorbed by tantalum in a somewhat different manner than nitrogen. Whereas nitrogen is taken up very slowly below 1600° K, oxygen is absorbed quite readily at 1000° K, and with extreme rapidity at 1800° K. Absorption is quite complete up to 20 volumes, the residual pressures being negligible. Further absorption at 1800° K (which takes place with great rapidity) leads to the formation of a compound. This is shown by the plots for the variation in resistance with gas content shown in Fig. 7. The cold resistance increases rapidly with concentration up to 20 volumes and then much more slowly.

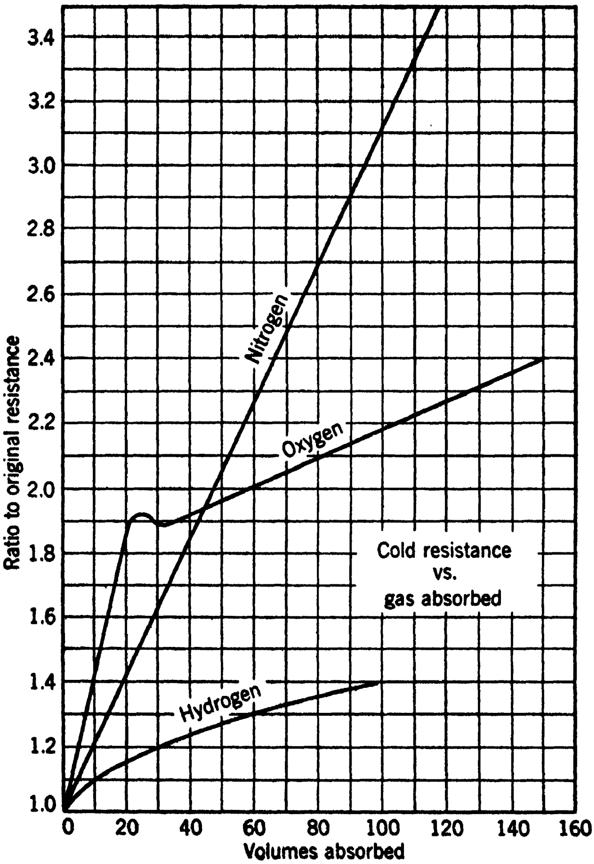

FIG. 7. Variation in resistance of tantalum with gas content. Curves plotted for nitrogen, oxygen, and hydrogen. Resistance given as ratio to the resistance of the gas-free filament. (Andrews.)

Here, again, there is evidence of the formation of an oxide, presumably Ta_2O_5, which would correspond to about 2500 volumes of oxygen per volume of metal.

The dissolved oxygen, that is, the first 20 volumes absorbed, can be re-evolved if the filament is operated in vacuum at 2200-2300° K.

It was shown in Table 9.16 that, at room temperature and atmospheric pressure, 1 volume of tantalum can dissolve about 765 volumes *hydrogen*, and that this solubility becomes about 50 times less at temperatures above 1000° C. Furthermore, it was shown in the same connection that the hydrogen is dissolved in the atomic form, since the solubility at constant temperature varies with the square root of the pressure.

Further confirmation of this conclusion was obtained by Mrs. Andrews in a series of observations which are described as follows:

> At the pressures used, 50 microns or less, no hydrogen was absorbed when the tantalum was heated in the gas; but if an auxiliary filament of tungsten was run in the same bulb at a high temperature so as to dissociate some of the hydrogen and the tantalum filament was run at the same time at 800° K to 1200° K, hydrogen was absorbed by the tantalum. Solubility was greater at the lower temperatures. At any given temperature absorption would take place until an equilibrium was established. Addition of more hydrogen caused increased absorption. The action was exactly similar to the absorption of nitrogen except that equilibrium was established between the dissolved hydrogen and the external pressure of *atomic* hydrogen. That is, if equilibrium was established with the tungsten filament running at a constant temperature, say 2400° K, and the tantalum also constant, at say 1000° K, and the temperature of the tungsten filament was then increased, to, say, 2600° K, thus increasing the fraction of the hydrogen dissociated, the tantalum absorbed hydrogen further until a new equilibrium was established. If the tungsten filament was lowered in temperature, the tantalum would immediately evolve gas to establish again an equilibrium, or if the current was taken off the tungsten filament, the tantalum one being left at 1000° K, gas would be evolved from the tantalum until practically all that had been absorbed had reappeared.
>
> The hydrogen curve in Fig. 7 shows that the resistance at room temperature rises less rapidly with hydrogen concentration than for either oxygen or nitrogen. It can be assumed that this is due to the small atomic volume of the hydrogen, so that a given number of molecules dissolved in the metal would strain the lattice less than larger atoms. There was no evidence of any compound up to the maximum concentrations of hydrogen reached.

Another interesting observation made in this investigation was that the rate of absorption was much less for a fresh filament than for one that had been subjected to sorption followed by desorption. Similar observations have been made in this laboratory by H. Huthsteiner in the sorption of hydrogen by tantalum and also by zirconium.

Above 1400° K, water vapor is decomposed by tantalum, with absorption of the oxygen and evolution of the hydrogen.

The reaction between tantalum and hydrocarbons such as benzene and naphthalene has also been investigated by Mrs. Andrews. The results obtained are quite similar to those obtained with tungsten and hydrocarbon vapors. A tantalum filament heated in a low pressure of the hydrocarbon vapor between 2000° K and 2800° K forms two carbides. The first one has the composition Ta_6C_5 and has an electrical resistivity at room temperature about 12 times that of pure tantalum. Further treatment in hydrocarbon vapor leads to the formation of the carbide TaC, which has a resistivity at room temperature about 1.2 times that of the metal. Both carbides have very high melting points (4000–4100° K) and are extremely brittle.

PART B. ELECTRICAL CLEAN-UP OF GASES

6. PHENOMENA IN COLD-CATHODE DISCHARGE TUBES

The gradual disappearance of gas in a low-pressure gaseous discharge tube was first observed by J. Plücker in 1858. As the pressure decreases, the voltage required to pass current through the tube increases, and finally the tube becomes "non-conducting"—at least with the voltage available. In the gas-filled Roentgen tube this phenomenon was known as "hardening," since the X-rays emitted increase in hardness, or penetrating power, with increase in the voltage required to operate the tube.

A large number of investigators have dealt with this phenomenon and a great variety of explanations has been offered.[48] The observations made by these investigators and the different interpretations given form the subject of the following sections.

However, before we can discuss all this work, it is necessary to consider briefly the mechanism of electrical conduction in gas discharge such as that which occurs in a Geissler tube. The carriers of electric charges consist of both electrons and positive ions. Because of their greater mobility and smaller mass, the electrons contribute by far the larger fraction of the current. Of special interest is the characteristic manner in which the voltage is distributed along a long tube in which a positive column discharge occurs. Figure 8, based on observations made by C. G. Found and J. D. Forney,[49] shows the potential distribution in a discharge in nitrogen at 0.5 mm pressure. The tube diameter was 6 cm, and the current, 5 ma. The distribution of light intensity along the tube is shown at the bottom. While that region in the discharge, known as the positive column, produces most of the light, a considerable fraction of the overall voltage is consumed in the narrow region adjacent to the cathode which is designated the "cathode dark space." This *cathode drop* varies from about 50 to 400 volts and higher, depending on the nature of both the electrode and gas, the pressure, area of cathode, and current. There is a slight gradient in the Faraday dark space, but under certain conditions this may become zero or even negative. Throughout the positive column there is a practically constant positive voltage gradient. The voltage drop at the anode may be positive, zero, or negative, depending upon the current density and other factors.

---

[48] A very comprehensive report of the earlier work on this topic has been given by E. Pietsch, *Ergeb. der exakt. Naturw.*, **5**, 213 (1926).

[49] *A.I.E.E. Trans.*, **47**, 855 (1928).

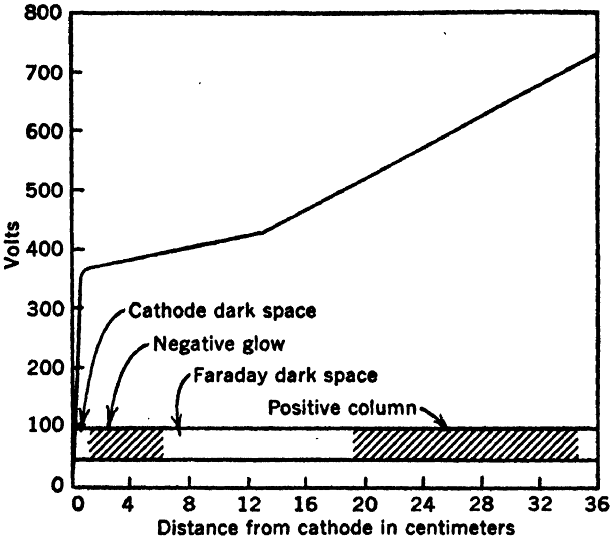

FIG. 8. Distribution of potential in positive column discharge in nitrogen (Found and Forney).

However, it is always very small compared to the cathode drop.

In the cathode fall region the ions are accelerated in accordance with the relation

$$\tfrac{1}{2}m_p v_p^2 = Ve, \tag{1a}$$

that is,

$$v_p = 1.390 \cdot 10^6 \sqrt{\frac{V}{M}} \quad \text{cm} \cdot \text{sec}^{-1}, \tag{1b}$$

where m_p and v_p denote the mass and velocity, respectively, of the positive ion, e denotes the charge on an electron or singly charged positive ion, V denotes the voltage drop, and M denotes the molecular weight of the gas in which the positive ions are produced.

Thus, for H_2^+, $v_p = 9.790 \cdot 10^5\sqrt{V}$ cm · sec⁻¹, and for N_2^+, $v_p = 2.626 \cdot 10^5\sqrt{V}$ cm · sec⁻¹. Comparing equation 1*b* with the relation deduced in Chapter 1 for the root-mean-square velocity,

$$v_r = 15{,}794\sqrt{\frac{T}{M}} \quad \text{cm} \cdot \text{sec}^{-1},$$

it follows that for any ion, independently of the value of M, the equivalent absolute temperature is given by the relation

$$T = 7.734 \cdot 10^3 V. \tag{2}$$

That is, the energy of the positive ion corresponds to that of the normal molecule at a very high temperature. This fact is of fundamental importance in most of the explanations which have been given of electrical clean-up phenomena.

The ions are produced as a result of collisions between electrons emitted from the cathode and gas molecules. For every gas there is a minimum value of the energy of the electrons at which such ionization occurs, and this is designated the *ionization potential* (V_i). (See discussion in Chapter 6, section 7.) The values of V_i vary from 3.87 volts for cesium vapor to 24.48 for helium. The velocity, v_e, acquired by an electron accelerated through a potential drop of V volts is given by the equation, similar to 1*a* and 1*b*,

$$\tfrac{1}{2}m_0 v_e^2 = Ve, \tag{3a}$$

where m_0 denotes the mass of the electron. That is,

$$v_e = 5.9314 \cdot 10^7 \sqrt{V} \quad \text{cm} \cdot \text{sec}^{-1}. \tag{3b}$$

At voltages below V_i, electrons colliding with the gas molecules are able to excite them, if they have the proper energy, to higher energy states (or levels), and it is by spontaneous transitions from these levels to lower levels (including the normal state of the atom or molecule) that spectral lines are emitted.[50]

Figure 9 shows such an energy-level diagram for *mercury*. When electrons emitted from the cathode collide with mercury atoms, no interchange of energy occurs until the electrons have been accelerated through a potential of 4.9 volts. At this energy two excited states are produced,

---

[50] A discussion of the Bohr theory of the origin of spectral lines is given in a large number of treatises, for instance, H. Semat, *Introduction to Atomic Physics*, Rinehart and Co., New York, 1946, and S. Dushman, Chapter II, *Treatise on Physical Chemistry*, Vol. I, edited by H. S. Taylor and S. Glasstone, D. Van Nostrand Company, New York, 1942.

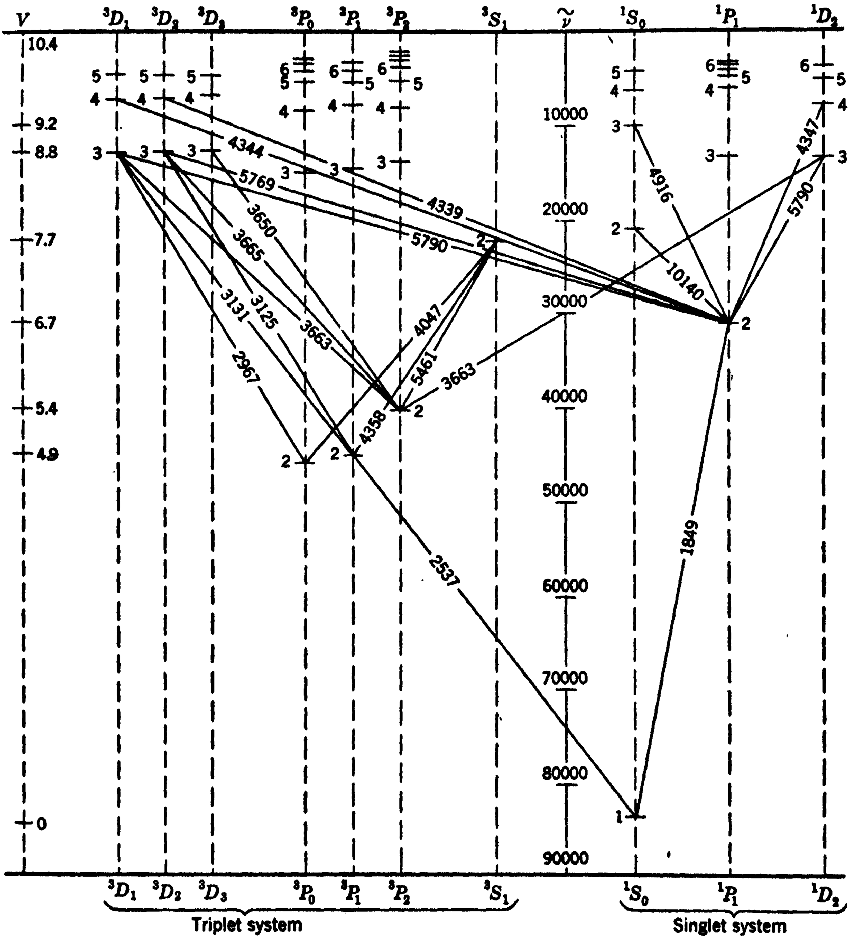

FIG. 9. Energy levels and lines in arc spectrum of mercury. Levels are designated by wave numbers, $\tilde{\nu}$, or electron-volts, V, required for their excitation.

designated 2^3P_0 and 2^3P_1, of which the first one is metastable since no spontaneous transitions can occur to the lowest ($^1S_0$) or normal state. On the other hand, a transition from the 2^3P_1 to the normal state is accompanied by emission of the ultraviolet line λ2537. As the accelerating voltage on the electrons is increased beyond 4.9 volts, excited states of higher energy content are produced, thus giving rise to the different spectral lines (indicated in the diagrams by lines between the energy levels). At 10.4 volts one of the electrons in the outer "shell" of the atom is completely removed, leaving a mercury ion (Hg^+).

The frequency of the line emitted as a result of any one transition is given by the relation,

$$h\nu = \Delta V \cdot e, \tag{4a}$$

that is,

$$\nu = 10^8\, c\lambda^{-1} = 2.4185 \cdot 10^{14}\, \Delta V \text{ sec}^{-1} = c\Delta\tilde{\nu} \tag{4b}$$

where $h = 6.624 \cdot 10^{-27}$ erg sec, c = velocity of light (cm/sec), ΔV is the difference in the voltages required to excite the higher- and lower-energy levels between which the transition occurs that gives rise to the spectral line (wavelength = λ in angstroms), and $\Delta\tilde{\nu}$ is the difference in wavenumbers ($\tilde{\nu}$) of the levels.

As mentioned above, the positive ions, when accelerated towards a negatively charged electrode or other surface, acquire considerable energy. It would therefore be only natural to assume that such high-speed particles might be driven into the surface of the cathode or glass walls (if the walls are negatively charged, as they usually are). This might therefore be one plausible explanation of the disappearance of gas in a discharge.

Furthermore, because of the high energy acquired in passing through the cathode fall, the positive ions actually cause a disintegration of the cathode. The "sputtered" deposit on the walls is undoubtedly capable of sorbing large quantities of gas. This therefore may be assumed to be another possible mechanism by which clean-up is effected.

But in addition a number of other mechanisms have been suggested. S. Brodetsky and B. Hodgson[51] have given the following list of the explanations that have been proposed:

1. Chemical action between the gas and the glass.[52]
2. Chemical action between the gas and the cathode.[53]
3. Chemical or mechanical action between the gas and the anode.[54,55,56]
4. Chemical action due to active nitrogen.[57]

---

[51] *Phil. Mag.*, **31**, 478 (1916).

[52] R. S. Willows, *Phil. Mag.*, **1**, 503 (1901).

[53] K. Mey, *Ann. Physik*, **11**, 127 (1903).

[54] C. A. Skinner, *Phil. Mag.*, **12**, 481 (1906).

[55] B. Hodgson, *Physik. Z.*, **13**, 595 (1912).

[56] V. L. Chrisler, *Physik. Z.*, **10**, 745 (1909); *Phys. Rev.*, **29**, 461 (1909).

[57] S. E. Hill, *Proc. Phys. Soc. London*, **25**, 35 (1912–1913).

5. Mechanical occlusion of the gas in the glass.[58]

6. Mechanical occlusion of the gas in the cathode.[59]

7. Mechanical occlusion of the gas in the disintegrated part of the cathode.[60]

In view of the relation between T and V expressed in equation (2), it would appear likely that ions may react chemically with other atoms with which they collide.

According to Langmuir[61] both the chemical and mechanical types of mechanisms are responsible for the clean-up of nitrogen in the presence of a hot tungsten cathode when an electric discharge passes. At higher pressures, the reaction is "electrochemical," the nitrogen combining with the tungsten to form the nitride WN_2. At very low pressures and high anode voltages, the action is apparently purely mechanical (Langmuir designates this the "electrical" clean-up). The nitrogen is driven into the glass in such a form that it can be recovered by heating. The action is thus apparently reversible, and only limited quantities of nitrogen can be cleaned up in this manner. The electrical clean-up, as distinguished from the electrochemical, also exhibits distinct fatigue effects.

It is quite probable that both these two types of clean-up occur simultaneously in practically all the cases where gases disappear during an electrical discharge, and we shall find that this point of view enables us to interpret to a large extent the many apparently contradictory results obtained by the different investigators.

Willows[62] observed that the amount of clean-up of gas in a discharge tube varied according to the nature of the glass from which the tube was made. The absorption was least in Jena glass, more in lead glass, and greatest in soda glass. At constant current, the amount of gas occluded was found to increase with decrease in pressure. The conclusion arrived at was that the clean-up is due to chemical reactions between the gases and the glass walls. In support of this view, Hill[63] has shown that absorption is observed with air in an electrodeless discharge. His experiments were carried out in the range of pressures varying from 0.4 mm to 0.04 mm of mercury. During these experiments the bulbs became covered with a dark deposit on the walls, presumably due to oxidation reactions. On exhausting these bulbs and filling them with hydrogen at about 1 mm pressure, the discharge caused a rapid disappearance of the gas and the deposit became lighter colored, which Hill accounted for by chemical reduction. Willows repeated Hill's experiments[64] with quartz vacuum tubes and observed that "a new quartz bulb does not absorb air, but if fed with repeated doses of hydrogen—which are absorbed when an electrodeless discharge is passed—it becomes very active. If discharges in hydrogen are alternated with those in air the bulb can be made to absorb large quantities of either gas and the activity with each gradually increases." Willows accounted for these results by assuming, as Hill did, alternate oxidation and reduction.

---

[58] A. A. Campbell Swinton, *Proc. Roy. Soc. London*, **A**, **79**, 134 (1907).

[59] E. Riecke, *Ann. Physik*, **15**, 1003 (1904).

[60] F. Soddy and T. D. Mackenzie, *Proc. Roy. Soc. London*, **A**, **80**, 92 (1908).

[61] *J. Am. Chem. Soc.*, **35**, 931 (1913).

[62] *Phil. Mag.*, **6**, 503 (1901).

[63] *Proc. Phys. Soc. London*, **25**, 35 (1912).

Mey[65] showed that when potassium and sodium amalgams are used as electrodes, compounds of these metals with hydrogen and nitrogen are formed during the discharge, and G. Gehlhoff[66] utilized this observation to purify rare gases (argon, helium, neon, etc.). In the presence of a glow discharge with a heated alkali metal as cathode, all the chemically active gases are removed from a mixture of chemically active and rare gases. Nitrogen is completely absorbed even with the alkali metal at ordinary temperatures. Complete absorption of hydrogen occurs with sodium at 290° C and with potassium at 175° C, and rubidium and cesium are effective at even lower temperatures. Gehlhoff assumed that chemical combination occurs between the vapors of the metals and the residual gases in an active state.

The absorption of hydrogen by sodium-potassium electrodes was also investigated by R. C. Gowdy.[67] Absorption was observed to occur when the alloy was used as cathode, and evolution when used as anode. The hydride is apparently decomposed by the cathode rays.

F. H. Newman[68] deposited different elements in a pure condition on the cathode of an electric discharge tube and then determined the absorption of different gases on passing an electric discharge. The minimum pressure at which clean-up was observed to occur varied around 0.1 to 1 mm of mercury.

Measurements were made to compare the amount of nitrogen gas absorbed by the element in the tube with the quantity of electricity passing in the circuit. Potassium, sodium, mercury, cadmium, antimony, magnesium, calcium, zinc, tin, phosphorus, sulfur, and iodine were tested in this way. The rates of absorption were very great with the last three elements. Hydrogen gas was also used in the tube, and absorption occurred with phosphorus, sulfur, and iodine.

---

[64] *Proc. Phys. Soc. London*, **28**, 124 (1915–1916).

[65] *Loc. cit.*

[66] *Ber. deut. physik. Ges.*, **13**, 271 (1911).

[67] *Phys. Rev.*, **4**, 401 (1914).

[68] *Engineering*, Jan. 14, 1921, p. 60; *Proc. Phys. Soc. London*, **32**, 190 (1919–1920); **33**, 73 (1920–1921).

Newman concluded from his experiments that the clean-up is due to chemical reactions between the elements present on the cathode and the gases which assume active modifications on the passage of an electric discharge.

In this connection it is interesting to refer briefly to the experiments carried out by R. J. Strutt[69] on the formation and properties of a chemically active modification of nitrogen. He observed that, on passing a condenser discharge through nitrogen at low pressures, a form of nitrogen is obtained which shows an intense yellow glow and is very active chemically. As is well known, nitrogen in the ordinary state is very inert chemically. It combines with other elements with difficulty and only under special conditions such as high temperature or high pressure. On the other hand, Strutt found that the nitrogen passed through the discharge tube under the above conditions was very active chemically. "Drawing it by the pump over a small pellet of phosphorus, a violent reaction occurs, red phosphorus is formed, and the yellow glow is quenched. At the same time the gas is absorbed." Similarly, active nitrogen combines readily with iodine, sulfur, and arsenic. There is no doubt, therefore, that the formation of active nitrogen must be taken into account in explaining clean-up effects in electrical discharges.

In a similar manner Newman accounted for the absorption of hydrogen by phosphorus, sulfur, and iodine, by assuming the formation of an active modification of the gas. This is probably the same form as that produced by G. L. Wendt and R. S. Landauer[70] in subjecting hydrogen to α-rays from radium emanation or to high-potential corona discharges.

These observations and the results obtained by Langmuir on the electrochemical clean-up of nitrogen by a heated tungsten cathode indicate that the above theory probably accounts for some of the clean-up effects observed in discharge tubes. As pointed out by G. W. C. Kaye:[71]

> It may be, also, that the action is stimulated by a species of electrolysis of the glass produced by the high-tension discharge playing over its surface. It is well known that glass may be readily electrolyzed by quite moderate potentials if the temperature of the glass is raised; and it is a matter of experience that the discharge seems to have an aging effect on the glass, to the detriment of subsequent working on the blowpipe. Such electrolysis might have a marked effect on the gas film which glass and other solids can condense on their surfaces.

It should be mentioned in this connection that some investigators have suggested that in a gas discharge even helium may become chemically active. E. H. Boomer[72] investigated the clean-up of helium in a hot-cathode discharge (see following section). A tungsten-filament cathode was used and an electron current of 5 to 10 ma at 1000 volts on the anode. It was observed that, in such a discharge in pure helium, the pressure was decreased from 4 to 0.1 mm. From a comparison of the loss in weight of the filament with the amount of helium cleaned-up, it was observed that the atomic ratio of tungsten to helium was about 1:2, "which led," according to the investigator, "to the belief that a distinct and stable compound of the formula WHe_2 exists." Since this combination was observed to be stable only at low temperatures (about that of liquid air) it would seem more probable that the helium was in an adsorbed condition.

---

[69] *Proc. Roy. Soc. London,* **A, 85,** 219 (1911), and subsequent papers.

[70] *J. Am. Chem. Soc.,* **42,** 930 (1920).

[71] *X-Rays,* 1918 Edition, Chapter VI.

[72] *Proc. Roy. Soc. London,* **A, 109,** 198 (1925).

That clean-up occurs as the result of reactions that are not chemical, however, is shown by the fact, observed by Soddy and Mackenzie,[73] that both pure helium and neon are also absorbed in electric discharge tubes. With aluminum electrodes, such as were used in their experiments, the electric discharge caused a considerable mechanical disintegration of the cathode and the portions of glass adjacent to the electrode became covered with a deposit of the metal in a finely divided state.

From the fact that the gases could be recovered by heating the tubes, Soddy and Mackenzie concluded that the gases were mechanically adsorbed by the deposits formed around the cathode. The finely divided metal formed by sputtering is thus assumed to behave like palladium or platinum black in the ordinary adsorption phenomena. That cathodically sputtered metals adsorb hydrogen during discharge has been shown by W. Heald,[74] and other investigators.

C. A. Skinner[75] found in his experiments that gas was evolved at the cathode and absorbed at the anode. The gas evolution occured at a rate given by Faraday's law, that is, 1 g of hydrogen for 96,500 coulombs. It is to be noted that with fresh electrodes a number of observers have found that

> there is often an initial evolution of gas, especially in hydrogen and nitrogen, or in any gas, with aluminum electrodes. But if the tube is used and then allowed to stand a while, on restoring the current, no initial evolution is found in most cases.

Chrisler[76] also concluded that the absorption in the discharge tube occurs at the anode. On the other hand, the weight of evidence points to the predominating influence of the cathode on the amount and rate of absorption. Hodgson[77] and Brodetsky and Hodgson[78] investigated the relation between amount of clean-up and current and also the effect of varying the chemical composition of the electrodes. The amount of gas absorbed per coulomb was observed to increase with decrease in pressure, as had previously been observed by Willows. The pressures at which these experiments were carried out varied from 2 mm to 0.03 mm approximately. A battery giving about 3200 volts was used as source of current, and the actual current strength varied from 0.008 to 0.002 amp. They found that the absorption varied with the rate of disintegration of the cathode, and no absorption was obtained in the absence of such disintegration. Furthermore, the absorption was observed to increase with increase in cathode drop. They therefore concluded, in agreement with Soddy and Mackenzie, that the major portion of the clean-up was due to adsorption of the gas by the metal sputtered from the cathode.

---

[73] *Proc. Roy. Soc. London*, **A**, **80**, 92 (1908).

[74] *Phys. Rev.*, **24**, 269 (1907).

[75] *Phil. Mag.*, **12**, 481 (1906); *Phys. Rev.*, **21**, 1, 169 (1905); *Physik. Z.*, **6**, 610 (1905).

[76] *Physik. Z.*, **10**, 745 (1909); *Phys. Rev.*, **29**, 461 (1909).

In his review Pietsch[79] has discussed very fully the investigations on the factors governing the intensity of sputtering of cathodes by positive ions, which were carried out during 1906–1914 by V. Kohlschütter and others. Other investigators apparently obtained quite different results. However, the observations made by L. Vegard[80] confirmed the generally held view that clean-up is due to sorption of gas by the metal sputtered from the cathode. He found that sorption is small as long as the cathode drop is below a certain "threshold" value. The rate of sorption apparently increased with increase in cathode drop, and the same parallelism held for the amount of cathodic sputtering. Thus, in oxygen, gold electrodes showed more sputtering than electrodes of platinum. At the same time, the rate of clean-up was greater with gold than with platinum. Vegard also observed that with helium there was a measurable clean-up which was, however, less than that obtained under similar conditions with either nitrogen or oxygen. With hydrogen both absorption and evolution were found to occur. "When a current of definite value has reduced the pressure to a given value, a larger current causes evolution, and a smaller one, absorption." This probably accounts to a certain extent for Skinner's observations.[81] Vegard concluded from his experiments that absorption occurs at the cathode and is somehow caused by high-velocity positive ions impinging on it. In other words, his explanation attempted to compromise between both the chemical and the mechanical theories.

---

[77] *Physik. Z.*, **13**, 595 (1912).

[78] *Phil. Mag.*, **31**, 478 (1916).

[79] *Ergeb. exakt. Naturwi.*, **5**, 213 (1926).

[80] *Ann. Physik*, **50**, 769 (1916).

[81] *Loc. cit.*

More recently, the *clean-up of rare gases* in a cold-cathode discharge tube has been investigated by H. Alterthum, A. Lompe, and R. Seeliger.[82] The discharge tube used was 2 cm in diameter and had hollow cylindrical electrodes made of thin sheet iron, which could be degassed with high-frequency heating. The cylinders were covered at the end nearest the seals by flat circular disks. Pressures were measured by means of a Pirani gauge, and the source of current was a transformer operated at 50 cycles and having an open-circuit voltage of 4500 volts. The pressures used were varied from several millimeters to 0.2 mm, and the currents, from 20 to 100 ma. In a tube containing neon at 7 mm pressure and operated at 100 ma, the voltage remained fairly constant at about 250 volts for several hundred hours. Then, as rate of clean-up increased, the voltage increased to 500 volts at 1000 hr and the pressure had decreased to less than 1 mm.

It was observed that in neon, at constant current, the rate of clean-up is low at the higher pressures but increases rapidly with decrease in pressure and finally becomes approximately independent of the pressure when it has decreased to about 3 mm.

The rate of clean-up was found to be proportional to the current and independent of the form and length of the discharge tube.

It was shown that the gas is cleaned up for the most part by the electrodes and, furthermore, that this clean-up occurs at the cathode. The fact that the clean-up did not occur on the glass walls and was independent of the amount of sputtering leads to the conclusion that the neon was *cleaned up as positive ions* driven into the cathode by the high cathode fall. This is in agreement with the observation that rate of clean-up increased with increase in cathode drop.

Similar observations were made with discharges in argon and helium. The rates of clean-up in the different gases at 2 mm and 100 ma were found to be in the ratios 0.4:1:10 for argon, neon, and helium, respectively. "This also," the investigators state, "is in agreement with the above hypothesis, since, the smaller the atoms (or ions), the more easily they will be able to penetrate into the metal and diffuse throughout it." It should also be added that the cathodic sputtering is greatest for argon and least for helium, which is another argument for the conclusions drawn from this investigation regarding the mechanism of clean-up.

In two subsequent papers,[83] Alterthum and Lompe investigated the effect of other factors on the clean-up of rare gases in a discharge tube such as that used in the previous work. In order to compare the data obtained under different conditions they defined a factor Z by means of the relation

---

[82] *Z. tech. Physik,* **17,** 407 (1936).

[83] *Z. tech. Physik,* **19,** 113, 116 (1938).

$$t = \frac{ZPV}{i}, \tag{5}$$

where t denotes the period (in hours) required to clean up PV mm · cm^3 with a discharge of i ma. Thus Z is a proportionality factor which corresponds to the period in hours required to decrease the quantity of gas by 1 mm · cm^3 with a discharge of 1 ma. The quantity Z involves all the factors that affect rate of clean-up, that is, nature of gas, nature of electrodes, variation in cathode drop with electrode shape, temperature of the electrodes, etc.

In carrying out the experiments the initial pressure in each case was 2 mm neon and the tube was then operated till the pressure had decreased to such a low value that the discharge could no longer pass. This gave the value of t, the time required to clean up the gas to a small fraction of its initial value. It was found that Z varied approximately linearly with inside area of the hollow cylindrical iron electrodes. The values of cathode drop and of Z were also determined for a large number of different metals constructed out of thin sheet similarly to the hollow sheet-iron electrode described above. No relation could be observed between the values of Z and the composition of the metal or the cathode drop.

From these observations made by Alterthum and his collaborators it may be concluded that electrical clean-up in the rare gases takes place by impact of positive ions on the electrodes.

7. CLEAN-UP IN ELECTRODELESS DISCHARGES

In order to eliminate the effect of electrodes a number of investigators have carried out experiments on clean-up in electrodeless discharges. Such discharges are obtained by coupling glass bulbs or rings containing the gas with coils carrying a high-frequency current, the frequency of which varies from 10^5 sec^{-1} to higher values.

G. Mierdel[84] used bulbs of glass and quartz to which were attached appendixes for cooling purposes. The clean-up was observed to be greatest for oxygen. With the appendix at liquid-air temperature the pressure decreased in less than a minute from 85 to 2 microns, and in order to maintain the discharge fresh oxygen had to be fed into the bulb. On warming the appendix to room temperature, most of the gas was reevolved. Mierdel considers the clean-up due to formation of ozone.

---

[84] *Ann. Physik*, **85**, 612 (1928).

With hydrogen, nitrogen, and air similar clean-up effects were observed, the amount of clean-up being least with hydrogen. Again, a considerable fraction of the absorbed gas was re-evolved on raising the temperature of the appendix. Mierdel accounts for the clean-up in hydrogen as due to formation of atomic hydrogen. This is condensed on the walls at liquid-air temperature and re-evaporates in the molecular form at room temperature. In the *case of argon no clean-up effect whatever was observed.*

With regard to the clean-up of hydrogen, E. Hiedemann,[85] working in Mierdel's laboratory, showed that the extent and rate of disappearance of the gas depends to a large extent on the nature of the preliminary treatment of the glass. Furthermore he observed a normal and "abnormal" clean-up effect. The normal is accounted for by the condensation of atomic hydrogen at low temperature; to explain the abnormal clean-up, it is suggested (on the basis of other investigations) that compounds of silicon and hydrogen (silanes) are formed at low temperatures.

The clean-up of hydrogen *at room temperature* was investigated by M. C. Johnson.[86] The pressure was measured by means of a very sensitive mercury manometer (described in Chapter 6). The range of the manometer was about 0.5 mm, with a detectable sensitivity of 10^{-4} mm. It was observed that the amount of hydrogen cleaned up under the influence of a high-frequency discharge was a maximum for any given tube immediately after the tube had been baked out at 300° C and thoroughly degassed. On repeating the bake-out and evacuation and letting in fresh hydrogen to the same initial pressure (about 0.1 mm) the amount of gas cleaned up was less and decreased still more with successive repetitions of bake-out and evacuation.

Taking into account the area available for adsorption, it was found that the maximum possible values of the fraction of the glass surface covered with a monolayer of atomic hydrogen were 0.66 and 0.36 for the two tubes used in the investigation.

8. ELECTRON EMISSION AND SPACE-CHARGE PHENOMENA IN HOT-CATHODE LOW-PRESSURE DEVICES

In a cold-cathode discharge tube the electrons are generated at the cathode by means of the positive ions which acquire a high velocity in the cathode-fall region. The ions cause sputtering of the cathode, and the sputtering is accompanied by a clean-up of the gas. If, however, a hot cathode is used, electrons are emitted by a mechanism analogous to the evaporation of atoms from a solid, and the cathode drop is reduced to a value which is, in general, only slightly higher than the ionizing potential (V_i) of the gas. Under certain conditions the cathode fall may be even less than V_i. As shown by A. W. Hull,[87] no sputtering occurs if the cathode drop is maintained below a certain critical value which depends upon the nature of the cathode and the composition of the gas. For instance, for thoriated tungsten cathodes this "disintegration voltage" is about 27 for neon ions and 17 for mercury ions.

---

[85] *Ann. Physik,* **8,** 456 (1931).

[86] *Proc. Roy. Soc. London,* **A, 123,** 603 (1929).

Before considering voltage clean-up phenomena in hot-cathode devices it is essential to review briefly certain fundamental characteristics of hot cathodes.[88]

The electron emission from a heated cathode varies with the absolute temperature in accordance with the relation

$$I = AT^2\epsilon^{-b_0/T}, \tag{1}$$

where $I =$ emission per unit area, at T degrees K, and A and b_0 are constants. This relation is more conveniently written in the form

$$\log I = \log A + 2\log T - \frac{b_0}{2.303T}\cdot \tag{2}$$

Table 5 shows values for I, the emission in amp/cm^2, as well as W, the watts radiated per cm^2, at a series of temperatures, for four types of cathodes.[89] Values of log A and of $b_0/2.303$ used in evaluating the emission data are given in the two lowest rows.

---

[87] *Gen. Elec. Rev.*, **32**, 213 (1929).

[88] The following references represent a selection of the vast literature which has been published on this topic.

1. A. L. Reimann, *Thermionic Emission*, John Wiley & Sons, New York, 1934.
2. L. R. Koller, *The Physics of Electron Tubes*, McGraw-Hill Book Company, 1937.
3. E. D. McArthur, *Electronics and Electron Tubes*, John Wiley & Sons, New York, 1936.
4. S. Dushman, *Rev. Modern Phys.*, **2**, 381 (1930); also *Encyclopædia Britannica*, 1946.
5. W. G. Dow, *Fundamentals of Engineering Electronics*, John Wiley & Sons, New York, 1937.

[89] The data were taken from the following sources:

Tungsten: H. A. Jones and I. Langmuir, *Gen. Elec. Rev.*, **30**, 310, 354, 408 (1927); S. Dushman, *loc. cit.;* A. L. Reimann, *loc. cit.*

Molybdenum: A. G. Worthing, *Phys. Rev.*, **28**, 190 (1946); S. Dushman, *loc. cit.;* A. L. Reimann, *loc. cit.*

Tantalum: M. D. Fiske, *Phys. Rev.*, **61**, 513, (1942); L. Malter and D. B. Langmuir, *Phys. Rev.*, **55**, 743 (1939).

Columbium: A. L. Reimann and C. K. Grant, *Phil. Mag.*, **22**, 34 (1936).

Thoriated tungsten (Th W): S. Dushman, *loc. cit.*

The thoriated tungsten is obtained by flashing a tungsten filament containing 0.5 to 1.5 per cent ThO_2 at a high temperature (above 2700° K) which reduces some of the oxide to metallic thorium. This is then followed by heating at 2100–2200° K, which causes a diffusion of thorium to the surface, where it forms a monatomic layer which possesses much higher electron emission than pure tungsten. At temperatures above about 2000° K the thorium evaporates at a rate which exceeds that of diffusion to the surface with a resultant decrease in electron emissivity.

In many electronic devices, an oxide-coated cathode is used, which consists of a nickel or nickel-alloy filament coated with a mixture of the carbonates of barium, strontium, and calcium. The filament must be "activated" by heat treatment in order to produce a monatomic film of barium which is the source of electrons. The values of A and b_0 for the activated emitter vary with composition of the coating, method of preparation, and nature of metal support.[90] The emission at 1000° K is usually found to lie, within a factor of 10, at the value of 10 ma/cm^2 for BaO, 1 ma/cm^2 for SrO, and 0.1 ma/cm^2 for CaO. The values of $b_0/2.303$ for BaO lie around 5500, and the values for SrO and CaO are higher. At temperatures above about 1200° K, the rate of evaporation of barium atoms increases rapidly with increase in temperature and the surface loses its activity.

The value of the space current passing from the hot cathode to the anode, in a good vacuum, is limited either by temperature saturation or by "space charge." The former may be calculated for a given area and temperature of cathode by means of equation 1 or 2. This emission is obtained, however, only if the anode voltage is sufficient to overcome the repulsion between electrons. As first shown by Langmuir (1913), the space-charge current is given by a relation of the form

$$i_s = sV^{3/2}, \tag{3}$$

where s is a constant, the value of which depends upon the geometry of the cathode and anode.

For instance, for parallel plane surfaces,

$$i_s = \frac{2.325 \cdot 10^{-6}}{d^2} V^{3/2} \quad \text{amp} \cdot \text{cm}^{-2}, \tag{4}$$

where d = distance (in centimeters) between the two electrodes. For a filamentary cathode of radius r_0 along the axis of a cylindrical anode of

---

[90] For a comprehensive discussion of oxide-coated cathodes, the reader should consult J. P. Blewett, *J. Applied Phys.*, **10**, 668, 831 (1939).

TABLE 5

ELECTRON EMISSION (I = AMPS/CM^2) AND W(= WATTS/CM^{-2})

	Tungsten		Molybdenum		Tantalum		Columbium		ThW
T	I	W	I	W	I	W	I	W	I
1000									$1.73 \cdot 10^{-7}$
1200									$3.95 \cdot 10^{-5}$
1400									$2.03 \cdot 10^{-3}$
1600	$9.27 \cdot 10^{-7}$	7.74	$2.39 \cdot 10^{-6}$	6.30	$9.1 \cdot 10^{-6}$	7.36	$2.19 \cdot 10^{-5}$	6.40	$4.06 \cdot 10^{-2}$
1800	$4.47 \cdot 10^{-5}$	14.2	$1.05 \cdot 10^{-4}$	11.3	$3.32 \cdot 10^{-4}$	13.3	$6.95 \cdot 10^{-4}$	11.4	0.428
2000	$1.00 \cdot 10^{-3}$	24.0	$2.15 \cdot 10^{-3}$	19.2	$6.21 \cdot 10^{-3}$	21.6	$1.16 \cdot 10^{-2}$	18.5	2.864
2200	$1.33 \cdot 10^{-2}$	38.2	$2.59 \cdot 10^{-2}$	30.7	$6.78 \cdot 10^{-2}$	34.2	0.115	29.9	
2400	0.116	57.7	0.215	47.0	0.509	51.3	0.800	45.3	
2600	.716	83.8	1.29	69.5	2.25	75.4	5.28	67.0	
2800	3.54	117.6	6.04	98.0	12.53	105.5	60.67	130.6	
3000	14.15	160.5	23.28	116.0	45.60	144.4			
	log A: 1.780		1.780		1.740		1.571		0.477
	$b_0/2.303$: 22,750		22,100		21,110		20,226		13,680

radius r (in centimeters), the current (in amperes) per centimeter length is given by the relation

$$i_s = 14.65 \times 10^{-6} \frac{V^{3/2}}{r\beta^2} \text{ amp/cm length,} \tag{5}$$

where β^2 is a function of r/r_0 which has the value 1 for $r/r_0 = \infty$.

The manner in which the electron current between the cathode and anode may be limited either by temperature of the cathode or by voltage between the two electrodes is illustrated by the plots in Fig. 10.[91] These plots give the variation in electron current observed from a tungsten filament 0.25 mm in diameter located along the axis of a cylinder 2.54 cm in diameter and 7.62 cm long. The maximum available electron current as a function of the temperature is given by the exponential

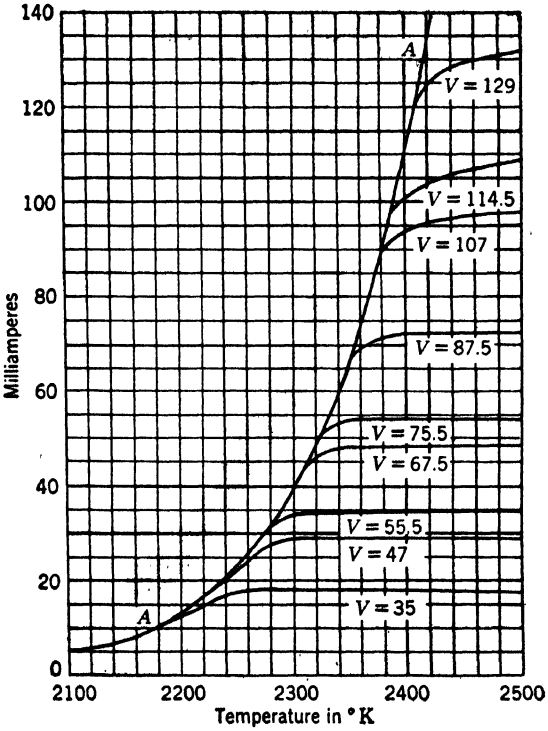

FIG. 10. Illustrating the limitation of electron current in a hot-cathode diode by (a) temperature of the cathode, as shown by the curve *AA*, or (b) anode volts, as shown by the horizontal lines for different values of the anode potential.

---

[91] S. Dushman, *Phys. Rev.*, **4**, 121 (1914).

curve. The horizontal plots give the space-charge-limited currents for different anode voltages. Curves such as shown in Fig. 10 are obtained only at extremely low pressures (usually of the order of 10^{-3} micron or less).

9. CLEAN-UP IN HOT-CATHODE DISCHARGES

When, however, the gas pressure exceeds a certain value (depending principally upon the nature of the gas and the geometrical dimensions of the device) some of the electrons no longer travel directly from the cathode to the anode. Collisions with gas molecules occur, and if the anode voltage exceeds the ionizing potential positive ions are produced which tend to neutralize a part or the whole of the negative space charge produced by the electrons; consequently, the electron current reaches the saturation value, corresponding to the temperature of the filament, at much lower voltages than when gas is not present.

These phenomena are illustrated by the following observations with a small hot-cathode high-vacuum rectifier (diode) in which a tungsten spiral was used as cathode and a molybdenum cylinder (enclosing the spiral) as anode. To the bulb containing these electrodes was attached an appendix containing a small amount of mercury, and the whole arrangement was exhausted to a very high vacuum. By immersing the appendix in liquid air the pressure of the mercury vapor could be reduced to such a low value that no ionizing effects occurred. Figure 11 shows the characteristics of the tube, under these conditions, at two different filament currents. It will be observed that at a filament current of 1.35 amp (curve *A*) the electron current varied with the anode voltage in accordance with the $\frac{3}{2}$ power relation. At a filament current of 1.25 amp, corresponding to a lower temperature, the electron current increased at first in accordance with the same voltage law and then tended to reach the value 38 ma corresponding to the emission for that particular temperature (curve *B*).

On removing the liquid air from the appendix, so that the mercury attained room temperature and the pressure in the device reached the value of about $2 \cdot 10^{-3}$ mm (corresponding to the vapor pressure of mercury at this temperature), the characteristic obtained with the filament at 1.25 amp was that shown in curve *C*. At 18 volts a distinct blue glow appeared, and at 26 volts this glow extended practically all the way down the appendix. It will be observed that, simultaneously with this appearance of blue glow, the electron current increased rapidly until it reached practically the same saturation value as that obtained under good vacuum conditions. That is, even at such a low pressure of mercury vapor, the space-charge phenomena practically disappeared and the saturation electron emission corresponding to 1.25-amp filament current was obtained at relatively low voltages.

Similar phenomena are observed in hot-cathode devices with all other gases. At very low pressures the electron current varies with the voltage according to the $\frac{3}{2}$ power law, but at higher pressures (ordinarily about 1 to 2 microns) blue glow appears as the voltage is raised above the ionizing potential and simultaneously with this blue glow the current increases rapidly, as shown in curve C, Fig. 11, to the saturation emission at the given filament temperature. In the case of most gases this blue glow does not ordinarily persist very long, owing to clean-up effects that ac-

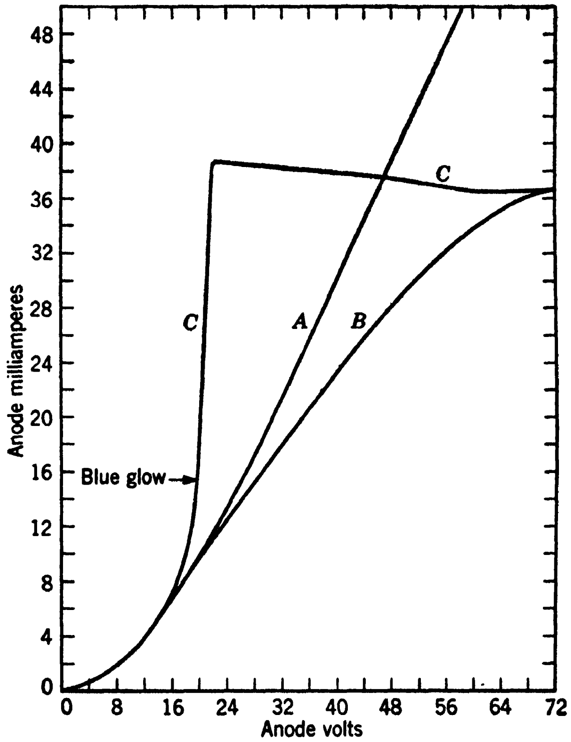

FIG. 11. Illustrating effect of mercury vapor on characteristics of hot-cathode diode. Curve A, space-charge limitation in good vacuum. Filament current, 1.35 amperes. Curve B, space-charge limitation at lower values of anode potential and temperature limitation at higher values of anode potential. Filament current, 1.25 amperes. Curve C, same filament temperature as curve B, but in the presence of mercury vapor at $P_\mu = 2.0$.

company the appearance of the glow, and consequently the electron current decreases again gradually until it attains the limiting value corresponding to space charge.

These clean-up phenomena that are observed in hot-cathode devices are extremely interesting, and they are of great technical importance. The experimental evidence obtained in this laboratory and by other investigators points to the conclusion that these effects are primarily due to the formation of ions by collisions between electrons and gas molecules. There is little or no evidence for any electrical clean-up below ionizing potentials.

Experiments along this line carried out in this laboratory some years ago showed that the factors governing clean-up are quite complex. In general, the rate of clean-up shows a tendency to increase with the anode voltage and with the electron current. In addition to these factors, the condition of the glass walls and the previous history of the glass bulb exert a profound effect on the rate of clean-up. The disappearance of gas by electrical clean-up is observed even at the very low pressures where space-charge effects are present and blue glow is therefore absent. Numerous observations in connection with hot-cathode devices have confirmed this conclusion. Thus a hot-cathode rectifier may be sealed off at 0.05 micron and, by subsequent operation with a current of a few milliamperes at 120 to 240 volts, the pressure will be found to decrease to 0.01 micron or less.

At any given electron current the residual gas pressure in the sealed-off tube reaches an equilibrium value which increases with the electron current. Part of this increase is probably due to an increased rate of evolution of gas from metal parts and glass walls until equilibrium is attained with the increased rate of clean-up. The pressure may thus be found to vary from 0.01 to as low as 0.0001 micron, depending upon anode voltage and electron current. Similar effects have been observed with the ionization gauge in using it to measure low pressures of chemically active gases, such as nitrogen, hydrogen, and oxygen. That this clean-up is not due in these cases to purely chemical reactions at the surface of the tungsten filament is easily shown by disconnecting the anode voltage, when the clean-up practically ceases. Moreover, this clean-up also occurs with the inert gases argon and helium.

A description of some observations made during some earlier experiments, by Mrs. M. R. Andrews, H. Huthsteiner, and the writer, may be of interest in this connection. In these experiments a tube containing two adjacent tungsten filaments was used, so that either filament could be made cathode, and the rate of clean-up was investigated for argon and nitrogen. Gas from a large reservoir was allowed to flow continuously through this tube at practically constant pressure, and the rate of clean-up was determined by collecting the gas after it left the tube. The pressures used in most of the experiments were so low that no blue glow effects were observed, and during any one set of observations both the electron current and the anode voltage were maintained constant. The magnitude of the current was varied in different runs from a few microamperes to several milliamperes, and the anode potential was varied from 25 to 250 volts. The rate of clean-up was observed to increase almost linearly with increase in pressure. With electron currents below a milliampere the rate of clean-up also varied linearly with the current, but it showed a tendency to increase much less rapidly with electron currents exceeding this value. At anode voltages in excess of 25, the rate of clean-up was observed to be practically constant and independent of the voltage. With freshly baked-out glass bulbs, the fatigue effects observed were quite pronounced. On covering the glass surface inside with a tungsten deposit (by evaporation of one of the filaments) the rate of clean-up was found to increase considerably, and much more gas could be cleaned up before fatigue effects occurred. The rate of clean-up of argon was found to be about half of that of nitrogen under otherwise similar conditions.

The following observations were made on a system consisting of a 5-in. bulb containing two adjacent tungsten filaments to which was attached an ionization gauge. The volume of the arrangement was about 1200 cm^3. After a thorough exhaust on the condensation pump, followed by a flashing of the filaments at a high temperature, argon at a pressure of $1.35 \cdot 10^{-3}$ mm of mercury was let into the system and the whole sealed off the pump. One of the tungsten filaments was then made cathode and raised to the temperature necessary to give an electron emission of 5 ma. With 250 volts on the other filament as anode, the pressures indicated in the following table were obtained at different intervals of time.

t (minutes)	P_μ	$k = \frac{1}{t} \log (P_{\mu 0}/P_\mu)$
0	1.35	
2	1.2	0.0255
4	1.05	0.0273
15	0.65	0.0212
27	0.36	0.0213
	Average =	0.0238

The approximate constancy of k in the last column shows that the rate of clean-up at any instant was proportional to the pressure.

Observations were made in the same manner with nitrogen. In one experiment, using 5 ma and 250 volts, the nitrogen cleaned up from a pressure of 8 to 1 micron in 35 minutes. In all these experiments, if, after cleaning up a certain amount of gas, more gas was let into the bulb, the rate of clean-up was observed to be much lower.

Regarding the mechanism of this clean-up, it is difficult to draw any positive conclusions. In the foregoing experiments there was no evidence to show that the gas was cleaned up at the cathode, as for instance by the formation of WN_2. This explanation would certainly not apply to argon; the gas was most probably driven into the walls. Subsequent heating rarely caused the evolution of as much gas as had been cleaned up, so that the ions must penetrate the glass quite deeply.

Observations similar to those mentioned have been obtained by other investigators working with hot-cathode devices. Thus W. H. Eccles, in a discussion of thermionic valves,[92] made the following very interesting comments regarding clean-up effects in these tubes:

> Many interesting phenomena are observed with the traces of residual gases always present even in the hardest of tubes. After running for some time with a given electron current to the positive electrode and a given voltage, a steady value for the pressure of the residual gas may be reached. If now the voltage is increased, but not sufficiently to overheat the positive electrode, the tube will harden, i.e., some of the residual gas will be absorbed. On the other hand, if the voltage is reduced, and particularly if the filament is simply heated without any voltage being applied to the positive electrode, the amount of residual gas will increase.
>
> These effects are well known to radiologists and various suggestions are put forward in explanation. But from the point of view of the development of the high-power valves, the whole problem requires careful investigation.
>
> The fact that an increasing voltage at the positive electrode hardens the valve leads to the conclusion that the effects are due to the action of the ionized gas. At these voltages the ions are positive, and their observed disappearance must be due to their being driven into the hot filament, or into the walls of the containing vessel. If they are driven into the filament, how are they retained with the filament at 2000° C? Is any chemical action involved, or is it the same process as the occlusion in the positive electrode? Or is it only the walls of the containing vessel that absorb the ions?
>
> A suggestion has been put forward by Dr. G. B. Bryan of the Physics Laboratory, at Royal Naval College, Greenwich, that the occlusion of the gases and the emission of positive ions from metallic surfaces at moderate temperature are closely related. He visualizes the process as follows: Some proportion of the gas to which the electrodes are exposed will probably be ionized hydrogen. A positive hydrogen ion is a very small heavy projectile with considerable powers of penetration. On striking the surface of a solid it will pass through the outer surface and pick up an electron, so becoming neutral. Now, however, it is a large body entrapped in among the atoms of the metal and unable to escape under ordinary conditions. But at moderate temperatures the electrons may be shed again, and the positive ion, being no longer en-

---

[92] *Radio Review*, 1, 26 (1919).

> cumbered by the outlying electron, can escape, so constituting the positive emission. One peculiar fact has frequently been observed by Dr. Bryan when exhausting a valve, viz., that a small liberation of occluded gas will give rise to a greater tendency to arcing than the introduction of a much greater quantity of ordinary air. If the gas liberated from the electrodes is already ionized, the observation is immediately explained.
>
> This theory is a very interesting one, and is one on which some light could be thrown by the entire removal of all traces of hydrogen. At present, however, it has never seemed possible to do this, as such extremely small quantities are involved; and possibly other ionized gases may be entrapped in the same way. If it is the outer electron that is lost, this would seem to be quite possible.

That the positive ions attain, under even moderate voltages, velocities which are much greater than those possessed by the corresponding molecules at ordinary temperatures, has already been pointed out in the discussion of electrical clean-up at higher pressures. It is therefore interesting to observe that Eccles and Bryan also suggested that this might be a possible explanation of the observed clean-up effects in hot-cathode devices.

On the other hand, in a paper by A. L. Hughes[93] another explanation was suggested which is to a certain extent equally probable. In these experiments the electrical clean-up of nitrogen and hydrogen was studied in a tube containing as cathode a platinum filament coated with BaO and SrO. In most of the experiments the whole tube was kept immersed in liquid air and the electron current was maintained constant in any one set of measurements. The rate of clean-up was found to decrease gradually during any run, owing to gradual saturation of the walls of the tube (as in the experiments mentioned previously). The initial pressures used in these experiments varied from 50 to 2 microns. The conclusions, as stated by Hughes, were as follows:

> For hydrogen, no disappearance was obtained unless the electrons had energy above 13 volts. The rate of disappearance rose rapidly as the energy of the electron was increased to about 70 volts, after which no rapid change was noted (the rate appeared to diminish somewhat when the energy of the electrons was raised from 150 to 300 volts). For nitrogen, the rate of disappearance was at first much less than for hydrogen, but when the energy of the electrons was raised sufficiently (roughly 200 volts) the rate of disappearance of the nitrogen exceeded that for hydrogen.

In explanation of the mechanism of clean-up Hughes concluded that "this disappearance is due to the splitting of the molecules into atoms when electrons collide with the molecules, and these atoms condense on the adjacent surfaces particularly if they are cold." This explanation would account for the observations made in the experiments by Mrs.

---

[93] *Phil. Mag.*, 41, 778 (1921).

Andrews and Huthsteiner that a charging up of the tungsten deposit on the walls, with either positive or negative potentials, produced no effect on the rate of clean-up of nitrogen. On the other hand, such an explanation could obviously not account for the clean-up of argon. Hughes also calculated the ratio between the number of molecules disappearing per unit time and the frequency of collisions between electrons and molecules. Figure 12 taken from his paper gives the relation between the value of this ratio (designated *b*) and the anode voltage, for both nitrogen and hydrogen. It is seen that, with approximately 250 volts on the anode, about one molecule disappeared for every six collisions, and presumably this molecule disappeared in the form of atoms. The theory that collisions between electrons and molecules may lead not only to the formation of ions but also to a dissociation of these molecules is extremely suggestive and may be a satisfactory explanation of the clean-up effects in some cases, but it is hardly possible that it is of general application.

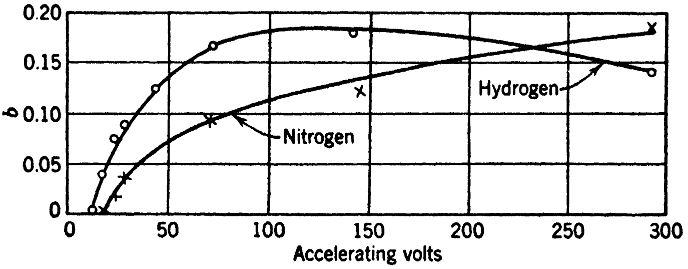

FIG. 12. Values of *b*, the ratio between number of molecules disappearing per unit time and frequency of collisions between electrons and molecules, as a function of the anode voltage, for hydrogen and nitrogen (Hughes).

Following up the results reported by Hughes, N. R. Campbell and E. G. New[94] also investigated the relation between rate of clean-up and rate of ionization of the gas in a hot-cathode triode. The cathode was, in most cases, a tungsten filament. It was surrounded by a nickel-wire spiral, similar to the grid of a receiving tube, and the third electrode was either a nickel cylinder surrounding the spiral, or a layer of silver, covering partially or almost completely the surface of the glass bulb. In the experiments the tube was used in the same manner as an ionization gauge, with the spiral positive to the filament and the cylinder negative, so that it collected positive ions. The anode voltage, V_a, ranged from 50 to 350 volts, and the ion collector voltage (V_c) was usually -2 volts. "The value of V_c, so long as it was of the right sign, was quite without effect on the experiments." The gas used in most of the experiments was nitrogen nearly free from argon.

---

[94] *Phil. Mag.*, **48**, 553 (1924).

The pressure was deduced, as in the ionization gauge, from the ratio between positive ion and electron currents and a calibration with a McLeod gauge. It was observed that at higher pressures the ratio of rate of decrease in pressure (n_1) to rate of ionization (n_2) was independent of pressure, and the order of magnitude of this ratio was about 1. At lower pressures the value of this ratio decreased rapidly with pressure and tended to approach zero. The value of the ratio was also found to be independent of V_a and of the arrangement of the electrodes. According to the investigators,

> It depends very greatly on the condition, but not very greatly on the material, of the walls of the vessel. The number of molecules disappearing is often greater than the number ionized. In argon there is no evidence of an absorption simply related to ionization. In hydrogen the facts are obscure, but it is probable that there is an electrical absorption more rapid than in nitrogen or carbon monoxide.

In spite of the observed proportionality between n_1 and n_2, Campbell and New do not believe that clean-up occurs by absorption of ions, although they are unable to suggest an alternative hypothesis. Of special interest in that connection are the following remarks, from their paper, with respect to the effect of heating the walls on the evolution of gas.

> If a vessel exhausted for several hours while maintained at (say) 360° C is sealed off, allowed to cool, and then maintained at (say) 100°, the pressure increases, rapidly at first and then more slowly, until after a period of many hours (say 100) an equilibrium pressure is attained which does not increase with time. If the vessel is now cooled, the pressure falls, rapidly at first and then more slowly; the original pressure at room temperature is not usually reached; there is some permanent evolution. If the heating and cooling are repeated, an equilibrium pressure, somewhat higher than before, is attained, and the final pressure reached on cooling is again somewhat greater. If, after the original heating at 100°, the temperature is raised to 200° C, the pressure will again reach equilibrium at a higher value. Permanent increases are produced by alternate heating and cooling; but there is some reason to believe that even this permanent evolution decreases as the cycle is repeated, and that finally a state would be obtained in which the equilibrium pressure is determined only by the temperature.
>
> These features are characteristic of all the well-exhausted vessels we have examined (except one, wholly anomalous and unexplained, which gave no change of pressure with temperature), whether or not gas has been made to disappear in them by the process studied here. In fact, we have never been able to satisfy ourselves that the absorption of gas by the discharge had any effect on the thermal evolution; it is certainly not true that, if two vessels are exhausted in apparently the same way and gas is absorbed in one and not in the other, that in which gas has been absorbed will always give the greater rise of pressure with temperature. In other words, we have no evidence that the gas absorbed by this process is capable of being restored by heating to any temperature under 300° C.

Nor does there appear to be any temperature below this limit at which the electrical absorption ceases; if the discharge is passed in the warm vessel absorption occurs, but at a smaller rate than at room temperature.

In the course of the experiments on "residual gas" many observations were made in which gas was alternately liberated by heating and absorbed by the discharge in the same closed vessel. On each repetition of the cycle the equilibrium pressure attained at any temperature during the leaking decreased, and the value of n_1/n_2 at any pressure during the absorption increased. The cycle on the whole tended to remove gas. If the facts are to be represented in terms of vapor pressure, the relation between thermal evolution and electrical absorption can be summed up in the statement that the discharge progressively decreases the vapor pressure of the vessel.

In a series of papers published by the research staff of the General Electric Company, Ltd., London,[95] the results have been reported of a comprehensive investigation of the relation between clean-up in hot-cathode devices and blue glow.

Very careful measurements were made of the voltages at which this glow sets in. "The first observations," it is stated,

proved that the glow potential is independent of the temperature of the filament and of the thermiomic emission from it in wide limits. If there is no thermionic emission, the glow does not appear of course until the spark potential of the gas is reached, but the change from this condition to that in which the glow occurs at the very much lower potential obtained with a hot cathode is so rapid that it could not be determined certainly whether the change was continuous or discontinuous. Once the lower value is obtained, no further change occurs even if the thermionic emission is increased 100-fold. There is no evidence that the glow potential depends at all on the thermionic emission, so long as it is great enough to give at all a glow potential distinct from the spark potential. On the other hand, the glow potential depends greatly on the pressure and on the nature of the gas.

Figure 13 shows the relation obtained in this investigation between the pressure and the glow potential for different gases. It will be observed that the potentials are plotted against the reciprocal of the pressures. The argon used contained 5 per cent nitrogen. The curves for hydrogen show the effects of slight traces of impurities. The glow potentials observed with increasing voltages were invariably somewhat higher than those observed with decreasing voltages, the maximum difference being obtained for argon, where it was about 10 volts at a pressure of 5 microns.

For mercury vapor the glow potential was observed to be always 32.5 volts, "whatever the nature of the gas with which it is mixed." Furthermore, the addition of any impurity to a gas was often observed to decrease the glow potential below that of either of the constituents. It was observed that the appearance of glow was essential for the occurrence of clean-up. The spectrum of the light emitted was always that of the gas having the lowest value of the glow potential. As will be observed from Fig. 13 the glow potential increases with decrease in pressure. Consequently, with a given voltage the clean-up continued only as long as this voltage exceeded the glow potential, and when the pressure decreased to such a value as to make the applied voltage lower than the glow voltage, the discharge and clean-up both ceased unless the voltage was increased.

---

[95] N. R. Campbell, *Phil. Mag.*, **41**, 685 (1921); N. R. Campbell and J. W. H. Ryde, *Phil. Mag.*, **40**, 585 (1920). Observations on the clean-up effect in the presence of blue glow have also been reported by C. F. Hagenow, *Phys. Rev.*, **13**, 415 (1919).

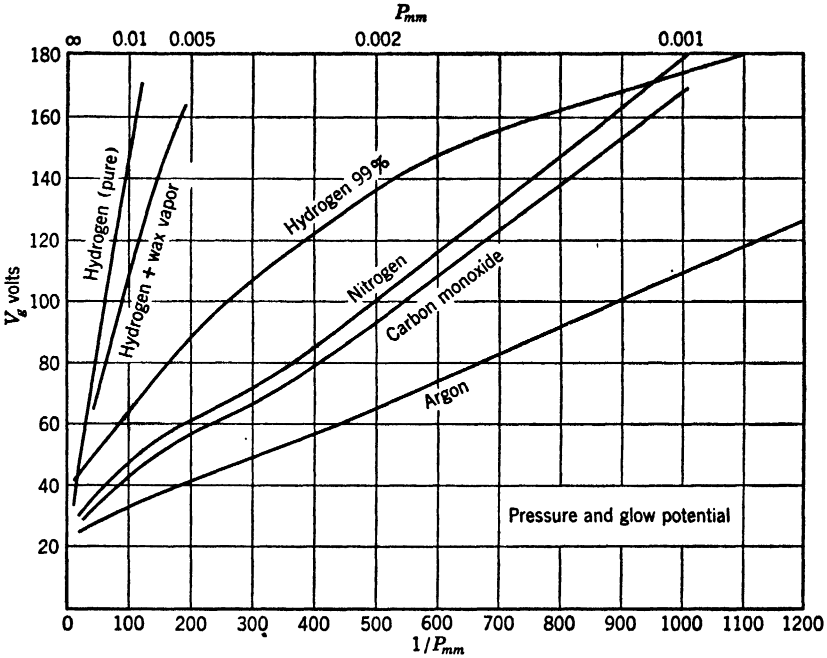

FIG. 13. Relation between glow potential, V_g, and reciprocal of P_{mm} for various gases (Campbell).

An important distinction was drawn in this investigation between the glow potential and that required for ionization.

> It is clear that the glow potential is not, like the ionization potential, a direct property of the individual atoms of the gas; it must also be a function of their mode of reaction with each other or with the walls of the vessel; for the glow potential is not, like the ionization potential, independent of the pressure. There is no evidence, therefore, that the glow represents a new form of ionization of the individual atoms.

Some interesting observations were recorded on the rate of disappearance of different gases in the presence of a glow discharge. In the case of carbon monoxide it was found that the gas cleaned up in consequence of the reaction $2CO = C + CO_2$, the carbon dioxide formed being adsorbed on the glass walls. The complete elimination of mercury vapor is essential for the occurrence of this reaction.

If mercury vapor is completely removed, the disappearance continues until the discharge stops, owing to the rise of the glow potential—at any rate, if a potential greater than 300 volts is not employed. If fresh carbon monoxide is admitted, it disappears again under the discharge at a rate apparently unchanged; a limit to the absorption has not been found, although a quantity has been adsorbed equal to at least five times that representing a monomolecular layer on the walls.

On baking the vessel to over 350° C, the greater part of the gas was re-evolved, mostly as carbon dioxide.

Nitrogen was observed to disappear in the same manner as carbon monoxide, "in apparently unlimited quantities." This disappearance was accompanied by some decrease in the filament diameter and a blackening of the bulb. Probably WN_2 was formed, as has been shown by Langmuir,[96] although Campbell has suggested that the clean-up may be due to an absorption of nitrogen by tungsten sputtered from the filament.

The rate of clean-up of argon was observed to be less than one-fifth that of nitrogen, and at the same time rapid blackening of the bulb occurred.

In both nitrogen and argon there is the intimate connection between cathode sputtering and absorption of gas which Vegard[97] has noted in the discharge without an incandescent cathode.

The observations with hydrogen in the absence of a discharge were in agreement with Langmuir's observations on the formation of atomic hydrogen.[98] Campbell observed, however, that in the presence of a discharge the rate of clean-up was much less than that obtained by purely thermal dissociation.

Very interesting phenomena were observed on passing a discharge in mercury vapor. In an otherwise thoroughly exhausted glass bulb, it was observed that under these conditions *hydrogen is liberated* from the walls. The fact that the discharge might evolve gas from the walls instead of causing it to disappear had already been noticed by Campbell as occurring to some extent in nitrogen, carbon monoxide, and argon. In the presence of mercury vapor this phenomenon was extremely marked.

---

[96] In *Trans. A.I.E.E.*, **32**, 1893 (1913), Langmuir has stated that "with voltages above 40 and pressures above 0.001 mm the nitrogen cleans up, provided the filament temperature exceeds 2000° K, and causes an attack on the negative end of the filament, producing a brown deposit of WN_2 on the bulb."

[97] *Ann. Physik*, **50**, 769 (1916).

[98] *J. Am. Chem. Soc.*, **37**, 1161 (1915).

And it should be noted that the gas thus liberated cannot be liberated by mere heating of the walls to their softening point; gas can be attached to the walls in some such way that it can be liberated by the discharge but not by heating. Of course, the attachment may consist of chemical combination; it is possible that glass contains hydrogen chemically combined, probably as water. But it should be observed that the hydrogen liberated, if piled up on the glass, would form a layer at least 25 molecules deep. Since the potential driving the discharge in these experiments was often as low as 50 volts, it is hardly to be expected that the electrons or ions could penetrate so far into the glass simply in virtue of the energy which they receive from the discharge. It seems easier to believe that a layer on the surface, subject to the action of these particles, is constantly renewed by diffusion from within.

The conclusions drawn by Campbell from these experiments were as follows:

(*a*) All gases can be made to adhere to glass by the discharge in such a way that part, at least, can be restored by heating the glass.

(*b*) The amount of gas that can be made so to adhere depends on the nature of the gas and on the state of the glass.

(*c*) The adhesion is not due primarily to chemical reaction, although such reaction (as in the conversion of CO to CO_2) may aid adhesion by converting the gas into another which adheres more readily.

(*d*) The discharge can also liberate gas from the walls, doubtless by bombardment of the charged particles, and some of the gas so liberated cannot be liberated by heating the glass to the softening point.

(*e*) The limit in the disappearance of the gas is reached when the rate at which gas is caused to adhere to the glass by the discharge becomes equal to the rate at which it is liberated by the bombardment.

That the clean-up effects are more pronounced in the presence of blue glow has been confirmed by work in this laboratory, but the rate of voltage clean-up in hot-cathode devices is quite appreciable even at very low pressures, as will be pointed out in a subsequent section. The actual values of the glow potentials as given in Fig. 13 are dependent on the geometry of the electrodes and size of bulb. For instance, blue glow in mercury vapor has been observed at as low as 18 volts, whereas the value obtained by Campbell at a pressure of 2 microns was 32.5 volts.

With regard to the relation between blue-glow potential and electron emission, Mrs. Andrews observed that in both argon and nitrogen the voltage required for the appearance of blue glow shows a tendency to decrease with increase in emission. At higher pressures it is possible to observe two glow potentials; at the lower of these, blue glow appears below the anode, and at the upper voltage the glow occurs both above and below the anode. Furthermore, with 250 volts on the anode, it was observed that the electron emission at which blue glow appeared varied approximately inversely as the pressure. Thus, at 45 microns of argon, the electron emission required to produce blue glow was about 0.15 ma, whereas at 4 microns the necessary emission was about 1.4 ma. In these measurements an ionization gauge was used, with the inner filament as cathode and the outer one as anode. At the same time the positive-ion current to the cylinder surrounding both filaments was measured, and it was observed that this current was approximately the same whenever blue glow appeared. This signifies that, for the appearance of glow in any device, it is apparently necessary to have a certain density of positive ions. This conclusion would also be in accord with the observation mentioned previously that the electron current required for blue glow to appear varies inversely as the pressure.

10. CLEAN-UP PHENOMENA IN VACUUM INCANDESCENT LAMPS

Very early in the development of the incandescent lamp it was realized that longer life could be obtained by improving the vacuum. On the other hand, it was evidently impractical from the point of view of cost to subject each lamp during the exhaust period to the rigorous treatment necessary to obtain a high vacuum. Actually, the pressure at which lamps were sealed off varied from as low as a few microns to 100 or even more.

In order to obtain a much better vacuum in the sealed-off lamps the method suggested by A. Malignani in 1894, which has been mentioned previously, was adopted. J. W. Howell and H. Schroeder[99] have described the process as follows:

> Malignani painted the inside of the exhaust tube of the lamp with red phosphorus. Then, when the filament was raised to high incandescence and the bulb was full of blue glow, he closed the connection between the pump and the lamp and heated the exhaust tube enough to vaporize the phosphorus. This drove the vapor inside the lamp, the blue glow disappeared and a good vacuum resulted.

This was the first recorded application of "getters."

The observations on electron emission and clean-up effects in hot-cathode tubes, discussed in the previous sections, obviously serve to explain, at least partly, the mechanism of the clean-up. The negative end of the filament emits electrons, and because of the high positive voltage on the other end of the filament ionization occurs and this is followed by clean-up.

The phenomena in vacuum tungsten lamps are similar to those observed in carbon lamps. In the older process the phosphorus was distilled into the lamp from a top tube with simultaneous flashing of the filament; the more recent process consists in coating the wire with an alcoholic suspension of red phosphorus and some salt (to prevent subsequent blackening by evaporated tungsten). After the lamp is exhausted and sealed off, it is flashed with gradually increasing voltage, and, as the phosphorus is volatilized from the filament, blue glow occurs and the residual gases are cleaned up.[100]

---

[99] *History of the Incandescent Lamp*, The Maqua Company, Schenectady, N. Y., 1927, p. 126.

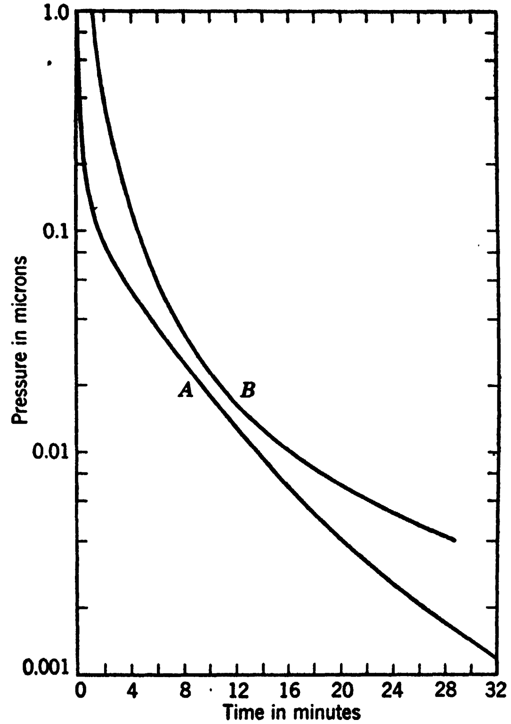

FIG. 14. Clean-up of residual air in 100-watt, 120-volt "ungettered" lamp. *A*, initial pressure 1 μ; *B*, initial pressure 5 μ.

Before discussing the theories that have been suggested in explanation of the function of phosphorus in cleaning up residual gases, it is of interest to mention some of the experimental results obtained by H. Huthsteiner and the writer on the rate of clean-up of gases in lamps under various conditions. Figure 14 shows the clean-up of residual air in a regular-type 100-watt, 120-volt lamp in which no phosphorus or other clean-up reagent was used. An ionization gauge attached to the lamp was employed to measure the pressure. Before introducing the air at a definite initial pressure, the lamp and ionization gauge were well exhausted by baking out at 360° C for 1 hour on the pump and flashing the filaments to a high temperature, thus eliminating gases occluded in the glass walls and filaments; the electrodes in the gauge were also well bombarded. Curve *A* shows the rate of clean-up with an initial pressure of 1 micron, and

---

[100] For similar observations see also S. Dushman, *Phys. Rev.*, **4**, 121 (1914); **5**, 212 (1915), and C. F. Hagenow, *Phys. Rev.*, **13**, 415 (1919).

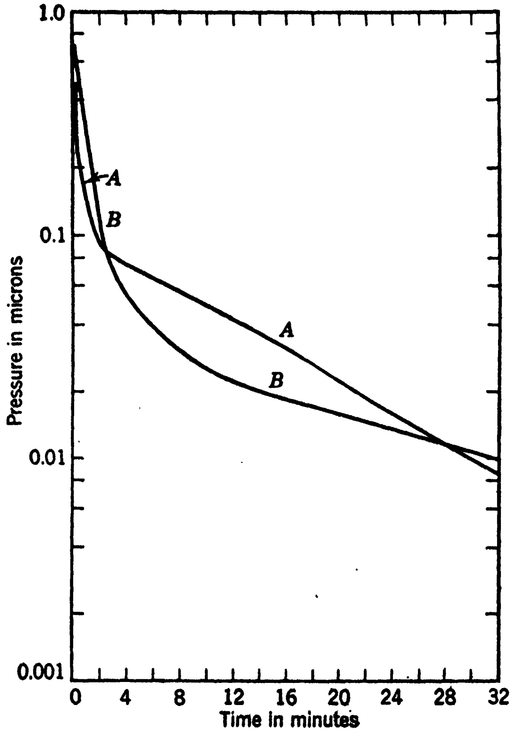

FIG. 15. Clean-up of residual air in 100-watt, 120-volt "gettered" lamp. *A*, initial pressure 10 μ; *B*, initial pressure 5 μ.

curve *B* with an initial pressure of 5 microns. The initial flash of blue glow disappeared in a fraction of a minute, and, as will be observed from the curves, most of the gas cleaned up in this period. The subsequent rate of clean-up was not so rapid. The flashing voltage used was 156 volts, corresponding to 130 per cent of the normal operating voltage.

Figure 15 shows the results obtained with a similar lamp in which red phosphorus served as getter. The lamp and gauge were exhausted as before, then air was admitted, the lamp removed from the pump, and a suspension of red phosphorus in alcohol painted on the leads just below the filament. The combination was then re-exhausted, given a 5-minute bake-out at 360° C, and sealed off. On flashing at 156 volts, the leads heated up sufficiently to volatilize the phosphorus and the clean-up curves shown in Fig. 15 were obtained.

In these cases, also, most of the gas cleaned up during the period of blue glow, as will be seen by comparing these results with those shown in Fig. 14; the initial rate of clean-up is much greater in the presence of phosphorus. In the lamp sealed off with air at 10 microns pressure, about 97 per cent of the gas disappeared in the first minute.

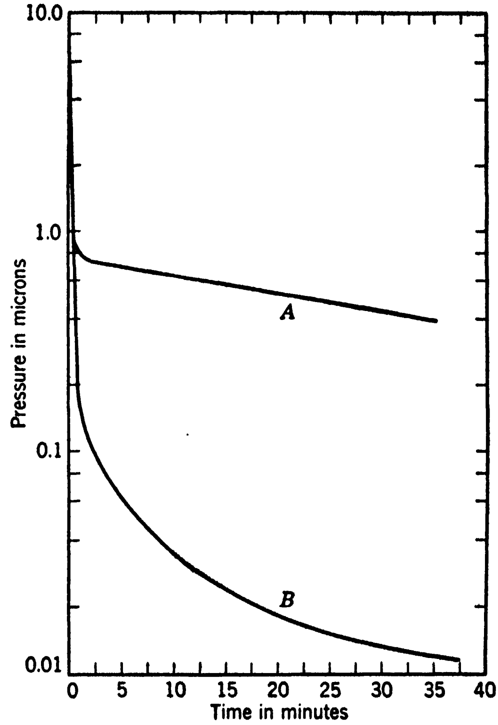

FIG. 16. Clean-up of argon (curve A) and of air (curve B) in 100-watt, 120-volt lamp gettered with phosphorus and flashed at 144 volts.

Figure 16 shows the difference in the rate of clean-up of argon and air. With argon (curve A) the initial pressure was 6.5 microns, and with air (curve B) the initial gas pressure was 4.5 microns. These observations also show the effect of phosphorus in accelerating the clean-up.

In general, over 90 per cent of the residual gas is cleaned up in a lamp during the blue-glow period, and the rate of clean-up during this time is much more rapid than that obtained subsequently. The final pressure attained on flashing varies from 0.01 to 0.001 micron. During life the pressure continues to decrease very slowly, and even after the filament burns out, there is no increase in pressure.

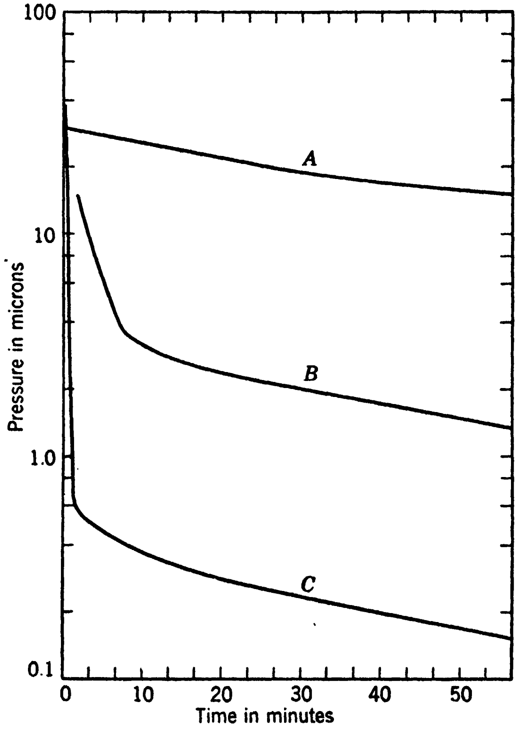

FIG. 17. Clean-up in two-filament diodes. Curve *A*, no red phosphorus, anode volts = 0; curve *B*, no red phosphorus, anode volts = 250; curve *C*, red phosphorus on leads of cathode filament, anode volts = 250.

Observations with different types of lamps have shown that there is no appreciable clean-up below 30 volts, but the rate of clean-up increases rapidly as the voltage is increased above this value and is extremely rapid in 220-volt lamps.

Any theory regarding the action of the phosphorus in incandescent lamps must primarily take into account the phenomena observed in hot-cathode devices. Figure 17 shows some results obtained with a two-filament diode (similar to that used in studying electrical clean-up effects without phosphorus) on the clean-up of residual air. Curve *A* served as the blank to take into account any purely chemical clean-up, while curves *B* and *C* show the effect of the presence of phosphorus. These observations show definitely that the phosphorus is most effective during the blue-glow period, as has already been emphasized in describing the clean-up phenomena in lamps. The similarity between curves *B* and *C* and those obtained in incandescent lamps also leads to the conclusion that the clean-up phenomena in the lamps and in hot-cathode devices must be quite similar in origin; that is, the reactions probably involve the formation of ions as an essential intermediate stage.

The action of phosphorus in a lamp is undoubtedly not very simple. It may be partly chemical, as probably some P_2O_5 is formed in the presence of residual oxygen and this would assist materially in eliminating water vapor and hydrogen. In some experiments carried out in this laboratory by Mackay and Huthsteiner it was observed that very large amounts of hydrogen could be cleaned up by the action of P_2O_5 vapor in a lamp and that a black deposit was formed on the walls. This deposit was assumed to consist of solid compounds of hydrogen and phosphorus, although no conclusive evidence for the assumption was obtained.

Also, as was mentioned in the discussion of clean-up effects at higher pressures, it is probable that under the influence of the discharge active modifications of the gases are produced which react readily with phosphorus. The fact that, according to Newman, phosphorus, sulfur, and iodine are most effective in cleaning up hydrogen, while these three substances have also been found to be very efficient "getters" in cleaning up residual gas in lamps, lends much support to this point of view.

Phosphorus itself is a very interesting substance chemically. As is well known, it exists in at least two forms at ordinary temperatures—the white and the red. The white, on being heated to just below 247° C, is converted into the red modification. The red form has an extremely low vapor pressure even at 300° C, whereas the white is quite volatile. Again, on passing a discharge through the vapor of white phosphorus it is converted into the red modification which deposits as a fine yellow to red coloration on the walls of the glass bulb. This phenomenon has been investigated very fully by V. Kohlschütter and A. Frumkin.[101]

Howell and Schroeder[102] in their discussion of the explanations that have been suggested for the getter action of phosphorus have remarked as follows:

> The residual gases in vacuum lamps, after sealing off, are, on the average, about 25 microns. In gettered lamps, this pressure will be reduced to less than 1 micron

---

[101] *Z. Elektrochem.*, **20**, 110 (1914).

[102] *Op. cit.*, p. 129.

> when the lamp has burned for a few seconds, provided the applied voltage is high enough. In lamps below 40 volts, the reaction is much slower and may be of a different nature. There is evidence that the reaction of the getter with the residual gas is not predominantly chemical, since such getters as phosphorus, silica, aluminum, or manganous oxide will, when applied to the filament as a getter, clean up such gases as hydrogen, nitrogen, carbon monoxide, carbon dioxide, oxygen, water vapor, and, to a lesser degree, argon, at about the same rate, and to about the same residual pressure, regardless of which getter or gas is used. Chemical action probably takes place between phosphorus and oxygen, and also water vapor. In addition to any action which may take place in the vapor phase, probably the most important reaction takes place on the bulb wall. When the lamps with phosphorus, silica, aluminum, or manganous oxide getter are burned, the getter having been thrown to the bulb wall and the gas having been cleaned up, a second clean-up can be obtained by admitting a small quantity of gas and again flashing the lamp. Only a limited quantity of gas can be made to disappear on a single coating of getter in this manner. It is believed that phosphorus has a continuing action during the life of the lamp in case any water vapor is liberated in its interior.
>
> The general conclusion is that the vacuum clean-up must be largely an adsorption, by the getter on the bulb wall, of gases activated in some manner by an electrical discharge of sufficiently high voltage. It is believed that the action of the phosphorus getter is solely to get and keep the vacuum, as it acts on gases only.

W. R. Whitney[103] has mentioned that arsenic, sulfur, and iodine act like phosphorus in cleaning up residual gases. In fact, any substance that can be sublimed readily can be used. The most plausible explanation would therefore be that (1) the vapor formed by volatilization of these substances assists in maintaining a glow discharge at lower residual gas pressures, and (2) the deposit formed by condensation of these vapors covers the gas driven into the walls (whether as positive ions or neutral dissociation products) and thus prevents any subsequent re-evolution of the absorbed gas.

An interpretation of the phenomena along these lines has been suggested by N. R. Campbell.[104] He found, in agreement with other investigators, that on passing a glow discharge through phosphorus vapor, it was converted into the red form, which deposits on the walls. Hydrogen, carbon monoxide, and nitrogen when mixed with phosphorus vapor cleaned up in the discharge very rapidly and in large amounts. An interesting observation (in accord with those made in this laboratory) was that "a lower final pressure can be reached with a given applied potential in the presence of phosphorus than in its absence." The explanation of this as given by Campbell is as follows:

> The absorption of gas ceases when the glow discharge ceases; and the glow discharge ceases when the falling glow potential becomes equal to the applied potential.

---

[103] *Trans. A.I.E.E.*, **31**, 1207 (1912).

[104] *Phil. Mag.*, **14**, 685 (1921).

> The admixture of phosphorus vapor with the gas increases the pressure corresponding to any given partial pressure of the gas and thus decreases the glow potential corresponding to that partial pressure. It therefore enables the discharge and the absorption of gas to continue when the partial pressure has fallen so low that, if the gas were present alone and its partial pressure were the total pressure, the potential applied could no longer be sufficient to maintain the discharge. When the partial pressure of the gas has fallen sufficiently, the phosphorus vapor, and not the gas, begins to disappear; and the disappearance of this vapor proceeds until the pressure of the phosphorus has fallen so low that the discharge can proceed no longer. And when the discharge ceases because the falling glow potential has become equal to the applied potential, it is not started again except by a very great increase of potential, owing to the wide difference between the falling and rising glow potentials in this vapor.

Furthermore, Campbell concluded that the reaction leading to the conversion of the phosphorus vapor into the red solid is reversible in the presence of the discharge. The equilibrium is pushed towards the vapor phase when the red phosphorus on the walls is bombarded by positive ions, so that

> as long as there is gas present in considerable quantity the conversion of white into red is never complete; there is always enough white phosphorus re-evaporating to maintain the discharge; and it is only when the gas has been greatly reduced in quantity that the equilibrium moves once more towards the solid phase, and a complete disappearance of all gaseous molecules is obtained.

This theory would account for the observation, often made in lamp practice, that clean-up effects can be made to occur in lamps in which red phosphorus is present on the bulb walls instead of on the leads or filament. The action would then be due to the bombardment of the red deposit by positive ions, with the resulting formation of a slight amount of vapor.

Regarding the chemical theory of the action of phosphorus, Campbell concluded that there is no evidence for any such theory and gave the following experimental observations to confirm this:

> (*a*) If the gas that has disappeared is restored, it is found to be in the same chemical state as it would have been if it had disappeared in the absence of phosphorus.
>
> (*b*) There is no simple relation between the quantity of gas that can be made to disappear and the quantity of phosphorus necessary for its disappearance. There is nothing approaching to a "law of constant proportions."
>
> (*c*) The amount of gas that will disappear depends very greatly on the surface condition of the walls of the discharge vessel.

As a working theory Campbell suggested that the red phosphorus covers the deposited gas and prevents it from being liberated again by bombardment. At the same time this red deposit provides a new surface on which gas can be absorbed. That the red phosphorus deposit adsorbs gas even in the absence of any discharge has been observed by the writer in a number of experiments.

From the point of view of this theory, it is therefore possible to account for the action of red phosphorus as used in lamp practice as follows: As is well known, the ordinary red phosphorus undoubtedly contains small traces of the white modification, as shown by the formation of P_2O_5 when it is exposed to air. Furthermore, when the glow discharge starts, some of the red phosphorus deposited on the walls becomes converted, as already stated, into the white form which volatilizes. This assists in maintaining the glow discharges at much lower residual gas pressures than is possible in the absence of phosphorus. The positive ions (or dissociation products, according to Hughes) formed in the discharge are driven into the walls and immediately become covered with the red deposit. The gas pressure is therefore reduced very rapidly and finally reaches a value at which no glow discharge can occur with the given applied potential.

E. Pietsch[105] has also mentioned, in this connection, the use of different salts, such as NaCl and NaF, in vacuum incandescent lamps. These salts, the evaporation of which results in a certain amount of clean-up, are also effective in preventing the evaporated tungsten from discoloring the glass walls.[106]

11. ELECTRICAL CLEAN-UP IN HOT-CATHODE TUBES AT VERY LOW PRESSURES

In all the earlier work discussed in the previous sections the clean-up was investigated at pressures in the range of 1 to 100 microns or even higher; the more recent work has dealt largely with voltage clean-up in the range 0.1 to 0.001 micron.

The arrangement used by W. v. Meyern[107] is shown in Fig. 18. It consisted of a tube with a tungsten filament cathode, K, and a platinum ring-shaped anode A, 2 cm in diameter. The discharge tube was set inside a solenoid (S) by means of which a field of 300 gauss could be obtained. Pressures were measured by means of an ionization gauge, and the voltage on the anode could be varied from 0 to 1000 volts.

In the presence of a magnetic field acting parallel to the axis of the tube the electron paths are elongated spirals, and consequently the electrons pass through the ring for a certain distance, then reverse their paths, and repeat this a number of times before they are collected by the anode. Hence the ionizing distance is very much greater than it would be in the absence of a magnetic field, and, as would be expected, the rate of clean-up is much more rapid in the presence of the magnetic field.

---

[105] *Loc. cit.*

[106] For discussion of the role of these salts, see L. Hamburger, *Proc. Royal Acad. Amsterdam*, **21**, 1062 (1919); **23**, 379 (1921); **25**, 463 (1923).

[107] *Z. Physik*, **84**, 531 (1933).

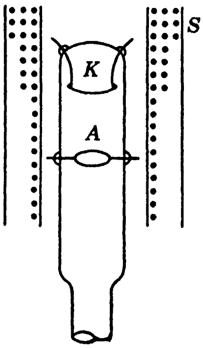

FIG. 18. Tube with hot cathode (K) and ring anode (A) in magnetic field produced by the solenoid (S). Clean-up observed in absence and also in presence of magnetic field (von Meyern).

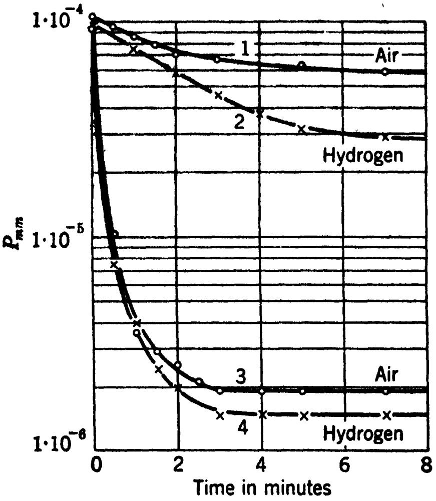

FIG. 19. Plot of P_{mm} (on log scale) versus time during clean-up of air and hydrogen in absence of magnetic field (curves 1 and 2) and in presence of magnetic field of 280 gauss (curves 3 and 4) (von Meyern).

Figure 19 illustrates the results obtained for air and hydrogen in the absence of a magnetic field (curves 1 and 2) and in the presence of a field of 280 gauss (curves 3 and 4). The initial pressure in all four cases was $1 \cdot 10^{-4}$ mm, and, as will be observed, the rate of clean-up in the presence of the field was approximately exponential during the first minute. The initial value of the electron current was 1.5 ma, and the anode potential was 820 volts for hydrogen and 900 volts for air. After the discharge was stopped the residual gas pressure remained at the low value for a while and then gradually increased to about $1.7 \cdot 10^{-5}$ mm in a period of several hours.

On heating the bulb to 200° C, all the absorbed gas was re-evolved; there was no appreciable absorption by the anode. A large fraction of the gas cleaned up in presence of a magnetic field was evolved if, after an equilibrium state was reached, the field was cut off. Evidently electrons striking the walls were able to remove gas previously absorbed.

The clean-up was found to improve with repetition of the sorption and desorption operations. If after cleaning up the gas from 10^{-4} to 10^{-6} mm, a fresh volume of gas was introduced at 10^{-4} mm, the rate of clean-up was decreased and the final equilibrium pressure increased. That is, the sorption phenomena exhibited fatigue effects. *In no case was the total amount of gas cleaned up more than a fraction of that required to form a monolayer on the walls,* and v. Meyern therefore concludes that all the observations can be interpreted, on the basis of Langmuir's views, as the establishment of an equilibrium between rate of condensation and rate of re-evaporation.

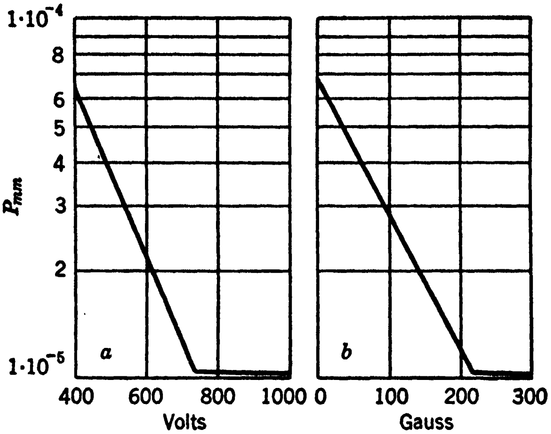

FIG. 20. Plot of final values of P_{mm} (on log scale) versus anode volts (*a*) and versus magnetic field (*b*) for clean-up of argon in tube shown in Fig. 18.

Confirming Campbell's conclusions, it was observed that clean-up occurred only at anode voltages in excess of the glow potential, V_g, which is defined by v. Meyern as that voltage at which the $V^{3/2}$ law (space-charge effect) is no longer followed. At this point the electron current increases rapidly, blue glow sets in, and clean-up occurs.

Since the value of V_g increases with decrease in pressure it is possible with a given anode voltage to clean up the gas to a point at which this voltage is equal to V_g, after which no further clean-up occurs. This could be observed only in the absence of a magnetic field. In the presence of a magnetic field it was observed that the electron current which could be drawn from the cathode (even on increasing its temperature) decreased to such a low value even with an anode voltage of 1000 that the rate of clean-up became very small. This decrease is due to the increased space-charge effect resulting from the presence of the magnetic field. In the absence of this field, the decrease in electron current with decrease in pressure was not observed.

These experiments on clean-up under the combined influence of high anode voltages and longitudinally directed magnetic fields were subsequently extended by v. Meyern[108] to helium, argon, and nitrogen in the range $5 \cdot 10^{-4}$ to $1 \cdot 10^{-7}$ mm. The same arrangement was used, but with a more sensitive ionization gauge. Before each set of observations on clean-up, the precaution was taken to bake out the tube for 1 hour at 360° C and for a short time at 400° C, in order to degas the glass walls as much as possible.

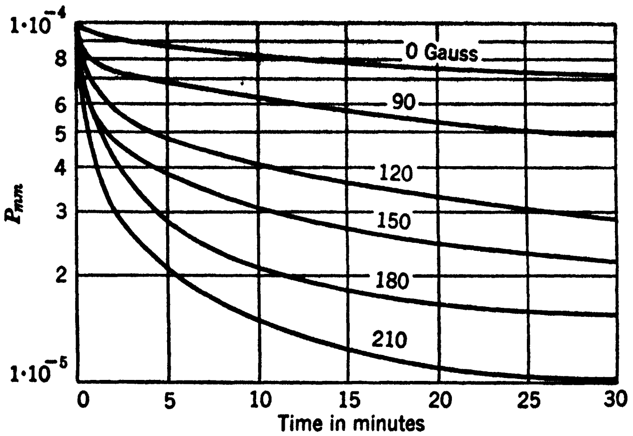

FIG. 21. Semi-log plots of pressure versus time for clean-up of argon at 800 volts at a series of values of the magnetic field (von Meyern).

Figure 20 shows the variation in the value of the final pressure obtained, as a function of (*a*) anode voltage and (*b*) magnetic field strength. These observations were made with argon, and the results obtained were similar to those for the other gases.

Figure 21 shows the rate of clean-up of argon at 800 volts as affected by variation in magnetic field strength. It was found that these curves could be represented very satisfactorily by the first-order rate equation

$$-\frac{dP}{dt} = k(P - P_e), \tag{1}$$

where P = pressure at any instant, P_e = equilibrium pressure, and k is a constant, the value of which depends upon the intensity of magnetic field and anode voltage. If we let P_i denote the initial pressure, then the integral has the form

---

[108] *Z. Physik*, **91**, 727 (1934).

$$\log\left(\frac{P_i - P_e}{P - P_e}\right) = \frac{kt}{2.303}. \tag{2}$$

The results obtained may be summarized as follows:

1. In the case of helium a slight clean-up (at an anode voltage of 800) was observed only in the presence of a magnetic field (240 gauss); argon was cleaned up at the same voltage even in the absence of a magnetic field. The fraction of the total surface of the tube covered with a monolayer, at equilibrium, increased from 0.37 to 3.1 per cent, with variation in initial pressure from $3.0 \cdot 10^{-5}$ to $4.0 \cdot 10^{-4}$ mm. At the same time, the equilibrium pressure varied from $1.33 \cdot 10^{-5}$ to $2.73 \cdot 10^{-4}$ mm.
2. In the absence of a magnetic field, and at the same anode potential, the clean-up of nitrogen was greater than that of argon. The fraction of the surface covered at equilibrium increased from 2.3 to 8.7 per cent, with increase in initial pressure from $1.0 \cdot 10^{-4}$ to $4.3 \cdot 10^{-4}$, and the equilibrium pressure varied from $7 \cdot 10^{-6}$ to $7.2 \cdot 10^{-5}$ mm.
3. In the presence of a magnetic field (240 gauss) all rates of clean-up were increased; the values of the total fraction of the surface were higher, varying from a maximum value of the fraction of the surface covered of 1.8 per cent for helium to 9.5 per cent for nitrogen, and the values of the equilibrium pressures attained were lower than in the absence of a magnetic field.
4. If the magnetic field was cut off, after clean-up had taken place, there was a considerable desorption of the glass walls due to electron bombardment.
5. The quantity of gas cleaned up was found to be proportional to the initial pressure.

More recently a comprehensive investigation of clean-up at pressures below 0.1 micron has been reported in two papers by H. Schwarz.[109] In the first of these the clean-up is shown to be dependent on negative charges on the glass walls. The walls become charged negatively by secondary emission, the efficiency of which increases with the energy of the primary electrons, and is lower, for the same electron energy, from a well-degassed surface than from one that is covered with a layer of gas. The positive ions are driven into the glass walls by the field, and it was found that in some cases the glass walls adsorb as much as 1.7 times that required to form a monolayer. It was furthermore observed that in a tube with metal walls no clean-up occurred.

[109] *Z. Physik,* **117,** 23 (1940); **122,** 437 (1944).

The second paper deals with clean-up in an ionization gauge, at very low pressures. Not only may positive ions be driven into the walls, but also these positive ions can drive out gases already sorbed in the walls, thus changing the composition of residual gases.

The electrical clean-up is intensified, as Schwarz has demonstrated, by increasing the ratio (i_p/i_e) of positive ion current to electron current for a given pressure. This may be accompanied either by change in design of gauge or by placing the gauge in a magnetic field, which increases the length of the electron paths.

The construction of gauge used in this investigation is shown in Fig. 22. The positive-ion collector was a cylinder made of sheet nickel 0.1 mm thick, 2 cm in diameter, and 3 cm long. The grid consisted of 18 turns of 0.3-mm-diameter nickel wire, wound in a spiral 0.75 cm in diameter and 3 cm long. Finally, the cathode, which was located along the common axis of both cylinder and grid, was a tungsten wire 0.2 mm in diameter and 5 cm long, connected to the leads H. The collector was maintained at -5 volts, and the grid at $+110$ volts, with respect to the negative end of the cathode. The temperature of the cathode was maintained at a value required to emit 1 to 2 ma electron current.

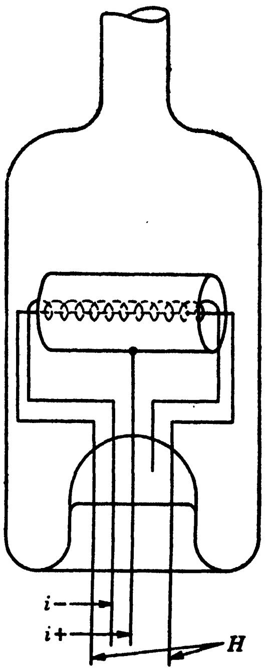

FIG. 22. Design of ionization gauge used in investigation on clean-up of gases at very low pressures (Schwarz).

In the case of *hydrogen*, there was observed a decrease in pressure, in 3 minutes, from 1.55 micron to $1.5 \cdot 10^{-2}$ micron, which resulted from dissociation in contact with the hot filament in the absence of any electron current. In the case of *argon* and in that of *nitrogen* clean-up occurred only when ionization was produced by the electrons from the hot cathode.

Another phenomenon, mentioned above, which was observed in these experiments, was that of *interchange* of molecules between the gas in the space and that already adsorbed on the walls. This was recognized by the change in the value of i_p/i_e at constant pressure, the pressure being measured by a Gaede molecular manometer. In one experiment nitrogen was cleaned up by successive introduction of fresh samples until complete saturation was attained at a pressure of a few tenths of a micron.

The gauge was then thoroughly evacuated and argon introduced at a pressure of 0.421 micron. Although the pressure as read by the molecular manometer remained practically constant, the value of the ratio i_p/i_e changed continuously, in such a manner as to indicate a substitution of argon for nitrogen in the walls, and finally most of the gas in the gauge consisted of nitrogen.

In another experiment there was an interchange in the opposite direction. Argon was cleaned up until the electrodes and glass walls were saturated. Then nitrogen was introduced, and it was found from the variation in the value of i_p/i_e, at constant pressure, that nitrogen was actually replacing the adsorbed argon, so that finally the gas in the gauge consisted almost wholly of argon.

On the basis of these observations Schwarz has drawn the conclusion that the ionization gauge is unreliable for the measurement of very low pressures. This conclusion is undoubtedly valid if the gauge is used to measure the pressure in a small volume. As pointed out, however, in Chapter 6, section 8, it is possible in general, by operating the gauge for very brief periods, to reduce to a minimum effects due to both chemical and electrical clean-up and thus to obtain data that are fairly reliable.

12. PRODUCTION OF EXTREMELY LOW PRESSURES IN SEALED-OFF DEVICES

In certain types of investigations, such as those dealing with thermionic and photoelectric emission, contact potentials, and secondary electron emission, it is absolutely essential to obtain surfaces that are as clean as possible. It is also necessary to maintain such a good vacuum that these surfaces shall not be contaminated by traces of residual gases, at least for a sufficiently long period to make certain that the observed data are characteristic of the clean surface.

Even at as low a pressure as 10^{-6} micron, the rate at which oxygen molecules at room temperature strike a surface is $3.6 \cdot 10^{11}$ molecules per cm^2 per sec. Assuming that the number of molecules required to form a monolayer is $8.26 \cdot 10^{14}$ (as indicated in Table 7.25), and that every molecule incident on the surface is adsorbed, 10 per cent of the surface would become covered with a layer of oxygen molecules in about 3.8 minutes. A contamination of this magnitude would decrease the photoelectric emission by a factor of the order of 10, at least, and thus lead to quite erroneous observations.

In the preceding chapters it has been shown that glass and all metals contain considerable amounts of dissolved gases (as well as adsorbed gases) and that the rate of evolution of these gases under vacuum conditions increases exponentially with the temperature. Some metals are more "gassy" than others, and in order to liberate the gas it may be necessary to heat them to temperatures at which the rate of volatilization is appreciable.[110] As emphasized in section 2 above, deposits obtained by volatilization may serve a very useful purpose as getters. But for proper functioning the getters should be preheated in order to eliminate any dissolved gases.

It should be borne in mind that the ultimate pressure obtained in any device represents an equilibrium state between the rate at which gas is evolved from glass walls and metal parts, and the rate at which these gases are removed, either by adsorption or pumping. Hence it is of extreme importance to take every precaution in investigations such as these under discussion to treat all parts of a system or device, while under exhaust, in such a manner that subsequent evolution of gases will be reduced to the minimum.

The story of the development of a vacuum technique adequate for the purpose mentioned begins with the epoch-making investigations of Langmuir and his associates, in 1912–1913. At that time a considerable number of physicists believed that electron emission from an incandescent metal surface at low pressures is due to the presence of residual traces of gas and that consequently this thermionic emission should disappear in a very good vacuum.[111]

In order to demonstrate the existence of a pure thermionic emission and the validity of the space-charge relation, Langmuir[112] used a bulb containing two hairpin tungsten filaments either of which could serve as electron emitter and the other as anode. During exhaust (by means of a Gaede rotary mercury pump) the bulb was heated for 1 hour at 360° C, which was as high a temperature as was practical without deformation of the bulb by atmospheric pressure. A liquid-air trap was placed between bulb and pump. The filaments were heated to 2700–2800° K in order to degas them, and the bulb was sealed off. In order to improve the vacuum, the filaments were aged at 2400° K for about 24 hours, which served to clean up the residual oxygen and nitrogen. "To still further improve the vacuum in some cases," Langmuir states, "the entire bulb was immersed in liquid air and the filaments again heated to high temperature for a short time." As shown subsequently by the writer,[113] observations taken with the molecular gauge indicated that the lowest pressure obtained in Langmuir's experiments was certainly well below about $4 \cdot 10^{-4}$ micron.[114]

---

[110] This topic is discussed at length in Chapter 11.

[111] The writer, who was associated with Dr. Langmuir at this time, could relate many amusing incidents regarding the ideas of some "famous" scientists and their reactions towards the results published at that period from this laboratory.

[112] *Phys. Rev.*, **2**, 450 (1913).

[113] *Phys. Rev.*, **5**, 212 (1915). See Chapter 6, section 4.

This technique which involves heating the glass during exhaust for 1 or more hours at about 360° C for soft glass (and at 500° C for Pyrex), heating the electrodes either by passage of current in the case of filaments or by electron bombardment to as high a temperature as practicable, sealing off the pump, and improving the vacuum in the sealed-off device by chemical or electrochemical clean-up—this procedure for obtaining a good vacuum became recognized practice.

One other contribution made by Langmuir to high-vacuum technique was the demonstration (discussed in Chapter 8) that in order to remove water vapor efficiently from the walls of glass vessels the heating during exhaust should be carried out in two or more stages of gradually decreasing temperatures. In that connection mention should also be made of Langmuir's suggestion regarding the heating of the glass bulb, to temperatures above those used normally, in a vacuum furnace, in order to prevent collapse of the walls.[115]

The procedure described above was applied by Langmuir in his investigations on electron emission from thoriated tungsten,[116] in which, in order to eliminate the effect of residual gases, the pressure had to be reduced to a value even below that required for observations on the emission from pure tungsten. In this case the improvement in vacuum was obtained by prolonged evaporation of tungsten at 2900° K with the bulb immersed in liquid air.

A slightly modified procedure was used by S. Dushman, H. N. Rowe, Jesse Ewald, and C. A. Kidner in their investigation on the thermionic emission from tungsten, molybdenum, and tantalum.[117] The tubular bulbs containing hairpin filaments were baked out during exhaust for 1 hour at 360° C. After the bulbs were cooled, the filaments were flashed for several minutes at temperatures just below those of noticeable volatilization (2700-2800° K for tungsten) and then maintained at slightly lower temperatures for 1 hour. Calcium was then volatilized from a spiral tungsten filament surrounding the metal. This formed a deposit on the walls and functioned, by means of flush seals in the glass, as anode.

---

[114] This corresponded approximately to the lowest pressure that could be measured by means of the gauge.

[115] U. S. Patent 994,010. This furnace is described by O. W. Richardson, *The Emission of Electricity from Hot Bodies*, Longmans, Green and Company, London, Second Edition, 1921.

[116] *Phys. Rev.*, **22**, 357 (1923).

[117] *Phys. Rev.*, **25**, 338 (1925).

After seal-off the filaments were aged at 2400° K for 24 hours and emission data were taken with the bulb immersed in liquid air.

For the determination of contact potentials between tungsten and adsorbed films of cesium and thorium on tungsten and oxygen-tungsten surfaces, Langmuir and K. H. Kingdon[118] used a tube containing two loop filaments surrounded by two cylindrical anodes. All metal parts were outgassed at high temperatures, and the observations were made with the tube immersed in liquid air.

We shall now consider some of the most recent publications which contain detailed descriptions of the technique used for obtaining very high vacuum.

In order to determine as accurately as possible the contact difference of potential between tungsten and barium and the electron-emission work function for barium, P. A. Anderson[119] developed a method for outgassing the surface by which highly reproducible measurements could be obtained.

The method of measurement may be described briefly as follows: A beam of low-velocity electrons was directed by an electron gun against a small area near the center of a strip of tungsten foil, and the current to the foil was plotted as a function of the retarding potential applied to the strip. As Anderson states,

> Any change in the work function of the (tungsten) surface, whether due to readsorption of gas or to the deposition of another metal, produces a shift of the straight-line portion of the curve by an amount equal to the contact difference of potential between the initial and final states of the surface.

An oven of molybdenum foil in which metallic barium could be vaporized was arranged in such a manner as to direct a stream of the vapor against the tungsten surface.

The procedure used for evacuation of the tube and preparation of the surfaces is described as follows:[120]

> During outgassing the tube was connected with a conventional pumping system which consisted of, numbering from the tube, *two liquid-air traps* in series, carbon dioxide trap, McLeod gauge, and Gaede two-stage mercury diffusion pump. There were, of course, *no waxed or greased joints between pump and tube.* The liquid-air trap nearest the tube showed no trace of condensed mercury at any time. *Before the barium was put into the oven* the tube was baked at 500° C for at least 48 hours and the metal parts were given a preliminary heating. The tube was then opened (at a sealed-off tip provided for this purpose), about 1.5 grams of barium placed in the oven, and the

---

[118] *Phys. Rev.*, **34**, 129 (1929).

[119] *Phys. Rev.*, **47**, 958 (1935).

[120] The features in this description which the writer considers of special importance from the point of view of vacuum technique are italicized.

> tube quickly sealed off and evacuated.... After re-evacuation the oven was glowed and the barium melted down thoroughly. The tube was then *baked again* for at least 60 hours at 350° C (a slow distillation of barium which destroys the insulation in the tube seems to occur at 500° C) and all of the tungsten strips were flashed intermittently.

Besides the test tungsten strip mentioned above there were two strips which surrounded the cathode in the electron gun. The maximum temperature used for the latter was 2200° K, while the test strip was flashed at 2800° K.

> During these treatments the molybdenum support wires became white hot and the tungsten leads themselves probably were heated sufficiently to effect a superficial heating of their surfaces. The tube was sealed from the pump while still hot and a fresh coat of barium immediately deposited on the walls of the oven chamber.
>
> The final cleaning of the tungsten ribbon was accomplished *after sealing off and immersing the tube in liquid air.*

After taking a series of measurements on the clean tungsten surface it was turned about an axis in order to receive the barium vapor jet emitted from the oven. Anderson states,

> In practically all cases the work function of a fresh barium film remained constant to within a few millivolts for periods of at least 20 or 30 minutes and continuation of the observations on a single film for an hour or more has failed to discover variations greater than this.

In order to measure the contact difference of potential between barium and silver, the procedure adopted by Anderson[121] was to evaporate films of each of these metals from separate ovens. He states,

> In work function investigations of the intermediate-melting-point metals (e.g., silver, copper, gold) by thermionic, photoelectric, and contact potential methods it has been customary to study massive specimens of the metals and to rely on prolonged heating for the outgassing and cleaning of these specimens. Consideration of the vapor-pressure curves for these metals and for the metallic salts and oxides which must be assumed to be present on the most carefully handled specimens (the oxides and salts of the alkali and alkaline-earth metals which are most likely to be present are especially effective in vitiating results and have, also, especially low vapor pressures) forces the conclusion that it is impossible to clean a massive specimen completely by such treatment no matter how it is prolonged. Our methods of measurement have been based, therefore, on the premise that it is possible to secure clean surfaces of these metals *only by fractional distillation in an adequate vacuum*, where an "adequate vacuum" is defined as one for which the rate of deposition of residual gas on the surface is so low as to produce no measurable change in the work function of that surface in the time required for its preparation and measurement.

As in the preceding investigation the tube was given a preliminary bake-out at 500° C for 48 hours, during evacuation.

---

[121] *Phys. Rev.*, **49**, 320 (1936).

> At intervals during this baking the electron gun was subjected to high-frequency heating at 1000° C or higher and the ovens were flashed at about 2000°. The tube was then opened, the silver and barium quickly introduced, and the tube reclosed and immediately re-evacuated. It was then subjected to seven or eight bakings of 8 hours each at about 350° C, between which were interspersed high-frequency heatings of the electron gun, flashings of the ovens at temperatures sufficient to melt down the barium and silver, and flashings of the electron emitter at temperatures well above its normal operating temperature. The tube was sealed from the pumping system while still hot and a fresh coat of barium immediately vaporized to the walls of the tube.

The measurements were taken with the tube immersed in liquid air, and, after the emitter had been operated long enough to establish steady emission, the barium oven was flashed to deposit a film of this metal. The reproducible characteristic data for this film having been obtained, the silver oven was flashed and the characteristics of the film of this metal were determined.

For the measurement of the contact difference of potential between barium and magnesium[122] Anderson adopted a design of tube somewhat more complicated than the tubes used in the two previous investigations, but the exhaust procedure was quite similar, except that an oil diffusion pump was used instead of a mercury pump. The tube was protected from oil vapors by *two long charcoal traps in series.* He states,

> These traps were of a new design[123] which permits heating the charcoal to incandescence in an all-Pyrex system. The behavior of this tube was indistinguishable from that of the others which were pumped with mercury vapor and protected by double liquid-air traps.

In a fourth publication,[124] dealing with the contact difference of potential between barium and zinc and the determination of the external work function for zinc, Anderson has emphasized the advantage of using *the emission from a pure tungsten surface as a criterion of good vacuum.* He states,

> It has been found in numerous published and unpublished results in this laboratory that tungsten, cleaned by flashing to 2800° K and then allowed to cool, invariably shows a drift of work function, but that, in well-gettered tubes, this drift does not become measurable until several minutes after flashing. In tubes immersed in liquid air the drift may be postponed for as much as 20 minutes.

The rate of deactivation of a thoriated-tungsten filament has been used in a similar manner by W. B. Nottingham[125] as a measure of the magnitude of the residual gas pressure, in connection with an investigation of the characteristics of willemite under electron bombardment. The experimental tube contained three cylindrical anodes with a common axis along which was located the thoriated filament. The two outer anodes were used as "guard rings," while the central anode had two small openings located opposite to each other. In one of these openings was placed a small glass plate on which the phosphor had been settled, while the other opening was used as a window for measuring the intensity of the luminescence produced by bombardment of electrons from the filament.[126]

---

[122] *Phys. Rev.*, **54**, 753 (1938).

[123] *Rev. Sci. Instruments*, **8**, 493 (1937). See Chapter 5, section 4.

[124] *Phys. Rev.*, **57**, 122 (1940).

[125] *J. Applied Phys.*, **8**, 762 (1937); also see *Phys. Rev.*, **55**, 203 (1939).

The procedure for evacuation was similar in many respects to that followed by Anderson. The metal parts were given a preliminary heat treatment, and the tube itself (made of Pyrex) with seven single lead tungsten-to-glass seals was connected to an exceptionally good vacuum system for the preliminary baking of 3 or 4 hours at 500° C.

The tube was then cracked open and the metal parts assembled on the leads. After inserting the test plate covered with the phosphor, "eight to ten aluminum-barium getter pellets[127] were welded in the form of a ring and mounted in a side tube."

As Nottingham states,

> After the tube was completely assembled and sealed back together at the "crack-off," the exhaust schedule lasting between 10 and 30 hours was started. After a 1-hour bake at 500° C and about 3 hours at 470° C, *during which time the liquid-air trap and the connection between it and the tube were also baked at the same temperature,*[128] liquid air was put on the trap and following this the "tube oven" and the "connection oven" were removed. The filament was then flashed and activated and the bombardment of the anodes begun. This was continued until a vacuum of the order of 10^{-8} mm of mercury was obtained with the first anode nearly at a "white heat" and the getter ring at as bright a red as was considered the maximum which would not explode the getter. During the early stages of heat treatment it was found that the gas given off rapidly deactivated the filament, as indicated by a considerable decrease in electron emission. The time required to bring about this deactivation served as a better indication of the condition of the tube than any measurements which could have been made with an ionization gauge. The tube was operated at about ten times the normal maximum load during this heat treatment in that 10 to 15 ma of electron current flowed from the filament to the anodes with a difference in potential between the filament and these collectors of 10,000 volts. . . . When it was found that under these conditions the filament remained well activated for a period of an hour

---

[126] The actual construction of the tube was more complicated than described in this discussion, but, in view of the fact that the topic of interest is the vacuum technique used, further details have been omitted.

[127] These were type C-400 barium-aluminum getters furnished by King Laboratories, Syracuse, N. Y. Nottingham states that these pellets "were found to be particularly satisfactory since they will withstand baking at 500° for long periods of time without appreciable evaporation before firing."

[128] Italicized by the writer.

or so, *the seal-off capillary was softened* and the getter ring heated to explode the getter. The tube was finally sealed off after another hour or so of heat treatment and pumping. After this rather vigorous exhaust schedule, the tube could be operated indefinitely at 10,000 volts with as much as 1 ma of current to the anodes without appreciable loss of activity of the cathode surface.

In connection with the exhaust, in this laboratory, of small Coolidge tubes it was observed that it was extremely important to give the seal-off constriction a prolonged torching before seal-off.

As is evident from the preceding discussion it is most important, in order to obtain as good a vacuum as possible, to give the glass a bake-out, and this should, preferably, be carried out over a prolonged period interrupted by periods of cooling. It is equally important to heat all metal parts to as high a temperature as possible, short of evaporation.

As mentioned in the previous chapter, it was demonstrated by Norton and Marshall that, after heating tungsten and molybdenum to a high temperature either in a vacuum or, preferably, *in an atmosphere of very pure, dry hydrogen,* these metals could be exposed to the atmosphere without adsorbing any considerable amount of gas. In fact, as will be discussed more fully in Chapter 12, a high-temperature treatment of metal parts in pure, dry hydrogen, when such treatment does not result in embrittlement (see preceding chapter), saves a good deal of time in the subsequent evacuation of devices containing these parts.

There are some other features in the exhaust procedures described above which should be emphasized strongly. One is the avoidance of waxed joints and stopcocks. If necessary, a stopcock should be introduced between the vapor pump and the mechanical pump. For introducing gas into a high-vacuum system a barometric mercury cut-off, with liquid-air trap between this and the system, should be used.

A second feature is the use of two liquid-air traps in series, so that the one nearest the experimental tube can be given a bake-out along with the tube.

Figure 23 shows a diagrammatic sketch of an exhaust system which has been designed and used by L. Apker, in this laboratory, in connection with an investigation on the work functions of semiconductors. The dashed rectangles indicate ovens that can be arranged to bake out different parts of the system. The following exhaust procedure, used by Apker, is based on the investigations carried out by Nottingham on high-vacuum technique.

Initially the tube *A*, gauge *G*, and the liquid-air traps *Tr*-2, and *Tr*-1 are given a prolonged bake-out at 500° C. Then the two lower ovens surrounding *Tr*-1 are removed, liquid air is put around it, and the bake-out is continued for a longer period on the rest of the system. At the end of this treatment, the upper oven is removed, all metal parts are heated by high-frequency and electron bombardment, and the tube is again heated at a moderate temperature.

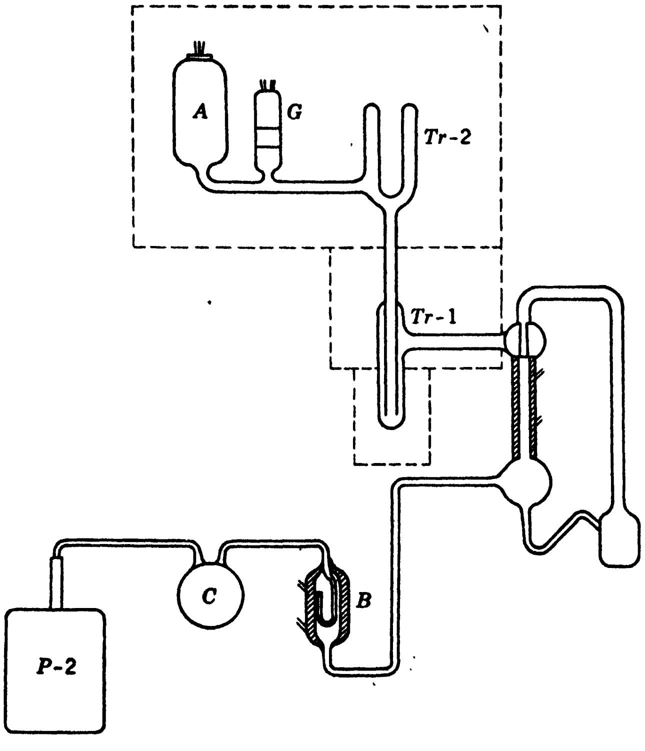

FIG. 23. Diagrammatic sketch of exhaust system for production of extremely low pressure (Nottingham, Apker). *A*, tube to be evacuated; *G*, ionization gauge; *Tr*-1 and *Tr*-2, liquid-air traps; *P*-1, mercury-vapor pump; and *P*-2 rotary oil pump. The bulbs *B* and *C* are used to prevent diffusion of oil vapor into the mercury-vapor pump.

If the tube is to be operated on the exhaust system, liquid air is applied to *Tr*-2 immediately after the last bake-out. If, however, the tube is to be sealed off, the constriction is heated to near the softening point of the glass for about 15 minutes, and pumping is continued for a couple of hours, with the tube hot. The getter is then flashed, liquid air is applied to *Tr*-2, and the tube is sealed off.

The pressure in a well-evacuated tube, as computed from the calibration of the ionization gauge with nitrogen, is approximately 10^{-8} mm of mercury.

It should be observed that the pump P-1 is of the type shown in Figs. 4.26 and 4.27. The bulbs B and C are used to take care of any oil that might back up from the mechanical pump P-2.

Apker has expressed the opinion, which is in agreement with earlier statements by Anderson and Nottingham, that *the constancy of emission from a clean tungsten surface is an even more sensitive indication of vacuum conditions* in the system *than the ionization gauge.*

CHAPTER 11

VAPOR PRESSURES AND RATES OF EVAPORATION

1. THERMODYNAMICAL RELATIONS

In connection with investigations and industrial developments in the field of high vacua, a knowledge of the vapor pressures of the materials used is often of great importance. Whether the problem concerns metals operated at high temperatures or gases and vapors at very low temperatures, information on the vapor pressures and rates of evaporation is frequently essential in order to be able to interpret results observed and also to guide the experimenter in the choice of metals for specific temperature requirements.

In discussing the available data on materials of interest in high-vacuum technique it has appeared to the writer to be most convenient to present this information in two sections. The first one deals with vapor pressures of metals and carbon, that is, mostly those materials which evaporate at appreciable rates only at temperatures above the normal range. The second one is devoted to a consideration of the vapor pressures of condensible and "non-condensible" gases at temperatures below the normal range. Thus, the data presented in the first part of this chapter are of interest in vacuum metallurgy, and in those investigations where it is desirable either to raise the temperature to as high a value as possible without obtaining appreciable evaporation or to actually evaporate some of the metal to form a thin deposit. On the other hand, it is of interest in using low-temperature traps to know the vapor pressures, at these temperatures, of gases which it is desired to eliminate from the vacuum system. Such data are presented in the second part of this chapter.

The methods that have been followed for the determination of vapor pressures have been described fully both in treatises on the subject of physical measurements and in a large number of publications. These methods differ according to the range of pressures under investigation and according to the volatility of the material in the temperature range under investigation. Of special interest in high-vacuum work are data on the temperatures corresponding to vapor pressures below 1 mm of mercury. For this reason most of the data given in this chapter are applicable to this range of pressures.

The methods for the determination of vapor pressures of metals have been reviewed by R. W. Ditchburn and J. C. Gilmour (2).[1] Most of them are based upon the application of Knudsen's relation for the rate at which molecules strike a surface, and some of these applications have been discussed in Chapter 1, section 6. The methods for the determination of low vapor pressures of oils have been discussed in a paper by F. H. Verhoek and A. L. Marshall.[2]

For highly refractory metals, such as tungsten, molybdenum, tantalum, and columbium, the vapor pressures have been deduced from determinations of the rate of loss in weight of filaments at constant temperatures. For these metals the principal problem has been the accurate determination of the temperature. An illustration of the extreme precautions that must be taken to secure such accuracy is given in the paper by A. L. Marshall, R. W. Dornte, and F. J. Norton (6) on the evaporation of iron and copper.

As will be discussed more fully in the following chapter, the most reliable method for correlating experimental observations on vapor-pressure data is based on the calculation of a function known as the *free energy*. Denoting this function by ΔF, the vapor pressure in *atmospheres* may be derived from values of ΔF (calories per g-mole) by means of the relation

$$\log P_{atm} = -\frac{\Delta F}{4.574T}. \tag{1}$$

In terms of other units of pressure, equation 1 takes the forms

$$\log P_{mm} = 2.8808 - \frac{\Delta F}{4.574T}, \tag{2a}$$

$$\log P_{\mu} = 5.8808 - \frac{\Delta F}{4.574T}, \tag{2b}$$

and

$$\log P_{\mu b} = 6.0057 - \frac{\Delta F}{4.574T}. \tag{2c}$$

In the range of vapor pressures below about 1 mm of mercury it has been observed that, for most materials, the vapor pressure can be represented as a function of T by the relation

---

[1] The numbers in parentheses in sections 1 and 2 refer to items in the list of references following Table 2.

[2] *J. Am. Chem. Soc.*, 61, 2737 (1939). See Chapter 6, section 3.

$$\log P = A - \frac{B}{T}, \tag{3}$$

where A and B are constants.

Comparing this relation with the first three equations it follows that, in the low-pressure range,

$$\Delta F = L_0 - IT, \tag{4}$$

where L_0, the latent heat of evaporation at $T = 0$, is determined by the relation

$$L_0 = 4.574B, \tag{5}$$

and I is an integration constant. Since I is usually expressed in terms of the pressure in atmospheres,

$$A = \log x + \frac{I}{4.574} \tag{6}$$

where x = conversion factor from atmospheres to the particular unit of pressure in which it is desired to express P. Thus, in equation 2*a*, $\log 760 = 2.8808$.

The great advantage of equation 3 is that it makes it possible to calculate very readily values of T corresponding to given values of P by means of the relation

$$T = \frac{B}{A - \log P}. \tag{7}$$

From the values of P, the rate of evaporation can be derived by means of the following equations:

Let W = rate of evaporation in $\mathrm{g \cdot cm^{-2} \cdot sec^{-1}}$, and M = gram-molecular weight. Then,

$$\log W = \bar{5}.6410 + 0.5 \log M + \log P_{\mu b} - 0.5 \log T \tag{8a}$$

$$= \bar{5}.7660 + 0.5 \log M + \log P_{\mu} - 0.5 \log T \tag{8b}$$

$$= C - 0.5 \log T - \frac{B}{T}, \tag{9}$$

where

$$C = A\,(\text{microbars}) + 0.5 \log M + \bar{5}.6410 \tag{10a}$$

$$= A\ (\text{microns}) + 0.5 \log M + \bar{5}.7660. \tag{10b}$$

Let μ = rate of evaporation in number of molecules or atoms per square centimeter per second. Then

$$\log \mu = 19.4208 + \log P_{\mu b} - 0.5 \log (MT) \qquad (11a)$$

$$= 19.5458 + \log P_{\mu} - 0.5 \log (MT) \qquad (11b)$$

$$= 23.7798 + \log W - \log M. \qquad (12)$$

For those metals for which *rates* of evaporation have been determined directly and can be represented by a relation of the form

$$\log W = A_1 - \frac{B_1}{T}, \qquad (13)$$

the values of the vapor pressure, in microns, have been calculated by means of equation 8*b*, that is,

$$\log P_{\mu} = 4.2340 + \log W + 0.5 \log \frac{T}{M}. \qquad (14)$$

From a plot of values of log P versus $1/T$ it was then possible to calculate values for the constants A, B, and C in equations 3 and 10*b*.

Since $P_{\mu b} = 1.333P_{\mu}$

$$\log P_{\mu b} = 0.1250 + \log P_{\mu}. \qquad (15)$$

In the tables in the following section *values of P are given in terms of microns.*

2. VAPOR-PRESSURE DATA AND RATES OF EVAPORATION FOR METALS AND CARBON

Until recently the most authoritative publication on this topic has been that by Kelley (1), which gives calculations of the free energy as a function of the temperature for all the metals for which data were available in 1935. Subsequently Ditchburn and Gilmour (2) published vapor-pressure data, based largely on further observations made between 1935 and 1941. In attempting to prepare tables of data for use in the present connection the writer based his conclusions largely on Kelley's calculations, modified in respect to certain metals by references mentioned in the publication by Ditchburn and Gilmour and in other sources.

However, unknown to the writer, Leo Brewer and a number of collaborators had prepared a report,[3] in connection with the war effort, in which all the available data had been reviewed with a great deal of care.

---

[3] The writer is indebted to Dr. W. M. Latimer for sending him a copy of the report, designated as number 3 in the list after Table 2.

This report gives values not only of the thermodynamic functions (total energy, entropy, free energy, etc.) but also of the temperatures in degrees Kelvin corresponding to the following range of values of P_{atm}: 10^{-6}, 10^{-5}, 10^{-4}, 10^{-3}, 10^{-2}, and 1 (that is, 0.76 μ, 7.6 μ, 76 μ, 0.76 mm, 7.6 mm, and 760 mm respectively). For a number of the metals there is excellent agreement between these values of T and those given by Kelley; for other metals, for which there are absolutely no observations available either on rates of evaporation or the boiling points, Brewer has deduced probable values, based on various considerations. Since, in such cases, even a "guess" is of undoubted value, the writer has made use of these deductions in calculating the data given in Tables 1 and 2.

From the values of T derived by Brewer for the series of values of P mentioned above the writer has calculated values of the constants A and B in equation 3 which are in most satisfactory agreement with the values for the range $P_{atm} = 10^{-6}$ to $P_{atm} = 10^{-3}$. Values of A (for the pressure in *microns*), B, and the constant C, defined by means of equation 10*b* above, are given in Table 1. The symbols l and s refer to the liquid and solid states, respectively. Values without such notation refer to both states.

By means of equation 7, values of t ($= T - 273$) were obtained for the range $P_\mu = 10^{-2}$ to $P_\mu = 10^3$, which are given in Table 2.

The values in the rows designated W were derived by means of equation 8*b*.

The second-last and the last columns give the melting points in degrees Centigrade (t_m) and the corresponding values of the vapor pressure, P_μ.

Where two sets of data are given for any one element, the one preferred by the writer is mentioned first. Thus, for rubidium and cesium, it is the writer's opinion that the most reliable data are those obtained by the positive-ion method (described in references 4 and 5). In Table 1 the first set of values of A and B refer to those deduced from the data given in these references; the values in parentheses were deduced from the data given by Brewer (3).

Finally, a list of the references mentioned in the second column of Table 2 is given immediately after this table. A much more comprehensive bibliography has been given in Brewer's report.[4]

---

[4] After the data given in Tables 1 to 5 had been calculated by the writer, a publication appeared by D. R. Stull (*Ind. Eng. Chem.*, **39**, 517 (1947) which gives data on the vapor pressures of 1200 organic and 300 inorganic compounds (including many of the elements). The data give the temperatures in degrees Centigrade corresponding to vapor pressures in the range 1 mm to 760 mm mercury. Also, there

The following notes contain comments on the data given in Tables 1 and 2 for a number of the metals.

TABLE 1

CONSTANTS IN RELATIONS FOR EVAPORATION OF METALS*

Metal	*A*	$10^{-3} \cdot B$	*C*	Metal	*A*	$10^{-3} \cdot B$	*C*
Li	10.50 (*l*)	7.480	6.687	Si	12.55 (*l*)	18.55	9.040
Na	10.71 (*l*)	5.480	7.157	Ti	11.25 (*s*)	18.64	7.856
K	10.36 (*l*)	4.503	6.922		11.98 (*l*)	20.11	
Rb	10.42 (*l*)	4.132	7.152	Zr	12.38 (*s*)	25.87	9.126
	(10.53 (*l*)	4.291)			13 04 (*l*)	27.43	
Cs	9.86 (*l*)	3.774	6.688	Th	12.52 (*l*)	28.44	9.469
	(10.02 (*l*)	3.883)		Ge	10.94 (*l*)	15.15	7.636
Cu	12.81 (*s*)	18.06	9.478	Sn	9.97 (*l*)	13.11	6.773
	11.72 (*l*)	16.58		Pb	10.69 (*l*)	9.60	7.614
Ag	12.28 (*s*)	14.85	9.063	V	13.32	26.62	9.940
	11.66 (*l*)	14.09		Cb	14.37 (*s*)	40.40	11.120
Au	11.65 (*l*)	18.52	8.563	Ta	13.00 (*s*)	40.21	9.895
Be	12.99 (*s*)	18.22	9.233	Sb_2	11.42	9.913	8.379
	11.95 (*l*)	16.59		Bi	11.14 (*l*)	9.824	8.066
Mg	11.82 (*s*)	7.741	8.279	Cr	12.88 (*s*)	17.56	9.504
Ca	11.30 (*s*)	9.055	7.868	Mo	11.80 (*s*)	30.31	8.557
Sr	11.13 (*s*)	8.324	7.867	W	12.24 (*s*)	40.26	9.138
Ba	10.88	8.908	7.715	U	12.88 (*l*)	25.80	9.834
Zn	11.94 (*s*)	6.744	8.614	Mn	12.25 (*s*)	14.10	8.886
Cd	11.78 (*s*)	5.798	8.571	Fe	12.63 (*s*)	20.00	9.270
B	14.13 (*s*)	21.37	10.423		13.41 (*l*)	21.40	
Al	11.99 (*l*)	15.63	8.471	Co	12.43	21.96	9.081
Sc	11.94	18.57	8.533	Ni	13.28 (*s*)	21.84	9.930
Y	12.43	21.97	9.171		12.55 (*l*)	20.60	
La	11.88 (*l*)	18.00	8.717	Ru	13.50	33.80	10.270
Ce	13.74 (*l*)	20.10	10.584	Rh	13.55	30.40	10.320
Ga	10.79 (*l*)	13.36	7.478	Pd	11.46	19.23	8.240
In	10.93 (*l*)	12.15	7.726	Os	13.59	37.00	10.500
Tl	11.15 (*l*)	8.92	8.066	Ir	13.06	34.11	9.970
C	14.06 (*s*)	38.57	10.370	Pt	12.633	27.50	9.544
Si	13.20 (*s*)	19.72	9.690				

* Values of *A* for the pressure in microns.

---

is attached a very comprehensive bibliography. Although for many of the elements the data given in the following tables agree very well with those given by Stull, there are considerable differences for others. This is especially true of those cases in which the decision involved a question of the reliability of the original data available in the literature.

TABLE 2

TEMPERATURES FOR GIVEN VALUES OF P_μ AND CORRESPONDING RATES OF EVAPORATION

Metal	Reference	P_μ:	10^{-2}	10^{-1}	1	10	100	1000	t_m	P_μ
Li	1 (2	t° C: W: t° C:	325 $6.28 \cdot 10^{-8}$ 353	377 $6.03 \cdot 10^{-7}$ 406	439 $5.76 \cdot 10^{-6}$ 467	514 $5.48 \cdot 10^{-5}$ 541	607 $5.18 \cdot 10^{-4}$ 632	725 $4.87 \cdot 10^{-3}$ 745)	179	$9 \cdot 10^{-7}$
Na	1	t° C: W:	158 $1.35 \cdot 10^{-7}$	195 $1.29 \cdot 10^{-6}$	238 $1.24 \cdot 10^{-5}$	291 $1.18 \cdot 10^{-4}$	356 $1.12 \cdot 10^{-3}$	437 $1.05 \cdot 10^{-2}$	98	$8.2 \cdot 10^{-5}$
K	1	t° C: W:	91 $1.91 \cdot 10^{-7}$	123 $1.83 \cdot 10^{-6}$	161 $1.75 \cdot 10^{-5}$	207 $1.67 \cdot 10^{-4}$	265 $1.57 \cdot 10^{-3}$	338 $1.48 \cdot 10^{-2}$	64	$9.8 \cdot 10^{-4}$
Rb	4 (3	t° C: W: t° C:	59.4 $2.96 \cdot 10^{-7}$ 70	88.5 $2.84 \cdot 10^{-6}$ 99	123 $2.71 \cdot 10^{-5}$ 135	165 $2.58 \cdot 10^{-4}$ 177	217 $2.43 \cdot 10^{-3}$ 230	283 $2.29 \cdot 10^{-2}$ 297)	38.5	$1.5 \cdot 10^{-3}$
Cs	5 3	t° C: W: t° C:	45 $3.77 \cdot 10^{-7}$ 50	74 $3.61 \cdot 10^{-6}$ 79	110 $3.44 \cdot 10^{-5}$ 115	153 $3.18 \cdot 10^{-4}$ 158	207 $3.07 \cdot 10^{-3}$ 211	277 $2.87 \cdot 10^{-2}$ 280	29	$1.5 \cdot 10^{-3}$
Cu	6, 3	t° C: W:	946 $1.33 \cdot 10^{-7}$	1035 $1.29 \cdot 10^{-6}$	1141 $1.24 \cdot 10^{-5}$	1273 $1.18 \cdot 10^{-4}$	1432 $1.13 \cdot 10^{-3}$	1628 $1.07 \cdot 10^{-2}$	1083	0.31
Ag	1	t° C: W:	767 $1.88 \cdot 10^{-7}$	848 $1.81 \cdot 10^{-6}$	936 $1.74 \cdot 10^{-5}$	1047 $1.67 \cdot 10^{-4}$	1184 $1.59 \cdot 10^{-3}$	1353 $1.50 \cdot 10^{-2}$	961	1.78
Au	1	t° C: W:	1083 $2.22 \cdot 10^{-7}$	1190 $2.14 \cdot 10^{-6}$	1316 $2.05 \cdot 10^{-5}$	1465 $1.96 \cdot 10^{-4}$	1646 $1.87 \cdot 10^{-3}$	1867 $1.77 \cdot 10^{-2}$	1063	$6 \cdot 10^{-3}$

Be	3, 7	*t*° C: *W*:	942 $5.03 \cdot 10^{-8}$	1029 $4.86 \cdot 10^{-7}$	1130 $4.68 \cdot 10^{-6}$	1246 $4.49 \cdot 10^{-5}$	1395	1582	1284	19.5
Mg	1	*t*° C *W*:	287 $1.21 \cdot 10^{-7}$	331 $1.17 \cdot 10^{-6}$	383 $1.12 \cdot 10^{-5}$	443 $1.08 \cdot 10^{-4}$	515 $1.02 \cdot 10^{-3}$	605 $9.71 \cdot 10^{-3}$	651	$2.2 \cdot 10^{3}$
Ca	1	*t*° C: *W*:	408 $1.42 \cdot 10^{-7}$	463 $1.37 \cdot 10^{-6}$	528 $1.31 \cdot 10^{-5}$	605 $1.25 \cdot 10^{-4}$	700 $1.19 \cdot 10^{-3}$	817 $1.12 \cdot 10^{-2}$	810	$8.75 \cdot 10^{2}$
	8	*t*° C:	462	523	594	680	784	—		
Sr	3	*t*° C: *W*:	361 $2.17 \cdot 10^{-7}$	413 $2.08 \cdot 10^{-6}$	475 $2.00 \cdot 10^{-5}$	549 $1.91 \cdot 10^{-4}$	639 $1.81 \cdot 10^{-3}$	750 $1.71 \cdot 10^{-2}$	771	$1.44 \cdot 10^{3}$
Ba	3	*t*° C: *W*:	418 $2.60 \cdot 10^{-7}$	476 $2.50 \cdot 10^{-6}$	546 $2.39 \cdot 10^{-5}$	629 $2.28 \cdot 10^{-4}$	730 $2.16 \cdot 10^{-3}$	858 $2.03 \cdot 10^{-2}$	717	76
	9	*t*° C:	485	549	625	716	829	961		
	10	*t*° C:	476	544	626	726	851	—		
Zn	1	*t*° C: *W*:	211 $2.15 \cdot 10^{-7}$	248 $2.07 \cdot 10^{-6}$	292 $1.98 \cdot 10^{-5}$	343 $1.90 \cdot 10^{-4}$	405 $1.81 \cdot 10^{-3}$	— —	419	$1.6 \cdot 10^{2}$
Cd	1	*t*° C: *W*:	148 $3.01 \cdot 10^{-7}$	180 $2.91 \cdot 10^{-6}$	220 $2.79 \cdot 10^{-5}$	264 $2.67 \cdot 10^{-4}$	321 $2.54 \cdot 10^{-3}$	— —	321	$1.0 \cdot 10^{2}$
Hg	11	*t*° C: *W*:	−23.9 $5.23 \cdot 10^{-7}$	−5.5 $5.50 \cdot 10^{-6}$	18.0 $4.84 \cdot 10^{-5}$	48.0 $4.61 \cdot 10^{-4}$	82.0 $4.39 \cdot 10^{-3}$	126 $4.14 \cdot 10^{-2}$	−38.9	$2.5 \cdot 10^{-3}$
B	3	*t*° C: *W*:	1052 $5.27 \cdot 10^{-8}$	1140 $5.11 \cdot 10^{-7}$	1239 $4.94 \cdot 10^{-6}$	1355 $4.76 \cdot 10^{-5}$	1489 $4.57 \cdot 10^{-4}$	1648 $4.38 \cdot 10^{-3}$	2000–2080	

TABLE 2. TEMPERATURES FOR GIVEN VALUES OF P_μ AND CORRESPONDING RATES OF EVAPORATION—*Continued*

Metal	Reference	P_μ:	10^{-2}	10^{-1}	1	10	100	1000	t_m	P_μ
Al	1	t° C:	724	808	889	996	1123	1279	660	$1.2 \cdot 10^{-3}$
		W:	$9.60 \cdot 10^{-8}$	$9.21 \cdot 10^{-7}$	$8.88 \cdot 10^{-6}$	$8.51 \cdot 10^{-5}$	$8.11 \cdot 10^{-4}$	$7.69 \cdot 10^{-3}$		
	3, 12	t° C:	843	929	1030	1148	1291	1465	660	$1.8 \cdot 10^{-5}$
		W:	$9.07 \cdot 10^{-8}$	$8.74 \cdot 10^{-7}$	$8.40 \cdot 10^{-6}$	$8.04 \cdot 10^{-5}$	$7.66 \cdot 10^{-4}$	$7.27 \cdot 10^{-3}$		
Sc	3	t° C:	1058	1161	1282	1423	1595	1804	1397	6.6
		W:	$1.07 \cdot 10^{-7}$	$1.04 \cdot 10^{-6}$	$9.94 \cdot 10^{-6}$	$9.51 \cdot 10^{-5}$	$9.07 \cdot 10^{-4}$	$8.40 \cdot 10^{-3}$		
Y	3	t° C:	1249	1362	1494	1649	1833	2056	1477	0.76
		W:	$1.41 \cdot 10^{-7}$	$1.36 \cdot 10^{-6}$	$1.31 \cdot 10^{-5}$	$1.25 \cdot 10^{-4}$	$1.20 \cdot 10^{-3}$	$1.14 \cdot 10^{-2}$		
La	3	t° C:	1023	1125	1242	1381	1549	1754	887	$2.3 \cdot 10^{-4}$
		W:	$1.91 \cdot 10^{-7}$	$1.84 \cdot 10^{-6}$	$1.77 \cdot 10^{-5}$	$1.69 \cdot 10^{-4}$	$1.61 \cdot 10^{-3}$	$1.53 \cdot 10^{-2}$		
Ce	3	t° C:	1004	1091	1190	1305	1439	1599	785	$5.5 \cdot 10^{-6}$
		W:	$1.93 \cdot 10^{-7}$	$1.87 \cdot 10^{-6}$	$1.80 \cdot 10^{-5}$	$1.74 \cdot 10^{-4}$	$1.67 \cdot 10^{-3}$	$1.60 \cdot 10^{-2}$		
Ga	3	t° C:	771	859	965	1093	1248	1443	30	0
		W:	$1.51 \cdot 10^{-7}$	$1.45 \cdot 10^{-6}$	$1.38 \cdot 10^{-5}$	$1.32 \cdot 10^{-4}$	$1.25 \cdot 10^{-3}$	$1.18 \cdot 10^{-2}$		
In	3, 13	t° C:	667	746	840	952	1088	1260	157	0
		W:	$2.04 \cdot 10^{-7}$	$1.96 \cdot 10^{-6}$	$1.87 \cdot 10^{-5}$	$1.79 \cdot 10^{-4}$	$1.69 \cdot 10^{-3}$	$1.60 \cdot 10^{-2}$		
Tl	1	t° C:	405	461	527	606	702	821	304	$5.0 \cdot 10^{-5}$
		W:	$3.20 \cdot 10^{-7}$	$3.08 \cdot 10^{-6}$	$2.95 \cdot 10^{-5}$	$2.81 \cdot 10^{-4}$	$2.67 \cdot 10^{-3}$	$2.52 \cdot 10^{-2}$		
C	3	t° C:	2129	2288	2471	2681	2926	3214		
		W:	$4.13 \cdot 10^{-8}$	$4.00 \cdot 10^{-7}$	$3.86 \cdot 10^{-6}$	$3.72 \cdot 10^{-5}$	$3.58 \cdot 10^{-4}$	$3.42 \cdot 10^{-3}$		

Si	3	t° C: W:	1024 $8.58 \cdot 10^{-8}$	1116 $8.29 \cdot 10^{-7}$	1223 $7.99 \cdot 10^{-6}$	1343 $7.68 \cdot 10^{-5}$	1485 $7.37 \cdot 10^{-4}$	1670 $7.01 \cdot 10^{-3}$	1410	31.6
Ti	3	t° C: W:	1134 $1.08 \cdot 10^{-7}$	1249 $1.04 \cdot 10^{-6}$	1384 $9.92 \cdot 10^{-6}$	1546 $9.47 \cdot 10^{-5}$	1742 $9.00 \cdot 10^{-4}$	1965 $8.53 \cdot 10^{-3}$	1727	84.3
Zr	3	t° C: W:	1527 $1.31 \cdot 10^{-7}$	1660 $1.27 \cdot 10^{-6}$	1816 $1.22 \cdot 10^{-5}$	2001 $1.17 \cdot 10^{-4}$	2212 $1.12 \cdot 10^{-3}$	2459 $1.07 \cdot 10^{-2}$	2127	40.7
Th	3	t° C: W:	1686 $2.01 \cdot 10^{-7}$	1831 $1.94 \cdot 10^{-6}$	1999 $1.86 \cdot 10^{-5}$	2196 $1.79 \cdot 10^{-4}$	2431 $1.71 \cdot 10^{-3}$	2715 $1.63 \cdot 10^{-2}$	1827	$9.3 \cdot 10^{-2}$
Ge	3	t° C: W:	897 $1.45 \cdot 10^{-7}$	996 $1.40 \cdot 10^{-6}$	1112 $1.34 \cdot 10^{-5}$	1251 $1.27 \cdot 10^{-4}$	1421 $1.21 \cdot 10^{-3}$	1635 $1.14 \cdot 10^{-2}$	959	$4.5 \cdot 10^{-2}$
Sn	3	t° C: W:	823 $1.92 \cdot 10^{-7}$	922 $1.84 \cdot 10^{-6}$	1042 $1.75 \cdot 10^{-5}$	1189 $1.66 \cdot 10^{-4}$	1373 $1.57 \cdot 10^{-3}$	1609 $1.47 \cdot 10^{-2}$	232	0
Pb	1	t° C: W:	483 $3.05 \cdot 10^{-7}$	548 $2.93 \cdot 10^{-6}$	625 $2.80 \cdot 10^{-5}$	718 $2.67 \cdot 10^{-4}$	832 $2.53 \cdot 10^{-3}$	975 $2.38 \cdot 10^{-2}$	328	$5.4 \cdot 10^{-6}$
V	3	t° C: W:	1465 $1.0 \cdot 10^{-7}$	1586 $9.6 \cdot 10^{-7}$	1725 $9.3 \cdot 10^{-6}$	1888 $8.9 \cdot 10^{-5}$	2079 $8.6 \cdot 10^{-4}$	2207 $8.2 \cdot 10^{-3}$	1697	0.65
Cb	14	t° C: W:	2194 $1.16 \cdot 10^{-7}$	2355 $1.08 \cdot 10^{-6}$	2539 $1.06 \cdot 10^{-5}$				2500	0.6
Ta	15, 16	t° C: W:	2407 $1.55 \cdot 10^{-7}$	2599 $1.48 \cdot 10^{-6}$	2820 $1.41 \cdot 10^{-5}$				2996	5.0
Sb_2	3	t° C: W:	466 $3.35 \cdot 10^{-7}$	525 $3.22 \cdot 10^{-6}$	595 $3.09 \cdot 10^{-5}$	678 $2.95 \cdot 10^{-4}$	779 $2.81 \cdot 10^{-3}$	904 $2.65 \cdot 10^{-2}$	630	2.82

TABLE 2. TEMPERATURES FOR GIVEN VALUES OF P_μ AND CORRESPONDING RATES OF EVAPORATION—*Continued*

Metal	Reference	P_μ:	10^{-2}	10^{-1}	1	10	100	1000	t_m	P_μ
Bi	3	t° C: W:	474 $3.08 \cdot 10^{-7}$	536 $2.96 \cdot 10^{-6}$	609 $2.84 \cdot 10^{-5}$	698 $2.71 \cdot 10^{-4}$	802 $2.57 \cdot 10^{-3}$	934 $2.43 \cdot 10^{-2}$	271	$1.20 \cdot 10^{-7}$
Cr	3, 12	t° C: W:	907 $1.22 \cdot 10^{-7}$	992 $1.18 \cdot 10^{-6}$	1090 $1.14 \cdot 10^{-5}$	1205 $1.09 \cdot 10^{-4}$	1342 $1.05 \cdot 10^{-3}$	1504 $1.00 \cdot 10^{-2}$	1900	$6.35 \cdot 10^{4}$
Mo	18	t° C: W:	1923 $1.29 \cdot 10^{-7}$	2095 $1.18 \cdot 10^{-6}$	2295 $1.12 \cdot 10^{-5}$	2533 $1.05 \cdot 10^{-4}$			2622	22.0
W	19	t° C: W:	2554 $1.47 \cdot 10^{-7}$	2767 $1.46 \cdot 10^{-6}$	3016 $1.45 \cdot 10^{-5}$	3309 $1.43 \cdot 10^{-4}$			3382	17.5
U	3	t° C: W:	1461 $2.16 \cdot 10^{-7}$	1585 $2.09 \cdot 10^{-6}$	1730 $2.01 \cdot 10^{-5}$	1898 $1.93 \cdot 10^{-4}$	2098 $1.85 \cdot 10^{-3}$	2338 $1.76 \cdot 10^{-2}$	1132	$3.24 \cdot 10^{-6}$
Mn	3	t° C: W:	717 $1.38 \cdot 10^{-7}$	791 $1.32 \cdot 10^{-6}$	878 $1.27 \cdot 10^{-5}$	980 $1.22 \cdot 10^{-4}$	1103 $1.17 \cdot 10^{-3}$	1251 $1.11 \cdot 10^{-2}$	1244	$9.04 \cdot 10^{2}$
Fe	3, 6	t° C: W:	1094 $1.29 \cdot 10^{-7}$	1195 $1.20 \cdot 10^{-6}$	1310 $1.10 \cdot 10^{-5}$	1447 $1.02 \cdot 10^{-4}$	1602 $1.01 \cdot 10^{-3}$	1783 $9.6 \cdot 10^{-2}$	1535	37.2
Co	3	t° C: W:	1249 $1.15 \cdot 10^{-7}$	1362 $1.11 \cdot 10^{-6}$	1494 $1.06 \cdot 10^{-5}$	1649 $1.02 \cdot 10^{-4}$	1833 $9.76 \cdot 10^{-4}$	2056 $9.28 \cdot 10^{-3}$	1478	0.76
Ni	3, 17	t° C: W:	1157 $1.18 \cdot 10^{-7}$	1257 $1.14 \cdot 10^{-6}$	1371 $1.10 \cdot 10^{-5}$	1510 $1.06 \cdot 10^{-4}$	1679 $1.01 \cdot 10^{-3}$	1884 $9.62 \cdot 10^{-3}$	1455	4.37

Ru	3	t° C: W:	1913 $126 \cdot 10^{-7}$	2058 $1.22 \cdot 10^{-6}$	2230 $1.18 \cdot 10^{-5}$	2431 $1.13 \cdot 10^{-4}$	2666 $1.08 \cdot 10^{-3}$	2946 $1.04 \cdot 10^{-2}$	2427	9.8
Rh	3	t° C: W:	1681 $1.34 \cdot 10^{-7}$	1815 $1.29 \cdot 10^{-6}$	1971 $1.25 \cdot 10^{-5}$	2149 $1.20 \cdot 10^{-4}$	2358 $1.15 \cdot 10^{-3}$	2607 $1.10 \cdot 10^{-2}$	1967	1.0
Pd	3	t° C: W:	1156 $1.59 \cdot 10^{-7}$	1271 $1.53 \cdot 10^{-6}$	1405 $1.47 \cdot 10^{-5}$	1566 $1.41 \cdot 10^{-4}$	1759 $1.34 \cdot 10^{-3}$	2000 $1.26 \cdot 10^{-2}$	1555	8.71
Os	3	t° C: W:	2101 $1.65 \cdot 10^{-7}$	2264 $1.60 \cdot 10^{-6}$	2451 $1.54 \cdot 10^{-5}$	2667 $1.48 \cdot 10^{-4}$	2920 $1.42 \cdot 10^{-3}$	3221 $1.36 \cdot 10^{-2}$	2697	13.5
Ir	3	t° C: W:	1993 $1.70 \cdot 10^{-7}$	2154 $1.65 \cdot 10^{-6}$	2340 $1.59 \cdot 10^{-5}$	2556 $1.52 \cdot 10^{-4}$	2811 $1.46 \cdot 10^{-3}$	3118 $1.39 \cdot 10^{-2}$	2454	3.55
Pt	3	t° C: W:	1606 $1.88 \cdot 10^{-7}$	1744 $1.81 \cdot 10^{-6}$	1904 $1.75 \cdot 10^{-5}$	2090 $1.68 \cdot 10^{-4}$	2313 $1.60 \cdot 10^{-3}$	2582 $1.52 \cdot 10^{-2}$	1774	0.16

For the following metals there is very good agreement between data deduced by Brewer and those deduced by Kelley: Li, Na, K, Rb, Cs, Mg, Ca, Ag, Au, Zn, Cd, Tl, and Pb.

For Cu, In, Fe, and Ni, the data given in the second reference (see the second column of Table 2) are those that must be regarded as most reliable, and they have been incorporated with only slight modifications in Brewer's deductions.

For aluminum and chromium, Brewer has placed much more reliance on the observations mentioned in reference 12 than would appear justifiable in the opinion of the writer. Some semi-quantitative determinations carried out in this laboratory on the rate of evaporation of aluminum appear to be in much better agreement with the deductions in reference 1 than with the observations recorded in 12. It is of interest to note that J. Fischer[5] has questioned the reliability of the experimental method used by Baur and Bruner and has given a number of reasons for distrusting their conclusions.

REFERENCES FOR DATA ON VAPOR PRESSURES OF METALS

1. K. K. Kelley, *Bureau of Mines Bulletin 383*, 1935.
2. R. W. Ditchburn and J. C. Gilmour, *Rev. Modern Phys.*, **13**, 310 (1941).
3. Leo Brewer, *The Thermodynamic and Physical Properties of the Elements*, Report for the Manhattan Project, 1946.
4. T. J. Killian, *Phys. Rev.*, **27**, 578 (1926).
5. J. B. Taylor and I. Langmuir, *Phys. Rev.*, **51**, 753 (1937).
6. A. L. Marshall, R. W. Dornte, and F. J. Norton, *J. Am. Chem. Soc.*, **59**, 1161 (1937).
7. R. Schumann and A. B. Garrett, *J. Am. Chem. Soc.*, **66**, 442 (1944); **67**, 2279 (1945).
8. E. Rudberg, *Phys. Rev.*, **46**, 763 (1934).
9. J. A. M. van Liempt, *Rec. trav. chim.*, **55**, 468 (1936).
10. E. Rudberg and J. Lempert, *J. Chem. Phys.*, **3**, 627 (1935).
11. *International Critical Tables*, Vol. 3, 306, 1928.
12. E. Baur and R. Bruner, *Helv. Chim. Acta*, **17**, 958 (1934).
13. J. S. Anderson, *J. Chem. Soc.*, **1943**, 141.
14. A. L. Reimann and C. K. Grant, *Phil. Mag.*, **22**, 34 (1936).
15. D. B. Langmuir and L. Malter, *Phys. Rev.*, **55**, 748 (1939).
16. M. D. Fiske, *Phys. Rev.*, **61**, 513 (1942).
17. H. L. Johnston and A. L. Marshall, *J. Am. Chem. Soc.*, **62**, 1382 (1940).
18. H. A. Jones, I. Langmuir, and G. M. J. Mackay, *Phys. Rev.*, **30**, 201 (1927).
19. H. A. Jones and I. Langmuir, *Gen. Elec. Rev.*, **30**, 354 (1927).
20. R. Speiser, Engineering Experiment Station, The Ohio State Univ., **19**, No. 5, p. 12 (1947).

---

[5] *Helv. Chim. Acta*, **18**, 1028 (1935).

For *carbon*, A. L. Marshall and F. J. Norton[6] have shown that their observations on rates of evaporation are most satisfactorily represented by the relation

$$\log W = 9.08 - \frac{39{,}500}{T}, \tag{1}$$

which, according to equation 1.5, yields the value $L_0 = 180{,}700$ cal/mole.

By correcting Marshall and Norton's value of L_0 for the dissociation of diatomic carbon, Brewer (3) deduced values of ΔF from which the writer has derived the vapor-pressure data given in Table 2.

The second row in Table 3 shows values of W calculated by means of equation 1 for the values of $t°$ C in Table 2. It should be observed, however, that for these values of W the vapor pressures cannot be those given at the head of the table, since the values of P_μ given in Table 2 are based on the assumption that all the carbon sublimes in the monatomic form. On the basis of equation 1 the values of W given in Table 2, which are *repeated in the third row* of Table 3, correspond to the values of $t°$ C given in the fourth row of this table.

TABLE 3

RATE OF EVAPORATION OF CARBON CALCULATED BY MEANS OF EQUATION 1

$t°$ C:	2129	2288	2471	2681	2926	3214
W:	$4.37 \cdot 10^{-8}$	$4.47 \cdot 10^{-7}$	$4.79 \cdot 10^{-6}$	$5.01 \cdot 10^{-5}$	$5.37 \cdot 10^{-4}$	$5.75 \cdot 10^{-3}$
W:	$4.13 \cdot 10^{-8}$	$4.00 \cdot 10^{-7}$	$3.86 \cdot 10^{-6}$	$3.72 \cdot 10^{-5}$	$3.58 \cdot 10^{-4}$	$3.42 \cdot 10^{-3}$
$t°$ C:	2127	2279	2453	2651	2881	3147

That there exists considerable doubt regarding the value for the heat of evaporation of carbon is evident from a review of this topic by H. D. Hagstrum.[7] From an interpretation of the band spectrum of carbon monoxide he has deduced for the heat of sublimation of carbon the value 135,700 cal/mole, and for the heat of sublimation into tetravalent carbon the value 232,100 cal/mole. These values are to be compared with the value 170,000 cal/mole for the heat of sublimation deduced by a number of previous investigators.

Antimony evaporates largely in the form of molecules, Sb_2, and the values of W given for this metal in Table 2 are based on this conclusion, that is, $M = 243.52$.

For barium it is of interest to note that Brewer's conclusions are in disagreement with those deduced from references 9 and 10. Similarly, there is considerable discrepancy between the two sets of values of $t°$ C for calcium.

---

[6] *J. Am. Chem. Soc.*, **55**, 431 (1933).

[7] *Phys. Rev.*, **72**, 947 (1947).

For beryllium the data calculated in Table 2 are based upon the results obtained by Schumann and Garrett (7). However, more recent data, published by R. Speiser (20) and based on unpublished results obtained by R. B. Holden, lead to the following values of $t°$ C for given values of P_μ:

P_μ:	10^{-2}	10^{-1}	1	10	60.3
$t°$ C:	911	992	1083	1189	1284(t_m).

These were calculated from the values (which differ from those in Table 1) $A = 13.805$, $10^{-3}B = 18.73$. (Evidently the values of t derived from the more recent publication are lower for given values of P_μ than those given in Table 2.)

Speiser's paper also contains an excellent review of the different methods used for the determination of the vapor pressures of metals, and Holden's results demonstrate that the value of the accommodation coefficient for beryllium is unity.

With reference to the data for Sc, Y, La, Zr, V, and Co, Brewer's comment is as follows:

> No vapor-pressure data are available, and the boiling point was estimated and the vapor-pressure data made consistent with known thermodynamic data. However, *all the temperatures given may be uniformly in error by several hundred degrees.*[8]

For a number of metals the only datum available is an approximate determination of the boiling point (Ge, B), or a statement in the literature that the metal is "markedly volatile" (Ti, Pd).

In a bulletin published by the National Research Corporation values are given for $t°$ C which as observed in their laboratory correspond to $P_\mu = 10$. Their values (designated NRC) compared with those given in Table 2 are as follows:

Metal:	Be	Zr	Ge	Sn	Pd	Ir
Table 2:	1246	2001	1251	1189	1566	2556
NRC:	1350	>2000	1300	1350	1550	>2400

Values of the temperature corresponding to $P_\mu = 1$, and to $P_{mm} = 1$, for a number of metals, have been published by W. J. Kroll[9] and A. Eucken,[10] respectively. Also, as mentioned previously, Ditchburn and Gilmour have deduced data similar to those given in Table 2. In view of the very great care taken by Brewer to consider all available observations that might have a bearing on this topic it appears to the writer that his conclusions should be regarded as much more trustworthy than those deduced by any previous investigators. For this reason no comparison is made between the data given in Table 2 and those published by other reviewers.

---

[8] Italics by the writer.

[9] *Trans. Am. Electrochem. Soc.*, **87**, 571 (1945).

[10] *Metallwirtschaft*, **15**, 27, 63 (1936).

Brewer has also calculated values of T_B, the boiling point (in degrees Kelvin), and of L, the heat of vaporization (cal/mole) at T_B. It will be observed that these values given in Table 4 are uniformly lower than the values of L_0 calculated from those of B in Table 1, since Brewer deduced his values on the basis of more rigorous arguments. Table 4 also gives values of T_1 and T_{10}, the temperatures (in degrees Kelvin) corresponding to $P_\mu = 1$ and $P_\mu = 10$, respectively. From these data, values have been derived of T_1/T_B, T_{10}/T_B, and L/T_B. The last column in the table gives values of Z, the atomic number. The value of L/T_B is designated the Trouton constant. As will be observed, the values of this constant are low for the alkali metals and considerably higher for carbon and the transition elements. For about half the total number of metals $L/T_B = 25 \pm 3$. It is also evident that the values of T_1/T_B and T_{10}/T_B increase with increase in value of L/T_B. That this is in accord with the Clapeyron relation may be demonstrated as follows:

From the second law of thermodynamics it follows that

$$\frac{d \ln P}{d\,(1/T)} = -\frac{L}{R_0}. \tag{2}$$

Assuming that L is a constant, this relation becomes

$$\frac{\log P_{\mu B} - \log P_\mu}{1/T - 1/T_B} = \frac{L}{4.574}, \tag{3}$$

where $P_{\mu B} = 7.60 \cdot 10^5$, and $\log P_{\mu B} = 5.881$.

Hence, for $P_\mu = 1$,

$$\frac{L/T_B}{26.71 + L/T_B} = \frac{T_1}{T_B}, \tag{4}$$

and for $P_\mu = 10$,

$$\frac{L/T_B}{22.14 + L/T_B} = \frac{T_{10}}{T_B}. \tag{5}$$

For $L/T_B = 25$, $T_1/T_B = 0.483$ and $T_{10}/T_B = 0.530$.

Table 5 gives a number of illustrations of the application of the last two equations, and, as will be observed, the agreement between the values thus calculated and those given in Table 4 is good, especially in

TABLE 4

ABSOLUTE TEMPERATURES CORRESPONDING TO THREE VALUES OF THE VAPOR PRESSURE, ALSO VALUES OF THE LATENT HEAT OF EVAPORATION, AND OF THE TROUTON CONSTANT

Element	T_1	T_{10}	T_B	T_1/T_B	T_{10}/T_B	L	L/T_B	Z
Li	712	787	1640	0.4342	0.4799	32,480	19.81	3
Na	511	564	1187	.4304	.4751	23,120	19.47	11
K	434	480	1052	.4128	.4562	18,880	17.95	19
Rb	396	438	952	.4160	.4601	18,110	19.02	37
Cs	383	426	963	.3977	.4424	16,320	16.94	55
Cu	1414	1546	2868	.4929	.5391	72,810	25.39	29
Ag	1209	1320	2485	.4863	.5311	60,720	24.42	47
Au	1589	1738	3239	.4907	.5365	81,800	25.25	79
Be	1403	1519	2780	.5047	.5464	73,900	26.59	4
Mg	656	716	1399	.4688	.5117	31,470	22.49	12
Ca	801	878	1755	.4564	.5003	36,740	20.94	20
Sr	748	822	1657	.4514	.4962	33,610	20.28	38
Ba	819	902	1911	.4286	.4721	35,665	18.66	56
Zn	565	616	1180	.4787	.5220	27,880	23.62	30
Cd	493	537	1038	.4750	.5175	23,870	23.00	48
Hg	291	321	634	.4590	.5063	13,980	22.06	80
B	1512	1628	2800	.5400	.5813	75,000	26.79	5
Al	1162	1269	2600	.4470	.4881	67,950	26.13	13
Sc	1555	1696	3000	.5183	.5654	80,000	26.67	21
Y	1767	1922	3500	.5048	.5618	90,000	25.71	39
La	1515	1654	3000	.5050	.5513	80,000	26.67	57
Ce	1463	1578	2800	.5225	.5635	73,000	26.07	58
Ga	1238	1366	2700	.4584	.5058	60,000	22.22	31
In	1113	1225	2440	.4560	.5020	53,800	22.05	49
Tl	800	879	1730	.4625	.5082	38,810	22.44	81
C	2744	2954	4775	.5746	.6186	180,000	37.70	6
Si	1496	1616	2750	.5434	.5876	71,000	25.82	14
Ti	1657	1819	3400	.4873	.5350	84,000	24.71	22
Zr	2089	2274	3850	.5426	.5906	120,000	31.17	40
Th	2272	2469	4500	.5049	.5487	130,000	28.89	90
Ge	1385	1524	2980	.4648	.5113	68,000	22.82	32
Sn	1315	1462	3000	.4383	.4874	70,000	23.33	50
Pb	898	991	2010	.4468	.4930	42,400	21.10	82
V	1998	2161	3800	.5259	.5687	106,000	27.89	23
Cb	2812	——	5400	.5207	——	155,000	28.77	41
Ta	3093	——	6300	.4910	——	183,000	29.05	73
Sb_2	868	951	1890	.4592	.5031	40,000	21.16	51
Bi	882	971	1900	.4641	.5110	42,600	22.42	83
Cr	1363	1478	2495	.5463	.5924	72,970	29.24	24
Mo	2568	2806	5077	.5058	.5527	128,420	25.29	42
W	3289	3582	5950	.5529	.6020	184,580	30.12	74
U	2003	2171	3800	.5270	.5714	110,000	28.95	92
Mn	1151	1253	2370	.4857	.5286	54,380	22.95	25
Fe	1583	1720	3008	.5264	.5719	84,620	30.94	26
Co	1767	1922	3370	.5243	.5703	93,000	27.60	27
Ni	1644	1783	3110	.5285	.5732	90,480	29.09	28

Element	T_1	T_{10}	T_B	T_1/T_B	T_{10}/T_B	L	L/T_B	Z
Ru	2503	2704	4500	0.5562	0.6011	148,000	32.90	44
Rh	2244	2422	4150	.5408	.5837	127,000	30.61	45
Pd	1678	1839	3440	.4877	.5346	89,000	25.87	46
Os	2724	2940	4900	.5559	.5999	162,000	33.06	76
Ir	2613	2829	4800	.5444	.5893	152,000	31.66	77
Pt	2177	2363	4100	.5310	.5761	122,000	29.76	78

view of the fact that, actually, L decreases with increase in T. However, the decrease in the value in the range $T = T_1$ to $T = T_B$ does not, in general, exceed more than a few per cent.

TABLE 5

RELATION BETWEEN THE VALUE OF L/T_B AND VALUES OF T_1/T_B AND T_{10}/T_B

Element	L/T_B	T_1/T_B		T_{10}/T_B	
		Eq. 4	Table 4	Eq. 5	Table 4
Cs	16.94	0.388	0.398	0.434	0.442
Li	19.81	.426	.434	.472	.480
Pb	21.10	.441	.447	.488	.493
Sn	23.33	.466	.438	.513	.487
Cu	25.39	.487	.493	.534	.539
V	27.89	.511	.526	.557	.569
W	30.12	.530	.553	.576	.602
Ru	32.90	.552	.556	.598	.601
C	37.70	.585	.575	.630	.619

3. GENERAL REMARKS ON VACUUM DISTILLATION OF METALS AND DEPOSITION OF FILMS

For the distillation of a metal in a vacuum, in order to purify it, W. J. Kroll[11] considers 1.8 mm of mercury as suitable for commercial operation. The temperature required for this purpose may be obtained from Table 2, and it will be observed that for some metals this pressure is attained below the melting temperature (or triple point)—that is, the solid sublimes—whereas other metals must be in the liquid state, at a temperature considerably above that of fusion.

Under these conditions, as will be discussed in the next section, nonvolatile metals can be purified of more-volatile constituents. For instance, tin can be freed from lead, since the temperatures at which the pressure is 1 mm is about 992° C for lead and about 1492° C for tin.

Also, during the process of distillation (or sublimation) dissolved gases are evolved and some compounds such as hydrides, nitrides, or oxides may be dissociated. (See discussion of dissociation pressures in the following chapter.)

---

[11] *Loc. cit.*

The deposition of thin films of metals by evaporation in vacuum has received considerable attention from a number of investigators. J. B. Strong[12] recommends, as the best condition for the deposition of a reflecting surface on glass or quartz, evaporation at a temperature, t_{10} (or T_{10}), corresponding to a *vapor pressure of about 10 microns.* Values of t_{10} (or T_{10}) have been given in Tables 2 and 4.

If the temperature used for evaporation is much in excess of the value t_{10}, there is danger of excessive sputtering (due, frequently, to too rapid evolution of sorbed gases) and the deposit may be both somewhat spongy and non-adherent to the surface of the glass, quartz, or other material on which condensation occurs.

In the presence of residual traces of gases having a pressure of a few microns or more, the deposit is also diffuse and extremely non-adherent, so that it can be rubbed off very readily. As mentioned in Chapter 10, section 2, such a diffuse deposit has many advantages for use as a "getter."

The rate of evaporation is decreased in presence of a gas at pressures exceeding 1 mm; and at higher pressures the rate of evaporation decreases to very low values. As is well known, this fact has been utilized in the development of the gas-filled tungsten-filament lamp.

The deposition of metal films by evaporation in a good vacuum has been utilized for the formation of exceptionally good reflecting surfaces on glass or quartz, and also for many other purposes.[13]

Very important contributions towards the development of a satisfactory technique, especially for the coating of glass with aluminum, have been made by Strong[14] and by C. H. Cartwright.[15]

Figure 1 shows a diagrammatic sketch of the arrangement used by Cartwright, which is suitable for the formation of deposits of Ag, Be, Cr, and Si. The evacuating system, shown at A, consists of a 1-in. steel base large enough to accommodate a 16-in. bell jar, a liquid-air trap, and a high-speed mercury-vapor pump. The seal between bell jar and plate may be made either by means of a low-melting-point wax or by means of a gasket of plastic material. The metal in the form of a bead is contained in a helical spiral made of 20-mil tungsten wire. By means of a mica shutter it is possible to give the metal a preliminary degassing at relatively low temperature without the danger of depositing any impurities on the glass. The vacuum attained should be 0.1 micron or better.

---

[12] *Procedures in Experimental Physics*, Prentice-Hall, New York, 1939, p. 169.

[13] Complete equipment for carrying out this technique is available commercially from at least two industrial organizations engaged in the production of vapor pumps and low-pressure gauges.

[14] *Rev. Sci. Instruments*, **2**, 189 (1931).

[15] *Rev. Sci. Instruments*, **3**, 298 (1932).

The electrical circuit is described as follows:

> The filament was heated by a transformer. A potential of about 200 volts was maintained between the filament and the metal base, as shown in Fig. 1*B*. This potential activated the hydrogen sometimes used for cleaning the metal to be evaporated and it was used to make the evaporating metal become luminous. The luminosity of the discharge in the metal vapor was a convenient measure of the rate of evaporation. With a proper rate of evaporation, the discharge was sufficiently bright to be seen in a well-lighted room. This discharge was similar to the discharge in a gas while sputtering except that here it was due to the metal vapor and therefore appeared only in parts of the bell jar in which the evaporating metal was present. The discharge seemed to cause an evaporated metal to adhere more tenaciously to glass.

C in Fig. 1 shows an alternative arrangement in which the liquid-air trap is replaced by an appendix containing activated charcoal and a tungsten or molybdenum boat is used instead of the spiral shown in *A*.

Strong has observed[16] that, if small pieces of aluminum wire are suspended along a tungsten spiral, then the fused aluminum adheres to the heating spiral in the form of globules.[17]

The use of a trough-shaped heating element of carbon or tungsten has been described by H. W. Edwards,[18] and H. B. DeVore[19] has modified this procedure by coating the tungsten spiral with alumina, in order to prevent alloying between the tungsten and the fused metal. A suspension of the oxide in a nitrocellulose binder is coated on the filament and the filament is heated at about 1700° C in hydrogen or in vacuum.

An interesting method for heating the metals has been described by H. M. O'Bryan.[20] Platinum, boron, molybdenum, as well as quartz are evaporated in vacuum from a graphite crucible which is raised to the desired temperature by bombardment with 4000-volt electrons emitted from an incandescent tungsten cathode. Figure 2 shows the essential details of the arrangement. The crucible (*b*) placed inside the tungsten spiral (*a*) may be heated to about 3500° C by an electron current of

---

[16] *Phys. Rev.*, **43**, 498 (1933).

[17] The application of this technique to the coating of glass mirrors is described in detail in *Procedures in Experimental Physics*, Chapter IV, in which are also described suitable procedures for the deposition by evaporation of a number of metals.

[18] *Rev. Sci. Instruments*, **4**, 449 (1933).

[19] *Rev. Sci. Instruments*, **9**, 202 (1938).

[20] *Rev. Sci. Instruments*, **5**, 125 (1934).

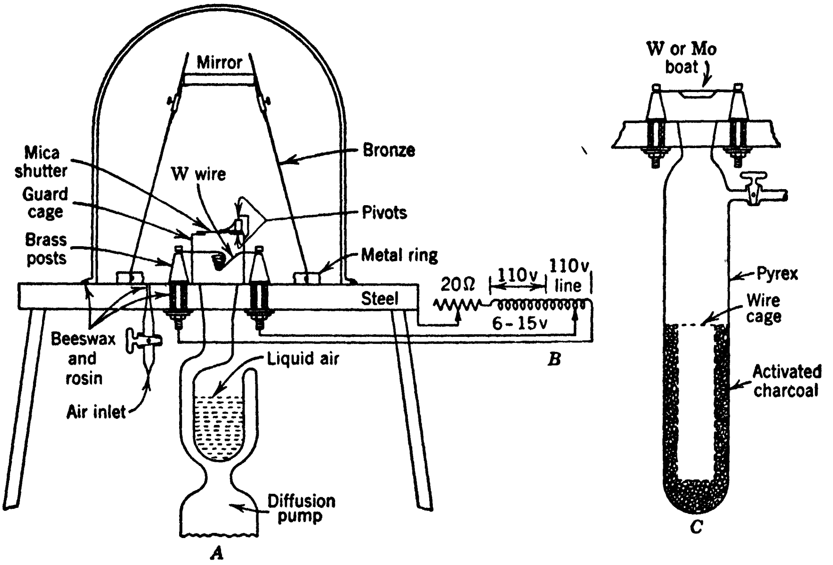

FIG. 1. Evaporating apparatus (Cartwright).

A. Evaporation is carried out by heating bead of metal in tungsten spiral. Deposit is formed on mirror near top of bell jar.

B. Electrical circuit for heating tungsten spiral and for obtaining glow discharge in the metal vapor.

C. Alternative arrangement in which liquid-air trap is replaced by appendix containing activated charcoal, and metal to be evaporated is placed in tungsten or molybdenum boat.

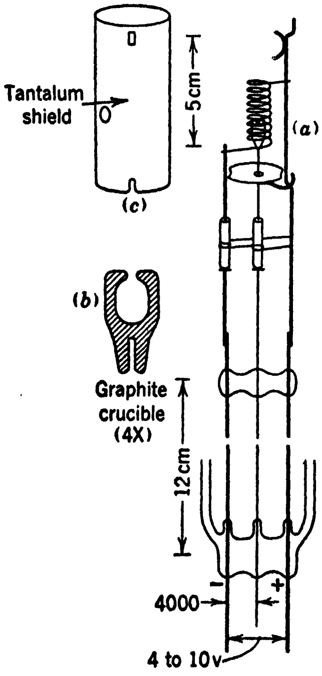

FIG. 2. Evaporating apparatus (O'Bryan). Metal to be evaporated is placed in graphite crucible (*b*) and bombarded by 4000-volt electrons using tungsten wire helix (*a*) as cathode. A tantalum shield (*c*) surrounds the cathode during bombardment.

100 ma. Complete details of the arrangement are described in the original paper.

Table 6 gives, as the author states,

> a partial list of substances which have been evaporated and their most obvious properties. Some elements which in the past have not been readily available in suitable form can now be examined for electrical and optical properties.

TABLE 6

MATERIALS EVAPORATED (O'BRYAN)

Material	Melting Point, ° C	Surface Appearance and Remarks
Boron	2300	Very bright, reflection superior to platinum.
Carbon (graphite)	3500	Amorphous, crucible partially melted.
Fused quartz	1700	Glossy surface, shows interference colors.
Molybdenum	2600	Fairly bright surface.
Chromium	1610	Characteristically bright.
Platinum	1755	Not as bright as chromium.
Vanadium	1710	Similar to chromium.
Cobalt	1480	Similar to chromium.
Nickel	1450	Not as bright as chromium.
Zirconium	1700	Similar to nickel.
Manganese	1260	Not as bright as nickel.
Boron carbide	2350	Melted, only slight gray deposit.
Silicon carbide	2200	Carbon residue, deposit green by transmission.

> None of the listed materials reacted to a great extent with graphite crucibles. Perhaps a thin layer of carbide was formed, lining the crucible, and preventing further reaction.

The problem of selecting a suitable filament material from which another metal can be evaporated successfully has been investigated by W. C. Caldwell.[21] As he points out,

> In order that a metal evaporate from a filament satisfactorily the metal must adhere to the filament, must have sufficient vapor pressure to evaporate while still at a temperature below the melting point of the filament material, and must not form an alloy with the filament which has a melting point below the temperature at which evaporation will ensue.

The conclusions reached, after investigation of nine filament materials and twenty-seven metals for evaporation, are summarized in Table 7.

It is of interest to note that, for a large number of the metals to be evaporated, filaments of the four most refractory metals (W, Ta, Mo, and Cb) were found to be suitable.

Results obtained in a very comprehensive investigation of techniques

---

[21] *J. Applied Phys.*, **12**, 779 (1941).

TABLE 7

SATISFACTORY FILAMENT MATERIALS FOR THE EVAPORATION OF VARIOUS METALS (LISTED IN ORDER OF MERIT ACCORDING TO CALDWELL)

Metal	Filaments	Metal	Filaments
Al	W, Ta, Mo, Cb	Pb	Fe, Ni, Chromel
Sb	Chromel, Ta, W	Mg	W, Ta, Mo, Cb
Ba	W, Ta, Mo, Cb	Mn	W, Ta, Mo, Cb
Be	Ta, W, Mo	Ni	W
Bi	Chromel, Ta, W	Pt	W
Cd	Chromel, Cb, Ta	Se	Chromel, Fe, Mo
Co	Cb	Ag	Ta, Mo, Cb, Fe
Cu	Cb, Mo, Ta	Sr	W, Ta, Mo, Cb
Ge	Ta, Mo	Te	W, Ta, Mo, Cb
Au	W, Mo	Tl	Ni, Fe, Cb, Ta
Fe	W	Th	Mo
Sn	Chromel	Ti	W, Ta
V	W, Mo	Zn	W, Ta, Mo, Cb

for the evaporation of metals have been reported by L. O. Olsen, C. S. Smith, and E. C. Crittenden, Jr.[22]

The evaporation system used consisted, as the authors state,

> of an 18-in.-diameter bell jar, pumping system, and vacuum gauges constructed along fairly standard lines. Twelve electrical terminals were brought into the jar and served to mount a number of independent filaments, allowing several evaporations to be done with one evacuation of the system. . . . A vacuum valve between the bell jar and the diffusion pump allowed air to be admitted to the bell jar without admitting it to the pumps. . . . A Pirani gauge in the fore-pumping line was used to follow the operation of the pumping system, and an ion gauge connected to the system through the base plate was used to observe the absolute pressure in the system during evaporation. Evaporations were carried out at pressures below $5 \cdot 10^{-5}$ mm of mercury.
>
> Three distinct types of heaters for evaporation were used in this study: open helical wire coils, close-wound conical wire baskets, and ceramic crucibles formed on wire baskets. Four metals, tungsten, iron, nickel, and Chromel, were used as bare wire coils and baskets; and the performance of two ceramics, Alundum and beryllium oxide, was studied in the form of crucibles.

These crucibles were prepared by painting a close-wound coil of tungsten with a water suspension of alumina or beryllium oxide and sintered at 1200° C to 1500° C after drying. "As far as these studies are concerned," the authors state, "Alundum appears to be by far superior to beryllium oxide, the latter being useful in the case of Alundum failure or, presumably, at high temperatures." The Alundum was actually used for evaporations up to about 1600° C, and the beryllium oxide for somewhat higher temperatures. Table 8, quoted from the original publication, presents a summary of the conclusions reached regarding the best methods for the evaporation of thirty-four elements.

---

[22] *J. Applied Phys.*, **16**, 425 (1945).

TABLE 8

SUGGESTED METHODS FOR EVAPORATION OF VARIOUS METALS (OLSEN, SMITH AND CRITTENDEN)

Metal	Method for Small Quantities	Method for Large Quantities
Aluminum	Helical coil of W	Helical tungsten coil
Antimony	Conical baskets of W, Ni, or Chromel	Alundum crucible
Arsenic	Alundum crucible	Alundum crucible
Barium	Conical baskets of W, Ni, Fe, or Chromel	Conical baskets of W, Ni, Fe, or Chromel
Beryllium	Conical basket of W	
Bismuth	Conical baskets of W, Fe, Ni, or Chromel	Alundum crucible
Calcium	Conical basket of W	Alundum crucible
Cadmium	Conical baskets of W, Ni, Fe, or Chromel	Alundum crucible
Carbon	Unsuccessful	Unsuccessful
Chromium	Conical basket of W	
Cobalt	Helical coil of W	Alundum or BeO crucible
Columbium	Helical coil of W	
Copper	Helical coil of W or conical basket of W	Alundum crucible
Germanium	Conical basket of W	Alundum crucible
Indium	Conical baskets of W or Fe	Alundum crucible
Iron	Helical coil of W	Alundum or BeO crucible
Lead	Conical basket of Fe	Alundum crucible
Magnesium	Conical baskets of W, Ni, Fe, or Chromel	Alundum crucible
Manganese	Conical basket of W	Conical basket of W or Alundum crucible
Molybdenum	Melting of molybdenum filament	
Nickel	Helical coil of W	Alundum or BeO crucible
Palladium	Helical coil of W	
Phosphorus (red)	Unsuccessful	Unsuccessful
Platinum	Helical coil of W	
Selenium	Conical baskets of W, Ni, Fe, or Chromel	Alundum crucible
Silicon	BeO crucible	BeO crucible
Silver	Helical coil or conical basket of W	Alundum crucible
Strontium	Conical basket of W	Large conical basket of W
Tellurium	Conical baskets of W, Ni, Fe, or Chromel	Alundum crucible
Thorium	Conical basket of W	Conical basket of W
Tin	Conical basket of W	Alundum crucible
Uranium	Conical basket of W	
Vanadium	Conical basket of W	Conical basket of W
Zinc	Conical baskets of W, Ni, Fe, or Chromel	Alundum crucible
Zirconium	Conical basket of W	

According to Strong, a good reflecting surface of aluminum is obtained with a thickness of about 1000 Å, and presumably the thickness required for surfaces of other metals is of the same order of magnitude. From the values for W given in Table 2, it should, therefore, be possible, for given area of deposit and temperature of evaporation, to calculate the time required to obtain the required thickness of the metal desired as a deposit.

In evaporating films from filaments of very refractory metals, like molybdenum, columbium, tungsten, or tantalum, in a vacuum, it is often necessary to keep the temperature constant. This is done by maintaining a constant value of the product $V\sqrt[3]{I}$, where V denotes the voltage drop along the filament, and I the heating current. For the metals mentioned, data are available for calculating both the current and the volts per centimeter length, for any given value of the diameter, as a function of T.[23]

For a considerable number of metals, radiation emissivities have been determined, by means of which the temperature can be calculated either from the value of the watts/cm^2 (in vacuum) or from "brightness temperatures" as measured by an optical pyrometer.[24]

4. VAPOR PRESSURES AND EVAPORATION PHENOMENA OF ALLOYS

According to the law of Raoult, which applies to dilute solutions, the vapor pressure of the solution is lower than that of the pure solvent by an amount which is proportional to the concentration of the solute. Let P_A and P_{AS} denote the vapor pressures of the pure solvent and solution, respectively, at any given temperature, and let x_B denote the mol-fraction of the solute present in the solution. Then, according to the law of Raoult,

$$\frac{P_A - P_{AS}}{P_A} = x_B = \frac{n_B}{n_A + n_B}, \tag{1}$$

where n_A and n_B denote the number of moles of solvent and solute respectively.

Since

$$x_A = \frac{n_A}{n_A + n_B}, \tag{2}$$

---

[23] See the list of references after Table 2, also the following: L. Malter and D. B. Langmuir, *Phys. Rev.*, **55**, 743 (1939), for tantalum, and *Temperature, Its Measurement and Control in Science and Industry*, Reinhold Publishing Corporation, New York, 1941, article by A. G. Worthing, p. 1164.

[24] See A. G. Worthing, *loc. cit.*

it follows from equation 1 that the following relation should be valid:

$$a_A = \frac{P_{AS}}{P_A} = x_A, \tag{3}$$

where a_A is designated the *activity* of A in the solution.

Applying these relations to a *binary* alloy in which one constituent A, which is present in larger proportion, is by far more volatile than B, we may regard B as solute, and consequently the decrease in vapor pressure of A should be in accordance with equation 1.

Furthermore, it follows, as a consequence of the application of the second law of thermodynamics, that corresponding to the decrease in vapor pressure of magnitude $P_A - P_{AS} = \Delta P_A$, there is an *increase* (ΔT_A) in the temperature at which the vapor pressure of the "solution" has a value of magnitude P_A. This increase is given by the relation

$$\frac{\Delta T_A}{\Delta P_A / P_A} = \frac{R_0 T_A{}^2}{L_A}, \tag{4}$$

where R_0 = molar gas constant (=1.9865 cal/mole) and L_A = heat of vaporization of A, in calories per mole.

From equations 4 and 1 it follows that

$$\Delta T_A = \frac{R_0 T_A{}^2 \cdot x_B}{L_A} = C_A T_A{}^2 x_B, \tag{5}$$

where C_A is a constant characteristic of the "solvent" A.

These relations should be applicable to both the solid and liquid states of the alloys, provided that the value of n_B is small compared with that of n_A.

If, furthermore, both A and B in the pure states possess vapor pressures which are of the same order of magnitude, we would expect to observe a decrease in vapor pressure of B due to addition of A as well as a decrease in vapor pressure of A due to addition of B.

Before proceeding with the discussion of particular illustrations of the above remarks, it is well to emphasize the fact that in this section the composition of an alloy is given in terms of *mol-fractions* rather than in terms of per cent by weight. Let q_A denote the per cent by weight of A and q_B, that of B, in a binary alloy. Then $q_A + q_B = 100$ and

$$q_A = \frac{100 x_A M_A}{x_A M_A + (1 - x_A) M_B} = \frac{100 x_A M_A}{x_A (M_A - M_B) + M_B}, \tag{6}$$

where M_A and M_B denote the gram-molar (or gram-atomic) masses.

Also, given the per cent by weight of each constituent, the mol-fractions can be deduced by means of the relation

$$x_A = \frac{q_A/M_A}{q_A/M_A + (100 - q_A)/M_B} = \frac{q_A}{q_A + (100 - q_A)M_A/M_B}. \tag{7}$$

An illustration of the application of equation 5 is found in the observations made by A. Schneider and U. Esch[25] on the rise in the boiling point of magnesium obtained by alloying it with different metals.

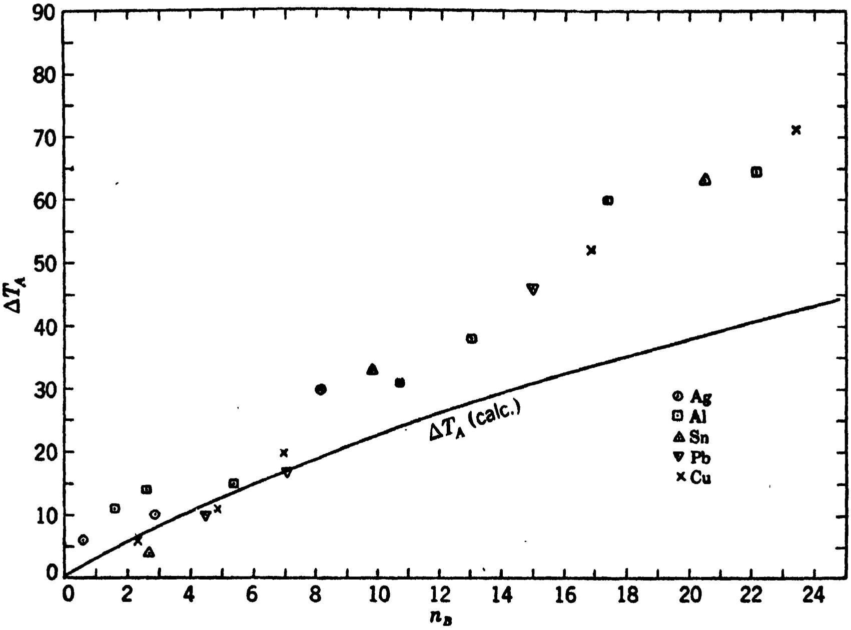

FIG. 3. Increase in boiling point of magnesium, in degrees Kelvin (ΔT_A), as a function of gram-atoms (n_B) of alloying metal per 1000 grams magnesium (Schneider and Esch).

The boiling point of pure magnesium at 760 mm pressure is 1380° K, and the latent heat of evaporation per gram-atom ($M = 24.32$) is 32,570 cal.

In this case, the composition was expressed in terms of n_B, the number of gram-atoms of the non-volatile constituent B per 1000 g of magnesium. Hence,

$$x_B = \frac{n_B}{n_B + 41.12},$$

---

[25] *Z. Elektrochem.*, **45**, 888 (1939).

and, consequently, the rise in boiling point according to equation 5 should be given by the relation

$$\Delta T_A = \frac{1.9865 \times (1380)^2}{32{,}570} \cdot x_B$$

$$= \frac{116.2 n_B}{n_B + 41.12}.$$

Figure 3 shows a plot of ΔT_A versus n_B, calculated by means of this relation, and also values actually observed for a number of alloys of magnesium with silver, aluminum, tin, lead, and copper in the liquid state. It will be observed that, with increase in the value of n_B, there is an increasing difference between the values of ΔT_A observed and those calculated. The discrepancy is such as to indicate a higher effective value of x_B than that calculated from the value of n_B.

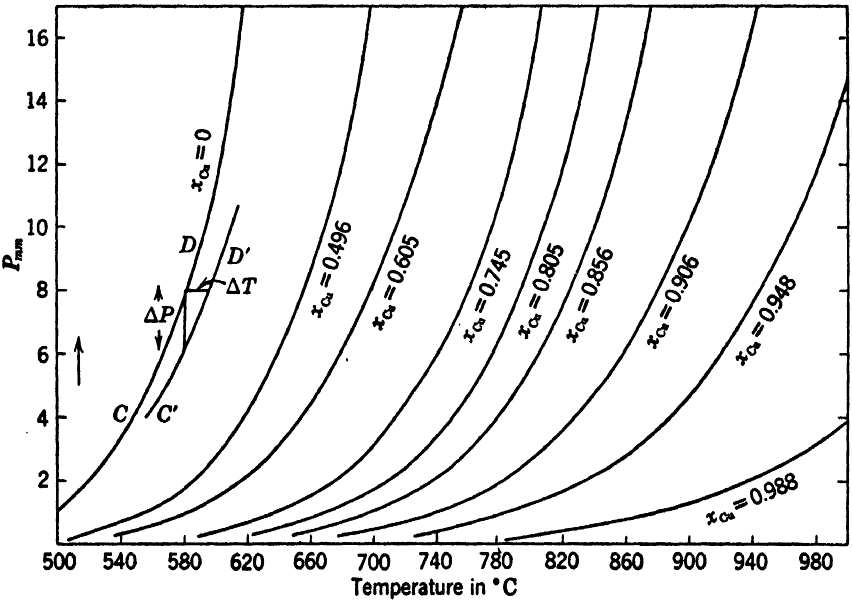

FIG. 4. Vapor pressure versus temperature plots for zinc-copper alloys for different values of x_{Cu}, the mol-fraction of copper. Curve CD is the vapor-pressure plot for pure zinc. For an alloy the vapor pressure for a given temperature is decreased by ΔP, and the temperature for a given value of the vapor pressure is increased by ΔT.

From the observations made by R. Hargreaves[26] on the vapor pressure of zinc in brasses, the curves shown in Fig. 4 have been plotted for a series of alloys in which the mol-fraction of copper in the alloy was varied from $x_{\text{Cu}} = 0.988$ to $x_{\text{Cu}} = 0.496$. The curve designated *CD* is a vapor-pressure plot for pure zinc (based on the vapor-pressure values deduced by Kelley[27]). For an alloy containing a very small mol-fraction of copper, the vapor-pressure plot would be represented by some curve such as $C'D'$, and the corresponding values of ΔT and ΔP have been indicated.

---

[26] *J. Inst. Metals*, **64**, 115 (1939).

As will be observed, the vapor pressure of zinc, at any given temperature, decreases with increase in x_{Cu}. Table 9 gives values of the activity of zinc for the series of brasses at 727° C, as defined by the relation

$$a_{\text{Zn}} = \frac{P_{\text{Zn}}}{90.3},$$

where P_{Zn} is the vapor pressure (in millimeters) as observed for the alloys and 90.3 mm is the vapor pressure, at this temperature, of pure zinc. The ratio

$$f_{\text{Zn}} = \frac{a_{\text{Zn}}}{x_{\text{Zn}}}, \tag{8}$$

is designated the *activity coefficient* and should be equal to 1 for an ideal solution.

TABLE 9

VALUES OF q_{Zn}, x_{Zn}, a_{Zn}, AND f_{Zn} FOR BRASSES AT 727° C

q_{Zn}	x_{Zn}	a_{Zn}	f_{Zn}	
5.3	0.052	0.0045	0.0865	
9.7	.094	.0086	.0915	
14.8	.144	.0185	.128	
20.0	.195	.0301	.154	
26.0	.255	.0545	.214	
38.0	.373	.134	.48	for β phase
			.33	for α phase
46.0	.453	.200	.46	
48.8	.481	.246	.51	
51.1	.504	.291	.58	

The values of a_{Zn} versus x_{Zn} have been plotted in curve *H*, in Fig. 5. Curve *A* shows a similar plot of data deduced from values of P_{Zn} observed at 700° C.[28] As will be observed, the values of a_{Zn} for zinc-copper alloys containing 0.8 mol-fraction of zinc or higher follow the relation predicted by equation 3 above. On the other hand, for values of x_{Zn} less than 0.8, the vapor pressures are lower than those calculated on the basis of equation 3, as shown by the observation that a_{Zn} is less than x_{Zn}.

---

[27] *Bur. Mines, Bull.* 383, 1935.

[28] A. Schneider and H. Schmid, *Z. Elektrochem.*, **48**, 627 (1942).

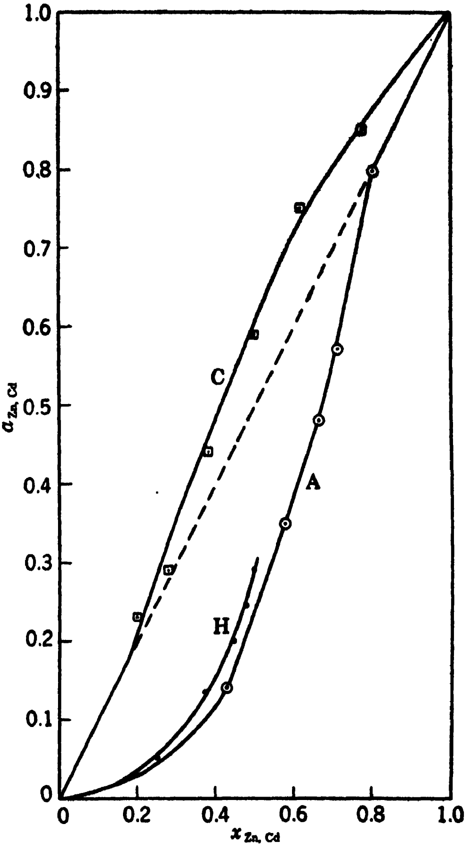

FIG. 5. Plots of the activities (a) of zinc and cadmium versus mol-fraction (x) for alloys with copper. Curve A, plot for zinc-copper alloys at 700° C; curve H, plot for zinc-copper alloys at 727° C (from data in Table 9), curve C, plot for cadmium-copper alloys in the range 700–850° C. The dashed line represents the values deduced on the basis of Raoult's law. (Curves A and C from Schneider and Schmid.)

Figure 6[29] shows the constitution of copper-zinc alloys, and, as is seen from the diagram, all the alloys containing up to about 69 per cent zinc are solid at 727° C. At 697° C, the alloys containing 30 per cent to 19.5 per cent copper exhibit a transition from the solid to the liquid state, and all alloys containing less than 19.5 per cent copper are fused at this temperature. Thus, according to curve A in Fig. 5, $f_{\text{Zn}} = 1$ for the alloys that are in the fused state at 700° C.

---

[29] *Metals Handbook*, 1939 Edition, p. 1367.

If $\log P_{\text{Zn}}$ for a given copper-zinc alloy is plotted versus $1/T$, a straight line is obtained, the slope of which yields a value of L, the heat of sublimation. Such a series of plots of the data shown in Fig. 4 leads, as shown by Hargreaves, to values of L ranging from 36,600 cal/g-atom for the alloy containing 1.2 per cent by weight of zinc to 31,500 cal/g-atom for the alloy containing 51.1 per cent zinc. The value for liquid zinc is 28,600 cal/g-atom.

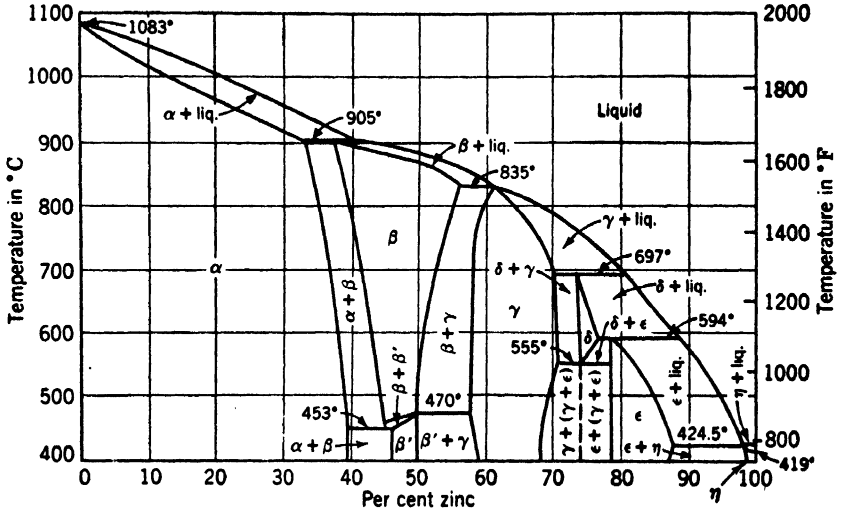

FIG. 6. Constitution diagram of copper-zinc alloys (*Metals Handbook*).

One important conclusion from these observations, which is valid for most alloys, is that in order to maintain the vapor pressure of zinc in a brass at, for instance, 1 mm, the temperature of evaporation must be increased continuously as the zinc content decreases. At 960° C, the vapor pressure of pure copper is about 10^{-5} mm (see Table 2), and, in the presence of even a small content of zinc, the vapor pressure of copper must be considerably smaller. Hence the elimination of the zinc becomes progressively more and more difficult with decreasing content in the alloy.

Curve C in Fig. 5 shows a plot of a_{Cd} for cadmium-copper alloys[30] in the range 700–850° C. At these temperatures all the alloys are in the fused state, and as will be observed f_{Cd} is greater than 1 for all alloys containing more than 0.2 mol-fraction of cadmium. That is, the vapor pressure of cadmium for these alloys is greater than that corresponding to equation 3.

---

[30] Schneider and Schmid, *loc. cit.*

The brasses are typical of binary alloys in which one constituent is practically non-volatile as compared with the other. An interesting illustration of a binary alloy in which this is not the case is furnished by the zinc-cadmium system, which has been studied by E. Burmeister and K. Jellinek.[31]

Table 10 gives the vapor pressures of zinc and cadmium at 682° C for the pure metals and three alloys. At this temperature the metals and alloys are above their melting points.

TABLE 10

VAPOR PRESSURES (IN MILLIMETERS) FOR ZINC-CADMIUM ALLOYS AT 682° C (BURMEISTER AND JELLINEK)

x_{Cd}	P_{Cd}	a_{Cd}	x_{Zn}	P_{Zn}	a_{Zn}	$P_{Zn} + P_{Cd}$
1	252	1	0	0	0	252
0.749	205	0.815	0.251	20.5	0.472	225.5
0.459	153	0.633	0.541	30.7	0.706	183.7
0.238	112	0.444	0.762	37	0.850	149
0			1	44	1	44

The values of the vapor pressures of the individual constituents and the total pressures are plotted in Fig. 7; Fig. 8 shows plots of the activities.

Similar plots of vapor pressures of fused tin-zinc alloys and tin-cadmium alloys[32] (at 700° C and 540° C, respectively) are shown in Fig. 9. In both these cases the values of f_{Zn} and f_{Cd} are greater than 1 for all the compositions.

Figure 10[33] shows plots of the activities of silver and magnesium in fused alloys and, for comparison, phase diagrams for these alloys. Similar plots are shown in Fig. 11[33] for the volatile constituents in fused alloys of lead-cadmium, lead-zinc, and bismuth-tin. The system lead-zinc is of special interest because of the limited solubility of zinc in lead.

The vapor pressures of aluminum-zinc alloys over the range of temperatures 600° C to 1100° C have been investigated by A. Schneider and E. K. Stoll.[34] Figure 12 shows plots of log P_{mm} versus $1/T$ for the three

---

[31] *Z. physik. Chem.*, **A**, **165**, 121 (1933).

[32] Burmeister and Jellinek, *loc. cit.*

[33] O. Kubaschewski, *Z. Elektrochem.*, **48**, 559, 646 (1942).

[34] *Z. Elektrochem.*, **47**, 527 (1941).

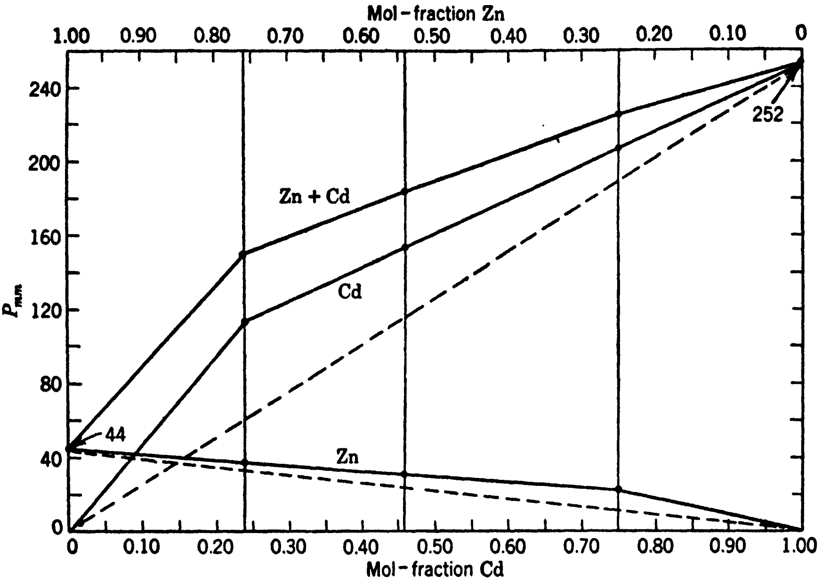

FIG. 7. Vapor pressures of zinc and cadmium and total vapor pressure for zinc-cadmium alloys at 682° C, plotted versus mol-fraction of each constituent (Burmeister and Jellinek).

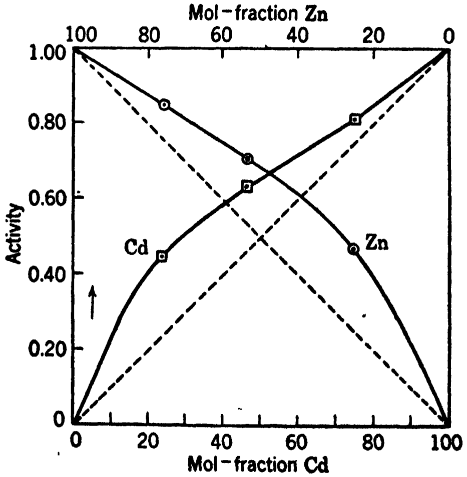

FIG. 8. Plots of activity versus mol-fraction for zinc and cadmium in zinc-cadmium alloys, corresponding to vapor-pressure plots in Fig. 7.

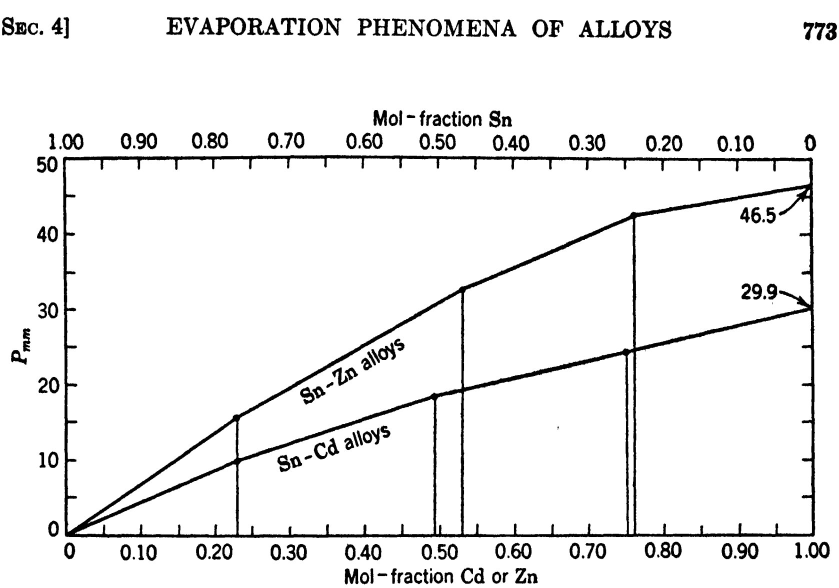

Fig. 9. Vapor pressure of zinc in tin-zinc alloys at 700° C, and vapor pressure of cadmium in tin-cadmium alloys at 540° C, plotted versus mol-fraction of zinc and cadmium respectively (Burmeister and Jellinek).

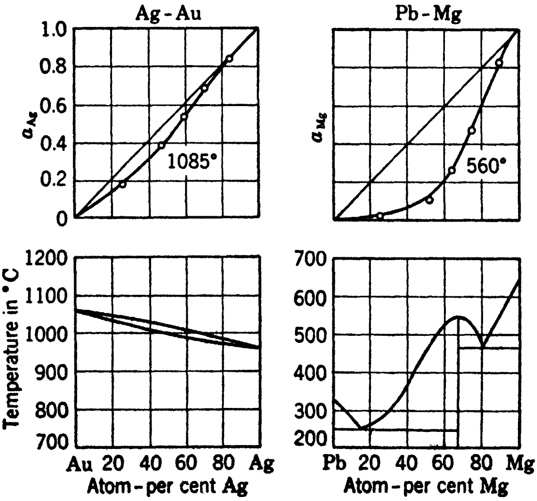

Fig. 10. Plots of the activity (a) versus atom-per cent for silver in fused silver-gold alloys at 1085° C, and for magnesium in fused lead-magnesium alloys at 560° C. Corresponding phase diagrams are shown below (from Kubaschewski).

alloys having the compositions:

2.12 atomic per cent Zn = 5.03 per cent by weight,
15.02 atomic per cent Zn = 30.0 per cent by weight,
49.04 atomic per cent Zn = 70.0 per cent by weight.

According to the constitution diagram shown in Fig. 13,[35] the alloy containing 5.03 per cent by weight zinc melts at about 608° C and equilibrium exists between the γ phase and the liquid to about 647° C.

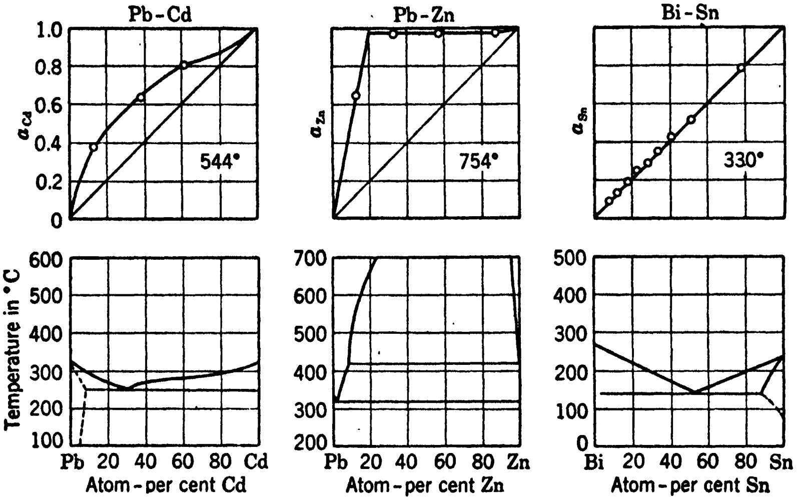

FIG. 11. Plots of the activity versus atom-per cent of cadmium in cadmium-lead alloys at 544° C, of zinc in zinc-lead alloys at 754° C, and of tin in bismuth-tin alloys at 330° C, with corresponding phase diagrams (from Kubaschewski).

Above this temperature the alloy is completely liquid. The plot in Fig. 12 shows that in this range of temperatures the vapor pressures are abnormally higher. A similar phenomenon is observed for the alloy containing 30 per cent by weight zinc in the range 513° C to 615° C, which is the range of existence of γ + liquid. For the alloy containing 70 per cent by weight zinc the γ + liquid range is from about 443° C to slightly above 500° C, and the log P_{mm} versus $1/T$ plot shows a deviation from the linear plot over this range of temperatures. The log P_{mm} versus $1/T$ plot for pure zinc shown in Fig. 12 is that for the liquid phase, since the melting point is 419.4° C.

Plots of a_{Zn} versus x_{Zn} for the aluminum-zinc system for 650° C and 800° C are shown in Fig. 14. As will be observed, the activities are higher than those predicted by Raoult's law.

---

[35] *Metals Handbook*, 1939 Edition, p. 1738.

Data on the vapor pressures of mercury over amalgams with a number of metals (for the range 300° C to 324° C) are given in *International Critical Tables*.[36] As shown by F. E. Poindexter[37] and A. L. Hughes and Poindexter,[38] "a sodium or potassium trap is almost, if not quite as effective as liquid air for stopping mercury vapor." Poindexter[39] has concluded, from plots of log P versus $1/T$ for a sodium amalgam containing a 50 per cent mol-fraction of sodium, that at 20° C the vapor

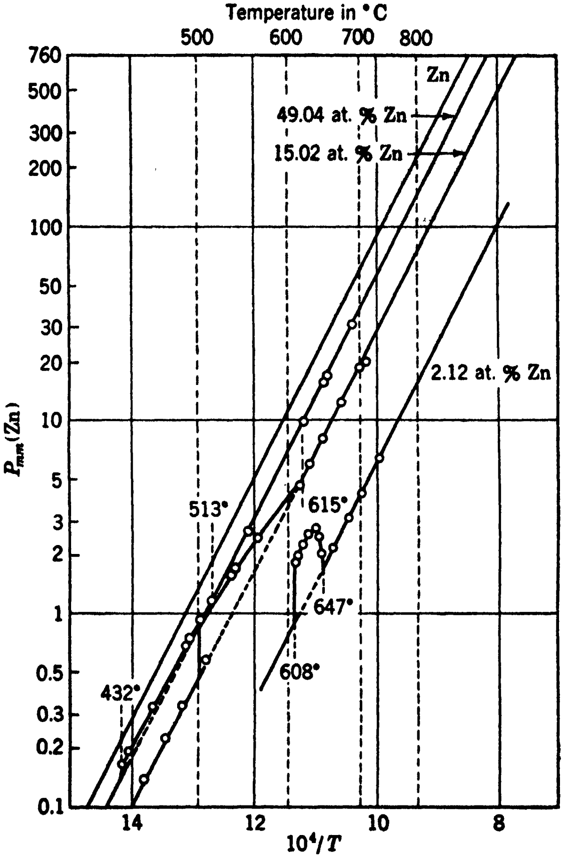

FIG. 12. Plots of P_{mm} (zinc) versus $1/T$ on semi-log scale for three zinc-aluminum alloys and for pure zinc (Schneider and Stoll).

---

[36] *International Critical Tables*, Vol. 3, p. 284 (1928).

[37] *J. Optical Soc. Am.*, **9**, 629 (1924).

[38] *Phil. Mag.*, **50**, 423 (1925); see Chapter 4, section 9.

[39] *Phys. Rev.*, **28**, 208 (1926).

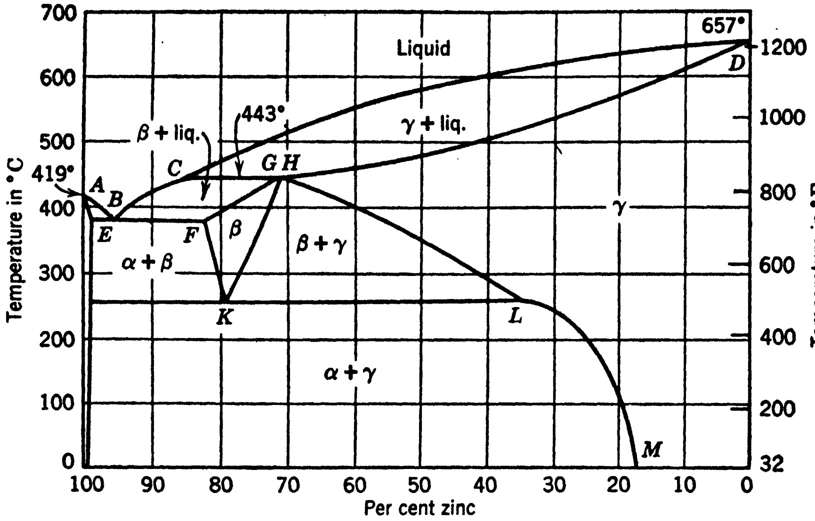

FIG. 13. Constitution diagram for zinc-aluminum alloys (*Metals Handbook*).

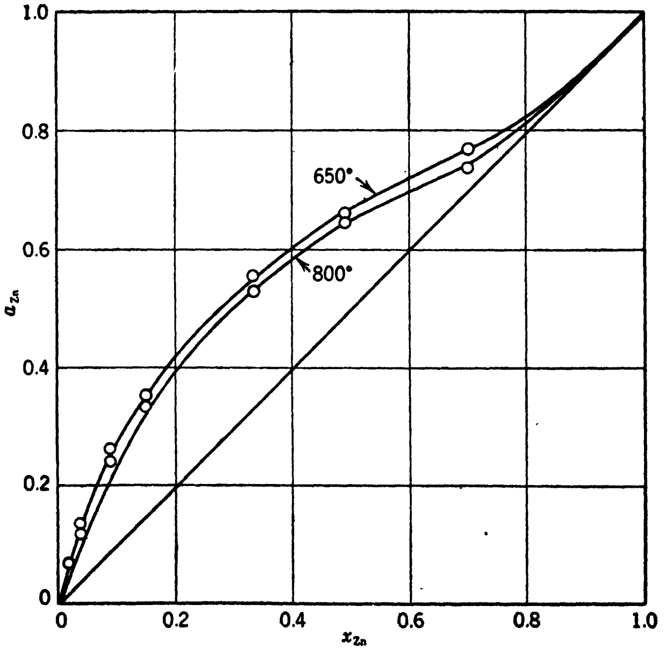

FIG. 14. Plots of activity of zinc (a_{Zn}) versus mol-fraction (x_{Zn}) in zinc-aluminum alloys.

pressure is $3 \cdot 10^{-8}$ mm mercury. However, in the case of the amalgams with other metals than those of the alkali group, the deviations from Raoult's law are not at all as great. The plots of a_{Hg} versus x_{Hg} are very similar to those shown for alloys of zinc-cadmium and some of the other metals.[40]

Frequently, in degassing parts made of high-melting-point alloys it is of considerable interest to be able to predict the relative volatilities of different constituents in a given alloy. From the preceding discussion it follows that at any given temperature the vapor pressure of each constituent in the alloy must be much lower than that for the pure metal. As a rough approximation the validity of Raoult's law may be assumed, that is, equation 3.

For instance, let us assume that we have an iron-manganese-carbon alloy containing 13 per cent by weight manganese and 0.20 per cent carbon.[41] Since the atomic weights of iron and manganese are 55.85 and 54.93, respectively, the mol-fraction of manganese is approximately 0.13. Hence, we may make the following assumptions:

1. Vapor pressure of Mn in alloy = 0.13 × (Vapor pressure of pure Mn).
2. Vapor pressure of Fe in alloy = 0.87 × (Vapor pressure of pure Fe).

From Table 2 it is seen that, at 1000° C, the vapor pressure of iron is about 10^{-3} micron, while that of manganese is about 10 microns. Therefore, in the alloy, the vapor pressures of manganese and iron will be approximately 1 micron and $9 \cdot 10^{-4}$ micron, respectively, and hence the manganese will evaporate about 1000 times more rapidly than the iron. The effect of the carbon may be neglected under these conditions.

As another illustration, let us consider an iron-nickel alloy containing 25 atomic per cent nickel. At 1200° C, the vapor pressures of iron and nickel are about 0.1 and 0.03 micron, respectively. Assuming the validity of Raoult's law, the vapor pressures of iron and nickel in the alloy would be about 0.075 and 0.008 micron, respectively. Consequently, we would conclude that the iron would evaporate about ten times as fast as the nickel.

In view of the fact that, as far as the writer is aware, there are no experimental data available on the rates of evaporation of alloys of the more refractory metals, the application of Raoult's law represents probably the only method by which any semiquantitative conclusion can be deduced in such cases.

---

[40] See also the following references: Na-Hg (375° C), K. Hauffe, *Z. Elektrochem.*, **46**, 348 (1940); K-Hg (300° C), Cd-Hg (284° C), J. S. Pedder and S. Barratt, *J. Chem. Soc.*, **1933**, 537; K-Hg (184° C–445° C), R. W. Millar, *J. Am. Chem. Soc.*, **49**, 3003 (1927).

[41] Constitution diagram given in *Metals Handbook*, 1939 Edition, p. 411.

Finally, mention may be made of the fact that, from observations on the relative rates of evaporation of different constituents of an alloy, it is possible to draw conclusions regarding relative vapor pressures. For example, the data in Table 2 show that copper has a much higher vapor pressure at any given temperature than gold. However, data have been published which indicate that the volatilities should be in the reverse order. Observations made in this laboratory on the evaporation of a gold-copper alloy containing equal proportions (by weight) of the two metals have shown that the copper evaporates almost completely before the gold even begins to evaporate and the temperature has to be increased in order to complete the evaporation. Hence, it must be concluded that the relative volatilities are in the order shown in the table.

Another illustration is furnished by the vapor pressure of chromium. The data shown for this metal in Table 2 are based on observations which the writer considers not very reliable. An investigation of the relative volatilities of the two metals in ferrochrome alloys would show whether the relative vapor pressures are in the order shown in Table 2 or in the reverse order. Similar observations on aluminum-silver alloys would be of help in deciding between the two sets of vapor-pressure data shown for aluminum.

5. VAPOR PRESSURES OF OXIDES AND OTHER INORGANIC COMPOUNDS

As in the case of metals, vapor pressures of a number of inorganic compounds of interest in vacuum technique can be calculated from free energy data given by Kelley[42] by means of equation 1.2*a* or 1.2*b*.

Table 11 gives data on some of these compounds, as obtained from the following sources:

1. K. K. Kelley, *Bureau of Mines Bulletin* 383, Washington.
2. B. H. Zimm and J. E. Mayer, *J. Chem. Phys.*, **12**, 362 (1944).
3. W. Kangro and H. W. Wieking, *Z. physik. Chem.*, **A**, **183**, 199 (1938–1939).
4. H. L. Johnston and A. L. Marshall, *J. Am. Chem. Soc.*, **62**, 1382 (1940).
5. J. P. Blewett, H. A. Liebhafsky, and E. F. Hennelly, *J. Chem. Phys.*, **7**, 480 (1939).

As in Table 2, the symbols *l* and *s* designate the liquid and solid states, respectively.

From their observations on the vapor pressures of four *solid* halides, in the range $T = 945°$ K to $T = 600°$ K, Zimm and Mayer deduced the following relations for vapor pressures.

---

[42] *Loc. cit.*

$$\begin{aligned}
\text{KCl:}\ \log P_{mm} &= 17.006 - 11{,}879/T - 2\log T.\\
\text{KBr:}\ \log P_{mm} &= 17.141 - 11{,}543/T - 2\log T.\\
\text{KI:}\ \log P_{mm} &= 17.277 - 11{,}263/T - 2\log T.\\
\text{NaCl:}\ \log P_{mm} &= 17.093 - 12{,}288/T - 2\log T.
\end{aligned}$$

From these relations two-term expressions were derived of the form

$$\log P_{mm} = A - \frac{B}{T}, \tag{1}$$

from which, in turn, values of $t°$ C were calculated for values of the pressure ranging from $P_\mu = 10^{-2}$ to $P_\mu = 100$, which are given in Table 11 in the rows designated by reference 2.

Kangro and Wieking found that their determination of the vapor pressures of the *fused* halides could be expressed in the form of equation 1 with the values of A (for the pressure in millimeters) and B given in Table 11. These were used to derive values of the pressure at the melting point. As will be observed these values are higher than those calculated from Kelley's values of ΔF. The table also gives the values of P_{mm} observed at 860° C, 950° C, and 990° C.

Johnston and Marshall deduced the following relation for the vapor pressure of NiO:

$$\log P_\mu = 16.079 - 7.67 \times 10^{-4}T + 7.21 \times 10^{-8}T^2 - \frac{25{,}586}{T},$$

which was used to calculate the values of P_μ given in the table.

In a booklet published by the National Research Corporation[43] are given vapor-pressure data obtained in their laboratory. These are listed at the bottom of Table 11. It is also stated in this publication that, for quartz, the temperature corresponding to a vapor pressure of 10 microns exceeds 2000° C. As will be observed, this conclusion is in considerable disagreement with vapor-pressure data given in Kelley's publication for fused silica.

Binary mixtures of compounds which are mutually soluble exhibit a decrease in the vapor pressure of each compound which is similar to that exhibited by binary alloys and which was discussed in the previous section. As an illustration of this phenomenon Table 12 gives vapor-pressure data for fused mixtures of KCl and NaCl as observed by Kangro and Wieking.[44]

---

[43] Cambridge, Mass., 1945.

[44] *Loc. cit.*

TABLE 11

VAPOR PRESSURES OF OXIDES, HALIDES, ETC.*

Compound	Melting Point, ° C	P_{mm} at M.P.	t° C for P_{mm} =		
			0.076	0.76	7.6
Al_2O_3 (1)	2050	0.347	(s)	2122 (l)	2351
SiO_2 (1)	1710	7.60			1710
MoO_3 (1)	795	7.50	661	726	801 (l)
LiF (1)	870	0.034	908 (l)	1031	1181
LiCl (1)	613	0.021	663 (l)	769	911
NaCl (1)	801	0.31	743 (s)	850 (l)	996
KCl (1)	776	0.44	704 (s)	806 (l)	948
RbCl (1)	718	0.23	——	777 (l)	917
CsCl (1)	646	0.14	——	730 (l)	864

	M.P., ° C	t° C for P_μ =				
		10^{-2}	10^{-1}	1	10	100
CaO (1)	2572	1583	1717	1873	2055	2271
SrO (1)	2430	1420	1258	1631	1757	1901
BaO (5)	1923	1150	1263	1395	1552	1742
P_4O_{10} (1)	358 (Sublimes)	42	63	87	116	149
AgCl (1)	455	479 (l)	536	607	690	790
NaCl (2)	801	479	532	592	662	745
KCl (2)	776	457	508	567	635	716

	A	B	P_{mm} at			
			M.P.	860° C	950° C	990° C
LiCl (3)	7.172	7187	0.12	6.7	10.9	30.2
NaCl (3)	7.906	8475	1.03	2.8	9.2	16.2
KCl (3)	7.245	7450	1.38	5.0	14.0	22.4
RbCl (3)	7.326	7809	0.28	2.7	8.6	14.0
CsCl (3)	8.302	8400	0.18	7.7	25.6	46.0

NiO (4)	P_μ:	10^{-6}	10^{-5}	10^{-4}	10^{-3}	10^{-2}	10^{-1}
	t° C:	943	1007	1069	1158	1248	1349

Data from NRC bulletin

Compound:	Sb_2S_3	CaF_2	Na_3AlF_6	Cr_2O_3	MgF_2	ZnS
M.p., ° C	550	1330	1000	1900	1395	1645
t° C for P_μ = 10	550	1400	1000	1900	1400	1200

---

* See also reference to Stull's publication in footnote 4, section 2.

TABLE 12

VAPOR PRESSURES OF FUSED MIXTURES OF KCL (A) AND NACL (B)

$t°$ C	$P_{mm}(A)$	$P_{mm}(B)$	Mol-Fraction in Per Cent	
			A	B
860	5.0	——	100	0
	3.7	0.7	74.5	25.5
	2.2	1.0	49.3	50.7
	1.1	1.9	25.6	74.4
	——	2.8	0	100
950	14.0	——	100	0
	8.9	1.9	74.4	25.6
	6.2	3.5	49.6	50.4
	3.1	6.5	25.8	74.2
	——	9.2	0	100
990	22.4	——	100	0
	13.0	4.9	75.9	24.1
	9.2	7.3	49.5	50.5
	6.7	9.8	24.3	75.7
		16.2	0	100

6. VAPOR PRESSURES AT LOW TEMPERATURES

In high-vacuum technique refrigerants are used to condense out a number of gases and vapors. Table 13 contains vapor-pressure data for ice and mercury. In each case two sets of values are given, one taken from *International Critical Tables*,[45] and the other derived from the expressions for ΔF calculated by K. K. Kelley.[46] According to the latter, the vapor pressure of ice is given by the relation

$$\log P_{mm} = 1.207 + 3.857 \log T + 3.41 \cdot 10^{-3} T + 4.875 \cdot 10^{-8} T^2 - \frac{2461}{T}.$$

The relations derived for the vapor pressure of mercury from Kelley's calculated expressions for ΔF are as follows:

$$\text{Liquid} \rightarrow \text{Gas:} \quad \log P_{mm} = 10.377 - 0.8254 \log T - \frac{3285}{T}.$$

$$\text{Solid} \rightarrow \text{Gas:} \quad \log P_{mm} = 9.453 - 0.2011 \log T - 6.558 \cdot 10^{-4} T - \frac{3379}{T}.$$

---

[45] *International Critical Tables*, Vol. 3, pp. 206 and 210. These data are also given in the *Handbook of Chemistry and Physics*, Chemical Rubber Publishing Company (1945), Cleveland, Ohio (designated RH), and in the *Handbook of Chemistry* by N. A. Lange, Handbook Publishers, Inc., 1941, Sandusky, Ohio (designated LH).

[46] *Loc. cit.*

TABLE 13

VAPOR PRESSURE OF ICE AND MERCURY AT LOW TEMPERATURES

$t°$ C	T	P_μ (KK)	P_μ (ICT)	$t°$ C	T	P_μ (KK)	P_μ (ICT)
Ice (H_2O)							
0	273.2		4579	−80	193.2	$4.13 \cdot 10^{-1}$	$4.0 \cdot 10^{-1}$
−10	263.2	1960	1950	−90	183.2	$7.45 \cdot 10^{-2}$	$7.0 \cdot 10^{-2}$
−20	253.2	779	776	−100	173.2	$1.10 \cdot 10^{-2}$	
−30	243.2	293.1	285.9	−110	163.2	$1.25 \cdot 10^{-3}$	
−40	233.2	99.4	96.6	−120	153.2	$1.13 \cdot 10^{-4}$	
−50	223.2	29.85	29.6	−130	143.2	$6.98 \cdot 10^{-6}$	
−60	213.2	8.40	8.08	−140	133.2	$2.93 \cdot 10^{-7}$	
−70	203.2	1.98	1.94	−150	123.2	$7.4 \cdot 10^{-12}$	
−78.5	194.7	0.53		−183	90.2	$1.4 \cdot 10^{-19}$	
Mercury (Hg)							
30	303.2	3.13	2.78	−38.9	234.3	$2.51 \cdot 10^{-3}$	
25	298.2	2.05	1.84	−45	228.2	$1.05 \cdot 10^{-3}$	
20	293.2	1.38	1.20	−50	223.2	$4.94 \cdot 10^{-4}$	
10	283.2	$5.62 \cdot 10^{-1}$	$4.90 \cdot 10^{-1}$	−60	213.2	$9.89 \cdot 10^{-5}$	
0	273.2	$2.22 \cdot 10^{-1}$	$1.85 \cdot 10^{-1}$	−70	203.2	$1.68 \cdot 10^{-5}$	
−10	263.2	$7.87 \cdot 10^{-2}$	$6.06 \cdot 10^{-2}$	−78.6	194.6	$3.13 \cdot 10^{-6}$	
−20	253.2	$2.64 \cdot 10^{-2}$	$1.81 \cdot 10^{-2}$	−80	193.2	$2.38 \cdot 10^{-6}$	
−30	243.2	$7.85 \cdot 10^{-3}$	$4.78 \cdot 10^{-3}$	−100	173.2	$2.39 \cdot 10^{-8}$	
−38.9	234.3	$2.51 \cdot 10^{-3}$	$1.24 \cdot 10^{-3}$	−183	90.2	$3.48 \cdot 10^{-29}$	

Table 14(*a*) gives vapor-pressure data for solid carbon dioxide according to C. H. Meyers and M. S. van Dusen.[47] The sublimation temperature of the solid at atmospheric pressure is −78.5° C.

The relation derived from Kelley's expression for ΔF is

$$\log P_{mm} = 8.882 + 0.8702 \log T - 3.891 \cdot 10^{-3} T - \frac{1408}{T}.$$

This has been used to calculate values of P for solid carbon dioxide in the range below −150° C, and Table 14(*b*) gives a comparison between these values (KK) and those given by Meyers and van Dusen (MVD).

Table 15(*a*) gives vapor pressures for the more common "non-condensible" gases.[48] Triple points are shown by asterisks.

[47] *J. Research Natl. Bur. Standards*, **10**, 381 (1933).

[48] Values for helium and neon taken from RH; values for hydrogen, nitrogen, carbon monoxide, argon, oxygen, and methane from LH. The data for krypton and xenon are taken from the paper by K. Peters and K. Weil, *Z. physik. Chem.*, **A**, **148**, 27 (1930). See also F. J. Allen and R. B. Moore, *J. Am. Chem. Soc.*, **53**, 2522 (1931), for the boiling points of these gases. Temperature-vapor pressure data for CS_2, SO_2, NH_3, CO_2, HCl, C_2H_4, CH_4, O_2, and N_2 are also given in FM.

TABLE 14(*a*)

Vapor Pressure of Solid Carbon Dioxide

Pressure in microns of mercury

t° C	0	1	2	3	4	5	6	7	8	9
−180	0.013	0.008	0.006	0.004	0.003	0.0017	0.0011	0.0007	0.0005	0.0003
−170	.37	.27	.20	.14	.10	.074	.052	.037	.026	.018
−160	5.9	4.6	3.6	2.7	2.1	1.58	1.19	.90	.67	.50
−150	60.5	48.8	39.2	31.4	25.1	19.9	15.8	12.4	9.8	7.6
−140	431	359	298	247	204	168	138	113	92	75

Pressure in millimeters of mercury

t° C	0	1	2	3	4	5	6	7	8	9
−130	2.31	1.97	1.68	1.43	1.22	1.03	0.87	0.73	0.61	0.51
−120	9.81	8.57	7.46	6.49	5.63	4.88	4.22	3.64	3.13	2.69
−110	34.63	30.76	27.27	24.14	21.34	18.83	16.58	14.58	12.80	11.22
−100	104.81	94.40	84.91	76.27	68.43	61.30	54.84	48.99	43.71	38.94
−90	279.5	254.7	231.8	210.8	191.4	173.6	157.3	142.4	128.7	116.2
−80	672.2	618.3	568.2	521.7	478.5	438.6	401.6	367.4	335.7	306.5
−70	1486.1	1377.3	1275.6	1180.5	1091.7	1008.9	931.7	859.7	792.7	730.3
−60	3073.1	2865.1	2669.7	2486.3	2314.2	2152.8	2001.5	1859.7	1726.9	1602.5
−50	—	—	—	—	—	—	—	3780.9	3530.2	3294.6

Triple point, —56,602 ± 0.005° C; 3885.2 ± 0.4 mm.

TABLE 14(*b*)

VAPOR PRESSURES OF SOLID CARBON DIOXIDE AT VERY LOW TEMPERATURES

$t°$ C	T	P_μ (KK)	P_μ (MVD)	t	T	P_μ (KK)	P_μ (MVD)
−150	123.1	61.94	60.5	−183	90.1	$4.2 \cdot 10^{-3}$	$4.0 \cdot 10^{-3}$
−160	113.1	7.30	5.9	−187	86.1	$7.9 \cdot 10^{-4}$	$7.0 \cdot 10^{-4}$
−170	103.1	$3.82 \cdot 10^{-1}$	$3.8 \cdot 10^{-1}$	−189	84.1		$3.0 \cdot 10^{-4}$
−175	98.1		$7.4 \cdot 10^{-2}$	−193	80.1	$5.85 \cdot 10^{-5}$	
−180	93.1		$1.3 \cdot 10^{-2}$	−196	77.1	$1.05 \cdot 10^{-5}$	

Kelley has given the following vapor-pressure relations for the *solid* state:

$$\text{Argon:} \quad \log P_{mm} = 7.620 - \frac{411.1}{T}\cdot$$

$$\text{Krypton:} \quad \log P_{mm} = 7.478 - \frac{555.2}{T}\cdot$$

$$\text{Xenon:} \quad \log P_{mm} = 8.00 - \frac{842}{T}\cdot$$

A chart showing plots of the vapor pressure versus temperature for a number of different gases in the range 100° C to −200° C has been published by E. Berl.[49]

Table 15(*b*) gives the temperature in degrees Centigrade for a series of values of the pressure in microns, as derived from Kelley's calculated values of ΔF. The values of t for 7600, 760, and 76 microns were taken from his tables; those for lower pressures were extrapolated from a plot of $\log P_\mu$ versus $1/T$ for the above values of P_μ. For argon, krypton, and xenon the two-term relations given above for the solid state were used. The last column in the table gives the boiling points according to Kelley for comparison with those given in the previous table.

Charts showing plots of vapor pressure versus the temperature in degrees Centigrade for a large number of gases and vapors of inorganic and organic compounds have been published by E. Berl.[50] Since these plots cover the range from −190° C to 200° C and from pressures above atmospheric to very low values, they should prove of value for information on the vapor pressures of those elements and compounds not discussed in the above review.

---

[49] *Chem. & Met. Eng.*, **51**, Oct., 132 (1944). See also *Chem. & Met. Eng.*, **53**, 130 (Jan., 1946), for table of boiling points of a number of elements and inorganic compounds.

[50] *Chem. & Met. Eng.*, **51**, 132–133 (October, 1944).

TABLE 15(*a*)

VAPOR PRESSURES OF GASES AT LOW TEMPERATURES

He	t° C	−271.1	−269.9	−268.9					
	P_{mm}	3	197	760					
H_2	t° C	−259.14	−258.46	−257.99	−257.21	−256.19	−254.73	−252.74	
	P_{mm}	51.4*	79.9	100	149.7	232.5	397.6	760	
Ne	t° C	−257.62	−257.48	−254.92	−253.16	−251.24	−250.22	−248.5	−245.92
	P_{mm}	0.55	2.4	7.8	28.2	91	148 (*s*)	325 (*l*)	760
N_2	t° C	−216.13	−213.18	−211.11	−210.90	−206.20	−202.16	−198.30	−195.82
	P_{mm}	21.8	47.0	71.9	96.4*	177.6	329.4	561.3	760
CO	t° C	−220.6	−209.1	−205.7	−192.0	(M.p. = −205.0)			
	P_{mm}	4	50	111.3	760				
A	t° C	−205.3	−200	−195.6	−189.3	−186.1	−185.9		
	P_{mm}	38.3	84.6	208.8	515.6*	672.7	760		
O_2	t° C	−215.73	−210.76	−205.82	−201.42	−196.39	−192.73	−187.61	−182.95
	P_{mm}	2.68 (*l*)	9.59	28.07	64.01	129.5	239.5	457.6	760
CH_4	t° C	−183.2	−182	−176	−170	−167	−165	−163	−161.5
	P_{mm}	70 (*s*)	94.0 (*l*)	190.5	353.2	468.2	559.3	663.8	760
Kr	t° C	−192	−188.5	−182.0	−169*	−165.3	−157.0	−151.8	−152.9
	P_{mm}	4.8	8.5	22.6	132.5	207.9	522.2*	760	760
Xe	t° C	−178.0	−162.0	−152.3	−138.0	−127.0	−118.1	−112.0	−109.1
	P_{mm}	0.3	3.0	10.0	60.0	185.0	373.5	615.5*	760

*Asterisks denote triple points.

TABLE 15(*b*)

TEMPERATURE IN DEGREES CENTIGRADE FOR PRESSURE IN MICRONS (KELLEY)

Gas	0.076	0.76	7.6	76	760	7600	B.P., °C
Ne				−259.3	−257.4	−254.9	−245.95
N_2	−242.1	−239.2	−236.0	−231.9	−226.8	−220.0	−195.78
CO	−238.5	−235.5	−232.0	−227.8	−222.7	−216.1	−191.5
A	−238.1	−234.8	−230.9	−226.0	−220.1	−212.1	−185.8
O_2	−237.3	−234.1	−230.3	−225.6	−219.7	−211.4	−183.0
CH_4	−229.1	−225.1	−220.1	−214.1	−206.5	−196.7	−161.4
Kr	−225.2	−220.7	−215.2	−208.4	−200.1	−188.9	−152.1
Xe	−203.6	−197.4	−189.9	−180.8	−169.6	−155.0	−108.0

Also R. V. Smith has published a vapor-pressure chart for volatile hydrocarbons[51] which shows values down to 10^{-2} mm plotted in accordance with the relation

$$\log P_{mm} = A - \frac{B}{T}.$$

7. BOILING POINT OF LIQUID AIR

Ordinary air consists of a mixture of 78.02 per cent nitrogen, 20.99 per cent oxygen, 0.94 per cent argon, and traces of hydrogen, carbon dioxide, and the other rare gases.[52] Hence the molecular percentage of oxygen is 23.5.

Since the boiling point of nitrogen is −195.78° C and that of oxygen −182.95° C, the "boiling point" of liquid air lies between these two values, depending on the composition. The earliest investigation on this topic was carried out by E. C. C. Baly.[53] More recently, B. F. Dodge and A. K. Dunbar[54] have repeated the measurements and extended the range to higher and lower pressures.

Table 16 gives the equilibrium compositions, as obtained in this investigation, for the range of temperatures from that of pure nitrogen to pure oxygen. Figure 15 shows a plot of these data.

At any given temperature the compositions of the vapor and liquid phases are given by the two points, such as *A* and *B*, on the line parallel to the axis of abcissas. For freshly produced liquid air, the composition

---

[51] *Bur. Mines Information Circular* 7215, August, 1942.

[52] Composition given in *International Critical Tables*, Vol. 1, p. 393. The density at 0° C and 1 atm is 1.2930 g · liter^{-1}.

[53] *Phil. Mag.*, **49**, 517 (1900).

[54] *J. Am. Chem. Soc.*, **49**, 591 (1927).

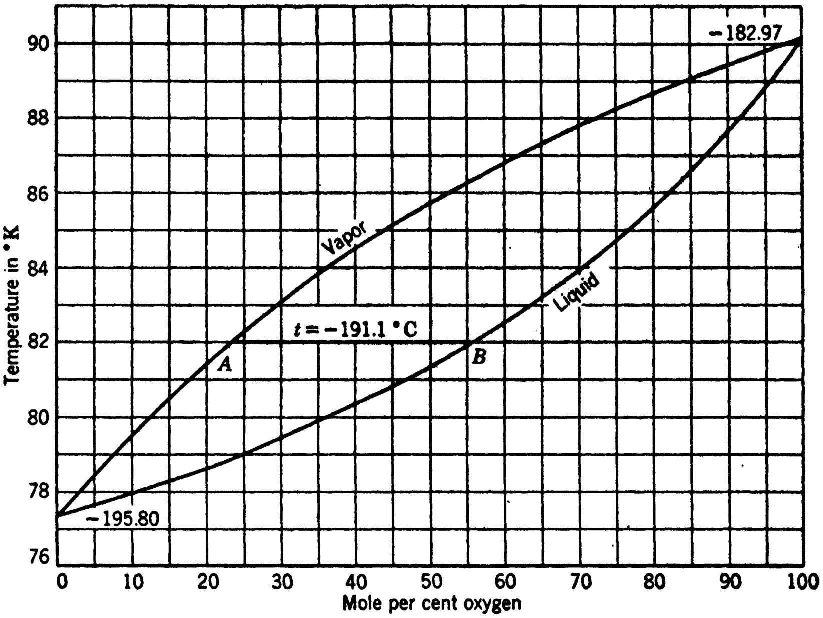

Fig. 15. Compositions of vapor and liquid phases for oxygen-nitrogen mixtures at 1 atm, showing corresponding boiling points (Dodge and Dunbar). For air the composition of the gas corresponds to *A*, and that of the liquid phase in equilibrium corresponds to *B*.

TABLE 16

Compositions of Vapor and Liquid Phases for Nitrogen-Oxygen Mixtures at 1 Atmosphere

T	$T - 273.13$	Mol-Fraction Oxygen in Liquid	Mol-Fraction Oxygen in Vapor
77.35	−195.78	0	0
77.86	−195.27	8.10	2.30
78.78	−194.35	21.60	6.50
79.72	−193.41	33.35	11.05
80.65	−192.48	43.38	15.65
81.60	−191.53	52.17	21.05
82.48	−190.65	59.53	26.26
83.38	−189.75	66.20	32.05
84.28	−188.85	72.27	38.40
85.22	−187.91	77.80	45.80
86.18	−186.95	82.95	54.00
87.15	−185.98	87.60	63.40
88.14	−184.99	91.98	73.90
89.18	−183.95	96.15	86.03
90.16	−182.97	100.00	100.00

of the liquid in equilibrium with air is 56 moles oxygen per 100 moles of the binary mixture; and the boiling point is (82 − 273.13[55] =) −191.1° C. However, as the liquid continues to evaporate it loses nitrogen much more rapidly than oxygen; the boiling point rises along the lower curve and ultimately attains the value −183° C, corresponding to the boiling point of pure oxygen. It is, therefore, strictly speaking, not correct to speak of the "temperature of liquid air," since this has no well-defined value.[56]

Furthermore, where liquid air is rectified,[57] as occurs in many industries, for the purpose of producing only nitrogen or oxygen alone, the liquid phase may be either of these, in a more or less purified state.

If the temperature of the liquid air surrounding a trap is below about −191° C and the exhaust system is opened to the atmosphere, air will condense in the trap and interfere with subsequent exhaust operation. *It is therefore always a safe rule to remove the refrigerant and permit the trap to reach room temperature before air is let into the system.* In fact it may be of considerable advantage to warm the trap moderately before letting in air, in order to remove any traces of water, mercury, carbon dioxide, etc., that may be condensed or adsorbed on the walls.

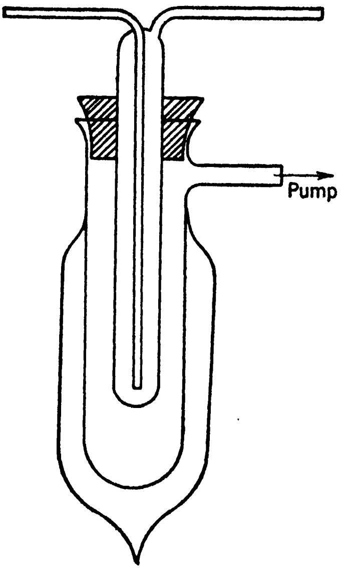

FIG. 16. Arrangement for lowering the temperature of liquid air (Klemenc).

According to A. Klemenc,[58] fresh liquid air is colorless and turns blue on evaporation of the nitrogen.

By reducing the pressure over the liquid air, the temperature may be reduced to −220° C. Figure 16, taken from the book by Klemenc, shows a simple arrangement for this purpose. The vapor pressures of pure oxygen and nitrogen at temperatures below their boiling points at 1 atm are given in Tables 15*a* and 15*b*.

---

[55] This is the value of the absolute temperature for 0° C, used by Dodge and Dunbar.

[56] For instance, the value is given as −187°C in FM. LH gives the value −190° C; RH gives the value −192° C.

[57] The subject of rectification of mixtures of O_2-N_2, O_2-A, CO-N_2, A-N_2, N_2-H_2, CO-H_2, and hydrocarbons is discussed at length by M. Ruhemann, *The Separation of Gases*, Clarendon Press, Oxford, 1940.

[58] *Die Behandlung und Reindarstellung von Gasen*, Leipzig, 1938.

8. VAPOR PRESSURES OF OILS, GREASES, AND WAXES

Oils. Data on the vapor pressures of oils used in vapor pumps have been given in Chapter 5.

The oils customarily used in rotary mechanical pumps, such as those described in Chapter 3, have vapor pressures of the order of 0.1 micron or less at room temperature.

Values obtained by H. Huthsteiner in this laboratory on a commercial transformer oil are given in Table 17. The Knudsen effusion method was used, and the vapor pressure was calculated from the loss in weight of the oil by assuming an average molecular weight of 142.

TABLE 17

APPROXIMATE VAPOR PRESSURES OF COMMERCIAL OIL

(*a*) Oil preheated to eliminate dissolved air and water:

$t°$ C:	100	74	57	34	
P_μ:	614	70–56	6	1	(extrapolated)

(*b*) Distilled out about ⅓ of the oil:

$t°$ C:	73	66	56	49	
P_μ:	25	8.5	2.6	1	(extrapolated)

(*c*) Distilled out about ¾ of the oil:

$t°$ C:	84	77	60	
P_μ:	2.8	1.0	0.1	(extrapolated)

The solubilities (α) of some of the more common gases in transformer oil, according to A. G. Loomis,[59] are shown in Table 18. By definition,

$$\alpha_t = \left(\frac{273.1}{t + 273.1}\right) \times \left(\frac{\text{g} \cdot \text{cm}^{-3} \text{ in liquid}}{\text{g} \cdot \text{cm}^{-3} \text{ in gas}}\right).$$

TABLE 18

SOLUBILITIES OF GASES IN TRANSFORMER OIL*

Values of $10^3 \alpha_t$

Gas	$t = 25$	$t = 50$	$t = 80$
H_2	51		69
N_2	84.8		91.6
O_2	156.2		148.5
CO_2	990	770	570

* A mineral oil of Pennsylvania base, 96 per cent saturated hydrocarbons and distilling between 300° C and 400° C. At 25° C, density is 0.840, and at 80° C, 0.800.

---

[59] *International Critical Tables,* Vol. 3, pp. 261–270 (1928).

Assuming that the pressure is 1 atm, the quantity (q) of gas in solution is $7.6 \cdot 10^2 \alpha_t$ micron · liters per cm^3 of liquid. Thus, for $\alpha_t = 50 \cdot 10^{-3}$, $q = 38$ micron · liters per cm^3. Also, all such blended oils always contain traces of more-volatile hydrocarbons. Consequently, any oil to be used in a vacuum pump must be "conditioned" for a certain period before attaining minimum vapor pressure.

Waxes and Greases. H. Mayer[60] has published results obtained with Ramsay grease. The material was treated for hours and days in vacuum, at a temperature above the melting point, in order to remove adsorbed gases and volatile products. The final values obtained for the vapor pressures were as follows:

$t°$ C:	38.8	34.0	29.0	25.0	21.4	16.5	12.6
P_μ:	0.32	0.15	0.073	0.05	0.035	0.015	0.011

G. Seydel[61] using the method for measuring vapor pressures devised by K. Neumann and E. Völker[62] obtained the following results for Apiezon fats. The freshly unpacked materials have an apparent vapor pressure of 10^{-5} mm. In a vacuum, at room temperature, the pressure decreases in a few hours to about $5 \cdot 10^{-7}$ mm. On heating to about 90° C, the more volatile compounds are removed rapidly and the pressure decreases to below 10^{-7} mm. At 130.5° C and 166.25° C, the vapor pressures observed for one sample were $0.5 \cdot 10^{-6}$ mm and $1.06 \cdot 10^{-5}$ mm, respectively. Extrapolation to room temperature yields a value between 10^{-10} and 10^{-11} mm.

Farkas and Melville[63] give the following data for compounds prepared by Technical Products, Ltd., England:

Grease L: 1 micron at 300° C; extrapolated value for 20° C, 10^{-8} micron. This has the same consistency as Vaseline and is used for sealing ground joints and lubricating taps.

Grease M: 1 micron at 200° C and 10^{-4} micron at 20° C. This is stated to be "similar to L, but less expensive."

Grease N: vapor pressure not given, but low enough for thermionic experiments.

"Sealing wax W is a black pitchlike material which softens at 80–90° C. At 180° C its vapor pressure is about 1 micron, which would imply a vapor pressure less than 10^{-5} micron at room temperature. It is useful for sealing windows to vacuum apparatus, and for making joints between silica and glass tubing."

J. Yarwood[64] gives the following data for Apiezon compounds supplied by Technical Products, Ltd.:

---

[60] *Z. Physik*, **67**, 264 (1931).

[61] *Z. tech. Physik*, **16**, 107 (1935).

[62] *Z. physik. Chem.*, **A**, **161**, 33 (1932). This method is described in Chapter 6, section 3.

[63] FM, p. 67.

[64] JY, p. 105.

Apiezon L is a grease supplied in metal tube containers. In use, a thin film of the grease is worked between well-fitting cone or flange joints till no "air lines" remain. Vapor pressure = $5 \cdot 10^{-6}$ mm Hg at 20° C. Apiezon M and N are similar, rather more viscous greases, more suitable if room temperature is above 20° C. If Apiezon M grease is baked in vacuum at 90° C for 2 hours its vapor pressure can be reduced to 10^{-8} mm Hg. These greases must be kept free from contact with air when not in use: they give more trouble due to occluded air than to high vapor pressure. Suitable for use in glass and metal stopcocks. A stopcock will give continual use up to 3 months if properly greased.

Apiezon Q compound is a plasticine-like substance consisting of graphite mixed with the low-vapor-pressure residues of paraffin oil distillation products. It is a semi-solid compound which can be readily pressed with the fingers round a joint in glass or metal to render it vacuum-tight.

Vapor pressure at 20° C = 10^{-4} mm Hg. Becomes too liquid for use at temperatures above 30° C.

Apiezon W wax has a very low vapor pressure ($<10^{-8}$ mm Hg at 20° C). It is a hard substance, supplied in sticks, very useful for semi-demountable joints in glass or metal where fusing or welding is impossible because of high temperatures necessary. It is applied to the joint at 100° C. It is best to heat the surface as well as the wax if a fairly permanent, gas-tight joint is required not liable to develop cracks. Softening point = 60–70° C. Soluble in xylene.

Khotinsky cement is a mixture of shellac and pitch obtained from Caroline tar. Softens at 50° C. Comparatively insoluble in usual organic liquids and common acids. Useful for joints at temperatures below 40° C.

Picein, a hard black wax of vapor pressure = 10^{-8} mm Hg at 20° C and 3–10 mm at 50° C. Softens at 50° C. Chemically inert to usual organic liquids and inorganic acids. Used similarly to "W" wax.

According to W. Espe and M. Knoll,[65] the vapor pressure of *Picein* at 20° C is about 0.3 to 0.4 micron. They also give the following values for the vapor pressure in microns of Apiezon M and L at different temperatures:

Apiezon M (degassed 2 hours at 90° C):
10^{-5} to 10^{-9} at 20° C, $6 \cdot 10^{-3}$ at 90° C, and ≈ 1 at 150° C.
Apiezon L (degassed several hours at 90° C):
Approximately 10^{-7} at 20° C, 10^{-4} at 90° C, and $2 \cdot 10^{-3}$ at 150° C.

Actually, these materials usually contain so much adsorbed gas and volatile vapor that an accurate determination of vapor pressure is difficult. This remark is illustrated by the data obtained by R. M. Zabel.[66] In carrying out the measurements, the cement was placed in a cylindrical tube (inside surface 284 cm^2) and exhausted through a glass tube having a conductance of 42 cm$^3 \cdot$ sec^{-1} for air. An ionization gauge reading at 23° C was taken 2½ hours after starting the exhaust. In terms of the gauge calibration for nitrogen, the values of the pressure observed were as follows:

---

[65] *Werkstoffkunde der Hochvakuumtechnik*, Julius Springer, Berlin, 1936, p. 224.

[66] *Rev. Sci. Instruments*, **4**, 233 (1933).

	MICRONS
Picein, m.p. 105° C	0.3
m.p. 80° C	0.34
Beeswax and rosin (1:1)	0.47
Glycol-phthalic anhydride resin	0.72
de Khotinsky (hard)	1.28
Glyptal lacquer (Baked 4 hours at 200° C)	0.17
Stopcock grease	0.60

The only question about these results is whether the vapor pressures observed would not have been much lower if the exhaust had been continued for a longer time before the reading was taken. Also, because of lack of information regarding the interpretation of the observed values of the ratio of positive ion to electron current, the actual pressures may have been much greater than those given above.

The Distillation Products, Inc., give for the vapor pressure of their product "Celvacene-Light" (melting point 90° C) the value 10^{-3} to 10^{-4} micron (at room temperature) as a lower limit after prolonged exhaust. For Celvacene-Heavy (melting point about 130° C) the vapor pressure is stated to be "even lower than that of the Celvacene-Light."

CHAPTER 12

DISSOCIATION PRESSURES OF OXIDES, HYDRIDES, AND NITRIDES AND RATES OF OXIDATION

1. FREE AND TOTAL ENERGY

In Chapter 9 mention was made of the fact that many metals react with hydrogen, nitrogen, and oxygen, forming compounds. Since, in general, these compounds are exothermic, they tend to dissociate with increase in temperature. Some of the oxides volatilize at temperatures so low that dissociation occurs only in the vapor phase; water is one of the most important illustrations of this type of oxide. However, for an oxide, nitride, or hydride which exists as a solid over a considerable range of temperatures there exists at any given temperature a dissociation pressure which represents an equilibrium between the compound, the gas, and the metal.

We are especially interested in the conditions for the reduction of oxides by hydrogen (or carbon monoxide). Obviously this involves the consideration of the two reactions: (*a*) dissociation of oxide, yielding oxygen and metal; and (*b*) reaction of oxygen with hydrogen, yielding water vapor.

Since such problems can be dealt with most adequately from the point of view of certain thermodynamical concepts, it is necessary before considering the reactions themselves to discuss briefly these fundamental ideas by the application of which it has been found possible to obtain solutions of the problems.

In any chemical (or physical reaction) heat is absorbed or liberated. Let ΔH denote the change in energy involved, in terms of calories. For exothermic reactions, ΔH is negative; for endothermic reactions, positive. For a long time the belief existed that, given a choice of different possible reactions, that reaction will occur for which ΔH has a maximum negative value; that is, it was assumed that the amount of heat liberated is a measure of the probability of occurrence of a given reaction. The quantity ΔH is known as the *total energy* change and corresponds to the quantity measured calorimetrically. This is given in tables of heats of formation, heats of evaporation, and so forth. However, from considerations based on the second law of thermodynamics, it has been shown that the direction and extent of a reaction are governed by the sign and magnitude of the change in *free energy*, designated by ΔF. The conclusion deduced may be stated as follows: A reaction can occur at constant temperature and pressure *only if the value of ΔF is negative.* That is, *the free energy must decrease.*[1] The values of ΔH and ΔF are ordinarily given in calories per mole.

From the second law of thermodynamics it follows that, at any given temperature and *constant pressure,*

$$\frac{d\Delta F}{dT} = \frac{\Delta F - \Delta H}{T}, \tag{1a}$$

that is,

$$\Delta F = \Delta H + T\frac{d\Delta F}{dT}. \tag{1b}$$

Dividing both sides of this equation by T^2, we obtain the relation

$$\frac{\Delta F}{T^2} - \frac{1}{T}\frac{d\Delta F}{dT} = \frac{\Delta H}{T^2};$$

that is,

$$\frac{d}{dT}\left(\frac{\Delta F}{T}\right) = -\frac{\Delta H}{T^2} \tag{2}$$

or

$$\frac{d(\Delta F/T)}{d(1/T)} = \Delta H. \tag{3}$$

Equations $1a$ and $1b$ constitute the Gibbs-Helmholtz relation. It states the relation between the change in free energy, the change in total energy, and the temperature coefficient of the free energy. Since, according to the *third law* of thermodynamics, $d\Delta F/dT = 0$ at $T = 0$, it follows that $\Delta F_0 = \Delta H_0$, where the subscript indicates that these values apply to $T = 0$.

At any higher temperature, the condition may occur that ΔF is negative, *in spite of a positive value of ΔH,* because of the fact that the second term on the right-hand side of equation 1*b* is negative and greater numerically than ΔH.[2]

---

[1] These concepts are discussed comprehensively in different treatises on thermodynamics, such as the following:

1. G. N. Lewis and M. Randall, *Thermodynamics*, McGraw-Hill Book Company, New York, 1923.
2. L. E. Steiner, *Introduction to Chemical Thermodynamics*, McGraw-Hill Book Company, New York, 1934.
3. R. R. Wenner, *Thermochemical Calculations*, McGraw-Hill Book Company, New York, 1941.

Equations 2 and 3 express the *Clausius-Clapeyron* relation, which may be stated as follows: Given a plot of $\Delta F/T$ versus $1/T$, then ΔH corresponds to the slope of the curve for any value of T.

In general, the value of ΔH will change with temperature because of the difference in heat capacities of products and reactants and also because of the variation in these quantities with temperature. We can express ΔH in the form,

$$\Delta H = \Delta H_0 + aT + bT^2 + cT^3 + \cdots, \tag{4}$$

where a, b, c, etc., are constants, characteristic of the reaction under consideration, which may be derived from specific-heat measurements.

In consequence of equations 2 and 3, it follows that we can express the change in free energy in the form

$$\Delta F = \Delta H_0 - aT \ln T - bT^2 - \frac{c}{2} T^3 \cdots - IT, \tag{5}$$

where I is an integration constant,[3] and ln denotes the natural logarithm.

Thus, from a knowledge of the constants ΔH_0, a, b, c, etc., and I, it is possible to calculate ΔF for a given reaction. Theoretically, at least, it is possible in this manner to deduce the value of ΔF for any desired temperature from a single determination of ΔF at some other temperature and from calorimetrically measured values of the constants in equation 4.

We shall now illustrate the application of the above relations to certain typical physical and chemical reactions.

Evaporation of Solids or Liquids. For the evaporation of a solid or liquid, the vapor pressure is uniquely determined by the temperature, and, as shown in any treatise on thermodynamics,

$$\Delta F = -R_0 T \ln P_{atm} \tag{6}$$

Assuming that $\Delta H = \Delta H_0$, a constant, it follows from equation 5 that

$$-R_0 T \ln P_{atm} = \Delta H_0 - IT,$$

that is,

$$\log P_{atm} = \frac{I}{2.30 R_0} - \frac{L_0}{2.30 R_0 T}, \tag{7}$$

---

[2] This actually occurs in the case of some batteries.

[3] This method of formulation for ΔF is a consequence of the application of the third law of thermodynamics.

where $L_0 = \Delta H_0$ = latent heat of evaporation in calories per gram atom (or gram mole) at $T = 0$, $R_0 = 1.9865$ cal/gram atom, and $2.30 \cdot R_0 = 4.574$. Evidently the last equation can be written in the more general form

$$\log P_{atm} = A - \frac{B}{T}, \tag{8}$$

which has been used in the previous chapter.

Dissociation of an Oxide. Let us consider a "non-volatile" oxide in equilibrium, at a given temperature, with oxygen at a pressure designated by P_{atm} (O_2) and the metal, which is assumed to be nonvolatile at the temperature under consideration. The reaction is customarily written in the form

$$m\text{M} + n\text{O}_2 \rightarrow \text{M}_m\text{O}_{2n}. \tag{9}$$

In general heat will be evolved (ΔH will be negative) in the reaction between the metal and oxygen.

For the determination of P_{atm} (O_2), we have the relation

$$\Delta F_n = nR_0T \ln P_{atm} (O_2), \tag{10}$$

where ΔF_n is the change in free energy per mole M_mO_{2n}.

Hence

$$\log P_{atm} (O_2) = \frac{1}{n} \frac{\Delta F_n}{4.574T},$$

and the equilibrium pressure, in millimeters of mercury, is given by

$$\log P_{mm} (O_2) = 2.881 + \frac{1}{n} \frac{\Delta F_n}{4.574T}. \tag{11}$$

For instance, for the reaction

$$\text{M} + 0.5\text{O}_2 \rightarrow \text{MO} + \Delta F,$$

where M represents a divalent metal, and ΔF is the free energy increase per gram mole MO,

$$\log P_{atm} (O_2) = \frac{2\Delta F}{4.574T}.$$

Dissociation of Water Vapor. Let ΔF_W denote the free energy increase, per gram mole H_2O, for the reaction

$$\text{H}_2 + 0.5\text{O}_2 \rightarrow \text{H}_2\text{O}. \tag{12}$$

Then,

$$\Delta F_W = -R_0T \ln K_W, \tag{13}$$

where

$$K_W = \frac{P_{atm}\,(H_2O)}{P_{atm}\,(H_2)\,\sqrt{P_{atm}\,(O_2)}}. \tag{14}$$

Reduction of an Oxide by Hydrogen. Let us now consider the reaction

$$2nH_2 + M_mO_{2n} \rightarrow 2nH_2O + mM. \tag{15}$$

ΔF_H, the free energy change per gram mole M_mO_{2n}, is given by the relation

$$\Delta F_H = -2nR_0T \ln K_H, \tag{16}$$

where

$$K_H = \frac{P(H_2O)}{P(H_2)} = \frac{(H_2O)}{(H_2)}. \tag{17}$$

Since K_H is evidently *independent* of the units used for the measurement of pressure, it has been frequently expressed in the following discussion by the notation $(H_2O)/(H_2)$ as shown in the last equation. It will also be observed that

$$\Delta F_H + \Delta F_n = 2n\Delta F_W,$$

corresponding to the fact that the net result of reactions 9 and 15 is the reaction

$$nO_2 + 2nH_2 \rightarrow 2nH_2O.$$

That is, values of ΔF for a series of reactions are additive, like values of ΔH. Thus, from known values of ΔF_W and of ΔF_H it is possible to calculate ΔF_n, and similarly it is possible to calculate ΔF_H from determinations of ΔF_W and ΔF_n.

Dissociation of an Oxide of a Volatile Metal. As an illustration, let us consider the reaction

$$Ba\ (g) + 0.5O_2 \rightarrow BaO\ (s), \tag{18}$$

where s and g denote the solid and gaseous phases, respectively. This reaction is of importance in connection with the activation process in oxide-coated cathodes.

Let ΔF_0 denote the change in free energy, per gram mole BaO, of the reaction

$$Ba\ (s) + 0.5O_2 \rightarrow BaO\ (s), \tag{19}$$

and let ΔF_v denote the free energy, per gram atom Ba, of the reaction

$$Ba\ (g) \rightarrow Ba\ (s). \tag{20}$$

Then $\Delta F_1 = \Delta F_0 + \Delta F_v$ = free energy, per gram mole BaO, of the reaction indicated in equation 18.

If the reaction is carried out in a volume maintained at temperature T,

$$\Delta F_1 = R_0 T \ln K_1, \tag{21}$$

where

$$K_1 = P_{atm}\,(\mathrm{Ba})\,\sqrt{P_{atm}\,(\mathrm{O_2})}. \tag{22}$$

Hence

$$\Delta F_1 = 4.574T\,(\log P_{mm}\,(\mathrm{Ba}) + 0.5 \log P_{mm}\,(\mathrm{O_2}) - 4.3212). \tag{23}$$

Since $P_{mm}\,(\mathrm{O_2}) = 0.5 P_{mm}\,(\mathrm{Ba})$, it follows from the last equation that

$$\log P_{mm}\,(\mathrm{Ba}) = 2.982 + \frac{\Delta F_1}{6.861T}\cdot \tag{24}$$

Let $P_{mm}'\,(\mathrm{Ba})$ denote the vapor pressure of solid (or liquid) barium at T. Then, since

$$\log P_{mm}'\,(\mathrm{Ba}) = 2.881 + \frac{\Delta F_v}{4.574T}, \tag{25}$$

we can also express equation 24 in the form

$$\log P_{mm}\,(\mathrm{Ba}) = 1.061 + \tfrac{2}{3} \log P_{mm}'\,(\mathrm{Ba}) + \frac{\Delta F_0}{6.861T}\cdot \tag{26}$$

Since ΔF_0 is a large negative magnitude, the last equation shows that the vapor pressure of barium in equilibrium with solid BaO must be considerably less than the vapor pressure of solid (or liquid) barium metal at the same temperature, T.

2. FREE AND TOTAL ENERGY OF FORMATION OF WATER VAPOR

Thus, it is of importance, in connection with the calculations on the dissociation of metallic oxides and their reduction by hydrogen, to determine the relation for ΔF_W as a function of the temperature.

Values of ΔF for reaction 12 have been deduced by a number of investigators. The first (and oldest) is that given by Lewis and Randall,[4] which has the form

$$\frac{\Delta F_W}{T} = -\frac{57{,}410}{T} + 2.165 \log T + 1.65 \cdot 10^{-3} T - 3.7 \cdot 10^{-7} T^2 + 3.92. \tag{1}$$

---

[4] *Op. cit.*, p. 485.

The relation deduced by J. Chipman[5] is

$$\frac{\Delta F_W}{T} = -\frac{57{,}120}{T} + 6.333 \log T - 7.5 \cdot 10^{-4} T - 6.65, \tag{2}$$

while the relations for ΔH_W and ΔF_W deduced by M. de K. Thompson[6] are as follows:

$$\Delta H_W = -56{,}565 - 1.6027T + 0.3647 \cdot 10^{-3} T^2 - 45.59 \sqrt{T}, \tag{3}$$

$$\Delta F_W = -56{,}565 + 3.692\, T \log T - 0.3647 \cdot 10^{-3} T^2 - 91.175 \sqrt{T} + 2.724T. \tag{4}$$

TABLE 1

VALUES OF FREE AND TOTAL ENERGY FOR DISSOCIATION OF STEAM

T	$-\Delta H_W$	$\Delta H_W + 56{,}565$	$-\Delta F_W$	$\Delta F_W + 56{,}565$
0	56,565	0	56,565	0
298	57,798	−1233	54,638	1,927
600	58,513	−1948	51,143	5,422
800	58,903	−2338	48,625	7,940
1000	59,245	−2680	46,010	10,555
1200	59,543	−2978	43,341	13,224
1400	59,860	−3295	40,618	15,947
1600	60,019	−3454	37,869	18,696
1800	60,203	−3638	35,080	21,485
2000	60,351	−3786	32,294	24,271

Table 1 gives values of ΔH_W and ΔF_W for the formation of water vapor according to equations 3 and 4. From ΔF_W, K_W, as defined by equation 1.14, may be calculated by means of the relation

$$\log K_W = -\frac{\Delta F_W}{4.574T}. \tag{5}$$

Figure 1 shows plots of $X = \Delta H_W + 56{,}565$ and of $Y = \Delta F_W + 56{,}565$ versus T. In accordance with the third law of thermodynamics,

$$\Delta F_0 = \Delta H_0 = -56{,}565$$

Table 2 gives for comparison values of $\Delta F_W/T$ calculated by means of equations 1 and 2 and from the values in Table 1. The sixth column gives values of $-\Delta F_W/T$ at higher temperatures as deduced by A. R.

---

[5] *J. Ind. Eng. Chem.*, **24**, 1013 (1932).

[6] *The Total and Free Energies of Formation of the Oxides of Thirty-Two Metals*, The Electrochemical Society, New York, 1942. This source has been used for a number of the calculations given in this chapter.

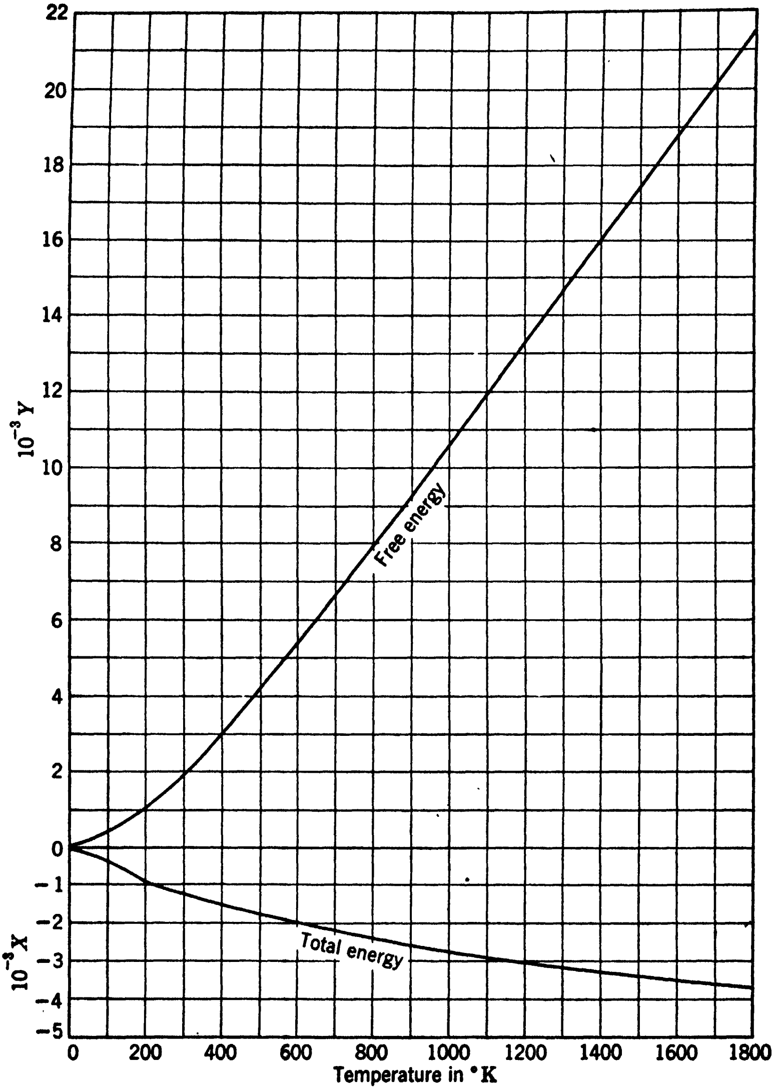

FIG. 1. Plots of free energy and total energy versus temperature, for reaction $H_2\,(g) + 0.5O_2\,(g) \rightarrow H_2O\,(g)$. Ordinates give values of $10^{-3}Y = 10^{-3}\Delta F_W + 56.565$ and $10^{-3}X = 10^{-3}\Delta H_W + 56.565$.

Gordon.[7] The seventh column gives values of log K_W derived from the values of $-\Delta F_W/T$ calculated by means of equation 4.

---

[7] *J. Chem. Phys.*, **1**, 308 (1933).

As will be observed there is very good agreement between the values of $-\Delta F_W/T$ derived from the relations deduced by different investigators. The agreement is especially good between the values deduced from equation 3 and those deduced by Gordon.

A plot of $-\Delta F_W/T$ versus $1/T$ (values given in Table 2) shows that for the range $T = 600$ to $T = 2000$ all the data can be represented very satisfactorily by the two-term relation

$$\frac{\Delta F_W}{T} = 13.98 - \frac{59{,}990}{T}, \tag{6}$$

that is,

$$-\log K_W = 3.057 - \frac{13{,}110}{T}, \tag{7}$$

TABLE 2

VALUES OF $\Delta F_W/T$, LOG K_W AND OF 100α AT 760 MM AND 0.76 MM

T	$10^3/T$	$-\Delta F_W/T$				$\log K_W$	100α	
		Eq. 1	Eq. 2	Eq. 4	Gordon		$P_{mm} = 760$	$P_{mm} = 0.76$
298	3.356			183.3		40.07		
600	1.667			85.24		18.63	$4.79 \cdot 10^{-11}$	$4.79 \cdot 10^{-10}$
800	1.250	60.47	60.13	60.78		13.29	$1.74 \cdot 10^{-7}$	$1.74 \cdot 10^{-6}$
1000	1.000	45.72	45.52	46.01		10.06	$2.47 \cdot 10^{-5}$	$2.47 \cdot 10^{-4}$
1200	0.8333	35.80	36.00	36.12		7.896	$6.86 \cdot 10^{-4}$	$6.86 \cdot 10^{-3}$
1400	0.7143	28.70	28.50	29.01	29.05	6.342	$7.43 \cdot 10^{-3}$	$7.43 \cdot 10^{-2}$
1600	0.6250	23.33	22.11	23.67	23.67	5.175	$4.47 \cdot 10^{-2}$	$4.47 \cdot 10^{-1}$
1800	0.5556	19.14	19.12	19.49	19.48	4.261	$1.82 \cdot 10^{-2}$	$1.82 \cdot 10^{-1}$
2000	0.5000	15.80	15.88	16.15	16.12	3.530	$5.59 \cdot 10^{-1}$	(5.59)

which is similar in form to the two-term expression for $\log P$ as a function of $1/T$. (See Fig. 2 for plot of $-\Delta F_W/T$ versus $1/T$.)

The degree of dissociation (α) at given values of the temperature and total pressure is derived as follows:

From 1 mole H_2O vapor, at pressure P_{atm}, there are produced at equilibrium $(1 - \alpha)$ moles H_2O, α moles H_2, and 0.5 mole O_2. Hence, total number of moles at equilibrium is $(1 + 0.5\alpha)$, and it follows from equation 14 that

$$K_W = \frac{(1 - \alpha)(2 + \alpha)^{1/2}}{\alpha^{1.5}\sqrt{P_{atm}}}, \tag{8}$$

that is,

$$\alpha^3 = \frac{(1-\alpha)^2(2+\alpha)}{K_W{}^2 P_{atm}}. \tag{9}$$

For $\alpha \ll 0.01$,

$$\alpha^3 = \frac{2}{K_W{}^2 P_{atm}} = \frac{1520}{K_W{}^2 \cdot P_{mm}}. \tag{10}$$

From these relations it follows that, at constant temperature, α varies inversely as $P^{1/3}$.

The last two columns in Table 2 give values of 100α, the per cent dissociation at $P_{mm} = 760$ mm and $P_{mm} = 0.76$ mm, respectively, calculated by means of the relations

$$\log \alpha = 0.1003 - \tfrac{2}{3} \log K_W \ \ (\text{for } P_{mm} = 760),$$

and

$$\log \alpha = 1.1003 - \tfrac{2}{3} \log K_W \ \ (\text{for } P_{mm} = 0.76).$$

The value of α for $T = 2000$ and $P_{mm} = 0.76$ is only approximate, since equation 10 is no longer valid for such large values of α.

In the presence of hydrogen or oxygen, the degree of dissociation of the water vapor is depressed, as may be deduced from the following considerations.

Let β = number of moles added O_2 per mole H_2O, and let α_1 denote the degree of dissociation obtained as a result of the presence of additional oxygen. Then,

$$K_W = \frac{(1-\alpha_1)}{\alpha_1 \sqrt{P_{atm}}} \sqrt{\frac{2+\alpha_1+2\beta}{\alpha_1+2\beta}}. \tag{11}$$

For $\alpha_1 \ll 0.01$, and β large compared to α_1, this equation leads to the relation

$$\alpha_1{}^2 = \frac{1}{K_W{}^2 P_{atm}} \left(\frac{1+\beta}{\beta}\right). \tag{12}$$

Comparing this with equation 9 it follows that, for the same value of P,

$$\left(\frac{\alpha_1}{\alpha_0}\right)^2 = \frac{\alpha_0}{2}\left(\frac{1+\beta}{\beta}\right), \tag{13}$$

which shows that α_1 must always be considerably less than α_0, where α_0 denotes the degree dissociation of in the absence of excess of either oxygen or hydrogen.

3. DISSOCIATION PRESSURES OF OXIDES OF SILVER, MERCURY, AND PALLADIUM

K. S. Pitzer and W. V. Smith[8] have reviewed the different observations which have been made on the dissociation pressure of *silver oxide*, Ag_2O, in accordance with the equation

$$2Ag + 0.5O_2 \rightarrow Ag_2O.$$

According to A. F. Benton and L. C. Drake[9] the dissociation pressure is 1 atm at $T = 463$. The earlier observations of G. N. Lewis[10] gave the value $P_{atm} = 20.5$ for $T = 575$. From these two values we obtain the relation for the dissociation pressure

$$\log P_{mm} = 9.614 - \frac{3118}{T}. \tag{1a}$$

This is to be compared with the relation

$$\log P_{mm} = 9.200 - \frac{2925}{T} \tag{1b}$$

deduced by M. de K. Thompson,[11] and with the relation

$$\log P_{mm} = 9.166 - \frac{2859}{T} \tag{1c}$$

deduced by F. G. Keyes and H. Hara[12] from their observations at higher temperatures and at pressures ranging from 74 to more than 200 atmospheres.

Table 3 shows pressures deduced for lower values of T by means of equation 1*a*.

The dissociation of *mercuric oxide* in accordance with the equation

$$Hg\ (g) + 0.5O_2 \rightarrow HgO$$

has been measured over the range 360° C to 500° C by a number of investigators, including G. B. Taylor and G. A. Hulett.[13]

In the absence of liquid mercury, the pressure of mercury, P_{mm1}, is

---

[8] *J. Am. Chem. Soc.*, **59**, 2633 (1937).

[9] *J. Am. Chem. Soc.*, **54**, 2186 (1932).

[10] *J. Am. Chem. Soc.*, **28**, 139 (1906).

[11] *Op. cit.*

[12] *J. Am. Chem. Soc.*, **44**, 479 (1922).

[13] *J. Phys. Chem.*, **17**, 565 (1913); also see *International Critical Tables*, Vol. 7, p. 259.

twice P_{mm2}, *the pressure of oxygen. Consequently,*

$$P_{mm1} = \frac{P_{mmt}}{3}$$

where P_{mmt} = total pressure. Also, in accordance with the mass law, for any given temperature,

$$K = \tfrac{2}{3}P_{mmt}\sqrt{\tfrac{1}{3}P_{mmt}} \tag{2a}$$

and

$$\sqrt{P_{mm2}} = \frac{K}{P_{mm1}}. \tag{2b}$$

From the plot of log P_{mmt} versus $1/T$, we obtain the relation

$$\log P_{mmt} = 9.745 - \frac{4960}{T}. \tag{3}$$

TABLE 3

DISSOCIATION PRESSURES OF OXIDES OF SILVER, MERCURY, AND PALLADIUM

$Ag_2O \rightarrow 2Ag + 0.5O_2$		$HgO \rightarrow Hg\ (g) + 0.5O_2$			$PdO \rightarrow Pd + 0.5O$	
T	P_{mm} (O_2)	T	P_{mmt}	P_{mm} (O_2)	T	P_{mm} (O_2)
324.3	1	633.1	90.2	0.168	1042	100
361.9	10	600	30.1	$2.16 \cdot 10^{-2}$	946	10
409.5	100	575	13.2	$5.80 \cdot 10^{-3}$	866	1
446.1	422	550	5.3	$1.05 \cdot 10^{-3}$	799	0.1
463	760	525	2.0	$9.45 \cdot 10^{-5}$	742	0.01
575	15,238	500	0.67	$2.86 \cdot 10^{-5}$	691	0.001

This was used to calculate the values of P_{mmt} for temperatures below 360° C, which are given in the fourth column in Table 3.

From these values of P_{mmt} values of K were derived, and from these, in turn, values of P_{mm}, given in the fifth column, for the condition in which *liquid* mercury is present. In that case, the value of P_{mm1} in equation 2*b* is determined by the *vapor pressure* of mercury at the given value of T. The values of P_{mm1} were taken from the standard tables, and, as will be observed, the oxygen pressure is decreased considerably; that is, the degree of dissociation of HgO is decreased in the presence of liquid mercury.

The dissociation pressures of *palladium monoxide*, PdO, have been measured by L. Wöhler.[14] His data are in satisfactory agreement with the relation

---

[14] *Z. Elektrochem.*, **12**, 781 (1906).

$$\log P_{mm} = 11.86 - \frac{10{,}280}{T}. \tag{4}$$

Table 3 shows the values of T, as calculated by means of this equation, for a range of pressures.

4. DISSOCIATION AND REDUCTION OF OXIDES OF COPPER

The reactions involved, with the corresponding designations[15] for the free energies, are as follows:

$$2Cu + 0.5O_2 \rightarrow Cu_2O + \Delta F_1.$$

$$Cu_2O + 0.5O_2 \rightarrow 2CuO + \Delta F_2.$$

$$Cu + 0.5O_2 \rightarrow CuO + \Delta F_3.$$

$$H_2 + CuO \rightarrow H_2O + Cu + \Delta F_{H3}.$$

$$H_2 + 2CuO \rightarrow H_2O + Cu_2O + \Delta F_{H2}.$$

$$H_2 + Cu_2O \rightarrow H_2O + 2Cu + \Delta F_{H1}.$$

Evidently,

$$\Delta F_3 = 0.5(\Delta F_1 + \Delta F_2). \tag{1}$$

$$\Delta F_{H3} = \Delta F_W - \Delta F_3 = \Delta F_W - 0.5(\Delta F_1 + \Delta F_2). \tag{2}$$

$$\Delta F_{H2} = \Delta F_W - \Delta F_2. \tag{3}$$

$$\Delta F_{H1} = \Delta F_W - \Delta F_1. \tag{4}$$

Furthermore, if we let P_{mm} (O_2) designate the pressure of oxygen at equilibrium at temperature T, then

$$\log P_{mm}(O_2) = 2.881 + \frac{2}{4.574} \cdot \frac{\Delta F}{T}, \tag{5}$$

where $\Delta F = \Delta F_1$, ΔF_2 or ΔF_3. Also

$$\log K_H = \log \frac{P(H_2O)}{P(H_2)} = \log \frac{(H_2O)}{(H_2)}$$

$$= -\frac{\Delta F_H}{4.574T}, \tag{6}$$

where ΔF_H corresponds to ΔF_{H1}, ΔF_{H2}, or ΔF_{H3}.

---

[15] Similar notation is used in the following tables.

The melting point of Cu_2O is 1235° C at 0.6 mm, and the eutectic melts at 1065° C.[16]

From the equations given above it is seen that values of ΔF_3 and ΔF_H can be calculated from values of ΔF_1, ΔF_2, and ΔF_W. Values of ΔF_W and of $\Delta F_W/T$ are given in Tables 1 and 2, respectively.

Values of ΔF_1 for the range 300° K to 1357° K have been determined by application of equations 4 and 6, that is, from measurements of the ratio K_H in the reduction of Cu_2O to Cu (solid) by hydrogen.[17] From these data M. de K. Thompson[18] has deduced the relation

$$\frac{\Delta F_1}{T} = -\frac{40{,}716}{T} + 2.695 \log T - 1.545 \cdot 10^{-3}T + \frac{85.68}{\sqrt{T}} + 6.967. \quad (7)$$

From a plot of $\Delta F_1/T$ versus $1/T$, it is observed that the values can be represented very satisfactorily by the two-term relation

$$\frac{\Delta F_1}{T} = 14.50 - \frac{39{,}110}{T} \quad (8)$$

For the range 273° K to 1353° K (the eutectic point), Thompson has deduced the relation

$$\frac{\Delta F_2}{T} = -\frac{34{,}610}{T} + 5.367 \log T - 3.91 \cdot 10^{-3}T + \frac{85.68}{\sqrt{T}} + 11.11, \quad (9)$$

which can also be represented by the relation, similar to 8,

$$\frac{\Delta F_2}{T} = 23.18 - \frac{31{,}900}{T}. \quad (10)$$

TABLE 4

VALUES OF FREE ENERGY FOR OXIDATION OF CU AND Cu_2O

T	$10^3/T$	$-\Delta F_1/T$	$-\Delta F_2/T$	$-\Delta F_3/T$	$-\Delta F_W/T$
298	3.3557	118.46	87.92	103.19	183.3
600	1.6667	50.82	30.51	40.67	85.24
700	1.4286	41.38	22.56	31.97	71.27
800	1.2500	34.32	16.67	25.49	60.78
900	1.1111	28.77	12.16	20.46	52.49
1000	1.0000	24.50	8.60	16.55	46.01
1100	0.9091	20.96	5.76	13.36	40.62
1200	0.8333	18.05	3.428	10.74	36.12
1300	0.7692	15.59	1.516	8.60	32.31

---

[16] A phase diagram for the system Cu + Cu_2O is shown by F. N. Rhines and C. H. Mathewson, *Metals Technol.*, **1**, Technol. Publication 534, 1934.

[17] C. G. Maier, *J. Am. Chem. Soc.*, **51**, 194 (1929), also M. Randall, R. F. Nielsen, and G. H. West, *J. Ind. Eng. Chem.*, **23**, 388 (1931).

[18] *Op. cit.*

Table 4 gives values of $\Delta F_1/T$ and $\Delta F_2/T$ calculated by means of equations 7 and 9, respectively. From these values those of $\Delta F_3/T$ have been calculated in accordance with equation 1. The last column in the table gives the values of $\Delta F_W/T$ taken from Table 2, with additional values of T not given in that table. From the plots shown in Fig. 2 it is observed that, to a very good degree of approximation, the values of $\Delta F/T$ plotted versus $1/T$ lie on straight lines, in accordance with equations 8 and 10. However, the actual values given in Table 4 were used to calculate the dissociation pressures of the oxides, P_{mm} (O_2), and values of K_H shown in Table 5. These were derived by means of equations 5 and 6 above.

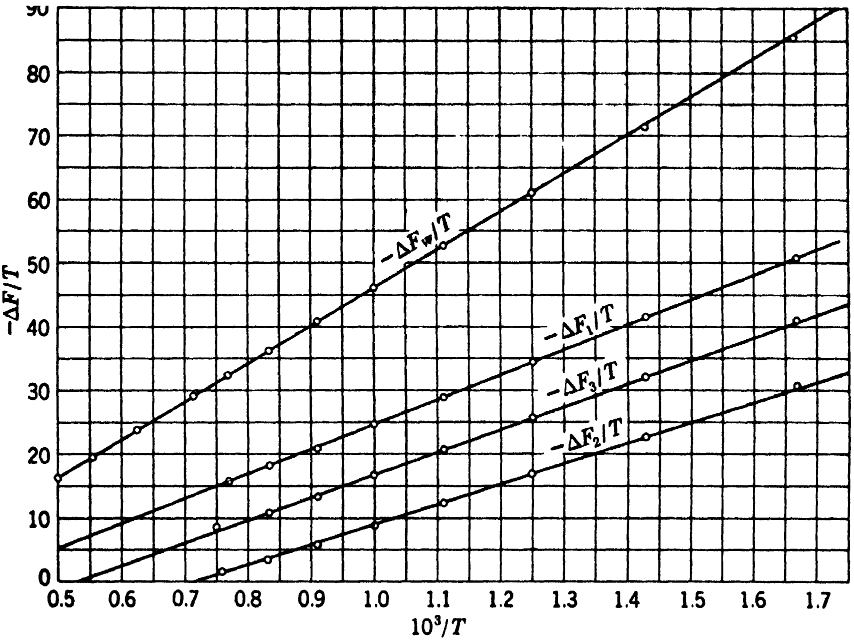

FIG. 2. Plots of $-\Delta F/T$ versus $1/T$ for formation of water vapor (ΔF_W), oxidation of Cu to Cu_2O (ΔF_1), oxidation of Cu_2O to CuO (ΔF_2), and oxidation of Cu to CuO (ΔF_3).

It will be observed that, for any given temperature, the value of $P_{mm}{}^2$ in the sixth column is equal to the product of the values of P_{mm} in the second and fourth columns, and a similar relation applies to the values of $K_H = (H_2O)/(H_2)$. It may be demonstrated very easily that these relations follow from equation 1.

The values given in Table 5 for the dissociation pressure of CuO to

TABLE 5

OXYGEN PRESSURES AND EQUILIBRIUM CONSTANTS FOR DISSOCIATION AND REDUCTION OF OXIDES OF COPPER

	$2Cu + 0.5O_2 \rightarrow Cu_2O$ $Cu_2O + H_2 \rightarrow 2Cu + H_2O$		$Cu_2O + 0.5O_2 \rightarrow 2CuO$ $2CuO + H_2 \rightarrow Cu_2O + H_2O$		$Cu + 0.5O_2 \rightarrow CuO$ $CuO + H_2 \rightarrow Cu + H_2O$	
T	P_{mm} (O_2)	$(H_2O)/(H_2)$	P_{mm} (O_2)	$(H_2O)/(H_2)$	P_{mm} (O_2)	$(H_2O)/(H_2)$
600	$4.57 \cdot 10^{-20}$	$3.36 \cdot 10^{7}$	$3.63 \cdot 10^{-11}$	$9.12 \cdot 10^{11}$	$1.26 \cdot 10^{-15}$	$5.56 \cdot 10^{9}$
700	$6.17 \cdot 10^{-16}$	$3.42 \cdot 10^{6}$	$1.02 \cdot 10^{-7}$	$4.47 \cdot 10^{10}$	$7.94 \cdot 10^{-12}$	$3.91 \cdot 10^{8}$
800	$7.41 \cdot 10^{-13}$	$6.10 \cdot 10^{5}$	$3.90 \cdot 10^{-5}$	$4.39 \cdot 10^{9}$	$5.37 \cdot 30^{-9}$	$5.18 \cdot 10^{7}$
900	$2.00 \cdot 10^{-10}$	$1.54 \cdot 10^{5}$	$3.65 \cdot 10^{-3}$	$6.55 \cdot 10^{8}$	$8.63 \cdot 10^{-7}$	$1.00 \cdot 10^{7}$
1000	$1.48 \cdot 10^{-8}$	$5.04 \cdot 10^{4}$	$1.32 \cdot 10^{-1}$	$1.51 \cdot 10^{8}$	$4.42 \cdot 10^{-5}$	$2.75 \cdot 10^{6}$
1100	$5.21 \cdot 10^{-7}$	$1.99 \cdot 10^{4}$	2.30	$4.22 \cdot 10^{7}$	$1.10 \cdot 10_{-}{}^{3}$	$9.12 \cdot 10^{5}$
1200	$9.77 \cdot 10^{-6}$	$8.93 \cdot 10^{3}$	24.10	$1.40 \cdot 10^{7}$	$1.53 \cdot 10^{-2}$	$3.54 \cdot 10^{5}$
1300	$1.15 \cdot 10^{-4}$	$4.53 \cdot 10^{3}$	165.2	$5.40 \cdot 10^{6}$	$1.32 \cdot 10^{-1}$	$0.5 \cdot 10^{5}$

Cu_2O are in good agreement with those obtained by H. W. Foote and E. K. Smith[19] and also with those published by E. Brody and Th. Millner.[20]

The values derived for the dissociation pressures of Cu_2O are in reasonable agreement with those given by F. Halla[21] but differ from those calculated by J. Gundermann, K. Hauffe, and C. Wagner[22] from emf measurements at high temperatures. Table 6 shows their values as compared with those derived by interpolation of the data in Table 5.

N. P. Allen and T. Hewitt[23] have calculated the dissociation pressures of Cu_2O from determinations of the constant K_H for the reaction between steam and *molten* copper. Their results are also shown in the last three rows of Table 6 and, for comparison, the values calculated by extrapolation of the data in Table 5.

As will be observed, the dissociation of CuO to Cu_2O is the only one of the three dissociation reactions for which the pressures of oxygen are sufficiently high at temperatures of 900° K and above to be of interest in actual exhaust operations. On the other hand, the fact that the values of K_H are very large in the three reductions, even at 1300° K, indicates that reduction of the oxides to metal occurs very readily, even when the hydrogen contains considerable percentages of water vapor. If, however, the ratio $(H_2O)/(H_2)$ is in excess of that derived in Table 5, oxidation occurs rather than reduction. For instance, at 1200° K, a hydrogen-steam mixture will oxidize copper if the value of this ratio is greater than $8.93 \cdot 10^3$.

TABLE 6

COMPARISON OF DISSOCIATION PRESSURES OF Cu_2O IN TABLE 5 AND OBSERVED VALUES

T	Values of P_{mm} (O_2) from Table 5	Values of P_{mm} (O_2) from Other Sources	
1073	$2.1 \cdot 10^{-7}$	$1.9 \cdot 10^{-6}$	Gundermann, etc.
1173	$4.6 \cdot 10^{-6}$	$4.4 \cdot 10^{-5}$	
1273	$6.2 \cdot 10^{-5}$	$4.8 \cdot 10^{-4}$	
1337	$5.5 \cdot 10^{-4}$	$1.4 \cdot 10^{-4}$	Allen and Hewitt
1363	$1.45 \cdot 10^{-3}$	$3.7 \cdot 10^{-4}$	
1423	$1.55 \cdot 10^{-2}$	$1.4 \cdot 10^{-3}$	

The fact that in the reduction of the oxides of copper by hydrogen the reaction can occur even in the presence of a relatively large percentage of steam is in contrast to the observation with other oxides, as will be emphasized in the subsequent discussion.

---

[19] *J. Am. Chem. Soc.*, **30**, 1344 (1908).

[20] *Z. anorg. Chem.*, **164**, 86 (1927).

[21] *Z. anorg. Chem.*, **180**, 83 (1929).

[22] *Z. physik. Chem.*, **B**, **37**, 148 (1937).

[23] *J. Inst. Metals*, **51**, 257 (1933).

Although the reduction of CuO by hydrogen begins at 200° C, the temperature actually used in practice is about 500° C, since the velocity of chemical reactions increases rapidly with the temperature. It should be observed that thermodynamic calculations, such as those made above, supply *no criterion whatever regarding the velocity of a reaction.*

As a rough approximation for determining the possibility of a chemical reaction, it is a usual procedure to calculate the magnitude and sign of the *total energy* change (thermochemical heat of reaction). For the oxides of copper the values of this energy change, designated by ΔH (calories per gram atom of oxygen), are as follows:

$$Cu + 0.5O_2 \rightarrow CuO - 34{,}890 \text{ cal},$$

$$2Cu + 0.5O_2 \rightarrow Cu_2O - 39{,}900 \text{ cal}.$$

Since $H_2 + 0.5O_2 \rightarrow H_2O\ (g) - 57{,}826$ cal, it follows that

$$Cu_2O + H_2 \rightarrow 2Cu + H_2O - 17{,}926 \text{ cal},$$

$$0.5\ CuO + H_2 \rightarrow 0.5\ Cu + H_2O - 40{,}381 \text{ cal},$$

and

$$2CuO + H_2 \rightarrow Cu_2O + H_2O - 27{,}946 \text{ cal}.$$

That is, in all cases *heat is evolved,* and the reduction is exothermic, with a large decrease in the value of ΔH. Consequently we can safely predict that reduction will proceed readily at a sufficiently high temperature.

One other consideration that should be mentioned in this connection is the effect of hydrogen on the physical properties of copper. As stated in Chapter 9, section 15, hydrogen "embrittlement" of copper is a phenomenon familiar to metallurgists, and therefore in the high-temperature treatment of copper in order to eliminate oxides precautions should be taken to avoid this effect.

5. DISSOCIATION OF OXIDES OF IRON AND THEIR REDUCTION BY HYDROGEN

The reactions of iron which have to be considered are the following:

(I*a*) $$Fe + 0.5O_2 \rightarrow FeO \quad (\Delta F_1,\ P_{mm1}).$$

(I*b*) $$FeO + H_2 \rightarrow Fe + H_2O \quad (\Delta F_{H1},\ K_{H1}).$$

(II*a*) $3FeO + 0.5O_2 \rightarrow Fe_3O_4 \quad (\Delta F_2, P_{mm2}).$

(II*b*) $Fe_3O_4 + H_2 \rightarrow 3FeO + H_2O \quad (\Delta F_{H2}, K_{H2}).$

(III*a*) $2Fe_3O_4 + 0.5O_2 \rightarrow 3Fe_2O_3 \quad (\Delta F_3, P_{mm3}).$

(III*b*) $3Fe_2O_3 + H_2 \rightarrow 2Fe_3O_4 + H_2O \quad (\Delta F_{H3}, K_{H3}).$

(IV*a*) $3Fe + 2O_2 \rightarrow Fe_3O_4 \quad (\Delta F_4, P_{mm4}).$

(IV*b*) $Fe_3O_4 + 4H_2 \rightarrow 3Fe + 4H_2O \quad (\Delta F_{H4}, K_{H4}).$

(V*a*) $2Fe + 1.5O_2 \rightarrow Fe_2O_3 \quad (\Delta F_5, P_{mm5}).$

(V*b*) $Fe_2O_3 + 3H_2 \rightarrow 2Fe + 3H_2O \quad (\Delta F_{H5}, K_{H5}).$

The corresponding values of ΔF, P_{mm} (the dissociation pressure of the oxide), and $K_H = (H_2O)/(H_2)$ are indicated by the symbols in parentheses.

Relations for the calculation of ΔF_1, ΔF_2, etc., have been derived by J. Chipman and D. W. Murphy.[24] From the values of ΔF_1, etc., thus derived, values of P_{mm1}, P_{mm2}, etc., can be calculated by means of relations similar to equations 1.11 and 4.5.

Actually the values of ΔF_1, ΔF_2, etc., have been derived from observations on the values of K_{H1}, K_{H2}, etc. By combining the values of ΔF_{H1}, ΔF_{H2}, etc., thus obtained, with those of ΔF_W, it is possible to derive values for ΔF_1, ΔF_2, etc., by means of relations similar to those in section 4 above.

In deriving the values of ΔF_1 and of the corresponding values of P_{mm1} (the dissociation pressure for FeO), the values of K_{H1} used were those published by J. B. Austin and M. J. Day,[25] which are in substantial agreement with those observed by P. H. Emmett and J. F. Schultz[26] and also by Chipman and S. Marshall.[27] These values are shown in the second column of Table 7, and the corresponding values of P_{mm1} are shown in the third column.

From energy considerations it follows that, for any given value of T, the five different values of ΔF must satisfy the following relations:

$$3\Delta F_1 + \Delta F_2 = \Delta F_4 \qquad (1)$$

---

[24] *J. Ind. Eng. Chem.*, **25**, 319 (1933).

[25] *J. Ind. Eng. Chem.*, **33**, 23 (1941). This gives values of K_{H1} over the range 400° C to 1300° C. The values given in Table 7, which are only slightly different from those published in 1941, are taken from a more recent paper by Austin, published by the American Society for Metals, Cleveland, Ohio, in the Symposium on Controlled Atmospheres, 1942.

[26] *J. Am. Chem. Soc.*, **52**, 4268 (1930).

[27] *J. Am. Chem. Soc.*, **62**, 299 (1940).

and

$$2\Delta F_4 + \Delta F_3 = 3\Delta F_5. \tag{2}$$

Using the expression for $\Delta F_4/T$ derived by Chipman and Murphy[28] and a plot of $\Delta F_1/T$ versus $1/T$, derived as described above, the following empirical relations were derived for $\Delta F_2/T$, $\log P_{mm2}$ and $\log K_{H2}$:

$$\frac{\Delta F_2}{T} = 25.55 - \frac{70{,}780}{T} \tag{3}$$

$$\log P_{mm2} = 14.05 - \frac{30{,}940}{T} \tag{4}$$

$$\log K_{H2} = 2.635 - \frac{2531}{T}\cdot \tag{5}$$

Values of K_{H2} and P_{mm2} (the dissociation pressure of oxygen for reaction II*a*) calculated by means of these relations are shown in Table 7.

Thompson has summarized the results of experimental observations on the values of K_{H2}, obtained by several investigators, and has deduced from these data the relation, valid over the range 863° K to 1335° K,

$$\log K_{H2} = 3.25 - \frac{3070}{T}\cdot \tag{6}$$

This is a very rough approximation, since the limits of error in the two constants, according to Thompson, are ±0.38 and ±300, respectively.

L. Wöhler and O. Balz[29] determined values of K_{H2} for the range 913° K to 1223° K. A plot of their results yields the relation

$$\log K_{H2} = 2.41 - \frac{1960}{T}\cdot \tag{7}$$

Values of K_{H2} derived by means of these last two equations are as follows:

T:	1400	1300	1200	1100	1000	900
K_{H2} (Th):	11.4	7.76	4.90	3.55	1.51	0.69
K_{H2} (W & B):	10.2	7.94	6.03	4.27	2.82	1.74

Evidently these values are considerably higher than those in Table 7.

From the expression for $\Delta F_4/T$, which was mentioned above, values of P_{mm4} and K_{H4} have been calculated; they are shown in Table 8. From a review of determinations made by different investigators of values of K_{H4}, Thompson has derived the following relation, which is valid only in the range 706° K to 838° K:

---

[28] *Loc. cit.*

[29] *Z. Elektrochem.*, **27**, 406 (1921).

$$4 \log K_{H4} = 5.59 - \frac{6019}{T}. \tag{8}$$

The two values given in the fourth column of Table 8 have been derived by means of this relation.

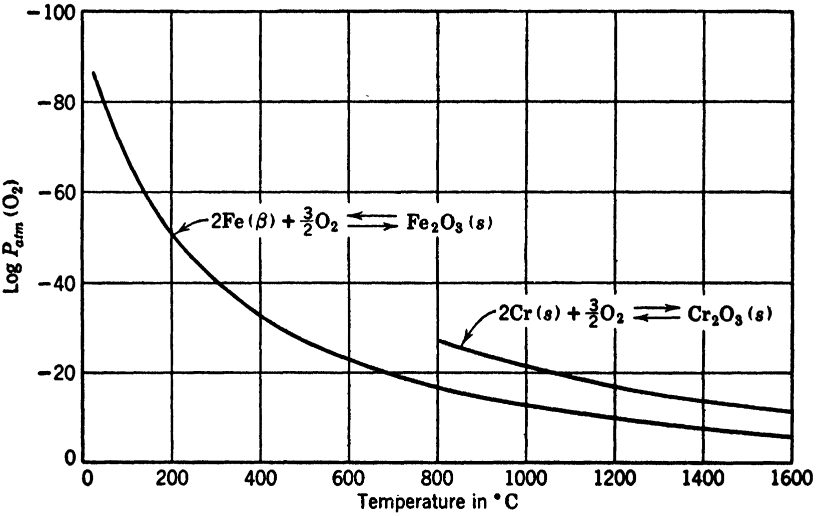

FIG. 3. Plots of log of dissociation pressures versus temperature for Fe_2O_3 (to Fe) and for Cr_2O_3 (to Cr) (Gulbransen).

The values of P_{mm5} and K_{H5} given in Table 8 were derived by means of the relation derived for ΔF_5 by Chipman and Murphy. Figures 3 and 4 show plots of the dissociation pressure of Fe_2O_3, P_{atm5}, and of K_{H5} respectively, as deduced by E. A. Gulbransen[30] from the relation for ΔF_5 given by J. Chipman and D. W. Murphy.[31]

From the values of $\Delta F_5/T$ and $\Delta F_4/T$, those of $\Delta F_3/T$ were calculated by means of equation 2. However, a comparison of the values thus derived with those obtained by O. C. Ralston[32] shows considerable disagreement. This result is not surprising in view of the fact that any

[30] *Trans. Electrochem. Soc.*, **82**, 375 (1942).
[31] *Ind. Eng. Chem.*, **25**, 326 (1933).
[32] *Bur. Mines*, Bulletin 296, Washington, 1929.

TABLE 7

DISSOCIATION PRESSURES OF OXIDES OF IRON AND EQUILIBRIUM CONSTANTS FOR REDUCTION BY HYDROGEN (I.)

Reactions Ia and Ib (FeO : Fe)			Reactions IIa and IIb (Fe_3O_4 : FeO)			Reactions IIIa and IIIb (Fe_2O_3 : Fe_3O_4)		
T	K_{H1}	P_{mm1}	T	K_{H2}	P_{mm2}	T	K_{H3}	P_{mm3}
1373	0.743	$5.0 \cdot 10^{-11}$	1400	6.71	$8.7 \cdot 10^{-9}$	1400	18.8	$7.0 \cdot 10^{-8}$
1273	.662	$7.6 \cdot 10^{-13}$	1300	4.92	$1.8 \cdot 10^{-10}$	1200	16.8	$4.6 \cdot 10^{-11}$
1200		$7.1 \cdot 10^{-14}$	1200	3.35	$1.9 \cdot 10^{-12}$	1100	15.7	$4.8 \cdot 10^{-13}$
1173	.582	$1.7 \cdot 10^{-14}$	1100	2.16	$8.3 \cdot 10^{-15}$	1000	14.4	$2.2 \cdot 10^{-15}$
1073	.499	$1.2 \cdot 10^{-16}$	1000	1.27	$1.3 \cdot 10^{-17}$	900	12.9	$2.1 \cdot 10^{-18}$
973	.422	$2.6 \cdot 10^{-19}$	900	0.66	$4.6 \cdot 10^{-19}$	800	11.4	$4.8 \cdot 10^{-20}$
923	.376	$7.2 \cdot 10^{-21}$						
873	.340	$1.5 \cdot 10^{-22}$						
823	.283							

errors in the expressions for ΔF_4 and ΔF_5 are magnified considerably in the calculation of ΔF_3 by means of equation 2.

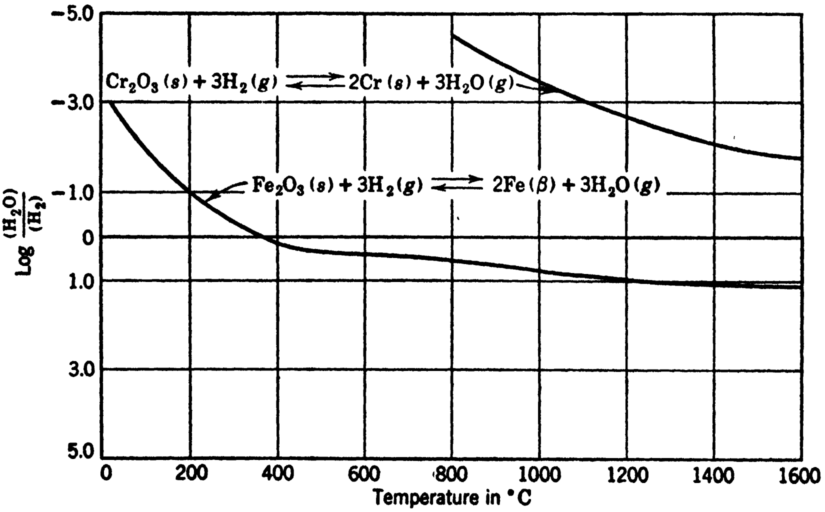

FIG. 4. Plots of log of ratio $(H_2O)/(H_2)$ versus temperature for equilibrium over the systems Fe_2O_3-Fe and Cr_2O_3-Cr (Gulbransen).

Consequently, more reliance has been placed on the experimental determinations of K_{H3} made by Wöhler and Balz.[83] These values,

---

[83] *Loc. cit.*

TABLE 8

DISSOCIATION PRESSURE OF OXIDES OF IRON AND EQUILIBRIUM CONSTANTS FOR REDUCTION BY HYDROGEN (II.)

T	$Fe_3O_4 : Fe$			$Fe_2O_3 : Fe$	
	Reactions IV*a* and IV*b*			Reactions V*a* and V*b*	
	P_{mm4}	K_{H4}	K_{H4} (Th)	P_{mm5}	K_{H5}
1400	$3.47 \cdot 10^{-10}$	1.340		$1.26 \cdot 10^{-8}$	8.00
1200	$1.51 \cdot 10^{-13}$	0.984		$4.68 \cdot 10^{-12}$	5.30
1100	$1.12 \cdot 10^{-15}$	.785		$3.16 \cdot 10^{-14}$	3.90
1000	$2.88 \cdot 10^{-18}$	.603		$5.75 \cdot 10^{-17}$	2.70
900	$2.00 \cdot 10^{-21}$	.398		$3.98 \cdot 10^{-20}$	1.78
800	$2.14 \cdot 10^{-25}$	.275	0.328	$6.17 \cdot 10^{-24}$	1.45
700	$1.59 \cdot 10^{-30}$	.159	.177		

which are represented satisfactorily by the empirical relation

$$\log K_{H3} = 1.569 - \frac{411.1}{T} \tag{9}$$

are given in the second last column of Table 7. By means of the relation

$$\log P_{mm3} = 2.881 + 2(\log K_{H3} - \log K_W) \tag{10}$$

values of P_{mm3} (dissociation pressure of Fe_2O_3 to Fe_3O_4) were calculated; they are given in the last column.

These pressures are extremely low compared with those published by P. T. Walden.[34] Thus Walden gives the value $P_{mm3} = 5.0$ mm at $T = 1373$, and correspondingly higher values for higher temperatures. However, these values of P_{mm3}, if correct, would lead to impossibly high values of K_{H3} (of the order of 10^5 at $T = 1400$).

That the data in Tables 7 and 8 on the dissociation pressures of the oxides of iron are in agreement with observations on the oxidation of iron at different temperatures is pointed out in section 11 below, especially in the discussion of Fig. 7. This diagram should therefore be consulted in connection with the above calculations.

Summarizing the results derived in Tables 7 and 8, the following conclusions may be drawn:

1. The dissociation pressures of the oxides of iron are extremely low, even at 1400° K.

2. The values of the ratio of the concentration of H_2O to that of H_2 at equilibrium, while increasing with the temperature, are less than unity

---

[34] *J. Am. Chem. Soc.*, **30**, 1350 (1908).

for the reduction of Fe_2O_3 to Fe and highest for the reduction of Fe_2O_3 to Fe_3O_4.

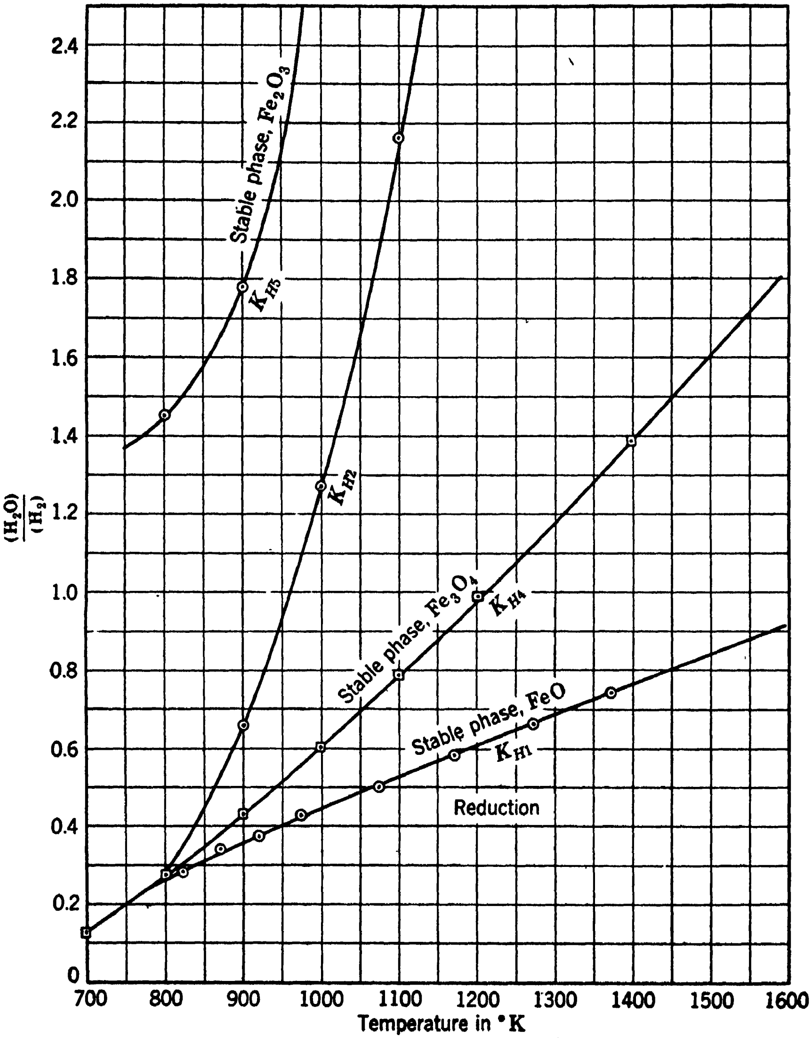

FIG. 5. Plots of equilibrium pressure ratios $(H_2O)/(H_2)$ versus temperature for the oxidation of iron by water vapor and reduction of oxides of iron by hydrogen. Curve K_{H1} for the system FeO-Fe; curve K_{H2} for the system Fe_3O_4-FeO; K_{H4} for the system Fe_3O_4-Fe; Curve K_{H5} for the system Fe_2O_3-Fe.

Figure 5 shows plots of K_{H1}, K_{H2}, and K_{H4} over the range $T = 700°$ to $T = 1400°$. For values of $(H_2O)/(H_2)$ less than those given by the plot for K_{H1}, FeO is *reduced by hydrogen.* The region between the plots for K_{H1} and K_{H4} corresponds to oxidation to FeO, and, in the region between the plots for K_{H4} and K_{H2}, Fe_3O_4 is reduced to FeO. In the region between the plots for K_{H5} and K_{H4}, Fe_3O_4 is the oxide formed by the action of steam on Fe or FeO. Finally, in order to obtain Fe_2O_3, the ratio $(H_2O)/(H_2)$ must exceed the values determined by the plot for K_{H5}.

The data on thermochemical heats of formation indicate that in all these reactions *heat is evolved* (ΔH is negative) when the reaction proceeds in the direction of oxidation by steam. The magnitudes of the energy of reaction in calories per mole H_2O are as follows:

$$\text{(I}b\text{)} \qquad Fe + H_2O \rightarrow FeO + H_2 - 6214.$$

$$\text{(IV}b\text{)} \qquad \tfrac{3}{4}Fe + H_2O \rightarrow \tfrac{1}{4}Fe_3O_4 + H_2 - 8661.$$

$$\text{(V}b\text{)} \qquad \tfrac{2}{3}Fe + H_2O \rightarrow \tfrac{1}{3}Fe_2O_3 + H_2 - 5741.$$

Thus for these reactions, deductions based on the fact that heat is evolved are not at all valid. Actually, the course of each reaction depends upon the value of the ratio $(H_2O)/(H_2)$ in the gas, that is, on the magnitude and sign of ΔF_H.

6. DISSOCIATION AND REDUCTION OF OXIDES OF NICKEL AND COBALT

H. L. Johnson and A. L. Marshall[35] have measured the dissociation pressures of *nickel oxide* according to the reaction

$$Ni + 0.5O_2 \rightarrow NiO.$$

From these values, those of $K = (H_2O)/(H_2)$ have been derived for the reaction

$$NiO + H_2 \rightarrow Ni + H_2O.$$

Both sets of data are given in Table 9.

For the analogous reactions for *cobalt,* the relations given by Thompson for the free energy of formation of CoO have been used. Values of $\Delta F_1/T$, P_{mm} (O_2), and K_H are given in Table 9.

The dissociation pressures for NiO in Table 9 are considerably lower than the values observed by H. W. Foote and E. K. Smith.[36] According to them the values of P_{mm} (O_2) are as follows:

---

[35] *J. Am. Chem. Soc.*, **62**, 1382 (1940).

[36] *J. Am. Chem. Soc.*, **30**, 1344 (1908).

$t°$ C:	1000	1100	1200	1245
P_{mm}:	2.0	5.5	13.0	18.0

The thermochemical heat of formation of NiO is 57,830 cal/mole. Comparing this with the value 57,826 for H_2O, it is evident that these data are altogether inadequate for the purpose of predicting the direction of the reaction

$$NiO + H_2 \rightleftarrows Ni + H_2O.$$

TABLE 9

DISSOCIATION PRESSURES FOR OXIDES OF NICKEL AND COBALT AND EQUILIBRIUM CONSTANTS FOR THEIR REDUCTION

NiO			CoO			
T	P_{mm} (O_2)	K_H	T	$-\Delta F_1/T$	P_{mm} (O_2)	K_H
1440	$5.9 \cdot 10^{-7}$	30.2	800	53.18	——	45.7
1495	$2.5 \cdot 10^{-6}$	29.0	1000	39.15	$5.8 \cdot 10^{-15}$	31.4
1511	$3.8 \cdot 10^{-6}$	28.9	1200	29.73	$7.6 \cdot 10^{-11}$	25.1
1529	$5.6 \cdot 10^{-6}$	28.2	1400	22.92	$7.2 \cdot 10^{-8}$	21.6
1566	$1.4 \cdot 10^{-5}$	27.9	1600	17.75	$1.32 \cdot 10^{-5}$	19.2
			1700	15.59	$1.16 \cdot 10^{-4}$	—

The values derived for K_H from the values of ΔF_1, which are given in the third column of Table 9, lead to the conclusion that hydrogen reduced NiO very readily at high temperatures, and, since K_H evidently increases with decrease in temperature, the reduction must occur even more readily at lower temperatures.

The oxide of cobalt is also reduced at all temperatures by hydrogen, as shown by the values of K_H given in the last column of Table 9. Wöhler and Balz[37] obtained the value $K_H = 14.0$ for $T = 723$, which is lower than that calculated from the value of $\Delta F_1/T$.

The higher oxide, Co_3O_4, dissociates at moderately high temperatures according to the equation

$$Co_3O_4 \rightleftarrows 0.5O_2 + 3CoO.$$

Two sets of values are quoted by Thompson[38] for the dissociation pressures; they are given in Table 10.

From plots of log P_{mm} versus $1/T$, the relations are derived that are shown in the lowest row in the table. The corresponding values of ΔH,

---

[37] *Loc. cit.*

[38] *Op. cit.*, p. 24.

TABLE 10

DISSOCIATION PRESSURES OF Co_3O_4

Set I		Set II	
T	P_{mm} (O_2)	T	P_{mm} (O_2)
1128	23	1073	10
1170	81	1123	28
1201	174	1183	183
1233	438	1223	521
		1243	765
$\log P_{mm} = 16.725 - 17{,}350/T$		$\log P_{mm} = 16.109 - 16{,}420/T$	

the heat of reaction, are 34,500 and 32,600 cal/mole Co_3O_4, which are in satisfactory agreement with thermochemical data.

Obviously Co_3O_4 is readily reduced by hydrogen at moderate temperatures.

7. DISSOCIATION AND REDUCTION OF OXIDES OF MANGANESE, CHROMIUM, MOLYBDENUM, AND TUNGSTEN

There are at least four oxides of manganese, which may be regarded as successive stages of oxidation of manganese or successive stages in the reduction of MnO_2. These reactions and the temperature ranges in which *dissociation* have been observed are as follows:[39]

$$MnO \rightarrow Mn + 0.5O_2 \quad \text{very high temperatures,}$$

$$Mn_3O_4 \rightarrow 3MnO + 0.5O_2 \quad \text{above 1300° C,}$$

$$3Mn_2O_3 \rightarrow 2Mn_3O_4 + 0.5O_2 \quad \text{900–1000° C,}$$

$$2MnO_2 \rightarrow Mn_2O_3 + 0.5O_2 \quad \text{500–900° C.}$$

Thus, according to Krüll, dissociation of MnO_2 is already perceptible (but occurs at a very slow rate) at 500° C and occurs very rapidly at 900° C.

Though M. de K. Thompson has deduced equations for the free energy of each of the oxides from the elements, the values of $\Delta F/T$ deduced from these equations are apparently not sufficiently accurate to be in accord with the above observations for the temperature ranges in which dissociation occurs. However, the values of $\Delta F/T$ calculated for the formation of MnO lead to the conclusion that, at $T = 1400$, P_{mm} (O_2) $= 1.5 \cdot 10^{-20}$ mm; that is, the dissociation pressure is negligibly small.

---

[39] F. Krüll, *Z. anorg. Chem.*, **208**, 134 (1932); also A. Simon and F. Fehér, *Z. Elektrochem.*, **38**, 137 (1932).

According to Wöhler and Balz,[40] the value of K_H for the reaction

$$Mn_3O_4 + H_2 \rightarrow 3MnO + H_2O$$

at $T = 723$ is 34.6. Hence, the dissociation pressure of Mn_3O_4 at this temperature is calculated to be about $1.4 \cdot 10^{-24}$ mm.

A. F. Kapustinskü and K. S. Bayushkina[41] have measured the dissociation pressures for the reaction

$$2MnO_2 \rightarrow 0.5O_2 + Mn_2O_3,$$

and their results are represented by the relation

$$\log P_{mm} = 11.007 - \frac{6897}{T} \cdot$$

Values of the dissociation pressure, in millimeters, calculated from this relation are as follows:

$t°$ C:	575	527	427
P_{mm} (O_2):	760	244	14

Chromium forms the two very stable oxides CrO and Cr_2O_3. The equilibrium constant of the reaction

$$2Cr + 3H_2O \rightarrow Cr_2O_3 + 3H_2$$

has been measured by G. Grube and M. Flad.[42] Table 11(a) gives the results obtained by them and values of P_{mm} (O_2), calculated from these results by Thompson.

TABLE 11(a)

OXIDATION OF CHROMIUM BY WATER VAPOR

T	P_{mm} (H_2)	P_{mm} (H_2O)	$\log P_{mm}$ (O_2)
1168	740.3	0.101	−24.13
1241	730.3	.173	−22.29
1275	734.7	.243	−21.42

That is, at equilibrium at 1168° K, there is present only about 1 part of water vapor in 7400 parts of hydrogen, by volume. Consequently, any moisture present in hydrogen in excess of this concentration must oxidize metallic chromium. This reaction has therefore been used to obtain the extremely pure hydrogen required for many annealing and firing processes.

---

[40] *Loc. cit.*

[41] *J. Phys. Chem.* (*U.S.S.R.*), **11**, 77 (1938).

[42] *Z. Elektrochem.*, **45**, 835 (1939).

C. G. Maier[43] has calculated the free-energy relations for the above reaction and also for the reaction

$$CrO + H_2 \rightarrow Cr + H_2O.$$

Table 11(*b*) gives values of the equilibrium constants $K_H = (H_2O)/(H_2)$ deduced by him for the above reaction and for the reaction

$$Cr_2O_3 + H_2 \rightarrow 2CrO + H_2O$$

TABLE 11(*b*)

EQUILIBRIUM CONSTANTS FOR REDUCTION OF OXIDES OF CHROMIUM

T	Cr_2O_3-Cr		CrO-Cr		Cr_2O_3-CrO	
	log K_H	P_{mm} (H_2O)	log K_H	P_{mm} (H_2O)	log K_H	P_{mm} (H_2O)
1000	-4.883	$9.95 \cdot 10^{-3}$	-5.62	$1.82 \cdot 10^{-3}$	-3.42	0.288
1200	-3.80	0.121	-4.34	$3.47 \cdot 10^{-2}$	-2.72	1.45
1400	-3.073	0.643	-3.47	0.257	-2.27	4.07
1600	-2.478	2.53	-2.77	1.29	-1.92	9.12
1800	-2.048	6.79	-2.25	4.27	-1.65	17.0
2000	-1.463	14.9	-1.84	11.0	-1.44	27.5

Assuming that P_{mm} (H_2) = 760, the values of log K_H yield the values of $P_{mm}(H_2O)$ that are given in the table.

Figures 3 and 4 in section 5 give plots of values of K_H and of the dissociation pressures for Cr_2O_3 as deduced by Gulbransen[44] from the relation for ΔF given by J. Chipman.[45]

For the oxidation of *molybdenum* according to the reaction

$$Mo + 2H_2O \rightarrow 2H_2 + MoO_2,$$

the relation given by Thompson for the value of ΔF leads to the following results:

T:	900	1000
$(H_2O)/(H_2)$:	86.3	246

Hence, at these temperatures the oxide is reduced by hydrogen.

For the oxidation of *tungsten* according to the reaction

$$W + 2H_2O \rightarrow 2H_2 + WO_2,$$

---

[43] *Bur. Mines Bulletin* **436**, **1942**.

[44] *Loc. cit.*

[45] *Trans. Am. Soc. Metals*, **22**, 425 (1934).

Smithells[46] has deduced the relation

$$\log \frac{(H_2O)}{(H_2)} = 0.845 - \frac{1111}{T}$$

which leads to the following results:

T:	1000	1200	1400	1600	1800
$(H_2O)/(H_2)$:	0.542	0.830	1.12	1.42	1.69

For the reaction

$$2WO_2 + H_2O \rightarrow H_2 + W_2O_5,$$

the value of the ratio $(H_2O)/(H_2)$, according to Thompson, is about 1.22 at $T = 1000$.

Hence, it follows that at these temperatures water vapor oxidizes readily not only tungsten but also the oxide WO_2 to the higher oxide W_2O_5.

8. REDUCTION OF OXIDES BY CARBON MONOXIDE, OTHER REDUCING ATMOSPHERES, AND CARBON

For the reduction of oxides, carbon monoxide or some other reducing atmosphere may be used, under certain conditions, to replace hydrogen. Indeed, in industrial metallurgical practice this is often done. The chemical reaction involved with a divalent metal (such as iron or nickel) is

I $$MO + CO \rightarrow M + CO_2.$$

Let ΔF_C denote the free energy increase for the reaction

II $$CO + 0.5O_2 \rightarrow CO_2,$$

and let ΔF_O denote the free energy of formation of the oxide per gram atom of oxygen. Then the free energy for reaction I is

$$\Delta F_R = \Delta F_C - \Delta F_O,$$

which is analogous to the relation

$$\Delta F_H = \Delta F_W - \Delta F_O$$

given in section 1 above for the reduction by hydrogen.

In this case, if we assume that both metal and oxide are not volatile in the range of temperatures under consideration, the equilibrium constant,

---

[46] *Tungsten, a Treatise on Its Metallurgy, Properties, and Applications*, Van Nostrand, New York, 1936. The relation given for log K is quoted from the paper by G. E. Moore, *J. Chem. Phys.*, **9**, 427 (1941), on the reduction of MgO by tungsten in vacuum.

$$K_R = \frac{P(\mathrm{CO_2})}{P(\mathrm{CO})} = \frac{(\mathrm{CO_2})}{(\mathrm{CO})}, \tag{1}$$

is determined by means of the relation

$$\begin{aligned}\log K_R &= -\frac{1}{4.574} \cdot \frac{\Delta F_R}{T}.\\ &= -\frac{1}{4.574T}(\Delta F_C - \Delta F_O),\end{aligned} \tag{2}$$

where ΔF_C is determined from observations of the values of the equilibrium constant

$$K_C = \frac{P_{atm}\,(\mathrm{CO_2})}{P_{atm}\,(\mathrm{CO})\,\sqrt{P_{atm}\,(\mathrm{O_2})}} \tag{3}$$

by means of the relation

$$\Delta F_C = -4.574T \log K_C.$$

From the relation for ΔF_C given by Thompson, we obtain values which, for the range $T = 600$ to $T = 1500$, can be represented (with a difference not exceeding 0.2 per cent) by the linear relation

$$\Delta F_C = -67{,}600 + 20.84T. \tag{4}$$

Even at 2000° K, the value derived from this equation is only about 1 per cent less than that calculated by means of the more elaborate relation derived by Thompson.

Comparing the last equation with equation 2.6 for ΔF_W, it is evident that, in the reduction of oxides by carbon monoxide, the value of the ratio $(\mathrm{CO_2})/(\mathrm{CO})$ for a given temperature is of the same order of magnitude as that of the ratio $(\mathrm{H_2O})/(\mathrm{H_2})$ for the reduction of oxides by hydrogen. This is shown for the *reduction of FeO* by the data in the second and third columns in Table 12, which are taken from publications by J. B. Austin and M. J. Day.[47]

Besides hydrogen and carbon monoxide, other types of reducing atmospheres are often used in metallurgical practice. The equilibrium constants for three of these reducing gases taken from the publication by Austin and Day, are shown in the last three columns of Table 12. It should be observed that in the water-gas reaction the atmosphere will

---

[47] See footnote 25.

TABLE 12

EQUILIBRIUM CONSTANTS FOR THE REDUCTION OF FEO BY HYDROGEN AND CARBON MONOXIDE AND FOR THREE OTHER REACTIONS

$t°$ C	$K_1^* = (H_2)/(H_2O)$	$K_2^* = (CO)/(CO_2)$	$K_3 = \frac{(H_2)(CO_2)}{(H_2O)(CO)}$	$K_4 = \frac{P_{atm}{}^2\,(CO)}{P_{atm}\,(CO_2)}$	$K_5 = \frac{P_{atm}{}^2\,(H_2)}{P_{atm}\,(CH_4)}$
400	9.12**	0.74**	12.3	$9 \cdot 10^{-5}$	$5.66 \cdot 10^{-2}$
500	4.68**	0.96**	4.88	$4.7 \cdot 10^{-3}$	$4.22 \cdot 10^{-1}$
600	2.99	1.17	2.55	$9.6 \cdot 10^{-2}$	$2.09 \cdot 10^{0}$
700	2.38	1.53	1.56	$1.06 \cdot 10^{0}$	$7.16 \cdot 10^{0}$
800	2.00	1.90	1.05	$7.48 \cdot 10^{0}$	$2.01 \cdot 10$
900	1.72	2.24	0.765	$3.767 \cdot 10$	$4.83 \cdot 10$
1000	1.51	2.57	0.589	$1.465 \cdot 10^{2}$	$1.024 \cdot 10^{2}$
1100	1.37	2.88	0.474	$4.634 \cdot 10^{2}$	$1.920 \cdot 10^{2}$
1200	1.26	3.21	0.395	$1.244 \cdot 10^{3}$	$3.35 \cdot 10^{2}$
1300	1.18	3.49	0.339	$2.951 \cdot 10^{3}$	$5.47 \cdot 10^{2}$

Reactions: (1) $Fe + H_2O \rightarrow FeO + H_2$.
(2) $Fe + CO_2 \rightarrow FeO + CO$.
(3) $CO + H_2O \rightarrow CO_2 + H_2$ Water-gas reaction.
(4) $C + CO_2 \rightarrow 2CO$ Producer-gas reaction.
(5) $CH_4 = C + 2H_2$ Decomposition of methane.

* It will be observed that the ratios K_1 and K_2 given in the table are the *reciprocals* of K_{H1} and K_R respectively as defined previously. It should also be stated that the data designated with two asterisks are probably not very accurate since the stable phase at temperatures of 400° C and 500° C is Fe_3O_4, not FeO.

be oxidizing or reducing according as the values of the ratios P_{CO}/P_{CO_2} or P_{H_2}/P_{H_2O} are less than, or greater than, the individual values of K_1 and K_2 shown in the table.

Both the producer-gas reaction (leading to formation of carbon monoxide) and the decomposition of methane are evidently favored by increase in temperature.

Table 13 taken from the treatise by N. R. Stansel[48] gives the composition of a number of gaseous mixtures used in industrial metallurgical operations.

TABLE 13

COMMERCIAL REDUCING GASES AND THEIR ANALYSIS

	Constituents, Per Cent by Volume							
Gas	CH_4	C_2H_6	C_2H_4	CO_2	CO	H_2	O_2	N_2
Natural gas, Ohio	80.5	18.2						1.3
Natural gas, Penna.	67.6	31.3						1.1
Manufactured coal gas	40		4.2	0.50	6.0	46.0	0.50	1.5
Water gas	2			4	45.0	45.0	0.50	2
Blue water gas				3.5	43.4	51.8		1.30
Carburetted water gas	20		12.05	0.22	25.9	36.50	0.03	3.24
Producer gas (bit.)	2.5		0.4	2.5	27	12.0	0.3	55.3
Producer gas (anth.)	0.31		0.31	6.57	25.07	18.73		49.01
Oil gas	58.3		17.4			24.3		
Blast-furnace gas				14.48	22.81	5.07		57.6

The composition of commercial producer gas varies according as the coal used is bituminous or anthracite. The active components are carbon monoxide and hydrogen, while about half the mixture is nitrogen.

Coke-oven gas consists mainly of hydrogen and methane, and the carbon monoxide content ranges from 5 to 9 per cent.

As will be observed, the composition of commercial water-gas mixtures is very close to the theoretical, which is equal parts of hydrogen and carbon monoxide.

Carburetted water gas contains, in addition to the constituents mentioned in the table, 2 per cent benzene.

The selection of an atmosphere for any particular service involves a number of considerations of a practical nature which are discussed by Stansel. In using such gas mixtures for the high-temperature treatment of metal parts for application in high-vacuum devices or systems, every precaution must be taken to avoid deleterious chemical and physical effects.

---

[48] *Industrial Electric Heating*, John Wiley & Sons, New York, 1933.

In a series of papers on the topic "Gases and Metals and Their Influence,"[49] which treat briefly many of the topics presented in this and previous chapters, H. Lepp has also discussed the reactions of oxides with hydrogen, carbon monoxide, and other reducing gases.[50] Whereas hydrogen can react in only one way, viz., that which leads to the formation of water, carbon monoxide can also react with the metal obtained by reduction of the oxide.

For example, with iron and nickel, carbon monoxide forms the carbonyls $Fe(CO)_5$ and $Ni(CO)_4$, respectively. These reactions occur at low temperatures (about 200° C); the products are volatile and dissociate readily at relatively low temperatures.

At about 500° C to 600° C, carbon monoxide may react with metals to form carbides. For example, we have the reactions

$$3Fe + 2CO \rightarrow Fe_3C + CO_2$$

and

$$4Ni + CO \rightarrow Ni_3C + NiO,$$

as well as the oxidation reaction,

$$Ni + CO_2 \rightarrow NiO + CO.$$

At the melting point of iron, the equilibrium for the reaction,

$$4Fe + CO \rightarrow FeO + Fe_3C$$

is definitely displaced to the right.

Hence, from the point of view of eliminating oxides from metal parts which are intended for use in high-vacuum devices, carbon monoxide should be used with considerable caution. The same remark applies to other reducing atmospheres obtained by cracking hydrocarbon gases. For example, methane reacts with iron according to the equation

$$3Fe + CH_4 \rightarrow Fe_3C + 2H_2$$

to form the carbide. This is the well-known process of cementation.

In a similar manner the reaction between certain oxides and carbon leads to the formation of carbides. For instance, C. H. Prescott has studied the two reactions

$$ZrO_2 + 3C \rightarrow ZrC + 2CO^{51}$$

---

[49] *Metal Ind. London*, **53**, 27, 59, 79, 103, 131 (1938).

[50] *Metal Ind. London*, **53**, 103 (1938).

[51] *J. Am. Chem. Soc.*, **48**, 2534 (1926).

and

$$ThO_2 + 4C \rightarrow ThC_2 + 2CO.^{52}$$

For the first reaction, he obtained the following relation for the pressure of carbon monoxide in atmospheres:

$$\log P_{atm} = 8.592 - \frac{16{,}580}{T}, \tag{5}$$

and, for the second, the relation

$$\log P_{atm} = 8.069 - \frac{19{,}325}{T}. \tag{6}$$

From these relations the following values for the pressure of carbon monoxide are deduced for a series of values of T. The second row gives the values for the reduction of ZrO_2; the third row, those for the reduction of ThO_2:

T:	1600	1800	2000	2200	2400
(Reduction of ZrO_2), P_{atm} (CO):	$1.7 \cdot 10^{-2}$	$2.4 \cdot 10^{-1}$	2.00	11.35	—
(Reduction of ThO_2), P_{atm} (CO):	$1 \cdot 10^{-4}$	$4.6 \cdot 10^{-2}$	$2.55 \cdot 10^{-2}$	0.191	1.04

Thus ZrO_2 is much more readily reduced by carbon than ThO_2. The values of ΔF corresponding to relations 5 and 6, as derived by Prescott, are:

$$\Delta F = 151{,}800 - 78.68T \tag{7}$$

and

$$\Delta F = 176{,}970 - 73.892T, \tag{8}$$

respectively.

Quite frequently it is of interest to know the order of magnitude of the free energy for the reduction of an oxide by some metal. For example, the reaction

$$2MgO\ (s) + W\ (s) \rightarrow 2Mg\ (g) + WO_2\ (s)$$

has been investigated by G. E. Moore.[53] He determined the vapor pressure of magnesium as a function of T and observed that there is a remarkable agreement between these values and those derived from calculated values of ΔF for the reaction. The following approximate

[52] Prescott and W. B. Hincke, *J. Am. Chem. Soc.*, **49**, 2744 (1927).

[53] *J. Chem. Phys.*, **9**, 427 (1941). See footnote 46 for reference to reduction of WO_2 by H_2.

values of the vapor pressure in millimeters of mercury were obtained from the plot given in the publication:

T:	1400	1600	1800
P_{mm}:	10^{-8}	$2 \cdot 10^{-6}$	$1 \cdot 10^{-4}$

Similar reactions for which both experimental data and calculations of ΔF would be extremely desirable for a better understanding of electron emission phenomena in good vacuum are the following:

$$ThO_2 + W \rightarrow Th + WO_2,$$

$$BaO + C \rightarrow Ba + CO,$$

and

$$BaO + CO \rightarrow Ba + CO_2.$$

9. DISSOCIATION OF HYDRIDES OF THE ALKALI AND ALKALINE-EARTH METALS

In Chapter 9 a comparison was made between the heats of formation of the so-called hydrides of the titanium group of metals and the hydrides of the alkali and alkaline-earth metals. These hydrides are formed when hydrogen is passed over the heated metals, so that the metal functions as a "getter" or chemical clean-up reagent. (Getters were discussed in Chapter 10.) At higher temperatures these hydrides dissociate, and at each temperature there exists an equilibrium pressure.

Dissociation Pressures of NaH and KH. These have been measured by F. G. Keyes[54] and more recently by E. F. Sollers and J. L. Crenshaw[55] who have also measured the dissociation pressures of the deuterides. Since the results obtained in these two investigations are in very good agreement we can, for the purpose of extrapolation to lower temperature, use the empirical relations derived in the more recent investigations, which are as follows:

$$\text{For NaH,} \quad \log P_{mm} = 11.9250 - \frac{6318.41}{T}. \tag{1}$$

$$\text{KH,} \quad \log P_{mm} = 11.6535 - \frac{6185.57}{T}. \tag{2}$$

$$\text{NaD,} \quad \log P_{mm} = 13.1994 - \frac{6915.0}{T}. \tag{3}$$

$$\text{KD,} \quad \log P_{mm} = 12.1977 - \frac{6318.68}{T}. \tag{4}$$

---

[54] *J. Am. Chem. Soc.*, **34**, 779 (1912).

[55] *J. Am. Chem. Soc.*, **59**, 2015 (1937) (KH and KD); **59**, 2724 (1937) (NaH and NaD).

Table 14 gives values of the dissociation pressures calculated by means of these relations.

As will be observed, the dissociation pressure of the deuterides are approximately twice those of the corresponding hydrides, while for the two hydrides the temperatures corresponding to a given value of the pressure are very closely the same.

TABLE 14

Dissociation Pressures of Sodium and Potassium Hydrides and Deuterides

	t° C:	380	360	340	320	300	280
NaH	P_{mm}:	178	88.1	41.6	18.7	7.9	3.2
NaD	P_{mm}:	407	189.3	83.2	34.7	13.6	5.0
KH	P_{mm}:	152	76.5	36.7	16.7	7.2	3.0
KD	P_{mm}:	343	164.9	78.0	35.0	14.8	5.9

t° C for P_μ =

	10^3	10^2	10	1	10^{-1}	10^{-2}	10^{-3}
NaH	256.6	215.6	180.5	150.1	123.6	100.1	79.2
KH	257.8	215.9	180.1	149.1	122.2	98.4	77.4

According to different investigators, sodium absorbs hydrogen appreciably at 100–200° C, and the rate of absorption increases with the temperature.[56]

Dissociation Pressures of CaH_2. There is a considerable literature on this topic, which has been reviewed by P. Remy-Genneté in a series of papers.[57] Besides the determinations made by him, careful measurements have also been made by C. A. Kraus and C. B. Hurd[58] and by Hurd and K. E. Walker.[59]

The results of each of these investigations can be represented by the relation

$$\log P_{mm} = A - \frac{B}{T} \tag{5}$$

where the values of A and B are shown in the second and third columns of Table 15.

The values of A and B in the first row are those derived by Kraus and Hurd; the two other pairs of values were derived by the writer from the plots shown in the original publications. From these values of A and B, the data given in the rest of the table were calculated.

---

[56] "The production of NaH and some of its reactions" is discussed by V. L. Hansley and P. J. Carlisle, *Chem. Eng. News*, **23**, 1332 (1945).

[57] *Ann. chim. France*, **19**, 263–352 (1933).

[58] *J. Am. Chem. Soc.*, **45**, 2559 (1923).

[59] *J. Am. Chem. Soc.*, **53**, 1681 (1931).

TABLE 15

DISSOCIATION PRESSURES OF CaH_2

			t° C for P_{mm} =					
Investigators	A	B	10	1	10^{-1}	10^{-2}	10^{-3}	10^{-4}
Kraus and Hurd	11.14	10,660	779	684	605	538	480	431
Hurd and Walker	11.79	11,160	761	673	599	536	481	434
Remy-Genneté	12.66	12,130	767	685	615	554	500	455

Hurd derived from the second set of measurements the value $Q = 50{,}000$ cal/mole for the heat of formation of CaH_2, which is higher than the value 46,200 obtained calorimetrically by earlier investigators.

F. Ephraim and E. Michel[60] attempted to measure dissociation pressures of LiH, SrH_2, and BaH_2 but encountered difficulties due to the fact that these hydrides form solid solutions with the metals. The only definite conclusion they could deduce was that for a given value of the dissociation pressure the corresponding temperatures are much lower for the other alkaline-earth hydrides than for CaH_2. For instance, at 677° C, the minimum value observed for the dissociation pressure of BaH_2 was about 270 mm as compared with about 1 mm for CaH_2 at this temperature.

10. DISSOCIATION PRESSURES OF NITRIDES

The alkali and alkaline-earth metals combine with nitrogen directly to form quite stable nitrides, as indicated by the fact that the reactions are strongly exothermic. The nitrides of copper, silver, mercury, and lead are endothermic compounds and very explosive. A number of other nitrides, such as those of iron, chromium, and manganese, are decomposed at comparatively low temperatures, while a considerable number, such as AlN, and TiN are extremely stable.

According to K. Becker,[61] the nitrides of metals of Groups IV, V, and VI in the periodic arrangement can be prepared by heating the metal powder to about 1100–1200° C in a current of nitrogen or of a gas, such as ammonia, which yields nitrogen by thermal decomposition at higher temperatures.[62] An alternative method is to heat a mixture of the oxide of the metal with carbon in a stream of nitrogen.[63]

---

[60] *Helv. Chim. Acta,* **4,** 900 (1921).

[61] *Hochschmelzende Hartstoffe und ihre technische Anwendung,* Berlin, Verlag Chemie, 1933, published by Authority of the Alien Property Custodian.

[62] The "nitriding" process is described in the following publications: V. O. Homerberg, *Metals Handbook,* p. 1071, American Society for Metals, 1939; C. F. Floe, *Trans. Am. Soc. Metals,* **32,** 134 (1944).

[63] A description of this method has been published by E. Friederich and L. Sittig. *Z. anorg. allgem. Chem.,* **143,** 293 (1925). See also C. Agte and K. Moers, *Z. anorg, allgem. Chem.,* **198,** 233 (1931).

The nitrides of molybdenum and tungsten are prepared by heating the metals in NH_3, while Friederich and Sittig have prepared the following nitrides by heating a mixture of the oxide and carbon in nitrogen at 1200° C: TiN, VN, BN, Si_3N_4, LaN, ZrN, ScN, CbN, and CeN.

In Table 16 data are given on the melting points and dissociation pressures. For information on the former use has been made of a tabulation by L. Brewer, LeRoy Bromley, P. Gilles and N. Lofsgren.[64] The values of ΔF for a number of the nitrides have been derived by K. K. Kelley.[65] From these data values of the dissociation pressure have been derived by means of the relation

$$\log P_{mm} = \frac{\Delta F}{4.574T} + 2.881, \tag{1}$$

where ΔF is the free energy *per mole* N_2 for the reaction

$$xM + N_2 \rightarrow M_xN_2. \tag{2}$$

References to the book by Becker are indicated in Table 16 by the number (3); additional references are given in the following remarks in connection with the data in the table on page 832.

BN sublimes at 3000° C.

Ca_3N_2: Data derived from the relation for the dissociation pressures given by C. A. Kraus and C. B. Hurd, *J. Am. Chem. Soc.*, **45**, 2559 (1923).

CbN, Mo_2N, ScN, W_2N, and Yn: The values of the integration constant, A, in equation 9.5 for log P_{mm} are indicated in reference 1 as doubtful.

Si_3N_4: Data derived from the relation for the dissociation pressures given by W. B. Hincke and L. R. Brantley, *J. Am. Chem. Soc.*, **52**, 48 (1930). In the range 1606° K to 1802° K, the dissociation pressure was observed to vary from 0.27 mm to 5.49 mm.

Iron and manganese form more than one nitride for each element. For iron the following are known: Fe_4N, Fe_3N, and Fe_2N. The value of ΔF for Fe_4N has been determined from the equilibrium pressures of H_2 and NH_3 in the reaction[66]

$$2Fe_4N + 3H_2 \rightarrow 8Fe + 2NH_3,$$

which is used for the preparation of the nitride. For the reaction

$$4Fe(\alpha) + 0.5N_2 \rightarrow Fe_4N$$

---

[64] A report, *Thermodynamic and Physical Properties of Nitrides, Carbides, Sulfides, Silicides, and Phosphides*, prepared for the Manhattan Project. The writer is indebted to Dr. W. M. Latimer for sending him the above report. This report is indicated in Table 16 as reference 1.

[65] *Bur. Mines Bulletin* 407, Washington, 1937. This is indicated in the table as Reference 2.

[66] Complete details of the observations and calculations are given by Kelley, *loc. cit.*

TABLE 16

MELTING POINTS AND TEMPERATURES FOR GIVEN VALUES OF DISSOCIATION PRESSURES OF NITRIDES

Nitride	M.P.		$t°$ C for P_{mm} =				
	°C	Reference	1	10^{-1}	10^{-2}	10^{-3}	Reference
AlN	2230	1	1487	1374	1275	1187	2
Ba_3N_2			1002	923	855	794	2
Be_3N_2	2200	1	2208	2015	1848	1704	2
BN	3000 (*s*)	1	1340	1193	1075	927	2
Ca_3N_2	900	1	1235	1147	1069	1000	Kraus and Hurd
CbN			1946	1770	1620	1491	1
CeN			2196	2029	1884	1756	2
CrN			719	646	582	533	2
LaN			2010	1855	1721	1602	2
Li_3N_2			896	835	778	727	2
Mg_3N_2			1602	1472	1359	1260	2
Mo_2N			329	283	243	209	1
ScN	2650	1	1880	1734	1607	1495	1
Si_3N_4	1900	2	1421	1282	1164	1060	Hincke and Brantley
Sr_3N_2			1154	1058	975	902	2
TaN	3070 ± 50	3	1921	1746	1599	1460	2
Th_3N_4			2401	2206	2037	1890	2
TiN	2950 ± 50	3	2912	2689	2489	2331	2
U_3N_4			2267	2070	1950	1753	2
VN	2050	3	1242	1127	1024	933	2
W_2N			344	296	256	221	1
YN			1990	1838	1704	1587	1
ZrN	2985 ± 50	3	2603	2390	2205	2046	2

Kelley's expression for ΔF leads to the relation

$$\log P_{mm} = -\frac{1688}{T} - 7.12 \log T + 3.914 \cdot 10^{-3} T + 26.30, \qquad (3)$$

which leads to the value $P_{mm} = 992$ for 25° C, and to much higher values of the dissociation pressure at higher temperatures. According to P. H. Emmett, S. B. Hendricks, and S. Brunauer,[67] the dissociation pressures in *atmospheres* calculated for a series of temperatures are as follows:

$t°$ C:	420	444	460	525
P_{atm}:	4250	4300	5400	5600

---

[67] *J. Am. Chem. Soc.*, **52**, 1456 (1930).

Obviously Fe_4N is unstable at ordinary temperatures and atmospheric pressure.

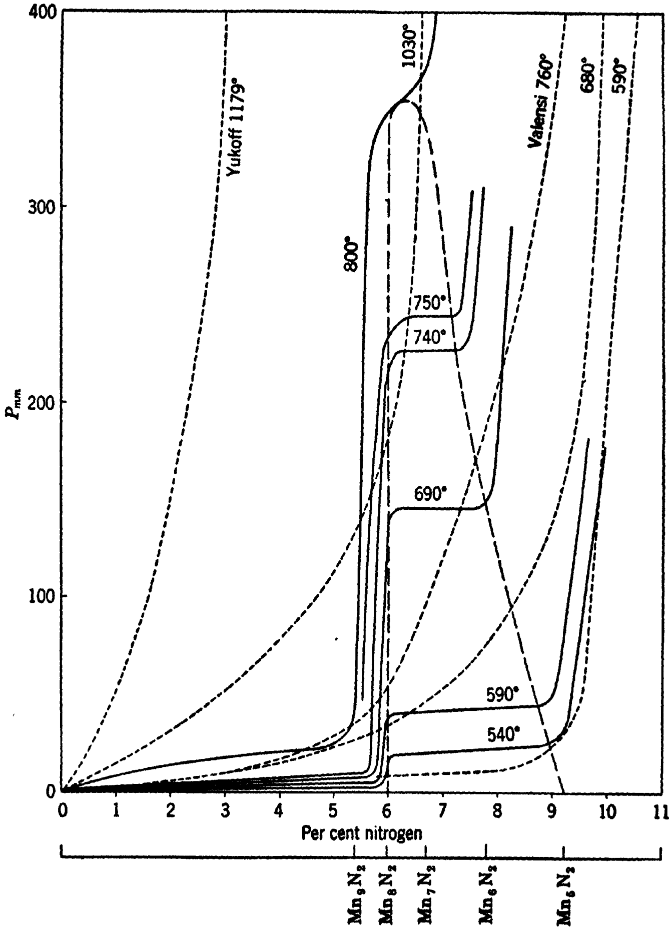

FIG. 6. Isotherms for the nitrogen-manganese system (Schenck and Kortengräber).

As Kelley has pointed out, an approximate calculation of the free energy for the formation of Fe_2N leads to the conclusion that this nitride is not as stable at room temperature as Fe_4N.

The formation of *nitrides of manganese* has been investigated in considerable detail by R. Schenck and A. Kortengräber.[68] Figure 6, from their paper, shows a series of isotherms for the range 540° C to 800° C corresponding to the dissociation pressures of the series of nitrides ranging from Mn_5N_2 to Mn_9N_2. The dotted curves represent isotherms obtained by previous investigators.

---

[68] *Z. anorg. allgem. Chem.*, **210**, 273 (1933).

As Kelley has stated,[69] there is some question regarding the existence of Mn_5N_2, since very valid arguments have been advanced by C. G. Maier[70] for the conclusion that this is actually a mixture of manganese and Mn_3N_2. Furthermore, the equilibrium pressure for the reaction

$$3Mn + N_2 \rightarrow Mn_3N_2$$

depends upon whether the Mn_3N_2-Mn system consists of an amorphous solid solution (Case A) or mixed crystals (Case B). The relations derived by Kelley for each of these cases are as follows:

$$\text{Case A:} \quad \log P_{mm} = 5.102 - \frac{2242}{T}. \tag{4}$$

$$\text{Case B:} \quad \log P_{mm} = 8.854 - \frac{7314}{T}. \tag{5}$$

Assuming the formation of Mn_5N_2, the relation derived by Kelley is

$$\log P_{mm} = 10.84 - \frac{12{,}630}{T}. \tag{6}$$

Table 17 gives values of t in degrees Centigrade corresponding to different values of P_{mm} for each of these reactions. The only conclusion that may be drawn from these data is that the nitrides of manganese are not very stable even at moderately high temperatures (below 1000° C).

TABLE 17

TEMPERATURES IN DEGREES CENTIGRADE FOR GIVEN VALUES OF THE DISSOCIATION PRESSURE, FOR NITRIDES OF MANGANESE

	t° C Calculated according to		
P_{mm}	Eq. 4	Eq. 5	Eq. 6
10	276	658	1010
1	168	553	892
10^{-1}	96	469	794
10^{-2}	44	401	711

A. Fry[71] has reported on the temperatures of dissociation of a number of nitrided metals and alloys. His results are shown in Table 18. The second column in this table gives the percentage nitrogen calculated for the completely nitrided metal.

---

[69] *Op. cit.*, p. 38.

[70] *Bur. Mines Inf. Circ.* 6769, Washington, 1934. Reference quoted by Kelley.

[71] *J. Iron Steel, Inst. London,* **125**, 191 (1932).

TABLE 18

DECOMPOSITION TEMPERATURES IN DEGREES CENTIGRADE OF NITRIDED IRON, MANGANESE, ALUMINUM, AND IRON ALLOYS IN VACUUM

Composition of Alloy	Per Cent Nitrogen	Decomposition		Per Cent Nitrogen in	
		Starts at	Ends at	Gas	Residue
Nitrided electrolytic Fe	6.7	400–500	700–800	6.88	0.005
Nitrided metallic Mn	11.8	500	700	11.6	1.9
Nitrided Al	14.6	>1000	—	—	14.4
Nitrided electrolytic Cr	10.6	600	—	4.1	6.8
Nitrided ferrochromium	8.2	400–500	—	4.8	4.1
Nitrided ferrotungsten	3.6	600	—	2.9	0.6
Nitrided ferrotitanium	4.1	600	—	0.9	3.4
Nitrided ferrovanadium	7.9	400–500	—	1.6	6.3

From these experiments Fry concludes that "the chemical affinity of nitrogen for the elements investigated decreases approximately in the following order: aluminum, titanium, chromium, tungsten, manganese, and iron." According to the data in Table 16, the order of aluminum and titanium should be reversed, since TiN dissociates at much higher temperatures than AlN.

11. PARABOLIC LAW OF RATES OF OXIDATION

To the experimenter in vacuum technique the presence of oxides on metal surfaces or in solution in the metals is of importance because these oxides not only adsorb large volumes of oxygen and other gases but also decompose more or less gradually at higher temperatures. It is therefore of interest to review the observations that have been made on rates of formation of oxide layers as affected by the nature of the metal, pressure of oxygen, and temperature.[72]

One of the earliest and most important investigations in this field was carried out by N. B. Pilling and R. E. Bedworth.[73] They pointed out that the behavior of a metal with respect to oxidation is controlled by the porosity of the oxide formed. The porosity depends upon the value of the ratio

---

[72] In German publications these phenomena are designated "Anlaufvorgänge," that is, "tarnishing reactions."

[73] *J. Inst. Metals*, **29**, 529 (1923); *J. Ind. Eng. Chem.*, **17**, 372 (1925).

$$\alpha = \frac{nV_m}{V_0}, \tag{1}$$

where V_0 = atomic volume of metal (= atomic weight/density).
V_m = molar volume of oxide (= molar weight/density).
n = number of metal atoms per molecule of oxide.

If α is less than 1, the oxide is physically discontinuous. It forms a porous layer through which oxygen permeates very readily. For $\alpha > 1$, the oxide forms as a homogeneous layer and the rate of oxidation depends upon diffusion through this layer. For the oxides of Li, Na, K, Rb, Cs, Ca, Ba, Sr, and Mg, α is less than 1; for all other oxides α is greater than 1.

Oxides of porous structure offer no resistance to the passage of oxygen to the surface of the metal, and as a result the rate of growth of the layer of oxide is constant at any given temperature. Denoting the increase in weight per unit area by W, the *linear law* states that, for a given temperature,

$$W = k_1 t, \tag{2}$$

where t = time elapsed, and k_1 is a constant.

As shown by Pilling and Bedworth the oxidation of calcium obeys this law. The values of k_1 observed for the oxidation in air at three different temperatures were as follows:

t° C	k_1 ($g \cdot cm^{-2} \cdot hr^{-1}$)
300	$3.12 \cdot 10^{-4}$
400	$6.84 \cdot 10^{-4}$
500	$1.90 \cdot 10^{-3}$

In the case of magnesium ($\alpha = 0.84$), the value observed for k_1 (in the same units) was $5.2 \cdot 10^{-4}$ at 500° C. However, they reported difficulties in obtaining reproducible results because of the evaporation of the metal. More recently E. A. Gulbransen[74] has described the results of experiments at temperatures of 400° C to 500° C and at pressures of 0.2 to 20 cm. of oxygen. Using a vacuum microbalance technique it was observed that, at 474° C and higher, the oxidation rate followed a linear law. At temperatures of 450° C and lower, protective coatings were formed, but after an "induction period" the oxidation followed a linear law. The observed rates of oxidation (in terms of $g \cdot cm^{-2} \cdot hr^{-1}$) were as follows:

---

[74] *Trans. Electrochem. Soc.*, **87**, 589 (1945).

500°	O_2 pressure 20 cm	$7.20 \cdot 10^{-5}$
475	O_2 pressure 20 cm	$6.84 \cdot 10^{-6}$
475	O_2 pressure 2 cm	$2.88 \cdot 10^{-6}$

Over the range 425° C to 500° C, it was observed that a plot of log k_1 versus $1/T$ is linear, thus indicating an activation energy for the oxidation.

For metals for which the oxide coating is compact ($\alpha > 1$), the rate of oxidation depends on the rate of diffusion of oxygen through the layer already formed. Hence, the relation between W and t should be of the form[75]

$$W^2 = k_2 t, \tag{3}$$

where k_2 is a constant for any given temperature. This relation, known as the *parabolic law*, was first observed by G. Tammann[76] and was confirmed by the observations made by Pilling and Bedworth on rates of oxidation of copper, nickel, and iron, which are summarized in Table 19.

The table gives values of k_2 in terms of $(\mathrm{g} \cdot \mathrm{cm}^{-2})^2\,\mathrm{hr}^{-1}$. The copper was soft electrolytic sheet and wire; both pure electrolytic and "Grade A" nickel were used, and electrolytic iron as well as Armco. The oxidation of copper was carried out in oxygen at 710 mm, and in air (oxygen pressure = 155 mm); for nickel, oxygen at 710 mm was used for both samples, and for iron, oxygen at 710 mm was used to obtain the data shown in the sixth and seventh columns, while the last column gives data for the oxidation of armco in air.

From plots of log k_2 versus $1/T$, the values of the *activation* energy, E_A, were calculated, which are given in the lowest row of Table 19.

Combining this result with equation 3 it follows that the rate of oxidation of *copper in air* is given by the relation

$$\log W = 1.0821 + 0.5 \log t - \frac{4603}{T}, \tag{4}$$

where W = gain in weight, in $\mathrm{g} \cdot \mathrm{cm}^{-2}$, after t minutes at the temperature $T°\ K$.

As will be observed the value of k_2 at any given temperature is highest for iron and lowest for nickel. This is in accord with the general observation that the rate of oxidation of nickel is very low compared with that of copper or iron. (For this reason nickel is a very much more satisfactory metal for use in vacuum tubes than either of the other metals.)

---

[75] A detailed discussion of the derivation of this equation is given by K. Heindlhofer and B. M. Larsen, *Trans. Am. Soc. Steel Treating*, **21**, 865 (1933).

[76] *Z. anorg. Chem.*, **111**, 78 (1920).

TABLE 19

RATE OF OXIDATION CONSTANT, k_2, $(\text{GM} \cdot \text{CM}^{-2})^2 \cdot \text{HR}^{-1}$, FOR COPPER, NICKEL, AND IRON

	Copper		Nickel		Iron		
$t°$ C	Oxygen	Air	Electrolytic	A	Electrolytic	Armco	Armco (air)
600	$1.13 \cdot 10^{-6}$						
700	$5.86 \cdot 10^{-6}$	$2.68 \cdot 10^{-6}$			$1.7 \cdot 10^{-5}$		
800	$3.14 \cdot 10^{-5}$	$2.70 \cdot 10^{-5}$	$9.3 \cdot 10^{-8}$		$1.0 \cdot 10^{-4}$	$1.95 \cdot 10^{-4}$	$1.06 \cdot 10^{-4}$
900	$1.27 \cdot 10^{-4}$	$1.10 \cdot 10^{-4}$	$7.6 \cdot 10^{-7}$	$1.9 \cdot 10^{-6}$	$6.5 \cdot 10^{-4}$	$1.01 \cdot 10^{-3}$	$4.90 \cdot 10^{-4}$
950	$2.68 \cdot 10^{-4}$			$3.4 \cdot 10^{-6}$			
1000	$6.02 \cdot 10^{-4}$	$4.60 \cdot 10^{-4}$	$3.4 \cdot 10^{-6}$	$6.8 \cdot 10^{-6}$		$4.30 \cdot 10^{-3}$	$2.05 \cdot 10^{-3}$
1100			$1.33 \cdot 10^{-5}$				
E_A =	39,000	42,100	48,000	39,000	43,000		

The proximate compositions of the oxide layers were found to be as follows:

Copper:	98.1 per cent Cu_2O +	1.9 per cent CuO.
Nickel:	90.3 per cent NiO +	9.7 per cent Ni_3O_4.
Iron:	48.2 per cent FeO +	51.8 per cent Fe_3O_4.
Iron:	60.2 per cent FeO +	39.8 per cent Fe_3O_4.

Evidently these results are in agreement with the conclusions regarding the formation of these oxides which have been stated in sections 4 and 5.

E. M. Wise[77] has stated that "nickel does not oxidize appreciably in air until a temperature of 400° C to 500° C is reached and even then the oxidation is slow and the oxide is adherent and protective." In fact, the data in Table 19 show that at 900° C to 1000° C the rate constant for iron is about 1000 times that for nickel.

The effect of pressure of oxygen on the value of k_2 for copper is shown by a comparison of the data for $P_{mm}\ (O_2) = 710$ and $P_{mm}\ (O_2) = 155$, in the second and third columns in Table 19. The effect of further decrease in pressure is shown by the data in Table 20.

TABLE 20

EFFECT OF OXYGEN PRESSURE ON THE VALUE OF THE RATE CONSTANT, k_2, FOR COPPER AT 800° C

P_{mm}:	710	155	19.7	2.60	1.07	0.24	0.24	0.070
$10^5 k_2$:	3.22	2.70	2.10	2.08	1.90	0.91	0.59	(0.006)

Evidently, the value of k_2 decreases only slowly with decrease in pressure until the pressure is decreased to 1 mm or less, which indicates that the rate of oxidation is not limited (except at very low pressure) by the rate at which molecules of oxygen strike the surface but rather by a diffusion process in the oxide layer.

The validity of the parabolic law was also confirmed by the observations made by J. S. Dunn[78] on the oxidation of copper and brass in the ranges 580–880° C and 209–284° C. The value observed for the activation energy was about 40,000 calories, which agrees with that derived from the measurements made by the previous investigators.

Similar results have been obtained by different investigators for a number of oxidations, such as the following:[79] cobalt and tungsten, in the range 700–1000° C, and chrome metal (98 per cent chromium) at 1000° C.

---

[77] *Proc. Inst. Radio Engrs.*, **25**, 714 (1937).

[78] *Proc. Roy. Soc. London*, **A**, **111**, 203, 210 (1926).

[79] *Review of Oxidation and Scaling of Heated Solid Metals*, Department of Scientific and Industrial Research, London, 1935.

In connection with his investigation on the oxidation of magnesium, Gulbransen[80] observed that the rate of oxidation of aluminum at 475° C and 6 mm O_2 also follows the parabolic relation.

The rate of oxidation of iron and some of its alloys has been investigated by K. Heindlhofer and B. M. Larsen.[81] The results for specimens of commercially pure iron in air, over the range 550–1100° C, were in agreement with the parabolic law, and all the observations could be represented as a function of the time, t (in minutes), and the absolute temperature, T, by a relation, similar to equation 4, of the form

$$\log W = 0.7993 + 0.5 \log t - \frac{3907}{T}, \tag{5}$$

From this relation it follows that, for $T = 1000$ and $t = 100$ minutes, $W = 7.8 \cdot 10^{-3}$, whereas it follows from equation 4 that, for the same values of T and t, the gain in weight of copper is $W = 3.0 \cdot 10^{-3}\ \text{g} \cdot \text{cm}^{-2}$, which is in agreement with the observations in Table 19.

The same investigators also observed that the rates of oxidation were substantially the same in carbon dioxide, steam, and oxygen as in air.

With regard to the composition of the oxide formed, it would be expected, from the conclusions regarding the conditions for the formation of the oxides of iron stated in section 5, that with increasing oxygen content the order of formation would be FeO for thin films, followed by Fe_3O_4 for thicker films, and finally some Fe_2O_3 at the outer surface of the oxide layer.

In their paper, Heindlhofer and Larsen have shown a phase diagram, based largely on the work of L. B. Pfeil,[82] for the Fe-O system which is reproduced in Fig. 7, with the following remarks:

> Below the equilibrium diagram is placed a photomicrograph of a section through the scale layer formed on pure iron at about 1050° C (1925° F); it shows three distinct layers—a thin Fe_2O_3 skin on the right, then a layer of Fe_3O_4, and a much thicker layer of FeO in which a decreasing amount of dissolved Fe_3O_4 has separated in cooling as we move toward the extreme left, where the scale was originally in contact with the metal. Since the scale, formed as it is by a diffusion process, can contain only those mixtures of iron and oxygen which form homogeneous single-phase solutions at the scaling temperature (1050° C in this example) the composition at the several boundaries in the scale should correspond with those represented by the intersection of a horizontal at 1050° C with the several lines of the FeO diagram. The curves given in Fig. 7 then represent qualitatively the course of decreasing oxygen

---

[80] *Loc. cit.*

[81] *Loc. cit.*

[82] *J. Iron Steel Inst. London*, **119**, 501 (1929); **123**, 237 (1931).

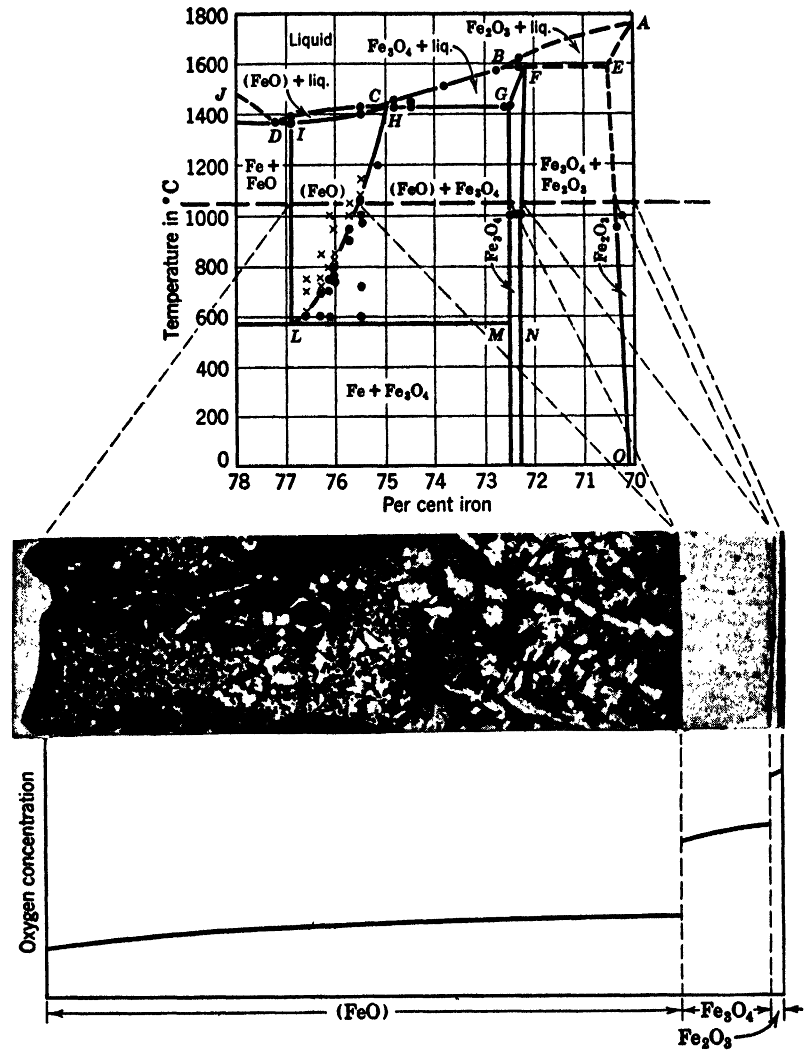

FIG. 7. Fe-O diagram according to Pfeil (modified by Heindlhofer and Larsen). Upper part gives the equilibrium diagram, and below is shown a photomicrograph of a section through the scale layer formed by oxidation. The dotted lines are drawn from the different layers in the scale to the equilibrium diagram. The lower curve represents qualitatively the course of decreasing oxygen content between outside and inside of the scale shown in the photograph.

content between outside and inside of the scale. Since the scale on pure iron (or carbon steel) contains nothing but iron and oxygen the iron content rises in proportion to the drop in oxygen content. The outside scale surface should be pure Fe_2O_3, containing 69.9 per cent iron, which can dissolve Fe_3O_4 (or extra iron atoms, which amounts to the same thing) up to about 70.4 per cent iron. There is, at the Fe_2O_3-Fe_3O_4 boundary, a sharp rise in iron content to about 72.3 per cent iron; a gradual rise through the Fe_3O_4 layer to around 72.6 per cent iron; another sudden rise at the Fe_3O_4-FeO boundary to 75.6 per cent iron which represents FeO saturated with oxygen; finally a gradual rise to 76.9 per cent iron, which is the composition of FeO, containing a little extra oxygen in solution, that is in equilibrium with iron at 1050° C. This inner FeO layer consists of one phase while at the temperature of scaling, but on cooling the solubility of the excess oxygen decreases with the consequent separation of crystals of magnetite which constitute the bright areas in this layer in the picture of Fig. 7.

Now, imagine a surface of iron exposed instantly to air at, say, 1050° C (1925° F). The first small amount of oxygen combining with the iron dissolves in the surface layer, but almost immediately a layer of FeO forms which grows by taking up more oxygen at its outside, and iron at its inside, surface. As this FeO layer grows thicker, oxygen diffuses in more slowly from the surface in contact with the atmosphere, and the oxygen concentration at the surface rises to the saturation value for oxygen in FeO. A layer of Fe_3O_4 then begins to form, which (always assuming that excess oxygen at a pressure above that of the dissociation pressure of Fe_2O_3 is supplied to the surface) becomes saturated with oxygen at its outside surface, where it oxidizes further to form a skin of Fe_2O_3. As soon as this outer skin has absorbed oxygen up to saturation the complete series of possible scale layers is formed and from this time on the *boundary conditions* in the scale are practically fixed at 69.9 per cent iron at the outside, and about 76.9 per cent iron at the inside, surface of the scale.

These remarks are in accord with the deductions regarding values of the oxygen pressure in Tables 7 and 8 above. From these tables it is observed that the values of the pressure of oxygen for the different reactions for $T = 1200°$ K are as follows:

$$\mathrm{FeO{:}\,Fe},\ 7.1 \cdot 10^{-14}\ \mathrm{mm}\ (\text{corresponding to } \Delta F_1),$$

$$\mathrm{Fe_3O_4{:}\,FeO},\ 1.9 \cdot 10^{-12}\ \mathrm{mm}\ (\text{corresponding to } \Delta F_2),$$

and

$$\mathrm{Fe_2O_3{:}\,Fe_3O_4},\ 4.6 \cdot 10^{-11}\ \mathrm{mm}\ (\text{corresponding to } \Delta F_3),$$

From equation 1.11, which relates the value of P (O_2) with that of ΔF, it follows that

$$-\Delta F_1 > -\Delta F_2 > -\Delta F_3;$$

that is, the stability of the oxides decreases as we pass from FeO to Fe_3O_4.

With regard to alloys of iron, Heindlhofer and Larsen state that

Nickel up to 35 per cent or aluminum up to around 5 to 7 per cent reduces scaling only moderately, to perhaps around one-half to one-third of the amount for pure iron, with the square root of time relationship approximately followed. Aluminum above 12 to 14 per cent cuts the scaling rate down to a magnitude of $\frac{1}{100}$ of that for pure iron, and a 27 per cent chromium-iron alloy is nearly as effectively protected against scale growth at temperatures up to above 1200° C as these high-aluminum alloys.

E. A. Gulbransen[83] has also studied the rate of oxidation of iron by means of a vacuum microbalance which he devised for this purpose and which had a sensitivity of about $1 \cdot 10^{-6}$ g. The observations were carried out in the range 25° C to 400° C and at pressures of oxygen varying from about 8 mm to about 15 cm. In agreement with other investigators, Gulbransen found that the rate was not affected to any considerable extent over this range of pressures. He did, however, observe that the rate of oxidation could be represented more satisfactorily by a modification of equation 3 of the form

$$W^2 = k_2 t + k_3, \tag{6}$$

where k_3 is a constant which corresponds to a very rapid initial oxidation that precedes the diffusion process.

The samples of iron (99.95 per cent Fe) used by Gulbransen had a thickness of 0.13 mm and total surface area of 14.5 cm^2, were annealed in hydrogen at 875° C, placed in a chamber which could be evacuated to 10^{-5} mm, and degassed at 700° C before oxygen was admitted at the desired pressure.

The initial gain in weight (in 10^{-6} g $\cdot$ cm^{-2}) for $t = 0$ (approximately) was observed to increase with temperature of oxidation as follows:

25° C	2–3
100	4–6
200	10
300	20–40
400	50–100

These values are approximate, and the lowest value for any given temperature corresponds, in most cases, to that observed at 8.0 mm, while the higher value was observed at 8.2 or 15.2 cm pressure (air at 1 atm).

After this preliminary oxidation the rate of oxidation was observed to follow the parabolic law, in accordance with equation 6.

With regard to the oxidation at 25° C, Gulbransen makes the following remarks:

> The experiments add further evidence to the large body of knowledge concerning the presence of oxygen films on metals at room temperature. The films form very rapidly on clean and degassed surfaces with only slight increase in weight after the

---

[83] *Trans. Electrochem. Soc.*, 81, 327 (1942).

first few minutes of oxidation. The films appear stable to evacuation (to 10^{-5} mm) and further addition of oxygen at 25° C.

Assuming that the adsorption is due to the beginning of a Fe_3O_4 lattice, the film thickness formed after 6 minutes' oxidation at room temperature is between 2 Å and 15 Å thick.

Using the microbalance technique, Gulbransèn has studied the formation and stability of oxide films on iron, stainless steel, and chrome iron.[84]

The equilibrium oxygen pressure over Fe_2O_3 (solid) and Cr_2O_3 (solid) as calculated by him are shown in Fig. 3, while Fig. 4 shows values of the equilibrium pressure ratio $(H_2O)/(H_2)$ over these oxides.[85] As Gulbransen points out,

> It is of interest to note that at temperatures below 1000° C the oxides are stable to the best vacua obtainable today. Also, the reaction of water vapor with chromium is favorable over the complete temperature range, but with iron, only at low temperatures. The reduction of Fe_2O_3 (solid) is feasible even at low temperatures. Cr_2O_3 (solid) reduction is extremely unfavorable except at the highest temperatures.

These remarks are in accord with the conclusions stated in sections 5 and 7 above.

Some of the observations made in this investigation are the following:

A film formed at room temperature in oxygen at 0.76 micron, corresponding to an oxygen gain of $0.22 \cdot 10^{-6}$ g · cm^{-2} (theoretical thickness of 15 Å), was found to be stable to a vacuum of $5 \cdot 10^{-3}$ micron and to a temperature of 600° C. This film was readily reduced by hydrogen at 600° C.

Films formed on iron at 800° C and at pressures as low as 3.5 microns and 0.25 micron oxygen were observed to be stable to pressures as low as $5 \cdot 10^{-3}$ micron.

Even in a vacuum of $5 \cdot 10^{-3}$ micron a sample of high-chrome iron was observed to increase in weight when heated at 600° C, thus confirming the conclusion, based on free-energy considerations, of the stability of Cr_2O_3. In fact it is extremely difficult to obtain a good enough vacuum in which chromium will not oxidize.

Plots of W^2 versus t for the oxidation of pure iron (at 300° C), chrome iron, and stainless steel (at 650° C) showed that the oxidation rates approach the parabolic law after an initial period, in accordance with equation 6.

In a still more recent paper[86] Gulbransen has discussed his observation on rates of oxidation from the point of view of the transition state theory of reaction rates developed by H. Eyring and associates.[87] This theory leads to the following relation for the rate constant:

---

[84] *Trans. Electrochem. Soc.*, **82**, 375 (1942). This paper gives a bibliography of papers dealing with the different methods that have been used to investigate the thickness and structure of adsorbed oxygen films on metals.

[85] These plots correspond to the data in Tables 8 and 11, respectively.

[86] *Trans. Electrochem. Soc.*, **83**, 301 (1943).

$$\log k_2 = \log (k_0T) + 2 \log \lambda - \frac{\Delta S}{4.574} - \frac{E_A}{4.574T}, \qquad (7)$$

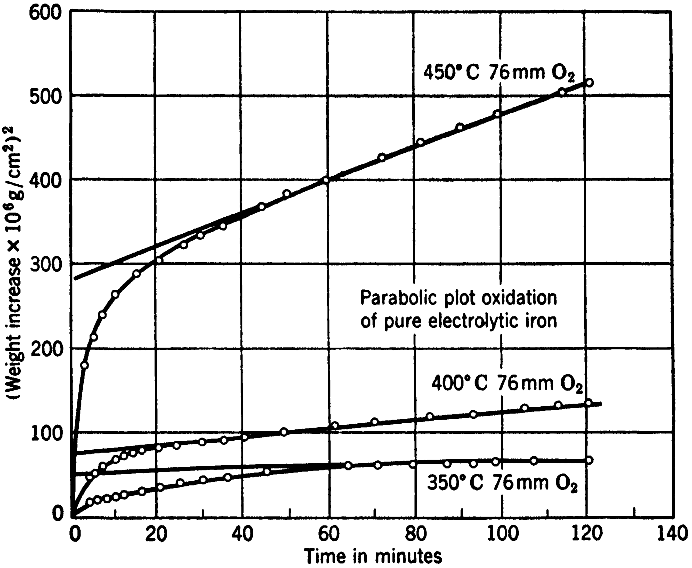

FIG. 8. Illustrating parabolic law for oxidation of pure electrolytic iron (Gulbransen).

where $k_0 = k/h$ (k = Boltzmann constant, h = Planck constant), λ denotes a length of the order of interatomic distances, ΔS = change in entropy, and E_A = activation energy. Thus $k_0\lambda^2T$ has the dimensions of a diffusion constant (D).

Rates of oxidation were determined at a series of temperatures and 76 mm of oxygen for samples of pure electrolytic iron, stainless steel, and copper. Figures 8 and 9 show parabolic plots of W^2 (W expressed in 10^6 g · cm^{-2}) versus t for electrolytic iron and stainless steel, respectively. From these plots, the values of k_2, E_A (cal/mole) ΔS (cal/° C), were calculated that are shown in Table 21. The values of ΔS were calculated by means of values of $D = k_0\lambda^2$, which were derived by application of certain theoretical relations deduced by N. F. Mott.[88] The values of D are given in the last column of the table.

---

[87] See the treatise by S. Glasstone, K. J. Laidler, and H. Eyring, *The Theory of Rate Processes*, McGraw-Hill Book Company, New York, 1941.

[88] *Trans. Faraday Soc.*, **36**, 472 (1940).

It will be observed that in these experiments the values of the temperature for comparable values of k_2 were lowest for copper, much higher for iron, and still higher for stainless steel, thus indicating that the last metal is less readily oxidized than iron and this in turn is far less readily oxidized than copper.

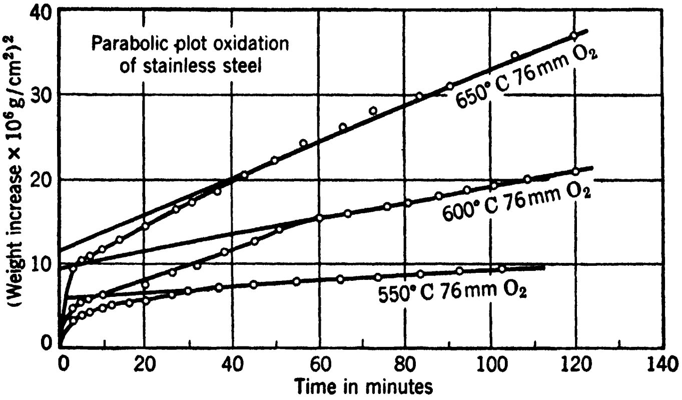

FIG. 9. Illustrating parabolic law for oxidation of stainless steel (Gulbransen).

The interesting feature in these data, from a theoretical point of view, is the negative value for the entropy change. This would seem to indicate that oxidation is accompanied by a *more ordered* arrangement in the system. In this respect, these results are similar to those observed for the sign of ΔS in experiments by the writer on creep in metals.[89]

TABLE 21

RATE CONSTANTS, ACTIVATION ENERGIES, ENTROPIES, AND DIFFUSION CONSTANTS FOR OXIDATION OF METALS

Metal	P_{mm} (O_2)	t° C	$10^{15}k_2$	E_A	ΔS	D (cm$^2\cdot$sec^{-1})
Iron	76	350	2.63	22,600	−31.2	$3.70\cdot10^{-9}$
		400	8.98	22,600	−31.6	$3.35\cdot10^{-9}$
		450	33.4	22,600	−31.6	$3.66\cdot10^{-9}$
Stainless steel	76	550	0.55	29,600	−35.2	$0.66\cdot10^{-9}$
		600	1.7	29,600	−35.6	$0.68\cdot10^{-9}$
		650	3.52	29,600	−35.6	$0.60\cdot10^{-9}$
Copper	152	139	2.86	24,900	−6.6	$4.65\cdot10^{-4}$
(preliminary)		169	23.4	24,900	−6.8	$5.44\cdot10^{-4}$

---

[89] *J. Applied Phys.*, **15**, 108 (1944).

The oxidation of iron at high temperatures by CO_2, NO, SO_2, O_2, and water vapor has been investigated by K. Fischbeck, L. Neundenbel, and F. Salzer.[90] Only for oxidation by moist carbon dioxide was the parabolic relation confirmed. In the other reactions secondary effects led to deviations from this relation. Plots of log (dW/dt) versus $1/T$ for the initial rates of oxidation were observed to be linear for the α-iron range of temperatures, with an abrupt decrease in the α-γ range.

Stainless steels[91] are especially oxidation-resistant alloys containing from 3.75 to 28 per cent chromium; some of the high-chromium alloys contain, in addition, from 6.00 to 25.00 per cent nickel.

The high-temperature oxidation of two such alloys has been investigated by H. M. McCullough.[92] The alloys, designated as types 304 and 410, have the following chemical compositions:

PER CENT	TYPE 304	TYPE 410
Carbon	0.037	0.081
Manganese	1.23	0.43
Phosphorus	0.019	0.013
Sulfur	0.010	0.012
Silicon	0.45	0.38
Nickel	9.01	—
Chromium	18.19	12.70

Figure 10 shows plots of oxidation tests at 1800° F (982° C) and variable oxygen concentrations. The ordinates, W, correspond to the total weight gain in grams/square inch in 6 hours, and the abscissas, C, correspond to the per cent oxygen concentration. It is of interest to observe that these data can be represented by the empirical relations:

$$W = k'C^{0.38} \text{ for type 410,}$$

and

$$W = k'C^{0.55} \text{ for type 304,} \quad \text{where } k' \text{ is a constant.}$$

Also a plot of log W versus $1/T$ yields a straight line, thus indicating that the amount of oxidation increases with temperature in a manner similar to that expressed in equation 4 above. This plot shows that

---

[90] *Z. Elektrochem.*, **40**, 517 (1934).

[91] See discussion of these alloys by O. K. Parmiter in *Metals Handbook*, 1939 Edition, pp. 533–543.

[92] *Engineering Experiment Station News*, **19**, No. 5, p. 38 (1947). This preliminary report of the results obtained has been supplemented by information in a private communication for which the writer is indebted to Mr. McCullough, who has carried out this investigation as a Research Fellow, under the direction of Dr. M. G. Fontana, on a contract between the Office of Naval Research and the Ohio State Research Foundation.

"both steels could be used in an oxygen atmosphere up to 20 per cent and 1600° F (871° C) satisfactorily."

In view of the results obtained by Heindlhofer and Larsen, which were discussed above, it is of interest to describe some of the observations reported by McCullough on the nature of the oxidation layer.

> The properties [he states] of oxides formed in a low oxygen concentration are much different than those formed in a high oxygen concentration. Specimens which were treated for 2 hr in a 2 per cent oxygen atmosphere followed by a treatment for 6 hr in a 20 per cent oxygen atmosphere showed a smaller weight gain for the over-all 8-hr period than the specimens treated for 6 hr in the straight 20 per cent oxygen atmosphere. This smaller weight gain indicates that at the lower concentrations a more compact protective oxide is formed which resists the more severe attack at higher concentrations.

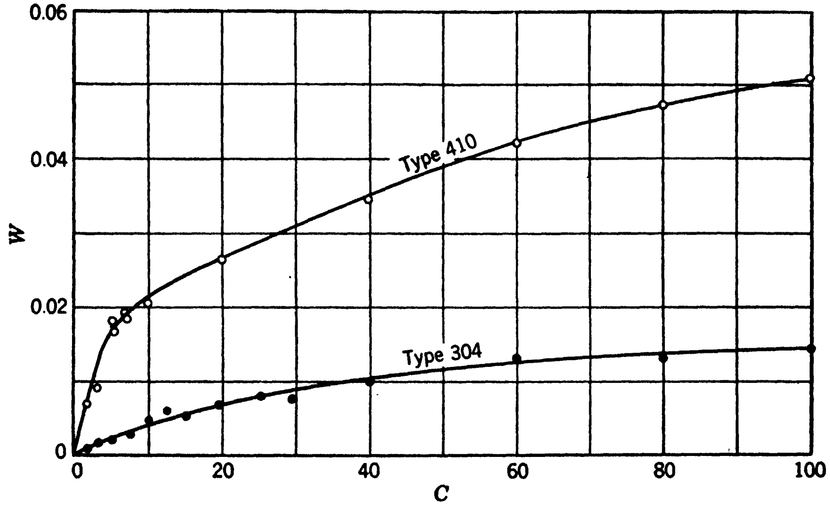

FIG. 10. Oxidation tests on types 304 and 410 stainless steel at 982° C. Weight increase in grams/sq in. in 6 hours (*W*) plotted versus per cent oxygen concentration (*C*) (McCullough).

Type 410 specimens were heated at 1149° C in 3, 20, and 95 per cent oxygen atmospheres for 6 hr to produce heavy oxide layers which could be separated from the metal. Table 22 shows a chemical analysis of the layers formed, at each concentration of oxygen, by this treatment.

> This chemical analysis shows that the compact protective oxide formed at the low oxygen concentrations is of the chrome spinel type and the porous unprotective oxide formed at the high oxygen concentrations is more of the Fe_2O_3 type. . . . These tests demonstrate that chromium in this type of steel is the main benefactor in the resistance to high-temperature oxidation.

TABLE 22

CHEMICAL ANALYSIS OF LAYERS FORMED ON TYPE 310 AT 2100° F (1149° C)

	Outside Layer Oxygen Concentration (%)			Inside Layer Oxygen Concentration (%)		
Composition	3.0	20.0	95.0	3.0	20.0	95.0
Metallic iron	0.13	0.26	0.16	0.48	0.38	0.31
FeO	——	——	——	1.31	6.35	0.74
Fe_2O_3	75.83	78.16	77.76	12.38	3.01	8.83
Fe_3O_4	3.78	0.93	19.48	——	——	——
$FeO{\cdot}Cr_2O_3$	16.62	19.31	1.86	84.74	91.00	87.25

12. LOGARITHMIC LAW OF RATES OF OXIDATION

In 1922, G. Tammann[93] proposed a relation for rate of oxidation of the form

$$W = k_4 \log (at + 1), \tag{1}$$

where k_4 and a are constants for any given temperature.

This relation has been found to be in agreement with observations on the oxidation of zinc by W. H. J. Vernon, E. I. Akeroyd, and E. G. Stroud.[94] The experiments were carried out with samples of very pure metal (99.947 per cent zinc) in air, over the range 25–400° C. The specimens used were in the hard (as-rolled) and annealed conditions, and were furthermore given an abrasion treatment or etched.

Figure 11 shows "straight plots" (W versus t) of experiments with abraded specimens in either annealed or as-rolled conditions. In these plots W denotes the increase in weight in *milligrams per 100 cm²* during the period t in *hours*.

From the form of equation 1 it is seen that, for $at \gg 1$, this equation approximates the relation

$$W = k_5 \log a + k_5 \log t. \tag{2}$$

Hence a plot of W versus $\log t$ should become linear for large values of t. Such linear plots were actually obtained for the observed values of W, whereas the plots of W^2 versus t were parabolic instead of linear. From the plots of W versus $\log t$ it was possible to derive values of a and k_5, and Fig. 12 shows a series of plots of W versus $\log (at + 1)$, thus deduced, for abraded specimens, in the range 275° C to 400° C, and for comparison the experimentally observed points.

---

[93] *Z. anorg. Chem.*, **124**, 25 (1922), **169**, 42 (1928); Tammann and W. Köster, *Z. anorg. Chem.*, **123**, 196 (1922).

[94] *J. Inst. Metals*, **65**, 301 (1939).

For temperatures above 225° C, the logarithmic law was found to be in very good agreement with the experimentally observed values of W and t; for temperatures below 225° C, the agreement was not so good.

Regarding the effects of temperature and of surface conditions, the investigators have made the following statement:

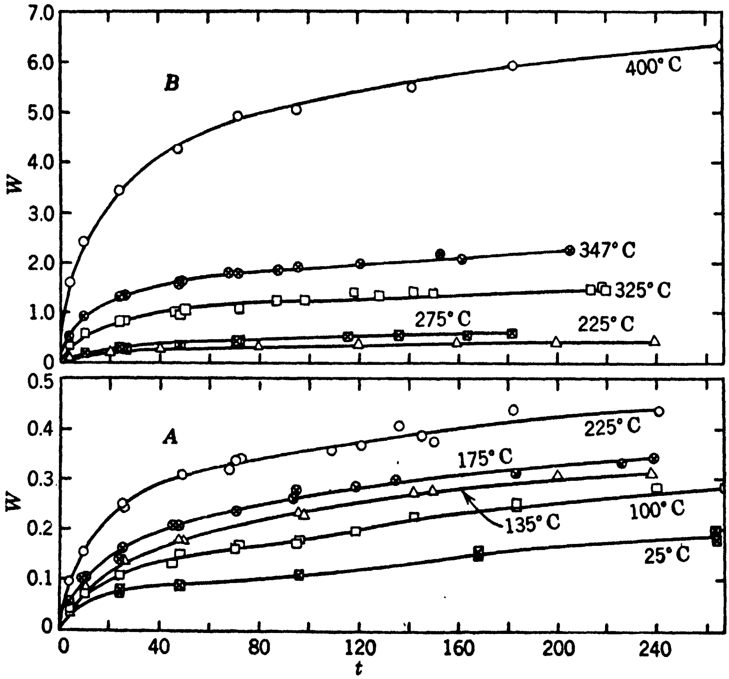

FIG. 11. Plots of weight increase in milligrams per 100 cm^2 (W) versus time in hours (t) for oxidation of abraded specimens of pure zinc. Curves A at 25° C to 225° C; curves B at 225° C to 400° C. (Points refer indiscriminately to specimens in either annealed or as-rolled conditions) (Vernon, Akeroyd, and Stroud.)

The relationship between oxidation and temperature above 225° C is represented by the equation:

$$\frac{d \ln W}{dT} = -\frac{Q}{R_0 T^2}, \tag{3}$$

a straight line (of identical slope and differing only slightly quantitatively for etched and abraded specimens) being obtained when logarithms of weight increments after an arbitrary time are plotted against reciprocals of absolute temperature. Below 225° C the relationship depends remarkably upon surface conditions.

A theory to account for both the logarithmic law and the parabolic law has been suggested by N. F. Mott.[95] Since this theory is intimately related to that of Wagner, it will be duscussed in the following section.

A. L. Dighton and H. A. Miley[96] found that in the oxidation of abraded copper surfaces in the range 180° C to 288° C the rate follows the parabolic law until a certain thickness (varying from 3000 Å to 9000 Å is built up and then changes to the logarithmic law.

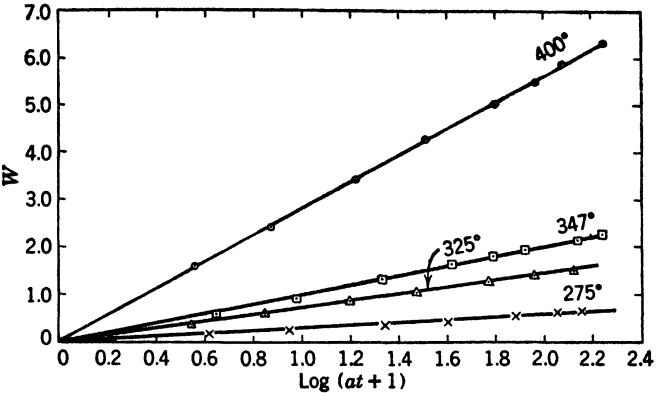

FIG. 12. Plots of W versus log $(at+1)$ for observations plotted in curves B in Fig. 11. Straight lines correspond to the equation $W = k \log (at + 1)$. Plotted points are experimental values (Vernon, Akeroyd, and Stroud).

A. H. White and L. H. Germer[97] used electron diffraction technique to measure the rate of oxidation of thin copper films in pure dry oxygen at room temperature and 20 mm pressure. They found that the thickness (x) of the oxide coating increases according to the logarithmic equation

$$x = 4 + 6.5 \log t, \tag{4}$$

where t is measured in minutes and is greater than 2, and x is measured in angstrom units. This leads to a limiting thickness of about 50 Å in one year.

According to B. Lustman,[98] who has reviewed the experimental results obtained by different investigators on rates of formation of thin oxide films, and has compared these with results on rate of growth of thick films, the two processes of film formation are "essentially different with respect to time and temperature effect on rate of formation." As is evident from the previous remarks in this section, the logarithmic law applies to some cases and the parabolic law to others. Lustman has suggested that probably a diffusional mechanism alone does not control the rate of growth of thick films.

---

[95] *Trans. Faraday Soc.*, **36**, 472 (1940).

[96] *Trans. Electrochem. Soc.*, **81**, 321 (1942).

[97] *Trans. Electrochem. Soc.*, **81**, 305 (1942).

[98] *Trans. Electrochem. Soc.*, **81**, 359 (1942).

On the other hand, according to U. R. Evans,[99]

> The logarithmic law occurs when the conditions needed for parabolic thickening are absent (e.g., on zinc), and is believed to be due to the outward passage of interstitial matter through flaw paths or zones of loose structure in the outer part of the oxide film; the actual rate of passage along a given path is regulated by the rate of crossing a less pervious inner film of constant thickness and is independent of the thickness of the outer film. If such an obstruction occurs, however, passage along the path in question becomes impossible, and clearly the chance of obstruction of a given path will increase with the film thickness. It can be shown that the growth rate will fall off with film thickness in accordance with the logarithmic law.
>
> Where a film, like that on aluminum, possesses a highly protective character (connected with its ideal composition and high electrical resistance), the formation of discrete cracks becomes an important factor in film growth. Such cracking occurs in films on other metals.

13. IONIC THEORY OF RATES OF OXIDATION

In all the preceding discussion it has been assumed that rate of oxidation is controlled by rate of diffusion of molecules of the oxidizing atmosphere through the oxide layer. C. Wagner[100] has given a quantitative explanation of the rate of growth of oxide films in which it is shown that the governing factor is the *mobility of positively charged ions* (such as Cu^+, Fe^+, etc.) *through the film lattice towards the oxide-gas surface.*[101]

On the basis of this theory, C. Wagner and K. Grünewald[102] deduced an equation for the rate of oxidation, which is a modification of equation 11.3 and has the form

$$W^2 + k_4W = k_2t. \tag{1}$$

Furthermore according to Wagner the constant k_2 in this equation may be calculated from the transport numbers of the ions and electrons, the electrical conductivity, and the free energy of formation of the oxide.

---

[99] *Trans. Electrochem. Soc.*, **83**, 335 (1943).

[100] *Z. physik. Chem.*, **B**, **21**, 25 (1933), and subsequent papers in the same journal by Wagner and coworkers.

[101] Reviews of Wagner's theory are contained in the following publications: W. Jost, *Diffusion und chemische Reaktion in festen Stoffen*, Theodor Steinkopff, Dresden and Leipzig, 1937; T. P. Hoar and L. E. Price, *Trans. Faraday Soc.*, **34**, 867 (1938); L. E. Price, *Chem. Ind.*, **56**, 796 (1937); N. F. Mott and R. W. Gurney, *Electronic Processes in Ionic Crystals*, Clarendon Press, Oxford, 1940, Chapter VIII.

[102] *Z. physik. Chem.*, **B**, **40**, 455 (1938).

The mechanism of the reactions involved in the oxidation of copper to Cu_2O may best be understood by means of the following quotation from a paper by Wagner and H. Hammen.[103]

> An oxygen molecule from the gas phase combines with four electrons from inside the Cu_2O phase, to form two oxygen ions ($O^{=}$) at the surface. Simultaneously four copper ions (Cu^+) migrate to the surface from the oxide phase and these metal ions combine with the oxygen ions to form an extension, towards the outside, of the Cu_2O lattice. Thus for every oxygen molecule taken up we find four vacancies previously occupied by Cu^+ ions and four other vacancies previously occupied by electrons.

Let us designate a Cu^+ ion vacancy by Cu_v^+ and a place in the lattice occupied by a Cu^+ ion by Cu_l^+, and similarly, by e_l^- and e_v^-, spaces filled by electrons and vacated by electrons, respectively. Then the reaction which occurs in the oxidation of copper may be written in the symbolic form

$$O_2\ (g) + 4e_l^- = 2O_l^= + 4Cu_v^+ + 4e_v^-.$$

Evidently the concentrations (designated in the following remarks by square brackets) of ions and electrons must be equal. Denoting these by $[y]$, it follows from the mass law that

$$[y]^8 = \text{constant}\ P;$$

that is,

$$[y] = KP^{1/8}, \tag{2}$$

where P denotes the *pressure of oxygen* in the gas phase.

This relation gives an interpretation of the observation that the electrical conductivity of Cu_2O actually varies as the seventh root of the pressure, and indicates that in the Cu_2O lattice there is a deficiency in Cu^+ ions as compared with the stoichiometric formula; that is, there is an excess of oxygen in the lattice. Since the concentration of vacancies $[Cu_v^+]$ increases with the pressure, it also follows that in the Cu_2O lattice $[Cu_v^+]$ is greatest at the oxide-gas surface and least at the metal-oxide interface. As a result there is a migration of vacancies from the outside to the surface of the metal, or, what is equivalent, a migration of Cu^+ from the metal outwards to the oxide-gas boundary. Furthermore the rate of migration must increase with the pressure.

A calculation by Wagner and Grünewald[104] of the rate constant, k_2, shows that, in the range of pressures of oxygen 0.228 to 63.1 mm of mercury, the calculated value is in reasonably good agreement with that observed.

In the case of zinc oxide, the electrical conductivity *decreases with in-*

---

[103] *Z. physik. Chem.*, **B**, **40**, 197 (1938).

[104] *Loc. cit.*

crease in pressure of oxygen. This indicates that, in the ZnO lattice, there is a *deficiency* of *oxygen ions*, or excess, over the stoichiometric relation, of Zn^{++} ions. Consequently the concentration of Zn^{++} ions is lowest at the surface oxide-gas, and highest at the surface metal-oxide. Increasing the pressure of oxygen while depressing the concentration of Zn^{++} at the outer surface of the oxide cannot seriously affect the concentration gradient of Zn^{++} ions through the film. Hence it would be expected that the constant k_2 would not be altered sensibly by varying the pressure of oxygen. Wagner and Grünewald actually observed that a fiftyfold decrease in pressure had no effect on the rate of oxidation.

The oxidation of nickel to NiO is similar to that of copper to Cu_2O. The conductivity increases with increase in pressure of oxygen, and Wagner and Grünewald calculated that the rate constant k_2 should vary as $P^{1/6}$. Observations by the same investigators showed an increase in k_2 with pressure which was, at least qualitatively, in agreement with this conclusion.

Experimental evidence for the actual motion of metal ions towards the gas-oxide surface has been obtained by L. B. Pfeil[105] in the oxidation of iron and by Wagner[106] in the formation of Ag_2S.

For continuous growth of the oxide film it is necessary that electrons as well as metal ions shall pass through the oxide to the outer surface. N. F. Mott[107] has discussed the different mechanisms by which the electrons can be transmitted into and through the oxide layer. The rate of migration depends upon the ratio between the "work function" for emission of electrons, ϕ, from the metal and the energy E required to bring a positive ion from the metal to an interstitial position in the oxide.

Mott has shown that, for $\phi > E$, the rate of growth of the film should follow a logarithmic law, while for $\phi < E$ the parabolic law should apply.[108]

[105] *J. Iron Steel Inst., London,* **119,** 501 (1929); **123,** 237 (1931).

[106] *Z. physik. Chem.,* **B, 21,** 37 (1933).

[107] *Trans. Faraday Soc.,* **36,** 472 (1940).

[108] The discussion in this section has touched only briefly on a topic which has received attention from a large number of investigators. Further references are to be found in a number of papers in *Trans. Electrochem. Soc.,* **81,** 305–413 (1942), and in the different references cited above.

NOTE

Significance of the designations for reference books is explained on the pages indicated:

CC, 1
CS, 547
EHK, 1
FM, 48
JG, 387
JHJ, 1
JY, 94
LBL, 1
LD, 67
LH, 781
McB, 387
RB, 111
RH, 781
SB, 387

NAME INDEX

Abbott, T. A., 377
Adam, N. K., 416
Adzumi, H., 118
Agte, C., 830
Akeroyd, E. I., 849, 850, 851
Alexander, P., 159, 165, 206, 208, 209, 210, 213, 214
Alleman, G., 626, 633
Allen, F. J., 782
Allen, H. S., 451
Allen, N. P., 563, 605, 645, 646, 809
Allmand, A. J., 396, 486
Altherthum, H., 697, 698
Anderson, J. S., 752
Anderson, P. A., 247, 249, 733, 734, 735, 736, 739
Anderson, R. B., 430, 486, 487
Anderson, W. A., 642
Andrade, E. N. da C., 205
Andrew, J. H., 445
Andrews, D. H., 445
Andrews, M. R., 286, 358, 514, 607, 630, 634, 659, 680, 681, 683, 684, 685, 686, 687, 706, 710, 715
Angerer, E. V., 295
Anhorn, V. J., 258, 264
Antropoff, A., 415
Apker, L., 359, 737, 738, 739
Archbutt, S. L., 646
Archer, C. T., 45
Armbruster, M. H., 269, 394, 398, 407, 412, 421, 422, 434, 437, 438, 449, 554, 556, 557, 558, 559, 560, 561, 562
Arner, L. H., 647
Aten, A. H. W., Jr., 531
Austin, J. B., 398, 412, 421, 422, 438, 449, 811, 823
Avogadro, 3
Azarian, G. J., 569

Backhurst, I., 192
Bacon, J., 659
Bagley, G. D., 174
Baker, W. C., 189
Baly, E. C. C., 786
Balz, O., 812, 814, 818, 820
Bancroft, F. E., 230
Bangham, D. H., 452
Bardeen, J., 73
Barker, M. E., 471
Barkhausen, H., 340
Barr, W. E., 258, 264
Barratt, S., 777
Barrer, R. M., 111, 421, 453, 503, 504, 505, 507, 508, 531, 535, 536, 547, 552, 609, 610, 620, 623
Bartholomeyczyk, W., 316
Barton, E. H., 137
Basch, R., 36
Baukloh, W., 554, 567
Baule, B., 40
Baur, E., 752
Bayushkina, K. S., 820
Beams, J. W., 290
Becker, J. A., 226, 247, 329, 404
Becker, K., 830
Beckwith, J. B., 463
Bedworth, R. E., 835, 836, 837
Beebe, R. A., 461, 464
Beeck, O., 453
Bell, J., 217
Benton, A. F., 396, 413, 549, 550, 593, 803
Berenyi, L., 432, 433
Bergner, E., 574, 586, 587, 605
Berl, E., 784
Bessel-Hagen, E., 137
Bessey, W. H., 27
Best, N. R., 15
Bever, M. B., 564, 566
Bielz, F., 26
Bircumshaw, L. L., 555, 569
Birge, R. T., 3
Bleakney, W., 352
Blears, J., 168, 250, 251, 252, 253, 356, 357

Blewett, J. P., 701, 778
Blodgett, K. B., 54, 60, 480
Blythswood, Lord, 451
Bodenstein, M., 273
Bohr, N., 689
Boltzmann, L., 3, 9, 845
Boomer, E. H., 694
Borelius, G., 610, 616, 617
Born, M., 26
Bowden, F. P., 454
Bowie, R. M., 342, 343, 361
Boyle, R. A., 254
Braaten, E. O., 535, 610, 614
Bradley, R. S., 437
Bramley, A., 72, 623
Brantley, L. R., 831, 832
Braun, H., 555, 569
Braune, H., 36
Bray, R. I., 460
Brewer, A. K., 72
Brewer, L., 743, 744, 752, 753, 754, 755, 831
Briesemeister, S., 646
Briggs, H., 470, 471
Briggs, L. J., 508, 509
Bright, H. C., 650
Brode, R B., 352
Brodetsky, S., 691, 696
Brody, E., 809
Bromley, Le Roy, 831
Brower, T. E., 619, 639
Brown, Boveri and Company, 332
Brown, G. P., 117, 255, 256, 257
Brown, J. R. C., 461, 496
Brüche, E., 286, 310, 311
Brüning, H., 575, 579, 589, 598, 599
Brüning, K., 555, 568
Bruining, H., 531
Brunauer, S., 42, 44, 387, 398, 399, 409, 413, 415, 421, 424, 425, 426, 427, 428, 431, 432, 433, 436, 446, 447, 448, 449, 450, 453, 454, 456, 457, 458, 460, 461, 465, 475, 476, 479, 500, 501, 528, 832
Bruner, M., 272
Bruner, R., 752
Bruns, R., 471
Bryan, G. B., 708
Buckley, O. E., 333
Bunsen, R. W., 508, 509
Bunting, E. N., 524
Burch, C. R., 127, 218, 223
Burger, H. C., 316
Burmeister, E., 771, 772, 773
Burrage, L. J., 396
Burrows, G., 221, 260, 263
Burt, F. P., 452
Burt, R., 535
Byck, H. T., 198, 199, 228

Caldwell, W. C., 761, 762
Campbell, N. R., 320, 321, 650, 710, 711, 712, 713, 714, 715, 722, 723, 726
Campbell-Swinton, A. A., 692
Carlisle, P. J., 829
Cartwright, C. H., 521, 522, 523, 758, 760
Carver, E. K., 262
Central Scientific Company, 141, 215
Chaney, N. K., 467, 468, 469, 470
Chaplin, R., 396
Chapman, S., 1, 27, 30, 32, 33, 41, 45, 67, 68, 70, 71, 74
Chaston, J. C., 646
Chaudron, G., 628, 630
Cheng, G. K., 117
Chipman, J., 597, 606, 798, 811, 813, 821
Chrisler, V. L., 691, 695
Clark, G. F., 535, 610, 613
Clark, R. E. D., 434, 509
Clark, R. J., 271
Claude, G., 466, 488, 491, 492, 493
Claus, W., 646
Clausing, P., 90, 96, 98, 99, 100, 101, 102, 166, 167, 453
Clough, J. H., 657
Clusius, K., 68, 71
Cobine, J. D., 11, 333
Compton, K. T., 351, 352, 353
Coolidge, A. S., 269, 286, 482, 483, 484, 485, 499, 500
Coons, C. E., 276
Copley, M. J., 168, 202, 203, 230, 231, 341
Cowling, T. G., 1, 28, 30, 32, 33, 41, 45, 68, 71
Crawford, W. W., 190, 202, 245
Crenshaw, J. L., 828
Crigler, E., 445
Crittenden, E. C., Jr., 762, 763
Crookes, W., 126, 293
Czochralski, J., 555, 569

Dalton, R. H., 524, 525, 648
Daly, M., 494, 595
Danner, P. S., 670
Danz, W., 577
Darlington, C. J., 626, 633
Day, M. J., 811, 823
Daynes, H. A., 45, 48
Dayton, B. B., 131, 166, 167, 168, 221, 222
De Boer, J. H., 600, 670
De Graaf, J. E., 666, 667, 668
DeGroat, C. T., 193, 250
Deitz, V. R., 276, 465
Deming, H. G., 610
DeVore, H. B., 759
Dewar, J., 293, 440, 466, 488, 491, 493
DeWitt, T., 460
Dickel, G., 68, 71
Dickens, B. G., 45, 48, 49, 54, 57
Dickinson, R. G., 653
Dighton, A. L., 851
DiNardo, A., 117
DiPietro, W. O., 653
Distillation Products, Inc., 127, 131, 218, 220, 221, 222, 233, 234, 235, 236, 237, 342, 792
Ditchburn, R. W., 741, 743, 752, 754
Dodge, B. F., 786, 787, 788
Dootson, F. W., 68
Dornte, R. W., 741, 752
Dorsey, F. M., 467, 495
Doughty, E. G., 379
Douglas, R. W., 525
Dow, W. G., 700
Downing, J. R., 161, 347
Drake, L. C., 803
Dryer, W. P., 117
DuMond, J. W. M., 301, 302, 367, 368
Dunbar, A. K., 786, 787, 788
Dunlap, G. C., 317
Dunn, J. S., 839
Dunnill, S., 470
Dunoyer, L., 67, 151, 154, 169, 270, 271
Durand, E., 15
Durau, F., 528, 548
Dushman, S., 154, 191, 258, 291, 334, 336, 348, 349, 350, 352, 353, 356, 376, 515, 544, 595, 625, 632, 655, 658, 680, 689, 700, 703, 706, 717, 731, 732, 846
Dux, W., 273

Eccles, W. H., 708
Edwards, C. A., 607
Edwards, H. W., 230, 759
Edwards, W., and Co., 271
Egerton, A. C., 22
Ehrke, L. F., 656, 663, 664, 665, 666, 668, 671
Eichner, C., 610, 614
Eitel-McCullough, 239
Eklund, S., 159
Ellett, A., 166, 324, 342
Elliott Company, 169, 171, 173
Ellis, O. W., 645
Eltenton, G. C., 159, 162
Embree, N. D., 221, 222, 245, 277
Emmett, P. H., 44, 424, 428, 456, 457, 458, 460, 461, 463, 475, 476, 479, 486, 487, 500, 529, 811, 832
Encyclopædia Britannica, 137, 138, 139, 154, 205
Enringer, G., 621, 623
Enskog, D., 30, 68, 74
Ephraim, F., 830
Epremian, E., 569
Erickson, J. L., 570, 647
Esch, U., 766
Espe, W., 791
Estermann, I., 21, 101, 198, 199, 228, 444
Eucken, A., 45, 431, 754
Evans, U. R., 852
Ewald, J., 732
Eyring, H., 409, 845

Farkas, A., 48, 111, 263, 272, 273, 276, 648, 650, 790
Fast, J. D., 600, 670, 671, 672
Favre, P. A., 440, 449
Fehér, F., 264, 819
Ferguson, J. B., 535
Filby, E., 538, 539
Finn, A. N., 524
Firth, J. B., 453, 468, 487, 488, 496
Fischbeck, K., 847
Fischer, E. A., 465
Fischer, J., 752
Fiske, M. D., 700, 752
Flad, M., 820
Fleming, Arthur P., 221, 251
Floe, C. F., 564, 566, 606, 830
Flosdorf, E. W., 269, 271

Fogel, C. M., 344
Fonda, G. R., 79, 80, 81
Fontana, M. G., 847
Foord, S. G., 273, 274
Foote, H. W., 809, 817
Footitt, F. F., 524
Forney, J. D., 687, 688
Foster, A. G., 430
Found, C. G., 334, 336, 349, 352, 353, 356, 359, 687, 688
Fowler, R. H., 409, 589, 590, 591
Fox, K., 653
Francis, M., 270
Frank, H. S., 529
Frankenburg, W. G., 394, 395, 406
Frazer, J. C. W., 269, 529
Frazer, J. H., 529
Frazer, R. G. J., 26, 27
Fredlund, E., 301, 313
Freeman, I. R., 465
Freneau, P., 169, 171, 172, 173
Freundlich, H., 388, 396, 400, 424
Friederich, E., 830, 831
Friesen, S. v., 155
Frumkin, A., 471, 721
Fry, A., 834, 835
Fukusima, M., 554
Furry, W. H., 68, 73

Gaede, W., 39, 90, 110, 126, 137, 138, 139, 151, 152, 154, 176, 178, 179, 180, 182, 184, 191, 204, 213, 249, 270, 309, 310
Gaines, J. M., 601
Gale, D. I., 15
Galstaun, L. S., 575, 579
Garrett, A. B., 752, 754
Gay-Lussac, 66
Gehlhoff, G., 693
General Electric Company, 192, 193, 250, 254
Germer, L. H., 851
Gill, E. W. B., 340
Gilles, P., 831
Gillespie, L. J., 68, 69, 575, 579
Gilmour, J. C., 741, 743, 752, 754
Glasser, J., 341
Glasstone, S., 409, 689, 845
Gleysteen, L. F., 465
Glockler, G., 73
Goes, K., 151
Goetz, A., 354
Gordon, A. R., 800, 801
Gordon, E., 647
Gordon, N. T., 317
Gotta, A., 574, 575
Gowdy, R. C., 693
Grähling, K., 499
Grant, C. K., 700, 752
Green, C. B., 329
Green, R. L., 521
Gregg, S. J., 387, 396, 401, 415, 498, 500
Gregory, H., 45
Grew, K. E., 71
Grigorovici, R., 275
Grimsehl, E., 138
Grogan, J. D., 646
Grube, G., 820
Grünewald, K., 852, 853, 854
Gulbransen, E. A., 813, 814, 821, 836, 840, 843, 844, 846
Guldner, W. G., 672
Gundermann, J., 809
Guntz, M., 670
Gurney, R. W., 852
Gutbier, 593

Haase, G., 267, 268
Haase, Th., 263, 315, 316, 331, 332
Haber, F., 283, 284, 285
Haedrich, 175
Hägg, C., 581, 582, 584
Hagen, C., 267
Hagen, H., 554, 555, 556, 562, 563, 575, 589
Hagenacker, J., 604
Hagenow, C. F., 712, 717
Hagstrum, H. D., 753
Hahner, C., 524
Hale, C. F., 319
Hall, F. P., 575
Hall, M. N. A., 575, 584, 585, 673
Halla, F., 809
Ham, W. R., 536, 610
Hamacher, H. E., 364
Hamaker, H. C., 531, 666, 667, 668
Hamburger, L., 724
Hamlin, M. L., 262
Hammen, H., 853
Hand, P. G. T., 486

Hansley, V. L., 829
Hanson, D., 646
Hara, H., 803
Hargreaves, R., 767, 770
Harkins, W. D., 463, 464
Harmsen, H., 111
Harris, J. E., 517, 518, 519, 521
Harrison, G. O., 262
Harteck, B. P., 273
Harvey, E. N., 465
Hauffe, K., 777, 809
Havens, J. R., 15
Haworth, L. J., 371
Heald, W., 695
Hecker, J. C., 220, 222, 277
Heindlhofer, K., 837, 840, 841, 842, 848
Heller, S., 279
Hendricks, B. C., 610
Hendricks, S. B., 832
Henglein, A., 283
Hennelly, E. F., 323, 778
Henry, D. C., 419, 424, 489
Henry, W., 401, 424
Hering, E., 261
Herty, C. H., Jr., 601
Hertz, G., 111, 177
Herzfeld, K. F., 74, 84, 177
Hessenbruch, W., 627
Heuse, W., 261, 270
Heuser, E., 538
Hewitt, T., 809
Hickey, J. S., 385, 386
Hickman, K. C. D., 23, 127, 165, 218, 219, 220, 223, 224, 225, 227, 230, 232, 236, 244, 245, 247, 249, 263, 277, 355
Hiedemann, E., 699
Hill, S. E., 691, 692, 693
Hincke, W. B., 827, 831, 832
Hipple, J. A., 346, 379, 384
Hittorf, W., 126
Ho, T. L., 180, 200, 201, 202, 229
Hoag, J. B., 360
Hoar, T. P., 852
Hodgson, B., 691, 696
Hogg, J. L., 281
Hogness, T., 535
Hoitsema, C., 594
Holden, R. B., 754
Holley, C. E., 73
Holm, V. C. F., 650
Holstmark, J., 243
Holweck, F., 154
Homerberg, V. O., 830
Homfray, I., 392, 409, 420, 435, 437, 439, 466, 468, 473, 474, 475, 478, 481, 499
Honig, J. M., 463
Honig, R. E., 112
Houtz, C. C., 542, 543, 544
Howard, H. C., 652
Howell, J. W., 680, 716, 721
Huber, H., 574
Hückel, E., 436, 448
Hughes, A. L., 216, 304, 305, 709, 710, 724, 775
Hukawa, S., 672
Hulett, G. A., 481, 485, 803
Hull, A. W., 700
Humphreys, H. R., 246
Hunsmann, W., 326
Hunten, K. W., 216
Huntley, A. G., 595
Huntoon, R. D., 342
Hurd, C. B., 829, 830, 831, 832
Hustrulid, A., 377
Huthsteiner, H., 285, 353, 356, 491, 515, 676, 678, 686, 706, 717, 721, 789

Ibbitson, D. A., 453, 504, 505, 507
Ibbs, T. L., 48, 67, 68, 71
Ihmori, T., 509
Iliin, B., 435
Iwasé, K., 554, 555, 569

Jackson, C. G., 273
Jacobs, R. B., 222, 377, 378, 384
Jaeckel, R., 241, 249, 250
Jaycox, E. K., 226, 247, 340, 341, 360
Jeans, J. H., 1, 37, 54, 68, 74, 75, 76, 81
Jellinek, K., 151, 261, 273, 771, 772, 773
Johansen, E., 318
Johnson, E., 173
Johnson, F. M. G., 272, 555, 570, 603, 604, 607, 611
Johnson, H. H., 647
Johnson, H. L., 817
Johnson, M. C., 262, 699
Johnson, T. H., 215
Johnston, H. L., 680, 752, 778, 779
Johnston, J., 535
Jones, H., 578

Jones, H. A., 20, 54, 59, 63, 64, 80, 352, 675, 700, 752
Jones, L. T., 189
Jones, R. C., 68, 73
Jordon, L., 638
Jossem, E. L., 535, 612
Jouan, R., 610
Jura, G., 463, 464

Kälberer, W., 499
Kahlbaum, G. W. A., 137
Kalähne, E., 646
Kangro, W., 778, 779
Kannuluik, W. G., 45
Kapff, S. F., 222
Kapustinskü, A. F., 820
Katz, J. R., 508
Kaufmann, —, 138
Kaufmann, A. R., 647
Kaye, G. W. C., 37, 159, 192, 694
Kearsley, W. K., 360
Kelley, K. K., 743, 752, 768, 778, 779, 781, 784, 786, 831, 833, 834
Kennard, E. H., 1, 11, 24, 33, 35, 37, 40, 51, 52, 55, 74, 76, 81, 93, 99
Kenty, C., 272, 371, 652, 653
Kerschbaum, F., 283, 284, 285
Keyes, F. G., 447, 803, 828
Kidner, C. A., 515, 658, 676, 732
Kieffer, R., 498
Killian, T. J., 752
King, E. B., 286, 287
Kingdon, K. H., 551, 733
Kinney Manufacturing Company, 134, 142
Kirschfeld, L., 555, 574, 575, 582, 583
Kistler, S. S., 465
Klages, G., 315, 316
Klemenc, A., 788
Klingler, E., 276
Klose, W., 110
Klumb, H., 258, 263, 305, 306, 307, 308, 315, 316, 331, 332
Knauer, F., 26, 322
Knoll, M., 791
Knudsen, M., 18, 21, 51, 56, 57, 58, 59, 66, 88, 90, 93, 110, 111, 151, 152, 262, 294, 295, 296, 441, 442
Köster, W., 849
Kohlschutter, V., 696, 721
Koller, L. R., 373, 700
Kornfeld, G., 276
Korsunsky, M., 166
Kortengräber, A., 833
Kraemer, E. O., 529
Kratz, H., 392, 393, 401, 470, 488, 499
Kraus, C. A., 192, 829, 830, 831, 832
Kroll, A. E., 173
Kroll, W. J., 754, 757
Krüll, F., 819
Krumbhaar, W., 605
Kruyt, H. R., 446, 449
Kubaschewski, O., 554, 574, 630, 771, 773, 774
Kuipers, G., 236
Kundt, A., 39, 281
Kuper, J. B. H., 360, 370
Kurth, E. K., 191
Kurz, K., 340

Laby, 37
Lacher, J. R., 575, 576, 577, 578, 579, 580
Ladenburg, E., 272
Lafferty, J. M., 107, 361, 363
Laidler, K. J., 409, 845
Lamb, A. B., 467, 470, 501, 502, 503, 504
Lampson, C. W., 360, 361, 373
Landauer, R. S., 694
Lane, C. T., 317
Lange, N. A., 42, 781
Langmuir, D. B., 20, 700, 752, 764
Langmuir, I., 18, 20, 40, 54, 59, 60, 61, 62, 63, 78, 80, 127, 128, 133, 184, 185, 188, 204, 206, 213, 283, 291, 292, 352, 372, 389, 400, 401, 402, 403, 404, 405, 407, 410, 411, 412, 413, 414, 416, 417, 418, 419, 424, 430, 437, 439, 440, 441, 442, 443, 451, 458, 469, 508, 509, 510, 511, 527, 547, 551, 613, 625, 643, 654, 673, 674, 675, 676, 677, 678, 679, 680, 681, 682, 683, 692, 700, 701, 714, 731, 732, 733, 752
Larose, P., 611
Larsen, B. M., 619, 639, 837, 840, 841, 842, 848
Latimer, W. M., 743, 831
Lawton, E. J., 372
Leblanc, M., 169
Ledebur, A., 639
Lederer, E. A., 668, 669, 670

Lee, H., 554, 562
Lehmann, E., 272
Lehner, S., 528, 529
Leithauser, G., 318
Lemon, H. B., 467, 480
Lempert, J., 752
Lendle, A., 480
Lepp, H., 607, 826
Lewis, G. N., 46, 794, 798, 803
Licht, W., Jr., 34
Liebhafsky, H. A., 778
Liempt, J. A. M., van, 620, 752
Lindblom, S., 610, 616, 617
Littleton, J. T., 521
Littman, 656
Litton Engineering Company, 223
Littwin, W., 310, 311
Livingston, H. K., 42, 457, 463
Lobb, G. W., 217
Lockenvitz, A. E., 230, 295, 303
Loeb, L. B., 1, 40, 51, 53, 54, 76, 101
Loevenger, R., 103
Loewenstein, L. C., 170
Lofsgren, N., 831
Lombard, V., 610, 614
Lompe, A., 697
Longhurst, E. C., 216
Lonius, A., 76, 77, 78
Loomis, A. G., 789
Loschmidt, 8, 77
Lowry, H. H., 401, 432, 433, 481, 485, 488
Luckmeyer-Hasse, L., 554, 561, 567
Luebke, E. A., 371
Lustman, B., 851, 852

Maass, O., 31, 538, 539
Mach, E., 170
Mackay, G. M. J., 62, 80, 657, 678, 721, 752
Mackenzie, T. D., 692, 695
Magnus, A., 392, 393, 401, 420, 424, 470, 488, 498, 499
Maier, C. G., 806, 821, 834
Malignani, A., 654, 716
Malter, L., 20, 230, 231, 700, 752, 764
Manley, J. H., 371
Manley, J. J., 264, 530, 531
Manning, J. E., 486
Marcuvitz, N., 230, 231
Margulis, N., 353
Markham, E. C., 413
Marshall, A. L., 20, 221, 222, 277, 278, 598, 599, 624, 632, 633, 635, 636, 637, 640, 648, 737, 741, 752, 753, 778, 779, 817
Marshall, M. J., 447
Marshall, S., 45, 811
Martin, E., 554, 568, 599
Martin, L. K., 45
Martin, S. L. H., 575, 584, 585, 673
Mathewson, C. H., 600, 601, 602, 806
Matignon, C., 670
Matricon, M., 165, 194, 195, 197, 200
Maxwell, J. C., 9, 40, 66, 74, 77, 111
Mayer, H., 790
Mayer, J. E., 778
McAdams, W. H., 90
McArthur, E. D., 700
McBain, J. W., 387, 388, 431, 435, 445, 446, 452, 453, 454, 455, 461, 465, 466, 468, 471, 487, 488, 495, 496, 498, 538, 575
McCullough, H. M., 847, 848
McHaffie, I. R., 528, 529
McIntosh, D., 272
McKinney, P. V., 549
McLean, D. A., 542, 543, 544
McLeod, H., 264
Mellen, G., 347
Melville, H. W., 48, 263, 272, 273, 276, 648, 650, 790
Merica, P. D., 603
Metropolitan-Vickers Electrical Company, 127, 218, 221, 222, 239, 241, 243, 251, 358
Mey, K., 691, 693
Meyer, F. A., 360
Meyer, G., 139
Meyer, L., 682
Meyern, W. v., 724, 725, 726, 727
Meyers, C. H., 782
Michel, E., 830
Michelson, W. A., 331
Mierdel, G., 698, 699
Miley, H. A., 851
Millikan, R. A., 40, 83
Millner, T., 809
Mitchell, A. C. G., 653
Modderman, J. G., 446, 449

Moeller, F., 555, 562, 563, 564, 569
Mönch, G., 258
Moers, K., 830
Moll, W. J. H., 316
Molthan, W., 206, 207
Mond, L., 592
Montgomery, C. G., 360
Montgomery, D. D., 360
Moore, G. E., 822, 827
Moore, J. W., 290
Moore, R. B., 782
More, K. R., 246
Morey, G. W., 509, 523
Morgan, S. O., 401, 488
Moritz, H., 554, 555, 558, 565, 566, 596, 598
Morrell, J. H., 340
Morse, R. S., 174, 216, 247, 256, 342, 343, 647
Mott, N. F., 578, 845, 851, 852, 854
Müller, E., 422, 592, 593
Müller, R., 554, 567
Müller-Goldegg, G., 574
Mündel, C. F., 261, 262
Murmann, H., 321, 322, 330
Murphy, D. W., 597, 811, 812, 813
Murphy, E. J., 545

Nambo, J., 672
National Research Corporation, 127, 161, 237, 238, 240, 347, 779
Naughton, J. J., 648, 649, 650
Navias, L., 520, 521
Neale, S. M., 540, 541, 544
Nelson, H., 374, 375
Nelson, R. B., 361, 372, 373, 374
Nemsome, P. T., 538
Neumann, K., 279, 790
Neumann, R., 137, 239, 258, 271
Neundenbel, L., 847
New, E. G., 710, 711
Newberry, K., 262
Newman, F. H., 693, 694, 721
Newton, Isaac, 28
Nicol, J., 609, 610
Nielsen, R. F., 806
Nier, A. O., 72, 377, 380
Niggli, P., 524
Nikitin, 548
Northrup, D. L., 215
Norton, F. J., 598, 599, 624, 633, 635, 636, 637, 640, 648, 651, 652, 731, 741, 752, 753
Nottingham, W. B., 204, 205, 358, 359, 735, 736, 738, 739

O'Bryan, H. M., 759, 760, 761
O'Connor, E. A., 454
Olmstead, P. S., 432, 433
Olsen, L. O., 762, 763
Onsager, L., 68, 73
Orr, W. J. C., 450
Ott, E., 538
Overbeck, W. P., 360
Owens, A. E., 498

Palmer, W. G., 434, 509
Pangburn, J., 514
Parmiter, O. K., 847
Parnell, T., 609, 610
Partington, J. R., 46, 53
Patrick, W. A., 269, 434, 498, 529
Pauling, L., 507
Payne, J. H., 96, 165, 192
Pearce, J. N., 465
Pearson, G. L., 329
Pearson, T. G., 263
Pedder, J. S., 777
Pell-Walpole, W. T., 646
Penning, F. M., 345, 346
Peters, K., 399, 472, 782
Pfeil, L. B., 840, 841, 854
Pfund, A. H., 271
Philip, J. C., 470
Philips Lamp Company, 192
Phillips, A., 600, 601
Phipps, T. E., 202, 230, 341
Picard, R. G., 364, 365
Pickels, W. M., Jr., 301, 302, 367, 368
Pickett, G., 430
Pidgeon, L. M., 499, 501
Pietsch, E., 681, 687, 696, 724
Pihlstrand, F., 554
Pilling, N. B., 835, 836, 837
Pirani, M., 258, 271, 318, 586, 640, 641
Pitzer, K. S., 803
Planck, M., 845
Plesset, M. S., 26
Plücker, J., 687
Poindexter, F. E., 216, 775

Poiseuille, J. L. M., 66, 84, 87, 90
Polanyi, M., 431, 432
Prescott, C. H., Jr., 648, 826, 827
Preston, W. C., 498
Price, L. E., 852
Prytherch, W. E., 646
Prytz, K., 262

Quarrell, A. G., 554, 562

Ralston, O. C., 813
Ramm, W., 243
Ramsay, W., 592
Randall, M., 46, 794, 798, 806
Ransley, C. E., 610, 612, 613, 614, 615, 616, 618, 620, 622, 623
Rao, K. S., 499, 501
Raoult, 764, 774, 777
Rayleigh, 261, 270
Rees, A. L. G., 575, 584, 585, 673
Reeve, L., 638
Reidenour, L. N., 344, 360, 361, 373
Reiff, H. J., 272
Reimann, A. L., 326, 655, 661, 662, 663, 700, 752
Remy-Genneté, P., 829, 830
Reuter, F. W., Jr., 371, 652, 653
Reynolds, N. B., 349, 350, 351, 352, 359
Reynolds, O., 89
Rhines, F. N., 600, 601, 642, 643, 806
Rice, C. W., 64
Rice, M. J., 465
Richardson, L. B., 409, 437, 439, 473, 478
Richardson, L. F., 301
Richardson, O. W., 609, 610, 732
Rideal, E. K., 414, 454
Riecke, E., 692
Riegger, H., 293, 301
Roberts, J. K., 54, 551
Robertson, W. D., 569
Rodebush, W. H., 276
Roell, E., 574, 583, 584
Roentgen, P., 555, 562, 563, 564, 569
Roeser, W. F., 535, 536
Rohn, W., 315
Rohn, W. J. P., 627, 646
Rosenberg, P., 267, 268, 269
Rosenhain, W., 646
Rothstein, J., 515
Rowe, H., 488, 489, 490, 493, 494, 496, 497
Rowe, H. N., 732
Royds, R., 173
Ruckes, W., 90
Rudberg, E., 752
Ruder, W. E., 293
Ruggles, W. A., 191, 372
Ruhemann, M., 788
Rumpf, E., 315
Russell, A. S., 536
Russell, N. O., 189
Ryde, J. W. H., 712
Ryder, H. M., 262, 275, 610, 625, 648

Salzer, F., 847
Sameshima, J., 119
Sanford, C. R., 165, 227
Savage, R. H., 496
Scheel, K., 261, 270
Schenck, H., 554, 561, 567
Schenck, R., 833
Schieferdecker, W., 593
Schilling, W. G., 46, 53
Schmid, H., 768, 769, 770
Schmidt, O., 504
Schneider, A., 766, 768, 769, 770, 771, 775
Schofield, T. H., 646
Schroeder, H., 680, 716, 721
Schroeder, H. J., 241
Schuil, A. E., 35, 43, 458
Schultz, J. F., 811
Schulz, E. H., 628
Schumacher, E. E., 517, 518, 519, 521
Schumann, R., 752, 754
Schuster, C., 499
Schutte and Koerting Company, 174
Schutze, W., 111
Schwab, G. M., 681
Schwabe, K., 422, 592, 593
Schwartz, H. A., 647
Schwarz, H., 258, 305, 306, 307, 308, 368, 728, 729, 730
Scott, D. H., 284
Scott, E. J., 326
Sebastian, J. J., 652
Seelinger, R., 276, 697
Seeman, W., 332
Semat, H., 689
Seybolt, A. U., 601, 602, 647

Seydel, S., 158
Shakespear, G. A., 48
Shaw, P. E., 283
Sheldon, H. H., 470
Shenk, W. E., 619, 639
Sheppard, S. E., 538
Sherwood, R. G., 189, 297, 299, 300, 512, 513, 514, 515, 521
Sherwood, T. K., 117
Shields, J., 592
Shields, J. R., 169, 171, 172, 173
Shiels, D. O., 486
Shrader, J. E., 189, 262, 275, 297, 299, 300, 512, 516
Siegbahn, S., 155
Sieverts, A., 554, 555, 556, 557, 558, 560, 562, 563, 564, 565, 566, 568, 570, 574, 575, 577, 579, 581, 582, 583, 584, 586, 587, 589, 596, 598, 599, 604, 605
Sihvonen, V., 682, 683
Simon, A., 264, 819
Simon, F., 445
Simon, H., 354
Simons, J. H., 536, 603, 604
Simpson, O. C., 27, 202, 230
Sittig, L., 830, 831
Skaneateles Manufacturing Co., 260
Skinner, C. A., 691, 695, 696
Skinner, E. N., 601
Slack, C. M., 656, 663, 664, 665, 666, 668, 671
Slater, I. G., 646
Smallwood, H. M., 74, 84, 177
Smith, A. E., 453
Smith, C. S., 762, 763
Smith, D. P., 552
Smith, E. K., 809, 817
Smith, H. E., 269, 529
Smith, J. H., 67
Smith, N. M., 360
Smith, P. C., 364
Smith, P. L., 537
Smith, P. T., 352
Smith, R. V., 786
Smith, W. R., 460
Smith, W. V., 803
Smithells, C. J., 547, 550, 551, 568, 570, 572, 580, 589, 590, 591, 596, 600, 609, 610, 612, 613, 614, 615, 616, 618, 620, 621, 622, 623, 637, 822
Smittenberg, J., 67, 554, 559, 560
Smoluchowski, M. v., 51, 54, 63, 90, 151
So, Misamiclu, 320, 339
Soddy, F., 654, 656, 657, 658, 692, 695
Sollers, E. F., 828
Sommermeyer, K., 276
Speiser, R., 752, 754
Spencer, L., 610
Stanley, L. F., 322
Stansel, N. R., 825
States, M. N., 96
Stauffer, R. A., 653
Steacie, E. W. R., 555, 570, 603, 604, 607
Stechert, D. G., 34
Stefan, 74
Steiner, L. E., 794
Steinhäuser, K., 631
Stern, O., 26, 322
Stevens, C. M., 377
Stewardson, E. A., 275
Stimson, H. F., 192
Stinson, L. S., 171, 174
Stintzing, H., 258
Stock, A., 138
Stodola, A., 170
Stokes, F. J., Machine Company, 144
Stokes, J. J., Jr., 536
Stoll, E. K., 771, 775
Street, A. C., 645
Strickland-Constable, R. F., 682, 683
Stringfellow, W. A., 540, 541, 544
Strong, J. B., 758, 759, 764
Stroud, E. G., 849, 850, 851
Strutt, R. J., 694
Stuart, H. A., 42, 43, 44
Stull, D. R., 744, 745, 780
Sullivan, H. M., 134
Summerhays, W. E., 48, 76
Sutherland, W., 32, 33, 34, 36, 37, 41, 76, 281
Sykes, C., 230

Tammann, G., 837, 849
Taylor, G. B., 803
Taylor, H. S., 480, 549, 552, 689
Taylor, J. B., 27, 752
Taylor, N. W., 537
Taylor, T. I., 73
Technical Products, Ltd., 790
Teckentrup, C. H., 548

Teller, E., 424
Tenney, H. M., 202, 230
Thiesen, M., 261
Thomas, H. A., 346, 379, 383, 384
Thompson, H. C., 323
Thompson, J. G., 650
Thompson, M. de K., 799, 803, 806, 812, 813, 817, 819, 820, 821, 822
Thornhill, F. S., 460
Timiriazeff, A., 40, 293
Titoff, A., 409, 432, 435, 437, 439, 446, 468, 473, 475, 477, 478, 479, 481
Todd, B. T., 521
Todd, G. W., 295
Todd, H. C., 635
Tompkins, F. C., 66, 67
Tonks, L., 418, 424
Torrey, A. C., 31
Torricelli, 137
Travers, M. W., 466
Trump, J. G., 317
T'sai, L. S., 535
Tsien, Hsue-Shen, 35
Tullis, D. R., 646

Uhlig, H. H., 643, 649
Ulrey, D., 512
Urry, W. D., 535
Utterback, C. L., 262

Vacher, H. C., 638, 650
Valentiner, S., 593, 594
Valko, E. I., 538, 544
Van Atta, C. M., 134, 215
Van Atta, L. C., 215
Van Cleave, A. B., 31
van der Waals, 41, 43
Van Dusen, M. S., 782
Van Valkenburg, H. E., 364
Van Voorhis, C. C., 351, 352, 353, 535
Vegard, L., 696
Vekshinsky, S., 166
Verhoek, F. H., 20, 221, 222, 277, 278, 741
Vernon, W. H. J., 849, 850, 851
Villachon, A., 628
Villars, D. S., 551
Voege, W., 315
Völker, E., 279, 790
Voigt, G. Q., 524
Volmer, M., 192, 279, 409, 417, 444

Wagner, C., 809, 851, 852, 853, 854
Wakeman, A. C. R., 70
Walden, P. T., 815
Walker, K. E., 829, 830
Walker, M. K., 680
Wall, F. T., 73
Waltenberg, R. G., 603
Wamsley, D. H., 668, 669, 670
Warburg, E., 39, 281, 318, 509
Ward, A. F. H., 437, 438
Warfield, C. N., 15
Washburn, E. W., 524
Watson, W. W., 246
Webber, R. T., 317
Weigle, J. J., 26
Weil, K., 399, 472, 782
Weinhart, H. W., 340, 341, 360
Weise, E., 327
Weisz, C., 316
Welch, W. M., Scientific Company, 144, 263
Welterer, G., 287, 288, 289, 290
Wendt, G. L., 694
Wenner, R. R., 794
Wentzel, W., 36
West, G. D., 294
West, G. H., 806
Westin, S., 243
Westmeyer, H., 316
Weyl, W. A., 536, 537
Weyssenhoff, J., 441, 442
Wheeler, A., 453
Wheeler, D. W., 66, 67
White, A. H., 851
White, T. A., 396, 549, 550
White, W. C., 385, 386
Whitney, W. R., 722
Wicking, H. W., 778, 779
Wiedmann, M. L., 54
Wilcock, D. F., 253
Wilkins, F. J., 419, 421, 437, 438
Williams, A. M., 419, 420, 424, 435, 436, 489
Williams, G. A., 535
Williams, H. B., 189
Williams, T. W., 346, 379, 383
Willows, R. S., 691, 692, 693, 696
Wilson, R. E., 467, 470, 480

Winkler, O., 496, 497
Wing, A. K., Jr., 361
Wise, E. M., 637, 639, 839
Witt, R. K., 445
Witty, R., 239
Wöhler, L., 804, 812, 814, 818, 820
Wood, R. W., 441, 442, 443
Woodhouse, J. C., 501, 502, 503, 504
Woodrow, J. W., 297, 299, 301, 494
Woonton, G. A., 216
Wooten, L. A., 461, 672
Worcester, W. G., 379
Work, L. T., 175
Workman, O., 470
Worthing, A. G., 700, 764
Wyman, L. L., 641, 642

Yarwood, J., 94, 159, 162, 232, 258, 272, 345, 790
Young, A. H., 329, 349, 350, 352, 544
Young, J. L., III, 290

Zabel, R. M., 229, 324, 791
Zapf, G., 554, 558, 577, 596, 598
Zehnder, L., 138
Zeise, H., 409, 415, 422, 437, 439, 473, 479, 527, 528, 593
Zimm, B. H., 778
Zollers, S. M., 364
Zuhr, H. F., 377, 378, 384

SUBJECT INDEX

Figures in italics indicate sections dealing with the topics.

Absolute gauge for determination of vapor pressures, 276, 278
Absorbent, definition of, 388
Absorption, definition of, 388; *see also* Solubility
Accommodation coefficient α, for condensation, 20, 404, 442
  for adsorption, 442
  for clean-up of oxygen by tungsten, 674
  for thermal conduction, 51, 54, 55
Activity, definition of, 765
Activity coefficient, definition of, 765, 768
Adatoms, average life of (τ_1), 413
  definition of, 404
Adsorbate, definition of, 388
Adsorbents, measurement of surface of, by electrical method, *454*
    by multimolecular adsorption, *456*
  particle sizes of, 461
  sorption of, in relation to boiling point, 389
  surface area of, 454, 455, 456, 459, 462, 463, 464
Adsorption, accommodation coefficient for, 442
  activated, on finely divided metals, 548
  application of potential theory to, *431*
  characteristic curve for, 432
  definition of α for, 412
  definition of σ for, 412
  discontinuities in, 396
  heat of, *390*; *see also* Heat of adsorption
  multimolecular, *424*, *431*
  of argon, krypton, neon on charcoal, 399
  of carbon dioxide on wood charcoal, 393
  of gases, on charcoal, *see* Charcoal
    on glass, 413
    on ionic crystals, 450
    on mica, 413
  of hydrogen on tungsten powder, 395
  of nitrogen, carbon monoxide, and argon on silver, 394
Adsorption, of nitrogen on coconut charcoal, 392
  of nitrogen on different catalysts, 428
  of nitrogen on mica, 409
  of nitrogen on steel, 398
  of oxygen, carbon monoxide, and carbon dioxide on silica, 414
  on charcoal in relation to boiling point of adsorbent, 389
  physical, definition of, *387*
    on finely divided metals, *547*
  rate of, *451*
  temperature variation of, *434*
  units and conversion factors for amount adsorbed, 391
  values of α, for, 413, 438
  values of σ_1, for, 413, 438
  values of τ_1, for, 413
  van der Waals type of, *387*
Adsorption constants, values of, from isotherms, 399, 400, 408, 413
Adsorption isobar, 390, 435
Adsorption isostere, definition of, 390
  Williams' relation for, 436
Adsorption isotherm, definition of, 390
  equation for, of Armbruster-Austin, 421
    of Brunauer-Emmett-Teller, *424*
    of Euken-Polanyi, 431
    of Freundlich, *396*
    of Henry, 401
    of Langmuir, *401*
    of Magnus, 420
    of Palmer-Clark, 434
    of Patrick, 434
    of Tonks, *416*
    of Wilkins, 419
    of Williams-Henry, *419*
    of Zeise, 415, 422
  for dissociated molecules, 411
  for inhomogeneous surface, 410
  for multimolecular adsorption, *424*, *431*

Adsorption isotherm, hyperbolic equation for, *401*
  parabolic equation for, *396*
  summary of equations for, 424
Adsorption potential, 431
Air, boiling point of liquid, *786*
  density of, at 1 atm, 19
  variation in pressure of, with height, 15, 16
Alkali metals, use of, as substitutes for liquid air, 216
Alloys, constitution diagrams of, for bismuth-tin, 774
    for copper-zinc, 770
    for lead-cadmium, 774
    for lead-magnesium, 773
    for lead-zinc, 774
    for silver-gold, 773
    for zinc-aluminum, 776
  of copper-tin, solubility of hydrogen in, 564
  of iron-manganese, solubility of hydrogen in, 567
  of iron-molybdenum, solubility of hydrogen in, 568
  of iron-nickel, solubility of hydrogen in, 561
  vapor pressures of, *764*
Alphatron gauge, *345*
Aluminum, effect of alloying elements on solubility of hydrogen in, 569
  solubility of hydrogen in, 569
  solubility of nitrogen in, 600
Amalgams, use of, as high-vacuum cutoff, 217
    as substitutes for liquid air, *216*
Analcite, *see* Chabasite
Analysis of gases in metals, methods of, *648*
Atmosphere, unit of pressure, 4
Avogadro constant N_A from value of *e*, *8*
Avogadro's law, 3

b, coefficient of van der Waals, 41
Baffles, design of, for oil-vapor pumps, *246*, 248
Bar, unit of pressure, 4
Batalum getter, 666, 668
Beams, molecular, 26, 27
Beryllium, vapor-pressure data for, 747, 754
Boltzmann constant *k*, 2, 3, 8, 15
Brownian motions, theory of, *81*

Carbon, vapor-pressure data for, 748, 753
Carbon dioxide, vapor-pressure data for solid, 783, 784
Carbon filament, reaction of, with oxygen, 682
Carbon monoxide, clean-up of, by tungsten, 676
  diffusion of, through iron, 611
  reduction of oxides by, 824, 826
Cathode drop, 688
Cathodes, oxide-coated, slumping of, due to gas from glass, *531*
Cellulose, heat of sorption of water vapor by, 544
  rate of desorption of water vapor from, 544
  sorption and desorption isotherms for water vapor in, 539
  sorption and desorption phenomena in, *538*
  thermal decomposition of, *545*
Cerium, solubility of hydrogen in, 574, 586
Chabasite, dehydrated, sorption by, *500*
    in relation to molecular size of adsorbate, 504, 506
    sorption of argon, hydrogen, and nitrogen by, 503
    sorption of carbon dioxide, hydrogen, and oxygen by, 503
    sorption of hydrocarbons by, 505
Characteristic curve for adsorption, 432
Charcoal, activated, chemisorption by, 496
    isotherms for sorption of nitrogen by, 392
    porosity of, 471
    preparation of, *467*
    purification of, 470
    sorption and desorption of water vapor for, 486, 487
    sorption by, at low pressures, 472, 478, 479, *488*
    sorption constants for adsorbates on, 478, 479

- Charcoal, activated, sorption of air by, 480
  - sorption of ammonia by, 477
  - sorption of argon by, 472, 474
  - sorption of carbon dioxide by, 474, 477, 489
  - sorption of carbon monoxide by, 474, 476, 490, 493
  - sorption of ethylene by, 474, 475
  - sorption of helium by, 474
  - sorption of hydrogen by, 468, 472, 477, 488, 490, 491, 492, 493, 496
  - sorption of methane by, 475
  - sorption of neon by, 492, 493
  - sorption of nitrogen by, 472, 474, 476, 477, 480, 487, 489, 490, 491, 492, 493, 496
  - sorption of oxygen by, 476, 480, 489
  - sorption of rare gases by, 472
  - structure of, *467*
  - surface area of, 479
  - use of, in high-vacuum systems, *493*
  - isotherms for sorption of rare gases by, 399
  - sugar, sorption of oxygen by, 481
    - sorption of water vapor by, 482
  - wood, sorption of carbon dioxide by, 393
- Charcoal trap, Anderson's design of, 247
- Charles' law, 3
- Chemical clean-up, by aluminum, 665
  - by barium, 665, 667
  - by batalum, 666, 668
  - by calcium, 656
  - by evaporated metals, *656*, 665
  - by incandescent filaments, *673*
  - by KIC getter, 666, 668
  - by magnesium, 656, 662, 665
  - by misch metal, 665
  - by sodium, 661
  - by thorium and uranium, 665
  - by zirconium and titanium, 670
  - of gases, *654*
- Chemical equilibria, free and total energy of, *793*
- Chemisorption, 446
  - by charcoal, 496
  - of hydrogen by tungsten, 551
  - of oxygen by tungsten, 551
- Chlorine, dissociation of, 679
- Chromium, rate of oxidation of, *see* Oxidation
  - solubility of hydrogen in, 568
- Clausing's factor K, 98, 99
- Clausius-Clapeyron relation, 795
- Clean-up, chemical, *654; see also* Chemical clean-up
  - electrical, *see* Electrical clean-up
  - of gases by palladium black, *595*
- Cobalt, solubility of hydrogen in, 562
  - solubility of oxygen in, 601
- Coconut charcoal, *see* Charcoal
- Coefficient, f, of Maxwell, 39, 40
  - of accommodation, *see* Accommodation coefficient
  - of heat conductivity, *see* Thermal conductivity of gases
  - of interdiffusion D_{12}, method for determination of, 77
    - relation of, to δ, 75, 76
    - variation of, with temperature, 77
  - of self-diffusion D_{11}, relation for, 74
  - of slip, 39, 87
  - of thermal separation, definition of, 68
    - relation of, to force constants between molecules, 69
      - to molecular diameters, 70
      - to ratio of hot to cold temperature, 68
  - of viscosity η, relation of, to coefficient of diffusion, 74
      - to L, mean free path, 29, 30, 31
      - to molecular diameter δ, 31, 32
      - to thermal conductivity λ, 45
    - values of, 36, 37
    - variation of, with temperature, 31, 32, 36, 37
- Cold-cathode discharge, clean-up phenomena in, *691*
- Collision cross section of molecules, *see* Number of molecules, per monolayer
  - for electrons, 42, 43
  - for molecules, 42
- Collision frequency of molecules ω, 25, 36
- Collisions, rate of, per unit volume, 37, 38
- Columbium, solubility of hydrogen in, 574, 585
- Condensation, accommodation coefficient for, 20, 404, 442

Condensation pump (Langmuir), *184*
Conductance F, *see* Flow of gases
  for cylindrical tubes, as a function of a/P, 113, 114, 117
  for flow of gases, at low pressures, 90
    at normal pressures, 84
  for free-molecule flow, as a function of M, 94, 104
    Clausing's factor K for, 98, 99
    experimental tests of formulas for, 110
    of liquid-air trap, 106
    of orifices, 91, 92, 94, 95, 105
    of short tubes, 96, 98
    of slits, 102
    of tubes in series, 125
Constitution diagrams of alloys, *see* Alloys
Contact gettering, 656
Conversion factors, for amount adsorbed, 391
  for amount of gas in iron, 630
  for quantity of gas, 6
  for R_0, 5
  for units of pressure, 4, 5
  for viscous flow, 85
  from grams/liter to oz/cu ft, 5
Conversion units for solubility of gases in metals, 553
Cooling trap, *see* Baffles; Charcoal trap; Liquid-air trap
  use of refrigerant with, 215
Copper, diffusion of hydrogen through, 616
  molten, effect of alloying metal on solubility of hydrogen in, 564
    solubility of sulfur dioxide in, 605
  rate of oxidation of, *see* Oxidation
  solubility of hydrogen in, 563
  solubility of oxygen in, 601

Decrement type of viscosity gauge, *281*
Degassing, of cast metals, methods for, 646
  of metals, rates of, *618*, 624, 633
Densities of gases, values of, derived from M, 7, 19
Density of atmosphere as a function of height, 15
Design of vacuum systems, *134*
Desorption, definition of, 388
  rates of, *618*
Deuterium, solubility of, in palladium, 577
Diameters of molecules, *see* Molecules
Diffusion, and condensation, role of, in vapor pumps, *204*
  of gases, *see* Coefficient of interdiffusion
    in a vapor stream, Gaede's theory of, 176
    kinetic theory of, 74
    through metals, *607*
      effect of pressure and temperature on, 609
      effect of surface treatment on, 613
      rates, 611
    through quartz and glasses, *531*, 534, 536
  of hydrogen through palladium, 611, 612
  thermal, *see* Thermal diffusion
Diffusion constant for air in mercury vapor, 178
Diffusion constants, for gases in metals, *618*
  for oxygen in oxide coatings, 846
Diffusion pump of Gaede, *182*
Dispersal gettering, 656
Displacement, free air, of pump, 136
Dissociation, degree of, for water vapor, 796, 801
  of chlorine by hot filament, 679
  of hydrogen by hot filament, 677
  of oxygen by hot filament, 680
Dissociation pressures, of hydrides, *828*
  of nitrides, *830*
  of oxides, *796*
Distillation, effect of pressure on rate of, 23
  in vacuum, rate of, 23
Distribution function, for energy, 12
  for velocities, 9, 12
Distribution law for particles, with height, 15
Distribution laws for molecular velocities, *9*
Dubrovin gauge, 263

Effusion, rate of, through an orifice, 21
  through a porous diaphragm, *118*
Ejector pump, design of oil-vapor, 236
Ejector pumps, steam-jet, *169*
Electrical clean-up, in cold-cathode discharge, *691*
    by sputtering, 696
  in electrodeless discharge, 692, 698
  in hot-cathode discharges, *704*
    at very low pressures, *724*
    effect of magnetic field on, 726
    effect of voltage on, 726
    mechanism of, 708
    rate of, 707, 727
    relation of, to glow potential, 712
      to ionization, 709
  in ionization gauge, 729
  in vacuum incandescent lamps, *716*
  of gases, *687*
Electrical discharges, clean-up and gas evolution in, 713
Electron, charge of, 8
Electron emission, from hot cathodes, *699*
  from tungsten, effect of oxygen on, 372
Electrons, velocity of, in relation to potential drop, 689
Energy, free, and total, for chemical equilibria, *793*
      for formation of water vapor, *798*
    of evaporation, relation of, to vapor pressure, 741
    of reactions, *793*
  total, of evaporation, *see* Heats of evaporation
Energy levels in atomic spectra, 690
Energy loss due to thermal conductivity, *see* Thermal conductivity of

  of molecules, average, 2
    distribution law for, 12
Equation of state, for ideal gases, 2, 3
  for monolayer, 417
  of van der Waals, 41, 417
Equilibrium constants, for carbon-carbon dioxide reaction, 824
  for dissociation of methane, 824
  for dissociation of water vapor, 801
Equilibrium constants, for hydrogen-carbon dioxide reaction, 824
  for reduction of oxides by hydrogen, *see* Oxides
Esters for oil-vapor pumps, formulas for, 220
  vapor pressures of, 222
Evaporation, free energy of, in relation to vapor pressure, *795*
  of metals in vacuum, filament materials for, 761
  rate of, effect of pressure on, *78*
    in relation to vapor pressure, *18*
  rates of, of alloys, *764*
Exhaust, rate of, through orifice or tube, *121*
  speed of, 129
  time constant for, 123
Exhaust pressure of pump, 128
Expansion of wire, use of, in low-pressure gauge, 330

Faraday constant F, 8
Film theory of heat conduction of gases, *59*, 63
Film thickness for heat conduction from wires, 61, 64
Flow, of air, rate of, through cylindrical tube, as a function of a/L, 113
  of gases, *see* Conductance F
    at intermediate pressures, *111*
    free-molecule, *90*
    rate of, units for measurement of, 6
    through porous diaphragms, *118*
    turbulent, *89*
    viscous, *84*
Force constants in law, μr^{-s}, 70
Free air displacement of pump, 136
Free-molecule flow, of gases, *90*
  through an orifice, spatial distribution of, 167
Free-molecule heat conductivity, 52
  values of, 53
Free path of molecules, distribution law for, *24*

Gas, density of, relation for, 7
  mass of, incident per cm^2 per sec, 19
  quantity of, units for measurement of, 6

Gas constant R_0, *3*
Gas discharge, distribution of potential in cold-cathode type of, 687
  use of, to indicate low pressures, *258*
Gaseous mixtures, separation of, by effusion, 21
    by porous diaphragm, 110
    by thermal diffusion, 67
Gases, amount of, in cast metals, *644*
  Charles' law for, 3
  content of, in glass, *see* Glasses
  diffusion of, through metals, *607*
    through quartz and glasses, *531*
  flow of, *see* Flow of gases; Conductance F
  in metals, amount and composition of, *624*, 633
    methods for analysis of, *648*
  law of ideal, *1*
  low-temperature distillation method for analysis of, *650*
  sorption of, by chabasite, *see* Chabasite
    by charcoal, *see* Charcoal
    by metals, *552; see also under different gases*
    by silica gel, *see* Silica gel
  specific heats of, 46
  units for solubility of, in metals, 553
  values of densities of, derived from M, 19
  values of γ for, 46
  van der Waals equation for, 41
Gauge, absolute, for determination of vapor pressures, 276
Gauges, *366*
  decrement type of, *281*
  heat conductivity, *313*
  involving linear expansion of wire, *330*
  ionization, *332; see also* Ionization gauges
  Knudsen, *294*
    DuMond and Pickels form of, 302
    Hughes form of, 305
    Klumb-Schwarz form of, 305
    Lockenvitz form of, 303
    Shrader and Sherwood form of, 299
    Woodrow form of, 297
  mechanical type of, 272
Gauges, mercury, McLeod type of, *264; see also* McLeod gauge
    Rayleigh form, 260
    sensitive forms of, *263*
    Shrader and Ryder optical lever, 261, 262
  molecular, 291
  Molvakumeter type of, 309
  Pirani-Hale, *318*
    Reimann design of, 326
    Thompson-Hennelly modification of, 323
  quartz fiber, 284
  quartz spiral form of, 273
  quartz surface, 286
  radiometer (Knudsen) type of, *293*
    theory of, 310
  ranges of pressure for different types of, 367
  thermistor, 329
  thermocouple, *315*
  thin-wall type of, design by Foord, 214
    design by Grigorovici, 274
    design by Scheel and Heuse, 275
  viscosity type of, *279*
Getter, type C-400 barium-aluminum, 736
  use of phosphorus as, 716, 720
Getters, application of, in vacuum technique, *654; see also* Chemical clean-up
  batalum, 666, 668
  contact type of, 656
  disperse type of, 656
  KIC, 666, 668
  technical, 668
Gibbs-Helmholtz relation, 794
Glass, adsorption of gases on, 527
  adsorption on, 413
  evolution of hydrogen chloride from, 531
  sorption of water vapor by, 528, 530
Glasses, bake-out schedule for (Langmuir), 511
  composition of, in relation to gas content, 517, 521, 525, 526
  diffusion of gases through, *531*
  evolution and sorption of gases by, *509*, 512, 524

Glasses, gas evolution from, after evacuation, 516
  used in vacuum devices, composition of, 527
Glow potential, *see* Electrical clean-up
Gram-molar volume V, 3
Graphite, amount and composition of gases in, 636
Greases for use in vacuum technique, vapor pressures of, *790*

Halides, vapor pressures of, 780
Heat, mechanical equivalent of, J_{15}, 6
  of adsorption, differential and integral, 448
    of carbon dioxide on charcoal, 447
    of oxygen on charcoal, 447
    of water vapor on charcoal, 485
    on metal surfaces, 449
    (sorption), 390, *445*
      relation of, to boiling point, 449
        to heat of evaporation, 446, 449
  of evaporation, of carbon, 753
    relation of, to heat of sorption, 446
  of solution, of oxygen in cobalt, 603
    of sulfur dioxide in copper, 606
  of sorption of water vapor by cellulose, 544
Heat conductivity gauges, *see* Gauges
Heat conductivity of gases, *see* Thermal conductivity of gases
Heats, of evaporation for metals, 756
    relation of, to vapor pressures, 742
  of formation of hydrides, 588
  of formation of hydrogen alloys, 588
  of solution of hydrogen in metals, 591
    of Group A, 554
Henry's law, 401, 473
Ho coefficient for speed of vapor pump, 168, 200, 245, 246
Hot-cathode discharges, clean-up in, *see* Electrical clean-up
Hot cathodes, electron emission from, *699*
  space-charge phenomena at, 701
Hydrides, dissociation pressures of, *828*
  heats of formation of, 588
Hydrogen, activated adsorption of, on tungsten, 551
  clean-up of, by tantalum, 686
Hydrogen, diffusion of, through metals, *611*
  dissociation of, 677
  embrittlement of metals by, *640*
  equilibrium constants for reduction of oxides by, 797; *see also* Oxides
  heat of reaction of, with palladium, 576, 579
  heat of sorption of, by iron, 558
    by metals, 554, 591
    by molybdenum, 568
    by nickel, 560
    by platinum, 570
    by silver, 571
  in metals, effect of, on electrical resistance, 588
    theory of solubility of, *589*
  isobars for solubility of, in metals of Group A, 571
    in metals of Group B, 573
  isotherms for solutions of, in titanium, 581
    in vanadium, 582
  reduction of oxides by, *see* Oxides
  solubility of, in aluminum, 569
    in chromium, 568
    in cobalt, 562
    in columbium, 574, 584
    in copper, 563
    in iron, 555
    in iron-manganese alloys, 567
    in iron-molybdenum alloys, 568
    in iron-vanadium alloys, 583
    in manganese, 565
    in metals, effect of temperature on, 554
    in metals of Group A, *553*
    in metals of Group B, *572*
    in molten copper alloys, 564
    in molybdenum, 568
    in nickel, 559
    in palladium, 575
    in palladium alloys, 580
    in palladium-like metals, 591
    in platinum, 570, 592
    in platinum black, 593
    in rare-earth metals, 574, 585
    in silver, 570
    in tantalum, 574
    in thorium, 574, 587

- Hydrogen, solubility of, in titanium, 574
    - in vanadium, 574
    - in zirconium, 574, 583, 585
  - sorption of, by metals, effect of pressure on, 554
    - by palladium black, 593
  - types of interaction of, with metals, 552
- Hydrogen alloys, heats of formation of, 588, 591
- Hydrogen-palladium system, isotherms for, 576
  - theory of, 578

- Ice, vapor-pressure data for, 782
- Incandescent filaments, clean-up by, *673*
- Ionization, probability of, 351
- Ionization gauge, electrical clean-up in, 729
  - interchange phenomena in, 729
- Ionization gauges, *332*
  - Alphatron type, 347
  - Barkhausen oscillations in, 340
  - calibration of hot cathode, 349
  - control circuits for, *359*
  - control types of circuit for, 334
  - Dushman-Found design of, 336
  - Fogel, design of, 344
  - Jaycox-Weinhart, design of, 341
  - Morse-Bowie, design of, 343
  - Penning cold-cathode, 345
- Iron, diffusion of hydrogen through, 617
  - rate of oxidation of, *see* Oxidation
  - solubility of hydrogen in, 555
  - solubility of nitrogen in, 596
  - solubility of oxygen in, 601
- Isobar, definition of, 390; *see also* Adsorption
- Isostere, definition of, 390; *see also* Adsorption
- Isosteres for sorption of water vapor by sugar charcoal, 483
- Isotherm, *see* Adsorption isotherm
- Isotherms for sorption of water vapor by sugar charcoal, 484, 485

- Jets, design of, for oil-vapor pumps, *241*

- Katharometer, 48, 76
- Kelvin temperature scale, 3, 5
- Kinematic viscosity, 35
- Kinetic theory of gases, derivation of relation for pressure, 2
  - fundamental postulates of, 1
- Knudsen gauge, *294*; *see also* Gauges, Knudsen

- Lamps, vacuum incandescent, clean-up in, *716*
- Lanthanum, solubility of hydrogen in, 574, 586
- Law, of distribution, for energy, 12
    - for free paths, 25
    - for molecular velocities, 9
    - for particles, with height, 15
  - of repulsive force between molecules, 70
- Leak detectors, *370*
  - use of halogen in positive-ion type of, 385
  - use of helium ionization gauge for, 376
  - use of hydrogen ionization gauge for, 374
  - use of mass spectrometer for, *377*
  - use of oxygen in, 372
  - use of Pirani gauge for, 371
- Light, velocity of, 8
- Liquid air, boiling point of, *786*, 788
- Liquid-air trap, conductance of, for flow of gases, 106
  - design of low-resistance, 215
  - substitutes for, 216
- Logarithmic decrement of viscosity, definition of, 282
- Loschmidt number, 8
- Low-temperature distillation method of gas analysis, 650

- Magnetic field, effect of, on electrical clean-up, 726
- Manganese, solubility of hydrogen in, 565
- Manometers for low pressures, *258*; *see also* Gauges
- Mass spectrometer, use of, for leak detection, *377*
- McLeod gauge, *264*; *see also* Gauges
  - calibration of capillary of, 270, 271
  - constants for different dimensions of, 267

McLeod gauge, determination of pressure of condensible gases by, 269
  extremely sensitive design of, 268, 269
  method for, eliminating sticking of mercury in, 268
  Pfund's modification of, 271
  sticking of mercury in capillary of, 267
  swivel form of, 271, 272
Mean free path, L, *see also* Free path of molecules
    as reciprocal of absorption coefficient, 25
    calculation of, from velocity of sound, 35
    effect of temperature on, 32
    experimental determination of, 26
    in gaseous mixtures, 38
    relation of, to coefficient of viscosity, 28, 33
      to molecular diameter, 31, 32
      to pressure, 33
    values of, 36
  of air in mercury vapor, 184, 187, 206
  of air in oil vapors, 225
  of electron, 42, 338
  of ion, 338
Mechanical equivalent of heat J_{15}, 6
Mercury, vapor-pressure data for, 782
Mercury manometers, 260
Merit factor of pumps, 136
Metals, amount and composition of gases in, *624*, *633*
  amount of gases in cast, *644*
  determination of oxygen in, *637*
  diffusion of gases through, *611*
  embrittlement of, by hydrogen, *640*
  methods for vacuum distillation of, *757*
  methods of analysis of gases in, *648*
  methods of degassing of, 646
  sorption of gases by, 552
  sorption of hydrogen by, *552*; *see also* Hydrogen
  vapor-pressure data for, *753*, 754
Methane, degree of dissociation of, 824
Mica, adsorption on, 407
Microbar, unit of pressure, 4
Mixture of gases, separation of components in, by effusion, 110
    by thermal diffusion, 67
Molecular areas, values of, 459
Molecular beams, 27
Molecular diameter δ, from coefficient of interdiffusion, 76
  from density, 42, 43
  from van der Waals constant, 42, 43
  relation of, to coefficient of viscosity, 32
    to mean free path, *31*, 32
  Sutherland relation for, 32
  values of, 36, 43
Molecular gauge, 291
Molecular heat conductivity, values of, 53
Molecular pumps, *see* Pump; Pumps
Molecular velocities, average values of, v_a, 10, 19
  distribution laws for, 9
  most probable values of, 10
  relation of, to velocity of sound, 13
  root-mean square values of, 10
Molecules, average kinetic energy of, 2
  collision cross section of, for electrons, 43
  collision-frequency of, ω, 34, 36
  dimensions of, from sorption data, 506, 507
  masses of, 19
  number of, per cm^3, 9
    per monolayer, 36, 43
  random (Brownian) motions of, 81
  rate of incidence of, per cm^2, 17, 19
  repulsive force constants for, in mixtures, 70
Mol-fraction, definition of, 765
Molvakumeter, 309
Molybdenum, reactions of, with gases, 676, 679
  solubility of hydrogen in, 568
  solubility of nitrogen in, 599
Momentum, rate of transfer of, in gas at low pressure, 39
    in gas at normal pressure, 29
Monolayer, definition of, 388
  equation of state for, 417
  equivalent volume for, 391
  number of molecules per, 391, 459
Multimolecular adsorption, *422*, *431*
Multimolecular adsorption method for determination of surface of adsorbents, *456*

Newton, unit of force, 4
Nickel, rate of oxidation of, *see* Oxidation
  solubility of hydrogen in, 559
Nitrides, dissociation pressures of, *830*
Nitrogen, active, 694
  clean-up of, by molybdenum, 676
    by tantalum, 683
    by tungsten, 675
  diffusion of, through metals, 611
  solubility of, in aluminum, 600
    in iron, 596
    in molybdenum, 599
    in tungsten, 599
    in zirconium, 600
  sorption isotherms for, by charcoal, 392
Nitrogen-oxygen mixtures, boiling points of, *786*
Non-condensible gases, vapor-pressure data for, 785, 786
Number of molecules, per monolayer, N_S, 36, 43, 391, 412, 459
  per unit volume, 9

Occlusion, definition of, 388; *see also* Solubility
Oil, vapor pressures of commercial, 789
Oils for vapor stream pumps, 220, 222
  adsorption of, on metals, 225
  conditioning of, 223
  silicones, *253*
  stability of, 223, 249
  ultimate pressures of, 224, 251
  vapor pressures of, 221, 222
Optical-lever mercury manometers, 261, 262
Oxidation, effect of pressure on rate of, 839
  ionic theory of rate of, *852*
  linear law for rate of, *836*
  logarithmic law for rate of, *849*
  parabolic law for rate of, *837*
  rate of, for iron, 840
Oxide, of magnesium, reaction of, with tungsten, 827
  of mercury, dissociation pressures of, 803
  of palladium, dissociation pressures of, 804
  of silver, dissociation pressures of, 803
Oxides, composition of, for layers on copper, 839
    for layers on iron, 839, 841
    for layers on nickel, 839
    for layers on steel, 849
  equilibrium constants for reduction of, by hydrogen, 797
  of chromium, dissociation pressures of, 813, 820, 844
    reduction of, by hydrogen, 814, 821
  of cobalt, dissociation pressures of, 818
    reduction of, by hydrogen, 818
  of copper, dissociation pressures of, *805*
    reduction of, by hydrogen, *805*
  of iron, dissociation pressures of, *810*, 844
    reduction of, by hydrogen, *810*
  of manganese, dissociation pressures of, 819
    reduction of, by hydrogen, 819
  of molybdenum, reduction of, by hydrogen, 821
  of nickel, dissociation pressures of, *817*
    reduction of, by hydrogen, 817
  of tungsten, reduction of, by hydrogen, 821
  porosity of, in relation to rate of oxidation, 835
  reduction of, by carbon, 638, 826
    by carbon monoxide, 826
    by reducing atmospheres, *822*
  vapor pressures of, *778*
Oxygen, activated adsorption of, on tungsten, 551
  clean-up of, by tantalum, 685
    by tungsten, 673
  determination of, in metals, *637*
  diffusion constants for, in oxide coatings, 846
  diffusion constants of, through silver, 611
  dissociation of, 680
  effect of, on emission from tungsten, 372
  reaction of, with carbon, 682
  solubility of, in cobalt, 601
    in copper, 600
    in iron, 601
    in silver, 603

Palladium, diffusion of hydrogen through, 611, 612, 615
  solubility of hydrogen in, 574, 575
Palladium black, preparation of, 594
  sorption of hydrogen by, 593
  use of, in clean-up of gases, 595
Palladium-hydrogen system, isotherms for, 576
  theory of, *578*
Paper, sorption of water vapor by, *see* Cellulose
  thermal decomposition of, 545
Parabolic equation for adsorption isotherm, *396*
Permeability, for gases, definition of, 532
  of porous diaphragms, 120
  of Pyrex for gases, values of, 534
  of silica for gases, values of, 534
Persorption, definition of, 507
Philips ionization manometer, 345
Phosphorus, mechanism of clean-up by, 720
  use of, as getter in vacuum lamps, 716
Physical adsorption, *see* Adsorption
Pirani gauge, *318*; *see also* Gauges
Platinum, solubility of hydrogen in, 570, 592
Poiseuille law, *84*
Porous diphragms, rate of flow of gases through, *118*
  separation of gases by, 110
Positive ions, velocity of, in relation to cathode drop, 689
Potential theory, application of, to adsorption, *431*
Pressure, effect of, on rate of evaporation of metals, 78
    on sorption of hydrogen by metals, 554
  kinetic-theory relation for, 2, 3
  units of, 4, 5
  variation of, with height of atmosphere, 15, 16
Pressures, measurement of low, *see*

  production of extremely low, *730*
  use of gas discharge as indicator of low, *258*
Probability of ionization, 351
Pump, degree of vacuum attainable with, 128
  exhaust pressure of, 128
  oil-vapor, simple form of, 219
  speed of, 129
    methods for determination of, *159*
Pumps, mechanical type, *126*
    Cenco High-vacuum, 141
    free air displacement of, 136
    Gaede molecular, 151
    Gaede rotary mercury, 138
    Gaede rotary oil, 139
    Geissler-Toepler, 137
    Holweck molecular, 154
    Kinney rotary oil, 142
    merit factor of, 136
    Siegbahn molecular, 155
    Sprengel mercury, 137
    Stokes Microvac, 144
    Welch Duo-seal, 144
  mercury-vapor, Alexander, 211
    arc type of, 189
    Copley, 202
    Crawford, 190
    diffusion and condensation in, *204*
    divergent nozzle types, speeds of, 204
    effect of fore-pump pressure, on fine pressure of, 196
      on speed of, 195
    effect of heater watts, on fine pressure of, 193
      on speed of, 213
    effect of nozzzle design on speed of, *198*
    Estermann-Byck, 199
    Gaede diffusion, *182*
    Ho coefficient for speed of, 200
    Langmuir condensation, *184*
    Kurth-Ruggles, 191
    multistage, 191
    performance characteristics of, *193*
    scattering of vapor at nozzle of, 207
  oil-vapor, booster type, 235, 239
    conditioning of, 223
    design of baffles for, 246, 248
    design of jets for, *241*, 243
    Eimac type, 239
    ejector design, 236
    Embree jet for, 244

Pumps, oil-vapor, fractionating type, 224, 230
    of Distillation Products, Inc., 232, 237
    of Malter and Marcuvitz, 230
    of National Research Corporation, 238
  liquids for use in, 220, 222
  Metrovac type, 241
  non-fractionating type, *226*
    Copley et alii, 230
    Estermann and Byck, 228
    Zabel, 229
 steam-jet, ejector, *169*

Quantity of gas, units for measurement of, 6
Quartz, diffusion of gases through, *531*
Quartz fiber gauge, 284
Quartz powder, sorption of water vapor by, 508, 509
Quartz surface gauge, 286
 calibration curves for, 289

Radiometer type of gauges, theory of, 294, *310*; *see also* Knudsen gauge
Random motions of molecules, *81*
Raoult, law of, 764
Rare gases, clean-up of, in cold-cathode discharge, 697
Rate, of degassing of wire, 621
 of distillation, variation of, with pressure, of gas, 23
 of evaporation, effect of pressure on, 78, 80
  relation of, to vapor pressure, *18*, 742
 of exhaust through tubes and orifices, *121*
 of flow as a function of the pressure, 111, 118; *see also* Flow of gases
 of incidence of molecules, 17, 19
 of sorption, by adsorbents, *451*
  in capillaries, 453
Rates, of evaporation of metals and carbon, *743*
 of oxidation, *see* Oxidation
 of sorption and desorption, *618*
Ratio C_p/C_v, values of, 46

Reducing atmospheres, composition of, 825
 equilibrium constants for reduction of iron oxide by, 824
Reduction of oxides, *see* Oxides; Equilibrium constants
 by carbon monoxide, 826
Resistance of tubes and orifices to flow of gases, *see* Conductance F
Reynolds number, 89
Rotating disk type of gauge, 291

Self-diffusion of a gas, *see* Diffusion
Separation of gases, by effusion, 21
 by thermal diffusion, 67
Silica, adsorption on, 414
Silica gel, and silicates, sorption by, *498*
 sorption of argon by, 499
 sorption of carbon dioxide by, 498, 499
 sorption of water vapor by, 499, 500, 501
Silicone oils, chemical composition of, *253*
 speeds of pumps with, 256
 use of, in vapor pumps, *253*, 255
 vapor pressures of, 254
Silver, adsorption on, 394
 diffusion of oxygen through, 611
 solubility of hydrogen in, 570
 solubility of oxygen in, 603, 604
Size of molecules, *see* Molecular diameter δ
Skanascope, 260
Solubility, of gases in metals, *see under individual metals and gases*
 of hydrogen in metals, *552*; *see also* Hydrogen
  theory of, *589*
Sorption, by glass, *see* Glass
 definition of, 387; *see also* Absorption; Adsorption; Solubility
 heat of, *see* Heat of adsorption
 Henry's law for, 401
 of hydrogen by metals, *552*; *see also* Hydrogen
 rate of, 451, 618
  in capillaries, 453
Sound, relation of velocity of, to mean free path, 35
  to molecular velocities, 13

Space-charge phenomena in hot-cathode devices, 701
Specific heats of gases, values of, 46
Spectral lines, theory of origin of, 690
Speed, of exhaust for diffusion pump, 178, 181
  of pump, definition of, 129
    effect of streaming on determination of, 166
    for different oils and mercury, 256, 257
    Ho coefficient for, 200
    intrinsic, 130; *see also* Pumps
    methods for determination of, *159*
Sputtering in cold-cathode discharge, 696
Steam-jet ejector pumps, *169*
Steel, rate of oxidation of, *see* Oxidation
Streaming, of gas through an orifice, spatial distribution in, 167
  of mercury vapor through a nozzle, 206, 208
Substitutes for liquid-air trap, 216
Sulfur dioxide, solubility of, in molten copper, 605
Surface of adsorbents, *see* Adsorbents
Sutherland constant, *see* Molecular diameter
  definition of, 32
  values of, 36

Tantalum, effect of dissolved gases on resistance of, 685
  solubility of hydrogen in, 574, 586
Temperature, effect of, on adsorption, *434*
    on sorption of hydrogen by metals, *589*
Temperature scale, of Kelvin, 2
  of Rankine, 5
Thermal conductivity of gases, at low pressures, *48*, 52, 53
  at normal pressures, *44*
  film-theory of, *59*
  kinetic-theory relation for, 44
  values of, 46, 49
  variation of, with temperature, 46, 60
Thermal diffusion, *67*
  application of, to separation of isotopes, 72
  coefficient of thermal separation in, 68
Thermal separation, coefficient of, *see* Coefficient of thermal separation
Thermal transpiration, *65*
  effect of pressure on, 67
Thermionic emission, *see* Electron emission
Thermionic halogen vapor detector, *385*
Thermistor gauge, 329
Thermomolecular flow, *65*
Thorium, solubility of hydrogen in, 574, 587
Time constant for exhaust, *123*
Titanium, chemical clean-up by, 670
Titanium-hydrogen system, isotherms for, 581
Tor (Torr), unit of pressure, 4
Trouton constant, 755
Tungsten, reactions of incandescent, with gases, *675*
  solubility of nitrogen in, 599
  sorption of hydrogen by, 395
Turbulent flow of gases, *89*

Units, of pressure, 4, 5
  of quantity of gas, 6; *see also* Conversion factors

Vacuscope, 272
Vacustat, 272
Vacuum, production of very high, *730*
Vacuum cut-off, use of amalgams in, 217
Vacuum systems, design of, *134*
  use of charcoal in, 493
van der Waals constant b, 41
  relation of, to molecular diameter, 41
van der Waals equation for gases, 41, 417
Vanadium-hydrogen system, isotherms for, 582
Vapor pressure, relation of, to free energy, 741, 795
    to rate of evaporation, 18, 740
  variation of, with temperature, *740*
Vapor-pressure data, for beryllium, 747, 754
  for carbon, 748, 753
  for commercial oil, 789
  for metals, *743*
Vapor pressures, at low temperatures, *781*

Vapor pressures, at low temperatures,
      of ice, 782
    of mercury, 782
    of non-condensible gases, 785
    of rare gases, 784, 785
    of solid carbon dioxide, 783, 784
  of alloys, *764*
  of halides, *780*
  of oils, absolute method for determination of, 277
    for vapor-stream pumps, 222
  of oxides, *778*
  of silicones, 254
  of waxes and greases, *790*
  temperatures corresponding to given, *743*, 755, 756
Vapor-stream pumps, *see* Pumps
Velocities of molecules, *see* Molecular velocities
Velocity, of light, 8
  of sound, 13, 35
Viscosity, coefficient of, *see* Coefficient of viscosity
  kinematic, 35
Viscosity gauges, *see* Gauges
Viscous flow, *see* Flow of gases
Water vapor, free and total energy for formation of, *798*, 807
  rate of evolution of, from cellulose, 544, 545
  sorption and desorption of, in cellulose, *538*
  sorption of, *see under individual adsorbents*
    by charcoal, 482
    by different adsorbents, 500
    by glass, 528
    by quartz, 508
    by silica gel, 499, 500, 501
    by silicates, 508
Water-vapor cycle in tungsten lamp, 679
Waxes for use in vacuum technique, *790*
Wood charcoal, *see* Charcoal
Wood pulp, sorption of water vapor by, *see* Cellulose

Zeolites, sorption by, *see* Chabasite
Zirconium, chemical clean-up by, *670*
  solubility of hydrogen in, 574, 583, 585
  solubility of nitrogen in, 600

DATE OF ISSUE

This book must be returned within 3, 7, 14 days of its issue. A fine of ONE ANNA per day will be charged if the book is overdue.

For Reference
Only.

This book is issued for
3 DAYS ONLY.